

Ilya Volodyaev
Eduard van Wijk
Michal Cifra
Yury A. Vladimirov *Editors*

Ultra-Weak Photon Emission from Biological Systems

Endogenous Biophotonics and Intrinsic Bioluminescence



Ultra-Weak Photon Emission from Biological Systems

Ilya Volodyaev • Eduard van Wijk •
Michal Cifra • Yury A. Vladimirov
Editors

Ultra-Weak Photon Emission from Biological Systems

Endogenous Biophotonics and Intrinsic
Bioluminescence

 Springer

Editors

Ilya Volodyaev
Department of Embryology
Faculty of Biology
Moscow State University
European Medical Center
Moscow, Russia

Michal Cifra
The Czech Academy of Sciences
Institute of Photonics and Electronics
Prague, Czech Republic

Eduard van Wijk
MeLuNa Research
Wageningen, The Netherlands

Yury A. Vladimirov
Department of Medical Biophysics
Faculty of Fundamental Medicine
Moscow State University
Moscow, Russia

ISBN 978-3-031-39077-7 ISBN 978-3-031-39078-4 (eBook)
<https://doi.org/10.1007/978-3-031-39078-4>

© Springer Nature Switzerland AG 2023

This work is subject to copyright. All rights are reserved by the Publisher, whether the whole or part of the material is concerned, specifically the rights of translation, reprinting, reuse of illustrations, recitation, broadcasting, reproduction on microfilms or in any other physical way, and transmission or information storage and retrieval, electronic adaptation, computer software, or by similar or dissimilar methodology now known or hereafter developed.

The use of general descriptive names, registered names, trademarks, service marks, etc. in this publication does not imply, even in the absence of a specific statement, that such names are exempt from the relevant protective laws and regulations and therefore free for general use.

The publisher, the authors, and the editors are safe to assume that the advice and information in this book are believed to be true and accurate at the date of publication. Neither the publisher nor the authors or the editors give a warranty, expressed or implied, with respect to the material contained herein or for any errors or omissions that may have been made. The publisher remains neutral with regard to jurisdictional claims in published maps and institutional affiliations.

This Springer imprint is published by the registered company Springer Nature Switzerland AG
The registered company address is: Gewerbestrasse 11, 6330 Cham, Switzerland

Paper in this product is recyclable.

Preface

While this book was being prepared and written, the world changed several times, in ways both big and small.

Lev Belousov, our dear friend and colleague, has passed away, and we cannot but dedicate this work to him. Fritz-Albert Popp, a complex and controversial figure in science, but definitely a man of great magnitude with a vision who inspired many, is also no longer with us. Regrettably, Yuri Vladimirov, an originator and, until very recently, a towering figure in the field of bioluminescence, has been unable, due to an illness, to produce a large proportion of the book. The same is true of some other authors whose so much-anticipated contributions never materialized for various reasons, much to our chagrin. And yet somehow, as if by magic and against all odds, the book began to slowly take its current shape and form.

The events on a larger scale were no less dramatic. We have seen the COVID pandemic come and go, witnessed the onset of a horrendous, disgraceful war unleashed by my (IV) country against Ukraine, and finally, a heinous terrorist attack on Israel that transcends all boundaries of good and evil. At this very moment while the wars are still raging unabated, we cannot but feel enormous shame and grief over the unfolding tragedies and complete uncertainty of what lies ahead.

However, in less turbulent times, this book might have never seen the day. It unites under one cover individual scholars and research groups, who share little common ground and rarely agree to participate in any joint activities, be it a conference or a publication. However, we, both editors and participating authors, are convinced that the physical truth is one. Divergent or even controversial as data and their interpretation sometimes might be, we all believe them to coalesce one day into a unified and universally embraced paradigm – similar or dis-similar to views we espouse today.

For this reason, the current project contains both universally recognized and undisputed science, as well as undertakes forays into specific and often controversial areas. Meticulous attention has been paid to primary sources (in some cases, almost completely inaccessible today), for the original works contain valuable information that has occasionally been lost or been subject to misrepresentation down through the years.

We express profound appreciation to Prof. Belousov's son and widow, Sergey and Susanna, for permanent and unrestricted access to the library and archives of their family: Lev Belousov, Anna Gurwitsch and Alexander Gurwitsch, as well as to Alexander Krasnovsky Jr. for his critique and advice, and Nikolay Nadtochiy for his thorough linguistic assistance. We also thank our universities and research institutes: the Embryology Department of Moscow State University and the European Medical Center (IV), the Institute of Photonics and Electronics of the Czech Academy of Sciences (MC) and Meluna Research (EW) for their support, and especially our near and dear ones for the understanding and endless patience they showed us whenever we had to divert our attention from our family commitments to the book.

Our very special thanks go to Merry Stuber and her team from Springer Nature for their kindness and generosity with our delays and hassles, as well as the unwavering support they have been showing us along the way.

In the scientific field, we are thankful for the honor of having been around our teachers and mentors: Lev Belousov and Yury Vladimirov (IV), Roeland Van Wijk (EW) and Jiří Pokorný (MC), as well as Fritz-Albert Popp, and Emilio Del Giudice, all of whom we consider distinguished personalities and visionaries in science.

We would be happy to dedicate this book to the unity and mutual support of people, which is most vivid in science, and which is especially and urgently needed in stormy times. And on a very special note, to those distinguished people that have created this research area and developed it to the present-day state:

Alexander, Lidia and Anna Gurwitsch,
Tiberius Reiter and Denes Gabor,
Otto Rahn,
Gleb Frank,
Rene Audubert,
Sergey Konev,
Boris Tarusov and Alexander Zhuravlev,
Yury Vladimirov,
Rostislav Vasil'ev,
Janusz Slawiński and Danuta Slawińska,
Britton Chance,
Terence Quickenden and Rod Tilbury,
Jiří Pokorný,
Robert Allen,
Lev Belousov,
Fritz-Albert Popp,
Roeland Van Wijk,
Marco Bischof,
Humio Inaba and Masaki Kobayashi,
Francesco Musumeci,
Hugo Niggli,
Rajendra Bajpai,
Larissa Brizhik,
Emilio Del Giudice,
Vladimir Voeikov,
Daniel Fels,
Yu Yan.

It is our hope that these people, so starkly different in their perspectives and perceptions and yet invariably outstanding, will not object to finding their names listed together in token of respect and appreciation.

For, at the end of the day, the truth and physical reality are one, and peace, progress and unity of people are our shared imperative worth working and living for.

Moscow, Russia
Wageningen, The Netherlands
Prague, Czech Republic

Ilya Volodyaev
Eduard Van Wijk
Michal Cifra

Contents

| | | |
|--|--|------------|
| 1 | Introduction | 1 |
| | Ilya Volodyaev | |
| Part I History of UPE Research | | |
| 2 | Mitogenetic Rays | 7 |
| | Ilya Volodyaev and Elena V. Naumova | |
| 3 | Oxidation, Free Radicals and Ultraweak Luminescence | 27 |
| | Ilya Volodyaev | |
| 4 | Biophotons and the International Institute of Biophysics (IIB) | 49 |
| | Roeland van Wijk and Eduard van Wijk | |
| Part II Physics of Light and Light Research | | |
| 5 | Physics of Photon Emission | 61 |
| | Ilya Volodyaev and Yury A. Vladimirov | |
| 6 | Chemiluminescence as a Tool for Free Radical Research | 83 |
| | Dmitry Izmailov and Ilya Volodyaev | |
| 7 | Highly Sensitive Imaging and Spectral Analysis of UPE from Biological Systems and Their Application | 95 |
| | Masaki Kobayashi | |
| Part III Molecular Mechanisms of UPE | | |
| 8 | Free Radicals in Biology | 107 |
| | Ilya Volodyaev and Yury A. Vladimirov | |
| 9 | Ultraweak Luminescence from Aqueous Systems | 123 |
| | Ilya Volodyaev and Yury A. Vladimirov | |
| 10 | Chemiluminescence in Oxidation of Hydrocarbons: Mechanistic Fundamentals | 131 |
| | Ilya Volodyaev, Alexei Trofimov, and Yury A. Vladimirov | |
| 11 | Chemiluminescence in Oxidation of Fatty Acids and Lipids | 157 |
| | Ilya Volodyaev and Yury A. Vladimirov | |
| 12 | Chemiluminescence in Protein Oxidation | 189 |
| | Ilya Volodyaev and Yury A. Vladimirov | |

| | | |
|--|---|-----|
| 13 | Emitters of Endogenous Biological Chemiluminescence: Quantum Chemical Modeling Insights | 213 |
| | Homa Saeidfirozeh, Francesco Lelj, Michal Cifra, and Azizollah Shafiekhani | |
| 14 | Enzymatic Sources of Free Radicals | 219 |
| | Ilya Volodyaev and Yury A. Vladimirov | |
| Part IV UPE Research in Life Science | | |
| 15 | Luminescence of Animal Tissues and Vegetable Oils | 265 |
| | Alexander I. Zhuravlev and Ilya Volodyaev | |
| 16 | Ultraweak Photon Emission from the Human Body in Relation to Anatomy and Histology | 277 |
| | Roeland van Wijk and Eduard van Wijk | |
| 17 | Chronobiological Aspects of Spontaneous Ultra-Weak Photon Emission in Humans: Ultradian, Circadian and Infradian Rhythms | 289 |
| | Felix Scholkmann | |
| 18 | Autoluminescence in Seedlings: Applications | 305 |
| | Cristiano de Mello Gallep | |
| 19 | Application Potentiality of Delayed Luminescenc in Medicine, Biology, and Food Quality Researches | 313 |
| | Rosaria Grasso, Francesco Musumeci, Agata Scordino, and Antonio Triglia | |
| Part V Mitogenetic Effect and Related Phenomena: Unresolved Problems of UPE | | |
| 20 | Mitogenetic Effect in Biological Systems | 329 |
| | Ilya Volodyaev, Irina I. Kontsevaya, and Elena V. Naumova | |
| 21 | Physical Properties of Mitogenetic Radiation | 361 |
| | Elena V. Naumova and Ilya Volodyaev | |
| 22 | Secondary, Degradation and Necrobiotic Radiation | 387 |
| | Elena V. Naumova and Ilya Volodyaev | |
| 23 | Mitogenetic Research in Medicine: Radiation of Blood and Cancer Diagnostics | 403 |
| | Elena V. Naumova, Maira S. Aristanbekova, and Ilya Volodyaev | |
| Part VI Nonchemical Distant Interaction Hypothesis: Pro et Contra | | |
| 24 | The Possible Functions of Electromagnetic Cell Communication | 427 |
| | Daniel Fels | |
| 25 | Understanding Fritz-Albert Popp's Biophoton Theory from the Viewpoint of a Biologist | 435 |
| | Yu Yan | |

| | | |
|------------------------------|---|-----|
| 26 | Limits to Information Transfer Through Biological Autoluminescence | 441 |
| | Ondřej Kučera | |
| 27 | Quantum Nonlocality and Biological Coherence | 447 |
| | Sergey Mayburov | |
| Part VII Perspectives | | |
| 28 | Integrating Ultraweak Photon Emission in Mitochondrial Research | 461 |
| | Roeland Van Wijk and Eduard P. A. Van Wijk | |
| 29 | Selected Biophysical Methods for Enhancing Biological Autoluminescence | 475 |
| | Hadi Sardarabadi, Fatemeh Zohrab, Petra Vahalova, and Michal Cifra | |
| 30 | Upconverting Nanoparticles as Sources of Singlet Oxygen | 489 |
| | Cássio Cardoso Santos Pedroso, Sayuri Miyamoto, Amanda da Anunciação Farhat, Eduardo Alves de Almeida, Hermi Felinto Brito, and Paolo Di Mascio | |
| 31 | Delayed Luminescence as a Tool to Study the Structures of Systems of Biological Interest and Their Collective Long-Living Excited States | 505 |
| | Rosaria Grasso, Francesco Musumeci, Agata Scordino, and Antonio Triglia | |
| | Index | 519 |

Contributors

Maira S. Aristanbekova Saratov Regional Center for the Prevention and Control of AIDS, Saratov, Russia

Michal Cifra The Czech Academy of Sciences, Institute of Photonics and Electronics, Prague, Czech Republic

Amanda da Anunciação Farhat Departamento de Bioquímica, Instituto de Química, Universidade de São Paulo, São Paulo, SP, Brazil

Eduardo Alves de Almeida Departamento de Bioquímica, Instituto de Química, Universidade de São Paulo, São Paulo, SP, Brazil

Hermi Felinto Brito Departamento de Química Fundamental, Instituto de Química, Universidade de São Paulo, São Paulo, SP, Brazil

Paolo Di Mascio Departamento de Bioquímica, Instituto de Química, Universidade de São Paulo, São Paulo, SP, Brazil

Daniel Fels Independent Researcher, Binningen, Basel, Switzerland

Cristiano de Mello Gallep Faculdade de Tecnologia, Universidade de Campinas, Limeira, SP, Brazil

Rosaria Grasso Department of Physics and Astronomy “Ettore Majorana”, University of Catania, Catania, Italy

Dmitry Izmailov Moscow State University, Moscow, Russia

Masaki Kobayashi Tohoku Institute of Technology, Sendai, Japan

Irina I. Kontsevaya Francysk Skaryna Gomel State University, Gomel, Republic of Belarus

Ondřej Kučera Institut de recherche interdisciplinaire de Grenoble, Commissariat à l'énergie atomique et aux énergies alternatives (CEA), Grenoble, France

Department of Engineering Technology, South East Technological University, Waterford, Ireland

Francesco Lelej La.M.I. and LaSCAMM INSTM Sezione Basilicata, Dipartimento di Chimica, Università della Basilicata, Potenza, Italy

Sergey Mayburov Lebedev Institute of Physics, Moscow, Russia

Sayuri Miyamoto Departamento de Bioquímica, Instituto de Química, Universidade de São Paulo, São Paulo, SP, Brazil

Francesco Musumeci Department of Physics and Astronomy “Ettore Majorana”, University of Catania, Catania, Italy

Elena V. Naumova Rzhanov Institute of Semiconductor Physics, Russian Academy of Science, Siberian Branch, Novosibirsk, Russia

Cássio Cardoso Santos Pedroso The Molecular Foundry, Lawrence Berkeley National Laboratory, Berkeley, CA, USA

Departamento de Bioquímica, Instituto de Química, Universidade de São Paulo, São Paulo, SP, Brazil

Homa Saeidfirozeh J. Heyrovský Institute of Physical Chemistry, Czech Academy of Sciences, Prague, Czech Republic

Hadi Sardarabadi Faculty of Medicine, Cellular and Molecular Research Center, Qom University of Medical Sciences, Qom, Iran

Felix Scholkmann Biomedical Optics Research Laboratory, Department of Neonatology, University Hospital Zurich, University of Zurich, Zurich, Switzerland

Institute of Complementary and Integrative Medicine, University of Bern, Bern, Switzerland

Agata Scordino Department of Physics and Astronomy “Ettore Majorana”, University of Catania, Catania, Italy

Azizollah Shafiekhani Department of Physics, Alzahra University, Tehran, Iran

Antonio Triglia Department of Physics and Astronomy “Ettore Majorana”, University of Catania, Catania, Italy

Alexei Trofimov Emanuel Institute of Biochemical Physics, Russian Academy of Sciences, Moscow, Russia

Petra Vahalova Institute of Photonics and Electronics of the Czech Academy of Sciences, Prague, Czechia

Eduard Van Wijk Meluna Research, Wageningen, The Netherlands

Roeland van Wijk Meluna Research, Wageningen, The Netherlands

Yury A. Vladimirov Moscow State University, Moscow, Russia

Ilya Volodyaev Moscow State University, Moscow, Russia

Yu Yan Meluna Research B.V. Business & Science Park Wageningen, Wageningen, The Netherlands

Alexander I. Zhuravlev Moscow State University, Moscow, Russia

Fatemeh Zohrab Department of Medical Science, Qom Branch, Islamic Azad University, Qom, Iran

Introduction

Ilya Volodyaev

“Ultraweak photon emission (UPE),” “biophoton emission,” “biological autoluminescence (BAL),” “biochemiluminescence (BCL),” etc. are different terms for the phenomenon of *intrinsic (spontaneous) photon emission of extremely low intensity, which is characteristic of all biological systems as well as many model objects*. The system composition, its state, and external conditions determine its intensity, spectrum, and, possibly, other physical properties, but the phenomenon itself remains universal. This brief introduction outlines the main historical milestones and basic concepts in the field of ultraweak luminescence. A detailed presentation of these issues will be given in the later parts of the book.

1.1 Historical Lines

The UPE studies, like any other area of scientific activity, were marked by milestone discoveries that shaped the course of scientific research for many years ahead. Looking back, we can identify several individual strands of research, each one starting out and evolving more or less independently and finally merging in the last decades of the twentieth century.

The first strand starts with purely biological questions, addressed by an outstanding Russian biologist A.G. Gurwitsch (1874–1954): What causes a single cell to unfold into a complex, well-organized living organism? Why do cells divide at the right time and in the right place? This led A.G. Gurwitsch to formulate the hypothesis of the so-called mitogenetic radiation (MGR) and set up a number of various experiments, which resulted in long-term studies undertaken by many scientists in the period 1923–1950s. The history of this line is described in Chap. 2.

The second strand is dedicated to free radicals and free-radical processes. Here, the first stage can probably be called the peroxidation theory by A.N. Bach and G. Engler (1897),

who were the first to suggest that oxidation of organic molecules yields unstable peroxide compounds. The second stage is the radical chain reactions theory formulated by N.N. Semenov (1928, 1934), who showed that free radical particles appearing in a system can participate in whole chains of concurrent reactions and, using his theory, explained the Bach–Engler peroxidation kinetics. The next important step was the theory of liquid-phase oxidation of hydrocarbons and fats, developed by N.M. Emanuel (1961, 1965), and the large-scale research of radical reactions in liquid-phase hydrocarbons by R.F. Vasil’ev and group (1960s and further). Finally, the modern stage in the study of free radical processes in lipids and biological systems in general was undoubtedly largely predetermined by the works of B.N. Tarusov, who hypothesized the decisive role of lipid chain oxidation in the action of ionizing radiation and other damaging factors on the cell (1954–1957).

The third research line – physical research of biological autoluminescence – should go back to the first attempts of A.G. Gurwitsch’s MGR physical detection. These were performed by B. Rajewsky (1930, 1931) and G.M. Frank (1932), who invented special photosensitive modifications of Geiger–Muller counters, and later developed by H. Barth (1936), R. Audubert (1938), and others (see more in Chap. 21). However, only with the invention of photomultiplying tubes did this direction really begin to flourish, starting with the works of B.L. Strehler and W. Arnold (1951), L. Colli and U. Facchini (1954), Yu.A. Vladimirov and F.F. Litvin (1959), and the group of A.I. Zhuravlev and B.N. Tarusov (1960s). These works can be considered the beginning of the modern period in biological autoluminescence studies per se (see Chap. 3).

Finally, the fourth research line, also ideologically going back to A.G. Gurwitsch’s works, is the research of F.A. Popp et al. (1970s–1990s), who attempted to discover the physical properties of biological autoluminescence and to explain its supposed ability for light-mediated communication. Chapter 4 is devoted to this aspect of the story.

I. Volodyaev (✉)
Moscow State University, Moscow, Russia

Over time, these lines have appeared and disappeared and have weirdly intertwined – both helping and, at times, conflicting with each other. Our current knowledge, as well as what we still do not know, is the result of this bizarre historical process of scientific development.

1.2 The Physics of Photon Emission

Any quantum of luminescence is generated during radiative relaxation of the excited state of some molecule. Lower-energy excited states relax non-radiatively, releasing energy to the vibrational and rotational degrees of freedom of the surrounding molecules (Fig. 1.1b). Excited states that have sufficient energy for photon generation are electronic, in which one or more electrons occupy a higher orbital (Fig. 1.1c, d).

The phenomenon of luminescence can be classified according to the initial source of the excitation energy and the physical properties of the relaxation process.

According to the origin of electronic excitation, luminescence can be classified into:

- **Photoluminescence** – excitation is generated by external light
- **Thermoluminescence** – excitation is generated by sample heating (which requires a system with previously stored energy from external processes)
- **Electroluminescence** – excitation is generated by transmission of electric current through the sample

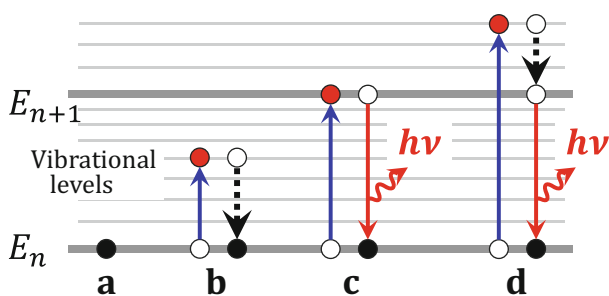


Fig. 1.1 A diagram of energy levels and transitions in a molecule. E_n is the ground (unexcited) electronic level of the molecule; E_{n+1} is the excited electronic level; and the vibrational excited energy levels are shown for both E_n and E_{n+1} . a – ground (unexcited) state, b – (spontaneous) transition to a vibrationally excited state and its non-radiative relaxation (without photon emission), c – transition to the electronically excited-state E_{n+1} upon absorbing a large portion of energy and its radiative relaxation (accompanied by photon emission – luminescence), d – transition to a vibrational sublevel of E_{n+1} and its relaxation in two stages: (1) rapid non-radiative relaxation to E_{n+1} and (2) radiative relaxation from E_{n+1} to E_n

- **Sonoluminescence** – excitation results from the impact of ultrasound on the fluid
- **Mechanoluminescence** – excitation is generated by mechanical forces acting on a solid object
- **Chemiluminescence** – electronic excitation states are generated by chemical (free radical) processes

In the case of biological autoluminescence, this excitation energy almost entirely comes from chemical processes within the system, which automatically categorizes it as chemiluminescence (**biochemiluminescence**, as it is usually called). Other luminescence types can also be observed in biological systems under special conditions (or in specific parts, like photosynthetic complexes). Moreover, though it is obviously incorrect to call them all spontaneous (intrinsic, auto-) luminescence, in the end, they can turn out contributing to the internal processes that lead to photon generation and autoluminescence. All this is associated with the electronic excitation energy transfer between molecules (or supramolecular complexes) and will be discussed further in Chap. 5.

According to the physical properties of radiant relaxation, luminescence can be classified into:

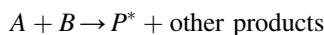
- Fluorescence – if the radiant relaxation is not accompanied by electron spin changes (either singlet–singlet or triplet–triplet relaxation)
- Phosphorescence – if the outer electron spin is inverted during relaxation (triplet–singlet or (very rarely) singlet–triplet relaxation)

Phosphorescence belongs to what is called the spin-forbidden process, which means that its probability is many orders of magnitude lower than for fluorescence. This manifests in different excited-state lifetimes, depending on the available electronic relaxation ways. Typically, the states in which a molecule relaxes fluorescently have a characteristic lifetime in the order of $10^{-9} - 10^{-8}$ s, whereas those in which a molecule can relax only phosphorescently (i.e., with spin inversion) have a characteristic lifetime in the order of $10^{-4} - 10^1$ s. This will also be discussed in Chap. 5.

In addition, many living organisms, such as fireflies, bacteria, and some marine species, are capable of emitting quite strong light as a result of specialized enzymatic reactions. In these cases, electronically excited states appear during the reaction of a highly specialized enzyme with its specific substrate, with a very high radiative relaxation quantum yield. This glow is called bioluminescence, but, due to its high intensity, it is not related to UPE.

1.3 The Chemistry of Photon Emission: Chemiluminescence in Biological Systems

As mentioned above, biological autoluminescence is almost exclusively chemiluminescence. Its appearance means that the energy released at one of the stages of the chemical processes within a system is sufficient to form one of the reaction products in an electronically excited state:



It is the relaxation of this product's electronically excited state that leads to photon generation:



These relaxation processes are independent of way that the P^* molecule is excited and can proceed from the singlet level S_1 (fluorescence – since in most cases, the ground state is singlet), triplet T_1 (phosphorescence), and, in rare cases, follow anti-Stokes pathways (see Sect. 5.2.5). In addition, naturally, the processes of excitation energy transfer between molecules or parts of one molecule, non-radiative relaxation, luminescence quenching due to interaction with other molecules, etc. are possible (see Chap. 5). Therefore, endogenous biological chemiluminescence has very low quantum yields, which determines its ultralow intensity.

Let us note several key features of biochemiluminescence (BCL):

1. In general, chemiluminescence, including BCL, originates from the relaxation of electronically excited states of certain reaction products. These excited states arise due to electron transfer between parts of the same molecule or different molecules – recombination of previously separated charges or unpaired electrons.
2. In biological systems, under normal conditions, only recombination of free radicals (e.g., lipid radicals, amino acid radicals) is sufficiently exothermic to generate electronically excited states.
3. Free radicals are typically very reactive and attack the nearest organic molecule, accepting an electron from it (or giving it an electron, if it is a stronger oxidant). As a result, this neighboring molecule turns out to become a free radical and attacks the next molecule in its turn. Thus, a single free radical can potentially originate a chain process of one-electron oxidation of many organic molecules in the system.
4. This complete oxidation in biological samples usually doesn't happen due to the presence of antioxidants, and

free radical recombination, thus terminating this chain reaction.

5. At the same time, some free radical products – usually, organic hydroperoxides – can also decompose to form new free radicals. This can lead to the chain process's branching and an explosive increase in its speed.

Thus, free radical processes are potentially highly dangerous to a cell, and the fact that they can be monitored by detecting the accompanying chemiluminescence has important applications, both for research and for medicine. Nowadays, the prominent role of free radical reactions in body aging and in the development of almost all advanced-age diseases has become obvious. This is largely due to the improvement of direct and indirect methods of detecting free radicals in biological objects and model systems.

1.4 The Dual Role of Free Radicals

Yet, as we now know, free radicals not only cause damage to cellular structures but also act as contributors to the proper functioning of living cells. A number of crucial enzymatic processes, such as respiratory chain functioning, or peroxidase action, go through free radical states and fundamentally cannot proceed otherwise. This means that free radicals are inevitably present in biological systems, as well as free radical processes, including branched-chain peroxidation and radical recombination, generating light quanta. Thus, autoluminescence is also a profound intrinsic quality of biological systems.

While accumulating new knowledge, a lot of initial ideas about the mechanism of the radicals' formation and their subsequent reactions have changed. Twenty years ago, most researchers were convinced that free radicals' generation was mainly catalyzed by iron and other transition metal ions (see Chaps. 8 and 11). Nowadays, it has become obvious that the main source of free radicals is reactions involving metalloprotein enzymes, including heme proteins (see Chap. 14).

The same applies to the notion of targets for free radicals. It was believed that due to the radicals' high chemical activity, their action is nonspecific and always destructive. This resulted in common generalizing terms, such as "oxidative stress" or "reactive oxygen species (ROS)," suggesting the randomness and complexity of the radicals' destructive action on living cells and bodies. Yet, data obtained in recent years have shown quite different facts: the *in vivo* action of various radicals can be much more specific, aimed at benefiting the living body and ensuring the survival of the species.

Much information has been accumulated on the radicals' role in an individual cell's life as well as on the relationship between systemic and local manifestations of excessive radical formation (oxidative stress). This has formed the basis for a number of analytical methods for assessing the level of free radicals in the human body under various pathological conditions.

In this context, the early works on the supposed signaling role of UPE, initiated by the pioneering studies of A.G. Gurwitsch on the so-called mitogenetic effect and mitogenetic radiation, partly discredited by inept followers and forgotten by the scientific community for several decades, are perceived in an unexpectedly new way. Chapter 2 and Parts V and VI are devoted to these studies, their modern rethinking, and reflections on possible further development.

The relatively late discovery of such a universal phenomenon as UPE (in 1923 by A.G. Gurwitsch and again in 1954 by L. Colli and U. Facchini, in 1959 by Yu.A. Vladimirov and F.F. Litvin, and in 1961 by B.N. Tarusov, A.I. Zhuravlev, and A.I. Polivoda) is associated with its extremely low intensity ($\sim 10^0 - 10^3$ quanta/s/cm²) and complex requirements for both equipment and research workflow. An interesting and diverse history of this issue is further described in Chap. 3.

1.5 Summary

Light appears in biological systems in course of electronically excited states relaxation. Outside of special external influences, the main mechanism for their generation is free radical chain reactions, including branched-chain mechanisms. Moreover, even under external influences, almost all light generation processes in biological systems have free radical stages. As it is now known, such stages (usually extremely short-living and therefore inaccessible to the researcher) are characteristic of most biochemical processes, and "working with free radicals" is one of the most important aspects of cell life.

The proper functioning and life of a cell itself largely depends on the balance between suppression and activation of free radical processes. In this sense, the free radicals appearing and utilized in the cell, are reminiscent of nuclear power plants: the enormous possibilities and colossal efficiency of normally proceeding processes are associated with no less colossal risks if they get out of control.

The molecular mechanisms of chemiluminescence and the processes associated with free radical formation and chemical transformations will be discussed in detail in Part III. In the next Part I, we will provide a historical review of this research area's emergence and development.

Part I

History of UPE Research



2.1 Introduction: On the History of Mitogenesis

Ultraweak photon emission (UPE) from biological systems was predicted (Gurwitsch 1911, 1922) and first observed (Gurwitsch 1923) by a distinguished Russian biologist Alexander Gurwitsch. The main particularity of his work, which was both successful and posed serious problems, was that the UPE was detected with biological, but not physical, detectors. The “biological detector” (plant meristem, microbial or tissue culture) demonstrated higher rate of cell proliferation when put in optical contact with a UPE source, called “inductor.” This phenomenon was termed “mitogenetic effect” (MGE) and was soon attributed to ultraviolet UPE due to its ability to propagate only straightly in uniform media, disappear if the two interacting objects were separated with any material opaque in the UV (including glass), and preserve when they were separated with quartz, while being chemically isolated (Gurwitsch 1924a; Reiter and Gabor 1928b) (see below). Thus, the term “mitogenetic radiation” (MGR) was suggested (Gurwitsch 1924a), which was actively used for more than 30 years, and was later considered inexact by the author (Gurwitsch and Gurwitsch 1999), because of its connection with phenomena not related to mitogenesis:

1. Besides tissues and cultures with high mitosis rate, MGR was observed for excited muscles and nerves (Siebert 1928a; Anikin 1926); stressed, dying, or resorbed tissues (Blacher and Bromley 1931; Gurwitsch and Gurwitsch 1948, 1959); and some chemical reactions (Wolff and Ras 1932; Potozky 1932; Braun 1934). The authors

concluded that “the ability to emit ultraweak ultraviolet rays is an extremely common property of most chemical processes, regardless of whether it is a simple oxidation of inorganic substances in a test tube, or splitting of complex protein bodies in a living organism” (Rodionov and Frank 1934).

2. Besides stimulation of mitoses, MGR could cause quite different effects in the recipient object: mitotic suppression (Acs 1933), decrease of nerve conduction (Gurwitsch 1937), increase of permeability of plant cell walls (Potozky 1936), appearance of malformations in embryo development (Magrou 1932), etc.

The biological way of “detecting” UPE, initially suggested due to the very role the UPE was presumed to play in the living organisms, appeared extremely problematic for the whole field and doubtful in the eyes of many researchers. Its main disadvantages were obvious subjectiveness and laborious methods of observation, vulnerable to subtle deviations from the procedure. At the same time, as physiology and molecular biology were actually in their infancy, the procedure itself was usually described rather vaguely (e.g., “20-hour-old yeast culture on wort agar” without any information on its physiological state or medium content), and experimental details and results were frequently alternating with explanations and reflections on the topic. It was probably due to this uncertainty that many authors experienced periods of unexplained irreproducibility of their results, which later gave way to periods of sustained success.

The materials and methods of some “early works” were partially cleared up in Rahn (1936) and Gurwitsch (1968) and, nowadays, analyzed in Volodyaev and Belousov (2015) and Volodyaev et al. (2021) (see also Part V).

Having once tried to reproduce MGE and failed (Volodyaev et al. 2013) and determined to put an end to this topic for ourselves, one of us (IV), together with the late Lev Belousov, plunged into thorough reading of the “old literature” on MGE. Unexpectedly, we found so many

I. Volodyaev (✉)

Biological Faculty of M.V. Lomonosov Moscow State University, Moscow, Russia

E. V. Naumova

Rzhanov Institute of Semiconductor Physics, Russian Academy of Science, Siberian Branch, Novosibirsk, Russia

important methodical details that we had missed, that our main conclusion happened to be the following: “if the mitogenetic effect existed, under our experimental conditions, it was sure not to manifest.” That is, we had done everything *not* to confirm the effect, only because we had not paid enough attention to methodical details of the early works.

Though detailed methodical recommendations had been given in Gurwitsch (1929) and Reiter and Gabor (1928b), most of the “negative works” we managed to get and study (Hollaender and Claus 1937; Taylor and Harvey 1931; Kreuchen and Bateman 1934; Richards and Taylor 1932; Quickenden and Tilbury 1985; Quickenden et al. 1989) also contained critical deviations from these methods, that would have guaranteed their failure in MGE verification. Our experience in this area, together with both positive and negative works, analyzed from methodical viewpoint is given in Chap. 20, and also in Volodyaev and Belousov (2015).

At the same time, the biological method of “UPE detection” appeared extremely sensitive, as it let the authors discover UPE as weak as $10\text{--}1000\text{ photons/s}^{-1}\text{ cm}^{-2}$, 15 years before the first stable success in its physical detection (Barth 1936; Barth 1937; Grebe et al. 1937; Audubert 1938), and 30–40 years before what is presently considered its proof (Colli and Facchini 1954; Vladimirov and Litvin 1959; Tarusov et al. 1961).

Notwithstanding lack of general recognition of MGE, and complete mistrust of some researchers, one has to admit that the basic data on MGE were actually never refuted in later works and seemingly do not contradict them. Moreover, many results and conclusions of early works were proven later or appeared to have curious parallels in what is known now: the phenomenon of UPE from biological systems (see Part IV), free-radical processes as its source (see Part III), the existence of peptide tumour markers in blood (see Chap. 23), etc. These facts command respect to early experiments and attract interest to their broader revisiting and thorough investigation at the up-to-date level. With this in mind, we now aim to go through a brief, yet evidence-based summary of the history of MGE research, and come to some general discussion closer to the end of the book (Chaps. 20, 21, 22, and 23).

2.2 A Brief History of the Mitogenetic Research

Here, we briefly describe the history of mitogenetic radiation, in a concise form, with illustrations from the now almost inaccessible original works.

2.2.1 1910s–1923 – Before the Beginning

2.2.1.1 A.G. Gurwitsch’s Reflections on the Factors Inducing Mitosis and Organizing Its Temporal Orderliness in Tissues. His Concept of Two Mitotic Factors: “Factor of Cell Readiness” and “Initiation Factor”

In Russia, the 10s–20s of the twentieth century are associated with global historical upheavals: participation in the First World War, two revolutions, and the Civil War. A famous histologist and morphologist, a world-famous scientist, A.G. Gurwitsch received invitations from leading world universities, including personal offers from Wilhelm Ru to replace him in his position. Yet, he remained in Russia.

In 1918, he left the ruined Petrograd to the newly founded Taurida University in Simferopol, where he was to spend very fruitful years, among the great scientists V.I. Vernadsky, V.A. Obruchev, S.I. Metalnikov, and V.I. Palladin and his outstanding pupils A.A. Lyubishchev, G.M. Frank, and others.

Here, during extensive histological observations, A.G. Gurwitsch discovered the following pattern. While neighboring cells in a tissue or embryo can divide independently (Fig. 2.1a), several nuclei surrounded by a single membrane – in multinucleated cells (Fig. 2.1a, b) or syncytia (Fig. 2.1c, d) – always divide synchronously (Gurwitsch 1926).

This observation led the author to formulate his “two-factor theory of mitosis.” According to this, in order to start mitosis, the cell requires two independent factors:

1. The endogenous “readiness factor” – meaning all the processes of synthesis <and replication> that must be completed in advance (Gurwitsch 1926)
2. The exogenous “initiation factor” – an external impulse that must somehow affect the cell membrane and trigger the (already prepared) mitosis in all the nuclei surrounded by it (Gurwitsch 1926)

The “readiness factor” was obvious even at that time (long before the DNA discovery), while the search for the hypothetical “initiation factor” prompted A.G. Gurwitsch to the following experiments.

2.2.1.2 Experiments Indirectly Confirming the Existence of the “Initiation Factor” and the Two-Factor Theory of Mitosis. Rationale That the “Initiation Factor” Should Be Radiation

A.G. Gurwitsch obtained the first indirect evidence for the existence and possible nature of the initiation factor in experiments with onion roots (*Allium cepa*). If an onion

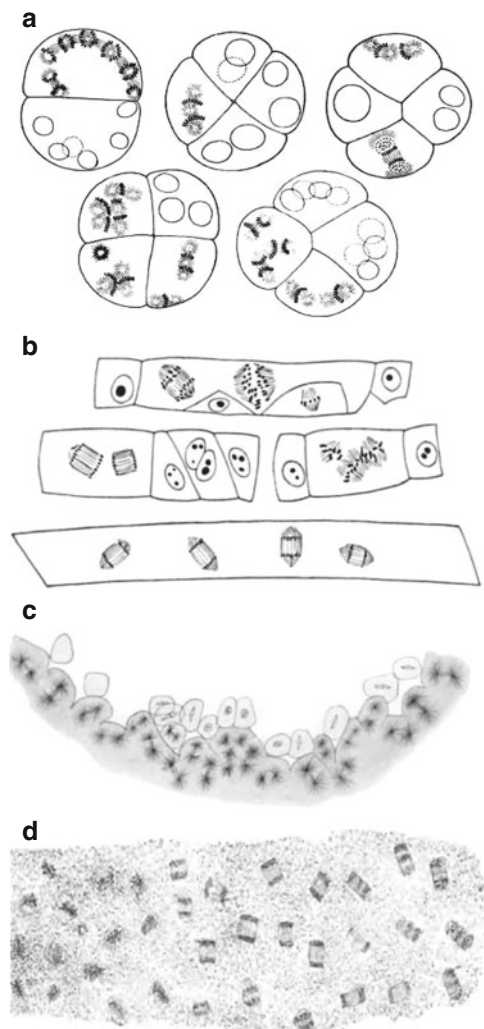


Fig. 2.1 Observations that led A.G. Gurwitsch to the “two-factor theory of mitosis”: (a) Synchronous mitoses of nuclei in one blastomere; asynchronous mitoses in different blastomeres (*Sea urchin* embryos). (b) Synchronous mitoses in multinucleated cells (*Ricinus* root). (c, d) Synchronous mitoses in syncytia (c – *Belone acus* periblast, d – *Fritillaria imperialis* embryo sac). (Adapted from Gurwitsch (1926). Copyright 1926, with permission from Springer Nature)

root was separated from the bulb, or the bulb was narcotized or killed with local boiling, the mitoses in the onion root meristem were suppressed. Yet, even a small viable piece of the sole remaining on the root base, was enough to maintain mitoses in the root meristem (Gurwitsch 1926). Thus, cell division in the onion root meristem required a certain external impulse, apparently coming from the bottom of the bulb.

On the physical nature of the “initiation factor,” Gurwitsch considered two possible alternatives:

1. A chemical ligand, sensed by membrane receptors

2. A kind of radiation, sensed by a “mosaic” of membrane-associated receivers by means of resonant absorption (the question how such a radiation could spread in the tissue was addressed later – see below)

In a series of histological observations on longitudinal sections of onion roots, the author showed that the probability of detecting a meristem cell in the state of mitosis decreases linearly with its length and exponentially increases with its distance from the bottom of the bulb (Gurwitsch 1923). Interpreting this pattern, through a complex chain of reasoning (Gurwitsch 1926), he concluded that the initiation factor should be resonantly acting on something spatially distributed in the membrane and suggested it to be a kind of radiation.

2.2.1.3 The First Experimental Evidence in Favour of the Radiant Nature of the Initiation Factor

The first attempts to test the hypothesis that the initiation factor is radiant, were carried out on frog cornea (apparently *Rana temporaria*). It was known that a wound applied to the corneal epithelium stimulates mitosis in the surrounding tissue. Varying the size and type of wound, Gurwitsch obtained the following results (Gurwitsch 1923):

- A burn wound, applied to the cornea led to suppression of mitoses in the nearest cells (quite soon) and stimulation of mitoses 3–4 days later.
- Too strong wounds gave only suppression.
- Accurate linear cuts had no effects on the cornea, but they “screened” a part of it from the mitosis-stimulating influence of the burn wound (Fig. 2.2), “as if the initiation factor were linearly spreading through the tissue.”

The author’s conclusions from the results were as follows (Gurwitsch 1926):

1. The existence of the initiation factor is indirectly confirmed; its (additional) source in the tissue is the wound surface;
2. The initiation factor propagates linearly in the medium, i.e., apparently, is radiation (the critical question how such a radiation could spread in the tissue was addressed much later – see below).

Thus, the “two-factor theory of mitoses” was preliminary considered right, and the initiation factor was supposed to be some kind of radiation. This brought the author to his famous “Grundversuch” – “onion experiment.”

2.2.2 1923–1928 – Discovery and First Surge of Interest in MGE and MGR

2.2.2.1 The First Observation of Mitogenetic Effect on Onion Roots and the Surge of Interest in the Newly Found Phenomenon

After obtaining preliminary data, indirectly supporting the existence and radiant nature of the initiation factor, Gurwitsch turned to direct experimental verification of this

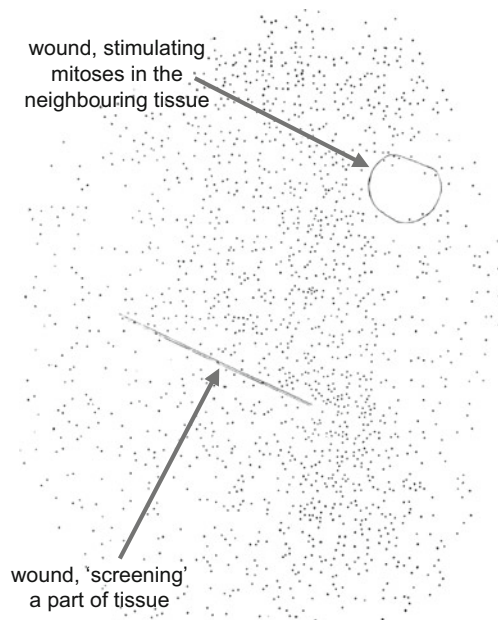
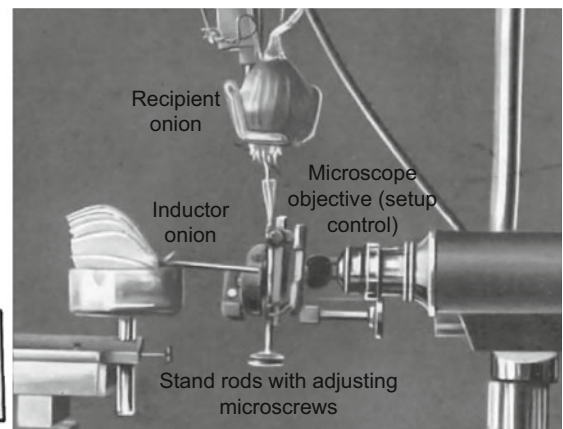
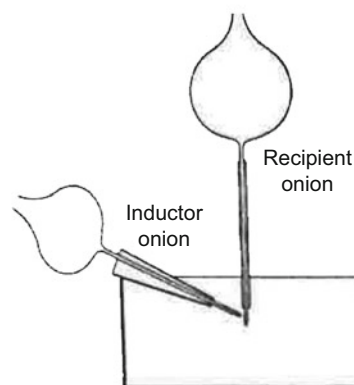


Fig. 2.2 Spatial distribution of mitoses (dots) in *frog* cornea (*Rana temporaria*) after applying a round burn wound (“stimulating mitoses in the surrounding tissue”) and a “linear, most accurate” wound (“screening a part of tissue from the influence of the round wound”). (Adapted from Gurwitsch (1923). Copyright 1923, with permission from Springer Nature)

Fig. 2.3 “Onion experiment” for detecting the supposed initiation factor. (a) Scheme of experimental setup. (Adapted from Gurwitsch (1926). Copyright 1926, with permission from Springer Nature). (b) Photo of experimental setup. (Adapted from Gurwitsch (1923). Copyright 1923, with permission from Springer Nature)



hypothesis. For this, he needed to create conditions under which the hypothetical induction factor would be partially irradiated beyond the biological system and could affect another one, in which (if it was competent) the frequency of mitoses should increase (Gurwitsch 1923).

The onion root was chosen as the first (“inductor”) object, because in it (see above) the radiation was supposedly propagated from the bottom of the bulb to the tip and, therefore, could be partially radiated into the space. The onion root was also chosen as the second (“recipient”) object, because, in the absence of obvious defects, the “perfectly straight root” is radially symmetric and, according to the author, the difference in the number of mitoses between any two halves of any transverse cut does not exceed 3%.

The experimental design and photograph of the setup are shown in Fig. 2.3 (the roots mutual position was precisely controlled with adjusting microscrews and a horizontal microscope).

The cross-sectional diagram of the control and induced onion roots in the induction region is shown in Fig. 2.4. The difference in the number of mitoses between the two halves of the root is shown in Fig. 2.5 (a – induced root, b – control, noninduced root). One can see considerably more mitoses in the induced half of the recipient root, and no difference in the control.

Thus, the presence of an inductor root near the division zone of the recipient root led to a stable effect: stimulation of mitoses in the induced half of the recipient. This phenomenon proved the existence of the initiation factor and was called the “mitogenetic effect” (MGE).

Soon, the MGE was confirmed by other authors (for a review, see (Reiter and Gabor 1928b)), not only on onion roots but also on other objects. However, its physical nature still required verification.

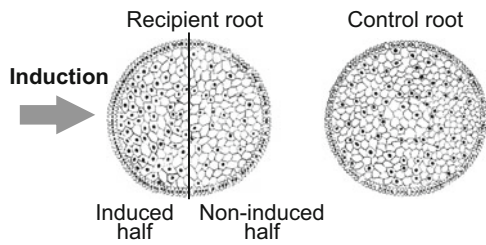


Fig. 2.4 Results of the “Onion experiment” for detecting the supposed initiation factor. A scheme of the cross-section of intact (control) and induced (recipient) onion roots after the experiment; mitoses marked. The number of mitoses at the “induced” half is definitely higher than at the “noninduced” half. (Adapted from Reiter and Gabor (1928a) and Gurwitsch and Gurwitsch (1932). Copyright 1932, with permission from Springer Nature)

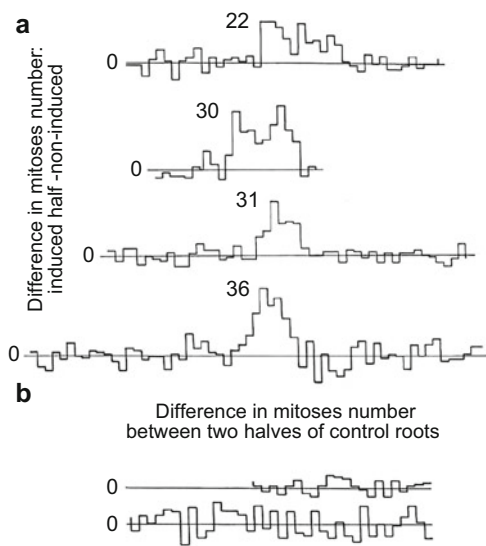


Fig. 2.5 Results of the “Onion experiment” for detecting the supposed initiation factor. Difference between the number of mitoses in two halves of the roots: (a) Recipient root: “induced” half–“noninduced” half (as the original figures contain no division values along axes, the numbers at plots were taken from the accompanying raw data tables). (b) Control (noninduced) onion root: random fluctuations around 0. (Adapted from Gurwitsch (1923). Copyright 1923, with permission from Springer Nature)

2.2.2.2 Evidence That MGE-Producing Factor Is Ultraweak Photon Emission in the UV Range; Appearance of the Term “Mitogenetic Radiation” (MGR)

In subsequent experiments, the authors turned to study the nature of the factor causing MGE (Gurwitsch 1924a; Reiter and Gabor 1928b; Frank 1929).

The MGE was preserved, when the inductor and the recipient were separated with quartz plates (Fig. 2.6), even when they were completely chemically isolated (Figs. 2.7 and 2.8). Separation of the inductor and the recipient with UV-opaque materials having various transparency windows

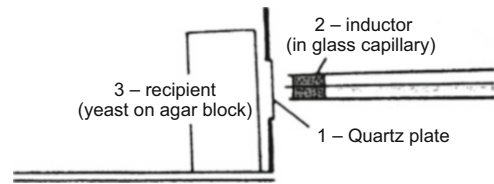


Fig. 2.6 Physical properties of mitogenetic effect: evidence that it is produced by UPE in the UV range. The inductor and the recipient are separated with quartz. (Adapted from Gurwitsch (1929). Copyright 1929, with permission from Elsevier)

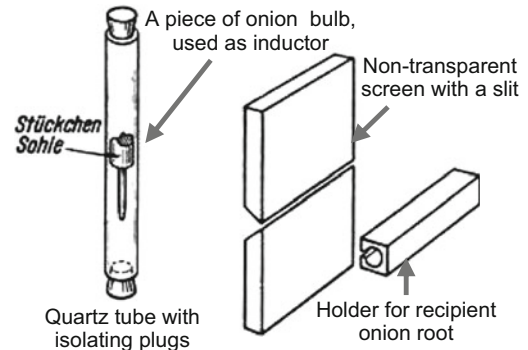


Fig. 2.7 Physical properties of mitogenetic effect: evidence that it is produced by UPE. The inductor is placed inside a quartz tube with isolating plugs. (Adapted from Reiter and Gabor (1928b). Copyright 1928, with permission from Springer Nature)

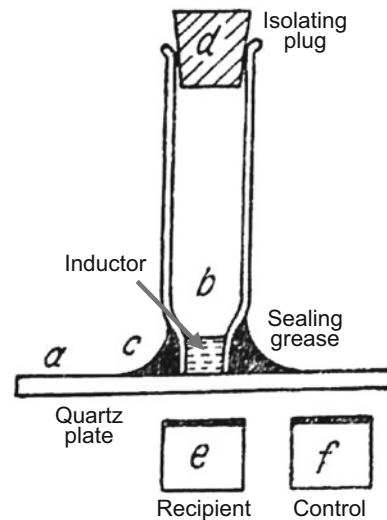


Fig. 2.8 Physical properties of mitogenetic effect: evidence that it is produced by UPE. The inductor is placed inside an isolated bottle with quartz bottom; the recipient is placed under the quartz bottom of the inductor; the control is placed next to the recipient. (Adapted from Blacher and Bromley (1931). Copyright 1931, with permission from Springer Nature)

(glass, wood, gelatin etc.) led to complete disappearance of MGE. Straightforward propagation (Fig. 2.7), reflection in UV mirrors (mercury and others) (Figs. 2.9 and 2.10) and

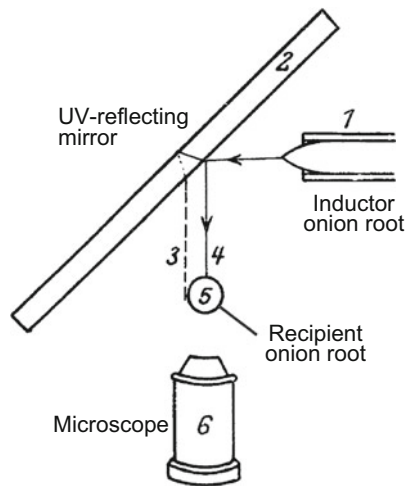


Fig. 2.9 Physical properties of mitogenetic radiation: reflection in mirrors. Experimental setup from Gurwitsch (1926). (Adapted from Gurwitsch (1926). Copyright 1926, with permission from Springer Nature)

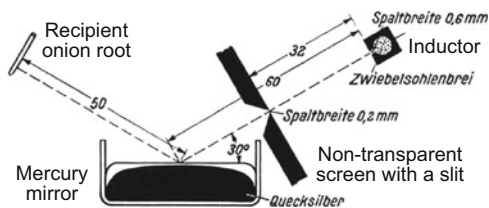


Fig. 2.10 Physical properties of mitogenetic radiation: reflection in mirrors. (Adapted from Reiter and Gabor (1928b). Copyright 1928, with permission from Springer Nature)

UV-like refraction in quartz prisms (Fig. 2.11) also corroborated the conclusion that the acting factor should be electromagnetic radiation belonging to the UV range (Gurwitsch 1926, 1929; Reiter and Gabor 1928b). Later, it was also confirmed by observation of MGE produced by weak UV radiation from artificial sources (see below and Chap. 20) and spectral analysis of MGE-inducing radiation from both biological and physical sources (see below and Chap. 21). A.G. Gurwitsch called this radiation mitogenetic (MGR).

2.2.2.3 Search for and Discovery of Other Inductors, Recipients, and Noninductors of MGE

As the existence of the initiation factor was supposed universal (Gurwitsch 1926), experiments on obtaining MGE began to be carried out at different objects and in different combinations. Below is a short list of recipients, inductors, and noninductors – those objects that didn't cause any MGE in the recipient (for more details on the conditions for obtaining the effect and requirements for objects, see Chap. 20).

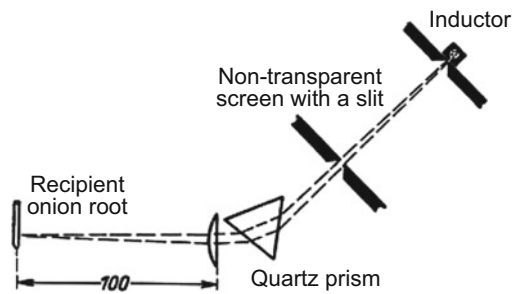


Fig. 2.11 Physical properties of mitogenetic radiation: refraction in quartz prisms. (Adapted from Reiter and Gabor (1928b). Copyright 1928, with permission from Springer Nature)

- **Recipients** – yeast (Siebert 1930; Baron 1926), bacterial cultures (Wolff and Ras 1931b; Sewertzowa 1928), corneal epithelium of frogs, tritons, rats (Gurwitsch and Anikin 1928)
- **Inductors** – yeast (Baron 1926), bacteria (Sewertzowa 1928; Acs 1931), eggs and embryos of different species (Magrou et al. 1929; Gurwitsch 1924d), blood (Sorin 1926; Potozky and Zoglina 1929), malignant tumours (Siebert 1928b; Gurwitsch and Gurwitsch 1928; Reiter and Gabor 1928b)
- **Noninductors** – blood of cancer patients (Gurwitsch and Salkind 1929; Siebert 1930; Gesenius 1930), internal organs of adult animals (Gurwitsch and Gurwitsch 1932), nongrowing or slowly growing cultures (Gurwitsch and Gurwitsch 1932)

Also, a number of works have shown MGE at interaction of organisms of different taxa (Siebert 1928a; Gurwitsch and Gurwitsch 1924), as well as “nonmitogenetic effects” of MGE: influence of growing bacterial cultures on embryo growth, teratosis, etc. (Magrou 1932; Wolff and Ras 1934).

Therefore, MGE appeared not species-specific and not associated with any highly-specific signals, “dictating to a cell or tissue what to do.” On the contrary, it turned out more like a “nonspecific primitive yes/no signal, triggering the recipient to start the process, determined by the other context.”

2.2.2.4 Spread of Work on MGE and MGR

Initially after MGE discovery, its study was conducted only by a narrow circle of A.G. Gurwitsch's close associates in Taurida University – his wife L.D. Gurwitsch (1924b, c) and daughter N.A. Gurwitsch (1924d), G.M. Frank (1925), S.J. Salkind (1925) and a few others. Their leaving for Moscow with appointment of A.G. Gurwitsch to the post of the Histology Department head, Moscow University (1924), gave rise to development of this small group into an advanced scientific school on mitogenesis.



Fig. 2.12 “Days of Soviet Science” in Berlin (1927). Sitting: 1st – C. Vogt, 2nd – A.V. Lunacharsky, 3rd – F.G. Schmidt-Ott, 4th – N.A. Semashko, 5th – M.P. Koltsova, 6th – wife of A.A. Borisyak. Standing: 1st – A.G. Gurwitsch, 2nd – P. P. Lazarev, 3rd – A. Einstein, 6th – A.F. Samoilov, 10th – A.I. Abrikosov, 12th – Ambassador of USSR in Germany N.N. Krestinsky, 13th – A.Ye. Fersman, 14th–

N.K. Koltsov, 16th – A.V. Palladin, 17th – V.N. Ipatyev, 19th – A.A. Borisyak, 20th – L.Ya. Brusilovsky, 21st – A.Ye. Chichibabin, 23rd – P.M. Nikiforov, 24th – V.I. Vernadsky, 25th – I.I. Schmalgausen. (From the personal archive of A.G. Gurwitsch, with the permission of his heirs)

Later, this problem attracted interest of various scholars around the world. A brilliant talk of A.G. Gurwitsch at the “Days of Soviet Science” in Berlin (1927), participated by A. Einstein, V.I. Vernadsky, and other outstanding people (see Fig. 2.12), stimulated further dissemination of knowledge about MGR and research spreading. At this time, several teams started their works on MGR, including the groups of J. Magrou (The Pasteur Institute, Paris), W.W. Siebert (The Medical Clinic of Berlin University, now Charité), A.F. Ioffe (State Physical-Technical Radiology Institute, now Ioffe Physical-Technical Institute, St. Petersburg), D. Gabor (Siemens&Halske AG, now Siemens AG, Berlin). Research by the physicist D. Gabor (later Nobel laureate) and the physician T. Reiter, and their monograph on MGE (Reiter and Gabor 1928b) had a strong impact on the field.

Also the first critical papers by H. Guttenberg (1928a, b) and his pupil B. Rossmann (Rossmann 1928) from Botanical Institute of Rostock University were published (their arguments and counter-critique see in Chap. 20).

Altogether, during the period of 1923–1928, the scope of works on MGE comprised verification of MGE; proofs of ultraviolet radiation as its mediator; wide diversification of the known biological inductors, noninductors, and recipients; and development of experimental methods.

2.2.3 1928–1938 – “The Golden Age of MGR”

2.2.3.1 Advancement of MGR Research

The next decade witnessed a burst of activity and significant progress in MGR research. “Nothing among biological works from your country attracts so much attention of scientific world as your works” – wrote A. Bethe, Director of the Institute of Physiology, Frankfurt am Main University, in

his letter to A.G. Gurwitsch in 1930 (Gavrish 2003). From 1929 to 1938, Gurwitsch was 11 times nominated for the Nobel Prize for his works on MGE and once failed to get just two votes to the prize (Nobel Prize Nomination Database).

The heated international discussion of that period was accompanied by multiple verifications of all key experiments in authoritative laboratories. MGR study was a fundamentally interdisciplinary field and attracted well-known experts in biology, physics, chemistry, physiology, and medicine. For instance, a famous physicist S.I. Vavilov summed up the results of an outstanding chemist R. Audubert as the final proof of A.G. Gurwitsch’s findings (Gurwitsch and Gurwitsch 1948) (see Chap. 21).

The development of interest to MGE and MGR led to series of works by various authors in the USSR, the United States, Germany, France, the Netherlands, Italy, and other countries. The most extensive research was conducted in the USSR (Moscow, Leningrad) and in Germany (Berlin, Frankfurt am Main); significant contribution was made by the groups of the microbiologist L.K. Wolff (Utrecht University, Netherlands) and the bacteriologist O. Rahn (Cornell University, USA). The total number of publications on these topics was more than 1000 (e.g., the dissertation of Moissejewa on MGR (Moissejewa 1960) contains more than 1000 references), including several dozen books and more than 50 publications in “top journals” (e.g., at least a dozen in Nature (Braun 1934; Copisarow 1932; Gurwitsch 1933; Gurwitsch and Gurwitsch 1939; Gurwitsch et al. 1965; Heinemann 1934; Prokofiewa 1934; Wolff and Ras 1934; Hill 1933; Bateman 1934; Gates 1929; Anonim 1937).

At the same time, although many of these publications confirmed the results of Gurwitsch (Reiter and Gabor 1928a; Tuthill and Rahn 1933; Ferguson and Rahn 1933; Wolff and Ras 1931b; Loos 1930), some other authors didn’t succeed in

obtaining MGE and published negative works (Taylor and Harvey 1931; Moissejewa 1931a, b; Rossmann 1928). According to the assessment (Maxia 1940), "...Several hundreds of confirming results coming from different countries... <were> opposed by barely a couple of dozen reports of negative results" (cited from Gurwitsch and Gurwitsch (1999)).

There was also a number of false-positive papers inevitable for such a surge of interest. The most detailed critical analysis of publications on MGE was presented in a series of papers by A. Hollaender (Hollaender and Schoeffel 1931; Hollaender and Claus 1935, 1937; Hollaender 1936, 1939; Hollaender and Duggar 1938). It is worth mentioning that being the most consistent critic of false-positive papers on MGE, he clearly stated that "we cannot believe that the phenomenon should be relegated to the limbo of an ignominious past, merely on the ground that some of the evidence presented by possibly overenthusiastic supporters is inconsistent" (Hollaender and Claus 1935). Moreover, he didn't claim MGE generally false even after his own failure to observe this effect (Hollaender and Claus 1937) (though later this work appeared the most crucial for the whole area). A. Gurwitsch also was indignant at plenty of emerged negative and positive publications with fundamental methodical errors (Gurwitsch and Gurwitsch 1999).

Among the critical papers of this period, the analytical reviews (Hollaender 1936; Bateman 1935) can be recommended as the most thorough ones.

A detailed analysis of critical works is given later in Chaps. 20 and 21. Here, we give only a summary assessment of the reliability of the results on onion roots, conducted in Schwemmlé (1929) (Fig. 2.13). In all experiments analyzed by the author, the difference in the number of mitoses

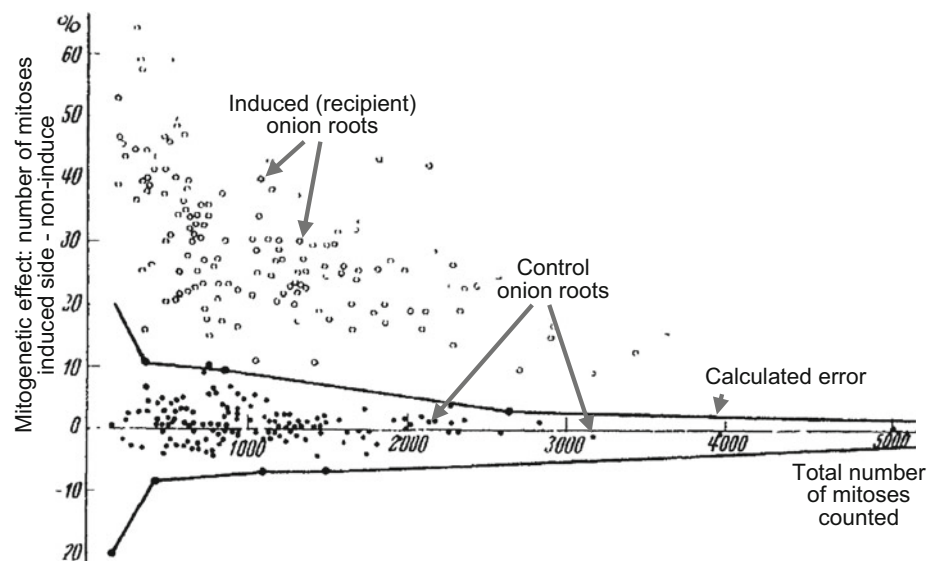
between two halves of control roots fell into the area of the calculated error, while the difference in the number of mitoses between the induced and noninduced sides of the recipient root exceeded the limits of this region. The author concluded that results of MGE experiments on onion roots are reliable (Schwemmlé 1929).

Besides verification of onion experiments, there was intensive further development of yeast (Tuthill and Rahn 1933; Baron 1930; Gurwitsch and Gurwitsch 1934) and bacterial (Ferguson and Rahn 1933; Wolff and Ras 1933b; Sewertzowa 1928, 1931) "MGR detection technique," more universal and less laborious and subjective than that based on onion roots. Thus, in the early 1930s, onion recipients in MGE research were almost completely superseded by yeast in the USSR and by bacterial ones in Europe and the United States. Their extensive use made it possible to elaborate and describe complicated experimental conditions for observing MGR (see methods in (Rahn 1936; Gurwitsch and Gurwitsch 1934; Gurwitsch 1945, 1968), and their present-day reanalysis in Chap. 20 and (Volodyaev and Belousov 2015; Volodyaev et al. 2021)). All this potentiated broadening of research activities and wide application of MGE for studying biochemical and physiological processes (see Chaps. 22 and 23, and (Gurwitsch and Gurwitsch 1934, 1959)).

In 1928–1938, the topics of MGE and MGR research were greatly diversified:

- Development of spectral analysis and its application to study nerve and muscle activity
- Physical detection of MGR
- Discovery of UV-chemiluminescent reactions
- Attempts to apply MGR to medical diagnostics; analysis of physiological states and biochemical processes in vivo

Fig. 2.13 The results of all publications of the Gurwitsch school devoted to MGE on onion roots by 1929. The filled circles are control roots; the hollow circles are recipients in MGE experiments. Each point is the result of one experiment. All control experiments fall within the area of the calculated error; all induced roots fall outside this area. Thus, in all the experiments analyzed, the result is reliable. (Adapted from Rahn (1936). Copyright 1936, with permission from Springer Nature)



- Study of MGR at stress conditions (“degradation MGR”) and its difference from physiological MGR
- Discovery of “secondary MGR,” emitted by some systems after exposure to MGR from other sources (see more in Chap. 22)

Theoretical efforts to comprehend extensive experimental data led to the concepts of free-radical mechanisms of MGR generation and “nonequilibrium molecular constellations” (i.e., delocalized electron-excited states) in biological systems (details and references see below).

The main focus of research works visibly shifted from biology to physics, chemistry and medicine. Several authoritative medical teams joined the field, for instance, the group headed by R. Seyderhelm, Director of Hospital of the Holy Spirit (Frankfurt am Main, Germany) (Heinemann 1932, 1934, 1935; Seyderhelm 1932; Seyderhelm et al. 1932; Heinemann and Seyderhelm 1933, 1934). Blood as the most commonly used object of medical tests and easily available active inductor of MGE had already got the top priority among biological inductors, MGR of blood in various physiological and pathological states was studied in-depth (Siebert 1930; Gurwitsch and Salkind 1929; Yefimov and Letunov 1934; Golshmid 1934; Gurwitsch and Gurwitsch 1934) and led to the discovery of the first tumour marker (Gurwitsch and Gurwitsch 1937; Siebert and Seffert 1937). Also wide-scale experiments were devoted to application of MGR spectral analysis to nerve and muscle activity research.

In this period, the trend of proceeding from study of MGE per se to its application as an analytical and diagnostic method began to show, and strengthened later on. As A. Gurwitsch stated “We suggest that... the use of the mitogenetic method will prevail and will gradually push into the background... the question of mitogenesis itself” (Gurwitsch and Gurwitsch 1999).

2.2.3.2 Further Development of the MGR Spectral Analysis

After rough estimations of MGR spectral range, its spectral composition was further studied with spectrographs, in which the photographic plates were replaced with series of biological detectors – which were onion roots in the first

Fig. 2.14 “Mitogenetic spectral analysis.” Scheme of experimental setup. (Adapted from Frank (1929) and Gurwitsch and Gurwitsch (1932). Copyright 1932, with permission from Springer Nature)

experiments (Reiter and Gabor 1928a), and usually yeast cultures later (Frank 1929) (see scheme of experimental setup in Fig. 2.14 and examples of spectra in Figs. 2.15 and 2.16).

Thus, according to the data of both groups, the MGR spectra belonged to UV. The differences in specific spectral regions with mitogenetic activity between (Reiter and Gabor 1928b) and (Frank 1929) (compare the spectra in Figs. 2.15 and 2.16) are apparently due to different recipients (onion roots in Reiter and Gabor (1928b) and agar yeast cultures in Frank (1929)), and other methodological details (see more in Chaps. 20 and 21). Yet, the general conclusion was similar: the MGE was stimulated by ultraweak UV light emitted from the inductor.

Later, with improvement of spectral resolution, the authors were able to obtain MGR spectra of a wide range of chemical systems and biological inductors and construct a database of their “spectral fingerprints” (Ponomarewa 1931; Kannegiesser 1931; Decker 1936; Billig et al. 1932; Braun 1934) – see Fig. 2.17. Analyzing these data, Gurwitsch, following (Frankenburger, 1933) made another assumption, which was more than 30 years ahead of the emergence of modern concept. They suggested that different bands in the MGR spectra correspond to different excited states generated in the system, mostly by recombining free radicals. It is these excited states that determine the wavelength of photon emission, rather than any special qualities of the ongoing processes (Gurwitsch and Gurwitsch 1934, 1959) (see more in Chap. 21).

The mitogenetic spectral analysis opened up the possibility of noninvasive study of biochemical processes in living organisms, which was widely used for system analysis (Gurwitsch and Gurwitsch 1934, 1959; Gurwitsch 1968) and medical diagnostics (Gurwitsch and Gurwitsch 1938; Gurwitsch et al. 1947). As A. Gurwitsch wrote, “contrary to any biochemical methods, the analysis is made not after, but during the functioning” (Gurwitsch and Gurwitsch 1934).

2.2.3.3 The Negative Side: Drawbacks of Biological Detection of MGR

Yet, not everything was so smooth. As it was already mentioned in introduction, biological detection of MGR had a number of serious disadvantages, that caused a lot of

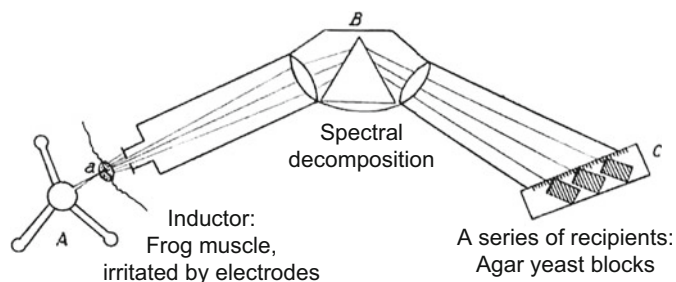


Fig. 2.15 MGR spectrum from rat sarcoma, obtained using onion roots as biological detectors. (Adapted from Reiter and Gabor (1928b). Copyright 1928, with permission from Springer Nature)

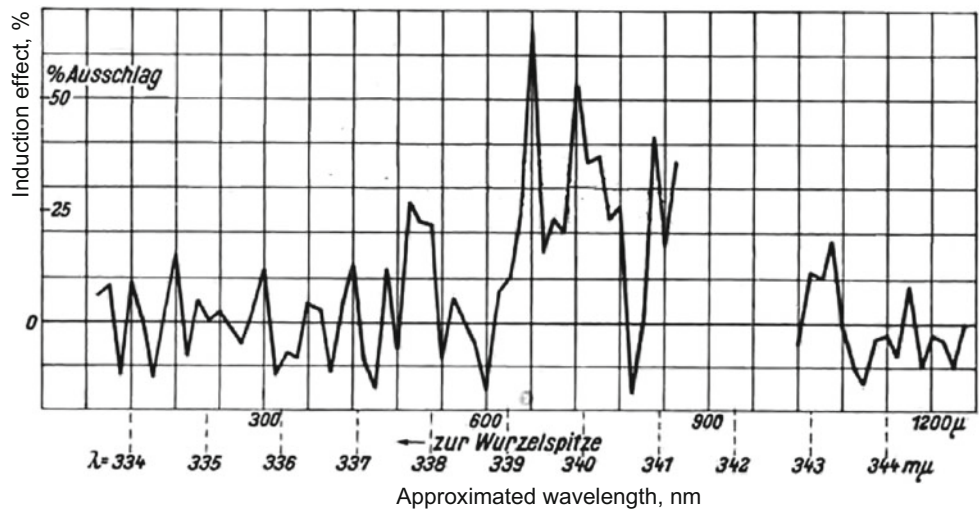


Fig. 2.16 MGR spectrum from frog muscle in tetanus state, obtained using agar yeast cultures as biological detectors. (Adapted from Frank (1929) and Gurwitsch and Gurwitsch (1932). Copyright 1932, with permission from Springer Nature)

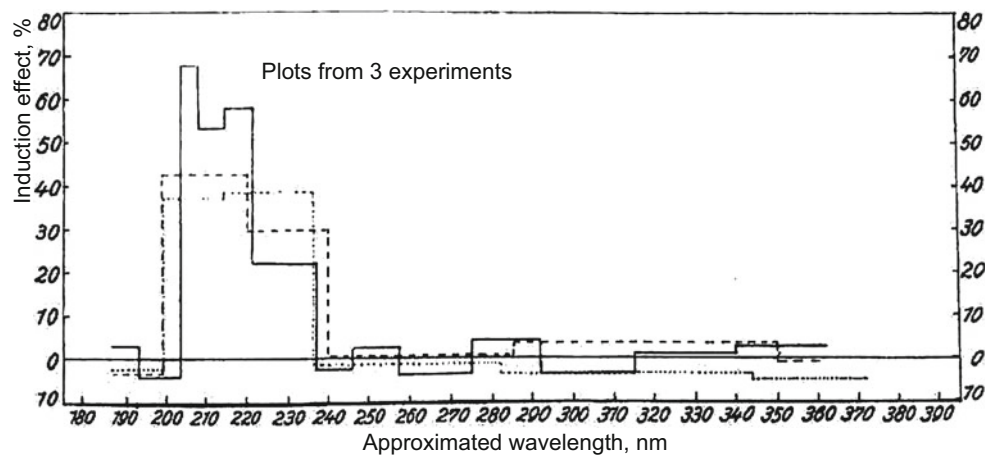
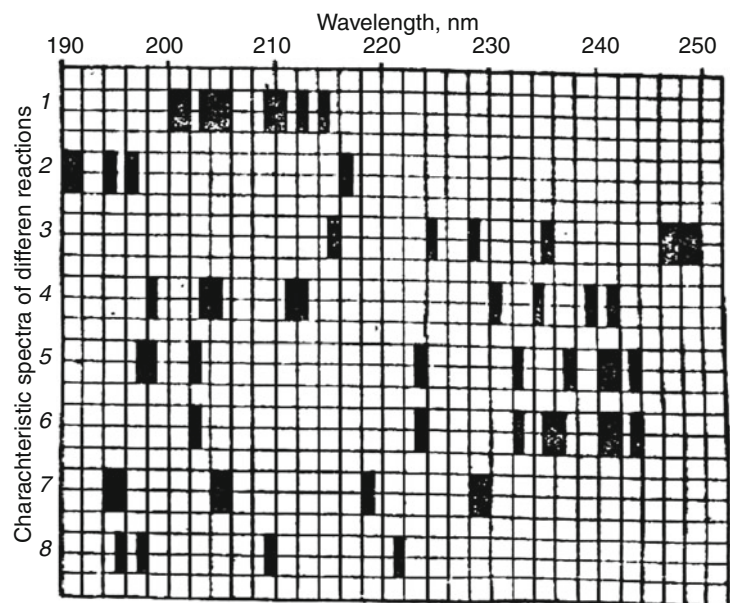


Fig. 2.17 Mitogenetic spectra of several characteristic biochemical inductors: 1 – creatine phosphate breakdown; 2 – glycolysis; 3 – phosphatase exposure on nucleic acids and lecithin; 4 – fluorescence of peptide bond; 5 – enzymatic breakdown of maltose; 6 – enzymatic breakdown of sucrose; 7 – breakdown of urea; 8 – lipolysis. (Reprinted from Gurwitsch and Gurwitsch (1959). Copyright 1959, with permission from Springer Nature)



criticism and led to some distrust to the phenomenon. Much later, this skeptical attitude resulted in significant oblivion of the fundamental works and perception of the whole area as pseudoscience.

Here are the main drawbacks of biological detection of MGR:

2.2.3.3.1 Subjectiveness

As the very effect was “detected” by people, visually comparing the “MGR-stimulated” organism (culture) to the “non-irradiated” control, a lot of criticism was (rightly) focused on possible mistakes and even (unconscious) falsification that could be made by researchers (Hollaender and Claus 1935; Bateman 1935). Yet, a number of MGR works were performed at quite high quality standards, with appropriate controls, blind detection and good statistical analysis (Tuthill and Rahn 1933; Ferguson and Rahn 1933; Wolff and Ras 1931a, 1933a; Chariton et al. 1930; Schwemmler 1929).

2.2.3.3.2 Slurred Experimental Conditions and Too Much Speculation Mixed with Real Data

In the 1920s–1930s, the experimental conditions were usually described rather vaguely, e.g., “20-hour-old yeast culture on wort agar at room temperature” without any information on its physiological state or medium content. As O. Rahn wrote, “Unfortunately, it was not stated that 12 °C is considered a normal room temperature in Moscow and Leningrad, and investigators following such directions literally, and at American room temperatures, would doubtless have obtained an entirely different physiological stage” (Rahn 1934a).

The experimental details and results were frequently alternating with explanations and reflections on the topic, which made impression of a science-fiction literature, simultaneously far from the mainstream of contemporary science and too hypothetical. Bibliographic references in publications of Gurwitsch’s school and some other researchers were often incomplete or even absent, though updated data were usually discussed quite carefully in the body of the article (see, e.g., (Gurwitsch and Gurwitsch 1934)).

The materials and methods of some “early works” were partially cleared up in Rahn (1936) and Gurwitsch (1968) and, nowadays, carefully analyzed in Volodyaev and Belousov (2015) (see Part V).

2.2.3.3.3 Problems with Reproducibility

All the authors of positive works pointed out that the experimental conditions had to be very carefully adjusted and methods of biological detection were extremely vulnerable to any subtle deviations from procedures. Moreover, nearly all the leading researchers – Gurwitsch (Gurwitsch and Gurwitsch 1934, 1959), Rahn (1934a, 1936), Wolf (1932) and others, which headed laboratories with extensive

experience of positive experiments, honestly reported periods of unexplained failures in getting any effect. As Rahn wrote, “Professor Gurwitsch has told the author that in his experience <MGE failures> usually remained for several days, or even for a number of weeks, and it was impossible to produce even the simplest mitogenetic effect. Eventually the culture reacted normally again. . .” Doctor Heinemann, after a very successful diagnosis of cancer by the absence of blood radiation. . . with yeast as recipient, suddenly experienced a complete lack of reaction, and none of the various attempts to obtain normal reactions proved successful, not even the testing of a large number of different yeast cultures. . . Professor Werner Siebert’s many successful experiments with yeast detector have been mentioned in many chapters of this book. But with him, too, the yeast suddenly ceased to react. . . Gurwitsch and his group also had long periods of negative results in their laboratory, which came and went at irregular intervals. (Rahn 1936).

A. Gurwitsch suggested that these days of failures related to the changes in radiofrequency background, L. Wolff and G. Ras explained them by specific changes of biological detectors themselves, some other authors named climate variations as probable reason, etc. (Rahn 1936). In any case, it should be clearly stated that some important factor (or factors) influencing MGE had not been determined.

Thus, despite significant successes in the field of mitogenesis, including insights that were decades ahead of their time, the direction critically required objective methods of physical detection and validation of biological data.

2.2.3.4 The First Works on Physical Detection of Ultraweak Photon Emission (MGR)

Beginning from the first experimental evidence that MGE is caused by weak UV radiation (MGR), the researchers’ natural desire was to observe MGR with physical methods. In the first attempts made on photographic plates, no positive results were obtained, even with multiday exposures (Taylor and Harvey 1931; Magrou 1930a, b; Reiter and Gabor 1928a). As indicated in Frank and Rodionow (1932), “In experiments of Protti (1930), the source of radiation was blood on glass wool. . ., the exposure lasted 70 hours . . . <However>, the blood in vitro loses its ability to <induce MGE> after 10–15 min, and after spending many hours in the atmosphere of oxygen, phenomena completely different from MGR can appear. . . In the experiments of Brunetti (Brunetti and Maxia 1930), the effect on the photographic plate was observed after preliminary intense illumination of the object. Apparently, <in both works> MGR did not act on the photographic plate, and the blackening was the result of phosphorescence or chemiluminescence (probably in visible spectral range).” The use of photocells gave no results either (Schreiber and Friedrich 1930; Chariton et al. 1930; Kreuchen and Bateman 1934).

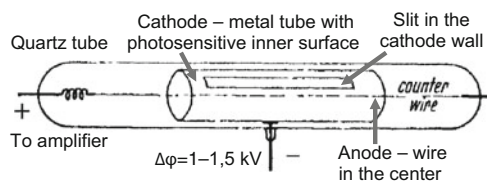


Fig. 2.18 Photosensitive modification of the Geiger–Müller counter proposed by Rajewsky (1931). (Adapted from Rahn (1936). Copyright 1936, with permission from Springer Nature)

The first successful attempt of physical registration of MGR was made by Rajewsky (1930, 1931) with the help of a photosensitive modification of the recently proposed Geiger–Müller counters (Geiger and Müller 1928a, b). The counter cathode was a metal cylinder with a cut-through window, the inner surface of the cathode being covered with a photosensitive layer (Fig. 2.18). The thin-wire anode was placed in the center of the cylinder. The potential difference between the cathode and the anode reached 1.5 kV. The entire structure was placed in a quartz flask filled with an inert gas.

The MGR source was placed outside the flask opposite the window in the cathode, so that the MGR emitted by it passed through the window to the photosensitive layer. A quantum of light entering the photo layer knocked out an electron from it, which accelerated in the counter field and led to an avalanche-like gas ionization detected by an electrometer and an automatic counter (Frank and Rodionow 1932).

Using this setup, the author was able to detect radiation from the onion root, onion gruel and carcinoma and estimate its intensity at $\sim 10\text{--}100$ quanta/s (Rajewsky 1931).

Similar devices were constructed in other laboratories (Frank and Rodionow 1932; Barth 1936; Grebe et al. 1937; Audubert 1938). By selecting the photosensitive layer, the resistance value, the gas composition, etc., the authors managed to get devices sensitive in the spectral region of MGR (Fig. 2.19). With these, they got reliable results of UPE detection from MGE inductors (Fig. 2.20), comparing it to no UPE from noninductors (Fig. 2.21). The parameters of UPE estimated in Audubert (1938) were: intensity $\sim 100\text{--}1000$ quanta \cdot s $^{-1}$ \cdot cm $^{-2}$ and wavelength $\sim 230\text{--}240$ nm (according to the data given in Audubert (1938), it should be somewhere between 200 and 280 nm).

As discussed below (and also in Chaps. 20 and 21), significant doubts in the very existence of MGR were arising due to difficulties in its physical detection. However, the described photosensitive modifications of Geiger–Müller counters let the researchers overcome this problem and obtain stable results on the MGR physical detection. As academician S.I. Vavilov concluded: “Emission of ultraviolet rays in many chemical reactions and biological processes is completely confirmed by usual physical methods.

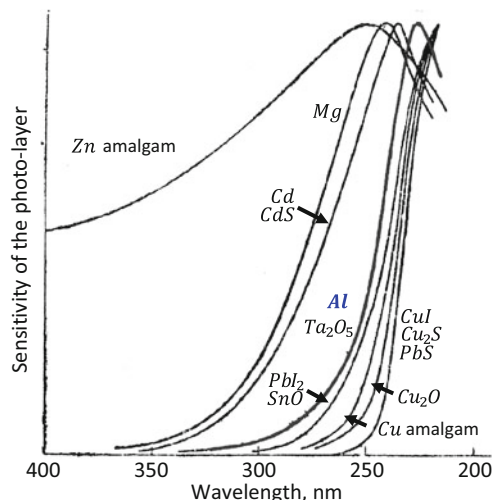


Fig. 2.19 Sensitivity spectra of modified Geiger–Müller counters with various photo-sensitive layers (the photosensitivity spectrum of the setup used in Figs 2.20 and 2.21 is highlighted in blue). (Adapted from Audubert (1938). Copyright 2006, with permission from John Wiley and Sons)

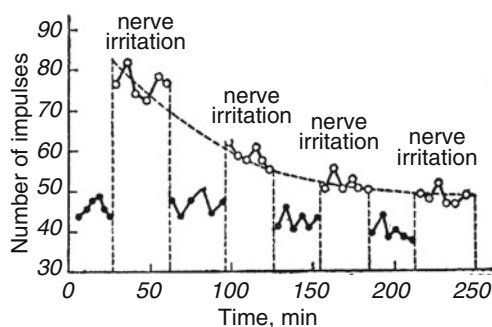


Fig. 2.20 UPE from a periodically irritated frog nerve (Aluminum photocathode, see sensitivity spectrum at Fig. 2.19). The UPE intensity was estimated as ~ 100 quanta \cdot s $^{-1}$ \cdot cm $^{-2}$; the UPE wavelength was estimated as 230–240 nm. (Adapted from Audubert (1938). Copyright 2006, with permission from John Wiley and Sons)

...Wavelengths observed by Audubert belong to the same spectral range that was stated in Gurwitsch’s laboratory” (Gurwitsch and Gurwitsch 1948).

Thus, the initiation factor proposed by Gurwitsch was convincingly identified by the end of the 1930s.

2.2.3.5 Obtaining MGE from Physical Sources of UV

As data on the physical nature of MGR were accumulated, its imitation by physical sources became no less important and obvious. The first attempts of it were made in Frank and Gurwitsch (1927) and Reiter and Gabor (1928a). The authors used spark discharges of aluminum (Frank and Gurwitsch 1927; Reiter and Gabor 1928a), zinc and cadmium (Chariton et al. 1930), as well as mercury, amalgam, or silver arc lamps

Fig. 2.21 UPE from frog nerve, killed with ethanol, and periodically irritated identically to Fig. 2.20 (Aluminum photocathode, see sensitivity spectrum at Fig. 2.19). (Adapted from Audubert (1938). Copyright 2006, with permission from John Wiley and Sons)

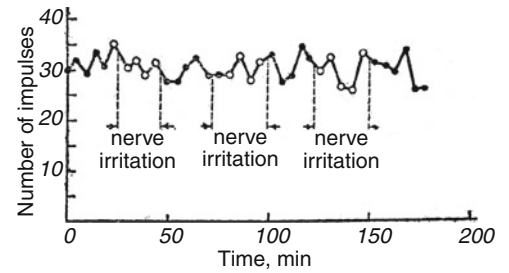


Fig. 2.22 Device for conducting stimulation of MGE by radiation from a physical source (silver arc lamp). (Adapted from Reiter and Gabor (1928b). Copyright 1928, with permission from Springer Nature)

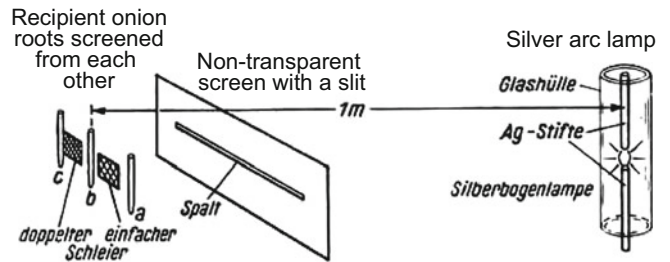
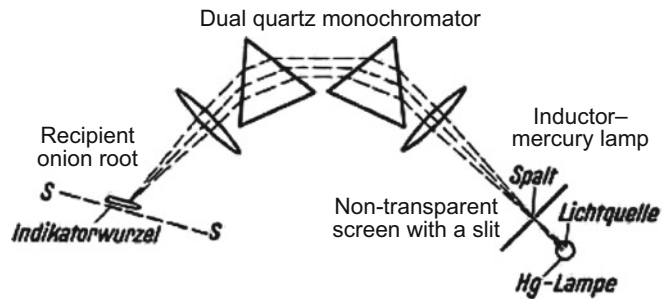


Fig. 2.23 Device for inducing MGE by narrow-band radiation from a physical source (mercury lamp). (Adapted from Reiter and Gabor (1928b). Copyright 1928, with permission from Springer Nature)



(Reiter and Gabor 1928b) as sources of ultraviolet radiation (the device schemes are shown in Figs. 2.22 and 2.23).

Despite technical difficulties (the need to attenuate light from the lamp by 10^{10} times or more, the dangers of exposure to extraneous light, the need to control the state of the biological recipient, etc.), the authors managed to obtain MGE from physical sources and construct the dependence of MGE on the wavelength (Fig. 2.24, according to Reiter and Gabor (1928b)) and both the wavelength and the intensity (Fig. 2.25, according to Chariton et al. (1930)) of the stimulating radiation.

The differences in specific spectral regions with mitogenetic activity between the data (Reiter and Gabor 1928b) and (Chariton et al. 1930) (compare the spectra in Figs. 2.24 and 2.25), are apparently due to the attenuation method used (i.e., final intensities of the inducing light) and different recipients (onion roots in Reiter and Gabor (1928b) and yeast in Chariton et al. (1930)).

Another important feature was that MGE from physical UV sources was observed only at intensities several orders of magnitude higher than those estimated for MGR in the

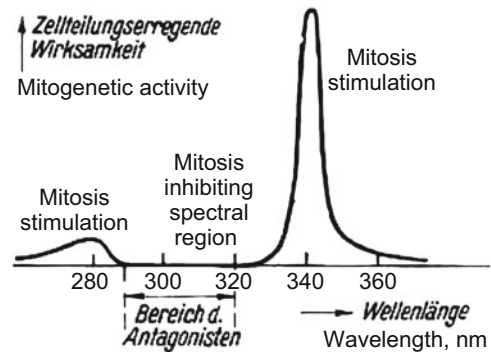
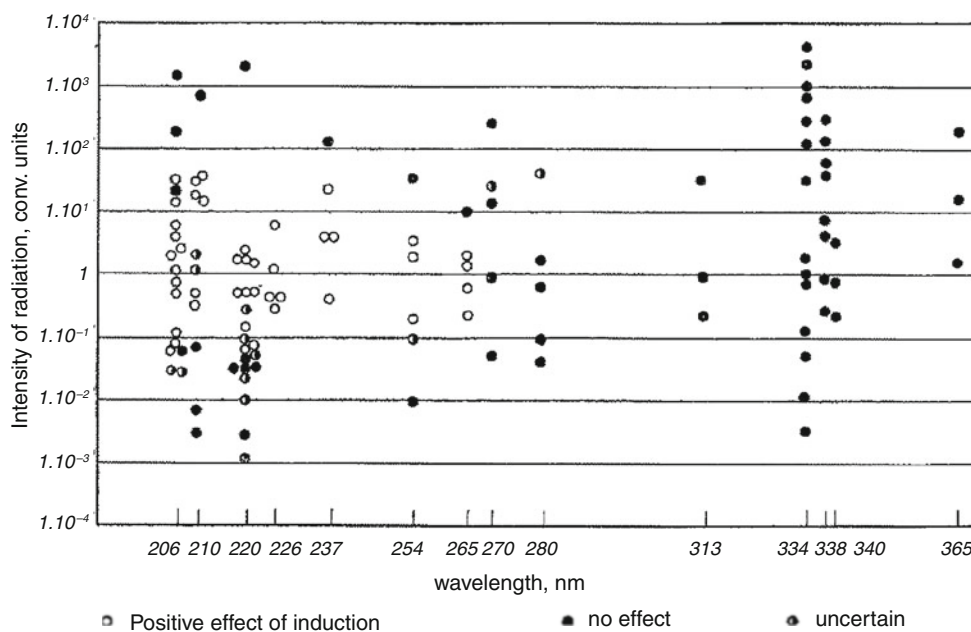


Fig. 2.24 Spectra of mitogenetic activity of ultraweak UV light from physical sources. (Adapted from Reiter and Gabor (1928b). Copyright 1928, with permission from Springer Nature)

experiments with Geiger–Muller counters. The authors interpreted this as evidence that MGR had some special properties that light from physical sources did not have – specific spectrum, some kind of temporal dynamics, etc. (Chariton et al. 1930).

Fig. 2.25 Spectra of mitogenetic activity of ultraweak UV light from physical sources (1 conv.unit equals to 10^{-14} ampere of photocurrent). (Reprinted from Chariton et al. (1930). Copyright 1930, with permission from Springer Nature)



Anyway, both groups obtained reproducible MGE from physical UV sources, which gave the final proof of mitogenetic activity of ultraweak UV.

2.2.3.6 Applied Research Related to MGE: Cancer Quencher

In addition to studying the basic MGE and its physical properties, the authors made some practical observations. Thus, they found that in most cases the blood of a healthy person or animal was a stable inductor of MGE. Yet, the blood of cancer patients ceased to emit MGR. The same effect was observed in mice with inoculated or induced tumors long before the onset of apparent clinical or histological presentation of cancer (Gurwitsch and Gurwitsch 1938). The disappearance of MGR from the blood of cancer patients was caused by formation of a specific substance (or substances) quenching MGR, supposedly due to the disruption of free-radicals generation. It was called the “cancer quencher,” which was the first blood tumour marker ever proposed (Gurwitsch and Gurwitsch 1937; Siebert and Seffert 1937; Gurwitsch et al. 1947).

2.2.3.6.1 “Degradation MGR”

In addition to standard MGE inductors, almost any biological system appeared possessing a short-term inducing ability under external destructive or stressful effects: mechanical pressure, cooling, passing electric current, etc. (Gurwitsch and Gurwitsch 1948, 1959). This phenomenon, called by the authors “degradation MGR,” could be observed during a limited time, then showed some refractory period and if the impact was reversible, could be reobtained after a long time of “system recovery” (see more in Chap. 22).

Gurwitsch interpreted “degradation MGR” as evidence of the nonequilibrium state of biological systems, destroyed by the externally applied stressful influences, with the appearance of free radicals – sources of MGR (Gurwitsch and Gurwitsch 1948, 1959).

2.2.3.7 The Results of the “Golden Age”

Thus, by the end of the 1930s, the MGE research led to the following results:

- The effect had been confirmed in various laboratories on a number of biological objects.
- MGR spectra were obtained using biological recipients (“detectors”).
- Ultraweak luminescence from MGE inductors was recorded in the spectral range of 180–340 nm with intensity of $\sim 10\text{--}10^3$ quanta \cdot s $^{-1}$ \cdot cm $^{-2}$, which roughly corresponded to indirect estimates of MGR.
- MGE was obtained from ultraweak radiation of physical sources in the spectral range of MGR estimates.
- The MGR phenomenon began to be used as a research method in biochemistry and physiology and showed its potential for medical diagnostics.

Based on the experimental data on MGR, the following suggestions were made:

- MGR was suggested resulting from recombination of free radicals.
- Biological systems were assumed to be in nonequilibrium (electron-excited) states, and capable of emitting MGR quanta when these states were disturbed.

2.2.4 1938–1948 – “The Sunset of MGR”

2.2.4.1 Criticism

Notwithstanding the large number of publications, confirming MGE, its accurate verification demanded a lot of subtle conditions to be fulfilled. As A.G. Gurwitsch wrote, “With the remarkable exception of the studies of a few authors who really contributed to the new discipline (among them we may mention Magrou and Magrou, Ziebert, Blacher, Wolf, and Zirpolo), all the other numerous tests – with either positive or negative conclusions – led the authors to express doubt” (Gurwitsch and Gurwitsch 1943) (cited from a later English reprint: (Gurwitsch and Gurwitsch 1999)).

At the same time, the “nonclassicality” of the MGE phenomena naturally aroused skepticism in the scientific community, especially given the vague wording and low level of some works. There were a number of negative publications attempting to verify MGE (Taylor and Harvey 1931; Richards and Taylor 1932; Nakaidzumi and Schreiber 1931; Kreuchen and Bateman 1934; Gray and Ouellet 1933; Lorentz 1929; Westenberg 1935; Hollaender and Claus 1937; Moissejewa 1960), some of which had a significant impact on public opinion. Methodical mistakes of the “negative works” were partly analyzed in Rahn (1934a, 1936), and Zalkind (1940), yet were mostly ignored by Gurwitsch: “We believe that there are no words, harsh enough to condemn those authors who, having set themselves the goal of verifying the existence of the phenomenon, not only ignored our methodological instructions for experimental setup, but acted contrary to them, i.e., used methods that we had explicitly warned against” (Gurwitsch and Gurwitsch 1943) (not translated in Gurwitsch and Gurwitsch (1999)). Detailed analysis and critics of early works will be given in Chaps. 20, 21, 22, and 23. Though most of their negative results could be well explained by incorrect experimental conditions (physiological state of the cells, structure of physical detectors, etc. – see more in Chaps. 20 and 21) (Rahn 1934a, b; Gurwitsch and Gurwitsch 1948, 1999; Barth 1934; Zalkind 1940), they were followed by sharply negative consequential reviews of the topic (Bateman 1935; Anonim 1937; Moissejewa 1960).

2.2.4.2 Geopolitics

Fast decline of works on MGE in Germany began soon after Hitler’s accession to power because of the emigration of the leading researchers (D. Gabor, T. Reiter, M. Heinemann and others). Some of researchers left this area in favour of other ones, including military topics (A.F. Ioffe, G.M. Frank, A. Hollaender, O. Rahn, R. Audubert). Audubert left the field, explaining that because of technical limitations his further research would do little other than laboriously accumulate very similar evidence of the phenomenon. The prewar

aggravation of international relations cast the shadow of “Soviet science” over the MGE.

Naturally, with the beginning of WWII, research on MGE completely stopped in Western Europe and the United States, and none of these laboratories returned to this topic after WWII and during the Cold War. In contrast to the previous period, in 1938–1948, Soviet researchers were mostly published in Russian (Gurwitsch and Gurwitsch 1945, 1948), and a lot of their works remained unknown to the “western scientists” for decades (e.g., (Gurwitsch and Gurwitsch 1943) was translated only in 1999 (Gurwitsch and Gurwitsch 1999)), while many others are still untranslated). In spite of this scientific isolation, hard times of war, evacuation of A.G. Gurwitsch and his colleagues from Leningrad, and inevitable reduction of research activities, these years were still fruitful for mitogenesis in the USSR. The main subjects of this period were: MGE spectral analysis with the focus on nerve activity and carcinogenesis (Gurwitsch et al. 1947; Gurwitsch and Gurwitsch 1945), development of cancer diagnostics and accumulation of clinical data on its successful application (Pesochensky 1942; Avchina 1950; Gurwitsch et al. 1947), and theoretical attempts to explain extensive experimental data previously collected (Gurwitsch 1947a, b). Gurwitsch was awarded with the highest scientific award of the USSR for works on MGE and cancer study (Stalin Prize, 1941).

In this period, physicians actively joined the field, more than 12 dissertations on “cancer quencher” were written including such a prominent one as Doctor of Medical Science dissertation by B.S. Pesochensky defended in Military Medical Academy in the besieged Leningrad (Pesochensky 1942). Experimental cancer studies and data obtained in the leading clinics of the USSR demonstrated that the cancer diagnostic with detection of “cancer quencher” by MGE-methods had specificity and sensitivity of >95% (see Chap. 23). Due to the language barrier, the “cancer quencher” research, probably the most attractive from the point of view of practical applications, remained almost unknown to the western readers.

In the USSR, the postwar raise of research marked with significant growth of publication activity soon gave place to dramatic decline due to political reasons. For a long time, Gurwitsch had been immune to the regular charges of being “bourgeois vitalist” (Lepeshinskaya 1926; Tokin 1933) due to his recognition as a world-known scientist. With ceasing of his worldwide fame and the rise of power of O.B. Lepeshinskaya and other followers of T.D. Lysenko, these charges became really threatening. Mitogenetic researches were persecuted altogether with genetics after the decisions of the “August session of VASKhNIL” (All-Union Academy of Agricultural Sciences) in 1948. In this time, many scientists suffered from political persecution

in the USSR; Gurwitsch had to retire from the post of Director of Institute of Experimental Biology.

2.2.5 After 1948 – After the Sunset

Although the mitogeneticists were never repressed as hard as geneticists in the USSR, the August VASKhNIL session appeared to have a more severe impact on its further progress. While the success of genetics in the Western countries made soviet officials revise their perception of this science, the mitogenetic research was both denounced as “Soviet obscurantism” in the West, and stigmatized as a “bourgeois science” in the USSR. Works on MGE were still continued in several labs in the USSR where some new publications were appearing (Gurwitsch 1968; Avchina 1950; Troitskii et al. 1961; Konev 1965; Gurwitsch et al. 1965). Yet, the scope of work was incomparable to the large-scale research conducted before WWII and even in wartime. The main topics worked on were application of the invented photomultiplying tubes as extremely sensitive detectors of UPE (Gurwitsch et al. 1965; Troitskii et al. 1961), and cancer diagnostics in clinics (Avchina 1950).

Soon, visible UPE from biological systems was discovered, and its mechanisms and general prevalence investigated (Colli and Fachini 1954; Tarusov et al. 1961; Vladimirov 1967; Boveris et al. 1981). This part of the story is given in the following Chap. 3. The main point we would like to mention here is that the newly discovered visible UPE was actually never contrasted to MGR at the evidence level, and never disproved its existence.

Though later a number of authors accidentally stumbled upon this topic anew, they mostly exhausted their interest by finding the most easily accessible critical prewar articles (Hollaender and Claus 1937; Anonim 1937; Bateman 1935; Hollaender 1936) assuring them of the falsity of the original works (which they had never read). As written in Metcalf and Quickenden (1967), “These studies were originated by Gurwitsch and are still carried on in the Soviet Union, but almost ceased in Britain and the United States in the 1930s after much careful but negative work (Lorenz 1934; Gray and Ouellet 1933; Hollaender and Claus 1937). Nobody there was able to stimulate cell division with weak ultraviolet light or to detect radiation from rapidly dividing cells with photoelectric or biological detectors” (references saved). Yet, further deepening into the topic and their own positive experimental results made these authors acknowledge the validity of early works and show much more respectful attitude to them (e.g., (Quickenden and Hee 1981)).

However, after 1948, almost all attempts to verify MGE were sporadic and demonstrated lack of knowledge of early works. It should be noted that the early literature on MGE became rather rare, and it was extremely difficult to track

research chains and find methodical descriptions. The more so, that Gurwitsch and his pupils when citing other works, usually named only the authors without presenting full bibliographic references.

Interestingly, many scientific results obtained in the “Golden age” of MGE were rediscovered with novel scientific methods, but mostly without reference to early MGE researchers (see below).

2.3 Epilogue: The Paradoxes of Mitogenesis

The story of the mitogenetic effect is full of contradictions. On the one hand, it may seem one of the fallacies of the old days. Yet, a lot of data from the “old days” appeared anticipating much later discoveries (UPE from biological systems, its free-radical nature, peptide tumour markers, two-photon processes, etc.). On the other hand, it may seem solid science, forgotten by accident and/or due to historical troubles. Yet, there were a number of badly done works (both positive and negative) that compromised the whole topic. The very chain of reasoning, that led to the concept of MGE, being the result of constant deep reflection on the processes of cell division and morphogenesis, is actually full of strange and quite doubtful conclusions. As A.G. Gurwitsch wrote, “What may be instructive in our case is that blunders frequently intervened in the chain of our deductions, sometimes in its most crucial links. This happened repeatedly after the discovery of the phenomenon and in the course of its further investigation. . . It is difficult to understand now, how such a chain of arbitrary and physically rather naive reasoning could have led us to a valid result – discovery of the radiation” (Gurwitsch and Gurwitsch 1999).

Experimental development of the topic was also quite contradictory. As the field of research was quite new, the methodical details were usually not well understood by the authors themselves. Due to the vague procedure descriptions overcrowded with irrelevant information, many of those who wanted to verify the original MGR works missed important recommendations, and lost the effect from the very beginning. Though a number of very serious authors were unsuccessful in obtaining the phenomenon (Taylor and Harvey 1931; Richards and Taylor 1932; Nakaidzumi and Schreiber 1931; Kreuchen and Bateman 1934; Gray and Ouellet 1933; Lorentz 1929; Westenberg 1935; Hollaender and Claus 1937; Moissejewa 1960), most (if not all) of their negative results were quite explainable in the course of the “mitogenetic reasoning” (Rahn 1934a, b; Gurwitsch and Gurwitsch 1948, 1999; Barth 1934; Zalkind 1940), and the “negative works” often directly violated the methods previously developed in “positive works.” Interestingly, one of the seemingly most persuasive parts of the critique, the “proof” that the phenomenon of biological UPE is physically impossible (Bateman

1935; Hollaender and Claus 1937; Taylor and Harvey 1931) turned out wrong, as the physically detected UPE from living systems became a well-established fact already in the 1960s (Vladimirov 1967). Many theoretical arguments against experimental results on MGE also failed to stand the test of time, for instance, Bateman's caustic critique of Gurwitsch's experimental results on secondary radiation (see Chap. 22) that violated Stokes law as "fluorescence hitherto unknown... we are seriously asked to believe in its existence" (Bateman 1935) (existence of anti-Stokes processes was predicted and proved much later).

On the one hand, the critique of MGE and MGR mainly became obsolete, and we can clearly state that the key experiments have never been disconfirmed in a conclusive way. On the other hand, most of MGE and MGR experiments cannot be considered absolutely correct without modern verification because of significant advances in biological methods, more stringent requirements for evidence, and statistical processing of data. We consider that the results of early authors must not be taken for granted but surely worth of serious attention and thorough verification with the focus on factors affecting MGE and improving reproducibility.

Trying to make the real situation as clear as possible, in the following parts, we address the topics of UPE in general (the now classic works on free-radical processes accompanied by UPE, which originated from attempts to test MGR on PMTs – Chap. 3 and Part III), its occurrence in nature (Part IV), physical mechanisms (down to quantum dynamical models, which have become achievable only recently, thanks to the development of computer technology – Part III), and applications (Parts IV and VII). Later, we will return to the unsolved mystery of mitogenesis, discussing methodical details of early works, their results and applications, controversies, and problems (Parts V and VI). Finally, we will outline the sudden parallels between the early works and the presently well-established data and come to perspectives and new approaches in this area of science (Part VII). The future will show if there was the baby thrown out with the bath water of mitogenetic works.

References

- Acs L (1931) Über die mitogenetische Strahlung der Bakterien. *Centr Bakt I Abt Orig* 120 (1/2):116–124
- Acs L (1933) Über echte mitogenetische Depressionen. Bakterienantagonismus und mitogenetische Strahlung. *Zentralblatt für Bakteriologie, Parasitenkunde und Infektionskrankheiten* 127: 342–350
- Anikin AW (1926) Das Nervensystem als Quelle mitogenetischer Strahlung. *Wilhelm Roux' Archiv für Entwicklungsmechanik der Organismen* 108 (4):609–616. <https://doi.org/10.1007/bf02080166>
- Anonim (1937) Mitogenetic rays? *Nature* 140 (3554):1007–1008. <https://doi.org/10.1038/1401007c0>
- Audubert R (1938) Die Emission von Strahlung bei chemischen Reaktionen. *Angewandte Chemie* 51 (11):153–163. <https://doi.org/10.1002/ange.19380511102>
- Avchina EE (1950) On the prognostic value of the reaction of quenching of the mitogenetic radiation of blood in the treatment of uterine cancer: *Cand. Med. Sci. dissertation* (in Russian). Leningrad
- Baron MA (1926) Über mitogenetische Strahlung bei Protisten (16. Mitteilung über mitogenetische Strahlung). *Wilhelm Roux' Archiv für Entwicklungsmechanik der Organismen* 108 (4):617–633. <https://doi.org/10.1007/bf02080167>
- Baron MA (1930) Analyse der mitogenetischen Induktion und deren Bedeutung in der Biologie der Hefe. *Planta: Archiv für wissenschaftliche Botanik* 10 (1):28–83. <https://doi.org/10.1007/bf01911536>
- Barth H (1934) Versuche zum physikalischen Nachweis von mitogenetischer Strahlung. *Archive of Biological Sciences Ser B* 35 (1):29–36
- Barth H (1936) Physikalische Versuche zum Problem der mitogenetischen Strahlung. *Biochemische Zeitschrift* 285:311–339
- Barth H (1937) Physical studies on the question of mitogenetic radiation problem (in Russian). *Archive of Biological Sciences* 46 (1): 153–177
- Bateman JB (1934) Mitogenetic Radiation and Bioluminescence. *Nature* 133 (3371):860. <https://doi.org/10.1038/133860a0>
- Bateman JB (1935) Mitogenetic radiation. *Biological Reviews* 10 (1): 42–71. <https://doi.org/10.1111/j.1469-185X.1935.tb00476.x>
- Billig E, Kannegiesser N, Solowjew L (1932) Die Spektralanalyse der mitogenetischen Strahlung bei Pepsinverdauung und bei der Spaltung von Glycyl-Glycin durch Erepsin. *Hoppe-Seyler's Zeitschrift für physiologische Chemie* 210 (5–6):220–227. <https://doi.org/10.1515/bchm2.1932.210.5-6.220>
- Blacher LJ, Bromley NW (1931) Resorptionsprozesse als Quelle der Formbildung. IV. Mitogenetische Ausstrahlungen bei der Schwanzregeneration der Urodelen. *Wilhelm Roux' Archiv für Entwicklungsmechanik der Organismen* 123 (2):240–265. <https://doi.org/10.1007/bf00644902>
- Boveris A, Cadenas E, Chance B (1981) Ultraweak chemiluminescence: a sensitive assay for oxidative radical reactions. *Fed Proc* 40 (2): 195–198
- Braun AD (1934) Lipolysis as a source of mitogenetic radiation. *Nature* 134 (3388):536. <https://doi.org/10.1038/134536d0>
- Brunetti R, Maxia C (1930) Sulla fotografia e la eccitazione delle radiazioni del Gurwitsch. *Atti della Società fra i Cultori delle Scienze Mediche e Naturali in Cagliari* 32:50–57
- Chariton J, Frank G, Kannegiesser N (1930) Über die Wellenlänge und Intensität mitogenetischer Strahlung. *Naturwissenschaften* 18 (19): 411–413. <https://doi.org/10.1007/bf01501123>
- Colli L, Facchini U (1954) Light emission by germinating plants. *Il Nuovo Cimento* 12 (1):150–153. <https://doi.org/10.1007/bf02820374>
- Copisarow M (1932) Radiation and enzyme activity. *Nature* 130 (3296): 1001–1002. <https://doi.org/10.1038/1301001b0>
- Nobel Prize Nomination Database <https://www.nobelprize.org/nomination/archive>. Accessed 22 Aug, 2023
- Decker G (1936) Über die Schärfe mitogenetischer Spektren. *Protoplasma* 25 (1):515–527. <https://doi.org/10.1007/bf01839124>
- Ferguson AJ, Rahn O (1933) Zum Nachweis mitogenetischer Strahlung durch beschleunigtes Wachstum von Bakterien. *Archiv für Mikrobiologie* 4 (1–4):574–582. <https://doi.org/10.1007/bf00407563>
- Frank G (1929) Das mitogenetische Reizminimum und -maximum und die Wellenlänge mitogenetischer Strahlen. *Biologisches Zentralblatt* 49:129–141
- Frank G, Rodionow S (1932) Physikalische Untersuchung mitogenetischer Strahlung der Muskeln und einiger Oxydationsmodelle. *Biochemische Zeitschrift* 249 (4/6):323–343

- Frank GM (1925) Über Gesetzmäßigkeiten in der Mitosenverteilung in den Gehirnbräuen im Zusammenhange mit Formbildungsprozessen. *Archiv für mikroskopische Anatomie und Entwicklungsmechanik* 104 (1):262–272. <https://doi.org/10.1007/bf02108500>
- Frank GM, Gurwitsch AG (1927) Zur Frage der Identität mitogenetischer und ultravioletter Strahlen. *Wilhelm Roux' Arch Entwickl Mech Org* 109 (3):451–454. <https://doi.org/10.1007/bf02080806>
- Frankenburger W (1933) Neuere Ansichten über das Wesen photochemischer Prozesse und ihre Beziehungen zu biologischen Vorgängen. *Strahlenther Onkol* 47 (2):233–262
- Gates RR (1929) Zellteilung und Strahlung. *Nature* 124 (3115):50–51. <https://doi.org/10.1038/124050a0>
- Gavrish OG (2003) Gurwitsch and true story of biological field (In Russian). *Chemistry and life (Khimija i zhizn')* 5:32–37
- Geiger H, Müller W (1928a) Das Elektronenzählrohr. *Physikalische Zeitschrift* 29:839–841
- Geiger H, Müller W (1928b) Elektronenzählrohr zur Messung schwächster Aktivitäten. *Die Naturwissenschaften* 16 (31):617–618
- Gesenius H (1930) Über die Gurwitsch-Strahlung menschlichen Blutes und ihre Bedeutung für die Carcinom-Diagnostik. *Biochemische Zeitschrift* 226 (4–6):257–272
- Golshmid KL (1934) Mitogenetic radiation of blood in pellagra (In Russian). In: *Collected works of Perm Medical Institute "Pellagra"*. Perm Medical Institute, Perm, pp 105–137
- Gray J, Ouellet C (1933) Apparent mitogenetic inactivity of active cells. *Proceedings of the Royal Society of London Series B, Containing Papers of a Biological Character* 114 (786):1–9. <https://doi.org/10.1098/rspb.1933.0067>
- Grebe L, Krost A, Peukert L (1937) Versuche zum physicalischen Nachweis der mitogenetische Strahlung. *Strahlenther apie* 60: 575–571
- Gurwitsch A (1933) Mitogenetic radiation of nerve. *Nature* 131 (3321): 912–913. <https://doi.org/10.1038/131912a0>
- Gurwitsch AA (1947a) An attempt of constructing a model of non—equilibrated molecular constellations and of degradation radiation (In Russian). In: Gurwitsch AG (ed) *Collected volume on mitogenesis and theory of biological field*. Pub.house of the USSR Academy of Medical Sciences, Moscow, pp 92–101
- Gurwitsch AA (1968) [The problem of mitogenetic emission as an aspect of molecular biology] *Problema mitogeneticheskogo izlucheniya kak aspekt molekuliarnoj biologii* (in Russian). *Meditsina*, Leningrad
- Gurwitsch AA, Eremeev VF, Karabchievsky YA (1965) Ultra-weak emission in the visible and ultra-violet regions in oxidation of solutions of glycine by hydrogen peroxide. *Nature* 206 (4979): 20–22. <https://doi.org/10.1038/206020b0>
- Gurwitsch AG (1911) Untersuchungen über den zeitlichen Faktor der Zellteilung. *Arch EntwMech Org* 32:447–471
- Gurwitsch AG (1922) Über Ursachen Der Zellteilung Roux' *Arch Entwicklmech Organ* 52:167–181
- Gurwitsch AG (1923) Die Natur des spezifischen Erregers der Zellteilung. *Archiv für mikroskopische Anatomie und Entwicklungsmechanik* 100 (1–2):11–40. <https://doi.org/10.1007/bf02111053>
- Gurwitsch AG (1924a) Physikalisches über mitogenetische Strahlen. *Archiv für mikroskopische Anatomie und Entwicklungsmechanik* 103 (3–4):490–498. <https://doi.org/10.1007/bf02107498>
- Gurwitsch AG (1926) Das Problem der Zellteilung physiologisch betrachtet, vol 11. *Monographien aus dem Gesamtgebiet der Physiologie der Pflanzen und der Tiere*. Julius Springer, Berlin
- Gurwitsch AG (1929) Methodik der mitogenetischen Strahlenforschung. In: *Abderhalden E (ed) Handbuch der biologischen Arbeitsmethoden, vol V. vol 2/2*. Urban & Schwarzenberg, Berlin, Wien, pp 1401–1470
- Gurwitsch AG (1937) *Mitogenetic Analysis of the Excitation of the Nervous System*. N. V. Noord-Hollandsche Uitgeversmaatschappij, Amsterdam
- Gurwitsch AG (1945) Physical and chemical bases of mitogenetic radiation (in Russian). *Bulletin of the USSR Academy of Sciences: Physics* 9 (4–5):335–340
- Gurwitsch AG (1947b) The concept of “whole” in the light of the cell field theory (In Russian). In: Gurwitsch AG (ed) *Collected volume on mitogenesis and theory of biological field*. Pub.house of the USSR Academy of Medical Sciences, Moscow, pp 141–147
- Gurwitsch AG, Gurwitsch LD (1928) Über ultraviolette Chemolumineszenz der Zellen im Zusammenhang mit dem Problem des Carcinoms. *Biochemische Zeitschrift* 196 (4–6.):257–275
- Gurwitsch AG, Gurwitsch LD (1932) Die mitogenetische Strahlung, vol 25. *Monographien aus dem Gesamtgebiet der Physiologie der Pflanzen und der Tiere*. Springer-Verlag Berlin Heidelberg, Berlin. <https://doi.org/10.1007/978-3-662-26146-0>
- Gurwitsch AG, Gurwitsch LD (1934) Mitogenetic radiation (Mitogeneticheskoe izlucheniye) (in Russian). VIEM publishing house, Leningrad
- Gurwitsch AG, Gurwitsch LD (1937) [Mitogenetic analysis of cancer cell biology] *Mitogeneticheskij analiz biologii rakovoj kletki* (In Russian). VIEM publishing house, Moscow
- Gurwitsch AG, Gurwitsch LD (1938) Quencher in cancer patients' blood, its value for diagnostic value and anti-quencher (in Russian). *Archive of Biological Sciences* 51 (3):40–44
- Gurwitsch AG, Gurwitsch LD (1939) Ultra-Violet Chemi-Luminescence. *Nature* 143 (3633):1022–1023. <https://doi.org/10.1038/1431022b0>
- Gurwitsch AG, Gurwitsch LD (1943) Twenty Years of Mitogenetic Radiation: Emergence, Development, and Perspectives (in Russian). *Success of modern biology* 16 (3):305–334
- Gurwitsch AG, Gurwitsch LD (1945) [Mitogenetic radiation: physical and chemical bases and applications in biology and medicine] (Mitogeneticheskoe izlucheniye: fizikokhimicheskije osnovy i prilozheniya v biologii i meditsine) (in Russian). *Medgiz*, Moscow
- Gurwitsch AG, Gurwitsch LD (1948) [An introduction to the teaching of mitogenesis] *Vvedeniye v ucheniye o mitogeneze* (in Russian). USSR Academy of Medical Sciences Publishing House, Moscow
- Gurwitsch AG, Gurwitsch LD (1959) Die mitogenetische Strahlung (Mitogenetic radiation). *VEB Gustav Fischer Verlag*, Jena
- Gurwitsch AG, Gurwitsch LD (1999) *Twenty Years of Mitogenetic Radiation: Emergence, Development, and Perspectives* (translation from [Uspekhi Sovremennoi Biologii] *Advances in Contemporary Biology*, 1943, 16 (3):305–334). *21st Century Science and Technology Magazin* 12 (3):41–53
- Gurwitsch AG, Gurwitsch LD, Zalkind SY, Pesochensky BS (1947) [The teaching of the cancer quencher: Theory and clinics] *Ucheniye o rakovom tushitele: Teorija i klinika* (in Russian). USSR Academy of Medical Sciences Press, Moscow
- Gurwitsch AG, Gurwitsch N (1924) Fortgesetzte Untersuchungen über mitogenetische Strahlung und Induktion. *Archiv für mikroskopische Anatomie und Entwicklungsmechanik* 103 (1):68–79. <https://doi.org/10.1007/bf02107090>
- Gurwitsch L (1924b) Untersuchungen über mitogenetische Strahlen. *Archiv für mikroskopische Anatomie und Entwicklungsmechanik* 103 (3):483–489. <https://doi.org/10.1007/bf02107497>
- Gurwitsch L, Anikin A (1928) Das Cornealepithel als Detektor und Sender mitogenetischer Strahlung. 25. Mitteilung über mitogenetische Strahlung und Induktion. *Wilhelm Roux' Arch Entwickl Mech Org* 113 (4):731–739. <https://doi.org/10.1007/bf02252023>
- Gurwitsch LD (1924c) Die Wertverteilung des Feldbegriffes zur Analyse embryonaler Differenzierungvorgänge. *Archiv für mikroskopische Anatomie und Entwicklungsmechanik* 101 (1/3):40–52

- Gurwitsch LD, Salkind S (1929) Das mitogenetische Verhalten des Blutes Carcinomatoser. *Biochemische Zeitschrift* 211 (1–3): 362–372
- Gurwitsch N (1924d) Über zweifache Verwertung embryonaler Elemente im Laufe der Embryogenese. *Anatomischer Anzeiger* 58: 32–39
- Guttenberg Hv (1928a) Die Theorie der mitogenetischen Strahlen. *Biologischen Zentralblatt* 48:31–39
- Guttenberg Hv (1928b) Schlußwort zur Arbeit von B. Rossmann. Wilhelm Roux' Archiv für Entwicklungsmechanik der Organismen 113:414–418
- Heinemann M (1932) Cytagenin und "mitogenetische Strahlung" des Blutes. *Klinische Wochenschrift* 11 (33):1375–1378. <https://doi.org/10.1007/bf01815913>
- Heinemann M (1934) Physico-chemical test for mitogenetic (Gurwitsch) rays. *Nature* 134 (3392):701. <https://doi.org/10.1038/134701b0>
- Heinemann M (1935) Physico-chemical test for mitogenetic (Gurwitsch) rays. *Acta Brevia Nederland* 5:15
- Heinemann M, Seyderhelm R (1933) Weitere Untersuchungen über die Mitogenetische Strahlung des Blutes unter besonderer Berücksichtigung der "Strahlungen" des Blutes von Carcinomkranken. *Klinische Wochenschrift* 12 (25):990–990. <https://doi.org/10.1007/bf01876282>
- Heinemann M, Seyderhelm R (1934) Mitogenetische Strahlung des Blutes und "Strahlungen" des Blutes Carzinomkranker. *Archive of Biological Sciences Ser B* 35 (1):106–112
- Hill AV (1933) The Physical Nature of the Nerve Impulse. *Nature* 131 (3310):501–508. <https://doi.org/10.1038/131501a0>
- Hollaender A (1936) The problem of mitogenetic rays. In: Duggar B (ed) *Biological effects of radiation*, vol 2. 1 edn. McGraw-Hill Book Company, Inc., NY, London, pp 919–958
- Hollaender A (1939) The present status of mitogenetic radiation. *Radiology* 32 (4):404. <https://doi.org/10.1148/32.4.404>
- Hollaender A, Claus WD (1935) Some Phases of the Mitogenetic Ray Phenomenon. *Journal of Optical Society of America* 25:270–286
- Hollaender A, Claus WD (1937) An experimental study of the problem of mitogenetic radiation, vol 100. *Bulletin of the National research council of the National academy of sciences*, Washington
- Hollaender A, Duggar BM (1938) The effects of sublethal doses of monochromatic ultraviolet radiation on the growth properties of bacteria. *Journal of Bacteriology* 36 (1):17–37
- Hollaender A, Schoeffel E (1931) Mitogenetic rays. *The Quarterly Review of Biology* 6 (2):215–222
- Kannegiesser N (1931) Die mitogenetische Spektralanalyse. I. *Biochemische Zeitschrift* 236:415–424
- Konev SV (1965) The nature and biological importance of ultraweak luminescence of a cell (In Russian). In: *Bioluminescenssiya*. Trudy MOIP, vol 21. "Nauka", Moscow, pp 181–185
- Kreuchen KH, Bateman JB (1934) Physikalische und biologische Untersuchungen über mitogenetische Strahlung. *Protoplasma* 22 (1):243–273. <https://doi.org/10.1007/bf01608868>
- Lepeshinskaya OB (1926) [Militant vitalism. On book of Prof. Gurwitsch Voinstvujuschij vitalizm. O knige prof. Gurvicha (In Russian). "Northern publisher", Vologda
- Loos W (1930) Untersuchungen über mitogenetische Strahlen. *Jahrb Wiss Bot* 72 (4):611–664
- Lorentz E (1929) Investigation on mitogenetic radiation by means of a photoelectric counter tube. *Physical Reviews* (44):329–329
- Lorenz E (1934) Search for Mitogenetic Radiation by Means of the Photoelectric Method. *The Journal of general physiology* 17 (6): 843–862. <https://doi.org/10.1085/jgp.17.6.843>
- Magrou J (1930a) Actions biologiques à distance 1. – Les faits. *Bulletin de d'Institut Pasteur* 28 (9):393–405
- Magrou J (1930b) Actions biologiques à distance 2. – Les interprétations. *Bulletin de d'Institut Pasteur* 28 (10):441–448
- Magrou J (1932) Action à distance et embryogenèse. *Radiobiologia* 1: 32–38
- Magrou MJ, Magrou MM, Reiss MP (1929) Action à distance de divers facteurs sur le développement de l'œuf d'Oursin. *Compte Rendu de l'Academie des Sciences* 189:779
- Maxia C (1940) Quadro sinottico delle ricerche sull' "effetto Gurwitsch". *Scritti biologici* 15:186–220
- Metcalf WS, Quickenden TI (1967) Mitogenetic Radiation. *Nature* 216 (5111):169–170. <https://doi.org/10.1038/216169a0>
- Moisseejewa M (1931a) Zur Theorie der Mitogenetischen Strahlung I. *Biochemische Zeitschrift* 241:1–13
- Moisseejewa M (1931b) Zur Theorie der Mitogenetischen Strahlung II. *Biochemische Zeitschrift* 243 (1–3):67–87
- Moisseejewa MN (1960) [Mitogenetic rays and mitogenetic methods] Mitogeneticheskije luchi i mitogeneticheskij metod (in Russian). Abstract of dissertation (Doctor of Biological Sciences). Kiev
- Nakaidzumi M, Schreiber H (1931) Untersuchungen über das mitogenetische Strahlungsproblem II. *Biochemische Zeitschrift* (237):358–379
- Nobel Prize Nomination Database (2021) <https://www.nobelprize.org/nomination/archive>. Accessed 22 Aug, 2021.
- Pesochensky BS (1942) [The phenomenon of the mitogenetic radiation quenching in blood in cancer and "precancer"] Fenomen mitogeneticheskogo tushenija krovi pri rake i "predrakovykh sostojanijakh": Dr.Med. Sci. Dissertation (in Russian). Leningrad Oncological Institute, Leningrad
- Ponomarewa J (1931) Die mitogenetische Spektralanalyse. III. Mitteilung: Das detaillierte glykolytische Spektrum. *Biochemische Zeitschrift* 239:424
- Potozky A (1932) Untersuchungen über den Chemismus der mitogenetischen Strahlung. II. Mitteilung: Die mitogenetischen Spektren der Oxydationsreaktionen. *Biochemische Zeitschrift* 249: 282–287
- Potozky A (1936) Über Beeinflussung der Zellpermeabilität durch mitogenetische Bestrahlung. *Protoplasma* 25 (1):49–55. <https://doi.org/10.1007/bf01839030>
- Potozky A, Zoglina I (1929) Untersuchungen über die mitogenetische Strahlung des Blutes. *Bioch Ztschr* 211 (4–6):352–361
- Prokofiewa EG (1934) Mitogenetic Radiation of the Urea-Urease System. *Nature* 134 (3389):574–574. <https://doi.org/10.1038/134574a0>
- Protti G (1930) I raggi mitogenetici nell' emoinnesto e prime loro fotografie. In: *Comunicazione alla Seduta scientifica dell' Ospedale Civile di Venezia*, XVIII, Venezia, Stamperia Carlo Rertotti,
- Quickenden TI, Hee SSQ (1981) On the Existence of Mitogenetic Radiation. *Speculat Sci Technol* 4 (5):453–464
- Quickenden TI, Matich AJ, Pung SH, Tilbury RN (1989) An attempt to stimulate cell division in *Saccharomyces cerevisiae* with weak ultraviolet light. *Radiat Res* 117 (1):145–157. <https://doi.org/10.2307/3577283>
- Quickenden TI, Tilbury RN (1985) An attempt to stimulate mitosis in *Saccharomyces cerevisiae* with the ultraviolet luminescence from exponential phase cultures of this yeast. *Radiation Research* 102: 254–263
- Rahn O (1934a) The Disagreement in mitogenetic experiments, a problem in bacterial physiology. *Journal of Bacteriology* 28 (2):153–158
- Rahn O (1934b) The physico-chemical basis of biological radiations. In: *Cold Spring Harbor Symposia on Quantitative Biology*, Vol. II Berlin, pp 226–240. <https://doi.org/10.1101/SQB.1934.002.01.029>
- Rahn O (1936) Invisible radiations of organisms, vol 9. *Protoplasma Monographien*. Gebrüder Bornträger, Berlin

- Rajewsky B (1930) Anordnung zur Messung kleinster Lichtintensitäten. *Zeits f Physik* 63:576
- Rajewsky B (1931) Zur Frage des physikalischen Nachweises der Gurwitsch-Strahlung. In: Dessauer F (ed) *Zehn Jahre Forschung auf dem physikalisch-medizinischen Grenzgebiet*. Georg Thieme Verlag, Leipzig, pp 244–257
- Reiter T, Gabor D (1928a) Ultraviolette Strahlen und Zellteilung. *Strahlenther apie* (28):125–131
- Reiter T, Gabor D (1928b) Zellteilung und Strahlung. Sonderheft der Wissenschaftlichen Veröffentlichungen aus dem Siemens-Konzern. Springer-Verlag, Berlin. <https://doi.org/10.1007/978-3-642-50832-5>
- Richards OW, Taylor GW (1932) "Mitogenetic rays" – a critique of the yeast-detector method. *The Biological Bulletin* 63 (1):113–128
- Rodionov S, Frank GM (1934) On the measurements of mitogenetic radiation by means of a photoelectron counter (In Russian). *Archive of Biological Sciences Ser B* 35 (1):277–288
- Rossmann B (1928) Untersuchungen über die Theorie der mitogenetischen Strahlen. *Wilhelm Roux' Archiv für Entwicklungsmechanik der Organismen* 113 (2):346–405. <https://doi.org/10.1007/bf02081074>
- Salkind SJ (1925) Weitere Untersuchungen über mitogenetische Strahlen und Induktion. *Archiv für mikroskopische Anatomie und Entwicklungsmechanik* 104 (1):116–120. <https://doi.org/10.1007/bf02108494>
- Schreiber H, Friedrich W (1930) Über Nachweis und Intensität der mitogenetischen Strahlung. *Biochem Zeitsch* (227):386–400
- Schwemmler J (1929) Mitogenetische Strahlen. *Biologisches Zentralblatt* (49):421–437
- Sewertzowa LB (1928) Über den Einfluss der mitogenetischen Strahlung auf die Vermehrung der Bakterien. *Biologisches Zentralblatt* 49:212–225
- Sewertzowa LB (1931) Influence du rayonnement mitogénétique sur la vitesse de multiplication des bactéries. *Annales Inst Pasteur* 46:337–371
- Seyderhelm R (1932) Über einen durch ultraviolette Bestrahlung aktivierbaren, antianämisch wirkenden Stoff im Blut. *Klinische Wochenschrift* 11:628–631
- Seyderhelm R, Kreitmar, H (1932) Über einen durch U.V.-Bestrahlung aktivierbaren antianämischen Stoff im Blute. *Naunyn-Schmiedebergs Archiv für experimentelle Pathologie und Pharmakologie* 167:106–107
- Siebert W, Seffert H (1937) Zur Frage der Blutstrahlung bei Krankheiten, insbesondere bei Geschwülsten. *Biochemische Zeitschrift* 289 (6/2):292–293
- Siebert WW (1928a) Über die mitogenetische Strahlung des Arbeitsmuskels und einiger anderer Gewebe. *Biochemische Zeitschrift* 202:115–122
- Siebert WW (1928b) Über eine neue Beziehung von Muskeltätigkeit und Wachstumsvorgängen. *Zeitsch Klin Med* (109):360–370
- Siebert WW (1930) Die mitogenetische Strahlung des Blutes und des Harns gesunder und kranker Menschen. *Biochemische Zeitschrift* 226 (4–6):253–256
- Sorin AN (1926) Zur Analyse der mitogenetischen Induktion des Blutes. *Wilhelm Roux' Archiv für Entwicklungsmechanik der Organismen* 108 (4):634–645. <https://doi.org/10.1007/bf02080168>
- Tarusov BN, Polivoda AI, Zhuravlev AI (1961) Study on ultra weak spontaneous luminescence of animal cells (in Russian). *Biofizika (Russ)* 6 (4):490–492
- Taylor GW, Harvey EN (1931) The theory of mitogenetic radiation. *Biolog Bull* 61 (3):280–293
- Tokin BP (1933) [Mitogenetic rays] *Mitogeneticheskije luchy* (In Russian). State Medical Publishing House,
- Troitskii NA, Konev SV, Katibnikov MA (1961) Studies on ultraviolet hemiluminescence of biological systems (In Russian). *Biofizika* 6: 238–240
- Tuthill JB, Rahn O (1933) Zum Nachweis mitogenetischer Strahlung durch Hefesprossung. *Archiv für Mikrobiologie* 4 (1–4):565–573. <https://doi.org/10.1007/bf00407562>
- Vladimirov YA (1967) Ultraweak luminescence accompanying biochemical reactions (English translation of "Sverkhslabye svecheniya pri biokhimicheskikh reaktsiyah" USSR Academy of Sciences, Institute of Biological Physics. Izdatel'stvo "Nauka" Moscow, 1966). NASA, C.F.S.T.I., Springfield, Vermont
- Vladimirov YA, Litvin FF (1959) Investigation of very weak luminescence in biological systems. *Biophysics* 4 (5):103–109
- Volodyaev IV, Belousov LV (2015) Revisiting the mitogenetic effect of ultra-weak photon emission. *Frontiers in physiology* 6 (00241): 1–20. <https://doi.org/10.3389/fphys.2015.00241>
- Volodyaev IV, Belousov LV, Kontsevaya II, Naumova AE, Naumova EV (2021) Methods of studying ultraweak photon emissions from biological objects. II. Methods based on biological detection. *Biophysics* 66 (6):920–949
- Volodyaev IV, Krasilnikova EN, Ivanovsky RN (2013) CO2 mediated interaction in yeast stimulates budding and growth on minimal media. *PLoS One* 8 (4):e62808. <https://doi.org/10.1371/journal.pone.0062808>
- Westenberg J (1935) Die "slide-cell" Methode von Wolff und Ras zum Nachweis von Gurwitsch-Strahlen. N.V. Noord-Hollandsche Uitgeversmaatschappij, Amsterdam
- Wolff LK (1932) Mitogenetische stralen. *Neederl Tijdschrift voor Geneeskunde* 76 (27):3278–3287
- Wolff LK, Ras G (1931a) Einige Untersuchungen über die mitogenetischen Strahlen von Gurwitsch. *Ztrbl f Bakt I* 123:257–270
- Wolff LK, Ras G (1931b) Über Gurwitsch-Strahlen bei Bakterien. *Acta Brevia Neerlandica de physiologia, pharmacologia, microbiologia* 1 (7):136–137
- Wolff LK, Ras G (1932) Über Gurwitschstrahlen bei einfachen chemischen Reaktionen. *Biochemische Zeitschrift* 250:305–307
- Wolff LK, Ras G (1933a) Über mitogenetische Strahlen. IV. Über Sekundärstrahlung. *Zentralblatt für Bakteriologie, Parasitenkunde und Infektionskrankheiten* 128:305–313
- Wolff LK, Ras G (1933b) Über mitogenetische Strahlen. V. Über die Methodik zum Nachweis von Gurwitschstrahlen. *Zentralblatt für Bakteriologie, Parasitenkunde und Infektionskrankheiten* 128:314–319
- Wolff LK, Ras G (1934) Effect of Mitogenetic Rays on Eggs of *Drosophila melanogaster*. *Nature* 133 (3361):499–499. <https://doi.org/10.1038/133499a0>
- Yefimov VV, Letunov SP (1934) Effects of work, fatigue, and rest on the blood emission of Gurwitsch's rays (In Russian). *Archive of Biological Sciences Ser B* 35 (1):157–168
- Zalkind SY (1940) Antimitogenetic monography (in Russian). *Archive of Biological Sciences* 57 (2–3):124–127

Ilya Volodyaev

3.1 Biological Oxidation

Oxidation of organic compounds with molecular oxygen is the main and ultimately the only source of energy in the body of animals and humans. Fortunately, this process does not occur spontaneously due to its high activation energy. This is caused, in turn, by the tight double bond between the two oxygen atoms in the molecule, which has to be somehow broken before it enters into a chemical reaction. The O = O bond breaking energy is 117 to 118 kcal/mol (Berezin et al. 1966). In addition, the oxidation substrate also has to be activated: e.g., the C – H bond break formally requires from 75 to 100 kcal/mol (Berezin et al. 1966).

A hundred years ago, there was a well-known discussion between O. Warburg and H.O. Wieland regarding what is activated during biological oxidation – hydrogen atoms of the substrate, or molecular oxygen? This discussion was resolved by the discovery of the entire electron transport system (respiratory chain) in animal cells. On the one side of this chain, the substrate hydrogen is activated by dehydrogenases, and on the other side, oxygen is activated by terminal oxidases, including the Warburg respiratory enzyme (Warburg 1948).

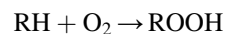
3.1.1 Peroxidation

Elucidating the respiratory chain structure and oxidative phosphorylation as a linking bridge between cellular oxidation and energy storage diverted researchers' attention for some time from other oxidation pathways of biologically important compounds and, in particular, from free-radical peroxidation. Meanwhile, the peroxide theory, formulated back in 1896–1897 by A.N. Bach (Fig. 3.1) and G. Engler (Bach 1897), was essentially the first theory of biological oxidation.

I. Volodyaev (✉)
Moscow State University, Moscow, Russia

The basic idea of this theory was that upon oxygen activation, only one rather than two chemical bonds are broken in the O₂ molecule, thus forming the –O – O– peroxide group, which is added to the oxidizing compound as a whole, forming its peroxide.

Indeed, from the 1930s to 1950s, the works of a number of researchers (see, e.g., (Berezin et al. 1966)) showed that the main or even the only primary products of nonenzymatic oxidation of organic compounds with molecular oxygen are hydroperoxides formed in the following reaction:



In the first stages of oxidation of olefins, alkylaromatic and hydroaromatic compounds, hydroperoxides account for 92% to 98% of all oxidation products, and only later, when these primary products begin to undergo further transformations, other products accumulate. In the oxidation of saturated hydrocarbons, hydroperoxides are also the only primary molecular reaction products (Emanuel et al. 1965).

3.1.2 Radical Chain Mechanism

The second stage in research of peroxidation processes is associated with the name of N.N. Semenov (Fig. 3.2), who developed the theory of branched chain reactions (Semenov 1934). As we will see further (Chap. 10), the chain, free-radical nature is characteristic for all peroxidation processes.

A classic example of free-radical chain reactions is light-activated interaction of hydrogen and chlorine vapors (Nernst 1918). A quantum of light absorbed by chlorine causes its photolysis, generating two chlorine atoms, each with an unpaired electron. Each of them attacks a nearby molecule, generating HCl and a hydrogen atom in case this molecule is H₂; the hydrogen atom attacks further molecules, etc.:

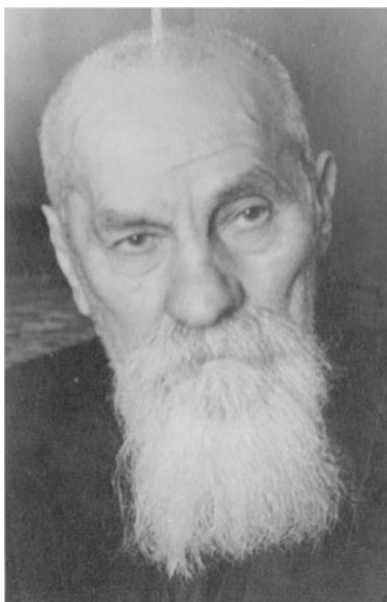


Fig. 3.1 A.N. Bach (1857–1946). (Reprinted from Bach, https://commons.wikimedia.org/wiki/File:%D0%90%D0%BB%D0%B5%D0%BA%D1%81%D0%B5%D0%B9_%D0%9D%D0%B8%D0%BA%D0%BE%D0%BB%D0%B0%D0%B5%D0%B2%D0%B8%D1%87_%D0%91%D0%B0%D1%85.jpg. Accessed 28 April 2023)

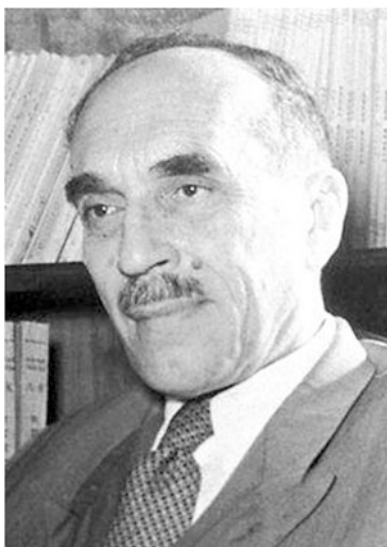
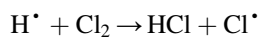
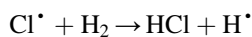
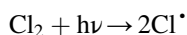


Fig. 3.2 N.N. Semenov (1896–1986). (Reprinted from Semenov, https://commons.wikimedia.org/wiki/File:Nikolay_Semyonov_Nobel.jpg. Accessed 28 April 2023)



Obviously, the quantum yield of the elementary act of this reaction (photolysis of the chlorine molecule) cannot be higher than unity. But due to the chain mechanism of the process, the gross quantum yield of HCl formation can reach

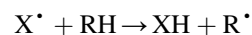
values of $10^6 - 10^7$ at room temperature. Thus, the chain process, which is “carried out” by the free radicals H^{\bullet} and Cl^{\bullet} , is accompanied by the formation of millions of product molecules for each radical formed in the system, i.e., the length of such a chain reaction reaches $\geq 10^6 - 10^7$.

A similar kind of proof of the chain reaction mechanism was obtained in the case of photo-induced peroxidation of a number of organic compounds. Thus, in the presence of oxygen, illumination of cyclohexene solution leads to formation of 8 peroxide molecules per each absorbed photon, and of ethyl linoleate – to 90 peroxide molecules per photon (Emanuel et al. 1965). It is quite obvious that in these cases, the primary photochemical formation of active intermediate products (radicals) leads to the development of a chain reaction with the formation of many product molecules:



Other possible initiators of peroxidation are: photosensitizer molecules, which are decomposed under the action of light, generating radicals; ionizing radiation; and a number of chemical reactions (Vladimirov 1965; Vladimirov et al. 1970a, b). All these agents actually accelerate peroxidation of organic compounds and can therefore be called pro-oxidants.

Despite the variety of factors attributed to pro-oxidants, their action is always based on generating radicals able to interact with the molecules of the oxidized compound, forming its free radical:



3.2 Free Radicals

3.2.1 The Existence of Free Radicals

Historically, the first report on the existence of a stable particle with an unpaired electron was made back in 1900 by M. Gomberg (Fig. 3.3a), who proved the existence of a triphenylmethyl free radical (Fig. 3.3b) (Gomberg 1900).

At the end of his famous report “An instance of trivalent carbon: triphenylmethyl” (Gomberg 1902), the author wrote: “This work will be continued and I wish to reserve the field for myself.” While nineteenth-century chemists respected such claims, the field discovered by the author, free-radical chemistry and later, free-radical biology, appeared so comprehensive, that not only was he alone unable to master the entire field, but even 120 years later, with the participation of thousands of researchers, work in this area is still far from complete.

Nevertheless, the existence of free radicals for a long time not only raised doubts, but was openly denied by many researchers. In 1915, V. von Richter in his monograph “Organic Chemistry” wrote: “The assumption of the existence of free radicals, capable of existing alone and playing a special role in chemical reactions, has long been abandoned.” (von Richter et al. 1915). In 1926, C.W. Porter in his book “The Carbon Compounds” also said: “Negative results gradually established the doctrine that a free carbon radical was incapable of independent existence.” (Porter 1926).

Apparently, the main interest in free radicals as intermediate products of organic reactions was formed in the late 1920s–early 1930s when, in a series of works by the group of F. Paneth (e.g., (Paneth and Hofeditz 1929; Paneth 1934; Paneth and Lautsch 1935)) and soon by F.O. Rice et al. (1932), the possibility of obtaining a number of carbon-

containing radicals in free form was unequivocally proved (see (Ihde 1967)).

In general, by the end of the 1930s, there was no longer any doubt that free radicals are intermediate products of photochemical and pyrolytic reactions (see, e.g., (Terenin 1947)).

3.2.2 Biological Role

Predicting the important role of free radicals in biology is attributed to L. Michaelis, who in a series of publications formulated the concept that all redox reactions of organic compounds proceed through the stage of free radicals as a result of the molecules one-electron oxidation or reduction (Michaelis 1935, 1940; Michaelis et al. 1939; Michaelis and Hill 1933). This statement was based on experiments with potentiometric titration of semiquinones, intermediate products of quinone reduction (Michaelis and Hill 1933). Simultaneously, the existence of the semiquinone radical as an obligatory intermediate product of quinone oxidation was shown by V.L. Levshin (1935a, b). Today, we know that ubisemiquinone radicals are indeed involved in electron transfer along the mitochondrial respiratory chain.

At the same time, J. Frankenburger (1933), R. Audubert (1939) and A.G. Gurwitsch (reviewed in (Gurwitsch and Gurwitsch 1948)), working on the problem of the so-called mitogenetic radiation (see Chap. 2), argued that free radicals are indispensable participants in generation of biological autoluminescence quanta. This statement also found full confirmation in the science of our time (see Chaps. 8, 9, and 10).

3.2.2.1 Free Radicals in Photobiology

Another important step of research on the biological role of free radicals is the work on primary photobiological processes carried out by A.A. Krasnovsky (Fig. 3.4).

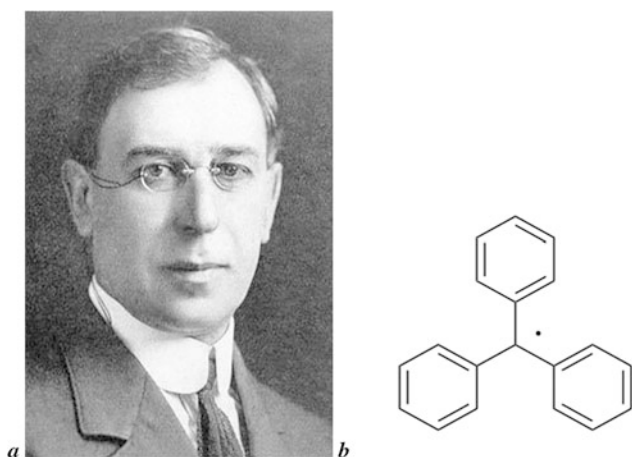


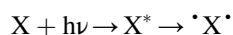
Fig. 3.3 Moses Gomberg (1866–1947) (a) and triphenylmethyl (b) – the first case of stable free radical, discovered by him. (Reprinted from Wikipedia, https://en.wikipedia.org/wiki/Moses_Gomberg. Accessed 6 Jan 2022)

Fig. 3.4 A.A. Krasnovsky (1913–1993). (From the personal archive of A.A. Krasnovsky Jr., with permission)

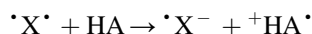


The author showed that chlorophyll can be reversibly reduced by electron donors under excitation with light (in an alkaline environment) and proposed the following mechanism for this process (Krasnovsky 1948):

1. Absorption of a quantum of light by chlorophyll (X) and its transition to a triplet biradical state



2. Acceptance of an electron from a donor (HA) with the formation of radical ions (green form of photo reduced chlorophyll, stable at temperatures less than -40 °C):



3. Attachment of a proton with the formation of the final reduced (red) form of chlorophyll:



Nowadays, this mechanism is well-known, and the reaction is named after A.A. Krasnovsky. In essence, this scheme laid down the basic concept of the primary stages of a number of photobiological processes (see also (Krasnovsky 1960)). In all of them, absorption of a photon, and the accompanying transition of the chromophore to an excited state, leads to the primary formation of free radicals, while more stable molecular products are formed later.

The following works on photo-induced luminescence of amino acids, peptides and proteins, carried out by the group of Yu.A. Vladimirov together with A.A. Krasnovsky (see Sect. 3.5.4), fully confirmed these assumptions.

3.2.2.2 Pathological Role of Free Radicals

In 1956–1957, D. Harman showed the role of free radicals in the body aging (Harman 1956, 2001) and in atherosclerosis development (Harman 1957). The author's conclusions were based on the fact that the lifespan of laboratory animals increased when they were fed with antioxidants (which were already known to inhibit reactions involving radicals, formed, in particular, under the influence of ionizing radiation).

In 1957, B.N. Tarusov (Fig. 3.5) suggested that the effect of ionizing radiation on the body is based on the initiation of radical chain reactions (Tarusov 1954, 1957). A number of facts spoke in favor of this, in particular, the incommensurability of energy costs of the radiation action (which are very small) and the body response (damage to a number of important functions and death). The substrate for chain reactions could be lipids, for which the possibility of such reactions had already been established (Tarusov 1957).



Fig. 3.5 B.N. Tarusov (1900–1977). (From the personal archive of A.A. Krasnovsky Jr., with permission)

Indeed, later in the works of Tarusov and colleagues, as well as a number of other authors, exposure of tissues to ionizing radiation was shown to stimulate both free-radical formation (detected by graft copolymerization, EPR, and chemiluminescence) and accumulation of lipid peroxides (Zhuravlev 1963; Polivoda and Sekamova 1962). At the same time, accumulating peroxides were observed during irradiation of whole animals (Tarusov et al. 1961a), homogenates of tissues, and during oxidation of suspensions of subcellular particles: microsomes, mitochondria, and lysosomes (Desai et al. 1964a, b; Tappel 1965; Tappel and Sawant 1963).

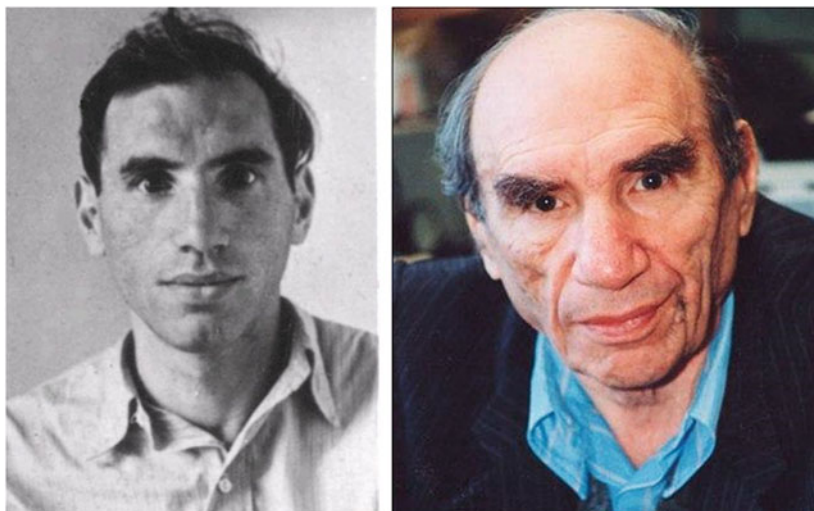
Ultraviolet radiation had a similar effect, causing formation of free radicals in biological systems and accumulation of peroxides in mitochondria suspensions (Marzoev et al. 1971, 1973; Roshchupkin et al. 1973) and in the stroma of erythrocytes (Korchagina and Vladimirov 1971).

3.2.3 Direct Detection of Free Radicals

Free radicals appearing in dry proteins irradiated with ionizing radiation were directly demonstrated by L.A. Blumenfeld (Fig. 3.6) and A.E. Kalmanson in 1958–1959 by the method of electron paramagnetic resonance, with the help of a specially constructed device (Blyumenfel'd and Kalmanson 1957, 1958). Yet, due to the high reactivity of radicals, the EPR method proved to be insufficiently sensitive to detect EPR signals in living cells and even in biochemical systems.

Direct EPR observation of free radicals in biological systems became possible many years later, thanks to the development of the spin trapping approach (Janzen and Blackburn 1968).

Fig. 3.6 L.A. Blumenfeld (1921–2002). (Reprinted from Lev Aleksandrovich Blumenfeld – quotes (in Russian) <https://citaty.info/man/lev-aleksandrovich-blyumenfeld>. Accessed 28 April 2023)



Spin traps are compounds (A) which transform, upon interaction with highly active radicals (R^{\bullet}), into stable spin adducts (RA^{\bullet}), which can be detected with EPR. One of the most important types of spin traps are those derived from iminoxyl radical ($>NO^{\bullet}$) surrounded by hydrophobic groups screening it, first synthesized in 1970 by E.G. Rozantsev (1970; Rozantsev and Sholle 1971). The characteristic triplet EPR signal of iminoxyl radicals has a fine structure that, within certain limits, depends on the structure of the captured radical. Thanks to the RA^{\bullet} stability, in a system where R^{\bullet} free radicals are formed the RA^{\bullet} stationary concentration is many times higher than that of the “original” free radicals R^{\bullet} . This allows the researcher to study adduct radicals (and, indirectly, initial radicals) in biological systems where direct detection of active radicals is impossible.

The use of iminoxyl radicals as spin traps allowed A.N. Saprin and L.H. Piette to show formation of free radicals during lipid peroxidation in liver microsomes (Saprin and Piette 1977) and A.N. Osipov and colleagues to show the appearance of lipid radicals while decomposition of lipid hydroperoxides by Fe^{2+} ions (Osipov et al. 1980).

Thus, free radicals were gradually proven and well accepted to be important “players” in both photobiological and a number of physiological processes.

3.3 Biological Autoluminescence

3.3.1 Before PMT (1930s–1940s)

However, evidence for the role of free radicals in biological systems came even earlier through the discovery of ultraweak luminescence arising from their recombination.

As already mentioned, the first works on UPE from biological systems belong to mitogenetic studies (see Chap. 2). Purely biological experiments on the interaction

of biological objects due to the alleged mitogenetic radiation were soon replaced by works on its physical detection (Rajewsky 1930, 1931, 1932; Frank and Rodionow 1931, 1932; Rodionov and Frank 1934), which gave variable results due to the ultra-low intensity of the radiation (Kreuchen and Bateman 1934; Lorenz 1934). The lack of equipment for detecting ultraweak light fluxes at that time, forced the authors to invent appropriate photodetectors by themselves. The most sensitive detectors appeared to be special photosensitive modifications of Geiger–Muller counters, which allowed measuring as low intensities as 10 to 100 quanta/s (Rajewsky 1931, 1932; Frank and Rodionow 1932; Rodionov and Frank 1934; Audubert 1938). However, these devices were found very capricious, and sometimes, an assembled counter was enough to carry out just one experiment, after which it lost sensitivity (Rodionov and Frank 1934; Barth 1937; Audubert 1938).

It was the observed UPE at a number of chemical reactions that led to formulating the energy paradox: luminescence with photon energy reaching 120 to 130 kcal/mol was observed during chemical reactions with the enthalpy of ≤ 30 kcal/mol. A solution to this problem was first proposed by J. Frankenburger (1933), who suggested that radiation quanta are generated during rare side processes involving free radicals. The same considerations were further developed by R. Audubert (1939) and A.G. Gurwitsch (Gurwitsch and Gurwitsch 1948), anticipating further development of science by 20 to 30 years (see Chaps. 8, 9, 10, 11, and 12).

3.3.2 First Works on Photomultipliers (1950s)

A new stage in UPE research began with the invention of photomultiplier tubes (PMT). The idea of using secondary electron radiation to amplify the primary weak electron flux belongs to J. Slepian (1923). The use of this secondary

amplification in combination with the photoelectric effect (generating the primary electron flux) led to the invention of PMT. Such a device was proposed and designed in the 1930s, independently by L.A. Kubetsky (invention (Kubetsky 1930); implementation (Kubetsky 1937)) and by H. Iams and B. Salzberg (1935). Since then and up to now, PMT-type devices remain the most sensitive detectors of ultraweak light fluxes and are used as a reference for evaluating the efficiency of other photodetectors.

W. Arnold and B.L. Strehler can be considered pioneers in the study of weak photon emission of biological objects using PMT (Strehler 1951; Strehler and Arnold 1951). The setup developed by these authors consisted of a photomultiplier entirely placed in a glass Dewar flask with liquid nitrogen, in which a transparent (not silvered) window was left. A test tube or a capillary of the flow system was fixed in front of this window. The pulses coming from the PMT were recorded by a counter (Arthur and Strehler 1957; Strehler 1951). With this light detector, the authors studied bioluminescence of the firefly and bacteria, and also discovered the long-term afterglow of green leaves (Strehler 1951; Strehler and Arnold 1951).

The detected “photosynthetic luminescence” was a relatively intense UPE caused by reverse photochemical reactions in chloroplasts. The study of the photon emission that occurs during dark biochemical reactions (except for the specific mechanisms of bioluminescence) was not carried out by the authors, and such a task, apparently, was not posed.

The truly spontaneous emission of biological systems was first detected with the use of a PMT by L. Colli and U. Facchini in 1954 (Colli and Facchini 1954). The authors used an end-face photomultiplier cooled with solid carbon dioxide and recorded photon emission from germinating plants in the visible spectral region (450–650 nm). This differed from both groups of studies cited above. Thus,

Rajewsky (1931, 1932), Frank and Rodionow (1932), Siebert and Seffert (1933), Rodionov and Frank (1934), Barth (1934, 1936, 1937), Glasser and Barth (1938), and Audubert (1938) worked with photon emission in the UV spectral range, and Strehler (1951), Strehler and Arnold (1951), and Arthur and Strehler (1957) observed weak luminescence of previously illuminated objects. Contrary to that, the ultraweak photon emission detected by Colli and Facchini (1954) and Colli et al. (1955) was a true visible-range autoluminescence generated by dark biochemical reactions.

3.3.3 “Soviet School” of Biochemiluminescence (1959–1970s)

3.3.3.1 Beginning

Studies of ultraweak luminescence of biological systems were started with the work of Yu.A. Vladimirov and F.F. Litvin in 1959 (Vladimirov and Litvin 1959) (Figs. 3.7 and 3.8).

Seeking, on the one hand, to verify the data on mitogenetic radiation (see Chap. 2) and, on the other hand, to elucidate the role of excited states in biochemical reactions, the authors developed a special highly sensitive photodetection equipment consisting of a liquid nitrogen-cooled photomultiplier and a pulse counter (Fig. 3.9). The device could detect luminous fluxes as low as 1.7 quanta/s in the spectral region of 400 to 550 nm and 8.5 quanta/s in the region of 650 to 850 nm.

Using the instrument developed, the authors confirmed Strehler’s data on prolonged (up to an hour or more) leaf afterglow (Strehler 1951; Strehler and Arnold 1951) and on riboflavin chemiluminescence under the action of hydrogen peroxide (Strehler and Shoup 1953).

Fig. 3.7 Yu.A. Vladimirov (born 08/18/1932). (From the personal archive of Yu.A. Vladimirov, with permission)

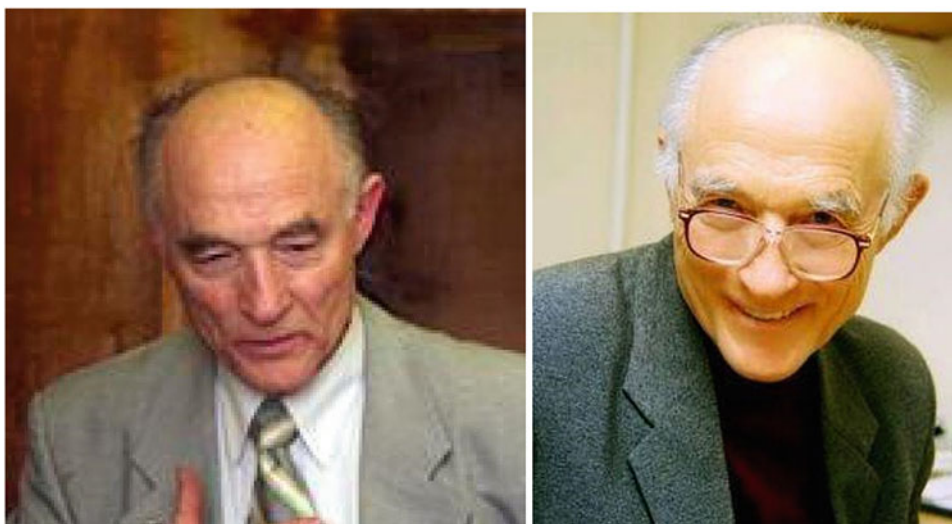


Fig. 3.8 F.F. Litvin (born 05/15/1929). (a) Reprinted from Litvin Felix Fedorovich (in Russian), <http://letopis.msu.ru/peoples/4384>. Accessed 28 April 2023 (b) from the personal archive of Yu.A. Vladimirov, with permission

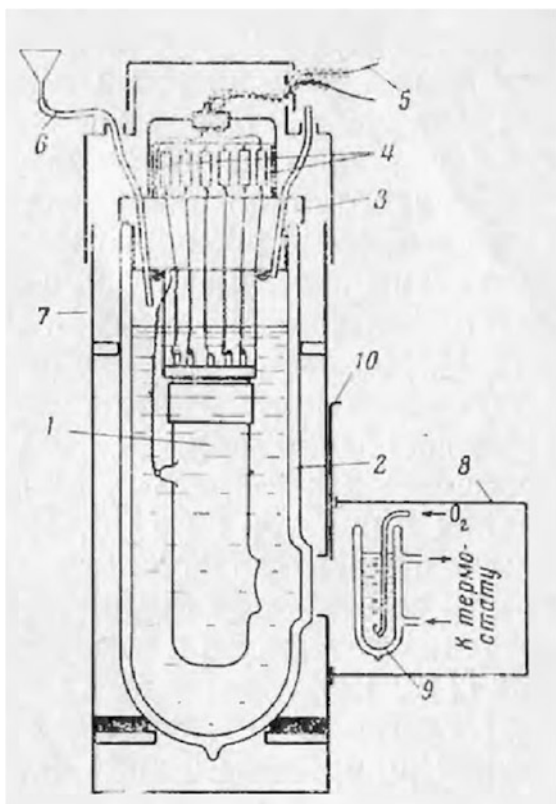


Fig. 3.9 Schematic of the setup for studying ultraweak luminescence (Vladimirov and Litvin 1959, 1964). 1 – photomultiplier; 2 – Dewar vessel with liquid nitrogen; 3 – foam plug; 4 – voltage divider; 5 – high voltage input and signal output; 6 – rubber tube with a funnel for liquid nitrogen; 7 – outer metal casing; 8 – opaque camera for the object; 9 – thermostatically controlled object cuvette; 10 – curtain and light filter. (Reprinted with permission from Vladimirov and Litvin (1964). Copyright 1964, the authors)

They also discovered the afterglow of dry proteins (Vladimirov and Litvin 1959) and their low-temperature phosphorescence (Vladimirov and Litvin 1960), which was the first work related to the UPE of proteins and amino acids and subsequently led to an important series of works on amino acid free radicals (see Sect. 3.5.4). Further, they showed chemiluminescence during the dark processes accompanying chlorophyll photochemical reactions (Krasnovsky et al. 1961; Litvin et al. 1960) and confirmed the data of L. Colli and U. Facchini on UPE from bean sprouts. Later, in an attempt to record chemiluminescence of yeast suspension cultures in the dark, they discovered light-induced luminescence of yeast, which was closely related to cellular metabolism (Vladimirov et al. 1962).

3.3.3.2 B.N. Tarusov's Group

The same technique of UPE detection was applied in a series of works by B.N. Tarusov, A.I. Zhuravlev (Fig. 3.10) and coworkers, started in 1961. The authors were the first to successfully record true autoluminescence of animal tissues (not induced by light) using PMT (Tarusov et al. 1961b, 1962). They also found that UPE intensity always increased with increasing the sample temperature, which definitely showed its nonenzymatic nature. For instance, UPE from homogenates of different rat tissues became detectable only at the temperature higher than 50 °C (Tarusov et al. 1961b, 1962).

At the same time, exposing animals to ionizing radiation greatly increased UPE from their tissue homogenates and whole organs, making it significant even at 37 °C (Tarusov et al. 1961a, 1962). UPE was also observed from the liver of a living rat with an opened abdominal cavity, and its intensity was also significantly higher for irradiated animals (Tarusov

Fig. 3.10 A.I. Zhuravlev (born 01/28/1930). (a) From the personal archive of A.I. Zhuravlev, with permission; (b) from the author's personal archive



Table 3.1 Ultraweak luminescence of some irradiated and unirradiated objects

| Object | Dose, Röntgen | Temperature, °C | UPE, <i>imp/min</i> | Background, <i>imp/min</i> |
|------------------------|-----------------|-----------------|---------------------|----------------------------|
| Mouse liver | 0 | 38 | 100–150 | 20–30 |
| | 700 | 38 | 160–250 | 20–30 |
| Canine liver lipids | 0 | 60 | 305–340 | 60–80 |
| | 4200 | 60 | 1800–2050 | 60–80 |
| Mouse liver homogenate | 0 | 50 | 60–70 | 20–30 |
| Olive oil | 0 | 60 | 205–240 | 40–55 |
| | 3×10^5 | 60 | 400–440 | 40–55 |
| Oleic acid | 0 | 60 | 860–1200 | 60–80 |
| Sunflower oil | 0 | 60 | 60–90 | 20–30 |

Reprinted with permission from Tarusov et al. (1961a)

et al. 1961a, 1962). This perfectly matched Tarusov's earlier assumption that the main mechanism of radiation damage to biological systems is initiation of uncontrolled free-radical chain peroxidation (Tarusov 1954, 1957).

Also, spontaneous luminescence was recorded from lipids upon oxidation with oxygen (Zhuravlev 1962b, 1965a, b; Tarusov and Zhuravlev 1965), including lipid extracts from animal tissues (Tarusov et al. 1961a, b). Importantly, the lipid UPE, as well as UPE from tissue homogenates, was suppressed by antioxidants (Zhuravlev 1960), including those naturally present in biological tissues (Zhuravlev et al. 1961, 1964; Zhuravlev and Filippov 1965).

Some of the results obtained by this group are given in Table 3.1.

Altogether, the authors proved the following statements:

- Animal tissues are sources of spontaneous UPE of nonenzymatic nature.
- UPE from animal tissues is stimulated by factors, initiating free-radical processes (ionizing radiation, UV of high intensity, chemical sources of free radicals, like hydrogen peroxide, etc.).

- UPE from animal tissues is suppressed by antioxidants.

All these data showed that UPE from animal tissues was generated in the process of lipid peroxidation, a free-radical chain process, spontaneously taking place in tissues, and activated/initiated with heating, ionizing radiation, etc. As we know now, these ideas appeared completely correct, and a significant part of biological autoluminescence is actually generated during lipid peroxidation.

3.4 Delayed Luminescence: Phosphorescence and Photochemiluminescence

Although this may seem strange, a very important role in the study of biological autoluminescence was played by a seemingly extraneous direction of research – the afterglow of irradiated systems, typically called “delayed luminescence.” It was this very research line that provided an understanding of the structure of molecule energy levels, the properties of electronically excited states, the mechanisms of

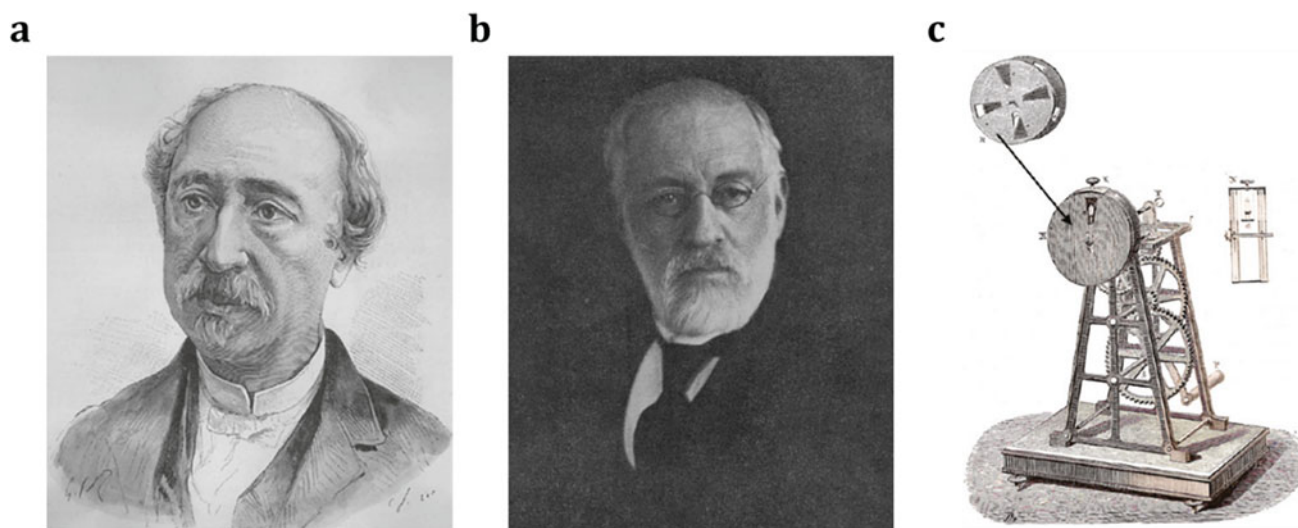


Fig. 3.11 (a) E. Becquerel (1820–1891), (b) E.E.G. Wiedemann (1852–1928) and (c) a picture of the first phosphoroscope. ((a), (c) Reprinted with permission from Valeur and Berberan-Santos (2011).

Copyright 2011 American Chemical Society; (b) Reprinted with permission from Seemann (1930))

phosphorescence and photochemiluminescence, and, ultimately, the structure of amino acid radicals and the mechanisms of their recombination.

3.4.1 Delayed Luminescence Phenomena

While the standard photo-excited fluorescence is observed exactly during photoexcitation (and the corresponding excited state has a very short lifetime – $\sim 10^{-9}$ s), delayed luminescence may last from microseconds to hours after the end of photoexcitation and is actually a number of different phenomena, combined only by duration.

Such phenomena have been known for more than two centuries and were initially called phosphorescence, though it is not necessarily related to what we now call it. The first device for investigating such afterglow without incident light exposure was developed by E. Becquerel (Fig. 3.11a) in 1858 and called phosphoroscope (Fig. 3.11c). This let the author make the first systematic observations on long-lasting luminescence induced by external light (Becquerel 1867) (see and more in (Krasnovsky (Jr) 2014; Harvey 1957)).

Later, E. Wiedemann (Fig. 3.11b) suggested a common term **luminescence** for any photon emission not associated with general body heating (Wiedemann 1888) (i.e., differentiated luminescence from what we now call black body radiation). He also suggested the modern terms **photo-**, **chemi-**, **electro-**, **thermo-**, and **triboluminescence** and classified photoluminescence according to its lifetimes:

- **Fluorescence** – instantaneous luminescence of an irradiated substance (observed in liquid and gaseous substances)

- **Phosphorescence** – long-lived emission of preirradiated substances (previously observed only in solids)

While at present E. Wiedemann’s “phosphorescence” would be subdivided into **phosphorescence**, **delayed fluorescence** and **photochemiluminescence**, according to its exact mechanisms and spectra (see Sect. 5.2), his unified classification made a huge breakthrough in the luminescence research.

Importantly, the author showed that practically all fluorescent substances are also capable of phosphorescence, if “solidified” by mixing with gelatine and drying (see (Wiedemann 1888) and references therein). Thus, “one can convert a fluorescent body into a phosphorescent one by restricting the free mobility of its molecules” (Wiedemann 1888).

This was also confirmed by G.C. Schmidt, who achieved phosphorescence from dye solutions, super-cooled to a rigid glassy state (Schmidt 1896), and E. Tiede, who formed glassy states of dye solutions at room temperature by mixing them with fused boric acid and showed phosphorescence from them (Tiede 1920; Tiede and Wulff 1922).

3.4.2 Phosphorescence and Delayed Fluorescence

Important data were achieved from spectral studies of luminescence (Wawilow and Lewschin 1926; Delorme and Perrin 1929). Besides the main fluorescent spectral band, phosphorescent substances showed a second spectral component, at longer wavelengths, which could be well observed at low temperatures, but gradually disappeared

Fig. 3.12 Luminescence spectra of fluorescein in boric acid and the corresponding Perrin–Jablonski diagram. (a) – Phosphorescence spectra of fluorescein in boric acid at (1) 20 °C and (2) -40 °C; (b) – Energy diagram of fluorescein in boric acid. (Reprinted with permission from Lewis et al. (1941). Copyright 1941, American Chemical Society)

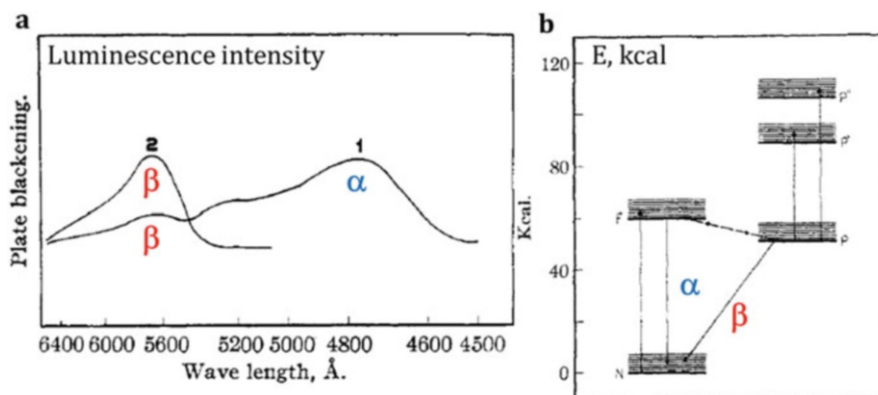
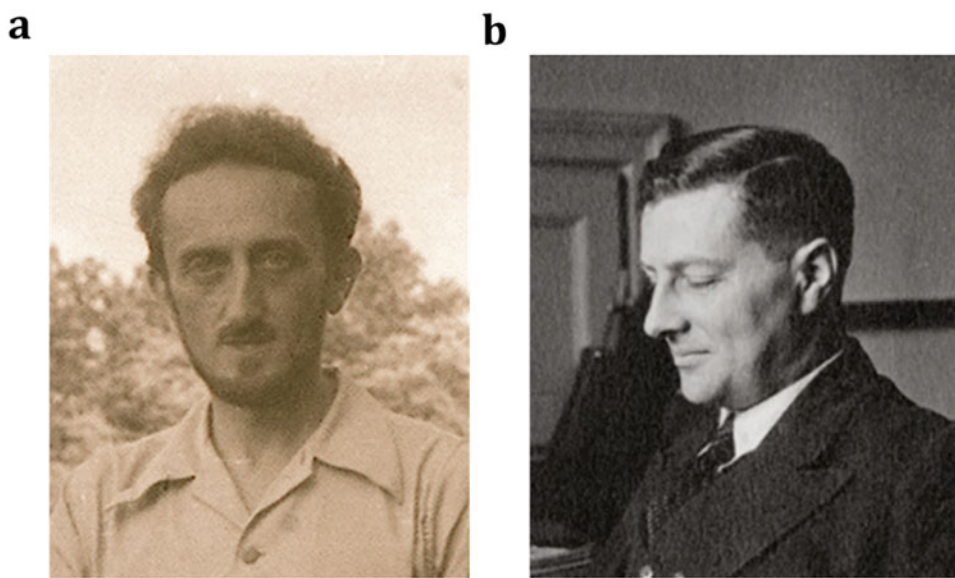


Fig. 3.13 (a) Francis Perrin (1901–1992), (b) Aleksander Jablonski (1898–1980). ((a) Reprinted from Wikipedia, [https://de.wikipedia.org/wiki/Francis_Perrin_\(Physiker\)](https://de.wikipedia.org/wiki/Francis_Perrin_(Physiker)) <https://isaran.ru/?q=ru/person&guid=64A681C2-F526-3600-B100-E7EF1A7F25F7>. Accessed 6 Janspiepr146 2022), (b) reprinted from Lumipedia, http://www.lumipedia.org/index.php?title=Jab%C5%82o%C5%84ski_Aleksander <https://isaran.ru/?q=ru/person&guid=64A681C2-F526-3600-B100-E7EF1A7F25F7>. Accessed 6 Janspiepr146 2022)



as the temperature rose (see Fig. 3.12a). F. Perrin (1929; Delorme and Perrin 1929) (Fig. 3.13a) explained this by another, lower-energy, excited state of the dye molecule, which he called metastable: the longer wavelength component was attributed to its direct radiative relaxation, while the “fluorescence-like” band was attributed to its thermal activation to the standard fluorescent excited state. These ideas were finalized by A. Jablonski (1935) (Fig. 3.13b), who formed the present-day picture of energy levels – Perrin–Jablonski diagram (see Fig. 3.12b).

The fact that phosphorescence was generated at relaxation of a single electron-excited state (rather than recombination of certain species, or a chemical reaction) was reliably shown by the groups of S.I. Vavilov and V.L. Levshin (Wawilow and Lewschin 1926; Levshin and Vinokurov 1934; Levshin 1936; Schischlowski and Wawilow 1934), and later by N. Lewis et al. (1941) (Fig. 3.14b). The authors showed that the true phosphorescence decay (if not mixed with photochemiluminescence) fits perfectly into the exponential curve, indicating the monomolar mechanism of photon

emission – i.e., that phosphorescence is generated by relaxation of a single electron-excited state.

Thus, by the 1940s, it was reliably shown that phosphorescence occurs during the relaxation of a certain metastable state, the energy of which is lower than the energy of the usual excited fluorescent state, and the lifetime for some reason is much longer. This corresponded to the longer-wavelength band of delayed luminescence (β in Fig. 3.12). The “fluorescence-like band” (α in Fig. 3.12) appeared at thermal excitation from the metastable state to the standard fluorescent state and radiant relaxation from there was exactly the same as for standard fluorescence, and only slowed down by the previous electron transition to the metastable level and back.

3.4.3 The Triplet State

However, none of the above authors could explain the unusually long lifetime of the metastable state. This was done by

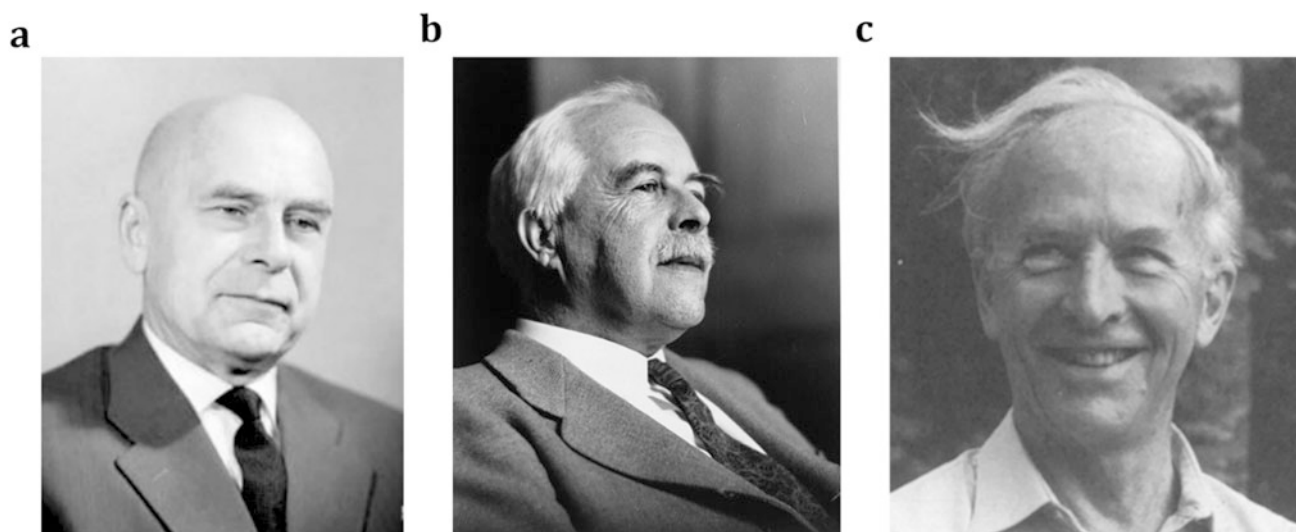


Fig. 3.14 (a) A.N. Terenin (1886–1967), (b) G.N. Lewis (1875–1946) and (c) M. Kasha (1920–2013). (Reprinted with permission from (a) Terenin (2022), (b) (This Month in Physics History. December

18, 1926: Gilbert Lewis coins “photon” in letter to Nature 2012). (c) Reprinted from (Demchenko et al. 2014). Copyright 2014, with permission from John Wiley and Sons))

A.N. Terenin (see Fig. 3.14a) in 1943 (Terenin 1943), and independently by N. Lewis and M. Kasha in 1944 (Lewis and Kasha 1944) (see Fig. 3.14b, c).

Based on huge experimental material, collected by that time, and on their own extensive research (see also (Lewis et al. 1941; Lewis and Lipkin 1942; Lewis and Calvin 1945; Kasha 1947; Terenin 1943), the authors came to the following conclusions (quotes from (Lewis and Kasha 1944)):

- “All of the normal and excited states of a molecule fall into two classes of different multiplicity”: **singlet, S** (with all electrons coupled, and 0 spin), and **triplet, T** (with two uncoupled electrons with parallel spins on the outermost orbitals).
- The lowest level of all is stable; the lowest level of the other class is metastable.
For the vast majority of substances, the **stable state is singlet**; the **metastable state is triplet**. For several specific molecules (O_2 , S_2 , SO , and organic biradicals), opposite to that, the stable state is triplet; the metastable state is singlet.
- Standard absorption and emission occur between two levels of the same multiplicity: S–S or T–T. The S–T or T–S absorption and emission are quasi-forbidden for spin reasons and thus have much lower probability (but can be observed under specific conditions – e.g., (Lewis and Kasha 1945)).
- The S–S (or T–T) photon emission is **fluorescence**.
- The T–S and S–T emission is **phosphorescence**. “Phosphorescence has been found, not in every molecule, but in all sorts of molecules, complex or simple, organic or inorganic.”

The incomparably longer lifetime of the phosphorescent states (due to the spin ban for T–S transitions) makes them susceptible to quenching, and the dissipative process becomes rate-determining. That is why phosphorescence is mostly observed from solid or rigid glassy states, in which “the main function of rigidity is to protect the molecules in the phosphorescent state from the process of dissipation” (Lewis and Kasha 1944). However, using specific substances and conditions allows observing both phosphorescence and S–T absorption at room temperature and even in liquid and gaseous states (Lewis and Kasha 1945).

Besides the abovementioned numerous chemical, kinetical and spectroscopic data, supporting this scheme, it was unambiguously confirmed by the fact that the phosphorescent state acquired paramagnetic properties (Lewis and Calvin 1945).

Thus, due to the outstanding works of A.N. Terenin and G.N. Lewis et al., by the middle of the 1940s, the metastable phosphorescent state was confidently identified as triplet (for the molecules, whose ground state is singlet; and on the contrary, singlet, for triplet molecules). The unusually long lifetime of such states is due to the spin ban for their radiative relaxation; and the fact that they are mainly observed at low temperatures is explained by their thermal excitation to the standard fluorescent state under warmer conditions.

3.4.4 Photochemiluminescence

However, phosphorescence and delayed fluorescence appeared not the only processes caused by UV irradiation. In addition to the main process of phosphorescence –

Table 3.2 Comparison of the main qualities of two types of photo-induced photon emission from proteins

| Radiation property | Standard phosphorescence | Second component (“Phosphorescence of very long duration”) |
|--|--|--|
| Duration, s | Trp – 3 s (all pH) Tyr – 3 s (acidic media); <1 s (alkaline media) Phe – <0.1 s | $10^2 - 10^3$ s (at 77 °C) No (at higher T) |
| Decay function | Exponent | Inverse power function |
| Main spectral maxima, nm | 418; 440 nm | |
| Sensitivity to pH | Spectral maxima depend on pH: 417 nm (acidic media) 418; 440 nm (alkaline media) | Alkaline media – intense emission (Trp, Tyr) Weak or no emission in acidic media |
| Sensitivity to the protein composition | Trp or Tyr necessary; Otherwise – No | |
| Source | Relaxation from T_1 : Trp (++) Tyr (+) Phe (?) Other amino acids – No | e^- + amino acid radical-cation recombination: Trp (all pH) Tyr (alkaline media) Phe – No Other amino acids – No |

Based on the data in (Debye and Edwards John 1952; Debye and Edwards 1952)

relaxation of electronically excited triplet states, UV irradiation can cause three more types of events – dissociation of molecules into: (1) two radicals, (2) positive and negative ions, and (3) a positive ion and an electron (Lewis and Lipkin 1942).

While generally these phenomena are a subject of pure photobiology, the last variant, UV-induced dissociation of a molecule into a radical-cation and an electron, appeared of utmost importance for investigating the autoluminescence of amino acids and proteins.

While measuring phosphorescence of frozen amino acids and proteins at 77 °C, P. Debye and J.O. Edwards observed a second component of their photon emission with several principal differences from the classical phosphorescence (Debye and Edwards John 1952; Debye and Edwards 1952) (Table 3.2). The authors denoted it as “phosphorescence of very long duration” (Debye and Edwards John 1952).

As had already been known, the standard phosphorescence intensity is mostly independent of pH and temperature per se (aside from the quenching effects) and shows an exponential decay function after the end of the excitation. All this corresponds to its mechanism of monomolecular reaction – relaxation of a T_1 electron-excited state. Contrary to that, the second component – “phosphorescence of very long duration” (Debye and Edwards John 1952), is only observed at very low temperature and at alkaline pH. It also shows an inverse power decay function, which corresponds to a bimolecular reaction – recombination of the generated radicals or an organic cation-radical with an electron, ejected from the molecule by the exciting light. At the temperature of liquid nitrogen this component is well pronounced, at higher temperatures it is not, due to immediate recombination of the charged particles within the system. This dramatic dependence on the temperature is the main quality that makes this component distinguishable from standard phosphorescence.

Also, along with the decay function, it most directly characterizes its recombination mechanism. The authors attributed this phenomenon to recombination of electrons and radical cations, dissociated under the UV action, similarly to that previously shown for simpler substances (Lewis and Lipkin 1942; Harris et al. 1935).

3.5 Plexus of Lines: Mechanisms of UPE

3.5.1 Aqueous Systems

In the 1960s–1970s, the four lines of research described above, on free radicals, on peroxidation, on biological autoluminescence and on photo-induced photon emission, gradually intertwined into a single, sheathed and multifaceted field of science. Today, it also contains organic and quantum chemistry (see Chaps. 10, 11, 12, and 13), quantum mechanics (Chap. 13), and methods of mathematical modeling and digital signal processing.

Yet, the beginning of the *mechanistic research* on UPE per se should be attributed to the first works on simplest inorganic model systems carried out by W.W. Siebert and H. Seffert (Siebert 1934), R. Audubert (1938, 1939) and other “mitogenetic authors” (Chap. 2). These works were later continued and expanded by J. Stauff and H. Schmidkunz with the use of highly sensitive PMTs (Stauff 1964; Stauff and Reske 1964; Stauff and Rümmler 1962; Stauff and Schmidkunz 1962a, b; Stauff et al. 1963; Stauff and Wolf 1964). It was these works that brought the idea of free-radical recombination as the mechanism of UPE (see Chaps. 8, 10). They also stated the importance of oxygen for this phenomenon and explained the ultralow intensity of UPE: it is generated during very rare high energy side reactions (not in the main chemical process taking place

in the system), mostly involving oxygen-containing free radicals (see Chap. 9). Needless to say, this is very close to what we know now.

3.5.2 Hydrocarbons and Lipids

The study of the UPE accompanying peroxidation processes was initiated by the above works of Yu.A. Vladimirov et al. (Vladimirov and Litvin 1959; Vladimirov and L'vova 1965) and B.N. Tarusov, A.I. Zhuravlev et al. (Zhuravlev 1962a, 1963, 1965a, b; Zhuravlev et al. 1965; Zhuravlev and Korzhenko 1963). Independently, research of the luminescence accompanying lipid oxidation and peroxidase reactions was started by the groups of G. Anhström (Ahnström and Natarajan 1960) and R. Nilsson (Nilsson et al. 1964).

Simultaneously with these studies, R.F. Vasil'ev (Fig. 3.15), V.Ya. Shlyapitokh and colleagues began a systematic mechanistic study on chemiluminescence from model organic systems, mostly – solutions of aromatic hydrocarbons and their derivatives (Allabutayev et al. 1965; Vasil'ev 1963, 1965a, b, c, d; Vasil'ev and Vichutinskii 1962a; Vassil'ev and Vichutinskiy 1962; Vasil'ev et al. 1959, 1961, 1963; Vasil'ev and Rusina 1964a, b; Zakharov and Shlyapintokh 1961; Entelis et al. 1960; Shliapintokh et al. 1960; Vassil'ev 1962; Vasil'yev 1963) (see Chap. 10). Using a highly sensitive photo-detector, based on an end-face photomultiplier cooled with dry ice (Vasil'ev 1965c; Vasil'ev et al. 1961), the authors recorded UPE accompanying a number of reactions, including thermal decomposition of organic hydroperoxides in solutions, decomposition and oxidation of organic compounds in the gas phase, electrochemical reactions, dissolution,

condensation, and polycondensation (Vassil'ev et al. 1959; Shliapintokh et al. 1960).

The main stages of the chain peroxidation process, considered by the authors (and already known from other methods – see Sects. 3.1 and 3.2) were as follows:

Taking into consideration the observed UPE intensity, and the amount of hydroperoxides produced during this process, R.F. Vasil'ev calculated the approximate total quantum yield of luminescence (the number of quanta released for each molecule of the formed peroxide), which appeared as low as 10^{-8} (Vasil'ev 1963, 1965a). In full agreement with the reasoning of R. Audubert and J. Stauff, the author concluded that only some of the above reactions (Table 3.3) are accompanied by luminescence, namely (according to the enthalpy calculations), free-radical recombination (4, 5 and 6 in Table 3.3). Moreover, the presence of oxygen even at low concentrations gave reaction 6 an overwhelming advantage, also shown by calculations (see Sect. 10.3 for more details). All these conclusions are fully confirmed by modern data, including those based on complex quantum chemical models.

Table 3.3 The main stages of hydrocarbon chain peroxidation, considered by the group of R.F. Vasil'ev

| | | |
|---|--|--------------------|
| 1 | $X^{\bullet} + RH \xrightarrow{k_1} XH + R^{\bullet}$ | Chain initiation |
| 2 | $R^{\bullet} + O_2 \xrightarrow{k_2} ROO^{\bullet}$ | Chain peroxidation |
| 3 | $ROO^{\bullet} + RH \xrightarrow{k_3} ROOH + R^{\bullet}$ | |
| 4 | $R^{\bullet} + R^{\bullet} \xrightarrow{k_4} \text{inactive products}$ | Chain termination |
| 5 | $R^{\bullet} + ROO^{\bullet} \xrightarrow{k_5} \text{inactive products}$ | |
| 6 | $ROO^{\bullet} + ROO^{\bullet} \xrightarrow{k_6} \text{inactive products}$ | |

where X^{\bullet} is chain initiator, RH hydrocarbon, R^{\bullet} hydrocarbon radical, ROO^{\bullet} peroxy radical, $ROOH$ hydroperoxide

Fig. 3.15 R.F. Vasil'ev (born in 1929). (From the personal archive of A.V. Trofimov, with permission)



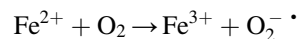
3.5.3 Mitochondria and Animal Tissues

Developing the above works on biological autoluminescence (see Chap. 2 and Sect. 3.3), different groups investigated spontaneous photon emission of homogenates and pieces of animal liver tissue (Cadenas et al. 1980a, b), as well as isolated mitochondria and microsomes (Boveris et al. 1980; Sławińska and Sławiński 1987; Vladimirov 1996; Vladimirov and Sherstnev 1991). Importantly, in full accordance with Vasil'ev's data on hydrocarbons, UPE from mitochondria was associated with formation of lipid peroxides (Suslova et al. 1969, 1970); Vladimirov et al. 1969a, b, suggesting a similar mechanism of chain peroxidation.

At the same time, accumulation of lipid peroxides in the system depended on the presence and valence of iron ions (Vladimirov et al. 1968, 1969a). Analyzing the complex chemiluminescence dynamics after adding micromolar amounts of Fe^{2+} to the mitochondrial suspension (Fig. 3.16), the authors compared it with accumulating peroxidation products, and iron oxidation, and came to the following conclusions:

- Lipid oxidation is a radical chain process, developing in the lipid layer of mitochondrial membranes, and forming fatty acid hydroperoxides.

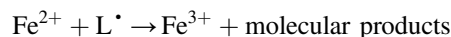
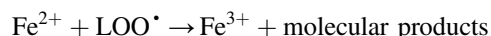
- Fe^{2+} ions play several important roles in such systems:
 - They initiate peroxidation by reacting with oxygen:



- They branch lipid peroxidation chains, making the process self-accelerating (Suslova et al. 1969; Vladimirov et al. 1969a);



- At high concentrations, they can also react with lipid radicals, thus breaking the peroxidation chains and suppressing UPE.



It's worth mentioning that the role of iron impurities in lipid peroxidation in mitochondria and microsomes was also discussed in the biochemical studies of Hochstein, Ernster and Hunter in 1963–1964 (Hochstein and Ernster 1963; Hochstein et al. 1964).

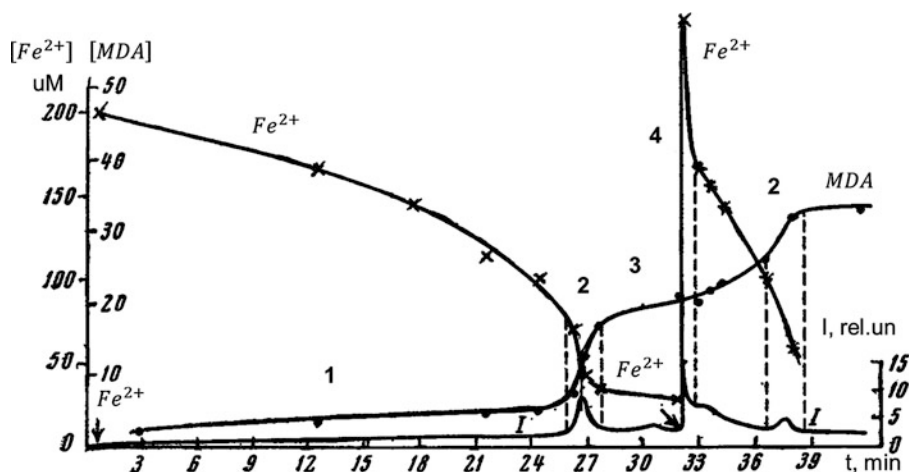


Fig. 3.16 Chemiluminescence, Fe^{2+} and a marker of lipid peroxidation (malondialdehyde, MDA) dynamics in the mitochondria suspension after adding 0.2 mM Fe^{2+} . The incubation mixture composition: 1 ml of mitochondria suspension in 10 ml of 105 mM NaCl and 20 mM Tris buffer, pH 7.5. Temperature 20 °C. 1–4 – stages of luminescence dynamics: 1 – latent period, 2 – “slow flash,” 3 – period of luminescence

inhibition, 4 – “fast flash” after Fe^{2+} injection. Along the axes: $[Fe^{2+}]$ – concentration of Fe^{2+} ions, μM ; $[MDA]$ – MDA concentration, μM ; I – chemiluminescence intensity, rel. units; t (min) – time after adding the mitochondria into the test tube. Arrows indicate the moments of Fe^{2+} injection. (Reprinted from Vladimirov et al. (1969a), with permission from the authors)

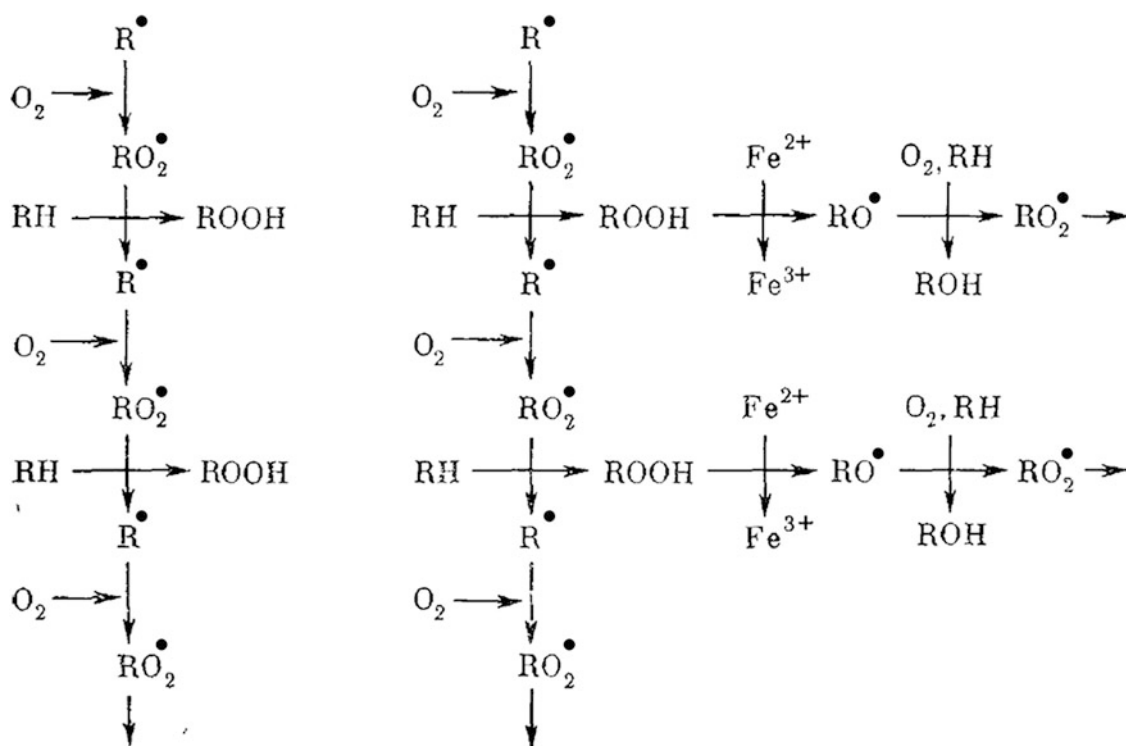


Fig. 3.17 Scheme of lipid peroxidation without Fe²⁺ (with unbranched chains) and in its presence (with branched chains). (Reprinted from Vladimirov et al. (1969a), with permission from the authors)

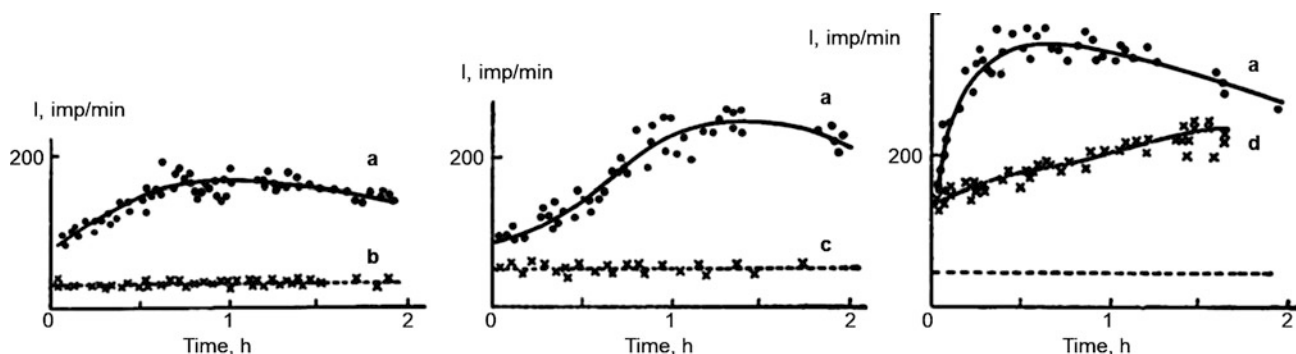


Fig. 3.18 The influence of various factors on the luminescence of the mitochondrial suspension (Vladimirov and L'vova 1964). a – complete system (mitochondria suspended in the incubation medium containing 1.2 mg/ml ATP, 2 mg/ml succinate, 2.9 mg/ml glutamate, 0.005 M MgCl₂, tris- and phosphate buffer, pH 7.4); b – the same, in the presence

of 0.2 mg/ml EDTA; c – the same as a, in the absence of ATP; d – the same as a, in the absence of substrates. The dashed line on all graphs is background signal from PMT (“dark count”). (Reprinted from Vladimirov and L'vova (1964), with permission from the authors)

The scheme of nonbranched and branched chain reactions of lipid peroxidation, constructed in these works, is shown in Fig. 3.17 (for a detailed review and a step-by-step chart featuring its architecture, see Chap. 11).

Another important issue arising in these works, is the origin of “the very first” free radicals in the system (i.e., the chain initiation mechanisms).

While the above-mentioned one-electron oxygen reduction by Fe²⁺ was definitely very important in model systems,

it was highly unlikely to play a prominent role in the cell. The first data on this topic were obtained by the group of Yu. A. Vladimirov already in the 1960s, by comparing mitochondrial UPE and respiration activity. Undisturbed mitochondria appeared a strong source of UPE under conditions supporting oxidative phosphorylation (i.e., in the presence of oxygen and oxidation substrates). Yet, when at least one necessary component was excluded from the system, the UPE became dramatically weaker or even undetectable (Fig. 3.18).

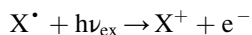
Inhibitors of the mitochondrial respiratory chain also suppressed UPE (Vladimirov and L'vova 1964; L'vova and Vladimirov 1966). Thus, the authors showed that mitochondrial electron-transport chain generates free radicals during its normal functioning, anticipating the presently known role of free radicals in many enzymatic processes and normal cell life (see below and Chaps. 8 and 14).

Thus, the peroxide, free-radical mechanism of light generation during spontaneous autoluminescence of biological systems was unambiguously shown in a number of studies by various authors and repeated the mechanism of UPE generation in model systems. At the same time, in biological systems, the respiratory chain (as well as other enzymatic processes) deserved special attention in the processes of free-radical generation.

3.5.4 Amino Acids and Proteins

At about the same time (1964–1970), developing the photochemical studies of G.N. Lewis and others (see Sect. 3.4), and photobiological research of A.A. Krasnovsky (see Sect. 3.2.2), Yu.A. Vladimirov, D.I. Roshchupkin and coauthors performed a study of photo-induced luminescence of amino acids and proteins (Vladimirov 1965; Vladimirov et al. 1970a, b).

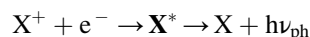
As is known, one of the simplest photochemical reactions, photoionization of organic compounds, results in formation of a radical cation X^+ and an electron e^- captured by the medium molecules (solvated electron):



where $h\nu_{\text{ex}}$ is the excitation light.

This reaction is reversible, the products are unstable: at room temperature, the lifetime of a hydrated electron is 25 to 50 μsec and that of organic radicals, including aromatic amino acids, about 100 μsec (Grossweiner et al. 1963a, b).

At the temperature of liquid nitrogen (77 K), solvated electrons are captured by traps in the frozen solvent and become incomparably more stable. Gentle heating of such samples leads to recombination of electrons and cation radicals and generation of UPE. This phenomenon is called low-temperature thermoluminescence (Vladimirov and Roshchupkin 1964; Roshchupkin and Vladimirov 1965) and appears phosphorescence (Vladimirov et al. 1966, 1970a, b):



Illumination of such a system with a weak red light leads to another type of UPE, containing both fluorescent and phosphorescent components (Agaverdiyev and Tarusov

1965; Aksentzev et al. 1966; Vasil'ev 1963), which could be called anti-Stokes photoluminescence (since the luminescent light is of shorter wavelengths than the exciting light). Here, in full accordance with Audubert's considerations (Audubert 1938), the energy of the emitted quantum is the sum of the reaction energy and the activation energy.

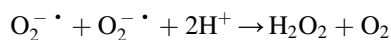
Using the method of pulsed photolysis, the authors also recorded absorption spectra of amino acid radicals, appearing in the reaction course as intermediate products (Aksentzev et al. 1967). Thus, they discovered free radicals of tyrosine, tryptophane, and phenylalanine formed in this system; showed their structure and mechanisms of elimination (Vladimirov et al. 1966, 1970a, b); and observed UPE at their recombination with solvated electrons (see Chap. 12).

All these data were obtained due to a special device, constructed by D.I. Roshchupkin and Yu.A. Vladimirov (Vladimirov and Roshchupkin 1962): a highly sensitive PMT-based photodetector, combined with a Dewar flask for placing the sample in liquid nitrogen with the possibility of its controlled evaporation (Fig. 3.19).

Today we know that tyrosine and tryptophan radicals are not just exotic species, formed in model systems as above. They are constantly appearing in various enzymes both at reactions with other radicals and in course of their normal functioning (e.g., compounds I and II of peroxidases – see Chap. 14). Thus, the reactions initiated by amino acid radicals, including free-radical peroxidation of organic substances and free-radical recombination, are normally present in the cell and, moreover, tightly controlled (see below). Importantly, the above-described luminescence at recombination of amino acid radicals with electrons can be used as a prototype for the processes of photon generation in proteins (see Chap. 12).

3.5.5 Enzymatic Generation of Free Radicals

All of the above results, surprisingly, did not have a big impact on biochemical science: biochemists, as they say, “did not see” free-radicals point-blank, just as they “did not see” biological membranes at that time either. Both of these issues fell out of sight, because common biochemical methods did not include electrochemical measurements, chemiluminescence, or radiospectroscopy, including EPR. Therefore, for the biochemical scientific community, the superoxide dismutase discovery by J.M. McCord and I. Fridovich in 1969 (McCord and Fridovich 1969a, b, 1970), an enzyme that converts two superoxide radicals into molecules of hydrogen peroxide and dioxygen:



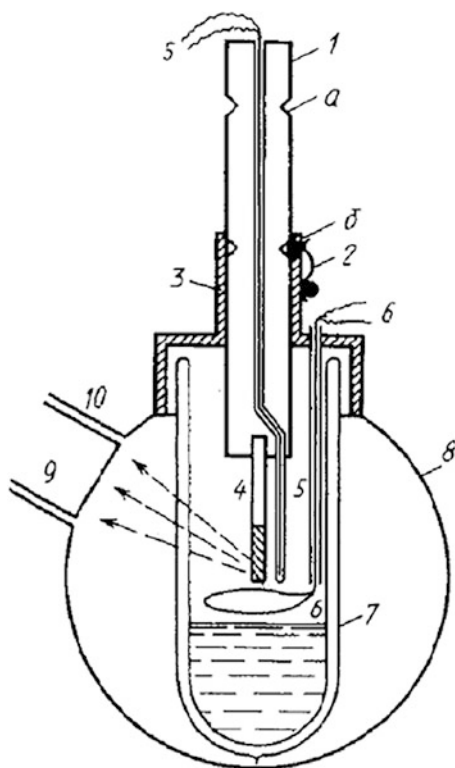


Fig. 3.19 Scheme of the device for measuring UPE at free-radical recombination at low temperatures. 1 – Movable rod; 2 – Spring fixing the rod in positions a or b when it moves in an opaque sleeve; 3; 4 – Sample with a solution frozen with liquid nitrogen (77 K) and irradiated at 77 K with ultraviolet rays; 5 – Thermocouple, controlling the temperature around the sample; 6 – Heater, with which liquid nitrogen can be partially evaporated, to increase the local temperature around the sample; 7 – Dewar vessel; 8 – Light-insulated sphere coated from the inside with a light-reflecting compound; 9 – Photocathode of a photomultiplier that measures the light emitted by the sample when it is heated (dashed arrows); 10 – Photomultiplier casing (not shown completely). (Reprinted from Vladimirov and Potapenko (1989), with permission from the authors)

became a complete sensation. It became clear that since there is a special enzyme (by the way, extremely widespread in all taxa), then superoxide, although it is a free radical, plays a large biological role.

The previously shown phagocyte respiratory burst (Sbarra and Karnovsky 1959; Baldrige and Gerard 1932) was soon connected to intense generation of reactive oxygen species (ROS): $O_2^- \cdot$ (Allen et al. 1972; Babior et al. 1973; Goldstein et al. 1975) and H_2O_2 (Iyer et al. 1961; Baehner et al. 1975), showing their first-discovered important role in the body – efficient and quick microbial killing.

Yet, this appeared to be far from their only role in the cell. ROS were shown to be enzymatically generated not only in phagocytes, but in plenty of other cell types (both immune and nonimmune), with no direct functions of bacterial killing. Moreover, the generated ROS were playing various and highly important regulatory roles (see Chap. 14). Nowadays

we know their irreplaceable role in respiration (Turrens 1997; Yankovskaya et al. 2003), immune system functioning (Panday et al. 2015), xanthine oxidase (George and Struthers 2009), and peroxidase (Cormier and Prichard 1968; Furtmuller et al. 2004; Vladimirov and Proskurnina 2009) reactions, in many of which free radicals are not only generated, but are included into the enzyme functioning cycle. As each of these free-radicals-operating enzymes deserves a special attention, we will discuss them more thoroughly in a special chapter (Chap. 14).

At the same time, free radicals are highly reactive and consequently quite dangerous compounds. Their decisive role in the emergence and development of many diseases has been revealed – those of brain, heart, kidneys, lungs, liver, blood, cancer, diabetes, disorders of the immune system and so on. Thick monographs with thousands of cited articles (Halliwell and Gutteridge 2015) and a number of highly rated specialized journals (“Free Radical Biology & Medicine,” “Free Radical Research,” “Redox Report: Communications in Free Radical Research,” “Free Radical Research Communications,” and others) have appeared. The ultraweak luminescence of biological systems, in addition to its own scientific significance, has acquired the role of a supersensitive method for observing free-radical processes directly in their course.

References

- Agaverdiyev AS, Tarusov BN (1965) Ultraweak chemiluminescence of wheat stems in dependence on temperature (In Russian). *Biofizika* 10 (2):351
- Ahnström G, Natarajan AT (1960) Chromosome Breakage induced by electrolytically produced Free Radicals. *Nature* 188 (4754): 961-962. doi:<https://doi.org/10.1038/188961a0>
- Aksentsev SL, Vladimirov YA, Olenev VI, Fesenko EE (1967) Study of the primary photoproducts of aromatic amino acids by the method of flash photolysis at 80 °K. *Biophysics* 12 (1):64-70
- Aksentzev SL, Vladimirov YA, Olenev VI (1966) Ionization of aromatic aminoacids under influence of ultraviolet radiation. In: Frish SE (ed) *Optika i spektroskopija* [Optics and Spectroscopy]. Academy of Sciences of the USSR, Leningrad, pp 57-64
- Allabutayev KA, Vasil'ev RF, Vichutinskiy AA, Rusina IF (1965) Chemiluminescence mechanism of oxidative reactions in solutions (In Russian). In: *Bioluminescencesiya. Trudy MOIP* [Bioluminescence. MOIP Reports], vol 21. Nauka, Moscow, pp 8-*
- Allen RC, Sjernholm RL, Steele RH (1972) Evidence for the generation of an electronic excitation state(s) in human polymorphonuclear leukocytes and its participation in bacterial activity. *Biochem Biophys Res Commun* 47:679-684
- Terenin A.N. (photo). From: <https://isaran.ru/?q=ru/person&guid=64A681C2-F526-3600-B100-E7EF1A7F25F7> <https://isaran.ru/?q=ru/person&guid=64A681C2-F526-3600-B100-E7EF1A7F25F7>. Accessed 6 Jan 2022
- Arthur WE, Strehler BL (1957) Studies on the primary process in photosynthesis. I. Photosynthetic luminescence; multiple reactants. *Arch Biochem Biophys* 70 (2):507-526. doi:[https://doi.org/10.1016/0003-9861\(57\)90140-6](https://doi.org/10.1016/0003-9861(57)90140-6)

- Audubert R (1938) Die Emission von Strahlung bei chemischen Reaktionen. *Angewandte Chemie* 51 (11):153–163. doi:<https://doi.org/10.1002/ange.19380511102>
- Audubert R (1939) Emission of ultra-violet rays by chemical reactions. *Transactions of the Faraday Society* 35 (213):197–206
- Babior BM, Kipnes RS, Curnutte JT (1973) Biological defense mechanisms. The production by leukocytes of superoxide, a potential bactericidal agent. *J Clin Invest* 52 (3):741–744. doi:<https://doi.org/10.1172/jci107236>
- Bach AN (1897). *Zhurnal Rossijskogo fiziko-khimicheskogo obshchestva [Journal of Russian Physico-chemical Society]* 29 (373)
- Baehner RL, Murrmann SK, Davis J, Johnston RB, Jr. (1975) The role of superoxide anion and hydrogen peroxide in phagocytosis-associated oxidative metabolic reactions. *J Clin Invest* 56 (3): 571–576. doi:<https://doi.org/10.1172/JCI108126>
- Baldrige CW, Gerard RW (1932) The extra respiration of phagocytosis. *American Journal of Physiology-Legacy Content* 103 (1): 235–236. doi:<https://doi.org/10.1152/ajplegacy.1932.103.1.235>
- Barth H (1934) Versuche zum physikalischen Nachweis von mitogenetischer Strahlung. *Archive of Biological Sciences Ser B* 35 (1):29–36
- Barth H (1936) Physikalische Versuche zum Problem der mitogenetischen Strahlung. *Biochemische Zeitschrift* 285:311–339
- Barth H (1937) Physical studies on the question of mitogenetic radiation problem (in Russian). *Archive of Biological Sciences* 46 (1):153–177
- Bequerel E (1867) *La lumière, ses causes et ses effets*. Firmin Didot frères, fils et cie, Paris
- Berezin IV, Denisov ET, Emanuel' NM (1966) Oxidation of Cyclohexane. Pergamon Press, Oxford
- Blyumenfel'd LA, Kalmanson EA (1957)? (In Russian). *Biofizika (Russ)* 2 (5):552–565
- Blyumenfel'd LA, Kalmanson EA (1958) Electron paramagnetic resonance spectra of biological objects. Effect of denaturation on the e.p.r. spectra of irradiated proteins. *Biophysics* 3 (1):81–85
- Boveris A, Cadenas E, Reiter R, Filipkowski M, Nakase Y, Chance B (1980) Organ chemiluminescence: noninvasive assay for oxidative radical reactions. *Proceedings of the National Academy of Sciences of the United States of America* 77 (1):347–351. doi:<https://doi.org/10.1073/pnas.77.1.347>
- Cadenas E, Boveris A, Chance B (1980a) Low-level chemiluminescence of bovine heart submitochondrial particles. *The Biochemical journal* 186 (3):659–667. doi:<https://doi.org/10.1042/bj1860659>
- Cadenas E, Boveris A, Chance B (1980b) Low-level chemiluminescence of hydroperoxide-supplemented cytochrome c. *The Biochemical journal* 187 (1):131–140. doi:<https://doi.org/10.1042/bj1870131>
- Colli L, Facchini U (1954) Light emission by germinating plants. *Il Nuovo Cimento* 12 (1):150–153. doi:<https://doi.org/10.1007/bf02820374>
- Colli L, Facchini U, Guidotti G, Lonati RD, Arsenigo M, Sommariva O (1955) Further measurements on the bioluminescence of the seedlings. *Experientia* 11 (12):479–481
- Cormier MJ, Prichard PM (1968) An investigation of the mechanism of the luminescent peroxidation of luminol by stopped flow techniques. *The Journal of biological chemistry* 243 (18):4706–4714
- Debye P, Edwards JO (1952) Long-Lifetime Phosphorescence and the Diffusion Process. *The Journal of chemical physics* 20 (2): 236–239. doi:<https://doi.org/10.1063/1.1700385>
- Debye P, Edwards John O (1952) A Note on the Phosphorescence of Proteins. *Science* 116 (3006):143–144. doi:<https://doi.org/10.1126/science.116.3006.143>
- Delorme R, Perrin F (1929) Durées de fluorescence des sels d'uranyle solides et de leurs solutions. *Journal de Physique et le Radium* 10 (5): 177–186. doi:<https://doi.org/10.1051/jphysrad:01929001005017700>
- Demchenko AP, Heldt J, Waluk J, Chou P-T, Sengupta PK, Brizhik L, del Valle JC (2014) Michael Kasha: von Photochemie und Blumen bis Spektroskopie und Musik. *Angewandte Chemie* 126 (52): 14542–14551. doi:<https://doi.org/10.1002/ange.201405222>
- Desai ID, Calvert CC, Scott ML (1964a). *Arch Biochem and Biophys* 108:60
- Desai ID, Sawant PL, Tappel AL (1964b). *Biochim et biophys acta* 86: 277
- Emanuel NM, Denisov YT, Mayzus ZK (1965) Tsepnyje reaktzii okislenija uglevodorodov v zhidkoj faze (In Russian) [Chain reactions of hydrocarbons in liquid phase]. *Nauka, Moscow*
- Entelis SG, Shlyapintokh VY, Karpukhin ON, Nesterov OV (1960) Chemiluminescence in reactions of acid chloranhydrides with amines and ketones (In Russian). *Zhurnal Fizicheskoi Khimii [Journal of Physical Chemistry]* 34 (7):651
- Bach A.N. (photo). From: https://commons.wikimedia.org/wiki/File:D0%90%D0%BB%D0%B5%D0%BA%D1%81%D0%B5%D0%B9_%D0%9D%D0%B8%D0%BA%D0%BE%D0%BB%D0%B0%D0%B5%D0%B2%D0%B8%D1%87_%D0%91%D0%B0%D1%85.jpg. Accessed April 28, 2023
- Frank G, Rodionow S (1931) Über den physikalischen Nachweis mitogenetischer Strahlung und die Intensität der Muskelstrahlung. *Die Naturwissenschaften* 19 (30):659–659. doi:<https://doi.org/10.1007/BF01516035>
- Frank G, Rodionow S (1932) Physikalische Untersuchung mitogenetischer Strahlung der Muskeln und einiger Oxydationsmodelle. *Biochemische Zeitschrift* 249 (4/6):323–343
- Frankenburger W (1933) Neuere Ansichten über das Wesen photochemischer Prozesse und ihre Beziehungen zu biologischen Vorgängen. *Strahlenther Onkol* 47 (2):233–262
- Furtmuller PG, Jantschko W, Zederbauer M, Jakopitsch C, Arnholt J, Obinger C (2004) Kinetics of interconversion of redox intermediates of lactoperoxidase, eosinophil peroxidase and myeloperoxidase. *Jpn J Infect Dis* 57 (5):S30–31
- George J, Struthers AD (2009) Role of urate, xanthine oxidase and the effects of allopurinol in vascular oxidative stress. *Vasc Health Risk Manag* 5 (1):265–272
- Glasser O, Barth H (1938) Studies on the problem of mitogenetic radiation. *Radiology* 30 (1):62–67. doi:<https://doi.org/10.1148/30.1.62>
- Goldstein IM, Roos D, Kaplan HB, Weissmann G (1975) Complement and immunoglobulins stimulate superoxide production by human leukocytes independently of phagocytosis. *J Clin Invest* 56 (5): 1155–1163. doi:<https://doi.org/10.1172/JCI108191>
- Gomberg M (1900) An instance of trivalent carbon: triphenylmethyl. *Journal of the American Chemical Society* 22 (11):757–771. doi: <https://doi.org/10.1021/ja02049a006>
- Gomberg M (1902) On trivalent carbon. *Journal of the American Chemical Society* 24 (7):597–628. doi:<https://doi.org/10.1021/ja02021a001>
- Grossweiner LI, Swenson GW, Zwicker EF (1963a) Photochemical generation of the hydrated electron. *Science* 141 (3583): 805–806. doi:<https://doi.org/10.1126/science.141.3583.805>
- Grossweiner LI, Zwicker EF, Swenson GW (1963b) Photochemical production of the solvated electron in ethanol. *Science* 141 (3586): 1180. doi:<https://doi.org/10.1126/science.141.3586.1180>
- Gurwitsch AG, Gurwitsch LD (1948) *Vvedeniye v ucheniye o mitogeneze (in Russian) [An introduction to the teaching of mitogenesis]*. USSR Academy of Medical Sciences Publishing House, Moscow
- Halliwell B, Gutteridge JMC (2015) *Free Radicals in Biology and Medicine*. 5rd edn. Oxford University Press,
- Harman D (1956) Aging: a theory based on free radical and radiation chemistry. *J Gerontol* 11 (3):298–300. doi:<https://doi.org/10.1093/geronj/11.3.298>
- Harman D (1957) Atherosclerosis: a hypothesis concerning the initiating steps in pathogenesis. *J Gerontol* 12 (2):199–202

- Harman D (2001) Aging: overview. *Annals of the New York Academy of Sciences* 928:1-21
- Harris L, Kaminsky J, Simard RG (1935) The Absorption Spectrum of Malachite Green Leucocyanide and the Mechanism of the Dark Reaction after Photolysis. *Journal of the American Chemical Society* 57 (7):1151-1154. doi:<https://doi.org/10.1021/ja01310a001>
- Harvey EN (1957) A history of luminescence from the earliest times until 1900. Philadelphia : American Philosophical Society, Philadelphia
- Hochstein P, Ernster L (1963) Adp-Activated Lipid Peroxidation Coupled to the Tpnh Oxidase System of Microsomes. *Biochem Biophys Res Commun* 12:388-394
- Hochstein P, Nordenbrand K, Ernster L (1964) Evidence for the involvement of iron in the ADP-activated peroxidation of lipids in microsomes and mitochondria. *Biochem Biophys Res Commun* 14:323-328
- Iams H, Salzberg B (1935) The Secondary Emission Phototube. *Proceedings of the Institute of Radio Engineers* 23 (1):55-64. doi:<https://doi.org/10.1109/JRPROC.1935.227243>
- Iyer GYN, Islam MF, Quastel JH (1961) Biochemical Aspects of Phagocytosis. *Nature* 192 (4802):535-541. doi:<https://doi.org/10.1038/192535a0>
- Jabłoński A (1935) Über den Mechanismus der Photolumineszenz von Farbstoffphosphoren. *Zeitschrift für Physik* 94 (1):38-46. doi:<https://doi.org/10.1007/BF01330795>
- Janzen EG, Blackburn BJ (1968) Detection and identification of short-lived free radicals by an electron spin resonance trapping technique. *J Am Chem Soc* 90 (1):5909-5910. doi:<https://doi.org/10.1021/ja01023a051>
- Kasha M (1947) Phosphorescence and the role of the triplet state in the electronic excitation of complex molecules. *Chemical reviews* 41 (2):401-419. doi:<https://doi.org/10.1021/cr60129a015>
- Korchagina MV, Vladimirov YA In: Simpozium "Svobodnoradikal'nyje sostoyaniya i ih rol' pri lucheovom porazhenii i zlokachestvennom roste" (Symposium "Free-radical states and their role in radiation injury and malignant growth". "5-8 January". M., 1971, crp. 49, 5-8 January 1971. p 49
- Krasnovsky (Jr) AA (2014) Phosphorescence of triplet chlorophylls. In: Kadish KM, Smith KM, Guillard R (eds) *Handbook of Porphyrin Science with Applications to Chemistry, Physics, Materials Science, Engineering, Biology and Medicine*, vol 33. World Scientific Publishing, Singapore, pp. 77-165
- Krasnovsky AA (1948) Reversible photochemical reduction of chlorophyll with ascorbic acid (in Russian). *Rep Acad Science USSR LX* (3):421-424
- Krasnovsky AA (1960) The reaction of reversible photochemical reduction of chlorophyll, its analogues and derivatives (in Russian). *Adv Chemistry XXIX* (6):736-759
- Krasnovsky AA, Litvin FF, Vladimirov Y, A. (1961) Application of photon counter for measurements of chlorofillum chemiluminescence in photobiologic reactions. V Intern biochem Congress, Abstracts II (sections 14-28):484-485
- Kreuchen KH, Bateman JB (1934) Physikalische und biologische Untersuchungen über mitogenetische Strahlung. *Protoplasma* 22 (1):243-273. doi:<https://doi.org/10.1007/bf01608868>
- Kubetsky LA (1930) Certificates No. 24040 and No. 45765. Application for Patent 74242.
- Kubetsky LA (1937) Multiple Amplifier. *Proceedings of the Institute of Radio Engineers* 25 (4):421-433. doi:<https://doi.org/10.1109/JRPROC.1937.229045>
- L'vova OF, Vladimirov YA (1966) Ultra-weak luminescence of mitochondria and its relation to biochemical processes (In Russian). Svobodnoradikal'nye protsessy v biologicheskikh sistemah Trudy MOIP [Free-Radical Processes in Biological Systems MOIP Reports] 16:214-217
- Blumenfeld L.A. (photo). From: <https://cityinfo.man/lev-aleksandrovich-blyumenfeld>. Accessed April 28, 2023
- Levshin VL (1935a). *Acta phys chim URSS* 2:221
- Levshin VL (1935b). *Acta phys chim URSS* 1:685
- Levshin VL (1936) Recherches sur la décroissance de la luminescence et le mécanisme d'émission de différentes substances. *Acta Phys Polonica* (5):301-317
- Levshin VL, Vinokurov (1934). *Physik Z Sowjetunion* 10:10
- Lewis GN, Calvin M (1945) Paramagnetism of the phosphorescent state. *Journal of the American Chemical Society* 67 (7):1232-1233. doi:<https://doi.org/10.1021/ja01223a513>
- Lewis GN, Kasha M (1944) Phosphorescence and the Triplet State. *Journal of the American Chemical Society* 66 (12):2100-2116. doi:<https://doi.org/10.1021/ja01240a030>
- Lewis GN, Kasha M (1945) Phosphorescence in Fluid Media and the Reverse Process of Singlet-Triplet Absorption. *Journal of the American Chemical Society* 67 (6):994-1003. doi:<https://doi.org/10.1021/ja01222a032>
- Lewis GN, Lipkin D (1942) Reversible Photochemical Processes in Rigid Media: The Dissociation of Organic Molecules into Radicals and Ions. *Journal of the American Chemical Society* 64 (12):2801-2808. doi:<https://doi.org/10.1021/ja01264a025>
- Lewis GN, Lipkin D, Magel TT (1941) Reversible Photochemical Processes in Rigid Media. A Study of the Phosphorescent State. *Journal of the American Chemical Society* 63 (11):3005-3018. doi:<https://doi.org/10.1021/ja01856a043>
- lhde AJ (1967) The History of Free Radicals and Moses Gomberg's Contributions. *Pure and Applied Chemistry* 15:1-13
- Litvin F.F. (photo). From: <http://letopis.msu.ru/peoples/4384>. Accessed April 28, 2023 2023
- Litvin FF, Vladimirov YA, Krasnovsky AA (1960) Chlorofillum chemiluminescence in photochemical reactions (In Russian). *Uspekhi fizicheskikh nauk [Advances in Physical Sciences]* 71(1):149-156
- Lorenz E (1934) Search for Mitogenetic Radiation by Means of the Photoelectric Method. *The Journal of general physiology* 17 (6):843-862. doi:<https://doi.org/10.1085/jgp.17.6.843>
- Jabłoński A. (photo). From: http://www.lumipedia.org/index.php?title=Jab%C5%82o%C5%84ski_Aleksander <https://isaran.ru/?q=ru/person&guid=64A681C2-F526-3600-B100-E7EF1A7F25F7>. Accessed 6 Jan 2022
- Marzoev AI, Roshchupkin DI, Vladimirov YA In: Simpozium "Svobodnoradikal'nyje sostoyaniya i ih rol' pri lucheovom porazhenii i zlokachestvennom roste" (Symposium "Free-radical states and their role in radiation injury and malignant growth", 5-8 January 1971. p 69
- Marzoev AI, Roshchupkin DI, Vladimirov YA (1973) Effect of UV light on biological membranes. II. Effect of irradiation on the chemiluminescence of mitochondria (In Russian). *Biofizika* 18 (2):258-263
- McCord JM, Fridovich I (1969a) Superoxide dismutase. An enzymic function for erythrocyte (hemocuprein). *The Journal of biological chemistry* 244 (22):6049-6055
- McCord JM, Fridovich I (1969b) The utility of superoxide dismutase in studying free radical reactions. I. Radicals generated by the interaction of sulfite, dimethyl sulfoxide, and oxygen. *The Journal of biological chemistry* 244 (22):6056-6063
- McCord JM, Fridovich I (1970) The utility of superoxide dismutase in studying free radical reactions. II. The mechanism of the mediation of cytochrome c reduction by a variety of electron carriers. *The Journal of biological chemistry* 245 (6):1374-1377
- Michaelis L (1935) Semiquinones, the Intermediate Steps of Reversible Organic Oxidation-Reduction. *Chemical reviews* 16 (2):243-286
- Michaelis L (1940) Occurrence and significance of semiquinone radicals. *Ann NY Acad Sci* 40:39

- Michaelis L, Hill ES (1933) Potentiometric studies on semiquinones. *Journal of the American Chemical Society* 55 (4):1481-1494
- Michaelis L, Schubert M, Granick S (1939) The free radicals of the type of Wurster's salts. *Journal of the American Chemical Society* 61 (8): 1981-1992
- Nernst WZ (1918). *Elektrochem* 24:335
- Nilsson R, Frøholm L, Gronowitz S, Hoffman RA, Nilsson L (1964) On the Mechanism of Peroxidase Catalyzed Oxidations Studied by Means of Chemiluminescence Measurements. *Acta Chemica Scandinavica* 18:389-401
- Osipov AN, Moravskii AP, Shuvalov VF, al. e (1980) Study of peroxide radical death kinetics in lipids (in Russian). *Biofizika (Russ)* 25 (2): 234–238
- Panday A, Sahoo MK, Osorio D, Batra S (2015) NADPH oxidases: an overview from structure to innate immunity-associated pathologies. *Cellular & Molecular Immunology* 12:5-23. doi:<https://doi.org/10.1038/cmi.2014.89>
- Paneth F, Hofeditz W (1929) Über die Darstellung von freiem Methyl. *Berichte der deutschen chemischen Gesellschaft (A and B Series)* 62 (5):1335-1347. doi:<https://doi.org/10.1002/cber.19290620537>
- Paneth FA (1934) The use of free methyl and ethyl in chemical synthesis. *Transactions of the Faraday Society* 30 (0):179-181. doi:<https://doi.org/10.1039/TF9343000179>
- Paneth FA, Lautsch W (1935) 83. Free organic radicals in the gaseous state. Part VI. Attempts to prepare various free radicals: the existence of free benzyl. *Journal of the Chemical Society (Resumed)* (0): 380–383. doi:<https://doi.org/10.1039/JR9350000380>
- Perrin F (1929). La fluorescence des solutions. *Ann Phys, Vol. 10, No 12*, 169–275
- Polivoda AI, Sekamova EN (1962) [Ultraweak luminescence (450–700 nm) of surviving and homogenized liver tissue in normal conditions and following the action of ionizing radiation] (in Russian). *Radiobiologiya* 2 (6):801-810
- Porter CW (1926) *The Carbon Compounds: A Textbook of Organic Chemistry*. Ginn
- Rajewsky B (1930) Eine neue Messanordnung für kleinste Lichtintensitäten. *Strahlenther Onkol* 39:194-200
- Rajewsky B (1931) Zur Frage des physikalischen Nachweises der Gurwitsch-Strahlung. In: Dessauer F (ed) *Zehn Jahre Forschung auf dem physikalisch-medizinischen Grenzgebiet*. Georg Thieme Verlag, Leipzig, pp 244-257
- Rajewsky B (1932) Zum Problem der mitogenetischen Strahlung. *Zeitschrift für Krebsforschung* 35 (1):387-394. doi:<https://doi.org/10.1007/bf01792230>
- Rice FO, Johnston WR, B.L. E (1932) The thermal decomposition of organic compounds from the standpoint of free radicals, II, Experimental evidence of decomposition of organic compounds into free radicals. *J Am Chem Soc* 54:3529
- Rodionov SF, Frank GM (1934) *Voprosy svetobiologii i izmereniya sveta. [Problems of Light Biology and Light Measurement]* (In Russian). Gostekhizdat, Moscow-Leningrad
- Roshchupkin DI, Marzoev AI, Vladimirov YA (1973) Effect of UV-radiation on biological membranes. I. Disruption of oxidative phosphorylation and changes in protein state during radiation of isolated mitochondria (In Russian). *Biofizika*, 18 (1):83-88
- Roshchupkin DI, Vladimirov YA (1965) Investigation of primary photochemical processes in proteins-II. Reactions in frozen solutions of aromatic amino acids and proteins at 77-200 °K. *Biophysics* 10 (1): 50-58
- Rozantsev EG (1970) *Svobodnyie iminoksil'nyie radikaly [Free iminoxil radicals]*. Khimiya, USSR
- Rozantsev EG, Sholle VD (1971) Advances in chemistry of nitroxil radicals (in Russian). *Uspekhi Khimii [Advances in Chemistry]* 40 (3):417–443
- Saprin AN, Piette LH (1977) Spin trapping and its application in the study of lipid peroxidation and free radical production with liver microsomes. *Archives of biochemistry and biophysics* 180 (2): 480-492. doi:[https://doi.org/10.1016/0003-9861\(77\)90063-7](https://doi.org/10.1016/0003-9861(77)90063-7)
- Sbarra AJ, Karnovsky ML (1959) The biochemical basis of phagocytosis. I. Metabolic changes during the ingestion of particles by polymorphonuclear leukocytes. *The Journal of biological chemistry* 234 (6):1355-1362
- Schischlowski AA, Wawilow SI (1934). *Physik Z Sowjetunion* (5):379-392
- Schmidt GC (1896). *Annal Physik* 58:103–130
- Seemann HJ (1930) Eilhard Wiedemann geb. 1. August 1852—gest. 7. Januar 1928. *Isis* 14 (1):166-186
- Semenov NN (1934) Chain reactions (In Russian). *Goskhimizdat, Moscow*
- Shliapintokh VY, Vassil'ev RF, Karpukhine ON, Postnikov LM, Kibalko LA (1960) La chimiluminescence de processus chimiques lents. *J Chim Phys* 57 (11–12):1113
- Siebert W (1934) Die "mitogenetische" Strahlung des Blutes. In: Hirschfeld H, Hittmair A (eds) *Handbuch der allgemeinen Hämatologie*, vol 2. Urban & Schwarzenberg, Berlin, Wien, p 1339
- Siebert WW, Seffert H (1933) Physikalischer Nachweis der Gurwitsch-Strahlung mit Hilfe eines Differenzverfahrens. *Naturwissenschaften* 21 (9):193-194. doi:<https://doi.org/10.1007/bf01504200>
- Stawińska D, Sławiński J (1987) Ultraweak photon emission in model reactions of the in vitro formation of eumelanins and pheomelanins. *Pigment cell research* 1 (3):171-175. doi:<https://doi.org/10.1111/j.1600-0749.1987.tb00409.x>
- Slepian J (1923) Hot Cathode Tube. United States Patent No US1450265A. Application filed April 18, 1919. Serial No. 291,158. <https://patents.google.com/patent/US1450265A/en>
- Stauff J (1964) Lumineszenz and Energieübertragung angeregter Zustände von Proteinen. *Ber Bunsenges phys chem* 68 (8–9):773
- Stauff J, Reske G (1964) Lumineszenz von Hefe. *Naturwissenschaften* 51 (2):39
- Stauff J, Rümmler G (1962) Chemilumineszenz von Oxydationsreaktionen. II. Die Spektren der Reaktionen Harnstoff + Hypohalgenit, Formaldehyd + H₂O₂ und NaOH + H₂SO₄ + O₂. —, 34, N 1–4, 67, 1962. *Z Physikal Chemie (BRD)* 34 (1–4):67
- Stauff J, Schmidkunz H (1962a) Chemilumineszenz von Oxydationsreaktionen. I. Qualitative Beobachtungen und Analyse der Reaktion Harnstoff + Na-Hypochlorit. *Z Physikal Chemie (BRD)* 33 (5/6):273
- Stauff J, Schmidkunz H (1962b) Chemilumineszenz von Oxydationsreaktionen. III. Mitt. Sauerstoff-van der waals-Assoziat als möglicher Träger der Chemilumineszenz. *Z Physikal Chemie (BRD)* 35 (4–6):295
- Stauff J, Schmidkunz H, Hartmann G (1963) Chemiluminescence in oxidation reactions. *Nature* 198:281
- Stauff J, Wolf H (1964) Konformationsabhängige Phosphoreszenz und Chemilumineszenz einiger Proteine. *Z Naturforsch* 19b (2):87
- Strehler BL (1951) The luminescence of isolated chloroplasts. *Archives of biochemistry and biophysics* 34 (2):239-248
- Strehler BL, Arnold W (1951) Light production by green plants. *The Journal of general physiology* 34 (6):809-820
- Strehler BL, Shoup CS (1953) The chemiluminescence of riboflavin. *Archives of biochemistry and biophysics* 47 (1):8
- Suslova TB, Olenev VI, Korchagina MV, Vladimirov YA (1970) Chemiluminescence connected with the formation of lipid peroxides in biological membranes. IV. Role of the change of iron valency in these processes (In Russian). *Biofizika*, 15 (4):622-628
- Suslova TB, Olenev VI, Vladimirov Iu A (1969) [Chemiluminescence accompanied by the formation of lipid peroxides in biological membranes. I. Luminescence of mitochondria in the presence of Fe²⁺]. *Biofizika*, 14 (3):510-516
- Tappel AL (1965). *Federat Proc* 24:73
- Tappel AL, Sawant PL (1963). In: *Ciba Found. Sympos. on Lysosomes*. Churchill Ltd., London, p 78

- Tarusov BN (1954) Fundamentals of biological effects of radioactive radiation. Medgiz, Moscow
- Tarusov BN (1957). Uspekhi Sovremennoi Biologii (in Russian) [Advances in Contemporary Biology] 44:173
- Tarusov BN, Polivoda AI, Zhuravlev AI (1961a) Detection of chemiluminescence in the liver of irradiated mice (In Russian). Radiobiologiya 1 (1):150-151
- Tarusov BN, Polivoda AI, Zhuravlev AI (1961b) Study on ultra-weak spontaneous luminescence of animal cells (in Russian). Biofizika (Russ) 6 (4):490-492
- Tarusov BN, Polivoda AI, Zhuravlev AI, Sekamova EN (1962) Ultraweak spontaneous luminescence in animal tissue (in Russian). Tsitologiya 4:696-699
- Tarusov BN, Zhuravlev AI (1965) Biochemiluminescence of lipids (In Russian). In: Bioluminescentsiya. Trudy MOIP [Bioluminescence. MOIP Reports], vol 21. Nauka, Moscow, p 125
- Terenin AN (1943) Photochemical processes in aromatic compounds (in Russian). Acta Physicochim USSR 8 (1):210-241
- Terenin AN (1947) Fotokhimiya krasiteley i rodstvennykh organicheskikh soyedineniy [Photochemistry of Dyes and Related Organic Compounds] (In Russian), Gostekhizdat, Moscow-Leningrad
- This Month in Physics History. December 18, 1926: Gilbert Lewis coins "photon" in letter to Nature (2012). APS News 21 (11)
- Tiede E (1920) Phosphoreszenz der Borsäure. (III. Mitteilung zur Kenntnis anorganischer Lumineszenz-Erscheinungen.). European Journal of Inorganic Chemistry 53 (11):2214-2216
- Tiede E, Wulff P (1922) Bortrioxyd-Hydrate als Bestandteil hochphosphoreszenz-fähiger, organische Verbindungen enthaltender Systeme. Berichte der deutschen chemischen Gesellschaft (A and B Series) 55 (2):588-597. doi:<https://doi.org/10.1002/cber.19220550239>
- Turrens JF (1997) Superoxide production by the mitochondrial respiratory chain. Biosci Rep 17 (1):3-8
- Valeur B, Berberan-Santos MN (2011) A Brief History of Fluorescence and Phosphorescence before the Emergence of Quantum Theory. Journal of Chemical Education 88 (6):731-738. doi:<https://doi.org/10.1021/ed100182h>
- Vasil'ev RF (1965a) Chemiluminescence in solutions I. Methods of identification of excited states (In Russian). Opt Spektrosk+ 18 (2): 236-244
- Vasil'ev RF (1965b) Chemiluminescence in solutions II. Identification of the excited state in reactions of liquid-phase oxidation (In Russian). Opt Spektrosk+ 18 (3):415
- Vasil'ev RF (1965c) Photoelectric apparatus for investigating weak luminescence (In Russian). In: Bioluminescentsiya. Trudy MOIP [Bioluminescence. MOIP Reports], vol 21. Nauka, Moscow, p 170
- Vasil'ev RF (1965d) Some problems in the mechanism of chemiluminescence. (In Russian). In: Bioluminescentsiya. Trudy MOIP [Bioluminescence. MOIP Reports], vol 21. Nauka, Moscow, p 198
- Vasil'ev RF, Karpukhin ON, Shlyapintokh VY (1961) An apparatus for measuring weak light fluxes (In Russian). Zhurnal Fizicheskoy Khimii [Journal of Physical Chemistry] 35 (2):461
- Vasil'ev RF, Vichutinskii AA (1962a) The enhancement of chemiluminescence by the addition of luminescent substances (In Russian). Zh Fiz Khim 36 (8):1799-1800
- Vasil'yev RF (1963) Spin-orbit coupling and intermolecular energy transfer. Nature 200 (4908):773
- Vasil'ev RF (1963) Lyuminestsentsiya pri khimicheskikh reaktsiyakh v rastvorakh (In Russian)[Luminescence Accompanying Chemical Reactions in Solutions]: Doctoral Dissertation. Moscow
- Vasil'ev RF, Rusina IF (1964a) The chemiluminescence mechanism for the oxidation of organic matter in solution (In Russian). Doklady AN SSSR 156 (6):1402-1405
- Vasil'ev RF, Rusina IF (1964b) The chemiluminescence of molecular oxygen during the oxidation of organic matter (In Russian). Izv AN SSSR, Seriya Khim 9:1728
- Vasil'ev RF, Vichutinskii AA (1962b) The chemiluminescent method of measuring the relations of elementary constants in liquid hydrocarbon oxidation reactions (In Russian). Doklady AN SSSR 145 (6): 1301
- Vasil'ev RF, Vichutinskiy AA, Cherkasov AS (1963) Chemiluminescence activated by anthracene derivatives. Doklady AN SSSR 149 (1):124
- Vasil'ev RF (1962) Secondary processes in chemiluminescent solutions. Nature 196 (4855):668
- Vasil'ev RF, Karpuchin ON, Shlapintoch VJ (1959) Chemiluminescence accompanying reactions of thermal decomposition (In Russian). Doklady AN SSSR 125 (1):106
- Vasil'ev RF, Vichutinskiy AA (1962) The nature of the relationship between chemiluminescence and oxidation by molecular oxygen (In Russian). Doklady AN SSSR 142 (3):615
- Vladimirov Y, A., Suslova TB, Olenev VIC, Z.P. (1968) Dependence of processes of lipidic peroxide formation in membranes of mitochondria from the state of nonheme iron. In: Sergeev PV (ed) Structure and function of biological membranes. Pirogov Medical State Institute, Moscow, pp 15-16
- Vladimirov YA (1965) Fotokhimiya i lyuminescentsiya belkov [Photochemistry and luminescence of proteins] (In Russian). Nauka, Moscow
- Vladimirov YA (1996) Intrinsic (low-level) chemiluminescence. In: Punchard NAaK, F.J. (ed) Free radicals. A practical approach. Oxford University Press, Oxford, New York, Tokyo, pp 65-82
- Vladimirov YA, Ai-Ke H, Roshchupkin DI (1966) Investigation of the primary photochemical processes in proteins-IV. Luminescence spectra of primary and end photo products of aromatic amino acids and proteins. Biophysics 11 (2):268-276
- Vladimirov YA, L'vova OF (1964) Ultraweak luminescence and oxidative phosphorylation in mitochondria (In Russian). Biofizika (Russ) 9 (4):506-507
- Vladimirov YA, L'vova OF (1965) Study of ultraweak luminescence of homogenates and liver pulp (In Russian). In: Frank GM (ed) Biofizika kletki [Biophysics of the Cell]. Nauka, Moscow, pp 74-83
- Vladimirov YA, Litvin FF (1959) Investigation of very weak luminescence in biological systems. Biophysics 4 (5):103-109
- Vladimirov YA, Litvin FF (1960) Long-lived phosphorescence of aromatic amino-acids and proteins at low temperatures. Biophysics 5 (2):151-159
- Vladimirov YA, Litvin FF (1964) Fotobiologiya i spektral'nyye metody issledovaniya. Praktikum po obshchey biofizike. [Photobiology and Spectral Research Methods. Workbook on General Biophysics] (In Russian). vol 8. Vysshaya shkola, Moscow
- Vladimirov YA, Litvin FF, Man-ch'i T (1962) The role of excited states and the nature of ultraweak luminescence in biological systems. Biofizika+ 7 (6):675-682
- Vladimirov YA, Potapenko AY (1989) Fiziko-khimicheskije osnovy fotobiologicheskikh protsessov [Physico-chemical basis of photobiological processes]. Vysshaya shkola, M
- Vladimirov YA, Proskurnina EV (2009). Uspekhi Biologicheskoy Khimii [Advances in Biological Chemistry] 49:341-388
- Vladimirov YA, Roshchupkin DI (1962) Study of luminescence and primary photochemical reactions in proteins (In Russian). Paper presented at the XI soveshchaniye po lyuminestsentsii. Tezisy dokladov [Eleventh Conference on Luminescence. Summaries of Reports], Moscow,
- Vladimirov YA, Roshchupkin DI (1964) Study of primary photochemical processes in proteins 1. Two photochemical reactions in aromatic amino acids. Biophysics 9 (3):305-316

- Vladimirov YA, Roshchupkin DI, Fesenko EE (1970a) Mechanism of ultraviolet radiation effects on proteins (In Russian). *Biofizika* 15 (2):254-264
- Vladimirov YA, Roshchupkin DI, Fesenko EE (1970b) Photochemical reactions in amino acid residues and inactivation of enzymes during U.V.-irradiation. A review. *Photochem Photobiol* 11 (4):227-246
- Vladimirov YA, Sherstnev MP (1991) Biophysical chemiluminescent analysis. In: Lopukhin YM (ed) *Soviet Medical Reviews/Section B. Physicochemical Aspects of Medicine. Vol.2, Part 5.* Harwood Academic Publishers GmbH, London, pp 1–43
- Vladimirov YA, Suslova TB, Olenev VI (1969a) Chemiluminescence associated with the formation of lipid peroxides in biological membranes. II. The role of Fe²⁺ in the development of chain oxidation of lipids and of ultra-weak luminescence (In Russian). *Biofizika* 14 (5):836-845
- Vladimirov YA, Suslova TB, Olenev VI, Cheremisina ZP (1969b). In: *Mitochondrii, Biokhimicheskiye funktsii v sisteme kletochnyh organell [Mitochondria. Biochemical functions in the system of cell organelles]*. Nauka, Moscow, p 203
- Von Richter V, Anschuetz R, Schroeter G, Meerwein H, Smith EF, Spielmann PE, d'Albe EEF (1915) *Organic Chemistry; or, Chemistry of the Carbon Compounds.* P. Blakiston's Son & Company,
- Warburg OH (1948) *Schwermetalle als Wirkungsgruppen von Fermenten.* Werner Saenger, Berlin
- Wawilow SJ, Lewschin WL (1926). *Z Phys* 35:920-936
- Wiedemann E (1888) Ueber Fluoreszenz und Phosphoreszenz I. Abhandlung. *Annalen der Physik* 270 (7):446-463. doi:<https://doi.org/10.1002/andp.18882700703>
- Perrin F. (Photo). From: [https://de.wikipedia.org/wiki/Francis_Perrin_\(Physiker\)](https://de.wikipedia.org/wiki/Francis_Perrin_(Physiker)). Accessed 6 Jan 2022
- Gomberg M. (photo). From: https://en.wikipedia.org/wiki/Moses_Gomberg. Accessed 6 Jan 2022
- Yankovskaya V, Horsefield R, Tornroth S, Luna-Chavez C, Miyoshi H, Leger C, Byrne B, Cecchini G, Iwata S (2003) Architecture of succinate dehydrogenase and reactive oxygen species generation. *Science* 299 (5607):700-704. doi:<https://doi.org/10.1126/science.1079605>
- Zakharov IV, Shlyapintokh VY (1961) Chemiluminescence in the diphenylethane hydroperoxide decay reaction and its relationship to the kinetics of the process (In Russian). *Kinetika i Kataliz [Kinetics and Catalysis]* 2 (2):165
- Zhuravlev AI (1960) The role of antioxidants in primary radiobiological effects (In Russian). In: *Trudy simpoziuma "Rol' perekisey i kisloroda v nachal'nykh stadiyakh radiobiologicheskogo effekta" ["Transactions of the Symposium "The Role of Peroxides and Oxygen in the Initial Stages of the Radiobiological Effect"]*. AN SSSR Publishing House, Moscow, p 55
- Zhuravlev AI (1962a) Determination of free radicals in fats. *Zh Prikl Khim* 35 (5):1153
- Zhuravlev AI (1962b) Ultraweak chemiluminescence of antibiotics in lipids (In Russian). *Antibiotiki* 7 (11):1023
- Zhuravlev AI (1963) Lipid model of radiation injury and radioprotective prevention. In: *Primary mechanisms of biological effects of ionizing radiations*, vol 7. Acad.Sc. USSR, Moscow, pp 93–101
- Zhuravlev AI (1965a) An anomaly of lipid chemiluminescence (In Russian). In: *Bioluminescentsiya Trudy MOIP [Bioluminescence. MOIP Reports]*, vol 21. Nauka, Moscow, p 133
- Zhuravlev AI (1965b) Problems on bioluminescence (In Russian). In: *Bioluminescentsiya Trudy MOIP [Bioluminescence. MOIP Reports]*, vol 21. Nauka, Moscow, p 184
- Zhuravlev AI, Filippov YN (1965) Chemiluminescence and antioxidative properties of human lipids (In Russian). In: *Bioluminescentsiya Trudy MOIP [Bioluminescence. MOIP Reports]*, vol 21. Nauka, Moscow, p 75
- Zhuravlev AI, Filippov YN, Simonov VV (1964) Chemiluminescence and antioxidation properties of human lipids (In Russian). *Biofizika*, 9 (6):671
- Zhuravlev AI, Korzhenko VS (1963) Chemiluminescence of lipids and growth rate of Oriental salmon. *Doklady AN SSSR [Rep Acad Science USSR]* 152 (2):457
- Zhuravlev AI, Polivoda AI, Tarusov BN (1961) The mechanism of inactivation of radicals and peroxides by natural tissue antioxidants. *Radiobiologiya* 1 (3):321
- Zhuravlev AI, Veselovsky VA, Koshcheyenko NN (1965) Bioluminescence. In: *Bioluminescentsiya. Trudy MOIP [Bioluminescence. MOIP Reports]*, vol 21. Nauka, Moscow, p 19



Biophotons and the International Institute of Biophysics (IIB)

4

Roeland van Wijk and Eduard van Wijk

4.1 Formation of the Form

To illustrate the global history, we should travel through 200 years of biology focusing on “Formation of the Form” unfolding itself from anatomy and physiology to the discovery of the cell and back to embryology. This ultimately led to the discovery of mitogenetic radiation. Subsequently, the latest century presents in four major parts representing progress in the understanding of “universal biological light” as it unfolded during alternating periods of active and inactive research within the interconnected disciplines of biology, chemistry, and physics. It paralleled the second part of the journey that began in the early 1900s vis-à-vis a better understanding of a biological organism as a system. This perspective accepted a field of organization with properties specific to the totality of the form, not solely about the particles that make up the form. In searching for a nonmechanical/nonparticle regulatory principle, an alternative principle developed: a morphogenetic field based on radiation. Although this part of the journey offers many fascinating scientific explorations, it took a long time and many developments in physics before biology definitively and internationally, in the 1970s, accepted the existence of universal ultraweak biological radiation. At that time, one could finally begin to document the richness of information from measurements of biological photon emission. The new photovoltaic and multiplier technologies connected photon emission with the biochemistry of oxygen and oxygen reactive species. The role of reactive oxygen species (ROS) became known during this part of the journey. With the advent of modern technology and increasing knowledge of the relationship between mitochondrial functioning and glycolysis, cancer might be interpreted as a mitochondrial dysfunction. Although the link between photon emission as part of the reactive oxygen dependent processes and tumor development

was more firmly established, the question whether photon emission is able to regulate the mitotic process required an additional concept: the specific properties of an electromagnetic field. At that time, it was not part of molecular cell biology. We must now include another interface between biology and physics. However, during this part of the journey, the original interest in the informational content of biophotons related to “form” was perhaps forgotten, or at least it was no longer obvious, or when present, only an issue of minor importance.

However, from the 1930s on, it became evident that biological systems can emit electromagnetic waves and can also have sensitive physiologic responses to the entire spectral range. The organism embodies diverse interconnections of electromagnetic fields (in addition to the known diverse biochemical connections). Research data suggested that the “optical photon emission window” may, then, offer a view of the electromagnetic interaction field with the way a body develops and keeps its “shape” within the ceaseless shifting metabolism of material. It was this journey at the end of the 1970s that suggested the possibility of integrating all previous scientific hypotheses resulting in the revival of the photon field concept.

The role of the photon field in metabolic and cell biological regulation was considered, bringing expertise simultaneously from biology, chemistry, and physics. The idea emerged that a biological system not only has the property of emission but also the capacity to store (or trap) photons. The trapping, as a photochemical process, may influence metabolic events. It resulted in a cell resonance cancer theory. Data supported the fact that tumor cells with a lower degree of differentiation have a high-short storage and a low-long-term resonance system capacity. In biophysics, field/matter interaction studies focused on protein and DNA levels as well as on the process of differentiation. The cancer problem marks the beginning of the International Institute of Biophysics (IIB).

R. van Wijk · E. van Wijk (✉)
Meluna Research, Wageningen, The Netherlands
e-mail: evanwijk@melunaresearch.nl

The “optical window” provides a key to understanding the organization of living systems. It creates a challenge to collaborate on the theme of photon emission from animal and human systems linking it to metabolism in health and disease. Since the late 1990s, such collaboration has resulted in novel techniques that can both estimate the human body emission pattern as well as novel procedures to analyze the language of human light. Present developments focus on the relationship to life style, health, and disease.

4.2 Revival of the Photon Field Concept: Toward an Integration of Sciences

4.2.1 Linking the Photon Field to Biochemistry

Since Presman published his pioneer work entitled *Electromagnetic Fields and Life* (1970), it became more and more evident that biological systems can emit electromagnetic waves and also provide sensitive responses throughout the whole spectral range from the extremely slow fluctuations (with frequencies of the order of a few Hertz and below) up to the extremely short waves in the UV region (and even possibly above). A variety of experimental facts (documented over almost two decades) hinted at the existence of “biological resonances” that can give rise to sensitive reactions in biological systems under the influence of electromagnetic waves. It seemed that nature used such waves for regulatory processes, or more generally, for communication within living systems. It became evident that research on “electromagnetic fields and life” and “photon emission in living systems” calls for the collaboration of at least three sciences: mathematics (cybernetics and information theory) in regard to the term “communication,” physics referring to “electromagnetic fields” and biology (biochemistry, quantum chemistry) with reference to “biological systems.” This collaboration should then be considered as a composite field dealing with all of these phenomena and should be entitled, “Electromagnetic Bio-Information.” At least, this was the opinion of Fritz-Albert Popp who invited scientists (mostly German of diverse disciplines: biologists, biochemists, physicians, and physicists familiar with these problems) to meet in Marburg, Germany. The conference, entitled “Electromagnetic Bio-Information” took place on September 5, 1977. It was the first conference dealing in a multidisciplinary way with this subject.

At the conference, the topic of ultraweak photon emission was intensively discussed. In particular, Popp promoted extending the concept of photon emission within the realms of cell communication and regulation (by referring to the possibility that chemical substances may influence cellular processes by interfering with a cell’s electromagnetic field). Popp’s major scientific interest was to study the chemical

induction of carcinogenesis. Data had already documented both that cancer cells were intense radiation sources and proliferating cell cultures radiate more intensely than do those wherein growth has ceased. Such data corresponded to Popp’s hypothesis (formulated in the mid-1970s) regarding photon storage of coherent modes within biological systems as well as a role of photon fields in growth regulation (particularly in carcinogenesis). His interest was mainly theoretical.

4.2.2 Linking Biochemiluminescence with Biophotochemical Reactions

Another field of interest was the existence of (at that time) a new type of coupled reactions in biology: simultaneous occurrence of a biochemiluminescence reaction and a biophotochemical reaction. A large body of theoretical as well as experimental arguments converged on these new types of coupled reactions in biology. These new types of coupled reactions corresponded to the concept of “photobiochemistry without light” (already having been labeled for a few years based on the major work of Cilento in the early 1970s). Those studies bridged the gap between modern (in system terminology such as synergy, coherence, etc.) molecular aspects and the localized biochemical view point. His work demonstrated that in biological systems, excited molecules can transfer their excitation energy to other biomolecules and thereby trigger amplification mechanisms and/or promote photochemical processes in the dark.

It was becoming more and more clear that living organisms are endowed with extremely complex, efficient, and indeed very ingenious devices for transforming and transmitting energy. They all are part of a continuous energy flow. In the course of this energy flow, numerous articulated chemical reactions of diverse types take place. It was known that thermodynamically endergonic reactions may occur simultaneously with exergonic reactions in the metabolic process. All of such ideas have a great heuristic value and open new horizons in the holistic interpretation of biological electromagnetic radiations. They support a possible triggering and regulating role of photons in biochemical activity.

All of the above led Popp to postulate that biological systems generally have the capacity to coherently store photons which come from the external world. It required the development of special equipment in combination with the photomultiplier tube to prove his ideas. The equipment would need to facilitate the exposure of a biological system to a (light) radiation source. This may lead to a storage of photons in the system, which, after exposure, start to emit. The emission depends on the capacity of photon storage. Such storage capacity could be derived from the decay

constant of the emission process. Popp's subsequent hypothesis emphasized that the emission of such biophotons is qualitatively and quantitatively linked to a changing metabolic state later.

4.2.3 Photons and Information

Photon signals as such are not inconsistent with communication. Real communication, however, is only possible when the receptor cell is able to process signals. There are indications that this is indeed true. The most widely known examples of photon effects on physiological processes are photosynthesis and the vision process. Moreover, enzymatic processes that are not connected with photosynthesis (as well as the vision processes) are also influenced by photons. At that time, it was already documented in the literature that photons could cause a change in the conformation of proteins. Since the biochemical activity of a protein is correlated with its conformation, it was not difficult to understand why photons influence or even regulate biochemical processes in enzymes. As to other reactions of live cells (when exogenously stimulated by light), the influence by those stimuli upon cell biological processes seem to be based on complicated mechanisms.

Most important, discussion began at the 1977 Conference about the regulatory role of photons, thereby indirectly stimulating a revival of interest in the Gurwitsch concept. The search for evidence of the "informational character" of ultraweak photon emission in biological systems reappeared. How did this develop in the following decade?

4.3 Internationalization of the New (Informational) Photon Field Research

4.3.1 Beginning: The First Symposium

It is the year 1985. Experimental activities in physics, biology, and chemistry (regarding photon emission) developed during the last decade in many places of the world. Looking at the utilization of interdisciplinary communication, one cannot deny that it was indispensable in order to understand the complex problem of electromagnetic radiation in biosystems. Simultaneously, it still was very difficult, since a satisfactory comprehensive model of the phenomenon was still lacking and the mutual sharing of information between the Eastern and Western European scientific worlds continued to be absent. For the latter reason, several Polish researchers, in cooperation with the Polish Academy of Science, began to organize the First International Symposium on Photon Emission from Biological Systems. It was held in Wroclaw, January 24–26, 1986.

Many researchers were not willing to consider the aspect of informational potential of emitted radiation. The status of that research seemed only at the beginning stage. Two levels reflecting the research at that time were clearly based on a dichotomy of the conceptual approach to photon emissions: (1) the biochemical level, claiming that biological luminescence is an adventitious emission associated with exergonic oxidation reactions and has no function in the energetics of biochemistry or regulation, and (2) the biophysical level, assigning informative and regulative roles to the electromagnetic field within living organisms and interpreting the phenomenon in terms of nonlinear thermodynamics and optics.

Janusz Slawinski symbolized the status of photon emission research as an iceberg. So far, one could not take into account all possible interactions of electronically excited states and photons within the components of a very complex biological system and medium. We still have a long way to go to develop our knowledge about cooperative, weak molecular interactions: (1) how they contribute to the generation of excited states and photons and (2) how they result from the action of endogenous electromagnetic fields. Such limitations are also due to our lack of knowledge about cybernetic models which eventually might describe couplings, feedbacks, and account for the changes of the photon field within very dense, heterogeneous media (i.e., in cells). Therefore, today's status of this research is truly not more than the tip of an iceberg. The submerged portion represents the hidden part of the photon field and its properties. Ultimately, the conviction evolved to the interdisciplinary communication between physics, biology, and chemistry of photon emission that it was indispensable to finally understand the complexity of electromagnetic radiation in biosystems.

4.3.2 Collective Works: *Experientia*

The opportunity for such interdisciplinary communication was then further extended via an initiative of *Experientia*, an interdisciplinary journal for life sciences (in 1997 renamed, *Cellular and Molecular Life Sciences*). The editors of that journal, recognizing the developments (internationally) within that research arena regarding ultraweak photon emission from living organisms, asked Popp (1987) to coordinate a multiauthor review about Biophoton Emission. The review appeared July 15, 1988. Major subjects included (1) low-level luminescence as a new discipline in photobiochemistry and consequently, the reactions and biochemical source(s) responsible for this phenomenon (J. Slawinski); (2) photobiochemistry without light radiation from (and within) biological matter, long-range interactions and energy dissipation (G. Cilento); (3) coherent transfer of photon energy and its origin from a coherent electromagnetic field (F. A. Popp and K. H. Li and others); (4) the

experimental findings of correlations between photon emission and biological functions (R. Van Wijk, D. H. J. Schamhart, and W. B. Chwirot); (5) technological aspects (H. Inaba); and (6) the relationship between photon emission and models as originally proposed by A. G. Gurwitsch (A. A. Gurwitsch).

Meanwhile, the same organizers of the First International Symposium took the initiative to organize a second international meeting entitled "The International School on Biological Luminescence." It was held from June 20 to June 23, 1989, Wroclaw. The objective was to bring together more scientists from all of the interdisciplinary fields leading to many additional overviews of bioluminescence and photon emission. It considerably broadened the joint research within the fields of physics, chemistry, biology, biocybernetics, and medicine.

Since the second Polish meeting included many applications in medicine, a second multiauthor review in *Experientia* was organized around several medical issues. Van Wijk coordinated the review entitled "Biophoton Emission, Stress and Disease." It was published December 1, 1992. It focused on stress-perturbed systems, within bacteria to man, including disease states. Perturbations of the organisms were initiated by mechanical, temperature, oxidative, chemical, and photochemical stress. In most instances, a perturbation of homeostasis gave rise to an increase in photon emission. The biological stressors included chemical, physical, emotional (psychological), and infections that cause an increase in endogenous free-radical production. The stress related photon emission was reviewed for bacterial and low eukaryotic systems (R. N. Tilbury) and higher eukaryotic systems (J. Slawinski). Photon emission in relationship to stress and disease was reviewed by E. M. Lilius and P. Marnilla. Van Wijk and Van Aken reviewed photon emission in the field of tumor biology. The more fundamental basis of the photonic response from stress-perturbed biosystems was presented by Popp utilizing his feedback model coupling radiationless chemical pumping of energy (from the cytoplasmic metabolism in DNA) with the DNA conformation dependent regulation of the metabolic activity of a cell (thus closing the feedback loop).

4.3.3 Conclusion

The growing research activities and international collaboration between scientists of different disciplines during the period 1977–1992 (plus the conferences and multiauthor reviews in this period) can be seen as the beginning to discern the richness of information which can be retrieved from measurements of photon emission.

4.4 The Photon Energy Storage Concept

4.4.1 Photon Storage in Tumor Biology

In 1976, Cilento postulated the existence of a new type of coupled reaction in biology related to light excitation. The postulate was based on simultaneous occurrence of biochemiluminescence and biophotochemical reactions as well as the occurrence of excited electronic states in dark biological processes (photobiochemistry without light). It eventually became clear that living organisms are, indeed, endowed with ingenious and efficient devices for transforming and transmitting energy. Since it is known that different states of organization also exist within tumors, it implies that they also function not only with shifts in energy flow patterns but also in the coupling of biochemiluminescence and biophotochemical reactions.

Effective intracellular photon trapping is expected to influence metabolic and cellular events. It has been hypothesized that the actual number of photons trapped (i.e., the efficacy of photon trapping) also actually continues to change within the process of carcinogenesis. In order to experimentally study these ideas, it was suggested to fill the photon stores by artificially illuminating the cells. If photons are actually trapped, the properties of the trapping mechanism(s) are reflected during delayed emission. Precise analysis of post irradiation photon emission should demonstrate photon storage characteristics of a biological system.

Testing the hypothesis required the development of special equipment. The important technique for estimating light-induced delayed emission was the double shutter system in combination with a sensitive photomultiplier tube. In Popp's laboratory, such equipment was initially constructed by Ruth. After excitation, a shutter imposed between a light source and sample is rapidly closed, while, a second shutter between sample and the photomultiplier tube is almost immediately opened and the recording of delayed photon emission begins.

To study the photon trapping in tumor development, an experimental model (including cell lines from the same tissue, but with different degrees of differentiation) must be available.

The experimental cell model was established in the early 1970s by Van Wijk and colleagues. It included four hepatoma cell lines commonly named H35, HTC, MH1C1, and RLC. On the basis of their degree of differentiation systematically evaluated both at the level of cell morphology and functioning (ultrastructure of the cytoplasm, mitochondrial volume and structure, glycolytic and gluconeogenic functions, enzyme activities, growth and division potential, and sensitivity for hormones) the series of rat hepatoma cell lines definitively illustrated the "Molecular Correlation Con-

cept” at the level of cells *in vitro*. The liver characteristics partially persisted in a coordinated manner in the well differentiated hepatoma cells H35 and MH1C1. Whereas in the poorly differentiated cell lines, HTC and RLC, the differentiation characteristics were lost.

4.4.2 Degree of Differentiation and Photon Storage Capacity

This cell model system regarding loss of differentiation in tumor development was utilized to study the relationship between the state of differentiation and the photon storage capacity. This comparative study focused on three types of cells from fully differentiated (liver cells) to very poorly differentiated cells (HTC hepatoma cells) with the well differentiated H35 cells as an example of an intermediate state. In 1983, a long-term cooperation of the research groups of Popp (Kaiserslautern, Germany) and Van Wijk (Utrecht, Netherlands) began. The light-induced photon emission reflecting the photon storage capacity was studied after preilluminating the cells with visible light. The studies focused on (1) total number of photons emitted after preillumination and (2) the kinetics of the light-induced delayed photon emission. The studies were published in 1987–1990.

The kinetics of delayed luminescence were estimated using several cell densities. For all of these cell types, the decay curve of the delayed photon emission could best be described as hyperbolic rather than exponential. As expected, the total emission differed between cell types. The comparison of the two hepatoma cell lines documented that the poorly differentiated HTC cells both had a higher total photon emission and also a more rapid decay than the well differentiated H35 cells. The situation with the hepatocytes was even more complex. At higher cell density, total counts were even less than the cuvette counts. These data illustrated a basic phenomenon in studies with mammalian cells: “photon sucking.”

In the 1990s, more (nonhepatoma) mammalian cell lines were studied regarding their emission (i.e., decay dynamics and total photon emission). The data confirmed the “photon storage” model proposed by Popp and Nagl in the early 1980s. According to this model (which was initially described in terms of a resonator cavity), a high-quality resonant system loses only a small amount of its energy (photons) per unit time. A less quality system (due to the malfunction of the feedbacks) will give a larger response to the (light) stimulus.

4.4.3 Cell Types

Focusing now on total emission in relationship to density as well as the question whether these values are indicative of cell transformation, a third analysis was made of 17 mammalian cell types present in the Utrecht Laboratory (Van Wijk and colleagues). The study included cell lines (1) derived from different organisms (cat, human, monkey, mouse, rat, etc.); (2) derived from different types of tissue (heart, kidney, liver, etc.) and (3) derived from tumor and normal cells. Total photon emission was estimated for each cell line at different cell densities. In all cases, the cells displayed an increasing delayed photon emission almost linear to the increasing cell density. It ranged from 4 up to more than 100 photons per 10^4 cells. The data suggested that light-induced delayed photon emission is a general phenomenon in suspensions of mammalian cells. The question was: why do differences exist between the cell types.

A relationship between delayed photon emission and species of origin was not observed. Instead, a relationship between emission intensity and a specific cell type was most obvious. Cells of mesodermal origin (fibroblast/endothelial), either obtained from primary cultures of dissociated cells or derived from monolayer cultures of established cell lines, demonstrated the highest values. The other group of cell types (of nonmesodermal origin) included normal cells and tumor cells. In general, the lowest delayed emissions were observed from normal cells. Tumor cells demonstrated an intermediate range.

The data led to the conclusion that (1) tumor cells have higher delayed emissions than normal cells and (2) that a special class of cells exist (of mesodermal origin) that have an even higher emission than the tumor cells. Why did the tumor cells tend toward an energy balance which was expressed mostly by mesenchymal cells? This may be important to understand the underlying, cellular, and structural conditions.

4.4.4 The “Photon Sucking” Phenomenon in Early Development

The challenge to understand the photon emission during body pattern formation in development remained almost untouched until Lev Belousov at the Lomonosov Moscow State University focused on photon emission in relationship to early development. He referred to the classic Gurwitsch data in his own theory of early development (wherein average intensity of spontaneous photon emission decreases). Simultaneously, the intensity of a degradational radiation increased

(which might be initiated vis-à-vis slightly reversible damaging influences) suggesting the destruction within the collective states of each domain. Such domains are progressively generated and enlarged during development. Belousov hypothesized that they have properties of “photon sucking.” Along this line, it is of interest that already in the early 1990s, Mae-Wan Ho documented progressive decrease in spontaneous photon emission in *Drosophila* eggs. In 1997–1998, the same trend was also described by Belousov regarding chicken embryos and fish (*Misgurnus fossilis*) eggs plus their embryos. In this description of the developmental changes, Belousov utilized the Fourier spectra of photon emission to describe the progressive enlargement of the collective excitation domains (the increased interaction of coupled oscillators). Fourier spectra of different stages of fish embryos significantly differ from each other.

Belousov’s studies of chicken eggs and their shells documented that a hen’s egg, irrespectively of whether it contains a developing embryo (or was nonfertilized) did emit after it had absorbed daylight. Within many hours a considerable amount of photons appeared, primarily in the red spectral range. The only significant emitter was the shell (both yolk and embryo emit two orders of magnitude less, whereas egg whites do not emit photons at all). However, only in dead eggs and nonfertilized eggs, the rate of photon emission of a whole intact egg is approximately equal to that of its isolated shell. Whole, second day fertilized eggs primarily emit many more photons than their isolated shells. The 9 day fertilized eggs appear in a reverse manner. Hence, during early stages, an egg’s interior stimulates, whereas during later stages, it suppresses its shell emission. This latter effect may be due to active absorption (“sucking”) of photon energy from the shell by the embryo. By hyperbolic decay criteria, emission was considered highly coherent. The obvious explanation is the crystalline structure of the shell. The same is not true for a fresh nonfertilized egg. Consequently, only a developing egg can support coherence of shell emitted light.

Similarly, nonadditive relationships between the emission of developing embryos and egg membranes have been observed in amphibians. In the gastrula stage, the amount of photon emission of the isolated egg shell is smaller than that of embryos plus their shells. However, the advanced neurula stage embryos demonstrate the reverse. This, again, might point to an increase in “photon sucking” during development. Egg shells (besides their routine protective role) seem to act as storages and transformers of an external light.

By analyzing Fourier spectra of ultraweak photon emission from different stages of fish embryos, Belousov demonstrated significant differences. He interpreted such differences as follows: Immediately after fertilization, a

single powerful oscillator containing many harmonics becomes active. At the end of the cleavage period, the single oscillator exchanges to a large set of smaller ones which are, at first, noncorrelated with each other. Later, these oscillators again become coupled, this time including only a few dominating frequencies. These latter events are then associated with the beginning of active behavior simultaneous to the functioning of a central nervous system.

Belousov finally compared the Fourier patterns of ultraweak photon emission from cell cultures of fibroblasts and cardiomyocytes. He demonstrated that in such cell cultures, important substances for growth and differentiation (e.g., fibroblast growth factor) could influence the cell Fourier spectra (although the average rates of photon emission remained the same). He also demonstrated changes in Fourier spectra utilizing substances and conditions that might influence cytoskeleton structures (i.e., cytochalasin, colchicine, and trypsin).

4.5 The Two Examples – Biophotons in Cancer and in Embryonal Development – Belong to the Major Challenge of The International Institute of Biophysics (IIB)

It was important to manage the interdisciplinary research in an orderly manner. The cooperation and the excitement of the researchers worldwide resulted in the production of a series of scientific books (see Table 4.1). The choice to write books instead of articles has sometimes been criticized. It was argued that information provided in books can have a smaller impact as supposed to materials published in peer-reviewed articles. However, the participating researchers were, almost without exception, professors, associate professors, or senior scientists at distinguished universities. Therefore, books presented the possibility to strategically share important information publicly regarding the umbrella theme of “Life, Electromagnetic Fields and Light.”

Acknowledgments In order to author this chapter, we owe a special debt of gratitude to a large number of professors, associated professors and senior scientists, cooperating scientifically vis-à-vis the International Institute for Biophysics (and Biophotons): Rajendra P. Bajpai (North Eastern Hill University, Shillong, India), Lev. V. Belousov (Moscow State University, Moscow, Russia), Larissa Brizhik (Ukrainian National Academy of Sciences, Kyiv, Ukraine), Marco Bischof (Viadrina University, Frankfurt an der Oder, Germany), Jiin-Ju Chang (Chinese Academy of Sciences, Beijing, P.R. China), Barbara W. Chwirot (Nicholas Copernicus University, Torun, Poland), Mitsuo Hiramatsu (Hamamatsu Photonics K.K., Hamamatsu, Japan), G.J. Hyland (University of Warwick, Coventry, England), Masaki Kobayashi (Tohoku Technical University, Sendai, Japan), Michael Lipkind (Kimron Veterinary Institute, Beit Dagan, Israel), Takahiro

Table 4.1 The scientific cooperation in biophoton research: leading conferences, corresponding book volumes, and the International Institute of Biophysics

| Year | Location | Title | Editors | Publisher |
|------|-----------------------------|--|--|--|
| 1986 | Wroclow, Poland | Photon Emission from Biological Systems | B. Jezowska-Trzebiatowska, B. Kochel, J. Slawinski, W. Strek | World Scientific, Singapore, 1987 |
| 1989 | Wroclow, Poland | Biological Luminescence | B. Jezowska-Trzebiatowska, B. Kochel, J. Slawinski, W. Strek | World Scientific, Singapore, New Jersey, London, Hong Kong, 1990 |
| 1992 | Kaiserslautern, Germany | Recent Advances in Biophoton Research and its Applications | F.A. Popp, K.H. Li, Q. Gu | World Scientific, Singapore, New Jersey, London, Hong Kong, 1992 |
| 1994 | | Bioelectrodynamics and Biocommunication | Mae-Wan Ho, F.A. Popp, U. Wanke | World Scientific, Singapore, New Jersey, London, Hong Kong, 1994 |
| 1994 | Moscow, Russia | Biophotonics, Non-equilibrium and Coherent Systems in Biology, Biophysics, Biotechnology | L.V. Belousov, F.A. Popp | Bioinform Services Co., Russia 1995 |
| 1995 | Neuss, Germany | Current Development of Biophysics | Ch. Zhang, F.A. Popp, M. Bischof | Hangzhou University Press, Hangzhou, 1996 |
| 1997 | Ilmenau, Neuss, Germany | Biophotons | J.J. Chang, J. Fish, F.A. Popp | Kluwer Academic Publishers, Dordrecht, Boston, London, 1998 |
| 1999 | Moscow, Russia | Biophotonics and Coherent Systems | L.V. Belousov, F.A. Popp, V. Voeikov, R. van Wijk | Moscow University Press, Moscow, 2000 |
| 1999 | Neuss, Germany | What is Life? | H.P. Durr, F.A. Popp, W. Schommers | World Scientific, New Jersey, London, Singapore, Hong Kong, 2002 |
| 2002 | Catania, Italy | Energy and Information Transfer in Biological Systems | F. Musumeci, L.S. Brizhik, Mae-Wan Ho | World Scientific, New Jersey, London, Singapore, 2003 |
| 2003 | Beijing, China | Biophotonics, Optical Science and Engineering for the 21st century | Xun Shen, R. Van Wijk | Springer, New York, 2005 |
| 2003 | Neuss, Germany | Integrative Biophysics, Biophotonics | F.A. Popp, L.V. Belousov | Kluwer Academic, Dordrecht, Boston, London, 2003 |
| 2004 | Simferopol, Crimea, Ukraine | Biophotonics and Coherent Systems in Biology | L.V. Belousov, V.L. Voeikov, V.S. Martynyuk | Springer, New York, 2007 |

Modified from Van Wijk (2014)

Makino (Shizuoka Agricultural Experiment Station, Tomigaoka, Japan), Franco Musumeci (University of Catania, Catania, Italy), Hugo Niggli (University Hospital, Lausanne, Switzerland), J. Pokorny (Academy of Sciences of Czech Republic, Prague, Czech Republic), Fritz-Albert Popp (International Institute of Biophysics, Neuss, Germany), Xun Shen (Chinese Academy of Sciences, Beijing, P.R. China), Janusz Slawinski (Poznan University of Technology, Poznan, Poland), Kwang-Sup Soh (Seoul National University, Seoul, South Korea), John Swain (Northeastern University, Boston, USA), Vladimir L. Voeikov (Lomonosov Moscow State University, Moscow, Russia), and Yu Yan (International Institute of Biophysics, Neuss, Germany).

Publications for Further Reading

General

- Popp, F. A., Becker, G., König, H. L., and Peschka, W. (Eds.) 1979. Electromagnetic Bio-Information. Urban & Schwarzenberg, München, Wien, Baltimore.
- Van Wijk, R. 2014. Light in Shaping Life – Biophotons in Biology and Medicine, Meluna Research, Geldermalsen.

Polycyclic Aromatic Hydrocarbons and Carcinogenesis: Selection in Historical Order

- Schmidt, O. 1938. Die Beziehungen zwischen Dichteverteilung bestimmter B-Elektronen und die Reaktivität bei aromatischen Kohlenwasserstoffen. *Z. Physik. Chem.* 39: 59.
- Schmidt, O. 1939. Beitrage zum Mechanismus der Anregungsvorgänge in der Krebskranken und gesunden Zellen. *Z. Physik. Chem.* 44: 194.
- Schmidt, O. 1941. Charakterisierung und Mechanismus der Krebs erzeugenden Kohlenwasserstoffe. *Naturwissenschaften* 10: 146.
- Pullman, A., and Pullman, B. 1955a. *Adv. Cancer Res.* 3: 117.
- Pullman, A., and Pullman, B. 1955b. Cancérisation par les Substances Chimiques et Structure Moléculaire. Masson, Paris.
- Pullman, A., and Pullman, B. 1955c. Electronic structure and carcinogenic activity of aromatic molecules; new developments. *Adv. Cancer Res.* 3: 117–169.
- Pullman, A., and Pullman, B. 1956. On a paper by Nagata, Fukui, Yonezawa and Tagashira: electronic structure and carcinogenic activity by aromatic molecules. *Cancer Res.* 16: 267–268.
- Pullman, A., and Pullman, B. 1962. Electron transfer and carcinogenesis. *Nature* 196: 228–229.
- Pullman, B. 1964. *Electron Aspects of Biochemistry*. Academic Press, New York, London.
- Pullman, A., and Pullman, B. 1963. *Quantum Biochemistry*. Interscience Publ., New York.
- Kumaki, K., Hara, S. I., Mizuno, K., and Tomioka, S. 1969. Relation between the hydroxylated position of aromatic compounds by monooxygenases and various electronic reactivity indexes. *Chem. Pharm. Bull. Tokyo* 17: 1571.
- Buu-Hoï, N. P., and Sung, S. S. 1970. A non-radiative photochemical model for polycyclic aromatic hydrocarbon-induced carcinogenesis. *Naturw.* 3: 135.
- Sung, S. S., and Buu-Hoï, N. P. 1970. Sur l'intervention possible d'un mécanisme photochimique dans le processus de cancérisation par les hydrocarbures aromatiques et leurs analogues hétérocycliques. *C.R. Acad. Sci. D* 270: 2052.
- Sung, S. S. 1975. Electronic excitation states and carcinogenicity in polycyclic aromatic hydrocarbons. *Ann. Soc. Scient. Bruxelles* 89 II: 319.
- Sung, S. S. 1977. What's wrong with the theoretical research on molecular mechanisms of the chemical cancerization process? *Arch. Geschwulstforsch.* 47: 109.

Resonance Theory of Carcinogenesis by F. A. Popp (Historical order)

- Popp, F. A. 1972a. MO-Rechnungen an 3,4-Benzpyren und 1,2-Benzpyren legen ein Modell zur Deutung der chemischen Karzinogenese nahe. *Z. Naturforsch.* 27b: 731.
- Popp, F. A. 1972b. Elektronische Struktur und karzinogene Aktivität von 3,4-Benzpyren und 1,2-Benzpyren. *Z. Naturforsch.* 27b: 850.
- Popp, F. A. 1972c. Ein Modell der Karzinogenese. *Strahlentherapie* 144: 208.
- Popp, F. A. 1973a. Zur Deutung der Karzinogenität aus dem UV-Spektrum von 3,4-Benzpyren und 1,2-Benzpyren. *Z. Naturforsch.* 28c: 165.
- Popp, F. A. 1973b. Ein Zusammenhang zwischen Anregungszuständen von Molekülen und biologischer Wirkung wie Strahsensibilisierung und Kanzerogenität. *Z. Naturforsch.* 28c: 517.
- Popp, F. A. 1973c. Zur Resonanzhypothese der Karzinogenese. *Strahlentherapie* 146: 582.

- Popp, F. A. 1973d. Weak Quantization. *J. Math. Phys.* 14: 604.
- Popp, F. A. 1974a. Erläuterungen zum Resonanzmodell der Karzinogenese. *Z. Naturforsch.* 29c: 454.
- Popp, F. A., Schaumlöffel, E., Böhm, P., Herrmann, K., and Kramer, J. 1974. Biosignale zur Steuerung des Zellstoffwechsels. Eine Resonanzhypothese der Karzinogenese. *Münch. Med. Wschr.* 116: 381–384.
- Popp, F. A. 1974b. Einige Möglichkeiten für Biosignale zur Steuerung des Zellwachstums. *Arch. Geschwulstforsch.* 44: 295.
- Popp, F. A., Bothe, B., and Goedecke, R. 1975. Prinzipien der Optimierung der Bestrahlungsplanung. *Strahlentherapie* 150: 389.
- Popp, F. A. 1976a. So konnte Krebs entstehen. *Bild der Wissenschaft* 1: 59.
- Popp, F. A. 1976b. Molecular Aspects of Carcinogenesis. In E. Deutsch, K. Moser, H. Rainer, A. Stacher (Eds.) *Molecular Base of Malignancy*. Thieme, Stuttgart.
- Popp, F. A. 1976c. Biophotonen. Ein neuer Weg zur Lösung des Krebsproblems. *Schriftenreihe Krebsgeschehen. Bd.6.* Verlag für Medizin (vfm), Heidelberg.
- Popp, F. A., and Ruth, B. 1976. Untersuchungen zur ultraschwachen Photonenmission aus biologischen Systemen. *Arzneimittelforsch./Drug Res.* 27: 933.
- Popp, F. A. 1977a. Krank sein – Wenn Zellen nicht mehr miteinander reden. *Bild der Wissenschaft* 8: 90.
- Popp, F. A., and Strauss, V. E. 1977. So konnte Krebs entstehen. DVA, Stuttgart.
- Popp, F. A. 1977b. A very significant correlation between carcinogenic activity of polycyclic hydrocarbons and certain properties of their transition states in the range of the lowest triplet states of the DNA. *Arch. Geschwulstforsch.* 47: 97.
- Popp, F. A. 1977c. Model studies in tumor incidence. *Arch. Geschwulstforsch.* 47: 106.

Photochemistry Without Light by C. Cilento (Historical Order)

- Cilento, C. 1974. Excited electronic states in dark biological processes. *Quart. Rev. Biophys.* 6: 485.
- Cilento, G. 1982. Electronic excitation in dark biological processes. In W. Adam and G. Cilento (Eds.) *Chemical and Biological Generation of Excited States*. Academic Press, New York, pp. 277–307.
- Adam, W., and Cilento, G. (Eds.) 1982. *Chemical and Biological Generation of Excited States*. Academic Press, New York.
- Adam, W., and Cilento, G. 1983. Four-membered ring peroxides as excited state equivalents: a new dimension in bioorganic chemistry. *Ang. Chem. int. Ed. (Engl.)* 22: 529–542.
- Cilento, G. 1984. Generation of electronically excited triplet species in biochemical systems. *Pure appl. Chem.* 56: 1179–1190.
- Cadenas, E., Sies, H., Campa, A., and Cilento, G. 1984. Electronically excited states in microsomal membranes: use of chlorophyll-a as an indicator of triplet carbonyls. *Photochem. Photobiol.* 40: 661–666.
- Baader, W. J., Bohne, C., Cilento, G., and Dunford, H. B. 1985. Peroxidase catalyzed formation of triplet acetone and chemiluminescence from isobutyraldehyde and oxygen. *J. biol. Chem.* 260: 10217–10225.
- Villablanca, M., and Cilento, G. 1985. Enzymatic generation of electronically excited states by electron transfer. *Photochem. Photobiol.* 42: 591–597.
- Adam, W., Baader, W. J., and Cilento, G. 1986. Enol of aldehydes in the peroxidase-oxidase promoted generation of excited triplet species. *Biochim. biophys. Acta* 881: 330–336.

- Baader, W. J., Bohne, C., Cilento, G., and Nassi, L. 1986. Enzymatic generation of triplet acetone: a window to photobiochemistry without light. *Biochem. Acta*. 14: 190–192.
- Nascimento, A. L. T. O., da Fonseca, L. M., Brunetti, I. L., and Cilento, G. 1986. Intracellular generation of electronically excited states. Polymorphonuclear leukocytes challenged with a precursor of triplet acetone. *Biochim. biophys. Acta* 881: 337–342.
- Salim-Hanna, M., Campa, A., and Cilento, G. 1987. The α -oxidase system of young pea leaves. *Pisum sativum* as generator of electronically excited states. Excitation in the dark under natural conditions. *Photochem. Photobiol.* 45: 695–702.
- Cilento, G. 1988. Photobiochemistry without light. *Experientia* 44: 572–576.

Photons and Information (Selected Early Papers in Historical Order)

- Arvanataki, A., and Chalazonitis, N. 1960. Photopotentiels d'excitation et d'inhibition de différents somata identifiables (Aplysia). *Activations monochromatiques*. Bull. de l'Institut Océanographique (Monaco) 1164.
- Benolken, R. M. 1961. Reversal of photoreceptor polarity recorded during the graded receptor potential response to light in the eye of *Limulus*. *Biophys. J.* 1: 551–564.
- Kikuchi, R., Naito, K., and Tanaka, I. 1962. Effect of sodium and potassium ions on the electrical activity of single cells in the lateral eye of the horseshoe crab. *J. Physiol. (London)* 161: 319–343.
- Chalazonitis, N. 1964. Light energy conversion in neuronal membranes. *Photochem. Photobiol.* 3: 539–559.
- Brown, A. M., and Brown, H. M. 1973. Light response of a giant *Aplysia* neuron. *J. Gen. Physiol.* 62: 239–254.
- Henkart, M. 1975. Light-induced changes in the structure of pigmented granules in *Aplysia* neurons. *Science* 188: 155–157.
- Oesterheld, D. 1976. Bacteriorhodopsin als Beispiel einer lichtgetriebenen Photonenpumpe. *Angew. Chem.* 88: 16–24.
- Gurwitsch, Photons and Nerves
- Gurwitsch, A. 1932a. Die mitogenetische Strahlung der optischen Bahn bei adäquater Erregung. *Pflügers Arch. Ges. Physiol.* 231: 254–264.
- Gurwitsch, A. 1932b. Die mitogenetische Strahlung des markhaltigen Nerven. *Pflügers Arch. Ges. Physiol.* 231: 234–237.
- Fischer, H. 1979. Photons as transmitter for intra- and intercellular biological and biochemical communication. In Popp F. A., Becker G., König, H. L., Peschka W., (Eds.) *Electromagnetic Bio-Information*. Urban & Schwarzenberg, München, Wien, Baltimore, pp. 175–180.
- B. Ruth: Experimental Investigations on Ultraweak Photon Emission p. 107.
- F. A. Popp: Photon Storage in Biological Systems p. 123.
- S. S. Sung: A Possible Biophotochemical Mechanism for Cell Communication p. 151.
- H. Fischer: Photons as Transmitter for Intra- and Intercellular Biological and Biochemical communication – The Construction of a Hypotheses p. 175.
- W. Kroy: The Use of Optical Radiation for Stimulation Therapy p. 181.
- U. Warnke, F. A. Popp: Some Aspects of magnetic Influences on Biological Systems p. 195.
- 1983 – Coherent Excitations in Biological Systems (International Symposium, Bad Neuenahr, November 29 – December 1, 1982) Edited by H. Fröhlich, F. Kremer (Springer Verlag – Berlin, Heidelberg, New York, Tokyo):
- H. Fröhlich: Coherence in biology p.1.
- F. Drissler and L. Santo: Coherent excitations and Raman effect p. 6.
- F. Kremer, C. Koschnitzke, L. Santo, P. Quick, and A. Poglitsch: The non-thermal effect of millimeter wave radiation on the puffing of giant chromosomes p. 10.
- W. Grundler, F. Keilmann, V. Putterlik, L. Santo, D. Strube and I. Zimmermann: Nonthermal resonant effects of 42 GHz microwaves on the growth of yeast cultures p. 21.
- G. Nimtz: On the microwave response of the *Drosophila Melanogaster* p. 38.
- S. M. Motzkin, L. Benes, N. Block, B. Israel, N. May, J. Kuriyel, L. Birenbaum, S. Rosenthal and Q. Han: Effects of low-level millimeter waves on cellular and subcellular systems p. 47.
- L. Genzel, F. Kremer, A. Poglitsch and G. Bechtold: Millimeter-wave and far-infrared spectroscopy on biological macromolecules p. 58.
- J. B. Hasted, S. K. Husain, A. Y. Ko, D. Rosen, E. Nicol, and J. R. Birch: Excitation of Proteins by electric fields p. 71.
- G. R. Welch and M. N. Berry: Long-range energy continua in the living cell Protochemical considerations p. 95.
- K. H. Li, F. A. Popp, W. Nagl, and H. Klima: Indications of optical coherence in Biological systems and its possible significance p. 117.
- E. Del Giudice, S. Doglia, and M. Milani: Self-focussing and ponderomotive forces of coherent electric waves: A mechanism for cytoskeleton formation and dynamics p. 123.
- F. Kaiser: Specific effects in externally driven self-sustained oscillating biophysical model systems p. 128.
- F. A. Sauer: Forces on suspended particles in the electromagnetic field p. 134.
- S. Rowlands: Coherent excitations in blood p. 145.
- J. S. Clegg: Intracellular water, metabolism, and cell architecture p. 162.
- D. B. Kell and G. D. Hitchens: Coherent properties of the membranous systems of electron transport phosphorylation p. 178.
- H. A. Pohl: Natural oscillating fields of cells p. 199.
- U. Zimmermann and W. M. Arnold: The interpretation and use of the rotation of biological cells p. 211.
- H. P. Schwan: Symposium on coherent excitations in biological systems: Some impressions and conclusions p. 222.
- 1987 – Photon Emission from Biological Systems (First International Symposium Wroclaw, Poland, January 24–26, 1986) Editors: B. Jezowska-Trzebiatowska, B. Kochel, J. Slawinski, W. Strek (World Scientific – Singapore, New Jersey, Hong Kong):
- J. Slawinski: Present status and prospects of PEBS' investigations p. 7.
- Z. W. Wolkowski: Hierarchical aspects of synergy and coherence in biological systems p. 22.
- K. H. Li: Physical basis of coherent radiations from biomolecules p. 51.
- F. A. Popp: On the coherence of ultraweak photon emission from living tissues p. 63.
- B. Kochel, E. Grabikowski, J. Slawinski: Analysis of photon-counting time series of low level luminescence from wheat leaves at high temperatures p. 96.

Internationalization of the New (Information) Photon Research

- 1979 – *Electromagnetic Bio-Information* (Symposium, Marburg, September 5, 1977) Edited by F. A. Popp, G. Becker, H. L. König, W. Peschka (Urban & Schwarzenberger – München, Wien, Baltimore):
- H. Breithaupt: Biological Rhythms and Communication p. 1.
- H. L. König: Bioinformation – Electrophysical Aspects p. 25.
- U. Warnke: Information Transmission by means of Electrical Biofields p. 55.
- W. Peschka: On Kinetobaric Effects and Bioinformational Transfer by Electromagnetic Fields p. 81.
- G. Becker: Communication between Termites by Means of Biofields and the Influence of Magnetic and Electric Fields on Termites p. 95.

- C. W. Smith, A. H. Jafary-Asl, R. Y. S. Choy, J. A. Monro: The emission of low intensity Electromagnetic radiation from multiple allergy patients and other biological systems p. 110.
- K. Fraczkowski, K. Gwozdz: Stimulated biomagnetic responses from brain stem and cortex as a consequence of electromagnetic radiations p. 127.
- D. H. J. Schamhart, R. van Wijk: Photon emission and the degree of differentiation p. 137.
- H. Klima, O. Haas, P. Roschger: Photon emission from blood cells and its possible role in immune system regulation p. 153.
- J. W. Dobrowolski, A. Ezzahir, M. Knapik: Possibilities of chemiluminescence application In comparative studies of normal and cancer cells with special attention to leukemic blood cells p. 170.
- M. I. Yanbastiev: On some applied-medical aspects of biophotonics p. 184.
- B. Yoda, Y. Goto, A. Saeki, H. Inaba: Chemiluminescence of smoker's blood and its possible Relationship to cigarette smoke components p. 199.
- J. W. Dobrowolski, J. Borkowski, S. Szymczyk: Preliminary investigation of the influence of laser light on the bioluminescence of blood cells. Laser stimulation of cumulation of selenium in tomato fruit p. 211.
- E. Celan, D. Gradinaru, B. Celan: The evidence of selective radiation emitted by a cell culture which destructively affects some tumoral cell lines p. 219.
- D. Slawinska, E. Polewski: Spectral analysis of plant chemiluminescence participation of polyphenols and aldehydes in light producing relations p. 226.
- S. Tryka, R. Koper: Luminescence of cereal grain subjected to the effect of mechanical loads p. 248.
- 1988 – Multi-author review on 'Biophoton emission' Coordinated by F. A. Popp. It was published in *Experientia* (volume 44, issue 7 (1988)):
- F. A. Popp: Introduction p. 543.
- A. A. Gurwitsch: A historical review of the problem of mitogenic radiation p. 545.
- H. Inaba: Super-high sensitivity systems for detection and spectral analysis of ultraweak photon emission from biological cells and tissues p. 550.
- J. Slawinski: Luminescence research and its relation to ultraweak cell radiation p. 559.
- G. Cilento: Photobiochemistry without light p. 572.
- F. A. Popp, K. H. Li, W. P. Mei, M. Galle and R. Neurohr: Physical aspects of biophotons p. 576.
- R. van Wijk and D. H. J. Schamhart: Regulatory aspects of low intensity photon emission p. 586.
- W. B. Chwirot: Ultraweak photon emission and anther meiotic cycle in *Larix europaea* (Experimental investigation of Nagl and Popp's electromagnetic model of differentiation) p. 594.
- W. Nagl: Concluding remarks p. 599.
- 1990 – Biological Luminescence (First International School on Biological Luminescence, June 20th to June 23rd, 1989 in Wroclaw, Poland) Editors: B. Jezowska-Trzebiatowska, B. Kochel, J. Slawinski and W. Streck. (World Scientific– Singapore, New Jersey, London, Hong Kong):
- Part I: Biophysical and biocybernetic:
- C. W. Smith: Coherence and Biocommunication p. 3.
- A. I. Zhuravlev: Spontaneous superlow chemiluminescence and creation of quantum biology p. 19.
- J. Slawinski: Ultraweak luminescence and perturbations of biohomeostasis p. 49.
- J. Slawinski and B. Kochel: Stochastic models of nonstationary photon emission from chemically perturbed living organisms p. 78.
- B. Kochel: Luminescence of perturbed living organisms: A memory function approach based on linear stochastic model of nonstationary photon emission processes p. 101.
- M. Usa, M. Kobayashi, R. Q. Scott, R. Hiratsuka, T. Maeda and Inaba: Ultraweak biophoton emission and bioelectrical activity in plant tissues p. 117.
- V. E. Orel: Triboluminescence as a biological phenomenon and methods for its investigation p.133.
- Part II: Biological:
- R. N. Tilbury: Ultraweak luminescence of yeast and bacteria p. 151.
- A. Ezzahir, M. Godlewski, T. Kwiecinska, Z. Rajfur, J. Slawinski and K. Scieszka: Photoinduced delayed luminescence from yeast *Saccharomyces cerevisiae* p. 173.
- M. Godlewski, Z. Rajfur, A. Ezzahir, D. Sitko and M. Krol: The influence of environmental conditions on the luminescence from *Saccharomyces cerevisiae* p. 182.
- D. Slawinska: Spectral analysis of ultraweak photon emission from plants p. 197.
- L. O. Bjorn, I. Panagopoulos and G. S. Bjorn: Ultraweak luminescence from plant tissue: spectral characteristics and effect of ultraviolet radiation, anaerobiosis and ageing p. 214.
- H. Reiber: Low-level luminescence from disintegrated brain cells – subcellular distribution and kinetics of the biophysical radiation p. 224.
- 1992 – Multi-author review on 'Biophoton emission, stress and disease' Coordinated by R. van Wijk. It was published in *Experientia* Volume 48, issue 11–12 (1992):
- R. van Wijk: Introduction to Biophoton emission, stress and disease p. 1029.
- R. N. Tilbury: The effect of stress factors on the spontaneous photon emission from microorganisms p. 1030.
- J. Slawinski, A. Ezzahir, M. Godlewski, T. Kwiecinska, Z. Rajfur, D. Sitko and D. Wierzuchowska: Stress-induced photon emission from perturbed organisms p. 1041.
- B. Kochel: Time-resolved luminescence of perturbed biosystems Stochastic models and perturbation measures p. 1059.
- Q. Gu and F. A. Popp: Nonlinear response of biophoton emission to external perturbations p. 1069.
- E. M. Lilius and P. Marnila: Photon emission of phagocytes in relation to stress and disease p. 1082.
- R. van Wijk and J. M. van Aken: Photon emission in tumor biology p. 1092.

Part II

Physics of Light and Light Research

5.1 Light and Electronic Excitation

5.1.1 Light

Light radiation is known to exhibit the properties of both an electromagnetic wave and a stream of particles propagating at the speed c . As an electromagnetic wave, it is characterized by wavelength λ (frequency ν), intensity, and polarization. As a particle flux, it is characterized by the energy and momentum of an individual particle and their statistical characteristics: distribution by energy, time of appearance, etc.

For individual photons, these properties are united by the famous Plank–Einstein (Eq. (5.1)) and de Broglie (Eq. (5.2)) relations:

$$E = h\nu = \frac{hc}{\lambda} \quad (5.1)$$

$$p = mc = \frac{E}{c} = \frac{h}{\lambda} \quad (5.2)$$

where h is Planck's constant ($6.626 \cdot 10^{-34} \text{ J} \cdot \text{s}$), c is the speed of light, p is momentum (as you know, a photon has no rest mass and exists only in the form of a particle propagating at the speed of c).

For macroscopic amounts of photons, more convenient units are those related to moles. The energy of 1 mole of photons is called *Einstein* (expressed in J/mol):

$$E = N_A h\nu = \frac{N_A hc}{\lambda} \quad (5.3)$$

where N_A is Avogadro's constant ($6.023 \cdot 10^{23} \text{ mol}^{-1}$).

As you can see, the value of one *Einstein* varies and depends on the wavelength of light. For instance, for radiation with $\lambda = 300 \text{ nm}$, 1 *Einstein* is 399 kJ/mol, and for

400 nm, it is 299 kJ/mol. If the radiation energy is expressed in *Einstein*, then numerically it is equal to the number of moles of photons.

The other common energy units used in biophotonics are electron volts (eV), kJ/mol, and kcal/mol.

1 eV = $1.602 \cdot 10^{-19} \text{ J}$ corresponds to the kinetic energy gained by a single electron accelerating from rest through an electric potential difference of 1 V. Numerically, it is equal to the charge of a single electron in coulombs.

1 cal (thermal) = 4.184 J is the amount of heat needed to raise the temperature of 1 g of water by 1 K. The commonly used value is $1 \frac{\text{kcal}}{\text{mol}} = 2.613 \cdot 10^{22} \text{ eV}$.

Light emission has a pronounced twofold nature. On the one hand, the appearance of a photon is always a single quantum process. On the other hand, the electromagnetic field or wave as such almost always corresponds to a plurality of photons, their ensemble. The statistical characteristics of this ensemble are of great importance: first of all, their distribution by energy and time of appearance. In wave representation, this corresponds to the spectrum of radiation (the dependence of its intensity on the wavelength) and modulation (the dependence of the intensity on time). In addition, since even a single photon is at the same time a wave packet of electromagnetic radiation, an important characteristic is also its polarization and, at the ensemble level, the polarization properties of the entire light flux.

According to conservation laws, the appearance of a photon (with its energy and momentum) is possible only with the corresponding losses of energy and momentum of its source. Aside from high-energy processes of particle creation and annihilation, this always corresponds to electronic transitions in certain atoms, molecules, or ions.

5.1.2 Energy Levels and Their Population

Each atom (molecule or ion) has a series of filled and free electron orbitals (Fig. 5.1).

I. Volodyaev (✉) · Y. A. Vladimirov
Moscow State University, Moscow, Russia

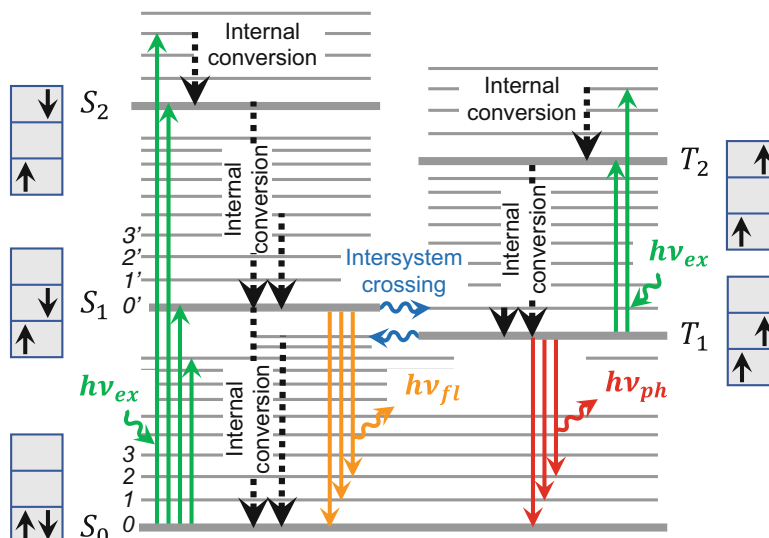


Fig. 5.1 Electronic transitions in molecules. S – singlet states (two electrons at the highest orbitals have opposite spins), T – triplet states (two electrons at the highest orbitals have equal spins). S_0 – the ground (unexcited) state (some molecules, e.g., oxygen have not singlet, but triplet ground state). S_1, S_2 and T_1, T_2 – excited singlet and triplet states, respectively. Spin direction of the excited electron is schematically shown near each level, in relation to the spin of the remaining electron. Bold horizontal lines – purely electronic energy levels, thin lines (0, 1,

2 ... or $0', 1', 2', \dots$) – vibrational levels. Vertical solid lines with arrows – energy transitions: green – absorption, orange and red – radiative transitions, accompanied by photon emission. Orange – fluorescence (without spin inversion, mostly $S_1 \rightarrow S_0$ transition); red – phosphorescence (with spin inversion, mostly $T_1 \rightarrow S_0$ transition). Black dotted vertical arrows – nonradiative relaxation of electronically excited states (Internal conversion). Intersystem crossing – electron transitions to the nearest levels with spin reversal

In the initial (unexcited) state, the molecules are at the lowest possible energy level (0 – S_0 in Fig. 5.1), that is, at the lowest vibrational sublevel of the ground state.

The probability of a spontaneous molecule transition to a higher energy level through heat (thermal excitation) is determined by the Boltzmann equation:

$$\frac{n}{n_0} = e^{-\frac{\Delta E}{k_B T}} \quad (5.4)$$

where n_0 and n are the number of molecules at the ground state and at the excited state, respectively; ΔE is the energy difference between the levels; k_B is the Boltzmann constant; and T is the absolute temperature.

In thermal equilibrium, practically all molecules are at the lowest vibrational sublevel of the lowest electronic level. For instance, in a phenylalanine molecule, for the nearest vibrational sublevels, $\Delta E \cong 0.1$ eV (at 300 K, 0.1 eV $\cong 3.8$ kT) and $n/n_0 = 2.2\%$. The population of the overlying electronic levels is obviously much less.

5.1.3 Electronic Transitions and Photon Emission

5.1.3.1 Excited States with Conserved Spin

From the ground state S_0 , a molecule can pass to different vibrational sublevels of the overlying electron orbitals (S_1, S_2 ,

etc.), by absorbing photons of the corresponding energy (Fig. 5.1, green arrows):

$$h\nu = \Delta E = E_2 - E_1 \quad (5.5)$$

where $h\nu$ is photon energy and E_2 and E_1 are the energies of the upper and lower levels, correspondingly.

These transitions are carried out with the electron spin conserved ($S_0 \rightarrow S_1$; $S_0 \rightarrow S_2$) and occur at characteristic times of $10^{-14} - 10^{-15}$ s (Dutoi et al. 2010). During the next $10^{-11} - 10^{-12}$ s, the excited molecule thermally equilibrates with the environment, and the relative population of the excited state sublevels begins to obey the Boltzmann equation (Eq. (5.4)). Thus, part of the excited state energy is immediately transferred to the thermal motion of the surrounding molecules (dissipated into heat). In Fig. 5.1, this is denoted as “internal conversion” from different levels to the lowest vibrational sublevel of the lowest excited state $0' - S_1$ (black dotted arrows).

The $0' - S_1$ state is more stable; its characteristic lifetime is usually $\sim 10^{-9} - 10^{-8}$ s. In the absence of further photochemical reactions or energy transfer to other molecules, it can undergo the following transitions:

- 1. Nonradiative relaxation.** The energy of the excited state is gradually wasted on oscillatory and rotational movements (i.e., thermal motion) of molecules (internal conversion arrows in Fig. 5.1).

2. **Fluorescence.** An electron passes from the excited state orbital S_1 to the ground state orbital S_0 “at once,” generating a fluorescence quantum (Fig. 5.1, orange arrows). The energy of this quantum is also determined by Eq. (5.5), if E_2 stands for the energy of the higher level. Since such a transition can occur at different vibrational sublevels of the ground state, the energies of the fluorescent photons can be slightly different, reflecting the positions of these sublevels and forming the so-called fine structure of the fluorescent spectrum.

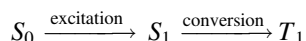
The **characteristic time** of fluorescent transitions is $\sim 10^{-9} - 10^{-8}$ s (determining the approximate lifetime of the S_1 excited state).

3. **Intersystem crossing.** Conversion to other excited states is accompanied by spin inversion, usually $S_1 \rightarrow T_1$ (Fig. 5.1, blue wavy lines). The energy of the T_1 triplet state is usually lower than that of S_1 , and though this transition is spin forbidden, it still occurs (at some lower probability) due to energy benefits.

5.1.3.2 Excited States with Inverted Spin

Excited states with reversed electron spin (mostly T_1 , if the ground state is singlet, S_0) are much more stable, for their relaxation demands a quantum-forbidden process of spin inversion. The existence of such metastable states, as well as the term “metastable” used for them, was first suggested by Delorme and Perrin (1929) and Jablonski (1933). Yet, the authors didn’t understand that these states were triplets and strongly opposed this hypothesis later, as did some other influential physicists of that time (see Lower and El-Sayed 1966; Krasnovsky 2018). The hypothesis of the triplet nature of this metastable state was formulated and partially proven by Terenin (1943) and Lewis and Kasha (1944) (see more in Chap. 2).

As the direct excitation $S_0 \rightarrow T_1$ is spin-forbidden, it is extremely unlikely: for example, for tryptophan, the absorption coefficient for $S_0 \rightarrow T_1$ transition is $\sim 10^9$ times lower than for the main absorption band corresponding to the $S_0 \rightarrow S_1$ transition. Thus, these levels are mostly populated through the singlet excited state:



The inverse relaxation transition $T_1 \rightarrow S_0$ is also highly unlikely; its probability is 4–9 orders of magnitude lower than for fluorescence. This determines the incomparably longer lifetime of such states, from 10^{-4} s to even hours.

In the liquid phase during this time, the energy of the excited triplet state is dissipated, and the electron returns to the ground state nonradiatively. Yet, in solid samples, as well

as in frozen liquid systems, a radiative transition $T_1 \rightarrow S_0$, accompanied by the emission of a phosphorescence quantum, can be observed.

Thus, in the absence of energy transfer to other molecules and photochemical reactions, triplet excited states can undergo the following transitions:

1. **Phosphorescence.** Radiative relaxation $T_1 \rightarrow S_0$, accompanied by photon generation (Fig. 5.1, red arrows). Being spin-forbidden and thus highly unlikely, it is observable only due to the great lifetime of the T_1 state. Since such a transition can occur at different vibrational sublevels of the ground state, the phosphorescence spectra have a certain fine structure.

The **characteristic time** of phosphorescence transitions is $\sim 10^{-4} - 10^1$ s (determining the approximate lifetime of the T_1 excited state);

2. **Intersystem crossing.** Spontaneous reverse conversion $T_1 \rightarrow S_1$ has an extremely low probability since, in addition to the spin-forbidden transition, S_1 usually has a higher energy than T_1 . However, pumping additional energy into the system, for example, in the form of heat or infrared radiation, makes this process possible. This transition is followed by all the possibilities of $S_1 \rightarrow S_0$ relaxation, including radiant, accompanied by photon emission. The latter is similar to fluorescence in spectrum (since it involves the same $S_1 \rightarrow S_0$ transition) and phosphorescence in kinetics (since it is preceded by very slow $S_1 \rightarrow T_1$ and $T_1 \rightarrow S_1$ transitions). This photon emission is called **delayed luminescence** (see Sect. 5.2.5).

In addition (if there is interaction between molecules in the system), nonradiative transfer (or migration) of energy from one molecule to another can also occur (see Sect. 5.4).

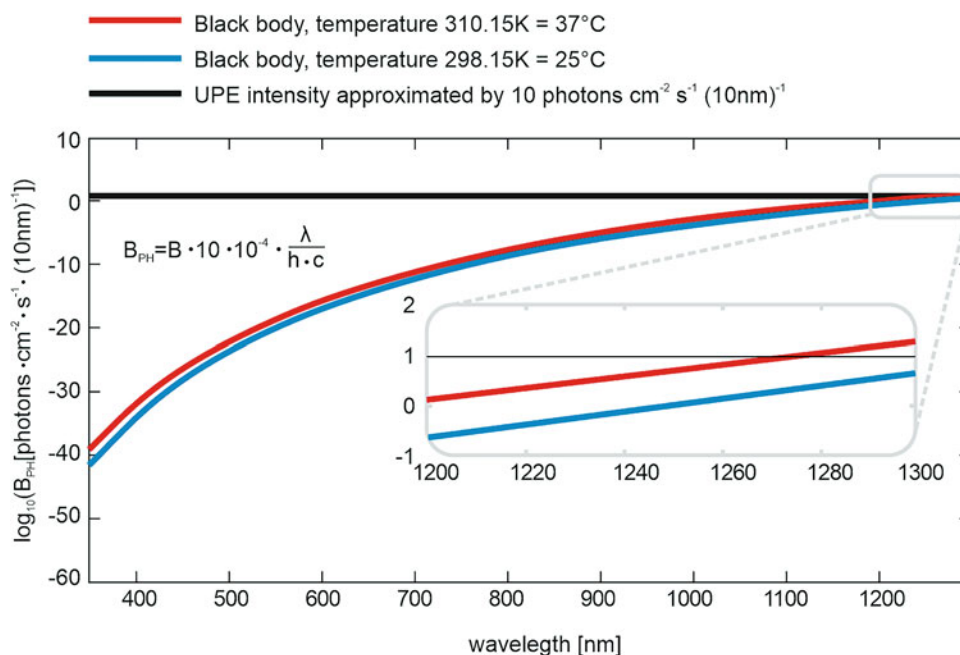
5.2 Luminescence

5.2.1 Definition and Classification

It is important to distinguish the luminescence phenomenon from other types of light emission. According to S.N. Vavilov (1950), the luminescence of a body in a given spectral region is an excess of radiation over thermal (blackbody-like) radiation, provided that this excess radiation has a finite duration that exceeds the period of light oscillations.

Spontaneous ultraweak photon emission (UPE), that is, biological autoluminescence, has very low intensity ($10^0 - 10^2$ photons \cdot s $^{-1}$ \cdot cm $^{-2}$) but is still incomparably higher

Fig. 5.2 Number of photons emitted to a hemisphere (2π steradians of solid angle and π steradians of projected solid angle) from the planar ideal blackbody at the temperatures 25 °C (blue line) and 37 °C (red line) versus biological autoluminescence, approximated by the flux of 10 photons \cdot s $^{-1}$ \cdot cm $^{-2}$ per band of 10 nm (solid line). The assumed intensity of ultraweak photon emission in the near-infrared region of the spectrum equals the intensity of blackbody radiation at 1337 nm for 25 °C and at 1281 nm for 37 °C. (Reprinted with permission from Cifra and Pospisil (2014). Copyright 2014 Elsevier)



than Planck's blackbody radiation in the visible and ultraviolet (UV) spectral range at physiological temperatures (Fig. 5.2). Thus, when detecting luminescence within this range, thermal radiation can be easily neglected.

As said above, there are two basic types of luminescence:

- Fluorescence (with conservation of spin: as a rule, $S_1 \rightarrow S_0$ transitions, but also $T_1 \rightarrow T_0$ transitions if the ground state is triplet).

Characteristic times: $10^{-9} - 10^{-8}$ s.

- Phosphorescence (with spin inversion: $T_1 \rightarrow S_0$ or $S_1 \rightarrow T_0$).

Characteristic times: $10^{-4} - 10^1$ s.

Besides, luminescence can be classified according to the origin of electronic excitation:

- *Chemiluminescence*: Electronic excitation states are generated by chemical (free radical) processes.
- *Photoluminescence*: Excitation is generated by external light.
- *Thermoluminescence*: Excitation is generated by sample heating and energy transfer.
- *Electroluminescence*: Excitation is generated by electric current.
- *Sonoluminescence*: Excitation is generated due to the system's exposure to ultrasound.
- *Triboluminescence*: Excitation is generated by surface friction.

Biological autoluminescence (spontaneous UPE from biological systems) belongs almost exclusively to the category of chemiluminescence.

5.2.2 Luminescence Spectra

The basic properties of luminescence are its spectra, that is, the energy distribution of emitted photons, and its kinetics, directly related to the lifetime of the excited states.

The luminescence spectrum (fluorescence or phosphorescence) is called the dependence

$$I_{\text{lum}} = f(\lambda) \text{ or } I_{\text{lum}} = f(\nu) \quad (5.6)$$

where I_{lum} is the luminescence spectral density, measured at a wavelength λ (frequency ν).

As the T_1 excited energy level usually has lower energy than S_1 , the phosphorescence has usually longer wavelengths than fluorescence (e.g., Fig. 5.3). At the same time, the excitation spectra of fluorescence and phosphorescence coincide (as the T_1 level is mostly populated through S_1 – see above) and obviously have shorter wavelengths (due to the loss of some excitation energy on inner conversion; see Fig. 5.1).

5.2.2.1 Laws of Luminescence

There are several empirical laws of luminescence: Stokes's law, Kashi's rule, Levshin's rule, and Vavilov's law. They are very helpful in luminescent research and can be easily explained by the diagram in Fig. 5.1 (see below).

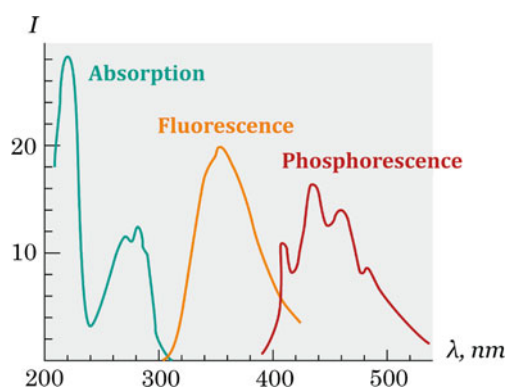


Fig. 5.3 Excitation (absorption), fluorescence and phosphorescence spectra of tryptophan. (Redrawn with permission from Vladimirov and Potapenko (1989), with mild modification. Copyright 1989, the authors)

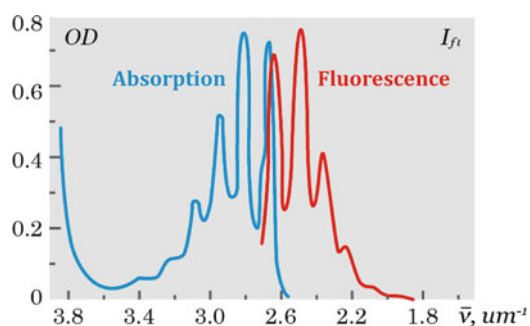


Fig. 5.4 Absorption and fluorescence spectra of anthracene (1 $\mu\text{g/ml}$) in ethanol. (Redrawn with permission from Vladimirov and Potapenko (1989). Copyright 1989, the authors)

According to **Stokes's law**, the fluorescence spectrum lies at longer wavelengths compared to the absorption spectrum of the same compound (Figs. 5.3 and 5.4). This means that the average energy of fluorescence quanta is less than that of absorbed quanta. In Fig. 5.1, this is evident in the larger average length of straight upward arrows (electronic transitions in light absorption) compared to downward-directed arrows (electronic transitions during fluorescence and phosphorescence). The reason for this (already discussed above) is that part of the absorbed photon energy is converted into thermal energy by the surrounding molecules.

According to **Kashi's rule**, the spectrum of fluorescence (and phosphorescence) does not depend on the wavelength of the exciting radiation (for photoluminescence). As said above, the emission of fluorescence (or phosphorescence) quanta always occurs at the lowest excited level of the given multiplicity, regardless of the level to which the electron was previously thrown. This means that the luminescence spectra generally do not depend on the method of excitation, including the wavelength of the exciting light (different vertical upward arrows in Fig. 5.1).

Vavilov's law states that the quantum yield of fluorescence does not depend on the wavelength of the exciting light.

The quantum yield of (photoinduced) fluorescence (φ_{fl}) is defined as:

$$\varphi_{fl} = \frac{N(\text{emitted quanta})}{N(\text{absorbed quanta})} \quad (5.7)$$

that is, the ratio of the number of emitted fluorescent quanta to the number of quanta absorbed by the sample.

The explanation for Vavilov's law is basically the same as for Kashi's rule. Any photon absorption leads to the formation of a molecule in an excited state. Due to the very high rate of thermalization of excess energy (inner conversion in Fig. 5.1), one can assume that any absorbed photon converts the molecule to the state S_1 . That is, the probability of $S_0 \rightarrow S_1$ transition upon absorption of a photon is equal to 1 and does not depend on the method of excitation, including the wavelength of the exciting light. Radiative transition of a molecule from the lowest sublevel of the excited state, accompanied by photon emission, occurs with a probability $\varphi_{fl} < 1$, which is the quantum yield of fluorescence. It is less than 1, since there is a certain probability ($1 - \varphi_{fl}$) of nonradiative transitions to the ground state or excited triplet state, transitions of excitation energy to neighboring molecules, etc.

The consequences of Vavilov's law and Kashi's rule are very "convenient" for researchers:

1. When studying photoluminescence, it is permissible to excite it with light with shorter wavelengths than the luminescence spectrum, which makes it possible to "separate" luminescence from direct scattering.
2. When studying chemiluminescence, the quantum yield of radiative relaxation can be considered equal to the quantum yield measured in photoluminescence experiments. Both of them are determined by the properties of the S_1 or T_1 levels, which do not depend on the way the molecule was excited.

Levshin's rule, also called the rule of mirror symmetry, states that fluorescence spectra are mirror-symmetric in shape to the long-wavelength band of the absorption spectrum if they are plotted in the frequency (energy) scale (see Fig. 5.4).

This phenomenon can be explained by the fact that the properties of a molecule, in particular the distance between vibrational sublevels and the probabilities of transitions to them, are mostly similar for molecules in the ground and electronically excited states. (In fact, excited molecules have a slightly altered structure of vibrational sublevels compared to molecules in the ground state, and the law of mirror symmetry is somewhat violated.)

5.2.2.2 Chemiluminescence Spectra

Recording chemiluminescence spectra (including biological UPE) is a very difficult technical task due to its extremely low intensity in most reactions. Most often, it is not possible to accurately measure the spectra at all because of the loss of light in the optical system. Interference filters are usually not suitable either, as they also transmit too little light. Therefore, weak chemiluminescence spectra, although coarse, are obtained using a series of light filters with a steep short-wavelength cutoff (cutoff filters). The long-wavelength transmission limits of these light filters typically lie outside the sensitivity range of light detectors and photomultipliers and thus can be assumed to be identical for all filters involved in the measurement.

The principle of recording chemiluminescence spectra with such edge filters is shown in Fig. 5.5.

Using the measured values of ΔS , the known λ and $\Delta\lambda$, and the photomultiplier sensitivity K_λ , we calculate I_λ . The resulting spectrum $I_\lambda = f(\lambda)$ looks like a histogram (Fig. 5.5), while the true, smooth spectrum corresponds to the outline of this bar graph.

In some cases, it is also possible to directly obtain chemiluminescence spectra using high-aperture monochromators and long-term signal accumulation (for some examples, see Chap. 6).

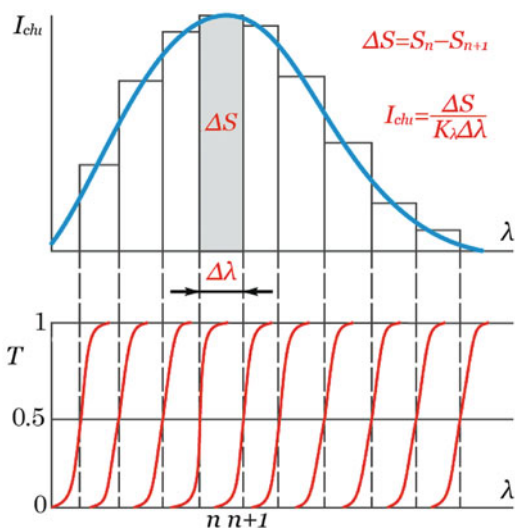


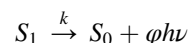
Fig. 5.5 Scheme for measuring chemiluminescence spectra using a series of edge light filters. At the top: the zones into which the chemiluminescence spectrum (envelope curve) is divided using light filters; I_{chl} is the intensity of chemiluminescence at a given wavelength λ ; ΔS is the light sum corresponding to the spectral interval $\Delta\lambda$; and K_λ is the photomultiplier sensitivity in the spectral region $\lambda_n - \lambda_{n+1}$. At the bottom: cutoff wavelengths of long pass light filters; T is transmission, and n is the serial number of the filter from left to right. (Redrawn with permission from Vladimirov and Potapenko (1989). Copyright 1989, the authors)

5.2.3 Luminescence Kinetics. The Lifetime of the Excited States

The lifetime of molecules in the excited state – τ , is obviously a very important characteristic. It can be used to judge the type of luminescence, the ratio of the probabilities of radiative and nonradiative relaxation, as well as the presence of absorbers in the system or the possibility of using them.

The main approach to its evaluation is measuring the luminescence kinetics $I_{\text{lum}}(t)$ after the end of photoexcitation.

Immediately after the action of the exciting light pulse, a certain number of molecules appear in the excited state S_1 , from which they begin to pass into the ground state S_0 , with the probability of photon emission φ , denoted as the quantum yield of luminescence. Each separately taken molecule will make this transition in its own time τ_i , that is, τ_i is the lifetime of the excited state of the given (i -th) molecule. If we consider the entire ensemble of molecules, then the process will have a probabilistic nature and will be described by the scheme:



where k is the probability of $S_1 \rightarrow S_0$ transition per unit time, and φ is the quantum yield of luminescence. The kinetics of this transition is similar to the kinetics of a first-order chemical reaction:

$$\frac{d[S_1]}{dt} = -k[S_1] \quad (5.8)$$

where $[S_1]$ is the quantity of excited molecules in the sample.

The value k has the dimension of frequency (s^{-1}), and its reciprocal $\tau = 1/k$ has the dimension of time and is the average lifetime of molecules in the excited state:

$$\tau = \frac{1}{k} = \langle \tau_i \rangle \quad (5.9)$$

From Eqs. (5.8) and (5.9), it follows:

$$\ln \frac{[S_1]_t}{[S_1]_0} = -\frac{t}{\tau}; [S_1]_t = [S_1]_0 e^{-t/\tau} \quad (5.10)$$

where $[S_1]_0$ and $[S_1]_t$ are the number of excited molecules at the initial moment and at the moment t .

The luminescence intensity is proportional to $d[S_1]/dt$, corrected for φ :

$$I_{\text{lum}} = \frac{d[h\nu]}{dt} = k\varphi[S_1] \quad (5.11)$$

Thus, the luminescence decay will also follow an exponential law:

$$\ln \frac{I_{\text{lum}}(t)}{I_{\text{lum}}(0)} = -\frac{t}{\tau}; I_{\text{lum}}(t) = I_{\text{lum}}(0) e^{-t/\tau} \quad (5.12)$$

where $I_{\text{lum}}(0)$ and $I_{\text{lum}}(t)$ are the luminescence intensity at time zero and after time t .

Box 5.1: Experimental Measurement of τ

One-Photon τ -Metry

1. The ratio of the initial value $I_{\text{lum}}(0)$ to the luminescence light sum S .

As can be seen from Eqs. (5.11) and (5.12), the luminescence light sum, that is, the total number of emitted light quanta is equal to:

$$S = \int_0^{\infty} I_{\text{lum}}(t) dt = I_{\text{lum}}(0) \cdot \tau \quad (5.13)$$

whence:

$$\tau = \frac{S}{I_{\text{lum}}(0)} \quad (5.14)$$

2. The time, the emission intensity decreases by the factor of e .

As can be seen from Eq. (5.12):

$$I_{\text{lum}}(\tau) = I_{\text{lum}}(0) \cdot e^{-1} \quad (5.15)$$

From where, τ is the point on the graph $I_{\text{lum}}(t)$, where the luminescence intensity is equal to $1/e$ ($\sim 37\%$) of the initial intensity $I_{\text{lum}}(0)$ (Fig. 5.6a).

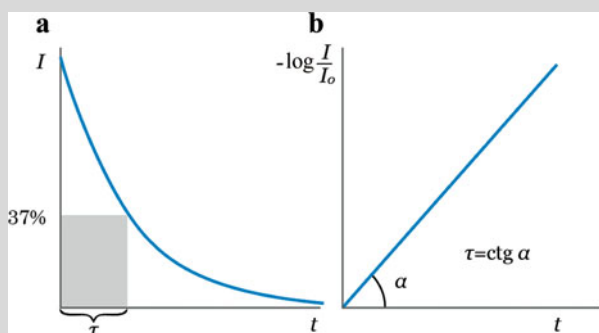


Fig. 5.6 Finding the lifetime (τ) of fluorescence. (Redrawn with permission from Vladimirov and Potapenko (1989). Copyright 1989, the authors)

Box 5.1 (continued)

3. The slope of the linear approximation $I_{\text{lum}}(t)$ in semi-logarithmic coordinates.

By taking the logarithm of Eq. (5.12), we get:

$$\begin{aligned} \ln I_{\text{lum}}(t) &= \ln I_{\text{lum}}(0) - \frac{t}{\tau} \\ \ln \frac{I_{\text{lum}}(t)}{I_{\text{lum}}(0)} &= -\frac{t}{\tau} \end{aligned} \quad (5.16)$$

Thus, the dependence $I_{\text{lum}}(t)$ in logarithmic coordinates along the y-axis is a straight line, the slope of which to the x-axis gives the value $1/\tau$ (Figs. 5.6b and 5.7).

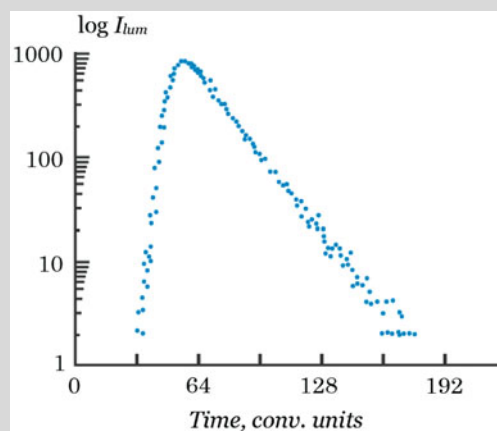


Fig. 5.7 Fluorescence decay of 8-methoxypsoralen in ethanol, measured by single-photon photometry. The y-axis is logarithmic. (Redrawn with permission from Vladimirov and Potapenko (1989). Copyright 1989, the authors)

As can be seen from the graph, on the whole $\log I_{\text{lum}}(t)$ is well approximated by a straight line (although individual points have their own random deviations). That is, the dependence of $I_{\text{lum}}(t)$ is exponential.

This method should be recognized as the best, since it uses all the experimentally recorded kinetics of $I_{\text{lum}}(t)$, and therefore, it is less sensitive to errors at individual points ($I_{\text{lum}}(0)$ or $I_{\text{lum}}(\tau)$ in methods 1 and 2).

If the curve $I_{\text{lum}}(t)$ differs from the exponential, this indicates additional effects complicating the system dynamics: excited state delocalization, energy migration to other molecules, photochemical processes, etc. In particular, there are often cases when the system under study contains several types of fluorescent molecules with different values of τ . Then the luminescence decay curve will be described by a linear combination of the corresponding exponential functions:

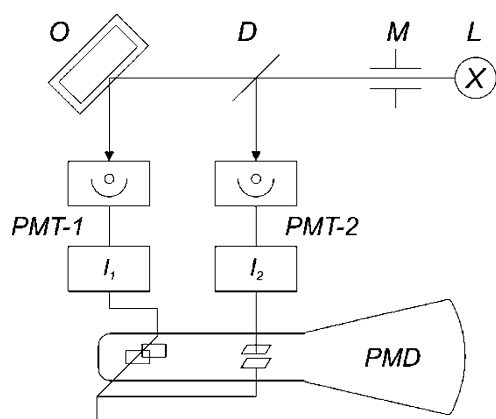


Fig. 5.8 Phase fluorometer. *D* semi-transparent mirror, *L* light source, *M* modulating device, *O* cuvette with the investigated object, *PMT-1* *PMT-2*, photomultipliers; and *PMD* phase-measuring device. (Redrawn with permission from Vladimirov and Potapenko (1989). Copyright 1989, the authors)

$$\ln I_{\text{lum}}(t) = \ln I_{\text{lum}}(0) - \sum_n (t/\tau_n) \quad (5.17)$$

To find each value of τ , it is necessary to decompose the total curve into individual exponents.

5.2.3.1 Phase τ -Metry

Phase τ -metry is based on splitting the exciting light beam, passing one part of the beam through the sample and comparing it with the second, reference part of it. The delay in the beam passing through the sample corresponds to the average lifetime of the excited state, τ .

In order to measure this delay, the light beam is premodulated with a high-frequency periodic function (see Fig. 5.8), so that:

$$I = I_0(1 + m \cos \omega t) \quad (5.18)$$

where ω is the circular modulation frequency ($\sim 10^8$ Hz), and m is the modulation depth coefficient (the ratio of the amplitude of the alternating component to the constant component). This modulated light flux is divided by a semi-transparent plate *D* into two parts: one (about 8%) is reflected from the plate and acts on the *PMT-2*, generating current that changes according to the described law. The other part of the light excites fluorescence in the cuvette *O*, and the fluorescence light falls on another receiver – *PMT-1*. The fluorescence light will also be modulated with a frequency ω , but since it is retained in the sample for an average lifetime τ , the modulation phase of the fluorescence light will lag behind the phase of the exciting light by some angle φ . Calculation shows that in this case, the modulation depth also slightly changes for fluorescence. Thus, the law of light change at the *PMT-1* receiver has the form:

$$\bar{f} = \bar{f}_0[1 + m\alpha \cos(\omega t - \varphi)] \quad (5.19)$$

where $\alpha < 1$.

With exponential law of fluorescence decay, the relationship between the phase shift φ , the factor α , and τ is simple:

$$\tan \varphi = \omega\tau; \alpha = \cos \varphi \quad (5.20)$$

That is, to measure τ , it is sufficient to measure the phase shift between the currents arising in the receivers *PMT-1* and *PMT-2*. This is carried out using phase-measuring devices.

5.2.4 Influence of Microenvironment on Luminescence Spectra and Quantum Yield

The environmental conditions surrounding the fluorescent molecules affect both the absorption and fluorescence spectra. The most important factors are the polarity and mobility of the surrounding molecules, and for liquid solutions, the dielectric constant and viscosity of the environment. Table 5.1 shows the positions of the maxima in the absorption (λ_a) and fluorescence (λ_f) spectra of the luminescent compound dimethylaminochalcone (DMC; see Fig. 5.9a) in solvents of different polarities (dielectric constant ϵ).

You can see the maxima in the absorption spectrum and especially in the fluorescence spectrum, shifting toward longer wavelengths with the increase in solvent polarity. An explanation of this phenomenon is given in Fig. 5.9.

The DMC molecule in the ground state has a relatively small dipole moment $\mu_0 \cong 1.7 \cdot 10^{-29}$ C · m, and, accordingly, is moderately solvated, that is, surrounded by oriented polar solvent molecules, such as water (Fig. 5.9b1). Photon absorption and the molecule excitation are accompanied by an increase in the molecule dipole moment to $\mu_{ex} \cong 7.7 \cdot 10^{-29}$ C · m (Fig. 5.9b2). This leads to polarization of the surrounding molecules, inductive displacement of their atoms in 10^{-12} – 10^{-13} s, and reorientation of the surrounding molecules (the solvation increase, Fig. 5.9b3), which takes $\sim 10^{-11}$ – 10^{-8} s. The waste of energy for all these processes leads to the

Table 5.1 Absorption and fluorescence maxima of the dimethylaminochalcone probe in different solvents

| Solvent | Dielectric constant ϵ | λ_a , nm | λ_f , nm |
|----------|--------------------------------|------------------|------------------|
| Heptane | 1.9 | 383 | 436 |
| Toluene | 2.4 | 402 | 472 |
| Butanol | 17.7 | 418 | 545 |
| Methanol | 32.7 | 418 | 547 |
| Water | 80 | 427 | 560 |

Adapted with permission from Vladimirov and Potapenko (1989). Copyright 1989, the authors

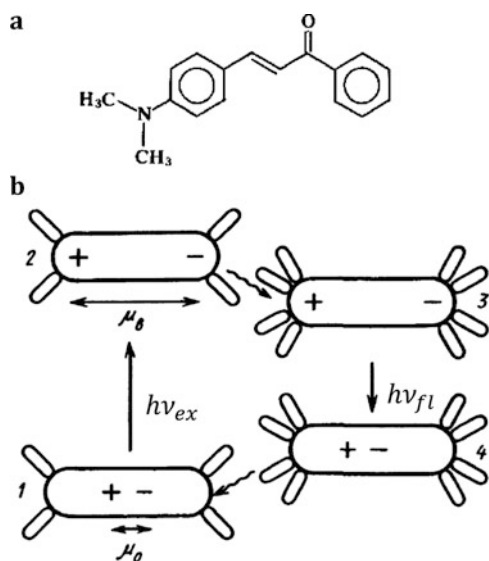


Fig. 5.9 Schematic explanation of the influence of solvent polarity on fluorescence. (a) Fluorescent molecule of dimethylaminochoalcone (DMC). (b) Changes in the dipole moment and solvation of a DMC molecule after absorption or emission of a photon: large ovals schematically denote DMC molecules and small ovals indicate solvent molecules. (Adapted with permission from Vladimirov and Potapenko (1989). Copyright 1989, the authors)

long-wavelength shift of the fluorescence band (short arrow at the transition 3–4 in Fig. 5.9b).

Upon excitation, the dipole moment can change in any way, both in magnitude and in direction; however, in almost all biologically interesting cases, it increases. As observed experimentally, the fluorescence band position depends on the solvent much stronger than the absorption band. For example, for tryptophan, the absorption spectrum is virtually independent of the solvent polarity (Fig. 5.10), while the fluorescence spectrum shifts by about 20 nm to longer wavelengths when changing from nonpolar to polar solvents (Fig. 5.11).

Obviously, this shift will be higher under the following conditions:

1. Large value of the difference $\mu_{ex} - \mu_0$.
2. The surrounding molecules have a high dipole moment.
3. The mobility of the surrounding molecules (the medium fluidity) and the lifetime of the excited molecules τ are large enough for the molecules of the medium to reorient themselves during the time τ .

Thus, the difference between the absorption and fluorescence maxima (shift according to Stokes's law) will be higher in the case of probes with a significant difference $\mu_{ex} - \mu_0$, long lifetime of the excited state, and in low-viscosity, polar media.

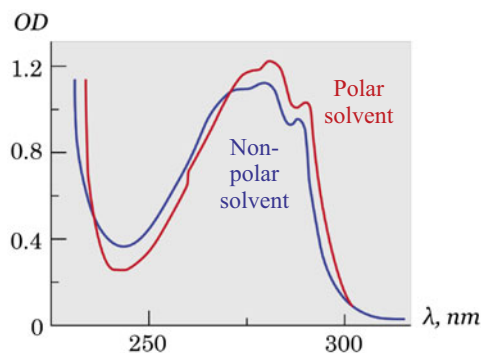


Fig. 5.10 Absorption spectra of tryptophan in water (red) and in 80% dioxane (blue). (Redrawn with permission from Vladimirov and Potapenko (1989). Copyright 1989, the authors)

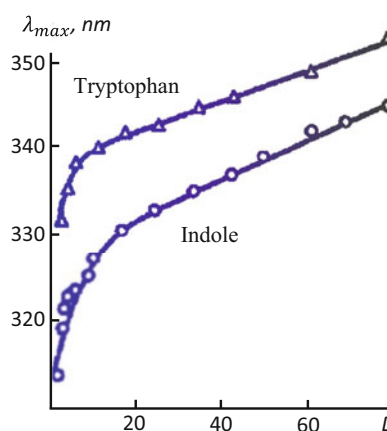


Fig. 5.11 Dependence of the position of the spectral maxima of tryptophan and indole fluorescence in water–dioxane mixtures. D is the dielectric constant of the mixture. (Redrawn with permission from Vladimirov and Potapenko (1989). Copyright 1989, the authors)

5.2.5 Special Cases of Luminescence

5.2.5.1 Delayed Luminescence

As mentioned above (Sect. 5.1.3), delayed luminescence is UPE generated at relaxation from the first electron-excited level with the same multiplicity as the ground state (similar to fluorescence), but at much greater characteristic times (similar to phosphorescence). The mechanism lies in the double electron transition $S_1 \rightarrow T_1 \rightarrow S_1$ (for S_0 ground state), which takes much time because of the spin ban in both transitions, and demands additional energy (heat or IR radiation), necessary for the energetically unfavorable reverse transition $T_1 \rightarrow S_1$.

Delayed luminescence was first observed at the measurement of the afterglow of luminescent compounds at different temperatures, for example, eosin solution in ethanol (Fig. 5.12). Their luminescence spectra have two distinct

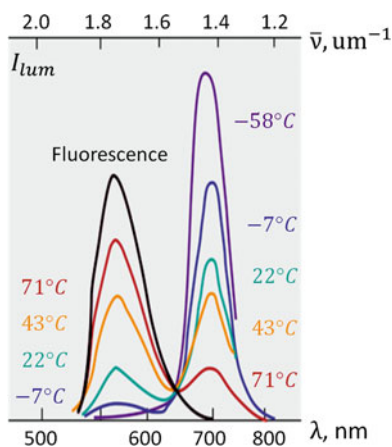


Fig. 5.12 Luminescence spectra of eosin in ethanol: (1) standard (“fast”) fluorescence at 22 °C; (2) long-lived emission at 71 °C; (3) at 43 °C; (4) at 22 °C; (5) at –7 °C; and (6) at –58 °C. The scale of intensities for 2–6 is 1000 times smaller than for 1. (Redrawn with permission from Vladimirov and Potapenko (1989). Copyright 1989, the authors)

Table 5.2 Processes of triplet state deactivation

| Eq. no. | Process | Scheme | Kinetic equation |
|---------|-----------------------------|--|--------------------------|
| 1 | Phosphorescence | $T_1 \xrightarrow{k_{ph}} S_0 + h\nu_{ph}$ | $\nu_{ph} = k_{ph}[T_1]$ |
| 2 | Delayed fluorescence | $T_1 \xrightarrow{k_{TS}} S_1 \rightarrow S_0 + h\nu_{fl}$ | $\nu_{TS} = k_{TS}[T_1]$ |
| 3 | Quenching with Q molecule | $T_1 + Q \xrightarrow{k_q} S_0 + Q$ | $\nu_q = k_q[T_1][Q]$ |

peaks, corresponding to (1) $S_1 \rightarrow S_0$ (Fig. 5.12, left peak) and (2) $T_1 \rightarrow S_0$ (Fig. 5.12, right peak) transitions. At low temperatures (Fig. 5.12, spectra –58 °C, –7 °C), the whole delayed luminescence is concentrated in the right ($T_1 \rightarrow S_0$) band. However, as temperature increases, the relative contribution of the left-hand peak increases, as molecules at the T_1 level have more chances for thermal excitation to higher vibrational sublevels and subsequent intercombinational conversion ($T_1 \rightarrow S_1$) (Fig. 5.12).

For a quantitative description of these phenomena, let us consider the kinetics of the triplet state deactivation processes (Table 5.2).

From the kinetic Eqs. 1 and 2 in Table 5.2, one can find the ratio of the intensities of delayed fluorescence to phosphorescence:

$$\frac{I_{dfl}}{I_{ph}} = \frac{\nu_{TS}}{\nu_{ph}} = \frac{k_{TS}}{k_{ph}} \quad (5.21)$$

which appears independent of quenching by extraneous molecules. The value of the constant k_{TS} should increase with increasing temperature, since the interconversion from

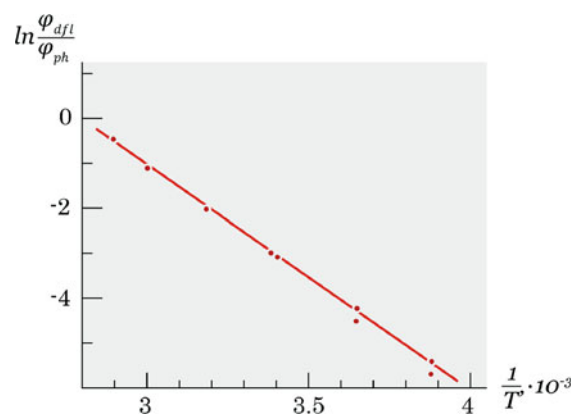


Fig. 5.13 Dependence of delayed eosin fluorescence in ethanol on temperature. (Redrawn with permission from Vladimirov and Potapenko (1989). Copyright 1989, the authors)

T_1 to S_1 state includes the process of thermal excitation of triplets to a higher vibrational level, from which the transition to S_1 occurs. Therefore, the constant k_{TS} can be represented as:

$$k_{TS} = A e^{-\frac{\Delta E}{RT}} \quad (5.22)$$

where A is a constant, ΔE is the activation energy of the transition to a higher vibrational level of the triplet state, and R is the universal gas constant.

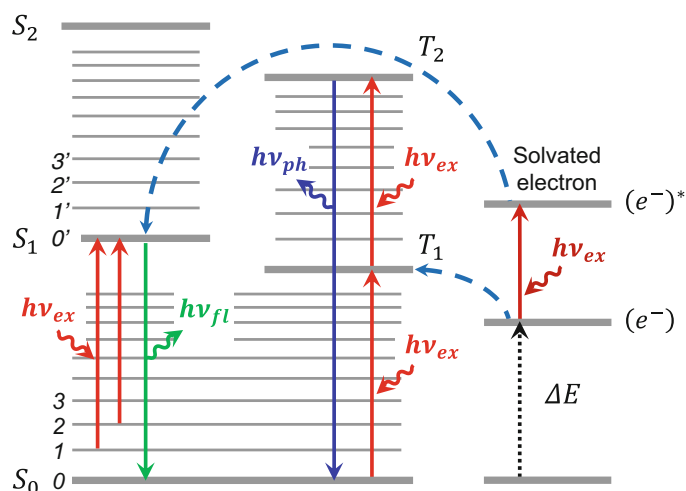
If we take into account that $k_{ph} = 1/\tau_0^{ph}$, where τ_0^{ph} is the radiational lifetime of triplets in the absence of quenching processes (see Sect. 5.3.4), for example, in a solid matrix at liquid nitrogen temperature, then we get:

$$\frac{\varphi_{dfl}}{\varphi_{ph}} = \varphi_{fl} \frac{k_{TS}}{k_{ph}} = \varphi_{fl} \tau_0^{ph} A e^{-\frac{\Delta E}{RT}} \quad (5.23)$$

Indeed, $\ln \varphi_{dfl}/\varphi_{ph}$ values, estimated from the spectra (Fig. 5.12) linearly depend on $1/T$ (Fig. 5.13). The ΔE value obtained from the graph slope coincides with the energy difference between the maxima of the two emission bands, thereby confirming the proposed mechanism.

The intensity of delayed fluorescence, as well as phosphorescence at room temperature, is extremely low due to the quenching of long-lived triplet states by oxygen molecules. Removal of oxygen, as well as increasing the medium viscosity, enhances delayed fluorescence and phosphorescence. So, for example, metalloporphyrins, included in the membranes of microorganisms, give delayed fluorescence with maxima at 590 and 630 nm and phosphorescence with maxima at 720 and 800 nm in the absence of oxygen (V.G. Petukhov, N.S. Osin, cited from Vladimirov and Potapenko 1989). Increasing the oxygen concentration in the medium suppresses both of them.

Fig. 5.14 The simplest possible mechanisms of anti-Stokes luminescence



5.2.5.2 Anti-Stokes Luminescence

Contrary to Stokes's law, there are quite specific processes in which the energy of the emitted quantum is greater than the energy of the absorbed quantum of light. This type of luminescence is called **anti-Stokes** or **upconverting**.

The simplest mechanism leading to such a phenomenon is the absorption of a quantum of light by molecules already in an excited state, either at nonzero vibrational sublevels of the ground electronic level S_0 (levels 1 and 2 in the example in Fig. 5.14) or at electronically excited levels (level T_1 in Fig. 5.14). Such processes, however, have extremely low efficiency due to the high rate of nonradiative relaxation of excited molecules and the low population of nonzero vibrational levels (see Sect. 5.1.2).

More complex but more efficient processes leading to anti-Stokes luminescence are associated with the transfer of energy to neighboring molecules or ions. Thus, solutions of tryptophan or tyrosine, frozen in liquid nitrogen and irradiated with UV, contain stabilized solvated electrons (e^- in Fig. 5.14). Upon careful heating of the system, these electrons recombine with the amino acid radical cations to form excited molecules (T_1 level in Fig. 5.14). If the system is additionally irradiated with red light, the solvated electron will move to a higher orbital ($(e^-)^*$ in Fig. 5.14) and, upon recombination, will be able to excite the amino acid molecule to the S_1 level.

Chapter 29 is devoted to other, more complex mechanisms of upconverting luminescence.

5.3 Nonradiative Relaxation: Luminescence Quenching

Quenching of luminescence refers to any process that reduces the luminescence intensity of a given substance. The main reason for it is the interaction of the luminescent compound molecules with other molecules in the medium, which can

generally be called quencher molecules. The action of most quencher molecules is based on perturbation of the luminophore electronic levels, an increase in the probability of nonradiative transitions (in particular, the $S_1 \rightarrow T_1$ transition), and the formation of nonluminescent quencher–luminophore complexes.

Understanding the processes of quenching is necessary for the study of real systems that contain a variety of different quenchers, distorting the luminescence picture. In practical terms, luminescence quenching can be used for experimental research on the molecular mechanisms of photon emission, which is often associated with the targeted introduction of quenchers into the system and the assessment of their effect on the system luminescence.

Besides, luminescence quenching can be used to study the diffusion of substances and their localization in the cell. If the luminophore is associated with a specific protein group or localized within certain organelles, its quenching can be used to estimate the protein conformation (i.e., the accessibility of the quencher to the molecule region where the luminophore is located) or the membrane permeability of these organelles.

5.3.1 Types of Quenching

Several different mechanisms of quenching can be distinguished:

1. **Reabsorption** is apparent quenching due to the absorption of luminescence quanta in the bulk of the sample itself. This trivial type of quenching carries little information about molecular processes. However, it becomes practically significant at high optical density or turbidity of the sample, as well as at a long optical path that a luminescence quantum must travel before leaving the sample.

2. **Dynamic quenching** is quenching caused by random collisions between **excited luminophore** molecules and **unexcited quencher** molecules, accompanied by a nonradiative transfer of excitation energy.
3. **Static quenching** is quenching associated with the formation of a nonluminescent complex between an **unexcited luminophore** molecule and a **quencher** molecule. Static quenching is often a complicating factor in dynamic quenching analysis.

Box 5.2: Quenching Molecules

The most active fluorescence quenchers include:

1. Heavy anions and cations, I^- , Br^- , Cs^+ , Cu^{2+} (facilitate the $S_1 \rightarrow T_1$ transition).
2. Paramagnetic ions and molecules, Mn^{2+} .
3. Oxygen. It refers to dynamic quenchers and quenches the fluorescence of almost all known fluorophores (Kautsky 1939; Cheng et al. 2020).
4. Hydrogen peroxide (Cavatorta et al. 1979), dinitrogen oxide, nitromethane (Dreeskamp et al. 1975), and nitroxides (Bieri and Wallach 1975; Green et al. 1973).
5. Aromatic and aliphatic amines are effective quenchers for the fluorescence of most unsubstituted aromatic hydrocarbons. In this case, quenching occurs due to the formation of a charge transfer complex in an excited electronic state (Knibbe et al. 1968).
6. Olefins (O'Connor and Ware 1976; Ware et al. 1974; Taylor 1971) and hindered saturated hydrocarbons (Gassman et al. 1981).
7. Halogens and halogenated substances: BrO_4^- (Winkler 1969), I^- (Lehrer 1971); chloroform, trichloroethanol (Eftink et al. 1977), bromobenzene (Medinger and Wilkinson 1965), methylmercury chloride (Lakowicz and Anderson 1980), and various compounds containing more than one chlorine atom (Lakowicz and Hogen 1980).
8. Purines, pyrimidines (Scott et al. 1970; Spencer and Weber 1972), *N*-methylnicotinamides, and *N*-alkylpyridinium, and picolinium salts (Davis 1973; Shinitzky and Rivnay 1977) can also be used as quenchers. For example, the fluorescence of flavin adenine dinucleotide (FAD) and reduced nicotinamide adenine dinucleotide (NADH) is quenched by the adenine moiety. The quenching of flavin fluorescence is due to both static and dynamic processes, while the quenching of dihydronicotinamide is mainly dynamic. Depending on the structural

Box 5.2 (continued)

- features of the compounds under study, the intramolecular complex in the ground state can be quite stable. As a consequence, both dynamic and static quenchings are often observed in FAD and NADH.
9. Solvent molecules. Usually, polar solvents such as water have the greatest quenching effect, apparently associated with the facilitation of the $S_1 \rightarrow T_1$ transition in the molecule of the fluorescent compound.

It should be noted that the quenching effect of solvent molecules is difficult to quantify. Since the luminescence of biologically important substances is always measured in one or another solvent, one can only compare the quantum yields of luminescence of a substance in different solvents. Since the solvent concentration is constant, the solvent quenching is always included in the process of "inner conversion" of excitation (see Fig. 5.1). Therefore, quenchers in a narrower sense are usually called not the solvent but the molecules of other compounds dissolved in it, whose increasing concentration reduces the quantum yield of luminescence.

Due to the fact that many substances can act as quenchers, it is possible to find a combination of luminophore and quencher for the task at hand. It is important to note that not all luminophores are quenched by any of the listed substances. The quenching effect depends on its mechanism due to the structure of individual molecules. This fact can be used to selectively quench a particular luminophore.

5.3.2 Reabsorption

Reabsorption is the absorption of luminescence quanta in the bulk of the sample, including photon absorption in the anti-Stokes region by the luminescent substance itself. It leads to a weakening of the luminescence intensity in the short-wavelength part of the spectrum (Fig. 5.15).

The nature of such distortions of the luminescence spectrum is completely determined by the absorption spectra of substances in the system. The reabsorption effect increases with an increase in the sample optical density in the luminescence detection region. Reabsorption will be maximal in the region where the luminescence and absorption spectra overlap, that is, in the short-wavelength part of the luminescence spectrum.

For a researcher, reabsorption is mostly a parasitic process; it complicates the study of system luminescence and

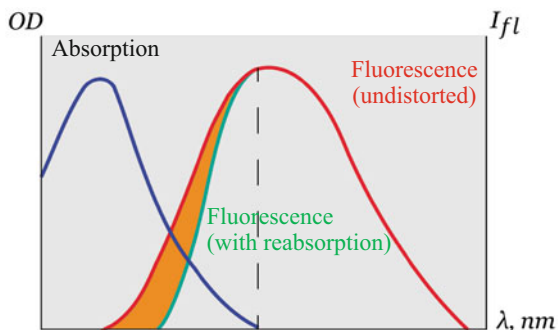


Fig. 5.15 Distortion of fluorescence spectra as a result of reabsorption: blue – absorption spectrum; red – undistorted fluorescence spectrum; and magenta – distorted fluorescence spectrum. (Redrawn with permission from Vladimirov and Potapenko (1989). Copyright 1989, the authors)

molecular processes, which are mostly analyzed by adding quenchers of other types. To reduce reabsorption, one should:

- Use samples with low optical density.
- Measure luminescence from the front wall of the cuvette.
- Excite luminescence at the maximum absorption of the substance (if it is photoluminescence).

5.3.3 Dynamic Quenching

Dynamic quenching (collisional quenching) is the transfer of energy from an excited molecule of a fluorophore F^* to an unexcited molecule of a quencher Q on their collision (Fig. 5.16):

A characteristic feature of this type of quenching is that the quantum yield of luminescence φ is directly proportional to the lifetime of the excited state τ (see below).

Let us consider a solution with a fluorophore F and a dynamic quencher Q , illuminated with a constant, exciting light. As relaxation of F from higher excited levels to S_1 occurs orders of magnitude faster than the $S_1 \rightarrow S_0$ transition, it is enough to consider only S_1 and S_0 levels of F (Fig. 5.17).

The vertical arrows in Fig. 5.17 show electronic transitions in F . The values k_f , k_{ic} , and k_q , are the rate constants of the corresponding transitions, respectively: k_f – accompanied by photon emission (fluorescence), k_{ic} – nonradiative relaxation due to inner properties of F , and k_q – nonradiative relaxation due to collision of the excited F^* with a quencher molecule Q .

Representing the above transitions in kinetic form, we get the following (see Table 5.3).

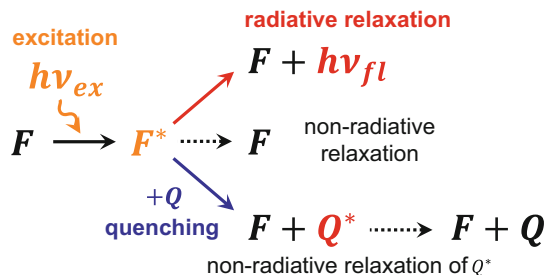


Fig. 5.16 Dynamic quenching of fluorescence. F , fluorophore molecule, F^* , electronically excited F , $h\nu_{ex}$, quantum of exciting light, $h\nu_{fl}$, quantum of fluorescence, Q , quencher molecule, and Q^* , electronically excited Q

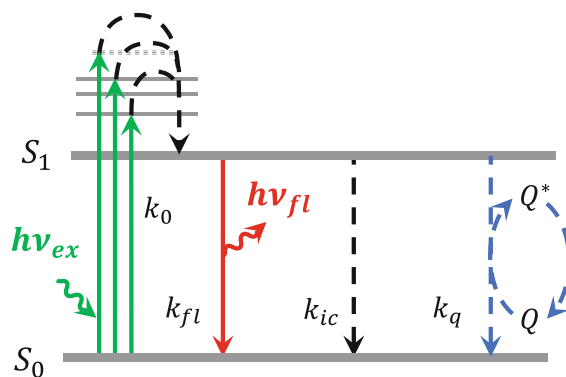


Fig. 5.17 Relaxation of an excited fluorophore molecule F in the presence of a quencher

$k_f, k_{ic}, k_q - S_1 \rightarrow S_0$ relaxation paths:
 k_f (fluorescence) – radiative relaxation (with emission of the fluorescence quantum $h\nu_{fl}$);
 k_{ic} (internal conversion) – nonradiative relaxation, due to the system internal properties;
 k_q – energy transfer to the Q molecule;
 $h\nu_{ex}$ – the exciting light quantum;
 $h\nu_{fl}$ – the fluorescence quantum.
 Solid lines are light absorption or emission. Dotted lines are nonradiative transitions

Table 5.3 Processes of electronic excitation and relaxation

| Process | Scheme | Kinetic equation |
|-----------------------------|-----------------------------------|-------------------------|
| Absorption of quanta | $S_0 + h\nu_{ex} \rightarrow S_1$ | $v_0 = k_0 I_0 [S_0]$ |
| Luminescence | $S_1 \rightarrow S_0 + h\nu_{fl}$ | $v_{fl} = k_{fl} [S_1]$ |
| Internal conversion | $S_1 \rightarrow S_0$ | $v_{ic} = k_{ic} [S_1]$ |
| Quenching with Q molecule | $S_1 + Q \rightarrow S_0 + Q$ | $v_q = k_q [S_1][Q]$ |

5.3.3.1 Luminescence Quantum Yield

If the system is under continuous illumination, it will finally get into a stationary state, and the total rate of $S_0 \rightarrow S_1$ excitation will be equal to the total rate of all $S_1 \rightarrow S_0$ transitions:

$$v_0 = v_{fl} + v_{ic} + v_q. \quad (5.24)$$

By definition, the quantum yield of photo-induced fluorescence is:

$$\varphi = \frac{\text{number of emitted quanta}}{\text{number of absorbed quanta}}.$$

The number of emitted quanta equals to the number of radiative transitions v_{fl} . Thus:

$$\varphi = \frac{v_{fl}}{v_0} = \frac{v_{fl}}{v_{fl} + v_{ic} + v_q} \quad (5.25)$$

Let us denote the fluorescence quantum yield in the presence of quencher as φ_q :

$$\varphi_q = \frac{k_{fl}}{k_{fl} + k_{ic} + k_q[Q]} \quad (5.26)$$

and in the absence of quencher as φ :

$$\varphi = \frac{k_{fl}}{k_{fl} + k_{ic}}. \quad (5.27)$$

Obviously, $\varphi > \varphi_q$.

Dividing Eq. (5.27) by Eq. (5.26), we obtain the Stern–Volmer equation for the degree of fluorescence quenching by the quencher Q :

$$\frac{\varphi}{\varphi_q} = \frac{k_{fl} + k_{ic} + k_q[Q]}{k_{fl} + k_{ic}} = 1 + \frac{k_q}{k_{fl} + k_{ic}}[Q] = 1 + K_{dyn}[Q], \quad (5.28)$$

where

$$K_{dyn} = \frac{k_q}{k_{fl} + k_{ic}}, \quad (5.29)$$

is the Stern–Volmer dynamic quenching constant.

Since this type of quenching involves only excited molecules of the fluorophore F^* , and the unexcited F molecules are not involved, the absorption of the fluorescent substance (total excitation rate v_0) does not depend on the quencher. Then Eq. (5.28) can be written in the form:

$$\frac{I}{I_q} = 1 + K[Q], \quad (5.30)$$

where I and I_q are the fluorescence intensities for the same method of excitation in the absence and presence of the quencher.

Equation (5.30) is commonly used in experimental work. Having measured the luminescence intensity in the absence of the quencher and at its various concentrations, the

dependence $I/I_q = f([Q])$ is plotted. In the absence of other processes that complicate the system, the graph will be a straight line with a slope equal to K_{dyn} , which can serve as a measure of the quencher efficiency.

5.3.3.2 Excited State Lifetime

As already mentioned, the average lifetime of the molecule's excited state is the reciprocal of the transition constant from the excited state to the ground state: $\tau = 1/k$ (Sect. 5.3.3, Eq. (5.9)).

If there were no nonradiative transitions, the $S_1 \rightarrow S_0$ rate would be determined only by the radiative transition rate constant k_{fl} (Fig. 5.17). The inverse value τ_0 is called the radiational lifetime of molecules in the excited state:

$$\tau_0 = \frac{1}{k_{fl}}. \quad (5.31)$$

If, in addition to radiative transitions, we “allow” the processes of internal conversion (arrow k_{ic} in Fig. 5.17), we'll get:

$$\tau = \frac{1}{k_{fl} + k_{ic}}. \quad (5.32)$$

Finally, if there is also a quencher Q :

$$\tau_q = \frac{1}{k_{fl} + k_{ic} + k_q[Q]}. \quad (5.33)$$

Comparing Eqs. (5.32) and (5.33), we can easily see that the quencher, accelerating the $S_1 \rightarrow S_0$ transition, decreases τ . Dividing Eq. (5.32) by Eq. (5.33), we obtain an analog of the Stern–Volmer equation for the ratio of the excited state lifetimes in the absence and presence of the quencher:

$$\frac{\tau}{\tau_q} = 1 + K_{dyn}[Q]. \quad (5.34)$$

Dividing Eq. (5.32) by Eq. (5.31), we obtain a similar expression for the (theoretical) ratio of the excited state lifetimes in the absence and presence of internal quenching (it coincides with Eq. (5.27) for the quantum yield of luminescence in the absence of the quencher):

$$\frac{\tau}{\tau_0} = \frac{k_{fl}}{k_{fl} + k_{ic}} = \varphi. \quad (5.35)$$

Similarly, dividing Eq. (5.33) by Eq. (5.31), we get (compare with Eq. (5.26)):

$$\frac{\tau_q}{\tau_0} = \frac{k_{fl}}{k_{fl} + k_{ic} + k_q[Q]} = \varphi_q. \quad (5.36)$$

5.3.3.3 Summary

Thus, regardless of the presence of luminescence quenchers, the luminescence quantum yield (φ in the absence of the quencher or φ_q in its presence) is the ratio of the excited state lifetime (with or without the quencher, respectively) to the radiational lifetime τ_0 . Obviously, for molecules of any given substance, τ_0 is the theoretical limit of the excited state lifetime, when the relaxation $S_1 \rightarrow S_0$ proceeds exclusively along the radiative path, that is, luminescence quantum yield $\varphi = 1$.

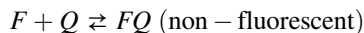
As already mentioned, in practice, quenching data are usually presented in the coordinates $I/I_q = f([Q])$, since I/I_q (which equals φ/φ_q in the first approximation), as expected, should linearly depend on the quencher concentration. The graph gives the y-axis cutoff equal to one and the slope equal to K_{dyn} (Eq. (5.34), see below, Fig. 5.18a). It is useful to note that $1/K_{dyn}$ is equal to the concentration of the quencher at which $\varphi/\varphi_q = 2$, that is, 50% fluorescence is quenched.

A straight-line dependence in the Stern–Volmer coordinates usually indicates the existence of one type of fluorophores in the solution. If two types of fluorophores are present, the Stern–Volmer plot deviates from linearity.

It is important to know that the linearity observed in the Stern–Volmer coordinates does not yet prove that fluorescence quenching is dynamic. In the next section, we will see that static quenching also gives a straight line in Stern–Volmer coordinates. In general, static and dynamic quenching can be distinguished by their dependence on temperature and viscosity, or, more preferably, by measuring the decay time of fluorescence (see Sect. 5.3.6).

5.3.4 Static Quenching

Static quenching is associated with the formation of nonfluorescent complexes FQ of an unexcited fluorophore molecule (F) with a quencher molecule Q :



Let us denote the equilibrium constant of this reaction (inverse to the $[FQ]$ dissociation constant) as K_{st} :

$$K_{st} = \frac{[FQ]}{[F][Q]}. \quad (5.37)$$

If the complexed form does not fluoresce and the absorption of F and the FQ complex does not differ, then the remaining fluorescence fraction (I_q/I) is determined by the noncomplexed part of the total amount of fluorophores $[F]/([F] + [FQ])$, that is,

$$\frac{I}{I_q} = \frac{[F] + [FQ]}{[F]} = 1 + \frac{[FQ]}{[F]}, \quad (5.38)$$

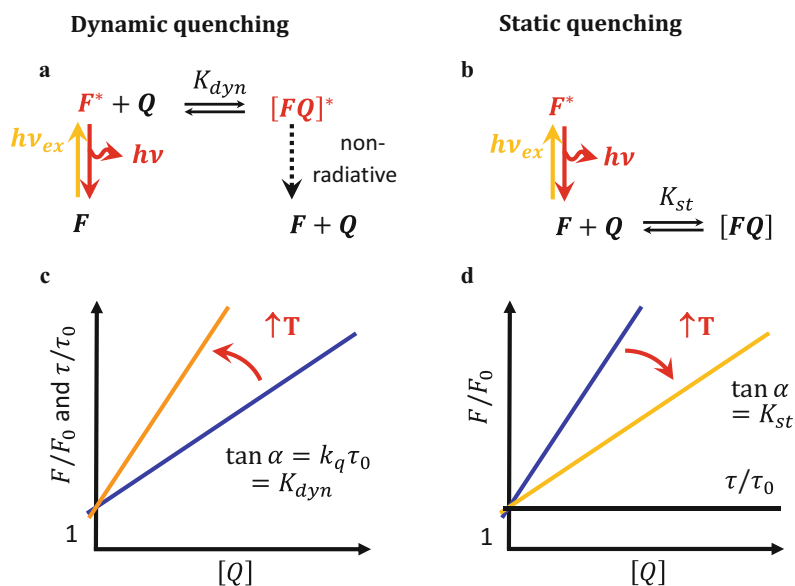
whence

$$\frac{I}{I_q} = 1 + K_{st}[Q], \quad (5.39)$$

and

$$\frac{\varphi}{\varphi_q} = 1 + K_{st}[Q], \quad (5.40)$$

Fig. 5.18 Comparison of dynamic and static quenching. (Adapted from Lakowicz (2006). Copyright 2006, with permission from Springer Nature)

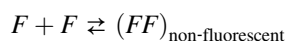


analogous to the Stern–Volmer equations (Eqs. (5.28) and (5.30)).

This is mostly fulfilled for low optical densities but is violated if the complex absorption differs from that of the fluorescent substance.

Thus, static and dynamic quenching cannot be distinguished by the dependence of the fluorescence intensity on the quencher concentration.

A particular case of static quenching is the so-called concentration quenching, which is associated with the formation of nonfluorescent dimers and larger aggregates of fluorophore molecules at high concentrations:



The phenomenon of concentration quenching is widespread and finds useful applications in a number of cases, for example, to observe the accumulation of certain fluorescent dyes by cells or mitochondria. As the substance accumulates, its concentration in the environment decreases. Inside cells or organelles, the dye concentration is very high, and nonfluorescent complexes are formed. Sometimes this picture is further complicated by the formation of nonfluorescent complexes with intracellular compounds, for example, hemoproteins.

5.3.5 Comparison of Static and Dynamic Quenching

As shown above (Eqs. (5.30) and (5.39)), fluorescence intensity during static and dynamic quenching depends on the quencher concentration in the same way, which makes it impossible to distinguish them by fluorescence quantum yield or intensity. Still, they can be distinguished by lifetimes depending on temperature, viscosity, and absorption spectra (Fig. 5.18):

- Under static quenching, complex-bound fluorophores (FQ) do not fluoresce, and only free fluorophores F do. Thus, the fluorescing states F^* remain unchanged, and, therefore, their lifetime remains equal to τ : $\tau/\tau_q = 1$. In contrast, for dynamic quenching $\tau/\tau_q = \varphi/\varphi_q$ (see above, Eqs. (5.28) and, (5.34)).
- Dynamic quenching is diffusion-dependent. Since an increase in temperature leads to an increase in diffusion coefficients, it can be expected that the bimolecular rate constant of quenching k_q in the equation $v_q = k_q[S_1][Q]$ will increase with increasing temperature, and hence, K_{dyn} will also increase. More precisely, one should expect that k_q will be proportional to T/η , since the diffusion coefficients are proportional to this ratio (the Stokes–Einstein equation, see, e.g., Lakowicz 1983).

In the case of static quenching, on the contrary, with an increase in temperature, the complex stability most likely decreases, and so does the value of K_{st} .

Another additional method for distinguishing static from dynamic quenching is a thorough analysis of the fluorophore absorption spectrum. Dynamic quenching affects only the fluorophore excited state, and it can be assumed that it will not change the absorption spectra. In contrast, the formation of a complex in the ground state often leads to a disturbance in the fluorophore absorption spectrum.

5.3.6 Mixed Dynamic and Static Quenching

In many cases, the fluorophore can be quenched both by collisions and by the formation of a complex with the quencher. A characteristic feature of the Stern–Volmer graph in such cases is the upward deflection and concavity with respect to the y-axis (Fig. 5.19). Residual fluorescence (I_q/I) is determined by the product of the fraction not bound in the complex (F) and the fraction not quenched by diffusion collisions.

Applying simultaneously the theory of dynamic (Sect. 5.3.4) and static quenching (Sect. 5.3.5), we get:

$$\frac{\varphi}{\varphi_q} = (1 + K_{\text{dyn}}[Q])(1 + K_{\text{st}}[Q]). \quad (5.41)$$

This modified form of the Stern–Volmer equation is a second-order equation with respect to $[Q]$, which explains the upward bending of the graph observed when the fluorophore is simultaneously quenched by both static and dynamic mechanisms.

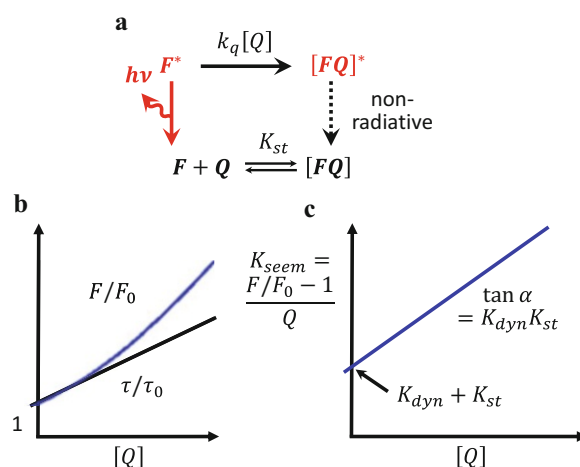


Fig. 5.19 Graphical dependencies for mixed dynamic and static quenching of fluorophores of the same species. (Adapted from Lakowicz (2006). Copyright 2006, with permission from Springer Nature)

The proportion of dynamic quenching in the observed fluorescence decrease can be determined from the change in the decay time, that is, by the dependence $\tau/\tau_q = 1 + K_{\text{dyn}}[Q]$. If there is no such data, then Eq. (5.41) can be converted to graphically define K_{st} and K_{dyn} . After multiplying the terms in parentheses, we get:

$$\frac{\varphi}{\varphi_q} = 1 + (K_{\text{st}} + K_{\text{dyn}})[Q] + K_{\text{st}}K_{\text{dyn}}[Q]^2 = 1 + K_{\text{seem}}[Q], \quad (5.42)$$

where K_{seem} is the apparent quenching rate constant, calculated for each quencher concentration:

$$K_{\text{seem}} = (K_{\text{st}} + K_{\text{dyn}}) + K_{\text{st}}K_{\text{dyn}}[Q]. \quad (5.43)$$

The plot of K_{seem} versus $[Q]$ is a straight line with a cutoff on the y-axis equal to $K_{\text{st}} + K_{\text{dyn}}$ and a slope equal to $K_{\text{st}}K_{\text{dyn}}$ (Fig. 5.19). Individual values of constants can be obtained by solving the system:

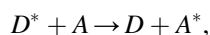
$$\begin{cases} K_{\text{st}} + K_{\text{dyn}} = K_{\text{seem}}(\text{at } [Q] = 0) \\ K_{\text{st}}K_{\text{dyn}} = \tan \alpha \end{cases}. \quad (5.44)$$

The dynamic component is usually chosen as a solution comparable in magnitude to the expected diffusion-controlled value, in dependence on temperature or viscosity, or according to other available information.

5.4 Nonradiative Relaxation: Energy Transfer

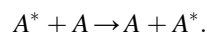
Another type of process affecting luminescence intensity and deeply connected to luminescence quenching is the transfer of electronic excitation between different molecules. A vivid example of this kind of process is dynamic quenching, discussed in Sect. 5.3.4.

In a general form, the transfer of electronic excitation energy between two molecules can be represented as a diagram



where D is the donor molecule; A is the acceptor molecule; and D^* and A^* are their electron-excited states.

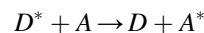
The initially excited molecule D^* passes into the ground (unexcited) state D , donating its excitation energy to the acceptor molecule A and exciting it to A^* . Donor and acceptor molecules can be either different or identical:



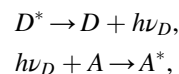
Energy transfer between identical molecules (which can be multiple) is called energy migration.

5.4.1 Basic Mechanisms of Energy Transfer

Energy transfer can occur either directly:



which is called **nonradiative energy transfer**, or through a luminescence quantum, emitted by D and absorbed by A :



which is called **radiative energy transfer**.

The latter mechanism has been discussed in Sect. 5.3.3 as reabsorption. As a rule, it does not carry information about the processes in the system and is only a complicating phenomenon that interferes with the investigation of the main molecular mechanisms.

Nonradiative energy transfer occurs either during kinetic collisions of the donor and acceptor molecules or due to resonant processes.

The first variant was described by Terenin and Ermolaev (1952) and was called **exchange-resonant energy transfer**. The second variant can be observed if the diffusion-dependent interaction of molecules is excluded, for example, in very viscous solutions or in a glassy matrix. It was described by Vavilov (1950), Galanin (1960), and Förster (1946, 1948, 1960), based on studies of solution fluorescence depolarization and sensitized fluorescence, and was called **inductive-resonant energy transfer**.

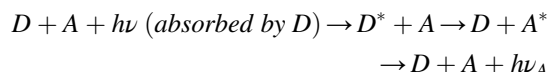
Energy transfer processes require rather sophisticated methods to study (see Terenin 1947, 1967):

1. Measuring the fluorescence polarization.
In viscous, dilute solutions with a sufficiently large distance between molecules, the polarization degree P is equal to the maximum P_0 . Yet, an increase in the solution concentration (i.e., a decrease in intermolecular distances) makes energy transfer more probable. Theoretical calculations show that even a single energy transfer between randomly oriented molecules causes an almost complete depolarization of the sample fluorescence.
2. Measuring the decrease in the donor fluorescence quantum yield in the presence of an energy acceptor.
This process can be carried out either by dynamic quenching (the Stern–Volmer mechanism; see Sect.

5.3.4) or by inductive-resonant energy transfer. In the latter case, the energy transfer does not depend on the medium viscosity, which allows it to be distinguished from dynamic quenching by using similar solutions with different viscosities.

- Measuring the sensitized luminescence of the energy acceptor.

Sensitized luminescence is photon emission by energy acceptor molecules under the action of radiation, absorbed mainly by donor molecules:



- Measuring a sensitized photochemical reaction: the active radiation is absorbed mainly by the donor molecules, and the acceptor molecules enter the photochemical process.
- Measuring the decrease in the decay time of the donor fluorescence (τ_D) in the presence of an acceptor, as well as the increase in τ_A upon excitation in the donor absorption band (since in the case of transfer from D^* to A , the time τ_A includes lifetime of donor molecules up to the moment of energy transfer + lifetime of the excited state of acceptor molecules).

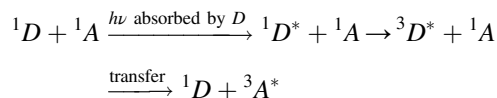
Here we will give a brief overview of the two main types of energy transfer mentioned above.

5.4.2 Exchange-Resonant Energy Transfer

The exchange-resonant transfer occurs only at direct contact of molecules and can be realized only if the electron shells of

the adjacent molecules D^* and A overlap. The transfer distance in the absence of diffusion is approximately 1.1–1.3 nm, which corresponds to acceptor concentrations of 0.2–0.3 M (Vladimirov and Potapenko 1989).

Exchange-resonant transfers can be either singlet–singlet or triplet–triplet. The triplet–triplet mechanism is more efficient because of the longer lifetime of the donor triplet excited state. Here is the scheme of the triplet–triplet transfer:

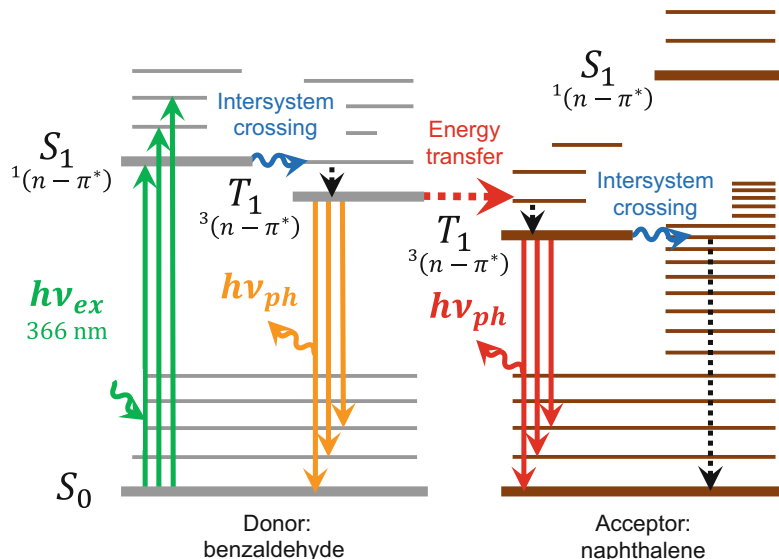


It was first experimentally observed through the successful selection of donor–acceptor pairs, in particular benzaldehyde and naphthalene, of which benzaldehyde has higher S_1 level than naphthalene, and lower T_1 level (Fig. 5.20).

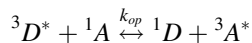
This allows selective $S_0 \rightarrow S_1$ excitation of benzaldehyde and further $T_1 \rightarrow T_1$ energy transfer between the molecules. Indeed, while naphthalene molecules absorb radiation with $\lambda < 310$ nm, benzaldehyde well absorbs light at $\lambda = 366$ nm. Thus, if this mixture is irradiated at $\lambda = 366$ nm, only donor molecules are excited, and direct excitation of acceptor is excluded. The singlet–singlet energy transfer from D^* to A is also highly improbable due to energy considerations. Still, the triplet–triplet energy transfer is quite favorable, as the T_1 level of benzaldehyde is above that of naphthalene. This was experimentally detected by naphthalene phosphorescence (see Terenin 1967).

In liquid solutions, triplet–triplet energy transfer was discovered by Bäckström and Sandros (1958, 1960; Sandros and Bäckström 1962), with 2,3-butanedione used as the

Fig. 5.20 Exchange-resonant energy transfer from benzaldehyde to naphthalene. (Redrawn with permission from Vladimirov and Potapenko (1989). Copyright 1989, the authors)



donor and various aromatic hydrocarbons with T_1 levels either below or above that of 2,3-butanedione, used as acceptors. In the absence of oxygen, 2,3-butanedione in benzene solutions is capable of bright phosphorescence at room temperature. If the acceptor T_1 level is lower than that of the donor, the donor phosphorescence is quenched by highly efficient $D \rightarrow A$ triplet–triplet energy transfer. If the energies of ${}^3D^*$ and ${}^3A^*$ are comparable, the resulting excited molecule ${}^3A^*$ can again transfer its excitation energy to the molecule 1D :



where k_{op} is the energy transfer rate constant. Thus, the observed transfer rate decreases. Finally, if the donor T_1 level is higher than that of the acceptor by 15 kJ/mol or more, the transfer requires thermal activation and is additionally decreased by reverse energy transfer from ${}^3A^*$ to 3D .

Currently, there are few examples of exchange-resonant energy transfer known for biological systems. Thus, Krasnovsky Jr. showed that the quantum yield of chlorophyll phosphorescence in the leaf is ~ 2000 times lower than in solution, supposedly due to quenching of the chlorophyll triplet excited states by carotenoids via the exchange-resonance transfer mechanism (see Krasnovsky and Kovalev 2014). Thus, carotenoids prevent the photogeneration of singlet oxygen by chlorophylls by quenching chlorophyll triplets, thereby protecting the photosynthetic apparatus from oxidative damage. Accordingly, carotenoid-free mutants of photosynthetic organisms are known to die in the light.

Triplet–triplet energy transfer in double-stranded DNA is also possible between nucleotides toward thymine, which contributes to the predominant formation of thymine dimers under UV irradiation of DNA (Xu and Nordlund 2000; Curutchet and Voityuk 2011).

The phenomenon of exchange-resonant energy transfer finds application in some biological experiments, in particular for the activation of chemiluminescence. Kuznetsov and Sevchenko (1962) showed exchange-resonant energy transfer in rare-earth metal chelates: from the organic ligand triplet state to the rare-earth ion. After that, the excited ion emits a bright luminescence. This phenomenon was used by Vladimirov (1967) to activate natural luminescence and experimentally observe free radical processes. The author added ions of Eu^{3+} to the suspension of biological particles, thus activating chemiluminescence by 2–3 orders of magnitude due to energy transfer from triplet ketones and aldehydes formed during chemical reactions, to Eu^{3+} .

5.4.3 Inductive-Resonant Energy Transfer

This mechanism consists of the resonant transfer of excitation energy from an excited donor molecule (D^*), forming a dipole, to an acceptor molecule (A), induced to form a dipole by electrostatic interactions with the neighboring D^* (Förster 1946, 1948, 1960).

This requires two types of conditions: resonance and induction. The resonance condition means that the energy difference between the ground and excited electronic levels of both molecules must be the same (the oscillators natural frequencies must coincide). The induction condition means that the interaction between molecules must be strong enough.

The energy transfer rate constant k_t is described by the Förster equation (Förster 1959):

$$k_{et} = \alpha \frac{\Phi^2}{R^6} \frac{\varphi_D}{\tau_D} \frac{S_{AD}}{S_D} \quad (5.45)$$

where α is the proportionality coefficient, n is the refractive index; φ_D is the quantum yield of donor fluorescence; τ_D is the donor excited state lifetime in the absence of energy transfer; Φ is the factor of mutual orientation of the electronic transition vectors in the donor molecule during emission and in the acceptor molecule during photon absorption; $S_{AD} = \int_0^\infty F_D(\bar{\nu}) \varepsilon_A(\bar{\nu}) \bar{\nu}^{-4} d\bar{\nu}$ is the overlap integral of the donor fluorescence and acceptor absorption spectra; $\bar{\nu}$ is the radiation frequency; ε_A is the molar absorption coefficient; F_D is the donor fluorescence intensity in relative units; $S_D = \int_0^\infty F_D(\bar{\nu}) d\bar{\nu}$ is the area under the donor fluorescence curve; and the use of the S_{AD}/S_D ratio allows one to normalize the donor fluorescence intensities when calculating the spectral overlap (Fig. 5.21).

Thus, for efficient energy transfer, the following rules must be met:

1. The energy donor D^* must be capable of luminescence (as the transfer probability is proportional to the rate constant of its radiative transition, φ_D).
2. The donor fluorescence spectrum $F_D(\nu)$ should overlap with the acceptor absorption spectrum $\varepsilon_A(\nu)$ (resonance condition).
3. The donor and the acceptor molecules must be sufficiently close (since the probability of energy transfer is inversely proportional to the sixth power of the distance R between them).
4. The donor and the acceptor must be well oriented relative to each other (orientation factor Φ^2):

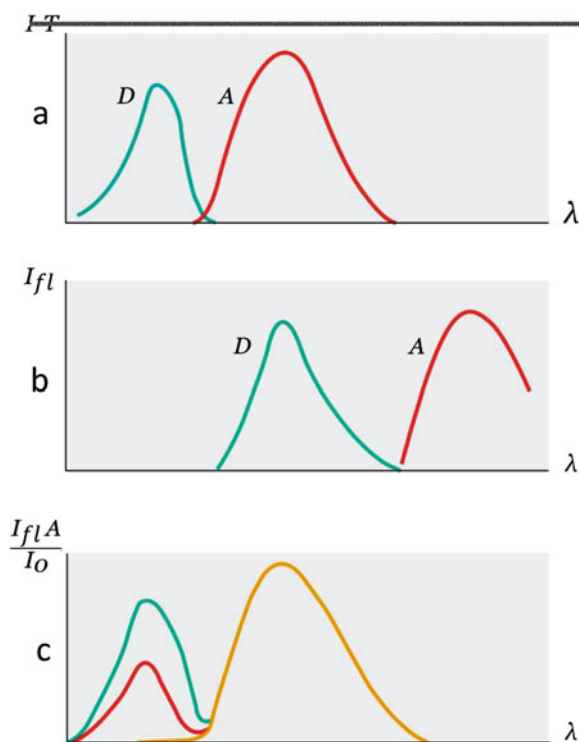


Fig. 5.21 Inductive-resonant energy transfer (D – donor and A – acceptor). (a) Absorption spectra; (b) fluorescence spectra; and (c) excitation of the acceptor fluorescence under conditions of: 100% energy transfer from the donor (magenta), partial transfer (red), and in the absence of transfer (yellow). (Redrawn with permission from Vladimirov and Potapenko (1989). Copyright 1989, the authors)

- If the dipole moments of the donor radiation and the acceptor absorption are perpendicular to each other, the energy transfer will not occur ($\Phi^2 = 0$).
- If the moment's direction coincides with the direction of the radius vector connecting D^* and A, the transfer probability is maximum ($\Phi^2 = 4$).
- In solutions with chaotic orientations of molecules and their rapid rotation $\Phi^2 = 2/3$.

5.4.4 Energy Transfer in Crystals

In 1931, Frenkel (1931a, b) came to the conclusion that electronic excitation in a system of identical molecules, such as crystals, is impossible to localize. He predicted that the excited state would inevitably transfer through the crystal and called it an **exciton**, similar to a particle.

Experimental evidence of exciton migration in crystals was obtained in the study of sensitized fluorescence in mixed crystals (see Terenin 1967). Weigert found that if anthracene crystals contain an impurity of tetracene as low as 0.1–0.001%, the crystal fluorescence spectrum coincides with the spectrum of tetracene, although anthracene absorbs all the exciting radiation (Luther and Weigert 1905). Another

example of exciton transfer was shown by the studies of Vladimirov (1957) in crystals of phenylalanine with an impurity of tryptophan.

Terenin showed that migration in crystals is possible not only between the singlet but also between the triplet levels of molecules, and the migration of such a triplet exciton is no less effective than the singlet one (see Terenin 1967). Thus, in benzene crystals, a singlet exciton can visit 10–100 molecules during its existence, while a triplet exciton can visit as many as 10^{11} – 10^{13} molecules, to a large extent, due to the longer lifetime of the triplet state. It undoubtedly indicates that between the molecules in the crystal, there is an extremely high probability of excited state energy transfer due to exchange interaction and a noticeable overlap of electron orbitals. This mechanism can be responsible for the energy transfer between nucleotides in coiled DNA under UV irradiation.

A biologically very important phenomenon of energy transfer takes place in two-dimensional crystals of chlorophyll, that is, in monomolecular films of chlorophyll in chloroplast membranes (Moya 1983). A quantum of light absorbed by any molecule from the “energy” of hundreds of molecules migrates between them until it hits the one, entering the photochemical center, where there is a whole set of participants in the photosynthesis primary reactions and where this photon energy is converted into chemical energy of photoproducts. Thus, energy migration is involved in the very process of photosynthesis, increasing its effectiveness by orders of magnitude (compared to model systems with forbidden energy transfer) (Vladimirov and Potapenko 1989; Nganou et al. 2017).

In semiconductor crystals, the excited state energy migrates by moving an electron in the conduction band and a hole in the valence band. Many attempts have been made to prove the semiconducting properties of biological systems such as protein molecules, nucleic acids, biomembranes, etc. As known, thermal excitation of molecules in a semiconductor leads to the conduction band population and the appearance of electronic conductivity ρ , which depends on temperature according to the equation

$$\rho = \rho_0 e^{-\frac{\Delta E}{2kT}} \quad (5.46)$$

This method was used to study the semiconducting properties of proteins, nucleic acids, and chloroplasts (see Vladimirov and Potapenko 1989; Terenin 1967). Electrical conductivity must be measured in dry films in order to exclude the possibility of electricity transfer by diffusing ions dissolved in water. It was shown that proteins have extremely high resistance at room temperature, that is, they behave like good insulators. The activation energy of electrical conductivity (the energy gap, ΔE) was found to be 2.6–3.1 eV. This indicated that proteins are semiconductors,

albeit bad. However, it was later found that when an electric current is passed through protein films, hydrogen is released at the cathode in an amount proportional to the passing current. Most likely, the activation energy of the electrical conductivity of protein films is nothing more than the activation energy of the ionization of various protein groups, which supply ions to the adsorbed water film surrounding the protein. Thus, there is currently no evidence of the semiconductor properties of biological objects.

References

- Bäckström HLJ, Sandros K (1958) The Quenching of the Long-lived Fluorescence of Biacetyl in Solution. *Acta Chemica Scandinavica* 12:823–832
- Bäckström HLJ, Sandros K (1960) Transfer of Triplet State Energy in Fluid Solutions. I. Sensitized Phosphorescence and Its Application to the Determination of Triplet State Lifetimes. *Acta Chemica Scandinavica* 14:48–62
- Bieri VG, Wallach DFH (1975) Fluorescence quenching in lecithin: cholesterol liposomes by paramagnetic lipid analogues: Introduction of new probe approach. *Biochim Biophys Acta* 389:413
- Cavatorta P, Favikka R, Mazzini A (1979) Fluorescence quenching of tryptophan and related compounds by hydrogen peroxide. *Biochim Biophys Acta* 578:541
- Cheng Y-H, Belyaev A, Ho M-L, Koshevoy IO, Chou P-T (2020) The distinct O₂ quenching mechanism between fluorescence and phosphorescence for dyes adsorbed on silica gel. *Physical Chemistry Chemical Physics* 22 (46):27144–27156. <https://doi.org/10.1039/DOCP05182A>
- Cifra M, Pospisil P (2014) Ultra-weak photon emission from biological samples: definition, mechanisms, properties, detection and applications. *Journal of photochemistry and photobiology B, Biology* 139:2–10. <https://doi.org/10.1016/j.jphotobiol.2014.02.009>
- Curutchet C, Voityuk AA (2011) Triplet-triplet energy transfer in DNA: a process that occurs on the nanosecond timescale. *Angewandte Chemie* 50 (8):1820–1822. <https://doi.org/10.1002/anie.201004732>
- Davis GA (1973) Quenching of aromatic hydrocarbons by alkylpyridinium halides. *J C S Chem Commun*:728
- Delorme R, Perrin F (1929) Durées de fluorescence des sels d'uranyle solides et de leurs solutions. *Journal de Physique et le Radium* 10 (5): 177–186. <https://doi.org/10.1051/jphysrad:01929001005017700>
- Dreeskamp H, Koch E, Zander M (1975) On the fluorescence quenching of polycyclic aromatic hydrocarbons by nitromethane. *ZNaturforsch* 30a:1311
- Dutoi AD, Cederbaum LS, Wormit M, Starcke JH, Dreuw A (2010) Tracing molecular electronic excitation dynamics in real time and space. *The Journal of chemical physics* 132 (14):144302. <https://doi.org/10.1063/1.3353161>
- Eftink MR, Zajicek JL, Chiron CA (1977) A hydrophobic quencher of protein fluorescence: 2,2,2-trichloroethanol. *Biochim Biophys Acta* 491:473
- Förster T (1946) Energiewanderung und Fluoreszenz. *Naturwissenschaften* 33 (6):166–175. <https://doi.org/10.1007/BF00585226>
- Förster T (1948) Zwischenmolekulare Energiewanderung und Fluoreszenz. 437 (1–2):55–75. <https://doi.org/10.1002/andp.19484370105>
- Förster T (1960) Transfer Mechanisms of Electronic Excitation Energy. *Radiation Research Supplement* 2:326–339. <https://doi.org/10.2307/3583604>
- Förster T (1959) 10th Spiers Memorial Lecture. Transfer mechanisms of electronic excitation. *Discussions of the Faraday Society* 27 (0): 7–17. <https://doi.org/10.1039/DF9592700007>
- Frenkel J (1931a) On the Transformation of light into Heat in Solids. I. *Physical Review* 37 (1):17–44. <https://doi.org/10.1103/PhysRev.37.17>
- Frenkel J (1931b) On the Transformation of Light into Heat in Solids. II. *Physical Review* 37 (10):1276–1294. <https://doi.org/10.1103/PhysRev.37.1276>
- Galanin MD (1960). In: *Proceedings of Phys. Institute of the USSR Academy of Sciences*, vol 12. p 3
- Gassman PG, Olson KD, Walter L, Yamaguchi R (1981) Photoexcitation of nonconjugated, strained, and saturated hydrocarbons. Relationship between ease of oxidation and quenching of naphthalene fluorescence by saturated hydrocarbons. *J Amer Chem Soc* 103: 4977
- Green JA, Singer LA, Parks JH (1973) Fluorescence quenching by the stable-free radical di-t-butyl nitroxide. *J Chem Phys* 58:2690
- Jablonski A (1933) Efficiency of Anti-Stokes Fluorescence in Dyes. *Nature* 131 (3319):839–840. <https://doi.org/10.1038/131839b0>
- Kautsky H (1939) Quenching of luminescence by oxygen. *Trans Faraday Soc*, 35:216
- Knibbe H, Rehm D, Weller A (1968) Intermediates and kinetics of fluorescence quenching by electron transfer. *Ber Bunsenges* 72:257
- Krasnovsky AA (2018) Singlet molecular oxygen: Early history of spectroscopic and photochemical studies with contributions of A.N. Terenin and Terenin's school. *J Photoch Photobio A* 354:11–24. <https://doi.org/10.1016/j.jphotochem.2017.07.013>
- Krasnovsky AA, Kovalev YV (2014) Spectral and kinetic parameters of phosphorescence of triplet chlorophyll a in the photosynthetic apparatus of plants. *Biochemistry-Moscow* 79 (4):349–361. <https://doi.org/10.1134/S000629791404004x>
- Kuznetsov VV, Sevchenko AN (1962) On the mechanism of energy migration in organic complexes of rare earths. In: *Physical problems of spectroscopy*, vol 1. Publishing house of the Academy of Sciences of the USSR, Moscow, pp 236–239
- Lakowicz JR (1983) *Principles of Fluorescence Spectroscopy*. Plenum Press, New York
- Lakowicz JR (2006) Quenching of Fluorescence. In: Lakowicz JR (ed) *Principles of Fluorescence Spectroscopy*. Springer US, Boston, MA, pp 277–330. https://doi.org/10.1007/978-0-387-46312-4_8
- Lakowicz JR, Anderson CJ (1980) Permeability of lipid bilayers to methylmercuric chloride: Quantification by fluorescence quenching of a carbazole-labeled phospholipid. *Chem Biol Interactions* 30:309
- Lakowicz JR, Hogen D (1980) Chlorinated hydrocarbon-cell membrane interactions studied by the fluorescence quenching of carbazole-labeled phospholipids: Probe synthesis and characterization of the quenching methodology. *Chem Phys Lipids* 26:1
- Lehrer SS (1971) Solute perturbation of protein fluorescence. The quenching of the tryptophan fluorescence of model compounds and of lysozyme by iodide ion. *Biochemistry* 10:3254
- Lewis GN, Kasha M (1944) Phosphorescence and the Triplet State. *Journal of the American Chemical Society* 66 (12):2100–2116. <https://doi.org/10.1021/ja01240a030>
- Lower SK, El-Sayed MA (1966) The Triplet State and Molecular Electronic Processes in Organic Molecules. *Chemical reviews* 66 (2):199–241. <https://doi.org/10.1021/cr60240a004>
- Luther R, Weigert F (1905) Über umkehrbare photochemische Reaktionen im homogenen System: Anthracen und Dianthracen. I. *J Zeitschrift für Physikalische Chemie*. 51U (1): 297–328. <https://doi.org/10.1515/zpch-1905-5119>
- Medinger T, Wilkinson F (1965) Mechanism of fluorescence quenching in solution I. Quenching by bromobenzene. *Trans Faraday Soc* 61: 620
- Moya I (1983) Energy Migration in Photosynthesis. In: Cundall R.B. DREe (ed) *Time-Resolved Fluorescence Spectroscopy in*

- Biochemistry and Biology. NATO Advanced Science Institutes Series (Series A: Life Sciences), vol 69. Springer, Boston, pp 741–754. https://doi.org/10.1007/978-1-4757-1634-4_40
- Nganou C, Lackner G, Teschome B, Deen MJ, Adir N, Pouhe D, Lupascu DC, Mkandawire M (2017) Energy Transfer Kinetics in Photosynthesis as an Inspiration for Improving Organic Solar Cells. *ACS applied materials & interfaces* 9 (22):19030–19039. <https://doi.org/10.1021/acsami.7b04028>
- O'Connor DV, Ware WR (1976) Exciplex photophysics III. Kinetics of fluorescence quenching of α -cyanonaphthalene by dimethylcyclopentane-1,2 in hexane. *J Amer Chem Soc* 98:4706
- Sandros K, Bäckström HLJ (1962) Transfer of Triplet State Energy in Fluid Solutions. II. Further Studies of the Quenching of Biacetyl Phosphorescence in Solution. *Acta Chemica Scandinavica* 12:958–968
- Scott TG, Spencer RD, Leonard NJ, Weber G (1970) Emission properties of NADH. Studies of fluorescence lifetimes and quantum efficiencies of NADH, AcPyADH, and simplified synthetic models. *J Amer Chem Soc* 92:687
- Shinitzky M, Rivnay B (1977) Degree of exposure of membrane proteins determined by fluorescence quenching. *Biochemistry* 16: 982
- Spencer RD, Weber G (1972) Thermodynamics and kinetics of the intramolecular complex in flavin adenine dinucleotide. In: A. Akeson AE (ed) *Structure and Function of Oxidation Reduction Enzymes*. Pergamon Press, New York, p 393
- Taylor GN (1971) Emission from aromatic hydrocarbon — diene and olefin exciplexes. *Chem Phys Lett* 10:355
- Terenin AN (1943) Photochemical processes in aromatic compounds (in Russian). *Acta Physicochim USSR* 8 (1):210–241
- Terenin AN (1947) *Fotokhimiya krasiteley i rodstvennykh organicheskikh soyedineniy* [Photochemistry of Dyes and Related Organic Compounds] (In Russian), Gostekhizdat, Moscow-Leningrad
- Terenin AN (1967) *Fotonika molekul krasiteley* [Photonics of dye molecules] (in Russian) Nauka, Leningrad
- Terenin AN, Ermolaev VL (1952). *DAN SSSR* [Reports of Acad of Sci USSR] 85:547
- Vavilov SI (1950) *Mikrostruktura sveta* [Microstructure of light] (in Russian). USSR Academy of Sciences Pub. house, Moscow
- Vladimirov JA, Potapenko AJ (1989) *Fiziko-himicheskie principy fotobiologicheskikh processov* [Physico-chemical principles of photobiological processes] (in Russian). Vyschaja shkola, Moscow
- Vladimirov Y. A. (1957) *Fotokhimicheskiye proysessy v belkovykh sistemah* [Photochemical processes in protein systems] (in Russian): PhD Thesis in biological sciences. Moscow
- Vladimirov YA (1967) *Ultraweak luminescence accompanying biochemical reactions* (English translation of “Sverkhslabye svecheniya pri biokhimicheskikh reaktsiyah” USSR Academy of Sciences, Institute of Biological Physics. Izdatel'stvo “Nauka” Moscow, 1966) NASA, C.F.S.T.I., Springfield, Vermont
- Ware WR, Watt D, Holmes JD (1974) Exciplex photophysics I. The α -cyanonaphthalene — olefin system. *J Amer Chem Soc* 96:7853
- Winkler MH (1969) A fluorescence quenching technique for the investigation of the configurations of binding sites for small molecules. *Biochemistry* 8 (2586)
- Xu D-G, Nordlund TM (2000) Sequence Dependence of Energy Transfer in DNA Oligonucleotides. *Biophys J* 78 (2):1042–1058. [https://doi.org/10.1016/S0006-3495\(00\)76663-X](https://doi.org/10.1016/S0006-3495(00)76663-X)

Chemiluminescence as a Tool for Free Radical Research

6

Dmitry Izmailov and Ilya Volodyaev

6.1 The Chemiluminescence Method

Chemiluminescence (CL) is photon emission accompanying chemical reactions. It is generated by chemical reaction products in an electronically excited state, with one of the electrons located at a higher energy level. Such an electron is prone to return to the main energy level and realize excess energy in the form of thermal or light radiation (Fig. 6.1).

In the overwhelming majority of cases, electron transition from an electronically excited state to the ground state is accompanied by thermal energy release. Yet, for some substances, a part of the energy is released in the form of light radiation. The photon emission accompanying electron transition from a higher energy level to the ground level is called luminescence, and luminescing substances are called luminophores (see Chap. 5).

To better understand the principles of luminescence-based methods, including CL, one should consider not only the very fact of light emission but also the origin of the luminophores' electronically excited states.

The ability of substances to emit light, i.e., luminescence, is of great scientific and practical importance, as it allows quantitative and qualitative analysis of their composition. Yet, first of all, the sources of the electronic excitation of molecules, i.e., the causes of electron transfer to a higher energy level, are important. Depending on the energy source for the electronically excited state, the following types of luminescence are distinguished:

- Irradiation with ionizing radiation – radioluminescence
- Irradiation with ultraviolet or visible light – photoluminescence
- Electric current transmission – electroluminescence
- Exposure to ultrasound – sonoluminescence, etc. (see Chap. 5)

In all these examples, the substance is exposed to external energy, absorbs it, goes into an electronically excited state, and then emits the same energy (with some losses) in the form of luminescence. Such research methods can be defined as “invasive” by the way the energy for luminescence is obtained: in all of them, the object is exposed to external energy, which is eventually converted into photon energy.

For such energetically invasive methods, several features can be identified:

- The measurements are of a relative nature, since the luminescence intensity depends not only on the object itself but also on the radiation intensity.
- Low radiation levels have to be measured at high background radiation levels, which can negatively affect the method's sensitivity.
- The measurement results can be significantly influenced by the characteristics of external radiation, such as stability of the source.
- Exposing an object to high energy radiation can lead to changes in the object itself, such as photochemical reactions, and distorted results.

Research methods in which an object is exposed to external energy are mainly used to determine relatively high stationary concentrations of substances.

Contrary to the above, the main feature of the CL phenomenon is that a substance in an electronically excited state (P^*) appears as a product of an internal chemical reaction (Scheme 6.1):

In the course of CL, the energy, already contained in the solution in the form of chemical bonds of the reacting substances (A and B), is emitted as light energy. Thus, with the CL method, one detects the photon emission originating from the system's intrinsic energy, which is released in course of a chemical reaction.

To measure CL, no external energy is acting on the object, therefore, the CL method is “non-invasive”, meaning the

D. Izmailov (✉) · I. Volodyaev
Moscow State University, Moscow, Russia

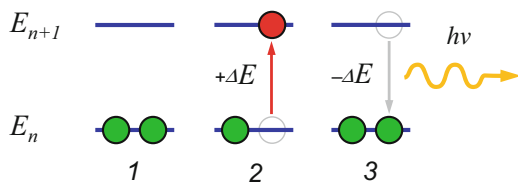
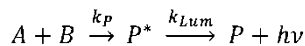


Fig. 6.1 Diagram of electronic energy levels and transitions during luminescence. (1) ground (unexcited) state, (2) transition to an excited state upon absorption of energy, and (3) transition to the ground state, accompanied by emission of a luminescence quantum



Scheme 6.1 Scheme of reactions leading to photon generation during chemiluminescence. k_P – chemical reaction rate constant and k_{Lum} – radiative relaxation rate constant of the excited product

means of energy supply for luminescence. Correspondingly, it has the following features:

- The measurements are absolute and do not depend on the luminescence background level, since the CL qualities relate only to the object and not to external energy sources.
- The sensitivity of the CL method depends only on the apparatus and can be significantly increased by technical means.
- It becomes possible to obtain fundamentally new information about the object's functional state by analyzing changes in the intensity of its own photon emission.

6.2 The Kinetic Chemiluminescence Method

Chemiluminescence is accompanied by a change in the investigated object's internal energy, since part of this energy is released in the form of light. These internal energy changes lead to a change in CL intensity, which turns out to be not a constant value and, as a rule, changes significantly during the measurement.

Such instability of the CL intensity causes certain difficulties in interpreting the experimental results. While in most "invasive" methods, the measurement results in a single value (determined by the level of exciting energy), the CL method, in most cases, means detecting photon emission for a long time, with changing intensity – i.e., observing the *chemiluminescence kinetics*.

The CL method registers the emission intensity I_{CL} – the flux of photons (formed during a chemical reaction), that hit the detector. The latter is proportional to the luminescent reaction rate and, accordingly, to the excited product's concentration:

$$I_{CL} \sim \nu_{Lum_reaction} = k_{Lum}[P^*] \quad (6.1)$$

In methods with an external source of irradiation, the concentration of electronically excited luminophores is constant, since it is proportional to the constant irradiation intensity. However, with CL, the excited product's concentration can change, since it depends on the rates of two successive reactions – the excited product formation and the luminescent reaction itself:

$$\frac{d[P^*]}{dt} = k_P[A][B] - k_{Lum}[P^*] \quad (6.2)$$

However, the time spent by the electron in the excited state is extremely short, and, therefore, the excited products quickly disappear and cannot accumulate, i.e., their disappearance rate is equal to their formation rate (see Chap. 8, Sect. 8.5.3). Thus, CL intensity reflects the rate of the luminescent reaction, which is equal to the rate of excited product formation:

$$I_{CL} \sim \nu_{Lum_reaction} = k_{Lum}[P^*] = k_P[A][B] \quad (6.3)$$

As we can see, the fundamental difference of the chemiluminescence method from other methods that use external sources to excite luminescence is that it reflects the intensity of the luminescent process rather than the concentration of any substance. The primary measured information for the CL method is the rate of the excited product formation, and the information on the substrate concentrations involved in it are secondary and can be mathematically calculated. Measuring the process rate allows using the CL method in two versions:

- *Non-kinetic chemiluminescence*: This is the measurement of the stationary process of excited product formation, for the purpose of quantitative analysis of the system's composition. This version of CL consists of creating conditions under which the rate of excited product formation is constant and proportional to the reagents' concentrations. This approach is similar to other methods with artificial luminescence excitation.
- *Kinetic chemiluminescence*: This comprises detecting the process's changing rate and subsequent mathematical analysis of the CL kinetics in order to determine the qualitative and quantitative characteristics as well as the mechanisms of the process under study. Changes in CL intensity carry essential information about the object's functional state, but it can only be obtained by mathematical analysis of the process kinetics, e.g., by means of mathematical modeling. Thus, kinetic chemiluminescence makes it possible to determine not only substance concentration but also the reaction rate constants in which they

participate as well as to elucidate possible reaction schemes.

6.3 Free Radical Chemiluminescence

The chemiluminescence method records the emission of the object's intrinsic energy, so it can be applied to objects that meet two basic requirements:

1. The object must contain certain potential energy that can be released into the environment.
2. There should be processes (reactions) in the object, converting this energy into light.

Free radicals fully meet these requirements, since they already possess the energy of an unpaired electron and strive to realize it through chemical interactions. The very fact of a free radical appearance indicates that the object under study contains internal energy, transformed into the energy of an unpaired electron as a result of certain processes.

The main way to realize the energy of an unpaired electron is to "find" another electron to pair up with, thus filling the electronic level. Yet, at least part of this energy can obviously be realized as light radiation. Thus, a free radical can be considered a luminophore in an electronically excited state, i.e., a particle potentially capable of emitting luminescence quanta (Fig. 6.2).

To a greater extent, this applies to radical anions that have received an extra electron. In radical anions, the main energy levels are filled with pairs of their own electrons, so an extra electron that turns a molecule into a radical can only be located at a higher (excited) electronic level.

The main difference between a luminophore and a radical anion lies in the population of the main electronic levels. In a luminophore, an electron can immediately move from the

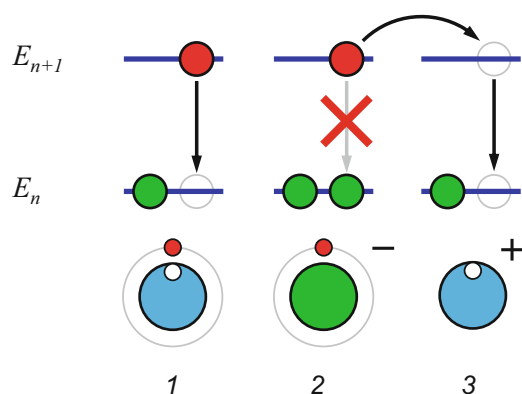


Fig. 6.2 Diagram of electronic energy levels and transitions during luminescence of a luminophore and free radicals: (1) a luminophore in an excited state, (2) an anion radical, and (3) a cation radical

upper excited level to the ground level with the emission of a luminescence quantum. In contrast, the ground level of a radical anion is completely occupied, so the free radical must transfer an electron with increased energy to another particle, i.e., get involved in a chemical reaction. A similar radical cation that has lost an electron from the ground energy level can act as such an electron acceptor with increased energy. Thus, the luminescence of free radicals can be caused by radical cations at the moment they receive a paired electron, which first occupies the upper energy level and then descends to the ground level with emission of a photon.

The formation of radical anions is associated with the appearance of free electrons, which is easy to imagine in a living organism, replete with potential electron donors – transition metal ions, the mitochondrial respiratory chain, NADPH oxidase, etc. Radical anions can be considered as carriers of an electron with potential energy, but they cannot independently realize this energy in the form of luminescence. To convert the energy of a radical anion into luminescence, it must interact with a radical cation, which has a vacant place at the main energy level.

It is more difficult to imagine the formation of radical cations capable of CL, since the detachment of one of the paired electrons from the molecule in most cases requires energy. Apparently, molecules with double bonds, for instance, the double bonds between two carbon atoms, can well act as sources of such luminescent radical cations. Breaking one of the double bonds transforms each of the carbon atoms into a radical cation with an unpaired electron at the main energy level (Fig. 6.3).

As everyone knows, double hydrocarbon bonds are present in the molecules of polyunsaturated fatty acids in lipid membranes, and this causes chemiluminescence of free radicals in many biological samples. The ability of some substances to convert free radical energy into luminescence and enhance it is probably also due to the presence of double bonds in them and the ability to form a luminescent radical cation. Such substances – chemiluminescence activators – will be discussed in more detail below (see Sect. 6.4.3).

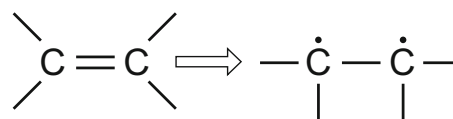


Fig. 6.3 Formation of a radical cation from double hydrocarbon bonds

6.4 Using Chemiluminescence to Study Free Radicals

6.4.1 In Vitro Detection of Free Radicals

Free radicals are extremely active particles with an unpaired electron and therefore exist in a free state for a very short time (fractions of a second). Biological samples intended for quantitative analysis of free radicals cannot be transported and stored, since free radicals completely disappear during the sampling time. Therefore, standard laboratory diagnostic methods, based on determining the stable concentration of substances or constant composition of the system (biochemical and clinical blood tests), are inapplicable for laboratory analysis of free radicals. Such structural (morphological) methods can only be used to determine the stable products of free radical oxidation of biological materials – markers of oxidative stress. However, this information is indirect and incomplete, since it reflects only the final result of a complex process.

The short lifetime of free radicals requires a different approach to laboratory diagnosis of free radical-related diseases. Instead of trying to quantify free radicals and their products, it is necessary to analyze the dynamic processes that involve free radicals. Laboratory diagnostics of oxidative stress should be functional, i.e., based on the study of the body's functional activity, associated with free radical formation and action. One of the most suitable methods for studying free radical processes is the CL method, since CL reflects the intensity of the ongoing processes and not the concentration of substances. However, its use for free radical research has a number of features associated with in vitro CL recording.

First, the biological material extracted from a living organism for laboratory analysis contains unnatural amount of free radicals. Indeed, while the previously formed free radicals quickly disappear, formation of the new ones is disrupted, since the conditions for their formation are violated or there are no sources of radicals. For example, when the material is removed, the supply of oxygen stops, so the formation of reactive oxygen species (ROS) becomes impossible. Thus, in vitro, it is necessary to restart (*initiate*) the process of free radical formation.

Second, the energy of free radicals is not always realized in the form of light. In biological materials, which contain many lipids and proteins, the free radical energy is mainly spent on the oxidation of the surrounding substrates. Therefore, to study the free radical processes in vitro, it is necessary to direct a significant part of the energy of free radicals to light emission, i.e., activate chemiluminescence.

Thus, when conducting chemiluminescence analysis of free radical processes in vitro, two main questions arise:

1. How to start the process of free radical formation outside a living organism?
2. How to make free radicals emit light?

To address these questions, two groups of substances are used – *chemiluminescence initiators* and *activators*.

6.4.2 Initiators of Chemiluminescence

As mentioned above, in the biological material extracted from the body, free radicals are no longer formed, and CL quickly decays. It can also be described as stopping the supply of energy needed to generate free radicals and subsequently emit light. To resume the processes of radical formation in vitro, a *chemiluminescence initiator* – a substance that initiates the onset of a chemical process accompanied by photon emission – is added to the test object. As a rule, the chemiluminescence initiator is a source of new energy for radical formation, so once it is completely used up, the CL also stops. In some situations, the test material contains enough energy to generate free radicals or is placed in a nutrient medium that is the source of energy. In these cases, a CL initiator plays the role of the source of the “very first radicals,” which later reproduce themselves due to the chain reaction.

A classic example of CL initiation is ferrous (Fe)-induced lipid peroxidation. If you add divalent ferrous ions (e.g., in the form of FeSO_4) to any lipid material, including those obtained from a living organism, the process of lipid peroxidation will start, accompanied by the formation of lipid radicals (see Chap. 11). The interaction of lipid radicals with each other (disproportionation) leads to CL. Here, ferrous ions initiate the formation of lipid radicals, as they are the primary source (donor) of unpaired electrons for the latter.

Another highly popular CL initiator is hydrogen peroxide, which is often added to biological samples as a source of radicals, mainly hydroxyl (OH^\bullet). In such methods, the biological material containing no free radical sources, but certain energy for their generation, is investigated. One can use this approach, e.g., to investigate the biological material's peroxidase activity.

CL initiators also include specific stimulators of cellular activity. Such initiators can be called “functional” (and not chemical), since they initiate a functional response of an independent biological unit (cell). In this case, the biological material contains both sources of free radicals and energy for their generation, but the process of radical formation itself is initiated only after the system receives a certain “signal.”

6.4.3 Activators of Chemiluminescence

As mentioned above, only a small fraction of free radical energy in biological materials is released as light. In this regard, the intrinsic biological CL is ultraweak and often cannot be recorded. In vitro, in order to convert a significant part of the free radical energy into photon emission, one can use special chemical substances – *chemiluminescence activators*, i.e. amplifiers of photon emission.

The most important characteristic of luminophores, i.e., substances capable of converting the energy of an electron into light radiation, is the luminescence quantum yield (ϕ_{lum}) – the proportion of electrons that convert the excitation energy into light energy of the total number of electrons in an excited state:

$$\phi_{lum} = \frac{N(\text{luminescent } e^-)}{N(\text{excited } e^-)} \quad (6.4)$$

The main characteristic feature of CL activators is a high quantum yield of luminescence, meaning a higher proportion of the energy received by the activator realized in the form of light.

On the one hand, CL activators interact with free radicals while competing with the biological oxidation substrate. On the other hand, acting as acceptors of the energy of unpaired electrons, CL activators convert much of it into photon emission due to the high quantum yield.

A classic example of CL activators is *luminol*, which is easily oxidized under the influence of any factors and, upon oxidation, emits light with a high quantum yield.

In addition to enhancing CL, activators are used to determine certain types of radicals. For example, *lucigenin* is a specific activator of superoxide radicals' CL and *coumarin 525* is a specific activator of lipid radicals' CL.

6.5 Performing Chemiluminescence Analysis

Chemiluminescence analysis of free radicals also has a number of features that should be taken into account in practice.

6.5.1 Composition of a Chemiluminescent System

Any chemiluminescent system consists of the following components:

- *A buffer*: This can be a chemical buffer or a physiological medium, ensuring the course of chemical reactions accompanied by luminescence. As is known, the quantum

yield of CL activators significantly depends on pH. Thus, it is necessary to maintain pH at a constant level during CL analysis. In purely chemical CL systems, containing no biological material, a constant pH is ensured by standard chemical buffers (phosphate, tris). In systems with biological objects (cells, tissues), standard physiological media are used (Hanks, Ringer's solution, etc.), which ensure normal physiological functioning of the biological material.

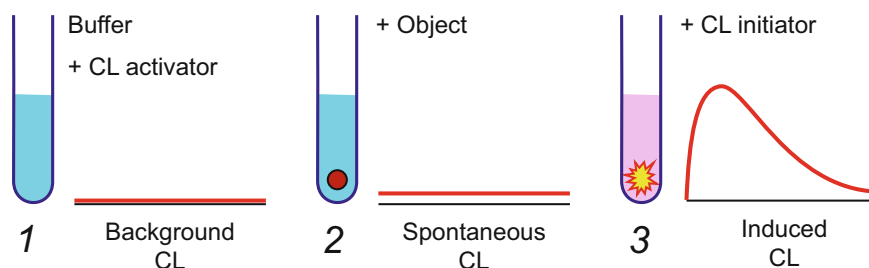
- *A chemiluminescence activator*: This is an oxidation substrate for free radicals, in which excited products are formed, followed by emission of light quanta.
- *A research object*: This can be biological materials or chemical agents that are the source of free radicals in a living organism or contribute to their formation (prooxidants).
- *A chemiluminescence initiator*: This is a chemical or physical factor, the appearance of which in a system leads to a significant increase in free radical formation and luminescence intensity. Transition metal ions, such as Fe and Co (which are sources of electrons for free radicals), or hydrogen peroxide (a direct source of free radicals) can be used as the chemical initiators of CL. As a physical initiator of chemiluminescence, one can consider, for example, temperature (in the case of thermal decomposition of certain substances, accompanied by free radical formation) or aeration of the solution with air or a gas mixture in order to provide the biological material with oxygen, a necessary participant in free radical processes.

Besides these main components, additional substances can be added to the chemiluminescent system, for example, *antioxidants* – substances that reduce the amount of free radicals. Antioxidants can be added to a CL system for two purposes: first, in order to study their effect in a known radical-producing system, and second, to determine the types of free radicals generated in the system under study. For example, adding superoxide dismutase (SOD) makes it possible to determine whether superoxide radicals are formed in the system.

6.5.2 Steps in Chemiluminescence Analysis

The sequence of mixing the components of a CL system and, accordingly, the sequence of measuring the CL signal is of fundamental importance for the CL analysis. Each CL assay should be carried out in stages by alternately adding reagents and measuring the corresponding chemiluminescence. Only such a step-by-step approach ensures adequate results and their correct interpretation. Figure 6.4 shows a general scheme for conducting a chemiluminescence analysis, which consists of three main stages:

Fig. 6.4 Stages of chemiluminescence analysis: (1) measurement of background chemiluminescence, (2) measurement of spontaneous chemiluminescence, and (3) measurement of induced chemiluminescence



1. First, a CL activator is added to the buffer and the *background chemiluminescence* is measured. The background luminescence reflects the activator's excited product formation in the absence of the research object (a putative source of free radicals). In a normal situation, the background emission should be absent or its level should be close to zero, which indicates, first of all, the absence of additional sources of free radicals. If the background luminescence is significantly higher than zero, then the buffer or activator can contain some additional components (impurities), generating free radicals, e.g., by self-oxidation. In such cases, one should abandon further use of these reagents, try to find out which of them (the buffer or the activator) is the source of the background emission, and prepare these solutions anew. Thus, the measurement of the background CL is mandatory for each study to identify other sources of luminescence, except for the research object. If the background CL is not measured, then it cannot be argued that the luminescence source is the research object but not other chemical reactions occurring in the buffer with the CL activator.
2. Second, the research object is added to the buffer with the activator, and its *spontaneous chemiluminescence* is measured. Spontaneous luminescence reflects the level of free radical formation in the research object before any impact on it, i.e., it reflects the intensity of spontaneous radical formation processes. In some studies, spontaneous chemiluminescence of biological objects is endowed with an independent diagnostic value. However, it should be borne in mind that spontaneous processes of radical formation can be caused not only by the physiological functioning of the biological material but to a large extent by the process of sample preparation associated with extraction from the body (mechanical and temperature effects, access to atmospheric oxygen, etc.). The level of spontaneous CL indicates, first of all, the research object's state when it enters the CL system. Thus, it is used as a baseline level of comparison with subsequent stages of CL analysis. In most cases, spontaneous CL has a low stationary level, close to the background emission. Its low level indicates that the object of

study is in a "quiet" (non-induced) state and that there are no extraneous CL initiators in the buffer. If the spontaneous CL intensity is high, or it shows a significant change (kinetics), then one can conclude that the research object has undergone some action or activation – either during sample preparation or when added to the CL system. Such cases, with pronounced spontaneous CL, can create difficulties during subsequent stages of CL analysis, since the already activated object may not respond to the putative initiators of CL. Thus, the measurement of the research object's spontaneous CL in the absence of a CL initiator is a mandatory requirement for each study and is necessary to determine its initial state.

3. Third, a CL initiator is added to the chemiluminescent system containing the buffer, the CL activator, and the research object. The *induced chemiluminescence* of the object is measured. The main subject of CL analysis is precisely induced CL, since it reflects the research object's behavior in the living organism and the physiological processes associated with the free radical formation. Induced CL, as a rule, has complex kinetics, and its intensity can change significantly during measurement, which is associated with a change in the research object's state. For purely chemical CL systems, a change in CL intensity is associated with a change in the concentration of the reacting substances. Usually, determining the rate constants of chemical reactions occurring in a living organism and the substances' initial concentration is of primary diagnostic value. In systems with biological objects, the induced CL kinetics reflects the ability of these objects to respond to an external stimulus or a physiological level of functioning.

The sequence of stages of CL analysis presented here, including the background measurement and both spontaneous and induced luminescence, provides control of the research object's initial state and allows to exclude the unrelated sources and initiators of CL in the system. The general approach to CL analysis is that one must be sure that the measured CL is the response of the test object to only one known CL initiator. Only in the case of such unambiguity can chemiluminescent data be used to assess the state and

behavior of the research object. If one can see overlapping CL signals from several sources or caused by different initiators, the interpretation of CL data becomes highly problematic.

6.6 Chemiluminescent Techniques

6.6.1 Free Radical Processes in a Living Organism

In a living organism, there are various processes accompanied by free radical formation and subsequent interaction with the surrounding substances. All of them can be described by a generalized diagram, which is shown in Fig. 6.5.

1. A cell's vital activity is associated with *primary radical* formation, such as a superoxide anion radical.
2. Chemical reactions of primary radicals lead to the formation of *secondary radicals* such as lipid radicals.
3. As a result of chemical transformations of primary and secondary radicals, stable *oxidation products* are formed, e.g., hydrogen and lipid peroxides.
4. Under the action of *prooxidants*, secondary radicals, such as lipid radicals, can again be formed from oxidation products.
5. The action of *primary antioxidants*, i.e., the body's own antioxidants, such as superoxide dismutase, is primarily aimed at eliminating primary radicals at the sites of their formation.
6. The action of *secondary antioxidants* received by the body from the outside is primarily aimed at eliminating secondary radicals.

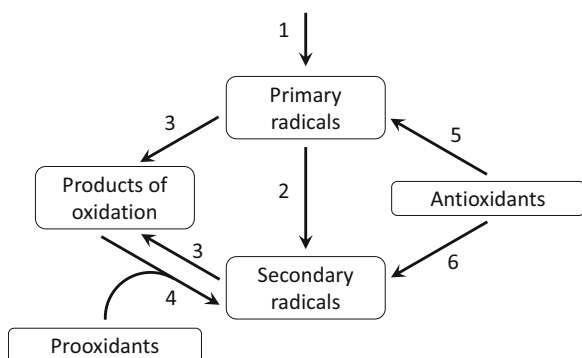


Fig. 6.5 Free radical processes in a living organism: (1) formation of primary radicals, (2) formation of secondary radicals, (3) formation of oxidation products, (4) action of prooxidants, (5) action of primary antioxidants, and (6) action of secondary antioxidants

The CL method allows studying all these free radical processes, but, for each of them, one should use an individual CL technique. It is very important in CL analysis to understand what kind of free radical process one or another technique is aimed at. The sequence of measurements and the correct choice of the activator and the initiator will largely depend on this.

In this section, we will provide a general description and the principles of CL techniques.

Tissue and cellular CL methods are used to study formation of primary radicals. The method of lipid peroxidation is used to study formation of secondary radicals. To determine oxidation products, methods of lipid peroxide detection are used. To determine the effect of prooxidants, one can use methods of peroxidase activity detection. To determine the effect of primary antioxidants, methods of measuring the activity of SOD and catalase can be used. The effect of secondary antioxidants is studied by evaluating their antioxidant capacity and activity.

6.6.2 Tissue Chemiluminescence

By the term “tissue chemiluminescence,” we mean the luminescence associated with superoxide radicals formed in the mitochondrial respiratory chain in the course of normal physiological process of oxidative phosphorylation. Unlike cellular chemiluminescence (see below), tissue chemiluminescence implies that the luminescence is caused by the natural vital activity of all tissue cells, rather than by a specific response of certain cell types to a certain effect.

The tissue CL technique involves the study of a whole area of a biological tissue (biopsy, section, punctate, etc.) that has not undergone mechanical or other preparations (homogenization etc.) and in which the cells' integrity and viability are preserved. The main approach of the tissue CL technique is to ensure the natural vital activity of a biological tissue in an *in vitro* study, similar to that in a living organism. When a biological tissue is removed from the body, its nutrients and oxygen supply are disrupted and the temperature regime changes. To restore these conditions of vital activity in the tissue CL method, a piece of tissue is incubated at 37 °C in a physiological medium (for example, Hanks' solution), which is additionally aerated with air or a gas mixture to maintain a certain level of oxygen saturation of the medium. The general application scheme of the method is shown in Fig. 6.6.

A fundamental feature of this approach is the possibility of detecting free radicals formed in the mitochondria using lucigenin, a CL activator specific for superoxide radicals. Possessing positive charge and the ability to penetrate lipid membranes, lucigenin enters cells and predominantly accumulates near the inner mitochondrial membrane, which has higher negative charge in absolute value. Thus, the

Fig. 6.6 The tissue chemiluminescence method: (1) a piece of tissue (biopsy), (2) an incubation medium with lucigenin, and (3) aeration of the incubation medium with air or a gas mixture

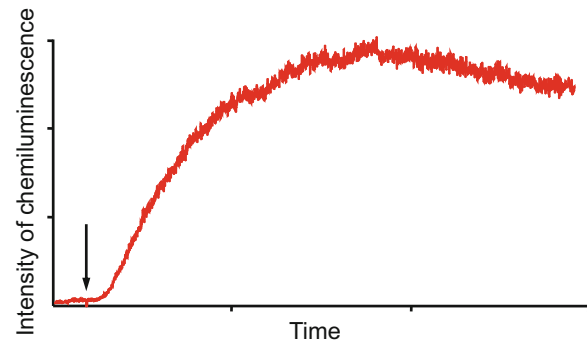
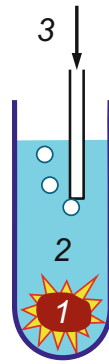


Fig. 6.7 Kinetics of cellular chemiluminescence. The arrow shows the moment when the stimulus was added (zymosan)

presence of lucigenin in the medium allows controlling superoxide radical formation, which accompanies the work of the mitochondrial respiratory chain.

In tissue CL, the activator is lucigenin, and oxygen in the incubation medium can be considered the CL initiator. The oxygen content in the medium can be controlled by changing the aeration intensity.

The tissue CL technique can be used to solve the following scientific and applied problems:

1. Determining tissue viability by the ability to restore the mitochondrial respiratory chain functioning

If blood supply to organs and tissues is violated, oxygen access to the cells stops and, accordingly, the mitochondrial respiratory chain work is disrupted. For some time of hypoxia, it can still be restored, i.e., the biological tissue remains viable. Yet, a prolonged state of hypoxia leads to structural disorders in cells, which can be characterized as a loss of tissue viability associated with irreversible disruption of the respiratory chain. The tissue CL method allows to determine the ability of a biological tissue in the hypoxia state, to restore respiratory chain work when oxygenation is restored. This means the ability to vitalize after normal physiological conditions are restored, for example, after the restoration of blood supply. The technique of tissue CL can be of great practical importance, for example, in surgery and transplantology to determine the ability to recover and engraft the operated and transplanted organs. One of the advantages of the tissue CL technique is the possibility of an early diagnosis of functional disorders in cell viability that precede structural disorders detected by morphological methods.

2. Evaluating the biological tissue resistance to hypoxia

The above approach to determining tissue viability can also be used to study the tolerance of various tissue types to hypoxia. The technique of tissue CL allows to vary the duration of hypoxia under experimental conditions, determining the time interval during which the viability of the tissue sample is maintained.

3. Determining the toxicity of various substances

The tissue CL technique allows one to determine the effect of various agents, for example, poisons and toxins, on the mitochondrial respiratory chain's functioning.

6.6.3 Cell Chemiluminescence

By the term “cellular chemiluminescence,” we mean the luminescence associated with the free radical formation by certain types of cells due to their specific responses to a certain stimulus. Cell CL methods are mainly used to assess the functional state of phagocytes (neutrophils, monocytes, etc.) and is based on the fact that the specific response of these cells to a stimulus or irritant is increase in the production of reactive oxygen species – “oxidative burst” (Fig. 6.7).

In cell CL approach, the CL activators used are either a nonspecific activator such as *luminol* or a specific activator such as *lucigenin* (determining the generation of superoxide radicals).

The CL initiators used are as follows:

- Opsonized zymosan (Schiffman et al. 1975)
- Phorbol 12-myristate 13-acetate (PMA) (the phorbol ester of myristic and acetic acids) (Dougherty and Niedel 1986)
- Polystyrene latex particles (O’Flaherty et al. 1979)
- Aggregated immunoglobulins (Smith et al. 1986)
- Calcium ionophores (Dougherty and Niedel 1986; Finkel et al. 1987; Kovalchuk et al. 1991)
- Unsaturated fatty acids and lysophospholipids (Englberger et al. 1987; Takahashi et al. 1991)
- BaSO₄ crystals, hydroxyapatites, and urates (Vladimirov and Sherstnev 1983; Vladimirov et al. 1989)
- Electrical breakdown of phagocyte membranes (Snyder and Bredt 1992)
- DAG (diacylglycerol) (Annaberdyeva et al. 1987), etc.

The cell CL technique can be used to solve the following scientific and applied problems:

1. Determine the cells' current state – whether the cells (for example, phagocytes) are in a quiescent or activated state
2. Determine the cells' ability to be activated by various stimuli and irritants – response to toxins, allergens, industrial dust, etc.
3. Dynamic monitoring of the body's state – a change in the degree of cell activation during treatment or exacerbation of diseases

6.6.4 Lipid Peroxidation

The chemiluminescent technique of iron-induced lipid peroxidation (LPO) is widely used in scientific research. In our classification, this approach can be referred to methods for studying the formation of secondary radicals, which include lipid radicals. The principle of the LPO technique is that the appearance of lipid radicals can be initiated in any lipid material by adding a source of electrons, e.g., transition metal ions. A usual case is adding Fe^{2+} , by introducing iron sulfate (FeSO_4) into the system. The appearance of electron donors in the system first leads to the formation of free radicals in the aqueous phase, such as superoxide and hydroxyl radicals, which then interact with lipid molecules and form lipid radicals. An essential feature of the lipid radical formation process is that it has a chain mechanism (Fig. 6.8, see more in Chap. 11).

The generated lipid radical interacts with a neighboring lipid molecule, converting it into another radical and being converted into a stable oxidation product – lipid hydroperoxide. Thus, the lipid radical that appears in some place moves along the neighboring lipid molecules forming a “chain” (a sequence) of oxidation. At the same time, the formed lipid peroxides can form new lipid radicals by interacting with electron donors such as iron ions. In general, the process of lipid oxidation has not only chain but also branched-chain

character, since new oxidation chains and new products can be formed from the oxidation products that have appeared. Such a branched-chain mechanism leads to a significant increase in the amount of formed lipid radicals compared to the amount of the initial radicals in the aqueous phase. This increase is due to the fact that electron donors, such as iron ions, are involved in two pathways of radical formation – initiation of new oxidation chains through primary radicals of the aqueous phase and branching of existing chains by reacting with oxidation products.

Another essential feature of lipid peroxidation is that the interaction (disproportionation) of lipid radicals with each other is accompanied by photon emission. Due to this, formation of lipid radicals can be directly detected by the CL method. The recorded CL intensity is proportional to the rate of reaction between two lipid radicals and, accordingly, to the square of their concentration:

$$I_{\text{CL}} \sim v_{\text{reaction}} = k[\text{LOO}]^2 \quad (6.5.5)$$

The luminescence accompanying the lipid radicals interaction is very weak (ultraweak); therefore, CL activators are used to enhance it. Good results in enhancing the lipid radicals' CL were obtained by physical activators from the group of coumarins, the best of which is coumarin 525.

The lipid peroxidation CL technique has become widespread due to its simplicity and effectiveness. In order to obtain a CL response, it is sufficient to take any biological material containing lipids (blood, serum, saliva, urine, etc.) and add a CL activator and ferrous sulfate to it. However, the main difficulty lies not in setting the measurement itself but in understanding and interpreting the results obtained.

Actually, the lipid peroxidation CL method was originally developed for the fundamental study of this process on model systems in vitro. However, the results and their interpretation obtained in artificial conditions on model systems cannot be directly transferred to the processes taking place in a living organism. In model systems, lipid peroxidation is induced by an artificially high concentration of iron ions, which does not exist in a living organism. If the same concentrations are added to a biological material, one cannot be sure to obtain the same peroxidation process in vitro, as the one existing in a living organism in vivo. In model systems, as a rule, purified lipids of high concentration are used, while the biological material contains a lot of other components and the concentration of lipids is relatively low. In this regard, the results obtained on the biological material may differ significantly from those on model systems.

The model kinetics of lipid peroxidation CL has a complex shape, which is shown in Fig. 6.9 (see Sect. 11.6 for more details). Immediately after the addition of Fe^{2+} ions, there is an intense, rapidly decaying flash of photon emission

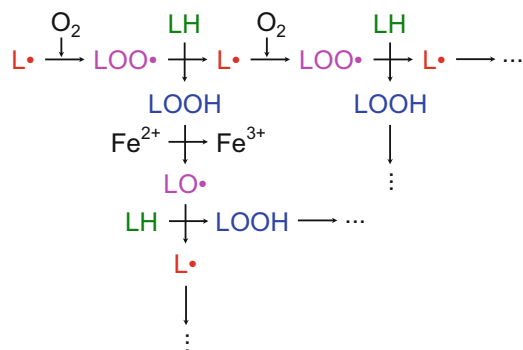


Fig. 6.8 A scheme of the branched-chain process of lipid peroxidation

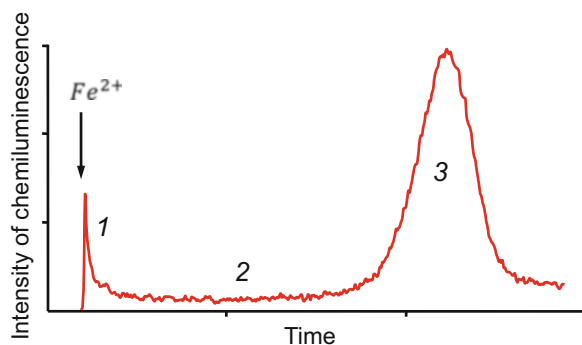


Fig. 6.9 The kinetics of lipid peroxidation chemiluminescence: (1) “fast flash”, (2) latent period, and (3) “slow flash”

called “fast flash” (phase 1 in Fig. 6.9). This is followed by a “latent period” of the absence of luminescence (phase 2 in Fig. 6.9) and then by a “slow flash,” a smooth increase and decrease of photon emission (phase 3 in Fig. 6.9).

Using mathematical modeling, we managed to decipher and explain such complex kinetics (Izmailov and Vladimirov 2002) (see Chap. 11 for more details):

1. The fast flash is associated with the presence of oxidation products in the lipid material – lipid hydroperoxides. Its amplitude depends on the amount of oxidation products present in the tested material, which can be used for diagnostic purposes to determine the degree of lipid oxidation.
2. The short duration of the fast flash and the onset of the latent period of complete luminescence suppression are due to the fact that the electron donors – iron ions – also exhibit an antioxidant effect, reacting with lipid radicals. This antioxidant effect is essential at high concentrations of Fe^{2+} ; therefore, the initial stage of iron-induced lipid peroxidation is characterized by complete suppression of luminescence. The fast flash of CL is observed anyway, due to the high content of oxidation products, but its amplitude can be largely suppressed by the antioxidant effect of high concentrations of iron ions.
3. The slow flash after the latent period appears due to a decrease in the Fe^{2+} concentration below a certain “critical” level, at which the antioxidant effect of iron ions is replaced by a prooxidant one (see Sect. 11.4). At concentrations above the critical level, iron ions are predominantly involved in oxidation chain-terminating reactions, interacting with lipid radicals. Contrary to that, at concentrations below the critical level, iron ions are predominantly involved in chain-branching reactions, interacting with lipid hydroperoxides and forming new oxidation chains.

Thus, the rise of the slow flash is due to the self-accelerating process of lipid radical formation (due to the

branching of oxidation chains). The decline of the slow flash is associated with complete disappearance of Fe^{2+} ions and is characterized only by the fact that new oxidation chains are no longer formed.

Deciphering the complex model kinetics of lipid peroxidation gives us understanding of how this technique can be used in practice to study biological materials. The kinetics of lipid peroxidation chemiluminescence allows one to obtain two main characteristics of the lipid material under study:

1. The amount of oxidation products, present in the lipid material, which is characterized by the amplitude of the fast flash
2. The oxidation capacity of the lipid material, i.e., its ability to form new chains and accelerate oxidation, which is characterized by the rate of rise and the amplitude of the slow flash

Obviously, these two characteristics of the lipid material must be determined separately, as they provide different information. The amount of oxidation products characterizes the intensity of the oxidation processes that take place in the body. The oxidation capacity characterizes the properties of the oxidized material itself. In order to individually determine these characteristics, it is necessary to obtain the CL kinetics, consisting of two clearly distinguishable flashes – fast and slow, i.e., having a pronounced latency period. However, when studying biological materials, one can quite often observe only one outbreak of chemiluminescence. This causes difficulties in interpreting the results, as there can be several reasons for this:

- The concentration of the added iron ions is below the “critical” level. In this case, the fast and the slow flashes merge together, so it becomes impossible to separate the radicals formed from the preexisting hydroperoxides and the newly generated ones. In this situation, it is necessary to increase the amount of added iron until there is a pronounced latency period between the two flashes.
- The concentration of iron ions is added significantly above the “critical” level. In this case, the latency period is very long and researchers often stop measuring the CL kinetics without waiting for the slow flash. This situation is also dangerous because high concentrations of iron, which have antioxidant effect, suppress the fast flash intensity, and, with a low oxidation state of the lipid material, the fast flash may even be absent. Thus, chemiluminescence accompanying iron-induced peroxidation cannot be detected at all, and disappointment in the technique ensues. In such a situation, it is necessary to increase the CL measurement duration and reduce the amount of added iron, possibly by several orders of magnitude.

- The concentration of lipid material is too low. In order for the peroxidation process to have a branched-chain character, the concentration of lipid material must be high. To continue the oxidation chain, a lipid radical must have high probability of meeting an unoxidized lipid molecule, i.e., there must be a lot of oxidation substrates around the radical. However, at low concentrations of the studied lipid material, the probability of oxidation of neighboring molecules is low and the oxidation process is not accelerated. Therefore, in studies with a low concentration of lipid material, a slow flash may be absent, since the oxidation is not of the chain nature. In such a situation, it is necessary to increase the lipid material concentration, either by eliminating its dilution or by measuring in small volumes.

Thus, the use of the CL technique of iron-induced lipid peroxidation for each type of research objects requires an individual approach involving the adjustment of iron and lipid concentrations.

6.6.5 Determining Oxidation Products

The oxidation products that can be determined by the CL method include hydroperoxides. In the lipid phase, these are lipid hydroperoxides formed from the secondary lipid radicals, and, in the aqueous phase, the oxidation product is hydrogen hydroperoxide as a metabolite of the primary superoxide radical.

The approach to lipid hydroperoxide determination is described above in the context of lipid peroxidation and is associated with the fact that the fast flash of CL from lipid systems is due to the presence of lipid hydroperoxides (Fig. 6.9, phase 1). Thus, to determine the amount of lipid hydroperoxides, the fast flash amplitude can be measured when iron ions are added to the lipid material.

To determine the concentration of hydrogen peroxide by the CL method, special enzymes can be used – peroxidases – e.g., horseradish peroxidase (see Chap. 14). Hydrogen

peroxide is the first substrate for peroxidase, and a CL activator, such as luminol, can be used as the second substrate. As a result of this peroxidase reaction, luminol products are formed in the excited state, which is realized by photon emission. Thus, by recording the CL intensity, it is possible to measure the rate of the peroxidase reaction, which is proportional to the concentration of hydrogen peroxide.

References

- Annaberdyeva EM, Polnikov IG, Puchkova TV, Sharov VS, Putvinskii AV, Vladimirov YA (1987). Bulletin of experimental biology and medicine 103 (4):452. doi:<https://doi.org/10.1007/Bf00842484>
- Dougherty RW, Nidel JE (1986). Cytosolic calcium regulates phorbol diester binding affinity in intact phagocytes. J Biol Chem 261 (9): 4097
- Englberger W, Bitter-Shermann L, Hadding W (1987). Internat J Immunopharm 9 (3):275
- Finkel T, Pabst M, Suzuki H, Guthrie L, Forehand J, Phillips W, Johnstone R (1987). J Biol Chem 310 (3):12589
- Izmailov DY, Vladimirov YA (2002) Mathematical modeling of the kinetics of chain lipid peroxidation in the presence of Fe²⁺. I. Basic model. Biol Membrany 19 (6):507–515
- Kovalchuk LV, Klebanov GI, Ribarov SR, Kreinina MV, Aptlsiauri NE, Gankovskaya LV, Shuikina EF, Karaseva MV, Vladimirov YA (1991). Biomed Sci 2 (3):11
- O'Flaherty JT, Showell HJ, Becker EL, Ward PA (1979) Neutrophil aggregation and degranulation. Effect of arachidonic acid. The American journal of pathology 95 (2):433–444
- Schiffman E, Corcoran BA, Wahe SM (1975). N-formylmethionyl peptides as chemoattractants for leucocytes. Proc Natl Acad Sci USA 72 (3):1059
- Smith RJ, Spziali SC, Ulrich RG, Bowman BJ (1986). Inflammation 10 (2):131
- Snyder SH, Bredt DS (1992) Biological roles of nitric oxide. Scientific American 266 (5):68–71, 74–77. doi:<https://doi.org/10.1038/scientificamerican0592-68>
- Takahashi R, Edagisshe K, Sato EF, Jnoue M, Matsuno T, Vtsumi K (1991). Arch Biochem and Biophys 285 (2):325
- Vladimirov YA, Sherstnev MP (1983). In: Chemiluminescence of animal cells. VINITI, M, p 176
- Vladimirov YA, Sherstnev MP, Piryazev AP (1989) Chemiluminescence of the leucocytes of whole blood stimulated by barium sulphate crystals. Biophysics 34 (6):1136–1140



Highly Sensitive Imaging and Spectral Analysis of UPE from Biological Systems and Their Application

7

Masaki Kobayashi

7.1 Introduction

Ultra-weak photon emissions (UPEs) from living organisms are spontaneous light emissions from chemically excited biomolecules in living bodies. The UPE intensity levels are 3–6 orders lower than the human eye threshold of recognition, which is roughly below 10^{-16} W/cm². UPEs, often designated as biophoton emissions (Popp 1988), are known to be associated with the production of reactive oxygen species (ROS), which are generated through intrinsic or extrinsic processes occurring in living bodies (Popp 1988; Pospíšil 2014). Normal metabolic processes, such as in mitochondrial energy metabolism, and ROS-related pathological effects are involved in photon emission mechanisms. Endogenously produced or exogenously produced ROS induce oxidative stress led by a redox imbalance, and cause various diseases. In contrast, the role of ROS as a signal mediator regulating physiological functions has attracted attention. Features associated with ROS generation suggest some UPE potential for noninvasive measurement of physiological and pathological states of a living body connected to diagnosis.

Imaging and spectroscopy of UPE are fundamentally important for discovering applications and for exploring their mechanisms. Efforts to develop techniques for imaging and spectroscopy have been undertaken from the early stage of UPE discovery. Since the 1960s, various UPE phenomena have been identified using photon-counting apparatus incorporating a photomultiplier tube (PMT). In this early stage, exertion characterizing the spatial and spectral properties of UPEs had been made using PMT base devices.

Supplementary Information: The online version contains supplementary material available at https://doi.org/10.1007/978-3-031-39078-4_7.

M. Kobayashi (✉)
Tohoku Institute of Technology, Sendai, Japan
e-mail: masaki@tohtech.ac.jp

In the 1980s, the development of imaging devices with sensitivity capable of resolving single-photon level light opened the door to practical UPE imaging (Kobayashi 2014). In Japan in the mid-1980s, Professor Inaba, a world UPE research pioneer, organized the “Inaba Biophoton Project,” promoted by the Japanese government as a part of the ERATO Program. He conducted advanced research by exploring UPE phenomena comprehensively with efforts in the fields of engineering, biochemistry, and biophysics. Given this historical background, technology for UPE analysis, including the development of detection technologies, such as single-photon counting for biophoton statistics analysis, two-dimensional (2D) imaging, and spectroscopy, have evolved. This chapter presents a review of novel techniques, particularly addressing UPE imaging and spectroscopy, with the characterization of the respective techniques and demonstration using experimentally obtained results. Those results indicate the feasibility of UPE applications in the fields of medicine, agriculture, and biology.

7.2 UPE Imaging System

Imagers for UPE detector devices are categorized as electron-tube-type image sensors and semiconductor image sensors. Electron-tube-type image sensors consist of a set of microchannel plates (MCP) for electron multiplication. Semiconductor image sensors are typically charge-coupled devices (CCD) with a function of long-time charge integration in the device. Electron-tube imagers consist of a photocathode for the conversion of photons into photoelectrons, MCP for electron multiplication, and an anode that has a function of identifying the two-dimensional position of multiplied electron-pulses hit on the anode, which corresponds to the position of the incident photon onto the photocathode. Electron-tube imagers designed for photon-counting imaging are generally designated as two-dimensional (2D) photon-counting tubes (Tuchiya et al.

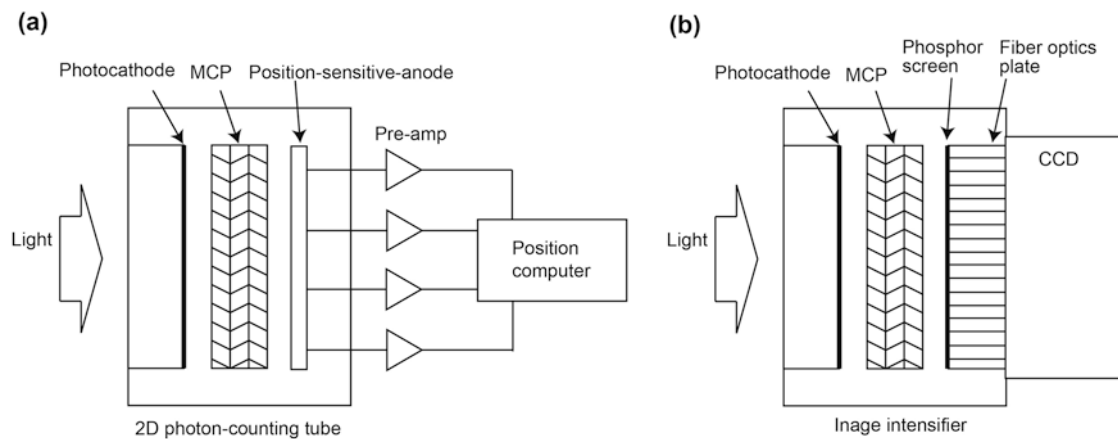


Fig. 7.1 (a) Schematic diagram showing the structure of a typical 2D photon-counting tube (b) Schematic configuration of a typical II-based 2D photon-counting imager

1985; Scott et al. 1989). Figure 7.1a presents a schematic diagram of the structure of a typical 2D photon-counting tube that is assembled with MCPs and a position-sensitive-anode to detect the position of the multiplied electron pulses for building a photon-counting image. Another electron-tube-type imager for UPE imaging that has been used (Ichimura et al. 1989; Suzuki et al. 1991; Amano et al. 1995) is a photon-counting imager that includes an image intensifier (II). The II is assembled with a photocathode, MCPs, and a phosphor screen. With the application of sufficient gain to the MCP, each photon that has fallen on the photocathode is converted to a bright spot on the screen. It is captured using a conventional imaging device such as a general CCD camera via a lens system or a fiber-optic plate. The spatial distribution of the number of bright spots produces a 2D photon counting image within the accumulation time. The schematic configuration of a typical II-based 2D photon-counting imager is presented in Fig. 7.1b. These electron-tube-type image sensors, which have the electron multiplication functionality, achieve ultra-weak light imaging at a single-photon level simultaneously with high temporal resolution.

However, CCD as a semiconductor imager, which has no electron multiplication function, has been used commonly recently for UPE imaging. The CCD developed for scientific measurements has a performance that is capable of detecting ultra-weak light on a single-photon level under cooling conditions (Kobayashi 2014; Kobayashi et al. 1997). Electron-multiplying CCD (EMCCD), which has a CCD structure equipped with a multiplication function, is commercially available. However, because of its limited sensor area and excess noise originating in the fluctuation of multiplication gain, it is unsuitable for UPE imaging for the targets that allow long time exposure. As another type of semiconductor image sensor, complementary metal-oxide-semiconductor (CMOS) image sensors are growing in use for consumer

cameras replacing CCD. Recently, the performance of scientific-grade CMOS image sensors has also progressed, along with the improvement of quantum efficiency and noise reduction technology. Nevertheless, in comparison with CCD, it remains insufficient for UPE applications.

This section presents a review of imaging devices of two types. Furthermore, a lens system, which is a key device that should be customized for UPE imaging, is described to design a UPE imaging apparatus.

7.2.1 Two-Dimensional Photon-Counting Imaging System

Actually, 2D photon-counting tubes have been used since the early 1990s. They are assembled with a uniform photocathode, a set of MCPs, and a position-sensitive anode that is sometimes a resistive anode or a position-sensitive detector (PSD). Spatial information of the X–Y coordinate of incident photons on the photocathode is calculated from signals of the position-sensitive anode. Incident photons form a 2D photon-counting image by accumulating the counts of the events on each image pixel. From the 1990s, Inaba's group revealed UPE images obtained from various living samples using an imaging system composed of the Imaging Photon Detector (IPD; Photech, UK), which is a 2D photon-counting tube characterized by a large active area of a photocathode with 40-mm diameter (Kobayashi et al. 1996, 1999a, b).

The minimum detectable photon-number or optical power of the 2D photon-counting imager is expressed as the following Eq. (7.1). It is derived from the signal-to-noise ratio (SNR; Eq. (7.2)) of the detector, which is restricted by the quantum efficiency of the photocathode and the shot noise of the dark current.

$$\langle \mathcal{N}_p \rangle_{\min} = \sqrt{\frac{\langle \mathcal{N}_d \rangle}{T}} \frac{1}{\eta} \quad (7.1)$$

$$P_{\min} = \sqrt{\frac{\langle \mathcal{N}_d \rangle}{T}} \frac{h\nu}{\eta}$$

$$\frac{S}{\mathcal{N}} = \frac{\eta \langle \mathcal{N}_p \rangle}{\sqrt{\eta \langle \mathcal{N}_p \rangle + \langle \mathcal{N}_d \rangle}} \sqrt{T} \quad (7.2)$$

In those equations, $\langle \mathcal{N}_p \rangle_{\min}$ and P_{\min} , respectively, represent the averaged minimum detectable photon-number reaching the detector per pixel in unit time and optical power per pixel. $\langle \mathcal{N}_d \rangle$ represents the averaged dark counts per pixel in unit time. η denotes the quantum efficiency of the photocathode. T represents the exposure time for imaging. h and ν , respectively, stand for Planck's constant and the light frequency. The minimum detectable photon-number is derived with condition $S/N = 1$.

The 2D photon-counting system has the performance of single-photoelectron detection in real time. It can analyze the spatiotemporal properties of photoelectron pulses, which are applicable to photon statistics and correlation analysis (Kobayashi et al. 1996). However, the spatial resolution of the 2D photon-counting system is restricted by the MCP

resolution and position-sensitive-anode or phosphor screen, which is generally worse than that of the cooled-CCD camera system described in the next section.

7.2.2 Cooled CCD Camera System

A scientific-grade CCD that provides high sensitivity adapted for astronomical observations is used for UPE imaging. The first UPE imaging using a CCD camera was reported by Kobayashi et al. (Kobayashi et al. 1997): a UPE image from a germinating soybean root was demonstrated with a liquid-nitrogen-cooled CCD camera. The scientific-grade CCD camera incorporates a back-illuminated-type large-area CCD with full-frame-transfer (FFT) architecture. To reduce the dark current, a cooling unit with cooling performance near -100°C is necessary, thereby achieving the detection of light at a single-photon level through long-term exposure. Although the CCD has no gain itself, its performance for weak light detection is comparable to that of the 2D photon-counting tube (Kobayashi et al. 1997). Figure 7.2 presents a typical UPE imaging system based on the cooled CCD camera.

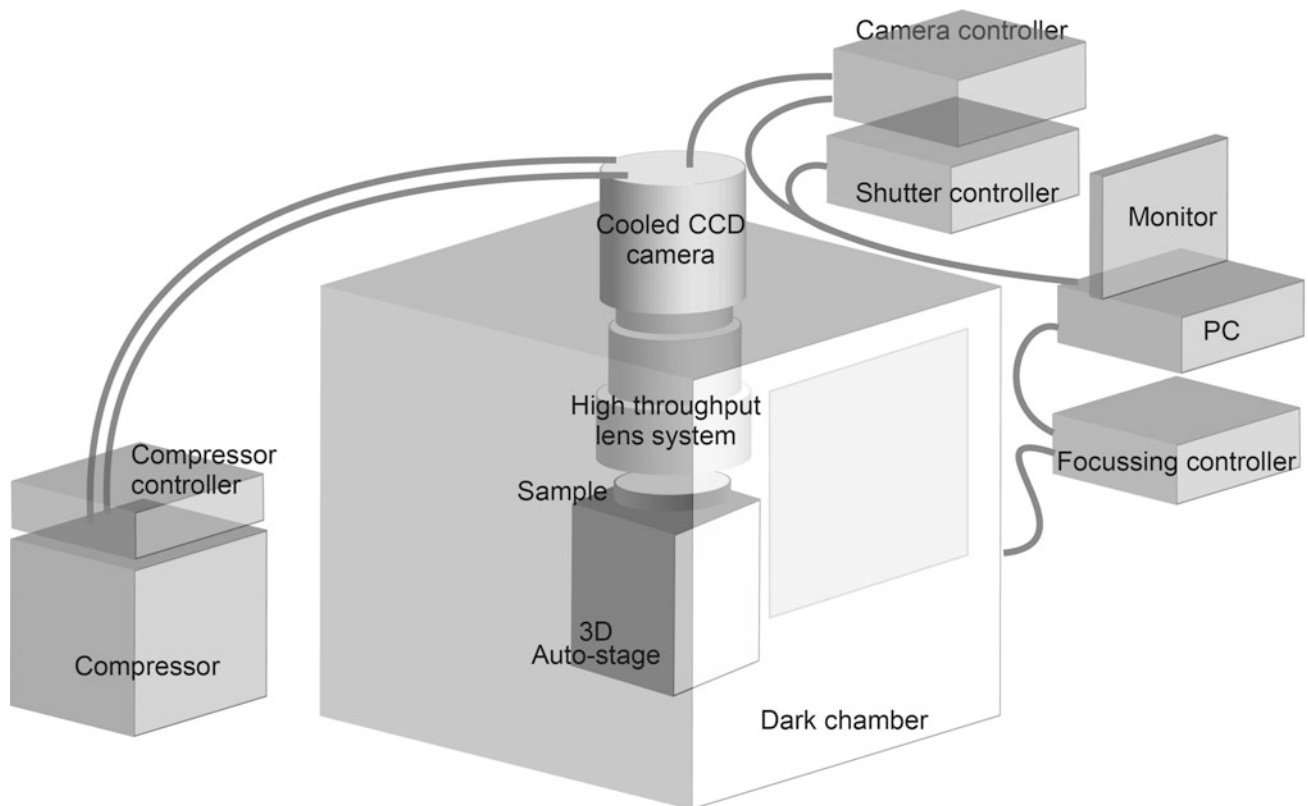


Fig. 7.2 Schematic illustration of the cooled-CCD-based UPE imaging system

A minimum detectable photon-number and optical power are presented as Eq. (7.3) under the condition of weak light measurement. It is derived from SNR, defined as Eq. (7.4).

$$\langle \mathcal{N}_p \rangle_{\min} = \frac{\sqrt{\langle \mathcal{N}_d \rangle \mathcal{T} + \mathcal{N}_r^2}}{\eta \mathcal{T}} \quad (7.3)$$

$$P_{\min} = \frac{\sqrt{\langle \mathcal{N}_d \rangle \mathcal{T} + \mathcal{N}_r^2}}{\eta \mathcal{T}} \frac{h\nu}{\eta} \quad (7.4)$$

$$\frac{S}{\mathcal{N}} = \frac{\eta \langle \mathcal{N}_p \rangle \mathcal{T}}{\sqrt{(\eta \langle \mathcal{N}_p \rangle + \langle \mathcal{N}_d \rangle) \mathcal{T} + \mathcal{N}_r^2}} \quad (7.4)$$

In those equations, \mathcal{N}_r is the root mean square (rms) readout noise of the output amplifiers that should be regarded as a part of the noise in addition to the shot noise. However, with the extension of the charge-integration time of the CCD, the effect of readout noise is reduced to be negligible. In this condition, the minimum detectable sensitivity reaches the shot-noise limit, which is similar to the 2D photon-counting tube (Eq. 7.1). Furthermore, because of its higher quantum efficiency and higher light-collection efficiency, it surpasses the performance of the 2D photon-counting tube. It originates in the large image area and back-illuminated structure of the CCD. Nevertheless, it requires long-duration exposure, restricting the time resolution of imaging as a disadvantage of CCD imaging. For spontaneous UPE observation, high temporal resolution is not primarily required. For that reason, the CCD is beneficial. Our group uses cooled CCD cameras providing a 2048×2048 pixel format with an image area of 27.6×27.6 mm ($13.5 \mu\text{m}$ square pixels) (CCD42-40; Teledyne e2v, UK). A liquid nitrogen system, a closed-cycle gas cooling system, or a thermo-electronic cooler is usually used for cooling the device, generally to about -100 °C. Recently, for convenience, a thermo-electronic cooler is generally used. For UPE applications, CCD is normally operated in a binning mode to shorten the integration time, which is a tradeoff for degrading the spatial resolution. The binning operation in the CCD can increase SNR without the addition of excess readout noise, in contrast with software binning conducted after image acquisition. It causes SNR degradation by the addition of excess readout noise.

For imaging applications, such as single-molecule fluorescence imaging, that require high speed, EMCCD with electron multiplication functionality is commonly used. It comprises an ion-impacted gain process for multiplication as a gain resistor equipped between a readout amplifier and a serial resistor. The benefit of EMCCD is that readout noise can be ignored by multiplication of the signal, allowing high-speed real-time imaging of weak light. However, the

additional noise originating in the fluctuation of gain, expressed as the excess noise factor, makes the SNR worse, as shown in Eq. (7.5) below.

$$\frac{S}{\mathcal{N}} = \frac{\eta \langle \mathcal{N}_p \rangle \mathcal{M} \mathcal{T}}{\sqrt{(\eta \langle \mathcal{N}_p \rangle + \langle \mathcal{N}_d \rangle) \mathcal{F}^2 \mathcal{M}^2 \mathcal{T} + \mathcal{N}_r^2}} \quad (7.5)$$

In that equation, M represents the gain. Also F denotes the excess noise factor, which depends on the gain. The minimum detectable photon-number is expressed as Eq. (7.6). With long-time exposure, it can be expressed as Eq. (7.7). Consequently, the minimum detectable photon-number in EMCCD becomes worse than CCD with a factor of \sqrt{F} . Actually, $F^2 \cong 2$ is known in the condition of $M > 20$ (Robbins and Hadwen 2003), demonstrating that the SNR of EMCCD is worse than CCD by a factor of $\sqrt{2}$.

$$\langle \mathcal{N}_p \rangle_{\min} = \frac{1}{\eta \mathcal{T} \mathcal{M}} \sqrt{\langle \mathcal{N}_d \rangle \mathcal{T} \mathcal{F}^2 \mathcal{M}^2 + \mathcal{N}_r^2} \quad (7.6)$$

$$\langle \mathcal{N}_p \rangle_{\min} = \frac{F}{\eta} \sqrt{\frac{\langle \mathcal{N}_d \rangle}{\mathcal{T}}} \quad (7.7)$$

Subsequently, the benefit of EMCCD is diminished for spontaneous UPE imaging, which requires a long exposure duration. Moreover, the small image area is an important shortcoming of EMCCD. If EMCCD could be operated in photon-counting mode similarly to silicon PMTs operated in Geiger mode and thereby achieving high detection efficiency, and if large area sensors were used, then EMCCD would be extremely useful for spontaneous UPE imaging.

7.2.3 Lens System

The selection of the lens system is crucially important for the UPE imaging system design. For spontaneous UPE imaging, the lens system should be selected with priority assigned to high throughput, representing the light collection efficiency determined by the f-number (or numerical aperture NA) and total transmittance of the lens elements. It restricts the spatial resolution. For that reason, it should be regarded as the minimum necessary spatial resolution. It is recommended that the specifically designed lens system be used for practical UPE imaging. Inaba's group developed three types of specially designed lens systems adapted for imaging the size of a human body to a soybean seed with magnifications of 1/20, 1/3, and 1.0. Optical design with minimization of the element number is crucially important to achieve improvement of the optical throughput. Kobayashi et al. reported the first UPE imaging of an in vivo rat brain (Kobayashi et al. 1999a, b), achieved using a specially designed 0.45 NA lens

system composed of six elements. It was designed to reach more than 88% of transmittance on the axis for throughput improvement. As a tradeoff against the throughput, the spatial resolution is constrained to approx. 5 line-pairs/mm in the 1.0 magnification lens.

7.3 UPE Spectral Analysis

Since the early stage of the discovery of UPE phenomena, spectral analyses have been demanded for elucidation of the UPE mechanisms, and especially for emission species identification. Commercially available spectroscopic devices, which usually use a diffraction grating, are unsuitable for UPE analysis because of the distinctive properties of UPE. Filter-type spectroscopy systems have been commonly used (Kobayashi et al. 2001; Kobayashi 2003; van Wijk and van Wijk 2005). Generally, they are composed of a series of optical filters, either high-pass or band-pass filters with a few tens of nanometers of resolution. This method can accept all directions of light irrespective of the incident angle, consequently being able to increase the effective area for improving the optical throughput. However, a mechanical system is necessary for filter exchange. This monochromatic scheme constrains the low temporal resolution determined by numerous filters that cover the observation wavelength range. Therefore, it is not suitable for spectroscopy of UPE, which has accompanying temporal variation. Therein, polychromatic spectroscopy which uses a diffractive grating equipped with a highly sensitive imaging device, is beneficial (Kobayashi et al. 2016; Scott and Inaba 1988; Nagoshi et al. 1992), because it is not affected by intensity variation during the measurement. It should be designed for UPE analysis, for which the optical throughput determined by the optical transparency of all elements and effective area for spectroscopy are primarily considered. The UPE sampling area is regulated by an optical input slit size (width and length). The effective area of the diffraction grating and the sensitivity of the imaging device are crucially important for the success of spectroscopy. However, the slit size expansion degrades the wavelength resolution, indicating the necessity of careful design considering the tradeoff relation between wavelength resolution and sensitivity.

7.3.1 Filter-Type UPE Spectral Analysis System

A filter-type spectral analysis system developed by Inaba's group and adapted for a wide wavelength range is described (Kobayashi et al. 2001; Kobayashi 2003). As the block diagram depicted in Fig. 7.3, two photomultiplier tubes

(PMT) bearing different spectral responses selected for single photon counting are equipped. The system is designed using colored glass filters that have sharp-cut-off transmittance properties of wavelengths. A set of 37 filters with different sharp-cut-off edge wavelengths of 250–850 nm is equipped. The spectral distribution is calculated after measurement by subtraction of the transmitted intensities in neighboring filters. The spectral responses of the two PMTs are, respectively, of wavelengths 300–900 nm (red-enhanced multi-alkaline) and 160–650 nm (ultraviolet-sensitive multi-alkaline). The filter inserted between PMT and the measurement sample is changed with the rotation of a disk on which 37 filters are mounted. Each rotation includes a through-hole position without a filter for correcting the intensity variation during measurements. After data correction with subtraction of the background emission of filters and spectral response of PMTs, integration of the intensity obtained in each filter is calculated to derive a spectral distribution. This system has a wavelength resolution of approximately 20–30 nm in the 300–700 nm range and 30–50 nm in the other UV and near-infrared regions of the wavelength.

7.3.2 Polychromatic Spectrum Analysis System Designed for UPE Study

The polychromatic spectral analysis system for UPE analysis based on a transmission-type grating is displayed schematically in Fig. 7.4. This is the system developed for UPE spectroscopy targeted to a human fingertip reported by Kobayashi et al. (Kobayashi et al. 2016). The salient features of this system include the use of lenses for optical systems and a large sampling area found by the 1-mm-wide and 20-mm-high entrance slit. Photons entering the slit are collimated using a collimator lens system designed to improve the NA and transmittance. The transmission-type diffraction grating, which has 300 lines/mm grooves with a 17.5° groove angle and active area of 50 mm × 50 mm, is inserted between the collimator lens and the condenser lens system. The transmission wavelengths are 400–900 nm with the efficiency of more than 40%; it has a peak at 550 nm with 75% efficiency. For polychromatic detection, the diffracted photons are focused on a cooled CCD camera through a condenser lens system. The CCD camera is the same camera used for UPE imaging described in the text above. It provides sufficient sensitivity performance for UPE imaging, which incorporates a back-illuminated-type 25 × 25 mm active area CCD (CCD42-40; e2v Inc., USA) with cooling performance capable of achieving –103 °C. The spectral sensitivity of the CCD covers 400–900 nm with a quantum efficiency of higher than 50%. With consideration of the spectral resolution, the

Fig. 7.3 Block diagram of the filter-type UPE spectral analysis system

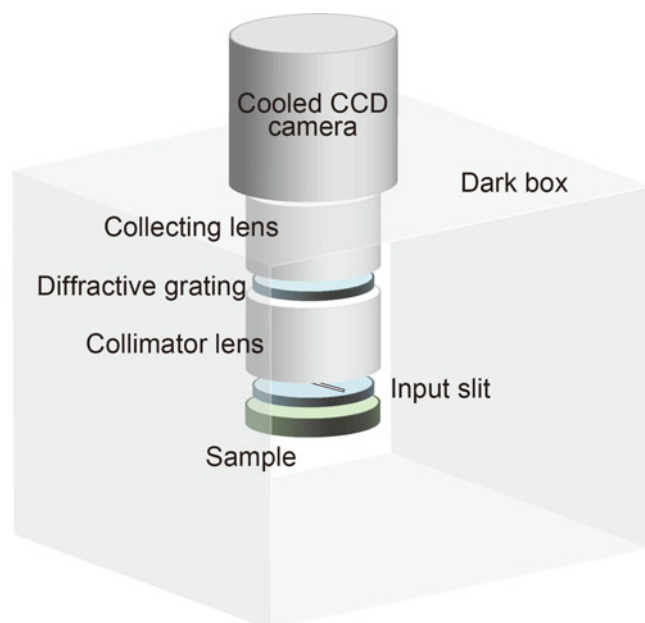
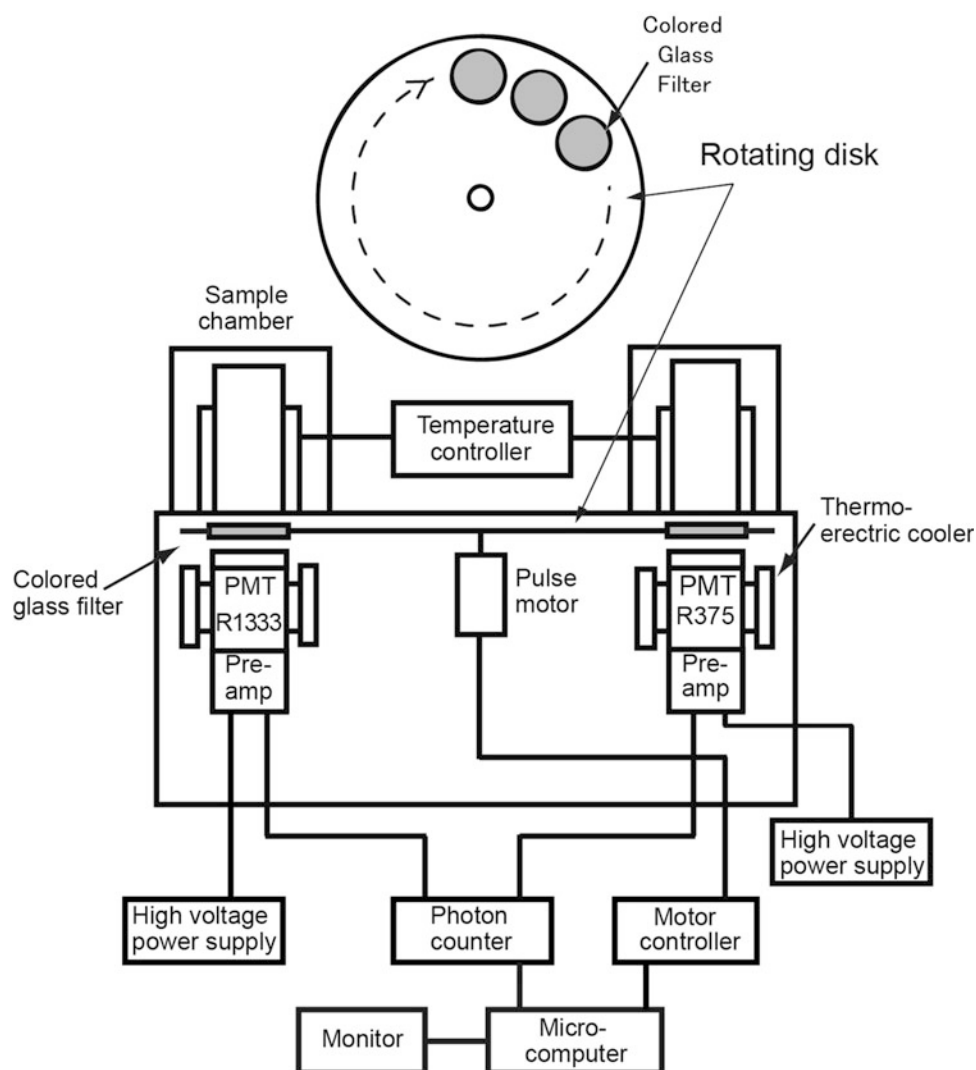


Fig. 7.4 Schematic illustration of the polychromatic spectral analysis system

CCD camera is operated with 8×8 binning mode, corresponding to the practical pixel size of $100 \times 100 \mu\text{m}$ and pixel number of 256×256 . The minimum detectable optical power within the slit area is estimated roughly as $1.0 \times 10^{-18} \text{ W}$, which is under measuring conditions of 20 min at 600 nm wavelength. Consequently, the peak-pair resolution of the wavelength for UPE analysis is approx. 80 nm. It is determined by the slit size, reciprocal linear dispersion (120 nm/mm), binned sizes of the CCD, and focal length of the condenser lens. To derive the UPE spectral distribution, the following sequence of data processing is demanded: (1) removal of cosmic-ray-induced hot noise from the image, (2) accumulation of CCD data along the vertical axis (height direction of the slit), (3) conversion of lateral pixel number to wavelength using calibration data, (4) background subtraction, (5) calibration of spectral properties ascertained according to the CCD response and the diffraction grating transmittance, (6) smoothing by a moving average within wavelength resolution to improve SNR.

7.4 Application of UPE Imaging and Spectral Analysis

7.4.1 UPE Images of Plants, Insects, Humans, and Other Mammals

As a demonstration of UPE imaging by the 2D photon-counting system and the cooled CCD camera system, UPE of plants, insects, humans, and other mammals are displayed in Figs. 7.5, 7.6, 7.7, and 7.8. Plant examples of UPE imaging are depicted respectively in Fig. 7.5a, b; the early stage of a germinating soybean representing respiratory activity and virally infected leaves induced by cucumber mosaic virus expressing physiological resistance, a hypersensitive response. These images were captured using the 2D photon-counting imaging system (Kobayashi et al. 2007).

Figure 7.6 is a UPE image of non-bioluminescent insects during metamorphosis, Lepidopteran swallowtail butterflies, the spangle; *Papilio protenor*, during morphogenetic

processes in larval–pupal ecdysis (pupation) (Usui et al. 2019). This result was observed using a cooled CCD imaging system. Characteristic patterns of UPE observed from a larva at 6 h before ecdysis (Fig. 7.6a), immediately before ecdysis (Fig. 7.6b), and a pupa 1 h after ecdysis (Fig. 7.6c) are depicted, respectively, representing physiological changes in the process of the preparation of molting, molting behavior of larva, and cuticle sclerotization of the pupa. Dynamics of UPE images representing the physiological changes regulating the metamorphosis from a larva to a pupa through a molting event are portrayed. Imaging was continued through 24 h with 5-min-exposure-time in each. All images were edited as moving pictures, depicting the spatiotemporal dynamics of specific UPE changes occurring during metamorphosis (see suppl. Videos 7.1 and 7.2).

As examples of UPE observed from animals, a UPE image of a normal rat brain (Fig. 7.7a) captured by the 2D photon-counting imaging system, a growing tumor observed from a cancer-cell-implanted nude mouse (Fig. 7.7b) (Takeda et al.

Fig. 7.5 UPE images of plants. (a) Early stage of a germinating soybean. (b) Cowpea leaves after viral infection, expressing the hypersensitive response

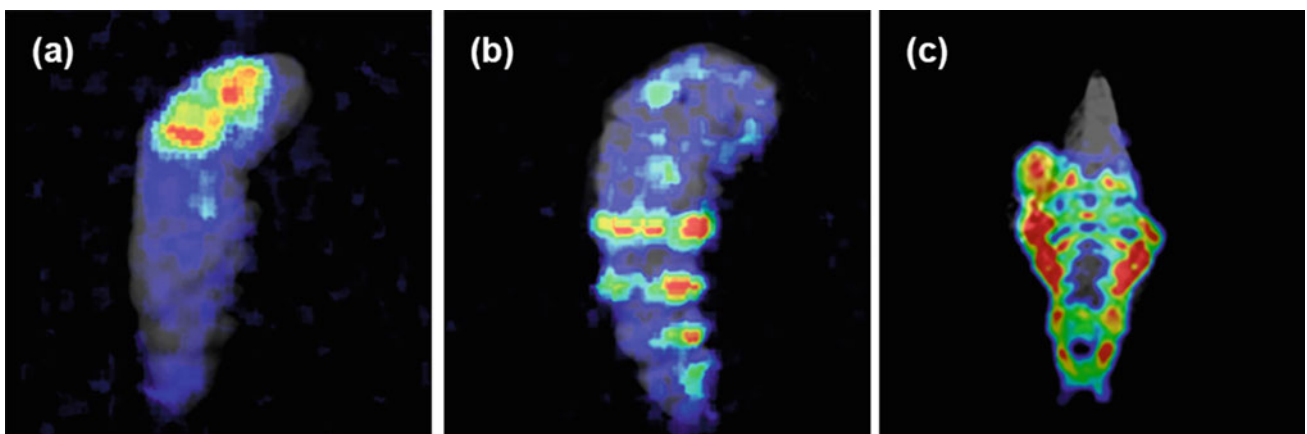
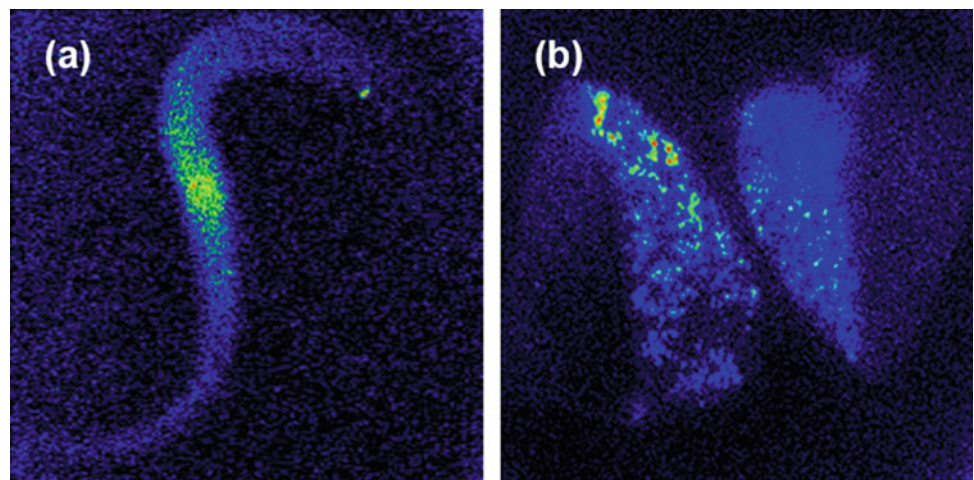


Fig. 7.6 UPE images of insects (Lepidopteran swallowtail butterflies, the spangle; *Papilio protenor*). All UPE images are superimposed on the pictures showing morphology of the insect. (a) 6 h before pupation of a

larva (larval–pupal ecdysis). (b) Right before the ecdysis of a larva. (c) 1 h after the ecdysis of a pupa

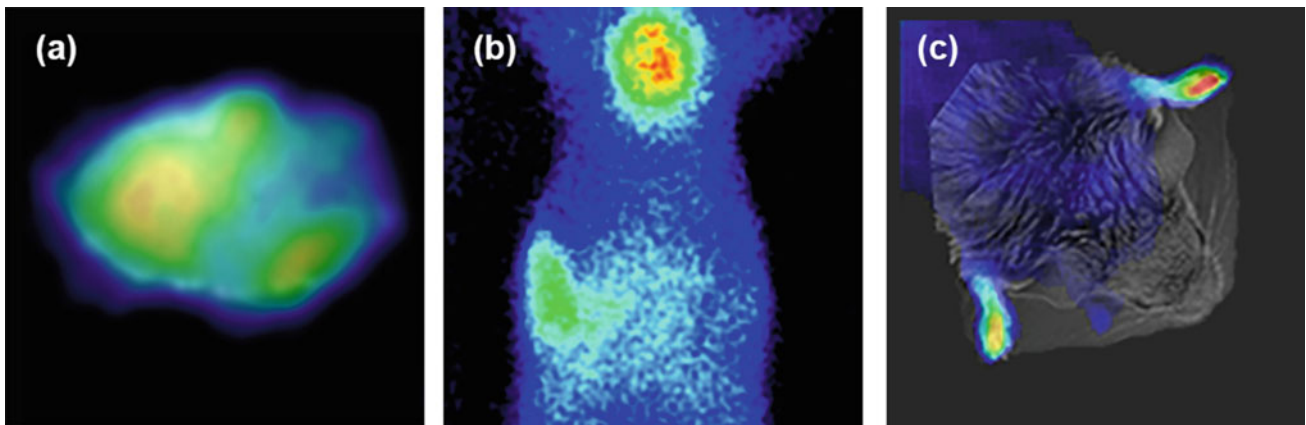
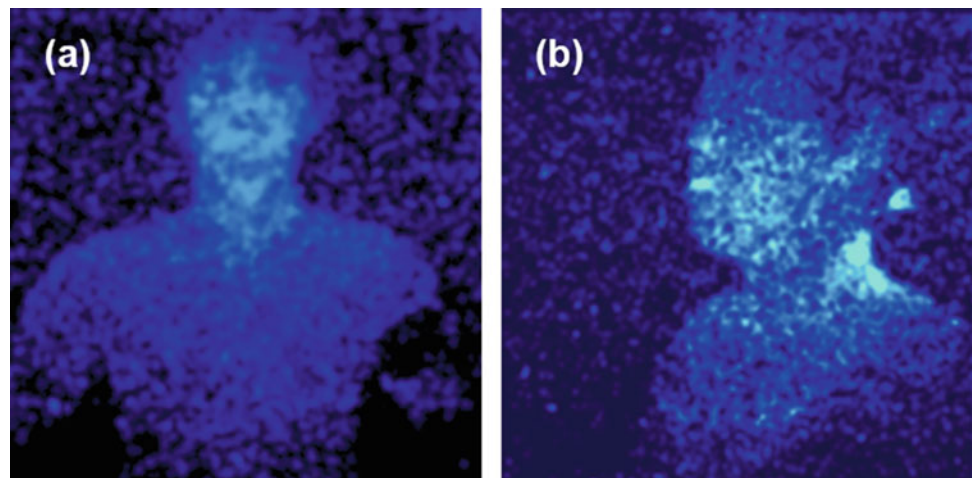


Fig. 7.7 UPE images of animals. (a) Normal rat brain observed through the skull under anesthesia. (b) Cancer-transplanted nude mouse. (c) Induced rheumatoid arthritis model mouse

Fig. 7.8 UPE images of a human body. (a) Spontaneous UPE of upper body (front view). (b) Spontaneous UPE of upper body (side view)



2004), and an artificially induced rheumatoid arthritis (RA) mouse (Fig. 7.7c) (Van Wijk et al. 2013) observed using the CCD system is portrayed. The latter two images depict the relation between the spontaneous UPE and pathological states associated with oxidative stress. Augmentation of UPE on the tumor is suggested, representing the proliferation activity of cancer cells caused by higher metabolic activity of cancer cells (Takeda et al. 2004). Regarding RA model mice, intense UPE was observed at the position corresponding to the foreleg joints, implying ROS production, which causes chronic inflammation by autoimmune disease.

A UPE image from the human body is displayed in Fig. 7.8. Spontaneous UPE images observed on the upper body in a normal healthy subject are depicted respectively as the front view and side view in Fig. 7.8a, b. The UPE intensity on the face is higher than the body under the head, implying different statuses of oxidative stress of skin between areas affected by the presence and absence of chronic UV exposure (Van Wijk et al. 2006; Kobayashi et al. 2009).

Figure 7.9 presents a comparison of a spontaneous UPE image (Fig. 7.9a) and a blue-light-induced UPE (or delayed luminescence; DL) image (Fig. 7.9b) observed on a human hand (Iwasa and Kobayashi 2018). The blue-light-induced UPE image was observed with a 5 min exposure time after irradiation of 3.9 J/cm^2 blue LED light (470 nm) on the fingertips (5 cm^2 irradiation area). The irradiated portion shows intense photon emissions that are three times higher than those of the non-irradiated portion (spontaneous UPE). Recently, blue light has become known to influence cells and tissues, leading to oxidative stress. Blue-light-induced UPE, which is inferred as derived through photosensitization reaction, might be an indicator of oxidative susceptibility of the skin. It can be inferred that UPE imaging is feasible for application to diagnose various diseases associated with oxidative stress. Exploration of UPE phenomena is progressing using the imaging system, including the evaluation of mechanisms (Tsuchida et al. 2019; Prasad 2011; Khabiri et al. 2008; Ou-Yang 2014).

Fig. 7.9 UPE images of a human hand. (a) Spontaneous UPE image. (b) Blue-light-induced UPE image (2.3 mJ 475 nm LED light was irradiated on two fingertips)

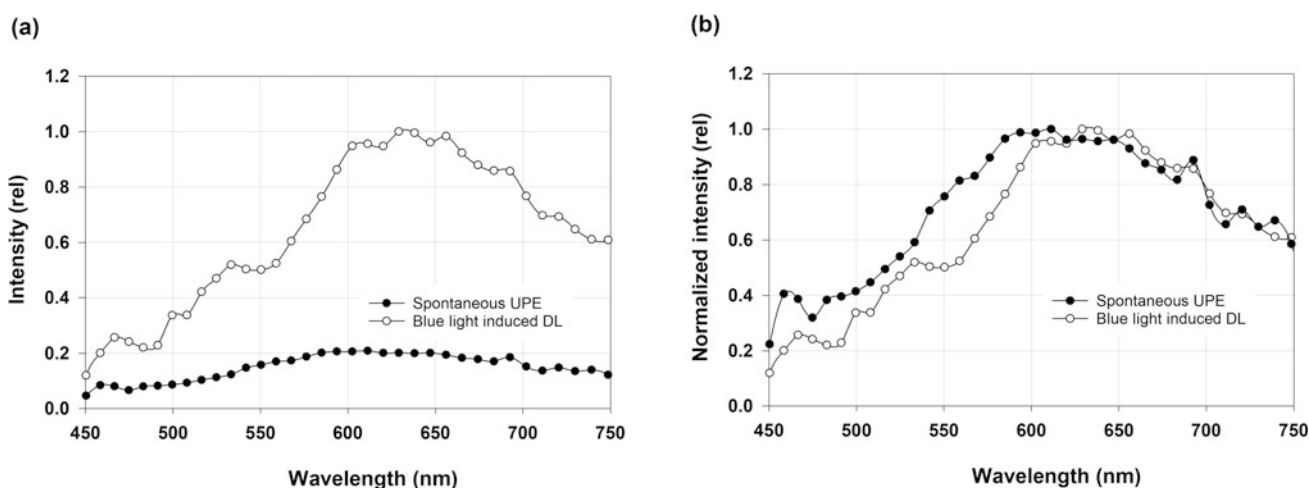
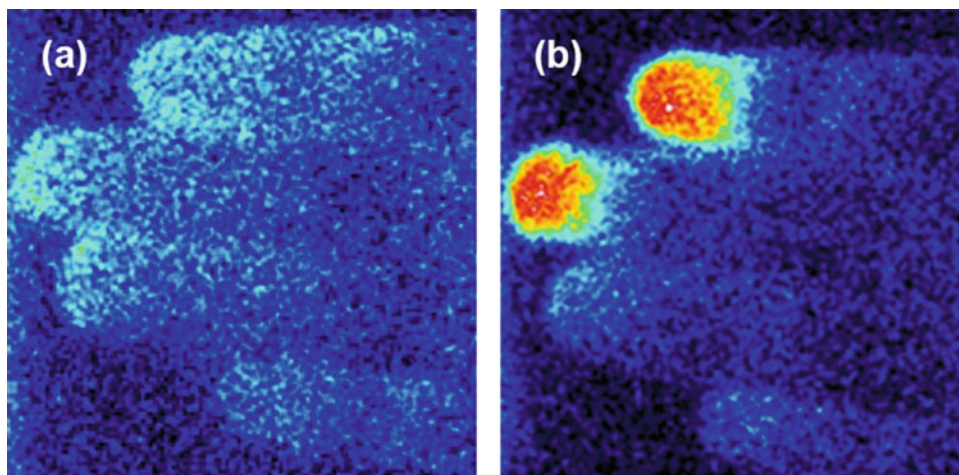


Fig. 7.10 UPE spectra of human hand observed using the polychromatic spectral analysis system. (a) Comparison between spontaneous and blue-light-induced UPE. (b) Comparison of them with intensity normalization in each

7.4.2 UPE Spectra of Human Skin

The UPE spectra of human skin, as observed on a fingertip, are displayed in Fig. 7.10, which depicts a comparison of spectra between spontaneous UPE and blue-light-induced UPE (Iwasa and Kobayashi 2018). These were acquired using a polychromatic spectral analysis system with the cooled CCD camera described in Sect. 7.3.2 (Kobayashi et al. 2016). A spontaneous UPE spectrum was observed with an exposure time of 15 min after 15 min dark adaptation in a darkroom. Blue-light-induced UPE was observed with 5 min exposure time after 13 mW and 3 min irradiation by a blue LED light. Figure 7.10a presents a comparison of these spectra, which highlights the difference in the intensities. To compare their spectral patterns, intensity normalization at peak intensity in each is conducted, resulting in Fig. 7.10b. In both spectral patterns, the major wavelength region of photon emissions is observed similarly at 600–750 nm, with a broad emission pattern across the visible wavelength.

However, a difference in spectral patterns was noticed at the spectral region of 500–600 nm: the blue-light-induced UPE composition ratio is smaller than that of spontaneous UPE (Kobayashi et al. 2016; Iwasa and Kobayashi 2018).

The photon emission species can be inferred from the spectral distribution. In spontaneous UPE, the region of 500–600 nm probably corresponds to melanin fluorescence, meaning that it is derived by Förster resonance energy transfer from the excited species originating in the lipid peroxidation process. The 600–700 nm region observed in both spontaneous and blue-light-induced UPE might derive from porphyrin compounds through energy transfer or direct excitation through photosensitization. As demonstrated here, the polychromatic spectral analysis has superiority for the application of UPE, which accompanies temporal changes such as light-induced UPE or DL. Polychromatic UPE spectroscopy, being a powerful tool for UPE application development, can facilitate the exploration of mechanisms with the identification of UPE species (Kobayashi et al. 2016).

7.5 Conclusion

Novel technologies of imaging and spectroscopy for UPE analysis were presented. Characterization of spatial, temporal, and wavelength properties of UPE is crucially important for developing UPE applications including mechanism exploration. This chapter provided a technical description with historical aspects of UPE measurement with a demonstration of images and spectra obtained from various biological samples using our developed systems. From our experience accumulated over more than 30 years, highly sensitive imaging devices and high-throughput lens systems are key devices used for imaging and spectroscopy. Particularly, commercially available lens systems are unsuitable for UPE detection, which should be originally designed or customized while aiming for the targets. Future advancements of imaging devices such as EMCCD and CMOS image sensors are expected to extend the potential for studies of UPE and their applications.

References

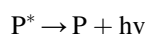
- Amano T, Kobayashi M, Devaraj B, Usa M, Inaba H (1995) Ultraweak biophoton emission imaging of transplanted bladder cancer. *Urol Res* 23: 315–318
- Ichimura T, Hiramatsu M, Hirai N, Hayakawa T (1989) Two-dimensional imaging of ultra-weak emission from intact soybean roots. *Photochem Photobiol* 50: 283–286
- Iwasa T, Kobayashi M (2018) Imaging and spectral analysis of ultraweak biophoton emission and delayed luminescence from human skin. In CLEO Pacific Rim 2018, W3A.131, Hong Kong Convention and Exhibition Centre, Hong Kong, 1 August 2018
- Khabiri F, Hagens R, Smuda C, Soltau A, Schreiner V, Wenck H, Wittern KP, Duchstein HJ, Mei W (2008) Non-invasive monitoring of oxidative skin stress by ultraweak photon emission (UPE)-measurement. I: mechanisms of UPE of biological materials. *Skin Res Technol* 14: 103–111
- Kobayashi M (2003) Spontaneous ultraweak photon emission of living organisms – biophotons – phenomena and detection techniques for extracting biological information. *Trends in Photochem Photobiol* 10: 111–135
- Kobayashi M (2014) Highly sensitive imaging for ultra-weak photon emission from living organisms. *J Photochem Photobiol B: Biology* 139:34–38. doi: <https://doi.org/10.1016/j.jphotobiol.2013.11.011>
- Kobayashi M, Devaraj B, Usa M, Tanno Y, Takeda M, Inaba H (1996) Development and applications of new technology for two-dimensional space-time characterization and correlation analysis of ultraweak biophoton information. *Frontiers Med Biol Engng* 7 (4): 299–309
- Kobayashi M, Devaraj B, Usa M, Tanno Y, Takeda M, Inaba H (1997) Two-dimensional imaging of ultraweak photon emission from germinating soybean seedlings with a highly sensitive CCD camera. *Photochem Photobiol* 65: 535–537
- Kobayashi M, Takeda M, Sato T, Yamazaki Y, Kaneko K, Ito KI, Kato H, Inaba H (1999a) In vivo imaging of spontaneous ultraweak photon emission from a rat's brain correlated with cerebral energy metabolism and oxidative stress. *Neurosci Res* 34: 103–113
- Kobayashi M, Takeda M, Sato T, Yamazaki Y, Kaneko K, Ito KI, Kato H, Inaba H (1999b) Two-dimensional photon counting imaging and spatiotemporal characterization of ultraweak photon emission from a rat's brain in vivo. *J Neurosci Meth* 93: 163–168
- Kobayashi M, Usa M, Inaba H (2001) Highly sensitive detection and spectral analysis of ultraweak photon emission from living samples of human origin for the determination of biomedical information. *Trans SICE E-1* (1) 214–220
- Kobayashi M, Sasaki K, Enomoto M, Ehara Y (2007) Highly sensitive determination of transient generation of biophotons during hypersensitive response to cucumber mosaic virus in cowpea. *J Exp Botany* 58: 465–472
- Kobayashi M, Kikuchi D, Okamura H (2009) Imaging of ultraweak spontaneous photon emission from human body displaying diurnal rhythm. *PLoS ONE* 4: e6256. doi: <https://doi.org/10.1371/journal.pone.0006256>
- Kobayashi M, Iwasa T, Tada M (2016) Polychromatic spectral pattern analysis of ultra-weak photon emissions from a human body. *J Photochem Photobiol B* 159: 186–190. <https://doi.org/10.1016/j.jphotobiol.2016.03.037>
- Nagoshi T, Watanabe N, Suzuki S, Usa M, Watanabe H, Ichimura T, Inaba H (1992) Spectral analysis of low level chemiluminescence of a short lifetime using a highly sensitive polychromatic spectrometer incorporating a two-dimensional photon-counting type detector. *J Photochem Photobiol* 56: 89–94
- Ou-Yang H (2014) The application of ultra-weak photon emission in dermatology. *J Photochem Photobiol B* 139: 63–70
- Popp FA (ed) (1988) Special issue on Biophoton emission. *Experientia* 44 (7):543–630
- Pospíšil P (ed) (2014) Special issue on Ultra-weak photon emission from living systems – from mechanism to application. *J. Photochem. Photobiol. B* 139:1–84
- Prasad A, Pospíšil P (2011) Two-dimensional imaging of spontaneous ultraweak photon emission from the human skin: role of reactive oxygen species. *J Biophotonics* 4: 840–849
- Robbins M, Hadwen B (2003) The noise performance of electron multiplying charge-coupled devices. *IEEE Trans Electron Devices* 50: 1227–1232
- Scott RQ, Inaba H (1988) Single photon counting imagery. *J Biolum Chemilum* 4: 507–511
- Scott RQ, Usa M, Inaba H (1989) Ultraweak emission imagery of mitosing soybeans. *Appl Phys B* 48: 183–185.
- Suzuki S, Usa M, Nagoshi T, Kobayashi M, Watanabe N, Watanabe H, Inaba H (1991) Two-dimensional imaging and counting of ultraweak emission patterns from injured plant seedlings. *J Photochem Photobiol B* 9: 211–217
- Takeda M, Kobayashi M, Takayama M, Suzuki S, Ishida T, Ohnuki K, Moriya T, Ohuchi N (2004) Biophoton detection as a novel technique for cancer imaging. *Cancer Sci* 95: 656–661
- Tsuchida K, Iwasa T, Kobayashi M (2019) Imaging of ultraweak photon emission for evaluating the oxidative stress of human skin. *J Photochem Photobiol B* 198: 111562. <https://doi.org/10.1016/j.jphotobiol.2019.111562>
- Tuchiya Y, Inuzuka E, Kurono T, Hosoda M (1985) Photon-counting imaging and its application. *Adv Electronics Electron Phys* 64A: 21–31
- Usui S, Tada M, Kobayashi M (2019) Non-invasive visualization of physiological changes of insects during metamorphosis based on biophoton emission imaging. *Scientific Reports* 9: 8576. <https://doi.org/10.1038/s41598-019-45007-3>
- van Wijk EPA, van Wijk R (2005) Multi-site recording and spectral analysis of spontaneous photon emission from human body. *Forsch Komplementärmed Klass Naturheilkd* 12: 96–106
- Van Wijk R, Kobayashi M, Van Wijk EP (2006) Anatomic characterization of human ultra-weak photon emission with a movable photomultiplier and CCD imaging. *J Photochem Photobiol B* 83: 69–76
- Van Wijk E, Kobayashi M, Van Wijk R, Van der Greef J (2013) Imaging of ultra-weak photon emission in a rheumatoid arthritis mouse model. *PLoS ONE* 8 (12): e84579. doi: <https://doi.org/10.1371/journal.pone.0084579>

Part III

Molecular Mechanisms of UPE

8.1 Introduction

As discussed above (see Part II), the appearance of any photon in a system is a consequence of the relaxation of some electronically excited state (EES):



Thus, the phenomenon of luminescence automatically requires constant appearance of electronic excitation within the system, and conditions for its further radiative relaxation (Scheme 8.1).

If the system is illuminated by external light, such electron-excited states (EES) may appear due to its absorption. This way is active in photosynthetic systems, in which there are many “adjustments” for inactivating EES to prevent uncontrolled dangerous processes with their participation (photochemical reactions).

Aside from this specific case, the main sources of electron excitation in biological systems are free-radical processes, proceeding by chain, including branched-chain mechanisms. Thus, spontaneous photon emission of biological systems, or biological autoluminescence (BAL), is almost exclusively chemiluminescence (see Chap. 5, Sect. 5.2).

Moreover, we can safely make the following statements:

1. In the absence of special external influences, all known cases of BAL relate specifically to chemiluminescence.
2. Spontaneous generation of EES in all known biological systems (and BAL at their relaxation) occurs as a result of free-radical processes, or at least with intermediate free-radical products. (A separate but very important case, photoinduced luminescence of photosystems also occurs through free-radical stages, although the initial energy comes from external illumination).

Thus, the phenomenon of biological autoluminescence is inextricably linked with free-radical processes, and the study of its mechanisms is almost entirely the study of free radicals.

Accordingly, this part of this book, devoted to molecular mechanisms of BAL, is actually a gradual step-by-step proof of the above statements. The next Chaps. 9, 10, 11, 12, 13, and 14, show detailed investigation of the origin of free radicals in different model and biological systems, as well as important, dangerous, and vital processes with their participation. For a better organization and a clear understanding of this huge and complicated material, this chapter is devoted to a general overview of the role of free radicals in biology, their classification and methods of experimental and theoretical work with them.

8.2 One-Electron Oxygen Reduction as a Source of Free Radicals

As is well known, “ordinary” molecules have two electrons in their upper filled electron orbital. It is the interaction of these paired electrons magnetic moments that ensure stability of chemical compounds. Contrary to that, free radicals are molecules containing one or more unpaired (single) electrons at the upper orbitals, which make them chemically active particles. The radical “seeks” to reclaim the missing electron, taking it from other molecules with which it collides, or to donate the unpaired electron to other species, with higher electron affinity.

Unlike most other molecules, oxygen in its ground state is triplet, 3O_2 , that is, it contains two unpaired electrons, forming a bi-radical. Thus, it is prone to accept two additional electrons, usually one by one, forming a number of intermediate species, that line up in a chain of one-electron oxygen reduction (Scheme 8.2).

I. Volodyaev (✉) · Y. A. Vladimirov
Moscow State University, Moscow, Russia

In the first step, the oxygen molecule (${}^3\text{O}_2$, Scheme 8.2a) accepts an electron, forming a mono-radical $\text{O}_2^- \cdot$ (Scheme 8.2b), which is also an anion, since the particle as a whole is negatively charged. The exact name of this molecular particle is radical dioxide, or dioxy, but the well-established name is superoxide anion-radical. Superoxide is involved in a variety of processes, both as an oxidizing agent and as a reducing agent (see Sect. 8.3.2). In addition, in neutral or acidic media, it quickly adds a proton, transforming into a neutral hydroperoxide radical $\text{HOO} \cdot$ (Scheme 8.2c). The latter forms hydroperoxide anion HOO^- upon further one-electron reduction (Scheme 8.2d). HOO^- , in its turn, attaches a proton, forming a neutral hydrogen peroxide molecule (Scheme 8.2e).

The scheme of the above reactions can be represented as follows (Scheme 8.3):

The H_2O_2 (HOOH) molecule also enters into further reactions, forming a whole spectrum of possible products, many of which are also radicals – including the most reactive radical $\text{OH} \cdot$.

In the presence of oxygen, this chain of reactions is one of the main sources of free radicals both in biological and in model systems.

8.3 Reactive Oxygen Species

All the radicals shown above (Scheme 8.2 and 8.3), as well as the hydrogen peroxide molecule and a number of other compounds, are usually classified as the family of reactive oxygen species (ROS).

Although the term itself is extremely widespread in the scientific literature, there is no clear generally accepted

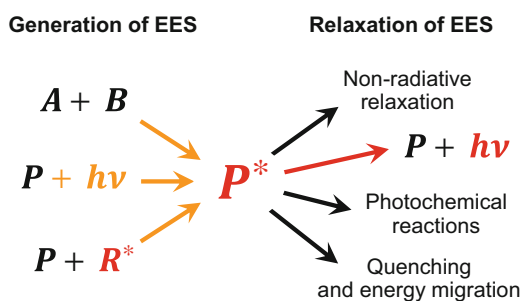
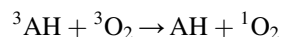
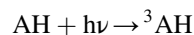
definition of it, and many authors put it in different meanings. Here we present the widest possible set of radicals and molecules attributed to ROS (Table 8.1). Some of these compounds would be more correctly attributed to active forms of other substances, which is what a number of authors are doing (see column 3).

8.3.1 Singlet Oxygen

As already discussed above, oxygen molecule in the ground, unexcited state is *triplet* (${}^3\text{O}_2$). Under the action of radiation in the near infrared region, the triplet oxygen passes into an excited, *singlet* state (${}^1\text{O}_2$) (see reviews (Krasnovsky 2007, 2015) for the history of its discovery, and its main properties). The energy difference between the ground state and singlet oxygen is 0.98 eV per molecule, which corresponds to a transition in the near IR range ($\lambda \cong 1270$ nm).

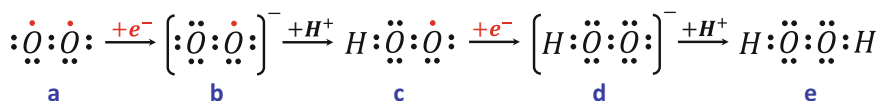
A direct transition between the singlet and triplet states is very unlikely due to spin exclusion. Therefore, direct ${}^3\text{O}_2 \rightarrow {}^1\text{O}_2$ excitation under the action of IR light practically does not occur, as well as spontaneous relaxation ${}^1\text{O}_2 \rightarrow {}^3\text{O}_2$ (the average lifetime of ${}^1\text{O}_2$ in the gas phase is estimated from minutes to dozens of minutes (Wang et al. 2020; Krasnovsky 2015)). In solutions, the molecules ${}^1\text{O}_2$ willingly enter into reactions with other molecules, and the ${}^1\text{O}_2$ lifetime is reduced to microseconds or less, primarily due to quenching by water molecules.

Singlet oxygen is chemically very active, which is used in photodynamic therapy of cancerous tumors (Krasnovsky 1998). The patient is given photodynamic sensitizers (hematoporphyrin, phthalocyanines), then the tumor site is irradiated with laser light, and the tumor tissue is selectively destroyed. This is a very effective method, especially in the postoperative period after surgical removal of the main tumor (Gunaydin et al. 2021). Upon irradiation, the sensitizer molecule (AH) transforms into an excited triplet state (${}^3\text{AH}$), reacts with molecular oxygen (which is in the ground, triplet state ${}^3\text{O}_2$), forming the extremely reactive singlet oxygen ${}^1\text{O}_2$:



Scheme 8.1 Generation and relaxation of electronically excited states (EES)

Scheme 8.2 One-electron oxygen reduction



Scheme 8.3 One-electron oxygen reduction

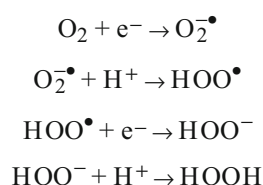


Table 8.1 Radicals and molecules classified as reactive oxygen species. Alternative options for classification are presented in the last column: RCS – reactive chlorine species, RNS – reactive nitrogen species, RLS – reactive lipid species

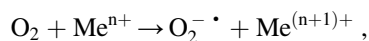
| Formula | Name | Alternative classification |
|--------------------------|-----------------------------------|----------------------------|
| $^1\text{O}_2$ | Singlet oxygen | ROS |
| $\text{O}_2^{\bullet -}$ | Superoxide anion-radical | ROS |
| H_2O_2 | Hydrogen peroxide | ROS |
| OH^{\bullet} | Hydroxyl radical | ROS |
| O_3 | Ozone | ROS |
| ClO^- | Hypochlorite | RCS |
| NO^{\bullet} | Nitrogen monoxide (nitric oxide) | RNS |
| ONOO^- | Peroxynitrite | RNS |
| L^{\bullet} | Alkyl (lipoalkyl) | RLS |
| LO^{\bullet} | Alkoxy (lipoxyl) | RLS |
| LOO^{\bullet} | Dioxil (peroxyl, lipoperoxil) | RLS |
| LOOH | Hydroperoxide (lipohydroperoxide) | RLS |

The $^1\text{O}_2$ molecule is further involved in the processes of damage to cancer cells.

8.3.2 Superoxide Anion-Radical

Superoxide anion-radical (radical dioxide or dioxy) is the first product in the chain of one-electron oxygen reduction (Scheme 8.2 and 8.3).

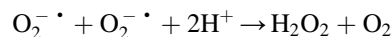
In the cell and in model systems, it is formed due to the reaction of oxygen with transition metals:



in the mitochondrial respiratory chain and during oxidation of NADPH with molecular oxygen using NADPH oxidase (see more in Chap. 14).

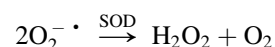
Superoxide has the properties of either an oxidizing agent or a reducing agent, depending on the partner. If there are no other partners, two superoxide molecules readily react with

each other, entering into a dismutation reaction, where one radical $\text{O}_2^{\bullet -}$ acts as an oxidizing agent, and the other one as a reducing agent:

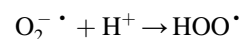


The spontaneous course of such a reaction is impeded by the electrostatic repulsion of two anions, and in proton-less media (nonpolar solvents, lipid layers of membranes or simply strongly alkaline media) superoxide radicals can exist for minutes or even hours.

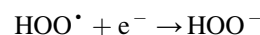
In the cell, the superoxide dismutation reaction is mainly enzymatic, due to catalysis by the enzyme superoxide dismutase (SOD, see Chap. 14):



In neutral and acidic media, superoxide anion quickly and spontaneously (without enzymes) attaches a proton, turning into a neutral hydroperoxide radical:



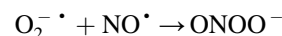
HOO^{\bullet} quickly attaches an electron to form the hydrogen peroxide anion:



By attaching a proton, this anion turns into a neutral molecule H_2O_2 :



Besides other reactions, superoxide readily reacts with nitric oxide, constantly produced in the cell, with a rate constant of $\sim 7 \times 10^9 \text{ M}^{-1}\text{s}^{-1}$ (Huie 1993), so that nearly every collision between these species results in an irreversible reaction:



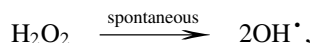
The formed peroxynitrite is a strong oxidizing and nitrating agent (Szabó et al. 2007), and its conjugated peroxynitrous acid homolyzes forming NO_2 and OH^{\bullet} (Beckman et al. 1990):



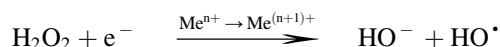
8.3.3 Hydrogen Peroxide and Hydroxyl Radicals

Hydrogen peroxide plays a huge role in the cell, including regulatory pathways.

Spontaneously, in the absence of enzymes, H_2O_2 can either undergo thermal decomposition:



which is highly unlikely under normal conditions, or one-electron reduction on transition metal ions in the *Fenton reaction* (Halliwell and Gutteridge 2015):



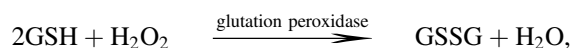
In particular, in the most common situation with iron ions:



In both of these reactions, an extremely chemically aggressive hydroxyl radical OH^\bullet , the most reactive of all ROS, is formed.

Hydroxyl radicals cause destruction in all vital cellular components. Penetrating into biological membranes, they initiate reactions of lipid chain oxidation, leading to membrane dysfunction, primarily as a barrier for ions and water-soluble molecules. In proteins, OH^\bullet oxidize thiol groups and histidine residues, thereby inactivating most of the enzymes. Acting on nucleic acids, OH^\bullet cause mutations. Many known mutagens act by forming hydroxyl radicals during their metabolism (Korkina et al. 1992; Moody and Hassan 1982; Reha-Krantz 2013). Thus, the Fenton reaction plays an important role in the development of a wide range of pathological processes.

In the cell, the most important reaction with the participation of H_2O_2 is glutathione oxidation, catalyzed by glutathione peroxidase:



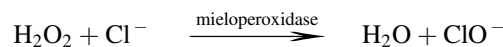
Glutathione plays the role of the main reservoir of sulfhydryl groups in the cell, and a decrease in its level leads to the oxidation of protein thiols and a change in activity of a number of enzymes. In addition, this reaction is accompanied by a decrease in redox potential.

Thus, the H_2O_2 molecule (and, accordingly, its precursor, $\text{O}_2^{\bullet -}$) plays the role of a regulator of a number of important processes in the cell, that is, behaves as a second messenger (see more in Chap. 14).

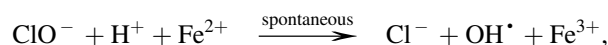
At the same time, being a potential source of the OH^\bullet radical, hydrogen peroxide can trigger many destructive processes.

8.3.4 Other Reactive Oxygen Species

Many authors also consider hypochlorite a reactive oxygen species. It is formed by the interaction of hydrogen peroxide with chloride ions under the action of myeloperoxidase:



In the presence of transition metals, ClO^- enters into the reaction, which was studied by A.N. Osipov and colleagues using the spin trap method (Osipov et al. 1993):



generating the OH^\bullet radical.

Considering the wide prevalence of Cl^- ions both in the cell and in the extracellular fluid, this path of OH^\bullet generation turns out to be no less and even more significant than the classical Fenton reaction.

Strictly speaking, hypochlorite could be attributed to active forms of chlorine, as well as peroxyxynitrite – to active forms of nitrogen.

Lipid radicals include three types of radicals – alkyl, alkoxy and dioxy radicals – which appear during lipid chain oxidation (see Chap. 11). Many authors also classify them as reactive oxygen species, although, in fact, these are more like reactive lipid species. Lipid hydroperoxides (LOOH) can also be classified as reactive lipid species, since they are easily involved in Fenton-like reactions, as well as subjected to the peroxidase action, thus forming lipid radicals and branching the lipid peroxidation chains. All these connections will be thoroughly covered in Chaps. 10 and 11.

8.4 Classification of Radicals

A convenient classification of free radicals occurring in the human body, and in biological systems in general, was proposed by Yu.A. Vladimirov (Vladimirov et al. 2017) (Fig. 8.1).

First of all, radicals formed in the cell and in the body as a whole can be divided into *natural*, spontaneously formed in the system, and *alien*, generated under certain external influences.

Fig. 8.1 Classification of free radicals in biological systems according to Yu.A. Vladimirov

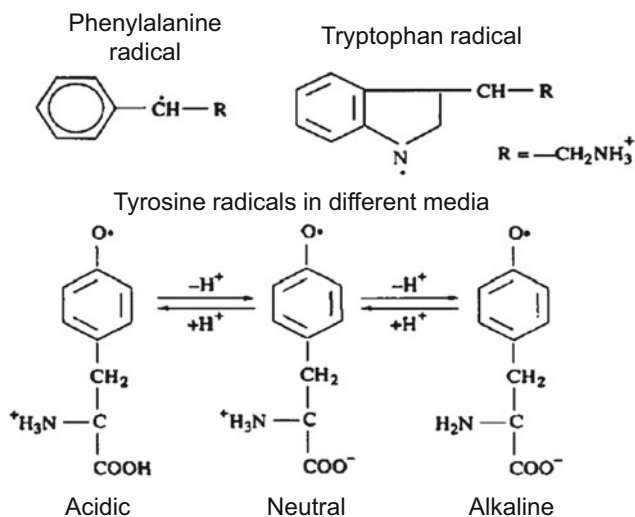
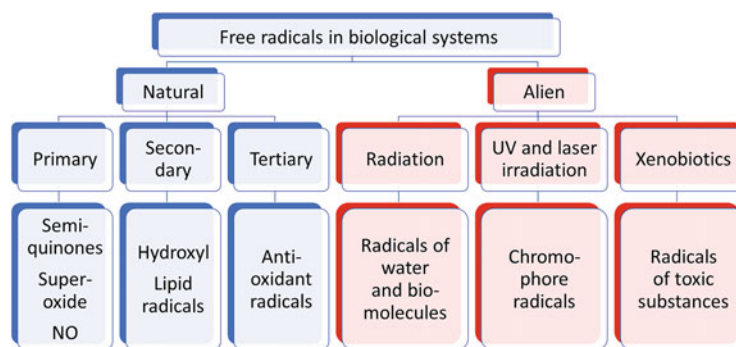


Fig. 8.2 Free radicals formed by the action of UV irradiation on amino acids. (Adapted from Vladimirov et al. (1966), with permission from the authors)

8.4.1 Alien Radicals

Alien radicals are those formed under the influence of adverse environmental factors: radiation or UV exposure, chemicals, etc. For instance, hard radiation produces water radicals and organic radicals; UV irradiation produces chromophore radicals, etc. The primary action of UV is photoionization, that is, “knocking out” an electron from a molecule. Thus, it ionizes aromatic amino acid residues in proteins, leading to formation of tyrosine, tryptophan, and phenylalanine radicals, through an intermediate state of radical-cation:



Formulas of aromatic amino acid radicals are shown in Fig. 8.2.

The formed radicals can react with adjacent amino acids, which leads to protein damage and to reactions of protein and/or lipid chain oxidation in the membrane structures of the cell.

When various poisons and toxins are metabolized in the body, they also form free radicals that destroy cells and tissues. For example, microsomal oxidation in the liver involves free-radical stages of the cytochrome P450 active center, which easily generate superoxide (see Chap. 14), but normally remain localized in the active center, causing no harm to the cell. Yet, in the presence of hepatotropic toxins, for example, carbon tetrachloride CCl_4 , radicals can escape from the active center of P450 and initiate chain oxidation of lipids, leading to the liver tissue destruction.

8.4.2 Natural Radicals

Natural radicals can be classified into primary, secondary, and tertiary.

8.4.2.1 Primary Radicals

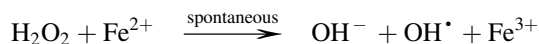
Primary radicals are those specially formed in the body as a result of enzymatic reactions. They are necessary for normal functioning of living cells and the body as a whole (see Chap. 14). These radicals include the following:

1. Respiratory chain electron carrier radicals: ubisemiquinone (Q^{\bullet}) and flavin radicals such as FAD^{\bullet} .
2. Superoxide $\text{O}_2^{\bullet-}$, formed by the enzyme NADPH oxidase in cell membranes, primarily of phagocytes, in the mitochondrial respiratory chain and on transition metal ions. $\text{O}_2^{\bullet-}$ is a source of other reactive oxygen species: hydrogen hydroperoxide H_2O_2 , hydroxyl radical OH^{\bullet} , singlet oxygen $^1\text{O}_2$, hypochlorite ClO^- .
3. Nitrogen monoxide NO^{\bullet} , which is synthesized by a group of enzymes called β -synthases. NO^{\bullet} is a natural factor in vascular relaxation and regulation of blood pressure. In particular, nitroglycerin, an important drug used in coronary artery disease, acts by stimulating NO^{\bullet} formation. Primary radicals are rapidly converted into molecular products, due to their high reactivity, and specific enzyme systems responsible for their further transformation (see Chap. 14). The formed molecular products are usually also chemically very active.

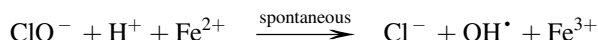
8.4.2.2 Secondary Radicals

Secondary radicals are formed when peroxide molecules and some other active compounds are broken down in one-electron reduction or oxidation processes. Hydroxyl and lipid radicals seem to play the most important role in biological systems.

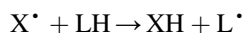
Hydroxyl radicals are formed in the *Fenton reaction* (Halliwell and Gutteridge 2015):



and in the *Osipov reaction* (Osipov et al. 1993):



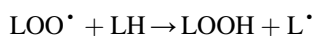
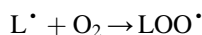
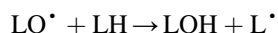
Lipid radicals (LO^\bullet , L^\bullet , and LOO^\bullet) are formed when lipid molecules (LH) are oxidized by other, already existing radicals:



(where X^\bullet is a primary radical, or in general any radical present in the system), as well as at the interaction of transition metal ions (e.g., Fe^{2+}) with lipid hydroperoxides (LOOH):



These reactions trigger a chain process of lipid peroxidation, which no longer requires primary radicals or metal ions and develops independently as long as there are lipids and molecular oxygen (see Chaps. 10 and 11):

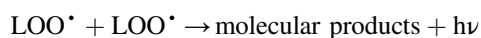


forming three types of radicals replacing each other in this chain: alkyl L^\bullet , alkoxy LO^\bullet , and dioxy LOO^\bullet .

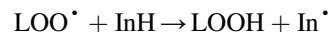
Lipid peroxides LOOH formed during this process, also react with Fe^{2+} and other metals, generating new peroxidation cycles $\text{L}^\bullet \leftrightarrow \text{LOO}^\bullet$.

Thus, an uncontrolled process of peroxidation can potentially lead to oxidation of all lipids in the membrane, a change in its viscosity and surface charge, and, as a result, to electrical breakdowns of the membranes and their destruction.

In nature, these processes are limited by recombination of free radicals, for example.,



and reactions with the so-called antioxidants – molecules that are readily oxidized by free radicals, turning them into molecules and forming relatively inert radicals of their own:



These processes will be discussed in more detail in Chaps. 10 and 11.

Other secondary radicals of utmost importance in the cell are *amino acid* and *protein radicals* formed during their oxidation by primary radicals (see above and also Chap. 12).

Secondary radicals have high chemical activity and, as a rule, harm the surrounding molecules, cells, and the body as a whole, participating in the chain processes of peroxidation.

8.4.2.3 Tertiary Radicals

Tertiary radicals are antioxidant radicals (“radical traps” or inhibitors of free-radical processes) – In^\bullet . They have a complex spatial structure, shielding the active site from the surrounding molecules, and therefore are much less reactive than secondary radicals. Thus, they “isolate” the unpaired electron and quench further development of oxidation chains.

The In^\bullet radicals themselves can be either beneficial or harmful, depending on the circumstances. In particular, α -tocopherol radicals can turn out to be prooxidants, reacting with lipid hydroperoxides (Izmailov and Vladimirov 2003).

8.5 Methods of Research on Free Radicals

Although free radicals themselves are not the direct subject of this monography, and the methods of their study – all the more, some of them will be immediately necessary for us in the subsequent sections. It was these methods that made the processes of light generation in biological systems available for discovery and research. Thus, without their understanding and application, some of the subsequent sections will be completely incomprehensible.

Therefore, here we devote a special section to the methods of free-radical research, with accents dictated by their necessity for the subsequent presentation.

These methods can be divided into three main categories: biophysical, biochemical methods and methods of kinetics and mathematical modeling.

8.5.1 Biophysical Methods

Biophysical methods can also be called direct methods, since they directly detect the presence of unpaired electrons in the system (the electron-spin resonance method), or the process of their recombination (chemiluminescence).

8.5.1.1 Electron-Spin Resonance

As is known, the electron-spin resonance (ESR) or electron-paramagnetic resonance (EPR) method is a classical approach for detecting particles with nonzero spin, including free radicals. Description and explanation of the method can be found elsewhere (Wertz 1986; Hammes and Hammes-Schiffer 2015; Weil and Bolton 2006), while here we emphasize its limitations in relation to the study of BAL generation.

As most of free radicals are very reactive, their stationary concentration is usually extremely low, even at a high rate of their appearance in the system. It is usually considered to be in average an order of magnitude less than the sensitivity threshold of the ESR method, which is estimated as $\sim 10^{-10} - 10^{-8}$ M (Mason and Fann, <https://www.niehs.nih.gov/research/resources/epresr/sensitivity/index.cfm>; Vladimirov 1967). Thus, classical ESR allows detecting radicals in biological systems only at their artificial initiation (i.e., under special model conditions), or in very specific situations, such as respiratory burst (Allen et al. 1972; Babior et al. 1973) (however, the new technologies arriving these years offer very promising prospects and might change the whole field in the nearest future (Probst et al. 2017)).

A successful modification of ESR for such issues is the spin trapping method (Janzen and Blackburn 1968; Saprin and Piette 1977; Haywood 2013). It consists in adding into the system special compounds, which react with the radicals to be detected, forming a new radical with a longer lifetime, known as a spin adduct. The added compound is called the spin trap.

Thus, adding a spin trap into the system greatly increases the concentration of unpaired electrons, making them detectable by ESR, but does not interfere with the processes leading to the generation of the studied radicals. Besides, there are spin traps that mainly react with a specific type of radicals, which makes it possible to detect them separately with rather high specificity (see more in Khramtsov (2018); Dikalov et al. (2018) and Samouilov et al. (2004)).

8.5.1.2 Chemiluminescence

As will be shown below, chemiluminescence (CL) necessarily occurs during recombination of certain types of free radicals. Accordingly, it clearly indicates the presence of these radicals in the system. On the one hand, this limits its applicability only to “luminescent radicals” (say, ROO^\bullet , but not R^\bullet – see Chap. 10); on the other hand, it makes CL a specific detection method, applicable for analysis of concrete processes and their mechanisms.

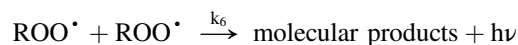
Other advantages of CL as a method for observing radicals are its noninvasiveness and kineticity. As a rule, CL detection does not require any processing of the system and is possible in dynamics (i.e., allows its real-time observation). That is why the discovery of chemiluminescence (Vladimirov and Litvin 1959; Tarusov et al. 1961a, b; Tarusov et al. 1962;

Vasil’ev 1965a, b) and its further use greatly simplified kinetic experiments, since in some cases, instead of sampling and analyzing the probes, it is enough to observe its luminescence kinetics.

8.5.1.2.1 Sensitivity

The sensitivity of CL, as a method to report free radicals in the system, can be roughly calculated as follows.

Let us consider lipid peroxidation – the process, responsible for the greatest proportion of biological autoluminescence (see Chaps. 10 and 11). As will be shown in Chap. 10, the main chemiluminescent reaction in this process is recombination of peroxide radicals:



whose rate equals:

$$v = k_6[\text{LOO}^\bullet]^2 \quad (8.1)$$

and the CL intensity is:

$$I_{hv} = N_A V_{\text{cuv}} \cdot \varphi_{\text{cl}} \cdot k_6[\text{LOO}^\bullet]^2 \quad (8.2)$$

where I_{hv} is CL intensity (photons/s), N_A – Avogadro number, V_{cuv} – cuvette volume (l), φ_{cl} – quantum yield of chemiluminescence, k_6 – reaction rate constant ($l \cdot \text{mol}^{-1} \cdot \text{s}^{-1}$), $[\text{LOO}^\bullet]$ – radical concentration (M).

The reaction rate constant k_6 and the quantum yield of CL φ_{cl} are obviously the two main parameters determining the CL intensity. Both of them can be estimated from extraneous data (Vasil’ev 1965a, b; Shlyapintokh et al. 1966).

For example, k_6 for a number of organic compounds at 15 °C is estimated as: $1.9 \times 10^7 l \cdot \text{mol}^{-1} \cdot \text{s}^{-1}$ (ethylbenzene), $5 \times 10^5 l \cdot \text{mol}^{-1} \cdot \text{s}^{-1}$ (ethyl linoleate), $2.8 \times 10^4 l \cdot \text{mol}^{-1} \cdot \text{s}^{-1}$ (cumene) (Shlyapintokh et al. 1966). φ_{cl} , which is defined as:

$$\varphi_{\text{cl}} = \frac{\text{number of emitted photons}}{\text{number of product molecules}} \quad (8.3)$$

can be represented as:

$$\varphi_{\text{cl}} = \varphi_{\text{ex}} \cdot \varphi_{\text{lum}} \quad (8.4)$$

where:

$$\begin{aligned} \varphi_{\text{ex}} &= \frac{\text{number of excited product molecules}}{\text{total number of product molecules}} \\ &\quad - \text{quantum yield of excitation} \\ \varphi_{\text{fl}} &= \frac{\text{number of emitted photons}}{\text{number of excited product molecules}} \\ &\quad - \text{quantum yield of luminescence} \end{aligned} \quad (8.5)$$

Both φ_{ex} and φ_{fl} can be estimated from other sources (Vasil'ev 1965a, b): $\varphi_{\text{ex}} = 10^{-5} \sim 10^{-4}$, $\varphi_{\text{fl}} = 10^{-4} \sim 10^{-3}$. Whence $\varphi_{\text{cl}} = 10^{-9} \sim 10^{-7}$ photons per formed product molecule, that is, per 2 radicals ROO^{\bullet} , disappearing in this reaction (Vasil'ev 1965a, b).

Altogether, from the approximated numbers above, one generated quantum of CL will correspond to $10^{-12} - 10^{-10}$ M, i.e. $10^{11} - 10^{13}$ reacted radicals:

$$[\text{LOO}^{\bullet}] \cong \sqrt{\frac{I_{\text{hv}}}{6 \times 10^{23} \cdot V_{\text{cuv}} \cdot (10^{-9} \sim 10^{-7}) \cdot (10^5 \sim 10^7)}} \quad (8.6)$$

Now if the photodetecting system collects $\sim 10\%$ of the total light emitted by the object (this depends on the optical system of the device and can be more), and the reaction cuvette is 10 ml, the minimal detectable concentration of radicals will be estimated as $10^{-9} \sim 10^{-11}$ M. This makes the CL method 1–2 orders of magnitude more sensitive than the classical ESR.

Another important difference between the methods is the information they give in general. While ESR detects the free-radical concentration as is, CL shows the rate of radical disproportionation. Importantly, the higher the radical reactivity (k_6 in Eq. 8.1), the lower their stationary detectable concentration is, and consequently, the less efficient is ESR and the more efficient the CL method.

8.5.1.3 Activated Chemiluminescence

In addition to analyzing intrinsic chemiluminescence (including its kinetics and spectral composition), a very informative method is the use of selective activators – molecules that “readily” react with certain free radicals, or accept the product excitation energy due to its physical transfer, and have a high quantum yield of luminescence. Their use appeared convenient if the system intrinsic CL is below the setup sensitivity threshold, if the researcher needs to reduce the volume of experimental material, or if it is necessary to reveal specific radicals involved in the process.

Widespread selective activators of CL are luminol (Allen and Loose 1976; Allred et al. 1980), lucigenin (Allen 1982) and coumarin derivatives (see more in Gomes et al. 2005 and Vladimirov and Proskurnina 2009). Other dyes such as eosin, fluorescein, and acridine orange are not selective, but these dyes can also be used in a number of cases. Thus, the measurement of chemiluminescence in combination with activators is a highly sensitive and selective technique for studying free-radical processes, similarly to spin trapping in ESR.

8.5.2 Biochemical Methods

Biochemical methods of free-radical research are mostly indirect, which is their obvious disadvantage comparing to ESR and CL. Yet, they can be quite useful in some situations (see below), and most importantly, it is these methods that allowed detailed studies of CL mechanisms, bringing it to the present state of a research method.

Biochemical methods are divided into biomarker and inhibitory. Biomarker analysis consists in detecting specific substances, generated during the process under study, which can be used to assess its efficiency and/or direction. Inhibitory analysis consists in introducing some highly specific substance, which suppresses a definite (known beforehand) stage of the process, detecting and analyzing its effect.

8.5.2.1 Biomarkers

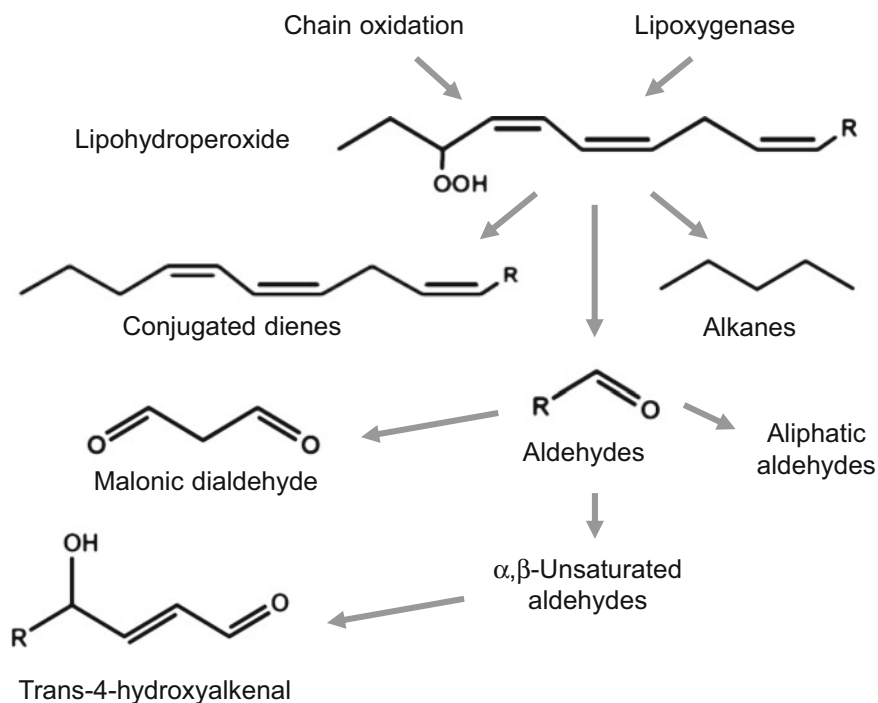
The biomarker approach is widely used in clinical free-radical research. These are chemicals that appear in the system as a result of radical attack on biologically important compounds: lipids, proteins, nucleic acids (see reviews (Kulikov and Grishina 2015; Proskurnina and Vladimirov 2015)). These processes are usually pathological, if it relates to medicine, and the biomarkers are mostly stable enough for chemical or spectroscopic detection. This determines their wide clinical application.

For instance, during oxidation of fatty acids, along with hydroperoxides, other compounds are formed: alcohols, ketones, aldehydes, epoxides, polymers, etc. (Badings 1960; Ellis 1950; Ellis et al. 1961; Evans 1961; Fenell and Skellon 1954; Karnojitzky and Vial 1966; Knight et al. 1951; King 1956; Perkins 1960) (see Fig. 8.3). All these substances can be quantitatively detected by chromatographic methods and mass-spectrometry.

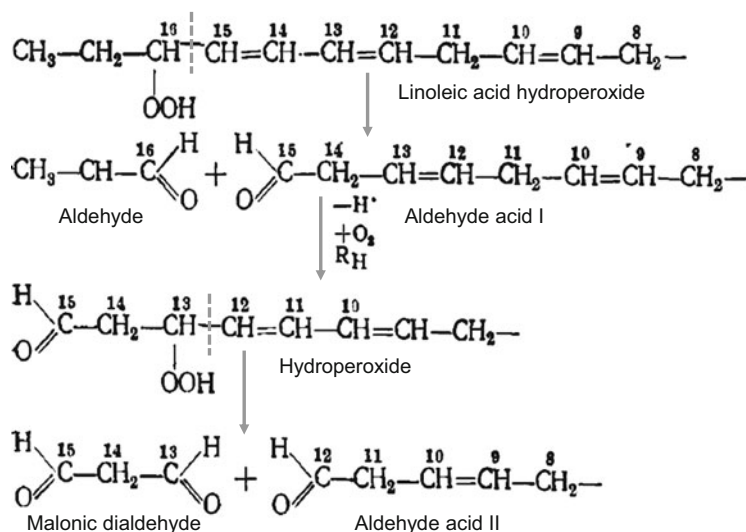
One of the most important marker reactions, which has been used in lipid peroxidation research for more than 50 years, is malonic dialdehyde (MDA), formed after a repeated radical attack on polyunsaturated fatty acids (PUFA) (Evans 1961; Mas-Bargues et al. 2021; Aguilar Diaz De Leon and Borges 2020) (see Fig. 8.4a).

Reacting with thiobarbituric acid (TBA), it gives a specific colored and fluorescent substance MDA-TBA₂ (Suslova 1971) (see Fig. 8.4b; see more in Mas-Bargues et al. (2021) and Aguilar Diaz De Leon and Borges (2020)). In PUFA oxidation it is formed in close relation with the free-radical processes and thus remains widely used as a marker for them. However, today we know that both MDA and TBA are rather nonspecific reactants, and in fact the colored reaction with TBA reflects a general presence of MDA-like species, commonly called TBARS (TBA-reactive substances), which cannot be used as the sole indicator of lipid peroxidation in complex biological samples (Mas-Bargues et al. 2021).

Fig. 8.3 Biomarkers of lipid peroxidation. (Reprinted with permission from Vladimirov et al. (2017). Copyright 2017, Vladimirov et al.)



a Appearance of MDA at lipid peroxidation



b TBA-reactive substances test

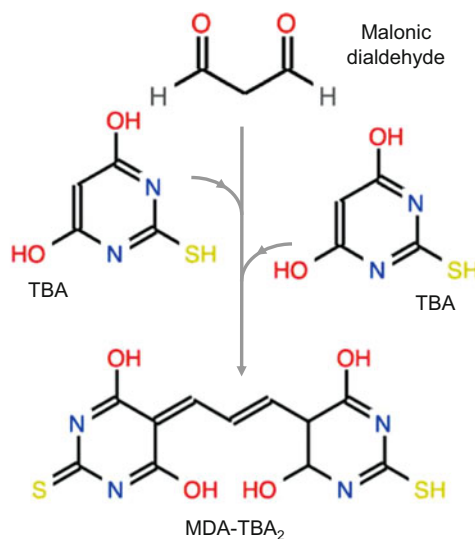


Fig. 8.4 Formation of malonic dialdehyde during the oxidation of linoleic acid (a) and a general scheme of its reaction with thiobarbituric acid (b). (a – reprinted from Vladimirov and Archakov (1972), with permission from the authors)

Yet, though lacking enough specificity (and sensitivity either), this reaction is still widely used for assessing the general rate of lipid and hydrocarbon peroxidation, which is quite convenient in combination with other methods (Forman et al. 2015).

In proteins, an important marker of free-radical oxidation is hydroxyphenylalanine, oxidized phenylalanine.

Phenylalanine is also oxidized enzymatically in the cell, without participation of radicals, but this leads to formation of para-hydroxyphenylalanine, that is, a natural amino acid tyrosine. If proteins containing phenylalanine are attacked by a hydroxyl radical, then various isoforms of hydroxyphenylalanine are formed, including ortho-hydroxyphenylalanine (sometimes called ortho-tyrosine), which is not normally present in the human body (Fig. 8.5).

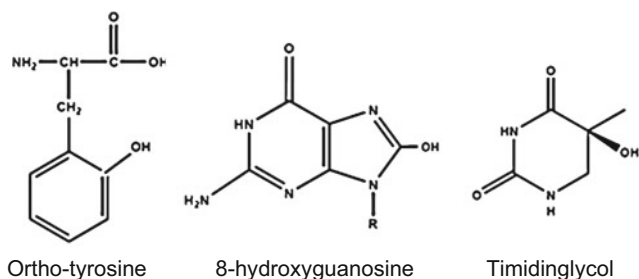


Fig. 8.5 Biomarkers of oxidative damage to proteins (o-tyrosine) and nucleic acids (8-hydroxyguanosine and thymidine glycol). (Reprinted with permission from Vladimirov et al. (2017). Copyright 2017, Vladimirov et al.)

A radical attack on nucleic acids leads to the formation of unusual derivatives of nitrogenous bases, for example, thymine or guanidine. Figure 8.5 shows the structural formulas of 8-hydroxyguanosine and thymidine glycol, substances that are absent in the blood under normal conditions.

8.5.2.1.1 Diene Conjugation

Diene conjugation is one of the most important markers for free-radical oxidation of polyunsaturated fatty acids (PUFA), an important component of biological membranes and blood lipoproteins. As known, PUFA are the least stable component of biological membranes and become the first targets for free radicals at their appearance. Therefore, detecting diene conjugation can be a sensitive test for the entire process of lipid peroxidation, which is of great importance both in normal cell metabolism and especially in the development of pathological conditions.

Besides, diene conjugation is a very accurate test specifically for free-radical processes (in contrast to other biomarker methods, which usually do not give complete confidence in the free-radical origin of the marker product). All this gives the diene conjugation method a special value and determines its wide use in free-radical research.

As is well known, the peculiarity of the PUFA chemical structure is double bonds, separated in the chain by the so-called methylene bridges ($-\text{CH}_2-$, see Fig. 8.6a). The carbon atoms in such bridges appear the most vulnerable targets for radical attack, as they have the weakest bonds with hydrogen atoms (Fig. 8.6a, see Chap. 10). A proton and an electron from this carbon atom are transferred to the radical (usually OH^\bullet), and the second, unpaired electron remains on the carbon. This electron is indistinguishable from the other four electrons that previously formed the neighboring double bonds, that is, a π -electron system of five identical electrons is formed (Fig. 8.6b-c). Such a compound is called alkyl radical (R^\bullet), and in case of lipids, it is denoted by L^\bullet . When molecular oxygen appears in the environment, it attacks R^\bullet in lateral positions of the π -electron system, as it is thermodynamically advantageous to form a

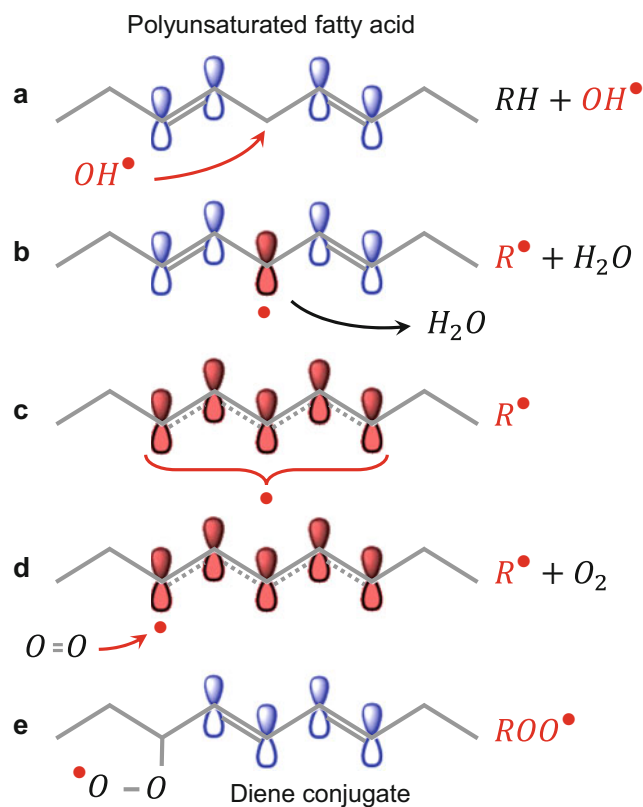


Fig. 8.6 Diene conjugation reaction scheme. (a) The site of the polyunsaturated fatty acid is attacked by a hydroxyl radical. (b) An alkyl radical of PUFA. (c) The unpaired electron is delocalized among the 5 carbon atoms with free π -orbitals. (d) A system of 5 carbon atoms containing a delocalized π electron is attacked by an oxygen molecule. (e) The lipoperoxyl radical, formed during the previous action, contains two conjugated double bonds (diene conjugate). (Adapted with permission from Vladimirov et al. (2017). Copyright 2017, Vladimirov et al.)

system of conjugated double bonds (Fig. 8.6d-e). As a result, a new radical ROO^\bullet appears, with the unpaired electron belonging to the oxygen atom (Fig. 8.6d, e). This can be proved by the ESR method, since the signal of radicals in which an unpaired electron belongs to carbon (R^\bullet) differs from the signal of radicals in which a single electron is “centered” on oxygen.

As a result of the above process, the remaining four π -electrons form a conjugated system (conjugated diene), which can be easily detected by spectrophotometry: conjugated dienes absorb at 233 nm, while unconjugated double bonds absorb only in very short wavelength UV (less than 200 nm) (O'Brien 1969; Freeman and O'Brien 1967; Recknagel and Ghoshal 1966a, b). As an example, Fig. 8.7 shows absorption spectra of the peroxidation products generated by irradiating a phospholipid suspension with UV. As once can see, 1–2 minutes of irradiation is enough to form diene conjugates with the absorption maximum at ~ 235 nm (Fig. 8.7, curves b, c). Further irradiation causes further photochemical transformation and appearance of

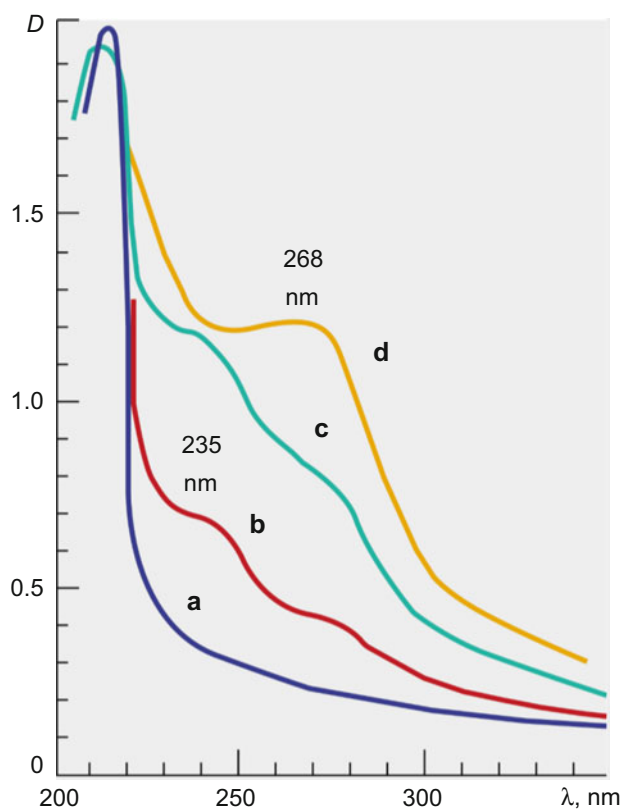


Fig. 8.7 Absorption spectra of freshly prepared phospholipid solutions in n-heptane, irradiated with a mercury quartz lamp for different time: a – without irradiation; b – 1 minute irradiation; c – 2 minutes irradiation; d – 22 minutes irradiation. (Redrawn with permission from Potapenko et al. (1972). Copyright 1972, the authors)

carbonyl compounds, absorbing at 260–280 nm (Fig. 8.7, curves c, d).

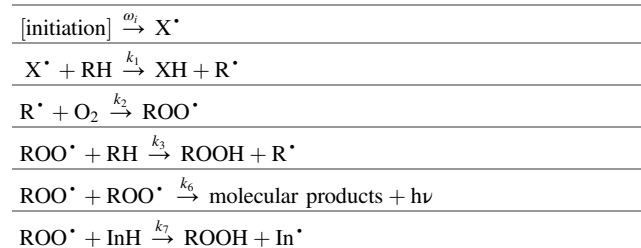
Altogether, since the appearance of conjugated dienes can occur *only* as a result of radical formation in the system (as above), their presence in the peroxidation products directly indicates the free-radical mechanism of PUFA peroxidation, which makes this method especially valuable for free-radical biology and medicine.

8.5.2.2 Inhibitory Analysis

The principle of inhibitory analysis is quite simple: a substance that intercepts radicals is introduced into the system, and the resulting changes are observed. For different radicals, one can find one or another interceptor-inhibitor. For instance, for superoxide anion-radical, it is the enzyme superoxide dismutase; for hydrogen peroxide, it is catalase; α -tocopherol or carotenoids can serve as traps for lipid radicals. Mannitol, benzoic acid, or ethanol are used to trap the hydroxyl radical.

Thus, the role of superoxide in phagocyte bacterial killing can be investigated by adding superoxide dismutase. As this experiment results in decreasing the number of killed

Table 8.2 Simplified diagram of peroxidation processes



Above the arrows are the rate constants of the processes

bacteria, an important role of superoxide in bacterial destruction is suggested.

For more information and practical recommendations see reviews (Emanuel 1976; Kostyuk and Potapovich 2009; Shinohara and Ishiguro 1989).

8.5.3 Kinetic and Simulation Methods

In the study of chain reactions, kinetic methods play a role that is perhaps even more important than in the study of any other chemical processes. The reason is that, unlike simple chemical transformations, chain processes cannot be divided into separate reactions and investigated with the common research techniques: isolating products at each stage, measuring stoichiometry, etc. In a chain reaction, initiation, chain development and termination occur simultaneously, and the researcher can judge about these basic elementary reactions only indirectly by the final macroscopic result: decrease in the initial compound, oxygen consumption, or accumulation of the final products. This is why to establish the mechanism of the process, one needs to study its kinetics, applying math simulation: construct a system of differential equations for the whole supposed set of elementary reactions, solve it under different conditions, and compare theoretical results to the experimental data. This allows one to draw conclusions about the mechanisms, and change, if necessary, the equations, and therefore the proposed scheme of the process.

Let us consider the simplified classic scheme of peroxidation processes (Table 8.2, see more in Chap. 10) and see what we can learn about it using this approach.

Here X^* are the primary radicals appearing in the system due to some initiation process with the rate ω_i , RH are organic molecules, subjected to peroxidation (usually lipids or hydrocarbons), R^* – their radicals, ROO^* – peroxy radicals, ROOH – hydroperoxides, InH and In^* – inhibitor and its radical. The above scheme is greatly simplified for convenience (a more complete scheme and its proof are given in Chap. 10); the rate equations are as follows (Table 8.3):

To study the behavior of such a reaction system, a number of techniques are used, the main of which are:

Table 8.3 Rate equations for a simplified peroxidation scheme (Table 8.2)

| | |
|---|---|
| 1 | $[\dot{X}^*] = \omega_i - k_1[X^*][RH]$ |
| 2 | $[RH] = -k_1[X^*][RH] - k_3[ROO^*][RH]$ |
| 3 | $[R^*] = k_1[X^*][RH] - k_2[R^*][O_2] + k_3[ROO^*][RH]$ |
| 4 | $[ROO^*] = k_2[R^*][O_2] - k_3[ROO^*][RH] - k_6[ROO^*]^2 - k_7[ROO^*][InH]$ |
| 5 | $[ROOH] = k_3[ROO^*][RH] + k_7[ROO^*][InH]$ |
| 6 | $[InH] = -k_7[ROO^*][InH]$ |

where, for any substance x , $[x]$ is its concentration, $\dot{[x]} \equiv \frac{d[x]}{dt}$ is the rate of its change

8.5.3.1 Give Priority to One of the Parallel Processes

If one of the components can be formed or consumed by several competing paths, the researcher can create special conditions under which one of these reactions will proceed incomparably faster than the others, and the rest can be neglected.

For example, in the initiation reaction $X^* + RH \xrightarrow{k_1} XH + R^*$ various radicals can act as initiator X^* :

- OH^* , formed in the Fenton and Osipov reactions, during ROOH thermal decomposition and in a number of other processes.
- HOO^* , generated at one-electron oxygen reduction.
- RO^* , formed during ROOH decomposition by transition metals: $ROOH + Fe^{2+} \rightarrow RO^* + OH^- + Fe^{3+}$, etc.

Each of these reactions has its own rate constant, and taking all of them into account makes even the first stage of initiation incredibly difficult. If the research task does not require simultaneous consideration of these processes, the system can be simplified to one or two main ways of initiation.

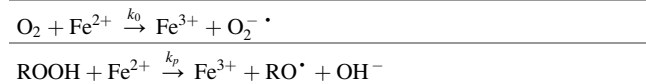
For instance, in Karpukhin et al. (1963) and Shlyapintokh et al. (1966), peroxidation in fatty acid or phospholipid suspensions was initiated by ionizing or UV irradiation of constant intensity. Because there were practically no other ways of initiation in the system, it can be assumed that:

$$\omega_i = \text{const} \sim I_{\text{illumination}}$$

In Emanuel et al. (1965); Emanuel and L'askovkaya (1961); Lemon et al. (1951); and Kern and Willersin (1955), also in suspensions, peroxidation was initiated by Fe^{2+} . Then the main reactions of initiation were (Table 8.4):

Thus, the initiation rate could be assumed as:

$$\omega_i = \mu k_0 [O_2] [Fe^{2+}] + \nu k_p [ROOH] [Fe^{2+}]$$

Table 8.4 Basic initiation reactions upon adding Fe^{2+} to model systems

where the constants μ and ν reflect the contribution of the resulting radicals $O_2^- \cdot$ and RO^* to further processes.

In the absence of oxygen, we get:

$$\omega_i = \nu k_p [ROOH] [Fe^{2+}]$$

In the presence of oxygen, but in the absence of ROOH, at the initial stages (when ROOH did not have time to accumulate due to peroxidation), we get:

$$\omega_i = \mu k_0 [O_2] [Fe^{2+}]$$

8.5.3.2 "Playing on Characteristic Times": Consider "Slow Variables" as Parameters

All reactions have their own rates and, accordingly, characteristic times of change of variables. If we are interested in the processes occurring during a time $\sim \tau_0$, then all variables with characteristic times $\tau \gg \tau_0$ can be considered parameters.

So, for example, in reactions (Table 8.4), with an excess of added Fe^{2+} , at the initial stages one can consider $[Fe^{2+}] \cong \text{const}$.

Then, in the absence of oxygen $\omega_i \sim [ROOH]$.

In the presence of oxygen, but in the absence of ROOH, $\omega_i \sim [O_2]$.

Later, however, the Fe^{2+} waste and the ROOH accumulation become significant, and the equation for ω_i becomes more complicated again.

$[LH] \cong \text{const}$ can often be considered as well.

8.5.3.3 "Playing on Characteristic Times": Tikhonov's Theorem for "Fast Variables"

Let us, again, consider processes occurring at characteristic times $\sim \tau_0$. Variables with $\tau \ll \tau_0$ are called "fast": they manage to change much faster than the "experimenter sees" and "instantly" reach a certain level determined by the balance of their formation and consumption and then remain at it. In physical chemistry this statement is known as the Bodenstein–Semenov principle; in mathematics, in a strict form, it follows from the Tikhonov theorem (Tikhonov 1952). This "quasi-stationary" state is determined by the parameters and the current value of the "slow" variables and, therefore, can gradually change.

Thus, the system dynamics is divided into three phases:

- The initial (very short) period – reaching the quasi-stationary state: fast variables (x_i) change from initial

Table 8.5 Quasi-stationary solutions of the associated system in Table 8.3

| | |
|----------------|---|
| 1 ^ˆ | $\omega_i - k_1[X^*][RH] = 0$ |
| 3 ^ˆ | $k_1[X^*][RH] - k_2[R^*][O_2] + k_3[ROO^*][RH] = 0$ |
| 4 ^ˆ | $k_2[R^*][O_2] - k_3[ROO^*][RH] - k_6[ROO^*]^2 - k_7[ROO^*][InH] = 0$ |

concentrations to a quasi-stationary state with slow variables remaining practically constant.

- The main period – the quasi-stationary state: slow variables change according to their equations; fast variables “instantly” reach their quasi-stationary state for each value of the slow variables.
- The final (short) period is a significant change in slow variables, at which the conditions for the Tikhonov theorem are violated.

8.5.3.4 Practical Application

In practice, such “fast” variables are often concentrations of free radicals, which generally react much faster than other molecules. Thus, the concentrations of X^* , R^* , and ROO^* , at a constant initiation rate, “instantly” (for most tasks immeasurably fast) reach such a quasi-stationary level, remaining almost constant until the entire RH pool is consumed, or new initiators appear. In Table 8.3, this allows replacing Eqs. 1, 3, and 4 with the following (Table 8.5):

Then from 1^ˆ:

$$[X^*] = \frac{\omega_i}{k_1[RH]} \quad (8.7)$$

(i.e., at a constant initiation rate, while the concentration of RH can be considered constant, $[X^*] = \text{const}$ also).

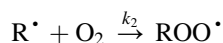
From 1^ˆ and 3^ˆ, we get:

$$\omega_i = k_2[R^*][O_2] - k_3[ROO^*][RH] \quad (8.8)$$

Then, the rate of the substrate consumption (reaction 2 in Table 8.3) will look like:

$$[\dot{RH}] = -k_1[X^*][RH] - k_3[ROO^*][RH] = -k_2[R^*][O_2] \quad (8.9)$$

and the substrate consumption rate (i.e., the rate of the entire peroxidation process) will be completely determined by the reaction



In a particular case, if there are no inhibitors in the system (which corresponds to model systems with hydrocarbon

suspensions), $[InH] = 0$, and Eq. 4^ˆ in Table 8.5 will take the form:

$$k_2[R^*][O_2] - k_3[ROO^*][RH] - k_6[ROO^*]^2 = 0$$

That is, $k_6[ROO^*]^2 = \omega_i$, and therefore:

$$[ROO^*] = \sqrt{\omega_i/k_6} \quad (8.10)$$

$$[R^*] = \frac{1}{k_2[O_2]} \left(\omega_i + \frac{k_3[RH]}{\sqrt{k_6}} \sqrt{\omega_i} \right)$$

Thus, the peroxidation rate will be:

$$\omega = -[\dot{RH}] = \omega_i + \frac{k_3[RH]}{\sqrt{k_6}} \sqrt{\omega_i} \quad (8.11)$$

If the initiation rate is small and $[RH]$ is large, then the predominant contribution to RH consumption will be made by the second term, and $[\dot{RH}] \sim \sqrt{\omega_i}$. It is this ratio shown in Emanuel et al. (1965), which was used as a proof of the very scheme of peroxidation processes.

Otherwise, if there are inhibitors in the system, then, as a rule, the rate of ROO^* disappearance is determined mainly by the reaction with InH, and not by recombination (as $[ROO^*]$ is very small in any case). Thus, the term $k_6[ROO^*]^2$ can be neglected, and eq. 4^ˆ in Table 8.5 will take the form:

$$k_2[R^*][O_2] - k_3[ROO^*][RH] - k_7[ROO^*][InH] = 0$$

That is, $k_7[ROO^*][InH] = \omega_i$, and therefore:

$$[ROO^*] = \frac{\omega_i}{k_7[InH]}$$

$$[R^*] = \frac{\omega_i}{k_2[O_2]} \left(\frac{k_3[RH]}{k_7[InH]} + 1 \right) \quad (8.12)$$

and the rate of peroxidation:

$$\omega = -[\dot{RH}] = \omega_i \left(\frac{k_3[RH]}{k_7[InH]} + 1 \right) \quad (8.13)$$

Thus, while in the absence of inhibitors, the peroxidation rate has two components: $\sim \omega_i$ and $\sim \sqrt{\omega_i}$, addition of inhibitors to the system makes the second component insignificant, replacing it with a component also proportional to ω_i .

8.5.3.5 Summary

In all cases, the original system is simplified by dividing it into relatively autonomous subsystems and a separate analysis of each of them. Using these methods, it is possible to investigate individual stages of the process: to check the correctness of specific kinetic equations and to obtain experimental values for the rate constants. Different variants of peroxidation process, depending on the concentrations of various components and rate constants, were analyzed in more detail in Vladimirov and Archakov (1972) and the literature cited there, and are also given further in Chaps. 10 and 11.

8.6 Summary and Announcement for the Next Chapters

As is well known, free radicals are the most reactive substances in the living cell, and thus the cause of damage and destruction. Their leading role in almost all elderly diseases and body aging is generally recognized and is the subject of numerous studies (Wei et al. 1989; Harman 1981; Beckman and Ames 1998; Valko et al. 2007; Smallwood et al. 2018; Tavassolifar et al. 2020). This set the generalized terms such as oxidative stress or reactive oxygen species.

At the same time, free radicals appeared important participants in regulation of living cells, triggering a lot of important processes (Iles and Forman 2002; Suzuki et al. 2011; Yang et al. 2012; Zhang et al. 2016). The general belief that their action is nonspecific and always destructive, was supplemented with new data: the action of various radicals can be unexpectedly specific, and most of the effects seem adapted by living nature for the benefit of the organism. Thus, superoxide radical, the main radical formed in living cells, serves as a source of hydrogen peroxide, which, in turn, is the main molecule that carries out redox signaling based on thiol-disulfide transitions in proteins (Finkel 2011; Fomenko et al. 2007; Weerapana et al. 2010). Lipid radicals participating in fatty acids oxidation turned out to be intermediate products in the biosynthesis of the most important lipid mediators (Xiao et al. 2011; Yu et al. 2009). Controlled cell death turned out to be triggered by radicals formed in the depths of lipoperoxidases, primarily cytochrome c in the complex with anionic lipids (Liu et al. 1996; Yang et al. 1997). These radicals generate other lipid radicals, whose action leads to the main events of apoptosis: a cascade of enzymatic reactions in the cytoplasm and the attraction of phagocytes to destroy the cell.

Research of free radicals, initially seeming impossibly difficult due to their high reactivity, appeared feasible mainly due to chemiluminescence and kinetic methods, which uncovered many sources of free radicals in the living cell.

The initial idea that the main catalysts for their appearance are transition metals, including iron, turned out too simplified and in many cases simply incorrect. The main sources of free radicals in real cells appeared reactions involving a wide range of enzymes, mainly metalloproteins, including heme proteins.

All this flurry of new data, as well as the classically accepted free-radical processes, will be discussed in the following chapters.

References

- Aguilar Diaz De Leon J, Borges CR (2020) Evaluation of Oxidative Stress in Biological Samples Using the Thiobarbituric Acid Reactive Substances Assay. *J Vis Exp* (159). doi:<https://doi.org/10.3791/61122>
- Allen RC (1982) Biochemiexcitation: Chemiluminescence and the Study of Biological Oxygenation Reactions. In: *Chemical and Biological Generation of Excited States*. pp 309–344. doi:<https://doi.org/10.1016/b978-0-12-044080-1.50015-8>
- Allen RC, Loose LD (1976) Phagocytic activation of a luminol-dependent chemiluminescence in rabbit alveolar and peritoneal macrophages. *Biochem Biophys Res Commun* 69 (1):245–252.
- Allen RC, Stjernholm RL, Steele RH (1972) Evidence for the generation of an electronic excitation state(s) in human polymorphonuclear leukocytes and its participation in bacterial activity. *Biochem Biophys Res Commun* 47:679–684
- Allred CD, Margetts J, Hill HR (1980) Luminol-induced neutrophil chemiluminescence. *Biochimica et biophysica acta* 631 (2):380–385
- Babior BM, Kipnes RS, Curnutte JT (1973) Biological defense mechanisms. The production by leukocytes of superoxide, a potential bactericidal agent. *J Clin Invest* 52 (3):741–744. doi:<https://doi.org/10.1172/jci107236>
- Badings HT (1960). *Nethese Milk Dairy J* 14:215
- Beckman JS, Beckman TW, Chen J, Marshall PA, Freeman BA (1990) Apparent hydroxyl radical production by peroxynitrite: implications for endothelial injury from nitric oxide and superoxide. *Proceedings of the National Academy of Sciences of the United States of America* 87 (4):1620–1624. doi:<https://doi.org/10.1073/pnas.87.4.1620>
- Beckman KB, Ames BN (1998) The free radical theory of aging matures. *Physiol Rev* 78 (2):547–581
- Dikalov SI, Polienko YF, Kirilyuk I (2018) Electron Paramagnetic Resonance Measurements of Reactive Oxygen Species by Cyclic Hydroxylamine Spin Probes. *Antioxid Redox Signal* 28 (15):1433–1443. doi:<https://doi.org/10.1089/ars.2017.7396>
- Ellis GW (1950). *Biochem J* 46:129
- Ellis R, Gadelis AM, Currie GT (1961). *J Food Sci* 26:131
- Emanuel NM (1976) Free radicals and the action of inhibitors of radical processes under pathological states and ageing in living organisms and in man. *Quarterly reviews of biophysics* 9 (2):283–308. doi:<https://doi.org/10.1017/s0033583500002420>
- Emanuel NM, Denisov YT, Mayzys ZK (1965) Tsepnyje reaktcii okislenija uglevodorodov v zhidkoj faze (In Russian) [Chain reactions of hydrocarbons in liquid phase]. Nauka, Moscow
- Emanuel NM, L'askovkaya YN (1961) Inhibition of lipid oxidation processes (In Russian) [Tormozhenije protsessov okislenija zhirov]. Pishchepronizdat, Moscow
- Evans CD In: *Chem. Symposium*, 1961. Campbell Soup. Co., Camden, N. Y., p 123
- Fenell AJ, Skellon JH (1954). *J Chem Soc*:3414
- Finkel T (2011) Signal transduction by reactive oxygen species. *J Cell Biol* 194 (1):7–15. doi:<https://doi.org/10.1083/jcb.201102095>

- Fomenko DE, Xing W, Adair BM, Thomas DJ, Gladyshev VN (2007) High-throughput identification of catalytic redox-active cysteine residues. *Science* 315 (5810):387–389. doi:<https://doi.org/10.1126/science.1133114>
- Forman HJ, Augusto O, Brigelius-Flohe R, Dennery PA, Kalyanaraman B, Ischiropoulos H, Mann GE, Radi R, Roberts LJ, Vina J, Davies KJA (2015) Even free radicals should follow some rules: A Guide to free radical research terminology and methodology. *Free Radical Bio Med* 78:233–235. doi:<https://doi.org/10.1016/j.freeradbiomed.2014.10.504>
- Freeman IP, O'Brien PJ (1967). *Biochem J* 102:9p
- Gomes A, Fernandes E, Lima JL (2005) Fluorescence probes used for detection of reactive oxygen species. *Journal of biochemical and biophysical methods* 65 (2–3):45–80. doi:<https://doi.org/10.1016/j.jbbm.2005.10.003>
- Gunaydin G, Gedik ME, Ayan S (2021) Photodynamic Therapy for the Treatment and Diagnosis of Cancer-A Review of the Current Clinical Status. *Frontiers in chemistry* 9:686303. doi:<https://doi.org/10.3389/fchem.2021.686303>
- Halliwell B, Gutteridge JMC (2015) *Free Radicals in Biology and Medicine*. 5rd edn. Oxford University Press,
- Hammes GG, Hammes-Schiffer S (2015) Principles of Nuclear Magnetic Resonance and Electron Spin Resonance. *Methods Biochem Anal* 55:289–313. doi:<https://doi.org/10.1002/9781118859148.ch13>
- Harman D (1981) The aging process. *Proceedings of the National Academy of Sciences of the United States of America* 78 (11):7124–7128. doi:<https://doi.org/10.1073/pnas.78.11.7124>
- Haywood R (2013) Spin-Trapping: Theory and Applications. In: Roberts GCK (ed) *Encyclopedia of Biophysics*. pp 2447–2453. doi:<https://doi.org/10.1007/978-3-642-16712-6>
- Huie REP, S. (1993) The reaction rate of nitric oxide with superoxide. *Free radical research* 18:195–199. doi:<https://doi.org/10.3109/10715769309145868>
- Iles KE, Forman HJ (2002) Macrophage signaling and respiratory burst. *Immunologic research* 26 (1–3):95–105. doi:<https://doi.org/10.1385/ir.26:1-3:095>
- Izmailov DY, Vladimirov YA (2003) The mathematical modeling of the kinetics of chain lipid peroxidation in the presence of Fe²⁺. II. Effect of antioxidants (In Russian). *Biol Membrany* 20 (4):349–358
- Janzen EG, Blackburn BJ (1968) Detection and identification of short-lived free radicals by an electron spin resonance trapping technique. *J Am Chem Soc* 90 (1):5909–5910. doi:<https://doi.org/10.1021/ja01023a051>
- Karnojitzky V, Vial C (1966). *Prod Probl Pharm* 21:245
- Karpukhin ON, Shlyapintokh VY, Zolotova NV, Kozlova ZG, Rusina IF (1963). *Zhurnal Fizicheskoy Khimii [Journal of Physical Chemistry]* 37:1636
- Kern W, Willersin H (1955). *Angew Chem* 67:573
- Khrantsov VV (2018) In Vivo Electron Paramagnetic Resonance: Radical Concepts for Translation to the Clinical Setting. *Antioxid Redox Signal* 28 (15):1341–1344. doi:<https://doi.org/10.1089/ars.2017.7472>
- King G (1956). *J Chem Soc*:587
- Knight HB, Colemann JE, Swern D (1951). *J Amer Oil Chemists's Soc* 28:498
- Korkina LG, Durnev AD, Suslova TB, Cheremisina ZP, Daugel-Dauge NO, Afanas'ev IB (1992) Oxygen radical-mediated mutagenic effect of asbestos on human lymphocytes: suppression by oxygen radical scavengers. *Mutat Res* 265 (2):245–253. doi:[https://doi.org/10.1016/0027-5107\(92\)90053-5](https://doi.org/10.1016/0027-5107(92)90053-5)
- Kostyuk VA, Potapovich AI (2009) Mechanisms of the suppression of free radical overproduction by antioxidants. *Front Biosci (Elite Ed)* 1:179–188. doi:<https://doi.org/10.2741/e17>
- Krasnovsky AA (2007) Primary mechanisms of photoactivation of molecular oxygen. History of development and the modern status of research (). *Biochemistry-Moscow* 72 (10):1065–1080. doi:<https://doi.org/10.1134/S0006297907100057>
- Krasnovsky AA (2015) Singlet oxygen and primary mechanisms of photodynamic and laser therapy In: Grigor'ev AI, Vladimirov YA (eds) *Basic sciences for medicine. Biophysical medical technologies*, vol 1. Max Press, Moscow, pp 173–218
- Krasnovsky AA, Jr. (1998) Singlet molecular oxygen in photobiochemical systems: IR phosphorescence studies. *Membr Cell Biol* 12 (5):665–690
- Kulikov AV, Grishina IV (2015) Application of biomarkers of oxidative stress for diagnostics of diseases (In Russian). In: *Fundamentalnyye nauki - meditsine: Biofizicheskije meditsinskije tekhnologii [Basic Sciences for medicine: Biophysical medical technologies]*. MAX Press, Moscow, pp 135–172
- Lemon HW, Kirby EM, Knapp RM (1951). *Canad J Techol* 29:523
- Liu X, Kim CN, Yang J, Jemmerson R, Wang X (1996) Induction of apoptotic program in cell-free extracts: requirement for dATP and cytochrome c. *Cell* 86 (1):147–157
- Mas-Bargues C, Escriva C, Dromant M, Borras C, Vina J (2021) Lipid peroxidation as measured by chromatographic determination of malondialdehyde. Human plasma reference values in health and disease. *Archives of biochemistry and biophysics* 709:108941. doi:<https://doi.org/10.1016/j.abb.2021.108941>
- Moody CS, Hassan HM (1982) Mutagenicity of oxygen free radicals. *Proceedings of the National Academy of Sciences of the United States of America* 79 (9):2855–2859. doi:<https://doi.org/10.1073/pnas.79.9.2855>
- O'Brien PJ (1969). *Canad J Biochem* 47:485
- Osipov AN, Yakutova ES, Vladimirov YA (1993) Formation of hydroxyl radicals on interaction of hypochlorite with ferrous ions. *Biophysics* 38 (3):383–388
- Perkins EQ. (1960). *Food Technol* 14:508
- Potapenko AJ, Roshchupkin DI, Kogon YA, Vladimirov YA (1972) Study of the effects of ultraviolet light on biomembranes. Registration of electroconductivity of biomolecular phospholipid membranes (In Russian). *Doklady AN SSSR (Rep Acad Science USSR)* 202 (4):882–885
- Probst S, Bienfait A, Campagne-Ibarcq P, Pla JJ, Albanese B, Barbosa JFDS, Schenkel T, Vion D, Esteve D, Mølmer K, Morton JLL, Heeres R, Bertet P (2017) Inductive-detection electron-spin resonance spectroscopy with 65 spins/ Hz sensitivity. 111 (20):202604. doi:<https://doi.org/10.1063/1.5002540>
- Proskurnina EV, Vladimirov YA (2015) Free radicals members of regulatory and pathologic processes (In Russian). In: *Fundamentalnyye nauki - meditsine: Biofizicheskije meditsinskije tekhnologii [Basic Sciences for medicine: Biophysical medical technologies]*. MAX Press, Moscow, pp 38–102
- Recknagel RO, Ghoshal AK (1966a). *Exper and Mol Pathol* 5:413
- Recknagel RO, Ghoshal AK (1966b). *Nature* 210:1162
- Reha-Krantz LJ (2013) Mutagens. In: Maloy S, Hughes K (eds) *Brenner's Encyclopedia of Genetics (Second Edition)*. Academic Press, San Diego, pp 528–532. doi:<https://doi.org/10.1016/B978-0-12-374984-0.00996-7>
- Samouilov A, Roubaud V, Kuppusamy P, Zweier JL (2004) Kinetic analysis-based quantitation of free radical generation in EPR spin trapping. *Anal Biochem* 334 (1):145–154. doi:<https://doi.org/10.1016/j.ab.2004.07.026>
- Saprin AN, Piette LH (1977) Spin trapping and its application in the study of lipid peroxidation and free radical production with liver microsomes. *Archives of biochemistry and biophysics* 180 (2):480–492. doi:[https://doi.org/10.1016/0003-9861\(77\)90063-7](https://doi.org/10.1016/0003-9861(77)90063-7)
- Shinohara R, Ishiguro I (1989) [Detection methods of free radical related substances and the system for their elimination]. *Rinsho Byori* 37 (9):1006–1012
- Shlyapintokh VY, Karpukhin ON, Postnikov LM, Zakharov IV, Vichutinskiy AA, Tsepalov VF (1966) *Hemiluminestentnyye*

- metody issledobaniya medlennykh himicheskikh protsessov [Chemiluminescent methods for studying the slow chemical processes]. Nauka, Moscow
- Smallwood MJ, Nissim A, Knight AR, Whiteman M, Haigh R, Winyard PG (2018) Oxidative stress in autoimmune rheumatic diseases. *Free radical biology & medicine* 125:3–14. doi:<https://doi.org/10.1016/j.freeradbiomed.2018.05.086>
- Suslova TB (1971) Chemiluminescent study of lipid peroxidation in mitochondrion membranes and oleic acid solutions., 2 Med Inst, Moscow
- Suzuki N, Miller G, Morales J, Shulaev V, Torres MA, Mittler R (2011) Respiratory burst oxidases: the engines of ROS signaling. *Curr Opin Plant Biol* 14 (6):691–699. doi:<https://doi.org/10.1016/j.pbi.2011.07.014>
- Szabó C, Ischiropoulos H, Radi R (2007) Peroxynitrite: biochemistry, pathophysiology and development of therapeutics. *Nature Reviews Drug Discovery* 6 (8):662–680. doi:<https://doi.org/10.1038/nrd2222>
- Tarusov BN, Polivoda AI, Zhuravlev AI (1961a) Detection of chemiluminescence in the liver of irradiated mice (In Russian). *Radiobiologiya* 1 (1):150–151
- Tarusov BN, Polivoda AI, Zhuravlev AI (1961b) Study on ultra-weak spontaneous luminescence of animal cells (in Russian). *Biofizika (Russ)* 6 (4):490–492
- Tarusov BN, Polivoda AI, Zhuravlev AI, Sekamova EN (1962) Ultraweak spontaneous luminescence in animal tissue (in Russian). *Tsitologiya* 4:696–699
- Tavassolifar MJ, Vodjgani M, Salehi Z, Izad M (2020) The Influence of Reactive Oxygen Species in the Immune System and Pathogenesis of Multiple Sclerosis. *Autoimmune Dis* 2020:5793817. doi:<https://doi.org/10.1155/2020/5793817>
- Tikhonov AN (1952) Systems of differential equations containing small parameters in the derivatives (In Russian). *Mat Sb (NS)* 31(73) (3): 575–586
- Valko M, Leibfritz D, Moncol J, Cronin MT, Mazur M, Telser J (2007) Free radicals and antioxidants in normal physiological functions and human disease. *Int J Biochem Cell Biol* 39 (1):44–84. doi:<https://doi.org/10.1016/j.biocel.2006.07.001>
- Vasil'ev RF (1965a) Chemiluminescence in solutions I. Methods of identification of excited states (In Russian). *Opt Spektrosk+18* (2): 236–244
- Vasil'ev RF (1965b) Chemiluminescence in solutions II. Identification of the excited state in reactions of liquid-phase oxidation (In Russian). *Opt Spektrosk+18* (3):415
- Vladimirov YA (1967) Ultraweak luminescence accompanying biochemical reactions (English translation of “Sverkhslabye svecheniya pri biokhimicheskikh reaktsiyah” USSR Academy of Sciences, Institute of Biological Physics. Izdatel'stvo “Nauka” Moscow, 1966). NASA, C.F.S.T.I., Springfield, Vermont
- Vladimirov YA, Ai-Ke H, Roshchupkin DI (1966) Investigation of the primary photochemical processes in proteins-IV. Luminescence spectra of primary and end photo products of aromatic amino acids and proteins. *Biophysics* 11 (2):268–276
- Vladimirov YA, Archakov AI (1972) Lipid peroxidation in biological membranes [Perekisnoe okislenie lipidov v biologicheskikh membranakh] (In Russian) (Perekisnoe okislenie lipidov v biologicheskikh membranakh). Nauka, Moscow
- Vladimirov YA, Litvin FF (1959) Investigation of very weak luminescence in biological systems. *Biophysics* 4 (5):103–109
- Vladimirov YA, Proskurnina EV (2009) Free radicals and cell chemiluminescence. *Biochemistry (Moscow)* 74 (13):1545–1566. doi:<https://doi.org/10.1134/s0006297909130082>
- Vladimirov YA, Proskurnina EV, Izmailov DY, Sozarukova MM, Dzhadtoeva AA, Vladimirov GK, Machneva TV (2017) Sources and targets of free radicals in human blood. MAX Press, Moscow
- Wang KK, Song S, Jung SJ, Hwang JW, Kim MG, Kim JH, Sung J, Lee JK, Kim YR (2020) Lifetime and diffusion distance of singlet oxygen in air under everyday atmospheric conditions. *Physical chemistry chemical physics: PCCP* 22 (38):21664–21671. doi:<https://doi.org/10.1039/d0cp00739k>
- Weerapana E, Wang C, Simon GM, Richter F, Khare S, Dillon MB, Bachovchin DA, Mowen K, Baker D, Cravatt BF (2010) Quantitative reactivity profiling predicts functional cysteines in proteomes. *Nature* 468 (7325):790–795. doi:<https://doi.org/10.1038/nature09472>
- Wei CE, Allen K, Misra HP (1989) Role of activated oxygen species on the mutagenicity of benzo[a]pyrene. *Journal of applied toxicology: JAT* 9 (3):169–173. doi:<https://doi.org/10.1002/jat.2550090306>
- Weil JA, Bolton JR (2006) Magnetic Interaction between Particles. *Electron Paramagnetic Resonance*. John Wiley & Sons. doi:<https://doi.org/10.1002/9780470084984.ch2>
- Wertz J (1986) *Electron Spin Resonance (Elementary Theory and Practical Applications)*. Springer Netherlands. doi:<https://doi.org/10.1007/978-94-009-4075-8>
- Xiao Y, Gu Y, Purwaha P, Ni K, Law B, Mallik S, Qian SY (2011) Characterization of free radicals formed from COX-catalyzed DGLA peroxidation. *Free radical biology & medicine* 50 (9): 1163–1170. doi:<https://doi.org/10.1016/j.freeradbiomed.2011.02.001>
- Yang J, Liu X, Bhalla K, Kim CN, Ibrado AM, Cai J, Peng TI, Jones DP, Wang X (1997) Prevention of apoptosis by Bcl-2: release of cytochrome c from mitochondria blocked. *Science* 275 (5303): 1129–1132
- Yang Y, Bazhin AV, Werner J, Karakhanova S (2012) Reactive oxygen species in the immune system. *Int Rev Immunol* 32 (3): 249–270. doi:<https://doi.org/10.3109/08830185.2012.755176>
- Yu Q, Purwaha P, Ni K, Sun C, Mallik S, Qian SY (2009) Characterization of novel radicals from COX-catalyzed arachidonic acid peroxidation. *Free radical biology & medicine* 47 (5):568–576. doi:<https://doi.org/10.1016/j.freeradbiomed.2009.05.023>
- Zhang J, Wang X, Vikash V, Ye Q, Wu D, Liu Y, Dong W (2016) ROS and ROS-Mediated Cellular Signaling. *Oxidative medicine and cellular longevity* 2016:4350965. doi:<https://doi.org/10.1155/2016/4350965>



Ilya Volodyaev and Yury A. Vladimirov

9.1 Sources of Biological Autoluminescence

9.1.1 Reactions Sources of UPE

The issue of the ultraweak photon emission (UPE) sources was raised already in 1920s, in the first works on the mitogenetic radiation, MGR (see Chap. 2). At first, as MGR was detected by a purely biological effect – stimulation of mitosis in the onion root by another onion root, which supposedly emitted it, A.G. Gurwitsch assumed that the source of MGR is a specific enzymatic reaction similar to luciferin / luciferase (Gurwitsch 1926; Frank and Salkind 1926). However, soon MGR was reported from other biological objects (plant sprouts, protist cultures, eggs of amphibia, brain of tadpoles, animal blood, working muscles, malignant tumours, etc.) (Gurwitsch and Gurwitsch 1926; Gurwitsch 1929; Siebert 1929), which meant that its source must be much more universal.

MGR was also reported from different tissues when peroxidase was added (see Reiter and Gabor 1928), which suggested the source of MGR to be oxidative processes (Reiter and Gabor 1928). Further investigation of model biochemical and chemical systems as sources of MGR (Frank and Rodionow 1932; Gerlach 1933; Audubert and Doormaal 1933; Barth 1937; Braunstein and Potozky 1934; Potozky 1932; Gurwitsch and Gurwitsch 1934b; Karpas 1929) supplemented their list with glycolysis, proteolysis, and even inorganic reactions (Table 9.1) (Gurwitsch and Gurwitsch 1934a).

Additional, more confident data (Frank and Rodionow 1932; Barth 1937) were collected after development of photosensitive modifications of Geiger–Muller counters (Rajewsky 1930; Rajewsky 1931a, b; Rodionov and Frank 1934), with the best, internationally recognized works belonging to R. Audubert (Audubert and Doormaal 1933; Audubert 1938, 1939). The author detected MGR from a

number of different redox reactions and estimated its absolute intensity at various wavelengths (Table 9.2).

Thus, by the middle of 1930s, UPE was reported from different model reactions, mostly of redox type.

Further progress in identifying sources of UPE was made in 1960s, after invention of PMT-based photodetectors (Kubetsky 1937; Iams and Salzberg 1935), and their first successful application to detecting UPE from biological samples (Strehler 1951; Strehler and Arnold 1951; Colli and Facchini 1954; Vladimirov and Litvin 1959; Tarusov et al. 1961). The main contribution to this issue can be attributed to the groups of J. Stauff, who was mostly investigating UPE from simple aqueous systems (Stauff 1964; Stauff and Reske 1964; Stauff and Rümmler 1962; Stauff and Schmidkunz 1962a, b; Stauff et al. 1963; Stauff and Wolf 1964), R.F. Vasil'ev and V.Ya. Shliapintokh, who studied in detail radical peroxidation and UPE in hydrocarbons (see next chapter). Table 9.3 represents redox reactions in water solutions, accompanied by UPE, according to J. Stauff et al. (Stauff and Schmidkunz 1962a).

9.1.2 Energy Considerations

The very fact of photon generation during the above reactions (Tables 9.1, 9.2, and 9.3) contains a serious 'energy paradox', first formulated by W. Frankenburger (Frankenburger 1933) and analysed by R. Audubert (Audubert 1939). According to the estimates of both authors, the enthalpy of the basic chemical reactions taking place in the system(s) was around of 0–30 kcal/mol. At the same time, they were accompanied by luminescence with $\lambda \cong 240\text{--}260$ nm and photon energy of 120–130 kcal/mol.

To solve this paradox, R. Audubert suggested (Audubert 1939) that the energy of the emitted quantum was summed from two components: the reaction enthalpy (Q or ΔH) and some activation energy of the process (E_a), which could be quite large (Eq. 9.1).

I. Volodyaev (✉) · Y. A. Vladimirov
Moscow State University, Moscow, Russia

Table 9.1 Reactions accompanied by ultraweak UV emission recorded by biological detectors (according to Braunstein and Pototskaya)

| |
|---|
| KMnO ₄ + H ₂ O ₂ |
| K ₂ Cr ₂ O ₇ + FeSO ₄ |
| HNO ₃ + FeSO ₄ [+H ₂ SO ₄] |
| KClO ₃ + Zn + NaOH |
| FeCl ₃ + NH ₂ OH · HCl |
| HgCl ₂ + SnCl ₂ |
| H ₂ O ₂ [+Pt] |

Adapted from Gurwitsch and Gurwitsch (1934b), with the permission of the heirs of the authors

Table 9.2 Reactions accompanied by chemiluminescence in the ultraviolet spectral region according to (Audubert 1939)

| Reaction | Intensity of emission, $\times 10^3 \frac{\text{counts}}{\text{sec}\cdot\text{cm}^2}$ | |
|--|---|-----------------------|
| | at $\lambda = 200$ nm | at $\lambda = 240$ nm |
| NaOH + HNO ₃ or H ₂ SO ₄ | 2–3 | 7–10 |
| K ₂ SO ₃ + O ₂ | 1.5–2 | – |
| Na ₂ S ₂ O ₃ + O ₂ | 1–1.5 | 7–10 |
| Pyrogallol + O ₂ | 1–1.5 | 10–15 |
| C ₂ H ₅ OH + HCrO ₄ | – | 70–100 |
| K ₂ C ₂ O ₄ + Br ₂ | – | 10–15 |
| K ₂ C ₂ O ₄ + I ₂ | – | 7–10 |
| Glucose + KMnO ₄ | 1.5–2 | – |

Adapted from Vladimirov (1967)

The measurements were carried out using a light-sensitive modification of Geiger–Muller counters (see Chaps. 2 and 21)

Table 9.3 Examples of reactions accompanied by weak chemiluminescence in the range of 250–650 nm (Stauff and Schmidkunz 1962a)

| Type of reaction | Reagents | I_{max} , rel. units | Duration of emission, min | Notes |
|--|---|-------------------------------------|---------------------------------|--|
| Interaction with atmospheric oxygen (air passed through the solution) | NaOH (1 M) + HCl (2 drops) | >200 | 1–2 | In the absence of oxygen, the neutralization reaction is not accompanied by emission |
| | NaOH (1M) + HCl (2 drops) + fluorescein | >400 | 10 | |
| | NaHSO ₃ (10 ⁻³ M) | >500 | – | – |
| | Na benzyl | >500 | 15–20 | – |
| | NaClO | 100 | – | – |
| Interaction with H ₂ O ₂ (2 ml 30% H ₂ O ₂ + 55 ml reagent solution) | Formaldehyde (15%) + NaOH (2 M) | – | 0.5 | Visible dark red glow |
| | Pyrogallol (10%) + NaOH (2 M) | >300 | 7 | – |
| | Fe ²⁺ + EDTA (catalyst) | >100 | 7 | – |
| | Fe ²⁺ + EDTA (catalyst) + gelatin (0.3%) | >200 | 0.3 | – |
| | Pyrogallol (10%) + NaOH (2 M) | >200 | 0.03–0.05 | – |
| Oxidation with NaClO (1 ml NaClO + 55 ml reagent solution) | Urea (0.05 M) | 200 | 2 | – |
| | Guanidine (0.05 M) | 200 | – | – |
| | Dimethylsulfoxide (90%) | >100 | 10–12 | Well seen emission |

Adapted from Vladimirov (1967)

Measurements were carried out using low-noise cooled photomultipliers

$$h\nu = E_a + Q \quad (9.1)$$

However, this suggested very high activation energy, which made the suggestion doubtful. Another concept for solving the ‘energy paradox’, proposed by Frankenburger (Frankenburger 1933) and supported by Audubert (Audubert 1939), was that UPE is generated at recombination of free

radicals, which might appear in course of very rare highly energetic side reactions, accompanying the main oxidation process.

Applying his idea of activation energy (Eq. 9.1) to recombination of two radicals, Audubert suggested the following expression (Eq. 9.2), with each radical already endowed with some activation energy in addition to the enthalpy of its generation.

$$h\nu = (E_a + Q)_{1\text{st radical}} + (E_a + Q)_{2\text{nd radical}} \quad (9.2)$$

Approximate implementation of Eq. 9.2 was shown for a number of oxidative processes (Audubert 1939) (however, with a very rough estimate of the photon energy: 145–150, 122–145, or 122–155 kcal/mol). At the same time, Eq. 9.1 could be attributed to luminescence in the visible spectral region (400–600 nm).

9.1.3 Summary

Thus, the general conclusions from the above data are as follows:

- UPE originates from a number of different chemical reactions, mostly of redox type.
- The exact mechanism of UPE generation is likely to be recombination of free radicals, appearing in course of very rare side processes accompanying the main reaction. The extremely low intensity of UPE is a consequence of the rarity of these adverse reactions.
- Biological autoluminescence is likely to be produced by such universal reactions, and not by specialized processes or structures in biological objects.

All this evidence, collected by the end of 1930s, anticipated the concepts developed in 1960s by the groups of J. Stauff and R.F. Vassil'ev, and appeared very close to what we know now.

9.2 Reactive Oxygen Species

9.2.1 The Role of Oxygen

The next step, clarification of the specific radicals responsible for photon generation, was mostly implemented in 1960s in the works of J. Stauff et al. (Stauff 1964; Stauff and Reske 1964; Stauff and Rümmler 1962; Stauff and Schmidkunz 1962a, b; Stauff et al. 1963; Stauff and Wolf 1964) and R.F. Vasil'ev et al. (Vasil'ev 1963; Vasil'ev 1965a, b, c, d; Vasil'ev and Vichutinskii 1962; Vassil'ev and Vichutinskiy 1962; Vasil'ev and Vichutinskii 1962; Vasil'ev et al. 1963; Vassil'ev et al. 1959; Vasil'ev et al. 1961; Vasil'ev and Rusina 1964a, b; Zakharov and Shlyapintokh 1961; Entelis et al. 1960; Shliapintokh et al. 1960; Vassil'ev 1962; Vasil'yev 1963; Vassil'ev and Vichutinskii 1962).

As easily calculated, the energy of a quantum of light is ~40–60 kcal/mol in the visible range and ~60–130 kcal/mol

Table 9.4 Examples of reactions – possible sources of luminescence in water systems and their energetics

| Reaction of free radical recombination | ΔH , kkal/mol | λ , nm of the corresponding photon |
|---|-----------------------|--|
| $2\text{OH}^{\bullet} \rightarrow \text{H}_2\text{O}_2$ | 47 | 617 |
| $2\text{HO}_2^{\bullet} \rightarrow \text{H}_2\text{O}_2 + \text{O}_2$ | 58 | 500 |
| $2\text{HO}_2^{\bullet} \rightarrow \text{H}_2\text{O}_2 + \text{O}_2^*$ | | |
| $\text{HO}_2^{\bullet} + \text{OH}^{\bullet} \rightarrow \text{H}_2\text{O} + \text{O}_2^*$ | 77 | 377 |

Adapted from Vladimirov (1967)

in the UV. This is a lot, even for free radicals, and significantly narrows the list of reactions, to be considered as possible sources of UPE. In aqueous solutions, according to J. Stauff, they are the following (Table 9.4).

Importantly, all these reactions involve oxygen-containing radicals (ROS, in modern terminology), which can arise (and, as is now known, constantly do) both in model water systems and in the cell.

Indirectly this statement was supported by the spectral studies of UPE from the above model reactions (Table 9.3) (Stauff and Rümmler 1962; Stauff and Schmidkunz 1962b; Brown and Ogryzlo 1965; Khan and Kasha 1964). The authors showed that these spectra for the most part very closely coincide with the absorption spectrum of the $(\text{O}_2)_2$ van der Waals complex (Table 9.5). That is, the allowed transitions of the emitters in these reactions have very close energy to the transitions upon excitation of $(\text{O}_2)_2$. Since such a coincidence of the vibrational levels structure of different molecules is extremely unlikely, the authors concluded that the oxygen van der Waals complexes should be direct sources of UPE, at least in some of the reactions. The reason for the transition of the oxygen molecule to different vibrational sublevels in different reactions was suggested to lie in different energetics of the processes, and the presence of a clear vibrational structure was explained by the fact that molecules of gaseous oxygen were excited on the surface of the bubbles released during the reaction (Khan and Kasha 1964).

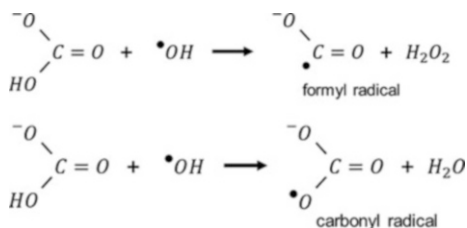
Thus, the UPE from model water systems is likely to originate from recombination of ROS, with the possible formation of excited unstable compounds like oxygen dimer $(\text{O}_2)_2$. Although it is not entirely clear how accurate the estimates of the chemiluminescence maxima could be, and why the luminescent relaxation occurred from various vibrational sublevels of the Van der Waals complex, and not from the lowest level, as it classically should be, Stauff's hypothesis anticipated the modern understanding of the role of ROS and molecular oxygen in UPE generation (see more on the present-day data on ROS and their basic reactions in Chap. 8).

Table 9.5 Position of the chemiluminescence maxima (λ_{chl}) of some model reactions and absorption maxima of the $(\text{O}_2)_2$ complex according to (Khan and Kasha 1964; Stauff and Rümmler 1962; Stauff and Schmidkunz 1962b)

| Chemiluminescent spectra of several model reactions in aqueous systems | | Absorption spectrum of $(\text{O}_2)_2$ complex | |
|--|-----------------------------|--|----------------------------|
| Reaction | λ_{chl} , nm | λ_{a} , nm | I_{a} , rel.units |
| $\text{H}_2\text{O}_2 + \text{Cl}_2$ [$+\text{OH}^-$] (Brown and Ogryzlo 1965) | 1300 1100 900 | Different electronic transitions in $(\text{O}_2)_2$ (Vasiljev 1967) | |
| $\text{H}_2\text{O}_2 + \text{Cl}_2$ [$+\text{OH}^-$] (Brown and Ogryzlo 1965) | 762, 770 | | |
| $\text{H}_2\text{O}_2 + \text{NaClO}$ [$+\text{OH}^-$] $\text{H}_2\text{O}_2 + \text{Cl}_2$ [$+\text{OH}^-$] (Brown and Ogryzlo 1965) | 703 703 | | |
| $\text{H}_2\text{O}_2 + \text{NaClO}$ $\text{H}_2\text{O}_2 + \text{Cl}_2$ [$+\text{OH}^-$] (Brown and Ogryzlo 1965) | 633, 634.8 633 | 630 | 60 |
| urea + NaClO | 580 | 578 | 75 |
| urea + NaClO | 535 | 533.5 | 25 |
| $\text{NaOH} + \text{H}_2\text{SO}_4 + \text{O}_2$ | 480 | 477.5 | 50 |
| $\text{NaOH} + \text{H}_2\text{SO}_4 + \text{O}_2$ | 360–390 | 381.5 | 30 |

Adapted from Vladimirov (1967). Supplemented with data from Brown and Ogryzlo (1965)

λ_{a} – absorption maximum wavelength, nm; I_{a} – absorption intensity, relative units

**Scheme 9.1** Possible mechanisms of free radical reactions involving carbonate

9.2.2 The Role of Carbonyl Radicals

Other important data were obtained by purging the above model systems with carbon dioxide, which sharply enhanced their UPE (Stauff et al. 1963, 1973). According to Stauff's hypothesis, this might be explained by the reaction between the radicals already present in the system and the bicarbonate ions formed from CO_2 . This reaction could happen in two ways with formation of either formyl or carbonyl radicals (Scheme 9.1).

To find out which of these two types of radicals can generate UPE upon recombination, the following experiment was set up. Formic acid or soda solutions were frozen with liquid nitrogen and exposed to ultraviolet irradiation, generating the corresponding free radicals (Scheme 9.2). Then, by careful heating of the sample, their partial recombination was obtained, after which the sample was again cooled to the temperature of liquid nitrogen.

The amount of radicals before and after heating was determined from the EPR spectra, and the amount of radicals recombined at heating (Δm) – from the difference between

them. In parallel with heating, UPE from the system was recorded.

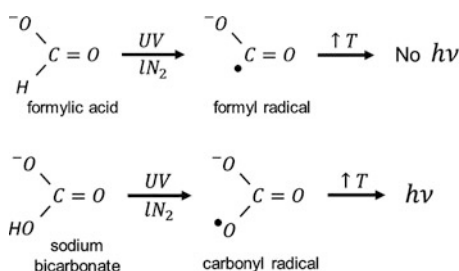
Obviously, the light sum of the luminescence S is proportional to the number of reacted radicals (Δm) or the square of this amount (for bimolecular reactions):

$$\begin{aligned} S &= k\varphi_{\text{lum}}\Delta m \\ S &= k\varphi_{\text{lum}}(\Delta m)^2 \end{aligned} \quad (9.3)$$

where k is a technical constant, reflecting the setup sensitivity in the current spectral region, and φ_{lum} is the luminescence quantum yield (which can be very different in different reactions).

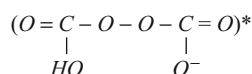
Of the two above reactions only Var.2 (with carbonyl radicals) was accompanied by UPE, while Var.1 (with formyl radicals) was not, although in both cases radicals were equally disappearing in the system according to the EPR data.

Thus, φ_{lum} for the product of carbonyl recombination was orders of magnitude higher than for that of formyl recombination, and the following conclusions can be drawn (Stauff et al. 1973):



Scheme 9.2 Verification of possible mechanisms of radical formation in reactions with carbonate

- UPE of the above model systems in the presence of CO_2 probably occurs due to recombination of two carbonyl radicals, with the formation of an intermediate unstable compound of the following type:



The latter undergoes radiant relaxation with a nonzero quantum yield.

- The very appearance of the carbonyl radicals additionally confirms that free radicals already existed in the solution, reacting with CO_2 at its appearance to form carbonyl radicals.

9.2.3 ROS and UPE

In accordance with the above data, all reactions in which ROS were known to be generated, were accompanied by UPE as well.

Thus, a number of authors have observed luminescence during the interaction of hydrogen peroxide with organic compounds at room temperature. In B.L. Strehler's works, luminescence was shown under the action of H_2O_2 on riboflavin, which was noticeably enhanced in the presence of iron and copper salts (Strehler and Shoup 1953); these data were confirmed by Yu.A. Vladimirov and F.F. Litvin (Vladimirov and Litvin 1959). Chemiluminescence under the action of H_2O_2 on glycine was recorded by A.A. Gurwitsch et al. (Gurwitsch et al. 1965). V.N. Benevolensky et al. detected UPE accompanying reaction of hydrogen peroxide with cysteine (Benevolenskiy et al. 1965).

Chemiluminescence under the action of hydrogen peroxide on proteins was observed by J. Stauff and H. Wolff (Stauff and Wolf 1964), as well as by I.I. Sapezhinskii and colleagues (Sapezhinskii et al. 1965). Since all these compounds are present in the tissues of animals and plants, it is natural that when hydrogen peroxide acts on them,

luminescence is also observed (becoming weaker as H_2O_2 decomposes) (Vladimirov et al. 1962; Popov 1965; Popov and Tarusov 1963).

Yu.A. Vladimirov showed luminescence accompanying the action of crystalline horseradish peroxidase on hydrogen peroxide in the presence of tyrosine (oxidation substrate) and upon decomposition of peroxide by catalase (Vladimirov et al. 1962); the same results were confirmed by K.P. Kachanova and A.P. Purmal (Kachanova and Purmal' 1964). Chemiluminescence under the action of peroxidase on hydrogen peroxide was observed by J. Stauff and H. Wolff (Stauff and Wolf 1964).

Although a number of authors were unable to reproduce some of these results (Popov 1965; Popov and Tarusov 1963), the reason for this may lie in the extremely high rate of catalase decomposition of peroxide; therefore, chemiluminescence can be recorded only if the process is sufficiently prolonged in time (at low concentrations of catalase and significant concentrations of H_2O_2) and if the luminescence is recorded immediately after mixing – conditions not fulfilled by the authors of unsuccessful experiments.

9.2.4 How Do These Data Relate to Biological Systems?

Since such an amount of peroxides, which is mostly used in model experiments (about 1%), never accumulates in the body, the mechanisms considered here may seem not related to the luminescence of tissues or cells. However, they are. Besides the above indirect data, there are others that indicate that the UPE is associated not with the decomposition of peroxide itself, but with the subsequent formation of peroxide radicals from molecules of *organic compounds present in the solution*. This is evidenced by the lack of proportionality between the rate of peroxide decomposition and the luminescence intensity both during the reaction (Meluzova and Knyazeva 1965) and when adding various catalysts.

As is now well known, the primary ROS radicals are the initiators of whole cascades of free radical processes involving many organic molecules. The catalytic decomposition of peroxide leads to the formation of radicals $\text{O}_2^{\cdot -}$ and HO_2^{\cdot} ,

which interact with organic compounds (impurities) and form peroxide radicals of the latter. The recombination of these radicals is accompanied by UPE (chemiluminescence), whose mechanism is close to that of luminescence in lipids and aromatic hydrocarbons (see Chaps. 10 and 11).

Peroxide compounds in the body can be formed not only as a result of H_2O_2 action but also under the action of ionizing radiation and, mainly, during catalytic oxidation reactions with the participation of specialized enzymes (see Chap. 14). Many of these processes are accompanied by UPE, which is analogous to that observed when hydrogen peroxide acts on the corresponding substrates.

9.3 Summary

Altogether, almost all the investigated reactions accompanied by UPE in model water systems were characterized by three features.

1. The chemiluminescence photon energy is much higher than the energy released in each elementary act of the main process.
2. The efficiency of UPE is very low: in most cases for each molecule entering the main reaction, 10^{-12} – 10^{-15} quanta are released, due to low quantum yields of both radical formation and radiative transition.
In cases when UPE from the same reaction was measured in different spectral ranges, one can conclude that *the quantum yield of UPE in UV is orders of magnitude lower than in the visible spectral range* (e.g. for the oxidation of propyl gallate or K_2SO_3 with molecular oxygen $\sim 10^{-15}$ quanta/radical in the UV (Audubert 1939) and 10^{-9} in the visible (Stauff et al. 1963)).
3. The presence of oxygen is necessary for chemiluminescence not only in cases when oxygen is a participant in the main process or when it can be released during the reaction (decomposition of peroxide, reactions involving hypochloride) but also in such reactions as neutralization of alkalis by acids (Stauff and Schmidkunz 1962a), when the main process does not involve oxygen at all.

All these facts were explained in the suggestion that a quantum is released not during the main chemical process, but as a result of very rare side reactions that lead to the formation of oxygen-containing free radicals (ROS). This scheme was confirmed by the study of free-radical processes and the analysis of chemiluminescence spectra.

Altogether, the role of ROS in UPE is as follows:

1. They are formed as by-products in a number of processes, up to the simplest redox reactions in water media;

2. They participate in recombination reactions, generating light quanta – both in the visible and, to a lesser extent, in the UV range;
3. They are initiators of free-radical chain processes with the participation of organic molecules, which, in turn, can also recombine with the formation of UPE quanta.

The next Chaps. 10, 11, and 12 describe such free-radical processes, involving different organic substances. Chapter 14 addresses enzymatic processes and participation of free radical compounds in real cell life.

References

- Audubert R (1938) Die Emission von Strahlung bei chemischen Reaktionen. *Angewandte Chemie* 51 (11):153–163. <https://doi.org/10.1002/ange.19380511102>
- Audubert R (1939) Emission of ultra-violet rays by chemical reactions. *Transactions of the Faraday Society* 35 (213):197–206
- Audubert R, Doormaal V (1933) Sur l'émission de rayonnement par les réactions chimiques. *Comptes Rendus des s* 196:1883–1885
- Barth H (1937) Physical studies on the question of mitogenetic radiation problem (in Russian). *Archive of Biological Sciences* 46 (1): 153–177
- Benevolenskiy VN, Koshcheyenko NN, Veselovskiy VA (1965) Chemiluminescence and toxicity of the reaction products of hydrogen peroxide and cysteine (In Russian). In: *Bioluminescencesiya. Trudy MOIP [Bioluminescence. MOIP Reports]*, vol 21. Nauka, Moscow, pp 112–*
- Braunstein AE, Potozky AP (1934) About specificity of mitogenetic radiation spectra in oxidation-reduction reactions (In Russian). *Archive of Biological Sciences, Ser B* 35 (1):73–86
- Brown RJ, Ogryzlo EA (1965). The yield of singlet oxygen in the reaction of chlorine with hydrogen peroxide. *Canad J Chem* 43: 2915. <https://doi.org/10.1139/v65-402>
- Colli L, Facchini U (1954) Light emission by germinating plants. *Il Nuovo Cimento* 12 (1):150–153. <https://doi.org/10.1007/bf02820374>
- Entelis SG, Shlyapintokh VY, Karpukhin ON, Nesterov OV (1960) Chemiluminescence in reactions of acid chloranhydrides with amines and ketones (In Russian). *Zhurnal Fizicheskoy Khimii [Journal of Physical Chemistry]* 34 (7):651
- Frank G, Rodionow S (1932) Physikalische Untersuchung mitogenetischer Strahlung der Muskeln und einiger Oxydationsmodelle. *Biochemische Zeitschrift* 249 (4/6):323–343
- Frank G, Salkind S (1926) Die Quellen der mitogenetischen Strahlung im Pflanzenkeimling (Источники митогенетического излучения в распадае растений). *Wilhelm Roux' Archiv für Entwicklungsmechanik der Organismen* 108 (4):596–608. <https://doi.org/10.1007/bf02080165>
- Frankenburger W (1933) Neuere Ansichten über das Wesen photochemischer Prozesse und ihre Beziehungen zu biologischen Vorgängen. *Strahlenther Onkol* 47 (2):233–262
- Gerlach W (1933) Physikalisches zum Problem der mitogenetischen Strahlung. *Sitzungsber Ges Morphol und Physiol [München]* 42:1–10
- Gurwitsch A, Gurwitsch L (1934a) L'analyse mitogénétique spectrale, vol 4. *Exposés de physiologie, IV; Actualités scientifiques et industrielles* 150. Hermann & Cie, Paris
- Gurwitsch AA, Eremeev VF, Karabchievsky YA (1965) Ultra-weak emission in the visible and ultra-violet regions in oxidation of solutions of glycine by hydrogen peroxide. *Nature* 206:20–22

- Gurwitsch AG (1926) Das Problem der Zellteilung physiologisch betrachtet, vol 11. Monographien aus dem Gesamtgebiet der Physiologie der Pflanzen und der Tiere. Julius Springer, Berlin
- Gurwitsch AG (1929) Methodik der mitogenetischen Strahlenforschung. In: Abderhalden E (ed) Handbuch der biologischen Arbeitsmethoden, vol V. vol 2/2. Urban & Schwarzenberg, Berlin, Wien, pp 1401–1470
- Gurwitsch AG, Gurwitsch LD (1926) Die Produktion mitogener Stoffe im Erwachsenen Tierischen Organismus 13 Mitteilung über mitogenetische Strahlung und Induktion. Wilhelm Roux' Archiv für Entwicklungsmechanik der Organismen 107 (4):829–832. doi: <https://doi.org/10.1007/BF02079917>
- Gurwitsch AG, Gurwitsch LD (1934b) Mitogeneticheskoje izluchenije [Mitogenetic radiation] (in Russian). VIEM publishing house, Leningrad
- Iams H, Salzberg B (1935) The Secondary Emission Phototube. Proceedings of the Institute of Radio Engineers 23 (1):55–64. <https://doi.org/10.1109/JRPROC.1935.227243>
- Kachanova ZP, Purmal' APZFK (1964) Study of catalase-active systems. Chemiluminescence accompanying the catalase process (in Russian). Zhurnal Fizicheskoi Khimii [Journal of Physical Chemistry] 38 (1):200
- Karpas AM (1929) Mitogenetische Strahlung bei Eiweißverdauung (Dritte Quelle der mitogenetischen Strahlung). Biochemische Zeitschrift 215 (4–6)
- Khan AU, Kasha M (1964) Rotational structure in the chemiluminescence spectrum of molecular oxygen in aqueous systems. Nature 204 (4955):241
- Kubetsky LA (1937) Multiple Amplifier. Proceedings of the Institute of Radio Engineers 25 (4):421–433. <https://doi.org/10.1109/JRPROC.1937.229045>
- Meluzova GB, Knyazeva LL (1965) Chemiluminescence investigation of the thermal decay of hydrogen peroxide in water (In Russian). In: Bioluminescenciya. Trudy MOIP [Bioluminescence. MOIP Reports], vol 21. Nauka, Moscow, pp 161–*
- Popov GA (1965) The use of the chemiluminescence method for studying oxidative reactions induced in a biosubstrate in dependence on the degree of its damage. In: Bioluminescenciya. Trudy MOIP [Bioluminescence. MOIP Reports], vol 21. Nauka, Moscow, pp 90–*
- Popov GA, Tarusov BN (1963) On the nature of spontaneous the luminescence of animal tissues (In Russian). Biofizika+ 8:317–320
- Potozky A (1932) Untersuchungen über den Chemismus der mitogenetischen Strahlung. II. Mitteilung: Die mitogenetischen Spektre der Oxydationsreaktionen. Biochemische Zeitschrift 249: 282–287
- Rajewsky B (1930) Anordnung zur Messung kleinster Lichtintensitäten. Zeits f Physik 63:576
- Rajewsky B (1931a) Ultraviolett-Strahlung des Eiweiss. Klinische Wochenschrift 10 (36):1672–1673. <https://doi.org/10.1007/bf01755391>
- Rajewsky B (1931b) Zur Frage des physikalischen Nachweises der Gurwitsch-Strahlung. In: Dessauer F (ed) Zehn Jahre Forschung auf dem physikalisch-medizinischen Grenzgebiet. Georg Thieme Verlag, Leipzig, pp 244–257
- Reiter T, Gabor D (1928) Zellteilung und Strahlung. Sonderheft der Wissenschaftlichen Veröffentlichungen aus dem Siemens-Konzern. Springer-Verlag, Berlin. <https://doi.org/10.1007/978-3-642-50832-5>
- Rodionov SF, Frank GM (1934) Voprosy svetobiologii i izmereniya sveta. [Problems of Light Biology and Light Measurement] (In Russian). Gostekhizdat, Moscow-Leningrad
- Sapezhinskii II, Silayev YV, Dontsova YG (1965) Mechanism of prolonged afterglow of ultraviolet irradiated solutions of serum albumin. Biophysics 10 (3):476–480
- Shliapintokh VY, Vasil'ev RF, Karpukhine ON, Postnikov LM, Kibalko LA (1960) La chimiluminescence de processus chimiques lents. J Chim Phys 57 (11–12):1113
- Siebert WW (1929) Aktionsstrahlung des Muskels und Wachstumswirkung des elektrodynamischen Feldes. Biochem Zeitsch 215 (1–3):152–161
- Stauff J (1964) Lumineszenz and Energieübertragung angeregter Zustände von Proteinen. Ber Bunsenges phys chem 68 (8–9):773
- Stauff J, Reske G (1964) Lumineszenz von Hefe. Naturwissenschaften 51 (2):39
- Stauff J, Rümmler G (1962) Chemilumineszenz von Oxydationsreaktionen. II. Die Spektren der Reaktionen Harnstoff + Hypohalgenit, Formaldehyd + H₂O₂ und NaOH + H₂SO₄ + O₂. —, 34, N 1—4, 67, 1962. Z Physikal Chemie (BRD) 34 (1–4):67
- Stauff J, Sander U, Jaeshke W (1973) Chemiluminescence of perhydroxyl- and carbonate-radicals. Chemiluminescence and bioluminescence Edited by Cormier M, Hercules D, Lee J - New York: Plenum Press:136–148
- Stauff J, Schmidkunz H (1962a) Chemilumineszenz von Oxydationsreaktionen. I. Qualitative Beobachtungen und Analyse der Reaktion Harnstoff + Na-Hypochlorit. Z Physikal Chemie (BRD) 33 (5/6):273
- Stauff J, Schmidkunz H (1962b) Chemilumineszenz von Oxydationsreaktionen. III. Mitt. Sauerstoff-van der waals-Assoziat als möglicher Träger der Chemilumineszenz. Z Physikal Chemie (BRD) 35 (4–6):295
- Stauff J, Schmidkunz H, Hartmann G (1963) Chemiluminescence in oxidation reactions. Nature 198:281
- Stauff J, Wolf H (1964) Konformationsabhängige Phosphoreszenz und Chemilumineszenz einiger Proteine. Z Naturforsch 19b (2):87
- Strehler BL (1951) The luminescence of isolated chloroplasts. Archives of biochemistry and biophysics 34 (2):239–248
- Strehler BL, Arnold W (1951) Light production by green plants. The Journal of general physiology 34 (6):809–820
- Strehler BL, Shoup CS (1953) The chemiluminescence of riboflavin. Archives of biochemistry and biophysics 47 (1):8
- Tarusov BN, Polivoda AI, Zhuravlev AI (1961) Study on ultra-weak spontaneous luminescence of animal cells (in Russian). Biofizika (Russ) 6 (4):490–492
- Vasil'ev RF (1965a) Chemiluminescence in solutions I. Methods of identification of excited states (In Russian). Opt Spektrosk+ 18 (2): 236–244
- Vasil'ev RF (1965b) Chemiluminescence in solutions II. Identification of the excited state in reactions of liquid-phase oxidation (In Russian). Opt Spektrosk+ 18 (3):415
- Vasil'ev RF (1965c) Photoelectric apparatus for investigating weak luminescence (In Russian). In: Bioluminescenciya. Trudy MOIP [Bioluminescence. MOIP Reports], vol 21. Nauka, Moscow, p 170
- Vasil'ev RF (1965d) Some problems in the mechanism of chemiluminescence. (In Russian). In: Bioluminescenciya. Trudy MOIP [Bioluminescence. MOIP Reports], vol 21. Nauka, Moscow, pp 198–*
- Vasil'ev RF, Karpukhin ON, Shlyapintokh VY (1961) An apparatus for measuring weak light fluxes (In Russian). Zhurnal Fizicheskoi Khimii [Journal of Physical Chemistry] 35 (2):461
- Vasil'ev RF, Vichutinskii AA (1962) The enhancement of chemiluminescence by the addition of luminescent substances (In Russian). Zh Fiz Khim 36 (8):1799–1800
- Vasil'yev RF (1963) Spin-orbit coupling and intermolecular energy transfer. Nature 200 (4908):773
- Vasil'ev RF (1963) Lyuminescenciya pri khimicheskikh reaktsiyakh v rastvorakh (In Russian)[Luminescence Accompanying Chemical Reactions in Solutions]: Doctoral Dissertation. Moscow
- Vasil'ev RF, Rusina IF (1964a) The chemiluminescence mechanism for the oxidation of organic matter in solution (In Russian). Dokl AN SSSR 156 (6):1402–1405
- Vasil'ev RF, Rusina IF (1964b) The chemiluminescence of molecular oxygen during the oxidation of organic matter (In Russian). Izv AN SSSR, Seriya Khim 9:1728

- Vasil'ev RF, Vichutinskii AA (1962) The chemiluminescent method of measuring the relations of elementary constants in liquid hydrocarbon oxidation reactions (In Russian). Doklady AN SSSR 145 (6): 1301
- Vasil'ev RF, Vichutinskiy AA, Cherkasov AS (1963) Chemiluminescence activated by anthracene derivatives. Doklady AN SSSR 149 (1):124
- Vasiljev RF (1967). In: Progress in Reaction Kinetics., vol 4. Pergamon, New York, p 305
- Vassil'ev RF (1962) Secondary processes in chemiluminescent solutions. Nature 196 (4855):668
- Vassil'ev RF, Karpuchin ON, Shlapintoch VJ (1959) Chemiluminescence accompanying reactions of thermal decomposition (In Russian). Doklady AN SSSR 125 (1):106
- Vassil'ev RF, Vichutinskii AA (1962) Chemiluminescence and oxidation. Nature 194 (4835):1276–1277
- Vassil'ev RF, Vichutinskiy AA (1962) The nature of the relationship between chemiluminescence and oxidation by molecular oxygen (In Russian). Doklady AN SSSR 142 (3):615
- Vladimirov YA (1967) Ultraweak luminescence accompanying biochemical reactions (English translation of "Sverkhslabye svecheniya pri biokhimicheskikh reaktsiyah" USSR Academy of Sciences, Institute of Biological Physics. Izdatel'stvo "Nauka" Moscow, 1966). NASA, C.F.S.T.I., Springfield, Vermont
- Vladimirov YA, Litvin FF (1959) Investigation of very weak luminescence in biological systems. Biophysics 4 (5):103–109
- Vladimirov YA, Litvin FF, Man-ch'i T (1962) The role of excited states and the nature of ultraweak luminescence in biological systems. Biofizika+ 7 (6):675–682
- Zakharov IV, Shlyapintokh VY (1961) Chemiluminescence in the diphenylethane hydroperoxide decay reaction and its relationship to the kinetics of the process (In Russian). Kinetika i Kataliz [Kinetics and Catalysis] 2 (2):165



Chemiluminescence in Oxidation of Hydrocarbons: Mechanistic Fundamentals

10

Ilya Volodyaev, Alexei Trofimov, and Yury A. Vladimirov

10.1 Introduction

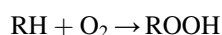
Reactive oxygen species formed in aqueous systems, are also formed in the cell. However, besides the rare “side reactions” investigated by J. Stauff (Stauff 1964; Stauff and Reske 1964; Stauff and Rümmler 1962; Stauff and Schmidkunz 1962a, b; Stauff et al. 1963; Stauff and Wolf 1964) (see Chap. 9), in the cell, ROS are also generated by enzymatic processes, and with much greater efficiency (see Chap. 14).

At the same time, the main source of biological auto luminescence (spontaneous ultraweak photon emission from biological systems) is not ROS themselves, but the processes of chain oxidation of organic molecules, triggered and supported by ROS. The main substrate for these processes is lipids in biological membranes, but proteins and other organic molecules are also susceptible to them.

The first and extremely important model object for the study of such processes is hydrocarbon solutions, discussed in this chapter; the second and closer model object is fatty acids, observed in Chap. 11, together with lipids in biological membranes and outside them.

10.2 Gross Reaction of Hydrocarbon Oxidation

The oxidation of hydrocarbons in general is represented by a very simple scheme:



However, it appeared to have certain special qualities.

I. Volodyaev (✉) · Y. A. Vladimirov
Moscow State University, Moscow, Russia

A. Trofimov
Emanuel Institute of Biochemical Physics, Russian Academy of Sciences, Moscow, Russia

First of all, when initiated with irradiation, it has unexpectedly high quantum yield, calculated as:

$$\varphi = \frac{\text{number of generated molecules of ROOH}}{\text{number of absorbed quanta}} \quad (10.1)$$

For example, for peroxidation of cyclohexene $\varphi = 8$, and for ethyl linoleate $\varphi = 90$ (Emanuel et al. 1965).

As the quantum yield of the primary photochemical process (φ_0) is obviously less than unity:

$$\varphi_0 < 1, \quad (10.2)$$

this undoubtedly suggests that the whole reaction of hydrocarbon peroxidation is a chain process. The primary photochemical reaction must be generating some active compounds that give rise to a chain reaction, with many product molecules formed:

| | |
|--|--------------------------------------|
| $\text{RH} + h\nu \rightarrow \text{R}^*$ | Chain initiation |
| $\text{R}^* + \text{RH} + \text{O}_2 \rightarrow \text{ROOH} + \text{R}^*$ (l times) | Chain reaction (l – chain length) |

Thus, the observed quantum yield must be interpreted as

$$\varphi = \varphi_0 l \quad (10.3)$$

where l is the chain length. Obviously, for the above examples with cyclohexene and ethyl linoleate, $l > 8$ and $l > 90$, respectively (probably even $l \gg 8$ and $l \gg 90$, since φ_0 can well be much less than 1).

The exact proof of the participation of free radicals R^* in the above chain reaction can be potentially obtained via electron spin resonance, but is quite complicated because of the high reactivity of R^* , and hence their very low concentration. However, it was confidently obtained by chemiluminescent methods, as well as by ESR with spin trapping (see below, and also Sect. 8.5).

10.3 Hydrocarbon Oxidation as a Free-Radical Chain Process

Altogether, in all free-radical chain processes, several stages can be distinguished:

1. Initiation – appearance of “the very first radical,” which will then react with the “next molecule”.
2. Chain development – the reaction of a radical with a neighboring molecule, forming a new radical, which enters into subsequent reactions (the same or different).
3. Chain branching – under some conditions, one radical can (directly or through intermediate stages) generate several new radicals at once, thereby increasing the number of simultaneously occurring processes.
4. Chain termination – the disappearance of a radical and the formation of conventional molecular products that do not enter into further reactions.

Naturally, all these stages coexist in time and space, and their activity is regulated by many external factors. Further, we will successively describe the known processes of hydrocarbon peroxidation, combine them into a single scheme, and show those reactions that are the sources of chemiluminescence in this process.

10.3.1 Initiation

Hydrocarbon peroxidation can be initiated by the following:

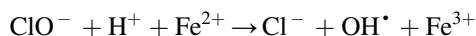
- Irradiation with ultraviolet light, especially in the presence of sensitizing molecules (even in small amounts). In biological systems, the role of such sensitizers can be played by many compounds, including aromatic amino acids, which easily form free radicals under UV irradiation (Vladimirov 1965; Vladimirov et al. 1970a; Vladimirov et al. 1970b).
- Ionizing radiation (Emanuel et al. 1965).
- All reactions leading to ROS generation:
 - One-electron reduction of molecular oxygen on transition metals



- Fenton reaction



- Osipov reaction

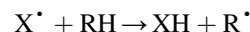


- In the cell or in the corresponding model systems – enzymatic pathways of ROS generation (see Chap. 14).
- Decomposition of peroxides and other compounds catalyzed by transition metals, for example,

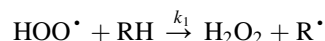
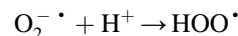


- Spontaneous decomposition of molecules, containing a relatively fragile bond – diazo compounds ($\text{R}_3\text{C} - \text{N} = \text{N} - \text{CR}_3$) and peroxides (the breaking energy of the O – O bond in peroxides is ~30–40 kcal/mol). This is especially effective at sufficiently high temperatures.

The radicals, generated in course of such reactions (here denoted as primary radicals – see Sect. 8.4), as a rule, quickly enter into further reactions:



In particular, for a superoxide anion-radical in a neutral or acidic medium:

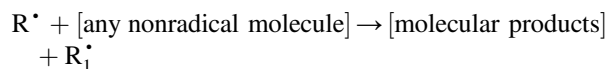


which is a very important reaction for all biological systems.

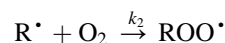
This starts the process of chain oxidation of organic compounds.

10.3.2 Chain Development

An important property of free radicals is that, no matter how many times a radical reacts with molecules, and how many molecular products are formed, a free radical (i.e., an unpaired electron) remains in the system:

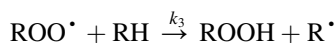


If there are oxygen molecules in the system, they readily react with hydrocarbon radicals, forming peroxide radicals:



with practically zero activation energy and extremely high rate constant ($k_2 \cong 10^7 - 10^8 \text{ l} \cdot \text{mol}^{-1} \cdot \text{s}^{-1}$) (Emanuel et al. 1965). Therefore, at oxygen concentrations in the system above 10^{-6} M , practically all R^\bullet radicals are converted into ROO^\bullet radicals (Vasil'ev and Vichutinskii 1962b; Vassil'ev and Vichutinskiy 1962) (see Box 10.1).

The ROO^\bullet radical can interact with a new molecule of the oxidizing compound, forming hydroperoxide ROOH and renewing the R^\bullet radical:



(It can obviously also interact with other radicals, but due to the incomparably higher concentration of RH , in most cases this is the dominating reaction).

This reaction also proceeds with a small activation energy (4–12 kcal/mol (Emanuel et al. 1965)) and with a rate constant k_3 varying from $0.03 \text{ l} \cdot \text{mol}^{-1} \cdot \text{s}^{-1}$ for trimethylheptane to $1900 \text{ l} \cdot \text{mol}^{-1} \cdot \text{s}^{-1}$ for benzaldehyde.

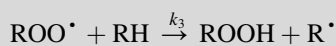
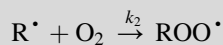
Alternating, these two reactions, involve more and more substrate molecules RH , and form more and more hydroperoxide molecules ROOH , while the number of radicals (R^\bullet and ROO^\bullet) remains unchanged (Scheme 10.1). This stage of the process is called chain prolongation, or chain development.

The whole process rate is determined by the slower reaction $\text{ROO}^\bullet + \text{RH}$. It is very important that the rate constant of this reaction depends on the chemical nature of the molecules R : it is lower for saturated hydrocarbons, and much higher for molecules with a large number of double bonds, which corresponds to the higher final rate of their oxidation.

Box 10.1. R^\bullet and ROO^\bullet : Calculation of Radical Concentrations

As both R^\bullet and ROO^\bullet radicals are highly reactive, their concentrations belong to the so-called fast variables (see Sect. 8.5.3.3), and quickly reach quasistationary state: $\frac{d[\text{R}^\bullet]}{dt} = 0$; $\frac{d[\text{ROO}^\bullet]}{dt} = 0$.

As the two dominating reactions, involving R^\bullet and ROO^\bullet are the following:



this means that in the first approximation:

$$k_2[\text{R}^\bullet][\text{O}_2] \cong k_3[\text{ROO}^\bullet][\text{RH}] \quad (10.4)$$

whence:

$$\text{Box 10.1 (continued)} \quad \frac{[\text{R}^\bullet]}{[\text{ROO}^\bullet]} \cong \frac{k_3[\text{RH}]}{k_2[\text{O}_2]} \quad (10.5)$$

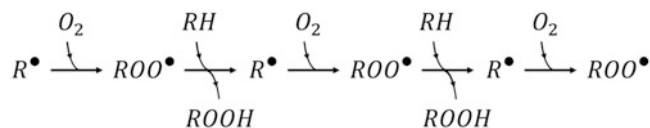
When studying the reactions of hydrocarbon peroxidation in the liquid phase, the substrate concentration $[\text{RH}]$ is usually 2–10 M, the atmospheric oxygen concentration $[\text{O}_2] \cong 10^{-2} \text{ M}$, and rate constants: $k_2 \cong 10^7 - 10^8 \text{ l} \cdot \text{mol}^{-1} \cdot \text{s}^{-1}$; $k_3 \cong 10^{-2} - 10^3 \text{ l} \cdot \text{mol}^{-1} \cdot \text{s}^{-1}$. Thus, the ratio of radical stationary concentrations is typically:

$$\frac{[\text{R}^\bullet]}{[\text{ROO}^\bullet]} \sim 10^{-1} - 10^{-7}$$

and $[\text{R}^\bullet]$ is practically always incomparably less than $[\text{ROO}^\bullet]$.

For instance, $[\text{R}^\bullet]/[\text{ROO}^\bullet] = 4.4 \times 10^{-4}$ at oxidation of ethyl linoleate, and 2×10^{-4} at oxidation of tetralin (Emanuel et al. 1965). Moreover, even at a hundred times decrease of $[\text{O}_2]$ to 10^{-4} M , the concentration of $[\text{R}^\bullet]$ in the system is still $\cong 1\%$ of $[\text{ROO}^\bullet]$. Thus, in most cases, the concentration of radicals $[\text{R}^\bullet]$ is considered vanishingly small and, accordingly, the role of reactions involving these radicals in chain termination (see below) is insignificant (see, e.g., Vasil'ev (1963)).

However, in biological systems, for example, in phospholipid membranes, the situation may be significantly different, since with close contact of oxidizing molecules, the $[\text{RH}]$ concentration becomes high, and the oxygen concentration in a number of cases, on the contrary, may be very low. In this case, $[\text{R}^\bullet]$ can become comparable to $[\text{ROO}^\bullet]$ (see Eq. 10.5), and further reactions involving $[\text{R}^\bullet]$ cannot be ignored any more.



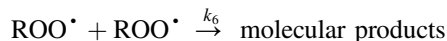
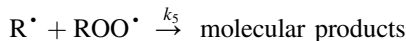
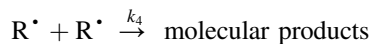
Scheme 10.1 Peroxidation: the chain prolongation stage

10.3.3 Chain Termination

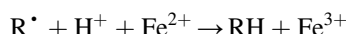
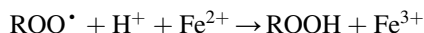
If free radicals always reacted only with new molecules, then a single radical in the presence of a sufficient amount of oxygen would sooner or later convert all organic molecules in a given sample into peroxides.

This does not happen because radicals can undergo additional reactions, namely:

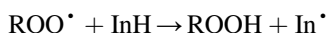
(a) Recombination with other radicals:



(b) Reaction with transition metal ions, for example:



(c) Reaction with molecules of the so-called antioxidants, such as α -tocopherol (denoted here as InH – inhibitor):



In the first two cases, radicals form molecular (nonradical) products, which stops the chain process. In the third case the generated radicals In^{\bullet} are inert (which is what defines the term antioxidants), and unable to react with new organic molecules. Thus, the In^{\bullet} radicals remain in the system until they are attacked by another radical, In^{\bullet} , R^{\bullet} , or ROO^{\bullet} . In any case, the chain is terminated.

Between the moment when a free radical appears, and the moment when it disappears, several successive reaction cycles involving R^{\bullet} and ROO^{\bullet} occur. Thus, for each radical that appears in the system several hydroperoxide molecules are formed. This number characterizes the chain length (l), which is limited by termination reactions and is shortened in the presence of antioxidants, which usually explains their action as inhibitors of free-radical processes.

10.3.4 Chain Branching

The considered picture characterizes chain oxidation with nonbranching chains. However, there are possible situations in which one radical generates two or more, thereby leading to the appearance of new parallel chains of peroxidation – to chain branching.

In particular, transition metals, catalyzing decomposition of hydroperoxides (formed in the chain reaction), generate new free radicals from the nonradical products:



Needless to say, these new radicals participate in new chain reactions, forming what is called degenerated branching of the chain process. In model experiments, in excess of Fe^{2+} ions, the reaction rate depends mainly on $ROOH$ concentration. Thus, as $ROOH$ is rapidly accumulated as the main chain product, the whole process gets self-accelerating, explosive character.

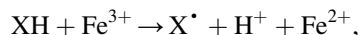
The analogy of this stage of peroxidation with an explosion is enhanced by the fact that the process is accompanied by luminescence (chemiluminescence). The latter, if recorded in time, allows one to study the reactions kinetics and mechanism.

In the cell, the chain branching rate is determined mainly by the presence of enzymes with transition metals in the lower oxidation state (see more in Chap. 14) and, to a lesser extent, by the concentration and localization of free Fe^{2+} ions. In model systems, this process is conveniently regulated by adding Fe^{2+} salts in the required concentration.

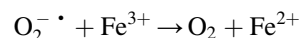
Fe^{2+} can also be regenerated due to sulfhydryl groups of membrane proteins:



by one-electron oxidation of different species (e.g., cysteine):

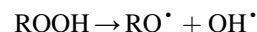


or reacting with superoxide (which is the opposite to initiation):



These reactions restore the Fe^{2+} pool and thus support the chain branching process.

In addition, peroxides can break down spontaneously:



However, at room temperature, the rate of this process is practically zero. It acquires any significance only at high temperatures and is therefore called thermal decomposition.

10.3.5 Summary and General Scheme of Peroxidation Reactions

Thus, the oxidation of hydrocarbons (as well as fatty acids, lipids, and a number of other organic molecules) by molecular oxygen is a free-radical chain process. The main evidences for that are as follows:

- The oxidation rate is increased by various radical-generating agents: lighting, ionizing radiation, substances

Table 10.1 Basic reactions of hydrocarbon free-radical peroxidation

| Process stage | Reactions | Rate-limiting reaction and effective reaction constant |
|-----------------|--|--|
| Initiation | $\text{Me}^{n+} + \text{O}_2 \xrightarrow{k_0} \text{Me}^{(n+1)+} + \text{O}_2^- \cdot$ | k_0 |
| | $\text{O}_2^- \cdot + \text{H}^+ \xrightarrow{k_{00}} \text{HOO} \cdot$ | |
| | $\text{HOO} \cdot + \text{RH} \xrightarrow{k_1} \text{H}_2\text{O}_2 + \text{R} \cdot$ | |
| Propagation | $\text{R} \cdot + \text{O}_2 \xrightarrow{k_2} \text{ROO} \cdot$ | k_3 |
| | $\text{ROO} \cdot + \text{RH} \xrightarrow{k_3} \text{ROOH} + \text{R} \cdot$ | |
| Chain branching | $\text{ROOH} + \text{Fe}^{2+} \xrightarrow{k_p} \text{RO} \cdot + \text{OH}^- + \text{Fe}^{3+}$ | k_p |
| | $\text{ROOH} \xrightarrow{k_T} \text{RO} \cdot + \text{OH} \cdot$ | |
| | $\text{RO} \cdot + \text{RH} \xrightarrow{k_5} \text{ROH} + \text{R} \cdot$ | |
| Termination | $\text{R} \cdot + \text{R} \cdot \xrightarrow{k_4} \text{P}^* \rightarrow \text{P}$ | k_6 |
| | $\text{R} \cdot + \text{ROO} \cdot \xrightarrow{k_5} \text{P}^* \rightarrow \text{P}$ | |
| | $\text{ROO} \cdot + \text{ROO} \cdot \xrightarrow{k_6} \text{P}^* \rightarrow \text{P} + h\nu$ | |
| | $\text{ROO} \cdot + \text{InH} \xrightarrow{k_7} \text{ROOH} + \text{In} \cdot$ | k_8 |
| | $\text{ROO} \cdot + \text{In} \cdot \xrightarrow{k_8} \text{Y}$ | |
| | $\text{ROO} \cdot + \text{H}^+ + \text{Fe}^{2+} \xrightarrow{k_9} \text{ROOH} + \text{Fe}^{3+}$ | k_9 |
| | $\text{R} \cdot + \text{H}^+ + \text{Fe}^{2+} \xrightarrow{k_{9a}} \text{RH} + \text{Fe}^{3+}$ | |
| Iron reduction | $2\text{RSH} + 2\text{Fe}^{3+} \xrightarrow{k_{10}} \text{RSSR} + 2\text{H}^+ + 2\text{Fe}^{2+}$ | k_{10} |
| | $\text{XH} + \text{Fe}^{3+} \rightarrow \text{X} \cdot + \text{H}^+ + \text{Fe}^{2+}$ | k_{11} |
| | $\text{Me}^{(n+1)+} + \text{O}_2^- \cdot \xrightarrow{k_{-0}} \text{Me}^{n+} + \text{O}_2$ | k_{-0} |

that produce radicals at decomposition, and transition metals.

- The process has characteristic stoichiometry: a single initiating quantum or molecule results in several product molecules.
- The reaction is suppressed by radical-binding compounds.

The rate of the whole process depends on the concentration of peroxide radicals, leading the oxidation chain. The product of this process is hydroperoxides, and the process is generally called peroxidation.

In conclusion, we present a list of chemical reactions, associated with hydrocarbon peroxidation, with the designation of the rate constants (Table 10.1 and Fig. 10.1).

10.4 Hydrocarbon Oxidation Is Accompanied by Photon Emission

Besides the free-radical chain nature, the above processes of hydrocarbon peroxidation are characterized by another quality of primary importance: they emit light, albeit of ultralow intensity. This was first observed in Vasil'ev et al. (1959) and Shliapintokh et al. (1960) and later appeared largely identical to biological autoluminescence (ultraweak photon emission of biological systems) (see, e.g., (Vladimirov and Archakov 1972; Fedorova et al. 2007; Hammond and White

2011)). The decisive role in this phenomenon (as well as in development of the radical chain process) is played by oxygen, that is, it is associated precisely with oxidation. For this reason, such kind of chemiluminescent processes is often called oxyluminescence, or oxychemiluminescence, OCL (Belyakov et al. 2004; Fedorova et al. 2007), of which we will use the latter term.

10.4.1 Identification of OCL Sources: General Steps

A major contribution to understanding the mechanism of OCL at hydrocarbon peroxidation was made by the group of R.F. Vasiliev (Vasil'ev 1963; Vasil'ev 1965a, b, c, d; Vasil'ev and Vichutinskii 1962b; Vassil'ev and Vichutinskiy 1962; Vasil'ev and Vichutinskii 1962a; Vasil'ev et al. 1963; Vassil'ev et al. 1959; Vasil'ev et al. 1961; Vasil'ev and Rusina 1964a, b; Vasiljev 1967). First of all, similarly to Frankenburger–Audubert's reasoning (see previous chapter), the authors emphasized that of all the reactions occurring simultaneously during chain peroxidation (see Table 10.1), the amount of energy sufficient to get an electronic-excited state, with further photon emission at its relaxation, is released only in three, namely, reactions of free-radical recombination (Table 10.2).

Fig. 10.1 Basic reactions of free-radical peroxidation of hydrocarbons

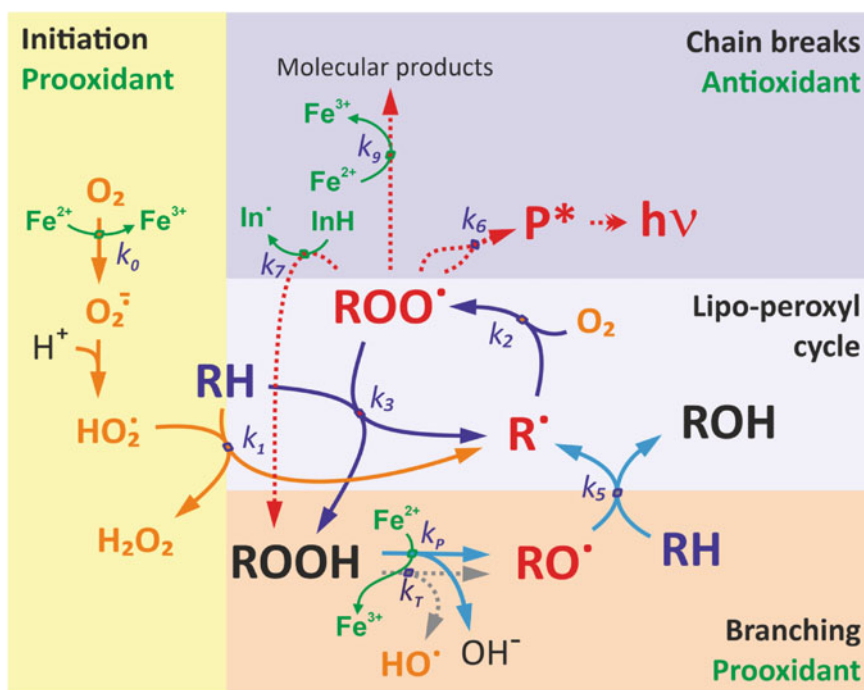


Table 10.2 Activation energy (E_a) and enthalpy (ΔH) of hydrocarbon peroxidation reactions

| Reaction | E_a , kcal/mol | ΔH , kcal/mol |
|----------|--|-----------------------|
| 1 | $X^{\cdot} + RH \rightarrow XH + R^{\cdot}$ | – |
| 2 | $R^{\cdot} + O_2 \xrightarrow{k_2} ROO^{\cdot}$ | +24 |
| 3 | $ROO^{\cdot} + RH \xrightarrow{k_3} ROOH + R^{\cdot}$ | –3 |
| 4 | $R^{\cdot} + R^{\cdot} \xrightarrow{k_4} \text{inactive products}$ | +60–90 |
| 5 | $R^{\cdot} + ROO^{\cdot} \xrightarrow{k_5} \text{inactive products}$ | +70 |
| 6 | $ROO^{\cdot} + ROO^{\cdot} \xrightarrow{k_6} O_2 + \text{inactive products}$ | +100 |

According to Vasil'ev (1963) and Vasil'ev (1965b)

Reactions with enough energy to generate a photon are No 4–6. The reaction that is actually the source of chemiluminescence is No 6.

However, as shown in Box 10.1, the presence of at least 10^{-4} M of oxygen makes concentration of R^{\cdot} incomparably smaller than that of ROO^{\cdot} , and reaction 6 becomes absolutely dominating among reactions 4–6 (Vasil'ev and Vichutinskii 1962b). Contrary to that, if the oxygen access to the system is stopped, the balance of radicals $R^{\cdot} \leftrightarrow ROO^{\cdot}$ quickly shifts toward R^{\cdot} , and then the chain termination occurs mainly as a result of reaction 4. Importantly, photon emission in the presence of oxygen is at least two orders of magnitude more intense than in its absence, though the chain peroxidation can be detected in both cases (Allabutayev et al. 1965; Vasil'ev 1965a). Thus, the main (if not the only) source of OCL at hydrocarbon oxidation is reaction 6, and the quantum yield of chemiluminescence in reactions 4 and 5 is at least two orders of magnitude lower.

Further, to identify the electron-excited states, responsible for luminescence in a given system, one usually

starts with finding the energy level structure of the emitter, which can be used as its fingerprints. For photoluminescence, this is obtained from its excitation spectra, emission spectra, luminescence quantum yields and luminescence kinetics, which allow constructing the whole Jablonski diagram for the emitter. However, in chemiluminescence studies, there is no external excitation, and thus, instead of the excitation spectrum, at best, the reaction energy is calculated. Besides, measuring the luminescence spectra and yields, and the excited state lifetime, is extremely complicated due to its vanishingly low intensity.

For hydrocarbon peroxidation, this difficult task was accomplished in a series of works by the group of R.F. Vasiliev (Vasil'ev 1963; Vasil'ev 1965a, b; Vasil'ev and Vichutinskii 1962b; Vasil'ev et al. 1963; Vasil'ev et al. 1959; Vasil'ev et al. 1961; Vasil'ev and Rusina 1964a).

10.4.2 Excited State Lifetime

As discussed in Chap. 5, the excited state lifetime, τ , is a very important characteristic. It allows to judge, whether the excited state is singlet (radiational lifetime $\tau_0 = 10^{-8} - 10^{-9}$ s) or triplet ($\tau_0 \geq 10^{-4}$ s), calculate probabilities of radiative and nonradiative relaxation, and analyze conditions for energy transfer in the system. In photoluminescence studies, τ can be obtained from the luminescence decay after the end of its excitation (see Sect. 5.2.3). Contrary to that, for chemiluminescence, this approach is obviously inapplicable, and one has to use indirect methods.

In Vassil'ev and Vichutinskii (1962), τ was evaluated from the effect of luminescence quenching by atmospheric oxygen. For this, hydrocarbon oxidation was carried out in a closed vessel at a constant initiation rate. The oxygen concentration decreased linearly with time (Fig. 10.2), meaning that the rate of the whole chain process remained constant until oxygen was almost completely depleted of in the medium (Vassil'ev and Vichutinskii 1962). Hence, stationary concentrations of excited products formed within the system (which are described by the so-called fast variables – see Sect. 8.5.3) must be also constant. At the same time, the UPE intensity was increasing with time till the very end of the process (Fig. 10.2), which could be explained only by UPE quenching with oxygen, which is maximal at the beginning, and decreases as oxygen is spent in the reaction course (Vassil'ev and Vichutinskii 1962). This fact per se, already suggests that the excited state should be triplet, as singlet-excited states are poorly quenched by triplet oxygen.

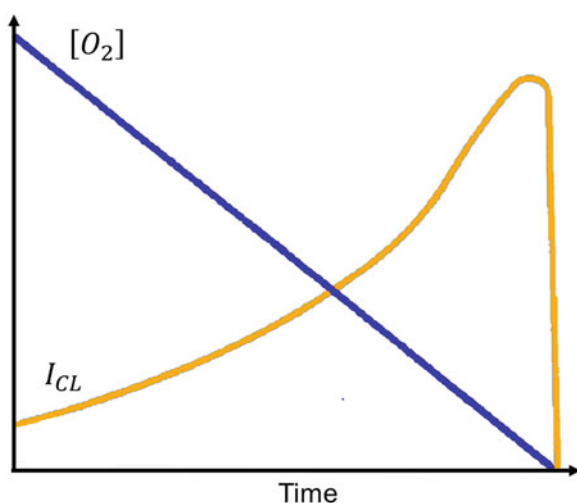


Fig. 10.2 Oxygen quenching of chemiluminescence at constant initiation rate. $[O_2]$ – oxygen concentration, I_{CL} – intensity of chemiluminescence. (Redrawn with permission from Vladimirov and Potapenko (1989). Copyright 1989, the authors)

Analysis of UPE kinetics in such a system shows, that the main part of it obeys the well-known Stern–Volmer equation for luminescence quenching (see Sect. 5.3.4):

$$\frac{I}{I_q} = \frac{\varphi}{\varphi_q} = 1 + \tau D_{O_2}[O_2] \quad (10.6)$$

where I and φ are the UPE intensity and quantum yield in the absence of the quencher (i.e., at low-oxygen concentrations); I_q and φ_q – the same in the presence of the quencher; τ is the lifetime of the excited state in the absence of the quencher; D_{O_2} is the oxygen diffusion coefficient.

Putting $I/I_q = f([O_2])$ on the graph, the authors found:

$$\tau D_{O_2} = 2 \cdot 10^3 \text{ l/mol.}$$

The value of D_{O_2} can be approximated from the studies on photoluminescence quenching by oxygen: $10^{10} \text{ l} \cdot \text{mol}^{-1} \cdot \text{s}^{-1}$ (for quenching fluorescence of aromatic hydrocarbons), $(4 - 5) \times 10^9 \text{ l} \cdot \text{mol}^{-1} \cdot \text{s}^{-1}$ (for quenching phosphorescence of the same compounds). Thus, the excited state lifetime of the molecule formed during chemiluminescence equals (Vassil'ev et al. 1959; Vasil'ev et al. 1961; Emanuel et al. 1965):

$$\tau \cong 10^{-7} \text{ s (if the product is in the singlet state), or}$$

$$\tau \cong 10^{-6} \text{ s (if the product is in the triplet state),}$$

of which the second variant is more likely.

10.4.3 Luminescence Quantum Yield

Obviously, the luminescence intensity largely depends on intramolecular deactivation of the excited state source of UPE (see Sect. 5.4). This effect was used by R.F. Vasil'ev and A.A. Vichutinskii to evaluate its luminescence quantum yield (Vasil'ev 1963; Vasil'ev and Vichutinskii 1962b; Vasil'ev et al. 1963) by comparing UPE from hydrocarbon solutions (cyclohexane or ethylbenzene) with and without luminescence activators (luminophores), for example, dibromoanthracene.

Adding even a small amount of activator to the oxidizing solution leads to energy transfer from the excited product to the activator, which further luminesces with its own quantum yield and spectrum (Fig. 10.3). This is analogous to dynamic quenching of the product excited state (see Sect. 5.3.4), but accompanied by intense luminescence of the energy acceptor.

Thus, the detected luminescence of the system gets additional spectral band ($h\nu_A$) and becomes more intense, as the

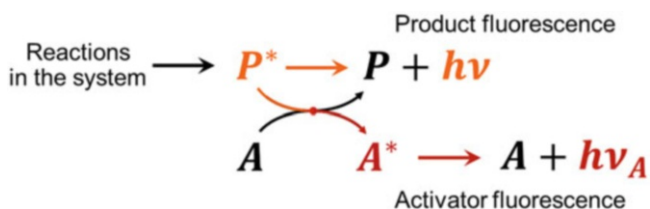


Fig. 10.3 Chemiluminescence in the system containing activator. P – the product of the chemiluminescent reaction; P^* – P in the excited state; A – activator (fluorophore); A^* – A in the excited state; $h\nu$ – fluorescence of the reaction product; $h\nu_A$ – fluorescence of the activator

luminescence quantum yield of the activator (φ_A) is always much higher than that of the product (φ_P): $\varphi_A \gg \varphi_P$. However, the rate of the chemical reaction itself does not change, since the activator does not undergo chemical transformations (which is very important, as it means that adding activators, we still observe the natural dynamics of the processes).

As the activator concentration increases, the intensity of its luminescence tends to a certain limit, which will be reached when all the excited molecules of the product P^* transfer their energy to the activator A . It is obvious that the chemiluminescence intensity in this case (I_A) will be as many times higher than that without the activator (I_P), as the quantum yield of the activator luminescence (φ_A) is greater than that of the product (φ_P):

$$\frac{I_A}{I_P} = \frac{\varphi_A}{\varphi_P} \quad (10.7)$$

where I_A and I_P are expressed in the number of photons/s.

As the luminescence quantum yield does not depend on the method of the molecule excitation (see Chap. 5); the value of φ_A can be obtained separately in experiments on photoluminescence. Based on these data, φ_P equals (Vasil'ev 1963; Vasil'ev 1965a, b; Vasil'ev et al. 1963):

$$\varphi_P \cong 10^{-4} - 10^{-3} \quad (10.8)$$

10.4.4 The Excited State Natural Lifetime

The low quantum yield of luminescence, calculated above, $\varphi_P \cong 10^{-4} - 10^{-3}$, means that the excited state P^* is effectively quenched in the system. Hence, the observed excited state lifetime ($\tau \cong 10^{-6} - 10^{-7}$, see Sect. 10.4.2) is actually much shorter than its natural lifetime in the absence of any quenching processes. As mentioned in Chap. 5, Sect. 5.3.4.2, the latter is called radiational lifetime – τ_0 (defined as the

lifetime of the excited state when the quantum yield of luminescence is unity), that can be calculated from the well-known ratio (see Sect. 5.3.4.2):

$$\varphi_{\text{lum}} = \frac{\tau}{\tau_0} \quad (10.9)$$

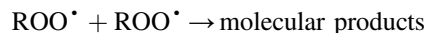
Here φ_{lum} is the luminescence quantum yield; τ is the observed excited state lifetime, and τ_0 is its radiational lifetime.

Thus, for the luminescent product of hydrocarbon peroxidation:

$$\tau_0 = 10^{-2} - 10^{-4} \text{ s} \quad (10.10)$$

which undoubtedly indicates that it should be in the triplet-excited state. So, we can conclude that hydrocarbon peroxidation is accompanied by formation of certain triplet-excited molecules (with $\tau_0 = 10^{-2} - 10^{-4}$ s), which are strongly quenched at room and higher temperatures, reducing the excited state lifetime to the observed $\cong 10^{-6}$ s.

These results are already quite useful in identification of the luminescent substance. As mentioned in Sect. 10.4.1, the only reaction capable of generating light quanta during the peroxidation process is the following:

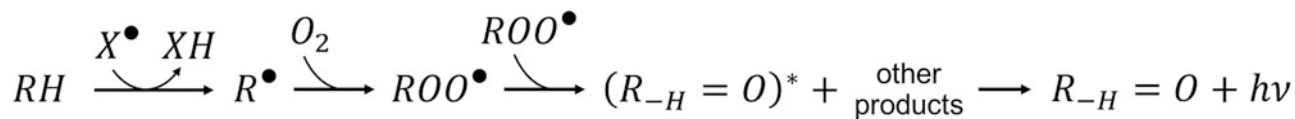


One of the products, possibly appearing within the system in the triplet-excited state is ketone molecules, whose properties match the above data very well. They have both high efficiency of the singlet–triplet transition, and the radiational lifetime of triplet-excited states $10^{-2} - 10^{-3}$ s. Thus, the following reaction scheme can be suggested (Scheme 10.2).

10.4.5 Luminescence Spectra: Triplet Ketones

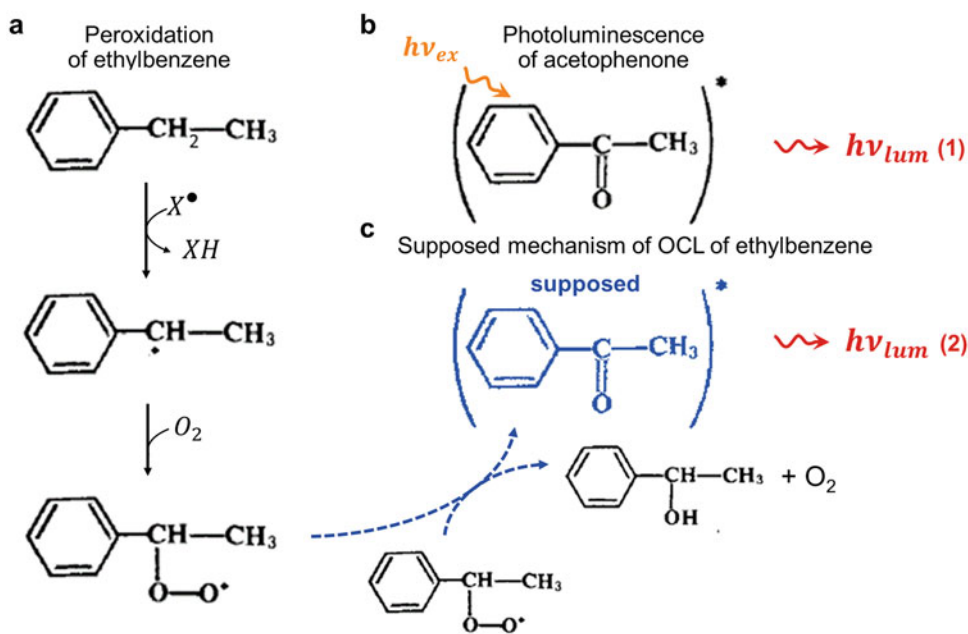
The above suggestion can be further tested by measuring spectra of OCL from different substances, and thus reconstructing the energy level structure of the luminescent molecules. As mentioned above, this is one of the most important steps in their identification, which can become a reliable proof of mechanism, if supplemented with additional data.

In full accordance with the suggested Scheme 10.2, the OCL spectra of ethylbenzene, cyclohexane, n-decan, and 2-butanone coincided with the photoluminescence spectra of the ketones supposedly formed during recombination of their peroxy radicals (Vasil'ev and Rusina 1964a; Vasil'ev 1965c) (e.g., Schemes 10.3 and 10.4).

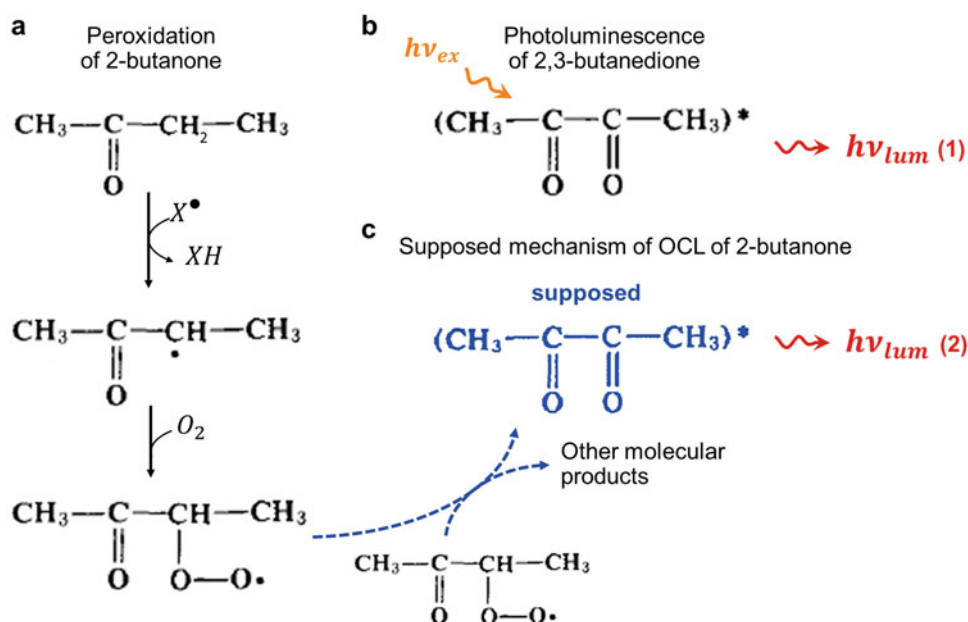


Scheme 10.2 The suggested scheme of UPE generation during peroxidation of hydrocarbons

Scheme 10.3 Comparison of oxychemiluminescence of ethylbenzene with photoluminescence of acetophenone. (a) The known processes, taking place during peroxidation of ethylbenzene. (b) Photoluminescence of acetophenone. (c) The supposed mechanism of chemiluminescence, accompanying peroxidation of ethylbenzene (a). The spectra of $h\nu_{lum}(1)$ and $h\nu_{lum}(2)$ match very well, which suggests, that the luminescent substance in c is identical to that in a



Scheme 10.4 Comparison of chemiluminescence of methyl ethyl ketone with photoluminescence of 2,3-butanedione. (a) The known processes, taking place during peroxidation of methyl ethyl ketone. (b) Photoluminescence of 2,3-butanedione. (c) The supposed mechanism of chemiluminescence, accompanying peroxidation of methyl ethyl ketone (a). The spectra of $h\nu_{lum}(1)$ and $h\nu_{lum}(2)$ match very well (see, Fig. 10.4a, curves 4 and 4'), which suggests, that the luminescent substance in c is identical to that in a



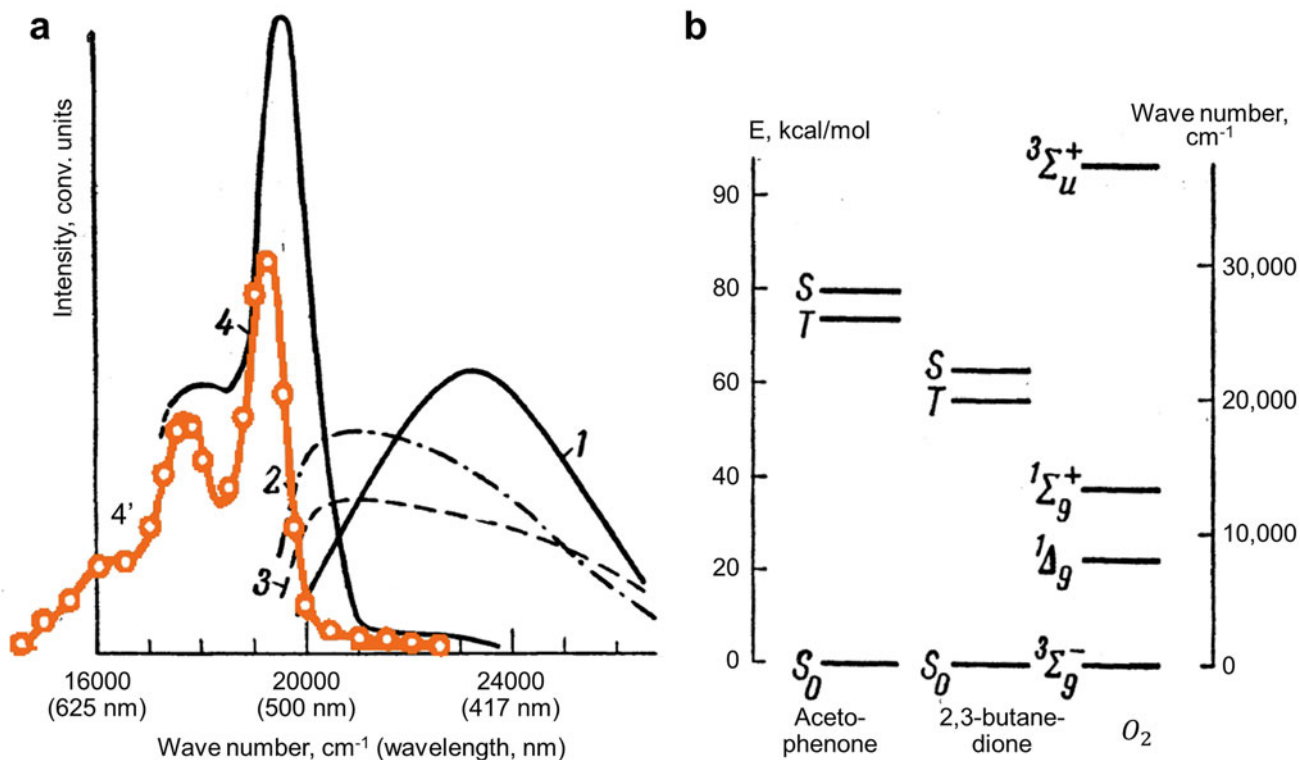


Fig. 10.4 Luminescence spectra (a) and energy levels (b) of some oxidized substances. (a) Oxychemiluminescence of: (1) ethylbenzene, (2) cyclohexane, (3) n-decan, (4) 2-butanone; (4') photoluminescence of 2,3-butanedione. (After Bäckström and Sandros (1960)). (b) – The lowest electron-excited states of the substances, supposedly generated

in electron-excited states during peroxidation of the above hydrocarbons (Schemes 10.3 and 10.4): acetophenone, 2,3-butanedione and oxygen. (Adapted from Vasil'ev and Rusina (1964b), with permission from the authors)

At the same time, chemiluminescence at peroxidation of different hydrocarbons had distinctly different spectra (see, e.g., Fig. 10.4a for OCL spectra of some of them, and Fig. 10.4b, for their lowest electron-excited states).

Important data can be obtained from the well resolved spectrum of 2,3-butanedione (or peroxidation of 2-butanone), obtained in the presence of oxygen (Fig. 10.4a, 4 and 4'). As is known, atmospheric (triplet) oxygen is quenching triplet states $\sim 10^4$ times efficiently than singlet states (Kellogg 1969). If singlet and triplet-excited states were present in equal amounts, the observed intensity of phosphorescence would be 10^4 times less than fluorescence. As the phosphorescence peak area (Fig. 10.4a, 4 and 4', left peak) is comparable to the fluorescence one (Fig. 10.4a, 4 and 4', right peak), the ratio of triplet to singlet ketones initially produced in the chemical reaction should be $\sim 10^4$ (Kellogg 1969). This is also generally confirmed by the observed OCL quenching by atmospheric oxygen (Kellogg 1969).

Thus, one of the main fractions of luminescent substances at OCL of hydrocarbons is their triplet-excited ketones,

generated at recombination of peroxy radicals (Schemes 10.3c and 10.4c).

10.4.6 Luminescence Spectra: Singlet Oxygen

However, besides the blue-green part of the spectrum (420–550 nm, characteristic of the carbonyl groups (Vasiljev 1967)), the above OCL had red and near infrared spectral bands – from 10% to 85% of all intensity (Niu and Mendenhall 1990; Koga et al. 1991; Howard and Ingold 1968). Some of them were characteristic of singlet oxygen (e.g., 1270 nm), others – similar to those attributed to the supposed oxygen dimers (O₂)₂ by J. Stauff (see Chap. 9) (Nakano et al. 1976).

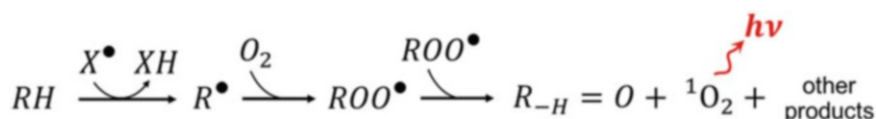
Generation of singlet oxygen at hydrocarbon peroxidation was indeed confidentially shown in a number of works (e.g., (Howard and Ingold 1968; Kanofsky 1984; Niu and Mendenhall 1990; Nakano et al. 1976)), both by specific trapping of ¹O₂ (9,10-diphenylanthracene) (Howard and Ingold 1968), and spectroscopically (Koga et al. 1991).

Table 10.3 Oxygen absorption and luminescence spectra in visible and near IR spectral regions, and their interpretation in terms of electron-vibrational transition

| | Absorption | | Luminescence | |
|----------|--------------------------|---|--------------------------|--|
| | $\lambda(I_{\max})$, nm | Electron-vibrational transition | $\lambda(I_{\max})$, nm | Electron-vibrational transition |
| Dimole | 381 | $[^1\Sigma(0)]_2 \leftarrow [^3\Sigma(0)]_2$ | 381 | $[^1\Sigma(0)]_2 \rightarrow [^3\Sigma(0)]_2$ |
| | 478 | $[^1\Sigma(0)^1\Delta(0)] \leftarrow [^3\Sigma(0)]_2$ | 477 | $[^1\Sigma(0)^1\Delta(0)] \rightarrow [^3\Sigma(0)]_2$ |
| | 533 | $[^1\Delta(0)^1\Delta(2)] \leftarrow [^3\Sigma(0)]_2$ | | |
| | 580 | $[^1\Delta(0)^1\Delta(1)] \leftarrow [^3\Sigma(0)]_2$ | 578 | $[^1\Delta(0)^1\Delta(1)] \rightarrow [^3\Sigma(0)]_2$ |
| | 631 | $[^1\Delta(0)]_2 \leftarrow [^3\Sigma(0)]_2$ | 634 | $[^1\Delta(0)]_2 \rightarrow [^3\Sigma(0)]_2$ |
| | | | 703 | $[^1\Delta(0)]_2 \rightarrow [^3\Sigma(0)^3\Sigma(1)]$ |
| Monomole | 762 | $^1\Sigma(0) \leftarrow ^3\Sigma(0)$ | 762 | $^1\Sigma(0) \rightarrow ^3\Sigma(0)$ |
| | | | 860 | $^1\Sigma(0) \rightarrow ^3\Sigma(1)$ |
| | 1070 | $^1\Delta(1) \leftarrow ^3\Sigma(0)$ | | |
| | 1270 | $^1\Delta(0) \leftarrow ^3\Sigma(0)$ | 1268 | $^1\Delta(0) \rightarrow ^3\Sigma(0)$ |
| | | | 1580 | $^1\Delta(0) \rightarrow ^3\Sigma(1)$ |
| | | | | |

Reprinted from Krasnovsky Jr. (1990), with permission from the author

Scheme 10.5 The suggested scheme of $^1\text{O}_2$ -mediated UPE generation during peroxidation of hydrocarbons



Oxygen dimoles were also supposed by some authors (e.g., (Nakano et al. 1976)), but were confidentially shown only at highly exothermic reactions, like $\text{H}_2\text{O}_2 + \text{Cl}_2$ and $\text{H}_2\text{O}_2 + \text{OCl}^-$, within the generated oxygen bubbles (Khan and Kasha 1966; Kasha and Khan 1970). The first group which has reliably shown singlet oxygen dimoles in liquid phase is that of A.A. Krasnovsky (Krasnovsky Jr and Neverov 1990), where they were stabilized by specific solvents, with whose molecules they formed complexes. These data were later confirmed in Chou et al. (1996) and Krasnovsky Jr. (2010).

In aqueous systems and within the cell generation of oxygen dimoles was supposed by a number of authors (Sander and Stauff 1971; Stauff et al. 1963; Stauff and Fuhr 1971; Seliger 1960, 1964; Nakano et al. 1976; Arnold et al. 1964; Furukawa et al. 1970), but in all cases remains unproven and supposedly relates either to oxygen dimoles appearing within the generated bubbles, or to excited carbonyls (see discussion in Krasnovsky (2007) and Koga et al. (1991)). The most reliable of these works is supposedly (Cadenas et al. 1983).

Altogether, the characteristic spectral bands of oxygen absorption and luminescence and their interpretation are summarized in Table 10.3.

Altogether, while oxygen dimoles in liquid systems remain mostly unobservable, one can definitely conclude that a fraction of oxygen molecules formed in course of peroxidation (see, e.g., Scheme 10.3), should be in singlet-

excited state. Thus, the above-suggested scheme of OCL (Scheme 10.2) should be supplemented with the following path (Scheme 10.5).

See more on the topic in Krasnovsky (2007).

10.4.7 Quantum Yield of Excitation

An important point in the above line of research is to calculate the probability of generation of the excited state source of OCL. As one can see, these quantum yields must be calculated separately for all luminescent states (e.g., for the above-mentioned triplet carbonyls and singlet oxygen).

As is well known, the chemiluminescence intensity (I) is related to the reaction rate (ω) by the expression:

$$I = \varphi_{\text{total}} \cdot \omega, \quad (10.11)$$

where φ_{total} is the general quantum yield of the chemiluminescent process (number of quanta produced per a single reacting molecule), I is expressed in the number of quanta, ω – in the number of molecules entering the reaction.

φ_{total} , in its turn, is representable as the product of quantum yields of excitation and luminescence per se:

Table 10.4 Total quantum yield of oxychemiluminescence at peroxidation of different hydrocarbons, calculated as $\varphi_{\text{total}} = \varphi_{\text{ex}} \cdot \varphi_{\text{lum}} = I/\omega$ in Eq. 10.11

| Molecule | Total quantum yield of CL $\varphi_{\text{total}} = I/\omega, \times 10^{-9}$ |
|----------------------|---|
| n-Heptane | 0.8 |
| n-Octane | 0.16 |
| n-Dodecane | 0.15 |
| Cyclohexane | 2.4 |
| Cyclododecane | 1.1 |
| Ethylbenzene | 0.9 |
| 2-Butanone | 7 |
| 2-Heptanone | 2.4 |
| Benzyl phenyl ketone | 8 |
| Cyclopentanone | 40 |

Reprinted with permission from Kellogg (1969). Copyright 1969, American Chemical Society
 I is expressed in the number of photons, ω in the number of molecules

$$\varphi_{\text{total}} = \varphi_{\text{ex}} \cdot \varphi_{\text{lum}} \quad (10.12)$$

Thus, knowing φ_{total} and φ_{lum} (calculated above for some cases, see Sect. 10.4.3), one can estimate the quantum yield of excitation as well – the probability of generating the excited state source of UPE from the reacting molecules.

The values of φ_{total} for OCL of triplet-excited ketones at peroxidation of different hydrocarbons are of the order of $10^{-8} - 10^{-10}$ (see Table 10.4), whence the excitation quantum yield is (Vasil'ev 1965b):

$$\varphi_{\text{ex}} = 10^{-4} - 10^{-6} \quad (10.13)$$

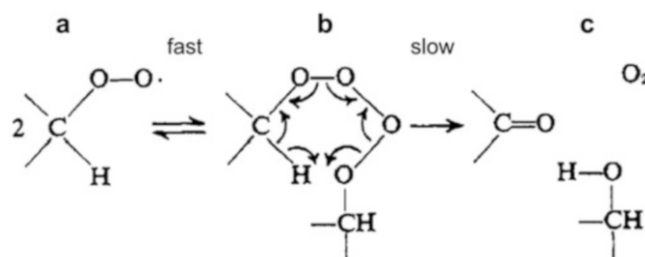
At the same time, singlet oxygen has quite high φ_{ex} (estimated as 3.5–14.0% in the case of simple alkylhydroperoxides (Niu and Mendenhall 1990)), but very low quantum yield of luminescence (10^{-6} at best (Krasnovsky 1981; Koga et al. 1991)), which gives a relatively low total intensity for singlet oxygen component of OCL.

Importantly, spectral bands observed at OCL of hydrocarbons, are also found in OCL at peroxidation of fatty acids and lipids in microsomes, suggesting some common mechanism in all these systems. See more in this respect further, and in Chap. 11.

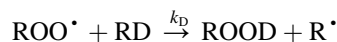
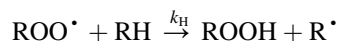
10.5 The Mechanism of Photon Emission

10.5.1 Russell's Tetroxide Mechanism

The exact mechanism of reaction between two peroxide radicals was suggested in 1957 by G. Russell in his elegant work (Russell 1957), based on comparison of kinetic characteristics of hydrocarbon peroxidation with hydrogen and deuterium isotopes:



Scheme 10.6 Russell's mechanism of chain termination at hydrocarbon peroxidation (Russell 1957). (Reprinted with permission from Howard and Ingold (1968). Copyright 1968, American Chemical Society)



This resulted in the famous Russell's tetroxide mechanism (Scheme 10.6), suggesting the following sequence of events for interaction of two hydroperoxide radicals:

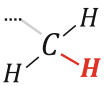
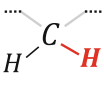
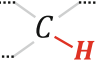
- Fast and reversible composition of unstable quasicyclic tetroxide (Scheme 10.6b);
- Slow and irreversible decomposition of the tetroxide; formation of ketone, alcohol, and oxygen (Scheme 10.6c). The ratio of the reaction rates was also confirmed by the group of Vasil'ev (Belyakov and Vassil'ev 1970).

Importantly, the **b** compound is singlet, as well as the *ground state* of the resulting ketones and alcohols, while the *ground state* of oxygen is triplet. Thus, according to Wigner's spin conservation rule, *it is impossible for all products to be in the ground state at the same time.*

The most possible variants are as follows:

- Unexcited ketone + unexcited alcohol + *singlet-excited oxygen* ($^1\Sigma_g^+$ or $^1\Delta_g$).

Table 10.5 Energies of C – H bonds in alkanes

| Type of C – H bond | Scheme | Energy, kcal/mol |
|--------------------|--|------------------|
| Primary |  | 98–100 |
| Secondary |  | 94–95 |
| Tertiary |  | ~91 |

Data from Fedorova et al. (2007)

- Triplet-excited ketone (n, π^*) + unexcited alcohol + unexcited (triplet) oxygen.

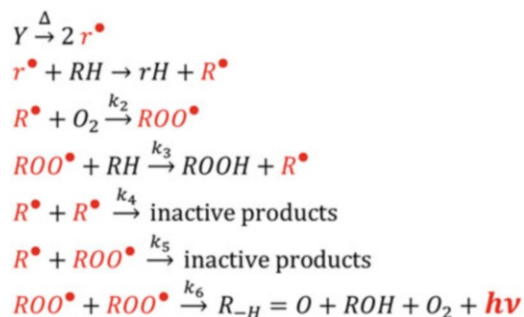
Exothermicity of the whole reaction is estimated over 100 kcal/mol (Howard and Ingold 1968; Vasil'ev 1963; Vasil'ev 1965b)), and probably even more (115–150 kcal/mol according to Kellogg (1969), 157 kcal/mol according to Russell (1957)). This is enough to generate any of the above electronically excited states: the energy excess of singlet oxygen over the triplet ground state is 37.5 kcal/mol for $^1\Sigma_g^+$ state and 22.5 kcal/mol for $^1\Delta_g$ (Howard and Ingold 1968); the energy excess of triplet-excited ketones over the singlet ground state is $\leq 75 - 80$ kcal/mol (Kellogg 1969; Belyakov and Vassil'ev 1970).

Thus, Russell's mechanism is energetically admissible, and required from spin considerations. Besides, and most importantly, it's in full accordance with the above data on luminescence spectra, excited states lifetimes and luminescence quantum yields (see Sect. 10.4).

10.5.2 Oxychemiluminescence of Saturated Hydrocarbons

The best investigated by now is oxidation of saturated hydrocarbons. As a free-radical chain process, it includes dozens of elementary stages (e.g., more than 40 in oxidation of alkyl aromatic hydrocarbons at 100 °C (Belyakov et al. 2004; Emanuel et al. 1967)). However, the only known reactions leading to generation of excited states (i.e., to photon emission), are reactions of free radicals' recombination, as those investigated by G.A. Russell (Russell 1957) and R.F. Vasil'ev (Vasiljev 1967; Vasil'ev 1970; Belyakov and Vassil'ev 1970; Vassil'ev and Vichutinskii 1962).

As is shown in Box 10.1, the presence of at least 10^{-4} M of oxygen in the system leads to complete dominance of the reaction between two peroxide radicals: $ROO^\bullet + ROO^\bullet$. Thus, this is the main reaction stage to be considered. The quantum yield of photon emission at this reaction is also 2–3 orders of magnitude higher than for $R^\bullet + ROO^\bullet$ or $R^\bullet + R^\bullet$



Scheme 10.7 Basic reactions of hydrocarbon peroxidation. Y – initiator, readily decomposed peroxide or azo compound used as a source of initiating free radicals r^\bullet

(Allabutayev et al. 1965; Vasil'ev 1965a), which makes it the most relevant stage for UPE research.

Though having important general features, the precise nature of this stage depends crucially on the radical structure, especially on the type of the weakest C – H bond in the hydrocarbon molecule, most subjected to oxidation. In specialized literature, it is customary to call such a bond *oxidizable functionality*, which we will use in the following. The energies of different C – H bonds in alkanes are shown in Table 10.5. The same trend persists for alkyl aromatic hydrocarbons, although in this case the binding energies are somewhat lower (Vasil'ev 2005; Belyakov 1970).

10.5.2.1 Secondary C – H Bonds

Hydrocarbons with a secondary C – H bond as an oxidizable functionality represent the most studied case of oxychemiluminescence (Vasiljev 1967; Vasil'ev 1970; Belyakov and Vassil'ev 1970; Belyakov 1970; Belyakov et al. 1978c; Mendenhall and Sheng 1991), which deserves consideration first. Ethylbenzene, PhCH_2CH_3 , was the first substrate whose oxidation followed by light emission was studied in detail (Vasiljev 1967; Vasil'ev 1970; Belyakov and Vassil'ev 1970; Belyakov 1970). In it, the $-\text{CH}_2-$ group is the oxidizable functionality, the $-\text{CH}_3$ group has just a nominal reactivity, and the C – H bonds in the aromatic ring

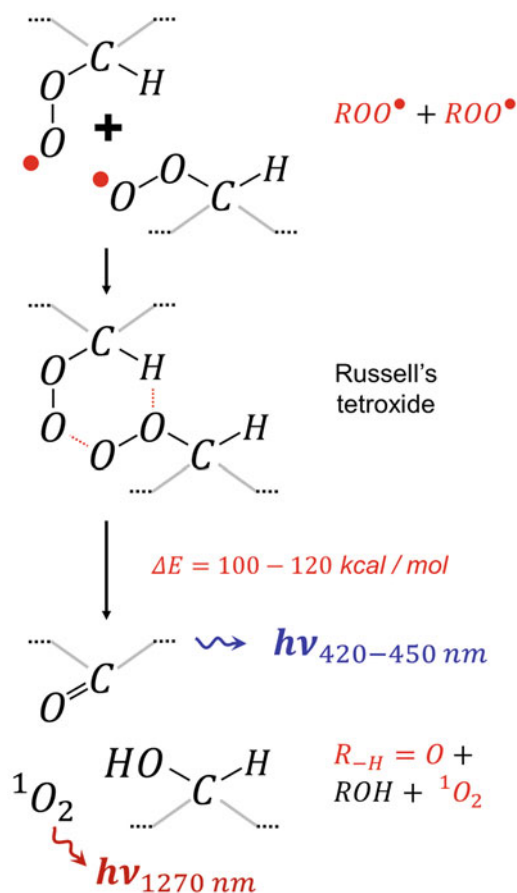


Fig. 10.5 Disproportionation of peroxide radicals with a secondary C – H bond as oxidizable functionality: Russell's mechanism

have very high energy, up to 103 kcal/mol, and are not involved in the oxidation process at all.

The reactions proceeding in this case, generally shown in Table 10.1, are repeated in Scheme 10.7.

For further discussion, it is mechanistically important that the peroxy radicals ROO^{\bullet} become the only chain carriers, and thus their recombination remains the only chain termination reaction at oxygen concentrations higher than 10^{-4} M (see Box 10.1). These peroxy radicals disproportionate according to the Russell mechanism via an intermediate tetroxide (see Sect. 10.5.1), the decomposition of which is sufficiently exothermic (100–120 kcal/mol) to form products in an excited state, namely ketone and singlet oxygen (Vasiljev 1967; Belyakov et al. 1978b) (Fig. 10.5). Alcohol, the third decomposition product, is formed unexcited, provided that the radicals ROO^{\bullet} do not possess any chromophore group.

Experimental evidence for the interference of tetroxide in ROO^{\bullet} disproportionation (Fig. 10.5) has been obtained from low temperature electron spin resonance (ESR) studies (Bennett and Summers 1973; Bennett et al. 1969; Adamic

et al. 1969). This chain termination mechanism is common to a wide variety of chemical and biological oxidation processes (Kanofsky 1986; Miyamoto et al. 2003). In this case, the excited ketone ($R-H = O^*$) is responsible for chemiluminescence in the visible range, which in most cases is phosphorescence from the state $^3(n, \pi^*)$ of the carbonyl group, while singlet oxygen emits infrared radiation from the state $^1\Delta_g$.

As mentioned in Sects. 10.4.5 and 10.4.6, the spectroscopic manifestation of the phosphorescence of chemically excited ketones is oxychemiluminescence bands in the 400–500 nm region with flat maxima around 420–450 nm. The spectroscopic manifestation of singlet oxygen is a band at 1270 nm (Kanofsky 1986; Miyamoto et al. 2003; Niu and Mendenhall 1990; Niu and Mendenhall 1992; Adam et al. 2005).

The quantum yield of triplet-excited ketones during hydrocarbon oxidation is usually $10^{-3} - 10^{-2}$, while that of singlet-excited ketones is several orders of magnitude lower (Belyakov and Vassil'ev 1970; Belyakov 1970). The quantum yield of singlet oxygen generation for primary and secondary peroxy radicals is generally ~ 0.1 (Kanofsky 1986; Niu and Mendenhall 1990; Niu and Mendenhall 1992; Adam et al. 2005) and does not depend on the radical structure, except for the cases of a heteroatom near the peroxy group, which reduces the 1O_2 yield (Niu and Mendenhall 1990; Niu and Mendenhall 1992; Adam et al. 2005).

10.5.2.2 Primary C – H Bonds

Hydrocarbons with a primary C – H bond as an oxidizable functionality, generally retain the salient features of the above mechanism (Adam et al. 2005; Belyakov et al. 1990a). The disproportionation of primary peroxy radicals also obeys the Russell mechanism, and the decomposition of the putative intermediate tetroxide is sufficiently exothermic to get excited carbonyl products and singlet oxygen (Adam et al. 2005; Belyakov et al. 1990a). (This is not so for hydrocarbons with an oxidizable tertiary bond, as they have no hydrogen atom to abstract for Russell's tetroxide formation – see Fig. 10.6 and the following section).

The excitation yields observed for primary peroxy radicals (approximately 0.1 for 1O_2 and 10^{-3} for carbonyls) are similar to those for secondary peroxy radicals (Adam et al. 2005; Belyakov et al. 1990a).

However, the overall chemiluminescence yield ($\varphi_{\text{total}} = \varphi_{\text{ex}} \cdot \varphi_{\text{lum}}$) measured for a representative case of methylbenzenes, appeared surprisingly low – 10^{-10} (Belyakov et al. 1990a). A detailed study of this unprecedented observation showed that such a negligible value is explained by the extremely short lifetime of the corresponding $^3(n, \pi^*)$ excited state of benzaldehydes, due to its high reactivity and efficient quenching by the π -system of benzene rings of substrates and the solvent (Belyakov et al.

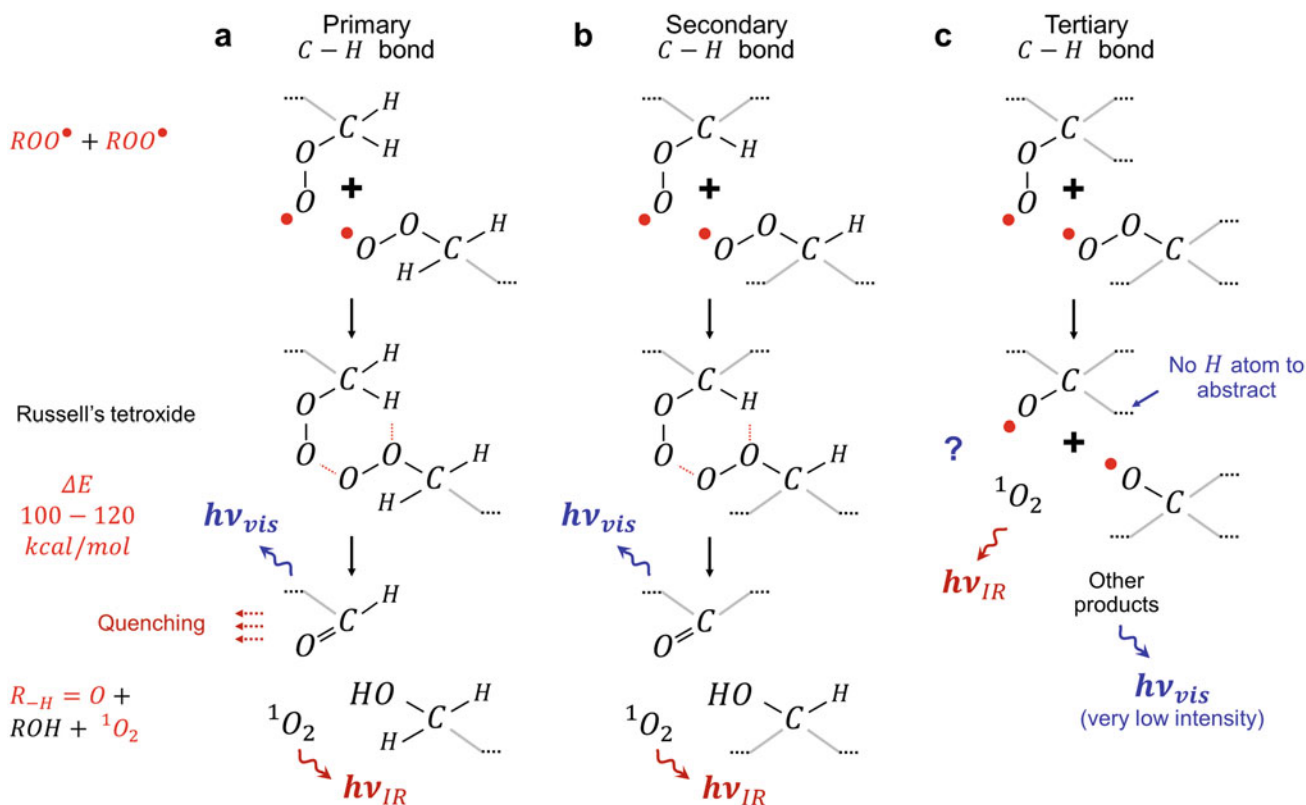
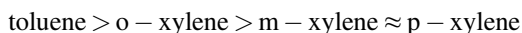


Fig. 10.6 Disproportionation of peroxide radicals with C – H bonds of different types

1990a). Indeed, the rate constants of intra- and intermolecular triplet–singlet quenching for the series:



correlate with the energy difference between the levels ${}^3(n, \pi^*)$ and ${}^3(\pi, \pi^*)$ (Belyakov et al. 1990a).

Thus, the general mechanism of disproportionation for primary peroxy radicals repeats the classical Russell's mechanism for secondary radicals. However, the formed triplet-excited carbonyls can be effectively quenched because of specific energy level structure. This determines the lower (sometimes dramatically lower) OCL intensity from the reaction.

10.5.2.3 Tertiary C – H Bonds

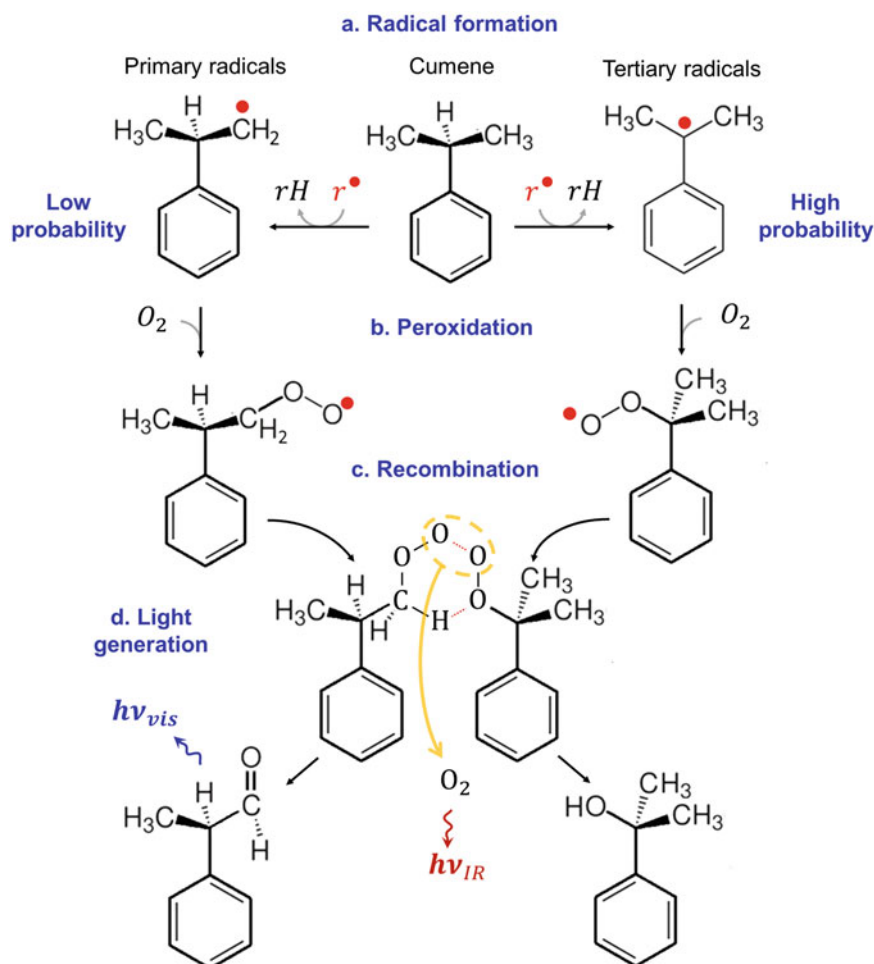
As mentioned above, tertiary peroxy radicals represent a special case for which the chemiluminescence mechanism depicted in Scheme 10.6 and Fig. 10.5 does not apply. Two cumene peroxy radicals, $\text{Ph}(\text{CH}_3)_2\text{COO}^\bullet$, which simulate the corresponding situation, cannot disproportionate through Russell's tetroxide, because they do not have an abstractable hydrogen atom in the immediate vicinity of peroxy (Fig. 10.6c) (Vasil'ev and Fedorova 2004). Nevertheless, free-radical oxidation of cumene is also accompanied by

chemiluminescence both in visible (Belyakov et al. 2004; Adam et al. 2005; Vasil'ev and Fedorova 2004; Belyakov et al. 1978a) and in infrared (Kanofsky 1986; Niu and Mendenhall 1992; Adam et al. 2005) regions due to generation of excited carbonyl and singlet oxygen molecules, respectively (see Fig. 10.7). The efficiency of chemiluminescence in the visible region (carbonyl) is one or two orders of magnitude lower than that for the case of the secondary C – H bond (Belyakov et al. 1978a). Singlet oxygen generation occurs with the yield of ~ 0.02 (Adam et al. 2005), which is several times lower than in the case of primary and secondary peroxy radicals.

Mechanistic alternatives to the standard (Russell's) chemiluminescence process include complex reaction schemes to account for the generation of an excited state (Kanofsky 1986; Niu and Mendenhall 1992; Adam et al. 2005; Vasil'ev and Fedorova 2004; Belyakov et al. 1978a). The mechanism inferred in Vasil'ev and Fedorova (2004) includes not only tertiary peroxy radicals, $\text{Ph}(\text{CH}_3)_2\text{COO}^\bullet$, but also primary ones $\text{PhCH}(\text{CH}_3)\text{CH}_2\text{OO}^\bullet$, formed as a result of hydrogen release from the methyl group of cumene, and subsequent capture of molecular oxygen (Fig. 10.7).

The steady-state concentration of primary radicals (Fig. 10.7, left part) is much lower than of tertiary, since the primary bond has higher energy, and the probability of its

Fig. 10.7 Cumene peroxidation and further recombination of radicals. (The mechanism suggested in Vasil'ev and Fedorova (2004))



breaking is much lower. However, the generated primary radicals quickly react with the tertiary radicals (which are much more common in the system), thus forming an asymmetric tetroxide with an abstractable hydrogen atom (Fig. 10.7c). This structural feature guarantees that such an intermediate will rapidly irreversibly decompose, with the formation of the excited aldehyde $PhCH(CH_3)CHO$, as in the case of secondary peroxy-radicals (Belyakov et al. 1978a) (Fig. 10.7d).

This mechanism was confirmed both experimentally by studying the cumene oxidation kinetics (Belyakov et al. 1978a) and computationally (Vasil'ev and Fedorova 2004) (see Fig. 10.8).

The energy profile of this reaction (Fig. 10.8, red curve – ΔH_f) shows distinct maximum, corresponding to the most unstable state of the heterocycle, and a sharp drop to the right from it. The general reaction exothermicity is ~ 95 kcal/mol.

In full accordance with the classical Russell mechanism, the following events occur in the six-membered heterocycle:

- The C^3O^2 bond goes from single to double (belonging to the forming ketone $R = O$): $n(C^3O^2) = 1 \rightarrow n(C^3O^2) = 2$.

- The O^1O^2 and O^5O^6 bonds are broken: $n = 1 \rightarrow n = 0$ (as the O^1O^6 splits off as a newly formed oxygen molecule).
- The O^1O^6 bond initially goes from $n = 1$ to $n = 2$ (which corresponds to the double bond in the singlet oxygen 1O_2) – the system moves on the singlet potential-energy surface. However, the intermediate state with the double bond appears unstable, and rapidly passes into the final product with $n = 1.5$ (which corresponds to the sesquialteral bond in the triplet oxygen 3O_2). Hence, the final lowest energy state:



demands intersystem crossing.

Importantly, as evident from Fig. 10.8, orders of all the bonds change simultaneously. Thus, the decomposition of tetroxide proceeds synchronously, rather than through the earlier proposed stepwise mechanism (Belyakov et al. 1978b), suggesting elimination of ROH from the tetroxide

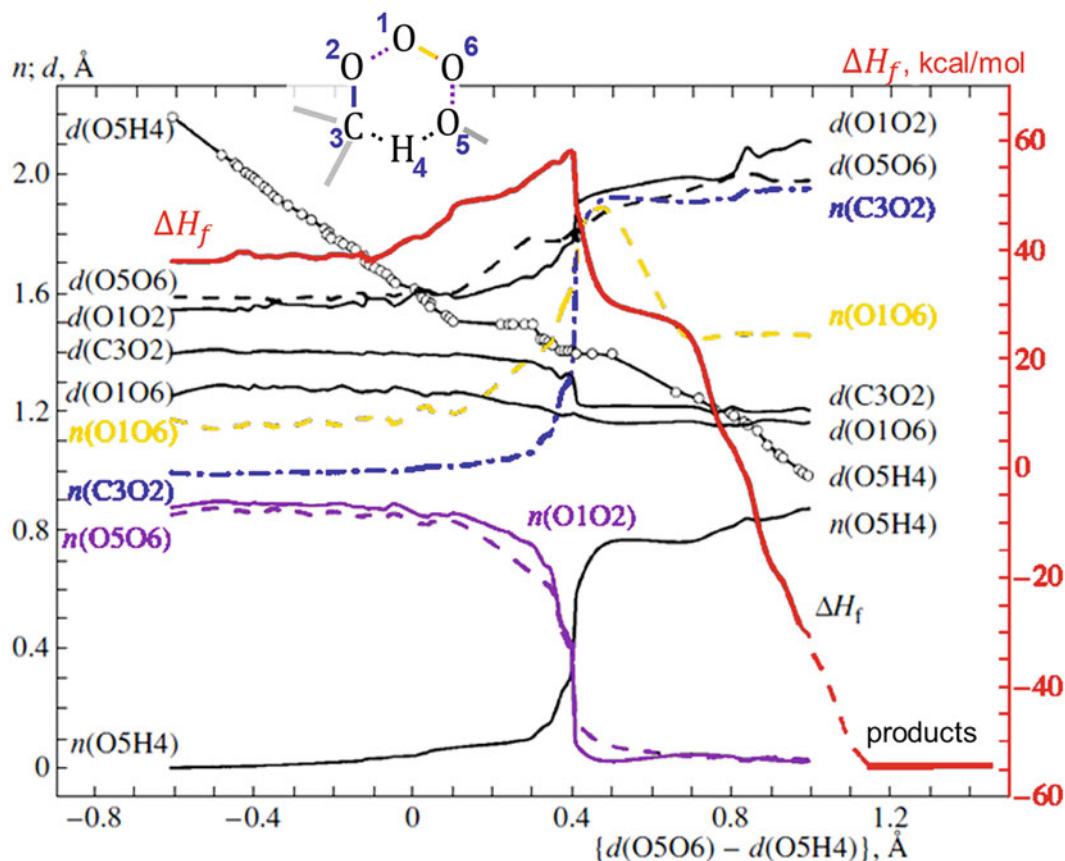


Fig. 10.8 Dependence of bond energies, bond lengths, and bond orders of the six-membered tetroxide center on the reaction coordinate of the Russell decomposition (the difference in the length of the breaking O^5O^6 bond and the forming O^5H^4 bond). The calculations were

performed by the PM3 method with Configuration interaction = 3HOMO + 3LUMO. (Adapted from Vasil'ev and Fedorova (2004). Copyright 2004, with permission from Pleiades Publishing, Ltd)

to yield relatively persistent biradical $^{\bullet}R-HOOO^{\bullet}$, whose cleavage leads to the ketone and O_2 molecules.

A query on the stepwise versus concerted mechanism of the tetroxide decomposition is general for the chemistry of cyclic peroxides. A prominent example is the cleavage of dioxetanes, which is a function of the molecular structure and exhibits concerted or stepwise features depending on substituents (Adam and Baader 1985). Very probably, the same pertains to the tetroxide, whose decomposition proceeds synchronously or stepwise also depending on the structure of this intermediate. Indeed, a wide body of evidence suggests the stepwise-cleavage mechanism of the six-membered tetroxide species formed by secondary peroxy radicals (Belyakov et al. 1978b), while the tetroxide Ph CH (CH₃) CH₂OOOOC (CH₃)₂ Ph, a particular case considered herein, decomposes synchronously (Vasil'ev and Fedorova 2004) (see Figs. 10.7 and 10.8).

10.5.2.4 Nonclassical Paths

Interestingly, deviations from the classical Russell mechanism can be found even at oxidation of hydrocarbons with the

“classical” secondary C – H bonds. In Belyakov et al. (1990b), the authors compared peroxidation of two structurally close hydrocarbons: (1) diphenylmethane and (2) fluorene, which, however, have important difference in photophysical qualities (Vasil'ev 2005; Belyakov et al. 1990b) (Table 10.6, Fig. 10.9).

As shown in Table 10.6, the first important difference between these two cases is the type of luminescence, the forming ketone is capable of. The T_1 triplet-excited state of benzophenone is of $^3(n, \pi^*)$ type, which makes it capable of phosphorescence, and consistent with the standard Russell mechanism. At the same time, the lowest triplet state of 9-fluorenone is of $^3(\pi, \pi^*)$ type, which is characterized by a very low probability of radiational relaxation (Andrews et al. 1978; Biczók and Bérces 1988; Kobayashi and Nagakura 1976). While the Russell mechanism implies that the carbonyl is formed either in the triplet-excited state, or in the ground state (see Sect. 10.5.1), this means, that oxidation of fluorene should not be accompanied by luminescence.

However, it is! Oxychemiluminescence of fluorene belongs to the range 400–600 nm, is suppressed by inhibitors

Table 10.6 Comparison of important qualities of diphenylmethane and fluorene

| | Diphenylmethane | Fluorene (in nonpolar solvents) |
|---|-----------------|--|
| Structural formula of the hydrocarbon | | |
| Ketone formed at peroxidation of the hydrocarbon | | |
| Available electronically excited states of the ketone | $^3(n, \pi^*)$ | $^1(n, \pi^*)$ $^3(n, \pi^*)$ $^3(\pi, \pi^*)$ |
| Possible type of luminescence | Phosphorescence | Fluorescence |

Data from Vasil'ev (2005), Belyakov et al. (1990b), Andrews et al. (1978), Biczók and Bérces (1988), Kobayashi and Nagakura (1976), Fedorova et al. (2007)

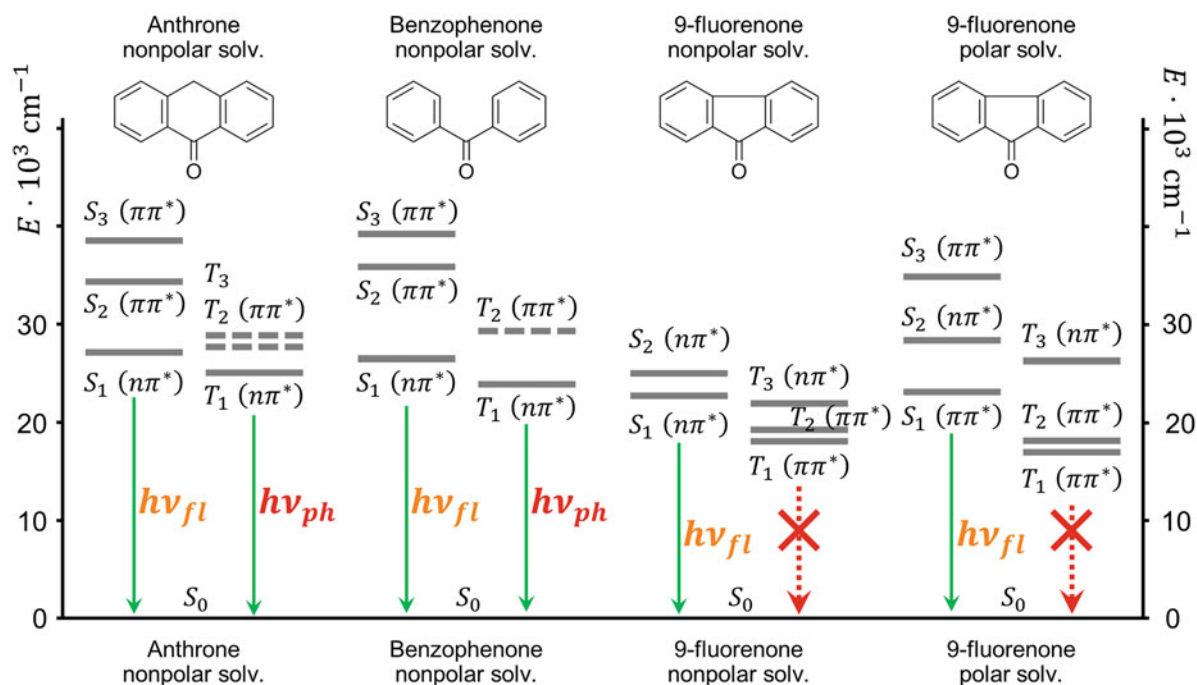


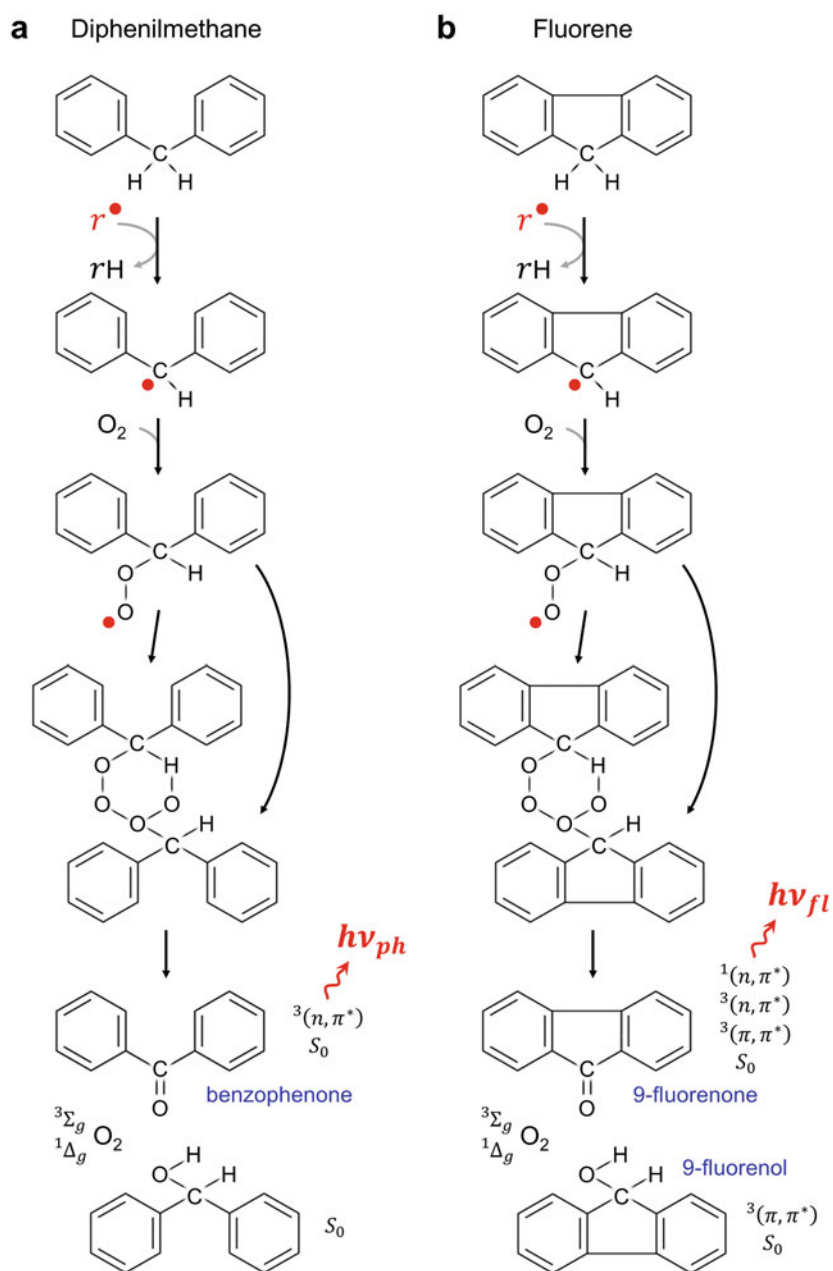
Fig. 10.9 Energy level diagrams for anthrone, benzophenone, and fluorenone in polar and nonpolar solvents. (Adapted from Kobayashi and Nagakura (1976), Copyright 1976, with permission from Elsevier)

of free-radical processes, and enhances with increasing concentrations of oxygen up to a certain plateau level (Belyakov et al. 1990b). All this convincingly shows that the source of fluorene OCL is recombination of peroxy radicals, similar to OCL of other hydrocarbons. However, unlike that, it is not suppressed by triplet quenchers (Belyakov et al. 1990b) – the radiational relaxation occurs from the S_1 state. Thus, OCL of fluorene is direct

fluorescence of fluorenone (Belyakov et al. 1990b), in accordance with Fig. 10.9, and contrary to the Russell mechanism.

The next question is whether the fluorescent (S_1) state of fluorenone is formed directly during the tetroxide cleavage, or through energy migration from the initially excited upper triplets. To test this, the authors selectively populated the upper (n, π^*) triplet state of fluorenone, by energy transfer from chemiexcited benzophenone (generated by peroxidation

Fig. 10.10 Mechanisms of oxidation of diphenylmethane and fluorene. (According to Belyakov et al. (1990b) and Fedorova et al. (2007))



of diphenylmethane – compare their energy structures in Fig. 10.9) (Belyakov et al. 1990b). The direct phosphorescence of benzophenone (observed in the absence of fluorene) was quenched according to Stern–Volmer’s rule (see Sect. 5.3.4), but the fluorescence of fluorenone did not increase. Thus, energy transfer from $^3(n, \pi^*)$ of bezophenone to $^3(\pi, \pi^*)$ of fluorenone occurred, but this did not lead to excitation of its $^1(n, \pi^*)$ fluorescent state. Hence, the fluorescent state of fluorenone generated at OCL of fluorene, can only appear directly in the course of tetroxide cleavage, rather than by intersystem crossing (Belyakov et al. 1990b) (Fig. 10.10).

The second noticeable difference between oxidation of diphenylmethane and fluorene is that in the first case, all

chromophores (carbonyl group and molecular oxygen) are formed in course of the reaction, while in the latter case there is also a chromophore (fluorenyl fragment), which remains unchanged during the oxidation process (Table 10.6). This raised the question of whether the energy released in the reaction is directed (partly) into this permanent chromophore, or is forming a molecular moiety in this chemical process a necessary condition for its chemical excitation? In this context, the possibility of excitation of alcohol (9-fluorenone) was of interest. Indeed, while the alcohol formed at oxidation of diphenylmethane (diphenylcarbinol) cannot be electronically excited for energetic reasons, generation of electronically excited fluorenone (at oxidation of fluorene) becomes energetically feasible due to the fluorenyl group. In addition, the

electronic excitation of alcohols during hydrocarbon oxidation had never been observed before, since in all previously studied cases alcohols did not possess chromophore groups, whose excitation is energetically possible.

As triplet-excited state of 9-fluorenol is of $^3(\pi, \pi^*)$ type, it is incapable of phosphorescence, and the only way of detecting it is via energy transfer to specific highly effective triplet state acceptors, like europium chelate $\text{Eu}(\text{TTA})_3\text{Phen}$ (the method of activated luminescence). This was also done in Belyakov et al. (1990b). Adding europium chelate to the oxidized fluorene increases photon emission from the system, and the intensity of activated luminescence correlates with that of spontaneous OCL at any parameters variation (Belyakov et al. 1990b; Fedorova et al. 2007). This shows that the reaction stage, responsible for the activated luminescence is the same as for spontaneous OCL – it also originates from the tetroxide cleavage.

Next, the $\text{Eu}(\text{TTA})_3\text{Phen}$ -activated luminescence is suppressed by triplet quenchers, which means that energy transfer to $\text{Eu}(\text{TTA})_3\text{Phen}$ occurs from a triplet-excited state of some molecule formed at the tetroxide cleavage. This could be one of the triplet-excited states of fluorenone, which (as shown above) cannot populate the $^1(n, \pi^*)$ fluorescent state of fluorenone according to El-Sayed rule. However, such energy transfer is endothermic by 5 kcal/mol, which makes it unlikely. Contrary to that, triplet-triplet energy transfer to the same acceptor from fluorenol is exothermic, and, therefore, energetically feasible and diffusion-controlled. This was confirmed by selective population of the triplet-excited states of fluorenone (analogous to the above experiments). This had no impact on the activated luminescence, and hence, the triplet-excited state donating energy to europium chelate could belong only to 9-fluorenol (Belyakov et al. 1990b).

Thus, the above studies show that virtually all energetically available excited states can be populated as a result of ROO^\bullet disproportionation. In the specific case of fluorene peroxidation, the chromophore group providing low-lying triplet-excited levels allows excitation of the third component of the tetroxide decomposition, alcohol.

Altogether, the fast and reversible appearance of intermediate Russell-type tetroxide occurs whenever it is physically possible – even at oxidation of hydrocarbons with primarily oxidized tertiary C – H bonds. However, the tetroxide can decompose along variable paths, depending on the available excited states of the products (determined by the oxidizable hydrocarbons structure). While the main paths are generation of triplet-excited carbonyls or singlet oxygen, there can be specific cases with generation of singlet-excited carbonyls, and even triplet-excited alcohols.

10.5.3 Oxychemiluminescence of Unsaturated Hydrocarbons

10.5.3.1 Two Components of OCL

The chemiluminescence yield upon oxidation of alkenes is one to three orders of magnitude lower than that of hydrocarbons with an oxidizable secondary C – H bond, and differs greatly for different compounds (Belyakov et al. 1983). However, the main difference is that in this case, along with the “classical” chemiluminescence generated at peroxy radical recombination according to the Russell mechanism, there is a significant fraction of OCL, that is not quenched by antioxidants (Belyakov et al. 1983). As is known, adding an antioxidant to the reaction mixture immediately suppresses the main “free-radical component” of OCL. Thus, the remaining emission can be called “molecular component” and investigated in the sense of its lifetime, quantum yield, etc.

Molecular component of OCL varies for different alkenes, and changes in course of the reaction: it is rather high in the presence of O_2 , but after oxygen is removed from the system and introduced again, the molecular component apparently decreases. If antioxidants are added into the reacting system, molecular component decreases exponentially with rate constants of the order of 10^{-4} s^{-1} (Belyakov et al. 1983), which suggests that it originates from some products of oxidation, “fueled” by free-radical processes, but stable enough to accumulate during the reaction. Evaluation of the characteristics of the emitter (lifetimes, quantum yields, and radiation constants) leads to values characteristic of the phosphorescence of carbonyl compounds (Belyakov et al. 1983).

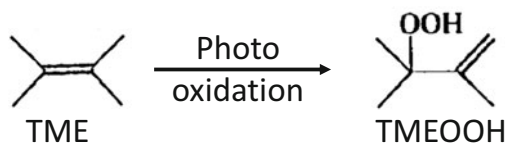
10.5.3.2 Oxidation of Unsaturated Hydroperoxides

In an extensive work (Timmins et al. 1997), the group of E.J.H. Bechara investigated the non-Russell OCL mechanism in more detail. The authors used a simple unsaturated hydroperoxide,

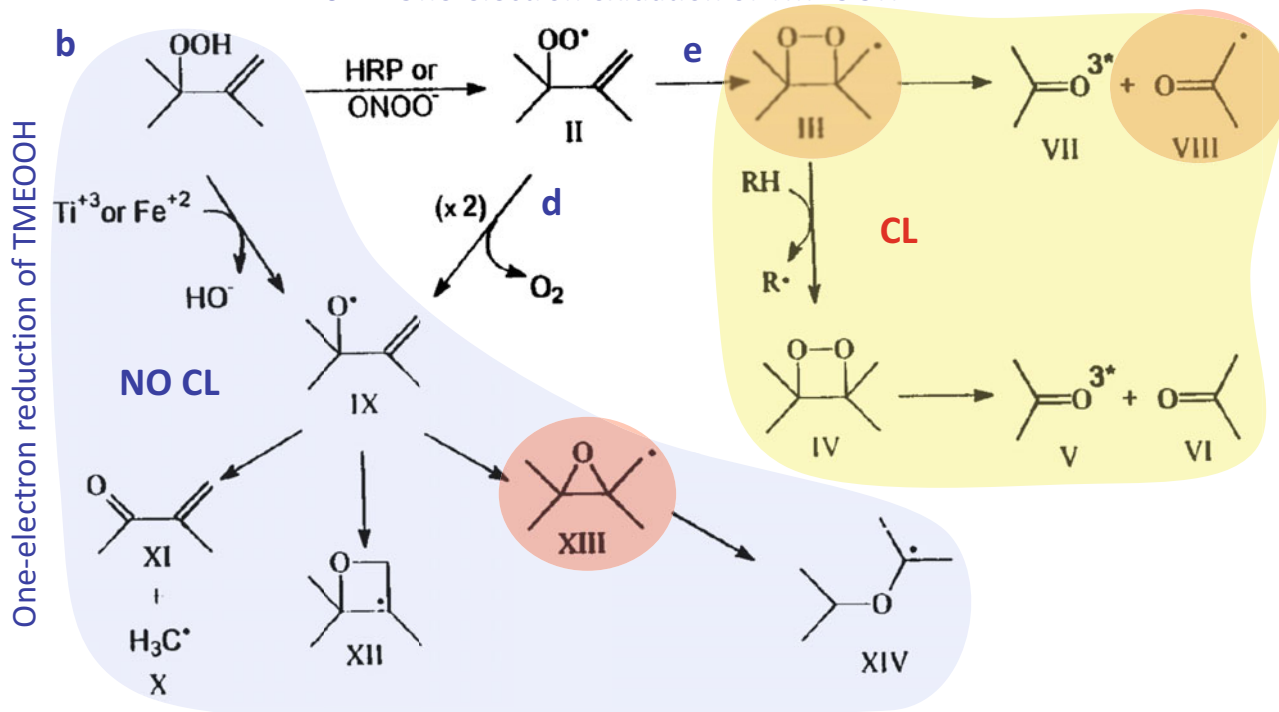
3-hydroperoxy-2,3-dimethyl-1-butene (TMEOOH), obtained at photo-oxidation of tetramethylethylene (TME) (see Fig. 10.11a). The main feature of TMEOOH is that the peroxy radical is centered on the tertiary carbon atom, and thus is incapable of the Russell-type cyclization (analogous to Fig. 10.6c). Consequently, the OCL from this system (if existing) is likely to be of non-Russell type, or at least have a detectable non-Russell component.

First, TMEOOH was subjected to one-electron *reduction* by Fe^{2+} or Ti^{3+} , generating an alkoxy radical TMEO^\bullet , followed by appearance of three types of radicals: CH_3^\bullet , RCH_2^\bullet , and $\text{R}_3\text{C}^\bullet$ (see Fig. 10.11c, species X, XII, XIII), detected by ESR spectra with spin trapping. This gave a general scheme of the possible reactions of TMEO^\bullet (see Fig. 10.11b).

a Generation of TMEOOH from tetramethylethylen



c One-electron oxidation of TMEOOH

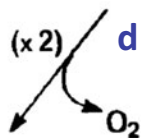
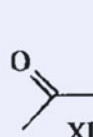


b

One-electron reduction of TMEOOH

Ti⁺³ or Fe⁺²

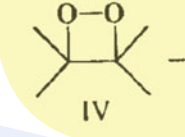
NO CL



e



CL



XIV

Fig. 10.11 Generation (a) and reactions of one-electron reduction (b) and one-electron oxidation (c) of the model unsaturated hydroperoxide, 3-hydroperoxy-2,3-dimethyl-1-butene (TMEOOH). (a) Generation of TMEOOH; (b) One-electron reduction of TMEOOH; (c) One-electron oxidation of TMEOOH; (d) Recombination of peroxy radicals TMEOO[•] with formation of peroxy radicals TMEOO[•]; (e) Cyclization of peroxy radicals TMEOO[•] with dioxetane formation. Species, used for spin-

adduct-based differentiation of paths: e (cyclization of the peroxy radical) and d (recombination of peroxy radicals), are marked with red. The recombination path is not accompanied by chemiluminescence (marked with blue), while the oxidation path is, of which the dioxetane formation is definitely accompanied by CL (marked with yellow). (Adapted from Timmins et al. (1997). Copyright 1997, with permission from American Chemical Society)

Next, TMEOOH was subjected to one-electron *oxidation* with the help of horseradish peroxidase (HRP), generating the TMEOO[•] radical (Fig. 10.11c). The radical products of this reaction, detected by ESR spectra with spin trapping, appeared mostly identical to those from the above one-electron reduction, suggesting the Russell-like path of recombination:



(see Fig. 10.11d). This recombination of peroxy radicals, similar to the classical Russell's path, is however different from it because of the lack of hydrogen atom to be subtracted from the reacting carbon (analogous to Fig. 10.6c). Thus, similarly to that for saturated hydrocarbons with oxidizable

tertiary C – H bonds, it is expected to have low yield of CL (which is an important prerequisite for the data below).

Besides this path, if TMEOOH was oxidized at a low-rate (with HRP added gradually, and at a low concentration), an additional radical adduct was detected, identified as another radical of RCH₂[•] type. Importantly, it never appeared during TMEOOH reduction, but only at oxidation. Thus, it was a product of TMEOO[•] further reactions, of which cyclization into a dioxetane is the most probable path (see Fig. 10.11e, species III). The same results were obtained when oxidizing TMEOOH with ONOO⁻.

Importantly, dominance of one of the two paths of TMEOO[•] reactions: (1) recombination, or (2) cyclization into dioxetanes, depended on the rate of the main oxidation reaction (proportional to HRP concentration). This was estimated by the ratio between the spin adducts formed at

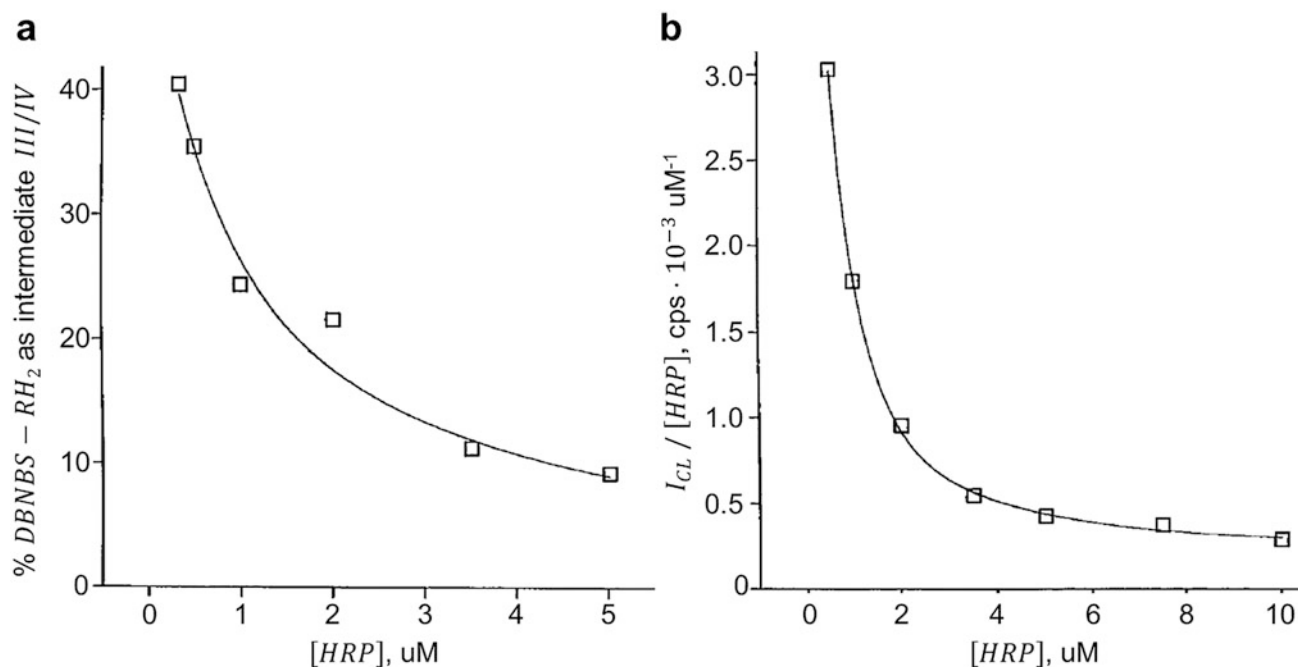


Fig. 10.12 Ratio of cyclization vs. disproportionation paths (Fig. 10.11e, d) and chemiluminescence intensity as functions of HRP concentration (determining the reaction rate). (a) Ratio of spin adducts $\frac{\text{III and/or VIII}}{\text{XIII}}$ (see Fig. 10.11) (i.e., the proportion of TMEOO[•] radicals undergoing cyclization) vs. HRP concentration. (b) CL intensity,

divided by HRP concentration (i.e., the proportion of TMEOO[•] radicals participating in CL) vs. HRP concentration. (Reprinted from Timmins et al. (1997). Copyright 1997, with permission from American Chemical Society)

these two paths (Fig. 10.11, species III and VIII for cyclization vs. species XIII for recombination).

At low oxidation rates (low concentrations of HRP) the cyclization path was quite pronounced (although the specific rate constants were not estimated), while at higher concentrations of HRP, recombination became more and more dominant (see Fig. 10.12a). This is quite understandable, as increase in the radical concentration leads to a quadratic increase in the probability of their encounter.

Similar data were obtained when oxidizing TMEOOH with ONOO⁻.

10.5.3.3 OCL in Oxidation of Unsaturated Hydroperoxides

The above reactions of TMEOOH oxidation were also accompanied by chemiluminescence (CL), which was identified as phosphorescence: it was suppressed by triplet quenchers, enhanced by triplet carbonyl acceptors, and not reacted to quenchers and enhancers of singlet-excited states. The excited state lifetime was estimated as 4 μs, which undoubtedly showed its triplet nature.

Importantly, CL was not observed at TMEOOH reduction, that is, it was not associated with any species from the blue region of Fig. 10.11. Moreover, using higher HRP concentrations (i.e., higher rates of TMEOO[•] generation)

led to a disproportionately small increase in CL intensity. The ratio of CL intensity to the HRP concentration, estimating the proportion of TMEOO[•] radicals involved in CL reactions, gave a curve surprisingly similar to the proportion of TMEOO[•] radicals undergoing cyclization (compare Fig. 10.12a, b). The same results were obtained if HRP was replaced with hematin or cytochrome c.

Thus, the chemiluminescent species was a triplet-excited molecule, generated within the TMEOOH cyclization path (Fig. 10.11e).

The authors also recorded the CL spectrum, and showed that it had a definite maximum around 450 nm, which is typical for triplet-excited carbonyls. All this, together with the above data of excited state lifetime, is in full accordance with the triplet-excited state of acetone, probably generated in course of the above reactions (see Fig. 10.11e, species V and VII).

Importantly, the product analysis using thin layer chromatography and gas chromatography, showed formation of acetone, which is only expected to be produced from the dioxetane intermediate (Fig. 10.11e, species III). Moreover, the yield of acetone was 18% at 1 μM of HRP, and dropped down to 6% at 10 μM of HRP, which fully confirms the above conclusions based on ESR and CL.

Altogether, due to the specific structure of the investigated species, precluding the classical Russell's mechanism of

OCL, the model system in Timmins et al. (1997) appeared especially effective in demonstrating the dioxetane path of OCL. Thus, it was convincingly shown that during the peroxidation of unsaturated hydrocarbon hydroxides, the dioxetane-mediated chemiluminescence pathway should be considered along with the Russell-type disproportionation of peroxy radicals.

10.6 Summary

Altogether, the studies of chemiluminescence accompanying hydrocarbon oxidation brought a detailed explanation of the main empirical regularities typical of CL processes in chemical and biochemical systems in general: low luminescence yield, the need for oxygen, and the proximity of spectra during oxidation of quite different compounds.

The role of oxygen consists in transforming the R[•] radicals, which recombine forming nonluminescent dimers RR, into ROO[•] radicals, which recombine forming luminescent ketones, or cyclize into excited dioxetanes, also capable of radiative relaxation.

Similar to Stauff's data on simpler substances (see Chap. 9), the OCL spectra here are very close. However, while Stauff explained it by formation of the same compounds (simple ROS) as a side effect in all reactions, here the generated excited carbonyls are different and depend on the hydrocarbons oxidized. Yet, for them, the luminescence spectra are mostly determined by the carbonyl group itself and little depend on the structure of the rest of the molecule, which explains their similarity for different substances.

At the same time, part of the luminescence is apparently due to the formation of singlet oxygen, and supposedly excited oxygen dimoles at peroxy radicals disproportionation, as in simple aqueous Stauff's systems.

References

- Adam W, Baader WJ (1985) Effects of Methylation on the Thermal Stability and Chemiluminescence Properties of 1,2-Dioxetanes. *Journal of the American Chemical Society* 107 (2):410–416. <https://doi.org/10.1021/ja00288a022>
- Adam W, Kazakov DV, Kazakov VP (2005) Singlet-oxygen chemiluminescence in peroxide reactions. *Chemical reviews* 105 (9): 3371–3387. <https://doi.org/10.1021/cr0300035>
- Adamic K, Howard JA, Ingold KU (1969) Absolute rate constants for hydrocarbon autoxidation. XVI. Reactions of peroxy radicals at low temperatures. *Can J Chem* 47 (20):3803
- Allabutayev KA, Vasil'ev RF, Vichutinskiy AA, Rusina IF (1965) Chemiluminescence mechanism of oxidative reactions in solutions (In Russian). In: *Bioluminescenciya. Trudy MOIP [Bioluminescence. MOIP Reports]*, vol 21. Nauka, Moscow, pp 8–*
- Andrews LJ, Deroulede A, Linschitz H (1978) Photophysical processes in fluorenone. *J Phys Chem-U.S.* 82 (21):2304–2309. <https://doi.org/10.1021/j100510a011>
- Arnold SJ, Ogryzlo EA, Witzke H (1964) Some New Emission Bands of Molecular Oxygen. *The Journal of chemical physics* 40 (6): 1769–1770. <https://doi.org/10.1063/1.1725394>
- Bäckström HLJ, Sandros K (1960) Transfer of Triplet State Energy in Fluid Solutions. I. Sensitized Phosphorescence and Its Application to the Determination of Triplet State Lifetimes. *Acta Chemica Scandinavica* 14:48–62
- Belyakov VA (1970) Ph.D. thesis. ICP USSR Acad. Sci.,
- Belyakov VA, Vasil'ev RF, Fedorova GF (1978a). *Dokl AN SSSR* 239: 344
- Belyakov VA, Vasil'ev RF, Fedorova GF (1978b). *Bull Acad Sci USSR Phys Ser* 42:138
- Belyakov VA, Vasil'ev RF, Fedorova GF (1978c). *High Energy Chem* 12:208
- Belyakov VA, Vasil'ev RF, Fedorova GF (1983) Chemiluminescence in the oxidation of unsaturated organic compounds in solution. *B Acad Sci Ussr Ch+ 32* (12):2429–2437. <https://doi.org/10.1007/BF00954469>
- Belyakov VA, Vasil'ev RF, Fedorova GF (1990a) *Sov J Chem Phys* 6: 1213
- Belyakov VA, Vasil'ev RF, Trofimov AV (1990b) Energy transfer from chemo-excited chromophore substituents spatially separated from the reaction center of the molecule (in Russian). *Bull Acad Sci USSR Phys Ser* 54:93
- Belyakov VA, Vasil'ev RF, Fedorova GF (2004) Kinetics of oxy-chemiluminescence and its use in the analysis of antioxidants. *Kinet Catal+* 45 (3):329–336. <https://doi.org/10.1023/B:KICA.0000032165.13080.c6>
- Belyakov VA, Vasil'ev RF (1970) Chemiluminescence in hydrocarbon oxidation in solution. A quantitative study of the excitation and emission steps. *Photochem Photobiol* 11 (3):179–192. <https://doi.org/10.1111/j.1751-1097.1970.tb05986.x>
- Bennett JE, Brown DM, Mile B (1969) The equilibrium between tertiary alkylperoxy-radicals and tetroxide molecules. *Journal of the Chemical Society D: Chemical Communications* (10):504–505. <https://doi.org/10.1039/C29690000504>
- Bennett JE, Summers R (1973) Electron spin resonance spectra of secondary alkylperoxy radicals. *Journal of the Chemical Society, Faraday Transactions 2: Molecular and Chemical Physics* 69:1043–1049. <https://doi.org/10.1039/F29736901043>
- Biczók L, Bérces T (1988) Temperature dependence of the rates of photophysical processes of fluorenone. *J Phys Chem-U.S.* 92 (13): 3842–3845. <https://doi.org/10.1021/j100324a033>
- Cadenas E, Sies H, Nastainczyk W, Ullrich V (1983) Singlet oxygen formation detected by low-level chemiluminescence during enzymatic reduction of prostaglandin G2 to H2. *Hoppe Seylers Z Physiol Chem* 364 (5):519–528. <https://doi.org/10.1515/bchm2.1983.364.1.519>
- Chou P-T, Wei G-T, Lin C-H, Wei C-Y, Chang C-H (1996) Direct Spectroscopic Evidence of Photosensitized O2 765 nm ($1\Sigma+g \rightarrow 3\Sigma-g$) and O2 Dimol 634 and 703 nm ($(1\Delta g)2 \rightarrow (3\Sigma-g)2$) Vibronic Emission in Solution. *Journal of the American Chemical Society* 118 (12):3031–3032. <https://doi.org/10.1021/ja952352p>
- Emanuel NM, Denisov ET, Maizus ZK (1967). *Liquid Phase Oxidation of Hydrocarbons*
- Emanuel NM, Denisov YT, Mayzus ZK (1965) Tsepnyje reaktsii okisleniya uglevodorodov v zhidkoj faze (In Russian) [Chain reactions of hydrocarbons in liquid phase]. Nauka, Moscow
- Fedorova GF, Trofimov AV, Vasil'ev RF, Veprintsev TL (2007) Peroxy-radical-mediated chemiluminescence: mechanistic diversity and fundamentals for antioxidant assay. *Arkhivoc* 8:163–215
- Furukawa K, Gray EW, Ogryzlo EA (1970) Singlet oxygen from discharge-flow systems. *Annals of the New York Academy of*

- Sciences 171 (1):175–187. <https://doi.org/10.1111/j.1749-6632.1970.tb39322.x>
- Hammond EG, White PJ (2011) A Brief History of Lipid Oxidation. *Journal of the American Oil Chemists' Society* 88 (7):891–897. <https://doi.org/10.1007/s11746-011-1761-8>
- Howard JA, Ingold KU (1968) Self-reaction of sec-butylperoxy radicals. Confirmation of the Russell mechanism. *Journal of the American Chemical Society* 90 (4):1056–1058. <https://doi.org/10.1021/ja01006a037>
- Kanofsky JR (1984) Singlet oxygen production by chloroperoxidase-hydrogen peroxide-halide systems. *Journal of Biological Chemistry* 259 (9):5596–5600. [https://doi.org/10.1016/s0021-9258\(18\)91055-0](https://doi.org/10.1016/s0021-9258(18)91055-0)
- Kanofsky JR (1986) Singlet Oxygen Production from the Reactions of Alkylperoxy Radicals. Evidence from 1268-nm Chemiluminescence. *Journal of Organic Chemistry* 51 (17):3386–3388. <https://doi.org/10.1021/jo00367a032>
- Kasha M, Khan AU (1970) The Physics, Chemistry, and Biology, of Singlet Molecular Oxygen. 171 (1):5–23. <https://doi.org/10.1111/j.1749-6632.1970.tb39294.x>
- Kellogg RE (1969) Mechanism of Chemiluminescence from Peroxy Radicals. *Journal of the American Chemical Society* 91:201 September 24, 1969 91 (20):5433–5436. <https://doi.org/10.1021/ja01048a005>
- Khan AU, Kasha M (1966) Physical Theory of Chemiluminescence in Systems Evolving Molecular Oxygen. *Journal of the American Chemical Society* 91:201 September 24, 1969 88 (7):1574–1576
- Kobayashi T, Nagakura S (1976) Picosecond time-resolved spectroscopy and the intersystem crossing rates of anthrone and fluorenone. *Chem Phys Lett* 43 (3):429–434. [https://doi.org/10.1016/0009-2614\(76\)80593-3](https://doi.org/10.1016/0009-2614(76)80593-3)
- Koga S, Nakano M, Uehara K (1991) Mechanism for the generation of superoxide anion and singlet oxygen during heme compound-catalyzed linoleic acid hydroperoxide decomposition. *Archives of biochemistry and biophysics* 289 (2):223–229. [https://doi.org/10.1016/0003-9861\(91\)90465-u](https://doi.org/10.1016/0003-9861(91)90465-u)
- Krasnovsky AA, Jr. (1990) Singlet molecular oxygen and primary mechanisms of photodynamic action of optical radiation (in Russian). In: *Modern problems of laser physics*, vol 3. All Union Institute of Science and Technology Information, Reviews on Science and Technology, Moscow, pp. 63–135
- Krasnovsky AAJ (1981) Quantum yield of photosensitized luminescence and radiative lifetime of singlet ($^1\Delta_g$) molecular oxygen in solutions. *Chem Phys Lett* 81 (3):443–445. [https://doi.org/10.1016/0009-2614\(81\)85647-3](https://doi.org/10.1016/0009-2614(81)85647-3)
- Krasnovsky AAJ (2007) Singlet oxygen and primary mechanisms of photodynamic therapy and photodynamic diseases. In: *Uzdensky AB (ed) Photodynamic therapy at the cellular level*. pp 17–62
- Krasnovsky Jr AA, Neverov KV (1990) Photoinduced dimol luminescence of singlet molecular oxygen in solutions of photosensitizers. *Chem Phys Lett* 167 (6):591–596. [https://doi.org/10.1016/0009-2614\(90\)85475-R](https://doi.org/10.1016/0009-2614(90)85475-R)
- Krasnovsky Jr AAN, K.V. (2010) On the mechanism of photosensitized luminescence of singlet oxygen dimols in air-saturated pigment solutions. *Biophysics* 55 (3):349–352. <https://doi.org/10.1134/s0006350910030012>
- Mendenhall GD, Sheng XC (1991) Yields of Excited Carbonyl Species from Alkoxy and from Alkylperoxy Radical Dismutations. *Journal of the American Chemical Society* 113 (23):8976–8977. <https://doi.org/10.1021/ja00023a073>
- Miyamoto S, Martinez GR, Medeiros MHG, Di Mascio P (2003) Singlet molecular oxygen generated from lipid hydroperoxides by the Russell Mechanism: Studies using ^{18}O -labeled linoleic acid hydroperoxide and monomol light emission measurements. *Journal of the American Chemical Society* 125 (20):6172–6179. <https://doi.org/10.1021/ja029115o>
- Nakano M, Takayama K, Shimizu Y, Tsuji Y, Inaba H, Migita T (1976) Spectroscopic Evidence for the Generation of Singlet Oxygen in Self-Reaction of sec-Peroxy Radicals. *Journal of the American Chemical Society* 98 (7):1974–1975. <https://doi.org/10.1021/ja00423a060>
- Niu Q, Mendenhall GD (1990) Structural Effects on the Yields of Singlet Molecular Oxygen ($^1\Delta_gO_2$) from Alkylperoxy Radical Recombination. *Journal of the American Chemical Society* 112 (4):1656–1657. <https://doi.org/10.1021/ja00160a070>
- Niu QJ, Mendenhall GD (1992) Yields of Singlet Molecular Oxygen from Peroxy Radical Termination. *Journal of the American Chemical Society* 114 (1):165–172. <https://doi.org/10.1021/ja00027a024>
- Russell GA (1957) Deuterium-isotope Effects in the Autoxidation of Alkyl Hydrocarbons. Mechanism of the Interaction of Peroxy Radicals. *Journal of the American Chemical Society* 79 (14):3871–3877. <https://doi.org/10.1021/ja01571a068>
- Sander U, Stauff J (1971). *Anales Asoc Quim Argent* 59:149
- Seliger HH (1960) A photoelectric method for the measurement of spectra of light sources of rapidly varying intensities. *Anal Biochem* 1:60–65. [https://doi.org/10.1016/0003-2697\(60\)90019-1](https://doi.org/10.1016/0003-2697(60)90019-1)
- Seliger HH (1964) Chemiluminescence of H_2O_2 -NaOCl Solutions. *The Journal of chemical physics* 40 (10):3133–3134. <https://doi.org/10.1063/1.1724975>
- Shliapintokh VY, Vassil'ev RF, Karpukhina ON, Postnikov LM, Kibalko LA (1960) La chimiluminescence de processus chimiques lents. *J Chim Phys* 57 (11–12):1113
- Stauff J (1964) Lumineszenz and Energieübertragung angeregter Zustände von Proteinen. *Ber Bunsenges phys chem* 68 (8–9):773
- Stauff J, Fuhr H (1971) Chemiluminescence from the Action of Singlet Oxygen ($^1\Delta_g$) on Chlorophyll a and some other Luminescing Substances. *Z Naturforsch Sect B J Chem Sci* 26 (3):260–263. <https://doi.org/10.1515/znb-1971-0317>
- Stauff J, Reske G (1964) Lumineszenz von Hefe. *Naturwissenschaften* 51 (2):39
- Stauff J, Rümmler G (1962) Chemilumineszenz von Oxydationsreaktionen. II. Die Spektren der Reaktionen Harnstoff + Hypohalogenit, Formaldehyd + H_2O_2 und $NaOH + H_2SO_4 + O_2$. —, 34, N 1–4, 67, 1962. *Z Physikal Chemie (BRD)* 34 (1–4):67
- Stauff J, Schmidkunz H (1962a) Chemilumineszenz von Oxydationsreaktionen. I. Qualitative Beobachtungen und Analyse der Reaktion Harnstoff + Na-Hypochlorit. *Z Physikal Chemie (BRD)* 33 (5/6):273
- Stauff J, Schmidkunz H (1962b) Chemilumineszenz von Oxydationsreaktionen. III. Mitt. Sauerstoff-van der waals-Assoziat als möglicher Träger der Chemilumineszenz. *Z Physikal Chemie (BRD)* 35 (4–6):295
- Stauff J, Schmidkunz H, Hartmann G (1963) Chemiluminescence in oxidation reactions. *Nature* 198:281
- Stauff J, Wolf H (1964) Konformationsabhängige Phosphoreszenz und Chemilumineszenz einiger Proteine. *Z Naturforsch* 19b (2):87
- Timmins GS, Dos Santos RE, Whitwood AC, Catalani LH, Di Mascio P, Gilbert BC, Bechara EJH (1997) Lipid peroxidation-dependent chemiluminescence from the cyclization of alkylperoxy radicals to dioxetane radical intermediates. *Chemical research in toxicology* 10 (10):1090–1096. <https://doi.org/10.1021/tx970075p>
- Vasil'ev RF (1965a) Chemiluminescence in solutions I. Methods of identification of excited states (In Russian). *Opt Spektrosk+* 18 (2):236–244
- Vasil'ev RF (1965b) Chemiluminescence in solutions II. Identification of the excited state in reactions of liquid-phase oxidation (In Russian). *Opt Spektrosk+* 18 (3):415
- Vasil'ev RF (1965c) Photoelectric apparatus for investigating weak luminescence (In Russian). In: *Bioluminescentsiya. Trudy MOIP [Bioluminescence. MOIP Reports]*, vol 21. Nauka, Moscow, p 170

- Vasil'ev RF (1965d) Some problems in the mechanism of chemiluminescence. (In Russian). In: Bioluminescentsiya. Trudy MOIP [Bioluminescence. MOIP Reports], vol 21. Nauka, Moscow, pp 198–*
- Vasil'ev RF (2005). In: Burlakova EB, Shilov AE, Varfolomeev SD, Zaikov GE (eds) Chemical and Biological Kinetics. New Horizons (in Russian), vol 1. Chemistry, Moscow, pp 453–493. **English Translation:** Brill, VSP: Leiden, The Netherlands, 2005
- Vasil'ev RF, Fedorova GF (2004) Asymmetric PhCH(CH₃)CH₂OOOC(CH₃)₂ as an intermediate in chain-termination processes and chemiluminescence excitation in the oxidation of cumene. *Kinet Catal* 45 (5):655–661. <https://doi.org/10.1023/B:KICA.0000044976.23380.cd>
- Vasil'ev RF, Karpukhin ON, Shlyapintokh VY (1961) An apparatus for measuring weak light fluxes (In Russian). *Zhurnal Fizicheskoy Khimii* [Journal of Physical Chemistry] 35 (2):461
- Vasil'ev RF, Vichutinskii AA (1962a) The enhancement of chemiluminescence by the addition of luminescent substances (In Russian). *Zh Fiz Khim* 36 (8):1799–1800
- Vasil'ev RF (1963) Luminescence Accompanying Chemical Reactions in Solutions (In Russian) [Lyuminescentsiya pri khimicheskikh reaktsiyakh v rastvorakh]: Doctoral Dissertation. Moscow
- Vasil'ev RF (1970) Chemiluminescence excitation mechanisms. *Russian Chemical Reviews* 39 (6):529–544. <https://doi.org/10.1070/RC1970v039n06ABEH002004>
- Vasil'ev RF, Rusina IF (1964a) The chemiluminescence mechanism for the oxidation of organic matter in solution (In Russian). *Dokl AN SSSR* 156 (6):1402–1405
- Vasil'ev RF, Rusina IF (1964b) The chemiluminescence of molecular oxygen during the oxidation of organic matter (In Russian). *Izvestiya AN SSSR, Seriya Khim* 9:1728
- Vasil'ev RF, Vichutinskii AA (1962b) The chemiluminescent method of measuring the relations of elementary constants in liquid hydrocarbon oxidation reactions (In Russian). *Doklady AN SSSR* 145 (6):1301
- Vasil'ev RF, Vichutinskii AA, Cherkasov AS (1963) Chemiluminescence activated by anthracene derivatives. *Doklady AN SSSR* 149 (1):124
- Vasil'ev RF (1967). In: Progress in Reaction Kinetics., vol 4. Pergamon, New York, p 305
- Vasil'ev RF, Karpuchin ON, Shlapintoch VJ (1959) Chemiluminescence accompanying reactions of thermal decomposition (In Russian). *Doklady AN SSSR* 125 (1):106
- Vasil'ev RF, Vichutinskii AA (1962) Chemiluminescence and oxidation. *Nature* 194 (4835):1276–1277
- Vasil'ev RF, Vichutinskii AA (1962) The nature of the relationship between chemiluminescence and oxidation by molecular oxygen (In Russian). *Doklady AN SSSR* 142 (3):615
- Vladimirov YA, Potapenko AJ (1989) Physico-chemical principles of photobiological processes Vyschaja shkola, (in Russian), Moscow
- Vladimirov YA (1965) Photochemistry and luminescence of proteins [Fotokhimiya i lyuminescentsiya belkov] (In Russian). Nauka, Moscow
- Vladimirov YA, Archakov AI (1972) Lipid peroxidation in biological membranes [Perekisnoe okislenie lipidov v biologicheskikh membranakh] (In Russian) (Perekisnoe okislenie lipidov v biologicheskikh membranakh). Nauka, Moscow
- Vladimirov YA, Roshchupkin DI, Fesenko EE (1970a) Mechanism of ultraviolet radiation effects on proteins (In Russian). *Biofizika* 15 (2):254–264
- Vladimirov YA, Roshchupkin DI, Fesenko EE (1970b) Photochemical reactions in amino acid residues and inactivation of enzymes during U.V.-irradiation. A review. *Photochem Photobiol* 11 (4):227–246

Ilya Volodyaev and Yury A. Vladimirov

11.1 Lipids and Fatty Acids

According to the available definitions, lipids are “loosely defined substances of biological origin that are soluble in nonpolar solvents” (IUPAC 1997), the main classes of which are glycerophospholipids (Fig. 11.1a), sphingolipids (Fig. 11.1b) and sterols (Fig. 11.1c). In the cell, they are an essential component of biological membranes, and also perform energetic, signaling functions, and participate in the formation of lipoproteins and other molecular complexes (Alberts et al. 2015).

The most common structural features of lipids are nonpolar hydrocarbon regions, that can be linear, formed by different fatty acids (with a different number of double bonds), or contain cyclic sections (like cholesterol) – see Fig. 11.2.

Importantly, the hydrocarbon tails composition determines the molecule shape, stability or reactivity, and, accordingly, the membrane physical properties: fluidity, local curvature, packing density of lipids, stabilization of lipoprotein domains, etc. (Fig. 11.3). All this plays a crucial role in cell functioning and dysfunction.

Besides, as is well known now, lipid composition is specific to different species, tissues, organelles and even layers of the same membrane (Fig. 11.4). Its violation (largely due to lipid peroxidation) is associated with severe diseases, including Alzheimer’s, Parkinson’s, mental retardation, etc. (See Harayama and Riezman 2018 for a review).

As will be shown below, it is the hydrocarbon residues, primarily the unsaturated fragments, that make lipids prone to peroxidation. The presence of double bonds, as well as the hydrocarbon chain branching, changes the nearest C – H bonds enthalpy, which makes certain atoms much more susceptible to oxidation. Thus, membranes with a high percentage of unsaturated lipids are more “liquid” and also more prone to oxidation. This can lead to serious disturbances in the membrane structure, up to their electrical

breakdowns and cell death, and directly affect the course of pathological conditions (Harayama and Riezman 2018; Vladimirov et al. 2017). All this gives additional importance to the processes of peroxidation as applied to biological systems.

11.2 Fatty Acid and Lipid Peroxidation: General Scheme

11.2.1 Peroxidation of Lipids and Fatty Acids: Evidence and Research Specificity

The simplest indication of peroxidation in fatty acid solutions and lipid systems is oxygen consumption without CO₂ release. In brain homogenates, this phenomenon was first discovered by Panimon and coworkers back in 1941 (cited in Suslova 1971). Also, characteristic biomarkers of peroxidation were found in tissue homogenates, mitochondrial and microsomal suspensions in the presence of oxygen: lipid hydroperoxides, TBA-active substances (see Sect. 8.5.2.1) (Kohn and Liversedge 1944), diene conjugates (Hashimoto and Recknagel 1968; Recknagel and Ghoshal 1966), etc. All these facts confidently point to peroxidation and precisely in the tails of unsaturated fatty acids (see below).

Theoretically, the mechanism of peroxidation should be directly extrapolated from hydrocarbons (see Chap. 10); however, its confident verification required careful studies, which also revealed some specific features of the oxidation of such “more biological” molecules. In addition, the study of peroxidation processes in cells and tissues has proved to be fraught with a number of additional difficulties.

First, the concentration of free radicals in the cell is much lower than when they are artificially generated in model systems, and therefore, their already quite difficult direct detection (see Sect. 8.5.1) becomes simply impossible. Fortunately, their appearance is associated with chemiluminescence during recombination, from which we can indirectly

I. Volodyaev (✉) · Y. A. Vladimirov
Moscow State University, Moscow, Russia

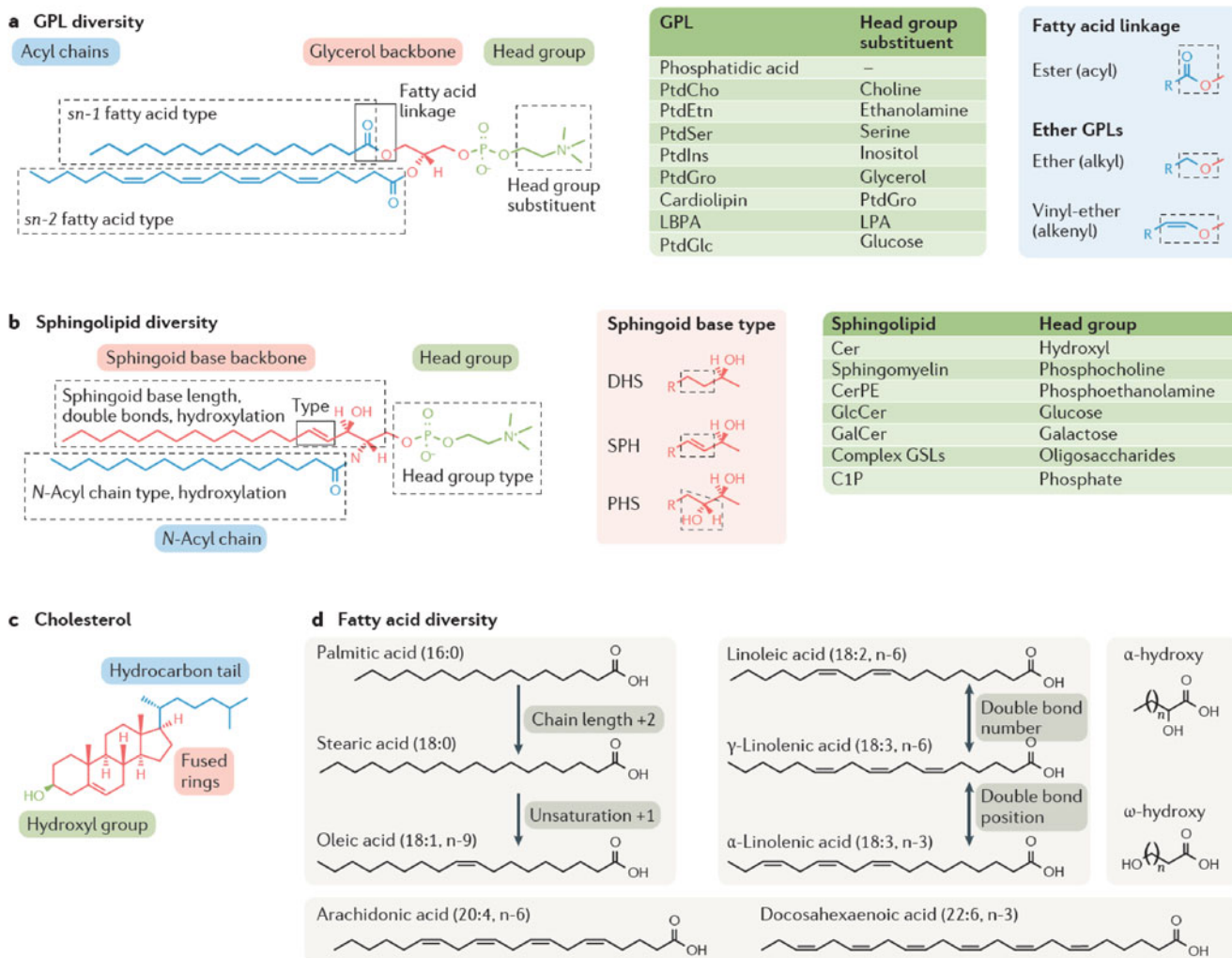


Fig. 11.1 Chemical diversity of membrane lipids in mammals: (a) glycerophospholipids; (b) sphingolipids; (c) cholesterol; (d) fatty acid structure and nomenclature. (Adapted from Harayama and Riezman (2018), Copyright 2018, with permission from Springer Nature)

judge the course of the whole chain process (see Sects. 6.4 and 8.5.3 and below). In addition, in some cases, natural chemiluminescence can be multiplied by using activators (see Sect. 6.4.3).

Second, membrane phospholipids are embedded in a complexly organized and chemically compound lipoprotein complex, and one cannot say in advance how this fact will affect the reactions course and mechanism. This makes it necessary to conduct research on various biological systems: mitochondrial and microsomal suspensions, cell membranes – and constantly compare these data with those obtained on simpler systems: phospholipid suspensions or fatty acid solutions.

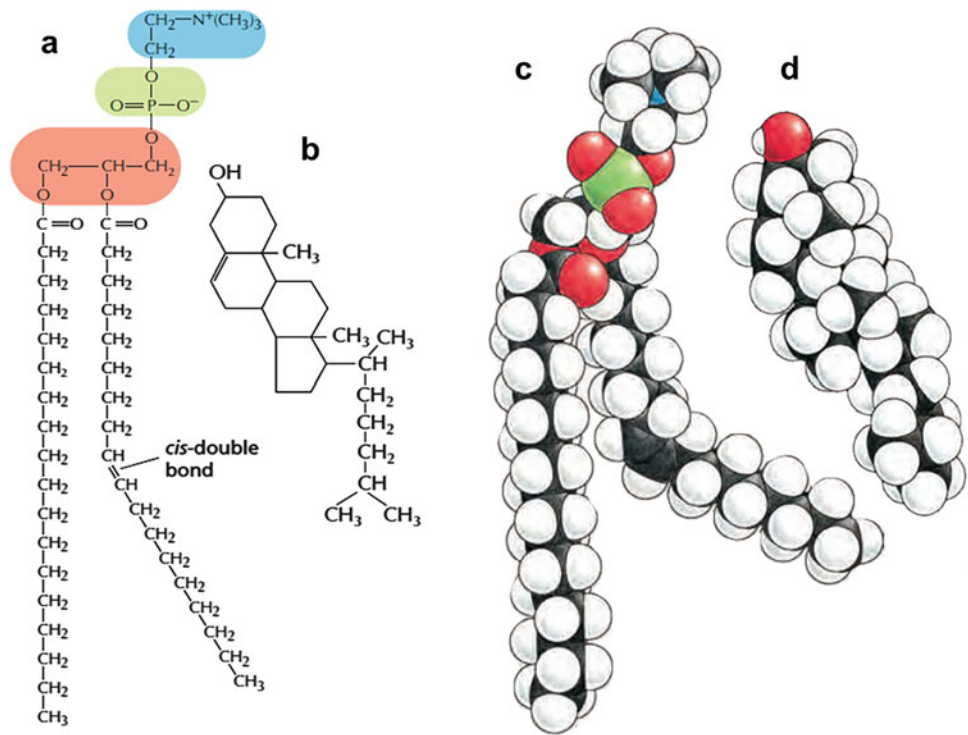
Third, peroxidation is a chain process and the appearance or disappearance of each of its free-radical participants leads to a change in the whole process, affecting concentration of

both radical and nonradical reaction products. Therefore, the study of chain reactions mechanism requires kinetic analysis, facilitated by the use of chemiluminescent methods, which allow continuous recording even for fast processes (see Chap. 6 and Sect. 8.5.3).

Thus, the experimental study of lipid peroxidation in biological membranes is a difficult, but in principle solvable issue. At the same time, the accompanying UPE, in addition to its own scientific significance, acquires even greater importance in the practical plane – as the most sensitive method for assessing the state and destruction of membranes, as well as a powerful tool for diagnosing medical pathology.

Further, instead of the above notation RH, R[•], ROO[•], etc. for arbitrary molecules and their radicals, the more specific designations LH, L[•], LOO[•], etc. will be used, indicating the participation of lipid (or, sometimes, fatty acid) molecules.

Fig. 11.2 Formula and model of phosphatidylcholine (a, c) and cholesterol (b, d). (Adapted from Alberts et al. (2015). Copyright 2015, with permission)

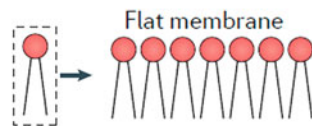


a Membrane curvature

Lipid species and spontaneous membrane curvature

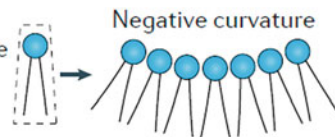
Cylindrical

- Phosphatidylcholine
- Phosphatidylserine



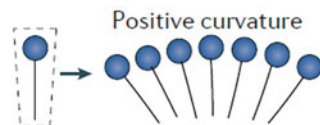
Conical

- Phosphatidylethanolamine
- Phosphatidic acid



Inverted-conical

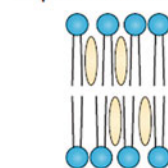
- Lyso-GPLs
- Phosphoinositides



b Fluidity and/or phase behaviour

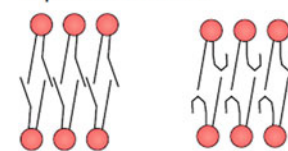
Model membranes

Liquid-ordered



- Saturated lipids
- Cholesterol

Liquid-disordered



Mono-unsaturated lipids

Poly-unsaturated lipids

Cells

Lateral heterogeneity
 • Initiated by proteins and stabilized by lipids
 • Driven by lipid immiscibility and phase separation?

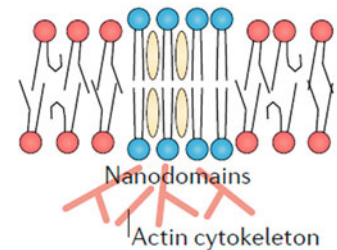


Fig. 11.3 Physical properties of membranes, determined by lipid composition: (a) local curvature; (b) phase behaviour. (Adapted from Harayama and Riezman (2018), Copyright 2018, with permission from Springer Nature)

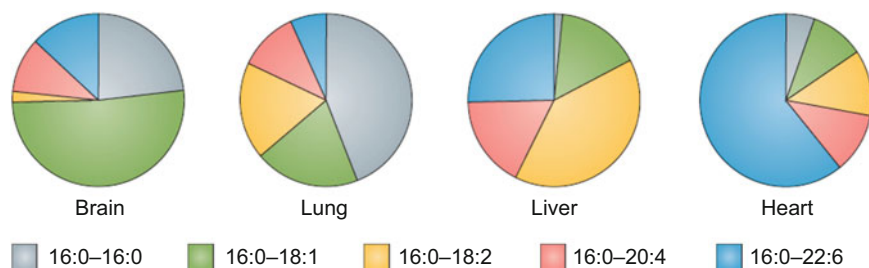


Fig. 11.4 Membrane lipid composition in cells of various organs in mice. The fatty acid structure is designated according to the XX:Y nomenclature, where XX is the number of carbons in the chain; Y is the number of double bonds (the level of chain desaturation). (Adapted from Harayama and Riezman (2018), Copyright 2018, with permission from Springer Nature)

Table 11.1 Oxidation rates for different fatty acid esters

| Compound | Structure | Maximal oxidation rate, conv. units |
|---------------------|-----------|-------------------------------------|
| Ethyl stearate | | $\sim 10^{-3}$ |
| Ethyl oleate | | 0.04 |
| Ethyl linoleate | | 1.63 |
| Ethyl linolenate | | 3.90 |
| Methyl arachidonate | | 7.78 |

Data from Holman and Elmer (1947)

11.2.2 Oxidizable Functionalities

In the oxidation of fatty acids, as well as fats of animal or vegetable origin, it is predominantly unsaturated fatty acids that undergo oxidation, and the faster, the higher the degree of unsaturation. Direct evidence of this was obtained back in 1947 by R.T. Holman and O.C. Elmer, who studied oxygen consumption by solutions of different fatty acids and their esters (Holman and Elmer 1947). Methyl oleate (with 1 double bond) was oxidized 11 times faster than ethyl stearate

(with no double bonds), and appearance of each new double bond accelerated the oxidation process several times more (Holman and Elmer 1947) (Table 11.1). A similar picture was observed during peroxidation of fatty acids, and phospholipids (Recknagel and Ghoshal 1966).

These results are easy to explain by experimental (Berkowitz et al. 1994) or theoretical (Pratt et al. 2003) estimation of the dissociation energies of the C – H bonds in different positions in hydrocarbon and fatty acid molecules (see Table 11.2).

Table 11.2 Bond dissociation energies for different hydrocarbons

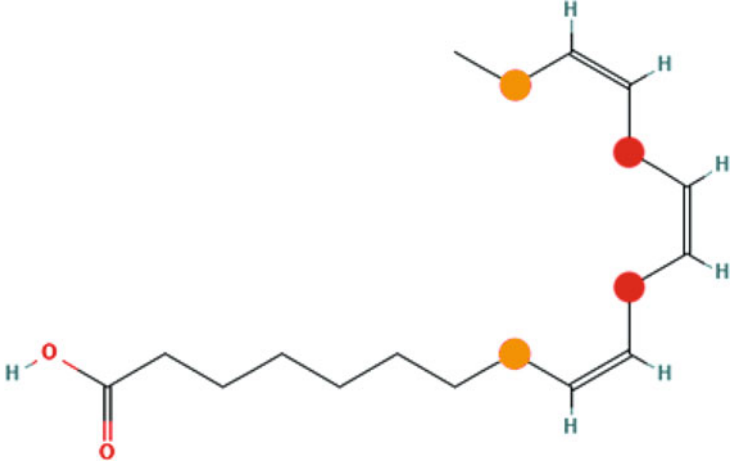
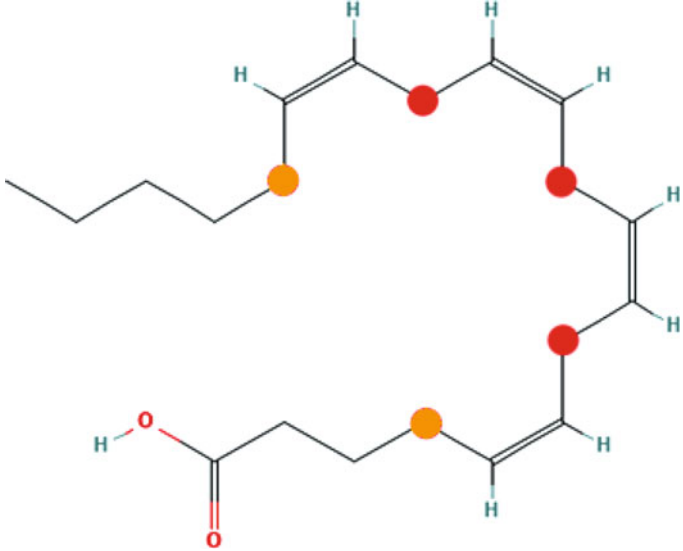
| Compound | Bond dissociation energy, kcal/mol | Source |
|---|------------------------------------|--|
| CH_3-H | 105 | Berkowitz et al. (1994) |
| CH_3-CH_2-H | 101 | Berkowitz et al. (1994) |
| $\begin{array}{c} CH_3-CH-CH_3 \\ \\ H \end{array}$ | 98.5 | Berkowitz et al. (1994) |
| $\begin{array}{c} CH_2=CH-CH_2 \\ \\ H \end{array}$ | 87-88.5 | Berkowitz et al. (1994), Pratt et al. (2003) |
| $\begin{array}{c} CH_2=CH-CH=CH-CH_2 \\ \\ H \end{array}$ | 81-83.5 | Pratt et al. (2003) |
| $\begin{array}{c} CH_2=CH-CH-CH=CH_2 \\ \\ H \end{array}$ | 72-77 | Pratt et al. (2003) |

Table 11.3 Structural formulas of unsaturated fatty acids. The most reactive carbon atoms are marked in: Red – the primary oxidizable functionalities (bis-allylic positions). Orange – the secondary oxidizable functionalities (mono-allylic positions)

| Fatty acid | Structure (the C atoms with the oxidizable C – H bond are marked in red and orange) |
|---------------|---|
| Oleic acid | |
| Linoleic acid | |

(continued)

Table 11.3 (continued)

| Fatty acid | Structure (the C atoms with the oxidizable C – H bond are marked in red and orange) |
|------------------|---|
| Linolenic acid |  |
| Arachidonic acid |  |

Thus, the main oxidizable functionality of unsaturated fatty acids are C – H bonds at α -carbon atoms, and preferably in bis-allylic positions. Oleic, linoleic, linolenic and arachidonic acids contain, respectively, 2, 3, 4 and 5 such α -carbon atoms (0, 1, 2 and 3 in bis-allylic positions – see Table 11.3), which explains the increase in their reactivity (with respect to peroxidation) with the increase in the number of double bonds (Holman and Elmer 1947).

11.2.3 Oxidation Scheme

As is known now, the mechanism of oxidation of unsaturated fatty acids can be imagined as follows (Farmer 1946; Farmer et al. 1942, 1943; Farmer and Sutton 1943, 1946):

- A radical attacks mainly an α -carbon, detaching the hydrogen atom from it and leaving an unpaired electron on the hydrocarbon (Fig. 11.5a, b).
- Since this electron does not differ from the π -electrons of the nearest double bond, the unpaired valence is delocalized, forming a system of three indistinguishable carbon atoms (Fig. 11.5c).
- The formed hydrocarbon radical can equally attach oxygen at either of the two extreme carbon atoms, forming two isomers (Fig. 11.5d, e).
- Importantly, while in one of them the double bond remains in its original position (Fig. 11.5 e2), in the other isomer it shifts by one bond toward the oxidized functionality (Fig. 11.5 e1). This can be used to unequivocally detect the reaction products (see below).

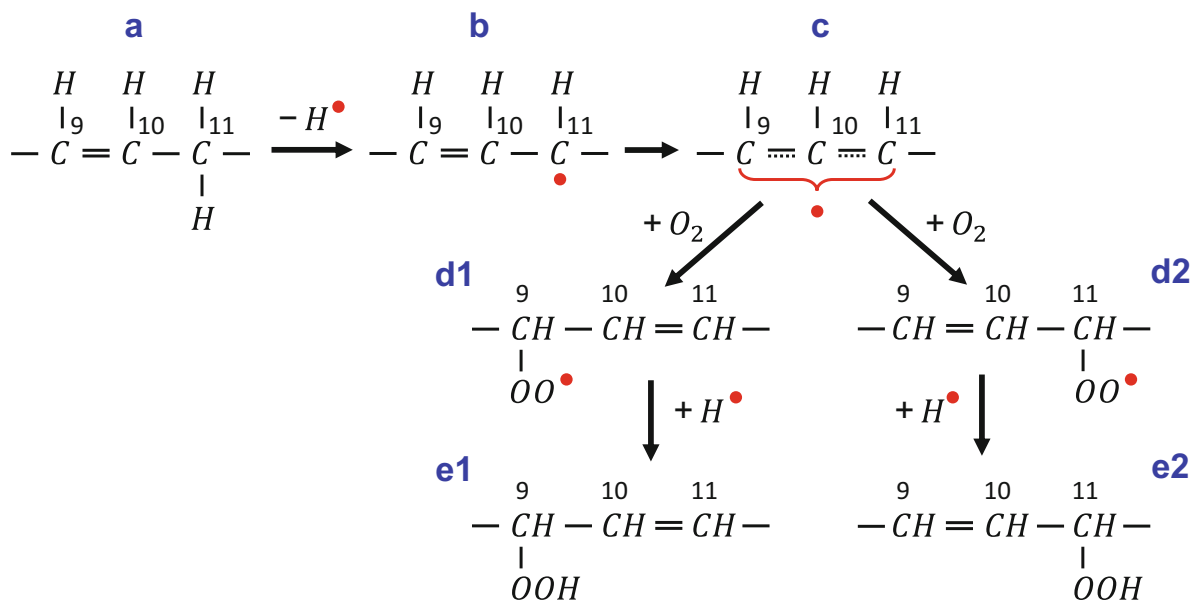


Fig. 11.5 Mechanism of oxidation of unsaturated fatty acids (using oleic acid as an example). $-H^\bullet$ – detachment of a hydrogen atom due to the attack of the molecule by another radical; $+O_2$ – attack of the three-carbon system with an unpaired electron by an oxygen molecule; $+H^\bullet$ –

detachment of a hydrogen atom from another molecule due to its attack by this peroxide radical. The first and last stages “close” the process, making it chain

Naturally, the same process can occur with the participation of each α -carbon in the fatty acid (Privett and Nickell 1959). However, as mentioned above, the bond dissociation enthalpy of the C – H bonds at the α -carbons between the double bonds (in the so-called bis-allylic positions) is ~ 5 – 15 kcal/mol lower than for mono-allylic positions (see Table 11.2) (Porter et al. 1994; Pratt et al. 2003). Thus, the primarily oxidizable functionalities in PUFA are C – H bonds at α -carbons between the double bonds. The radical attack on them leads to a specific 5-carbon delocalized intermediate state (Fig. 11.6c), which can be attacked by oxygen on any of the two extreme carbons (Fig. 11.6d). This results in two possible isomers of hydroxides with two conjugated double bonds (Fig. 11.6f), which can be detected by a specific maximum in the absorption spectrum at 233 nm (see Sect. 8.5.2.1). This spectral maximum is a reliable marker for PUFA peroxidation; moreover, as the resulting diene conjugation appears, in essence, during the free-radical stage of the process, it clearly indicates its free-radical mechanism.

The appearance of diene conjugates was shown at PUFA oxidation (Frankel 1962), as well as under UV irradiation of phospholipid suspensions (Potapenko et al. 1972) (see Fig. 8.6, Sect. 8.5.2.1). However, a quantitative verification of Fig. 11.6 also requires determining stoichiometric ratio of the amount of diene conjugates to the amount of hydroperoxides formed (or oxygen absorbed). For example, during the oxidation of linolenic acid, there are four α -carbon atoms, that can be subjected to the radical attack: two in mono-allylic positions (8 and 17), and two in bis-allylic

positions (11 and 14), of which only the latter form diene conjugates if attacked. Taking into consideration relatively higher reactivity of the bis-allylic positions, the ratio of the generated hydroperoxides (or consumed O_2) to the formed diene conjugates should be slightly less than two, which is well-confirmed experimentally (Frankel 1962; Frankel et al. 1961).

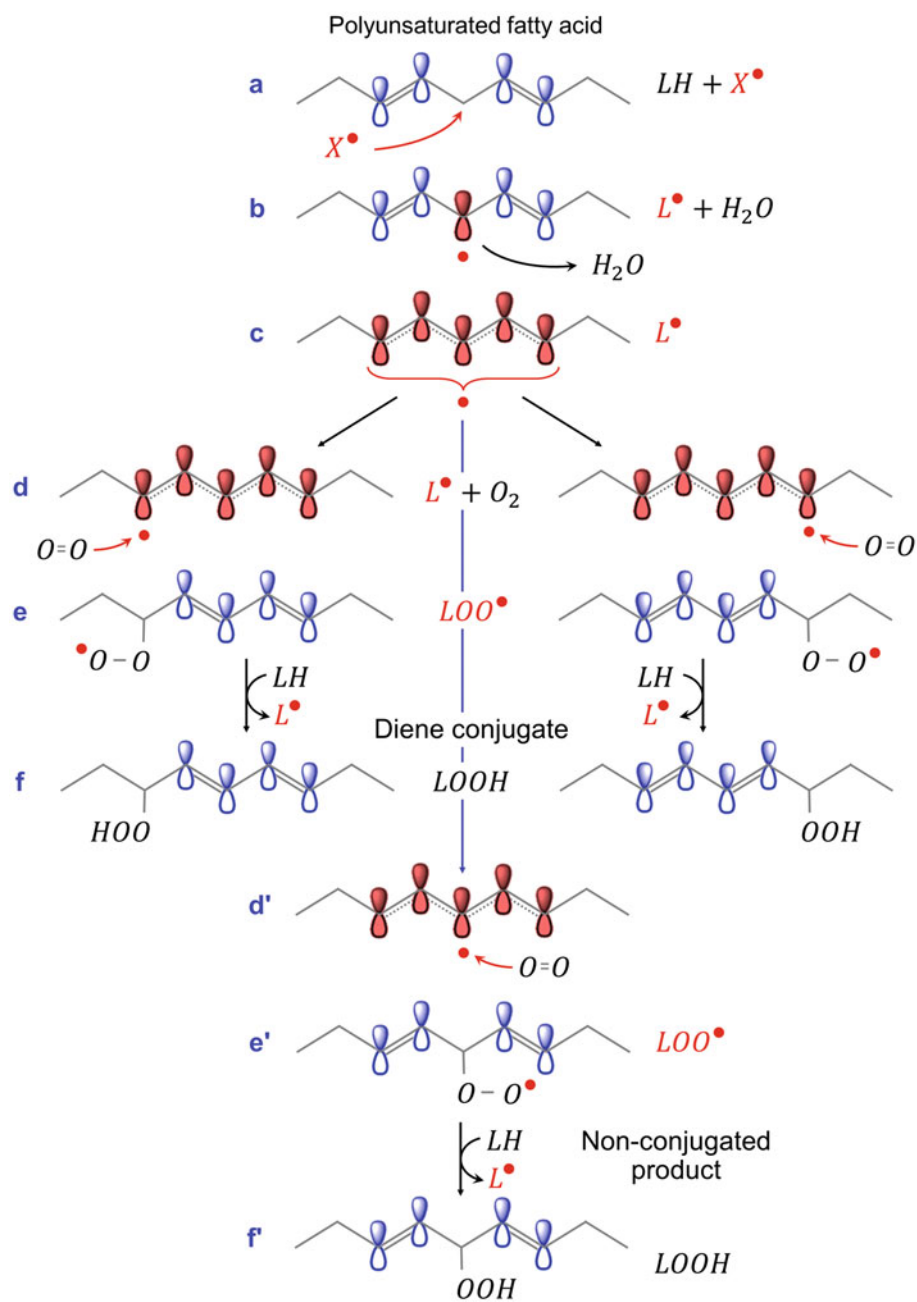
The third possible product – bis-allylic hydroperoxide (Fig. 11.6f') has been identified in the last two decades (Brash 2000; Tallman et al. 2009). However, it is generated only at exceptionally good hydrogen atom donors (like α -tocopherol) present in the system in high concentrations (above 0.1 M). Thus, it is a minor product under most conditions (see more in Yin et al. 2011).

11.3 Evidence for Free-Radical Chain Peroxidation

Figures 11.5 and 11.6 (and the data behind them) clearly show that oxidation proceeds according to a free-radical chain mechanism. However, the consistent proof of this statement requires several more conditions to be met:

1. “Abnormally high” yield of certain processes (e.g., formation of several hydroperoxide molecules and consumption of several oxygen molecules per a single absorbed quantum of initiating radiation, or per a single initiating molecule).

Fig. 11.6 Appearance of diene conjugates at peroxidation of polyunsaturated fatty acids (PUFA). (a) The PUFA bis-allylic α -carbon is attacked by a hydroxyl radical; (b) An alkyl radical of PUFA; (c) The unpaired electron is delocalized among 5 carbon atoms with free π -orbitals; (d) A system of 5 carbon atoms containing a delocalized π electron is attacked by an oxygen molecule; (e) The lipoperoxyl radical, formed during the previous action, contains two conjugated double bonds (diene conjugate); (f) Attack of the newly-formed lipoperoxyl radical on another molecule of fatty acids; formation of the peroxide molecule; (d'–f') Reactions possible in the presence of excellent H donors in high concentration: attack on the centrally located carbon and formation of nonconjugated products



2. Formation of specific reaction products (hydroperoxides, diene conjugates, TBA-active compounds, etc. – already shown above).
3. Direct detection of free radicals, at least when the oxidation is artificially enhanced.
4. Activation of peroxidation by increasing the concentration of free radicals (by exposure to ionizing or ultraviolet radiation, or by adding initiators of free-radical processes).
5. Suppression of peroxidation by introducing inhibitors of free-radical reactions (antioxidants).

11.3.1 Quantum Yield

Similarly to hydrocarbons (see Sect. 10.3), the most simple and visual evidence of free-radical nature of fatty acid oxidation is its quantum yield. If the process is initiated by UV and taking place in the presence of oxygen, its total (“gross”) quantum yield can be calculated as Eqs. 11.1 or 11.2 (which may give slightly different estimates because of possible side reactions, but generally coincide).

$$\varphi_{\text{total}} = \frac{\text{Number of molecules of absorbed oxygen}}{\text{number of absorbed quanta}} \quad (11.1)$$

$$\begin{aligned} \varphi_{\text{total}} \\ = \frac{\text{Number of molecules of generated hydroperoxide}}{\text{number of absorbed quanta}} \end{aligned} \quad (11.2)$$

Such quantum yields, calculated for different fatty acids and their esters, appeared abnormally high: e.g., $\varphi_{\text{total}} = 90$ for ethyl linoleate solution irradiated with $\lambda = 253.7$ nm, or $\varphi_{\text{total}} = 21$ for the same system irradiated with $\lambda = 365$ nm (Bateman and Gee 1948).

As the quantum yield of the primary photochemical process (φ_0) is definitely less than unity, the obtained total quantum yields mean that each absorbed quantum initiates a chain of reactions, consuming oxygen and producing hydroperoxides in each of its links with a certain probability. Then, obviously, the above “gross” quantum yield φ_{total} can be expressed as follows:

$$\varphi_{\text{total}} = \varphi_0 \cdot l \cdot \varphi_{\text{chain}} \quad (11.3)$$

where $\varphi_0 \leq 1$ is the quantum yield of the primary photochemical process, l is the chain length, $\varphi_{\text{chain}} \leq 1$ is the probability of the corresponding process (oxygen consumption or hydroperoxide generation) within each individual link of the chain process. Whence:

$$l = \frac{\varphi_{\text{total}}}{\varphi_0 \cdot \varphi_{\text{chain}}} \geq \varphi_{\text{total}} \quad (11.4)$$

Thus, for the above two examples, the chain length of the peroxidation process is $l \geq 90$ and $l \geq 21$, correspondingly (probably even $l \gg 90$ and $l \gg 21$).

For lipid peroxidation in microsomes, φ_{total} is less, but still more than unity: 3–4 moles of consumed O_2 per 1 mole of added NADPH (Hochstein and Ernster 1963; Hochstein et al. 1964), and from 3–4 to 10–12 moles of consumed O_2 per 1 mole of added Fe^{2+} , depending on its concentration (Vladimirov and Litvin 1963, 1964).

11.3.2 Oxidation Products

Besides the primary oxidation products – hydroperoxides, peroxidation of fatty acids gives other, minor products, generated later in the peroxidation process. These are alcohols, ketones, aldehydes and dialdehydes (including the above mentioned TBA-active products – see Sect. 8.5.2), epoxides, polymers, etc. (Badings 1960; Ellis 1950; Ellis

Table 11.4 The proportion of hydroperoxides in the total amount of methyl oleate peroxidation products (in the absence of catalysts at the temperature of 100 °C) depending on the oxidation duration

| Oxidation time, hours | Proportion of hydroperoxides, % |
|-----------------------|---------------------------------|
| 4 | 97.7 |
| 6 | 83.7 |
| 12 | 63.2 |

et al. 1961; Evans 1961; Fenell and Skellon 1954; Karnojitzky and Vial 1966; Knight et al. 1951; King 1956; Perkins 1960). A number of these substances can be used as biomarkers for peroxidation. In biological systems, formation of these compounds can be very important for changing or disrupting membrane structure and cell functioning in general.

Importantly, as mentioned above, hydroperoxides are formed first within the peroxidation process, while other compounds appear later on, after repeated radical attacks, or within other processes. This is indeed observed in the oxidation of fats and fatty acids and can be used as indirect evidence of free-radical nature of the process. For example, during oxidation of methyl oleate in the absence of catalysts at 100 °C, in the first hours of oxidation, hydroperoxides make up almost 98% of all oxidation products, while later this proportion decreases significantly (Swern et al. 1953) (Table 11.4).

This is also observed from the change in the absorption spectra of linoleic acid solution under the action of transition metals (O’Brien 1969). The initially appearing maximum at 235 nm (characteristic of diene conjugates) weakens with time, indicating their gradual decomposition, and a new maximum appears at 280 nm, showing formation of carbonyl compounds (Evans 1961).

11.3.3 Direct Detection of Free Radicals

As is discussed in Sect. 8.5.1, direct detection of free radicals in biological systems is extremely difficult because of their high reactivity and hence very low stationary concentration. However, it is possible to artificially increase it, by using spin trapping (Janzen and Blackburn 1968; Saprin and Piette 1977; Haywood 2013). This approach allowed to detect free radicals in practically all systems with active peroxidation: irradiated fatty acid solutions in the presence of oxygen (Zhuravlev 1962, 1965a, b; Tarusov and Zhuravlev 1965), fatty acid solutions with added pro-oxidants (Vladimirov 1965; Vladimirov et al. 1970a; Vladimirov et al. 1970b), suspensions of microsomes and mitochondria (Zhuravlev 1963; Polivoda and Sekamova 1962), tissue homogenates (Tarusov et al. 1961b, 1962), etc. Artificial enhancement of

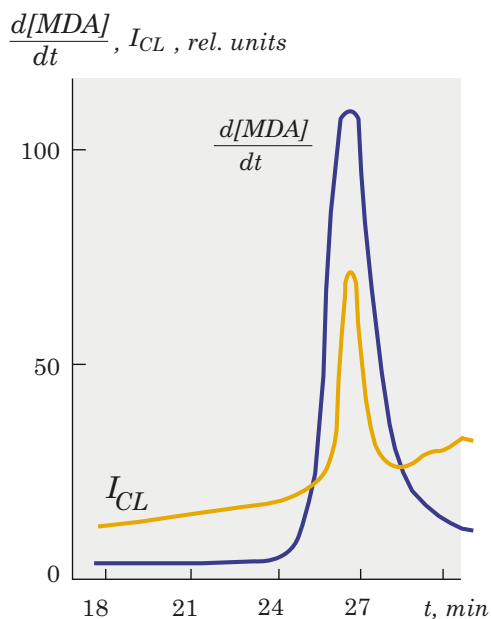
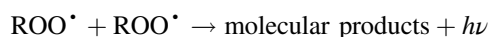


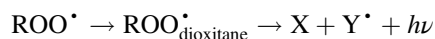
Fig. 11.7 Parallelism between the peroxidation rate ($d[\text{MDA}]/dt$) and the luminescence intensity (I_{CL}) at the “slow flash” stage of chemiluminescence (see Sect. 11.6) of the mitochondrial suspension in the presence of FeSO_4 . 1 – MDA formation rate; 2 – luminescence intensity. (Adapted from Vladimirov et al. (1969a), with permission from the authors)

peroxidation processes also increased the free-radical concentration (Tarusov 1954, 1957; Emanuel and L’askovkaya 1961).

Another, still more important approach to free-radical detection is chemiluminescence (CL). As discussed in Sects. 9.2 and 10.5, in chemiluminescent processes, photons are generated specifically within processes involving free radicals. For hydrocarbon oxidation, this is primarily recombination of peroxy radicals:



or (for unsaturated hydrocarbons) peroxy radical cyclization:



Thus, recording CL appears very close to direct detection of free radicals, and though its intensity is not directly proportional to $[\text{ROO}^\bullet]$ (because both mono- and bimolecular processes are involved in CL generation), it definitely reflects the general amount of peroxy radicals formed in the system.

CL at oxidation of fatty acids and lipids was first shown by the groups of Ahnstrom and Natarajan (Ahnström and Natarajan 1960), B.N. Tarusov (Tarusov et al. 1961a, b, 1962; Zhuravlev 1962, 1965a, b; Tarusov and Zhuravlev 1965) and Yu.A. Vladimirov (Vladimirov and L’vova 1965; Vladimirov et al. 1969b, 1971), and in a huge amount of

works since then. There is a good parallelism between the CL intensity and the rate of peroxidation in both fatty acid solutions and suspensions of microsomes and mitochondria (Fig. 11.7).

Thus, the lipid and fatty acid peroxidation is accompanied by generation of free radicals, and the rate of the process has a good parallelism with the radical concentration.

11.3.4 Increase in the Concentration of Free Radicals Stimulates Peroxidation

A further proof of the free-radical mechanism of oxidation is its acceleration when the system is exposed to radical-generating processes: ionizing radiation, UV and various pro-oxidants.

Irradiation of fats and tissues with ionizing radiation stimulates generation of free radicals, detected by graft copolymerization, ESR and chemiluminescence (Tarusov 1954, 1957). It also noticeably accelerates formation of hydroperoxides in fatty acid solutions (Zhuravlev 1960; Kudryashov et al. 1961), various tissue homogenates (Tarusov 1954, 1957), suspensions of subcellular particles and even whole animals (Tarusov 1954, 1957). Thus, free radicals, generated by ionizing radiation, accelerate fatty acid and lipid peroxidation in very different systems, from model solutions to whole animals.

Ultraviolet radiation had a similar effect, causing detectable formation of free radicals, accumulation of peroxides in mitochondrial suspensions (Marzoev et al. 1971, 1973; Roshchupkin et al. 1973) and in the stroma of erythrocytes (Korchagina and Vladimirov 1971).

Other well-known sources of free radicals are hydrogen peroxide (producing free radicals upon spontaneous decay), hydroperoxides of various substances (decomposing spontaneously, or, much faster, in the presence of transition metals, ascorbic acid, cysteine, reduced glutathione, etc. – see Sect. 11.4.1). Adding hydrogen peroxide to homogenates of various tissues enhances their oxychemiluminescence many times (i.e., increases the amount of recombining peroxide radicals) (Vasil’ev et al. 1961); adding peroxides of various substances to fatty acid solutions also increases their peroxidation rate (see, for example, (Emanuel and L’askovkaya 1961)). Incubating homogenates of various tissues with ascorbic acid or Fe^{2+} salts leads to lipid peroxides formation (Bernheim and Bernheim 1948; Bernheim et al. 1947; Wilbur et al. 1949; Ottolenghi 1959); adding Fe^{2+} salts, ascorbic acid, cysteine or reduced glutathione to suspensions of microsomes (Recknagel and Ghoshal 1966) or rat liver mitochondria (Santiago et al. 1968a, b; Forthney and Linn 1964; Hunter et al. 1963) leads to oxidation of unsaturated fatty acids (especially arachidonic and docosahexaenoic) (Recknagel and Ghoshal 1966), destruction of phospholipids

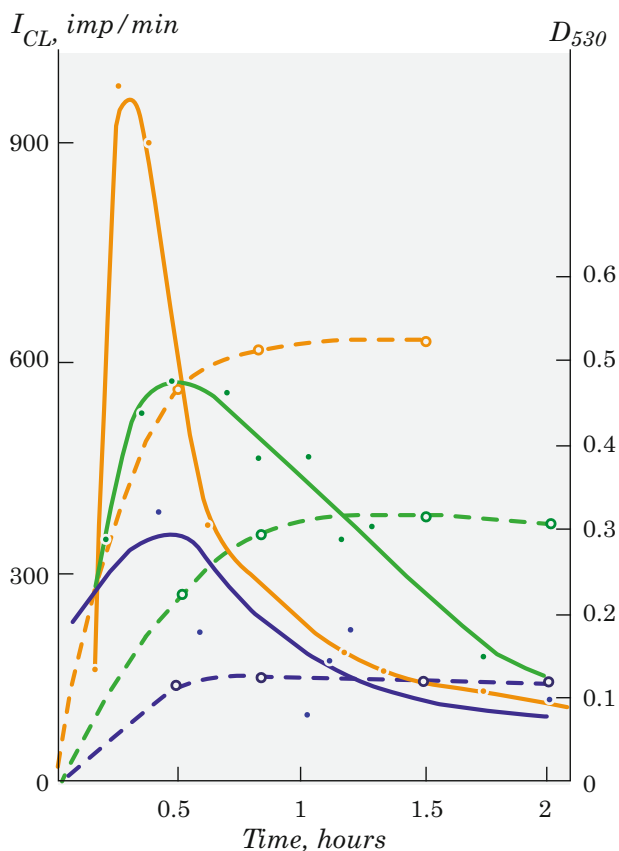


Fig. 11.8 Luminescence (solid lines) and accumulation of TBA-active substances, detected by optical density at 530 nm (dashed lines) in the mitochondria suspension in the presence of various concentrations of ascorbic acid. Blue – 10^{-5} M; green – 10^{-4} M; orange – 10^{-3} M. Incubation medium: 0.002 M K_2HPO_4 ; 0.005 M $MgSO_4$; 0.08 M KCl; 0.02 M ATP; 0.02 M glutamate; 0.02 M succinate. (Adapted from Vladimirov et al. (1966), with permission from the authors)

(especially phosphatidylethanolamine and phosphatidylcholine) (Santiago et al. 1968a, b) and enhancement of the system chemiluminescence (Vladimirov et al. 1966). Addition of ascorbic acid to mitochondrial suspensions also increases accumulation of TBA-active substances (products of radical lipid peroxidation – see Sect. 8.5.2) and chemiluminescence intensity (Fig. 11.8).

As is well-known, besides different external sources of free radicals, hydroperoxides, formed during fatty acid oxidation are also subjected to decomposition, generating free radicals (see Sects. 10.3.5 and 11.4.1). This gives the reaction a self-accelerating, “explosive” character, which has long been noted by many authors and is considered as one of the main arguments in favor of its free radical, chain nature (Emanuel and L’askovkaya 1961; Lundberg 1961). This can also be regulated by adding ions of Fe^{2+} , which catalyze decomposition of hydroperoxides (see Sect. 11.4.1).

So, altogether, an increase in the concentration of free radicals, obtained by practically any means, contributes to

an increase in lipid and separately fatty acid peroxidation, shown by a variety of different indicators.

11.3.5 Antioxidants Inhibit Peroxidation

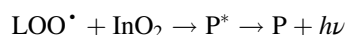
The fifth stage in proving the free-radical nature of the process is its suppression by antioxidants – substances that reduce the concentration of active free radicals.

Fatty acid oxidation can be effectively inhibited by adding various phenols, including ubiquinone and ubiquinol (Mellors and Tappel 1966), estrogenic steroid hormones (Zakharova et al. 1966), α -tocopherol (vitamin E) (Buzas et al. 1970; Mellors and Tappel 1966), etc. Addition of typical antioxidants to tissue homogenates, microsomal or mitochondrial suspensions also inhibits peroxidation. Thus, tocopherol and diphenylphenylenediamine suppress oxygen consumption and accumulation of TBA-active compounds in the microsomal fraction of rat liver (Carpenter et al. 1959; Hochstein and Ernster 1963) and in mitochondria (McKnight et al. 1965). Introducing such compounds as tocopherol, steroid hormones, butyloxytoluene, β -ionol or α -naphthol to tissue homogenates incubated in the presence of ascorbic acid prolongs the induction period in the accumulation of TBA-active compounds (Neyfakh 1963) and suppresses chemiluminescence (Zhuravlev et al. 1965; Tarusov and Zhuravlev 1965). The role of antioxidants, according to A.I. Zhuravlev’s data, could also be played by the antibiotics: tetracycline and penicillin (Zhuravlev 1962).

On the contrary, a decrease in the content of the natural antioxidant α -tocopherol during E-avitaminosis leads to an increase in the formation of lipid peroxides in homogenates (Bieri and Anderson 1960; Corwin 1962; Machlin 1961; Tappel and Zalkin 1959; Tappel 1955). Replacement of vitamin E with other antioxidants in animal food leads to inhibition of peroxidation and weakening of the signs of E-avitaminosis (Machlin 1961).

Thus, a decrease in the concentration of free radicals due to direct reactions of radicals with inhibitors or due to inactivation of pro-oxidants present in the system inhibits lipid peroxidation and accompanying chemiluminescence.

However, a number of publications (Zhuravlev 1965b; Zhuravlev and Tarusov 1962; Zhuravlev et al. 1965; Tarusov and Zhuravlev 1965) reported a short-time flash of luminescence at the very moment of adding antioxidants, such as β -mercaptoethylamine, β -mercaptoethylamine, adrenaline or lecithin. This flash was associated with reactions like:



where In^{\bullet} is the antioxidant radical.

Altogether, the totality of the presented data gives unambiguous evidence of the free-radical nature of fatty acid and lipid peroxidation, in full accordance with the model hydrocarbon systems (see Sect. 10.3).

11.4 The Dual Role of Transition Metals

11.4.1 Pro-Oxidant Role

11.4.1.1 Hydroperoxide Decomposition

As already mentioned in Sect. 10.3.5, transition metals are an effective agent that decomposes peroxides, forming free radicals. The catalytic effect of iron and copper salts on fatty acid peroxidation (in lipids or in free form) has been long noted by many authors (Emanuel and L'askovkaya 1961; Vladimirov et al. 1969a, b, 1971; Korchagina and Vladimirov 1971; Suslova 1971; Suslova et al. 1968; Thiele and Huff 1960). Moreover, their action is caused precisely by decomposition of hydroperoxides, since metal additives are effective only in their presence (Kern and Willersin 1955; Lemon et al. 1951). At the same time, Fe³⁺ salts have no effect (contrary to Fe²⁺) (Thiele and Huff 1960), suggesting the following dominating pro-oxidant reaction:



However, experiments with simultaneous addition of iron and other pro-oxidants (ascorbic acid, cysteine, glutathione, etc.) gave the following important data:

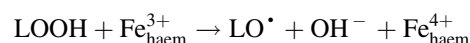
1. In the presence of ascorbate, Fe³⁺ ions also acquire a prooxidant activity equal to that of Fe²⁺ (Thiele and Huff 1960).
2. The pro-oxidant activity of ascorbate, cysteine and glutathione increases many times in the presence of Fe²⁺ (even at as low concentration as 10⁻⁶ M) (Forthney and Linn 1964; Ottolenghi 1959; Thiele and Huff 1960).
3. Fe²⁺ salts (at least in the form of admixtures), are necessary for peroxidation: binding of iron by such compounds as cyanide, EDTA, or o-phenanthroline leads to complete inhibition of peroxidation in all studied membrane systems (Vladimirov 1967; Vladimirov and L'vova 1964, 1965; Vladimirov et al. 1966; L'vova 1967; L'vova and Vladimirov 1966; Forthney and Linn 1964; Hochstein and Ernster 1963; Hochstein et al. 1964; Hunter et al. 1963, 1964a, b; Thiele and Huff 1960). Besides, both enzymatic and nonenzymatic formation of lipid peroxides in microsomes occurs only in the presence of Fe²⁺ (Hochstein et al. 1964).

Thus, the presence of iron salts at least in the form of admixtures (as in L'vova and Vladimirov 1966) not only enhances lipid peroxidation, but is necessary for it. The function of ascorbic acid, cysteine, or glutathione at their simultaneous addition with iron is to regenerate Fe²⁺ ions from the oxidized Fe³⁺ ions (see more discussion in Vladimirov and Archakov 1972). Contrary to that, in mitochondria iron is quickly extracted from the mitochondria themselves in the presence of cysteine (about a quarter of all nonheme iron in mitochondria – within 15 min) (Forthney and Linn 1964), and thus, lipid peroxidation proceeds well without its external addition (Forthney and Linn 1964; Vladimirov and Archakov 1972).

11.4.1.2 Hemin and Nonhemin Iron

Obviously, concentration of free iron ions in biological systems is incomparably lower than in model experiments, and the above data cannot be directly transferred to them. In biosystems, the key pro-oxidant role of transition ions passes to their complexes, among which those with porphyrins are of particular interest. Thus, the catalytic action of hemoglobin at peroxidation of unsaturated fatty acids appeared about 100 times higher than that of ferrous salts (Wills 1965); and peroxidation processes in fats were efficiently accelerated by chlorophyll and especially hemin compounds (Emanuel and L'askovkaya 1961). Importantly, hemoglobin, methemoglobin and hemin had approximately the same effect on peroxidation at equal molar concentrations (Emanuel and L'askovkaya 1961), which suggests that catalytic activity in various heme-containing compounds is manifested by the prosthetic groups.

Formally, the catalytic action of hemin compounds is due to a decrease in the activation energy. Thus, while in linoleate oxidation in the absence of a catalyst it was found to be 15.2 kcal/mol, in the presence of hemin compounds, it decreased to 3.3 kcal/mol (Tappel 1953). Similarly to ions of transition metals, hemin compounds accelerated decomposition of hydroperoxides with the formation of fatty acid radicals (Tappel 1953, 1955):



However, a number of important differences between hemin and nonhemin catalysis were found during their thorough comparison in homogenates of various tissues and fatty acid solutions (Wills 1965, 1966) (Table 11.5).

This allowed the authors to distinguish between heme and nonheme catalysis during peroxidation in various systems. Thus, adding linoleic acid to tissue homogenates resulted in both hemin and nonhemin catalysis of hydroperoxide decomposition (Wills 1966). At pH 7.4, the main role was probably played by hemin catalysis, since the addition of ascorbic acid

Table 11.5 Comparison of hemin and nonhemin peroxidation catalysis

| <i>Nonhemin</i> catalysis (Fe ²⁺) | <i>Hemin</i> catalysis (hemoglobin, cytochromes) |
|--|---|
| Addition of ascorbate, cysteine and glutathione dramatically stimulates peroxidation | Addition of ascorbate, cysteine and glutathione has no effect |
| Well-defined pH optimum at 5.5 (with ascorbate) or pH 4 (with cysteine) | Nondefined pH optimum from 5.5 to 8 |
| 2 × 10 ⁻³ M EDTA fully inhibits peroxidation | 2 × 10 ⁻³ M EDTA has no effect |

Adapted from Wills (1965), Copyright 1965, with permission from Elsevier

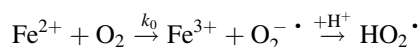
only reduced peroxidation, while EDTA did not completely inhibit the process. At pH 6, the proportion of nonhemin catalysis increased significantly (Wills 1966).

It is also interesting to compare relative catalytic activity of various transition metals and hemin compounds in the peroxidation of unsaturated fatty acids. For an emulsion of linoleic acid, the relative activity of Fe³⁺, Fe²⁺, Cu²⁺, V²⁺, Mn²⁺, Co²⁺ and hemoglobin was expressed, respectively, by the numbers 3; 5.8; 9.0; 13.9; 136, 170 and 10³ (Wills 1965). The ions Mg²⁺, Ni²⁺, Ca²⁺, Zn²⁺, Ag⁺, Cr³⁺, Sn²⁺, Pb²⁺, Ba²⁺, Sr²⁺ were found inactive (Wills 1965). It is characteristic that metals are located in exactly the same row according to their ability to decompose hydroperoxides of organic compounds (Hawkins 1961).

11.4.1.3 Initiating Peroxidation

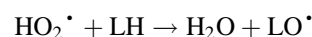
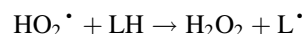
As we have just seen, transition metals and their porphyrin complexes efficiently decompose hydroperoxides, generating free radicals. The new peroxidation chains initiated by them can sooner or later lead to the oxidation of literally all available lipids and fatty acids due to chain branching (which does not happen in biological systems due to plenty of antioxidant substances, including the same transition metals – see below). However, all this does not remove the question of the source of the “very first” hydroperoxide molecule or, which is the same, of the production of primary free radicals.

Initiation of free-radical processes in both model and biological systems has been discussed in Sects. 8.2 and 10.3.1. Under model conditions it is known to happen due to action of various types of radiation or chemical pro-oxidants (Kalmanson 1963; Kayushin et al. 1970; Free radicals in biology 1963; Bray 1969; Ingram 1969; Wyard 1968; Sumarukov 1970), among which transition metals are quite efficient and widely used (see Vladimirov and Archakov 1972). In the presence of oxygen, Fe²⁺ ions are subjected to one-electron oxidation, generating O₂^{-•}, which quickly transforms into HO₂[•] in acidic media (Emanuel and Knorre 1962):

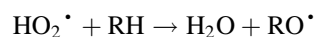


Though, in contrast to HO[•], the superoxyl radical HO₂[•] is not active enough and thus seems not so important for activation of organic compounds (Nilsson 1969a, b), nevertheless, its redox potential ($E_0 = +1500$ mV) is higher than that of, e.g., hydrogen peroxide ($E_0 = +900$ mV) (Sumarukov 1970), making it capable of oxidizing organic molecules, such as:

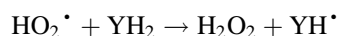
- Unsaturated fatty acids (see Vladimirov and Archakov 1972):



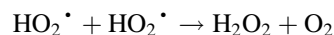
- Aromatic molecules (Yamazaki and Piette 1963):



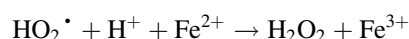
- Other important substances, like dihydroxy fumarate, indolyl acetate or triose reductone (Yamazaki and Piette 1963):



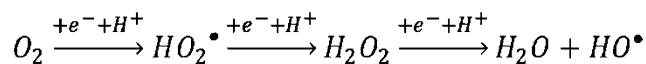
Yet, the yield of the above reactions is rather low, apparently due to the high disproportionation rate of HO₂[•] radicals ($k = 1.5 \times 10^7 \text{ M}^{-1}\text{s}^{-1}$):



as well as their further reduction by Fe²⁺ ions:



At the same time, H₂O₂ produced in some of the above processes is subjected to further reactions, including spontaneous and iron-induced decomposition (Fenton reaction):



Scheme 11.1 One-electron oxygen reduction



and enzymatic reduction (see more in Chap. 14).

Altogether, though this pathway gives a relatively low yield of free radicals in relation to oxidized Fe^{2+} , it leads to formation of all products of the sequential oxygen reduction (Scheme 11.1), each of them initiating lipid peroxidation in this or that way.

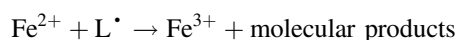
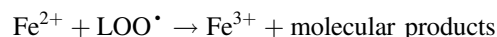
Importantly, the destructive effect of ionizing radiation, leading to numerous pathologies, including radiation sickness, is largely due to lipid peroxidation initiated through the described processes, and not by the direct effect of radiation (Kozlov 1969; Kudryashev 1960; Tarusov 1962).

At the same time, $O_2^-^\bullet$ and HO_2^\bullet radicals are also generated during functioning of many enzymatic systems: electron transfer chains (Free radicals in biology 1963; Bray 1969; Chetverikov et al. 1964; Knowles et al. 1969; Nilsson 1969a, b; Yamazaki and Piette 1963), peroxidases (Yamazaki and Piette 1963), etc. (Brzhevskaya and Nedelina 1969), which will be discussed in Chap. 14.

Altogether, while there are different factors, initiating free-radical processes, transition metals (both in free form, and as porphyrin complexes) play a key role in it, and in the absence of specific pro-oxidant external factors, can be called central pro-oxidants.

11.4.2 Antioxidant Role

However, the two types of pro-oxidant action, described above – chain initiation and chain branching, do not exhaust the role of transition metals in peroxidation processes. As mentioned in Sect. 10.3.4, when a free-radical encounters a transition metal ion (both in the free form, and as a complex), it can be further reduced by it, which turns out to be chain termination:



Such antioxidant role of iron in mitochondrial suspensions can be seen from peroxidation kinetics. Thus, adding Fe^{2+} to mitochondria suspensions leads to formation of

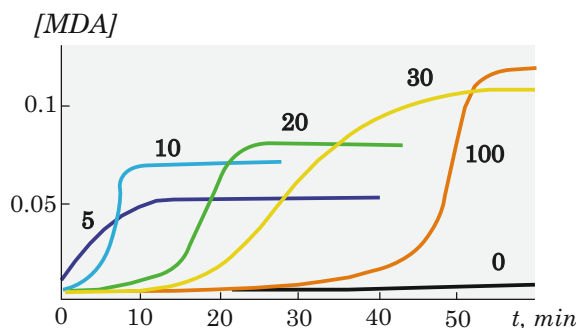


Fig. 11.9 Kinetics of accumulation of TBA-active products (malondialdehyde – MDA) in a suspension of mitochondria at various concentrations of added Fe^{2+} (concentration in μM is indicated on the curves). (Adapted from Hunter et al. (1963), under Creative Commons license. Copyright 1963, Elsevier)

malondialdehyde (a known biochemical marker of peroxidation – see Sect. 8.5.2) with a certain latent period, the longer, the more iron was added (Hunter et al. 1963) (see Fig. 11.9). While the latent period in itself is characteristic of all autocatalytic processes, its lengthening with Fe^{2+} concentration increase indicates the antioxidant aspect of iron action, i.e., its ability to react with free radicals.

The same conclusions follow from estimates of the peroxidation chain length. Thus, at oxidation of oleic acid (Cheremisina et al. 1972), as well as at enzymatic lipid peroxidation in microsomes or mitochondria (Hochstein and Ernster 1963; Hochstein et al. 1964), an increase in the iron concentration resulted in a significant reduction in chain length: from 10–20 at $[Fe^{2+}] \cong 10^{-5}$ to 2–4 at $[Fe^{2+}] \cong 10^{-4} - 10^{-3}$ (see Fig. 11.10) (Cheremisina et al. 1972) (for more information on chain length estimation see Sect. 11.6.2).

Besides the obvious effect “more iron – more radicals – higher probability of recombination – lower chain length,” an important (in fact, key) role in this phenomenon is played by the effect of chain termination on Fe^{2+} ions. Experimentally, this can be seen from the light sum of the fast flash of chemiluminescence after iron addition, which reflects the total number of LOO^\bullet radicals, participating in chemiluminescent processes (recombination or dioxetane formation – see Sect. 10.5). At $[Fe^{2+}] \leq 10^{-4}$, the light sum is proportional to the amount of added iron (see Fig. 11.10a), which shows its pro-oxidant role in decomposition of $LOOH$. However, at $[Fe^{2+}] > 10^{-4}$, further increase of $[Fe^{2+}]$ leads to a decrease of the lightsum, i.e., iron becomes a primarily antioxidant agent due to the dominating chain termination reaction (Cheremisina et al. 1972).

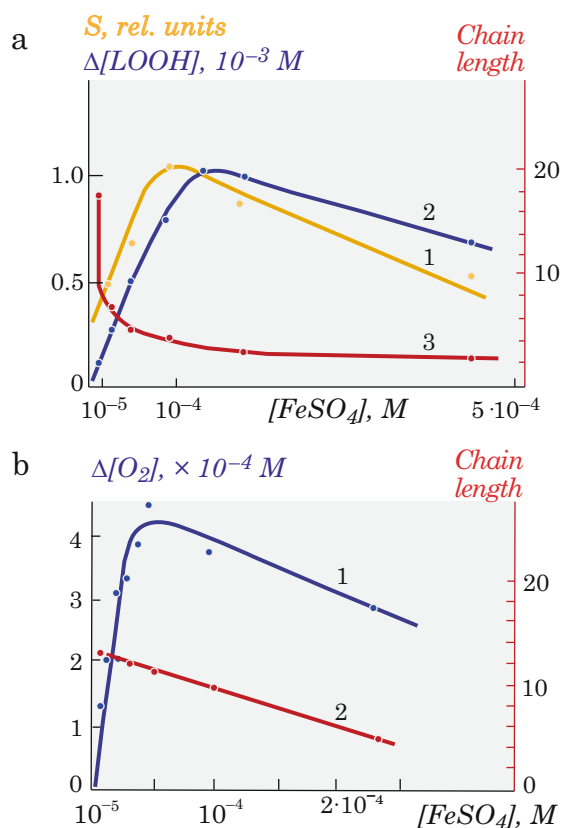


Fig. 11.10 Determination of peroxidation chain length after adding various amounts of FeSO_4 to (a) oleic acid; (b) mitochondria suspensions. (a) Orange – light sum of the fast UPE flash (S) after addition of FeSO_4 ; Blue – accumulation of LOOH ($\Delta[\text{LOOH}]$) during the fast flash when FeSO_4 is added to oxidized oleic acid; Red – lower estimate of the chain length l_{\min} (calculated from the amount of accumulated hydroperoxides, relatively to the amount of introduced iron). (b) Blue – oxygen consumption ($\Delta[\text{O}_2]$) during the fast UPE flash after addition of FeSO_4 ; Red – lower estimate of the chain length l_{\min} (calculated from the amount of consumed oxygen, relatively to the amount of introduced iron). (Adapted from Cheremisina et al. (1972), with permission from the authors)

11.4.3 Summary

Altogether, the whole data above can be explained by the following reactions (Table 11.6).

Of these reactions, one or another can become dominating, depending on the rate constants and initial conditions, i.e., concentration of substances. Detailed kinetic and model studies of this system can be found in Vladimirov and Archakov (1972), as well as in the original publications cited there. However, below we will give and further use some of the most important data from these works.

11.5 Chemiluminescence at Peroxidation of Lipids and Fatty Acids

11.5.1 CL Is Generated by Free-Radical Processes

Chemiluminescence at peroxidation of fatty acids was first shown as early as in 1960 by Ahnstrom and Natarajan (Ahnström and Natarajan 1960). Mixing vegetable oils of various origins with alkaline buffer solutions, they found a correlation between the oil mutagenic activity and intensity of CL at its oxidation. Yet, these observations did not answer the question of whether the luminescence was due to radical reactions, decomposition of peroxides, or some other reasons.

A more definite answer to the nature of luminescence during oxidation of fatty acids was given by systematic studies carried out by B.N. Tarusov, A.I. Zhuravlev, Yu.A. Vladimirov and coauthors.

First of all, the authors showed, that UPE from oils is activated upon heating and sharply intensifies after exposing them to ionizing radiation (Tarusov et al. 1961a), that is, under conditions of intensified peroxidation. Different pro-oxidants – transition metal ions, hydrogen peroxide, etc. also intensified UPE from fatty acids, oils and fats.

Table 11.6 Participation of iron ions in lipid peroxidation

| | | |
|----|---|---|
| 1 | $\text{Fe}^{2+} + \text{O}_2 \xrightarrow{k_0} \text{Fe}^{3+} + \text{O}_2^- \cdot \xrightarrow{+\text{H}^+} \text{HO}_2 \cdot$ | Initiation |
| 2 | $\text{Fe}^{2+} + \text{LOOH} \xrightarrow{-\text{OH}^- + \text{LH} - \text{LOH} + \text{O}_2} \text{Fe}^{3+} + \text{LOO} \cdot$ | Chain branching |
| 3 | $\text{LOO} \cdot + \text{LOO} \cdot \rightarrow \text{molecular products} + h\nu$ | Chain termination: Luminescent |
| 3a | $\text{LOO} \cdot \rightarrow \text{LOO} \cdot_{\text{dioxitane}} \rightarrow \text{X} + \text{Y} \cdot + h\nu$ | Radical cyclization; chain propagation Luminescent |
| 4 | $\text{LOO} \cdot + \text{Fe}^{2+} \rightarrow \text{Fe}^{3+} + \text{molecular products}$ | Chain termination: Nonluminescent |

Rows 1 and 2 – pro-oxidant Fe^{2+} reactions; Row 3 and 3a – luminescent (Fe^{2+} -independent) reactions; Row 4 – antioxidant Fe^{2+} reactions

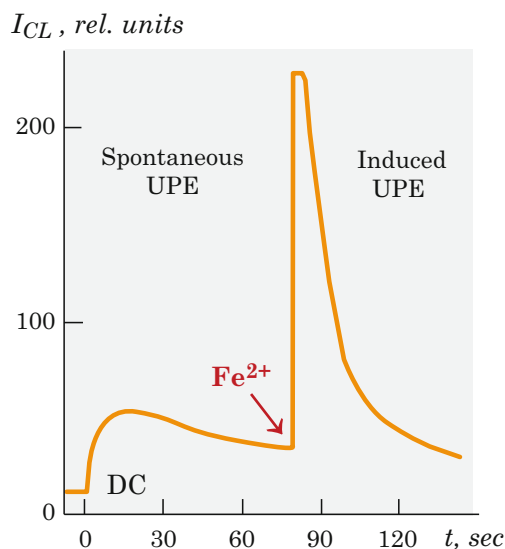


Fig. 11.11 A flash of oleic acid chemiluminescence, stimulated by addition of ferrous sulfate. At the time point indicated by the arrow, 1 ml of 10^{-2} M FeSO_4 was added to 10 ml of a 0.14% solution of oxidized oleic acid. DC – dark current. (Adapted from Vladimirov (1967), with permission from the authors)

Thus, adding Fe^{2+} salts to solutions of oleic acid, already containing hydroperoxides (accumulated in the system due to its preliminary UV irradiation, or heating in the presence of oxygen), led to a “fast flash” of UPE (Vladimirov et al. 1971; Korchagina and Vladimirov 1971) (Fig. 11.11). Moreover, the light sum of the flash linearly increased with the increase of the hydroperoxides amount in the solution (Vladimirov et al. 1969a, b, 1971; Korchagina and Vladimirov 1971; Suslova 1971; Suslova et al. 1968), in full accordance with the total amount of free radicals generated at their decomposition:



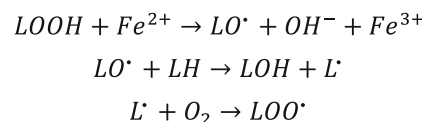
On the contrary, addition of typical antioxidants (β -ionol or β -naphthol), suppressing peroxidation, also suppressed chemiluminescence (Vladimirov et al. 1969b, 1971). Moreover, binding of Fe^{2+} ions due to the addition of EDTA and KCN to the system, inhibited accumulation of peroxides in fatty acid suspensions (Wills 1965) and mitochondria (Hochtein and Ernster 1963) and completely suppressed luminescence (Vladimirov and L'vova 1964; Vladimirov et al. 1966) (Table 11.7).

Thus, UPE from fatty acid solutions and lipids is generated at their peroxidation and with the participation of free radicals. So, it can be also called oxychemiluminescence, OCL, which we will use in the following.

Table 11.7 Luminescence intensity of the mitochondrial suspension 1 hour after adding various concentrations of EDTA

| EDTA concentration, M | I , imp/min |
|-----------------------|---------------|
| 0 | 268 |
| 10^{-6} | 340 |
| 10^{-5} | 76 |
| 10^{-4} | 64 |
| Dark current | 48 |

Adapted from Vladimirov (1967), with permission from the authors



Scheme 11.2 Peroxidation initiation reactions

11.5.2 Radicals Must Be Peroxide

Similarly to hydrocarbon solutions (see Sect. 10.3), OCL from fatty acids and lipids is observed only in the presence of oxygen when practically all radicals exist in the form of LOO^\bullet (Scheme 11.2, compare to Table 10.1 for hydrocarbon solutions).

Thus, in Vladimirov et al. (1971), the Fe^{2+} salts were added to fatty acid solutions (Fig. 11.12a) or mitochondria suspensions (see Fig. 11.12b), with previously accumulated hydroperoxides. This catalyzed peroxide decomposition, which however, was accompanied by luminescence only in the presence of atmospheric oxygen. Contrary to that, in the absence of oxygen, when all radicals exist as L^\bullet and LO^\bullet , no chemiluminescence was observed, and the subsequent air release was not accompanied by any UPE, which showed, that the radicals were not accumulating in the system, i.e., the recombination reactions themselves, apparently, proceeded (Fig. 11.12).

Thus, similarly to hydrocarbons, OCL was generated only in reactions involving peroxide radicals (reactions 3 and 3a in Table 11.6).

11.5.3 Mechanisms of Excitation

As is known now, similarly to unsaturated hydrocarbons, OCL of fatty acids and lipids has two distinct components: (1) Russell component, generated at recombination of peroxy radicals (Miyamoto et al. 2003), and (2) non-Russell component, accompanying relaxation of dioxetanes, formed during cyclization of peroxy radicals (see Sects. 10.5.2 and 10.5.3). In accordance with this, the OCL spectra of fatty acids are

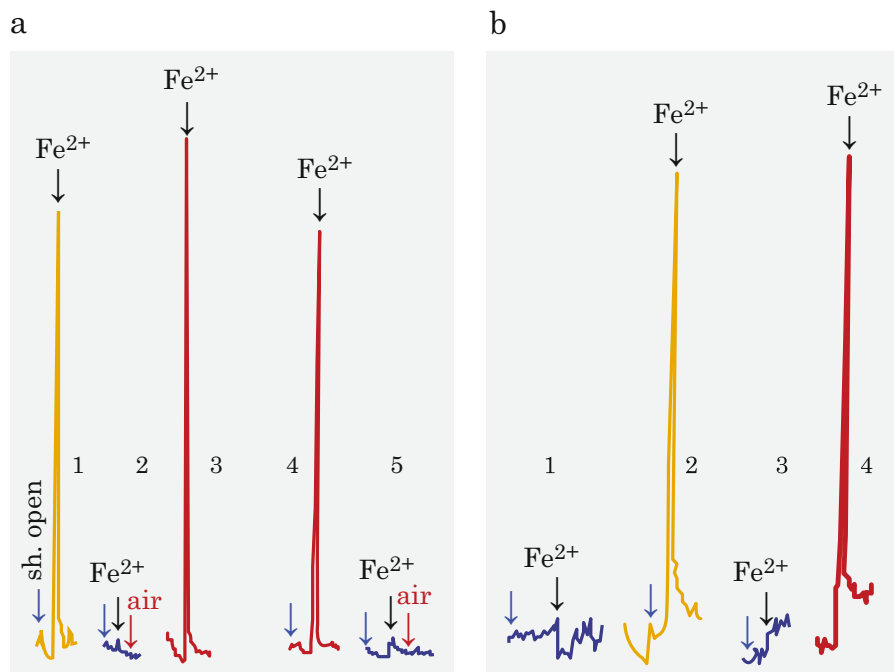


Fig. 11.12 “Fast flash” of chemiluminescence with the addition of FeSO_4 to: (a) Oleic acid (preincubated 35 min at 100 °C with air passing); (b) Mitochondria suspension (preincubated in a medium containing 20 mM KH_2PO_4 , 105 mM KCl and 1 mM FeSO_4 , pH 7.5, until the development of stationary luminescence). Black arrows indicate the moments of mixing oleic acid and iron sulfate (Fe^{2+}); Red

arrows indicate the moments of starting air; Blue arrows indicate the moment of opening the shutter in front of the photomultiplier window. Orange lines (a 1; b 2) – in the air; blue lines (a 2, 5; b 1, 3) – under vacuum, with subsequent air release; red lines (a 3, 4; b 4) – after air evacuation and subsequent release. (Adapted from Vladimirov (1967), with permission from the authors)

characterized by distinct spectral maxima, corresponding to luminescence of excited carbonyls and singlet oxygen or its dimers. For example, for oleic acid, the main maxima were found around 460, 550 and 600 nm (Ivanov and Petrushevich 1965, 1966); ~570 nm (oxygen dimol) and 1270 nm (singlet oxygen component) (Miyamoto et al. 2003).

An important spectroscopic study of CL from different systems was performed in Nakano et al. (1976). The authors showed distinct spectral peaks in OCL from linoleic acid solutions and microsomal lipids (Fig. 11.13), which mostly reproduced those in OCL at hydrocarbon peroxidation (Table 11.8). As discussed in Sect. 10.4.6, these spectral bands corresponded to oxygen electronic transitions, both from $^1\Sigma_g^+$ and $^1\Delta_g$ electron-excited states, as well as from dimol complexes.

The Russell’s mechanism of OCL generation in fatty acid solutions was also confirmed by using ^{18}O -labeled linoleic acid hydroperoxide, oxidized to $\text{L}^{18}\text{O}^{18}\text{O}^*$ peroxy radicals by Ce^{4+} . The obtained $\text{L}^{18}\text{O}^{18}\text{O}^*$ were further recombining according to Russell’s mechanism, and thus generating $^{18}\text{[}^1\text{O}_2\text{]}$, detected by DPA (9,10-diphenylanthracene) trapping and mass-spectrometry (Miyamoto et al. 2003) (Fig. 11.14). Thus, the detection of ^{18}O -labeled singlet oxygen confirmed the proposed mechanism.

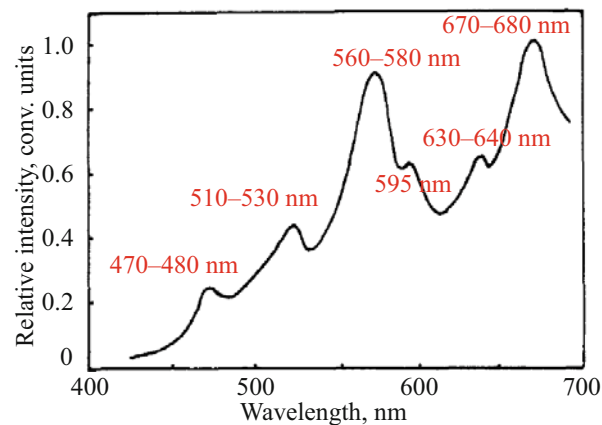


Fig. 11.13 UPE spectrum observed in the reaction of linoleic acid hydroperoxide with ceric ion. (Adapted from Nakano et al. (1976), under Creative Commons license. Copyright 1976, Elsevier)

However, similar to unsaturated hydrocarbons, Russell’s mechanism of peroxy radical disproportionation does not exhaust all paths of peroxidation. Generally speaking, the complicated structure of fatty acids and lipids permits multiple variants of molecule and radical encounters, as well as intramolecular rearrangements (see, e.g., Yin et al. 2011).

Table 11.8 Oxychemiluminescence from sec-butyl hydroperoxide, linoleic acid hydroperoxides and in the microsomal lipid peroxidation system. OCL initiated by $(\text{NH}_4)_2\text{Ce}(\text{NO}_3)_6$. Numbers in parentheses represent mean relative intensity

| Vibrational transition of $^1\text{O}_2$: $* * * \rightarrow 2(^3\Sigma_g^-)(0,0)$ | Wavelength of maximum intensity $\lambda(I_{\text{max}})$ | | |
|--|---|-----------------------------|-------------------------------|
| | Sec-butyl hydroperoxide | Linoleic acid hydroperoxide | Microsomal lipid peroxidation |
| $(^1\Sigma_g^+)(^1\Sigma_g^+)(0,0)$ | None | None | None |
| $(^1\Sigma_g^+)(^1\Delta_g)(0,0)$ | 480 (0.45) | 470 (0.26) | None |
| $(^1\Delta_g)(^1\Delta_g)(2,0)$ | 520–530 (1.0) | 520–530 (0.43) | 512–520 (0.30) |
| $(^1\Delta_g)(^1\Delta_g)(1,0)$ | 570 (0.62) | 570 (0.90) | 595 (0.85) |
| $(^1\Delta_g)(^1\Delta_g)(0,0)$ | 620–640 (0.66) | 640 (0.64) | 630 (1.00) |
| Unspecified transition | 670 (0.67) | 670 (1.00) | 680 (0.80) |

Adapted from Nakano et al. (1976), under Creative Commons license. Copyright 1976, Elsevier

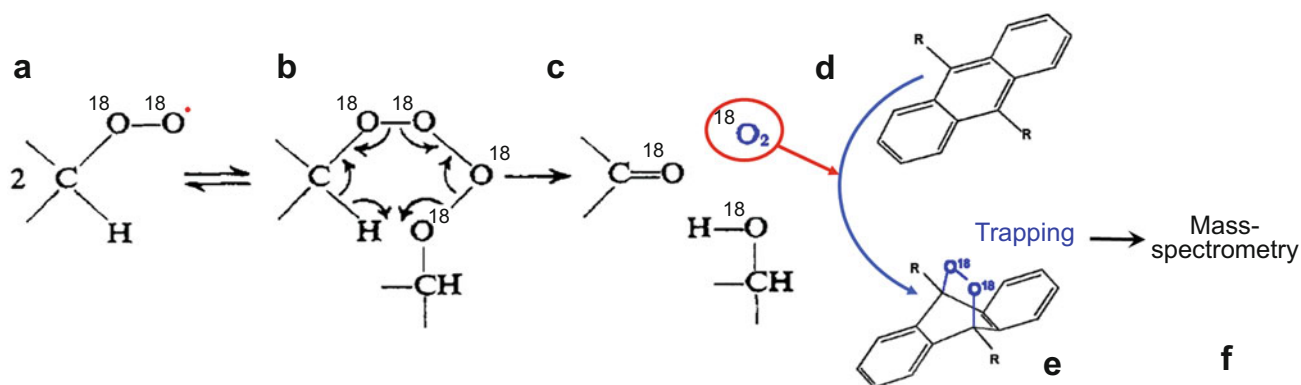


Fig. 11.14 Generation of ^{18}O -labeled singlet oxygen as an indicator of the Russell mechanism of peroxy radical recombination. (Adapted with permission from Howard and Ingold (1968). Copyright 1968, American Chemical Society)

However, the only process known to participate in CL is cyclization of alkyl radicals to excited dioxetanes, similar to unsaturated hydrocarbons (see Sects. 10.5.2 and 10.5.3) (Belyakov et al. 1983; Timmins et al. 1997; Fedorova et al. 2007). Altogether, the general scheme of peroxidation of polyunsaturated fatty acids (PUFA), as it is suggested now, is represented in Fig. 11.15.

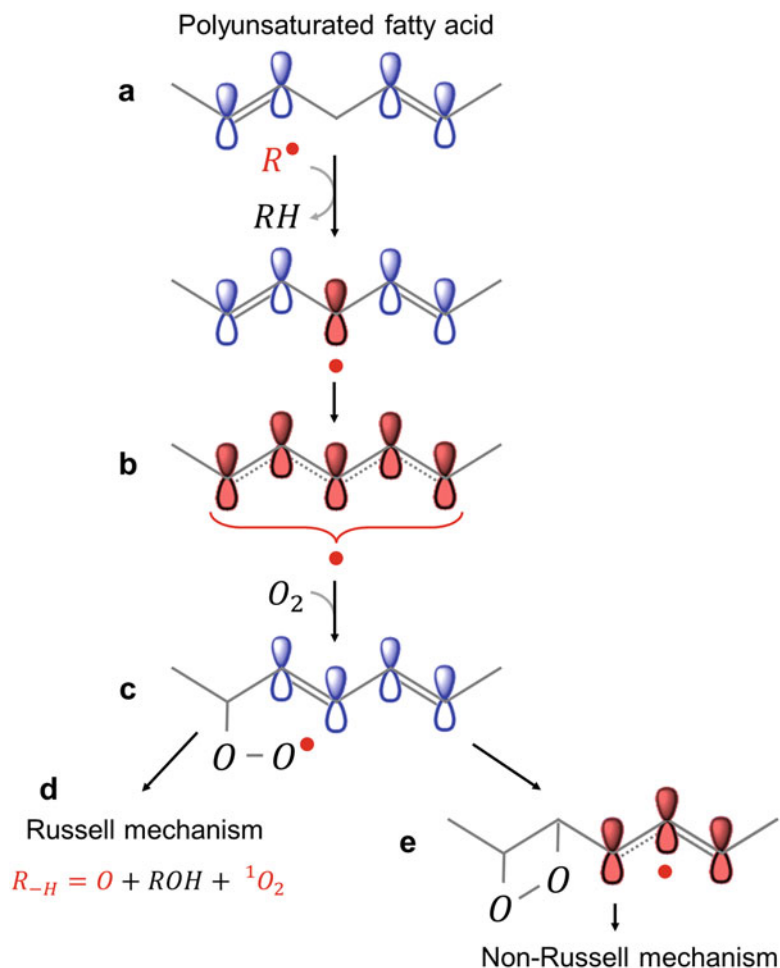
However, it should be said, that notwithstanding huge amount of information on peroxidation and OCL of organic substances, detailed mechanistical research on generation of electronically-excited states is still not enough. One of the latest original works on quantum-mechanical modeling of this process is represented later in this book (see Chap. 13).

11.5.4 Summary

Altogether, similar to the work on hydrocarbons, in fatty acids and lipids:

- Chemiluminescence quanta are formed during the recombination of LOO^\bullet radicals, as well as at relaxation of excited dioxetanes;
- Cessation of oxygen access shifts the balance $\text{L}^\bullet \leftrightarrow \text{LOO}^\bullet$ towards the radicals L^\bullet , which practically do not give light upon recombination;
- Transition metal ions stimulate decomposition of peroxides, forming free radicals and generating light in course of further processes with their participation.

Fig. 11.15 Mechanisms of generation of electronically excited states during oxidation of polyunsaturated fatty acids



11.6 Kinetics of Peroxidation and Chemiluminescence

The ratio of the pro- and antioxidant roles of iron can be studied by the methods of kinetics and kinetic modeling, in which chemiluminescence is one of the key characteristics, as it directly reflects the amount of peroxy radicals in the system (see Sects. 8.5.3, 10.3, 10.4, and above). Such kinetical research on lipid peroxidation in mitochondria, regulated by adding iron salts, was carried out in a series of works by Yu. A. Vladimirov et al. (see (Vladimirov et al. 1969a; Vladimirov and Archakov 1972) for the summary). Detecting CL kinetics, oxygen consumption, and periodically sampling the system for Fe^{2+} and malondialdehyde, the authors showed and analyzed a complex kinetics of the process (see below, Fig. 11.16).

11.6.1 Phases of Kinetic Curves

First of all, the chemiluminescence curve was conventionally divided into a number of phases, corresponding to different stages of luminescence kinetics. In Vladimirov et al. (1969a), the following names were proposed for them.

On the first addition of Fe^{2+} to a suspension containing no hydroperoxide:

1. Latency period
2. Slow flash of luminescence (autocatalytic acceleration of peroxidation and its decline)
3. Stationary luminescence

When readding Fe^{2+} (the system already contains hydroperoxides):

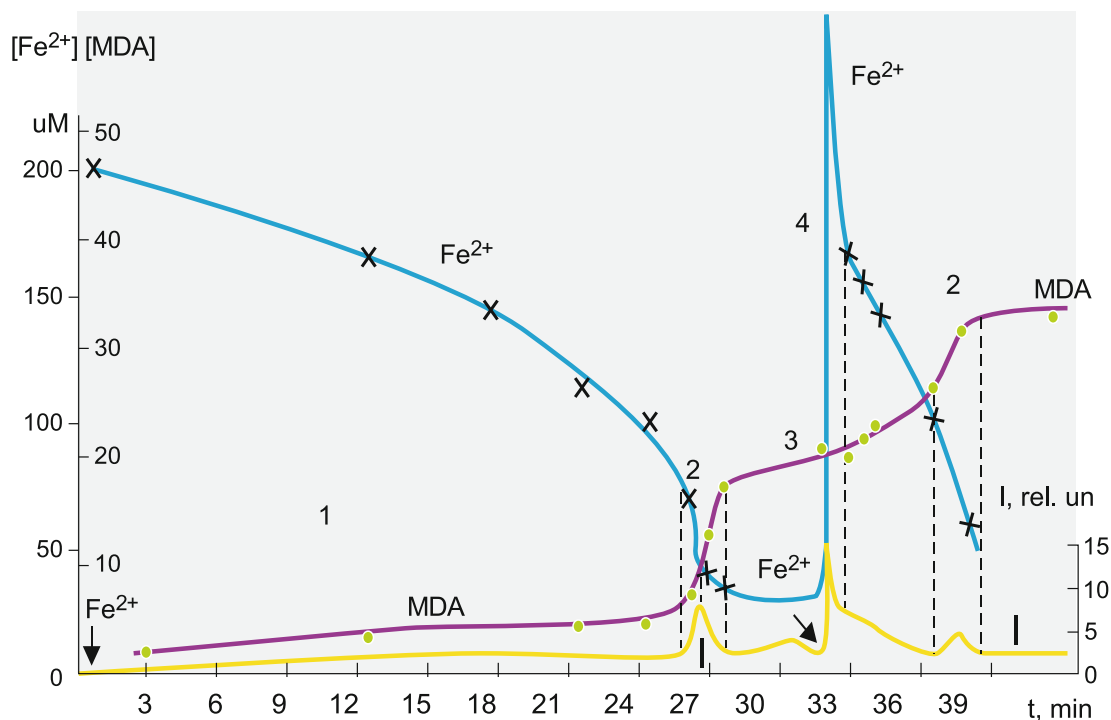


Fig. 11.16 Chemiluminescence (I , orange), change in the concentration of ferrous iron (Fe^{2+} , blue) and TBA-active substances (malondialdehyde, MDA, green) in mitochondria suspension after adding 0.2 mM Fe^{2+} . (Adapted from Vladimirov et al. (1969a), with permission from the authors)

1. Fast flash of luminescence
2. Suppression of luminescence
3. New slow flash
4. New level of stationary luminescence

Changes in luminescence intensity (i.e., LOO^\bullet concentration) were associated with changes in Fe^{2+} , LOOH concentration, accumulation of TBA-active substances (see Sect. 8.5.2) and oxygen consumption (Figs. 11.16 and 11.17).

In phase 1 (at the reaction beginning), there is a gradual oxidation of iron and oxygen consumption, relatively slow increase in the free-radicals concentration and accumulation of peroxides (Fig. 11.16). All these processes are gradually accelerated, so that at some point there is an explosive accumulation of peroxides, coupled with iron oxidation and accompanied by a flash of CL (“slow flash,” phase 2, see also Fig. 11.7). As iron in the system is oxidized, the process of peroxide accumulation slows down, and the luminescence intensity decreases (phase 3 – Figs. 11.16 and 11.17). The free-radical process remains at a more or less constant level, determined by the balance between the reactions of chain propagation:

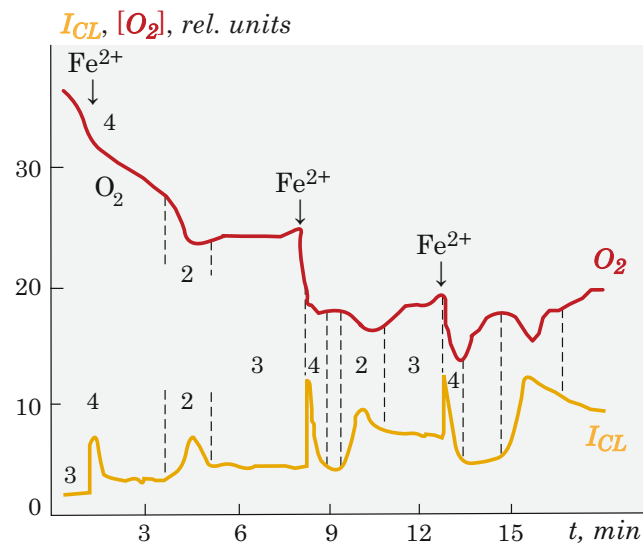
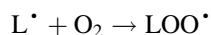
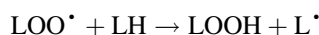
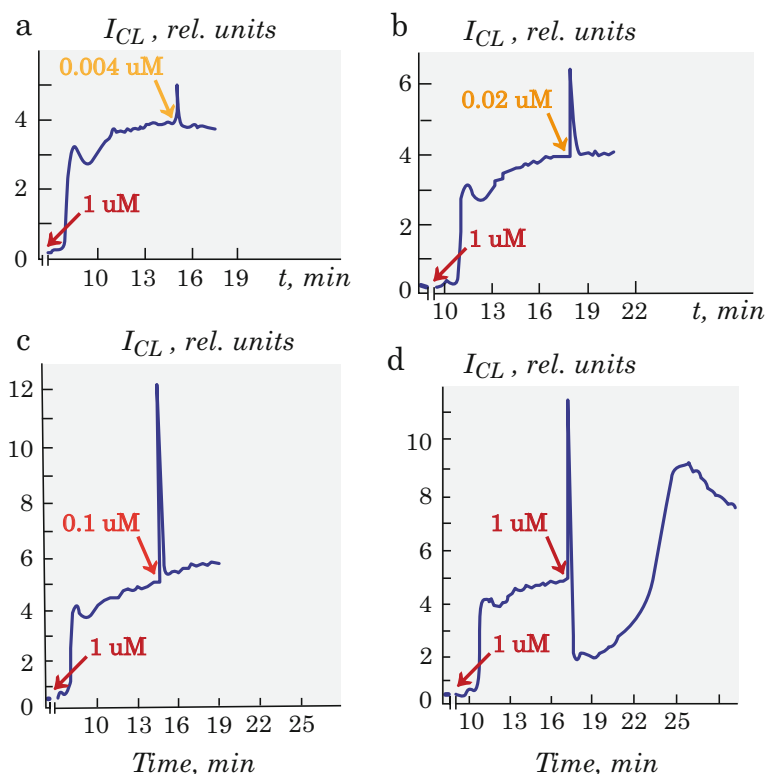
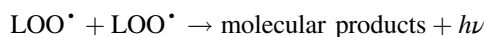
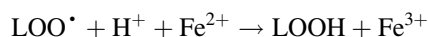


Fig. 11.17 Parallelism between luminescence (I_{CL} , orange line) and oxygen consumption by mitochondria (O_2 , red line) in the presence of Fe^{2+} ions. 2–4 – stages of luminescence kinetics. The arrows indicate the moments of FeSO_4 addition. The composition of the incubation mixture: 1 ml of a mitochondria suspension in 10 ml of 120 mM NaCl, 5 mM Tris buffer, pH 7.5, temperature 40°C . (Adapted from Vladimirov et al. (1969a), with permission from the authors)

Fig. 11.18 Effect of adding different amounts of FeSO_4 on mitochondrial CL (Suslova et al. 1970). The medium composition: 20 mM KH_2PO_4 , 105 mM KCl, pH 7.5, temperature 37 °C. Arrows indicate FeSO_4 additives. The concentration of added FeSO_4 is given in the figure. (Adapted from Vladimirov et al. (1969a), with permission from the authors)



and chain termination:



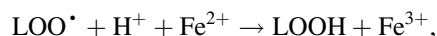
of which the radicals recombination increasingly dominates, as the iron is oxidized.

Adding a new portion of Fe^{2+} to the system leads to the “instantaneous” decay of accumulated peroxides:



and a “fast flash” of luminescence (phase 4).

At the same time, iron also enters into chain termination reactions:



which can lead to the subsequent CL suppression (phase 5), the longer and deeper, the higher the added iron concentration.

Experimentally, this issue was investigated in Suslova et al. (1970). A burst of chemiluminescence was recorded, when adding various amounts of FeCl_2 salt to the mitochondria suspension, preincubated in a medium already containing ferrous ions, so that a certain amount of lipid peroxides had previously accumulated in them. As seen in Fig. 11.18, when adding small amounts of iron (up to 10^{-4} M), the intensity of the “fast flash” increased with an increase in Fe^{2+} concentration, and no subsequent luminescence suppression was observed. However, with further increase of the introduced Fe^{2+} concentration, the fast flash intensity ceased to grow, and, conversely, the stationary luminescence was inhibited (phase 5), the deeper and more prolonged, the higher the added iron concentration (Suslova et al. 1970) (Fig. 11.19).

Thus, the added iron at concentrations less than 10^{-4} M acted mainly as a prooxidant, and at higher concentrations as an antioxidant.

Obviously, the luminescence suppression phase after the fast flash (phase 5) should strongly depend on the iron concentration: the higher its initial concentration, the longer the chain termination reaction on iron ions will dominate over the luminescent reactions, and the stronger the luminescence decay in phase 5 should be.

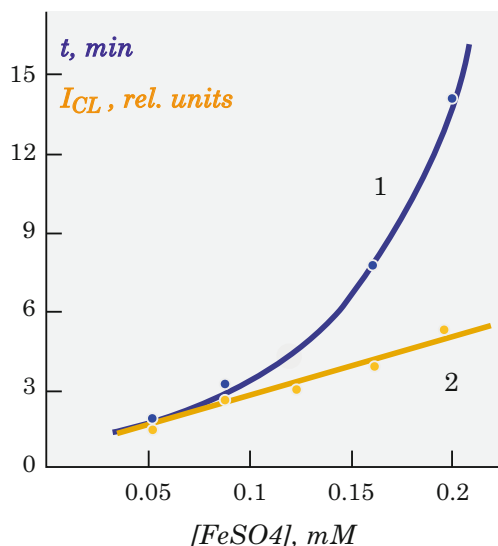


Fig. 11.19 Effect of the added Fe^{2+} concentration on the mitochondrial suspension CL: duration of the latency period (1) and the amplitude of the subsequent “slow flash” of CL (2). (Adapted from Vladimirov et al. (1969a), with permission from the authors)

Meanwhile, the radicals remaining in the system participate in the chain propagation reaction, during which new hydroperoxides are formed. The hydroperoxides, in turn, disintegrate with the participation of the remaining Fe^{2+} ions, which give a new phase of self-acceleration (phase 2).

11.6.2 Kinetic Modeling of Peroxidation

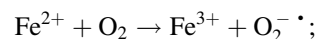
11.6.2.1 General Model

A correct modeling of the above data requires compilation and solution of differential equations describing the rates of all reactions involved (see Sect. 8.5.3). As shown above, for fatty acid peroxidation it should be generally similar to that for hydrocarbons (see Sect. 10.3.5), with addition of specific pro- and antioxidants present in the system, as well as CL reactions of non-Russell type (see Sect. 10.5.3). However, the use of model systems with a known specific composition and initial conditions can greatly simplify the mathematical problem (see Sect. 8.5.3). This approach has been consistently implemented in a comprehensive research of Yu.A. Vladimirov et al. with the above experimental data on model systems (Sect. 11.6.1) and subjected to mathematical modeling in Vladimirov et al. (1973) (see also Vladimirov and Archakov 1972).

The authors based on the following assumptions (see methods in Sect. 8.5.3):

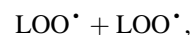
1. LH and O_2 are present in excess, and their concentration can be considered constant;

2. Of all pro- and antioxidants, only Fe^{2+} ions (introduced by the experimenter) are present in the system in sufficient quantities;
3. Initiation rate is determined by the reaction:

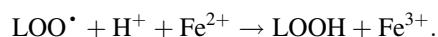


Further reactions of $\text{O}_2^{\cdot -}$ and/or HO_2^{\cdot} are incomparably faster;

4. All L^{\cdot} and LO^{\cdot} radicals immediately turn into LOO^{\cdot} , which has much less reactivity and longer lifetime (see Box 10.1). Thus, the stationary concentration of LOO^{\cdot} is incomparably higher than that of L^{\cdot} and LO^{\cdot} , and of all possible recombination processes, it is sufficient to take into account only



and of all the reactions of radicals with iron – only



5. The above points 3 and 4 mean, that concentrations of $\text{O}_2^{\cdot -}$, HO_2^{\cdot} , L^{\cdot} and LO^{\cdot} can be regarded as fast variables, and allow us applying Tikhonov’s theorem to them (see Sect. 8.5.3):

$$[\text{O}_2^{\cdot -}] \cong 0; [\text{HO}_2^{\cdot}] \cong 0; [\text{L}^{\cdot}] \cong 0; [\text{LO}^{\cdot}] \cong 0$$

where the concentration of (any) substance X is designated as $[X]$, and the rate of its change is designated as $\dot{X} \equiv \frac{d[X]}{dt}$.

This leads to the following simplified scheme of peroxidation reactions (Table 11.9), and the following system of kinetic equations (Table 11.10).

Further, applying Tikhonov’s theorem to fast variables and supposing quasi-constant concentrations for LH and O_2 , one gets the following scheme (Table 11.11) (Vladimirov et al. 1973).

Numerical solution of these equations with empirically selected values of the reaction rate constants (Table 11.12), gives the following kinetic curves (Fig. 11.20).

Comparing the obtained theoretical kinetics with experimental data (Fig. 11.20 vs. Fig. 11.16), one can see very good correspondence, suggesting the general correctness of the supposed reaction scheme.

A couple of special cases, important for practical use are given below.

Table 11.9 The main reactions of peroxidation in a model system of fatty acids or lipids in the presence of Fe^{2+}

| Process stage | No | Reaction |
|-----------------|----|---|
| Initiation | 0 | $\text{Fe}^{2+} + \text{O}_2 \xrightarrow{k_0} \text{Fe}^{3+} + \text{O}_2^- \cdot \xrightarrow{+\text{H}^+} \text{HO}_2 \cdot$ |
| | 1 | $\text{HO}_2 \cdot + \text{LH} \xrightarrow{k_1} \text{H}_2\text{O}_2 + \text{L} \cdot$ |
| Propagation | 2 | $\text{L} \cdot + \text{O}_2 \xrightarrow{k_2} \text{LOO} \cdot$ |
| | 3 | $\text{LOO} \cdot + \text{LH} \xrightarrow{k_3} \text{LOOH} + \text{L} \cdot$ |
| Chain branching | 4 | $\text{LOOH} + \text{Fe}^{2+} \xrightarrow{k_p} \text{LO} \cdot + \text{OH}^- + \text{Fe}^{3+}$ |
| | | $\text{LOOH} \xrightarrow{k_T} \text{LO} \cdot + \text{OH} \cdot$ |
| | 5 | $\text{LO} \cdot + \text{LH} \xrightarrow{k_5} \text{LOH} + \text{L} \cdot$ |
| Termination | 6 | $\text{LOO} \cdot + \text{LOO} \cdot \xrightarrow{k_6} \text{P}^* \xrightarrow{\eta} \text{P} + h\nu$ |
| | 9 | $\text{LOO} \cdot + \text{H}^+ + \text{Fe}^{2+} \xrightarrow{k_9} \text{LOOH} + \text{Fe}^{3+}$ |

Table 11.10 Kinetic equations for Table 11.9 (rates of fast variables are marked with the infinitesimal parameter ε – see Sect. 8.5.3)

| |
|--|
| $[\dot{\text{LH}}] = -k_1[\text{LH}][\text{HO}_2 \cdot] - k_3[\text{LH}][\text{LOO} \cdot] - k_5[\text{LH}][\text{LO} \cdot]$ |
| $\varepsilon[\dot{\text{L}} \cdot] = k_1[\text{LH}][\text{HO}_2 \cdot] - k_2[\text{L} \cdot][\text{O}_2] + k_3[\text{LH}][\text{LOO} \cdot] + k_5[\text{LH}][\text{LO} \cdot]$ |
| $[\dot{\text{LOO}} \cdot] = k_2[\text{L} \cdot][\text{O}_2] - k_3[\text{LH}][\text{LOO} \cdot] - k_6[\text{LOO} \cdot]^2 - k_9[\text{LOO} \cdot] \times [\text{Fe}^{2+}]$ |
| $\varepsilon[\dot{\text{LO}} \cdot] = k_p[\text{LOOH}][\text{Fe}^{2+}] - k_5[\text{LH}][\text{LO} \cdot] + k_T[\text{LOOH}]$ |
| $[\dot{\text{LOOH}}] = k_3[\text{LH}][\text{LOO} \cdot] - k_p[\text{LOOH}][\text{Fe}^{2+}] - k_T[\text{LOOH}]$ |
| $[\dot{\text{O}}_2] = -k_0[\text{Fe}^{2+}][\text{O}_2] - k_2[\text{L} \cdot][\text{O}_2]$ |
| $\varepsilon[\dot{\text{O}}_2^- \cdot] = k_0[\text{Fe}^{2+}][\text{O}_2] - k_{00}[\text{O}_2^- \cdot][\text{H}^+]$ |
| $\varepsilon[\dot{\text{HO}}_2 \cdot] = k_{00}[\text{O}_2^- \cdot][\text{H}^+] - k_1[\text{LH}][\text{HO}_2 \cdot]$ |
| $[\dot{\text{Fe}}^{2+}] = -k_0[\text{Fe}^{2+}][\text{O}_2] - k_p[\text{LOOH}][\text{Fe}^{2+}] - k_9[\text{LOO} \cdot][\text{Fe}^{2+}]$ |
| $I_{h\nu} = k_6\eta[\text{LOO} \cdot]^2$ |

Table 11.11 The final simplified system of kinetic equations for lipid peroxidation reactions at constant concentration of Fe^{2+}

| |
|--|
| $[\dot{\text{LOO}} \cdot] = k_0\rho[\text{Fe}^{2+}][\text{O}_2] + k_p[\text{LOOH}][\text{Fe}^{2+}] + k_T[\text{LOOH}] - k_9[\text{LOO} \cdot][\text{Fe}^{2+}] - k_6[\text{LOO} \cdot]^2$ |
| $[\dot{\text{LOOH}}] = k_3[\text{LH}][\text{LOO} \cdot] - k_p[\text{LOOH}][\text{Fe}^{2+}] - k_T[\text{LOOH}]$ |
| $[\dot{\text{Fe}}^{2+}] = -k_0[\text{Fe}^{2+}][\text{O}_2] - k_p[\text{LOOH}][\text{Fe}^{2+}] - k_9[\text{LOO} \cdot][\text{Fe}^{2+}]$ |
| $I_{h\nu} = k_6\eta[\text{LOO} \cdot]^2$ |

Adapted from Vladimirov et al. (1973), with permission from the authors

where ρ is initiation efficiency, i.e., the probability of generating an $\text{LOO} \cdot$ radical in a reaction chain initiated by oxygen reduction on iron: $\text{Fe}^{2+} + \text{O}_2$

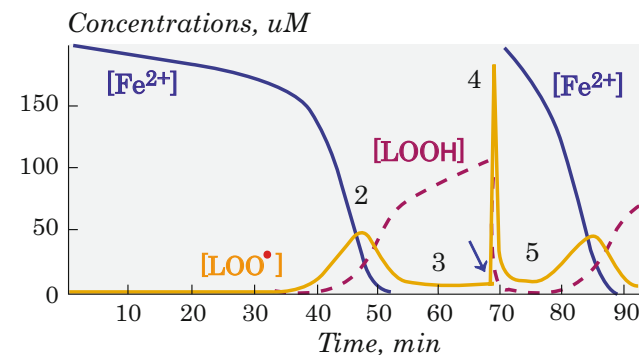
11.6.2.2 Branched and Unbranched Chain Reaction

If Fe^{2+} is introduced in relatively high concentration into a system, already containing hydroperoxides, the dominating radical-generating reaction at the initial stage will be iron-induced hydroperoxide decomposition:

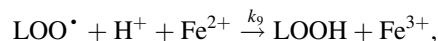
Table 11.12 Empirically selected values of the rate constants in the equations of Table 11.11

| | |
|-------------------|--|
| $k_0[\text{O}_2]$ | $4 \times 10^{-2} \text{ s}^{-1}$ |
| ρ | 5×10^{-5} |
| k_6 | $4 \times 10^5 \text{ l/mol} \cdot \text{s}$ |
| k_9 | $2 \times 10^4 \text{ l/mol} \cdot \text{s}$ |
| $k_3[\text{LH}]$ | 4.005 s^{-1} |
| k_p | $2 \times 10^4 \text{ l/mol} \cdot \text{s}$ |
| k_T | $2 \times 10^{-3} \text{ s}^{-1}$ |

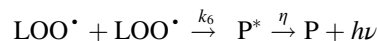
Adapted from Vladimirov et al. (1973), with permission from the authors

**Fig. 11.20** Mathematical modeling of the mitochondria OCL (Vladimirov et al. 1973) (compare with experimental data in Fig. 11.16). Blue line – $[\text{Fe}^{2+}]$, uM; fuchsia dashed line – $[\text{LOOH}]$, uM; orange line – $[\text{LOO} \cdot]$, generally reflecting the CL intensity. The blue arrow indicates the moment of iron addition. Process stages: 1 – latency period; 2 – “slow flash”; 3 – stationary luminescence; 4 – “fast flash”; 5 – luminescence suppression. (Adapted from Vladimirov et al. (1973), with permission from the authors)

while thermal decomposition of LOOH and iron-induced oxygen reduction will go incomparably slower, and can be neglected (see general reaction scheme in Table 11.9, and rate constants in Table 11.12). At the same time, chain termination will also occur primarily on Fe^{2+} :

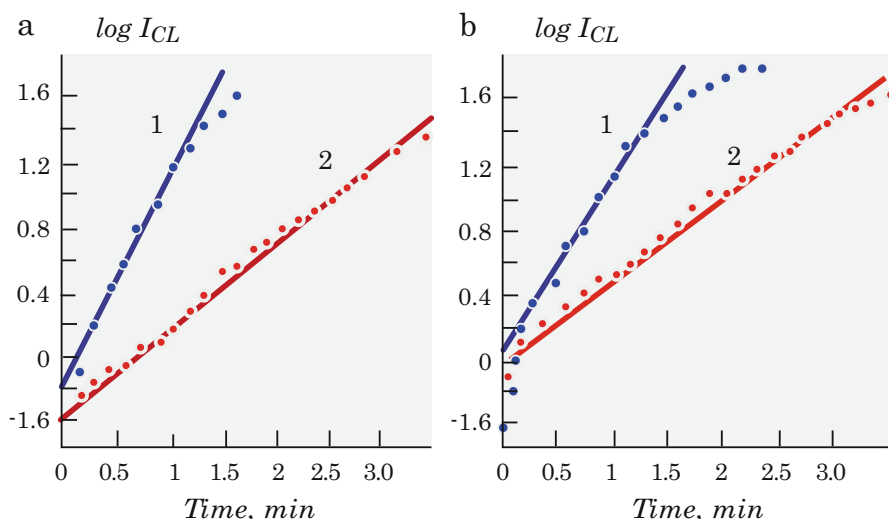


while radical recombination



can be neglected in the rate of $[\text{LOO} \cdot]$ change, as incomparably slower: initially, $[\text{Fe}^{2+}]$ is greater than $[\text{LOO} \cdot]$ by many orders of magnitude, while rate constants differ only by 10 times (see Table 11.12).

Fig. 11.21 Effect of α -tocopherol concentration and preincubation time on the initial kinetics of the mitochondria suspension “slow flash.” (a) concentration of α -tocopherol: $1-2 \times 10^{-7}$ M, $2-5 \times 10^{-7}$ M, (b) time of preincubation of α -tocopherol with mitochondria, 1–1 min, 2–2.5 min. I_{CL} – luminescence intensity, rel.un. (Adapted from Vladimirov et al. (1969c), with permission from the authors)



Assuming also, that at first

$$[\text{LH}] \cong \text{const}, [\text{O}_2] \cong \text{const}, \text{ and } [\text{Fe}^{2+}] \cong \text{const}$$

(while they are in excess in relation to radicals and hydroperoxides), and applying Tikhonov's theorem to $[\text{LOO}^{\bullet}]$:

$$[\text{LOO}^{\bullet}] \cong 0$$

(see Sect. 8.5.3), we get the following simplified equations:

$$k_P \nu [\text{LOOH}] [\text{Fe}^{2+}] = k_9 [\text{LOO}^{\bullet}] [\text{Fe}^{2+}] \quad (11.5)$$

$$[\text{LOOH}] = k_3 [\text{LH}] [\text{LOO}^{\bullet}] - k_P [\text{LOOH}] [\text{Fe}^{2+}] \quad (11.6)$$

where $\nu \leq 1$ is the probability of generating an LOO^{\bullet} radical in a reaction chain initiated by LOOH decomposition.

Solving this system, we get:

$$[\text{LOOH}] = [\text{LOOH}]_0 \cdot e^{\gamma t} \quad (11.7)$$

$$[\text{LOO}^{\bullet}] = [\text{LOO}^{\bullet}]_0 \cdot e^{\gamma t} = \frac{k_P \nu}{k_9} \cdot e^{\gamma t} \quad (11.8)$$

and for CL intensity:

$$I_{hv} = k_6 \varphi_{cl} [\text{LOO}^{\bullet}]^2 = I_0 \cdot e^{2\gamma t} \quad (11.9)$$

where φ_{cl} – is quantum yield of chemiluminescence, and

$$\gamma = \frac{k_3 [\text{LH}] k_P \nu}{k_9} - k_P [\text{Fe}^{2+}] \quad (11.10)$$

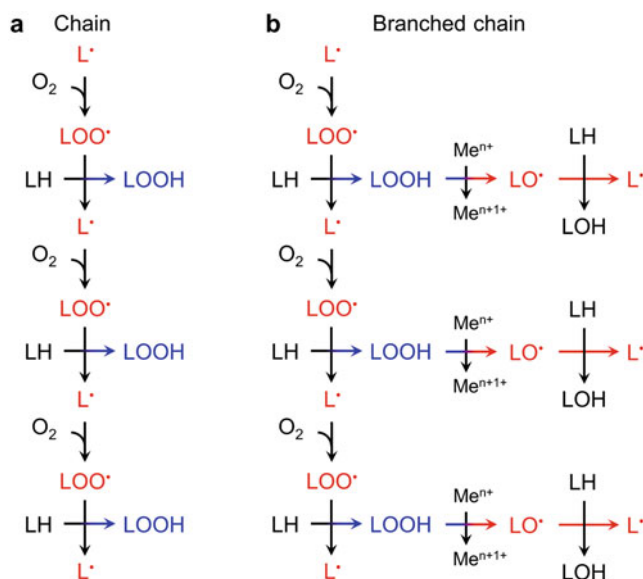
Thus, the initial phase of CL kinetics after adding Fe^{2+} salts to fatty acids or lipids (while Fe^{2+} remains in excess) should show exponential gain, which is indeed observed at the beginning of the “slow flash” (see Fig. 11.21). Later, the experimental data deviate from this dependence, because $[\text{Fe}^{2+}]$ decreases, and the above assumptions are not met any more. (Importantly, introduction of antioxidants, effectively decreasing free-radical concentration, decreases γ but does not change the exponential character of the initial phase of CL – see Fig. 11.21.)

The observed exponential development at the beginning of Fe^{2+} -initiated peroxidation can be easily explained:

- In the absence of pro-oxidants, peroxidation chains are unbranched, and either develop linearly, or terminate at radical disappearance (Scheme 11.3a).
- Adding Fe^{2+} (or any other catalyst for peroxide decomposition), leads to chain branching – i.e., generation of new radicals from the hydroperoxides produced in course of the chain reaction (Scheme 11.3b).

The rate of this branched chain reaction will increase exponentially all the time until the iron in the system is sufficiently oxidized, and the probability of chain branching considerably decreases.

Thus, introducing iron into the system of oxidizable fatty acids or lipids can cause its transition from a linear chain reaction to a branched chain reaction with explosive development. This role of iron has long been known to different authors and has been used as evidence of free-radical processes (e.g., (Vladimirov and Archakov 1972; Voeikov and Novikov 1998; Voeikov 2010)). However, as discussed in Sect. 11.4, transition metals, including iron, can act as both pro-oxidants and antioxidants, depending on the reactions in which they are primarily involved (see below).

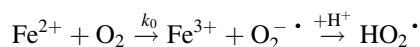


Scheme 11.3 Reactions of lipid peroxidation (Vladimirov et al. 1969a): (a) with unbranched chains, (b) with branched chains. (Adapted from Vladimirov et al. (1969a), with permission from the authors)

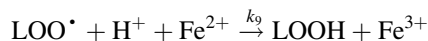
11.6.2.3 Trigger Role of Ferrous Iron in Chain Peroxidation Reactions

As discussed above, the dual role of iron is determined by its participation in reactions of the opposite type:

- pro-oxidant (radical-generating):



- and antioxidant (radical-eliminating):



The relationship between these two roles (i.e., between the rates of these reactions) is determined by iron concentration (see Sect. 11.4), which can be explained by the above expressions (Eqs. 11.7, 11.8, 11.9, and 11.10). Thus:

- If $\gamma = 0$, all the concentrations, as well as the CL intensity remain constant:

$$\begin{aligned} [\text{LOOH}] &= [\text{LOOH}]_0, [\text{LOO}^{\cdot}] = [\text{LOO}^{\cdot}]_0, \omega \\ &= \omega_0, I = I_0 \end{aligned} \quad (11.11)$$

- If $\gamma > 0$, i.e., $\frac{k_3[\text{LH}]k_p\nu}{k_9} > k_p[\text{Fe}^{2+}]$, the reaction is suppressed over time;
- If $\gamma < 0$, i.e., $\frac{k_3[\text{LH}]k_p\nu}{k_9} < k_p[\text{Fe}^{2+}]$, the reaction is exponentially accelerated.

That is, one can formulate the following conditions:

$$[\text{Fe}^{2+}] < \frac{k_3[\text{LH}]\nu}{k_9} \quad - \quad \text{activation} \quad (11.12)$$

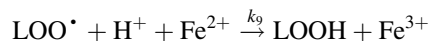
$$[\text{Fe}^{2+}] > \frac{k_3[\text{LH}]\nu}{k_9} \quad - \quad \text{inhibition} \quad (11.13)$$

which becomes more visual if we assume $\nu = 1$ (where ν is the probability of generating an LOO^{\cdot} radical upon LOOH decomposition). Then:

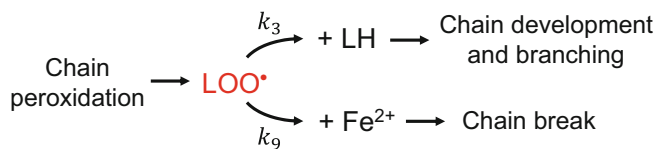
$$k_9[\text{Fe}^{2+}][\text{LOO}^{\cdot}] < k_3[\text{LH}][\text{LOO}^{\cdot}] \quad - \quad \text{activation} \quad (11.14)$$

$$k_9[\text{Fe}^{2+}][\text{LOO}^{\cdot}] > k_3[\text{LH}][\text{LOO}^{\cdot}] \quad - \quad \text{inhibition} \quad (11.15)$$

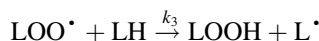
As one can see, $k_9[\text{Fe}^{2+}][\text{LOO}^{\cdot}]$ – is the rate of radical disappearance on iron:



and $k_3[\text{LH}][\text{LOO}^{\cdot}]$ – is the rate of lipid oxidation:



Scheme 11.4 The “fate decision” of the peroxide radical



If the first process prevails, the number of free radicals will decrease, and the chain oxidation will slow down. If the second process is more likely, the chain reaction will proceed with self-acceleration (as, besides preserving the existing radicals, hydroperoxides will be formed, and can be further decomposed by Fe^{2+} , with new radicals generated) – see Scheme 11.4.

Thus, the higher the Fe^{2+} concentration, the more probable the second reaction (and the second “fate” of the chain) is.

Switching the process from self-accelerating to slowing down with increasing iron concentration explains many features of the CL kinetics in mitochondria suspensions in the presence of ferrous ions:

- If the introduced iron concentration is less than the critical value: $[\text{Fe}^{2+}]_0 < \frac{k_3[\text{LH}]\nu}{k_9}$, the process proceeds with self-acceleration until all iron is oxidized and radicals begin to disappear due to recombination or chain termination on antioxidants. Thus, the “fast flash” of CL merges with the “slow flash.”
- If $[\text{Fe}^{2+}]_0 > \frac{k_3[\text{LH}]\nu}{k_9}$, the process is inhibited, and the CL is suppressed – the more, the more iron is initially introduced (Fig. 11.18).
- However, within the resulting period of suppression (or latency period), Fe^{2+} is still oxidized, and sooner or later, its concentration will drop below the $\frac{k_3[\text{LH}]\nu}{k_9}$ barrier. This switches the process into the self-accelerating regime.
- Initially, the autocatalytic peroxidation develops faster than exponentially, since the γ exponent itself grows with decreasing ferrous iron concentration (see Eqs. 11.8 and 11.10).
- When the chain length becomes large enough, and $k_P[\text{Fe}^{2+}] \ll \frac{k_3[\text{LH}]k_P\nu}{k_9}$, the kinetics becomes exponential, with $\gamma \cong \frac{k_3[\text{LH}]k_P\nu}{k_9}$ (see Eq. 11.10). This ends the “latent period” (induction period) and starts the “slow flash” of CL.

In other words, the CL decay in the end of the “fast flash,” its approximately constant intensity during the induction period, and its rise at the beginning of the “slow flash,”

correspond to changes in the γ exponent with a decrease in Fe^{2+} concentration (see Eqs. 11.7, 11.8, 11.9, and 11.10). Obviously, the more Fe^{2+} is added and the slower it is oxidized, the longer the induction period in CL development. This also fits other experimental data (e.g., (Hunter et al. 1963)).

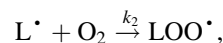
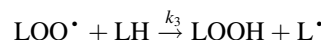
11.6.2.4 Chain Length Versus Fe^{2+} Concentration

As shown in Fig. 11.10, the chain length of peroxidation decreases with $[\text{Fe}^{2+}]$ increase, due to its termination on iron ions. This, can also get quantitative meaning within the framework of the above modeling.

First of all, let us make the definition of chain length more precise. If initiation and branching reactions result in appearance of ω_i M of LOO^{\bullet} radicals per second plus $k_P[\text{Fe}^{2+}][\text{LOOH}]$ M of LO^{\bullet} , each of which finally produces LOO^{\bullet} with probability ν , then the rate of LOO^{\bullet} formation will be:

$$\omega_i + k_P\nu[\text{Fe}^{2+}][\text{LOOH}] \text{ M/s}$$

If each of them participates in the chain reaction:

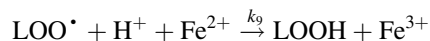
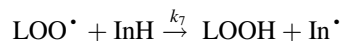


l times, thus generating $lk_3[\text{LH}][\text{LOO}^{\bullet}]$ M of hydroperoxide, then the value

$$l = \frac{k_3[\text{LH}][\text{LOO}^{\bullet}]}{\omega_i + k_P\nu[\text{Fe}^{2+}][\text{LOOH}]} \quad (11.16)$$

is the chain length.

The chain length depends both on the presence of antioxidants (InH) and on Fe^{2+} concentration, since the LOO^{\bullet} radicals react with both of these compounds. Considering both of these reactions:



and applying Tikhonov’s theorem ($[\dot{\text{LOO}}^{\bullet}] \cong 0$), we get:

$$\omega_i + k_P\nu[\text{Fe}^{2+}][\text{LOOH}] = k_9[\text{Fe}^{2+}][\text{LOO}^{\bullet}] + k_7[\text{InH}][\text{LOO}^{\bullet}] \quad (11.17)$$

Whence:

$$l = \frac{k_3[\text{LH}][\text{LOO}^*]}{\omega_i + k_p\nu[\text{Fe}^{2+}][\text{LOOH}]} = \frac{k_3[\text{LH}]}{k_9[\text{Fe}^{2+}] + k_7[\text{InH}]} \quad (11.18)$$

In the absence of inhibitors, except for Fe^{2+} , we obtain an even simpler expression:

$$l_0 = \frac{k_3[\text{LH}]}{k_9[\text{Fe}^{2+}]} \quad (11.19)$$

(l_0 – chain length in the absence of inhibitors other than iron).

It can be seen from this equation that the chain length decreases with increasing iron concentration, in full accordance with experimental data (see Fig. 11.10) (Cheremisina et al. 1972).

It is interesting to compare the expression Eq. 11.19 with the exponent γ in Eq. 11.8:

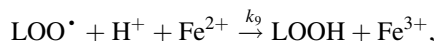
$$\begin{aligned} \gamma &= \frac{k_3[\text{LH}]k_p\nu}{k_9} - k_p[\text{Fe}^{2+}] = k_p[\text{Fe}^{2+}] \\ &\times \left(\frac{k_3[\text{LH}]\nu}{k_9[\text{Fe}^{2+}]} - 1 \right) = k_p[\text{Fe}^{2+}](\nu l_0 - 1) \end{aligned} \quad (11.20)$$

In other words, the longer the oxidation chain (l or, in the absence of InH, l_0) and the higher the chain nucleation rate ($k_p[\text{Fe}^{2+}]\nu$), the faster the chain oxidation develops.

Although an increase in iron concentration increases the rate of new chain formation due to hydroperoxide decomposition:



it also leads to a reduction in the chain length (Eqs. 11.18 and 11.19) due to chain termination:



so that as a result, the rate of the process development (γ) with increasing $[\text{Fe}^{2+}]$ may decrease and even become negative

One might wonder what the chain length would be if iron ions inhibited the process? Comparing Eq. 11.19 with Eqs. 11.12 and 11.13, we get:

$$\frac{k_3[\text{LH}]\nu}{k_9[\text{Fe}^{2+}]} = \nu l_0 > 1 \quad \text{– activation} \quad (11.21)$$

$$\nu l_0 < 1 \quad \text{– inhibition} \quad (11.22)$$

If $\nu = 1$, then we get an obvious conclusion that the process self-acceleration in the presence of Fe^{2+} corresponds to a chain length greater than unity, and at $l < 1$, the chains

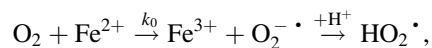
are predominantly terminated and the process as a whole is inhibited.

Thus, an increase in Fe^{2+} concentration leads to a reduction in the length of lipid oxidation chains, and at iron concentrations greater than the critical value $\frac{k_3[\text{LH}]\nu}{k_9}$ the chain length becomes less than unity, and peroxidation from self-accelerating turns into self-extinguishing.

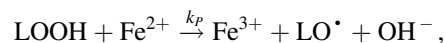
11.6.3 Summary

Altogether, the peroxidation complex kinetics and equally complex dependence on the initial conditions are elegantly explained in simple kinetic models. In the considered model systems, it is the Fe^{2+} ions that largely determine the course of peroxidation:

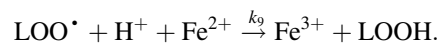
- Chain initiation at one-electron oxygen reduction:



- Chain branching at peroxide decomposition:



- And chain termination at reactions with peroxide radicals:



The first two (pro-oxidant) reactions result in chemiluminescence (through a chain of subsequent reactions – see Sect. 11.5), the last one (antioxidant) results in its suppression. This picture determines the following conditions:

- At $[\text{Fe}^{2+}] < 10^{-5} - 10^{-4}$, chain termination occurs mostly due to radical recombination, and is accompanied by CL.
- At $[\text{Fe}^{2+}] > 10^{-5} - 10^{-4}$ M, chain termination occurs mainly on iron ions; the CL light sum decreases, the CL decay becomes faster and exponential; the peroxidation chain length is reduced.

Thus, changes in iron concentration actually trigger the process from self-accelerating at low concentrations, to self-extinguishing at high total or local concentrations. All this is well explained by the above kinetic scheme.

11.7 Summary

Altogether, lipid peroxidation in biological systems repeats the key features of hydrocarbon peroxidation:

- Free-radical chain character
- Demand for oxygen
- Production of hydroperoxides
- Chemiluminescence

Similarly to unsaturated hydrocarbons, CL is generated in course of two processes:

- Russell-type peroxy radical recombination
- Peroxy radical cyclization into dioxetanes

Accordingly, the sources of CL are both carbonyl compounds and singlet oxygen, both as monomol and probably dimol complexes.

Transition metals are very important participants in this process, serving as both pro- and antioxidants, depending on their concentration. However, in real biological systems, the free iron ions considered above are mostly absent and replaced with other catalysts – heme molecules and various ROS-generating and ROS-utilizing enzymes, mostly associated with transition metals (see Chap. 14). This definitely modifies the reaction scheme, and reactions with Fe^{2+} have to be replaced with a set of reactions with different enzymes and other substances. Anyway, the general features are preserved, and the above model data appear very helpful in understanding more complex biological systems.

References

- Ahnström G, Natarajan AT (1960) Chromosome Breakage induced by electrolytically produced Free Radicals. *Nature* 188 (4754):961-962. <https://doi.org/10.1038/188961a0>
- Alberts B, Johnson AD, Lewis J, Morgan D, Raff M, Roberts K, Walter P (2015) *Molecular Biology of the Cell*. 6th Edition. Garland Science, Taylor and Francis Group, New York
- Badings HT (1960). *Nethese Milk Dairy J* 14:215
- Bateman L, Gee G (1948) A kinetic investigation of the photochemical oxidation of certain non-conjugated olefins. *Proc Roy Soc A* 195 (1042):376-391
- Belyakov VA, Vasil'ev RF, Fedorova GF (1983) Chemiluminescence in the oxidation of unsaturated organic compounds in solution. *B Acad Sci Ussr Ch+* 32 (12):2429–2437. <https://doi.org/10.1007/BF00954469>
- Berkowitz J, Ellison GB, Gutman D (1994) Three methods to measure RH bond energies. *The Journal of Physical Chemistry* 98 (11): 2744–2765. <https://doi.org/10.1021/j100062a009>
- Bernheim F, Bernheim MLC, Wilbur KM (1948) The reaction between thiobarbituric acid and the oxidation products of certain lipides. *J Biol Chem* 174:257. <https://pubmed.ncbi.nlm.nih.gov/18914082/>
- Bernheim F, Wilbur KM, Fitzgerald DB (1947) Studies on a new metabolite and its oxidation in the presence of ascorbic acid. *J Gen Physiol* 33:195. <https://doi.org/10.1085/jgp.31.2.195>
- Bieri JG, Anderson AA (1960) Peroxidation of lipids in tissue homogenates as related to vitamin E. *Arch Biochem and Biophys* 90:105. [https://doi.org/10.1016/0003-9861\(60\)90619-6](https://doi.org/10.1016/0003-9861(60)90619-6)
- Brash AR (2000) Autoxidation of methyl linoleate: identification of the bis-allylic 11-hydroperoxide. *Lipids* 35 (9):947–952. <https://doi.org/10.1007/s11745-000-0604-0>
- Bray RC (1969) Electron paramagnetic resonance in biochemistry. *Febs Lett* 5:1. [https://doi.org/10.1016/0014-5793\(69\)80278-4](https://doi.org/10.1016/0014-5793(69)80278-4)
- Brzhevskaya ON, Nedelina OS (1969) Investigation of the energy-dependent processes in metabolizing mitochondria by the EPR method. *Biophysics* 14 (3):472–476
- Buzas SK, Gol'dshtein NI, Kochur NA, Ivanov II, Petrusevich YM (1970). In: *Fiziko-khimicheskiye mekhanizmy zlokachestvennogo rosta*. Trudy MOIP [Physico-chemical mechanisms of malignant growth. MOIP Reports], vol 32. p 38
- Carpenter MP, Kitabchi AE, McCay PB, Caputto R (1959) The activation by tocopherol and other agents of ascorbic acid synthesis by liver homogenates from vitamin E-deficient rats. *J Biol Chem* 234: 2814. <https://pubmed.ncbi.nlm.nih.gov/13807882/>
- Cheremisina ZP, Olenov VI, Vladimirov Iu A (1972) Chemiluminescence coupled with the formation of lipid peroxides in biological membranes-VIII. Reactions of Fe^{++} and lipid peroxides at the stage of the "fast flash" of luminescence. *Biophysics* 17 (4):631–637
- Chetverikov AG, Kalmanson AE, Kharitonov IG, Blyumenfel'd LA (1964) Investigation by the EPR method of free radicals formed in biological specimens during enzymatic reactions. *Biophysics* 9 (1): 6–13
- Corwin LM (1962) Studies on peroxidation in vitamin E-deficient rat liver homogenates. *Arch Biochem and Biophys* 97 (1):51
- Ellis GW (1950) Autoxidation of the fatty acids. 3. The oily products from elaidic and oleic acids. The formation of monoacyl derivatives of dihydroxystearic acid and of $\alpha\beta$ -unsaturated keto acids. *Biochem J* 46:129. <https://doi.org/10.1042/bj0460129>
- Ellis R, Gaddis AM, Currie GT (1961) Carbonyls in Qxidizing Fat. IV. The Role of Various Fatty Acid Components in Carbonyl Generation. *J Food Sci* 26:131. <https://doi.org/10.1111/j.1365-2621.1961.tb00782.x>
- Emanuel NM, Knorre DG (1962) *Course of chemical kinetics*. Vyschaja shkola, Moscow
- Emanuel NM, L'askovkaya YN (1961) Inhibition of lipid oxidation processes (In Russian) [Tormozhenije protsessov okislenija zhirov]. Pishcheprozizdat, Moscow
- Evans CD In: *Chem. Symposium, 1961*. Campbell Soup. Co., Camden, N. Y., p 123
- Farmer EH (1946) Peroxidation in relation to olefinic structure. *Trans Faraday Soc* 42:228. <https://doi.org/10.1039/TF9464200228>
- Farmer EH, Bloomfield GF, Sundralingam A, Sutton DA (1942) The course and mechanism of autoxidation reactions in olefinic and polyolefinic substances, including rubber. *Trans Faraday Soc* 38: 348. <https://doi.org/10.1039/TF9423800348>
- Farmer EH, Koch HP, Sutton DA (1943) The course of autoxidation reactions in polyisoprenes and allied compounds. Part VII. Rearrangement of double bonds during autoxidation. *J Chem Soc* 541. <https://doi.org/10.1039/JR9430000541>
- Farmer EH, Sutton DA (1943) The course of autoxidation reactions in polyisoprenes and allied compounds. Part IV. The isolation and constitution of photochemically-formed methyl oleate peroxide. *J Chem Soc* 119. <https://doi.org/10.1039/JR9430000119>
- Farmer EH, Sutton DA (1946) The course of autoxidation reactions in polyisoprenes and allied compounds. Part XI. Double bond movement during the autoxidation of a mono-olefin. *J Chem Soc* 10. <https://doi.org/10.1039/JR9460000010>
- Fedorova GF, Trofimov AV, Vasil'ev RF, Veprintsev TL (2007) Peroxy-radical-mediated chemiluminescence: mechanistic diversity and fundamentals for antioxidant assay. *Arkivoc* 8:163–215. <http://dx.doi.org/10.3998/ark.5550190.0008.815>
- Fenell AJ, Skellon JH (1954) *J Chem Soc*:3414

- Forthney SR, Linn WS (1964) Role of ascorbate and cysteine on swelling and lipid peroxidation in rat liver mitochondria. *Arch Biochem and Biophys* 104 (2):241
- Frankel EN In: Symposium on Foods: Lipids and their Oxidation, Westport, Connecticut, 1962. AVI Publ. Co. Inc., p 51
- Frankel EN, Evans CD, Mc Connell DG, Selke E, Dutton HJ (1961) Autoxidation of Methyl Linolenate. Isolation and Characterization of Hydroperoxides. *J Org Chem* 26:4663. <https://doi.org/10.1021/jo01069a112>
- Free radicals in biology (In Russian) (1963). Inostrannaya literatura (Foreign literature), Moscow
- Harayama T, Riezman H (2018) Understanding the diversity of membrane lipid composition. *Nat Rev Mol Cell Bio* 19:281–296. <https://doi.org/10.1038/nrm.2017.138>
- Hashimoto S, Recknagel RO (1968) No chemical evidence of hepatic lipid peroxidation in acute ethanol toxicity. *Exper Mol Pathol* 8:225
- Hawkins EGE (1961) Organic Peroxides: Their Formation and Reactions. General and Industrial chemistry series D van Nostrand and Co, Princeton, New Jersey
- Haywood R (2013) Spin-Trapping: Theory and Applications. In: Roberts GCK (ed) *Encyclopedia of Biophysics*. pp 2447–2453. <https://doi.org/10.1007/978-3-642-16712-6>
- Hochstein P, Ernster L (1963) Adp-Activated Lipid Peroxidation Coupled to the Tpnh Oxidase System of Microsomes. *Biochem Biophys Res Commun* 12:388–394
- Hochstein P, Nordenbrand K, Ernster L (1964) Evidence for the involvement of iron in the ADP-activated peroxidation of lipids in microsomes and mitochondria. *Biochem Biophys Res Commun* 14: 323–328
- Hochstein P, Ernster L (1963) ADP-activated lipid peroxidation coupled to the TPNH. *Biochem and Biophys Res Commun* 12 (6):388
- Holman RT, Elmer OC (1947). The rates of oxidation of unsaturated fatty acids and esters. *J Amer Oil Chemists' Soc* 24:127. <https://link.springer.com/article/10.1007/BF02643258>
- Howard JA, Ingold KU (1968) Self-reaction of sec-butylperoxy radicals. Confirmation of the Russell mechanism. *Journal of the American Chemical Society* 90 (4):1056–1058. <https://doi.org/10.1021/ja01006a037>
- Hunter FE, Jr., Gebicki JM, Hoffsten PE, Weinstein J, Scott A (1963) Swelling and lysis of rat liver mitochondria induced by ferrous ions. *The Journal of biological chemistry* 238 (2):828–835
- Hunter FE, Jr., Scott A, Hoffsten PE, Guerra F, Weinstein J, Schneider A, Schutz B, Fink J, Ford L, Smith E (1964a) Studies on the Mechanism of Ascorbate-Induced Swelling and Lysis of Isolated Liver Mitochondria. *The Journal of biological chemistry* 239:604–613
- Hunter FE, Jr., Scott A, Weinstein J, Schneider A (1964b) Effects of Phosphate, Arsenate, and Other Substances on Swelling and Lipid Peroxide Formation When Mitochondria Are Treated with Oxidized and Reduced Glutathione. *The Journal of biological chemistry* 239: 622–630
- Ingram DJE (1969) Biological and biochemical applications of electron spin resonance Adam Hilger, London
- IUPAC (1997) Compendium of Chemical Terminology, 2nd ed. (the "Gold Book"). In: A. D. McNaught AW (ed). <https://doi.org/10.1351/goldbook>.
- Ivanov II, Petrusevich YM (1965) Study of chemiluminescent spectra of unsaturated fatty acids and some biolipids (In Russian). *Nauchnyje Doklady Vyschej Shkoly Biologicheskije nauki (Scientific Reports of higher schools Biological Sciences)* 3 (1):81–83
- Ivanov II, Petrusevich YM (1966) Study of chemiluminescent spectra of unsaturated fatty acids and some biolipids (In Russian). In: *Svobodnoradikal'nye protsessy v biologicheskij sistemah. Trudy MOIP [Free-Radical Processes in Biological Systems. MOIP Reports]*, vol 16. pp 13–15
- Janzen EG, Blackburn BJ (1968) Detection and identification of short-lived free radicals by an electron spin resonance trapping technique. *J Am Chem Soc* 90 (1):5909–5910. <https://doi.org/10.1021/ja01023a051>
- Kalmanson AE (1963). In: *Uspekhi biologicheskoy khimii*, vol 5. AN SSSR Publishing House, Moscow, p 289
- Karnojitzky V, Vial C (1966) *Prod Probl Pharm* 21:245
- Kayushin LP, L'vov KM, Pulatova MK (1970) Issledovaniye paramagnitnyh tsevtrov obluchennyh belkov (Study of paramagnetic centers of irradiated proteins). Nauka, Moscow
- Kern W, Willersin H (1955) *Angew Chem* 67:573
- King G (1956) A quantitative study of the autoxidation products of oleic acid. *J Chem Soc*:587
- Knight HB, Colemann JE, Swern D (1951). *J Amer Oil Chemists's Soc* 28:498
- Knowles PF, Gibson JF, Pick FM, Bray RC (1969) Electron-spin-resonance evidence for enzymic reduction of oxygen to a free radical, the superoxide ion. *The Biochemical journal* 111 (1):53–58
- Kohn HI, Liversedge M (1944) On a new aerobic metabolite whose production by brain is inhibited by apomorphine, emetine, ergotamine, epinephrine, and menadione. *J Pharmacol Methods* 82:292
- Korchagina MV, Vladimirov YA In: Simpozium "Svobodnoradikal'nyje sostoyaniya i ih rol' pri luchevom porazhenii i zlokachestvennom roste" (Symposium "Free-radical states and their role in radiation injury and malignant growth". 5–8 January". M., 1971, crp. 49, 5–8 January 1971. p 49
- Kozlov YP (1969). In: Kozlov YP (ed) *Fiziko-khimija lucheвого porazheniya [Physics and Chemistry of radiation injury]* (In Russian). Moscow University Press, Moscow, p 30
- Kudryashev YB (1960) Role of lipid radiotoxins in radiation toxic effect /Y.B. Kudryashev // *Radiotoxins*. - Moscow: Atomizdat, 1966. - Pp. 105–118
- Kudryashev YB, Mal'ts V, Goncharenko YN, Kakushkina ML, Lomsadze BA, Wen'-Dyuan' S, Syuey Yuj-hua, Dzen'-lyan' C (1961) The toxic effect of oleic acid and its oxidation products. *Radiobiologiya* 1 (1):78–94
- L'vova OF (1967) Study of ultraweak luminescence in homogenates, pulps and suspensions of liver mitochondria: Cand. of Med. Sci. Dissertation. Moscow
- L'vova OF, Vladimirov YA (1966) Ultra-weak luminescence of mitochondria and its relation to biochemical processes (In Russian). *Svobodnoradikal'nye protsessy v biologicheskij sistemah Trudy MOIP [Free-Radical Processes in Biological Systems MOIP Reports]* 16:214–217
- Lemon HW, Kirby EM, Knapp RM (1951). *Canad J Techol* 29:523
- Lundberg WO In: Symposium on Foods: Lipids and their Oxidation, Oregon, 1961. AVI Publ. Co., Inc., p 31
- Machlin LJ In: Symposium on Foods. Lipids and their Oxidation, Oregon, 1961. p 255
- Marzoev AI, Roshchupkin DI, Vladimirov YA In: Simpozium "Svobodnoradikal'nyje sostoyaniya i ih rol' pri luchevom porazhenii i zlokachestvennom roste" (Symposium "Free-radical states and their role in radiation injury and malignant growth", 5-8 January 1971. p 69
- Marzoev AI, Roshchupkin DI, Vladimirov YA (1973) Effect of UV light on biological membranes. II. Effect of irradiation on the chemiluminescence of mitochondria (In Russian). *Biofizika+* 18 (2): 258–263
- McKnight RC, Hunter FE, Oehlert WH (1965) Mitochondrial membrane ghosts produced by lipid peroxidation induced by ferrous ion. I. Production and general morphology. *J Biol Chem* 240: 3439. <https://pubmed.ncbi.nlm.nih.gov/14321385/>
- Mellors A, Tappel AL (1966). Quinones and quinols as inhibitors of lipid peroxidation. *Lipids* 1:282. <https://doi.org/10.1007/BF02531617>

- Miyamoto S, Martinez GR, Medeiros MHG, Di Mascio P (2003) Singlet molecular oxygen generated from lipid hydroperoxides by the Russell Mechanism: Studies using 18O-labeled linoleic acid hydroperoxide and monomol light emission measurements. *Journal of the American Chemical Society* 125 (20):6172–6179. <https://doi.org/10.1021/ja029115o>
- Nakano M, Takayama K, Shimizu Y, Tsuji Y, Inaba H, Migita T (1976) Spectroscopic Evidence for the Generation of Singlet Oxygen in Self-Reaction of sec-Peroxy Radicals. *Journal of the American Chemical Society* 98 (7):1974–1975. <https://doi.org/10.1021/ja00423a060>
- Neyfakh EA (1963). In: Trudy 8 Mezhdunarodnogo Protivorakovogo Kongressa (Proceedings of 8th International Anticancer Congress), vol 2. Medgiz, Moscow, p 141
- Nilsson R (1969a). *Biochim et biophys acta* 184:237
- Nilsson R (1969b) On the role of free radicals and hydrogen peroxide in some biological oxidations. *Roy. Univ., Stockholm*
- O'Brien PJ (1969) Intracellular mechanisms for the decomposition of a lipid peroxide. I. Decomposition of a lipid peroxide by metal ions, heme compounds, and nucleophiles. *Canad J Biochem* 47:485. <https://doi.org/10.1139/o69-076>
- Ottolenghi A (1959) Interaction of ascorbic acid and mitochondrial lipides. *Arch Biochem and Biophys*, 79:355
- Perkins EQ (1960). *Food Technol* 14:508
- Polivoda AI, Sekamova EN (1962) [Ultraweak luminescence (450–700 mmk) of surviving and homogenized liver tissue in normal conditions and following the action of ionizing radiation]. *Radiobiologiya* 2 (6):801–810
- Porter NA, Mills KA, Carter RL (1994) A Mechanistic Study of Oleate Autoxidation: Competing Peroxyl H-Atom Abstraction and Rearrangement. *Journal of the American Chemical Society* 116 (15): 6690–6696. <https://doi.org/10.1021/ja00094a026>
- Potapenko AJ, Roshchupkin DI, Kogon YA, Vladimirov YA (1972) Study of the effects of ultraviolet light on biomembranes. Registration of electroconductivity of biomolecular phospholipid membranes (In Russian). *Doklady AN SSSR (Rep Acad Science USSR)* 202 (4): 882–885
- Pratt DA, Mills JH, Porter NA (2003) Theoretical calculations of carbon-oxygen bond dissociation enthalpies of peroxy radicals formed in the autoxidation of lipids. *Journal of the American Chemical Society* 125 (19):5801–5810. <https://doi.org/10.1021/ja034182j>
- Privett OS, Nickell EC (1959) Determination of Structure and Analysis of the Hydroperoxide Isomers of Autoxidized Methyl Oleate. *Fette, Seifen, Anstrichmittel* 61:842. <https://doi.org/10.1002/lipi.19590611003>
- Recknagel RO, Ghoshal AK (1966) Lipoperoxidation as a vector in carbon tetrachloride hepatotoxicity. *Lab Invest* 15:132
- Roshchupkin DI, Marzoev AI, Vladimirov YA (1973) Effect of UV-radiation on biological membranes. I. Disruption of oxidative phosphorylation and changes in protein state during radiation of isolated mitochondria (In Russian). *Biofizika* 18 (1):83–88
- Santiago E, Guerra F, Macarulla JM (1968a). Effect of ascorbate on phospholipids during mitochondrial swelling and lysis. *Rev esp fisiol* 24:25
- Santiago E, Vazquez JJ, Guerra F, Macarulla JM (1968b). *Rev esp fisiol* 24:31
- Saprin AN, Piette LH (1977) Spin trapping and its application in the study of lipid peroxidation and free radical production with liver microsomes. *Archives of biochemistry and biophysics* 180 (2): 480–492. [https://doi.org/10.1016/0003-9861\(77\)90063-7](https://doi.org/10.1016/0003-9861(77)90063-7)
- Sumarukov GV (1970) Okislitelnoje ravnovesije i radiochuvstvitel'nost' organizmov [Oxidation balance and radio-sensitivity of organisms] (In Russian). Atomizdat, Moscow
- Suslova TB (1971) Chemiluminescent study of lipid peroxidation in mitochondrion membranes and oleic acid solutions., 2 Med Inst, Moscow
- Suslova TB, Olenev VI, Korchagina MV, Vladimirov YA (1970) Chemiluminescence connected with the formation of lipid peroxides in biological membranes. IV. Role of the change of iron valency in these processes (In Russian). *Biofizika* 15 (4):622–628
- Suslova TB, Olenev VI, Vladimirov YA (1968) Role of iron ions in chemiluminescence of lipids (In Russian). *Biofizika* 13 (4):723–726
- Swern D, Colemann JE, Knight HB, Riccinti C, Willits CO, Eddy CR (1953). *J Amer Chem Soc* 75:3135
- Tallman KA, Rector CL, Porter NA (2009) Substituent effects on regioselectivity in the autoxidation of nonconjugated dienes. *Journal of the American Chemical Society* 131 (15):5635–5641. <https://doi.org/10.1021/ja900040d>
- Tappel AL (1953). Oxidative fat rancidity in food products. I. Linoleate oxidation catalyzed by hemin, hemoglobin, and cytochrome c. *Food Res* 18:560. <https://doi.org/10.1111/j.1365-2621.1953.tb17751.x>
- Tappel AL (1955). Unsaturated lipid oxidation catalyzed by hematin compounds. *J Biol Chem* 217:721. <https://pubmed.ncbi.nlm.nih.gov/13271434/>
- Tappel AL, Zalkin H (1959) Lipid peroxidation in isolated mitochondria. *Arch Biochem and Biophys* 80:326. [https://doi.org/10.1016/0003-9861\(59\)90258-9](https://doi.org/10.1016/0003-9861(59)90258-9)
- Tarusov BN (1954) Fundamentals of biological effects of radioactive radiation. Medgiz, Moscow
- Tarusov BN (1957). *Uspekhi Sovremennoi Biologii (Advances in Contemporary Biology)* 44:173
- Tarusov BN (1962) Pervichnyje protsessy luchevego porazhenija (Primary processes of radiation injury) (In Russian). Atomizdat, Moscow
- Tarusov BN, Polivoda AI, Zhuravlev AI (1961a) Detection of chemiluminescence in the liver of irradiated mice (In Russian). *Radiobiologiya* 1 (1):150–151
- Tarusov BN, Polivoda AI, Zhuravlev AI (1961b) Study on ultra-weak spontaneous luminescence of animal cells (in Russian). *Biofizika (Russ)* 6 (4):490–492
- Tarusov BN, Polivoda AI, Zhuravlev AI, Sekamova EN (1962) Ultraweak spontaneous luminescence in animal tissue (in Russian). *Tsitologiya* 4:696–699
- Tarusov BN, Zhuravlev AI (1965) Biochemiluminescence of lipids (In Russian). In: *Bioluminescenciya. Trudy MOIP [Bioluminescence. MOIP Reports]*, vol 21. Nauka, Moscow, p 125
- Thiele EH, Huff JW (1960). *Arch Biochem and Biophys* 88:203
- Timmins GS, Dos Santos RE, Whitwood AC, Catalani LH, Di Mascio P, Gilbert BC, Bechara EJJ (1997) Lipid peroxidation-dependent chemiluminescence from the cyclization of alkyperoxy radicals to dioxetane radical intermediates. *Chemical research in toxicology* 10 (10):1090–1096. <https://doi.org/10.1021/tx970075p>
- Vasil'ev RF, Karpukhin ON, Shlyapintokh VY (1961) An apparatus for measuring weak light fluxes (In Russian). *Zhurnal Fizicheskoi Khimii [Journal of Physical Chemistry]* 35 (2):461
- Vladimirov YA (1965) Fotokhimiya i lyuminescenciya belkov [Photochemistry and luminescence of proteins] (In Russian). Nauka, Moscow
- Vladimirov YA (1967) Ultraweak luminescence accompanying biochemical reactions (English translation of "Sverkhslabye svecheniya pri biokhimicheskikh reaktsiyah" USSR Academy of Sciences, Institute of Biological Physics. Izdatel'stvo "Nauka" Moscow, 1966). NASA, C.F.S.T.I., Springfield, Vermont
- Vladimirov YA, Archakov AI (1972) Lipid peroxidation in biological membranes [Perekisnoe okislenie lipidov v biologicheskikh membranakh] (In Russian). Nauka, Moscow
- Vladimirov YA, Gutenev PI, Kuznetsov PI (1973) Mathematical modelling of kinetics of chain oxidation of biomembrane lipids in presence of Fe²⁺ ions. *Biofizika* 18 (6):1024–1029
- Vladimirov YA, Korchagina MV, Olenev VI (1971) Chemiluminescence accompanied by the formation of lipid peroxides in biological

- membranes. VII. Reaction accompanied by luminescence (In Russian). *Biofizika* 16 (5):952–955
- Vladimirov YA, L'vova O F, Cheremisina ZP (1966) Ultra-weak luminescence of mitochondria and its relation to enzymic oxidation of lipids (In Russian). *Biokhimiia* 31 (3):507–515
- Vladimirov YA, L'vova OF (1964) Ultraweak luminescence and oxidative phosphorylation in mitochondria (In Russian). *Biofizika* 9 (4): 506–507
- Vladimirov YA, L'vova OF (1965) Study of ultraweak luminescence of homogenates and liver pulp (In Russian). In: Frank GM (ed) *Biofizika kletki* [Biophysics of the Cell]. Nauka, Moscow, pp 74–83
- Vladimirov YA, Litvin FF (1963) The nature of ultraweak luminescence and the role of excited states of molecules in biological systems (In Russian). In: *Bioluminesentsiya. Simpozium 3-6 iyunya 1963. Tezisy dokladov.* [Bioluminescence. Symposium 3-6 June 1963. Summaries of Reports]. MOIP, Moscow, p 7
- Vladimirov YA, Litvin FF (1964) *Fotobiologiya i spektral'nyye metody issledovaniya. Praktikum po obshchey biofizike.* [Photobiology and Spectral Research Methods. Workbook on General Biophysics] (In Russian). vol 8. Vysshaya shkola, Moscow
- Vladimirov YA, Proskurnina EV, Izmailov DY, Sozarukova MM, Dzhadtoeva AA, Vladimirov GK, Machneva TV (2017) Sources and targets of free radicals in human blood. MAX Press, Moscow
- Vladimirov YA, Roshchupkin DI, Fesenko EE (1970a) Mechanism of ultraviolet radiation effects on proteins (In Russian). *Biofizika* 15 (2):254–264
- Vladimirov YA, Roshchupkin DI, Fesenko EE (1970b) Photochemical reactions in amino acid residues and inactivation of enzymes during U.V.-irradiation. A review. *Photochem Photobiol* 11 (4):227–246
- Vladimirov YA, Suslova TB, Olenev VI (1969a) Chemiluminescence associated with the formation of lipid peroxides in biological membranes. II. The role of Fe²⁺ in the development of chain oxidation of lipids and of ultra-weak luminescence (In Russian). *Biofizika* 14 (5):836–845
- Vladimirov YA, Suslova TB, Olenev VI, Cheremisina ZP (1969b). In: *Mitokhondrii, Biokhimicheskiye funktsii v sisteme kletochnykh organell* [Mitochondria. Biochemical functions in the system of cell organelles]. Nauka, Moscow, p 203
- Vladimirov YA, Tafel'shtein EE, Kozlov Iu P (1969c) [Effect of alpha-tocopherol on the chemiluminescence of mitochondria in the presence of Fe²⁺]. *Doklady Akademii nauk SSSR* 188 (5):1163–1165
- Voeikov VL (2010) Reactive oxygen species, water, photons and life. *Riv Biol* 103 (2–3):321–342
- Voeikov VL, Novikov CN (1998) Peculiarities of luminol- and lucigenin-dependent photon emission from nondiluted human blood. Propagation in Tissues III, SPIE Proceedings 3194:328–333. <https://doi.org/10.1117/12.301071>
- Wilbur KM, Bernheim F, Shapiro OW (1949) The thiobarbituric acid reagent as a test for the oxidation of unsaturated fatty acids by various agents. *Arch Biochem and Biophys* 24:305
- Wills ED (1965) Mechanism of lipid peroxide formation in tissues. Role of metals and haematin proteins in the catalysis of unsaturated fatty acids. *Biochim et Biophys Acta* 98 (2):238
- Wills ED (1966) Mechanisms of lipid peroxide formation in animal tissues. *Biochem J* 99:667. <https://doi.org/10.1042/bj0990667>
- Wyard SJ (1968) Electron spin resonance spectroscopy of animal tissues. *Proc Roy Soc A302*:355. <https://doi.org/10.1098/rspa.1968.0021>
- Yamazaki I, Piette LH (1963). The mechanism of aerobic oxidase reaction catalyzed by peroxidase. *Biochim et biophys acta* 77: 47. [https://doi.org/10.1016/0006-3002\(63\)90468-2](https://doi.org/10.1016/0006-3002(63)90468-2)
- Yin H, Xu L, Porter NA (2011) Free radical lipid peroxidation: mechanisms and analysis. *Chemical reviews* 111 (10):5944–5972. <https://doi.org/10.1021/cr200084z>
- Zakharova NA, Sholina SI, Kruglyakova KY, Karpukhin ON, Ananchenko SN, Limanov VY, Torgov IV, Emanuel NM (1966). *Izv Akad Nauk Otd khim nauk* 456
- Zhuravlev AI (1960) The role of antioxidants in primary radiobiological effects (In Russian). In: *Trudy simpoziuma "Rol" perekisey i kisloroda v nachal'nykh stadiyakh radiobiologicheskogo effekta* [Transactions of the Symposium "The Role of Peroxides and Oxygen in the Initial Stages of the Radiobiological Effect"]. USSR Academy of Sciences Publishing House, Moscow, p 55
- Zhuravlev AI (1962) Ultraweak chemiluminescence of antibiotics in lipids (In Russian). *Antibiotiki* 7 (11):1023
- Zhuravlev AI (1963) Lipid model of radiation injury and radioprotective prevention. In: *Primary mechanisms of biological effects of ionizing radiations*, vol 7. Acad.Sc. USSR, Moscow, pp 93–101
- Zhuravlev AI (1965a) An anomaly of lipid chemiluminescence (In Russian). In: *Bioluminesentsiya Trudy MOIP* [Bioluminescence. MOIP Reports], vol 21. Nauka, Moscow, p 133
- Zhuravlev AI (1965b) Problems on bioluminescence (In Russian). In: *Bioluminesentsiya Trudy MOIP* [Bioluminescence. MOIP Reports], vol 21. Nauka, Moscow, p 184
- Zhuravlev AI, Filippov YN, Simonov VV (1965) The mechanism of chemiluminescence of lipids (In Russian). *Biofizika (Russ)* 10 (2):246
- Zhuravlev AI, Tarusov BN (1962) The mechanism of the protective antioxidant effect of some compounds containing sulfur (In Russian). *Radiobiologiya* 2 (2):177



12.1 Introduction

As is known, proteins are the main nonwater component of practically all biological systems, accounting for definitely more than 50% (and often more than 80%) of their dry mass (see, e.g., Oh et al. 2022). Thus, they are anyway one of the main targets of any oxidative processes, including free radical (chemiluminescent) ones. And although membrane lipids were the first definitely shown source of chemiluminescence (CL, see previous chapter) (Tarusov and Zhuravlev 1965), now we know that proteins may well share with them the status of the most important substrate for free-radical oxychemiluminescence (OCL; see, e.g., Davies 2005, 2016).

In general, obviously, the more reactive a molecule or radical is, the more indiscriminate it is towards the oxidation substrate. Accordingly, the percentage of oxidizable molecules for the most reactive radicals (OH^\bullet and some others) is determined directly by their concentration, while that for less reactive species (e.g., $\text{O}_2^{\bullet-}$ or H_2O_2) is much more specific. This makes it possible to individually assess reaction rate constants for each oxidant and each of the cell compounds and correlate them with the latter's concentration.

As we know now, amino acids and proteins are oxidized by the radical chain mechanism, similar to lipids and hydrocarbons (see Chaps. 10 and 11), but with certain specificity. Their high content in the cell and the high reactivity of a number of free radicals generated within the cell make their peroxidation of utmost importance.

Interestingly, while the general statement of the first decades of CL research (the 1960s–1970s) was that all biochemiluminescence is generated by lipid peroxidation, the very first works related to biological ultraweak photon emission (UPE) – the mitogenetic research (see Chap. 2), declared cell protein reactions as its most important source.

12.2 Elements of Photophysics

Luminescence (the photon emission *per se*) can be called the opposite of photochemical processes. Therefore, one of the experimental approaches to studying photon generation at UPE processes can be the study of luminescence accompanying reverse photochemical reactions (i.e., the afterglow of light-, ultraviolet-, or γ -irradiated systems).

A molecule, hit by a quantum of exciting radiation, can be (1) electronically excited, (2) ionized, or (3) split into parts, with certain probabilities depending on its structure and the exciting quantum. This gives rise to a bunch of photochemical processes, of which here we will consider only those that are (1) reversible (not destroying chemical compounds in the system) and (2) leading to the generation of light quanta (see Table 12.1 and Fig. 12.1; see more in Chap. 5).

Thus, immediately after the end of photoexcitation, the system is left with a number of molecules in different excited states, which further relax to the ground state (S_0), or participate in different photochemical processes.

A radiant relaxation from an electron-excited state, either S_1 (Table 12.1, types 1, 3), or from T_1 (Table 12.1, type 2) is obviously a monomolecular process and thus gives an exponential decay kinetics (Wawilow and Lewschin 1926; Levshin and Vinokurov 1934; Levshin 1936; Schischlowski and Wawilow 1934). The photochemical processes (including recombination of the previously ejected electron with the remaining cation) are never monomolecular, and thus their decay kinetics is never exponential (Levshin 1936; Randall et al. 1945c). The simplest case of electron–cation recombination (Table 12.1, types 4, 5) gives an inverse power decay kinetics, being a pure biomolecular process (see, e.g., Randall et al. 1945a, b). The real decay kinetics can also be multi-component and thus more complicated, containing both monomolecular and bimolecular components with both fluorescent and phosphorescent spectra (see Nickel 1996, 1997 for an overview of these data and discussion).

I. Volodyaev (✉) · Y. A. Vladimirov
Moscow State University, Moscow, Russia

Table 12.1 Processes induced in a molecule by external illumination

| Excitation and energy migration | | Relaxation | | |
|---------------------------------|--|------------|--------------------------|--|
| Electronic excitation | $X(S_0) + h\nu_{ex} \rightarrow X(S_1)$ | 1 | Fluorescence | $X(S_1) \rightarrow X(S_0) + h\nu_{fl}$ |
| Intersystem crossing | $X(S_1) \rightarrow X(T_1)$ | 2 | Phosphorescence | $X(T_1) \rightarrow X(S_0) + h\nu_{ph}$ |
| Intersystem crossing (reverse) | $X(T_1) \xrightarrow{kT} X(S_1)$ | 3 | Delayed fluorescence | $X(S_1) \rightarrow X(T_1) \xrightarrow{kT} X(S_1) \rightarrow X(S_0) + h\nu_{fl}$ |
| Photo-dissociation | $X(S_0) + h\nu_{ex} \rightarrow X^+ + e^-$ | | Electron solvation | $X^+ + e^- \rightarrow X^+ + (e^-)_{solv}$ |
| Recombination | $X^+ + (e^-) \xrightarrow{kT} X(T_1)$ | 4 | Phosphorescence | $X^+ + (e^-)_{solv} \xrightarrow{kT} X(T_1) \rightarrow X(S_0) + h\nu_{ph}$ |
| Excitation and recombination | $X^+ + (e^-) \xrightarrow{h\nu_{IR}} X(S_1)$ | 5 | Anti-stokes fluorescence | $X^+ + (e^-)_{solv} \xrightarrow{h\nu_{IR}} X(S_1) \rightarrow X(S_0) + h\nu_{fl}$ |

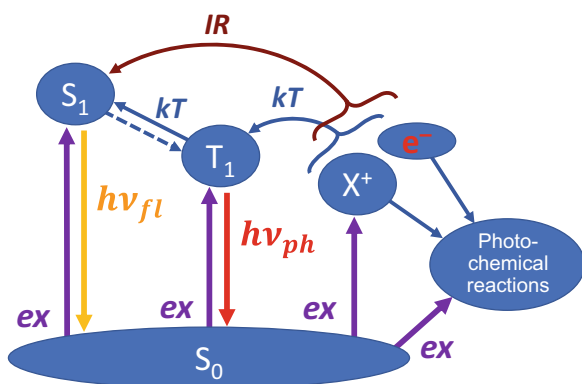


Fig. 12.1 Processes induced in a molecule by external illumination. S_0 , ground state; S_1 , singlet excited state; T_1 , triplet excited state; X^+ , radical cation formed at ejection of an electron (e^-); ex, radiative excitation; kT , thermal transitions (demanding additional energy); IR, infrared light-induced transition; $h\nu_{fl}$, fluorescence ($S_1 \rightarrow S_0$ radiative relaxation); $h\nu_{ph}$, phosphorescence ($T_1 \rightarrow S_0$ radiative relaxation)

12.3 Delayed Luminescence of Amino Acids Has Two Components

Standard fluorescence of amino acids and proteins has been known at least since the 1920s (Wels 1928) and is related to that of living cells and tissues (Wels and Jokisch 1930). The long-lasting afterglow of such systems, initially called phosphorescence (Giese and Leighton 1937), was later shown to have two distinctly different components (Debye and Edwards 1952a, b): “standard phosphorescence” and “phosphorescence of very long duration” (Table 12.2).

As one can see, the two types of photon emission can be distinguished by their decay kinetics – both the curve shape (decay function) and its dependence on temperature and pH:

- *The first type of emission* decays exponentially (suggesting that it is generated at a monomolecular reaction) and weakly depends on temperature and pH (suggesting that this reaction is the relaxation of certain electron-excited states).
- *The second type of emission* decays hyperbolically (suggesting that it is generated at a bimolecular reaction)

and has an observable duration only at very low temperatures (suggesting that this reaction is diffusion controlled, namely, recombination of certain species, formed under the action of the exciting light; at higher temperatures, it is not observed as an afterglow due to their immediate recombination).

However, the spectral characteristics of both types of emission are the same and coincide with the phosphorescence spectra of Trp and Tyr (suggesting that the final photon-generating state can be the T_1 state of these amino acids). Moreover, both types of emission are only observed in the presence of Trp or Tyr, at least as the slightest admixture (Debye and Edwards 1952a); emission from proteins coincides with that from Trp and Tyr solutions (supporting the above suggestion).

Thus, the first type of emission was identified as $T_1 \rightarrow S_0$ radiant relaxation of Trp and Tyr, excited by illumination (Debye and Edwards 1952a, b). The second type of emission was suggested to be also generated at $T_1 \rightarrow S_0$ radiant relaxation of Trp and Tyr but preceded by some kind of bimolecular process (see Wawilow and Lewschin 1926; Levshin and Vinokurov 1934; Levshin 1936; Schischlowski and Wawilow 1934; Randall et al. 1945a, b). The most probable candidate for this role is the recombination of an electron knocked out by the exciting radiation from Trp or Tyr and the remaining radical cation (analogous to simpler systems in Lewis and Lipkin 1942). This also explains its pH dependence.

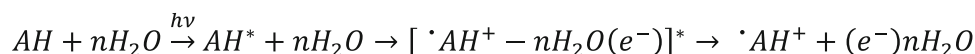
Thus, UV- or visible light-irradiated tryptophan, tyrosine, and probably phenylalanine are the sources of both phosphorescence and photochemiluminescence at the recombination of ejected electrons with radical cations. Moreover, even a slight admixture of these amino acids is sufficient for the afterglow of proteins or other amino acids (which possess no afterglow on their own), with parameters similar to those for Trp and Tyr. These processes are responsible for photo-induced delayed luminescence of amino acid (and partially protein) solutions, and most importantly (as we will see below), these are the prototypes of the terminal processes in the oxychemiluminescence of proteins.

The next section is devoted to an exact proof of the electron–radical cation mechanism.

Table 12.2 Comparison of the main qualities of two types of photo-induced photon emission from proteins

| Radiation property | Standard phosphorescence | Second component (“Phosphorescence of very long duration”) |
|---|---|--|
| Source | Trp (++), Tyr (+), Phe (?), Other amino acids – No | Trp (+, at all pH), Tyr (+, only in alkaline media), Phe – No, Other amino acids – No |
| Sensitivity to the protein composition | Trp or Tyr necessary for photon emission; Otherwise – No | |
| Spectral maxima, nm | 402; 418; 425; 440 nm | |
| Lifetime (time to reduce the intensity to 1/e of the original), s | Trp – 3 s (at all pH), Tyr – 3 s (in acidic media), < 1 s (in alkaline media), Phe – <0.1 s | 10 ² – 10 ³ s (at 77 °C) No emission (at higher T) |
| Sensitivity to temperature | Low | High: emission only at very low T |
| Sensitivity to pH | Low: observed at all pH, pH affects only the ratio of spectral maxima | High: alkaline media – intense emission (Trp, Tyr) acidic media – weak or no emission |
| Decay function | Exponent | Inverse power function |
| Mechanism | T ₁ → S ₀ relaxation | Recombination of electron with radical cation |

Based on data from Debye and Edwards (1952a, b)

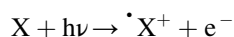


Scheme 12.1 Scheme of photoionization of organic compounds under the influence of UV. AH molecule; ^{*}AH⁺ radical cation; e⁻ solvated electron

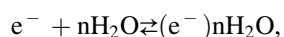
12.4 Photochemiluminescence of Deeply Frozen Trp and Tyr

12.4.1 Experimental Scheme

The simplest photochemical reaction, discussed above, is the photoionization of organic substances, forming a radical cation ^{*}X⁺ and a free electron e⁻:



The electron is immediately stabilized by solvation – reversible delocalization in a cluster of solvent molecules (Lewis and Lipkin 1942; Randall et al. 1945a, b):



which is still rather unstable (its lifetime at room temperature is ~25–50 μs (Grossweiner et al. 1963a, b)), and thus, at room temperature, can be detected only by the method of pulsed photolysis (see Grossweiner et al. 1963a, b), but not with standard phosphoroscopes (as in Debye and Edwards 1952a, b).

However, freezing the system to the temperature of liquid nitrogen (77 K) stabilizes the solvated electrons by the

so-called solvent traps (Randall et al. 1945a, b). The trapped solvated electrons slowly recombine with the radical cations, which results in a long afterglow of the irradiated frozen solutions of organic substances.

In a series of works (see, e.g., Roshchupkin and Vladimirov 1965; Vladimirov et al. 1970; Aksentzev et al. 1966), Yu.A. Vladimirov, D.I. Roshchupkin, and coauthors investigated this type of luminescence from deeply frozen amino acid solutions. The experimental scheme was as follows:

1. Amino acid solutions were frozen to 77 K.
2. The frozen solution was exposed to UV.
A UV-excited amino acid molecule donated an electron to the solvent (water) molecules, forming a radical cation ^{*}AH⁺ (Scheme 12.1). The electron transferred to the water molecule delocalized in a cluster of solvent molecules and stabilized because of the solvent’s frozen state (this state is called a solvated electron). Therefore, the radical cation and the solvated electron coexisted for some time without recombination.
3. Then the frozen solution was either heated gently or exposed to red or infrared (IR) light (λ = 600 – 990 nm). In the case of heating, the traps of the frozen solvent were destabilized, and the solvated electrons recombined with

the radical cations, generating weak luminescence in the 450 nm region (Roshchupkin and Vladimirov 1965; Vladimirov et al. 1970) (Scheme 12.2).

In the case of light exposure, luminescence was also observed, but its spectral maximum was shifted to 330 nm (Vladimirov et al. 1965) (Scheme 12.3).

Importantly, of all amino acids, both types of luminescence were observed only for tryptophan and tyrosine (Roshchupkin and Vladimirov 1965; Vladimirov et al. 1970; Aksentzev et al. 1966).

12.4.2 Energy Level Diagram

Comparing the spectra and decay times of the two observed types of luminescence, the authors developed the following diagram (Aksentzev et al. 1966) (see Fig. 12.2):

- The energy of the solvated electron is slightly lower than that of the triplet (T_1) excited amino acid molecule ${}^3\text{AH}^*$.
- Gentle heating in the first case provides the necessary activation energy for the electron to occupy T_1 , which can further radiantly relax to S_0 , generating a quantum of phosphorescence ($h\nu_{450\text{ nm}}$).
- The external IR light in the second case excites the solvated electron to the first excited level (e^-)*, lying above S_1 of the amino acid (${}^1\text{AH}^*$).
- Radiant relaxation from S_1 to S_0 is accompanied by generation of a fluorescence quantum ($h\nu_{330\text{ nm}}$).

The corresponding kinetic scheme of the reactions taking place in the system will look like this (Table 12.3).

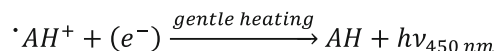
All this ideally corresponds to the above-mentioned luminescence characteristics as well as to the absorption spectra of intermediate reaction products obtained by pulsed photolysis at 89 K (Aksentzev et al. 1967).

Also, irradiation of the system with red light, along with the main fluorescence maximum ($h\nu_{330\text{ nm}}$), produces (much weaker) longer-wavelength phosphorescence ($h\nu_{450\text{ nm}}$). The intensities of the bands $h\nu_{330\text{ nm}}$ and $h\nu_{450\text{ nm}}$ correlate in the same way as in the case of optical excitation in the absorption band of amino acid molecules (Aksentzev et al. 1966), that is, the transition between the energy levels S_1 and T_1 obeys the usual laws.

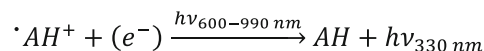
12.4.3 Conclusions

Altogether, experiments with deeply frozen amino acid solutions made it possible to separate the phases of ionization and recombination and, thus, to study in detail the electronically excited states of amino acids and their radiant relaxation.

As one can see, the luminescence during the interaction of solvated electrons with amino acid radical cations demonstrates a number of essential features similar to those of chemiluminescent systems:



Scheme 12.2 Thermo-induced UPE at recombination of an amino acid radical cation (${}^1\text{AH}^+$) with a solvated electron (e^-)



Scheme 12.3 Photo-induced UPE at recombination of an amino acid radical cation (${}^1\text{AH}^+$) with a solvated electron (e^-)

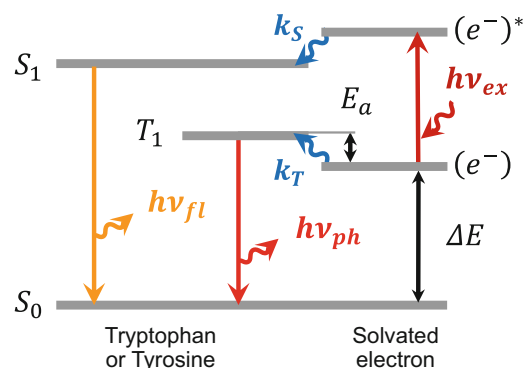


Fig. 12.2 Diagram of electronic levels and electronic transitions in aromatic amino acids irradiated by UV at 77 K. S_0 , amino acid in the ground state (AH in the text); S_1 , amino acid in the singlet excited state (${}^1\text{AH}^*$); T_1 , amino acid in the triplet state (${}^3\text{AH}^*$); (e^-) and $(e^-)^*$, solvated electron in the ground and excited states, the transition $(e^-) \rightarrow (e^-)^*$ occurs upon absorption of a quantum of red light (600–990 nm); the difference in the energy of the levels (e^-) and T_1 is equal to the thermoluminescence activation energy (E_a), the difference in the energy of the levels (e^-) and S_0 is equal to ΔE (see the text); $h\nu_{fl}$, fluorescence ($\lambda = 330\text{ nm}$), $h\nu_{ph}$, phosphorescence ($\lambda = 450\text{ nm}$), and $h\nu_{ex}$, excitation of a solvated electron by infrared or red light ($\lambda = 600 - 990\text{ nm}$)

Table 12.3 Scheme of reactions in aromatic amino acids irradiated with UV radiation at 77 K

| Process | Reaction scheme |
|--|---|
| UV-induced photoionization | $\text{AH} + h\nu_{280\text{ nm}} \rightarrow {}^1\text{AH}^+ + (e^-)$ |
| Thermo-induced phosphorescence | ${}^1\text{AH}^+ + (e^-) \xrightarrow{E_a} {}^3\text{AH}^* \rightarrow \text{AH} + h\nu_{ph}(450\text{ nm})$ |
| Photo-induced (anti-stokes) fluorescence | ${}^1\text{AH}^+ + (e^-) \xrightarrow{h\nu_{ex}(\lambda > 600\text{ nm})} {}^1\text{AH}^+ + (e^-)^* \rightarrow {}^1\text{AH}^* \rightarrow \text{AH} + h\nu_{fl}(330\text{ nm})$ |

1. An excited state arises during the recombination of previously separated charges, and an electron transferred to the acceptor molecule goes to the excited energy level rather than the ground level, making it a photon emitter.
2. The emitted photon energy ($T_1 \rightarrow S_0 + h\nu$) can exceed the average energy released during the chemical reaction (ΔE in Fig. 12.2) by the value of the activation energy E_a (see Fig. 12.2):

$$h\nu = \Delta E + E_a,$$

as was first proposed by R. Audubert (see Sect. 9.1.2).

3. Chemiluminescence from the triplet level of the emitter is more likely than from the singlet level, for reasons of a purely energetic nature.

Importantly, the UV-induced luminescence from amino acid solutions was obtained only from tyrosine and tryptophan, suggesting that these amino acids are the most likely contributors to protein chemiluminescence in living cells.

12.5 Photochemiluminescence of Amino Acids and Proteins at Room Temperature

12.5.1 Proteins and Amino Acids Luminesce at Room Temperature

At room temperature, a long-lasting photo-induced luminescence of protein solutions (at concentrations above 10 mg/ml) was occasionally found in Herberg (1958). This was in sharp contrast with the above data, where the recombinational CL was observed only at liquid nitrogen temperature (Debye and Edwards 1952a, b) or during a gentle warming from it (Roshchupkin and Vladimirov 1965; Vladimirov et al. 1970; Aksentzev et al. 1966), and any further heating led to its instant disappearance (within $10^{-9} - 10^{-6}$ s).

Moreover, in Herberg (1958) photo-induced luminescence of proteins was orders of magnitude more intense than that of pure Trp and Tyr, contrary to Debye and Edwards (1952a, b), where they practically coincided in intensity and dynamics.

Thus, the afterglow of proteins in Herberg (1958) appeared to be a more complicated phenomenon than the recombinational CL above (Sects. 12.3 and 12.4).

Similar phenomena – the long-lasting afterglow of irradiated proteins and amino acid solutions – were investigated by the groups of S.V. Konev (Konev and Katibnikov 1961; Katibnikov and Konev 1962), N.M. Emmanuel (Sapezhinskii et al. 1964; Sapezhinskii and Emanuel' 1965; Sapezhinskii et al. 1963; Sapezhinskii and Dontsova 1973), J. Slawinski (Slawiński et al. 1980), and

others. The solutions were preirradiated with UV (Sapezhinskii and Dontsova 1973; Sapezhinskii et al. 1964; Slawiński et al. 1980), γ -radiation (Sapezhinskii et al. 1963), or X-rays (Sapezhinskii et al. 1964), and the afterglow was observed for 5–15 min or more (up to several hours) at room temperature.

In some works (e.g., Sapezhinskii et al. 1964), the afterglow decay was described by hyperbolic functions, suggesting a bimolecular process – supposedly, recombination of radicals (as the lifetime of solvated electrons at room temperature was too low to consider recombination with them – see Sects. 12.3 and 12.4). In other works (Sapezhinskii et al. 1963; Sapezhinskii and Dontsova 1973; Slawiński et al. 1980), the afterglow decay was either exponential (Sapezhinskii et al. 1963; Sapezhinskii and Dontsova 1973) or a combination of several exponents (Slawiński et al. 1980), seemingly contradicting the above data on the recombinational nature and hyperbolic kinetics of CL (see Sects. 12.3 and 12.4).

Generally speaking, exponential decay kinetics can indicate three different situations:

- A monomolecular process (as in the case of standard phosphorescence; see Sects. 12.3 and 5.2).
- A process with a monomolecular rate-limiting reaction (as suggested in Sapezhinskii and Dontsova 1973).
- A complex multicomponent process in which the primary radicals give rise to certain chain reactions, and the luminescent species are “very far” from them (Sapezhinskii and Dontsova 1973; Slawiński et al. 1980). For such systems, the kinetics can be erroneously interpreted as purely exponential, especially considering certain experimental inaccuracies.

Below, we will see that all three variants may play a certain role in the current phenomenon.

12.5.2 Free-Radical Nature of Photochemiluminescence

The mechanisms of the above photochemiluminescence were investigated by several simultaneously working groups, of which great merit belongs to the works of I.I. Sapezhinsky et al. The data obtained by the authors can be structured as follows.

12.5.2.1 The Role of Free Radicals

1. UV-, γ -, and X-ray irradiation of protein solutions generate free radicals in them and cause luminescence of the system (Gordy et al. 1955; Gordy and Shields 1958; Blyumenfel'd and Kalmanson 1957; Roshchupkin and Vladimirov 1965).

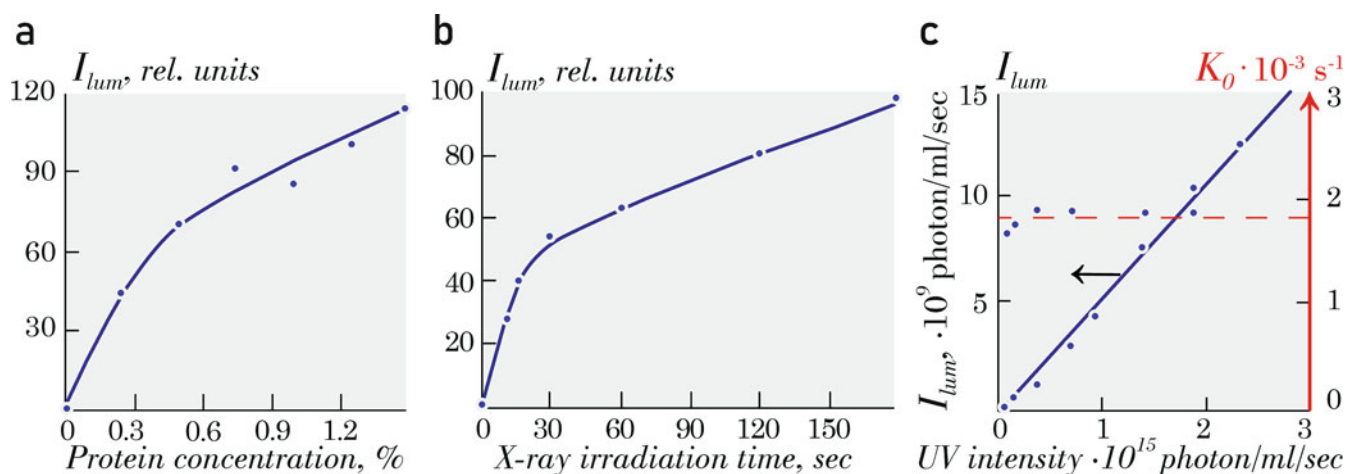


Fig. 12.3 Parameters of long-lasting afterglow of (a, b) protein or (c) dipeptide solutions. (a, b) Bovine serum albumin solutions, exposed to X-rays; (c) Gly-Trp solution, exposed to UV. (a, b) Relative luminescence intensity at 1 min after the end of irradiation as a function of (a) protein concentration and (b) duration of exposure. (c) Luminescence

intensity (blue, left y-axis) and rate constant of the rate-limiting radical reaction K_0 (red, right y-axis) as functions of the UV intensity. UV, ultraviolet. ((a, b) Adapted from Sapezhinskii et al. (1964) and (c) from Sapezhinskii and Dontsova (1973), with permission from the authors)

2. The higher the irradiation dose (both radiation intensity (Sapezhinskii and Dontsova 1973) and duration of exposure (Sapezhinskii et al. 1964)), the more radicals are generated in the system and the higher the luminescence intensity (see Fig. 12.3b, c).
3. Also, the higher the protein (or amino acid) concentration, the more radicals are generated in the system during its irradiation, and the higher the luminescence intensity (Sapezhinskii et al. 1964) (see Fig. 12.3a).
4. The addition of antioxidants (propyl gallate, isopropyl gallate, etc.) or cysteine to the system reduces the amount of free radicals in it as well as the luminescence intensity (Sapezhinskii et al. 1964).

All this suggests that photo-induced luminescence is generated with the participation of free radicals. In some works, the luminescence intensity was proportional to their concentration (Sapezhinskii et al. 1963), in others, to the square of it (Sapezhinskii et al. 1964), which reproduces the ambiguous situation with the afterglow decay. Importantly, while the luminescence intensity very well correlated with the radiation dose (Fig. 12.3), the decay dynamics (rate constant K_0 , calculated under the assumption of a unimolecular rate-limiting reaction) appeared invariable in a vast range of amino acid concentrations (Sapezhinskii and Dontsova 1973) and radiation doses (Fig. 12.3c, right). This suggests that while there can be different luminescence-generating paths, they are generally independent of irradiation regimes (within the tested conditions).

Thus, the protein photochemiluminescence also has a free-radical nature, similar to hydrocarbons (see Sect. 10.3) and lipids (see Sect. 11.3). At the same time, the inconsistency of

data on the kinetics of luminescence and its relation to the concentration of free radicals suggests a complex set of processes underlying photon generation in such systems.

12.5.2.2 Radicals Must Be Peroxide

The next important group of facts concerns oxygen.

1. Electron spin resonance (ESR) spectra of proteins irradiated in the absence of oxygen have the form of an unresolved doublet with a splitting of ~ 12 Oe (Gordy and Shields 1958). Blowing the system with oxygen converts this signal into a singlet, indicating the formation of peroxide radicals (Gordy and Shields 1958; Norman and Ginoza 1958). Thus (and expectedly), protein (amino acid) radicals also turn into a peroxide form in the presence of oxygen, similarly to hydrocarbons and lipids (see Box 10.1 in Chap. 10).
2. Protein solutions, irradiated in the presence of oxygen, give an afterglow several times more intense than in a vacuum or in an argon atmosphere (Sapezhinskii et al. 1963; Sapezhinskii and Emanuel' 1965). Blowing oxygen through a protein solution after it has been irradiated in a vacuum also gives a flash of luminescence (Sapezhinskii et al. 1963; Sapezhinskii and Emanuel' 1965). Thus, protein (amino acid) luminescence occurs precisely in the presence of peroxide radicals in the system, which also replicates the data on hydrocarbons.
3. Adding substances that selectively interact with peroxide radicals (e.g., ionol) decreases the system luminescence by several times (Sapezhinskii et al. 1963).

All this suggests that the radicals responsible for luminescence are specifically peroxy radicals (as for hydrocarbons

and fatty acids, see Chaps. 10 and 11), which is additionally confirmed by the following:

4. Irradiated proteins intensively consume oxygen. If the radicals in such a system are destroyed by heating (100 °C, 1 h; controlled by ESR), oxygen consumption stops (Sapezhinskii and Emanuel' 1965).
5. The lifespan of protein radicals is determined primarily by the penetration of oxygen into the sample (Gordy and Shields 1958). While in the presence of oxygen, the ESR spectrum lifetime is usually from several hours to 1 day, it can reach several months in anaerobic conditions (Sapezhinskii and Emanuel' 1965).
6. The reaction products include peroxides, confirming peroxidation reactions in the course of the process (Alexander et al. 1956), and carbonyl groups, likely to be formed at recombination of peroxide radicals (Alexander and Hamilton 1960).

Thus, the protein radicals formed within the system under UV-, γ -, or X-ray irradiation bind oxygen, turning it into peroxy radicals, which further participate in photon generation, supposedly including recombination reactions.

12.5.2.3 Peroxidation of Proteins is a Chain Process

The chain mechanism of peroxidation, well known for hydrocarbons and lipids (see Sects. 10.3, 11.2, and 11.3), can be additionally confirmed for fatty acids and proteins by estimating the process' total quantum yield φ_{total} (calculated as the number of consumed oxygen molecules divided by the number of disappeared radicals). For casein, φ_{total} was found to be equal to ~ 2 , and for serum albumin, ~ 3 (Sapezhinskii and Emanuel' 1965), which determines the minimal reaction chain length l_{min} equal to 2 and 3, respectively (compare Sect. 11.3.1). A decrease in the concentration of radicals also leads to an increase in l_{min} (~ 7 for casein) due to a lower probability of chain termination reactions (primarily recombination) (Sapezhinskii and Emanuel' 1965). Moreover, the real chain lengths can be many times greater than l_{min} due to the non-100% efficiency of the elementary processes within the chain as well as additional reaction paths (see more on the chain length estimation in Sects. 10.2, 11.3.1, and 11.6.2).

Thus, all the conditions necessary to prove the free-radical chain mechanism of protein peroxidation and accompanying luminescence are fulfilled – similarly to hydrocarbons and lipids. So, the photo-induced delayed luminescence of amino acids and proteins appeared to belong not only to the category of photochemiluminescence (i.e., luminescence, generated during chemical processes, induced by external light) but also to the subcategory of oxychemiluminescence

(OCL – i.e., luminescence generated at radical chain oxidation [peroxidation]).

12.5.3 Primary Mechanistic Data

12.5.3.1 Tryptophan Oxidation

A more detailed identification of the substances responsible for protein chemiluminescence is largely associated with spectral analysis. Thus, spectra of photochemiluminescence of tryptophan solutions reveal strong emission bands in the regions 380–420 nm and 460–520 nm, as well as some weaker bands around 575, 630, and 705 nm (Slawiński et al. 1980) (see Fig. 12.4).

These bands were mostly conserved for different irradiation times at 30 °C. However, irradiation at 44 °C led to the disappearance of the 380–420 nm band and the broadening of the longer wavelength bands (Slawiński et al. 1980) (compare Fig. 12.4a–d). This was associated with the photooxidation of tryptophan (observed by the gradual changes in absorption, fluorescence and phosphorescence spectra), and appearance of new oxidation products: kynurenine, kynurenic acid, *N*-formyl kynurenine, etc. (see more in Slawiński et al. 1980). Importantly, in all cases, the irradiation intensity and spectrum were similar, only the duration differed (which was shorter for Fig. 12.4d than for Fig. 12.4c). Thus, the observed photooxidation of Trp in Fig. 12.4d was caused not by irradiation per se but by free-radical processes stimulated by additional warming. Consequently, similar processes can be potentially initiated by other means, while the observed tryptophan oxidation and accumulation of oxidized species are likely to occur in non-photo-induced processes as well.

To interpret the obtained CL spectra, one needs to compare them to the standard photoluminescence spectra of tryptophan and its oxidation products (see Table 12.4). As one can see, the violet CL band (380–420 nm) matches both the tryptophan phosphorescence and fluorescence of its oxidation products; the cyan CL band (460–520 nm) fits well with the latter's phosphorescence.

Thus, besides direct Trp luminescence, the above oxidation products also participate in chemiluminescence during protein peroxidation. Indeed:

- They are chemically detected in peroxidized tryptophan solutions
- They can be witnessed by the dynamics of the system's absorption and luminescence spectra
- One can note the modified kinetics of photoinduced chemiluminescence, caused by accumulation of these products (see more in Slawiński et al. 1980 and refs. therein)

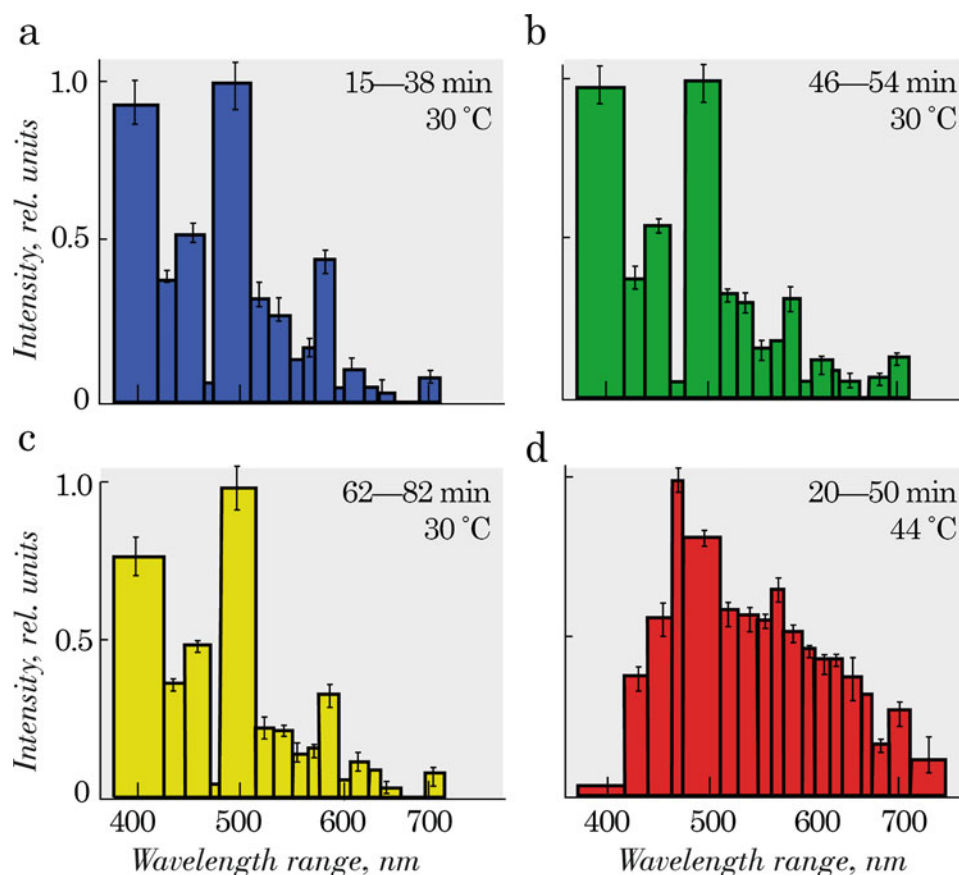


Fig. 12.4 Spectral distribution of chemiluminescence from the tryptophan solution after various irradiation times. Trp concentration 0.1 mM, pH 10.0, constant aeration. Irradiation with a high-pressure immersible ultraviolet lamp, integral intensity 10^{18} quanta/s. (a) 15–38 min irradiation (the luminescence spectrum is obtained at signal

accumulation throughout this period), temperature 30 °C; (b) 46–54 min irradiation, 30 °C; (c) 62–82 min irradiation, 30 °C; and (d) 20–50 min irradiation, 44 °C. (Adapted from Slawiński et al. (1980). Copyright 2004, with permission from John Wiley and Sons)

Table 12.4 Fluorescence and phosphorescence spectral maxima of certain products of tryptophan photooxidation

| Compound | Fluorescence λ_{\max} , nm | Phosphorescence λ_{\max} , nm |
|-----------------------------------|------------------------------------|---------------------------------------|
| Tryptophan | 350 | 433 |
| <i>N</i> -formyl kynurenine (NFK) | 430–445 | 445–460 |
| DL-3-hydroxy kynurenine (HK) | – | 480–520 |
| Kynurenic acid (KA) | 385 | 455–485 |
| Kynurenine (K) | 490 | |
| Xanthurenic acid (XA) | 460 | 495 |
| 3-Hydroxy-anthranilic acid (HAA) | 415 | 480–540 |
| Para-amino-salicylic acid (PAS) | 445 | |

12.5.3.2 Singlet Oxygen

However, the yellow and red CL components (575, 630, and 705 nm) cannot yet be interpreted from the above data. Of them, the red spectral bands might be attributed to the luminescence of singlet oxygen, which has been discussed as another important luminescent species in free-radical peroxidation (see Chap. 9 and Sects. 10.4.6 and 11.5.3).

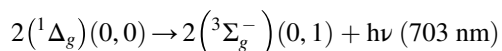
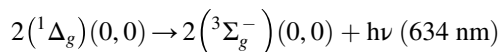
To estimate its role in a certain process, one can use two approaches:

1. Replace H_2O in the medium with D_2O ($^1\text{O}_2$ is known to be strongly quenched by H_2O and stabilized by its replacement with D_2O ; Merkel et al. 1972).
2. Use a standard H_2O -based medium with water-soluble quenchers of $^1\text{O}_2$ (e.g., NaN_3 or DABCO).

Repeating the above experiments with D_2O -based Trp solutions gave photochemiluminescence approximately

three times more intense than in standard H₂O solutions. Contrary to that, the addition of NaN₃ or DABCO diminished CL intensity by 10–15%. All this definitely suggests a singlet oxygen component in the detected protein luminescence.

At the same time, the 635 and 705 bands of the tryptophan photochemiluminescence fit well with the known luminescence bands at relaxation of oxygen dimoles (Sławiński et al. 1980), supporting the above conclusion:



12.5.3.3 General Scheme

Altogether, the basic scheme of protein oxidation appears very similar to that of hydrocarbons and lipids, being, however, also complicated by amino acid oxidation products. Here we present the simplest variant with radical recombination as the only source of light (see Table 12.5, compare Chaps. 10 and 11). However, below, we will complicate it according to some additional data.

Anyway, the given scheme does not necessarily mean a quadratic dependence on the incident radiation dose and a hyperbolic decay, typical for bimolecular reactions. Thus, a model in Sapezhinskii and Dontsova (1973) with the following assumptions:

- The luminescent reaction is the recombination of secondary peroxy radicals ROO[•], different from the primary ones (R₀[•]),

Table 12.5 Basic reactions of photo-induced peroxidation of proteins. R₀[•] is the initially formed (primary) radical, R[•] is any radical formed in the system (initially R₀[•], and then – any other radicals)

| Process stage | Reactions |
|--------------------|--|
| Initiation | R ₀ + hν _{ex} → R ₀ [•] + e ⁻ |
| | R ₀ [•] → R [•] |
| Propagation | R [•] + O ₂ $\xrightarrow{k_2}$ ROO [•] |
| | ROO [•] + RH $\xrightarrow{k_3}$ ROOH + R [•] |
| Disproportionation | ROO [•] + ROO [•] → P* → P + hν |
| | ROO [•] + ROO [•] → P + ¹ O ₂ → P + ³ O ₂ + hν |

Table 12.6 Characteristic parameters of photoluminescent processes

| Characteristic parameters / System and reference | Human serum albumin (Sapezhinskii 1969) | Gly-Trp dipeptide (Sapezhinskii and Dontsova 1973) |
|--|---|--|
| Quantum yield of radical formation, φ _{rad. form.} (radicals / UV quanta) | 5 · 10 ⁻³ | 3 · 10 ⁻² |
| Quantum yield of CL, φ _{CL} (CL quanta/reaction acts) | 10 ⁻⁷ | 6 · 10 ⁻⁸ |
| Activation energy, E _a (kcal/mol) | | 8 – 12 |

- The transition from primary to secondary radicals: R₀[•] K₀ → R[•] is the rate-limiting reaction,

gives solutions compatible with exponential decay and linear proportionality to the exciting radiation dose:

$$I_{\text{lum}} = I_{\text{ex}} \cdot \tau_{\text{ex}} \cdot \varphi_{\text{rad. form.}} \cdot \varphi_{\text{CL}} \cdot K_0, \quad (12.1)$$

where I_{lum} is the luminescence intensity; I_{ex}, intensity of the exciting light; τ_{ex}, duration of excitation; φ_{rad. form.}, quantum yield of radical formation (radicals/UV quanta); φ_{CL}, CL quantum yield (CL quanta/reaction acts); and K₀ is the rate constant of the rate-limiting reaction: R₀[•] K₀ → R[•].

This gives the following estimates (see Fig. 12.3):

$$K_0 \cong 1.8 \cdot 10^{-2} \text{ s}^{-1},$$

and

$$\varphi_{\text{rad. form.}} \cdot \varphi_{\text{CL}} \cong 2 \cdot 10^{-9} \frac{\text{CL quanta}}{\text{Exciting UV quanta}},$$

with the main quantum yields, calculated from these data given in Table 12.6 (see more in Sapezhinskii and Dontsova (1973).

At the same time, the luminescence intensity increases with increasing temperature, according to the following pattern (Sapezhinskii et al. 1964):

$$\log I_{\text{lum}} \sim -\alpha \frac{1}{T}$$

Thus, the luminescent reaction requires some activation energy, which can be calculated as in Table 12.6.

12.5.4 Conclusions

Altogether, the observed long-lasting afterglow of proteins was shown to be photo-induced oxychemiluminescence, which means that the mechanisms shown for it should be very close to those in non-photo-induced chemiluminescent systems. Though having much in common with the photochemiluminescence of deeply frozen amino acid solutions, this phenomenon appeared to have certain

specificities. While the chemiluminescent component of the amino acid afterglow was caused by the recombination of solvated electrons with radical cations and could be observed only under very specific conditions (very low temperature or very rigid molecular grid in the carrier), the protein afterglow appeared to be associated with recombination of a larger set of substances, all of which are free radicals. Actually, the electron–radical–cation recombination in amino acids appeared to be just a special and the simplest case of processes occurring in irradiated proteins. Moreover, the latter, besides recombination, involve chain development and probably chain branching (Lissi and Clavero 1990), similar to peroxidation of hydrocarbons and lipids.

12.6 Oxychemiluminescence of Amino Acids and Proteins

Naturally, the free-radical peroxidation processes observed in irradiated proteins basically correspond to those initiated by chemical oxidants, both introduced into the system from the outside and arising spontaneously during the cell's life. These reactions proved to be an important component of the free-radical processes in the cell and the accompanying oxychemiluminescence (OCL), which is known as the major fraction of biological autoluminescence in general.

Here we present data on the mechanisms of protein OCL accumulated to date, largely based on the works on photochemiluminescence discussed above.

12.6.1 Oxidation of Proteins and Amino Acids is Accompanied by Photon Emission

12.6.1.1 Photon Emission from Proteins and Amino Acids Is a Free-Radical Oxychemiluminescence

As shown in the previous section (Sect. 12.5), UV-, γ -, and X-ray irradiation of protein or amino acid solutions initiates their free-radical peroxidation, accompanied by ultraweak photon emission (UPE). The same picture can be achieved by various chemical initiators: hydroperoxides in the presence of transition metal ions (e.g., tert-butyl hydroperoxide + iron) (Barnard et al. 1993; Khabiri et al. 2008), ONOO⁻ (Watts et al. 1995), 2,2'-azobis(2-amidinopropane) dihydrochloride (AAPH) (Aspée and Lissi 2000, 2001), activated neutrophils (Barnard et al. 1993), etc.

Similar to photochemiluminescence, this UPE is suppressed by antioxidants and spin-traps: *N*-*t*-butyl- α -phenylnitron (Pollet et al. 1998), Trolox (Aspée and Lissi 2000, 2001), superoxide dismutase (Barnard et al. 1993), or scavengers of reactive oxygen species (e.g., U-78518-F (Barnard et al. 1993)).

The UPE intensity correlates with the oxidation rate, which can be estimated by amino acid consumption, oxygen uptake, or product accumulation (Aspée and Lissi 2000; Watts et al. 1995). It also increases with the concentration of the initiator (see Fig. 12.5a) and the substrate (amino acids or proteins – see Fig. 12.12).

Thus, UPE from protein and amino acid solutions is generated in the course of a free-radical oxidation process, i.e., it is OCL.

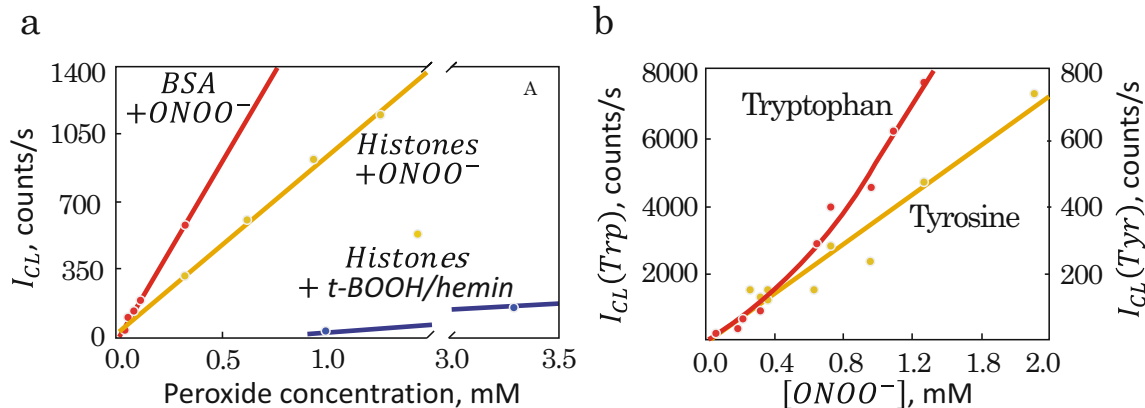


Fig. 12.5 Oxychemiluminescence (OCL) of proteins and amino acids initiated by different oxidizing substances: (a) tert-Butyl hydroperoxide (*t*-BOOH) or (b) ONOO⁻, in relation to their concentration. (a) BSA

and histones initiated by *t*-BOOH or ONOO⁻ and (b) tryptophan and tyrosine initiated by ONOO⁻. (Reprinted from Watts et al. (1995). Copyright 1995, with permission from Elsevier)

12.6.1.2 The Amino Acids: Sources of OCL

Of all amino acids, those most subjected to peroxidation are Trp, Tyr, Phe, His, Lys, Glu, Thr, Pro, Met, and Cys (Alvarez and Radi 2003; see also Davies 2016). However, attempts by several groups to measure OCL in different purified amino acid solutions gave different results.

In Pollet et al. (1998), definite OCL was detected only from tryptophan (repeating the above data on UV-induced CL; Sławiński et al. 1980), with very weak or even unreliable CL from other amino acids (sorted by CL intensity: Phe, Gln \geq Glu, Arg, Leu \geq His, Tyr, Ser, Asn, Lys \geq Val, Pro, Thr, Ala, Gly, 2-KG \geq Met \geq Ile) and no CL from Cys. The tested amino acid solutions were approximately 40–130 mM, oxidized with 600 μM ONOO⁻ at 30 °C, pH 7.4.

In Aspée and Lissi (2000), Barnard et al. (1993), and Watts et al. (1995), OCL was found mainly from tryptophan and tyrosine, while other amino acids showed inconsistent results (see Fig. 12.6):

- OCL from tryptophan was observed in all tested concentrations, from 1 μM (micromole/l) to 10 mM (Barnard et al. 1993; Watts et al. 1995; Aspée and Lissi 2000).
- OCL from tyrosine was observed only at a concentration of 1 mM, while 1–10 μM gave no signal, and concentrations above 5 mM were insoluble (Aspée and Lissi 2000).
- Oxidation of Gly, Ile, Phe, Ser, Asn, Glu, and Tyr gave certain weak CL, however, of nonconfident intensities:
 - Gly, Ile, Glu at 1 μM concentration
 - Ile, Asn at 1 mM
 - Phe, Ser, Asn, Glu at 10 mM

The amino acid solutions were oxidized with 20 mM 2,2'-azobis (2-amidinopropane) dihydrochloride (AAPH) at 27 °C, pH 7.4. The relative OCL intensities of different amino acids were independent of the general oxidation rate or time after the reaction started (Aspée and Lissi 2000).

Note that here the tested amino acid concentrations were from 1 μM to 10 mM, while in Pollet et al. (1998), they were \sim 100 mM.

In Khabiri et al. (2008), strong OCL was observed from Phe, Trp, His, and Cys solutions (the authors did not study Tyr) and very weak OCL from Lys and Thr (see Fig. 12.7a). However, the experimental conditions were very different from those in the above works. The amino acid solutions were \sim 3–10 mM (Trp, 1.2–2.5 mM), oxidized with 1 M H₂O₂ + 1 mM Fe²⁺, and pH 7.4. Thus, both much higher OCL intensities and intense OCL from Phe, His, and Cys are well explained by the great concentrations of H₂O₂ used by the authors.

An important issue shown in this work is non-additive OCL from amino acid mixtures (see Fig. 12.7b). For

example, a combination of Trp and His gave OCL 25 times more intense than the sum of their OCL, while Trp + Met gave OCL two times less intense than pure Trp. All this definitely shows intense energy migration between the molecules, with Trp supposedly playing the role of activator for His OCL in the first case and Met playing the role of Trp OCL quencher in the second case. Needless to say, such processes must play an important role in OCL from proteins and their combinations with other substrates (see some more examples in Khabiri et al. 2008).

Moreover, besides UPE, the authors detected oxidation products by mass spectrometry (Khabiri et al. 2008). Surprisingly, for Cys and His, the detected OCL was accompanied by a substantial accumulation of oxidation products, and for Trp and Phe, there were no oxidation products detected at comparable OCL. Unless there are specific artifacts or experimental biases, this can only suggest that CL quantum yield in oxidation of Trp and Phe is orders of magnitude higher than for Cys and His, making CL a more sensitive detector of Trp and Phe oxidation than even mass spectrometry (see Sect. 7.5.1 for a similar comparison of CL sensitivity to ESR).

This explains the discrepancy between Khabiri et al. (2008) and the above-mentioned works on the amino acid sources of OCL. While many amino acids can be oxidized, Trp and Phe (and Tyr, not investigated by the authors) are likely the primary OCL sources due to their high luminescence quantum yields. At the same time, other amino acids have incomparably lower luminescence quantum yields and thus mostly give no OCL at oxidation. Of them, His, Cys, and to a lesser extent Lys and Thr (and maybe some others, not investigated here) still have a certain probability of radiative relaxation, providing their oxidation with certain OCL. However, their OCL becomes observable only at very high oxidation rates, caused by huge concentrations of oxidizing agents, and is well detectable by mass spectrometry.

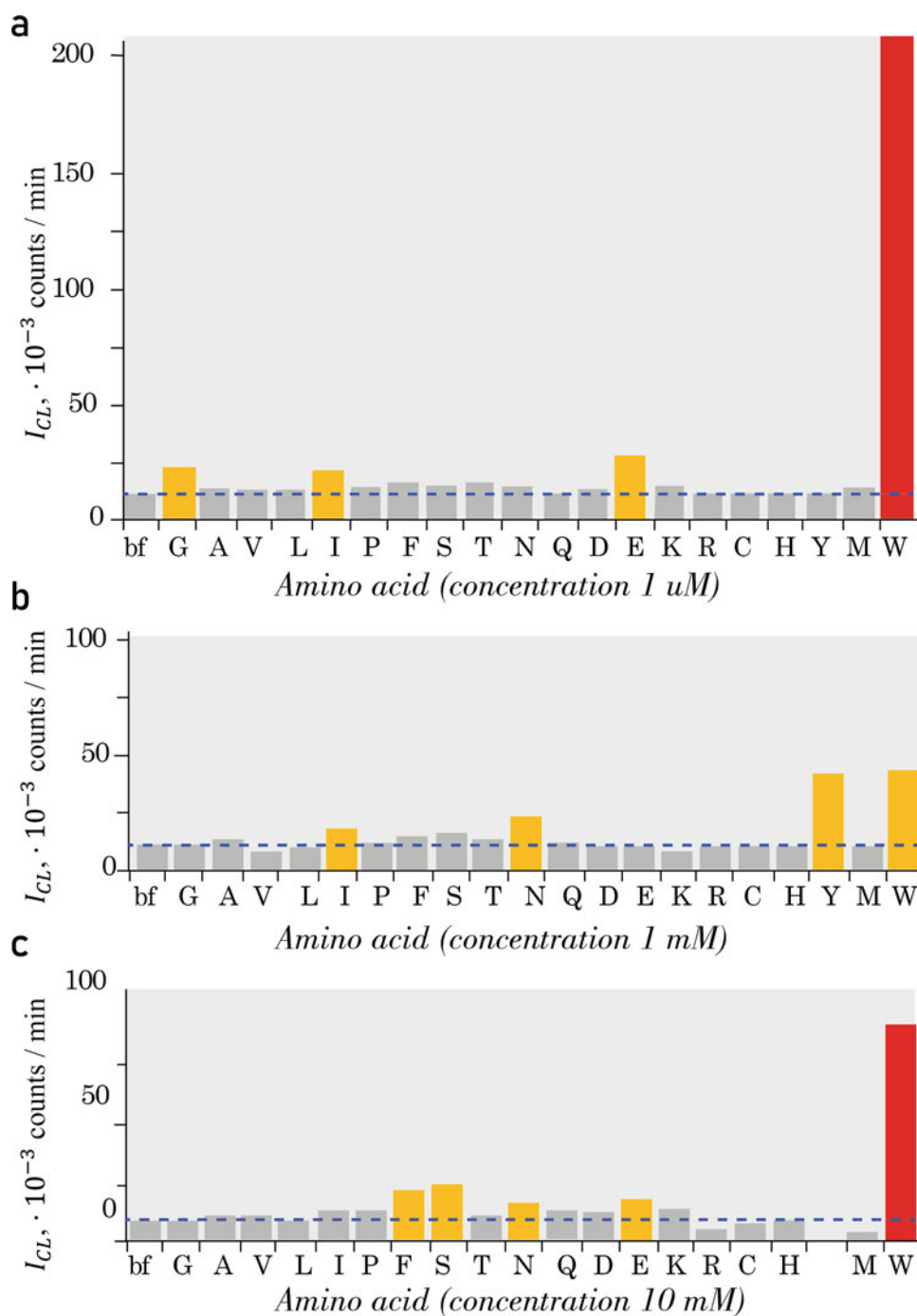
12.6.1.3 The Role of Oxygen: Peroxy Radicals and Singlet States

Similarly to hydrocarbons and lipids (see Sects. 10.3 and 11.5), the amino acid OCL is completely suppressed in anaerobic conditions (under nitrogen). Moreover, if oxidized luminescing solutions are purged by nitrogen, their OCL is instantly and totally quenched (Aspée and Lissi 2000).

On the other hand, bubbling oxygen through the system enhances OCL by 10–15% (Aspée and Lissi 2000).

This suggests that amino acid luminescent reactions also require peroxy radicals. However, not all OCL from amino acids and proteins is generated precisely at their recombination, as in Russell's mechanism. Below, we will see that a certain fraction of OCL, requiring peroxy radicals, is yet to be generated in non-Russell's paths.

Fig. 12.6 Intensity of oxychemiluminescence from different amino acid solutions of (a) 1 μ M, (b) 1 mM, and (c) 10 mM concentration. Measured after 50 min incubation in the presence of 20 mM AAPH. (Adapted from Aspée and Lissi (2000). Copyright 2000, with permission from John Wiley and Sons)



12.6.2 Spectra of Oxychemiluminescence

Rough spectra of OCL from protein and amino acid solutions were reported by several groups (Watts et al. 1995; Pollet et al. 1998; Aspée and Lissi 2000) and were generally in line with those obtained for photochemiluminescence (Sławiński et al. 1980) (see Sect. 12.5.3).

However, they had certain specificities connected to amino acid concentration. Thus, the OCL spectra of

tryptophan in the micromolar concentrations had a dominating region of <490 nm (see Fig. 12.8). As is known, this region contains fluorescence and phosphorescence bands of tryptophan and most of its oxidation products (see Sect. 12.5.3), but not of singlet oxygen, which emits red or IR light (Krasnovsky 2007).

Yet, higher concentrations of tryptophan, tyrosine (Aspée and Lissi 2000; Pollet et al. 1998), or bovine serum albumin (BSA; Watts et al. 1995) gave OCL with different spectra, in

Fig. 12.7 Intensity of OCL from different amino acid solutions and their combinations. (a) Pure 1% amino acid solutions (for Trp – 0.5%), oxidized by 1 M H₂O₂ + 1 mM Fe²⁺, OCL detected 40 s after Fe²⁺ addition, for 2 min. (b) Trp (0.25%) + various amino acids (0.5%), oxidized by 1 M H₂O₂ + 1 mM Fe²⁺, OCL detected 40 s after Fe²⁺ addition, for 2 min. (Adapted from Khabiri et al. (2008). Copyright 2008, with permission from John Wiley and Sons)

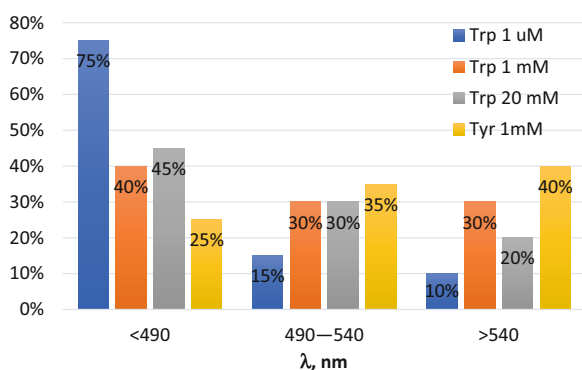
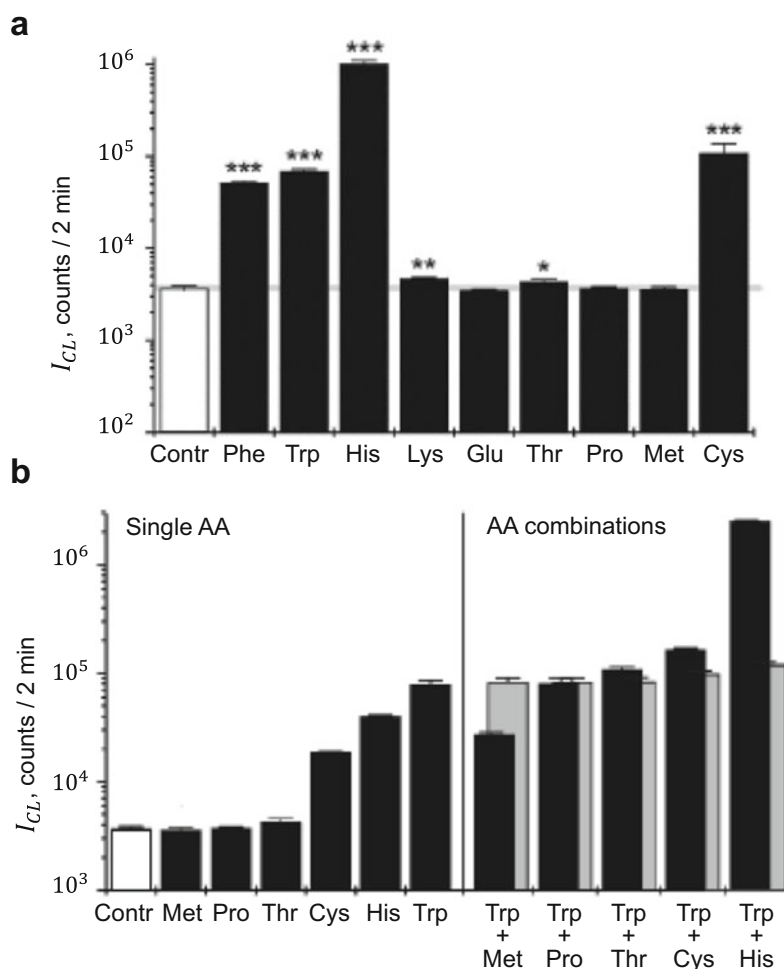


Fig. 12.8 Rough spectra of OCL from tryptophan and tyrosine solutions, initiated by AAPH. (Based on data from Aspée and Lissi (2000))

which $\geq 60\%$ lay in the region $\lambda \geq 490$ nm (Aspée and Lissi 2000; Pollet et al. 1998) (see Fig. 12.8).

This was generally confirmed in Khabiri et al. (2008), who worked with millimolar amino acid concentrations: 2.5 mM for Trp and ~ 5 –10 mM for the others (see Fig. 12.9a).

Interestingly, His showed a highly specific OCL spectrum, with a much higher 420–455 nm band and very low bands >490 nm, suggesting a highly excited carbonyl compound. At the same time, OCL from His + Trp had basically the same spectrum as pure Trp (see Fig. 12.9b), confirming the above suggestion of energy migration between different amino acids: here Trp plays the role of OCL activator, accepting energy from electron-excited states from the oxidized His and emitting it with its characteristic spectrum. As one can also see from Fig. 12.9b, a similar energy migration was likely happening from His to Cys, but with lower efficiency.

The OCL spectra of proteins obtained by the authors (Khabiri et al. 2008) (see Fig. 12.9c) are quite difficult to interpret: first, because of their roughness, and second, because of the complex interactions that probably occur between the amino acids within the protein. Here, one can only mention BSA, whose spectrum is close to that of pure Trp, and insulin, whose spectrum is quite close to that of Tyr. Importantly, in BSA, Trp indeed plays the role of the major luminophore, while in insulin, Tyr does (with no Trp contained by the protein) (see below, Sect. 12.6.4). However,

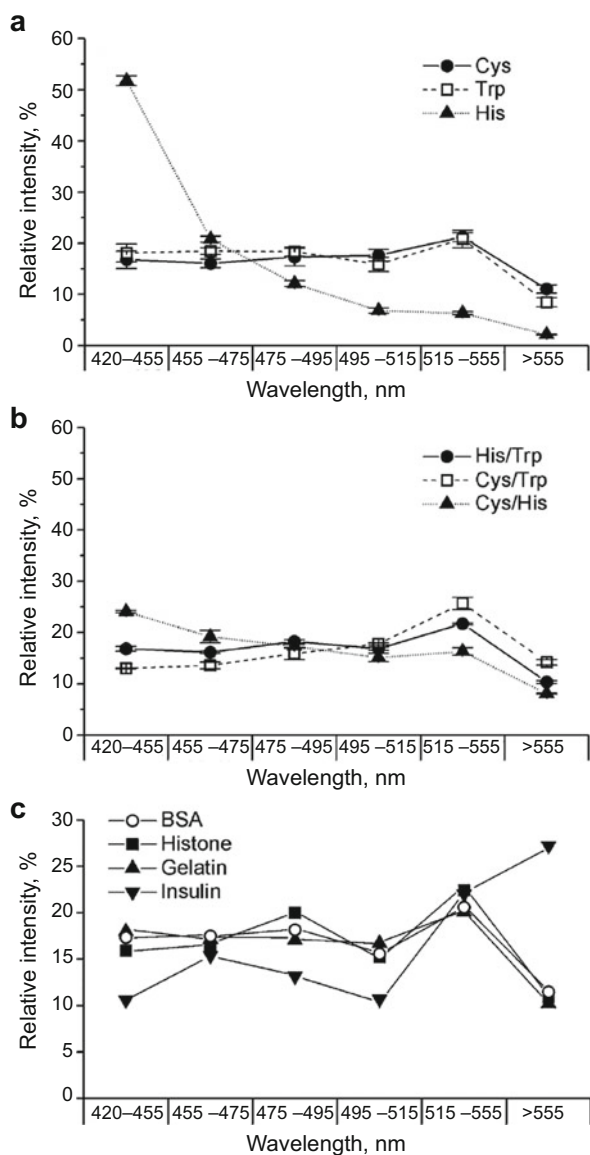


Fig. 12.9 Rough spectra of OCL from different amino acids and proteins, oxidized by 1 M H_2O_2 + 1 mM Fe^{2+} , OCL detected 40 s after Fe^{2+} addition, for 2 min. (a) Pure amino acid solutions; (b) combinations of amino acids; and (c) proteins (0.25% w/v; compare to their amino acid content given in Tables 12.7 and 12.8). (Adapted from Khabiri et al. (2008). Copyright 2008, with permission from John Wiley and Sons)

in general, protein OCL depends on the amino acid content, their solvent availability, and energy transfer processes as described above (see also Sect. 5.4).

In general, the interpretation of luminescent spectra is a complex and multifaceted issue, far from being solved in the case of amino acids and protein OCL (it has advanced much further for hydrocarbons; see Sect. 10.5).

Similarly to hydrocarbons and lipids, amino acid OCL contains bands emitted by various excited organic products (see Chaps. 10 and 11 and Sect. 12.5.3 of this chapter), as

well as those associated with singlet oxygen. Of these, the latter component can be easily estimated by comparing OCL in H_2O - and D_2O -based media (as in Sect. 12.5.3). Similarly to the above data on photochemiluminescence, the red component (>540 nm) of tryptophan's and tyrosine's OCL increases twofold if H_2O is replaced by D_2O , suggesting that a fraction of it is generated by singlet oxygen (Aspée and Lissi 2000). Also, the red spectral component is completely suppressed by Trolox, indicating its free-radical nature.

All this, combined with the need for oxygen (i.e., for the peroxy form of free radicals), suggests that the red spectral component is (at least partially) generated in Russell-type reactions, in which singlet oxygen is a known product (see Sect. 10.5.1). The upper estimate of this fraction is given by the proportion of the red spectral component (10–40%) for different systems, but it can be lower.

12.6.3 The Non-stationary Component of OCL

12.6.3.1 OCL Kinetics

As an initiator of peroxidation, AAPH is known to be a stable, Fe-independent source of peroxy radicals (Lissi et al. 1991), which is confirmed by the constant rate of oxygen uptake, substrate consumption, and product formation at AAPH-induced oxidation of amino acids and proteins (Aspée and Lissi 2000). For instance, at a concentration of 20 mM at 27 °C, it generates radicals at a stable rate of 0.25 $\mu\text{M}/\text{min}$ (Aspée and Lissi 2000; Lissi et al. 1991).

However, OCL from AAPH-oxidized tryptophan and tyrosine was found not to be stationary but increasing over time (see Fig. 12.10), suggesting either a self-accelerating process, as in the “slow flash” of lipid CL (see Sect. 11.6),¹ or accumulation of luminescent products (with the former likely to be responsible for most of the observed growth, but not excluding the latter).²

At the lowest tryptophan concentrations (~ 1 μM), this initial OCL increase is followed by a further decrease caused by substrate consumption, which is easily proven by repeated growth of OCL with the same kinetics after adding fresh tryptophan to the oxidized solution (see Fig. 12.11). Aside from this effect, OCL intensity for amino acid solutions is increasing every minute by several cpm, with the maximal

¹Note that in case of lipid CL, the CL enhancement in the “slow flash” reflects the chain process development, and further CL extinction is associated with depletion of the initiator Fe^{2+} . In contrast, in the amino acid CL studies, the peroxidation is initiated at a stable rate, and therefore, the phase of CL suppression does not occur.

²Unfortunately, the authors did not trace the kinetics of product accumulation and oxygen consumption in parallel with CL detection, as was done for lipid CL in Vladimirov's group (See Chap. 11), so the above conclusion remains a hypothesis.

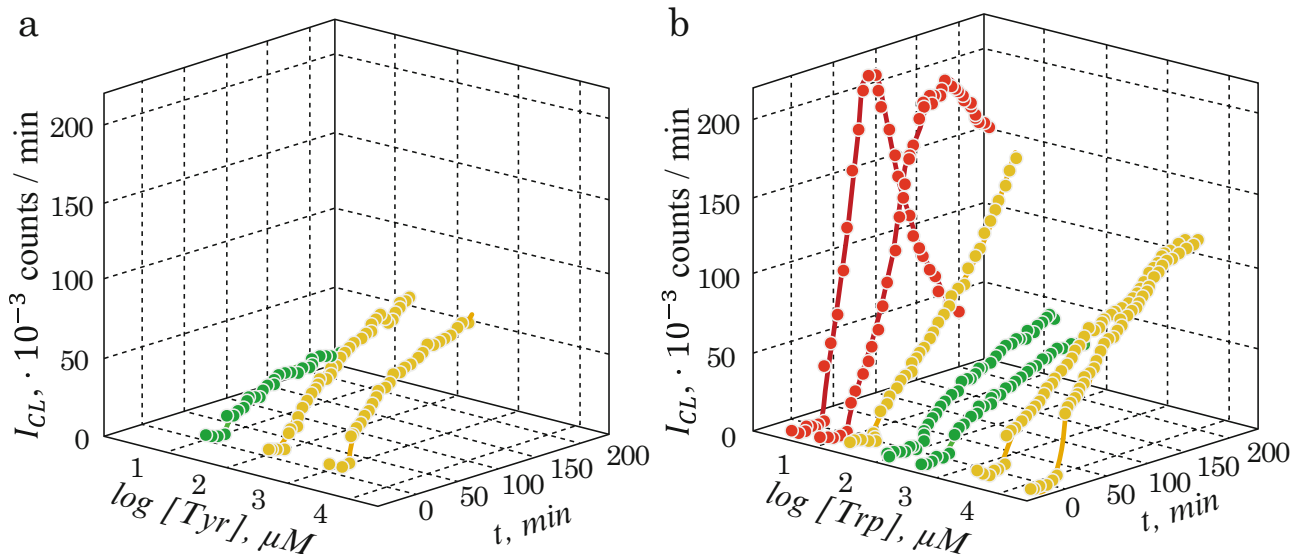


Fig. 12.10 Kinetics of oxychemiluminescence from amino acid solutions: (a) tyrosine, (b) tryptophan, at different concentrations of 20 mM. (Adapted from Aspée and Lissi (2000). Copyright 2000, with permission from John Wiley and Sons)

rate at the lowest concentrations of tryptophan (see Fig. 12.10b and also the discussion below).

The protein OCL exhibits an even more complex pattern with periods of increase and decrease depending on the protein composition (see below, Sect. 12.6.4).

12.6.3.2 The Role of Free Radicals and Peroxides

Similarly to lipids and hydrocarbons, the most part of amino acid and protein OCL is suppressed by free-radical scavengers (e.g., Trolox): ~90% for Tyr, ~75% for Trp, ~70% for BSA, etc. (Aspée and Lissi 2000, 2001) (see Fig. 12.12). This percentage was found independent of the time elapsed after the reaction start and the general OCL intensity. Thus, between 70% and 90% of the observed OCL is generated with the involvement of free radicals, and specifically peroxy radicals (as shown in Sect. 12.6.1), which may well be the Russel-type processes (see Sect. 10.5.1).

The remaining Trolox-independent OCL component (10–30%) is partially suppressed by glutathione (GSH), and totally suppressed by Ebselen (a known peroxidase-like compound), suggesting that it requires some peroxides (Aspée and Lissi 2000, 2001), similarly to the “fast flash” in lipid peroxidation (but with the difference that lipid hydroperoxides were decomposed by the added Fe^{2+} , while here iron is not present, compare Sect. 11.6).

At the same time, Trolox, added prior to AAPH, totally blocks any OCL (Aspée and Lissi 2000, 2001), suggesting that the peroxides, responsible for the second OCL component, also require free radicals to be generated, similarly to

amino acids. Oxidation held at a constant rate, determined by the concentration of 2,2'-azobis(2-amidinopropane) dihydrochloride,

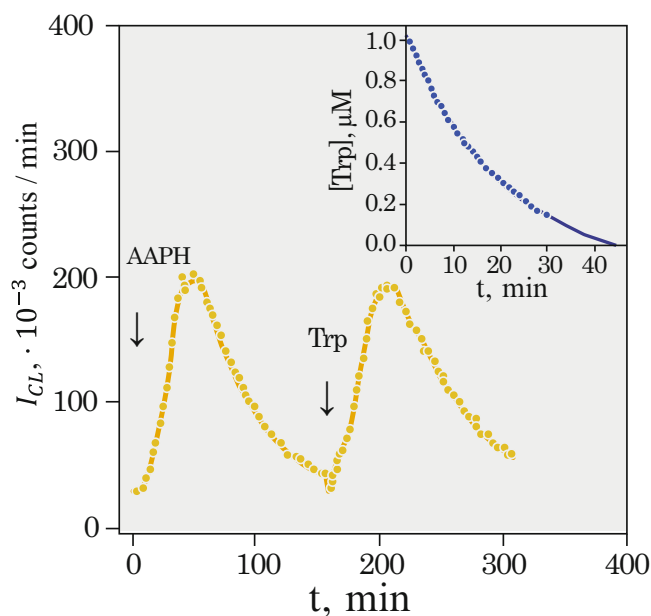


Fig. 12.11 OCL kinetics and substrate consumption. Tryptophan, 1 μM , AAPH 20 mM. (Adapted from Aspée and Lissi (2000). Copyright 2000, with permission from John Wiley and Sons)

lipid hydroperoxides decomposed during the “fast flash” of lipid CL (see Sect. 11.6).

Thus, both supposed sources of amino acid OCL – the peroxy-radical reactions (supposedly, the Russel-type recombination) and the peroxide decomposition (as well as the possible reactions of peroxy radicals with the accumulated peroxides) start from the initial free-radical peroxidation, initiated by AAPH (Aspée and Lissi 2000, 2001),

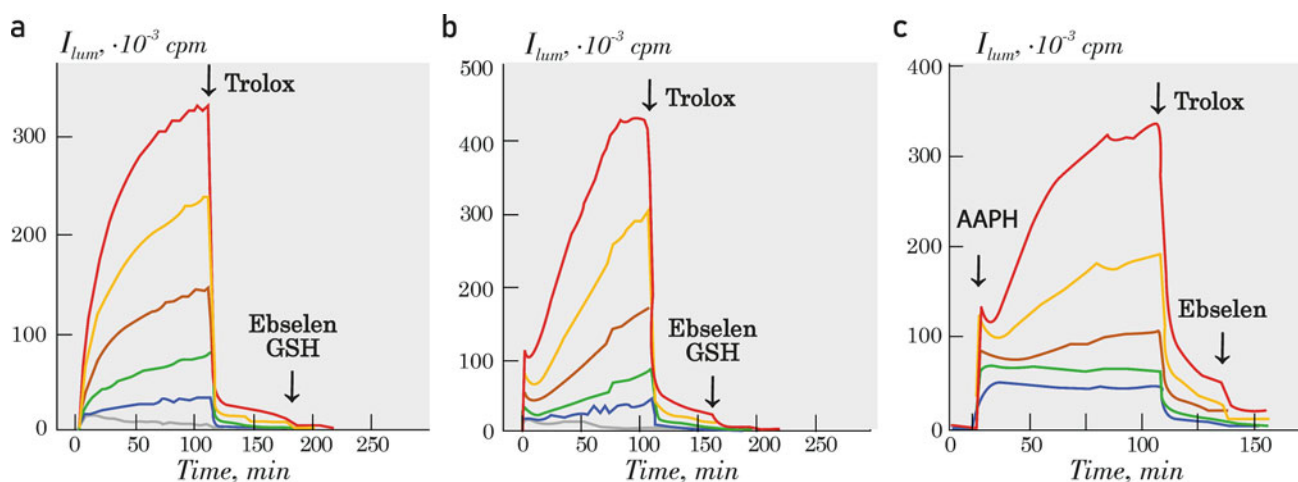


Fig. 12.12 Kinetics of OCL from (a) tyrosine, (b) tryptophan, and (c) BSA solutions at different oxidation rates (determined by the concentration of AAPH): blue, 10 mM; green, 20 mM; brown, 40 mM; orange,

80 mM; and red, 160 mM. (Adapted from Aspée and Lissi (2001). Copyright 2001, with permission from Springer Nature)

decomposing hydroperoxides (Barnard et al. 1993; Khabiri et al. 2008), or other initiators (e.g., Barnard et al. 1993; Watts et al. 1995).

Notably, the use of D₂O has no impact on the OCL kinetics (Figs. 12.10 and 12.12), supporting a minor role of singlet oxygen in OCL.

Interestingly, both the OCL spectra and the Trolox- and Ebselen-dependent fractions of OCL are practically independent of the elapsed time and general OCL intensity, suggesting that the general reaction scheme is quite stable in the system.

12.6.3.3 The Light Precursors' Lifetime

Interestingly, notwithstanding differences in the rate of OCL growth, the general shape of the OCL time profiles remained the same and was determined mostly by the amino acid (or protein) concentration (see Fig. 12.10). For Tyr and Trp, the lifetime of the light precursors, formed in the system, estimated from the OCL increase kinetics, is ~20 min (Aspée and Lissi 2000).

On the other hand, the decay kinetics after Trolox addition fits well to a bi-exponential function, with the first component (70–90% of all UPE intensity) having a lifetime of ~1–2 min and the remaining component having a lifetime of ~20 min for Tyr and Trp (Aspée and Lissi 2000) and from 30 to 120 min or more for different proteins (Aspée and Lissi 2001) (these times are practically independent of the initial OCL intensity). As shown above, the second component is totally quenched by Ebselen (which has the same effect when added both after and before Trolox) and thus can be attributed to the decomposition of peroxides.

The excellent matching between the above-calculated lifetimes:

- Of the accumulated light precursors
- Of the second (peroxide-associated) decay component

suggests that they relate to the same species, that is, peroxide-like compounds, accumulated in the system in the course of the reaction.

Importantly, for each of the systems, the spectral distribution was time-independent, suggesting that the reactions leading to OCL, as well as the proportion between OCL from different species, remained the same independently of the general OCL increase (Aspée and Lissi 2000).

12.6.4 OCL Depending on the Substrate

12.6.4.1 The Lowest Concentration Range: The Reaction Start

Obviously, at the lowest concentration of amino acids or proteins, the intensity of the OCL should positively correlate with concentration: the more substrate molecules – the higher the probability of oxidation acts – the higher the OCL intensity and/or the rate of its growth.

For tyrosine OCL, this pattern was observed at concentrations $<10^{-4}$ M (see Fig. 12.10); for tryptophan, the effect was not observed at the investigated concentrations (Aspée and Lissi 2000). However, as tryptophan solutions become reliable sources of OCL at concentrations 3–4 orders of magnitude lower than those of tyrosine (see Fig. 12.6), this range is likely to be shifted to concentrations $<10^{-7}$ – 10^{-6} (not investigated by the authors) (Aspée and Lissi 2000).

For protein solutions, the same regularity was shown within different concentration ranges (Aspée and Lissi 2001) (see Fig. 12.15):

Table 12.7 Composition of the investigated proteins

| Protein | Number of residues per protein molecule | | |
|---|---|-----|-----|
| | Total | Trp | Tyr |
| BSA (Majorek et al. 2012) | 583 | 2 | 20 |
| Phosphatase alkaline (Bradshaw et al. 1981) | 449 | 2 | 11 |
| Lysozyme (Kamei et al. 1988) | 117 | 6 | 3 |
| Ribonuclease A (Smyth et al. 1963) | 110 | 0 | 6 |
| Insulin (Nicol and Smith 1960) | 77 | 0 | 4 |

Table 12.8 Solvent surface accessibility of the Trp and Tyr in lysozyme, ribonuclease A, and insulin

| Protein | Residues | Σ | Solvent surface accessibility, % | | | |
|----------------|----------|----------|----------------------------------|-------|-------|------|
| | | | 80–60 | 60–40 | 40–20 | 20–0 |
| Lysozyme | Trp | 6 | | 1 | 1 | 4 |
| | Tyr | 3 | | | 2 | 1 |
| Insulin | Trp | 0 | | | | |
| | Tyr | 4 | 2 | 1 | | 1 |
| Ribonuclease A | Trp | 0 | | | | |
| | Tyr | 6 | | 2 | 1 | 3 |

Adapted from Aspée and Lissi (2001). Copyright 2001, with permission from Springer Nature

- BSA: $<10^{-6}$ M
- Lysozyme: $<10^{-5}$ M
- Phosphatase alkaline: $<10^{-6} - 10^{-5}$ M
- Insulin: $<10^{-6}$ M
- Ribonuclease A: $<10^{-3}$ M (if at all)

which is obviously connected to their amino acid content and (even more important) to the availability of Trp, Tyr, and other oxychemiluminescent residues to the oxidizing agents (see Table 12.7, see also the discussion below and Table 12.8, and Fig. 12.13).

12.6.4.2 Medium Concentration Range: The Chain Length

At higher concentrations, as mentioned above, the rate of OCL growth mostly decreases with concentration increase (see Fig. 12.11). This is observed for the following concentrations of (see also Fig. 12.15a):

Aminoacids:

- Tyrosine: $>10^{-4}$ M.
- Tryptophan: $10^{-6} - 10^{-4}$ M

Proteins:

- BSA: $10^{-6} - 10^{-5}$ M
- Lysozyme: $10^{-5} - 10^{-4}$ M
- Insulin: $10^{-6} - 10^{-4}$ M

At the same time, the minimal peroxidation chain length (l_0 , calculated as the average number of consumed oxygen

molecules divided by the average number of radicals introduced into the system) increases (see Fig. 12.15b for tryptophan; Aspée and Lissi 2001 for BSA). (Note, that l_0 is the lower estimate of the real chain length, which can be many times higher; see also Sects. 12.5.2 and 11.6.2).

This effect is quite understandable from the following point of view (compare Scheme 11.4). At each step, a free (peroxy) radical has a kind of fate decision:

- To participate in chain prolongation (for which it needs to meet another amino acid molecule).
- To take part in luminescent processes (which can be either radical recombination or something else).

As discussed above, non-peroxy radicals in the presence of oxygen are immediately turned into peroxy radicals (see Box 10.1, Sect. 10.3), while in anaerobic conditions, the luminescent path is replaced by other reactions not accompanied by luminescence (see Sect. 12.6.1).

Obviously, the higher the substrate concentration, the more likely the chain prolongation path is. Thus, within a certain range of substrate concentrations, the OCL intensity can well be negatively correlated with it (as in Fig. 12.14). However, whether this is the whole explanation for the phenomenon, or if there are additional quenching effects, is unknown.

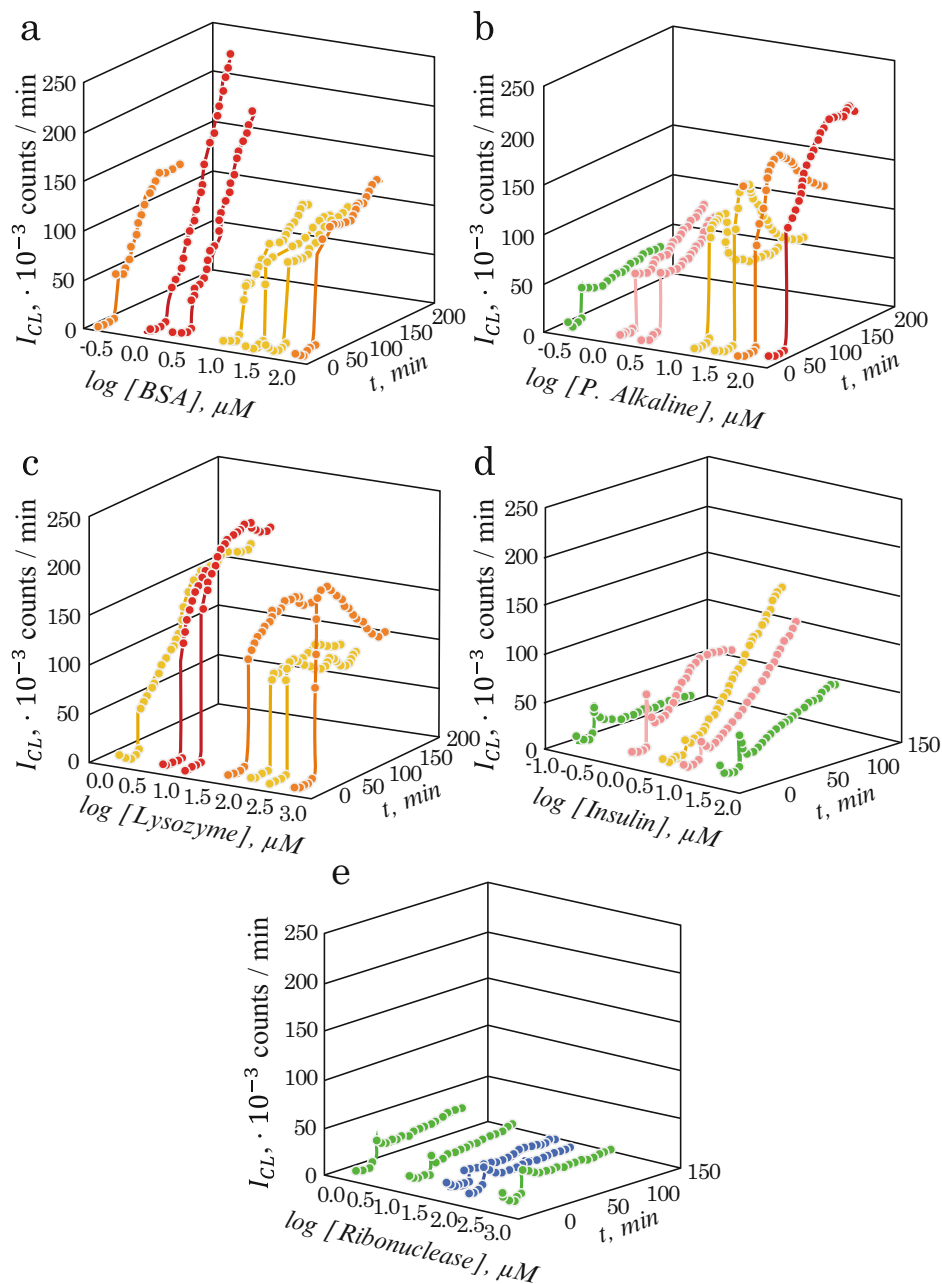
12.6.4.3 Higher Concentration Range: Oxidation Rate Increase

Further concentration increase can lead to different effects. For tryptophan, it is accompanied by an increase in the OCL growth rate at $[\text{Trp}] \geq 10^{-3}$ M. This is likely to be caused by the general oxidation rate increase (note that the minimal chain length is still increasing with concentration and even faster; see Fig. 12.14).

For tyrosine, this effect was not observed, probably due to reaching its solubility limit (Aspée and Lissi 2000).

For BSA, lysozyme, and alkaline phosphatase, the OCL pattern at high concentrations was similar to that of pure tryptophan (Aspée and Lissi 2001), which is quite understandable as tryptophan is likely to play a dominating role in their OCL (see Table 12.7).

Fig. 12.13 Kinetics of OCL from protein solutions: (a) BSA, (b) phosphatase alkaline, (c) lysozyme, (d) insulin, and (e) ribonuclease A at different concentrations. Oxidation held at a constant rate, determined by the concentration of AAPH (2,2'-Azobis(2-amidinopropane) dihydrochloride – 20 mM). (Adapted from (Aspée and Lissi 2001). Copyright 2001, with permission from Springer Nature)



For insulin and ribonuclease A, such a phase was not observed (Aspée and Lissi 2001). Importantly, both proteins do not contain Trp residues, and thus, the whole of their OCL (when it is observed) must be generated by Tyr and other residues. However, this does not exclude the possibility of observing this OCL pattern at still higher protein concentrations, which were not investigated by the authors (Aspée and Lissi 2001).

A deviation from this pattern of “higher concentration – higher oxidation rate – higher OCL intensity” should be seen at still higher substrate concentrations (which are obviously

individual for each substrate and each oxidation regime) due to such effects as energy transfer or concentration quenching (see Sects. 5.3 and 5.4). For Trp, oxidized by extremely high concentrations of decomposed H_2O_2 (1 M H_2O_2 + 1 mM Fe^{2+}), this concentration range was found to be $\geq 0.1\%$ w/v (i.e., ≥ 0.5 mM) (Khabiri et al. 2008), while for example, for His, it was still not achieved up to 1% w/v (6.5 mM; (see Fig. 12.15). Importantly, for other types of oxidizing agents, this concentration suppression effect was not observed even at much higher concentrations (see above).

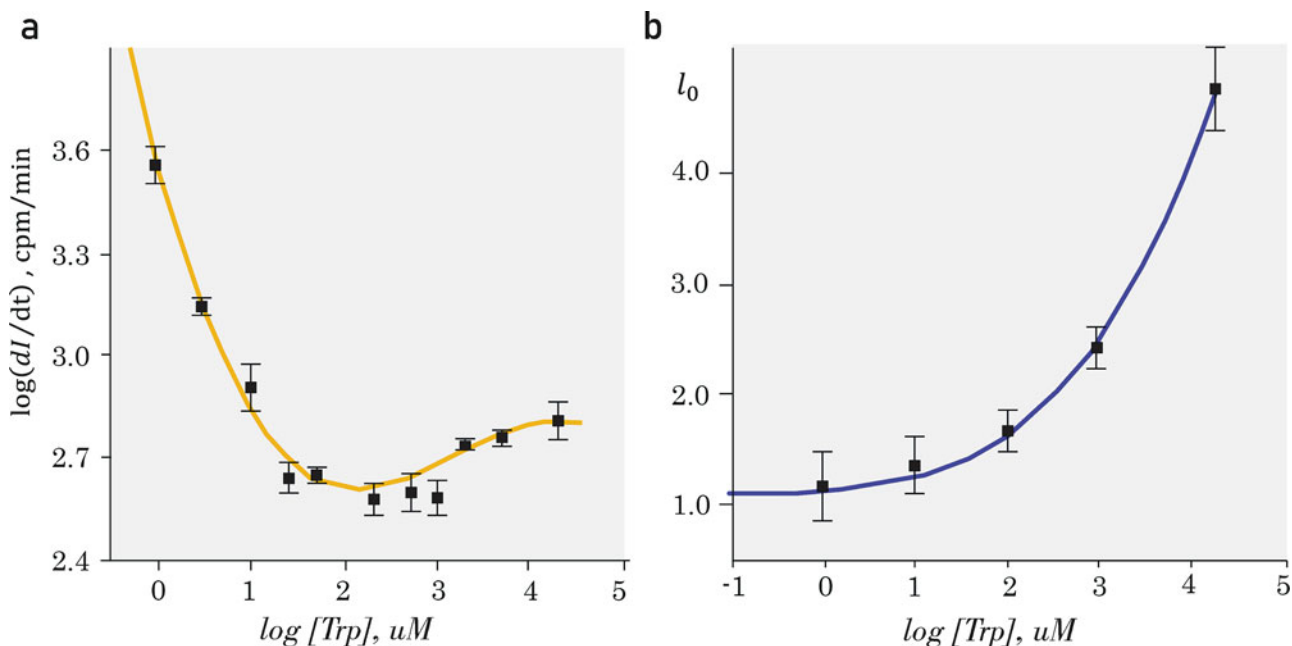


Fig. 12.14 Characteristics of tryptophan OCL. (a) Values of the initial rate of OCL increase for different concentrations of tryptophan. AAPH concentration is 20 mM. (b) Minimal chain length of the reaction (l_0),

calculated as the number of oxygen molecules consumed per radical introduced into the system. (Adapted from Asp e and Lissi (2000), with mild modification)

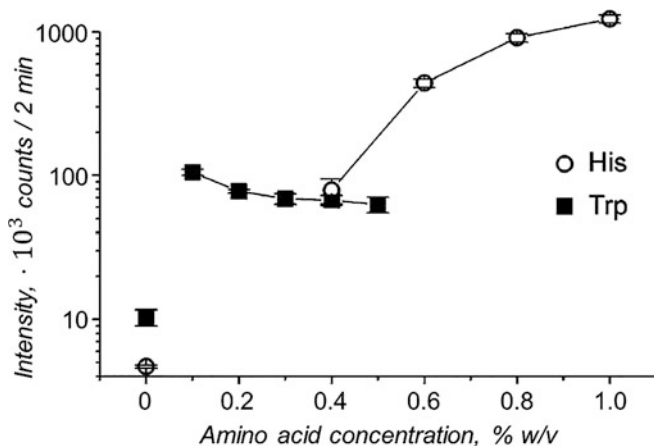


Fig. 12.15 Intensity of OCL from Trp and His solutions of various concentrations, oxidized by 1 M H_2O_2 + 1 mM Fe^{2+} (OCL detected 40 s after Fe^{2+} addition, for 2 min). (Adapted from Khabiri et al. (2008). Copyright 2008, with permission from John Wiley and Sons)

12.6.4.4 Proteins: Complicated OCL Kinetics

Altogether, as one can see, OCL from protein solutions gives much more variability than from pure amino acids. This is quite understandable, since of all amino acids, the luminescent ones are Trp, Tyr, and (to a lesser extent) several more, which can be contained in a protein in very different amounts and have very different availability for oxidation.

This is clearly seen from the comparison of OCL from lysozyme, ribonuclease A, and insulin, which have more or

less comparable lengths but different luminescent qualities (see Fig. 12.13 and Table 12.8):

- Lysozyme has six Trp residues, four of which are practically inaccessible to oxidation; one has 40–20% accessibility, but the remaining one should play a dominating role in OCL (as tryptophan is a much stronger source of OCL than tyrosine; see Sect. 12.6.1). The OCL pattern has much in common with that of Trp, which perfectly fits these structural data.
- Insulin has no Trp but four Tyr residues, of which two are highly available for oxidation and should make the molecule capable of OCL. In accordance with this, the protein is a good source of OCL, whose pattern is also quite similar to that of pure tyrosine.
- Ribonuclease A has no Trp and six Tyr residues, of which only two have 60–40% accessibility (note that Tyr is a much weaker source of OCL than Trp; thus, a Tyr residue with certain accessibility should mean OCL many times weaker than for a Trp residue under the same conditions). Accordingly, the protein gives very weak OCL, if at all.

Importantly, the lower oxidant availability of Tyr residues in ribonuclease A (compared to insulin) correlates both with its weaker OCL (under identical conditions) and with the lower rate of its Tyr residue consumption in the course of oxidation (see Fig. 12.16a). However, increasing the oxidation rate (by changing the AAPH concentration) led to a

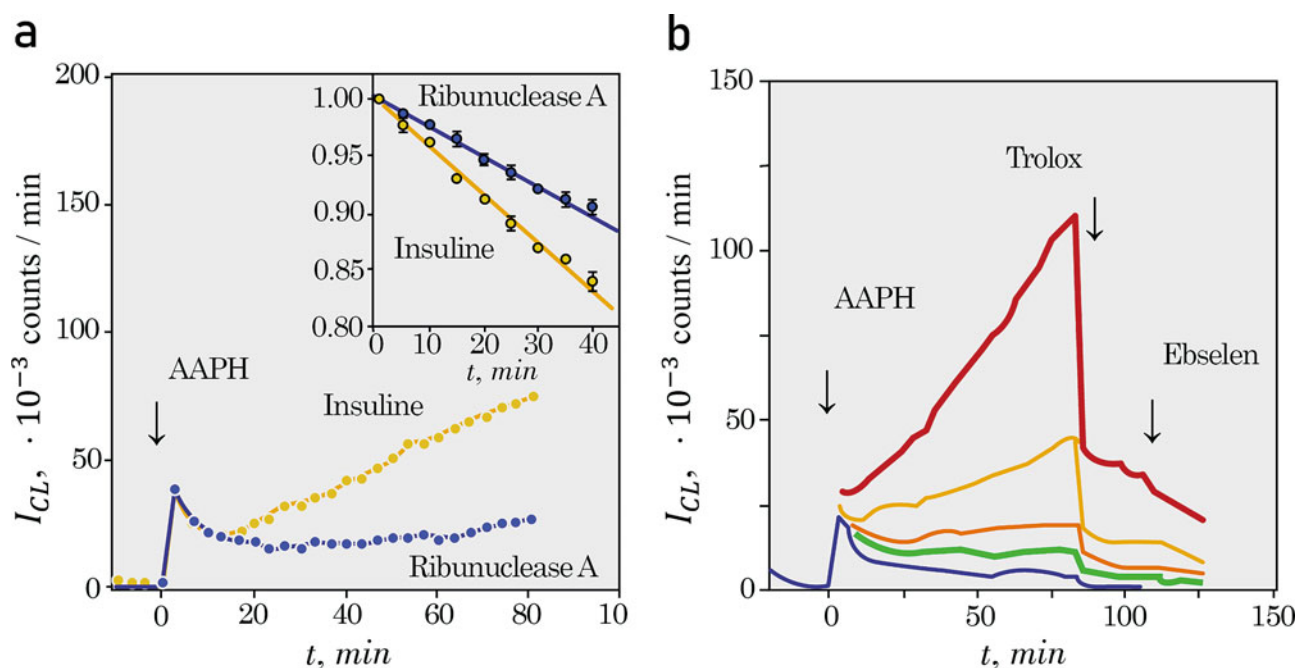


Fig. 12.16 OCL from ribonuclease A. (a) OCL from 1.33 μ M ribonuclease A and 2 μ M of insulin (AAPH concentration, 20 mM). The inset – tyrosine residue consumption evaluated from fluorescence measurement. (b) Kinetics of OCL from ribonuclease A solutions (1.33 μ M) at

different oxidation rates (determined by the concentration of AAPH): blue, 10 mM; green, 20 mM; brown, 40 mM; orange, 80 mM; and red, 160 mM. (Adapted from Aspée and Lissi (2001). Copyright 2001, with permission from Springer Nature)

detectable OCL from ribonuclease A, quite similar to that from insulin and other proteins but demanding a higher concentration of the oxidizing agent (see Fig. 12.16b; note the same picture in Khabiri et al. 2008).

Altogether, the OCL from protein solutions appeared to be very well explained by free-radical peroxidation of Trp and Tyr residues, taking into consideration their spatial arrangement and accessibility to free-radical attack. As Trp is a much better OCL source than Tyr, proteins containing Trp are generally better sources of OCL as well (however, solvent accessibility should be considered for final estimates).

At the same time, Trp and Tyr residues within the same molecule probably have different oxidation rates and kinetics, which may lead to several phases of the general OCL kinetics and complicated OCL curves. Moreover, oxidation of Phe, Cys, and His (and possibly Lys) is also accompanied by chemiluminescence, but it becomes detectable only at much higher oxidation rates.

All this is likely to be the main explanation for the variability of OCL kinetic patterns for different proteins.

12.6.5 Conclusions and the General Reaction Scheme

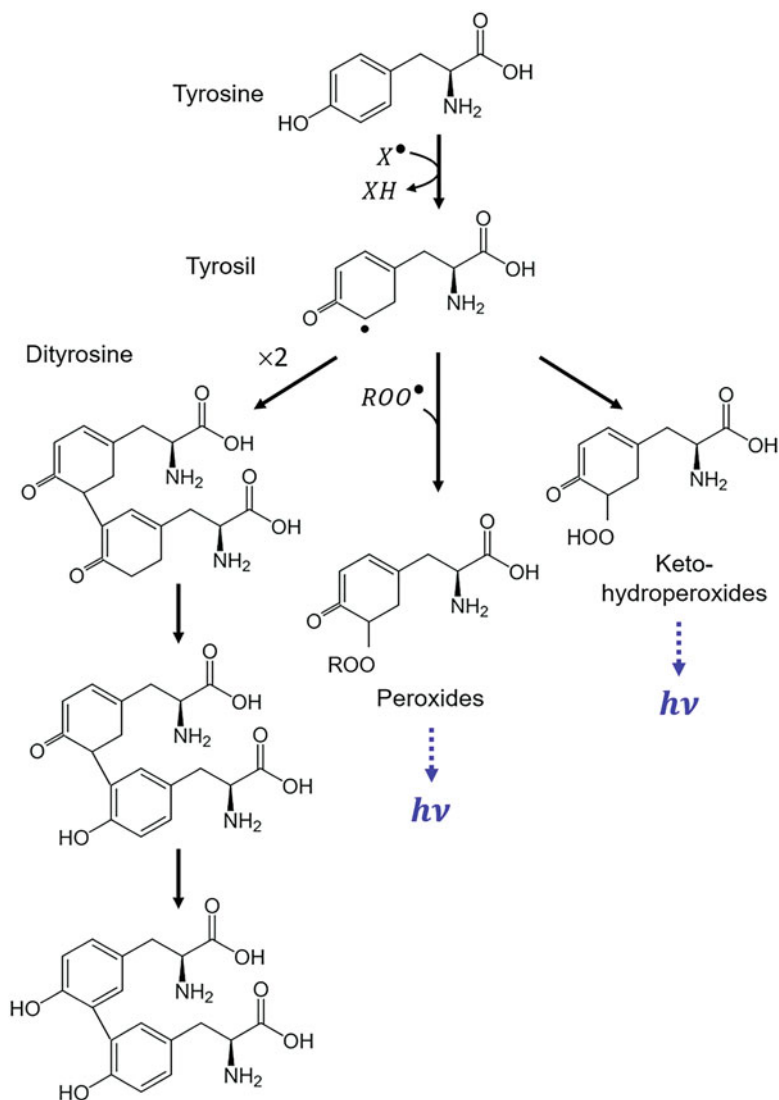
Thus, OCL from amino acids and proteins is generated in the course of at least two different types of processes:

1. Peroxy radical reactions (probably, recombination of the Russell type, but it doesn't exclude other possibilities). This component can be inhibited by Trolox at any stage;
2. Reactions of accumulated hydroperoxides, generating the truly molecular component of OCL. This component is insensitive to Trolox, and suppressed by Ebselen

Besides, this list may need to be supplemented with one more component: reactions of peroxy radicals with certain oxidation products (peroxides). This should be responsible for the Trolox- and Ebselen-dependent growing fraction of OCL. However, this needs to be studied further.

All these processes are initiated by the primary free radicals generated within the system by external stresses

Fig. 12.17 A supposed tyrosine oxidation scheme (after Aspée and Lissi 2000)



(irradiation or prooxidants), that give rise to chain peroxidation. In a real cell, they are also likely to be initiated by internal processes of enzymatic ROS generation (see Chap. 14).

The supposed oxidation schemes for tyrosine and tryptophan, according to Aspée and Lissi (2000), are given in Figs. 12.17 and 12.18, respectively.

OCL of proteins is generally reduced to a combination of OCL of tryptophan and tyrosine residues in their composition, taking into account their spatial positions and accessibility for free-radical attacks. Other oxidizable amino acids become important sources of OCL at higher oxidation rates but then can become even more dominant (see Fig. 12.15).

However, a final, exhaustive scheme of amino acid and protein peroxidation is still to be constructed (a more detailed discussion can be found in Aspée and Lissi 2000, 2001; Fedorova et al. 2007).

References

- Aksentsev SL, Vladimirov YA, Olenev VI, Fesenko EE (1967) Study of the primary photoproducts of aromatic amino acids by the method of flash photolysis at 80 °K. *Biophysics* 12 (1):64–70
- Aksentsev SL, Vladimirov YA, Olenev VI (1966) Ionization of aromatic amino acids under influence of ultraviolet radiation. In: Frish SE (ed) *Optika i spektroskopija* [Optics and Spectroscopy]. Academy of Sciences of the USSR, Leningrad, pp. 57–64
- Alexander P, Fox M, Stacey KA, Rosen D (1956) Comparison of Some Direct and Indirect Effects of Ionizing Radiations in Protein. *Nature* 178 (4538):846–849. doi:<https://doi.org/10.1038/178846a0>
- Alexander P, Hamilton LDG (1960) Irradiation of Proteins in the Solid State: II. Chemical Changes Produced in Bovine Serum Albumin. *Radiat Res* 13 (2):214–233. doi:<https://doi.org/10.2307/3570954>
- Alvarez B, Radi R (2003) Peroxynitrite reactivity with amino acids and proteins. *Amino Acids* 25 (3–4):295–311. doi:<https://doi.org/10.1007/s00726-003-0018-8>
- Aspée A, Lissi EA (2000) Kinetics and mechanism of the chemiluminescence associated with the free radical-mediated oxidation of

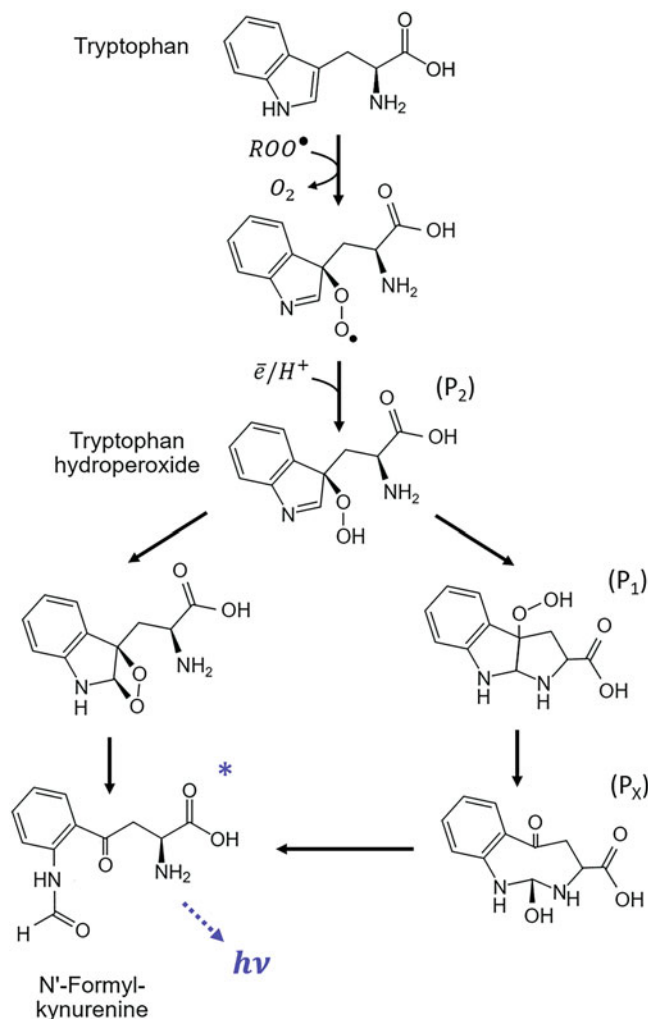


Fig. 12.18 A supposed tryptophan oxidation scheme (after Aspée and Lissi 2000)

- amino acids. *Luminescence* 15 (5):273–282. doi:10.1002/1522-7243(200009/10)15:5 < 273::aid-bio591 > 3.3.co;2-d
- Aspée A, Lissi EA (2001) Kinetics of the chemiluminescence associated to the reaction between peroxy radicals and proteins. *Journal of Protein Chemistry* 20 (6):479–485. doi:<https://doi.org/10.1023/A:1012554429450>
- Barnard ML, Gurdian S, Diep D, Ladd M, Turrens JF (1993) Protein and amino acid oxidation is associated with increased chemiluminescence. *Archives of biochemistry and biophysics* 300 (2): 651–656. doi:<https://doi.org/10.1006/abbi.1993.1090>
- Blyumenfel'd LA, Kalmanson EA (1957)? (In Russian). *Biofizika (Russ)* 2 (5):552–565
- Bradshaw RA, Fiorella C, Ericsson LH, Neumann PA, Piccoli SPS, Milton J., Shriefer K, Walsh KA (1981) Amino acid sequence of *Escherichia coli* alkaline phosphatase. *Proc Natl Acad Sci USA* 78 (6):3473–3477
- Davies MJ (2005) The oxidative environment and protein damage. *Biochimica et biophysica acta* 1703 (2):93–109. doi:<https://doi.org/10.1016/j.bbapap.2004.08.007>
- Davies MJ (2016) Protein oxidation and peroxidation. *The Biochemical journal* 473 (7):805–825. doi:<https://doi.org/10.1042/BJ20151227>
- Debye P, Edwards JO (1952a) A Note on the Phosphorescence of Proteins. *Science* 116 (3006):143–144. doi:<https://doi.org/10.1126/science.116.3006.143>
- Debye P, Edwards JO (1952b) Long-Lifetime Phosphorescence and the Diffusion Process. *The Journal of chemical physics* 20 (2): 236–239. doi:<https://doi.org/10.1063/1.1700385>
- Fedorova GF, Trofimov AV, Vasil'ev RF, Veprintsev TL (2007) Peroxy-radical-mediated chemiluminescence: mechanistic diversity and fundamentals for antioxidant assay. *Arkhivoc* 8:163–215
- Giese AC, Leighton PA (1937) Phosphorescence of cells and cell products. *Science* 85 (2209):428–429. doi:<https://doi.org/10.1126/science.85.2209.428-b>
- Gordy W, Ard WB, Shields H (1955) Microwave spectroscopy of biological substances. I. Paramagnetic resonance in x-irradiated amino acids and proteins. *Proceedings of the National Academy of Sciences* 41 (11):983. doi:<https://doi.org/10.1073/pnas.41.11.983>
- Gordy W, Shields H (1958) Electron Spin Resonance Studies of Radiation Damage to Proteins. *Radiat Res* 9 (6):611–625. doi:<https://doi.org/10.2307/3570707>
- Grossweiner LI, Swenson GW, Zwicker EF (1963a) Photochemical generation of the hydrated electron. *Science* 141 (3583): 805–806. doi:<https://doi.org/10.1126/science.141.3583.805>

- Grossweiner LI, Zwicker EF, Swenson GW (1963b) Photochemical production of the solvated electron in ethanol. *Science* 141 (3586): 1180. doi:<https://doi.org/10.1126/science.141.3586.1180>
- Herberg Richard J (1958) Phosphorescence in Liquid Scintillation Counting of Proteins. *Science* 128 (3317):199–200. doi:<https://doi.org/10.1126/science.128.3317.199>
- Kamei K, Hara S, Ikenaka T, Murao S (1988) Amino Acid Sequence of a Lysozyme (B-Enzyme) from *Bacillus subtilis* YT-251. *J Biochem* 104:832–836
- Katibnikov MA, Konev SV (1962). *Biofizika* (Russ) 7:270
- Khabiri F, Hagens R, Smuda C, Soltau A, Schreiner V, Wenck H, Wittern KP, Duchstein HJ, Mei WP (2008) Non-invasive monitoring of oxidative skin stress by ultraweak photon emission (UPE)-measurement. I: mechanisms of UPE of biological materials. *Skin Research and Technology* 14 (1):103–111. doi:<https://doi.org/10.1111/j.1600-0846.2007.00205.x>
- Konev SV, Katibnikov MA (1961) Prolonged afterglow of proteins and amino acids at room temperature-i. Kinetics of afterglow of proteins and amino acids. *Biophysics* 6 (5–6):715–722
- Krasnovsky AAJ (2007) Singlet oxygen and primary mechanisms of photodynamic therapy and photodynamic diseases. In: Uzdensky AB (ed) *Photodynamic therapy at the cellular level*. pp. 17–62
- Levshin VL (1936) Recherches sur la décroissance de la luminescence et le mécanisme d'émission de différentes substances. *Acta Phys Polonica* (5):301–317
- Levshin VL, Vinokurov (1934). *Physik Z Sowjetunion* 10:10
- Lewis GN, Lipkin D (1942) Reversible Photochemical Processes in Rigid Media: The Dissociation of Organic Molecules into Radicals and Ions. *Journal of the American Chemical Society* 64 (12): 2801–2808. doi:<https://doi.org/10.1021/ja01264a025>
- Lissi EA, Clavero N (1990) Inactivation of lysozyme by alkylperoxy radicals. *Free Rad Res Comms* 10 (3)
- Lissi EA, Salim-Hanna M, Faure M, Videlas LA (1991) 2,2'-Azo-bis-aminopropane as a radical source for lipid peroxidation and enzyme inactivation studies. *Xenobiotica* 21 (8):995–1001
- Majorek KA, Porebski PJ, Dayal A, Zimmerman MD, Jablonska K, Stewart AJ, Chruszcz M, Minor W (2012) Structural and immunologic characterization of bovine, horse, and rabbit serum albumins. *Mol Immunol* 52 (3–4):174–182. doi:<https://doi.org/10.1016/j.molimm.2012.05.011>
- Merkel PB, Nilsson R, Kearns DR (1972) Deuterium effects on singlet oxygen lifetimes in solutions. New test of singlet oxygen reactions. *Journal of the American Chemical Society* 94 (3):1030–1031. doi:<https://doi.org/10.1021/ja00758a072>
- Nickel B (1996) Pioneers in photochemistry: from the Perrin diagram to the Jablon- ski diagram. *EPA Newsletter* (58):9–38
- Nickel B (1997) Pioneers in photochemistry: from the Perrin diagram to the Jablon- ski diagram. Part 2. *EPA Newsletter* (61):27–60
- Nicol DS, Smith LF (1960) Amino-acid sequence of human insulin. *Nature* 187:483–485. doi:<https://doi.org/10.1038/187483a0>
- Norman A, Ginoza W (1958) Molecular Interactions in Irradiated Solids. *Radiat Res* 9 (1):77–83. doi:<https://doi.org/10.2307/3570782>
- Oh S, Lee C, Yang W, Li A, Mukherjee A, Basan M, Ran C, Yin W, Tabin CJ, Fu D, Xie XS, Kirschner MW (2022) Protein and lipid mass concentration measurement in tissues by stimulated Raman scattering microscopy. *Proceedings of the National Academy of Sciences of the United States of America* 119 (17): e2117938119. doi:<https://doi.org/10.1073/pnas.2117938119>
- Pollet E, Martynez JA, Metha B, Watts BPJ, Turrens JF (1998) Role of Tryptophan Oxidation in Peroxynitrite-Dependent Protein Chemiluminescence. *Archives of biochemistry and biophysics* 349 (1):74–80
- Randall JT, Wilkins MHF, Oliphant MLE (1945a) Phosphorescence and electron traps - I. The study of trap distributions. *Proceedings of the Royal Society of London Series A Mathematical and Physical Sciences* 184 (999):365–389. doi:<https://doi.org/10.1098/rspa.1945.0024>
- Randall JT, Wilkins MHF, Oliphant MLE (1945b) Phosphorescence and electron traps II. The interpretation of long-period phosphorescence. *Proceedings of the Royal Society of London Series A Mathematical and Physical Sciences* 184 (999):390–407. doi:<https://doi.org/10.1098/rspa.1945.0025>
- Randall JT, Wilkins MHF, Oliphant MLE (1945c) The phosphorescence of various solids. *Proceedings of the Royal Society of London Series A Mathematical and Physical Sciences* 184 (999):347–364. doi:<https://doi.org/10.1098/rspa.1945.0023>
- Roshchupkin DI, Vladimirov YA (1965) Investigation of primary photochemical processes in proteins-II. Reactions in frozen solutions of aromatic amino acids and proteins at 77–200 °K. *Biophysics* 10 (1): 50–58
- Sapezhinskii II (1969) Basic parameters of photochemiluminescence of protein solutions. *Khim Vys Energii* 3 (4):325–330
- Sapezhinskii II, Dontsova EG (1973) Photochemiluminescence of tryptophan-containing peptides and proteins during photooxidation. I. Kinetic regularities of chemiluminescence, peptide decomposition and formation of a series of products in glycyl-tryptophan solutions (In Russian). *Biofizika+18* (5):813–820
- Sapezhinskii II, Emanuel' NM (1965) The mechanism behind the recombination of the radicals of irradiated proteins in the presence of oxygen. *Dokl Akad Nauk SSSR* 165 (4):845–847
- Sapezhinskii II, Silaev YV, Emanuel' NM (1963) Interaction of radicals from irradiated protein and polymethylmetacrylate with oxygen and alkylphenols. *Dokl Akad Nauk SSSR* 151 (3):584–586
- Sapezhinskii II, Silaev YV, Emanuel' NM (1964) Long afterglow in aqueous solutions of proteins and synthetic polymers when irradiated by X-rays. *Dokl Akad Nauk SSSR* 159 (6):1378–1380
- Schischlowski AA, Wawilow SI (1934). *Physik Z Sowjetunion* (5): 379–392
- Slawiński J, Elbanowski M, Slawińska D (1980) Spectral characteristics and mechanism of chemiluminescence from tryptophan solutions induced by UV-irradiation. *Photochem Photobiol* 32 (2): 253–260. doi:<https://doi.org/10.1111/j.1751-1097.1980.tb04017.x>
- Smyth DG, Stein WH, Moore S (1963) The Sequence of Amino Acid Residues in Bovine Pancreatic Ribonuclease: Revisions and Confirmations. *Journal of Biological Chemistry* 238 (1): 227–234. doi:[https://doi.org/10.1016/s0021-9258\(19\)83984-4](https://doi.org/10.1016/s0021-9258(19)83984-4)
- Tarusov BN, Zhuravlev AI (1965) Biochemiluminescence of lipids (In Russian). In: *Bioluminescenciya. Trudy MOIP [Bioluminescence. MOIP Reports]*, vol 21. Nauka, Moscow, p 125
- Vassil'ev RF, Vichutinskii AA (1962) Chemiluminescence and oxidation. *Nature* 194 (4835):1276–1277
- Vladimirov YA, Aksentsev SL, Olenev VI (1965) Heat- and light-induced phosphorescence of proteins and aromatic amino acids irradiated with ultraviolet. *Biophysics* 10 (4):676–682
- Vladimirov YA, Roshchupkin DI, Fesenko EE (1970) Mechanism of ultraviolet radiation effects on proteins (In Russian). *Biofizika+15* (2):254–264
- Watts BP, Jr., Barnard M, Turrens JF (1995) Peroxynitrite-dependent chemiluminescence of amino acids, proteins, and intact cells. *Archives of biochemistry and biophysics* 317 (2):324–330. doi:<https://doi.org/10.1006/abbi.1995.1170>
- Wawilow SJ, Lewschin WL (1926). *Z Phys* 35:920–936
- Wels P (1928) Der Einfluß kurzweiliger Strahlen auf die Fluoreszenz von Eiweißkörpern und ihren Spaltprodukten. *Pflüger's Archiv für die gesamte Physiologie des Menschen und der Tiere* 219 (1): 738–752. doi:<https://doi.org/10.1007/BF01723455>
- Wels P, Jokisch M (1930) Der Einfluß der Quarzlampestrahlung auf die Fluoreszenz von Geweben und Zellen. *Pflüger's Archiv für die gesamte Physiologie des Menschen und der Tiere* 223 (1): 369–377. doi:<https://doi.org/10.1007/BF01794094>



Emitters of Endogenous Biological Chemiluminescence: Quantum Chemical Modeling Insights

13

Homa Saeidfirozeh, Francesco Lej, Michal Cifra, and Azizollah Shafiekhani

13.1 Introduction

The oxidation processes and the underlying chemical reactions that occur in organisms can generate molecules with electronically excited states that can emit light (Cilento 1973; Slawinska and Slawinski 1983; Vacher et al. 2018; Pospíšil et al. 2019; Cifra and Pospíšil 2014; Saeidfirozeh et al. 2018a). There is evidence that singlet oxygen (Miyamoto et al. 2007; Miyamoto et al. 2014) and triplet excited carbonyls (Vacher et al. 2018; Cilento and Adam 1995) are the two main excited state molecules that are primarily generated via chemiexcitation in biological systems. Although singlet oxygen emission spectra have been well-explored both experimentally (Schweitzer and Schmidt 2003; Adam et al. 2005; Losev et al. 1988) and theoretically (Schweitzer and Schmidt 2003; Minaev et al. 2009; Minaev 2017), there is no data on theoretical molecular-level calculations on emission from triplet excited carbonyls. The main physical parameter of interest that can be directly compared with experimental data is the emission spectrum of excited triplet carbonyls. Aldehydes are the most frequently analyzed carbonyls within this research field. Experimental evidence for electron-excited aldehydes generated through chemiexcitation suggests that the peak of

the emission is in the range of 400–450 nm (Bechara et al. 1979; Cilento 1984; Escobar et al. 1990). Spectra obtained by measuring the phosphorescence of aldehydes (excited states obtained by external light excitation) have confirmed this range (Oliveira et al. 1978; Schuh et al. 1984). There is also very extensive experimental evidence that carbonyls are generated during oxidative reactions – in fact, carbonylation is one of the well-accepted and widely used markers of oxidation of biomolecules (Rogowska-Wrzesinska et al. 2014; Purdel et al. 2014; Yan and Forster 2011). However, chemical detection of carbonyls does not provide information if the carbonyls were produced in an excited or ground state. Quantum chemical modeling of one of the processes (dioxetane decomposition), which is believed to generate excited state carbonyls, provides additional evidence that most of the excited state carbonyls are generated through chemiexcitation are in the triplet excited state (Farahani et al. 2013; Augusto et al. 2017). The triplet excited carbonyls may then undergo various decay pathways, including further reactions, transferring electron excitation energy to acceptors (Bohne et al. 1986; Durán and Cilento 1980) (which can then emit energy at longer wavelengths) or directly emitting the photon.

Molecular oxygen (O_2) is a known quencher of excited state carbonyls. Quenching takes place by excitation energy transfer from a carbonyl to O_2 and creating O_2 in an excited state (singlet oxygen, 1O_2) (Bastos et al. 2017; Gundermann and McCapra 1987). Various energy substrates of 1O_2 have also been claimed to be able to emit (1O_2 dimolar emission) at wavelengths that are (Khan and Kasha 1970) close to that of the carbonyl triplet excited state, hence creating ambiguity in the spectral evidence of carbonyl emission. Therefore, it is important to obtain a deeper theoretical understanding of the emission spectra of the carbonyl triplet excited state. Quantum mechanical modeling approaches are known to provide accurate predictions of the transitions between vibrational and electronic energy levels in molecules. Such an approach can be used to model the absorption and emission of photons

H. Saeidfirozeh (✉)

J. Heyrovský Institute of Physical Chemistry, Czech Academy of Sciences, Prague, Czech Republic
e-mail: homa.saeidfirozeh@jh-inst.cas.cz

F. Lej

La.M.I. and LaSCAMM INSTM Sezione Basilicata, Dipartimento di Chimica, Università della Basilicata, Potenza, Italy
e-mail: Francesco.lej@unibas.it

M. Cifra

The Czech Academy of Sciences, Institute of Photonics and Electronics, Prague, Czech Republic
e-mail: cifra@ufe.cz

A. Shafiekhani

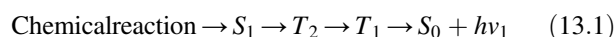
Department of Physics, Alzahra University, Tehran, Iran
e-mail: ashafie@alzahra.ac.ir

by molecules. Following our preliminary work (Saeidfirozeh et al. 2017; Saeidfirozeh et al. 2018b), the emission from the triplet excited states has been modeled in the case of the simplest molecules that contain carbonyl groups: formaldehyde, acetaldehyde, and acetone.

13.2 Chemiluminescence from Biological Systems as a Triplet Excited State Indicator

The lowest energy singlet excited state can undergo spin-orbit coupling (SOC), an intersystem crossing process into an energy state of higher spin multiplicity, which is known as a triplet state. The triplet state has a low transition probability (long decay time) to the ground state through the ‘dipole forbidden’ process because of the spin mismatch between the triplet and the singlet ground states. If it does not lose energy through non-radiative channels, it can decay radiatively to the singlet ground state with a ‘dipole forbidden’ but spin-orbit (SO) allowed transition. These transitions progress with significantly slower time scales because of the weakness of the SO interaction. If the quantum yield of these processes is large, it will release significant amounts of light over long time scales and create the so-called glow-in-the-dark effect.

As shown in Fig. 13.1, eventually, a chemical process can engender a new molecule in an excited state. If the system does not undergo a vibrational relaxation to the singlet ground state, a possible SOC interaction can allow a spin flip, moving it to the manifold of the triplet excited states. Within this manifold, because ‘dipole allowed transition’ is forbidden between states of different multiplicity, the system can perform further vibrational relaxation to the lowest energy triplet state, where it can reside for longer (on a molecular scale and compared with spin-allowed transitions) time. SOC can then allow a radiative process to S_0 , giving rise to photon emission. Thus, this phenomenon can be expressed as:



in which S_0 and S_1 are the singlet ground state and singlet excited state, respectively, T_1 and T_2 are the triplet excited states, and $h\nu_1$ is the vertical lowest energy. To calculate the correct energy related to the emission from the triplet state, first, the geometry of the molecule in both the ground and excited state needs to be optimized.

The carbonyls we selected to analyze (formaldehyde, acetaldehyde, and acetone) have different geometry in the ground and excited state. These molecules have a planar geometry in their singlet ground state, in which all the atoms are in the same plane (See S_0 energy level in Fig. 13.1).

However, in the first triplet excited state, these molecules show non-planar pyramidal geometry, in which they are bent with a τ (H-C-O-H) angle, (H-C-O-C) angle, and (C-C-O-C) angle in formaldehyde, acetaldehyde, and acetone, respectively (bent by approximately 35° compared with their planar configuration) (See T_1 energy level in Fig. 13.1). It is known that in these molecules, the $n \rightarrow \pi^*$ state is pyramidally distorted in the triplet excited state (Hadad et al. 1993). For more details about the electronic structure of these molecules, an interested reader is referred to (Demtröder 2010).

13.3 Computational Approach

All first principle calculations were performed with the Gaussian 16 Rev. B.01 program package (Frisch et al. 2016). Moreover, the wavefunctions were expanded with the 6311+g(d,p) triple-zeta valence Gaussian-type basis set with polarization and diffuse functions (Krishnan et al. 1980).

First, the geometry of the molecules in both the ground and the triplet excited state was optimized. Then the vibrational frequencies for these optimized geometries in both states were analyzed to confirm that all positive frequencies were obtained. Afterwards, the emission from the triplet excited state to the singlet ground state was calculated. Optimized geometries for both states and emissions’ spectra were calculated by using twelve methods (See Fig. 13.2) to determine how different levels of theory and basis set affect the results. Because the emission of these molecules has also been studied experimentally (Robinson and DiGiorgio 1958; Charlesby and Partridge 1965; Mano et al. 2014), we could make a comparison with our theoretical results.

As shown in Fig. 13.2, it is clear that the Møller-Plesset perturbation theory at second order (MP2) method for these three molecules has the best agreement with experiments. This method outperforms even the best available density functional theory (DFT) calculation (Goerigk and Grimme 2011).

Because water is the common environment in which these excited states are generated, we investigated the effect of water solvents on the emission spectra.

However, it is very difficult to study the effect of discrete water molecules on the photo-physical properties owing to the many possible water arrangements around the studied molecules, whereas we are interested in their average effect on these properties. To avoid any complexity owing to the interaction between water and our molecules, we used the implicit solvation model. To address this important aspect, we employed the Polarizable Continuum Model (PCM), which uses the integral equation formalism variant (IEFPCM). This method creates the solute cavity by using a set of overlapping spheres surrounding the molecule (Tomasi et al. 2005). The procedure uses a set of spheres centered on

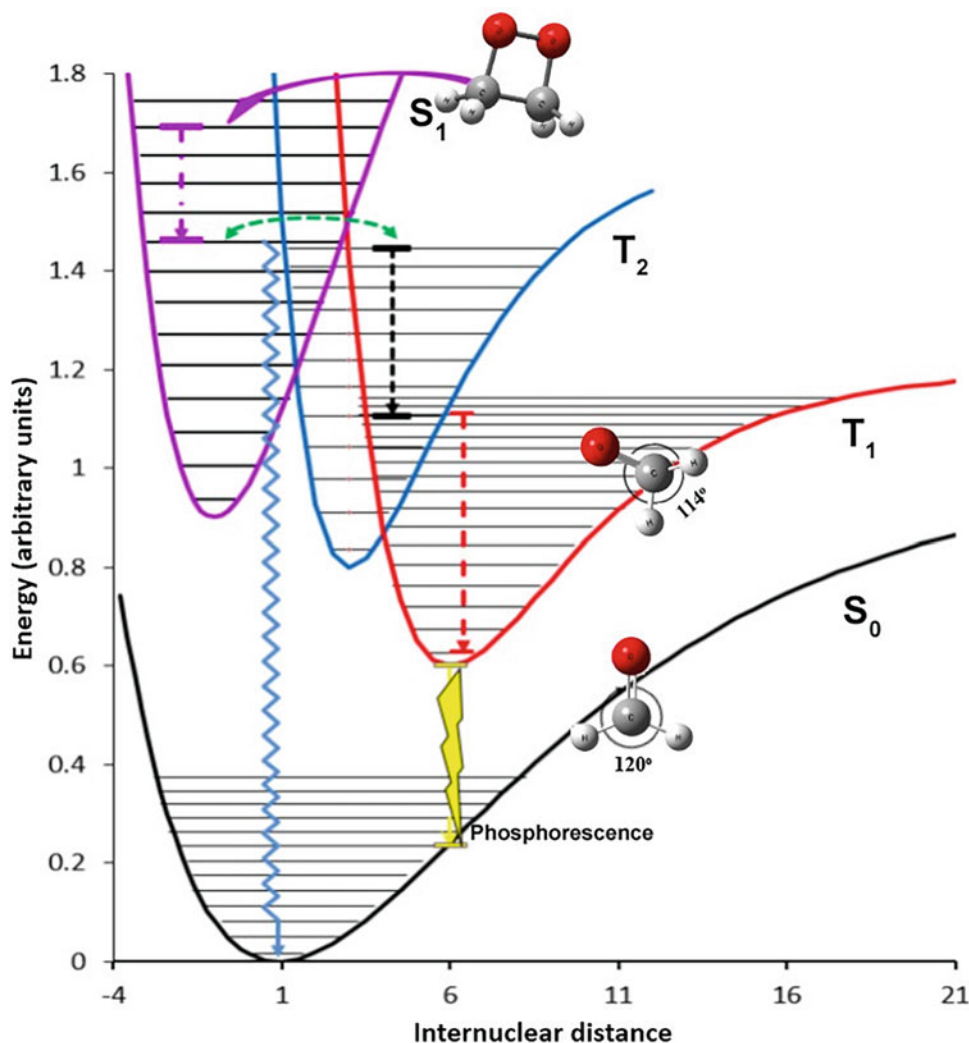


Fig. 13.1 Sketch of the possible Jablonsky-like energy plot of the adiabatic potential energy surface. S_0 and S_1 represent the singlet ground state and singlet excited state (black and purple lines), respectively. T_1 and T_2 represent the first and second triplet excited states (blue and red lines). T_2 could be assigned as any possible higher triplet excited state (Howarth et al. 2015). Abscissas-parallel thin lines within the Morse-like plots represent vibrational states associated with each adiabatic potential energy surface. The heavy purple arrow represents a possible chemical process (e.g., dioxetane decomposition) that engenders a carbonyl group in the S_1 state in some of its excited vibrational states. Dashed arrow lines represent vibrational cascades within each excited state. The double arrow green dashed line represents the intersystem

crossing process enabled by SOC between states of different multiplicity. Further internal conversion within T_2 and interstate transition to T_1 allow the system to reach a state of lower energy. The radiative transition from T_1 to S_0 (yellow 'bolt-like' line) is enabled owing to SOC between T_1 and S_0 . This radiative transition is the one that is suggested to give rise to photon emission from triplet excited carbonyls in endogenous chemiluminescence. A further non-radiative decay channel from S_1 is represented by the blue zig-zag line. See (Duben et al. 2013; Vo-Dinh and Cullum 2014; McLaren and Shugar 2016) for more information about excited states manifolds and transitions in general and (Ball 2014) for aldehydes, including the discussion of higher triplet states, such as T_2

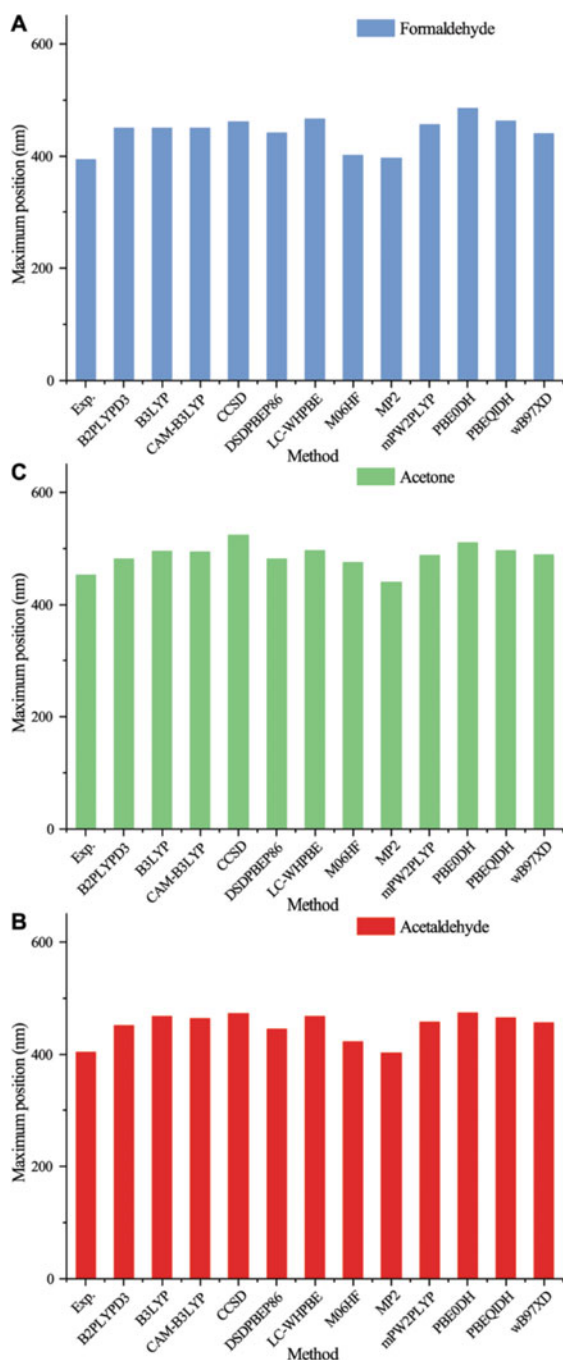


Fig. 13.2 The wavelength of the maximum (peak) in the water environment of the triplet emission spectra of the studied molecules for the different levels of theory used for its computation. The abbreviations of the theoretical approaches are labeled on the X-axis. The blue, red, and green bar charts refer to the peaks for formaldehyde, acetaldehyde, and acetone, respectively

each molecule atom and the inner surface defines the place where the reacting field of the solvent is computed. The

results of the calculated T_1 - S_0 emission spectra are shown in Fig. 13.3. The emission spectrum of the molecules in water is consistently blue-shifted compared with the gas phase for each of the three carbonyls. This finding might have relevance in biological systems: in enzymatic systems, it has been suggested that the excited state is generated from the substrate in the cavity of the enzyme (Baader et al. 1985). The static dielectric permittivity (which affects the polarizability) of the protein ($\epsilon_0 = 2-3$) (Zhao et al. 2011; Krivosudský et al. 2017) is typically much closer to the vacuum value than the static permittivity of water ($\epsilon_0 = 80$) (Ellison 2007; Cifra et al. 2019).

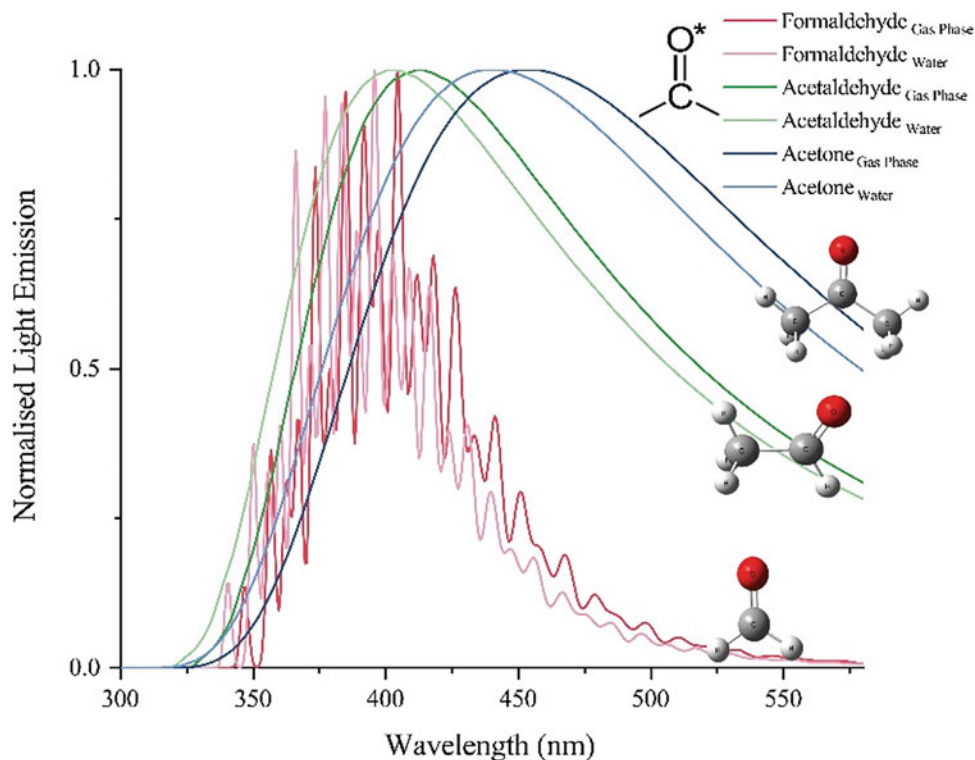
Furthermore, these results also showed that the presence of further methyl groups causes a shift of the spectra to longer wavelengths. Here, we should highlight that, in the case of formaldehyde, because the manifold of vibrational states is not as dense as in the case of larger molecules, the pattern of transitions between vibrational states belonging to the excited T_1 and the S_0 ground state is evident. In the case of acetaldehyde and acetone, the higher density of the vibrational states in T_1 and S_0 smooths out the plot, overriding the vibronic details. In general, our theoretical results match the experimental values obtained for the peak of the chemiluminescence in the blue region (400–450 nm), which is presumed to come from tripled excited carbonyls.

13.4 Conclusion

In this chapter, we demonstrated how modern quantum chemical approaches can provide a deeper understanding of the detected spectrum of biological chemiluminescence. We foresee that a massive application and computational screening of the spectra of various carbonyl species (as potential emitters) can potentially enable mechanistic interpretation of shifts of the emission spectra during various physiological states, diseases, or from various biological species. Such mechanistic understanding will foster the use of endogenous biological chemiluminescence in analytical, biotechnological, and biomedical applications.

Acknowledgements The authors gratefully acknowledge Dr. Rosendo Valero, who gave valuable suggestions and discussions during this research project. HS, on behalf of the Laboratory of High Resolution Spectroscopy, gratefully acknowledges ERDF/ESF ‘Centre of Advanced Applied Sciences’ (No. CZ.02.1.01/0.0/0.0/16_019/0000778). MC also acknowledges the Czech Science Foundation project no.20-06873X for major financial support. The authors are also participating in COST Actions CA1521 and the bilateral exchange project between the Czech and Slovak Academy of Sciences, no. SAV-18-11.

Fig. 13.3 Theoretical spectrum of T_1 - S_0 phosphorescence emission of formaldehyde, acetaldehyde, and acetone in the gas phase and water environments. Vibrational effects on the spectrum are visible in the case of formaldehyde (see text for more details)



References

- W. Adam, D.V. Kazakov, V.P. Kazakov, *Chemical Reviews* **105**(9), 3371 (2005). DOI <https://doi.org/10.1021/cr0300035>. URL <http://pubs.acs.org/doi/abs/10.1021/cr0300035>
- F.A. Augusto, A. Francés-Monerris, I. Fdez. Galván, D. Roca-Sanjuán, E.L. Bastos, W.J. Baader, R. Lindh, *Phys. Chem. Chem. Phys.* **19**(5), 3955 (2017). DOI <https://doi.org/10.1039/C6CP08154A>. URL <http://xlink.rsc.org/?DOI=C6CP08154A>
- W. Baader, C. Bohne, G. Cilento, H. Dunford, *Journal of Biological Chemistry* **260**(18), 10217 (1985). Publisher: ASBMB
- D.W. Ball, in *Physical Chemistry* (Cengage Learning, 2014), p. 523. Google-Books-ID: mULAAgAAQBAJ
- E.L. Bastos, P. Farahani, E.J. Bechara, W.J. Baader, *Journal of Physical Organic Chemistry* **30**(9), e3725 (2017). DOI <https://doi.org/10.1002/poc.3725>. URL <http://doi.wiley.com/10.1002/poc.3725>
- E.J. Bechara, O.M. Oliveira, N. Duran, R.C.D. Baptista, G. Cilento, *Photochemistry and Photobiology* **30**(1), 101 (1979). URL <http://onlinelibrary.wiley.com/doi/10.1111/j.1751-1097.1979.tb07121.x/full>
- C. Bohne, A. Campa, G. Cilento, L. Nassi, M. Villablanca, *Analytical biochemistry* **155**(1), 1 (1986)
- A. Charlesby, R. Partridge, *Proceedings of the Royal Society of London. Series A. Mathematical and Physical Sciences* **283**(1394), 312 (1965). Publisher: The Royal Society London
- M. Cifra, P. Pospíšil, *Journal of Photochemistry and Photobiology B: Biology* **139**, 2 (2014). DOI <https://doi.org/10.1016/j.jphotobiol.2014.02.009>. URL <https://www.sciencedirect.com/science/article/pii/S1011134414000463>
- M. Cifra, J. Průša, D. Havelka, O. Krivosudský, *IEEE Journal of Electromagnetics, RF and Microwaves in Medicine and Biology* **3**(2), 97 (2019). DOI <https://doi.org/10.1109/JERM.2018.2878379>
- G. Cilento, *Quarterly reviews of biophysics* **6**(04), 485 (1973)
- G. Cilento, *Pure and Applied Chemistry* **56**(9), 1179 (1984)
- G. Cilento, W. Adam, *Free Radical Biology and Medicine* **19**(1), 103 (1995)
- W. Demtröder, *Atoms, Molecules and Photons: An Introduction to Atomic-, Molecular-and Quantum Physics* (Springer-Verlag Berlin Heidelberg, 2010)
- A.J. Duben, L. Goodman, M. Koyanagi, in *Excited States*, ed. Edward C. Lim (Academic Press, 2013), p. 295
- N. Durán, G. Cilento, *Photochemistry and Photobiology* **32**(1), (1980). DOI <https://doi.org/10.1111/j.1751-1097.1980.tb03997.x>. URL <https://onlinelibrary.wiley.com/doi/abs/10.1111/j.1751-1097.1980.tb03997.x>. eprint: <https://onlinelibrary.wiley.com/doi/pdf/10.1111/j.1751-1097.1980.tb03997.x>
- W.J. Ellison, *Journal of Physical and Chemical Reference Data* **36**(1), 1 (2007). DOI <https://doi.org/10.1063/1.2360986>. URL <http://aip.scitation.org/doi/10.1063/1.2360986>
- J.A. Escobar, G. Cilento, A.L.T.O. Nascimento, *Photochemistry and Photobiology* **51**(6), 713 (1990). DOI <https://doi.org/10.1111/php.1990.51.6.713>. URL <http://doi.wiley.com/10.1111/php.1990.51.6.713>
- P. Farahani, D. Roca-Sanjuán, F. Zapata, R. Lindh, *Journal of Chemical Theory and Computation* **9**(12), 5404 (2013). DOI <https://doi.org/10.1021/ct4007844>. URL <http://pubs.acs.org/doi/abs/10.1021/ct4007844>
- M. Frisch, G. Trucks, H. Schlegel, G. Scuseria, M. Robb, J. Cheeseman, G. Scalmani, V. Barone, G. Petersson, H. Nakatsuji, others, *Gaussian 16* (Gaussian, Inc. Wallingford, CT, 2016)

- L. Goerigk, S. Grimme, *Physical Chemistry Chemical Physics* **13**(14), 6670 (2011). Publisher: Royal Society of Chemistry
- K.D. Gundermann, F. McCapra, in *Chemiluminescence in Organic Chemistry* (Springer, 1987), pp. 19–32
- C.M. Hadad, J.B. Foresman, K.B. Wiberg, *The Journal of Physical Chemistry* **97**(17), 4293 (1993). URL <http://pubs.acs.org/doi/abs/10.1021/j100119a010>
- A.J. Howarth, M.B. Majewski, C.M. Brown, F. Lelj, M.O. Wolf, B.O. Patrick, *Dalton Transactions* **44**(37), 16272 (2015). DOI <https://doi.org/10.1039/C5DT02691A>. URL <http://xlink.rsc.org/?DOI=C5DT02691A>
- A.U. Khan, M. Kasha, *Journal of the American Chemical Society* **92**(11), 3293 (1970)
- R. Krishnan, J.S. Binkley, R. Seeger, J.A. Pople, *The Journal of chemical physics* **72**(1), 650 (1980). Publisher: American Institute of Physics
- O. Krivosudský, P. Dráber, M. Cifra, *EPL (Europhysics Letters)* **117**(3), 38003 (2017). DOI <https://doi.org/10.1209/0295-5075/117/38003>. URL <http://stacks.iop.org/0295-5075/117/i=3/a=38003?key=crossref.3c28df9298d7a713ff4bb8db342852f2>
- A.P. Losev, I.M. Byteva, G.P. Gurinovich, *Chemical physics letters* **143**(2), 127 (1988). URL <http://www.sciencedirect.com/science/article/pii/0009261488870258>
- C.M. Mano, F.M. Prado, J. Massari, G.E. Ronsein, G.R. Martinez, S. Miyamoto, J. Cadet, H. Sies, M.H.G. Medeiros, E.J.H. Bechara, P. Di Mascio, *Scientific Reports* **4** (2014). DOI <https://doi.org/10.1038/srep05938>. URL <http://www.nature.com/articles/srep05938>
- A.D. McLaren, D. Shugar, in *Photochemistry of Proteins and Nucleic Acids: International Series of Monographs on Pure and Applied Biology, Volume 22* (Elsevier, 2016). Google-Books-ID: k3_ODAAAQBAJ
- B. Minaev, *Chemical Physics* **483-484**, 84 (2017). DOI <https://doi.org/10.1016/j.chemphys.2016.11.012>. URL <https://linkinghub.elsevier.com/retrieve/pii/S0301010416308394>
- B.F. Minaev, V.A. Minaeva, Y.V. Evtuhov, *International Journal of Quantum Chemistry* **109**(3), 500 (2009). DOI <https://doi.org/10.1002/qua.21783>. URL <http://doi.wiley.com/10.1002/qua.21783>
- S. Miyamoto, G.E. Ronsein, F.M. Prado, M. Uemi, T.C. Corrêa, I.N. Toma, A. Bertolucci, M.C.B. Oliveira, F.D. Motta, M.H.G. Medeiros, P.D. Mascio, *IUBMB Life* **59**(4), 322 (2007). DOI <https://doi.org/10.1080/15216540701242508>. URL <http://doi.wiley.com/10.1080/15216540701242508>
- S. Miyamoto, G.R. Martinez, M.H. Medeiros, P. Di Mascio, *Journal of Photochemistry and Photobiology B: Biology* **139**, 24 (2014). DOI <https://doi.org/10.1016/j.jphotobiol.2014.03.028>. URL <http://linkinghub.elsevier.com/retrieve/pii/S1011134414001742>
- O. Oliveira, M. Haun, N. Durán, P. O'Brien, C. O'Brien, E. Bechara, G. Cilento, *Journal of Biological Chemistry* **253**(13), 4707 (1978). Publisher: American Society for Biochemistry and Molecular Biology
- P. Pospíšil, A. Prasad, M. Rác, *Biomolecules* **9**(7), 258 (2019). DOI <https://doi.org/10.3390/biom9070258>. URL <https://www.mdpi.com/2218-273X/9/7/258>
- N.C. Purdel, D. Margina, M. Ilie, *Annual Research & Review in Biology* **4**(12), 2015 (2014)
- G.W. Robinson, V.E. DiGiorgio, *Canadian Journal of Chemistry* **36**(1), 31 (1958). Publisher: NRC Research Press
- A. Rogowska-Wrzesinska, K. Wojdyla, O. Nedić, C.P. Baron, H.R. Griffiths, *Free Radical Research* **48**(10), 1145 (2014). DOI <https://doi.org/10.3109/10715762.2014.944868>. URL <http://www.tandfonline.com/doi/full/10.3109/10715762.2014.944868>
- H. Saeidfirozeh, M. Cifra, A. Shafiekhani, *Free Radical Biology and Medicine* **108**, S103 (2017). DOI <https://doi.org/10.1016/j.freeradbiomed.2017.04.331>. URL <http://www.sciencedirect.com/science/article/pii/S0891584917305348>
- H. Saeidfirozeh, A. Shafiekhani, M. Cifra, A.A. Masoudi, *Scientific Reports* **8**(1), 16231 (2018a). DOI <https://doi.org/10.1038/s41598-018-34485-6>. URL <http://www.nature.com/articles/s41598-018-34485-6>
- H. Saeidfirozeh, M. Cifra, A. Shafiekhani, *Free Radical Biology and Medicine* **120**, S128 (2018b). DOI <https://doi.org/10.1016/j.freeradbiomed.2018.04.422>. URL <http://linkinghub.elsevier.com/retrieve/pii/S0891584918305872>
- M.D. Schuh, S. Speiser, G.H. Atkinson, *The Journal of Physical Chemistry* **88**(11), 2224 (1984)
- C. Schweitzer, R. Schmidt, *Chemical Reviews* **103**(5), 1685 (2003). DOI <https://doi.org/10.1021/cr010371d>. URL <http://pubs.acs.org/doi/abs/10.1021/cr010371d>
- D. Slawinska, J. Slawinski, *Photochemistry and Photobiology* **37**(6), 709 (1983)
- J. Tomasi, B. Mennucci, R. Cammi, *Chemical reviews* **105**(8), 2999 (2005). Publisher: ACS Publications
- M. Vacher, I. Fdez. Galván, B.W. Ding, S. Schramm, R. Berraud-Pache, P. Nau-mov, N. Ferré, Y.J. Liu, I. Navizet, D. Roca-Sanjuán, W.J. Baader, R. Lindh, *Chemical Reviews* **118**(15), 6927 (2018). DOI <https://doi.org/10.1021/acs.chemrev.7b00649>. URL <http://pubs.acs.org/doi/10.1021/acs.chemrev.7b00649>
- T. Vo-Dinh, B.M. Cullum, in *Biomedical Photonics Handbook: Biomedical Diagnostics* (CRC Press, 2014), p. 485. Google-Books-ID: IY_LBQAAQBAJ
- L.J. Yan, M.J. Forster, *Journal of Chromatography B* **879**(17–18), 1308 (2011). DOI <https://doi.org/10.1016/j.jchromb.2010.08.004>. URL <http://linkinghub.elsevier.com/retrieve/pii/S157002321000485X>
- H. Zhao, P.H. Brown, P. Schuck, *Biophysical Journal* **100**(9), 2309 (2011). DOI <https://doi.org/10.1016/j.bpj.2011.03.004>. URL <http://linkinghub.elsevier.com/retrieve/pii/S0006349511003146>



14.1 UPE from Living Cells

As shown in the previous sections, ultraweak photon emission (UPE) from living cells, i.e., biological autoluminescence (BAL), is observed under plenty of different conditions and includes several components. For most systems, the main fraction of BAL is oxychemiluminescence (OCL) from lipids (Tarusov et al. 1962; Vladimirov 1967; Cadenas 1984) (see more in Chap. 10). However, in certain cases, a dominating role is played by OCL from proteins, specifically from oxidation of Trp and Tyr residues (see Chap. 11). For instance, OCL at oxidation of lipoproteins has both lipid and protein components, the lipid component making up the main part of the general intensity, yet the protein OCL being also considerable (Pollet et al. 1998; Watts et al. 1995).

Sometimes, the lipid and protein fractions of OCL can be distinguished by kinetics – as for oxidized BSA in (Barnard et al. 1993), where it had two kinetically different components: (1) an OCL flash, lasting 5–75 min, and proportional to the fatty acid content; and (2) stationary luminescence after the flash, proportional to the protein content. In other cases, such distinction appears much more complicated. Then, the main instruments for analyzing sources of BAL are spectroscopic studies, as well as fractioning of the system, and use of specific inhibitors and activators (see Chap. 5 and Sect. 8.5).

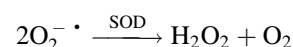
Anyway, as discussed above, BAL is generated by oxidative processes, involving free radicals, at least at some stages. However, though free-radical reactions are self-sustaining, there always must be a source of “the very first” – i.e., primary radicals. In model systems, these primary radicals are frequently generated by external impacts: irradiation or specific chemicals (see Sect. 8.4.1), while in biological systems, under natural conditions, the sources of primary radicals are mostly enzymatic (see Sect. 8.4.2), and the

radicals appearing in the system are reactive oxygen species (ROS), protein, and cofactor radicals (see Fig. 14.1 for an overall simplified picture of this). Below we will shortly discuss the mechanisms of enzymatic generation of these primary radicals, starting with immune system and the function of bacterial killing and finishing with ROS-dependent regulatory cascades.

14.2 ROS in Immune System: Bacterial Killing

One of the main sources of reactive oxygen species (ROS) in humans and animals are immune cells, namely, granulocytes, blood monocytes, and tissue macrophages (Yang et al. 2012; Babior 1978, 1984; Allen et al. 2000). The extensive literature on this topic comes back to the discovery of the respiratory burst – a dramatic increase in oxygen consumption at phagocytosis (Sbarra and Karnovsky 1959; Baldrige and Gerard 1932). Importantly, it is not aimed at any specific energy storage or use, but precisely at bacterial killing (Sbarra and Karnovsky 1959), involving intense generation of $O_2^- \cdot$ (Allen et al. 1972; Babior et al. 1973; Goldstein et al. 1975) and H_2O_2 (Iyer et al. 1961; Baehner et al. 1975).

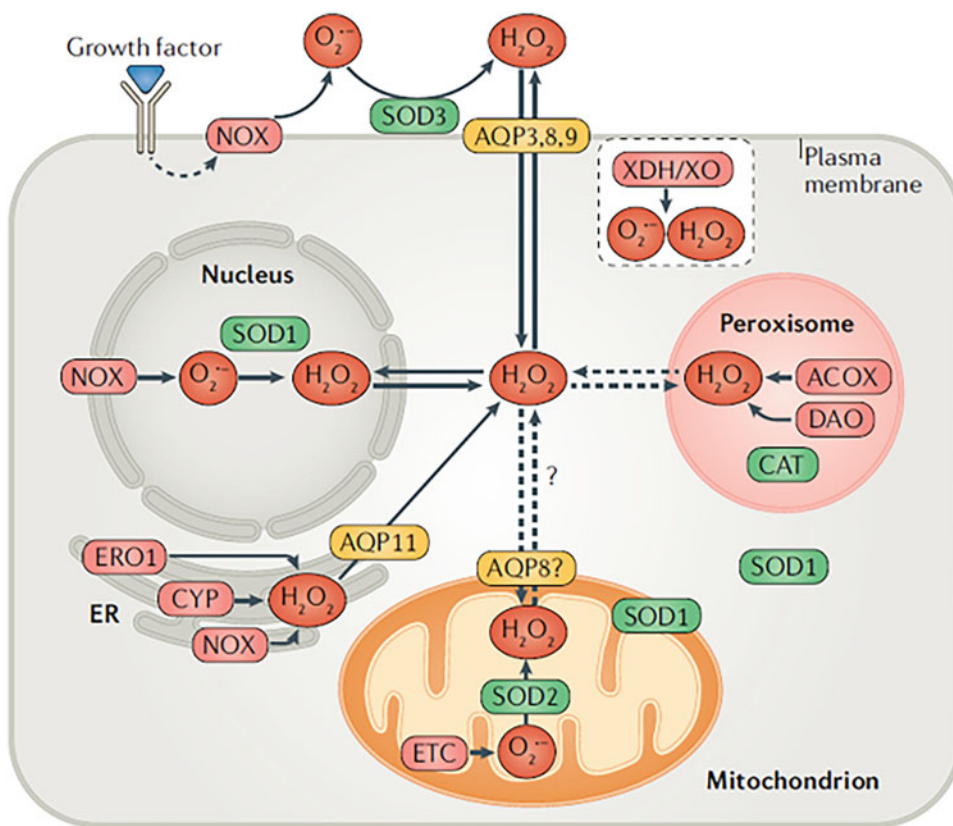
Methodically, the crucial point in this area was the discovery of superoxide dismutase (McCord and Fridovich 1969), catalyzing production of H_2O_2 from two superoxide anion-radicals:



This discovery, together with the already known catalase (Northrop 1925), reducing H_2O_2 to H_2O , brought all the advantages of inhibitory analysis into the field and resulted in a burst of investigations on the role of ROS in different reactions (McCord and Fridovich 1969; Hirata and Hayaishi 1971), and specifically in immune processes (Allen et al. 1972; Babior et al. 1973; Drath and Karnovsky 1975;

I. Volodyaev (✉) · Y. A. Vladimirov
Moscow State University, Moscow, Russia

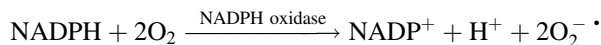
Fig. 14.1 Sources and targets of free radicals in a living cell: cell membranes, endoplasmic reticulum, mitochondria, and peroxisomes. ACOX, acyl-CoA oxidase; AQP, aquaporins; CAT, catalase; CYP, cytochrome P450-dependent monooxygenases; DAO, D-amino acid oxidase; ETC, electron-transport chain; ER, endoplasmic reticulum; ERO1, endoplasmic reticulum oxidoreductin 1; ETC, electron-transport chain; NOX, NADPH oxidase; SOD, superoxide dismutase; XDH, xanthine dehydrogenase/oxidase. The indicated list of participants is very far from complete; see more in the text. (Reprinted from (Sies and Jones 2020). Copyright 2020, with permission from Springer Nature)



Goldstein et al. 1975; Baehner et al. 1975; Root et al. 1975; Root and Metcalf 1977).

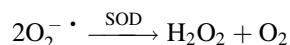
The presently well-known set of events at stimulated respiratory burst of phagocytes implies the following processes:

1. NADPH oxidase produces $O_2^{\cdot -}$ by transferring an electron from NADPH to oxygen dissolved in water (Allen et al. 1972):

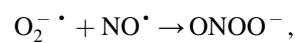


This reaction consumes all additional oxygen uptake at respiratory burst (Babior 1978).

2. The generated primary superoxide radicals are further dismutated by superoxide dismutase, forming hydrogen peroxide (McCord et al. 1971; Omar et al. 1992):



(with the reaction rate constant as high as $\sim 2 \times 10^9 \text{ M}^{-1} \text{ s}^{-1}$ (Fridovich 1975)), or react with NO, also generated at the respiratory burst (Carreras et al. 1994):

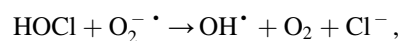
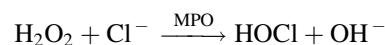


(with a still greater rate constant of $\sim 7 \times 10^9 \text{ M}^{-1} \text{ s}^{-1}$ (Huie 1993), so that nearly every collision between these species results in an irreversible reaction).

3. The produced ONOO^- is both a strong oxidant and a nitrating agent for macromolecules (see, e.g., (Szabó et al. 2007)), and if protonated, decomposes forming OH^{\cdot} radical (Beckman et al. 1990):

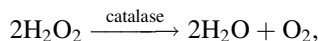
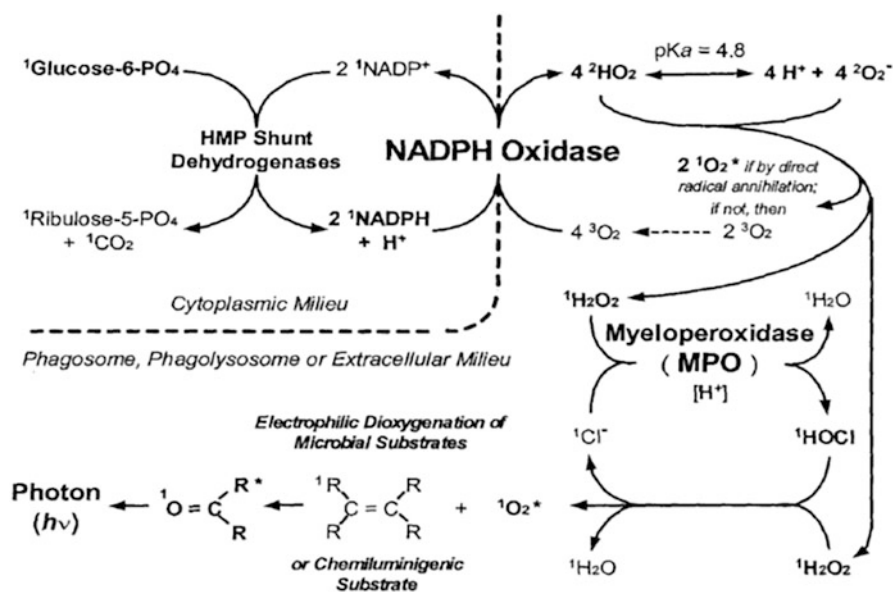


4. The produced H_2O_2 is further subjected to action of myeloperoxidase (Klebanoff 1999):

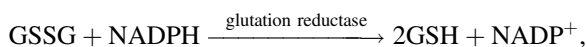
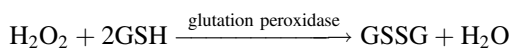


as well as catalase:

Fig. 14.2 The main enzymatic systems responsible for phagocyte microbicidal metabolism and oxygenation activities. (Reprinted with permission from (Allen et al. 2000). Copyright 2000, R.C. Allen et al.)



glutathione peroxidase–glutathione reductase system (Reed 1969):



Fenton reaction:



etc.

At immune response, all this leads to generation of singlet oxygen (Cadenas et al. 1981) and secondary radicals triggering free-radical oxidation of foreign particles (Iyer et al. 1961; Babior 1978; Root and Metcalf 1977; Dahlgren and Karlsson 1999) (Fig. 14.2; see also reviews (Allen et al. 2000; Dröge 2002; Yang et al. 2012)).

All this is accompanied by spontaneous UPE, lasting from several dozen minutes to several hours (see Fig. 14.3a), that can be activated by orders of magnitude with luminol, isoluminol, or other activators (see Fig. 14.3b).

Thus, the first discovered physiological source of UPE were activated phagocytes, actively producing reactive oxygen species in course of immune response. This process starts with NADPH oxidase, generating superoxide anion-radical, which is further involved in several reactions, producing other, more dangerous ROS, aimed at bacterial killing.

14.3 ROS in Signal Transduction

Until recently, bacterial killing was considered the only positive aspect of free-radical processes for the organism, and even that being connected to serious danger for the surrounding tissues (Arrigoni-Martelli 1985). Aside from that, ROS were considered a purely destructive agent arising under the influence of ionizing radiation, ultraviolet radiation, and a number of toxic substances and responsible for many diseases and aging (Harman 1956, 1981; Wei et al. 1989; Beckman and Ames 1998). Meanwhile, all the (already known) enzymes that work with ROS seemed to be nothing more than an ambulance for the cell, saving it from these harmful and dangerous species (see Fig. 14.4 for illustration).

However, today understanding of the ROS role in cell physiology and pathology has changed dramatically. Besides direct bactericidal action (see above), both $\text{O}_2^{\bullet -}$ and H_2O_2 have been shown to be important regulators of immune response (Kaul and Forman 1996; Torres and Forman 1999): activators of inflammation (Zhou et al. 2010; Tschopp and Schroder 2010; Bulua et al. 2011), natural killer activity (Duwe and Roder 1984; Duwe et al. 1985) (though not confirmed by some other authors (Ramstedt et al. 1984; Gibboney et al. 1988)), dendritic cells differentiation (Del Prete et al. 2008; Mantegazza et al. 2008; Kotsias et al. 2013; Matsue et al. 2003), activation, proliferation, function, and apoptosis of T cells (Williams and Kwon 2004; Tripathi and Hildeman 2004), etc. Importantly, their action appeared inter-related with increases in intracellular calcium, triggering IP3-mediated signaling and activating protein kinase C, i.e., the whole set of second messaging events (Murphy et al. 1995; Zhou et al. 1997; Girón-Calle and Forman 2000). Altogether, while in neutrophils, the main function of the

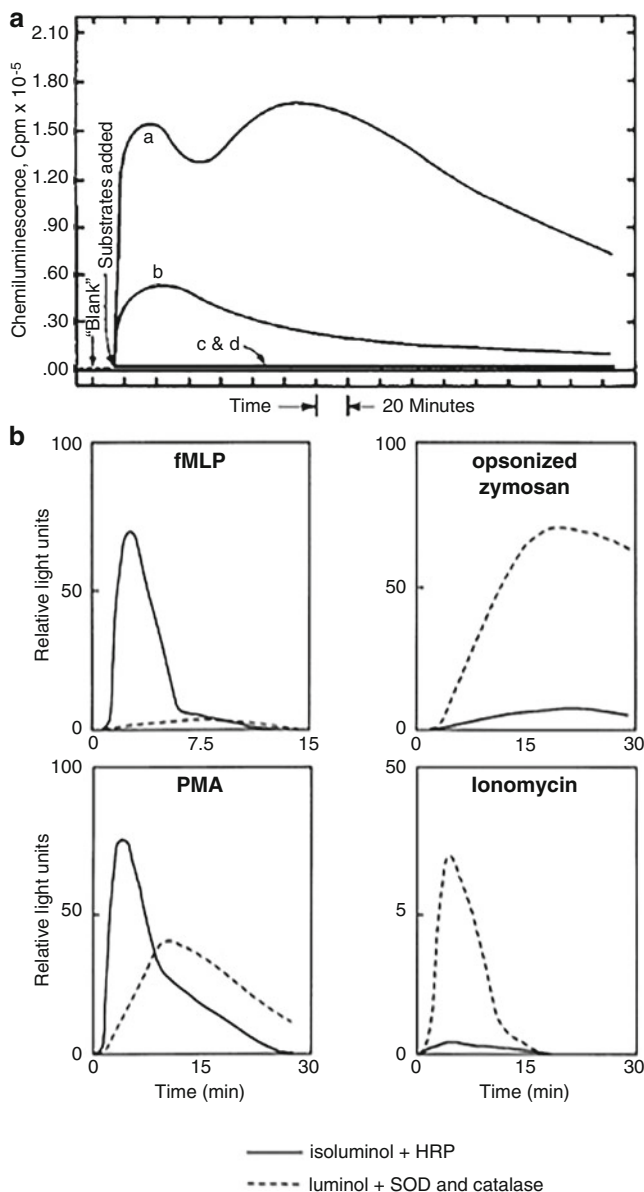


Fig. 14.3 Kinetics of spontaneous and activated UPE from polymorphonuclear leukocytes, obtained in different works (Allen et al. 1972; Dahlgren and Karlsson 1999). (a) spontaneous UPE (2.5×10^7 cells in 7 mL PBS), induced by addition of opsonized *P. shermanii* (curve a), opsonized latex particles (curve b) and nonopsonized *P. shermanii* (curve c) (from (Allen et al. 1972)). (b) activated CL of neutrophils, induced by various stimuli: fMLP (10^{-7} M), opsonized zymosan (10^7 /mL), phorbol myristate acetate (PMA, 5×10^{-8} M), and ionomycin (5×10^{-7} M), in relative units (from (Dahlgren and Karlsson 1999)). Solid line – extracellular chemiluminescence (activated by isoluminol, poorly penetrating into the cell due to its hydrophilic qualities, with addition of horseradish peroxidase). Dashed line – intracellular chemiluminescence (activated by luminol, easily penetrating into the cell, with extracellular chemiluminescence suppressed by superoxide dismutase and catalase). (a – reprinted from (Allen et al. 1972). Copyright 1972, with permission from Elsevier. b – reprinted from (Dahlgren and Karlsson 1999). Copyright 1999, with permission from Elsevier)

respiratory burst is still considered to be bactericidal, in other immune cells (for instance, macrophages, dendritic cells), it has become accepted as a primarily signaling process, linking different branches of the immune response (see more in (Iles and Forman 2002; Suzuki et al. 2011; Yang et al. 2012; Zhang et al. 2016; Forrester et al. 2018)).

Moreover, today, the prevalence of ROS appeared incomparably higher even than that. Besides immune cells, the family of NADPH oxidases (Nox/Duox) was found in many tissues, and participating in different regulatory cascades – from cell differentiation (Helfinger et al. 2017; Lardy et al. 2005; Li et al. 2006) to thyroid hormone biosynthesis (Ha et al. 2005), mechanotransduction of Ca^{2+} release in the heart (Prosser et al. 2011), epigenetic processes (Afanas'ev 2015), and beyond that (Sirokmány et al. 2016). In plants, NADPH-generated ROS activate Ca^{2+} channels, regulating their growth (Foreman et al. 2003). The famous oxidative burst at fertilization (Warburg 1908; Wong et al. 2004), as well as action of a number of growth factors (Lee 1998; Salmeen et al. 2003) were also found caused by NADPH oxidase activity, used for generation of $\text{O}_2^- \cdot / \text{H}_2\text{O}_2$ and further signal transduction. Moreover, growth factor signaling in general appeared deeply interrelated with the levels of $\text{O}_2^- \cdot$ and H_2O_2 , regulated by $\text{O}_2^- \cdot$ production and superoxide dismutase and catalase activity (Juarez et al. 2008) (see also review in (Marinho et al. 2014)).

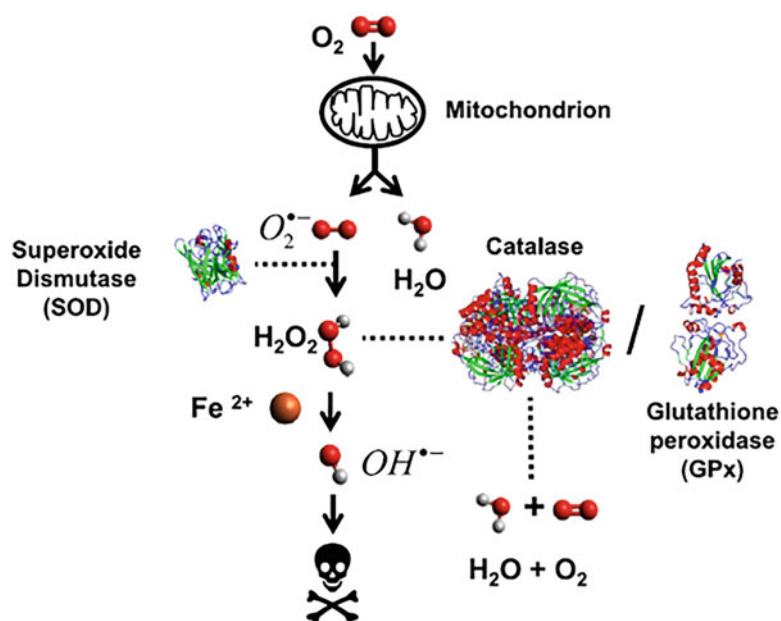
Besides Nox enzymes, a host of other intracellular enzymes were proven to be sources of ROS: the mitochondrial respiratory chain, xanthine oxidase, cyclooxygenases, cytochrome p450 enzymes, lipoxygenases, etc. (see below and also reviews in (Finkel 2011; Mittler et al. 2011; Forrester et al. 2018; Viña et al. 2013)). In all these enzymes, generation of ROS is a part of their normal physiological function, and in some cases – an integral stage of the enzymatic cycle (see below).

ROS signaling also appeared surprisingly widespread and evolutionary conserved among various species – from fungi and plants to mammals (Brown and Griendling 2009; Aguirre and Lambeth 2010; Foreman et al. 2003; Li et al. 2006), and even among yeast (Rinnerthaler et al. 2012) and prokaryotes (Hajjar et al. 2017; Juillan-Binard et al. 2017).

Importantly, the only clear function of NADPH oxidase family members known by now is regulated production of ROS, participating in bacterial killing (in phagocytes), intra- and intercellular signaling (see reviews in (Finkel 2011; Mittler et al. 2011; Viña et al. 2013)). Thus, their astonishing prevalence cannot be attributed to other circumstances besides their regulatory role.

Mechanistically, regulative action of so reactive and seemingly nonspecific destructive agents as ROS, is mostly due to relatively low reactivity and high diffusibility of H_2O_2 (see

Fig. 14.4 ROS as destructive factors in the cell. (Reprinted from (Sepasi Tehrani and Moosavi-Movahedi 2018). Copyright 2018, with permission from Elsevier)



also (Terada 2006; Cardoso et al. 2012)). The latter: (1) is enzymatically produced; (2) can travel at quite high distances, including preferential entry into the cell through aquaporin channels (Bienert et al. 2007; Miller et al. 2010); (3) has its levels precisely regulated by enzymes and antioxidants within the cell; and (4) has a specific action on external (not hidden in the protein globule) cysteine residues, likely playing the role of ROS receptors within certain proteins (Fomenko et al. 2007; Weerapana et al. 2010; Alderman et al. 2002) (see Fig. 14.5).

Indeed, H₂O₂ was shown to be a necessary mediator in a number of signaling paths, including MAPK and EGFR—ERK1/2 signaling, activated by UV irradiation and playing important role in UV defense of keratocytes (Peus et al. 1999; Devary et al. 1992; Heck et al. 2003, 2010), MAPK path in cardiac cell differentiation (Li et al. 2006), ROS-activated Ca²⁺ channels (Foreman et al. 2003), etc.

Moreover, the action of hydrogen peroxide can be different, and even opposite, depending on its concentration (e.g., (Zhou et al. 1997; Sies 2017), see reviews in (Sies and Jones 2020; Oxidative Stress Eustress and Distress 2019; Veal et al. 2007)), thus generating the whole world of redox signaling (Fig. 14.6).

All this, together with the enzymatic systems of ROS production and utilization, additional regulation by antioxidants, and, apparently, specific localization of sources and intended target of ROS (Woo et al. 2010; Mittler et al. 2011; Chen et al. 2008; Reddi and Culotta 2013), makes them an unexpectedly specific and very important line of second messaging and signal transduction in general.

In the following sections of this chapter, we discuss the mechanisms of action of certain ROS- and generally free-radical-generating enzymes in order to illustrate the

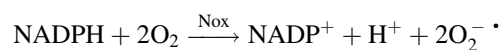
following basic statement: ROS and free radicals, in general, are constantly produced and utilized in the living cell, playing important regulatory functions and, at the same time, generating UPE at certain reactions. Figure 14.7 gives a basic scheme of this colossal free-radical/redox world of the cell.

14.4 ROS-Generating Enzymes

14.4.1 NADPH Oxidase

14.4.1.1 The Nox Complex and Its Role

NADPH oxidases (Nox family members) are transmembrane proteins that transport electrons across biological membranes to reduce oxygen to superoxide. Each oxidized NADPH molecule donates two electrons to the electron-transport chain, and each of these electrons is accepted by an oxygen molecule, resulting in the formation of superoxide:



NADPH oxidases have been identified in a wide variety of organisms, from mammals to nematodes, plants, fungi, and even bacteria (see a recently constructed phylogenetic tree of Nox enzymes in Fig. 14.8).

The Nox family members are classified into seven types, which have different structure and regulation and are differently distributed among taxons and in tissues (see Fig. 14.9). Some of them are constantly active (Nox4), others – activated as a stress-response via assembly of several domains into an active NADPH oxidase (Nox1–3, including the neutrophil

Fig. 14.5 Modifications of reactive cysteine residues as the basis for redox (ROS-mediated) signaling. (Reprinted from (Finkel 2011), under Creative Commons license. Copyright 2011, Rockefeller University Press)

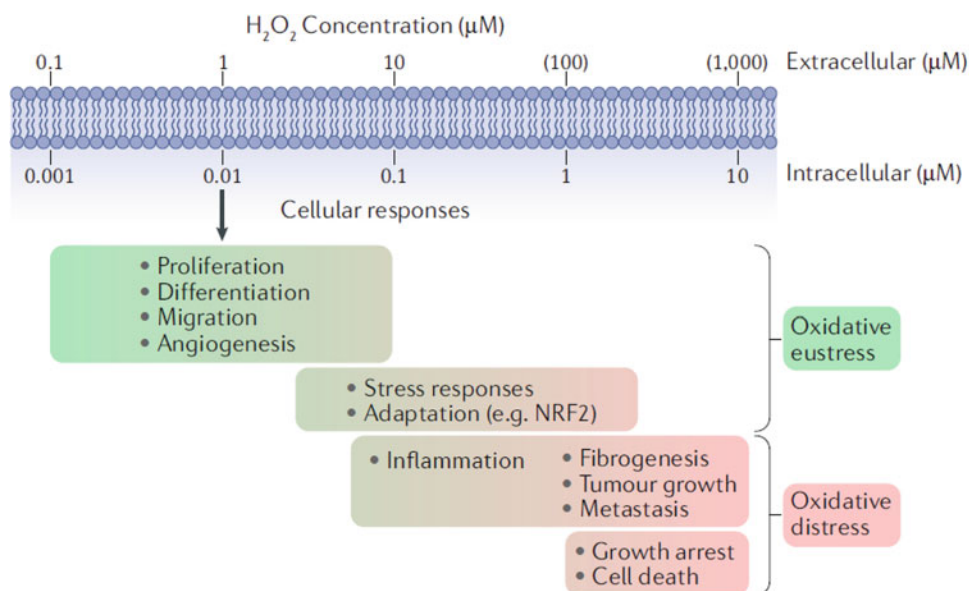
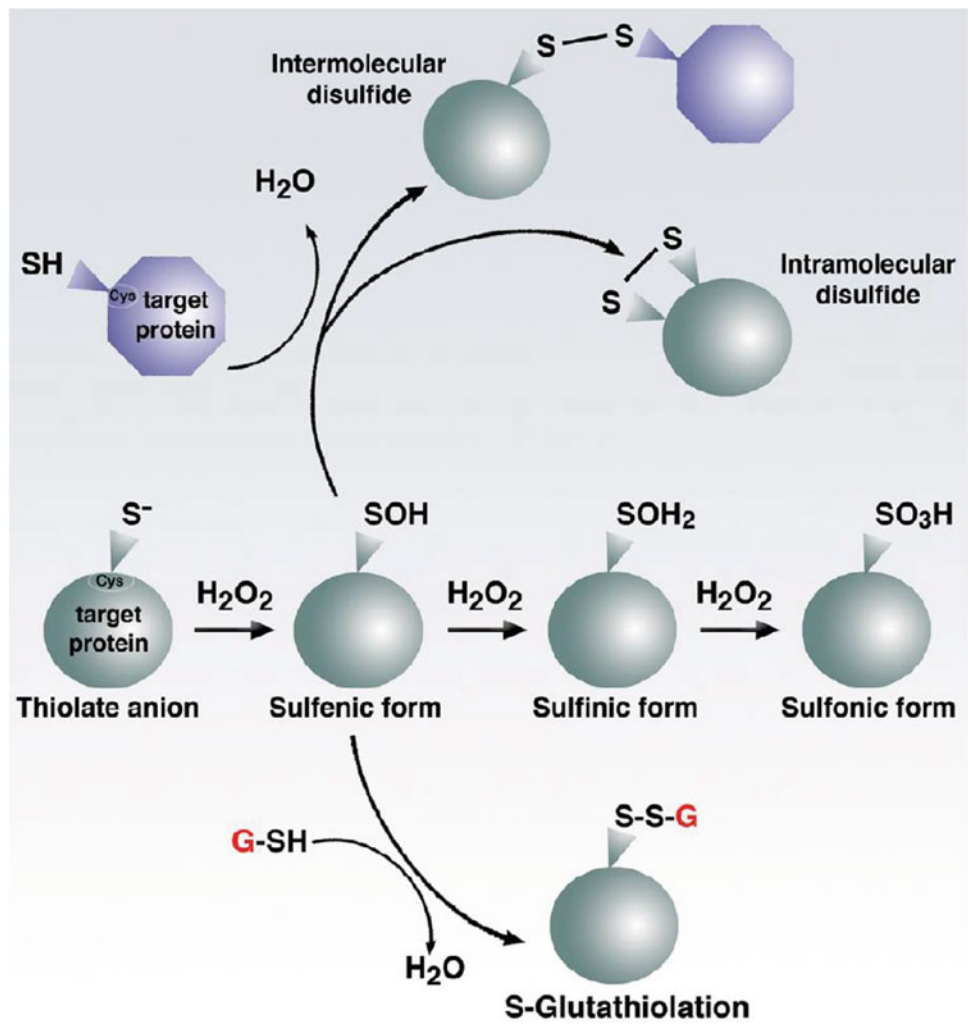


Fig. 14.6 The spectrum of possible actions of H₂O₂, depending on its concentration. “Oxidative eustress” (green) and “oxidative distress” (red) mark the physiological and pathophysiological modes. The intracellular physiological levels of H₂O₂ likely range between 1 and

100 nM; the arrow indicates H₂O₂ level in normally metabolizing liver (Sies 2017). (Reprinted from (Sies and Jones 2020). Copyright 2020, with permission from Springer Nature)

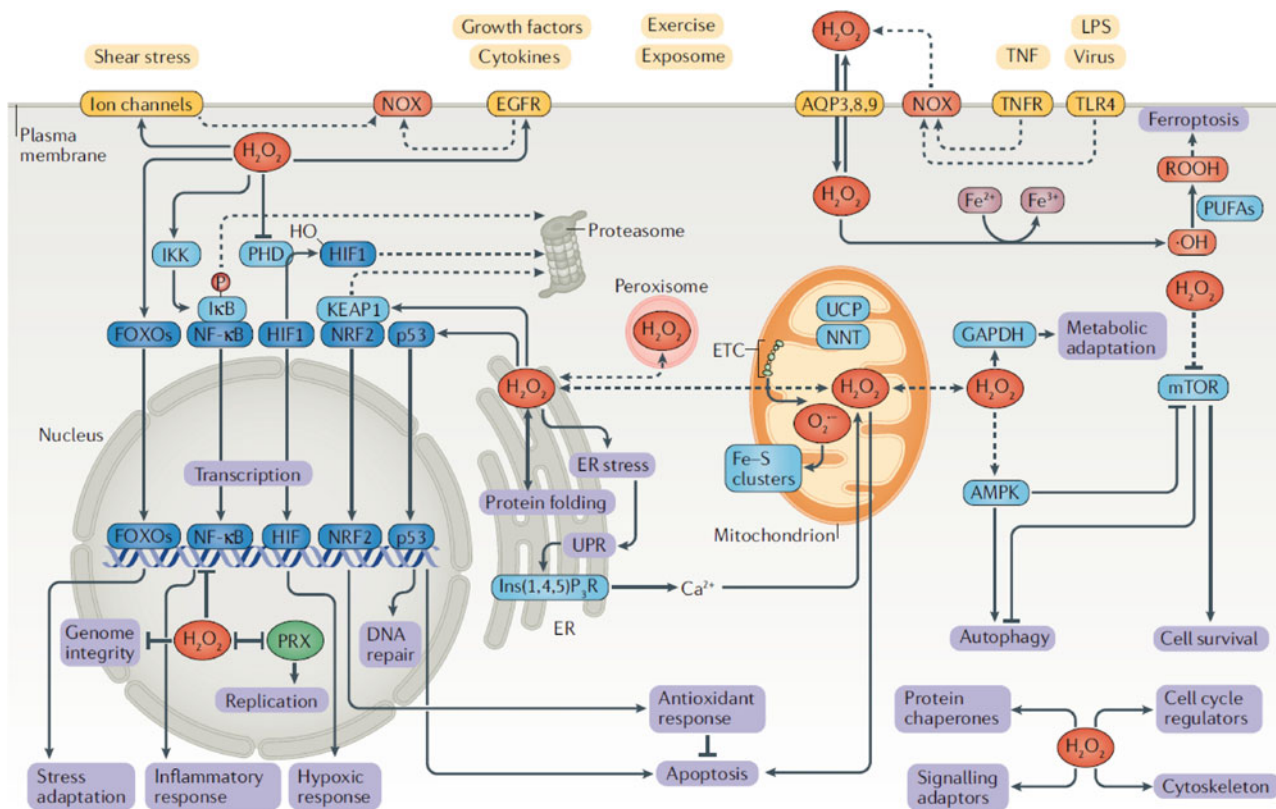


Fig. 14.7 ROS in cell signaling. AMPK, AMP-activated protein kinase; AQP, aquaporin; EGFR, epidermal growth factor receptor; ER, endoplasmic reticulum; ETC, electron-transport chain; FOXO, forkhead box protein O; GAPDH, glyceraldehyde 3-phosphate dehydrogenase; HIF, hypoxia-inducible factor; IκB, inhibitor of nuclear factor-κB; IKK, inhibitor of nuclear factor-κB kinase; Ins(1,4,5)P₃R, inositol 1,4,5-trisphosphate receptor; Keap1, kelch-like ECH-associated protein 1; LPS, lipopolysaccharide; mTOR, mammalian target of rapamycin;

NF-κB, nuclear factor-κB; NNT, nicotinamide nucleotide transhydrogenase; NOX, NADPH oxidase; NRF2, nuclear factor erythroid-2-related factor 2; PHD, prolyl hydroxylase; PRX, peroxiredoxin; PUFAs, polyunsaturated fatty acids; TLR4, Toll-like receptor 4; TNF, tumor necrosis factor; TNFR, tumor necrosis factor receptor; UCP, uncoupling protein; UPR, unfolded protein response. Dashed arrows indicate indirect processes. (Reprinted from (Sies and Jones 2020). Copyright 2020, with permission from Springer Nature)

oxidative burst oxidase Nox2), still others – activated by Ca²⁺ (Nox5). The basics of their function is shown in Fig. 14.10.

The physiological roles of Nox enzymes are diverse. In endothelial cells in the presence of superoxide, the amount of bioavailable NADPH decreases, which is directly involved in the regulation of blood pressure (Rabêlo et al. 2010; Di Meo et al. 2016). In the kidneys, ROS secreted by the Nox3 complex enhance the reabsorption of sodium chloride in the Henle loop (Gill and Wilcox 2006), ultimately modulating Na⁺/H⁺ exchange. In smooth muscle cells, Nox2 regulates cell proliferation and differentiation through the activation of the nuclear factor NF-κB and inducible NO synthase (Badran et al. 2020). Both of these enzymes are involved in the regulation of microglial proliferation and neuronal apoptosis during deprivation of nerve growth factor (NGF) (Di Meo et al. 2016). Also, NADPH oxidases activate repair of damaged tissues, inducing angiogenesis and cell proliferation (Fukai and Ushio-Fukai 2020).

Separate attention should be paid to the crosstalk between NADPH oxidase and pattern recognition receptors, which

include Toll-like receptors (TLR) and Nod-like receptors (Panday et al. 2015), leading to activation of various metabolic pathways and production of cytokines (Fukai and Ushio-Fukai 2020).

Thus, at present, there is no doubt that Nox family has a very important role both in the cell normal life and pathology (see more in reviews (Aguirre and Lambeth 2010; Belambri et al. 2018; Brown and Griendling 2009; Bedard and Krause 2007; Schröder 2020)).

14.4.1.2 The Phagocyte Nox2 Functioning

As mentioned above, in phagocytes, NADPH oxidase is represented by the Nox2 form, a multicomponent enzymatic complex embedded in the membrane lipid bilayer.

In resting cells, the NADPH oxidase subunits are distributed between the membrane (Rap1A and cytochrome b558 – p22^{phox} gp91^{phox} complex) and the cytosol (p40^{phox}, p47^{phox}, p67^{phox}, and Rac2), and the complex is inactive (see Fig. 14.11a). The complex assembly and function are activated in reply to diverse stimuli, acting through the

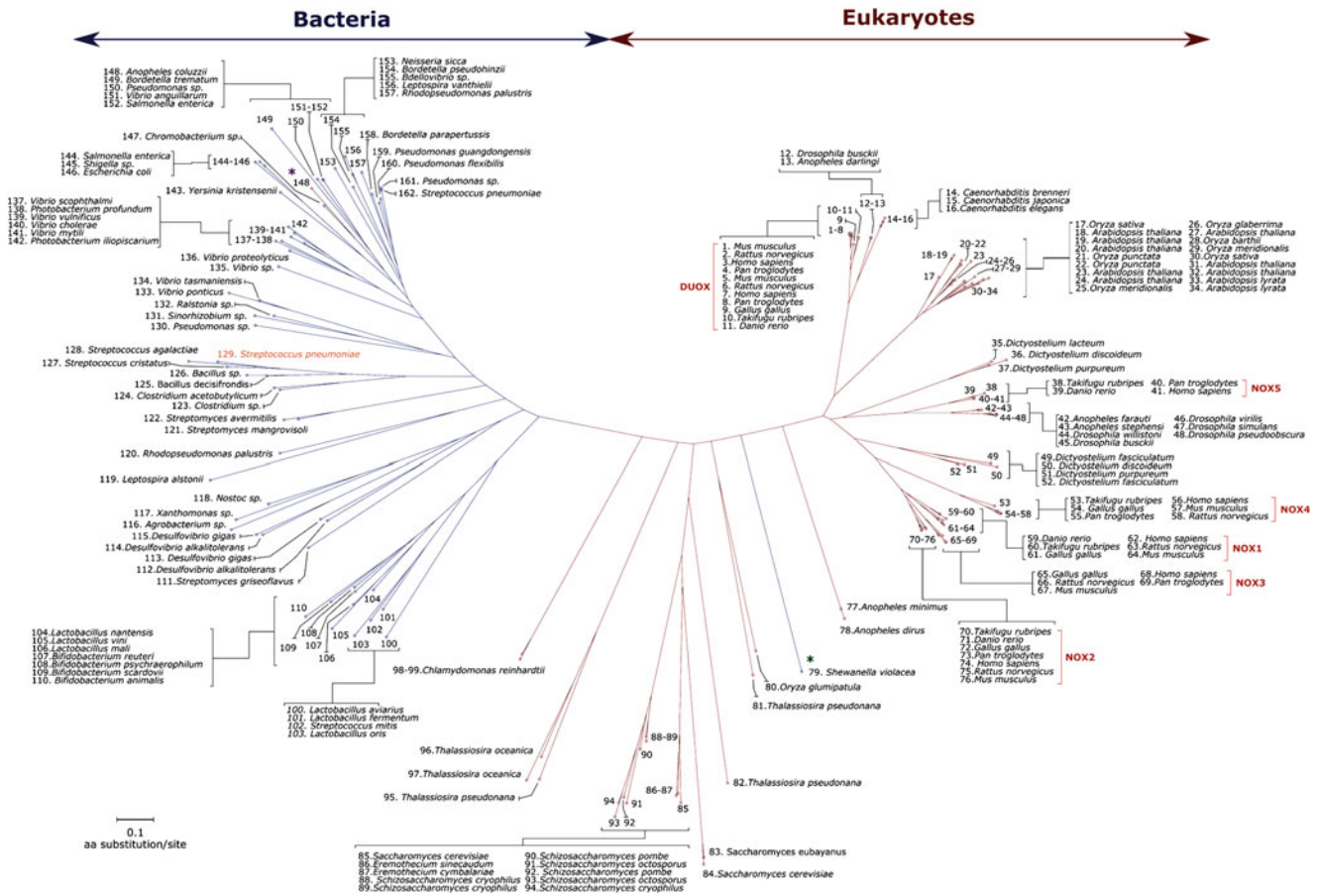


Fig. 14.8 Phylogenetic tree of the Nox family (from (Hajjar et al. 2017)). (Reprinted from (Hajjar et al. 2017), under Creative Commons license. Copyright 2017, American Society for Microbiology)

phagocyte receptor apparatus (Cree 1998; Bedard and Krause 2007). These stimuli are generally classified into:

- Corpuscular agents (e.g., latex particles, opsonized and nonopsonized zymosan, bacteria and their components, activated carbon).
- Soluble agents (e.g., fMLF, allergens, pyrogenal).

Triggering a cascade of intracellular mediators, the activating stimuli stimulate a rapid entry of calcium ions into the cell, activation of protein kinase C (PKC) and phospholipase A₂ (PLA₂). This leads to phosphorylation of the p47^{phox} and p67^{phox} proteins and migration of cytosolic subunits to the membrane, where they bind to the membrane domain, called cytochrome b₅₅₈. Thus, an active oxidase is formed (see Fig. 14.11b and (Cathcart 2004; Belambri et al. 2018) for detailed reviews).

Besides these natural stimuli, the complex association can be triggered by nonspecific agents, penetrating into the cell by passive diffusion and acting independently of receptors:

e.g., calcium ionophore A23187 and PKC FMA activator (Cree 1998).

The activated complex transfers electrons from NADPH on the C-terminal cytoplasmic domain of gp91 to FAD, then to cytochrome b₅₅₈, and finally to oxygen, which is determined by the redox potentials of the corresponding species (see Fig. 14.12).

Further, O₂^{-•} formed in phagocytes is quickly intercepted by other enzymes (superoxide dismutase, myeloperoxidase, etc.) and converted into secondary cytotoxic products necessary to destruct foreign microorganisms (Briheim et al. 1984). At the same time, as discussed above, the formed superoxide and hydrogen peroxide are involved in a wide variety of cell signaling and regulation of gene expression (Panday et al. 2015).

Deficiency of NADPH oxidase can lead to immunodeficiency (Giardino et al. 2017) (failure of the bacterial killing process). At the same time, excessive production of ROS leads to stress in the cell and serious diseases, up to autoimmune and neoplastic ones (Smallwood et al. 2018).

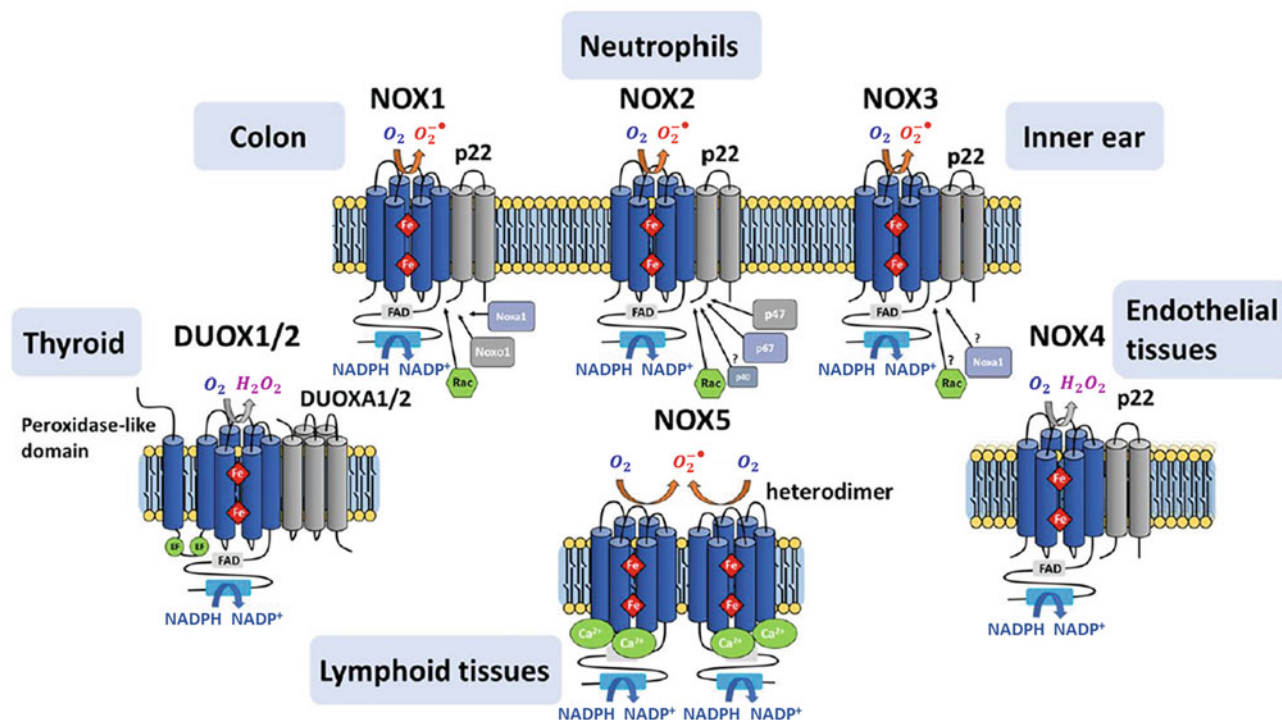


Fig. 14.9 Structure of different members of Nox family enzymes. (Adapted from (Vermot et al. 2021), under Creative Commons license. Copyright 2021, MPDI)

14.4.1.3 Summary

Thus, NADPH oxidases are a widespread family of enzymes, producing $O_2^{\bullet -}$ and H_2O_2 from molecular oxygen. While in phagocytes, its main function can be called bacterial killing due to the produced ROS reactivity and toxicity, in the vast majority of cells and organisms containing it, these functions are obviously absent and the only role of NADPH oxidases is ROS signaling.

14.4.2 Xanthine Oxidase

14.4.2.1 The XOR Complex and Its Role

Xanthine oxidase is one of two forms of the xanthine oxidoreductase (XOR) enzyme involved in purine catabolism – oxidation of hypoxanthine to xanthine and xanthine to uric acid.

The first of these forms, xanthine dehydrogenase (XD), transfers electrons from the oxidized base to the NAD^+ ion (Fig. 14.13, XD). The second form, xanthine oxidase (XO), transfers electrons to oxygen dissolved in water, thus generating $O_2^{\bullet -}$ and H_2O_2 (McCord and Fridovich 1968) (Fig. 14.13, XO).

Although the basal XOR level is low, it can increase during hypoxia, under the influence of interleukins-2 and -6, $TNF-\alpha$, lipopolysaccharides, and steroid hormones. The level of xanthine oxidase increases in many conditions, for

example, with ischemia of the extremities and heart failure. Circulating xanthine oxidase binds to glycosaminoglycans on the endothelial surface, which leads to increase of its pro-oxidant activity. This phenomenon is believed to play a role in endothelial damage (see reviews in (Harrison 2004; Bortolotti et al. 2021; Battelli et al. 2016)).

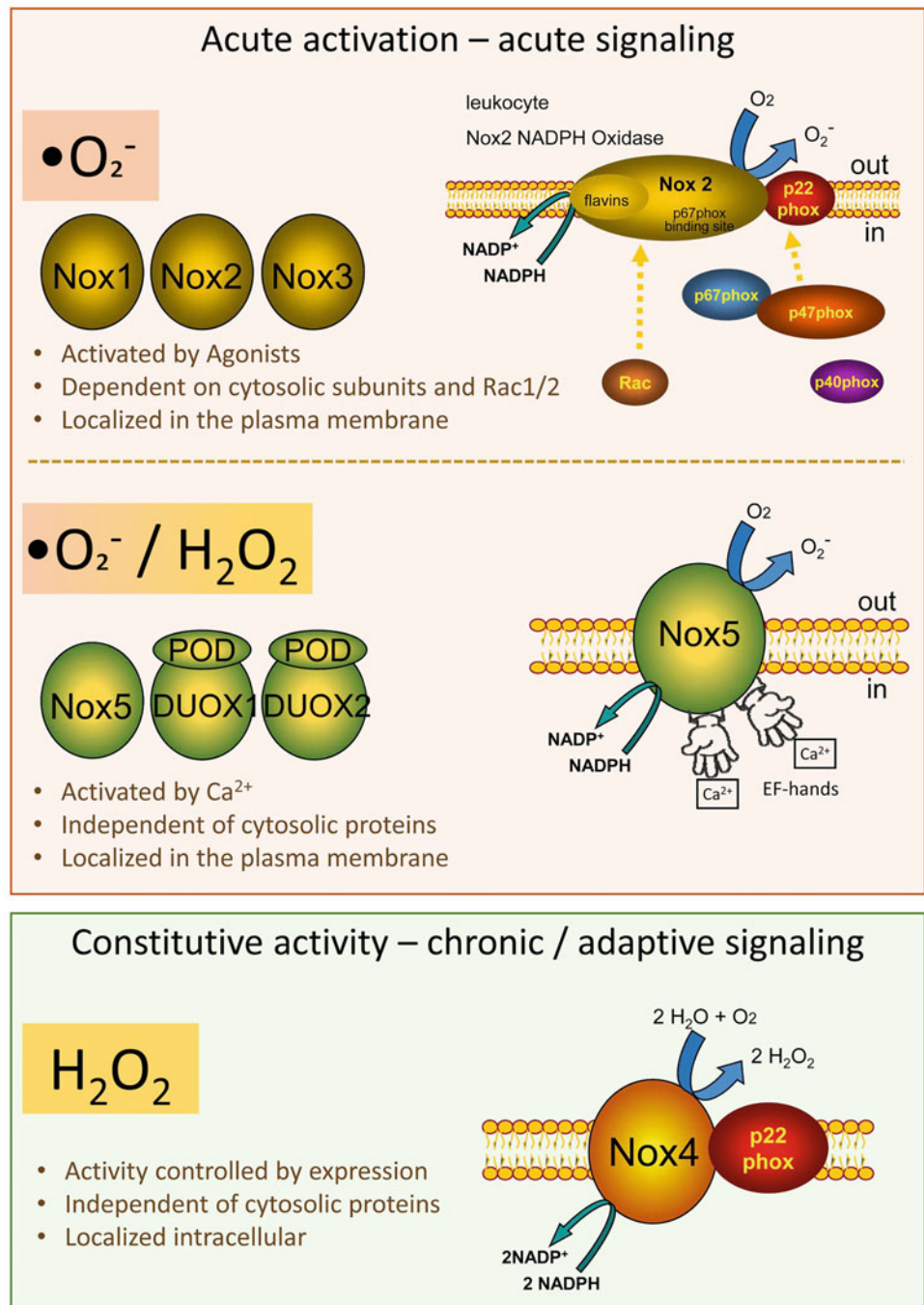
Active XOR is found in homogenates of many tissues: liver, spleen, intestines, kidneys, and muscles, as well as on the luminal surface of the vascular endothelium of many organs, including heart and brain (George and Struthers 2009).

It was shown that the level of urate is increased six-fold in atherosclerotic plaques. Free radicals produced by xanthine oxidase can be involved in the pathogenesis of many conditions, including reperfusion injury, multiple organ failure, and damage to the microcirculatory bed (Meneshian and Bulkley 2002). Presently, xanthine oxidase inhibitors are actively considered for the treatment of cardiovascular diseases (Labat-Robert and Robert 2014; Luna et al. 2019).

14.4.2.2 The XOR Structure and Functioning

XOR is a homodimer consisting of two 145 kDa subunits with pronounced cooperativity in both substrate binding and catalysis (Tai and Hwang 2004). Each of the subunits has an *N*-terminal domain with two iron-sulfur centers, a central domain with FAD, and a *C*-terminal domain with four

Fig. 14.10 Basic scheme of the Nox family classification, according to the activation mode. (Reprinted from (Schröder 2020), under Creative Commons license. Copyright 2020, Elsevier)



redox centers (Harrison 2002; Luna et al. 2019) (see Fig. 14.14).

The enzyme functioning is divided into reductive and oxidative half-reactions. The reductive half-reaction proceeds on the Mo-Co cofactor (Fig. 14.14a, c, blue domain), with electrons transferred from oxidized substrates (hypoxanthine or xanthine) to Mo and then to Fe_2S_2 clusters (Fig. 14.14b), serving for their “accumulation.” Thus, the enzyme can “accumulate” six excess electrons. The oxidative half-reaction occurs on the FAD-containing domain, where six

excess electrons are sequentially transferred to NAD^+ or oxygen.

As mentioned above, XOR exists in two interconverting but different forms: xanthine dehydrogenase (XD), which is directly expressed in the cell, and xanthine oxidase (XO), which is a posttranslational modification of XD.

The $XD \rightarrow XO$ transformation can occur in two ways:

- Reversible partial oxidation of thiol residues at low oxygen concentrations, in the presence of proinflammatory

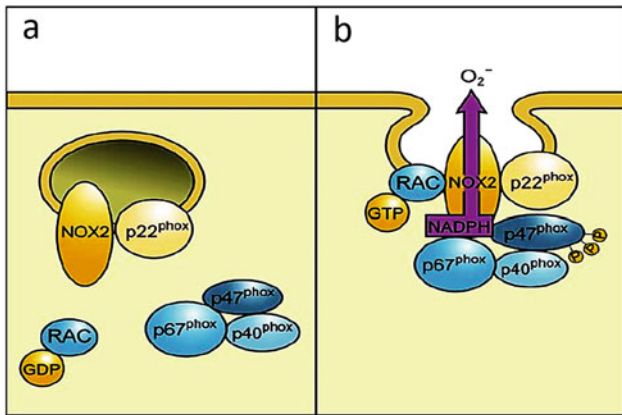


Fig. 14.11 Assembly and activation of the phagocyte Nox2 complex. (a) inactive disassembled complex; (b) active complex. (Reprinted from (Bedard and Krause 2007), under Creative Commons license. Copyright 2007, American Physiological Society)

mediators and under a number of other conditions (the sites marked with asterisks in Fig. 14.14c).

- Irreversible proteolytic cleavage at lysins (the sites indicated by arrows in Fig. 14.14c).

It is believed that both actions cause structural rearrangements of the other loop located close to the flavin ring, thus partially blocking access of NAD^+ to the FAD cofactor, changing the electrostatic environment of the active site and decreasing the enzyme affinity for NAD^+ (Nishino 1994; Ryan et al. 1997).

XD has high affinity for NAD^+ and restores oxygen only “according to the residual principle” – if NAD^+ does not contact the active center first. On the other hand, the reverse reaction $\text{NADH} \xrightarrow{-e^-} \text{NAD}^+$ can also occur on it with an efficiency reaching 40% of the direct reaction (Harris and Massey 1997).

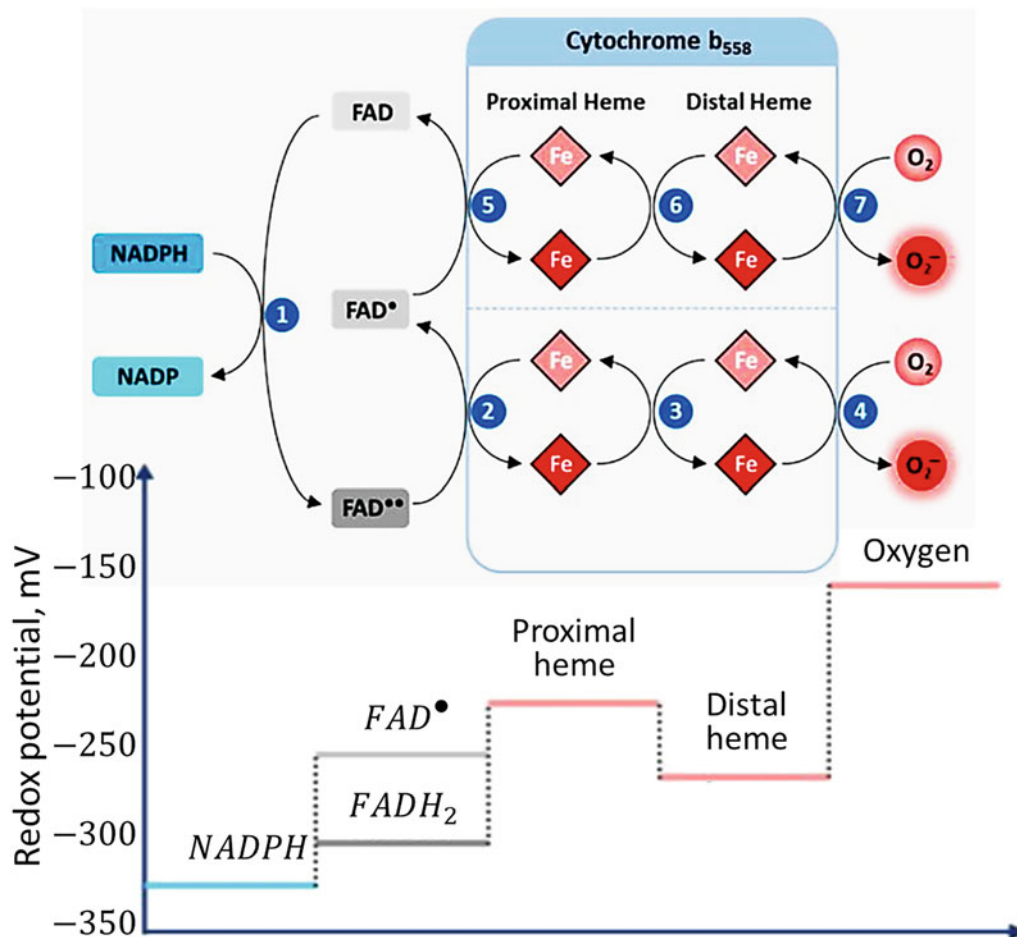


Fig. 14.12 Scheme of electron transport along the chain $\text{NADPH} \rightarrow \text{FADH}_2 \rightarrow \text{cytochrome b558} \rightarrow \text{O}_2$. Redox potentials for each transition are shown. Electron transfer from NADPH and FADH_2 occurs on the C-terminal cytoplasmic domain of gp91 on the inner side

of the membrane. Superoxide is generated by cytochrome b558 outside the membrane. (Adapted from (Vermot et al. 2021), under Creative Commons license. Copyright 2021, MPDI)

Fig. 14.13 Reactions catalyzed by two forms of xanthine oxidoreductase: XD, xanthine dehydrogenase; XO, xanthine oxidase. XD can also transfer electrons to oxygen, but with significantly lower efficiency than the main reactions

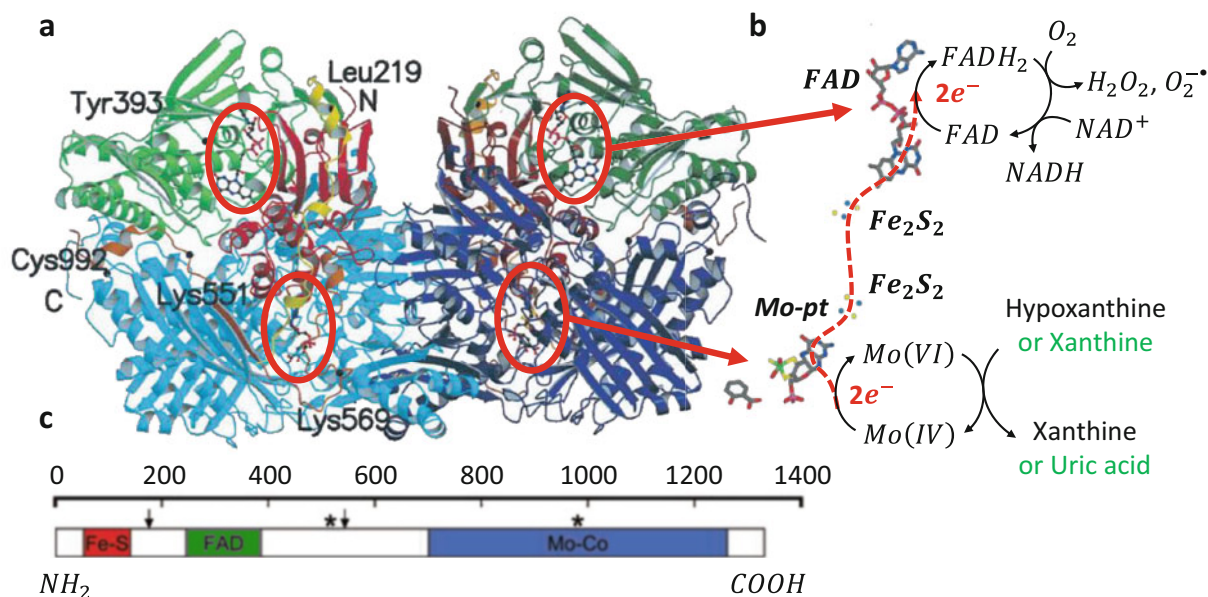
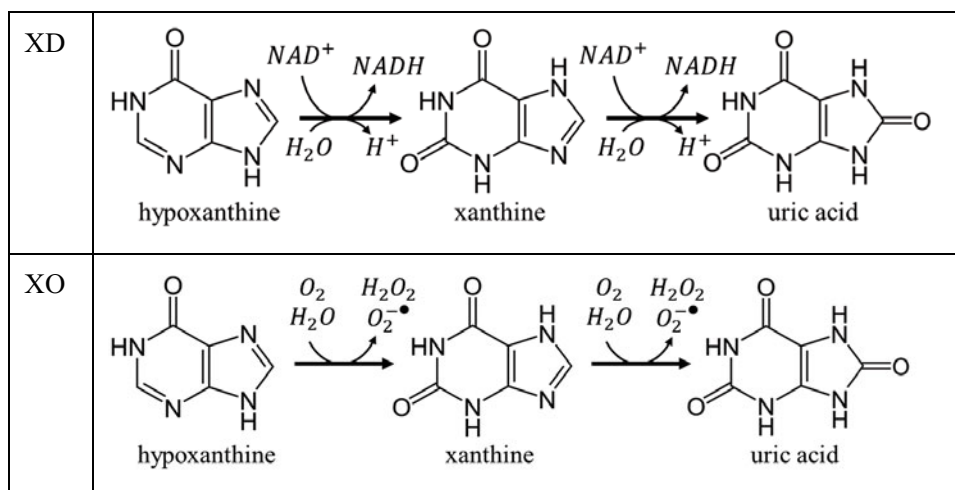


Fig. 14.14 Xanthine oxidoreductase. (a) Crystal structure of the enzyme homodimer (from (Enroth et al. 2000)). (b) Mutual position of cofactors in one XOR subunit and schematic path of electrons within the enzyme. Bottom – “reductive half-reaction” on Mo – Co: Hypoxanthine → Xanthine or Xanthine → Uric acid; in the middle – two iron-sulfur clusters Fe_2S_2 – “depot” of electrons; top – “oxidative half-reaction” on FAD: $NAD^+ \rightarrow NADH$, $O_2 \rightarrow O_2^{\cdot -}$ or $O_2 \rightarrow H_2O_2$. (c) Primary XOR protein sequence. Numbers – amino acid residues from

the N-terminus. Arrows – sites of proteolysis by trypsin during irreversible modification XD → XO (Lys186, Lys552). Asterisks are cysteine residues oxidized during reversible modification XD → XO (Cys535, Cys992). (a – Adapted from (Enroth et al. 2000), under Creative Commons license. Copyright 2000, the National Academy of Sciences. c – Adapted from (Berry and Hare 2004), under Creative Commons license. Copyright 2004, John Wiley and Sons)

XO has an extremely low affinity for NAD^+ and donates all electrons to oxygen. In this case, during the complete enzyme oxidation, the first four electrons are transferred to O_2 in pairs, generating two H_2O_2 molecules, and the last two electrons are transferred one at a time, generating two $O_2^{\cdot -}$.

14.4.2.3 Summary

Thus, xanthine oxidoreductase has two isoforms – xanthine dehydrogenase, participating in the cell metabolism, and

xanthine oxidase, producing $O_2^{\cdot -}$ and H_2O_2 from molecular oxygen. Switching between these isoforms can be both reversible and irreversible and is actively involved in cellular response to external stimuli, providing a rapid physiological mechanism of ROS signaling (see more in reviews (George and Struthers 2009; Bortolotti et al. 2021; Harrison 2004; Battelli et al. 2016)).

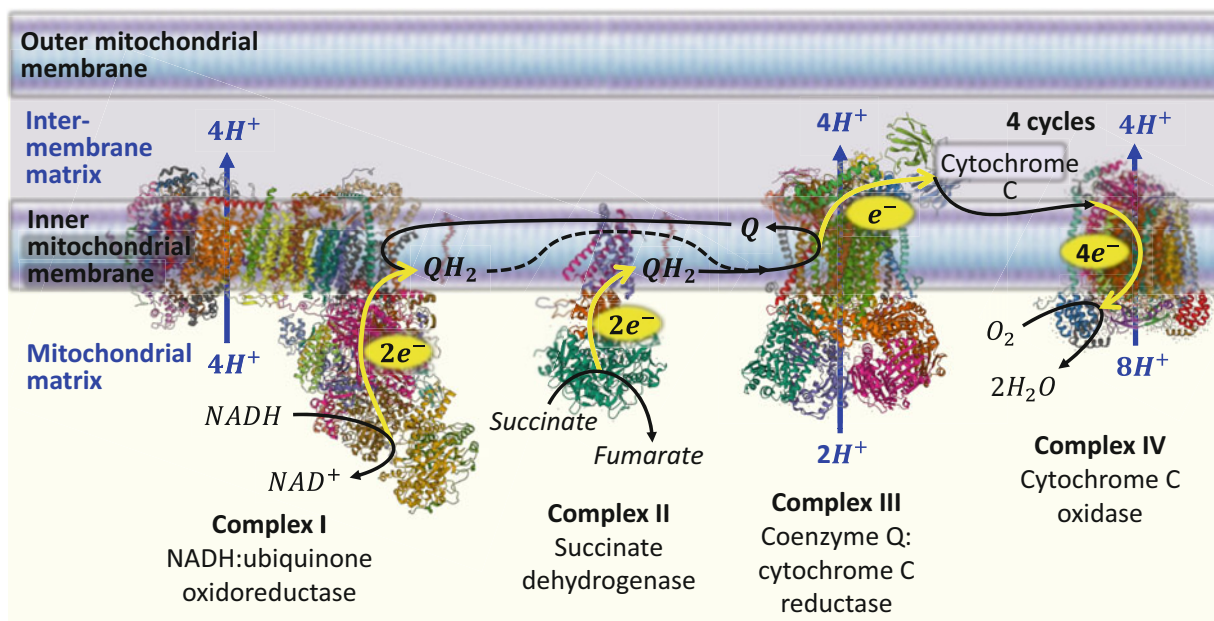


Fig. 14.15 The mitochondrial electron-transport chain

14.4.3 Respiratory Chain

14.4.3.1 The Respiratory Chain Structure and Its Function

The mitochondrial electron-transport chain (ETC) has been one of the most studied systems in cell energetics for decades, since its discovery and revealing basic mechanisms (Chance and Williams 1955; Hatefi et al. 1962; Mitchell 1961). As is well known, the general functions of this outstanding block of enzymes are:

- To subject organic substances, supplied by other biochemical paths, to a series of redox reactions, simultaneously pumping protons from the mitochondrial matrix into the intermembrane space, and, thus, creating an electrochemical gradient on the inner mitochondrial membrane.
- To relax the generated gradient, by letting the protons accumulated in the intermembrane space, back into the mitochondrial matrix, and simultaneously generate ATP.

The first function is played by the respiratory complexes I, II, III, and IV (see Fig. 14.15); the second function is played by complex V – the famous F_0F_1 ATP synthase. All these complexes are localized at the inner mitochondrial membrane, in its specific protrusions called cristae (see Fig. 14.16c). Their effective functioning is determined by their close and organized localization, dynamic (and/or static) assembly into supercomplexes and megacomplexes (respirasomes, see Fig. 14.16), as well as association with other proteins (Wang et al. 2010, 2019). All this is carefully regulated by different factors, and these regulatory paths are

still largely unknown and to be investigated (see, e.g., reviews in (Nesci et al. 2021; Brzezinski et al. 2021)).

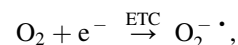
Altogether, the respiratory chain appeared a much more complicated system, than originally thought. Instead of a linear sequence of electron-transport events, it turned out to be a network of enzymatic complexes and their supramolecular associations, assembling, and disassembling under the action of various signaling factors, and participating in further signaling in their turn (see below; see also (Wu et al. 2020; Nesci et al. 2021; Lobo-Jarne and Ugalde 2018; Brzezinski et al. 2021) for reviews and discussion).

14.4.3.2 The Respiratory Chain Generates ROS

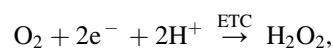
14.4.3.2.1 Sites of ROS Production

Formation of superoxide anion-radical and hydrogen peroxide by breathing mitochondria was demonstrated already in the 1970s (Boveris and Chance 1973; Loschen et al. 1971, 1974). It was soon shown to result from “premature leaking” of electrons from the electron-transport chain (e.g., (Cadenas et al. 1977; Chance and Oshino 1971; Loschen et al. 1974; Boveris and Cadenas 1975; Loschen et al. 1971)):

- Either singly



- Or in pairs:



of which the first reaction was considered dominant.

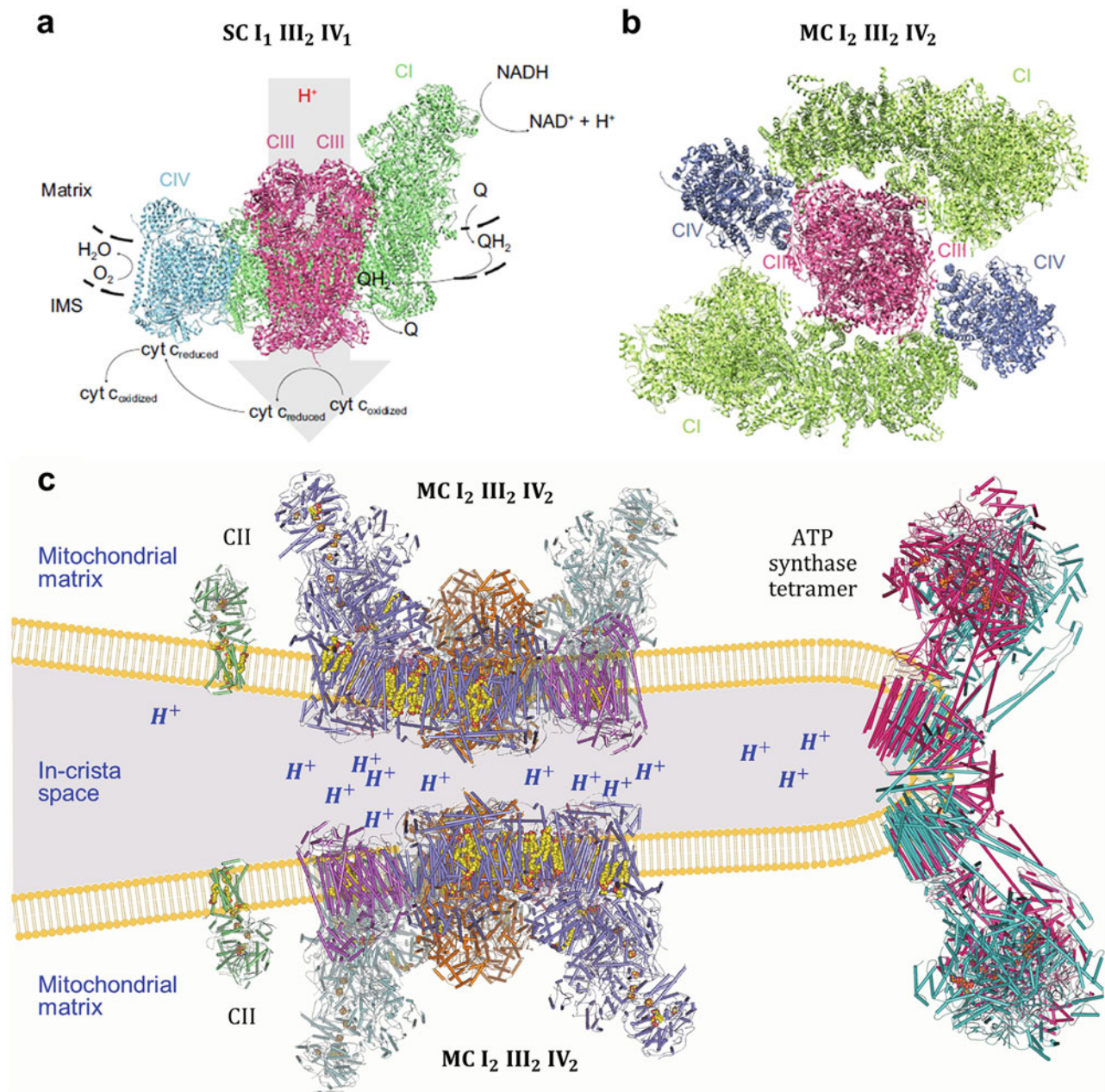


Fig. 14.16 Supramolecular organization of the mitochondrial respiratory chain. (a) SC I₁III₂IV₁ supercomplex – structure and scheme of functioning (side view – perpendicular to the membrane); (b) MC I₂III₂IV₂ megacomplex structure (top view – along the membrane);

(c) Mitochondrial crista organization: respiratory chain megacomplexes and ATP synthase rows. (Adapted from (Wu et al. 2020), under Creative Commons license. Copyright Springer, 2020)

The first discovered sources of such “electron leaking” were auto-oxidation of ubisemiquinone (see, e.g., (Chance et al. 1979)), and NADH-dehydrogenase activity (Turrens and Boveris 1980). Yet, by now, the list of ETC leak sites has expanded to at least 11 (see Fig. 14.17; the first two discovered sites are III_{Q0} and I_Q).

In accordance with the first works (Cadenas et al. 1977; Loschen et al. 1971, 1974; Chance and Oshino 1971; Boveris and Cadenas 1975), the majority of these sites produce O₂^{-•} (which can further react with NO, or be subjected to the

action of SOD); and yet, some sites directly produce H₂O₂, or a mixture of ROS. The currently known electron leakage products for these sites are as follows (Brand 2016):

- O₂^{-•} – sites I_F, III_{Q0}, G_Q
- Both O₂^{-•} and H₂O₂ – site II_F.
- Mostly O₂^{-•}, or a mixture of O₂^{-•} and H₂O₂ – sites O_F, P_F, B_F, A_F, I_Q.
- Unclear – sites E_F, D_Q.

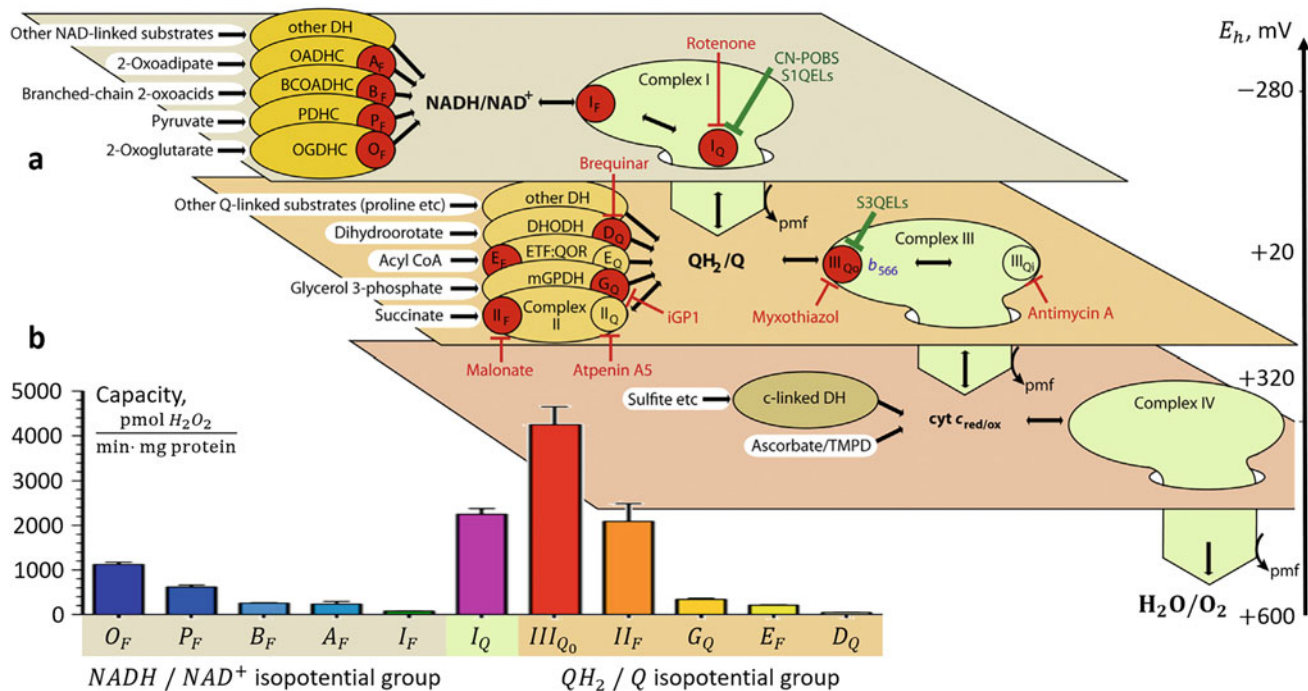


Fig. 14.17 Sites of $O_2^- \cdot / H_2O_2$ production in the mitochondrial electron-transport chain (ETC). (a) The scheme of the main leak sites in ETC, with their potential energies; (b) Maximal ROS-production capacities of different sites. Electrons are passed from the substrates to the chain through various dehydrogenases, shown as ovals. The redox centers are grouped into three approximately isotopotential planes (see energy scale on the right). At complexes I, III, and IV, electrons drop down from one isotopotential plane to another one and protons are pumped across the membrane. The electron leaking sites are marked with red circles. Specific inhibitors, typically used for research, are marked with red arrows. The ROS-production sites are labeled as follows: O_F, flavin in the 2-oxoglutarate dehydrogenase complex;

P_F, flavin in the pyruvate dehydrogenase complex; B_F, flavin in the branched-chain 2-oxoacid (or α -ketoacid) dehydrogenase complex; A_F, flavin in the 2-oxoadipate dehydrogenase complex; I_F, flavin in the NADH-oxidizing site of respiratory complex I; I_Q, ubiquinone-reducing site of respiratory complex I; III_{Q₀}, outer quinol-oxidizing site of respiratory complex III; II_F, flavin site of respiratory complex II; G_Q, quinone reducing site in mitochondrial glycerol 3-phosphate dehydrogenase; E_F, site in electron-transferring flavoprotein; D_Q, quinone reducing site in dihydroorotate dehydrogenase. See Goncalves et al. (2015) for more detailed information. (Adapted from (Brand 2016). Copyright 2016, with permission from Elsevier)

The majority of the produced ROS are vectorially released to the mitochondrial matrix (Brand 2016). However, the sites III_{Q₀} and G_Q are located on the outer side of the inner mitochondrial membrane and deliver $O_2^- \cdot$ partly to the mitochondrial matrix and partly to the cytosol. This generally corresponds to the earlier estimates that ~20–30% of the total mitochondrial ROS are directly released into the intermembrane space (Han et al. 2001).

14.4.3.2.2 ROS Production Rate

The first estimates of the ETC ROS production rate were ~10–20 nM/min/mg of protein (Boveris and Chance 1973; Cadenas et al. 1977; Boveris and Cadenas 1975), or 1–2% of the total electron flow (Boveris and Chance 1973; Chance et al. 1979), which were later adjusted down to 0.3–1 nM/min/mg of protein (Cadenas 2004).

However, all these data were obtained by using specific ETC inhibitors, or (later) genetically modified organisms, which affect the normal electron flow and alter the remaining ETC sites redox states. Indeed, addition of any ETC inhibitor

increases ROS production from the upstream sites (as they become more reduced) and decreases ROS production from the downstream sites (as they become more oxidized), thus making the estimated rates very (and unpredictably) far from natural.

Any ROS-producing site can be characterized by its maximal capacity, measured using optimal substrates and specific inhibitors (see Fig. 14.17b). However, this is also a very poor predictor for the native rates, which appeared several times lower and greatly dependent on the oxidized substrate and, accordingly, on the physiological state of the cell (Goncalves et al. 2015). Thus, in vivo rates of ROS production can only be estimated indirectly, by mimicking the substrate content corresponding to the cell's physiological state in question and using certain ETC components as endogenous reporters, whose redox states are previously correlated with the rates of ROS production at the current site (see (Quinlan et al. 2012, 2014; Goncalves et al. 2015; Brand 2016)). The rates of respiration and ROS production, measured for different

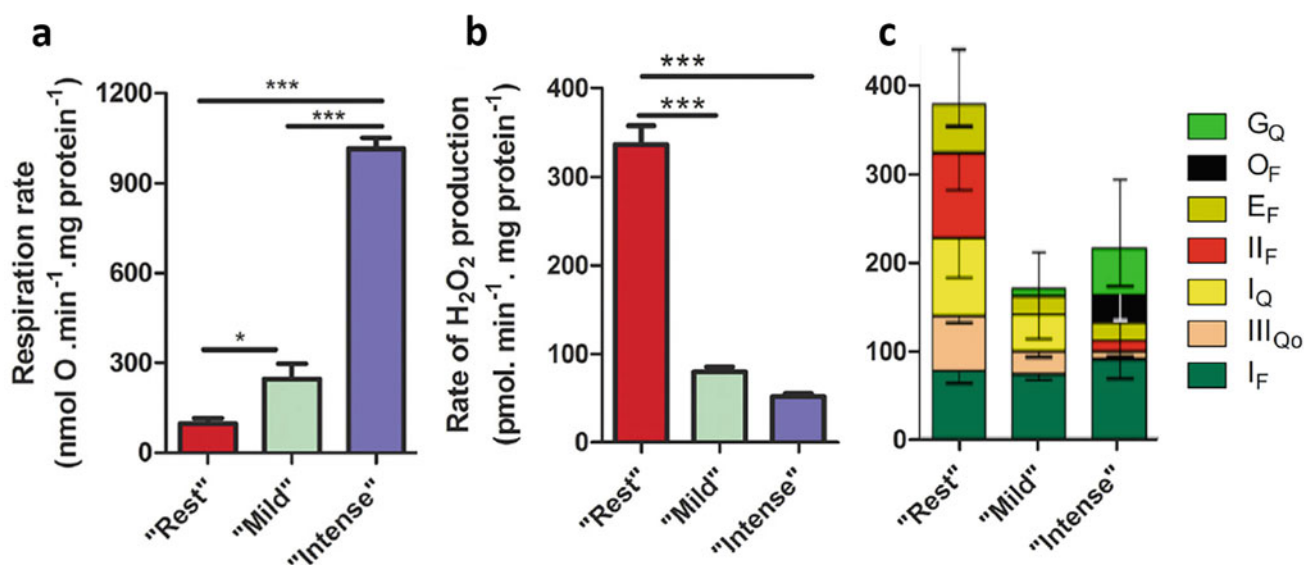


Fig. 14.18 Respiration and H_2O_2 production rates by isolated skeletal muscle mitochondria ex vivo in media mimicking rest, mild aerobic exercise, and intense aerobic exercise. (a) Respiration; (b) H_2O_2 production; (c) H_2O_2 production, corrected for the losses caused by the

activity of mitochondrial matrix peroxidases, and contributions of different sites (see Fig. 14.15). (Adapted from (Goncalves et al. 2015), under Creative Commons CC-BY license. Copyright 2015, Elsevier)

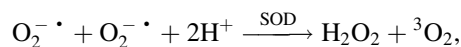
sites of ETC ex vivo, according to the above approach, are shown in Fig. 14.18.

An important consequence of the above data, is that, contrary to earlier hypotheses, the rates of ROS production cannot be used for diagnostics of mitochondrial dysfunction. The latter can be associated with both increase and decrease of ROS production, depending on its cause and affected point in the electron-transport chain (see more in (Brand and Nicholls 2011)). Besides, mitochondria have powerful antioxidant systems, which affect the observed ROS concentration and production rates (Starkov et al. 2014), making them even poorer indicators of the mitochondrial state.

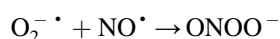
14.4.3.3 Further Reactions and Role of ROS

As stated above, the majority of the ETC sites produce $\text{O}_2^- \cdot$, which can be further subjected to different reactions:

- The action of superoxide dismutase (SOD), forming the neutral molecule of H_2O_2 , which can further diffuse into the cytoplasm (McCord and Fridovich 1969):



- Extremely fast, diffusion-limited reaction with NO (Kissner et al. 1997):

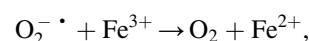


(NO is constantly produced by mitochondrial NO-synthases (Nitric Oxide 2010); its production rate is estimated as 0.2–0.9 nmol/min/mg of protein (Cadenas 2004), and the mitochondrial steady-state concentration of NO – as 20–50 nM (Poderoso et al. 1996)).

According to the estimates (Cadenas 2004), this reaction utilizes ~60–70% of mitochondrial $\text{NO} \cdot$ and ~15% of $\text{O}_2^- \cdot$.

The generated ONOO^- is further involved in reactions with NADH, QH_2 and GSH.

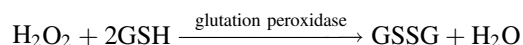
- Reduction of Fe^{3+} to Fe^{2+} :



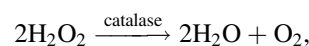
which is further involved in many free-radical-generating processes (see above).

H_2O_2 , formed either from $\text{O}_2^- \cdot$ at the SOD reaction, or directly by some of ETC sites, is further subjected to action of various enzymes:

- Peroxidases, including glutathione peroxidase (present in most organs of the human body):



- Catalase:



of which the first reaction is directly involved in signal transduction (see Sect. 14.3).

Initially, all these ROS-generating and ROS-involving reactions, obviously going against the main energetic function of the ETC, seemed purely parasitic, something like leakage from an electrical circuit with poor insulation (Boveris and Chance 1973). The generated $O_2^- \cdot$ and H_2O_2 were recognized as purely toxic agents (Boveris and Chance 1973), which the cell must dispose of as quickly as possible for the sake of its own life.

However, later they were shown to have important signaling functions. This applies to NO (Poderoso et al. 1996; Napoli et al. 2010), H_2O_2 (Boveris and Cadenas 2000), and $O_2^- \cdot$ (Cross et al. 1987). For instance, cytosolic concentrations of H_2O_2 modulate JNK signaling (Park et al. 2000), MAPK activity (Boyd and Cadenas 2002), and determine cell fate: proliferation, apoptosis or necrosis (Antunes and Cadenas 2001) (see more in Sect. 14.3). The peroxidase activity of cytochrome *C*, regulated by its interaction with the inner mitochondrial membrane, is a key regulator of the mitochondrial apoptotic path (Belikova et al. 2006) (see below and reviews, e.g., (Vladimirov et al. 2013)). For more examples of ROS-mediated signaling, see Sect. 14.3. Altogether, as stated by E. Cadenas already in 2004, “At present, $O_2^- \cdot$, H_2O_2 and NO are considered part of an integrated system of mitochondrial signaling for cellular regulation” (Cadenas 2004).

In this context, the topography of ROS production appeared of primary importance, regulating the downstream signaling cascades (Bleier et al. 2015; Schaar et al. 2015). As mentioned above, of all ROS-producing sites of ETC only III_{Q_0} and G_Q deliver a part of the generated $O_2^- \cdot$ to cytosole, which may mean their separate role in further signaling. However, this remains largely unknown.

14.4.3.4 Summary

Thus, besides its obvious main energetic role, electron-transport chain has a second, initially absolutely unexpected one – ROS signaling. While ETC ROS production has been known for decades, initially it was viewed as a mere imperfection – “electron leaking.” Yet, now there is mounting evidence of its signaling functions. Moreover, unlike most other ROS-generating systems, ETC produces $O_2^- \cdot$ and H_2O_2 in two important cell compartments at the same time: mitochondrial matrix and intermembrane space. This can well be the basis of spatial signal patterning, discussed above (see Sect. 14.3). Altogether, the dynamic balance between ETC electron transport and ROS generation is definitely an important physiological regulatory mechanism.

14.5 Enzymes, Utilizing ROS and Producing Other Free Radicals

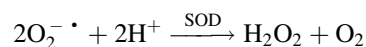
As discussed above, there are a number of enzymatic sources of reactive oxygen species in the cell, primarily, $O_2^- \cdot$ (typically playing the role of a primary radical) and H_2O_2 (playing the role of a second messenger in the so-called redox signaling cascades). These species, in their turn, are subjected to the action of different enzymes: superoxide dismutase, catalase, and various peroxidases.

Moreover, besides H_2O_2 , peroxidases are acting on organic peroxides, forming radicals of organic molecules as intermediate species. Similar biochemical pathways – with the generation of free radicals – are also known for cyclooxygenases and cytochromes. This side of the free-radical life of the cell is briefly touched upon in this section.

14.5.1 Superoxide Dismutase

14.5.1.1 What Is SOD?

Superoxide dismutases (SOD) are enzymes, producing H_2O_2 from two superoxide anion-radicals, $O_2^- \cdot$, by catalyzing their dismutation:



SOD is a universal family of enzymes, characteristic of practically all organisms living in the presence of oxygen, and frequently regarded “the first line of defense against ROS” (though this is not their only function).

SODs are typically classified into three subfamilies according to the catalytic metal ions in the active center: Cu/Zn (Potter and Valentine 2003), Mn or Fe (Miller 2012), and Ni (Wuerges et al. 2004) (see Fig. 14.19), which are differently distributed among taxa and in the cell (see Fig. 14.20).

The most ancient SOD, met in various bacteria and archaea, are Fe-SOD, or those functioning with both Fe and Mn. Besides, they are also found in various protists and plant chloroplasts.

Eukaryotic cells contain two different classes: Mn-SOD in mitochondria and Cu/Zn-SOD in the cytoplasm, peroxisomes and in the extracellular space (see (Miller 2012; Fridovich 1995; Wang et al. 2018) for more detailed reviews).

The mitochondrial (and prokaryotic) Mn-SODs are likely to have evolved from the ancient Fe-SOD, in response to diminished availability of Fe during the global change in the atmosphere from reducing to oxidizing (see (Miller 2012)). Indeed, the Mn-SOD has a much higher electron affinity than Fe-SOD, which makes it a better oxidant for the first half-

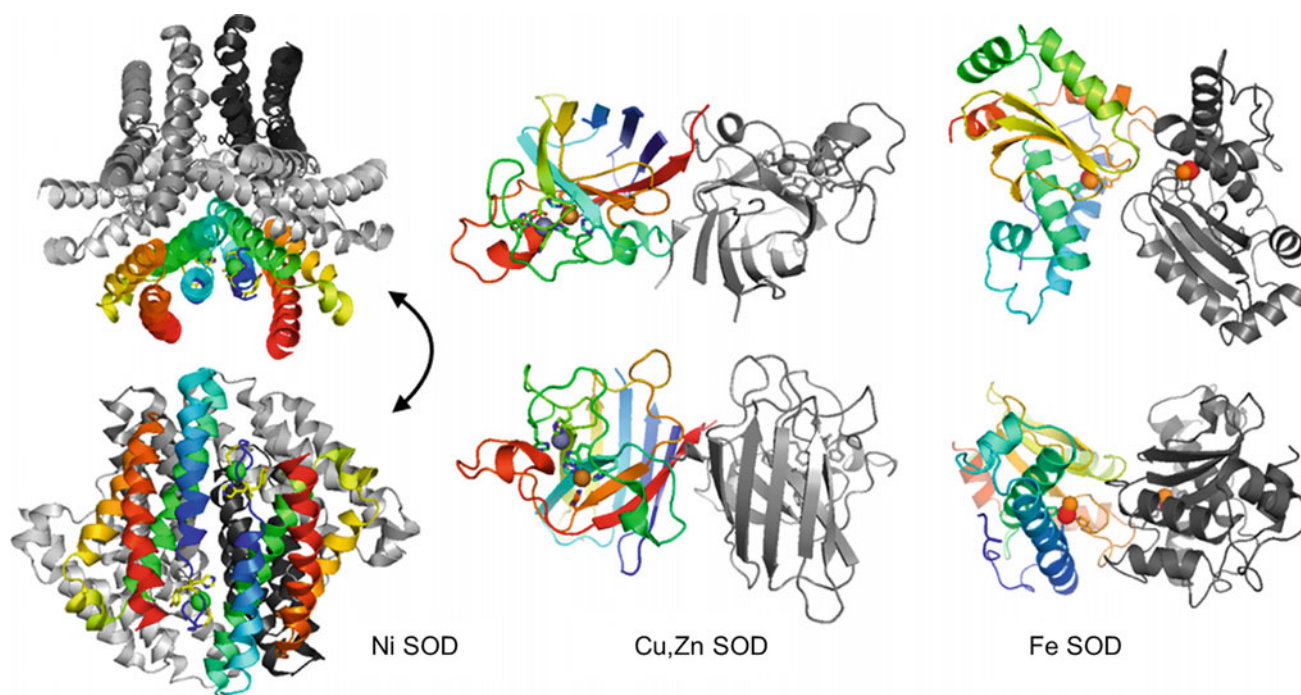
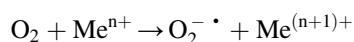
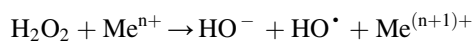


Fig. 14.19 General structure of the three classes of superoxide dismutases. (Reprinted from (Miller 2012), under Creative Commons license. Copyright 2012, John Wiley and Sons)

reaction with superoxide (see Table 14.1), and decreases its chances to participate in Fenton-like reactions:



That is, the Mn-SOD appear more prone to utilizing superoxide and less prone to producing it or other dangerous ROS, which must be a very important point for the oxidative environment (see more in a review (Miller 2012)). In animal cells, Mn-SOD is localized in mitochondria, where it can metabolize superoxide produced in the respiratory electron-transport chain.

The Cu/Zn-SODs have been found in cytoplasm, nucleus, peroxisomes, and in the extracellular space of animal tissues, as well as in plants, fungi, and certain bacteria (in which, however, it is very different from that of eukaryotes – see (Fridovich 1995; Miller 2012; Wang et al. 2018) for reviews).

14.5.1.2 SOD Role

Initially, the SOD function was considered to be defense from oxidative stress, by utilizing the primary radicals $\text{O}_2^{\bullet -}$. However, today, its participation in various cascades of redox signaling may be called no less important.

As for the protective function, $\text{O}_2^{\bullet -}$ per se is not a strong oxidative agent. Yet, besides being a univalent oxidant, it can also act as a univalent reductant, with plenty of different targets in the cell, which turns out a no less dangerous class of reactions. In vitro, $\text{O}_2^{\bullet -}$ reduces Fe^{3+} to Fe^{2+} , which further participates in Fenton-like reactions, producing the most dangerous ROS, HO^\bullet . In vivo, it also deactivates dehydrogenases, containing [4Fe – 4S] clusters in their active centers (e.g., aconitase and fumarase), and releases Fe^{2+} ions, which also enter Fenton reactions (see (Fridovich 1995; Liochev and Fridovich 1994)).

Indeed, the excess of $\text{O}_2^{\bullet -}$ is quite dangerous and associated with many pathologies in plenty of different species, from procaryotes to mammals and human (Dukan and Nyström 1999; Van Remmen et al. 2003; Elchuri et al. 2005; Yang et al. 2007). SOD-null mutants of bacteria, yeast, and various animals exhibit dioxygen-dependent auxo trophies and enhanced levels of mutagenesis (Farr et al. 1986; Hiraishi et al. 1992; Liu et al. 1992; Gurney et al. 1994). Many of them appear oxygen-intolerable, or have a shorter lifespan (Liu et al. 1992; Gurney et al. 1994) (see more in (Fridovich 1995) and references therein).

Parasitic bacteria and protists were shown to use SOD as a protectant against the oxidative burst of the host's immune system (Beaman et al. 1985; Filice et al. 1980). Interestingly, in certain species, SOD has been replaced with free Mn^{2+} ,

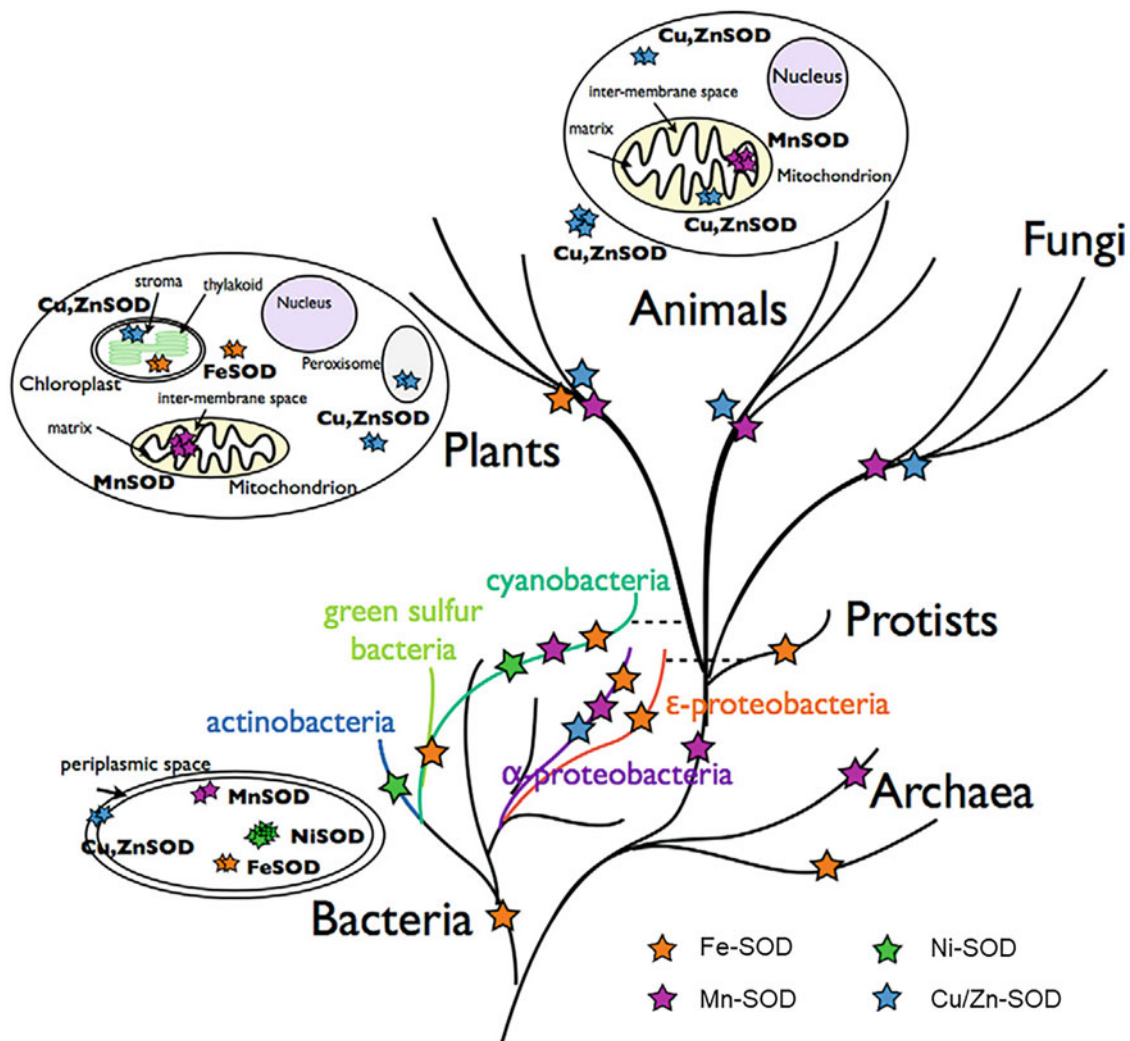


Fig. 14.20 Distribution of different classes of superoxide dismutases among taxa. The number of stars inside the ovals indicate the SOD quaternary states. (Reprinted from (Miller 2012), under Creative Commons license. Copyright 2012, John Wiley and Sons)

Table 14.1 Comparison of superoxide dismutation reactions: (a) spontaneous and (b) catalyzed by superoxide dismutase (data from (Fridovich 1975))

| Reaction | Concentration of reagents, M | Rate constant, $M^{-1}s^{-1}$ |
|---|--|-------------------------------|
| a Spontaneous dismutation $O_2^{\cdot -} + O_2^{\cdot -} \rightarrow \dots$ | $[O_2^{\cdot -}] \sim 10^{-10}$ | 2×10^5 |
| b SOD-catalyzed dismutation $O_2^{\cdot -} + O_2^{\cdot -} \xrightarrow{SOD} \dots$ | $[O_2^{\cdot -}] \sim 10^{-10}$ $[SOD] \sim 3 \times 10^{-5}$ | 2×10^9 |

which is reactant with $O_2^{\cdot -}$, but does not participate in Fenton chemistry (Archibald and Fridovich 1981).

At the same time, besides defending the cell from the direct toxic action of $O_2^{\cdot -}$, the SOD-mediated control of $O_2^{\cdot -} / H_2O_2$ signaling appears no less important (see Sect. 14.3).

14.5.1.3 SOD Functioning

Though $O_2^{\cdot -}$ is known to dismutate spontaneously, SOD-mediated reaction appears incomparably more effective, both because of the gain in the rate constant and due to its much higher concentration in the cell (Fridovich 1975) (see Table 14.1).

Table 14.2 The mechanism of SOD functioning: (a) the oxidative half-reaction (oxidizing the first $O_2^{\cdot -}$ to O_2); (b) reductive half-reaction (reducing the second $O_2^{\cdot -}$ to H_2O_2)

| | | |
|---|-------------------------|--|
| a | Oxidative half-reaction | $SOD \cdot Me^{3+} \cdot OH^- + O_2^{\cdot -} + H^+ \rightarrow SOD \cdot Me^{2+} \cdot OH_2 + O_2$ |
| b | Reductive half-reaction | $SOD \cdot Me^{2+} \cdot OH_2 + O_2^{\cdot -} + H^+ \rightarrow SOD \cdot Me^{3+} \cdot OH^- + H_2O_2$ |

A more detailed mechanism of reaction catalyzed by SOD is given in Table 14.2).

The elegance of SOD lies in the shift of its electron affinity between the two half-reactions, which allows it to use the same substrate ($O_2^{\cdot -}$) both as a reducing and as an oxidizing agent. Thus, SOD effectively oxidizes $O_2^{\cdot -}$ in the first half-reaction and reduces it in the second one.

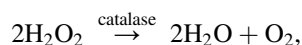
As $O_2^{\cdot -}$ is negatively charged, membranes are poorly permeable to it, and the cell needs to have SOD right in the compartment, where $O_2^{\cdot -}$ is generated. As mentioned above, in eukaryotes, different types of SOD are differently localized in the cell. The Cu,Zn-SOD is localized extracellularly and in the cytosole, protecting the cell from numerous external sources of $O_2^{\cdot -}$; Mn-SOD is localized in the mitochondria, protecting the cell from the internally generated ROS, and participating in redox signaling cascades.

Contrary to that, H_2O_2 is quite a stable and highly diffusible molecule that can easily penetrate membranes. As discussed above (see Sect. 14.3), its enzymatic production and removal provides site and time specificity for its action.

14.5.2 Catalase

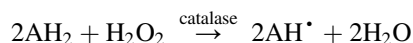
14.5.2.1 What Is Catalase?

Catalases are a universally present family of enzymes, catalyzing degradation of hydrogen peroxide to water and oxygen:



first discovered before 1900 (Loew 1900) and extensively studied after (see, e.g., reviews (Nicholls et al. 2000; Sepasi Tehrani and Moosavi-Movahedi 2018)). Catalases show extremely high reaction rates, with the maximal turnover number reaching $(16 - 44) \times 10^6 \text{ s}^{-1}$, but a surprisingly low affinity to H_2O_2 (see (Heck et al. 2010; Chelikani et al. 2004)).

Besides this reaction, at low concentrations of H_2O_2 catalases can possess certain peroxidase activity:



The second substrate, oxidized in course of this reaction, can be various hydrogen donors, such as alcohols, phenols, hormones, heavy metals, and nitrite. For most catalases, the rate of peroxidase reaction is very low and appears significant only at insufficient H_2O_2 concentrations.

Catalases are classified into for types (see reviews (Nicholls et al. 2000; Chelikani et al. 2004; Sepasi Tehrani and Moosavi-Movahedi 2018)):

- Monofunctional heme catalases* – the largest group of catalases, containing heme as prosthetic group. They are found in archaea, bacteria, fungi, plants, and animals; some of them also have minor peroxidase activity.
- Catalase peroxidases* – a large group of enzymes with significant catalase and peroxidase activity. They are found in bacteria and fungi.
- Nonheme catalases* – several enzymes, with Mn-rich active centers, found in several bacterial species.
- Minor catalases* – several heme-containing enzymes, mostly peroxidases, with minor (or even negligible) catalase activity (Arnao et al. 1990). Interestingly, the latter is observed even for the pure heme (though very weak), which may explain the catalase activity of nonspecialized enzymes (see more in (Nicholls et al. 2000)).

Examples of several different catalases can be seen in Fig. 14.21. Importantly, catalase activity strongly depends on its quaternary structure, for instance, mammalian catalases are active as homotetramer, while individual monomers are inactive (see discussion in (Heck et al. 2010)).

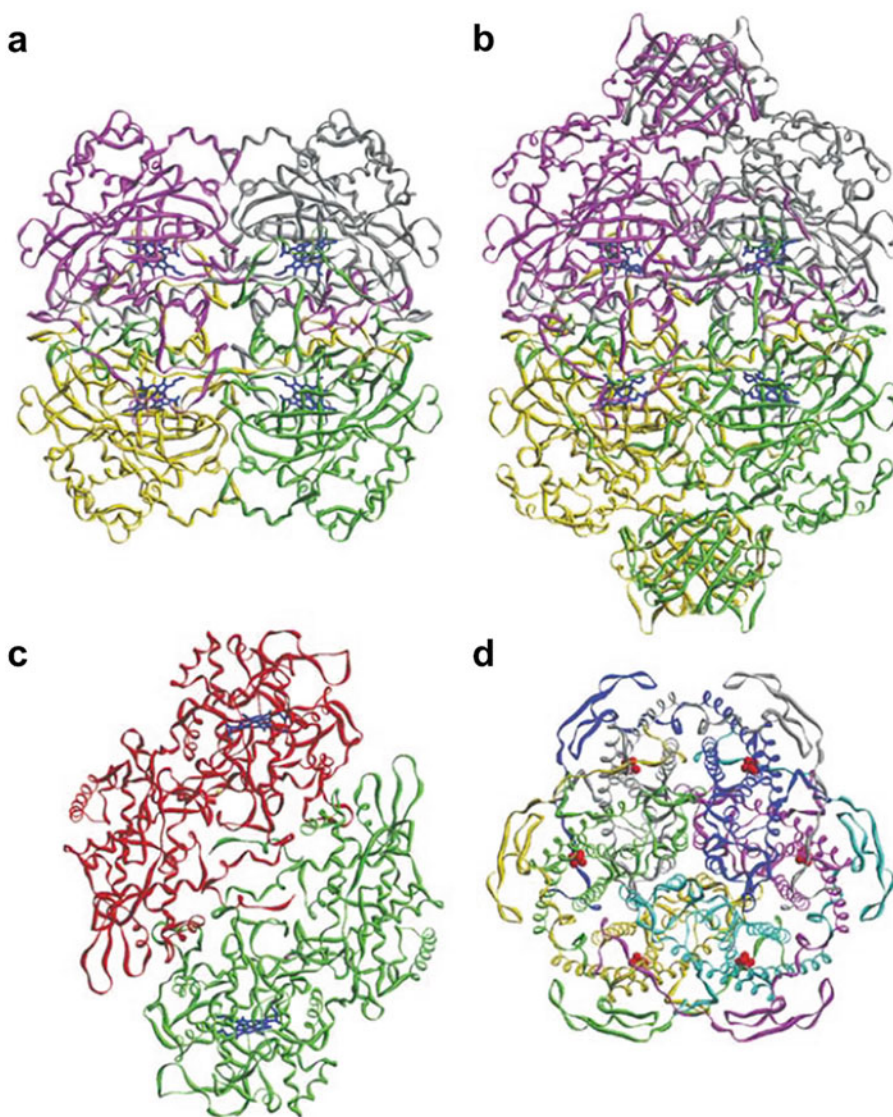
14.5.2.2 Catalase Role

Catalase can be called the first line of defense against ROS, particularly, H_2O_2 and OH^{\cdot} radical generated from it. However, this protective value becomes apparent mostly when the organism is exposed to oxidative conditions (see, e.g., (Izawa et al. 1996)). Catalase levels increase manifold at oxidative stress (Christman et al. 1985; Loewen et al. 1985; Schellhorn 1995), but can be also regulated by other factors, like substrate availability or the culture growth phase in bacteria (Loewen et al. 1985).

Importantly, the same cell often contains several catalase types, with different regulation and functions. For instance, *Escherichia coli* has two catalases (Loewen et al. 1985): HPII – a typical monofunctional catalase, weakly expressed during the culture growth and enhanced manifold in the stationary phase under aerobic conditions; and HPI – a catalase peroxidase, expressed on induction of oxidative stress.

In eukaryotes, catalase is mostly localized in peroxisomes (compromising ~16% of the total peroxisome protein (Fujiki et al. 1982)), but can also be found in the cytoplasm. Its redistribution between these compartments appeared tightly

Fig. 14.21 Overall structures of several typical catalases. (a) Tetrameric small subunit, heme-containing catalase, CatF; (b) Tetrameric large subunit, heme-containing catalase, HPII; (c) Dimeric catalase peroxidase, BpKatG; (d) Hexameric dimanganese catalase, LPC. (Reprinted from (Chelikani et al. 2004). Copyright 2004, with permission from Springer Nature)



regulated via several mechanisms (Hosoi et al. 2017; Dubreuil et al. 2020; Okumoto et al. 2020), with the following result: oxidative stress – catalase accumulation in the cytoplasm – catalase-mediated defense from ROS and activation of the downstream regulatory cascades (see more in reviews (Islinger et al. 2018; Fujiki and Bassik 2021)). This implies a protective role of peroxisomes at oxidative stress, as well as a specific branch of catalase-mediated redox signaling (Dubreuil et al. 2020; Okumoto et al. 2020).

Interestingly, some catalases (e.g., *E. coli*'s HPI) can also produce ROS when exposed to UVB (Heck et al. 2003; Heck et al. 2010), which might play an important role in UV-initiated ROS signaling and, further, UV defense of the organism (see below; see also (Peus et al. 1999; Devary et al. 1992)).

14.5.2.3 Catalase Functioning

The catalase reaction involves two stages: *reducing* the first molecule of H_2O_2 to water and *oxidizing* the second one to oxygen. For heme-containing catalases and catalase peroxidases, in the first half-reaction, H_2O_2 obtains two reducing equivalents: one from the iron atom (changing its valence to IV), and the other one from the porphyrin ring with the formation of a radical cation $Por^{•+}$ (Table 14.3a).

This forms a highly reactive intermediate *Compound I*, which can potentially oxidize different species, including a second molecule of H_2O_2 and various organic compounds. However, these oxidative reactions are largely limited by the fact that catalase active sites are deeply embedded in the rigid and stable beta-barrel structure of the protein. Substrates can reach the heme through two (or may be three) narrow

Table 14.3 The mechanism of catalase functioning: (a) formation of *Compound I* – reduction of the first H₂O₂; (b) reduction of *Compound I* and oxidation of the second H₂O₂; (c) formation of the inactive *Compound II*; (d) peroxidase activity of *Compound I* and (e) of *Compound II*

| | | |
|---|---|--|
| A | First half-reaction | $\text{Enz}(\text{Por} \cdot \text{Fe}^{\text{III}}) + \text{H}_2\text{O}_2 \rightarrow \text{CpdI}(\text{Por}^{\cdot\cdot} \cdot \text{Fe}^{\text{IV}} = \text{O}) + \text{H}_2\text{O}$ |
| B | Second half-reaction | $\text{CpdI}(\text{Por}^{\cdot\cdot} \cdot \text{Fe}^{\text{IV}} = \text{O}) + \text{H}_2\text{O}_2 \rightarrow \text{Enz}(\text{Por} \cdot \text{Fe}^{\text{III}}) + \text{H}_2\text{O} + \text{O}_2$ |
| C | Inactivation of Compound I to Compound II | $\text{CpdI}(\text{Por}^{\cdot\cdot} \cdot \text{Fe}^{\text{IV}} = \text{O}) + \text{e}^- \rightarrow \text{CpdII}(\text{Por} \cdot \text{Fe}^{\text{IV}} = \text{O})$ |
| | | $\text{CpdI}(\text{Por}^{\cdot\cdot} \cdot \text{Fe}^{\text{IV}} = \text{O}) + \text{e}^- + \text{H}^+ \rightarrow \text{CpdII}(\text{Por} \cdot \text{Fe}^{\text{IV}} - \text{OH}^+)$ |
| D | Peroxidase activity: step 1 | $\text{CpdI}(\text{Por}^{\cdot\cdot} \cdot \text{Fe}^{\text{IV}} = \text{O}) + \text{AH}_2 \rightarrow \text{CpdII}(\text{Por} \cdot \text{Fe}^{\text{IV}} - \text{OH}) + \text{AH}^{\cdot}$ |
| E | Peroxidase activity: step 2 | $\text{CpdII}(\text{Por} \cdot \text{Fe}^{\text{IV}} - \text{OH}) + \text{AH}_2 \rightarrow \text{Enz}(\text{Por} \cdot \text{Fe}^{\text{III}}) + \text{AH}^{\cdot} + \text{H}_2\text{O}$ |

channels, with a specific structure (Carpena et al. 2003; Ko et al. 1999), almost any changes in which disrupt the arrangement of water molecules in the channel and the enzyme functioning (see more in (Heck et al. 2010; Zámocký and Koller 1999; Chelikani et al. 2004)). This channel structure provides significantly better penetration of H₂O₂ over other substrates, giving a huge advantage to the second half reaction with H₂O₂ (Table 14.3 b).

However, at low H₂O₂ concentrations (typically <10 μM (Kremer 1970; Zámocký and Koller 1999)), there appears a noticeable chance for small organic molecules to access the catalase active center, and the enzyme obtains peroxidase activity, especially noticeable for catalase peroxidases (Kremer 1970) (Table 14.3d).

Besides the main reaction cycle, *Compound I* can undergo a one-electron reduction to the inactive *Compound II*, with the electron donated by the protein moiety to quench the reactive porphyrin radical (see Table 14.3c). *Compound II* returns to the enzyme basic state very slowly, which is the cause of catalase activity reduction over time (Jones and Suggett 1968).

The mentioned structural features of catalases – rigid beta-barrels, highly resistant to unfolding, make catalases surprisingly invulnerable to heating, denaturation and proteolysis. This is especially noticeable for the large-subunit monofunctional catalases, like *E. coli* HP11 (which is expressed in the culture stationary phase, with elevated protease levels, and, thus, really needs to be stable). At the same time, catalases are gradually inactivated by H₂O₂, manifesting at quite high concentrations: from 300 mM to 3 M for different enzymes, which is responsible for their gradual activity decrease under experimental conditions (see more in (Chelikani et al. 2004)).

Excitingly, under irradiation with UV light (even with physiological doses of UVB), catalases obtain ability to *produce* ROS (Heck et al. 2003). This effect was shown to be connected precisely with heme activity and depend on pH (with the lowest ROS production capacity at pH < 6 and the highest at pH 7–8). Catalase inhibitors also enhanced UVB-mediated ROS production; besides, the effect was observed for a catalase with NADPH cofactor and was not for a NADPH-independent catalase (Heck et al. 2010). While all these data are far from the final confident interpretation, the authors suggest that the absorbed UVB disrupts the

catalase channel native structure, giving preferential heme access to water molecules and stimulating heme-mediated ROS generation from them (Heck et al. 2010).

Paradoxically, while catalase was convincingly shown to *produce* ROS at UVB irradiation of keratinocytes (Heck et al. 2003), it has long been known as a strong UV *protectant* in these cells. This might mean that catalase-produced ROS are playing certain signaling roles, leading to UV protective effects in the cells.

14.5.3 Peroxidases

14.5.3.1 Peroxidases and Their Role

Peroxidases are a huge class of enzymes, closely related to catalases, including (at least some of) them, and belonging to the class of oxidoreductases (RedoxiBase). They catalyze different oxidative reactions, utilizing H₂O₂ or organic peroxides (ROOH) as electron acceptors and plenty of different substrates as donors – either in one-electron (Table 14.4a, b) or in two-electron (Table 14.4c, d) reactions. The one-electron donors include: aromatic phenols, phenolic acids, indoles, amines, sulfonates, proteins, and even metal cations (see, e.g., (Veitch 2004; de Oliveira et al. 2021)). The two-electron donors can be halides (Cl⁻, Br⁻, I⁻), thiocyanate (SCN⁻), and some others (e.g., (Roman and Dunford 1972, 1973)). Correspondingly, the peroxidase specificity is determined by the specific binding sites for the second substrate.

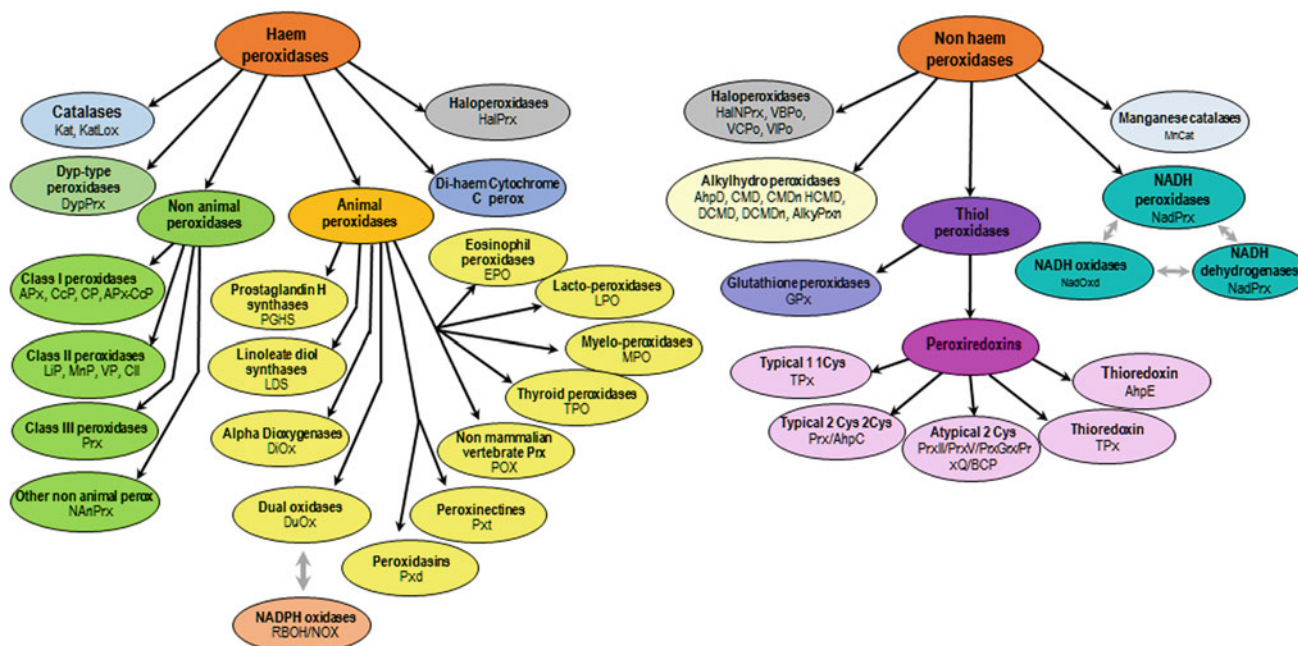
Some peroxidases can also catalyze H₂O₂ dismutation. However, the mechanism of these reactions is quite different from that of the typical monofunctional heme catalases (see Sect. 14.5.2) (Vlasits et al. 2010).

Peroxidases are extremely widespread and found in almost all living organisms, from prokaryotes to animals and human (Passardi et al. 2007). Within the cell they can be found both in the cytoplasm and in various organelles: peroxisomes, lysosomes, mitochondria, and even in the nucleus and cytoplasm, and also bound to plant cell walls and secreted into the extracellular space (see (de Oliveira et al. 2021; Zamocký et al. 2014; RedoxiBase)).

Notably, the same organism can contain several (many) different isoenzymes (e.g., at least 28 for Arabidopsis (Ostergaard et al. 1998)), differently expressed in organs

Table 14.4 Peroxidase reactions

| | | |
|---|------------------------|---|
| a | One-electron reactions | $\text{ROOH} + 2\text{AH}_2 \xrightarrow{\text{Peroxidase}} \text{ROH} + \text{H}_2\text{O} + 2\text{AH}^\bullet$ |
| b | | $\text{H}_2\text{O}_2 + 2\text{AH}_2 \xrightarrow{\text{Peroxidase}} 2\text{H}_2\text{O} + 2\text{AH}^\bullet$ |
| c | Two-electron reactions | $\text{ROOH} + \text{X}^- + \text{H}^+ \xrightarrow{\text{Peroxidase}} \text{ROH} + \text{HOX}$ |
| d | | $\text{H}_2\text{O}_2 + \text{X}^- + \text{H}^+ \xrightarrow{\text{Peroxidase}} \text{H}_2\text{O} + \text{HOX}$ |
| e | Catalase-like reaction | $2\text{H}_2\text{O}_2 \xrightarrow{\text{Peroxidase}} 2\text{H}_2\text{O} + \text{O}_2$ |

**Fig. 14.22** Peroxidase classification. (Adapted from (Savelli et al. 2019), under Creative Commons CC-BY license. Copyright 2019, Elsevier. See also (RedoxiBase))

and tissues, and at different physiological states (see (Veitch and Smith 2000)).

In plants, peroxidases participate in cell elongation, crosslinking of cell wall components (Fry 1987; Michon et al. 1997), its tightening and lignification (Michon et al. 1997; Wakamatsu and Takahama 1993). Expression of HRP is stimulated by wounding (Kawaoka et al. 1994; Lagrimini et al. 1987) and is involved in defense in physically damaged or infected tissues (Biles and Martyn 1993).

In various microorganisms, peroxidases promote virulence (e.g., (Brenot et al. 2004)). In mammals, they participate in immune response, metabolic regulation and various branches of signaling (see (Bae et al. 2011; Flohe and Ursini 2008)).

14.5.3.2 Peroxidase Classification

Peroxidases can be classified into heme and nonheme types (Koua et al. 2009) (see Fig. 14.22), which are further subdivided into classes and smaller clades. Interestingly, the most ancient bifunctional catalase peroxidases, forming the

basis of the peroxidase–catalase superfamily, evolutionarily were gradually losing their catalase activity (Vlasits et al. 2010) and finally formed the presently dominant class of monofunctional heme peroxidases (see Fig. 14.23). The important shift was probably attributed to the clade of hybrid-type A peroxidases, which lost the C-terminal domain, as well as the ability to dismutate hydrogen peroxide (Zamocky et al. 2014), and became monofunctional heme peroxidases (see asterisk in Fig. 14.23). Altogether, heme peroxidases include nearly ten thousand members belonging to three major classes and two hybrid types positioned between them (see Figs. 14.22 and 14.23). Of the best-known enzymes, they include myeloperoxidase (MPO), eosinophil peroxidase (EPO), lactoperoxidase (LPO), thyroid peroxidase (TPO), prostaglandin H synthase (PGHS), and peroxidasin (Nelson et al. 1994).

Nonheme peroxidases include vanadium- (Butler 1998, 1999) and selenium-containing (Stadtman 1990) enzymes and peroxiredoxines, which require no cofactors and instead

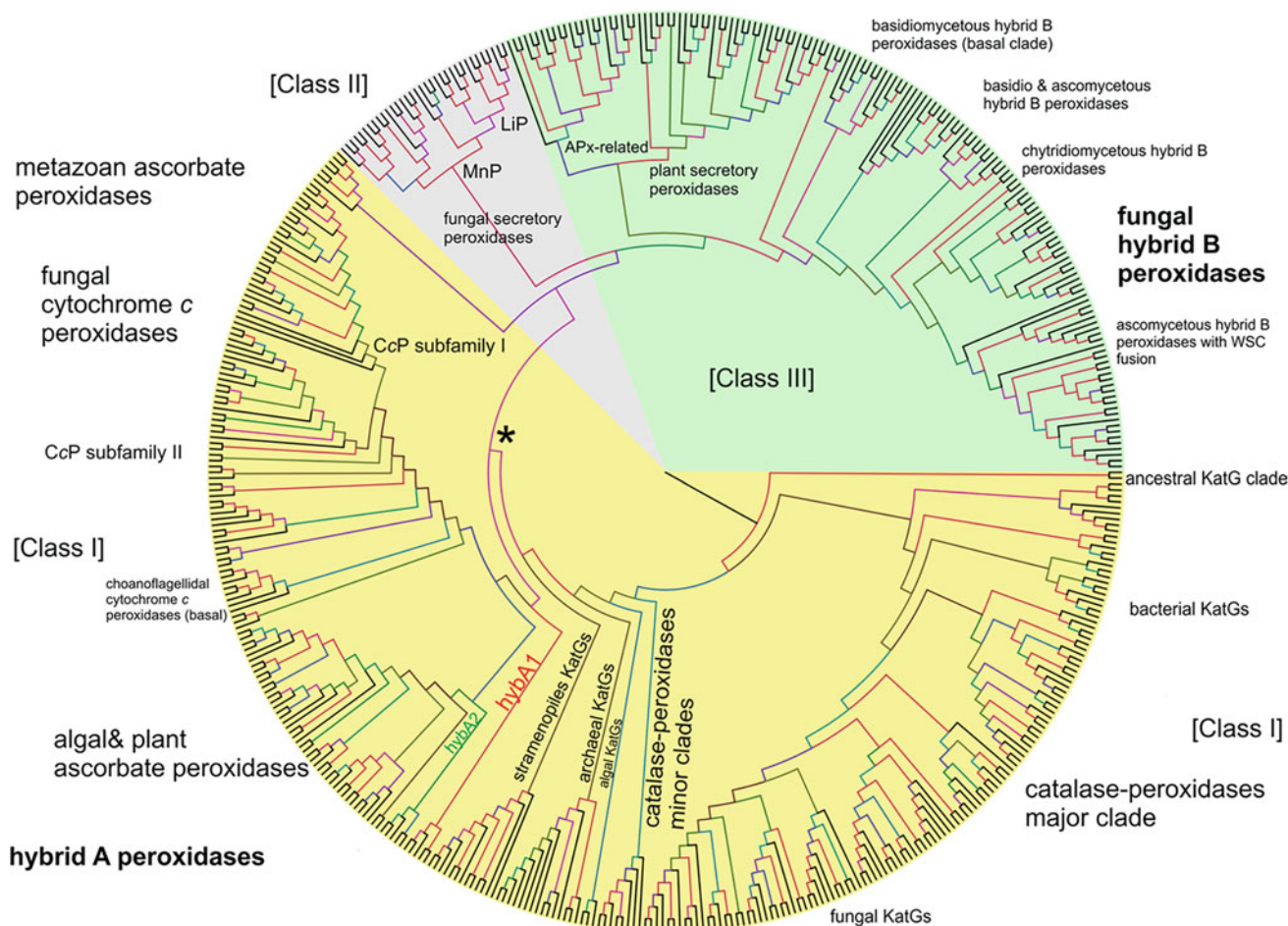


Fig. 14.23 Rooted maximum-likelihood tree for the peroxidase–catalase superfamily. Bootstrap values are presented in a color scheme for the ML output: red >90, violet >70, blue >50, green >30. Asterisk marks the evolutionary step when the bifunctionality and the

two-domain structure were lost. (Reprinted from (Zamocky et al. 2014), under Creative Commons CC-BY license. Copyright 2014, Springer Nature)

generate peroxidase-like activity by means of an active site cysteine residue (Choi et al. 1998).

The structure of some classical peroxidase enzymes is shown in Fig. 14.24.

14.5.3.3 Peroxidase Functioning

Although peroxidases differ in protein structure, active sites, and prosthetic groups, their catalytic mechanisms are largely similar and can be seen from a common perspective. The best studied peroxidase is horseradish peroxidase (HRP) (Veitch and Smith 2000), which can be used as an example of heme peroxidase functioning.

Generally, the peroxidase reaction involves two stages: (1) getting into the highly reactive state *Compound I*, by *reducing* the first substrate – H_2O_2 or $ROOH$; (2) returning to the enzyme resting state by *oxidizing* the second substrate, mostly, in two steps (see Table 14.5 and Fig. 14.25).

The first half-reaction is basically the same for all peroxidases and catalases. The enzyme active center is

oxidized by H_2O_2 (or another peroxide), generating the highly reactive *Compound I* (Table 14.5a), which is *two oxidizing equivalents above the resting state*. Peroxidases have very high affinity for H_2O_2 , and the direct reaction rate is very high ($1.2 \pm 0.4 \times 10^7$ L/mol/s, while the reverse reaction is very slow ($k_2 < 0.2$ s⁻¹), and the enzyme–substrate dissociation constant is less than 2×10^{-8}). Thus, the reaction is practically irreversible.

Further reaction consists in one-electron reduction of *Compound I* to *Compound II* and simultaneous oxidation of the first substrate molecule (Table 14.5b). This reaction can be quite variable, depending on the substrate, with the reaction rate differing from 0 to more than 10^5 L/mol/s (e.g., 3.0×10^4 L/mol/s for leucomalachite green and 1.8×10^5 L/mol/s for ascorbic acid (Chance 1952)).

The generated *Compound II* is also a powerful oxidant, one oxidizing equivalent above the resting state. It readily oxidizes the second substrate molecule, turning it into the free-radical form and returning to the *resting state*

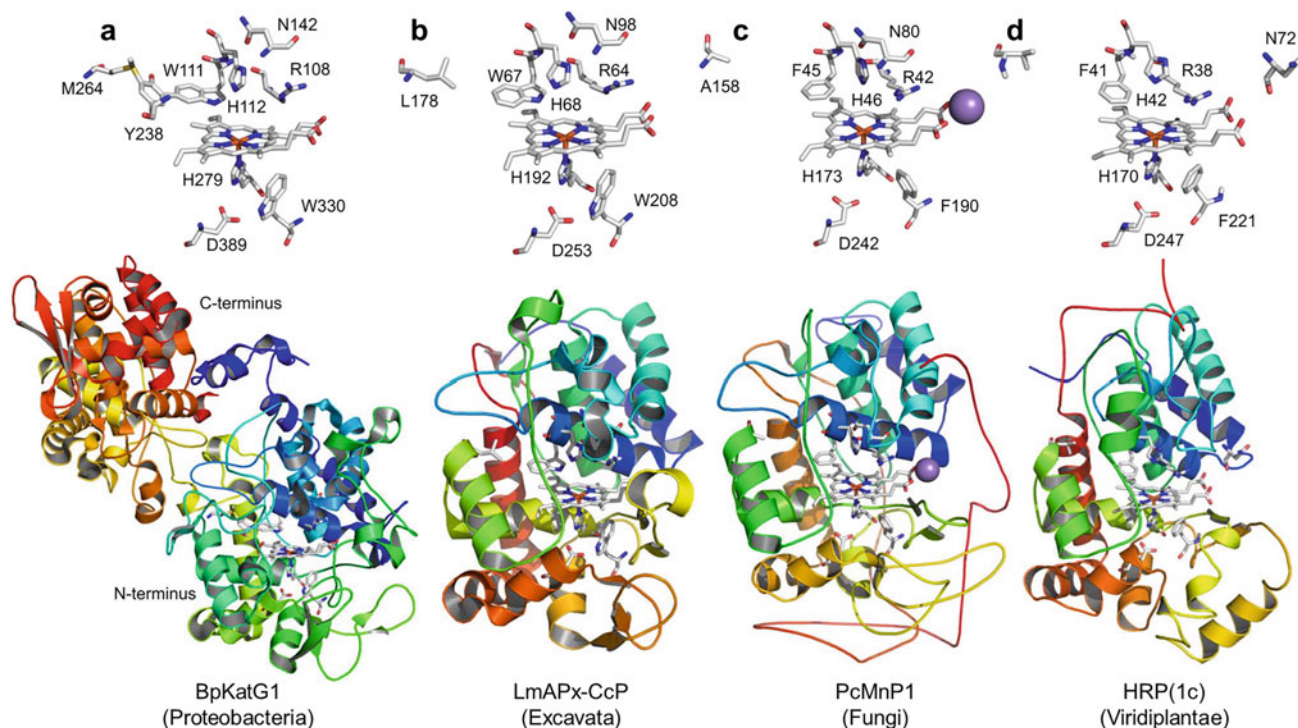


Fig. 14.24 Overall structures of several typical peroxidases (see Fig. 14.23 for phylogeny). (a, b) Class I peroxidases; (a) Bifunctional KatG from *Burkholderia pseudomallei*; (b) Hybrid-type A1 peroxidase from *Leishmania major*; (c) Manganese peroxidase from

Phanerochaete chrysosporium; (d) Horseradish peroxidase (from *A Armoracia rusticana*). (Reprinted from (Zamocky et al. 2014), under Creative Commons CC-BY license. Copyright 2014, Springer Nature)

Table 14.5 The mechanism of peroxidase functioning: (a) oxidation of the enzyme to *Compound I* – reduction of H_2O_2 ; (b) reduction of *Compound I* to *Compound II* – oxidation of the first substrate molecule; (c) reduction of *Compound II* to the resting state – oxidation of the second substrate molecule

| | | |
|---|--------------------------------|--|
| A | First half-reaction | $Enz(Por \cdot Fe^{III}) + H_2O_2 \rightarrow CpdI(Por^{+ \cdot} \cdot Fe^{IV} = O) + H_2O$ |
| B | Second half-reaction: step 1 | $CpdI(Por^{+ \cdot} \cdot Fe^{IV} = O) + AH_2 \rightarrow CpdII(Por \cdot Fe^{IV} = O) + AH^{\cdot} + H^+$ |
| C | Second half-reaction: step 2 | $CpdII(Por \cdot Fe^{IV} = O) + AH_2 + H^+ \rightarrow Enz(Por \cdot Fe^{III}) + AH^{\cdot} + H_2O$ |
| D | Free-radical product reactions | $2AH^{\cdot} \rightarrow A_2H_2$ |
| E | | $AH^{\cdot} + RH \rightarrow AH_2 + R^{\cdot}$ |

(Table 14.5c). Besides that, *Compound II* can be oxidized by another H_2O_2 molecule to *Compound III*, thus leading to the enzyme inactivation (see Fig. 14.25). This becomes quite probable under the excess of H_2O_2 , partially explaining the H_2O_2 -caused enzyme inactivation.

It is fundamentally important, that peroxidase functioning is inseparable from free-radical states. First, the peroxidase cycle involves a free-radical *Compound I*; second, the primary reaction product is a free radical in all cases of one-electron oxidation (Table 14.5b and c, AH^{\cdot}), i.e., for the vast majority of peroxidase reactions.

Thus, *Compound I*, in addition to reactions with the substrate, reducing it to *Compound II*, can interact with other species, giving rise to free-radical processes and/or leading to the enzyme inactivation. Moreover, active centers of both *Compound I* and *Compound II* tend to withdraw electrons

from the protein part (Furtmuller et al. 2004), thus producing protein radicals – mostly tyrosinyl or tryptophanyl (see Table 14.6, and Chap. 12 for more details on free-radical processes in proteins).

Next, as mentioned above, the primary product of the substrate oxidation (Table 14.5b and c) is a free-radical AH^{\cdot} in most peroxidase reactions, while molecular products are generated in further reactions. However, besides conventional reactions, AH^{\cdot} can either recombine, producing substrate dimers (Table 14.5d), or attack other molecules (Table 14.5e), starting a peroxidation cascade.

In the first case, the generated substrate dimers (A_2H_2 in Table 14.5 d) can also act as peroxidase substrates, thus producing dimer radicals and gradually forming oligomers and polymers. This is important, e.g., for crosslinking cell

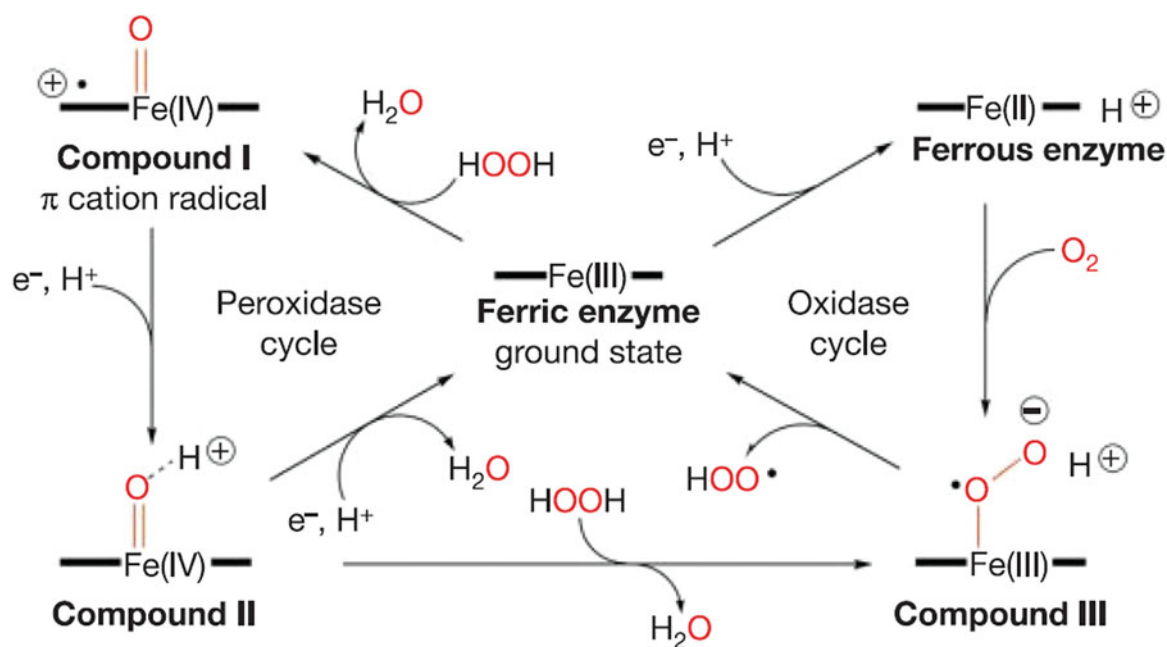


Fig. 14.25 Mechanism of reactions catalyzed by peroxidases (see also Table 14.5). (Reprinted from (Berglund et al. 2002). Copyright 2002, with permission from Springer Nature)

Table 14.6 Delocalizing electrons in Compounds I and II

| | | |
|---|-------------|---|
| a | Compound I | Protein · Por ²⁺ · Fe ^{IV} = O ↔ Protein ²⁺ · Por · Fe ^{IV} = O |
| b | Compound II | Protein · Por · Fe ^{IV} = O ↔ Protein ²⁺ · Por · Fe ^{III} = O |

wall components and lignification in plants (Fry 1987; Michon et al. 1997).

In the second case, the started free-radical cascades can deactivate the enzyme itself, as well as destruct cell membranes. For this reason, even though hydrogen peroxide is the natural substrate for peroxidases, it also disrupts the enzyme stability (Valderrama et al. 2002).

Thus, the vast majority of peroxidase reactions are going through free-radical stages – meaning both the enzyme (*Compound I* and to some extent *Compound II*), and the reaction products (AH[•]). Importantly, these stages are not only inevitable, but also mechanistically necessary.

Needless to say, besides their indispensable role in peroxidation, the free-radical species generated in course of peroxidation, also appear the origins of free-radical chain processes, involving both lipids (see Chap. 11), proteins (see Chap. 12), and other substances. Thus, they belong to the initial sources of biological autoluminescence processes.

14.5.4 Other Free-Radical-Producing Enzymes

14.5.4.1 Cyclooxygenases

Cyclooxygenases (prostaglandin-H-synthases) are enzymes that catalyze conversion of unsaturated fatty acids with four double bonds – arachidonic and duomo-gamma-linolenic acids, into prostaglandins through free-radical metabolites.

The enzyme cyclooxygenase carries out two catalytic reactions – cyclooxygenase and peroxidase. In the course of the cyclooxygenase reaction, two oxygen molecules are sequentially attached to the arachidonic acid molecule at positions C11 and C15. This is accompanied by cyclization of the carbon skeleton and the formation of an intermediate hydroperoxyl-endoperoxide. Further, during the peroxidase reaction, the 15-hydroperoxide group of prostaglandins PGG₂ is reduced to the hydroxyl group, forming PGH₂.

Intermediate free-radical products have been studied in vivo by electron spin resonance (ESR), gas chromatography and mass spectrometry (Xiao et al. 2011; Yu et al. 2009) (see Fig. 14.26).

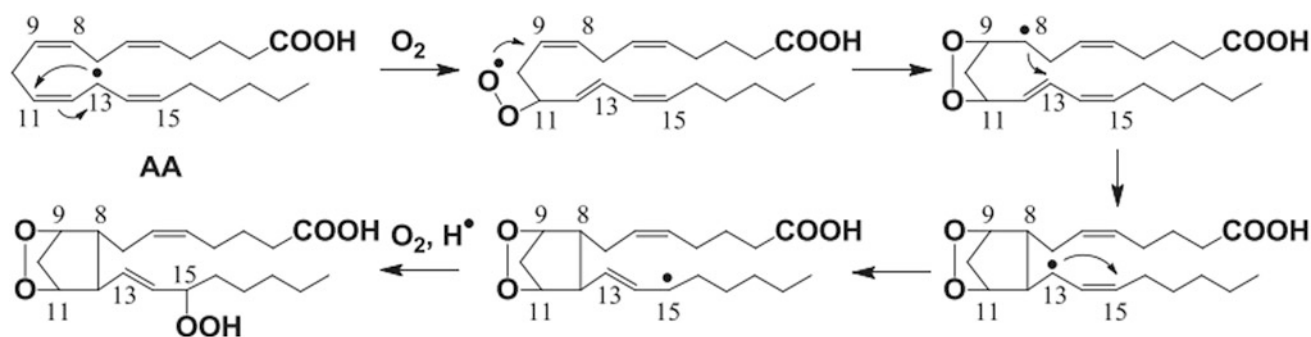
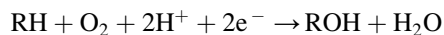


Fig. 14.26 The putative mechanism of arachidonic acid peroxidation into PGG₂ via free-radical products. (Reprinted from (Gu et al. 2013). Copyright 2013, with permission from Elsevier)

As one can see, these reactions also involve intermediate free-radical stages, also being potential sources of free-radical processes and BAL.

14.5.4.2 Cytochrome P450

The superfamily of cytochromes P450 includes a large group of enzymes that catalyze the oxidation of hydrophobic organic compounds: lipids, hormones, xenobiotics, and toxins. Basically, this is a monooxygenase reaction in which one oxygen atom is incorporated into the substrate and a water molecule is formed.



Two electrons are usually provided by NADPH, along two possible metabolic paths, realized in the endoplasmic reticulum and on the mitochondrial membrane. Namely, during microsomal oxidation, electrons are transferred to cytochrome P450 via cytochrome P450 reductase, an enzyme containing two cofactors: FAD and FMN. This electron transfer occurs with the participation of adrenodoxin reductase, a FAD-containing flavoprotein, and adrenodoxin, an iron-sulfur protein. The mechanism of cytochromes P450 operation includes six stages (see Fig. 14.27, see more in (Bae et al. 2011)):

1. The substrate binds to the protein active center in the immediate vicinity of the heme group, changing the active center conformation. The water molecule is replaced, and the iron becomes five-coordinated (stage 1).
2. A change in the spin state facilitates the transfer of an electron from NADPH through cytochrome P450 reductase or adrenodoxin, while the iron from the ferri-form is converted to the ferro-form (stage 2).
3. Ferrous iron binds oxygen, forming an oxo-complex with cytochrome (stage 3).
4. Then the second electron is transferred through cytochrome P450 reductase or adrenodoxin and a peroxo complex is formed (stage 4).

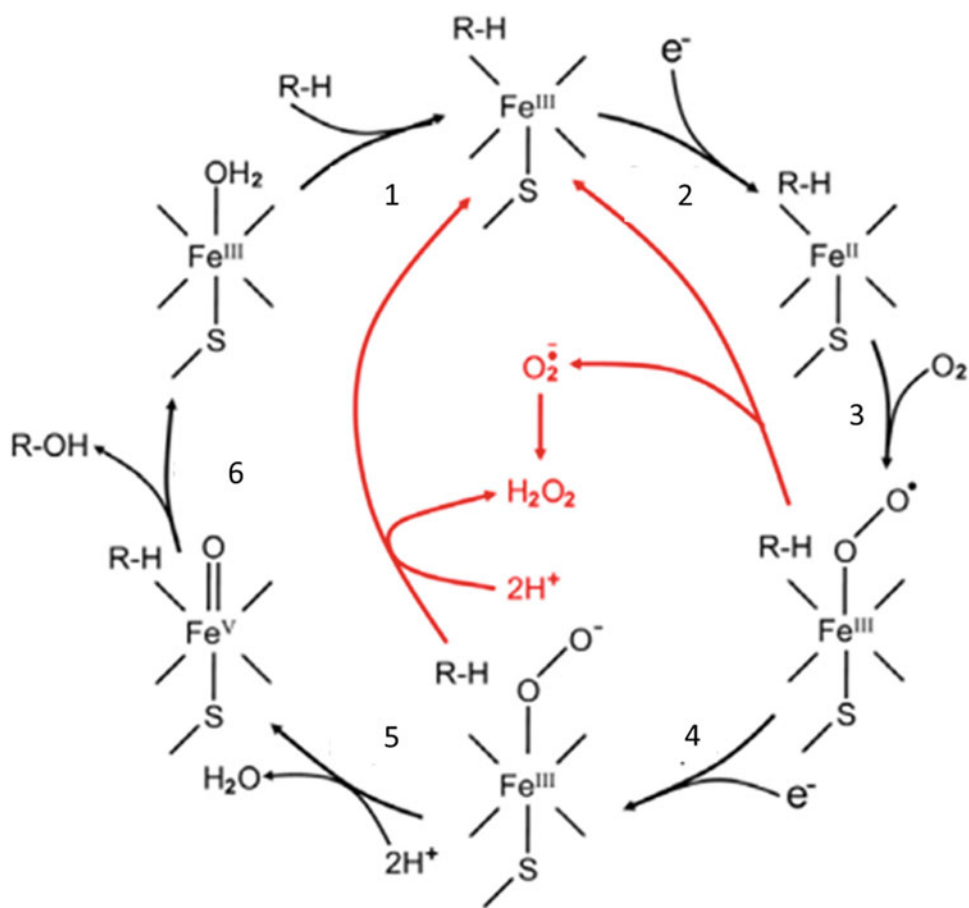
5. This peroxy group is rapidly protonated twice, which leads to heterolytic cleavage of the O – O bond with the formation of a water molecule and a highly reactive *Compound I* (stage 5) (Rittle and Green 2010).
6. The oxygen atom from *Compound I* is then incorporated into the RH substrate to form ROH (step 6).

Importantly, a significant part of oxygen leaves this cycle in the form of O₂^{-•} or H₂O₂. Alternatively, the product of one-electron oxygen reduction, the oxy complex (formed in step 3), breaks down to form O₂^{-•} (branch 1). Another way is the formation of H₂O₂ from the peroxy complex (branch 2). Thus, ROS production in the cytochrome P450 cycle is an inevitable phenomenon both in the presence and in the absence of substrates; however, the ROS yield depends on the type of cytochrome, substrate, pH, ionic strength, oxygen concentration, and other factors (Bae et al. 2011). The efficiency of electron transfer from NADPH to cytochrome P450 during monooxygenation is called the degree of conjugation.

In addition to the above, it should be noted that the cited scheme (Fig. 14.27) suggests an essentially peroxidase mechanism of substrate oxidation, except that the oxidizing agent is molecular oxygen, but not hydrogen peroxide, and *Compound I* is formed from hemoprotein in a bivalent state (Fe²⁺) rather than trivalent (Fe³⁺) (compare to Fig. 14.25). Meanwhile, the reaction of *Compound I* with a substrate molecule, as well as a similar reaction of the resulting *Compound II*, in the case of peroxidases directly leads to the formation of a substrate free radical, and the final oxidation product is formed in a process where radicals serve as intermediate products (see Sect. 14.5.3). Therefore, not only peroxidases and lipoxygenases but also cytochromes P450 can form radicals as intermediate products of substrate oxidation, including polyunsaturated fatty acids (compare to Fig. 14.26).

The products formed by the cytochrome P450 system during the oxidation of arachidonic acid and other

Fig. 14.27 Scheme of reactions catalyzed by cytochromes P450. (Reprinted from (Bae et al. 2011), under Creative Commons license. Copyright 2011, the Korean Society for Molecular and Cellular Biology)



polyunsaturated acids cleaved by phospholipase A2 are shown in Fig. 14.28.

The most active system of cytochrome P450 is observed in the liver cells, where the cytochrome itself and its reductase are located on the outer surface of the endoplasmic reticulum and are fixed by transmembrane anchor proteins. The cytochrome P450 system of mitochondria is located on the inner membrane and faces matrix. In cells of other organs, P450 is less represented, but even there, its amount is comparable to that of hemoproteins in the electron-transport chain. Thus, the amount of ROS produced by cytochrome P450 in our cells can be quite high.

14.5.5 Cytochrome C as a Peroxidase

14.5.5.1 Cytochrome C and Its Multiple Roles

As is known, cytochrome c (CytC) is an important component of the respiratory chain, carrying electrons from Complex III to Complex IV (see Sect. 14.4.3). It is a small globular hemoprotein of 94 to 114 amino acid residues for different species (see (Bushnell et al. 1990)), with variable (and evolutionary changing) amino-acid sequence. However, its tertiary structure is evolutionary conserved due to a well-

preserved set of key amino acid residues, determining its structure and function (see (Hannibal et al. 2016; Zaidi et al. 2014)).

Importantly, electron transport is far from the only function of cytochrome c. It was also shown to be a *strong and recoverable antioxidant*, defending mitochondria from excessively produced ROS by *oxidizing* $O_2^{\cdot -}$ to O_2 (Korshunov et al. 1999; Pereverzev et al. 2003) and either *oxidizing* or *reducing* H_2O_2 , depending on the CytC initial oxidation state (Wang et al. 2003).

Moreover, it appeared an important participant in the *mitochondrial oxidative protein folding* (the so-called *Mia* path – see (Mordas and Tokatlidis 2015)). The latter consists in delivery of protein precursors to the mitochondrial intermembrane space, and gradual oxidation of their *SH*-groups, forming disulfide bonds and, thus, folding the protein. Oxidation is performed by an essential oxidoreductase *Mia40*, which needs to further donate the delivered electron to restore its initial state, and for which CytC is one of the main terminal oxidants (see more in (Mordas and Tokatlidis 2015)).

Furthermore, CytC was shown to be the key participant of the mitochondrial apoptotic pathway, activated by a diversity of chemicals, drugs, and X- and UV-irradiation (see (Green

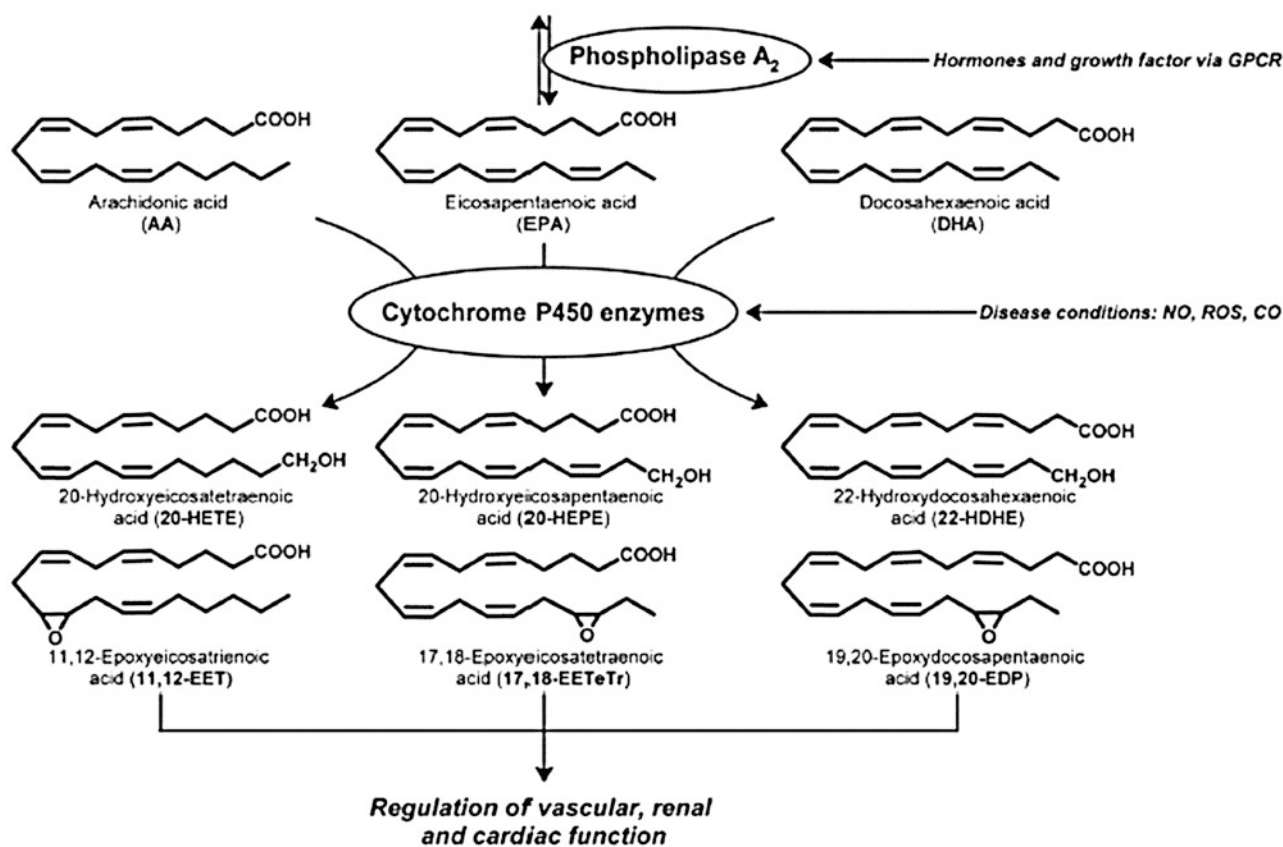


Fig. 14.28 Metabolism of arachidonic, eicosapentaenoic and docosahexaenoic acids by cytochrome P450 enzymes. The resulting products play a regulatory role in blood vessels, kidneys and heart. (Reprinted from (Poorani et al. 2016). Copyright 2016, with permission from Elsevier)

and Kroemer 2004)). All these upstream apoptosis-related stimuli are actually integrated by the all-or-nothing CytC release (Goldstein et al. 2000), activating downstream apoptotic machinery (Kagan et al. 2005). For this, CytC assembles a complex with cardiolipin (a mitochondria-specific phospholipid), referred to as *CytC-CL*, which has pronounced peroxidase activity. As will be shown below, *CytC-CL* specifically oxidizes cardiolipin of the inner mitochondrial membrane (Kagan et al. 2005; Kagan et al. 2009), stimulating its liquification, mitochondria swelling, the outer membrane permeabilization, and megapore formation (see (Green and Kroemer 2004)).

All this releases *CytC-CL*, Apaf-1, and other factors from the mitochondria into the cytoplasm (Goldstein et al. 2000), where they assemble apoptosomes (Li et al. 1997), activate caspases, and, thus, trigger apoptotic cascades (Kagan et al. 2005), ending with cell death and its capture by macrophages (see Fig. 14.29; see also reviews (Hannibal et al. 2016; Huttemann et al. 2011; Green and Kroemer 2004; Skulachev 1996, 1998; Liu et al. 1996; Yang et al. 1997)).

Thus, cytochrome *c* is a key component of the mitochondrial apoptotic pathway, initiated by formation of *CytC-CL* complex and cardiolipin peroxidation.

Besides all above, *CytC-CL* was also found an important regulator of several nonapoptotic (or preapoptotic) processes and redox signaling in general (Huttemann et al. 2011). For instance, being released into the cytoplasm, it further translocates to nuclei, upregulating protective response to nitrate stress (Godoy et al. 2009).

Thus, cytochrome *c* appears an amazingly multifunctional agent, integrating respiration, protein folding, anti- and pro-oxidant functions, and regulation of multiple processes, up to the life/death decisions.

Below we will dwell on the mechanisms of its proapoptotic function.

14.5.5.2 Cytochrome C in Apoptosis

14.5.5.2.1 Apoptosis in Short

As is known, the most common apoptotic path in vertebrates is mitochondrial, defined by the phenomenon of MOMP (mitochondrial outer membrane permeabilization), followed by the release of *cytochrome c* and other apoptotic factors from the intermembrane space, and further activation of caspase machinery (see (Green and Kroemer 2004; Kroemer and Reed 2000)). The exact timeline of these events can

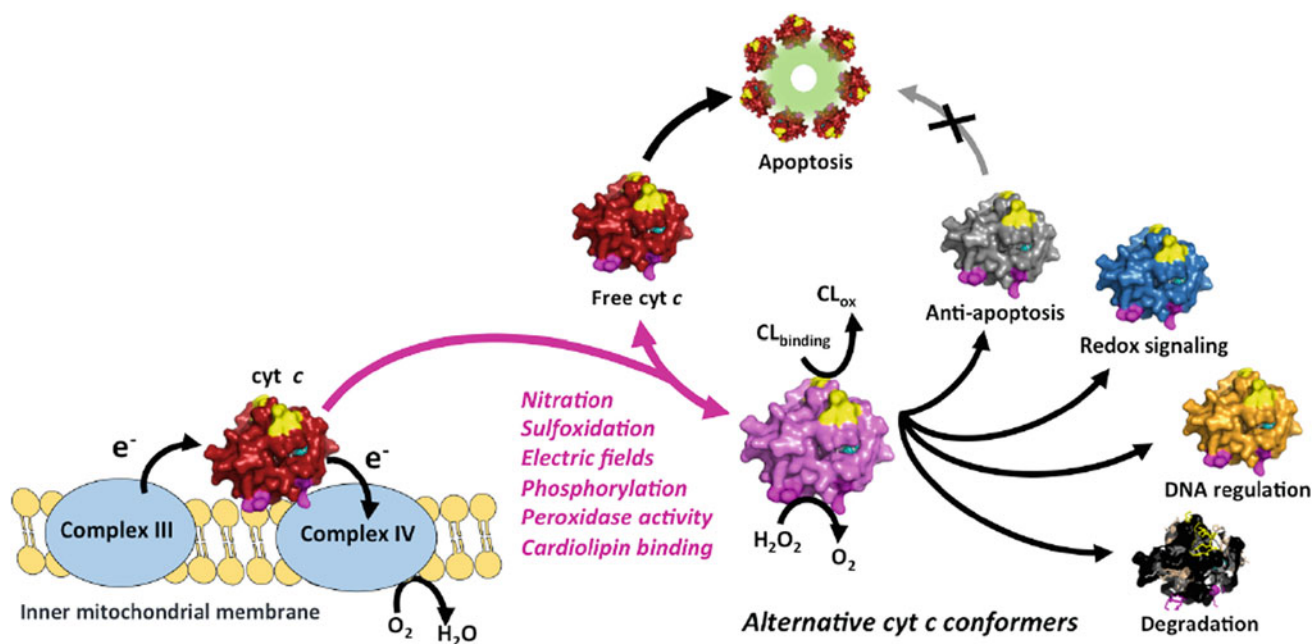


Fig. 14.29 The roles of cytochrome C in the cell. (Reprinted with permission from (Hannibal et al. 2016). Copyright 2016, American Chemical Society)

Table 14.7 The consequence and timing of the major apoptotic events in mouse embryonic cells, triggered by ACD (actinomycin D)

| | |
|---------|--|
| 0 h | Trigger of apoptosis |
| 6 h | Detectable <i>cardiolipin</i> (CL) oxidation |
| 8 h | <i>Cytochrome c</i> release from the intermembrane space into the cytoplasm |
| 8 h | <i>Caspase 3/7</i> activation |
| 9 h | <i>Phosphatidylserine</i> (PS) externalization on the mitochondrial membrane |
| 12–14 h | Mitochondrial membrane potential decrease |

Data from Kagan et al. (2005)

obviously vary in different cases, but the general sequence remains preserved. For instance, apoptosis in mouse embryonic cells, triggered by *actinomycin D* (ACD), shows the following pattern of events (Kagan et al. 2005) (see Table 14.7).

As is known, the factors triggering apoptosis, can substantially vary: from different chemicals and drugs to UV and ionizing radiation, as well as hypoxia, hyperthermia, viral infections, increased amount of free radicals (of different origin), etc. All of them lead to activation of intracellular proapoptotic factors and/or suppression of antiapoptotic ones, with the major role belonging to the *Bcl-2 apoptosis-regulating protein family* (see, e.g., (Alberts et al. 2015; Green and Kroemer 2004; Elmore 2007)).

14.5.5.2.2 CL Oxidation by CytC Is Necessary for Other Apoptotic Events

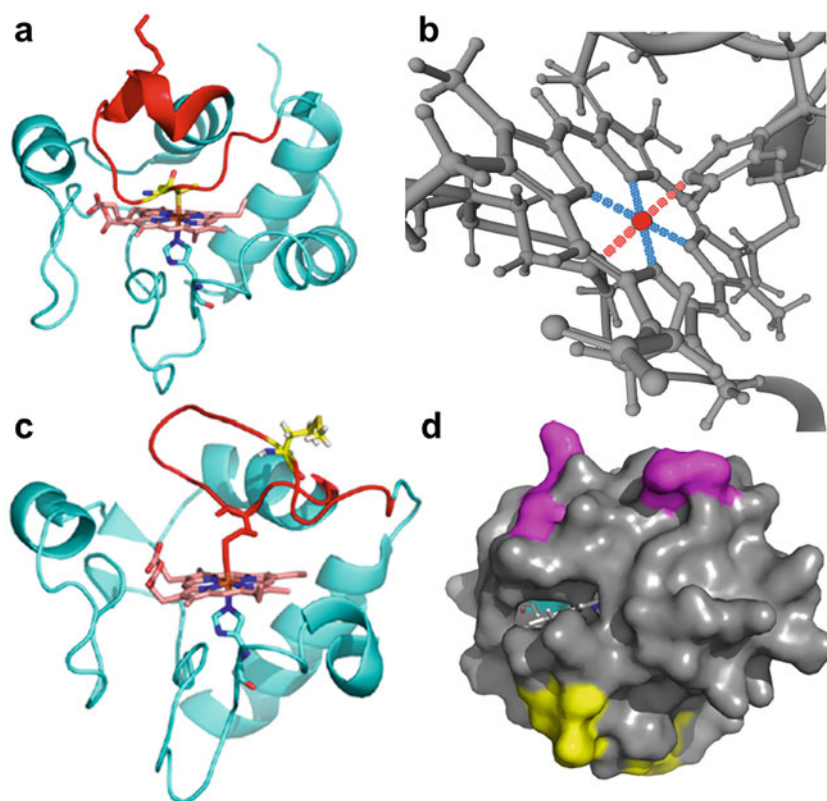
Importantly, all apoptosis triggers stimulate oxidation (peroxidation) of CL (but not other phospholipids present in

mitochondrial membrane), which can be assessed by formation of CL hydroperoxides or radical adducts (Kagan et al. 2005). Moreover, CL peroxidation occurs prior to other major apoptotic events (see Table 14.7) and is insensitive to caspase inhibitors, while CytC release and PS externalization are substantially suppressed by them (Kagan et al. 2005). Thus, CL oxidation is upstream of caspase activation (while other events are downstream of it).

Interestingly, a proapoptotic factor Bid (activated by *caspase 8*, and specifically targeted to mitochondria, where it stimulates CytC release) requires sufficient CL content in the membrane to bind it and is led to mitochondria specifically by their CL compound (Lutter et al. 2000).

At the same time, both CL peroxidation and further apoptotic events require CytC and are proportional to its content (Kagan et al. 2005). Indeed, the CytC knockout cells show no CL peroxidation, and cells with different levels of CytC suppression show proportional decrease of CL peroxidation

Fig. 14.30 Structure of cytochrome c. (a, c) General view: (a) “native” state; (c) “alternative,” partially unfolded state (from (Hannibal et al. 2016)). (b) Heme active center with 6-coordinated Fe (red circle). Blue bonds – with porphyrin ring; red bonds – with His18 and Met80. (d) Surface map, illustrating solvent accessibility: site A – magenta; site L – yellow. (a, c, d – Adapted with permission from (Hannibal et al. 2016). Copyright 2016, American Chemical Society)



and sensitivity to external apoptotic stimuli (e.g., ACD) (Kagan et al. 2005).

Thus, CL peroxidation in mitochondrial membranes, catalyzed by CytC (long before its release to the cytoplasm), is necessary for mitochondrial-type apoptosis and upstream of other major apoptotic processes.

14.5.5.2.3 The Alternative State of CytC

However, the standard (“native”) conformation of CytC has extremely low peroxidase activity, as the heme required for it is tightly embedded in the peptide. Moreover, its Fe atom is six-coordinated, having four bonds with the porphyrin ring and two more with His18 and Met80 of the peptide moiety (Zaidi et al. 2014; Hannibal et al. 2016) (see Fig. 14.30a, b). Thus, it appears practically inaccessible to other molecules, preventing any chemical reactions (but not the standard electron transfer, as it does not require direct contact of the heme Fe with the electron donor or acceptor) (Nantes et al. 1998).

However, addition of CL to CytC dramatically enhances CytC peroxidase activity (Belikova et al. 2006; Vladimirov et al. 2006b; Kagan et al. 2005) and causes generation of protein radicals, typical for the functioning of heme peroxidases (Kagan et al. 2005) (see Sect. 14.5.3). At the same time, it gets more reactive in general (Vladimirov et al. 2006a), showing that the active center becomes more accessible for different small molecules. All this strictly correlates with rupture of the Fe(heme)···S(Met80) bond (estimated by

the absorption band at 695 nm), and turning Fe into a 5-coordinated state (Kagan et al. 2005).

Moreover, breaking the Fe(heme)···S(Met80) bond by other means (addition of negatively-charged phospholipids or detergents, or excess of H₂O₂ – see (Vladimirov et al. 2006a, b)) also increases the CytC peroxidase activity, proportionally to the percentage of broken bonds (Vladimirov et al. 2006a, b). However, this “alternative-state” CytC appears 1 to 2 orders of magnitude less reactive than the real CytC-CL (at equal degree of Fe – S bond rupture) (Vladimirov et al. 2006a, b).

Thus, in CytC-CL, heme Fe is 5-coordinated (similar to that in heme peroxidases) and achievable for small molecules, including H₂O₂. This provides CytC-CL complex with peroxidase activity, which is proportional to the percentage of the broken Fe – S bonds (Vladimirov et al. 2006b), but not fully explained by it. There is an additional effect of binding CL, which dramatically increases CytC reactivity.

Interestingly, the CytC-CL interaction also shifts the CytC redox potential negatively by 350 to 400 mV (Basova et al. 2007), which strongly inhibits the CytC electron-transport capacity. Moreover, unlike the native-state CytC, CytC-CL complex is not efficient in scavenging superoxide anions and is not reduced by ascorbate (Basova et al. 2007).

Thus, formation of CytC-CL is really a major switch in the CytC functioning: from electron transport and antioxidant – to peroxidase and proapoptotic.

14.5.5.2.4 The CytC-CL Complex Structure

As is known, CytC contains four Tyr and one Trp residue. Yet, the native CytC, excited in their absorption bands, does not fluoresce, because their electron excitation is transferred to the closely located heme by the inductive-resonant mechanism (Vladimirov et al. 2013) (see their mutual location in Fig. 14.31a, see also Sect. 5.4). At the same time, CytC, denaturated by guanidine chloride, fluoresces well, because

these residues appear outside the Forster's radius relative to heme, and the excitation is not transferred to it any more.

A similar picture is observed for CytC-CL, in which Trp and three of four Tyr residues exhibit reliable fluorescence, though weaker than in guanidine chloride (Belikova et al. 2006; Vladimirov et al. 2013). These data are also confirmed by circular dichroism, IR spectroscopy, and X-ray scattering of CytC-CL (see (Vladimirov et al. 2013) and refs therein), which altogether clearly shows that CytC as part of the CytC-

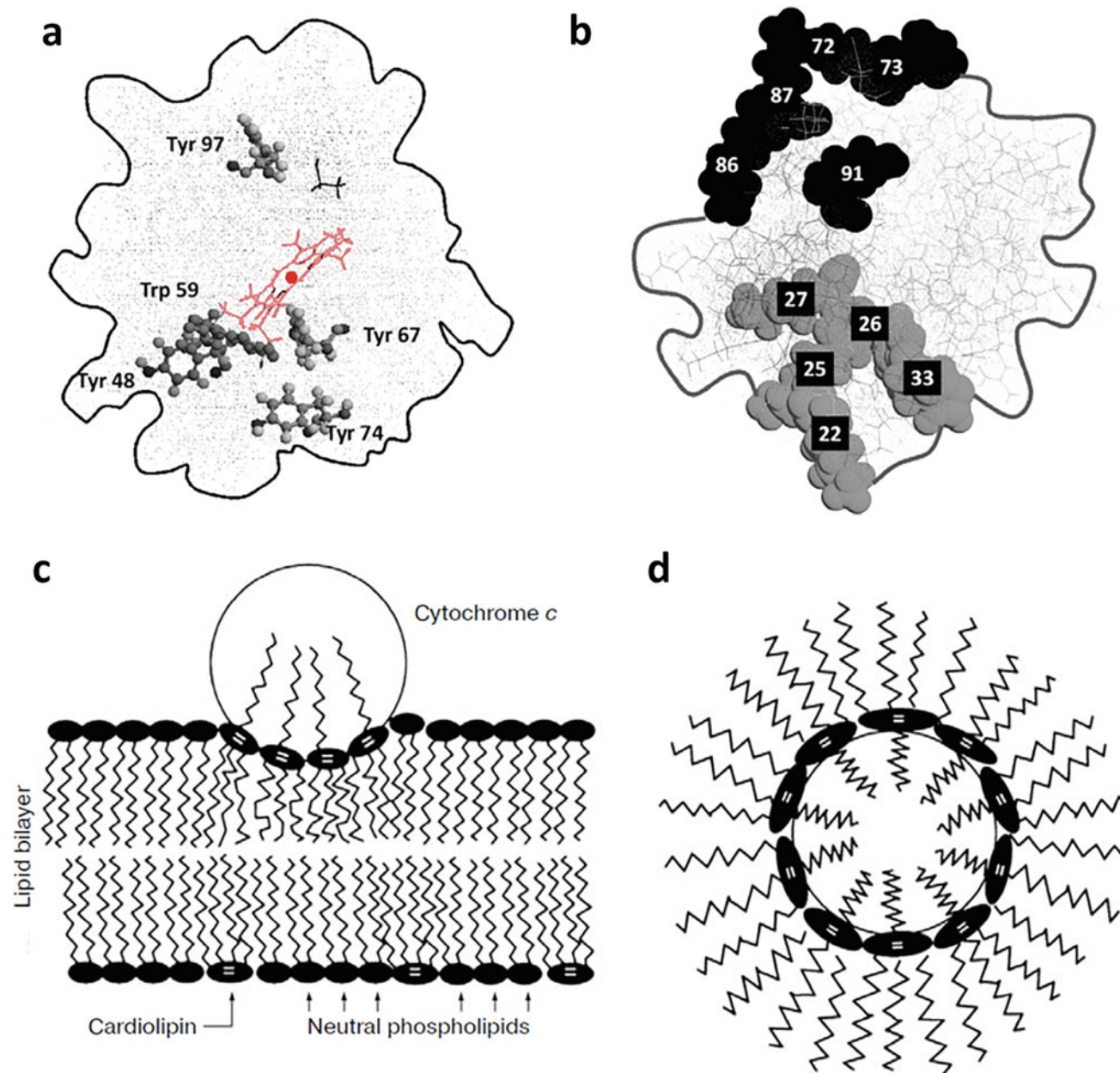


Fig. 14.31 Cytochrome c globule and its interaction with cardiolipin. (a) Location of heme, Tyr and Trp residues in the CytC globule; (b) Positively charged Lys residues in CytC; (c) Attachment of CytC globule to the CL-containing membrane, hydrophobic penetration of

CL chains into the CytC globule; (d) CytC-CL nanocomplex. (Reprinted from (Vladimirov et al. 2013). Copyright 2013, with permission from Springer Nature)

Table 14.8 The main dimensions in the CytC-CL complex (data from Vladimirov et al. (2011, 2019))

| “Native” CytC | TOCL length | CytC-CL globule | TOCL molecules per CytC | The supposed size of the CytC melted globule |
|---------------|-------------|-----------------|-------------------------|--|
| 3–4 nm | 2.8 nm | ~11 nm | 35–40 | ~5.5 nm |
| | | ~8 nm | 13–14 | ? |

CL is partially melted (unfolded) – compare Fig. 14.30a and c.

The exact mechanism of CytC-CL interaction includes several aspects (see reviews (Kagan et al. 2009; Vladimirov et al. 2013)):

1. *Electrostatic attraction.* CytC includes eight positively-charged Lys residues (see Fig. 14.31b), making its general charge +8 at neutral pH and attracting it to the negatively charged CL (Brown and Wuthrich 1977; Tuominen et al. 2002).
2. *Hydrophobic interactions.* As is known, CL consists of the polar head and four apolar fatty acid chains, of which one or two can penetrate the protein globule of CytC when forming the CytC-CL complex (Tuominen et al. 2002; Kalanxhi and Wallace 2007) (see Fig. 14.31c).

Yet, studying CytC-CL is actually complicated by two factors: (1) high heterogeneity and oxidizability of the natural CL, and (2) CL-induced peroxidase activity of CytC. All this makes research on their “natural mixtures” unreliable, which hindered further research progress for a long time (Vladimirov et al. 2013). It was finally overcome by using synthetic nonoxidizable tetraoleoylcardiolipin (TOCL), which forms standard complexes with CytC, but is not further oxidized by them, and, thus, does not interfere with their investigation (Kagan et al. 2005; Vladimirov et al. 2006a, b; Vladimirov et al. 2011).

3. *Nanocrystals.* Unexpectedly, adding TOCL to CytC water solution forms water-insoluble precipitate, with all properties of CytC-CL (Vladimirov et al. 2011). This precipitate has a microcrystal structure, with two crystal types: ~11 nm and ~8 nm in diameter. Only 11 nm crystals are observed at neutral pH (Vladimirov et al. 2011), while both 11 nm and 8 nm crystals can be found under acidic conditions (Vladimirov et al. 2019). These crystals have all the qualities of CytC-CL and contain CytC and CL in a strict proportion: ~35–40:1 for 11 nm crystals (Vladimirov et al. 2011) and ~13–14:1 for 8 nm ones (Vladimirov et al. 2019).

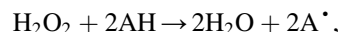
Importantly, the above nanocrystals are hydrophobic and can well penetrate into lipid bilayers (Vikulina et al. 2015; Vladimirov et al. 2017) (see also (Vladimirov et al. 2013)).

Summarizing these data, the authors concluded that CL should wrap the CytC molecule in CytC-CL, with polar heads facing inward and fatty acid tails outward (see Fig. 14.31d), and the exact number of CL molecules sterically determined and depending on chemical groups’ charges – i.e., on pH (Vladimirov et al. 2011). The known dimensions of CytC and TOCL (see Table 14.8), generally allow this model, but require the centrally-located CytC to be swollen by 30–50% in linear dimensions, comparing to its native state (see Table 14.8, the first and the last columns). Needless to say, this is exactly what is known from the above data on its “partially melted state.” Moreover, as apparently each molecule of CL has one of its fatty acid tails penetrating CytC, one can calculate the volume by which the CytC globule must swell while including all these hydrophobic tails. This corresponds to the experimental data quite well (Vladimirov et al. 2013).

Interestingly, with insufficient CL, the excessive CytC remains in the solution in the native state, suggesting that there are no intermediate complexes of CytC with CL (Vladimirov et al. 2011).

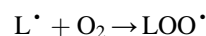
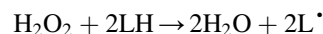
14.5.5.2.5 Lipid Radical Formation by the CytC-CL Complex

As mentioned above, the CytC-CL complex is a good peroxidase, i.e., catalyzes oxidation of various organic compounds by hydrogen peroxide (Belikova et al. 2006). In a simplified form, its reaction scheme is as follows (see more in Sect. 14.5.3):

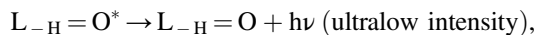


i.e., the first reaction products are free radicals of oxidized substrates.

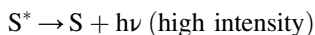
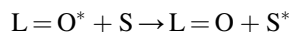
When polyunsaturated fatty acid residues serve as the reaction substrate (LH), alkyl radicals are formed (L^\bullet) and immediately react with molecular oxygen dissolved in the environment:



The appearance of peroxy radicals (LOO^\bullet) in the system can be detected by chemiluminescence during their recombination (see more in Sect. 11.5):

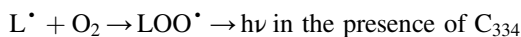
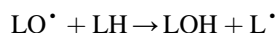
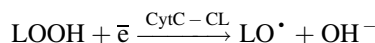


or in the presence of physical CL activators (sensitizers, S – see more in Sect. 8.5 and Chap. 5):



In our studies, we used strong physical activators, namely, isoquinolysine coumarins: C-525 (Vladimirov et al. 1992, 1995, 2000) and C-334 (Vladimirov et al. 2000). With this approach, we managed to show formation of lipid radicals in two reactions, catalyzed by CytC-CL (see Fig. 14.32):

1. Reduction of lipid hydroperoxides (LOOH) contained in natural CL:



2. CL peroxidation (denoted as LH) by H_2O_2 :

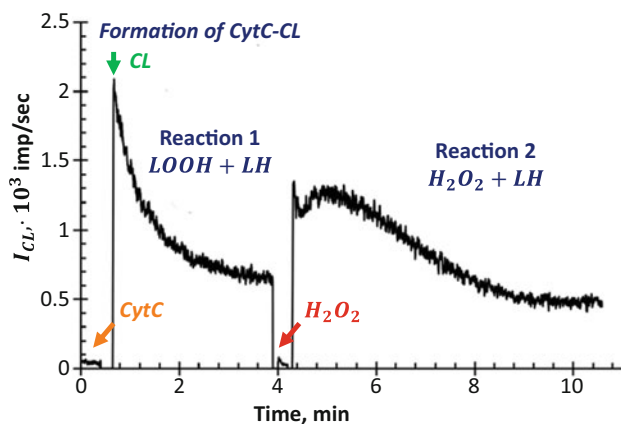
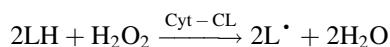
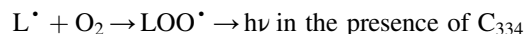


Fig. 14.32 Lipoyxygenase and lipoperoxidase activity of the CytC-CL complex. The chemiluminescence intensity (I_{CL}) reflects the concentration of lipoperoxyl radicals (LOO^{\bullet}) at any given time. The first flash of luminescence is associated with decomposition of the lipid hydroperoxides preexisting in the system (LOOH). The second flash is associated with LOO^{\bullet} formation in the peroxidase reaction ($\text{CL} + \text{H}_2\text{O}_2$), which begins when H_2O_2 is added to the system. (Reprinted from (Vladimirov et al. 2017). Copyright 2017, with permission from Springer Nature)



Interestingly, the initial stages of CytC-induced CL peroxidation (primarily to the general lipid-peroxidation stage) are practically insensitive to standard lipid antioxidants (Kagan et al. 2005), additionally showing that CytC CL peroxidation is not a standard lipid peroxidation (as described in Chap. 11), but a separate process specific for apoptosis.

14.5.5.2.6 CL Peroxidation Causes Membrane Permeabilization

As mentioned above, the peroxidase activity of CytC-CL is a key point in apoptosis triggering and development. The lipid radicals, generated in the membrane by this complex, initiate lipid chain peroxidation, which can even develop explosively in the presence of transition metals (see Sect. 11.4). All this leads to a quick mitochondrial membrane permeabilization, and further mitochondrial swelling (which are known to be important stages of apoptosis).

Interestingly, initially the cause for membrane permeabilization was believed to be Ca^{2+} entry into mitochondria (see review (Crompton 1999)), yet now the lipid-peroxidation mechanism is definitely known to play a leading role (see (Vladimirov et al. 2013, 2017)). Indeed, mitochondrial swelling is both caused by lipid peroxidation and stopped by antioxidants (Hunter et al. 1964; Schneider et al. 1964; Olenov et al. 1976) (see also review (Vladimirov et al. 1980)).

All this is followed by megapore formation, supposedly also caused by lipid peroxidation, and electrical breakdown of the oxidized and permeabilized membrane (see (Vladimirov 2017)). This causes quick release of CytC into the cytoplasm, lasting ~5 min (Goldstein et al. 2000), and leading to other proapoptotic factors release (Kagan et al. 2005) and apoptosome formation (see (Kroemer and Reed 2000)).

Thus, CytC indeed appears a major trigger, switching the cell from normal cell life (with CytC playing electron-transport and antioxidant roles), to apoptosis (with CytC playing the roles of peroxidase, initiator of membrane permeabilization and matrix swelling, and apoptosome formation).

14.5.5.3 Summary

Thus, the CytC-CL complex contains CytC in a specific state, with 5-coordinated Fe, better heme accessibility for small molecules, and partially melted protein globule (also referred to as “nonnative (alternative) conformations of CytC” (Hannibal et al. 2016), or “CytC alkaline transition” (Greenwood and Palmer 1965)). At physiological pH, this CytC globule is surrounded by 35 to 40 cardiolipin

molecules (the number seems exact, the range reflects the uncertainty of our data), with some of their fatty acid chains (supposedly, one per every CL molecule) penetrating the protein globule, which causes its melting. This state of CytC is an active peroxidase, specifically oxidizing the membrane CL (Kagan et al. 2005) and causing membrane permeabilization, matrix swelling, and further exit of Cyt-CL and other important proapoptotic factors. Altogether, this is the key and unavoidable stage of mitochondria-driven apoptosis.

14.6 Summary

Thus, today, the key role in appearance of free radicals in biological systems is attributed not to free iron ions or ionizing radiation (except in cases of severe pathology), but to enzymatic processes directly linked to the generation of free radicals. Moreover, the free radicals, initially considered purely destructive for the cell, associated with exposure to ionizing radiation, ultraviolet radiation or toxic substances, turned out an integral part of their normal functioning (in a way, confirming the old ideas of A.G. Gurwitsch – see Chap. 2). A significant part of the key enzymatic processes involve free-radical stages and are associated with ROS, lipid and protein radicals formation.

Accordingly, biological autoluminescence, arising from recombination of free radicals, turns out to be not only an indicator of destructive processes (which is really so) but also an accompaniment of natural processes. Being largely absorbed in the nearest environment, it is also partially emitted in the outer space, where it can be detected by technical means, and used to analyze the course of intracellular free-radical processes. The method of activated chemiluminescence is a great help in this complicated task.

Moreover, as the free-radical generation and utilization appears scrupulously regulated by lots of enzymes, and consequently so is the UPE, generated by them, one can fantasize the old Gurwitsch's hypothesis of the UPE signaling role (see Chap. 2) to be not that impossible, as it seemed two decades ago.

However, free-radical processes, being chain and, in particular, branched chain (primarily due to the decomposition of hydroperoxides generated as a “byproduct” during the chain development), carry a great potential danger. A branched chain process out of control can lead to massive oxidation of membrane lipids, disruption of their structure and function, and, as a result, cell death and development of severe body pathology. In this sense, the “use” of free-radical processes by the cell resembles the use of nuclear power plants by humans: the enormous possibilities and colossal efficiency of the processes are associated with no less colossal risks if they get out of control.

References

- Afanas'ev I (2015) Mechanisms of superoxide signaling in epigenetic processes: relation to aging and cancer. *Aging and disease* 6 (3): 216–227. doi:<https://doi.org/10.14336/AD.2014.0924>
- Aguirre J, Lambeth JD (2010) Nox enzymes from fungus to fly to fish and what they tell us about Nox function in mammals. *Free Radical Bio Med* 49 (9):1342–1353. doi:<https://doi.org/10.1016/j.freeradbiomed.2010.07.027>
- Alberts B, Johnson AD, Lewis J, Morgan D, Raff M, Roberts K, Walter P (2015) *Molecular Biology of the Cell*. 6th Edition. Garland Science, Taylor and Francis Group, New York
- Alderman CJ, Shah S, Foreman JC, Chain BM, Katz DR (2002) The role of advanced oxidation protein products in regulation of dendritic cell function. *Free radical biology & medicine* 32 (5):377–385
- Allen RC, Dale DC, Taylor FB (2000) Blood phagocyte luminescence: gauging systemic immune activation. In: *Methods in Enzymology*, vol 305. Academic Press, pp 591–629. doi:[https://doi.org/10.1016/S0076-6879\(00\)05515-4](https://doi.org/10.1016/S0076-6879(00)05515-4)
- Allen RC, Stjernholm RL, Steele RH (1972) Evidence for the generation of an electronic excitation state(s) in human polymorphonuclear leukocytes and its participation in bacterial activity. *Biochem Biophys Res Commun* 47:679–684
- Antunes F, Cadenas E (2001) Cellular titration of apoptosis with steady state concentrations of H(2)O(2): submicromolar levels of H(2)O(2) induce apoptosis through Fenton chemistry independent of the cellular thiol state. *Free radical biology & medicine* 30 (9): 1008–1018. doi:[https://doi.org/10.1016/s0891-5849\(01\)00493-2](https://doi.org/10.1016/s0891-5849(01)00493-2)
- Archibald FS, Fridovich I (1981) Manganese and Defenses against Oxygen Toxicity in *Lactobacillus plantarum*. *Journal of bacteriology* 145 (1):442451
- Arnao MB, Acosta M, del Rio JA, Varón R, García-Cánovas F (1990) A kinetic study on the suicide inactivation of peroxidase by hydrogen peroxide. *Biochimica et Biophysica Acta (BBA) - Protein Structure and Molecular Enzymology* 1041 (1):43–47. doi:[https://doi.org/10.1016/0167-4838\(90\)90120-5](https://doi.org/10.1016/0167-4838(90)90120-5)
- Arrigoni-Martelli E (1985) Pharmacology of free radical scavenging in inflammation. *Int J Tissue React* 7 (6):513–519
- Babior BM (1978) Oxygen-Dependent Microbial Killing by Phagocytes. *New England Journal of Medicine* 298 (12): 659–668. doi:<https://doi.org/10.1056/NEJM197803232981205>
- Babior BM (1984) The respiratory burst of phagocytes. *J Clin Invest* 73 (3):599–601. doi:<https://doi.org/10.1172/JCI111249>
- Babior BM, Kipnes RS, Curnutte JT (1973) Biological defense mechanisms. The production by leukocytes of superoxide, a potential bactericidal agent. *J Clin Invest* 52 (3):741–744. doi:<https://doi.org/10.1172/jci107236>
- Badran A, Nasser SA, Mesmar J, El-Yazbi AF, Bitto A, Fardoun MM, Baydoun E, Eid AH (2020) Reactive Oxygen Species: Modulators of Phenotypic Switch of Vascular Smooth Muscle Cells. 21 (22):8764
- Bae YS, Oh H, Rhee SG, Yoo YD (2011) Regulation of reactive oxygen species generation in cell signaling. *Mol Cells* 32 (6):491–509. doi:<https://doi.org/10.1007/s10059-011-0276-3>
- Baehner RL, Murrmann SK, Davis J, Johnston RB, Jr. (1975) The role of superoxide anion and hydrogen peroxide in phagocytosis-associated oxidative metabolic reactions. *J Clin Invest* 56 (3): 571–576. doi:<https://doi.org/10.1172/JCI108126>
- Baldrige CW, Gerard RW (1932) The extra respiration of phagocytosis. *American Journal of Physiology-Legacy Content* 103 (1): 235–236. doi:<https://doi.org/10.1152/ajplegacy.1932.103.1.235>
- Barnard ML, Gurdian S, Diep D, Ladd M, Turrens JF (1993) Protein and amino acid oxidation is associated with increased chemiluminescence. *Archives of biochemistry and biophysics* 300 (2): 651–656. doi:<https://doi.org/10.1006/abbi.1993.1090>

- Basova LV, Kurnikov IV, Wang L, Ritov VB, Belikova NA, Vlasova, II, Pacheco AA, Winnica DE, Peterson J, Bayir H, Waldeck DH, Kagan VE (2007) Cardiolipin switch in mitochondria: shutting off the reduction of cytochrome c and turning on the peroxidase activity. *Biochemistry* 46 (11):3423–3434. doi:<https://doi.org/10.1021/bi061854k>
- Battelli MG, Polito L, Bortolotti M, Bolognesi A (2016) Xanthine Oxidoreductase-Derived Reactive Species: Physiological and Pathological Effects. *Oxidative medicine and cellular longevity* 2016: 3527579. doi:<https://doi.org/10.1155/2016/3527579>
- Beaman BL, Black CM, Doughty F, Beaman L (1985) Role of superoxide dismutase and catalase as determinants of pathogenicity of *Nocardia asteroides*: importance in resistance to microbicidal activities of human polymorphonuclear neutrophils. *Infect Immun* 47 (1):135–141. doi:<https://doi.org/10.1128/iai.47.1.135-141.1985>
- Beckman JS, Beckman TW, Chen J, Marshall PA, Freeman BA (1990) Apparent hydroxyl radical production by peroxynitrite: implications for endothelial injury from nitric oxide and superoxide. *Proceedings of the National Academy of Sciences of the United States of America* 87 (4):1620–1624. doi:<https://doi.org/10.1073/pnas.87.4.1620>
- Beckman KB, Ames BN (1998) The free radical theory of aging matures. *Physiol Rev* 78 (2):547–581
- Bedard K, Krause KH (2007) The NOX family of ROS-generating NADPH oxidases: physiology and pathophysiology. *Physiol Rev* 87 (1):245–313. doi:<https://doi.org/10.1152/physrev.00044.2005>
- Belambri SA, Rolas L, Raad H, Hurtado-Nedelec M, Dang PM-C, El-Benna J (2018) NADPH oxidase activation in neutrophils: Role of the phosphorylation of its subunits. *Eur J Clin Invest* 48 (S2): e12951. doi:<https://doi.org/10.1111/eci.12951>
- Belikova NA, Vladimirov YA, Osipov AN, Kapralov AA, Tyurin VA, Potapovich MV, Basova LV, Peterson J, Kurnikov IV, Kagan VE (2006) Peroxidase activity and structural transitions of cytochrome c bound to cardiolipin-containing membranes. *Biochemistry* 45 (15): 4998–5009. doi:<https://doi.org/10.1021/bi0525573>
- Berglund GI, Carlsson GH, Smith AT, Szöke H, Henriksen A, Hajdu J (2002) The catalytic pathway of horseradish peroxidase at high resolution. *Nature* 417 (6887):463–468. doi:<https://doi.org/10.1038/417463a>
- Berry CE, Hare JM (2004) Xanthine oxidoreductase and cardiovascular disease: molecular mechanisms and pathophysiological implications (Topical review). *The Journal of physiology* 555.3:589–606. doi:<https://doi.org/10.1113/jphysiol.2003.055913>
- Bienert GP, Moller AL, Kristiansen KA, Schulz A, Moller IM, Schjoerring JK, Jahn TP (2007) Specific aquaporins facilitate the diffusion of hydrogen peroxide across membranes. *The Journal of biological chemistry* 282 (2):1183–1192. doi:<https://doi.org/10.1074/jbc.M603761200>
- Biles CL, Martyn RD (1993) Peroxidase, polyphenoloxidase and shikimate dehydrogenase isozymes in relation to the tissue type, maturity and pathogen induction of watermelon seedlings. *Plant Physiol Bioch* 31:499–506
- Bleier L, Wittig I, Heide H, Steger M, Brandt U, Drose S (2015) Generator-specific targets of mitochondrial reactive oxygen species. *Free radical biology & medicine* 78:1–10. doi:<https://doi.org/10.1016/j.freeradbiomed.2014.10.511>
- Bortolotti M, Polito L, Battelli MG, Bolognesi A (2021) Xanthine oxidoreductase: One enzyme for multiple physiological tasks. *Redox biology* 41:101882. doi:<https://doi.org/10.1016/j.redox.2021.101882>
- Boveris A, Cadenas E (1975) Mitochondrial production of superoxide anions and its relationship to the antimycin insensitive respiration. *Febs Lett* 54 (3):311–314. doi:[https://doi.org/10.1016/0014-5793\(75\)80928-8](https://doi.org/10.1016/0014-5793(75)80928-8)
- Boveris A, Cadenas E (2000) Mitochondrial production of hydrogen peroxide regulation by nitric oxide and the role of ubiquinone. *IUBMB life* 50 (4-5):245–250. doi:<https://doi.org/10.1080/713803732>
- Boveris A, Chance B (1973) The mitochondrial generation of hydrogen peroxide. General properties and effect of hyperbaric oxygen. *The Biochemical journal* 134 (3):707–716
- Boyd CS, Cadenas E (2002) Nitric oxide and cell signaling pathways in mitochondrial-dependent apoptosis. *Biol Chem* 383 (3-4): 411–423. doi:<https://doi.org/10.1515/bc.2002.045>
- Brand MD (2016) Mitochondrial generation of superoxide and hydrogen peroxide as the source of mitochondrial redox signaling. *Free radical biology & medicine* 100:14–31. doi:<https://doi.org/10.1016/j.freeradbiomed.2016.04.001>
- Brand MD, Nicholls DG (2011) Assessing mitochondrial dysfunction in cells. *The Biochemical journal* 435 (2):297–312. doi:<https://doi.org/10.1042/BJ20110162>
- Brenot A, King KY, Janowiak B, Griffith O, Caparon MG (2004) Contribution of glutathione peroxidase to the virulence of *Streptococcus pyogenes*. *Infect Immun* 72 (1):408–413. doi:<https://doi.org/10.1128/IAI.72.1.408-413.2004>
- Briheim G, Stendahl O, Dahlgren C (1984) Intra- and extracellular events in luminol-dependent chemiluminescence of polymorphonuclear leukocytes. *Infect Immun* 45 (1):1–5
- Brown DI, Griendling KK (2009) Nox proteins in signal transduction. *Free Radical Bio Med* 47 (9):1239–1253. doi:<https://doi.org/10.1016/j.freeradbiomed.2009.07.023>
- Brown LR, Wuthrich K (1977) NMR and ESR studies of the interactions of cytochrome c with mixed cardiolipin-phosphatidylcholine vesicles. *Biochimica et biophysica acta* 468 (3):389–410
- Brzezinski P, Moe A, Ädelroth P (2021) Structure and Mechanism of Respiratory III–IV Supercomplexes in Bioenergetic Membranes. *Chemical reviews* 121 (15):9644–9673. doi:<https://doi.org/10.1021/acs.chemrev.1c00140>
- Bulua AC, Simon A, Maddipati R, Pelletier M, Park H, Kim KY, Sack MN, Kastner DL, Siegel RM (2011) Mitochondrial reactive oxygen species promote production of proinflammatory cytokines and are elevated in TNFR1-associated periodic syndrome (TRAPS). *J Exp Med* 208 (3):519–533. doi:<https://doi.org/10.1084/jem.20102049>
- Bushnell GW, Louie GV, Brayer GD (1990) High-resolution three-dimensional structure of horse heart cytochrome c. *Journal of molecular biology* 214 (2):585–595
- Butler A (1998) Vanadium haloperoxidases. *Current Opinion in Chemical Biology* 2 (2):279–285
- Butler A (1999) Mechanistic considerations of the vanadium haloperoxidases. *Coordination Chemistry Reviews* 187 (1): 17–35. doi:[https://doi.org/10.1016/S0010-8545\(99\)00033-8](https://doi.org/10.1016/S0010-8545(99)00033-8)
- Cadenas E (1984) Biological chemiluminescence. *Photochem Photobiol* 40 (6):823–830. doi:<https://doi.org/10.1111/j.1751-1097.1984.tb04657.x>
- Cadenas E (2004) Mitochondrial free radical production and cell signaling. *Mol Aspects Med* 25 (1-2):17–26. doi:<https://doi.org/10.1016/j.mam.2004.02.005>
- Cadenas E, Boveris A, Ragan CI, Stoppani AO (1977) Production of superoxide radicals and hydrogen peroxide by NADH-ubiquinone reductase and ubiquinol-cytochrome c reductase from beef-heart mitochondria. *Archives of biochemistry and biophysics* 180 (2): 248–257
- Cadenas E, Wefers H, Sies H (1981) Low-Level Chemiluminescence of Isolated Hepatocytes. *Eur J Biochem* 119 (3):531–536. doi:<https://doi.org/10.1111/j.1432-1033.1981.tb05640.x>
- Cardoso AR, Chausse B, da Cunha FM, Luévano-Martínez LA, Marazzi TBM, Pessoa PS, Queliconi BB, Kowaltowski AJ (2012) Mitochondrial compartmentalization of redox processes. *Free Radical Bio Med* 52 (11):2201–2208. doi:<https://doi.org/10.1016/j.freeradbiomed.2012.03.008>

- Carpena X, Soriano M, Klotz MG, Duckworth HW, Donald LJ, Melik-Adamyany W, Fita I, Loewen PC (2003) Structure of the Clade 1 catalase, CatF of *Pseudomonas syringae*, at 1.8 Å resolution. *Proteins: Structure, Function, and Bioinformatics* 50 (3): 423–436. doi:<https://doi.org/10.1002/prot.10284>
- Carreras MC, Pargament GA, Catz SD, Poderoso JJ, Boveris A (1994) Kinetics of nitric oxide and hydrogen peroxide production and formation of peroxynitrite during the respiratory burst of human neutrophils. *Febs Lett* 341 (1):65–68. doi:[https://doi.org/10.1016/0014-5793\(94\)80241-6](https://doi.org/10.1016/0014-5793(94)80241-6)
- Cathcart MK (2004) Regulation of superoxide anion production by NADPH oxidase in monocytes/macrophages: contributions to atherosclerosis. *Arterioscler Thromb Vasc Biol* 24 (1):23–28. doi:<https://doi.org/10.1161/01.ATV.0000097769.47306.12>
- Chance B (1952) Oxidase and peroxidase reactions in the presence of dihydroxymaleic acid. *The Journal of biological chemistry* 197 (2): 577–589
- Chance B, Oshino N (1971) Kinetics and mechanisms of catalase in peroxisomes of the mitochondrial fraction. *The Biochemical journal* 122 (2):225–233. doi:<https://doi.org/10.1042/bj1220225>
- Chance B, Sies H, Boveris A (1979) Hydroperoxide metabolism in mammalian organs. *Physiol Rev* 59 (3):527–605.
- Chance B, Williams GR (1955) A Method for the Localization of Sites for Oxidative Phosphorylation. *Nature* 176 (4475):250–254. doi:<https://doi.org/10.1038/176250a0>
- Chelikani P, Fita I, Loewen PC (2004) Diversity of structures and properties among catalases. *Cellular and Molecular Life Sciences CMLS* 61 (2):192–208. doi:<https://doi.org/10.1007/s00018-003-3206-5>
- Chen IS, Huang SP, Jang-Liaw NH, Shen CN, Wu JH (2008) Molecular Evidence for Genetic Differentiation of the Opsariichthys Bidens Complex (Teleostei: Cyprinidae) in Southern China around South China Sea and the Validity of Opsariichthys Hainanensis. *Raffles B Zool*:215–223
- Choi HJ, Kang SW, Yang CH, Rhee SG, Ryu SE (1998) Crystal structure of a novel human peroxidase enzyme at 2.0 Å resolution. *Nature structural biology* 5 (5):400–406. doi:<https://doi.org/10.1038/nsb0598-400>
- Christman MF, Morgan RW, Jacobson FS, Ames BN (1985) Positive control of a regulon for defenses against oxidative stress and some heat-shock proteins in *Salmonella typhimurium*. *Cell* 41 (3): 753–762. doi:[https://doi.org/10.1016/s0092-8674\(85\)80056-8](https://doi.org/10.1016/s0092-8674(85)80056-8)
- Cree IA (1998) Phagocyte chemiluminescence. *Methods Mol Biol* 102: 179–187. doi:<https://doi.org/10.1385/0-89603-520-4:179>
- Crompton M (1999) The mitochondrial permeability transition pore and its role in cell death. *The Biochemical journal* 341 (Pt 2):233–249
- Cross CE, Halliwell B, Borish ET, Pryor WA, Ames BN, Saul RL, McCord JM, Harman D (1987) Oxygen radicals and human disease. *Annals of internal medicine* 107 (4):526–545. doi:<https://doi.org/10.7326/0003-4819-107-4-526>
- Dahlgren C, Karlsson A (1999) Respiratory burst in human neutrophils. *J Immunol Methods* 232 (1):3–14. doi:[https://doi.org/10.1016/S0022-1759\(99\)00146-5](https://doi.org/10.1016/S0022-1759(99)00146-5)
- de Oliveira FK, Santos LO, Buffon JG (2021) Mechanism of action, sources, and application of peroxidases. *Food Res Int* 143: 110266. doi:<https://doi.org/10.1016/j.foodres.2021.110266>
- Del Prete A, Zaccagnino P, Di Paola M, Saltarella M, Oliveros Celis C, Nico B, Santoro G, Lorusso M (2008) Role of mitochondria and reactive oxygen species in dendritic cell differentiation and functions. *Free radical biology & medicine* 44 (7):1443–1451. doi:<https://doi.org/10.1016/j.freeradbiomed.2007.12.037>
- Devary Y, Gottlieb RA, Smeal T, Karin M (1992) The mammalian ultraviolet response is triggered by activation of Src tyrosine kinases. *Cell* 71 (7):1081–1091. doi:[https://doi.org/10.1016/s0092-8674\(05\)80058-3](https://doi.org/10.1016/s0092-8674(05)80058-3)
- Di Meo S, Reed TT, Venditti P, Victor VM (2016) Role of ROS and RNS Sources in Physiological and Pathological Conditions. *Oxidative medicine and cellular longevity* 2016:1245049. doi:<https://doi.org/10.1155/2016/1245049>
- Drath DB, Karnovsky ML (1975) Superoxide production by phagocytic leukocytes. *J Exp Med* 141 (1):257–262. doi:<https://doi.org/10.1084/jem.141.1.257>
- Dröge W (2002) Free Radicals in the Physiological Control of Cell Function. *82* (1):47–95. doi:<https://doi.org/10.1152/physrev.00018.2001>
- Dubreuil MM, Morgens DW, Okumoto K, Honsho M, Contrepolis K, Lee-McMullen B, Traber GM, Sood RS, Dixon SJ, Snyder MP, Fujiki Y, Bassik MC (2020) Systematic Identification of Regulators of Oxidative Stress Reveals Non-canonical Roles for Peroxisomal Import and the Pentose Phosphate Pathway. *Cell reports* 30 (5): 1417–1433 e1417. doi:<https://doi.org/10.1016/j.celrep.2020.01.013>
- Dukan S, Nyström T (1999) Oxidative Stress Defense and Deterioration of Growth-arrested *Escherichia coli* Cells. *Journal of Biological Chemistry* 274 (37):26027–26032. doi:<https://doi.org/10.1074/jbc.274.37.26027>
- Duwe AK, Roder JC (1984) Involvement of hydroxyl free radical, but not superoxide, in the cytolytic pathway of natural killer cells. Revision of an earlier hypothesis. *Medical biology* 62 (2):95–100
- Duwe AK, Werkmeister J, Roder JC, Lauzon R, Payne U (1985) Natural killer cell-mediated lysis involves a hydroxyl radical-dependent step. *The Journal of Immunology* 134 (4):2637
- Elchuri S, Oberley TD, Qi W, Eisenstein RS, Jackson Roberts L, Van Remmen H, Epstein CJ, Huang T-T (2005) CuZnSOD deficiency leads to persistent and widespread oxidative damage and hepatocarcinogenesis later in life. *Oncogene* 24 (3):367–380. doi:<https://doi.org/10.1038/sj.onc.1208207>
- Elmore S (2007) Apoptosis: a review of programmed cell death. *Toxicol Pathol* 35 (4):495–516. doi:<https://doi.org/10.1080/01926230701320337>
- Enroth C, Eger BT, Okamoto K, Nishino T, Nishino T, Pai EF (2000) Crystal structures of bovine milk xanthine dehydrogenase and xanthine oxidase: Structure-based mechanism of conversion. *PNAS* 97 (20):10723–10728
- Farr SB, D'Ari R, Touati D (1986) Oxygen-dependent mutagenesis in *Escherichia coli* lacking superoxide dismutase. *Proceedings of the National Academy of Sciences of the United States of America* 83 (21):8268–8272. doi:<https://doi.org/10.1073/pnas.83.21.8268>
- Filice GA, Beaman BL, Krick JA, Remington JS (1980) Effects of human neutrophils and monocytes on *Nocardia asteroides*: failure of killing despite occurrence of the oxidative metabolic burst. *J Infect Dis* 142 (3):432–438. doi:<https://doi.org/10.1093/infdis/142.3.432>
- Finkel T (2011) Signal transduction by reactive oxygen species. *J Cell Biol* 194 (1):7–15. doi:<https://doi.org/10.1083/jcb.201102095>
- Flohe L, Ursini F (2008) Peroxidase: a term of many meanings. *Antioxid Redox Signal* 10 (9):1485–1490. doi:<https://doi.org/10.1089/ars.2008.2059>
- Fomenko DE, Xing W, Adair BM, Thomas DJ, Gladyshev VN (2007) High-throughput identification of catalytic redox-active cysteine residues. *Science* 315 (5810):387–389. doi:<https://doi.org/10.1126/science.1133114>
- Foreman J, Demidchik V, Bothwell JH, Mylona P, Miedema H, Torres MA, Linstead P, Costa S, Brownlee C, Jones JD, Davies JM, Dolan L (2003) Reactive oxygen species produced by NADPH oxidase regulate plant cell growth. *Nature* 422 (6930):442–446. doi:<https://doi.org/10.1038/nature01485>
- Forrester SJ, Kikuchi DS, Hernandez MS, Xu Q, Griendling KK (2018) Reactive Oxygen Species in Metabolic and Inflammatory Signaling. *Circulation research* 122 (6):877–902. doi:<https://doi.org/10.1161/CIRCRESAHA.117.311401>

- Fridovich I (1975) Superoxide Dismutases. *Annual Review of Biochemistry* 44 (1):147–159. doi:<https://doi.org/10.1146/annurev.bi.44.070175.001051>
- Fridovich I (1995) Superoxide radical and superoxide dismutases. *Annual Review of Biochemistry* 64 (1):97–112. doi:<https://doi.org/10.1146/annurev.bi.64.070195.000525>
- Fry SC (1987) Formation of Isodityrosine by Peroxidase Isozymes. *J Exp Bot* 38 (5):853–862. doi:<https://doi.org/10.1093/jxb/38.5.853> % J Journal of Experimental Botany
- Fujiki Y, Bassik MC (2021) A New Paradigm in Catalase Research. *Trends Cell Biol* 31 (3):148–151. doi:<https://doi.org/10.1016/j.tcb.2020.12.006>
- Fujiki Y, Fowler S, Shio H, Hubbard AL, Lazarow PB (1982) Polypeptide and phospholipid composition of the membrane of rat liver peroxisomes: comparison with endoplasmic reticulum and mitochondrial membranes. *J Cell Biol* 93 (1):103–110. doi:<https://doi.org/10.1083/jcb.93.1.103>
- Fukai T, Ushio-Fukai M (2020) Cross-Talk between NADPH Oxidase and Mitochondria: Role in ROS Signaling and Angiogenesis. 9 (8): 1849
- Furtmuller PG, Jantschko W, Zederbauer M, Jakopitsch C, Arnhold J, Obinger C (2004) Kinetics of interconversion of redox intermediates of lactoperoxidase, eosinophil peroxidase and myeloperoxidase. *Jpn J Infect Dis* 57 (5):S30–31
- George J, Struthers AD (2009) Role of urate, xanthine oxidase and the effects of allopurinol in vascular oxidative stress. *Vasc Health Risk Manag* 5 (1):265–272
- Giardino G, Cicalese MP, Delmonte O, Migliavacca M, Palterer B, Loffredo L, Cirillo E, Gallo V, Violi F, Pignata C (2017) NADPH Oxidase Deficiency: A Multisystem Approach. *Oxidative medicine and cellular longevity* 2017:4590127. doi:<https://doi.org/10.1155/2017/4590127>
- Gibboney JJ, Haak RA, Kleinhans FW, Brahmī Z (1988) Electron Spin Resonance Spectroscopy Does Not Reveal Hydroxyl Radical Production in Activated Natural Killer Lymphocytes. *Journal of Leukocyte Biology* 44 (6):545–550. doi:<https://doi.org/10.1002/jlb.44.6.545>
- Gill PS, Wilcox CS (2006) NADPH oxidases in the kidney. *Antioxid Redox Signal* 8 (9-10):1597–1607. doi:<https://doi.org/10.1089/ars.2006.8.1597>
- Girón-Calle J, Forman HJ (2000) Phospholipase D and priming of the respiratory burst by H₂O₂ in NR8383 alveolar macrophages. *Am J Respir Cell Mol Biol* 23 (6):748–754. doi:<https://doi.org/10.1165/ajrcmb.23.6.4227>
- Godoy LC, Munoz-Pinedo C, Castro L, Cardaci S, Schonhoff CM, King M, Tortora V, Marin M, Miao Q, Jiang JF, Kapralov A, Jemmerson R, Silkstone GG, Patel JN, Evans JE, Wilson MT, Green DR, Kagan VE, Radi R, Mannick JB (2009) Disruption of the M80-Fe ligation stimulates the translocation of cytochrome c to the cytoplasm and nucleus in nonapoptotic cells. *Proceedings of the National Academy of Sciences of the United States of America* 106 (8):2653–2658. doi:<https://doi.org/10.1073/pnas.0809279106>
- Goldstein IM, Roos D, Kaplan HB, Weissmann G (1975) Complement and immunoglobulins stimulate superoxide production by human leukocytes independently of phagocytosis. *J Clin Invest* 56 (5): 1155–1163. doi:<https://doi.org/10.1172/JCI108191>
- Goldstein JC, Waterhouse NJ, Juin P, Evan GI, Green DR (2000) The coordinate release of cytochrome c during apoptosis is rapid, complete and kinetically invariant. *Nat Cell Biol* 2 (3):156–162. doi:<https://doi.org/10.1038/35004029>
- Goncalves RL, Quinlan CL, Pervoshchikova IV, Hey-Mogensen M, Brand MD (2015) Sites of superoxide and hydrogen peroxide production by muscle mitochondria assessed ex vivo under conditions mimicking rest and exercise. *The Journal of biological chemistry* 290 (1):209–227. doi:<https://doi.org/10.1074/jbc.M114.619072>
- Green DR, Kroemer G (2004) The pathophysiology of mitochondrial cell death. *Science* 305 (5684):626–629. doi:<https://doi.org/10.1126/science.1099320>
- Greenwood C, Palmer G (1965) Evidence for the Existence of Two Functionally Distinct Forms of Cytochrome c Monomer at Alkaline pH. *Journal of Biological Chemistry* 240 (9):3660–3663. doi:[https://doi.org/10.1016/s0021-9258\(18\)97195-4](https://doi.org/10.1016/s0021-9258(18)97195-4)
- Gu Y, Xu Y, Law B, Qian SY (2013) The first characterization of free radicals formed from cellular COX-catalyzed peroxidation. *Free radical biology & medicine* 57:49–60. doi:<https://doi.org/10.1016/j.freeradbiomed.2012.12.004>
- Gurney ME, Pu H, Chiu AY, Dal Canto MC, Polchow CY, Alexander DD, Caliendo J, Hentati A, Kwon YW, Deng H-X, Chen W, Zhai P, Sufit RL, Siddique T (1994) Motor Neuron Degeneration in Mice that Express a Human Cu,Zn Superoxide Dismutase Mutation. 264 (5166):1772–1775. doi:<https://doi.org/10.1126/science.8209258>
- Ha EM, Oh CT, Bae YS, Lee WJ (2005) A direct role for dual oxidase in *Drosophila* gut immunity. *Science* 310 (5749):847–850. doi:<https://doi.org/10.1126/science.1117311>
- Hajjar C, Cherrier MV, Mirandela GD, Petit-Hartlein I, Stasia MJ, Fontecilla-Camps JC, Fieschi F, Dupuy J (2017) The NOX Family of Proteins Is Also Present in Bacteria. 8 (6):e01487–01417. doi:<https://doi.org/10.1128/mBio.01487-17>
- Han JY, Miura S, Akiba Y, Higuchi H, Kato S, Suzuki H, Yokoyama H, Ishii H (2001) Chronic ethanol consumption exacerbates microcirculatory damage in rat mesentery after reperfusion. *American journal of physiology Gastrointestinal and liver physiology* 280 (5): G939–948
- Hannibal L, Tomasina F, Capdevila DA, Demicheli V, Tórtora V, Alvarez-Paggi D, Jemmerson R, Murgida DH, Radi R (2016) Alternative Conformations of Cytochrome c: Structure, Function, and Detection. *Biochemistry* 55:407–428. doi:<https://doi.org/10.1021/acs.biochem.5b01385>
- Harman D (1956) Aging: a theory based on free radical and radiation chemistry. *J Gerontol* 11 (3):298–300. doi:<https://doi.org/10.1093/geronj/11.3.298>
- Harman D (1981) The aging process. *Proceedings of the National Academy of Sciences of the United States of America* 78 (11): 7124–7128. doi:<https://doi.org/10.1073/pnas.78.11.7124>
- Harris CM, Massey V (1997) The reaction of reduced xanthine dehydrogenase with molecular oxygen. Reaction kinetics and measurement of superoxide radical. *Journal of Biological Chemistry* 272: 8370–8379. doi:<https://doi.org/10.1074/jbc.272.13.8370>
- Harrison R (2002) Structure and function of xanthine oxidoreductase: Where are we now? *Free radical biology & medicine* 33 (6):774–797
- Harrison R (2004) Physiological Roles of Xanthine Oxidoreductase. *Drug Metab Rev* 36 (2):363–375. doi:<https://doi.org/10.1081/DMR-120037569>
- Hatefi Y, Haavik AG, Fowler LR, Griffiths DE (1962) Studies on the electron transfer system. XLII. Reconstitution of the electron transfer system. *The Journal of biological chemistry* 237:2661–2669
- Heck DE, Shakarjian M, Kim HD, Laskin JD, Vetrano AM (2010) Mechanisms of oxidant generation by catalase. *Annals of the New York Academy of Sciences* 1203:120–125. doi:<https://doi.org/10.1111/j.1749-6632.2010.05603.x>
- Heck DE, Vetrano AM, Mariano TM, Laskin JD (2003) UVB Light Stimulates Production of Reactive Oxygen Species: Unexpected Role For Catalase. *Journal of Biological Chemistry* 278 (25): 22432–22436. doi:<https://doi.org/10.1074/jbc.C300048200>
- Helfinger V, von Gall FF, Henke N, Kunze MM, Schmid T, Heidler J, Wittig I, Radeke HH, Marschall V, Anderson K, Shah AM, Fulda S, Brüne B, Brandes RP, Schröder K (2017) Hydrogen peroxide formation by Nox4 limits malignant transformation. bioRxiv:177055. doi:<https://doi.org/10.1101/177055>

- Hiraishi H, Terano A, Razandi M, Sugimoto T, Harada T, Ivey KJ (1992) Role of cellular superoxide dismutase against reactive oxygen metabolite injury in cultured bovine aortic endothelial cells. *The Journal of biological chemistry* 267 (21):14812–14817
- Hirata F, Hayaishi O (1971) Possible Participation of Superoxide Anion in the Intestinal Tryptophan 2,3-Dioxygenase Reaction. *Journal of Biological Chemistry* 246 (24):7825–7826. doi:[https://doi.org/10.1016/S0021-9258\(19\)45852-3](https://doi.org/10.1016/S0021-9258(19)45852-3)
- Hosoi KI, Miyata N, Mukai S, Furuki S, Okumoto K, Cheng EH, Fujiki Y (2017) The VDAC2-BAK axis regulates peroxisomal membrane permeability. *J Cell Biol* 216 (3):709–722. doi:<https://doi.org/10.1083/jcb.201605002>
- Huie REP, S. (1993) The reaction rate of nitric oxide with superoxide. *Free radical research* 18:195–199. doi:<https://doi.org/10.3109/10715769309145868>
- Hunter FE, Jr., Scott A, Hoffsten PE, Guerra F, Weinstein J, Schneider A, Schutz B, Fink J, Ford L, Smith E (1964) Studies on the Mechanism of Ascorbate-Induced Swelling and Lysis of Isolated Liver Mitochondria. *The Journal of biological chemistry* 239:604–613
- Huttemann M, Pecina P, Rainbolt M, Sanderson TH, Kagan VE, Samavati L, Doan JW, Lee I (2011) The multiple functions of cytochrome c and their regulation in life and death decisions of the mammalian cell: From respiration to apoptosis. *Mitochondrion* 11 (3):369–381. doi:<https://doi.org/10.1016/j.mito.2011.01.010>
- Iles KE, Forman HJ (2002) Macrophage signaling and respiratory burst. *Immunologic research* 26 (1-3):95–105. doi:<https://doi.org/10.1385/ir.26:1-3:095>
- Islinger M, Voelkl A, Fahimi HD, Schrader M (2018) The peroxisome: an update on mysteries 2.0. *Histochem Cell Biol* 150 (5):443–471. doi:<https://doi.org/10.1007/s00418-018-1722-5>
- Iyer GYN, Islam MF, Quastel JH (1961) Biochemical Aspects of Phagocytosis. *Nature* 192 (4802):535–541. doi:<https://doi.org/10.1038/192535a0>
- Izawa S, Inoue Y, Kimura A (1996) Importance of catalase in the adaptive response to hydrogen peroxide: analysis of acatalasaemic *Saccharomyces cerevisiae*. *Biochemical Journal* 320 (1):61–67. doi:<https://doi.org/10.1042/bj3200061>
- Jones P, Suggett A (1968) The catalase-hydrogen peroxide system. Kinetics of catalatic action at high substrate concentrations. *The Biochemical journal* 110 (4):617–620. doi:<https://doi.org/10.1042/bj1100617>
- Juarez JC, Manuia M, Burnett ME, Betancourt O, Boivin B, Shaw DE, Tonks NK, Mazar AP, Doñate F (2008) Superoxide dismutase 1 (SOD1) is essential for H₂O₂-mediated oxidation and inactivation of phosphatases in growth factor signaling. *PNAS* 105 (20):7147–7152. doi:<https://doi.org/10.1073/pnas.0709451105>
- Juillan-Binard C, Piccicocchi A, Andrieu J-P, Dupuy J, Petit-Hartlein I, Caux-Thang C, Vivès C, Nivière V, Fieschi F (2017) A Two-component NADPH Oxidase (NOX)-like System in Bacteria Is Involved in the Electron Transfer Chain to the Methionine Sulfoxide Reductase MsrP. *Journal of Biological Chemistry* 292 (6):2485–2494. doi:<https://doi.org/10.1074/jbc.M116.752014>
- Kagan VE, Bayir HA, Belikova NA, Kapralov O, Tyurina YY, Tyurin VA, Jiang J, Stoyanovsky DA, Wipf P, Kochanek PM, Greenberger JS, Pitt B, Shvedova AA, Borisenko G (2009) Cytochrome c/cardiolipin relations in mitochondria: a kiss of death. *Free radical biology & medicine* 46 (11):1439–1453. doi:<https://doi.org/10.1016/j.freeradbiomed.2009.03.004>
- Kagan VE, Tyurin VA, Jiang J, Tyurina YY, Ritov VB, Amoscato AA, Osipov AN, Belikova NA, Kapralov AA, Kini V (2005) Cytochrome c acts as a cardiolipin oxygenase required for release of proapoptotic factors. *Nature chemical biology* 1 (4):223–232
- Kalanxhi E, Wallace CJ (2007) Cytochrome c impaled: investigation of the extended lipid anchorage of a soluble protein to mitochondrial membrane models. *The Biochemical journal* 407 (2):179–187. doi:<https://doi.org/10.1042/BJ20070459>
- Kaul N, Forman HJ (1996) Activation of NF kappa B by the respiratory burst of macrophages. *Free radical biology & medicine* 21 (3):401–405. doi:[https://doi.org/10.1016/0891-5849\(96\)00178-5](https://doi.org/10.1016/0891-5849(96)00178-5)
- Kawaoka A, Kawamoto T, Ohta H, Sekine M, Takano M, Shinmyo A (1994) Wound-induced expression of horseradish peroxidase. *Plant cell reports* 13 (3-4):149–154. doi:<https://doi.org/10.1007/bf00239882>
- Kissner R, Nauser T, Bugnon P, Lye PG, Koppenol WH (1997) Formation and properties of peroxyxynitrite as studied by laser flash photolysis, high-pressure stopped-flow technique, and pulse radiolysis. *Chemical research in toxicology* 10 (11):1285–1292. doi:<https://doi.org/10.1021/tx970160x>
- Klebanoff SJ (1999) Myeloperoxidase. *Proceedings of the Association of American Physicians* 111 (5):383–389. doi:<https://doi.org/10.1111/paa.1999.111.5.383>
- Ko TP, Day J, Malkin AJ, McPherson A (1999) Structure of orthorhombic crystals of beef liver catalase. *Acta Crystallogr D Biol Crystallogr* 55 (Pt 8):1383–1394. doi:<https://doi.org/10.1107/s0907444999007052>
- Korshunov SS, Krasnikov BF, Pereverzev MO, Skulachev VP (1999) The antioxidant functions of cytochrome c. *FEBS Lett* 462 (1-2):192–198. doi:[https://doi.org/10.1016/S0014-5793\(99\)01525-2](https://doi.org/10.1016/S0014-5793(99)01525-2)
- Kotsias F, Hoffmann E, Amigorena S, Savina A (2013) Reactive oxygen species production in the phagosome: impact on antigen presentation in dendritic cells. *Antioxid Redox Signal* 18 (6):714–729. doi:<https://doi.org/10.1089/ars.2012.4557>
- Koua D, Cerutti L, Falquet L, Sigrist CJ, Theiler G, Hulo N, Dunand C (2009) PeroxiBase: a database with new tools for peroxidase family classification. *Nucleic Acids Res* 37 (Database issue):D261–266. doi:<https://doi.org/10.1093/nar/gkn680>
- Kremer ML (1970) Peroxidatic activity of catalase. *Biochimica et biophysica acta* 198 (2):199–209. doi:[https://doi.org/10.1016/0005-2744\(70\)90052-5](https://doi.org/10.1016/0005-2744(70)90052-5)
- Kroemer G, Reed JC (2000) Mitochondrial control of cell death. *Nature medicine* 6 (5):513–519. doi:<https://doi.org/10.1038/74994>
- Labat-Robert J, Robert L (2014) Longevity and aging. Role of free radicals and xanthine oxidase. A review. *Pathol Biol (Paris)* 62 (2):61–66. doi:<https://doi.org/10.1016/j.patbio.2014.02.009>
- Lagrimini LM, Burkhart W, Moyer M, Rothstein S (1987) Molecular cloning of complementary DNA encoding the lignin-forming peroxidase from tobacco: Molecular analysis and tissue-specific expression. *Proceedings of the National Academy of Sciences of the United States of America* 84 (21):7542–7546. doi:<https://doi.org/10.1073/pnas.84.21.7542>
- Lardy B, Bof M, Aubry L, Pacllet MH, Morel F, Satre M, Klein G (2005) NADPH oxidase homologs are required for normal cell differentiation and morphogenesis in *Dictyostelium discoideum*. *Biochimica et Biophysica Acta (BBA) - Molecular Cell Research* 1744 (2):199–212. doi:<https://doi.org/10.1016/j.bbamcr.2005.02.004>
- Lee JM (1998) Inhibition of p53-dependent apoptosis by the KIT tyrosine kinase: regulation of mitochondrial permeability transition and reactive oxygen species generation. *Oncogene* 17 (13):1653–1662
- Li J, Stouffs M, Serrander L, Banfi B, Bettiol E, Charnay Y, Steger K, Krause K-H, Jaconi ME (2006) The NADPH Oxidase NOX4 Drives Cardiac Differentiation: Role in Regulating Cardiac Transcription Factors and MAP Kinase Activation. *PLoS ONE* 1 (9):3978–3988. doi:<https://doi.org/10.1091/mbc.e05-06-0532>
- Li P, Nijhawan D, Budihardjo I, Srinivasula SM, Ahmad M, Alnemri ES, Wang X (1997) Cytochrome c and dATP-dependent formation of Apaf-1/caspase-9 complex initiates an apoptotic protease cascade. *Cell* 91 (4):479–489.

- Liochev SI, Fridovich I (1994) The role of $O_2^{\cdot -}$ in the production of HO^{\cdot} : in vitro and in vivo. *Free radical biology & medicine* 16 (1): 29–33
- Liu X, Kim CN, Yang J, Jemmerson R, Wang X (1996) Induction of apoptotic program in cell-free extracts: requirement for dATP and cytochrome c. *Cell* 86 (1):147–157
- Liu XF, Elashvili I, Gralla EB, Valentine JS, Lapinskas P, Culotta VC (1992) Yeast lacking superoxide dismutase. Isolation of genetic suppressors. *The Journal of biological chemistry* 267 (26): 18298–18302
- Lobo-Jarne T, Ugalde C (2018) Respiratory chain supercomplexes: Structures, function and biogenesis. *Semin Cell Dev Biol* 76:179–190. doi:<https://doi.org/10.1016/j.semcdb.2017.07.021>
- Loew O (1900) *Physiological studies of Connecticut leaf tobacco*. Washington government printing office
- Loewen PC, Switala J, Triggs-Raine BL (1985) Catalases HPI and HPII in *Escherichia coli* are induced independently. *Archives of biochemistry and biophysics* 243 (1):144–149. doi:[https://doi.org/10.1016/0003-9861\(85\)90782-9](https://doi.org/10.1016/0003-9861(85)90782-9)
- Loschen G, Azzi A, Richter C, Flohe L (1974) Superoxide radicals as precursors of mitochondrial hydrogen peroxide. *Febs Lett* 42 (1): 68–72
- Loschen G, Flohé L, Chance B (1971) Respiratory chain linked H_2O_2 production in pigeon heart mitochondria. *Febs Lett* 18 (2): 261–264. doi:[https://doi.org/10.1016/0014-5793\(71\)80459-3](https://doi.org/10.1016/0014-5793(71)80459-3)
- Luna G, Dolzhenko AV, Mancera RL (2019) Inhibitors of xanthine oxidase: scaffold diversity and structure-based drug design. *ChemMedChem*:10.1002/cmdc.201900034. doi:<https://doi.org/10.1002/cmdc.201900034>
- Lutter M, Fang M, Luo X, Nishijima M, Wang X (2000) Cardiolipin provides specificity for targeting of tBid to mitochondria. *Nat Cell Biol* 2:754–761
- Mantegazza AR, Savina A, Vermeulen M, Pérez L, Geffner J, Hermine O, Rosenzweig SD, Faure F, Amigorena S (2008) NADPH oxidase controls phagosomal pH and antigen cross-presentation in human dendritic cells. *Blood* 112 (12): 4712–4722. doi:<https://doi.org/10.1182/blood-2008-01-134791>
- Marinho HS, Real C, Cyrne L, Soares H, Antunes F (2014) Hydrogen peroxide sensing, signaling and regulation of transcription factors. *Redox biology* 2:535–562. doi:<https://doi.org/10.1016/j.redox.2014.02.006>
- Matsue H, Edelbaum D, Shalhevet D, Mizumoto N, Yang C, Mummert ME, Oeda J, Masayasu H, Takashima A (2003) Generation and Function of Reactive Oxygen Species in Dendritic Cells During Antigen Presentation. *The Journal of Immunology* 171 (6): 3010. doi:<https://doi.org/10.4049/jimmunol.171.6.3010>
- McCord JM, Fridovich I (1968) The reduction of cytochrome c by milk xanthine oxidase. *The Journal of biological chemistry* 243 (21): 5753–5760
- McCord JM, Fridovich I (1969) Superoxide dismutase. An enzymic function for erythrocyte (hemocuprein). *The Journal of biological chemistry* 244 (22):6049–6055
- McCord JM, Keele BB, Fridovich I (1971) An Enzyme-Based Theory of Obligate Anaerobiosis: The Physiological Function of Superoxide Dismutase. 68 (5):1024–1027. doi:<https://doi.org/10.1073/pnas.68.5.1024>
- Meneshian A, Bulkley GB (2002) The physiology of endothelial xanthine oxidase: from urate catabolism to reperfusion injury to inflammatory signal transduction. *Microcirculation* 9 (3):161–175. doi:<https://doi.org/10.1038/sj.mn.7800136>
- Michon T, Chenu M, Kellershon N, Desmadril M, Guéguen J (1997) Horseradish Peroxidase Oxidation of Tyrosine-Containing Peptides and Their Subsequent Polymerization: A Kinetic Study. *Biochemistry* 36 (28):8504–8513. doi:<https://doi.org/10.1021/bi963168z>
- Miller AF (2012) Superoxide dismutases: ancient enzymes and new insights. *Febs Lett* 586 (5):585–595. doi:<https://doi.org/10.1016/j.febslet.2011.10.048>
- Miller EW, Dickinson BC, Chang CJ (2010) Aquaporin-3 mediates hydrogen peroxide uptake to regulate downstream intracellular signaling. 107 (36):15681–15686. doi:<https://doi.org/10.1073/pnas.1005776107>
- Mitchell P (1961) Coupling of phosphorylation to electron and hydrogen transfer by a chemi-osmotic type of mechanism. *Nature* 191: 144–148. <https://www.nature.com/articles/191144a0>
- Mittler R, Vanderauwera S, Suzuki N, Miller G, Tognetti VB, Vandepoele K, Gollery M, Shulaev V, Van Breusegem F (2011) ROS signaling: the new wave? *Trends Plant Sci* 16 (6):300–309. doi:<https://doi.org/10.1016/j.tplants.2011.03.007>
- Mordas A, Tokatlidis K (2015) The MIA pathway: a key regulator of mitochondrial oxidative protein folding and biogenesis. *Accounts of chemical research* 48 (8):2191–2199. doi:<https://doi.org/10.1021/acs.accounts.5b00150>
- Murphy JK, Hoyal CR, Livingston FR, Forman HJ (1995) Modulation of the alveolar macrophage respiratory burst by hydroperoxides. *Free Radical Bio Med* 18 (1):37–45. doi:[https://doi.org/10.1016/0891-5849\(94\)00101-O](https://doi.org/10.1016/0891-5849(94)00101-O)
- Nantes IL, Faljoni-Alario A, Vercesi AE, Santos KE, Bechara EJ (1998) Liposome effect on the cytochrome c-catalyzed peroxidation of carbonyl substrates to triplet species. *Free radical biology & medicine* 25 (4-5):546–553
- Napoli C, Crimi E, Williams-Ignarro S, Nigris Fd, Ignarro LJ (2010) Chapter 23 - Nitric Oxide, Oxidative Stress, Immune Response and Critical Care. In: Ignarro LJ (ed) *Nitric Oxide (Second Edition)*. Academic Press, San Diego, pp 755–772. doi:<https://doi.org/10.1016/B978-0-12-373866-0.00023-X>
- Nelson RE, Fessler LI, Takagi Y, Blumberg B, Keene DR, Olson PF, Parker CG, Fessler JH (1994) Peroxidase: a novel enzyme-matrix protein of *Drosophila* development. *The EMBO journal* 13 (15): 3438–3447. doi:<https://doi.org/10.1002/j.1460-2075.1994.tb06649.x>
- Nesci S, Trombetti F, Pagliarani A, Ventrella V, Algieri C, Tioli G, Lenaz G (2021) Molecular and Supramolecular Structure of the Mitochondrial Oxidative Phosphorylation System: Implications for Pathology. 11 (3):242. doi:<https://doi.org/10.3390/life11030242>
- Nicholls P, Fita I, Loewen PC (2000) Enzymology and structure of catalases. In: *Advances in Inorganic Chemistry Volume 51. Advances in Inorganic Chemistry*. pp 51–106. doi:[https://doi.org/10.1016/s0898-8838\(00\)51001-0](https://doi.org/10.1016/s0898-8838(00)51001-0)
- Nishino T (1994) The conversion of xanthine dehydrogenase to xanthine oxidase and the role of the enzyme in reperfusion injury. *J Biochem* 116 (1):1–6. doi:<https://doi.org/10.1093/oxfordjournals.jbchem.a124480>
- Nitric Oxide (2010). Academic Press. doi:<https://doi.org/10.1016/C2009-0-02264-8>
- Northrop JH (1925) The kinetics of the decomposition of peroxide by catalase. *Journal of General Physiology* 7 (3):373–387. doi:<https://doi.org/10.1085/jgp.7.3.373>
- Okumoto K, El Shermely M, Natsui M, Kosako H, Natsuyama R, Marutani T, Fujiki Y (2020) The peroxisome counteracts oxidative stresses by suppressing catalase import via Pex14 phosphorylation. *Elife* 9. doi:<https://doi.org/10.7554/eLife.55896>
- Olenev VI, Suslova TB, Vladimirov YA (1976) Comparative study of different types of swelling of rat liver mitochondria. *Stud Biophys* 58 (2):147–161
- Omar BA, Flores SC, McCord JM (1992) Superoxide Dismutase: Pharmacological Developments and Applications. In: August JT, Anders MW, Murad F (eds) *Advances in Pharmacology*, vol 23. Academic Press, pp 109–161. doi:[https://doi.org/10.1016/S1054-3589\(08\)60964-3](https://doi.org/10.1016/S1054-3589(08)60964-3)

- Ostergaard L, Pedersen AG, Jespersen HM, Brunak S, Welinder KG (1998) Computational analyses and annotations of the Arabidopsis peroxidase gene family. *Febs Lett* 433 (1-2):98–102. doi:[https://doi.org/10.1016/s0014-5793\(98\)00849-7](https://doi.org/10.1016/s0014-5793(98)00849-7)
- Oxidative Stress. *Eustress and Distress* (2019). doi:<https://doi.org/10.1016/C2018-0-04253-X>
- Panday A, Sahoo MK, Osorio D, Batra S (2015) NADPH oxidases: an overview from structure to innate immunity-associated pathologies. *Cellular & Molecular Immunology* 12:5–23. doi:<https://doi.org/10.1038/cmi.2014.89>
- Park J, Choi HJ, Lee S, Lee T, Yang Z, Lee Y (2000) Rac-Related GTP-Binding Protein in Elicitor-Induced Reactive Oxygen Generation by Suspension-Cultured Soybean Cells. *Plant Physiol* 124 (2): 725–732
- Passardi F, Theiler G, Zamocky M, Cosio C, Rouhier N, Teixeira F, Margis-Pinheiro M, Ioannidis V, Penel C, Falquet L, Dunand C (2007) PeroxiBase: the peroxidase database. *Phytochemistry* 68 (12):1605–1611. doi:<https://doi.org/10.1016/j.phytochem.2007.04.005>
- Pereverzev MO, Vygodina TV, Konstantinov AA, Skulachev VP (2003) Cytochrome c, an ideal antioxidant. *Biochem Soc Trans* 31 (Pt 6): 1312–1315. doi:10.1042/
- Peus D, Meves A, Vasa RA, Beyerle A, O'Brien T, Pittelkow MR (1999) H₂O₂ is required for UVB-induced EGF receptor and downstream signaling pathway activation. *Free radical biology & medicine* 27 (11-12):1197–1202. doi:[https://doi.org/10.1016/s0891-5849\(99\)00198-7](https://doi.org/10.1016/s0891-5849(99)00198-7)
- Poderoso JJ, Carreras MC, Lisdero C, Riobo N, Schopfer F, Boveris A (1996) Nitric oxide inhibits electron transfer and increases superoxide radical production in rat heart mitochondria and submitochondrial particles. *Arch Biochem Biophys* 328:85–92. doi:<https://doi.org/10.1006/abbi.1996.0146>
- Pollet E, Martynez JA, Metha B, Watts BPI, Turrens JF (1998) Role of Tryptophan Oxidation in Peroxynitrite-Dependent Protein Chemiluminescence. *Archives of biochemistry and biophysics* 349 (1): 74–80. doi:<https://doi.org/10.1006/abbi.1997.0436><https://doi.org/>
- Poorani R, Bhatt AN, Dwarakanath BS, Das UN. (2016). COX-2, aspirin and metabolism of arachidonic, eicosapentaenoic and docosahexaenoic acids and their physiological and clinical significance. *European journal of pharmacology* 785:116–132. doi:<https://doi.org/10.1016/j.ejphar.2015.08.049>
- Potter SZ, Valentine JS (2003) The perplexing role of copper-zinc superoxide dismutase in amyotrophic lateral sclerosis (Lou Gehrig's disease). *Journal of biological inorganic chemistry : JBIC : a publication of the Society of Biological Inorganic Chemistry* 8 (4): 373–380. doi:<https://doi.org/10.1007/s00775-003-0447-6>
- Prosser BL, Ward CW, Lederer WJ (2011) X-ROS Signaling: Rapid Mechano-Chemo Transduction in Heart. 333 (6048): 1440–1445. doi:<https://doi.org/10.1126/science.1202768>
- Quinlan CL, Goncalves RL, Hey-Mogensen M, Yadava N, Bunik VI, Brand MD (2014) The 2-oxoacid dehydrogenase complexes in mitochondria can produce superoxide/hydrogen peroxide at much higher rates than complex I. *The Journal of biological chemistry* 289 (12):8312–8325. doi:<https://doi.org/10.1074/jbc.M113.545301>
- Quinlan CL, Treberg JR, Perevoshchikova IV, Orr AL, Brand MD (2012) Native rates of superoxide production from multiple sites in isolated mitochondria measured using endogenous reporters. *Free radical biology & medicine* 53 (9):1807–1817. doi:<https://doi.org/10.1016/j.freeradbiomed.2012.08.015>
- Rabêlo LA, Souza VN, Fonseca LJ, Sampaio WO (2010) Redox imbalance: NADPH oxidase as therapeutic target in blood pressure control. *Arquivos brasileiros de cardiologia* 94 (5):643–651, 684–693. doi:<https://doi.org/10.1590/s0066-782x2010000500018>
- Ramstedt U, Rossi P, Kullman C, Warren E, Palmblad J, Jondal M (1984) Free oxygen radicals are not detectable by chemiluminescence during human natural killer cell cytotoxicity. *Scand J Immunol* 19 (5):457–464. doi:<https://doi.org/10.1111/j.1365-3083.1984.tb00954.x>
- Reddi Amit R, Culotta Valeria C (2013) SOD1 Integrates Signals from Oxygen and Glucose to Repress Respiration. *Cell* 152 (1): 224–235. doi:<https://doi.org/10.1016/j.cell.2012.11.046>
- RedoxiBase <https://peroxibase.toulouse.inra.fr/>. Accessed 09 August 2022
- Reed PW (1969) Glutathione and the hexose monophosphate shunt in phagocytizing and hydrogen peroxide-treated rat leukocytes. *The Journal of biological chemistry* 244 (9):2459–2464. doi:[https://doi.org/10.1016/S0021-9258\(19\)78244-1](https://doi.org/10.1016/S0021-9258(19)78244-1)
- Rinnerthaler M, Büttner S, Laun P, Heeren G, Felder TK, Klinger H, Weinberger M, Stolze K, Grousl T, Hasek J, Benada O, Frydlova I, Klocker A, Simon-Nobbe B, Jansko B, Breitenbach-Koller H, Eisenberg T, Gourlay CW, Madeo F, Burhans WC, Breitenbach M (2012) Yno1p/Aim14p, a NADPH-oxidase ortholog, controls extramitochondrial reactive oxygen species generation, apoptosis, and actin cable formation in yeast. *Proceedings of the National Academy of Sciences* 109 (22):8658–8663. doi:<https://doi.org/10.1073/pnas.1201629109>
- Rittle J, Green MT (2010) Cytochrome P450 compound I: capture, characterization, and C-H bond activation kinetics. *Science* 330 (6006):933–937. doi:<https://doi.org/10.1126/science.1193478>
- Roman R, Dunford HB (1972) pH Dependence of the oxidation of iodide by compound I of horseradish peroxidase. *Biochemistry* 11 (11):2076–2082. doi:<https://doi.org/10.1021/bi00761a013>
- Roman R, Dunford HB (1973) Studies on Horseradish Peroxidase. XII. A Kinetic Study of the Oxidation of Sulfite and Nitrite by Compounds I and II. 51 (4):588–596. doi:<https://doi.org/10.1139/v73-089>
- Root RK, Metcalf J, Oshino N, Chance B (1975) H₂O₂ release from human granulocytes during phagocytosis. I. Documentation, quantitation, and some regulating factors. *J Clin Invest* 55 (5): 945–955. doi:<https://doi.org/10.1172/JCI108024>
- Root RK, Metcalf JA (1977) H₂O₂ Release from Human Granulocytes during Phagocytosis: Relationship to superoxide anion formation and cellular catabolism of H₂O₂: studies with normal and cytochalasin b-treated cells. *J Clin Invest* 60 (6):1266–1279. doi:<https://doi.org/10.1172/JCI108886>
- Ryan MG, Balendran A, Harrison R, Wolstenholme A, Bulkley GB (1997) Xanthine oxidoreductase: dehydrogenase to oxidase conversion. *Biochem Soc Trans* 25 (3):530s. doi:<https://doi.org/10.1042/bst025530s>
- Salmeen A, Andersen JN, Myers MP, Meng T-C, Hinks JA, Tonks NK, Barford D (2003) Redox regulation of protein tyrosine phosphatase 1B involves a sulphenyl-amide intermediate. *Nature* 423 (6941): 769–773. doi:<https://doi.org/10.1038/nature01680>
- Savelli B, Li Q, Webber M, Jemmat AM, Robitaille A, Zamocky M, Mathé C, Dunand C (2019) RedoxiBase: A database for ROS homeostasis regulated proteins. *Redox biology* 26:101247. doi:<https://doi.org/10.1016/j.redox.2019.101247>
- Sbarra AJ, Karnovsky ML (1959) The biochemical basis of phagocytosis. I. Metabolic changes during the ingestion of particles by polymorphonuclear leukocytes. *The Journal of biological chemistry* 234 (6):1355–1362. doi:[https://doi.org/10.1016/S0021-9258\(18\)70011-2](https://doi.org/10.1016/S0021-9258(18)70011-2)
- Schaar CE, Dues DJ, Spielbauer KK, Machiela E, Cooper JF, Senchuk M, Hekimi S, Van Raamsdonk JM (2015) Mitochondrial and cytoplasmic ROS have opposing effects on lifespan. *PLoS Genet* 11 (2):e1004972. doi:<https://doi.org/10.1371/journal.pgen.1004972>
- Schellhorn HE (1995) Regulation of hydroperoxidase (catalase) expression in *Escherichia coli*. *FEMS Microbiol Lett* 131 (2):113–119. doi:<https://doi.org/10.1111/j.1574-6968.1995.tb07764.x>
- Schneider AK, Smith EE, Hunter FE, Jr. (1964) Correlation of Oxygen Consumption with Swelling and Lipid Peroxide Formation When

- Mitochondria Are Treated with the Swelling-Inducing Agents Fe²⁺, Glutathione, Ascorbate, or Phosphate. *Biochemistry* 3:1470–1477. doi:<https://doi.org/10.1021/bi00898a014>
- Schröder K (2020) NADPH oxidases: Current aspects and tools. *Redox biology* 34:101512. doi:<https://doi.org/10.1016/j.redox.2020.101512>
- Sepasi Tehrani H, Moosavi-Movahedi AA (2018) Catalase and its mysteries. *Progress in Biophysics and Molecular Biology* 140:5–12. doi:<https://doi.org/10.1016/j.pbiomolbio.2018.03.001>
- Sies H (2017) Hydrogen peroxide as a central redox signaling molecule in physiological oxidative stress: Oxidative eustress. *Redox biology* 11:613–619. doi:<https://doi.org/10.1016/j.redox.2016.12.035>
- Sies H, Jones DP (2020) Reactive oxygen species (ROS) as pleiotropic physiological signalling agents. *Nat Rev Mol Cell Biol* 21 (7): 363–383. doi:<https://doi.org/10.1038/s41580-020-0230-3>
- Sirokmány G, Donkó Á, Geiszt M (2016) Nox/Duox Family of NADPH Oxidases: Lessons from Knockout Mouse Models. *Trends in Pharmacological Sciences* 37 (4):318–327. doi:<https://doi.org/10.1016/j.tips.2016.01.006>
- Skulachev VP (1996) Why are mitochondria involved in apoptosis? Permeability transition pores and apoptosis as selective mechanisms to eliminate superoxide-producing mitochondria and cell. *Febs Lett* 397 (1):7–10. doi:[https://doi.org/10.1016/0014-5793\(96\)00989-1](https://doi.org/10.1016/0014-5793(96)00989-1)
- Skulachev VP (1998) Cytochrome c in the apoptotic and antioxidant cascades. *Febs Lett* 423 (3):275–280. doi:[https://doi.org/10.1016/S0014-5793\(98\)00061-1](https://doi.org/10.1016/S0014-5793(98)00061-1)
- Smallwood MJ, Nissim A, Knight AR, Whiteman M, Haigh R, Winyard PG (2018) Oxidative stress in autoimmune rheumatic diseases. *Free radical biology & medicine* 125:3–14. doi:<https://doi.org/10.1016/j.freeradbiomed.2018.05.086>
- Stadtman TC (1990) Selenium biochemistry. *Annu Rev Biochem* 59: 111–127. doi:<https://doi.org/10.1146/annurev.bi.59.070190.000551>
- Starkov AA, Andreyev AY, Zhang SF, Starkova NN, Korneeva M, Syromyatnikov M, Popov VN (2014) Scavenging of H₂O₂ by mouse brain mitochondria. *J Bioenerg Biomembr* 46 (6): 471–477. doi:<https://doi.org/10.1007/s10863-014-9581-9>
- Suzuki N, Miller G, Morales J, Shulaev V, Torres MA, Mittler R (2011) Respiratory burst oxidases: the engines of ROS signaling. *Curr Opin Plant Biol* 14 (6):691–699. doi:<https://doi.org/10.1016/j.pbi.2011.07.014>
- Szabó C, Ischiropoulos H, Radi R (2007) Peroxynitrite: biochemistry, pathophysiology and development of therapeutics. *Nature Reviews Drug Discovery* 6 (8):662–680. doi:<https://doi.org/10.1038/nrd2222>
- Tai LA, Hwang KC (2004) Cooperative Catalysis in the Homodimer Subunits of Xanthine Oxidase. *Biochemistry* 43:4869–4876. doi:<https://doi.org/10.1021/bi035467b>
- Tarusov BN, Polivoda AI, Zhuravlev AI, Sekamova EN (1962) Ultraweak spontaneous luminescence in animal tissue (in Russian). *Tsitologiya* 4:696–699
- Terada LS (2006) Specificity in reactive oxidant signaling: think globally, act locally. *Journal of Cell Biology* 174 (5):615–623. doi:<https://doi.org/10.1083/jcb.200605036>
- Torres M, Forman HJ (1999) Activation of several MAP kinases upon stimulation of rat alveolar macrophages: role of the NADPH oxidase. *Archives of biochemistry and biophysics* 366 (2): 231–239. doi:<https://doi.org/10.1006/abbi.1999.1225>
- Tripathi P, Hildeman D (2004) Sensitization of T cells to apoptosis—A role for ROS? *Apoptosis* 9 (5):515–523. doi:<https://doi.org/10.1023/B:APPT.0000038033.14925.02>
- Tschopp J, Schroder K (2010) NLRP3 inflammasome activation: the convergence of multiple signalling pathways on ROS production? *Nature Reviews Immunology* 10 (3):210–215. doi:<https://doi.org/10.1038/nri2725>
- Tuominen EK, Wallace CJ, Kinnunen PK (2002) Phospholipid-cytochrome c interaction: evidence for the extended lipid anchorage. *The Journal of biological chemistry* 277 (11):8822–8826. doi:<https://doi.org/10.1074/jbc.M200056200>
- Turrens JF, Boveris A (1980) Generation of superoxide anion by the NADH dehydrogenase of bovine heart mitochondria. *The Biochemical journal* 191 (2):421–427. doi:<https://doi.org/10.1042/bj1910421>
- Valderrama B, Ayala M, Vazquez-Duhalt R (2002) Suicide Inactivation of Peroxidases and the Challenge of Engineering More Robust Enzymes. *Chemistry & Biology* 9 (5):555–565. doi:[https://doi.org/10.1016/S1074-5521\(02\)00149-7](https://doi.org/10.1016/S1074-5521(02)00149-7)
- Van Remmen H, Ikeno Y, Hamilton M, Pahlavani M, Wolf N, Thorpe SR, Alderson NL, Baynes JW, Epstein CJ, Huang T-T, Nelson J, Strong R, Richardson A (2003) Life-long reduction in MnSOD activity results in increased DNA damage and higher incidence of cancer but does not accelerate aging. *Physiological Genomics* 16 (1): 29–37. doi:<https://doi.org/10.1152/physiolgenomics.00122.2003>
- Veal EA, Day AM, Morgan BA (2007) Hydrogen peroxide sensing and signaling. *Mol Cell* 26 (1):1–14. doi:<https://doi.org/10.1016/j.molcel.2007.03.016>
- Veitch NC (2004) Horseradish peroxidase: a modern view of a classic enzyme. *Phytochemistry* 65 (3):249–259. doi:<https://doi.org/10.1016/j.phytochem.2003.10.022>
- Veitch NC, Smith AT (2000) Horseradish peroxidase. In: *Advances in Inorganic Chemistry*, vol 51. Academic Press, pp 107–162. doi:[https://doi.org/10.1016/S0898-8838\(00\)51002-2](https://doi.org/10.1016/S0898-8838(00)51002-2)
- Vermot A, Petit-Härtlein I, Smith SME, Fieschi F (2021) NADPH Oxidases (NOX): An Overview from Discovery, Molecular Mechanisms to Physiology and Pathology. *10 (6):890*. doi:<https://doi.org/10.3390/antiox10060890>
- Vikulina AS, Alekseev AV, Proskurnina EV, Vladimirov YA (2015) Cytochrome c-cardiolipin complex in a nonpolar environment. *Biochemistry-Moscow* 80 (10):1298–1302. doi:<https://doi.org/10.1134/s0006297915100107>
- Viña J, Borras C, Abdelaziz KM, Garcia-Valles R, Gomez-Cabrera MC (2013) The free radical theory of aging revisited: the cell signaling disruption theory of aging. *Antioxid Redox Signal* 19 (8): 779–787. doi:<https://doi.org/10.1089/ars.2012.5111>
- Vladimirov GK, Remenshchikov VE, Nesterova AM, Volkov VV, Vladimirov YA (2019) Comparison of the Size and Properties of the Cytochrome c/Cardiolipin Nanospheres in a Sediment and Non-polar Medium. *Biochemistry-Moscow* 84 (8):923–930. doi:<https://doi.org/10.1134/s000629791908008x>
- Vladimirov YA (1967) Ultraweak luminescence accompanying biochemical reactions (English translation of "Sverkhslabye svecheniya pri biokhimicheskikh reaktsiyah" USSR Academy of Sciences, Institute of Biological Physics. Izdatel'stvo "Nauka" Moscow, 1966). NASA, C.F.S.T.I., Springfield, Vermont
- Vladimirov YA (2017) Biological membranes – primary sources and targets of free radicals (Chapter 1) (In Russian). In: *Sources and targets of free radicals in human blood*. MAX Press, Moscow,
- Vladimirov YA, Arroyo A, Taylor JM, Tyurina YY, Matsura T, Tyurin VA, Kagan VE (2000) Quinolizin-coumarins as physical enhancers of chemiluminescence during lipid peroxidation in live HL-60 cells. *Archives of biochemistry and biophysics* 384 (1):154–162. doi:<https://doi.org/10.1006/abbi.2000.2109>
- Vladimirov YA, Nol' YT, Volkov VV (2011) Protein–lipid nanoparticles that determine whether cells will live or die. *Crystallogr. Rep.* 56 (4):553–559. doi:<https://doi.org/10.1134/S1063774511040250>
- Vladimirov YA, Olenev VI, Suslova TB, Cheremisina ZP (1980) Lipid peroxidation in mitochondrial membrane. *Advances in Lipid Research* 17:173–249. doi:<https://doi.org/10.1016/B978-0-12-024917-6.50011-2>
- Vladimirov YA, Proskurnina EV, Alekseev AV (2013) Molecular Mechanisms of Apoptosis. Structure of Cytochrome c-Cardiolipin Complex. *Biochemistry (Moscow)* 78 (10):1086–1097. doi:<https://doi.org/10.1134/s0006297913100027>

- Vladimirov YA, Proskurnina EV, Izmailov DY, Novikov AA, Brusnichkin AV, Osipov AN, Kagan VE (2006a) Cardiolipin activates cytochrome c peroxidase activity since it facilitates H₂O₂ access to heme. *Biochemistry-Moscow* 71 (9):998–1005. doi:<https://doi.org/10.1134/S0006297906090082>
- Vladimirov YA, Proskurnina EV, Izmailov DY, Novikov AA, Brusnichkin AV, Osipov AN, Kagan VE (2006b) Mechanism of activation of cytochrome c peroxidase activity by cardiolipin. *Biochemistry-Moscow* 71 (9):989–997. doi:<https://doi.org/10.1134/S0006297906090070>
- Vladimirov YA, Sarisozen C, Vladimirov GK, Filipczak N, Polimova AM, Torchilin VP (2017) The Cytotoxic Action of Cytochrome C/Cardiolipin Nanocomplex (Cyt-CL) on Cancer Cells in Culture. *Pharmaceutical Research* 34 (6):1264–1275. doi:<https://doi.org/10.1007/s11095-017-2143-1>
- Vladimirov YA, Sharov VS, Driomina ES, Reznitchenko AV, Gashev SB (1995) Coumarin derivatives enhance the chemiluminescence accompanying lipid peroxidation. *Free radical biology & medicine* 18 (4):739–745
- Vladimirov YA, Shestnev MP, Azimbaev TK (1992) [Evaluation of the anti-oxidative and antiradical activities of substances and biological objects using iron-initiated chemiluminescence] (in Russian). *Biophysics* 37 (6):939–944
- Vlasits J, Jakopitsch C, Bemroitner M, Zamocky M, Furtmuller PG, Obinger C (2010) Mechanisms of catalase activity of heme peroxidases. *Archives of biochemistry and biophysics* 500 (1):74–81. doi:<https://doi.org/10.1016/j.abb.2010.04.018>
- Wakamatsu K, Takahama U (1993) Changes in peroxidase activity and in peroxidase isozymes in carrot callus. *Physiol Plantarum* 88 (1):167–171. doi:<https://doi.org/10.1111/j.1399-3054.1993.tb01774.x>
- Wang Y, Branicky R, Noë A, Hekimi S (2018) Superoxide dismutases: Dual roles in controlling ROS damage and regulating ROS signaling. *J Cell Biol* 217 (6):1915–1928. doi:<https://doi.org/10.1083/jcb.201708007>
- Wang Y, Mohsen AW, Mihalik SJ, Goetzman ES, Vockley J (2010) Evidence for physical association of mitochondrial fatty acid oxidation and oxidative phosphorylation complexes. *The Journal of biological chemistry* 285 (39):29834–29841. doi:<https://doi.org/10.1074/jbc.M110.139493>
- Wang Y, Palmfeldt J, Gregersen N, Makhov AM, Conway JF, Wang M, McCalley SP, Basu S, Alharbi H, St Croix C, Calderon MJ, Watkins S, Vockley J (2019) Mitochondrial fatty acid oxidation and the electron transport chain comprise a multifunctional mitochondrial protein complex. *The Journal of biological chemistry* 294 (33):12380–12391. doi:<https://doi.org/10.1074/jbc.RA119.008680>
- Wang ZB, Li M, Zhao Y, Xu JX (2003) Cytochrome C is a hydrogen peroxide scavenger in mitochondria. *Protein Pept Lett* 10 (3):247–253. doi:<https://doi.org/10.2174/0929866033479013>
- Warburg O (1908) Beobachtungen über die Oxydationsprozesse im Seeigelei. *%J. 57* (1-2):1–16. doi:<https://doi.org/10.1515/bchm2.1908.57.1-2.1>
- Watts BP, Jr., Barnard M, Turrens JF (1995) Peroxynitrite-dependent chemiluminescence of amino acids, proteins, and intact cells. *Archives of biochemistry and biophysics* 317 (2):324–330. doi:<https://doi.org/10.1006/abbi.1995.1170>
- Weerapana E, Wang C, Simon GM, Richter F, Khare S, Dillon MB, Bachovchin DA, Mowen K, Baker D, Cravatt BF (2010) Quantitative reactivity profiling predicts functional cysteines in proteomes. *Nature* 468 (7325):790–795. doi:<https://doi.org/10.1038/nature09472>
- Wei CE, Allen K, Misra HP (1989) Role of activated oxygen species on the mutagenicity of benzo[a]pyrene. *Journal of applied toxicology* : JAT 9 (3):169–173. doi:<https://doi.org/10.1002/jat.2550090306>
- Williams MS, Kwon J (2004) T cell receptor stimulation, reactive oxygen species, and cell signaling. *Free radical biology & medicine* 37 (8):1144–1151. doi:<https://doi.org/10.1016/j.freeradbiomed.2004.05.029>
- Wong JL, Créton R, Wessel GM (2004) The oxidative burst at fertilization is dependent upon activation of the dual oxidase Udx1. *Dev Cell* 7 (6):801–814. doi:<https://doi.org/10.1016/j.devcel.2004.10.014>
- Woo HA, Yim SH, Shin DH, Kang D, Yu DY, Rhee SG (2010) Inactivation of peroxiredoxin I by phosphorylation allows localized H₂O₂ accumulation for cell signaling. *Cell* 140 (4):517–528. doi:<https://doi.org/10.1016/j.cell.2010.01.009>
- Wu M, Gu J, Zong S, Guo R, Liu T, Yang M (2020) Research journey of respirasome. *Protein & Cell* 11 (5):318–338. doi:<https://doi.org/10.1007/s13238-019-00681-x>
- Wuerges J, Lee JW, Yim YI, Yim HS, Kang SO, Djinovic Carugo K (2004) Crystal structure of nickel-containing superoxide dismutase reveals another type of active site. *Proceedings of the National Academy of Sciences of the United States of America* 101 (23):8569–8574. doi:<https://doi.org/10.1073/pnas.0308514101>
- Xiao Y, Gu Y, Purwaha P, Ni K, Law B, Mallik S, Qian SY (2011) Characterization of free radicals formed from COX-catalyzed DGLA peroxidation. *Free radical biology & medicine* 50 (9):1163–1170. doi:<https://doi.org/10.1016/j.freeradbiomed.2011.02.001>
- Yang J, Liu X, Bhalla K, Kim CN, Ibrado AM, Cai J, Peng TI, Jones DP, Wang X (1997) Prevention of apoptosis by Bcl-2: release of cytochrome c from mitochondria blocked. *Science* 275 (5303):1129–1132. doi:<https://doi.org/10.1126/science.275.5303.1129>
- Yang W, Li J, Hekimi S (2007) A Measurable Increase in Oxidative Damage Due to Reduction in Superoxide Detoxification Fails to Shorten the Life Span of Long-Lived Mitochondrial Mutants of *Caenorhabditis elegans*. *Genetics* 177 (4):2063–2074. doi:<https://doi.org/10.1534/genetics.107.080788>
- Yang Y, Bazhin AV, Werner J, Karakhanova S (2012) Reactive oxygen species in the immune system. *Int Rev Immunol* 32 (3):249–270. doi:<https://doi.org/10.3109/08830185.2012.755176>
- Yu Q, Purwaha P, Ni K, Sun C, Mallik S, Qian SY (2009) Characterization of novel radicals from COX-catalyzed arachidonic acid peroxidation. *Free radical biology & medicine* 47 (5):568–576. doi:<https://doi.org/10.1016/j.freeradbiomed.2009.05.023>
- Zaidi S, Hassan MI, Islam A, Ahmad F (2014) The role of key residues in structure, function, and stability of cytochrome-c. *Cell Mol Life Sci* 71 (2):229–255. doi:<https://doi.org/10.1007/s00018-013-1341-1>
- Zamocky M, Gasselhuber B, Furtmuller PG, Obinger C (2014) Turning points in the evolution of peroxidase-catalase superfamily: molecular phylogeny of hybrid heme peroxidases. *Cell Mol Life Sci* 71 (23):4681–4696. doi:<https://doi.org/10.1007/s00018-014-1643-y>
- Zámocký M, Koller F (1999) Understanding the structure and function of catalases: clues from molecular evolution and in vitro mutagenesis. *Prog Biophys Mol Biol* 72 (1):19–66. doi:[https://doi.org/10.1016/s0079-6107\(98\)00058-3](https://doi.org/10.1016/s0079-6107(98)00058-3)
- Zhang J, Wang X, Vikash V, Ye Q, Wu D, Liu Y, Dong W (2016) ROS and ROS-Mediated Cellular Signaling. *Oxidative medicine and cellular longevity* 2016:4350965. doi:<https://doi.org/10.1155/2016/4350965>
- Zhou H, Duncan RF, Robison TW, Gao L, Forman HJ (1997) Ca(2+)-dependent p47phox translocation in hydroperoxide modulation of the alveolar macrophage respiratory burst. *The American journal of physiology* 273 (5):L1042–1047. doi:<https://doi.org/10.1152/ajplung.1997.273.5.L1042>
- Zhou R, Tardivel A, Thorens B, Choi I, Tschopp J (2010) Thioredoxin-interacting protein links oxidative stress to inflammasome activation. *Nature immunology* 11 (2):136–140. doi:<https://doi.org/10.1038/ni.1831>

Part IV

UPE Research in Life Science

Alexander I. Zhuravlev and Ilya Volodyaev

15.1 Discovery and Scientific Significance of Biological Autoluminescence

In 1961, B.N. Tarasov and his collaborators discovered ultraweak photon emission (UPE) from animal tissues in visible and infrared ranges: from the surface of rat and rabbit brains and liver. Its photon energies are 30–80 kcal/mol (1.5–3.5 eV), which corresponds to the spectral range 1200–380 nm (Tarasov et al. 1961b, c).

In 1961, the authors discovered UPE from lipids in the same range (Tarasov et al. 1961a) and showed that they are the main source of UPE in our body. They are our inner sun.

15.1.1 The Problem of the Matter Composition

The problem that existed before 1961 was the data gap between physics and biology regarding the composition of matter. According to physics, the matter is mainly composed of:

- Protons and neutrons, which determine the mass.
- Electrons.
- Photons.

While the participation of protons, neutrons, and electrons in biological processes is beyond doubt, with photons, things have been much more complicated for a long time. As recently as 1960, Nobel Prize laureate Albert Szent-Gyorgyi stated that no one had yet been able to observe light emission in animal tissues (Szent-Györgyi 1960). However, literally, a year later, this statement was refuted, and biological autoluminescence gradually became recognized as a ubiquitous and well-proven phenomenon.

It was due to the technological progress in the 1950s–1960s that biologists began to widely use sensors invented by Lev Kubetsky for weak light fluxes – photomultiplier tubes (PMT). A PMT is an electronic vacuum lamp, in which L. Kubetsky combined two mechanisms: the photoelectric effect on the photocathode and dynatron emission, that is, knocking out 2–4 secondary electrons by each primary electron on several secondary internal electrodes – dynodes. PMT amplifies the signal by several million times.

For the detection of ultra-low light fluxes, the PMTs were usually immersed in liquid nitrogen in glass or quartz Dewars, which reduced their background noise. Yet, the initially constructed devices were unable to detect UPE from animal tissues and showed only UPE from more powerful sources.

The discovery of B.N. Tarasov’s group was enabled by the following invention:

1. They replaced the glass vessel with a foam one.
2. The photocathode was brought outside, excluding losses on two walls and in the nitrogen layer (Fig. 15.1).

This allowed the authors to record luminescence with a low intensity as $\sim 10\text{--}100$ quanta/sec/cm² in the spectral range of 380–1200 nm.

The discovery of light quanta and electronically excited states in living tissues solved the above problem formulated by A. Szent-Gyorgyi and helped bridge the gap between physics and biology, as far as matter composition is concerned.

15.1.2 The Energy Impasse and Bi-level Animal Bioenergetics

Another important problem, which existed for many years preceding the discovery of biological autoluminescence, was

A. I. Zhuravlev · I. Volodyaev (✉)
Moscow State University, Moscow, Russia

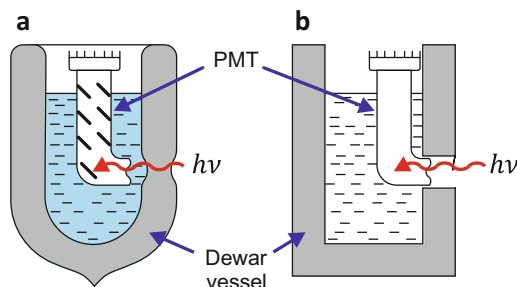
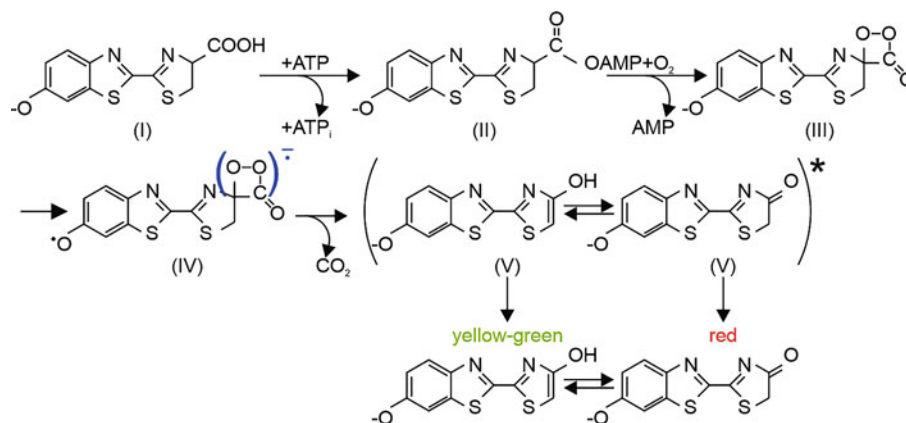
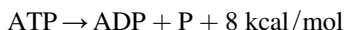


Fig. 15.1 The design of the unit for measuring ultra-weak light fluxes: (a) according to Yu.A. Vladimirov and R.F. Vasiliev; (b) according to B.N. Tarusov

Fig. 15.2 Mechanism of the luciferin-luciferase action. (Reprinted from Baldwin (1996). Copyright 1996, with permission from Elsevier)



the so-called energy paradox (Zhuravlev 2011). As is known, the energy of hydrolysis of high-energy bonds in the main energy currency of the cell, ATP is 8 kcal/mol:



This is ten times less than the energy of covalent bonds in the primary structure of biopolymers – proteins and DNA:

$$\Delta E = 70 - 90 \text{ kcal/mol}$$

Thus, it seemed in principle impossible to explain the elementary acts of metabolism – the breaking of a covalent bond due to ATP energy.

15.1.2.1 Bi-level Bioenergetics

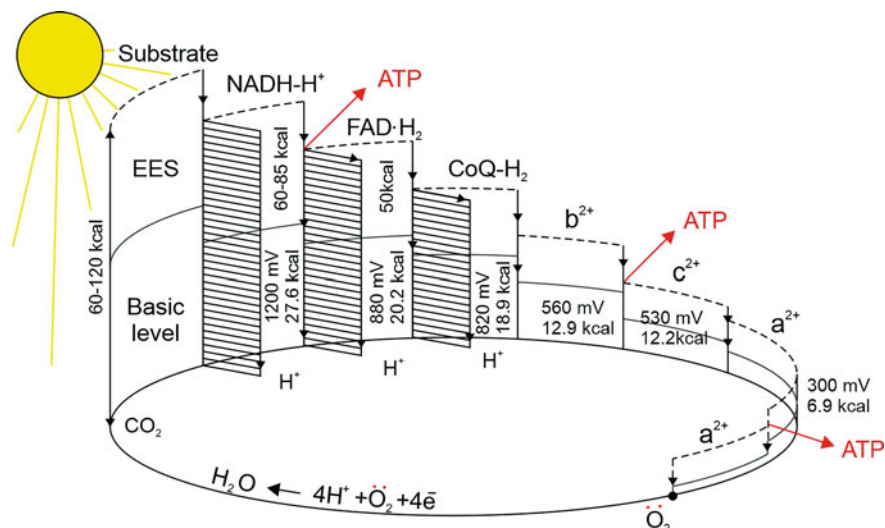
The solution to the problem lies in taking into account the electronically excited levels of molecules, the energy of which turns out to be sufficient both for breaking covalent bonds and for generating light quanta. This allowed us to formulate the concept of two-level bioenergetics, which we will first illustrate with a specific example of a firefly.

For the firefly, there is an apparent contradiction: the number of emitted yellow-green quanta with energies of 50–60 kcal/mol is almost equal to the number of decayed ATP (with energy ~8 kcal/mol), while obviously, ATP can in no way provide the energy of a photon. As we know now, in fact, ATP energy does not participate in photon generation. It is a trigger, activating luciferin, which is later oxidized with the peroxide formation and decay, and consequently, generation of electron-excited states (Fig. 15.2).

The ‘first energy level’ is the level of ATP, triggering the reaction; the ‘second energy level’ is the level of electron-excited states, producing photons.

Actually, many biological processes proceed in a similar manner, and can be decomposed in two different energy levels: the main one with low energy values and the electronically excited one with energies many times higher. Thus, the transport of electrons in the respiratory chain of mitochondria occurs both at the main levels with the energy difference of 27 kcal/mol (according to the difference in the redox potentials of H_2 and O_2) and at the electron-excited levels with an energy difference of 60–80 kcal/mol (Fig. 15.3).

Fig. 15.3 Bi-level bioenergetics of the respiratory chain



15.1.2.2 UPE and Mechanisms of Bi-level Energetics

The phenomenon of spontaneous UPE, manifesting the electron-excited states (EES), gave us the opportunity to propose a hypothesis about the general mechanism of such functioning. As a basis, we took the electron-exchange synthesis of EES developed in chemistry (Sharipov et al. 1990). Instead of chemical compounds, we took a lipid-protein complex that meets all the properties necessary for this. So, the step-by-step process should look as follows:

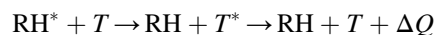
1. Interaction of ATP as a trigger with lipid-protein complexes with an increase in their oxygen affinity.
2. Addition of oxygen to the double bonds of the phospholipid with the formation of peroxide-dioxetane.
3. Peroxide in the ground state is an electron acceptor, which it easily receives from the reduced part of phospholipid fatty acid tails, creating a radical cation.
4. The attachment of an electron leads to the peroxide bond weakening.
5. The peroxide bond is broken to form two aldehyde groups, one of which is in an electronically excited state with an excess electron.
6. In the electronically excited state, the aldehyde is an electron donor and returns the electron to its original place.
7. The energy of the electronically excited state migrates to the protein, where it falls into the main trap of the electron excitation – tryptophan.

Thus, the protein is transformed into an active electronically excited state with an energy of 60–90 kcal/mol.

This mechanism is confirmed by the following facts:

1. Spontaneous emission of mitochondria and its enhancement, when oxidative phosphorylation is uncoupled by dinitrophenol (Tsvylev et al. 1974).
2. Generation of electron-excited states in mitochondrial respiratory enzymes (Boveris and Chance 1973).
3. Lipid-dependence of the membrane-bound enzyme's activity (Burlakova et al. 1978, 1980).

It becomes clear that the body needs a large number of protective quenchers of electron-excited states, inactivating them non-radiatively with their energy transformed into heat: heme, CO₂, ions Cl⁻, Br⁻, I⁻, carotene, O₂, amides in proteins, adrenaline:



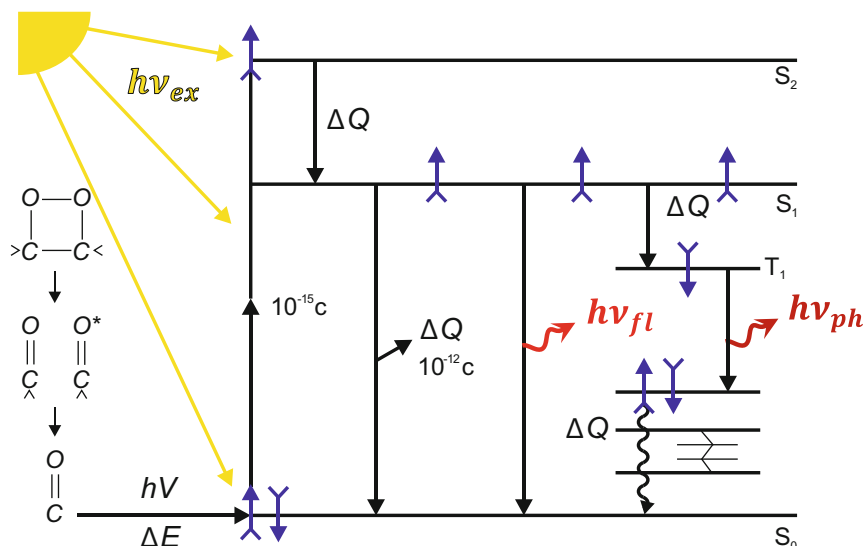
where T is the quencher molecule and ΔQ is heat.

15.1.3 Quantum Biology: A New Life Science

By this time these sporadic early works actually turned into a whole new area of quantum biology – a branch of biology that studies the participation of quantum physical effects, such as those involving electronic excited states and photons emitted by them. Now we see it as a single system of four main sections:

1. Biochemiluminescence studies, devoted to spontaneous endogenous (without any external physical and chemical influences) metabolic luminescence, mainly in the visible range: 380–1200 nm (started with B.N. Tarusov's works).
2. Photobiophysics (photonics, photobiology), devoted to the manifestation of electronic structures of substances

Fig. 15.4 Quantum biology: electronically excited states and quanta in the living world



by external visible and ultraviolet radiation with photosynthesis-induced electronically excited states (developed by A.S. Terenin, Yu.A. Vladimirov, S.V. Konev, and I.D. Volotovskiy).

3. Ultrasonic luminescence studies – research of water and aqueous systems luminescence (that is, the main environment of living organisms) under the influence of mechanical ultrasonic action (studied for low therapeutic modes of ultrasound by O.P. Tsvylev, A.I. Zhuravlev, and V.B. Akopyan).
4. Chemiluminescent analysis – identification of active metabolites by chemiluminescence generated during their interaction with probes: luminol, lucigenin, hydrogen peroxide, luciferin-luciferase system, etc.

This new (in my memory – A.Z.) and proved to be an all-encompassing life science makes it possible to study quantum processes in intact living systems and, thus, advance to fundamentally new levels in understanding the phenomenon of life (Fig. 15.4).

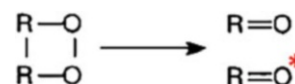
15.2 Mechanisms and Detection of Chemiluminescent Processes

15.2.1 Mechanisms

As mentioned above, the main source of UPE in the cell was considered to be lipid peroxidation, i.e. peroxidation of unsaturated fatty acid chains in them. The latter, both isolated and included in lipids, participate in two types of spontaneous processes. First, spontaneous free radical oxidation, the intermediate products of which are chemically determined peroxides ROOH, which, after accumulation, decompose to

the final products: aldehydes, ketones, alcohols, singlet oxygen, OH[•] radicals, and others (Kozin 1949; Emanuel and L'askovkaya 1961). Second, chemiluminescent processes – recombination of free radicals with the generation of EES.

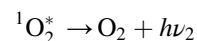
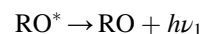
As shown by the studies of R.F. Vasiliev et al. on the example of hydrocarbons (Vasil'ev et al. 2002; Vasil'ev 1999; Fedorova 1979), the luminescence of auto-oxidizing systems is determined by the decomposition of peroxides, subsequent disproportionation of its products, with strong covalent bonds formed in the final products.



Some of the products turn out to be in a chemically active electronically excited state. These are mainly aldehydes, ketones (RO^{*}) and singlet oxygen (¹O₂^{*}).

The electronic excitation energy 35–90 kcal/mol (1.5–4.0 eV) is formed due to the difference between (1) the energy expended to break the weakened peroxide bonds –O~O– (40–50 kcal/mol) and (2) energy released during formation of the reaction products strong covalent bonds (80–95 kcal/mol).

After some time, electronically excited states relax, generating light quanta:



Thus, for spontaneous UPE, the preliminary formation of peroxides is necessary, which then decay with the formation

of electronically excited states (Zhuravlev 2011; Vasil'ev et al. 2002; Vasil'ev 1999).¹

15.2.2 What Part of Photon Emission Is Detected by the Device?

The intensity of spontaneous UPE, detected with experimental set-ups for measuring ultra-weak luminous fluxes (PMT), is defined by the following expression:

$$J = \omega \cdot k_{\text{ex}} \cdot k_{\text{lum}} \cdot k_{\text{PMT}} \cdot k_{\text{cathode}}$$

where:

ω – is the rate of peroxide decomposition, determined by the rate of free radical oxidation.

k_{ex} – quantum yield of excitation, equal to $\sim 10^{-4}$ ($10^{-3} - 10^{-5}$), according to R.F. Vasiliev (1963, 1965).

k_{lum} – quantum yield of luminescence, equal to $\sim 10^{-3}$ (Vasil'ev 1999; Fedorova 1979).

k_{PMT} – coefficient of light collection by PMT, equal to $\sim 4\%$, according to G.V. Margulis (Margulis 1972).

k_{cathode} – quantum yield of photocathode ($\sim 10\%$).

Calculations show that one pulse recorded by the photon counting device informs us about the decay of about one billion peroxides. Thus, one needs to have quite intense photo-generating processes going on in the system to be able to detect UPE.

Some technical tricks allow for improving characteristics of the experimental setups, but the main possibilities for increasing the system sensitivity lie at the biological level. Below we present the characteristics of spontaneous and enhanced luminescence of biological systems.

15.2.3 Spontaneous UPE

Luminescence is considered spontaneous if the rate of peroxides decay ω and the excitation constant k_{ex} are not affected by external factors, i.e. at the natural rate of electron-excited states generation $\omega \cdot k_{\text{ex}}$ (Zhuravlev 2011).

The intensities of spontaneous luminescence of various systems are given in Table 15.1.

When centrifuging tissue homogenates, the upper, lightest, lipid-rich layer emits light most intensely. Lipids were considered to be our 'inner sun', which determines the photon emission of all other biological objects.

Table 15.1 Intensity of spontaneous luminescence of various systems

| Object | Intensity of spontaneous UPE, photons/s/cm ² |
|-----------------|---|
| Tissue surfaces | ~ 10 |
| Blood serum | ~ 100 |
| Urine | $\sim 100-1000$ |
| Lipids | ~ 1000 |

Table 15.2 Spontaneous luminescence and activators

| Process | Scheme |
|---|--|
| Luminescence of primary electronically excited states (EES) | $\text{RO}^* \rightarrow \text{RO} + n_1 h\nu_1$ |
| Luminescence of activator | $\text{RO}^* + \text{A} \rightarrow \text{RO} + \text{A}^* \rightarrow \text{RO} + \text{A} + n_2 h\nu_2$ $n_2 \gg n_1$ |

15.2.4 How to Enhance Spontaneous UPE?

There are two different mechanisms for enhancing the spontaneous emission of the system: the use of activators and luminescent probes.

15.2.4.1 Activators

The use of activators was first proposed by R.F. Vasiliev (Vasil'ev and Vichutinskii 1962). *Activators* are substances that enhance spontaneous emission without changing k_{ex} . They intercept excitation from the primary EES RO^* , but do not affect generation of the EES or other processes in the system (Table 15.2). At the same time, activators have high luminescence quantum yield k_{lum} . Thus, they emit light at a much higher intensity, and with their own spectrum, but do not change the natural rate and dynamics of EES generation.

The known activators used in biological research are acridine orange, lanthanides, and europium.

15.2.4.2 Fluorescent Probes

Another option for enhancing spontaneous chemiluminescence was proposed by R.C. Allen (Allen 1989–1990). These are *luminescent probes* – substances that react with peroxides and ROS, generating their own EES. Thus, they increase k_{ex} , changing the concentration of primary EES and, consequently, break the spontaneity of radiation. Due to the high quantum yields of both excitation (k_{ex}) and emission (k_{lum}), luminescent probes multiply the intensity of UPE much more than activators: $n_3 \gg n_2 \gg n_1$.

One of the probes most widely used in chemiluminescence research is luminol (Fig. 15.5).

¹This is a personal interpretation of A.I. Zhuravlev. For the evidence-based schemes of molecular mechanisms, see Chaps. 8, 9, 10, 11, 12, 13, and 14 (editor's note).

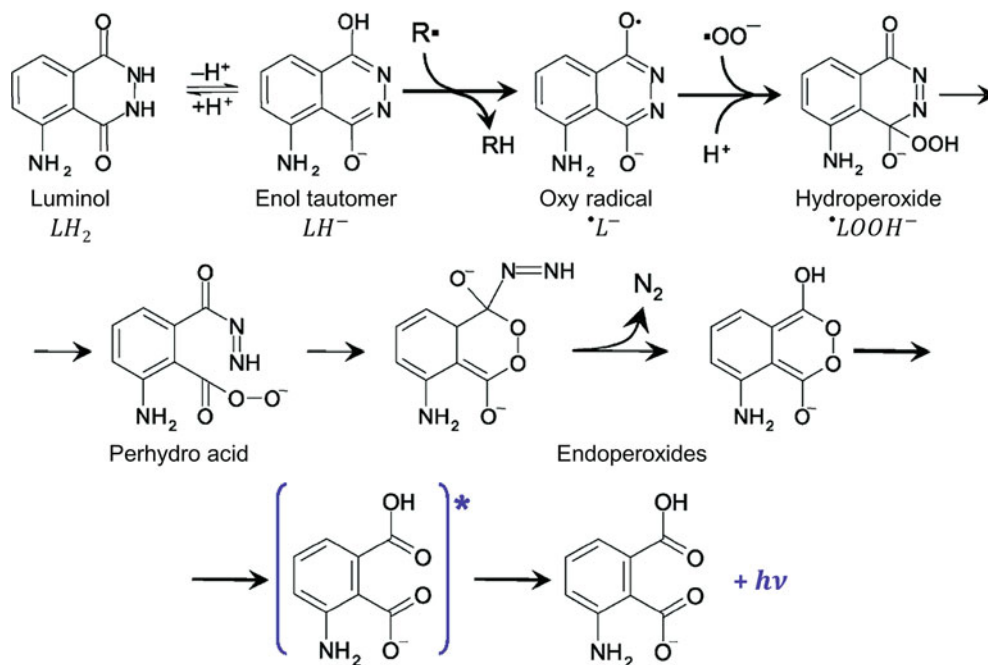


Fig. 15.5 Mechanism of luminol action. (Reprinted from Vladimirov and Proskurnina (2009). Copyright 2009, with permission from Springer Nature)

15.2.5 Informativeness of UPE

Spontaneous UPE informs the researcher about naturally occurring endogenous processes:

- Quantitatively – by its intensity.
- Qualitatively – by its spectrum.

The disadvantage of using spontaneous UPE is its low intensity.

As is known in physics, studying a molecular object, we change it and get an answer not from it or about it, but from the modified product we have created. A philosophical problem arises with the adequacy of the data we receive.

So, in the most common spectral studies in photobiology, we get an object, transfer it to an electronically excited state and receive an information response from this state, and not from the initial one. In contrast to this, spontaneous UPE contains information about those processes and substances that function without changes by chemical or physical external influences with their own intensity and spectrum.

Activated luminescence retains quantitative information about the process, while maintaining spontaneity, i.e. its intensity can be used for evaluating the intensity of natural EES-generating processes. Yet, it loses quality information, because it has the spectrum of the activator.

Luminol-dependent photon emission, most widely used by experimenters:

- Loses quantitative information about the process, because any probe reacts chemically only with a part of the free-radical and ROS products generated in the system.
- Loses qualitative information because it has its own spectrum.

Using luminol and other possible probes in UPE research allows chemiluminescent analysis of individual metabolites and their dynamics in health and disease. Yet, it is far from the research of spontaneous UPE in the full sense.

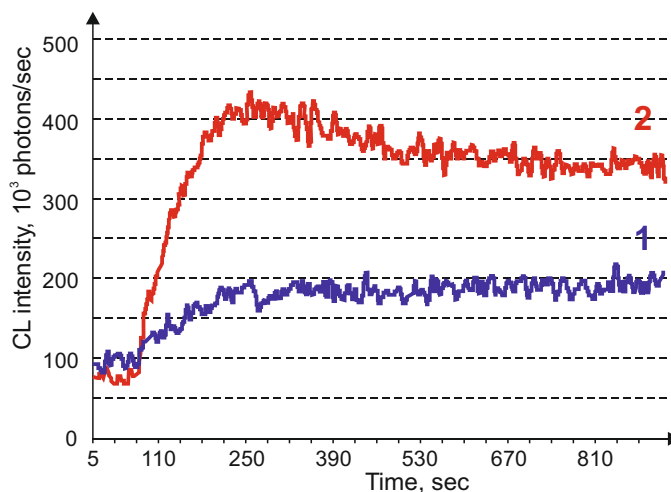
15.3 Autooxidation and UPE of Vegetable Oils

The spontaneous free-radical oxidation of unsaturated fatty acids is accompanied by two phenomena:

- Accumulation of peroxides, which can be detected chemically by iodometric titration. (Kozin 1949; Emanuel and L'askovkaya 1961).
- Spontaneous ultraweak luminescence (UPE), generated due to decay of a separate fraction of peroxides, which are chemically undetectable due to their instability (Zhuravlev 1957; Tarusov et al. 1961b; Zhuravlev 2011; Zhuravlev and Asanov 1991)².

²This is the author's (AZ) own classification; the current data are insufficient to classify peroxides into these two types (editor's note).

Fig. 15.6 Kinetics of chemiluminescence with the addition of 1 ml of H₂O₂ (3%) to 1 ml of native (1) and refined (2) sunflower oil



In model systems, e.g. oleic acid solutions, autoxidation starts at once and nearly all produced peroxides are chemically detectable. Contrary to that, the natural (unrefined) oils contain, in addition to triglycerides, a number of other substances, including carotenes, tocopherols, etc. that affect the rate of autoxidation. This leads to a pronounced induction period, during which the accumulation of chemically determined peroxides is completely suppressed, yet UPE is well observed. This suggests that unstable peroxides are formed and decay, generating electronically excited states, while stable peroxides are not formed. The presence of this induction period in oils indicates their bio-antioxidant activity.³ Practically, such bio-antioxidants can be determined by suppressing autoxidation of oleic acid, when added to it.

15.3.1 Autoxidation of Native Oils

With simultaneous determination of both chemiluminescence and autoxidation, we managed to investigate both oxidizability and antioxidant properties of different natural oils.

The sunflower oil exhibits a long (several days) induction period. Within this period chemically detectable peroxides do not accumulate in the system, but spontaneous UPE is observed (which manifests formation of unstable, chemically undetectable peroxides).

When hydrogen peroxide is added to the oils (to the final concentration of 1.5%), a multiple increase in chemiluminescence is observed. The refined sunflower oil, mostly devoid of antioxidants, enhances UPE from 10^5 to $4 \cdot 10^5$ quanta/s/

³By itself, the presence of a latency period is typical for all self-accelerating processes, so it does not prove the presence of antioxidant activity. The important feature is the length of this period and dynamics of further enhancement of the process. Actually, it's by analyzing these parameters that the author proves the antioxidant properties of natural oils (editor's note).

ml, while UPE intensity from unrefined oil is only doubled, from 10^5 to $2 \cdot 10^5$ quanta/s/ml (Fig. 15.6), which shows its high antioxidant capacity.

15.3.2 Autoxidation of Vegetable Oils with Different Habitat

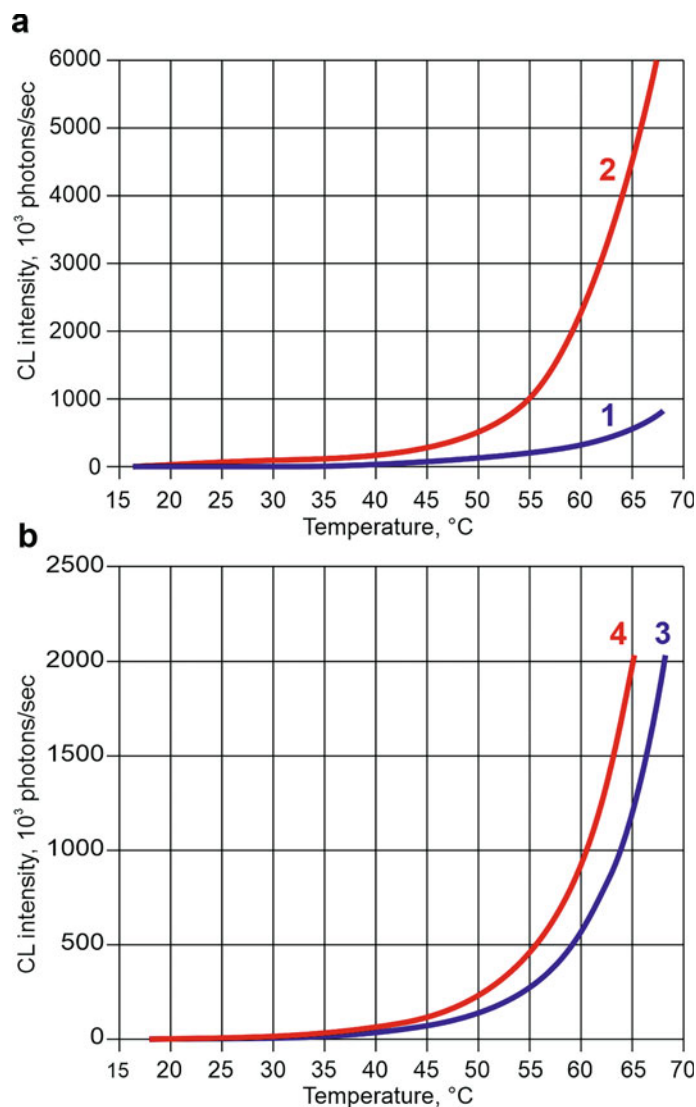
UPE, detected from oils, reflects their physicochemical characteristics, and the latter is tightly associated with the natural conditions in which the organism lives. The so-called *Ivanov's law*⁴ (Kozin 1949; Zhuralev 1957) says: lipids of northern plants and animals are more unsaturated than lipids of southern ones. This distinction was created evolutionarily, as more unsaturated lipids are 'more liquid' and freeze at lower temperatures. This is necessary for northern organisms so that they do not 'harden' at low temperatures. For animals hibernating, it is also necessary for returning to life with an increase in temperature in spring.

Indeed, the more southern olive oil, which contains mainly monounsaturated oleic acid, is more saturated (iodine number 75–88) than the more northern sunflower oil containing linolenic acid with three double bonds (iodine number 118–141). The northernmost linseed oil is even more unsaturated (iodine number 171–206) (Kozin 1949). Here we compare UPE and antioxidant qualities of these oils.

First of all, the more saturated olive oil (iodine number 75–88) gives UPE with lower intensity (26 quanta/second/ml), than the more unsaturated sunflower oil (iodine number 119–141, UPE intensity 57 quanta/second/ml) (Kozin 1949). For each of them, samples of refined oils, emit more intensely at all temperatures (Fig. 15.7). However, while the differences in olive oil are quite noticeable over the entire

⁴This might be the author's designation: we haven't found it in general literature (editor's note).

Fig. 15.7 Temperature dependence of chemiluminescence intensity for (1) native olive oil, (2) refined olive oil, (3) native sunflower oil, (4) refined sunflower oil



temperature range under study, in sunflower oil they become significant only at high temperatures.

15.3.3 Antioxidant Qualities of Different Vegetable Oils

An increase in UPE intensity from oils after refining (removal of pigments and other substances from them) shows the protective (antioxidant) effect of these impurities. This antioxidant effect can be determined after their complete oxidation at the end of the induction period, the length of which is a direct function of the amount of antioxidants and, possibly, quenchers in the system. However, the complete oxidation of these impurities takes several months. Therefore, the level of their antioxidant activity can instead be estimated by the effect they have on a model autooxidizing system, oleic acid. For this, the samples of these oils were added to oleic

acid in a ratio of 1:10 and both accumulation of stable peroxides and UPE intensity were measured over time (Fig. 15.8, Table 15.3).

Thus, unrefined (native) sunflower oil has the maximum antioxidant effect. It completely inhibits the accumulation of chemically titrated peroxides and significantly reduces the UPE intensity (which is not completely suppressed, however). Olive oil and refined sunflower oil have approximately the same antioxidant effect, reducing the spontaneous UPE intensity and inhibiting peroxides accumulation. Still, their antioxidant activity is much lower than that of unrefined sunflower oil, since they do not completely suppress accumulation of the peroxides.

Addition of 10% highly unsaturated northern flaxseed oil and fish oil to oleic acid completely suppresses accumulation of chemically titrated peroxides but weakly inhibits UPE, similar to unrefined sunflower oil (results not shown).

Fig. 15.8 Luminescence dynamics of oleic acid (1) and oleic acid with additives of various oils: olive (2), sunflower native (3), and sunflower refined (4)

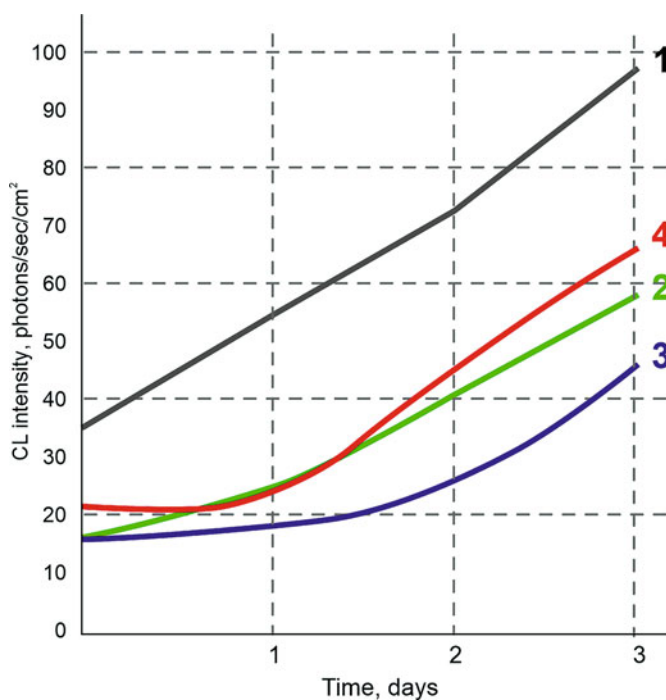


Table 15.3 Dynamics of the accumulation of chemically titrated peroxides for three days in the dark at 30 °C (peroxide number)

| Day | Oleic acid (control) | Oleic acid +10% olive oil | Oleic acid +10% refined sunflower oil | Oleic acid +10% non-refined sunflower oil |
|-----|----------------------|---------------------------|---------------------------------------|---|
| 1 | 4.0 | 5.0 | 6.0 | 6.0 |
| 2 | 39.0 | 9.8 | 9.8 | 5.8 |
| 3 | 87.0 | 15.0 | 13.8 | 5.8 |

Thus, for all oils, a high antioxidant activity is observed both in relation to the formation of chemically titrated peroxides and to unstable peroxides that decompose with subsequent luminescence.⁵ The antioxidant activity of native oils is always higher than that of purified–refined oils. The antioxidant activity of oils prepared from more northern plants appears higher than that of oils prepared from more southern plants. For example, the antioxidant activity of sunflower oil is higher than that of olive oil (more southern), but lower than that of linseed oil (more northern).

Thus, in the development of the above-mentioned Ivanov’s law, one more pattern can be formulated – *Zhuravlev’s rule* (Zhuravlev 2011, 2014): Fats of more northern plants and animals have a higher concentration of bio antioxidants and higher antioxidant activity.

This is also quite understandable. More unsaturated lipids, characteristic of more northern species, are oxidized easier and faster. To compensate for this ‘deficiency’, they need an

increased content of natural antioxidants – which is observed in experiments.

15.4 The Medical Use of the UPE Phenomena

In addition to the above data on the saturation and antioxidant activity of natural oils, the UPE phenomenon has made it possible to reveal a number of medically important phenomena. Today, UPE and its changes in various conditions can serve to assess important medical conditions, as well as for purely fundamental research. The field of quantum biology, mentioned above, is increasingly entering science and medicine, becoming an integral part. Here are some examples in which we were fortunate enough to be involved.

15.4.1 Stress

Already in 1974, it was found that with all types of emotional stress: pain, heat, food – the intensity of UPE from blood serum and urine increases, and characterizes the stress depth

⁵This is the author’s (AZ) own classification; the current data are insufficient to classify peroxides into these two types (editor’s note).

Table 15.4 The main characteristics of alimentary obesity as free-radical pathology in rats, obtained from blood plasma

| Group of the rats | Obesity (Lee index, g/cm) | Spont. UPE, imp/s | Activated UPE, imp/s | Diene conjugates, arb. units | Malondialdehyde, nM | Tocopherol, uM | Time of full haemolysis, s |
|---------------------------------------|---------------------------|-------------------|----------------------|------------------------------|---------------------|----------------|----------------------------|
| Control (main diet) | 132 | 1.86 | 7.6 | 2.57 | 2.24 | 4.2 | 670 |
| Main diet + diludin (12–14 mg/kg/day) | 234 | 1.62 | 7.3 | 1.85 | 1.8 | 5.9 | 688 |
| Main diet +50% fat | 430 | 6.27 | 41.56 | 9.10 | 9.0 | 1.6 | 280 |
| Main diet +50% fat + diludin | 366 | 2.68 | 8.57 | 4.08 | 4.0 | 2.2 | 505 |

1 – Control group (normal diet); 2 – Control group with additional antioxidants (diludin) in the diet; 3 – Alimentary obesity (diet enriched with fat by 50%); 4 – Alimentary obesity (diet enriched with fat by 50%) with additional antioxidants (diludin) in the diet

(Zhuravlev 1974). Inadequately high physical activity, even for top-qualification Olympics athletes, has a stressful effect, increasing UPE from blood serum and urine. Adequate loads (training), on the contrary, normalize metabolism, lowering high and increasing low levels of UPE from blood serum and urine (Zhuravlev 2011). The boundary between adequate and stress loads can be assumed by the UPE increase threshold.

Protection against stress is:

1. Adequate physical activity.
2. Antioxidants and extinguishers.

15.4.2 Obesity

A comprehensive study of obesity in rats was carried out by O.G. Yarosh (Yarosh 1996; Yarosh and Zuravlev 2003). Characteristic signs of free radical pathology have been shown for the group of obese rats (from a diet 50% richer in fat). This group had dramatic differences from control in all the main parameters, evaluating free-radical processes (see Table 15.4).

Thus, the main effects were:

1. Decrease in the level of tissue bioantioxidants (tocopherol) in obese rats.
2. Activation of free radical processes (a fourfold increase of blood plasma UPE) for obese rats and their suppression by antioxidants;
3. Accumulation of free radical products (diene conjugates; malondialdehyde) in obese rats.
4. Damage to cell membranes (dramatic decrease in hemolytic resistance of erythrocyte membranes to acetic acid), obviously caused by free-radical processes, activated in obese rats.
5. The effect of antioxidants was insignificant in healthy animals and sharply expressed in the normalization of all indicators – in the group of obese animals.

Of the investigated parameters, the most informative can be called UPE (both spontaneous and activated) from blood

plasma: both its enhancement in obesity and normalization under antioxidant action.

Of the studied antioxidants, lipoic acid, containing two sulfhydryl *SH* groups, showed the most pronounced preventive effect (data not shown).

We can conclude, that the main prophylactic and therapeutic agents for obesity, in addition to physical activity and dietary restrictions, should be antioxidants in the diet, compensating for the decrease in the level of tissue bioantioxidants.

Tissue bioantioxidants are not drugs, but metabolites, and their biological role and the laws of functioning of the bioantioxidant system are manifested when their level in tissues decreases below normal. The bioantioxidant system can be considered one of the immune systems of the organism.⁶

15.4.3 Nutritional Atherogenesis

Overfeeding rabbits with technical cholesterol causes food stress with increased serum luminescence. After 60–80 days, the body replaces active unsaturated fats and phospholipids with protective diluents: inert cholesterol and saturated fatty acids. At these initial stages of atherosclerosis, the luminescence intensity, and hence the free radical oxidation rate, decreases. With continuing the stress factor action, atherosclerosis develops, turning into pathology.

Yet, there is no need to remove cholesterol in such (or analogous) cases. It is necessary to remove the stressful causes activating free radical peroxidation and take antioxidants and quenchers.

15.4.4 Lesion – Proliferation – Cancer

In 1962, A.I. Zhuravlev showed that cancerous tissues emit less visible UPE, than tissues of normal organs (Zhuravlev et al. 1963).

⁶As above, this is a personal interpretation of the author (editor's note).

Normally, the products of weak free radical peroxidation are repressive regulators of cell division (Burlakova 1968). When tissue is damaged (incision, wound), the body seeks to restore the damage by accelerating cell proliferation due to the accumulation of antioxidants at the site of injury and a decrease in the repressive effect of free radical products (Zhuravlev 2011).⁷ Chronic damage leads to a constant increase in antioxidants and chronic proliferation. Chronic proliferation inevitably leads to the emergence of constantly and regularly dividing cancer tissue with the antioxidant levels increase and luminescence suppression. In this sense, the tumour is an antioxidant parasite.

15.4.5 Rejection of a Transplanted Organ

A multiple increases in the intensity of urine fluorescence manifests the onset of a rejection crisis of the transplanted kidney 2–3 days earlier than other clinical symptoms (Tsy-pin et al. 1975). This phenomenon allows to sharply reduce the dose of immunosuppressants and the risk of complications (Tsy-pin et al. 1975).

15.4.6 Chemiluminescence in the Antigen-Antibody Reaction

In 2000, A. Wentworth et al. found that in sensitized animals, all antibodies (type IgG) containing tryptophan and S – H groups, form superoxide radical anion $O_2^- \cdot$ in the antigen-antibody reaction (Wentworth et al. 2000). Subsequently, it transforms into H_2O_2 and singlet oxygen 1O_2 . They also showed that one-electron oxygen reduction by antibodies occurs without the participation of metal-intermediate oxidative processes, and argued that immunoglobulins can not only recognize, bind, and transport antigens, but also destroy it.

Later, O.G. Yarosh and A.I. Zhuravlev found spontaneous UPE at antigen—antibody reaction. They were using blood serum of rats sensitized with the human albumin and were adding the antigen – human albumin to the system (Yarosh 1996; Yarosh and Zhuravlev 2003). It was shown that during the interaction of antigen-sensitized blood serum, the intensity of spontaneous UPE, equal to 13 ± 1 impulses / s, significantly exceeds that for non-sensitized animals, which equals to only 5 ± 2 impulses/sec. The UPE intensification begins immediately after the reagents have been drained and begin to decrease after 15–20 min. When the reagents are stored, the effect persists for 2–3 days. Such prolonged luminescence suggests activation of free radical lipid oxidation in the system.

The ability of IgG to regulate free radical oxidation also shows its antioxidant activity due to the presence of sulfhydryl S – H groups (Zenkov et al. 2001).

15.5 Prospects

It is necessary to move from a quantitative to a qualitative spectral characteristic of biological autoluminescence. This is possible with an increase in the sensitivity of the experimental set-ups, first of all, due to an increase in the quantum yields of PMT photocathodes: from 10% to 70–90%, as well as by increasing light collection, etc.

This will allow qualitative spectral determination of individual molecular participants of chemiluminescent processes and quantum pathologies. We are moving from molecular biology to quantum biology. The future belongs to it.

References

- Allen RC (1989–1990) Chemiluminescence and the Study of Phagocytosis Biochemistry and Immunology. In: Biological Luminescence. World Scientific, Singapore, London, Hong-Cong, pp. 429–449
- Baldwin TO (1996) Firefly luciferase: the structure is known, but the mystery remains. *Structure* 4 (3):223–228. doi:[https://doi.org/10.1016/S0969-2126\(96\)00026-3](https://doi.org/10.1016/S0969-2126(96)00026-3)
- Boveris A, Chance B (1973) The mitochondrial generation of hydrogen peroxide. General properties and effect of hyperbaric oxygen. *The Biochemical journal* 134 (3):707–716. doi:<https://doi.org/10.1042/bj1340707>
- Burlakova EB (1968) Role of antioxidants in physical and chemical processes of regulation of cell expansion. In: *Fiziko-khimicheskiye osnovy avtoregulyatsii v kletkah* [Physics and chemistry of autoregulation in cells]. Nauka, Moscow, pp. 15–25
- Burlakova EB, Dzhalibova MI, Kobliakov VA, Koliada A, Molochkina EM (1978) Narusheniia v reguliatsii aktivnosti mikrosomal'nykh fermentov lipidami pri khimicheskom kantserogeneze v pecheni [Disorders in the regulation of the activity of microsomal enzymes by lipids during chemical carcinogenesis in the liver]. *Doklady Akademii nauk SSSR* 241 (2):477–480
- Burlakova EB, Molochkina EM, Pal'mina NP (1980) Role of membrane lipid oxidation in control of enzymatic activity in normal and cancer cells. *Advances in enzyme regulation* 18:163–179. doi:[https://doi.org/10.1016/0065-2571\(80\)90014-x](https://doi.org/10.1016/0065-2571(80)90014-x)
- Emanuel NM, L'askovkaya YN (1961) Inhibition of lipid oxidation processes (In Russian) [Tormozheniye protsessov okisleniya zhirov]. Pishchepronizdat, Moscow
- Fedorova GF (1979) Quantitative study of chemiluminescence from oxidation of hydrocarbons in solutions (abstract of a thesis). Institute of chemical physics, Moscow
- Kozin II (1949) Chemistry and commodity research of edible fats (in Russian). Gostorgizdat, Moscow
- Margulis GV (1972) Calculation of light collection from the cylindrical source of installation with photomultiplier FEU-42 as a detector. In: Zhuravlev AI (ed) *Sverkhslabije svechenija v biologii* [Ultraweak photon emissions in biology]. Nauka, Moscow, pp. 236–238
- Sharipov GL, Kazakov VP, Tolstikov GA (1990). *Khimiya i Khemilyuminestsentsiya 1,2-dioksetanov* [Chemistry and Chemiluminescence of 1,2-Dioxetanes]:252

⁷The author's personal interpretation (editor's note).

- Szent-Györgyi A (1960) Introduction to a Submolecular Biology. Academic Press.
- Tarusov BN, Polivoda AI, Zhuravlev AI (1961a) Detection of chemiluminescence in the liver of irradiated mice (In Russian). *Radiobiologiya* 1 (1):150–151
- Tarusov BN, Polivoda AI, Zhuravlev AI (1961b) Study on ultra-weak spontaneous luminescence of animal cells (in Russian). *Biofizika (Russ)* 6 (4):490–492
- Tarusov BN, Polivoda AJ, Zhuravlev AI (1961c) Low Intensity Radiations from Animal Tissues Their Mechanism and Kinetic Paper presented at the 1 International Biophysics Congress, Stockholm
- Tsvylev OP, Zubkova SM, Zhuravlev AI (1974) Registration of endogenous ultraweak emission of rat mitochondria in case of normal metabolism In: Ultraweak emission in medicine and agriculture. - Moscow University, Moscow, pp 49–58
- Tsylin AB, Rogatsky GG, Zhuravlev AI, Burdina GV, Asanov M (1975) Inventor's certificate "Method of transplant rejection diagnostics". USSR Patent
- Vasil'ev RF (1965) Chemiluminescence in solutions I. Methods of identification of excited states (In Russian). *Opt Spektrosk+* 18 (2): 236–244
- Vasil'ev RF (1999) The problem of transformation of chemical energy into light. Cyclical peroxides as model objects for quantum-chemical study of chemiexcitation processes (In Russian) *Kinetika i Kataliz [Kinetics and Catalysis]* 40 (2):192–200
- Vasil'ev RF, Vichutinskii AA (1962) The enhancement of chemiluminescence by the addition of luminescent substances (In Russian). *Zh Fiz Khim* 36 (8):1799–1800
- Vasil'ev RF (1963) *Lyuminesentsiya pri khimicheskikh reaktsiyakh v rastvorakh* (In Russian)[Luminescence Accompanying Chemical Reactions in Solutions]; Doctoral Dissertation. Moscow
- Vasil'ev RF, Naumov VV, Fedorova GF (2002) Molecular chemiluminescence of lipids and its influence on the determination of antioxidants. Paper presented at the Bioantioxidant-VI, Moscow
- Vladimirov YA, Proskurnina EV (2009) Free radicals and cell chemiluminescence. *Biochemistry (Moscow)* 74 (13):1545–1566. doi: <https://doi.org/10.1134/s0006297909130082>
- Wentworth AD, Jones LH, Wentworth P, Janda KD, Lerner RA (2000) Antibodies have the intrinsic capacity to destroy antigens. *Proceedings of the National Academy of Sciences* 97 (20): 10930. doi:<https://doi.org/10.1073/pnas.97.20.10930>
- Yarosh OG (1996) Spontaneous and activated biochemiluminescence and some parameters of lipid metabolism of blood of sows and rats with obesity: PhD thesis (Biological Sciences). Moscow
- Yarosh OG, Zuravlev AI (2003) Optimization of biochemiluminescence and free-radical oxidation in obesity. *Veterinariya [Veterinary]*
- Zenkov NK, Lankin VZ, Menshchikova EB (2001) Oxidative stress. IAPC Science / Interperiodics, Moscow
- Zhuravlev AI (1957) Influence of ionizing radiation on physicochemical and organoleptic properties of sunflower-seed oil. *Problems of nutrition* (4):60–64
- Zhuravlev AI (1974) Spontaneous metabolic ultraweak emission of blood plasma and blood serum in visible range In: Ultraweak emission in medicine and agriculture. - Moscow University, Moscow, pp 15–17
- Zhuravlev AI (2011) *Kvantovaya biofizika zhivotnykh i cheloveka [Quantum biophysics of animals and humans]*. Binom, Moscow
- Zhuravlev AI (2014) *Antioksidanty. Svobodnoradikalnaja patologiya [Antioxidants. Free-radical pathology]*. White Alves, Moscow
- Zhuravlev AI, Asanov MA (1991) Sensitivity and working characteristics of modern chemiluminometers. *Biophysics* 36 (3): 486–495
- Zhuravlev AI, Tarusov BN, Yesakova TD (1963) Novel physicochemical feature of cancer tissues. Paper presented at the Proceedings of VIII International Anti-cancer Congress, Moscow



Ultraweak Photon Emission from the Human Body in Relation to Anatomy and Histology

Roeland van Wijk and Eduard van Wijk

16.1 Introduction

Emission of ultraweak light from a human subject has been unequivocally demonstrated utilizing highly sensitive photomultiplier tubes and CCD imaging devices (Kobayashi 2003, 2005; Kobayashi et al. 2009; Rastogi and Pospisil 2011; Van Wijk 2014; Van Wijk and Van Wijk 2004, 2005; Van Wijk et al. 2006a, b, 2007, 2013, 2014). It is commonly accepted that ultraweak photon emission (UPE) is created within cells, in the mitochondrial compartments, when oxygen is available, and respiration takes place (Van Wijk et al. 2020). The biochemical production of photons in living cells has been explained by a two-step process: (a) reactions that lead to free oxygen radicals and their consecutive involvement in reactive oxygen species and lipid peroxidation reactions, and (b) formation of photons of different energy level depending on the excited molecular states that return to the ground state. In cells, it is a network of reactions that is responsible for the photon emission with wavelengths that are dependent on the energy, varying from (ultra) violet to infrared. For further details, the reader is referred to Chap. 28, from the same authors.

There is a severe gap in knowledge about the events taking place following the production of photons when dealing with complex organisms such as humans. Photons are commonly recorded non-invasively by a photomultiplier or imaging device that is directed towards and placed in proximity to the body but not touching the skin. The relevant questions regarding the gap can be formulated in two ways, depending on the point of view. The first is: Where do spontaneously emitted photons from a human body come from; ‘spontaneous’ being defined as not induced, for instance, by UV light or hydrogen peroxide treatment. The second is, starting from the other end: What happens with photons from the

metabolizing cells of body tissues? In this chapter, we focus on the gap in knowledge from the first point of view.

Most studies of non-invasively recorded UPE from a human body have focused on ‘photons originating from oxidative processes in skin’ following UV exposure (Sauermann et al. 1999; Rastogi and Pospisil 2011; Tsuchida et al. 2019). This induced UPE has commonly been studied in association with biological skin effects – both negative (erythema or skin aging) and positive effects (production of provitamin D3) – and utilizing data on the penetration depth of ultraviolet, visible and infrared radiation in biological tissue (Bruls et al. 1984; International Programme on Chemical Safety 1994). The conclusion is further confirmed by the (partial) inhibition of UPE if antioxidants were rubbed into the skin (Egawa et al. 1999; Evelson et al. 1997; Rastogi and Pospisil 2011; Sauermann et al. 1999). A recent imaging study has indicated that UV-induced UPE from human skin included UPE not only from the epidermis but also from the dermis layer (Tsuchida et al. 2019). The contributions of the dermis against total UPE is approximately 60–80% for UVA and 20–40% for UVB; differing contributions of UVA and UVB are explained by the higher transmittance of UVA in the dermis as compared with that of UVB.

The question about the spontaneous, i.e. non-induced UPE from the body, however, has remained unsolved. In this respect, the study on the influence of oxygen on UPE without excitation from outside may throw more light (Nakamura and Hiramatsu 2005). Lowering the oxygen concentration in the air around the palm of the hand using nitrogen gas as a replacement resulted in a decrease in the intensity of the UPE from the palm; about 40% of the UPE was based on external oxygen on the surface of the skin. The remaining 60% is from the inside of the skin. But does the latter part originate from the epidermis or the subjacent connective tissue layer – the derma, or perhaps from other connective tissue layers beneath the latter, such as the hypodermis or

R. van Wijk · E. van Wijk (✉)
Meluna Research, Wageningen, The Netherlands
e-mail: evanwijk@melunaresearch.nl

deeper structures such as deep fasciae, aponeuroses and periosteum (Standring 2008; Langevin and Huijing 2009).

In this respect, it must be taken into account that cell density is rather low in connective tissue as compared to the metabolically active cell layers of the epidermis. It is evident that in order to elucidate the entire mechanism of the spontaneous UPE emission, we need additional approaches. In this chapter, we have introduced an additional approach: comparing body regions with high and low UPE regarding anatomical properties of skin and underlying subjacent connective tissue layers. For this reason, we present first a short anatomical overview of the skin with reference to external light transport modeling.

16.2 Skin: Histology and Light Transport Modeling

The two layers of the skin – epidermis and derma – have different properties with respect to their pathway for photons, resulting from differences in scattering and absorption coefficients, which are highly wavelength dependent (Anderson and Parrish 1981). The different light properties are related to the differences in structure between the epidermis and dermis. In short, the epidermis varying from 0.07 to 0.12 mm in thickness on most parts of the body (on the palms and palmar surface of fingers it may reach 0.8 mm), is a stratified epithelium. Although the terminology of skin histology has changed regularly, we have in this chapter adapted the terminology of classic textbooks in histology (Maximow and Bloom 1960; Montagna 1956; Rothman 1954). From deep to superficial, we distinguish: (a) the layer of Malpighi (or stratum germinativum) touching the derma; (b) the granular layer (or stratum granulosum plus lucidum); and (c) the horny layer (or stratum corneum). The deepest layers of cells of the stratum germinativum are cylindrical; the cells above these, but still in the stratum germinativum, are polyhedral, and under the granular layer they become flattened. Mitotic figures occur rather frequently in this layer. The granular layer which continues to consist of flattened cells, contains cytoplasm with irregularly shaped granules of keratohyalin. With the gradual increase in size and number of granules, the nucleus disintegrates and metabolic activity is depressed. When cells have only the remains of the nucleus, they contain refractile eleidin droplets instead of the keratohyalin granules. Finally, at the outside, the epidermis is represented by the thick stratum corneum, consisting of layers of hornified cells, formed from keratin, a product of cellular proteins, the most peripheral part is constantly being desquamated. The epidermis is entirely devoid of blood vessels; it is nourished by the tissue fluid which penetrates the intercellular spaces of the Malpighian layer from capillaries in the underlying connective tissue.

The derma has a completely different structure. With an average thickness of approximately 1 to 2 mm (3 mm or more on the palms), the main dense portion of the derma is called the reticular layer. The reticular layer consists of bundles of collagenous fibers which form a dense network. The surface of the derma that is fused with the epidermis is called the papillary layer. In the papillary layer, the collagenous bundles are much thinner and more loosely arranged. The elastic fibers of the derma form abundant, thick networks between the collagenous bundles. Elastic fibers in the papillary layer are much thinner and form a continuous fine network under the epithelium. Cells are rather rare in the derma: most typical are fibroblasts.

Light transport modeling commonly used scattering coefficients measured from experimental techniques originating from Mie scattering due to collagen fibers and from Rayleigh scattering due to small tissue structures (Weber et al. 2011). The scattering coefficients and absorption coefficients are used to calculate photon distributions in scattering and absorbing media using a Monte Carlo modeling of a multi-layered skin model for modeling light transport, wherein elastic scattering results from inhomogeneities in the skin's index of refraction corresponding to the physical boundaries of anatomical features, such as collagen fibers. Such simulations also include the thickness of the epidermis and dermis depth (Ash et al. 2017). Those studies have shown that for external light, there is a greater absorption of shorter wavelength light at the front end of the epidermis which is due to the backscatter into the epidermis from the boundary of the dermal layer. The backscatter or reflection at the boundary layer is increased by the different refractive indices of the epidermis and dermis causing photons from the epidermis to the dermis to travel back again. The studies also indicated that once the light has passed through the boundary layer, its absorption rapidly reduces by greater than 50% for all wavelengths, due to the significantly increased mean free path in the dermis relative to the epidermis.

The light transport modeling studies have accentuated the situation for skin exposed to external light, but not, yet, for photon distributions of endogenously available photons, either produced by metabolizing cells locally or produced by other means. Models for endogenous production, transport and distribution of photons have not been developed. For this purpose, studies on the non-invasively recorded spontaneous photon emission in a comparison with local histology typing may be a first step. This chapter reviews three lines of research. First, the studies of the human body's UPE spatial characteristics. Second, the comparison of high-emitting locations with distinct anatomical features suggests a role for the fascial system. Third, the physiology of the fascial system is shortly described and related to studies on the temporal characteristic of human UPE.

16.3 Human Photon Emission Recording Technology Has Revealed an Anatomical UPE Body Pattern

The commonly reported UPE from human subjects is less than a few hundred photons per second per square centimeter (Cohen and Popp 1997; Jung et al. 2005; Zhao et al. 2016). For a photon at the visible wavelength of 500 nm, a photon count rate of 100 photons per second per square centimeter corresponds to an irradiance of $3.98 \cdot 10^{-17} \text{ W} \cdot \text{cm}^{-2}$ or $0.04 \text{ fW} \cdot \text{cm}^{-2}$. The extremely small intensity makes it impossible to detect UPE without highly sensitive photon-detecting devices and a completely darkened measurement environment. It is little known that this research started in the United Kingdom by Edwards and colleagues in 1989 (Edwards et al. 1989), addressing temporal and spatial fluctuations of human body photon emission. The protocol included a photomultiplier tube cooled to a temperature of $-23 \text{ }^\circ\text{C}$ in a light-tight dark room. The researchers reported spatial and temporal fluctuations but concluded that the sensitivity was not large enough to draw definite conclusions. In Germany, Popp and colleagues began the human UPE recordings in 1993 utilizing a temperature-controlled dark-room that included a bed upon which subjects were recorded in lying or sitting position (Markert 2000). The photomultiplier system with a 160–630 nm spectral sensitivity was hung on rails fixed on the ceiling and walls, allowing it to scan over any surface area of a subject. A spacer (a ring 7 cm high) at the front port of the photomultiplier tube not only facilitated the measurement of 9 cm diameter anatomic areas at a fixed distance but also avoided condensation (from perspiration) at the photomultiplier window. In 1994 and 1995, during the technological developments, the device was utilized to record emissions from 80 healthy subjects over various body areas confirming Edward's data of variations in intensity over various areas of the human body.

In 2000, the research groups of Van Wijk and Popp began to collaborate in an extensive systematic multi-site recording of human emission taking also more care for the subjects to be measured. A special pre-measurement protocol was developed to avoid delayed emission by dark adaption of the subject prior to positioning in the dark room. Moreover, when the photomultiplier tube was placed above the designated areas of the body, a time slot of at least 2 minutes was used for recording UPE (Van Wijk and Van Wijk 2004, 2005). Regarding the body locations for multi-site registration, a total of 29 sites were selected in such a way that the distribution of emission could be studied as right/left symmetry, dorsal/ventral symmetry, and the ratio between torso, head and extremities. The sequence of recording body locations was standardized beginning with the ventral side

and the forehead. The locations were measured by moving the photomultiplier from head to feet and at each level from right to left. When all ventral body locations were measured, the subject turned and all dorsal locations were measured, in the direction from feet to head. In such a routine each right site location was directly followed by the left location. It was evident that large differences in time did occur between the head and feet of the ventral side as well as the dorsal side. Even larger time differences (>1 hour) occurred between the dorsal and ventral body locations of the upper torso and the head.

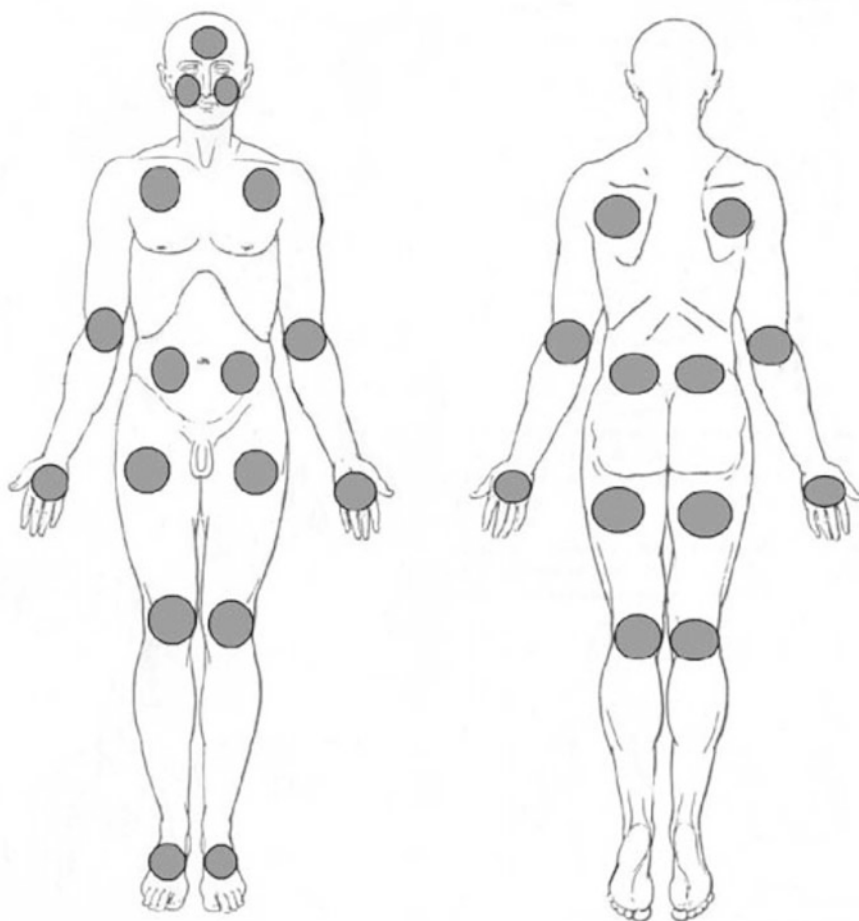
The recording of 29 selected body sites in the morning and in the afternoon of the same day was carried out for 4 (3 male and 1 female) subjects (Fig. 16.1).

Figure 16.2a–d demonstrates that variation in photon count over the body showed a systematic pattern for the four subjects. The thorax/abdomen region emitted the lowest intensity. In contrast, the upper extremities and the head region revealed the highest intensity. Generally, a high degree of left/right symmetry and (to a less degree) dorsal/ventral symmetry were observed. Higher values were also recorded for elbows, knees and feet, but in these cases, dorsal-ventral symmetry was not observed, whereas right-left symmetry in knees, hands and elbows remained. The loss in dorsal/ventral symmetry was typically observed in body parts that are more shaped, which may be interesting to clarify any relation between UPE and anatomy. This first systematic multi-site recording shows that each of the four participants has its own level of UPE and that the 'exceptional' UPE values belong to body parts that are characterized by their anatomical peculiarities. The minimal UPE values of the participants are much the same, 8–10 counts per second (cps) (including a background of 5–6 cps), whereas the exceptional values fluctuate more between the participants, reaching values between 14 and 40 cps.

The next study tested the hypothesis that the emission gradient of the superior part of the body represents a common human emission pattern and that hands and head are the highest UPE locations. In this multi-site UPE recording study, 60 healthy (male) human subjects participated and 12 anatomical locations were selected on the upper frontal torso, head and hands (Fig. 16.3) (Van Wijk et al. 2006a, 2006b).

As in the previous studies, photon emission of the abdomen was the lowest, values increased along the central axis rostrally to the throat, and the highest values were observed over the throat, cheeks and hands. For all subjects, data suggested that each individual anatomic position participated in the total emission with a predictable, constant percentage (independent of the total emission). Moreover, all subjects demonstrated a high degree of left/right symmetry.

Fig. 16.1 Map of locations for measurement of spontaneous photon emission over the anterior (left figure) and posterior (right figure) of the human body



More detailed body information came available from body photon emission imaging. Such technology was developed in Japan by Inaba and coworkers (Usa et al. 1994; Kobayashi et al. 1996; Inaba 1997). In a continuing process of improving UPE imaging technology, Kobayashi and colleagues reported the first human UPE images utilizing a highly sensitive, cryogenically cooled, charge-coupled device (CCD) camera system placed in a dark room (Kobayashi 2003; Kobayashi et al. 2009). It facilitated the imaging of the UPE from the upper torso, head, neck and arms (Fig. 16.4, see also Chap. 7 of this book) (Van Wijk et al. 2006a, b).

The images confirmed that UPE intensity around the face and neck was highest and gradually decreased over the torso and subsequently the abdomen (Fig. 16.4a) and to its lateral dimensions. Dorsally, the highest intensity was emitted from the neck (Fig. 16.4b). The image of the arm of the same subject illustrated how the low intensity of the body was extended over a large part of the arm increasing over the wrist and hand (Fig. 16.4c). Furthermore, novel interesting UPE information showed typical body locations that emitted far above or below the common range of an individual's emission. The most extreme UPE values are shown by the low-intensity eyes and the high-intensity fingernails

(Fig. 16.5). In the next paragraph, we discuss a few of these high-emission locations.

16.4 Considerations About a Relation Between High-Intensity UPE and Anatomy/Histology

The skin as a common boundary surface of the body shows transitions in the UPE intensity that is non-invasively recorded at typical locations, such as the knee, wrist, neck and hand sites. In most of these regions, the increased UPE is not easily explained by the active metabolizing cells of the epidermis. The structuring and thickness of epidermal layers in these regions are highly identical to the adjacent areas with altered light intensity. We concluded that, in general, epidermal photon production is not likely responsible for the typical locations with high emission intensity, and that we have to consider a possible role of tissue structure below the epidermis: the derma of the skin, and beneath it the hypodermis, consisting of collagenous and elastic fibers that pass directly into those of the derma. From histological data, it is commonly accepted that, where skin is flexible, the fibers are few;

and where it is closely attached to the underlying parts, such as on palms, they are thick and numerous (Singer 1935; Clemente 1985; Standring 2008). Furthermore, below the hypodermis, we find internal tissues and organs in close contact with the global organization of the fascia deeper in the body. Focusing on the fascial structure, it is also commonly accepted that the function of the fascia tends to dictate its structure. Fascia must be capable of significant distortion in multiple planes of direction and return rapidly to its native shape. This type of action is met by fascia constructed out of irregular connective tissue where the fibrous component is interwoven. This is opposed to the constructions containing

parallel arrays such as are seen in tendons, ligaments, aponeuroses and joint capsules. Due to the highly regular arrangement of collagen fibers in a tendon, ligament or aponeurosis, these structures can provide maximal resistance to stretch in *one or a limited* number of directions. Furthermore, the density of the fibrous component of the fascia will vary with its location and function. The fascia underlying the skin must be very movable and therefore has a lower density of collagenous fibers. Alternatively, the fascia that invests muscle, ligament, tendon or joint capsule is providing a stronger support role, the density of its collagen fibers being considerably higher.

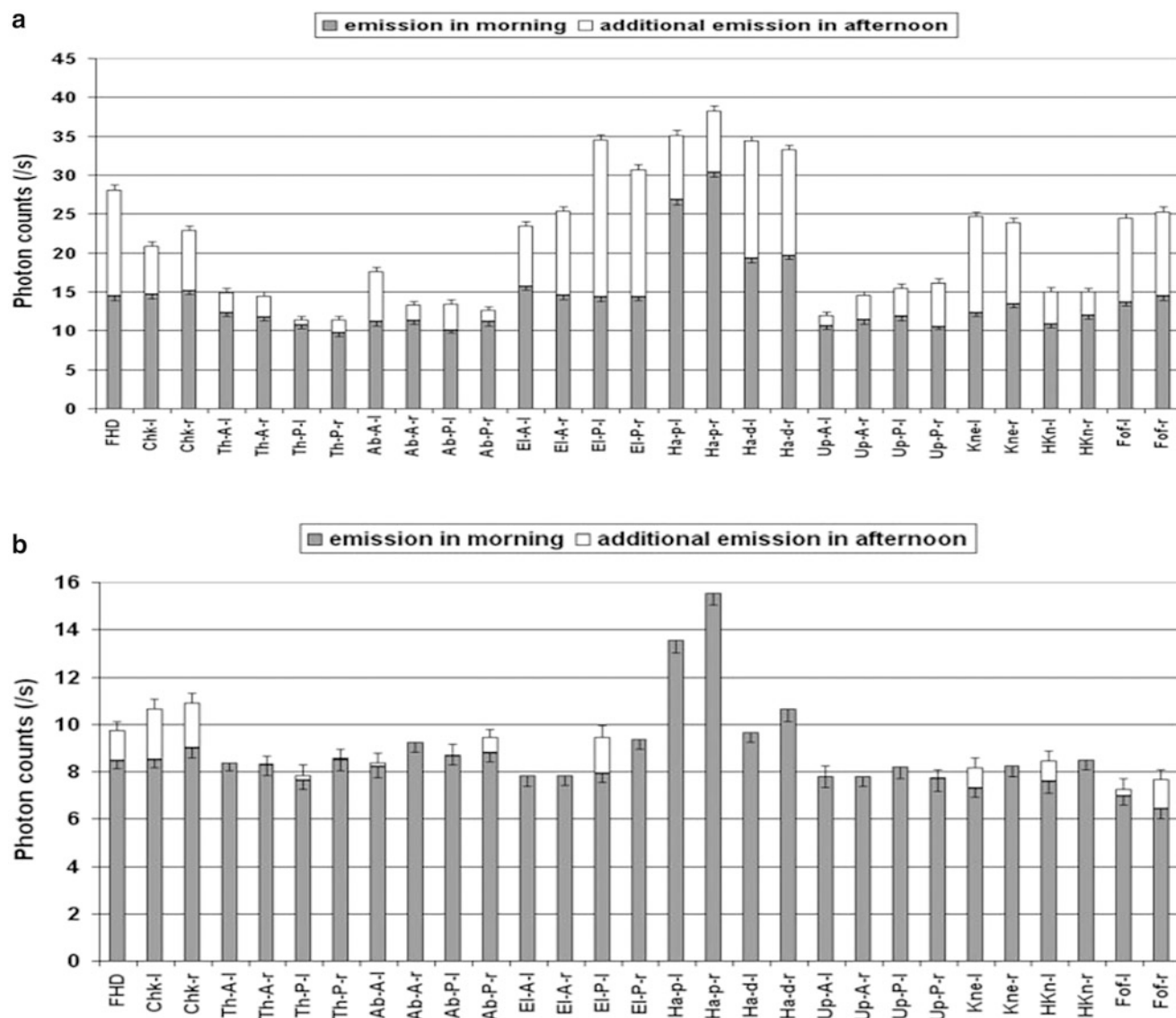


Fig. 16.2 Variation in photon counts over the body locations. The body locations on the left (l) and right (r) side were abbreviated as follows: forehead (FHD), cheek (Chk), thorax-anterior (Th-A), thorax-posterior, scapulae (Th-P), abdomen-anterior (Ab-A), abdomen-posterior, kidneys (Ab-P), elbow-anterior (El-A), elbow-posterior (El-P),

hand palm (Ha-p), hand dorsal (Ha-d), upper leg-anterior (Up-A), upper leg-posterior (Up-P), knee (Kne), hollow of knee (HKn) and foot frontal (Fof). Subfigure (a-d) represents the four subjects

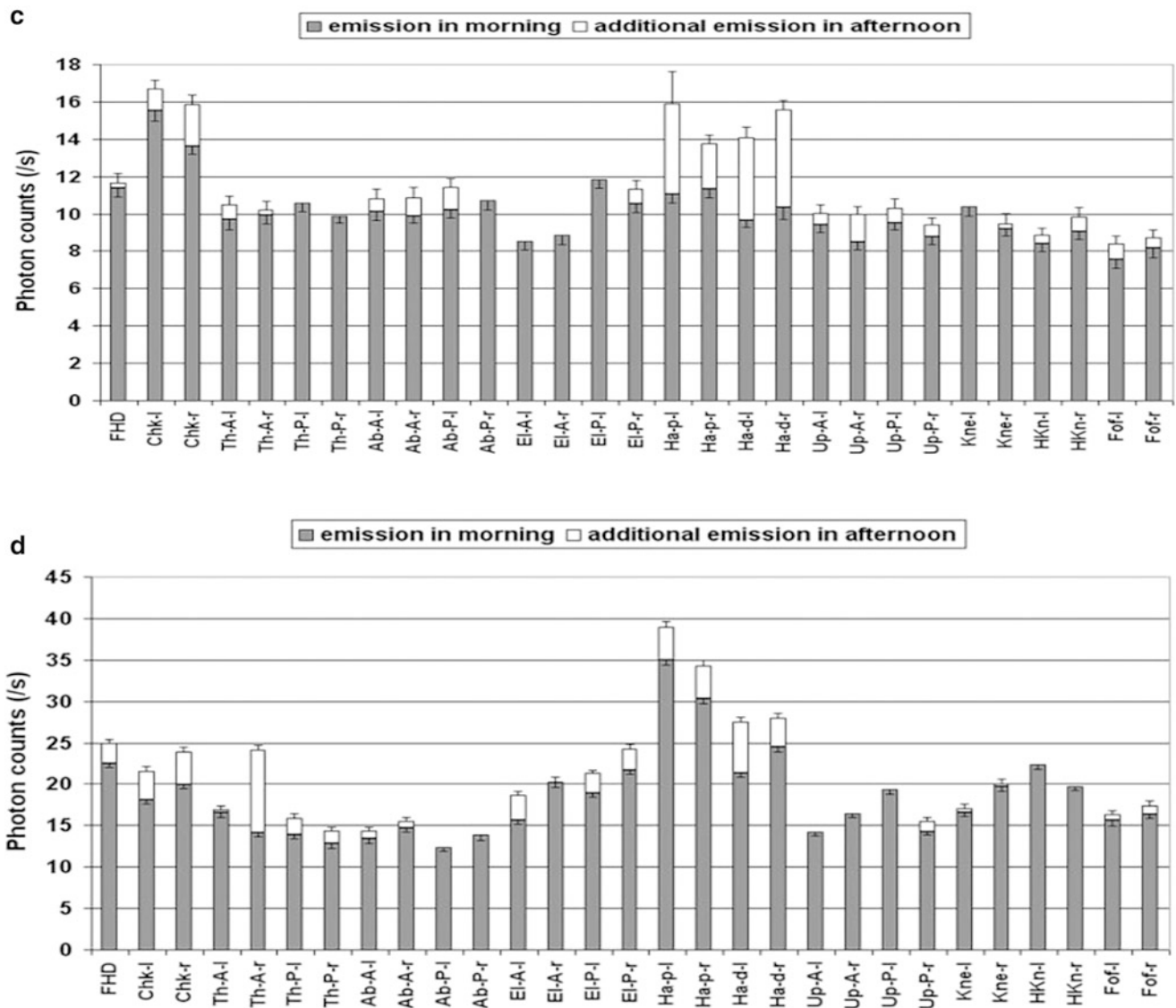


Fig. 16.2 (continued)

In continuing our considerations of a possible association of the fascial connective tissue, structure and increased UPE, we focus first on the neck region. The deep fasciae of the neck have been a controversial subject since their first description by Burns in 1824. Modern anatomical and surgical texts have continued the confusion by describing them inaccurately. Poirier (1912) has described these difficulties: ‘the cervical fasciae appear in a new form under the pen of each author who attempts to describe them’. In this paragraph, we follow a recent ‘Functional Atlas of the Human Fascial System’ (Stecco 2015) which also gives access to online video material (www.atlasfascial.com). The high-emitting neck region is characterized by three major fasciae: a superficial, middle and deep neck fascia. It is an interesting region because fascia structures cover not a single organ but

are investing multiple structures with different organizations. The superficial sheet lies directly below the skin and stretches as a continuation of the masseteric fascia from the mandible and the floor of the mouth over the interposition of the hyoid bone in a caudal direction, after which it is attached to the clavicle and the manubrium sterni and continues into the pectoral fascia. At the back, it covers the lateral cervical triangle and continues to the trapezius muscle. The middle neck fascia forms a firm triangular skirt in front of the cervical viscera. Cranially, it is fixed to the hyoid bone; caudally, it runs through the upper thoracic aperture behind the sternum and inserts at the manubrium sterni. The deep neck fascia is fixed to the anterior longitudinal ligament of the cervical spine and provides a connective tissue cover for the prevertebral muscles and the lateral neck muscles. Cranially,

Fig. 16.3 Map of 12 skin locations for measurement of photon emission over the anterior and posterior of the human body

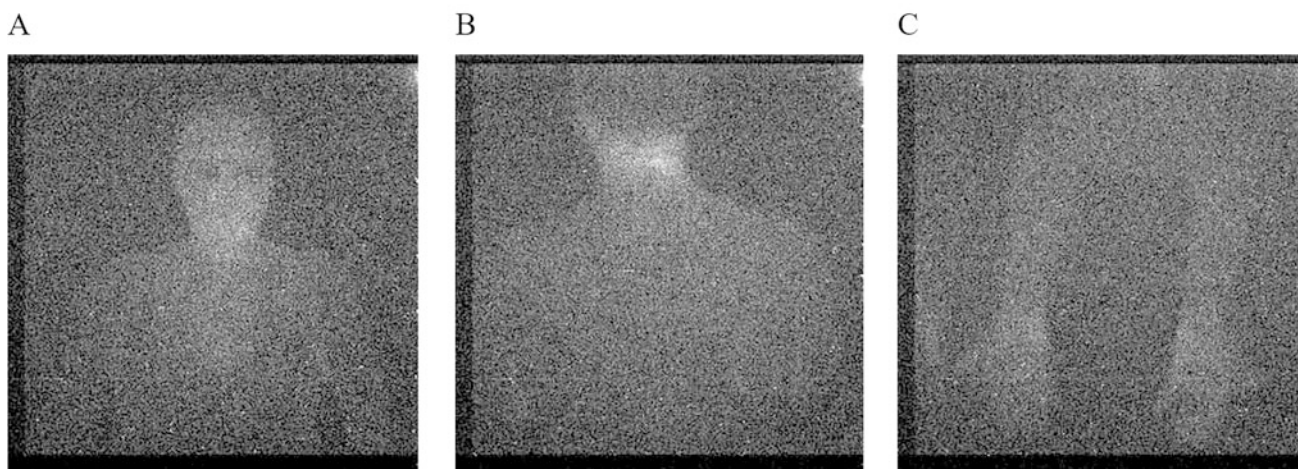
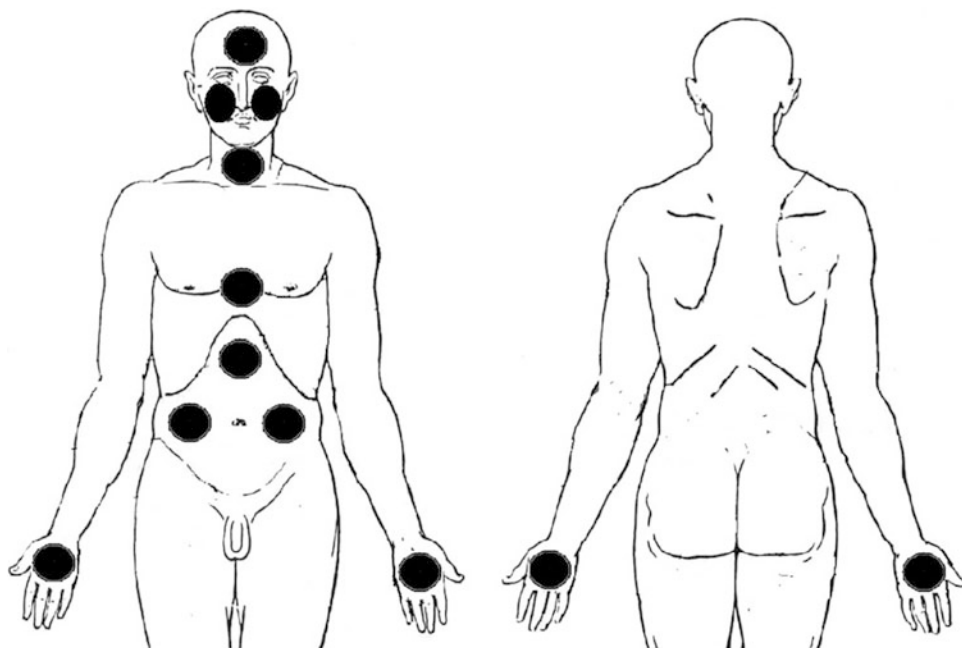


Fig. 16.4 Ultraweak photon emission of the ventral (a) and dorsal (b) head, torso, neck and arms (c) of a human subject

the deep neck fascia is fixed to the base of the skull; laterally, it is connected to the superficial sheet of the neck fascia. It is concluded that typically this unusual complex fascial structure is associated with an increased UPE strength.

Such complicated fascial structure is also recognized in the wrist/hand region (Stecco 2015). The brachial fascia and the antebrachial fascia form the deep fasciae of the arm. In the arm the antebrachial fascia appears as a thick layer of connective tissue, sheathing the flexor and extensor muscle compartments. The mean thickness of the antebrachial fascia is 0.75 mm, yet thickness increases in the wrist region (mean value 1.19 mm). Fiber bundles running in various directions form the antebrachial fascia. At the wrist, these bundles thicken and are arranged in multiple layers. In the palm, the

antebrachial fascia continues laterally and medially with the thenar and hypothenar fascia, and with the thick, transversal fiber bundles tensed between the eminences. In the mid-palm region, this thickening is continuous with the deep layer of the palmar aponeurosis. Such a description supports the suggestion that increased UPE occurs in regions with large fascial complexity.

Turning attention to the hand images (Fig. 16.4), it was observed that maximal photon emission was detected from the top of fingers, at the dorsal side at the nail area. This high intensity is remarkable because nails are horny plates, semi-transparent and consisting of closely welded, horny scales of cornified epithelial cells. The histology of the skin at the nail locations is different from common skin. The epidermis

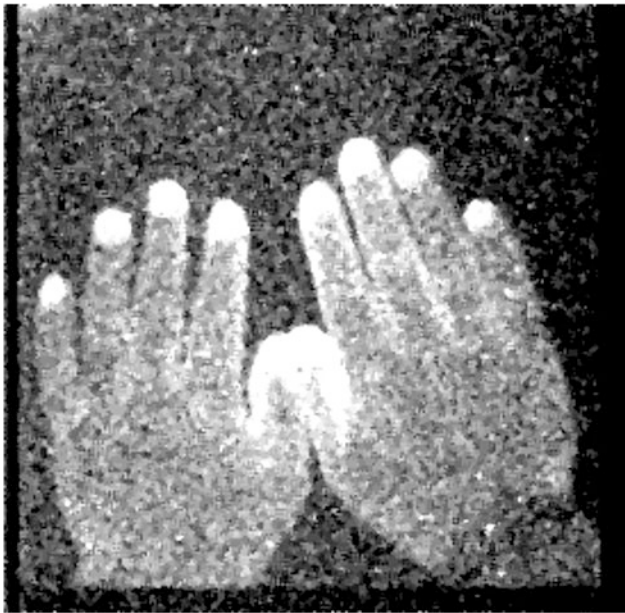


Fig. 16.5 Ultraweak photon emission of the dorsal hands and fingernails of a human subject

where the new formation of the nail proceeds, lining the proximal portion of the nail bed and corresponding roughly with the lunula, has the structure of skin with all its layers; accordingly, this region of the epithelium is called the nail matrix. At this location only are cylindrical and metabolically active cells with frequent mitoses. The stratum lucidum and the stratum granulosum do not continue along the lower surface of the nail plate. Instead, this entire mass becomes penetrated by parallel fibrils of a special ‘onychogenic’ substance. The nail covers the surface of the nail bed where the derma is directly fused with the periosteum of the phalanx. It illustrates clearly that UPE is not directly related to a growth region of the skin, but instead where the nail is fused with the derma and the periosteum.

To summarize these considerations, it can be stated that also other high-emission locations are characterized by their complex fascial structure. However, this will not be described here in detail. It is better to wait for more imaging research in this field in order to improve the argumentation of a relationship between the complexity of fascia and UPE strength. Instead, the next paragraph will focus on temporal aspects of UPE because this may be another approach to understanding the role of fascia in UPE.

16.5 The Fascia as a Global Organ with Temporal Characteristics

Our description in the previous paragraph suggests that it is possible to dissect the fascia network into hundreds of different sheets and bundles, provided one is sufficiently talented

in working with a surgical scalpel and given one has a clearly depicted guideline on where to place the cuts. However, when left without a dissection manual and looking at the tissue alone, it becomes apparent that all those whitish collagenous membranes and envelopes seem to act together as one interconnected fibrous network. The interconnected fascia has been recognized to include all the soft fibrous connective tissues that permeate the human body and blur the arbitrary demarcation lines between various components of the connective tissue (Schleip and Findley 2012; Stecco 2015).

But most important is the view that the fascial system is the largest system in the body, and it is the only system that touches all the organ systems. It is a metasystem, connecting and influencing all other systems, a concept with the potential to change our core understanding of human physiology (Langevin et al. 2001; Langevin and Yandow 2002). Diurnal and longer-duration rhythms in the fascial system exist and may prove to be an important element in orchestrating a body’s performance (Heine 2014) in anticipation of periodic feed/starvation, cold/hot temperature, rest/exercise and stress. The clock of fascia structure and functioning is under current exploration. This makes it interesting to consider the temporal fluctuations of human UPE.

In 1997, Cohen and Popp published the first systematic single-subject study addressing temporal variation in emission from both hands as well as forehead. They examined the subject daily during a 9-month period. The data demonstrated a clear preference for left/right-hand correlation. Frequency analysis of the spontaneous biophoton emission intensity revealed spectral components with longer-than-24-hours temporal characteristics ranging from 7 days and more (Cohen and Popp 1997, 2003). Seasonal variation of spontaneous photon emission of hands was studied by the South Korean team of Soh and colleagues performing monthly measurements of both sides of both hands of male subjects. It revealed changes over the year-long period with the lowest intensity in the autumn and the highest intensity appearing 6 months apart from the autumn (Jung et al. 2005). Fluctuations that occur during the day became the next piece of research. That question was studied by Cifra and coworkers recording every 2 h during 24 h the photon emissions of ventral and dorsal sites of both right and left hands (Cifra et al. 2007). The data suggested that emission intensity was high in the morning, decreased in the afternoon, rose during the evening and was again high at night. The time patterns for the left- and right-hand emissions showed a high degree of symmetry. A diurnal rhythm was also concluded from photon imaging studies of the face of human subjects recorded every 3 h during 24 h (Kobayashi et al. 2009). See also the Chap. 17 of F. Scholzman in this book.

Later studies have zoomed in on temporal fluctuations in detailed intensity spatial patterns of hand emission (Van Wijk et al. 2013). These studies were not aimed at a diurnal rhythm




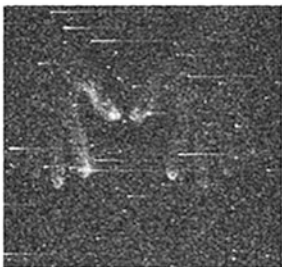







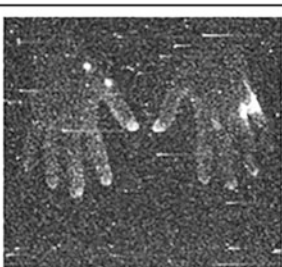
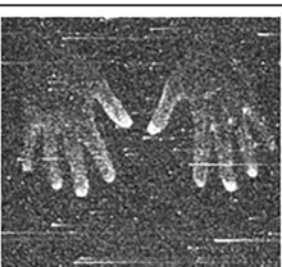
| Category 1 (low intensity) | Category 2 (intermediate intensity) | Category 3 (high intensity) |
|---|---|--|
| A  | F  | K  |
| B  | G  | L  |
| C  | H  | M  |
| D  | I  | |
| E  | J  | |

Fig. 16.6 The variability in ultraweak photon emission of the dorsal sides of the right and left hand of a single subject. In this collection of CCD images, each image was the first of a pair made on the same experimental day. The images are categorized by intensity. Category

1 represents five images with the lowest emission intensity. Category 3 represents three images with the highest photon emission intensity, and category 2 represents five images with intermediate overall intensity

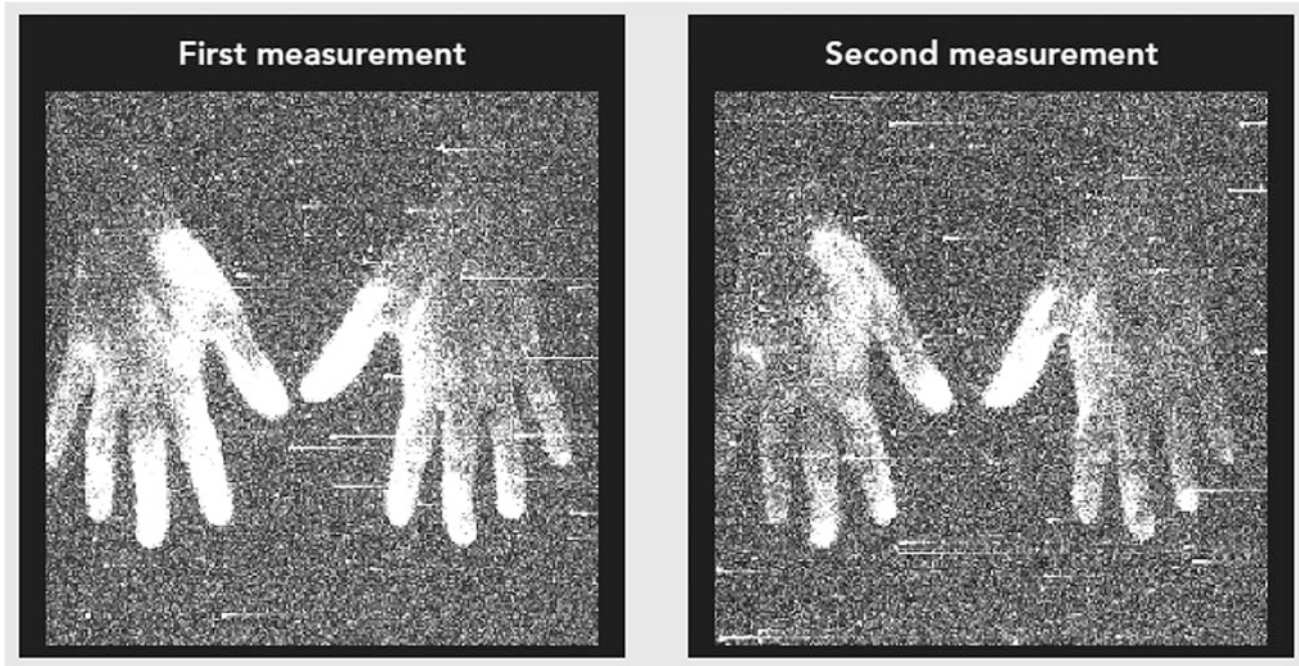


Fig. 16.7 Illustrative examples of changes (6 h between images) in ultraweak photon emission of the dorsal sides of the right and left hands of the same subject

but instead focused on whether short-term fluctuations (in hours) exist for the high-emitting fingers. The study followed a trial and error approach starting with a series of images consisting of 11 sets (made on 11 different days) of a single female subject captured throughout the year. On each experimental day, the subject was imaged twice. The time between those two imaging periods was variable ranging between a few minutes and 6 hours. Each set included therefore two images of the left and right dorsal sides of the hand. The first images each day provided a baseline image used for comparison with a second image made later that same day. The baseline images are presented in Fig. 16.6 demonstrating the high variability of hand emission intensity in a single person. The high variability offers the opportunity to study intensity patterns and to study changes in intensity and how these intensity changes relate to changes in the intensity pattern.

Figure 16.6 shows the systematic ordering in three categories of overall photon emission intensity: five images with the lowest intensity (category 1), three images with the highest intensity (category 3) and five images with intermediate overall intensity (category 2). In all cases, a high degree of similarity in the details of emission patterns was observed for the left and right hands. By zooming in on the specific patterns of the category 1 images, it was evident that, in general, the nails of one or more fingers and, in addition, the medial side of the thumb plus, in some cases, the lateral side of the index finger emitted more than the rest of the hand.

In the higher intensity UPE images the higher emission spread over a larger area as if the bright intensity has moved on the radial side towards the wrist. Although these images suggest that emission can differ in intensity following a fixed anatomic pattern, we need to compare two images made on the same experimental day in order to find evidence for the actual spreading of intensity in time. However, if hands were repeatedly imaged within 2 hours both the intensity and pattern of emission were indistinguishable. Only when the intermediate time was more than 2 hours, additional dynamics was observed. Figure 16.7 presents an example of two images taken 6 h apart. They illustrate a decrease in overall photon emission intensity and remarkably a decrease in emission from the thumb up to the wrist according to the pattern of spreading as discussed before.

16.6 Epilogue

Spontaneous UPE from a human body has been definitely demonstrated but it is not exactly known where this light comes from. Neither studies evaluating UV-induced UPE from the epidermis and dermis nor oxygen replacement studies have been able to elucidate the mechanism of spontaneous UPE. The new approach presented here is based on a comparison of high-UPE regions and low-UPE regions with respect to anatomical and histological properties of skin and the underlying subjacent connective tissue layers. In general,

the thorax/abdomen region emitted the lowest intensity. In contrast, the upper extremities and the head region revealed the highest intensity. Generally, a high degree of left/right symmetry and (to a less degree) dorsal/ventral symmetry were observed. The loss in dorsal/ventral symmetry (and not in right/left symmetry) was observed for elbows, knees and feet, typically body parts that are more shaped. Data also suggested that each individual anatomic position participated in the total emission with a predictable, constant percentage (independent of the total emission). More detailed body information became available from body photon emission imaging. The images showed novel UPE information, i.e. typical body locations that emitted far above or below the common range of an individual's emission, such as the high-intensity fingernails and low-intensity eyes, respectively.

With the exception of nails and eyes, the structuring and thickness of the epidermal layer of high-emission regions is highly identical with its adjacent areas with lower light intensity. We concluded that, in general, epidermal photon production does not explain the typical body photon emission pattern, and hence, we have to consider a possible role of tissue structures below the epidermis: the derma of the skin, and beneath it, the hypodermis and other fascial structures which have a very low cell density but instead consist mostly of collagenous and elastic fibers. In our considerations we followed a recent 'Functional Atlas of the Human Fascial System' (Stecco 2015) which also gives access to online video material (www.atlasfascial.com), in order to discuss the high-emitting neck region and the wrist/hand region. The first is characterized by the complexity of three major fasciae investing in multiple structures with different organizations. Such complicated fascial structure is also recognized in the wrist/hand region. The exceptionally high emission at the nail location confirms that UPE does not need to be directly related to a growth region of the skin, but instead is associated with a complex fusion of nail, derma and periosteum. It is suggested that also other high-emission locations are characterized by their complex fascial structure and that we have to wait for more detailed imaging research in this field. In this future research, we also suggest taking the temporal and diurnal aspects of UPE into account: the UPE spreading and contraction pattern in relation to fascial structures. Utilizing the hand and finger pattern of UPE, we have illustrated that such an approach is feasible.

The next step will be to focus on photon distribution modeling of endogenously produced photons, either produced by metabolizing epidermal cells locally and/or produced under the influence of the cell-poor connective tissue structures beneath. In such an agenda for human spontaneous photon emission research attention remains needed for the emission mechanism that may be hidden in the connective tissue.

References

- Anderson R, Parrish J (1981) The optics of human skin. *J Invest Dermatol* 77: 13–19.
- Ash C, Dubec M, Donne K, Bashford T (2017) Effect of wavelength and beam width on penetration in light-tissue interaction using computational methods. *Lasers Med Sci* 32:1909–1918.
- Bruls WAG, Slaper H, van der Leun JC, Berrens L (1984) Transmission of human epidermis and stratum corneum as a function of thickness in the ultraviolet and visible wavelengths. *Photochem Photobiol* 40: 485–494.
- Cifra M, Van Wijk EPA, Koch H, Bosman S, Van Wijk R (2007) Spontaneous ultraweak photon emission from human hands is time dependent. *Radioengineering* 16: 15–19.
- Clemente CD (1985) *Gray's Anatomy of the Human Body*. Philadelphia: Lea & Febiger.
- Cohen S, Popp FA (1997) Biophoton emission of the human body. *J Photochem Photobiol B* 40:187–189.
- Cohen S, Popp FA (2003) Biophoton emission of human body. *Indian J Exp Biol* 41:440–445.
- Edwards R, Ibsin MC, Jessel-Kenyon J, Taylor RB (1989) Light emission from the human body. *Comp Med Res* 3:16–19.
- Egawa M, Kohno Y, Kumano Y (1999) Oxidative effects of cigarette smoke on the human skin. *Int J Cosmet Sci* 21:83–98.
- Evelson P, Ordóñez CP, Llesuy S, Boveris A (1997) Oxidative stress and in vivo chemiluminescence in mouse skin exposed to UVA radiation. *J Photochem Photobiol B* 38: 215–219.
- Heine H (2014) *Lehrbuch der Biologischen Medizin: Grundlagen und Extrazelluläre Matrix*. Stuttgart: Haug-Verlag.
- Jung HH, Yang JM, Woo WM, Choi C, Yang JS, Soh KS (2005) Year long biophoton measurements: normalized frequency count analysis and seasonal dependency. *J Photochem Photobiol B* 78:149–154.
- Inaba H (1997) Photonic sensing technology is opening new frontiers in biophotonics. *Optical Reviews* 4:1–10.
- International Program on Chemical Safety, Environmental Health Criteria 160, Ultraviolet Radiation (1994), <http://www.inchem.org/documents/ehc/ehc/ehc160.htm>.
- Kobayashi M (2003) Modern technology on physical analysis of biophoton emission and its potential extracting the physiological information. In: Musumeci F, Brizhik LS, Ho MW (Eds) *Energy and Information Transfer in Biological Systems*. World Scientific Publishing, New Jersey, London, pp. 157–187.
- Kobayashi M (2005) Two-dimensional imaging and spatiotemporal analysis of biophoton. In: Shen X, Van Wijk R (Eds) *Biophotonics – Optical science and engineering for the 21st century*. Springer, New York, pp. 155–170.
- Kobayashi M, Devaraj B, Usa M, Tanno Y, Takeda M, Inaba H (1996) Development and application of new technology for two-dimensional space-time characterization and correlation analysis of ultraweak biophoton information. *Frontiers of Medical and Biological Engineering* 7:299–309.
- Kobayashi M, Kikuchi D, Okamura H (2009) Imaging of ultraweak spontaneous photon emission from human body displaying diurnal rhythm. *PLoS ONE* 7:e6256.
- Langevin HM, Churchill DL, Cipolla MJ (2001). Mechanical signaling through connective tissue: a mechanism for the therapeutic effect of acupuncture. *FASEB J* 15:2275–2282.
- Langevin HM, Yandow JA (2002) Relationship of acupuncture points and meridians to connective tissue planes. *Anat Rec (New Anat)* 269:257–265.
- Langevin HM, Huijing PA (2009) Communication about fascia: history, pitfalls, and recommendations. *International Journal of Therapeutic Massage and Bodywork* 2:3–8.
- Markert M (2000) Whole body measurements of biophoton emission. In: Belousov L, Popp FA, Voeikov V, Van Wijk R

- (eds) *Biophotonics and Coherent Systems*. Moscow University Press, Moscow, pp. 405–410
- Maximow AA, Bloom W (1960) *A textbook of histology*. WB Saunders Co, Philadelphia, London.
- Montagna W (1956) *The structure and function of skin*. Academic Press
- Nakamura K, Hiramatsu M (2005) Spontaneous ultraweak photon emission from human hand: influence of temperature and oxygen concentration on emission. *J Photochem Photobiol B* 80:156–160.
- Rastogi A, Pospisil P (2011) Spontaneous ultraweak photon emission imaging of oxidative metabolic processes in human skin: effect of molecular oxygen and oxidant defense system. *J Biomed Opt* 16: 096005. Doi: <https://doi.org/10.1117/1.3616135>.
- Rothman S (1954) *Physiology and Biochemistry of the Skin*. University of Chicago Press, Chicago.
- Sauermann G, Mei WP, Hoppe U, Stab F (1999) Ultraweak photon emission of human skin in vivo: Influence of topically applied antioxidants on human skin. *Methods in Enzymology* 300:419–428.
- Schleip R, Findley TW (2012) *Fascia: The Tensional Network of the Human Body*. Edinburgh: Churchill Livingstone
- Singer E (1935) *Fascia of the Human Body and Their Relations to the Organs they Envelop*. Philadelphia: Williams and Wilkins.
- Standring S (2008) *Gray's Anatomy*. Fortieth ed. Churchill Livingstone, London.
- Stecco C (2015) *Functional Atlas of the Human Fascial System*. Edinburgh: Churchill Livingstone
- Tsuchida K, Iwasa T, Kobayashi M (2019) Imaging of ultraweak photon emission for evaluating the oxidative stress of human skin. *J Photochem Photobiol B* 198:111562. <https://doi.org/10.1016/j.jphotobiol.2019.111562>.
- Usa M, Devaraj B, Kobayashi M, Takeda M, Ito H, Jin M, Inaba H (1994) Detection and characterization of ultraweak biophotons from life processes. In: Ohzu H, Komatsu S (eds) *Optical methods in biomedical and environmental sciences*. Elsevier, Amsterdam.
- Van Wijk R (2014) *Light in shaping life—Biophotons in biology and medicine*. Meluna Research, Geldermalsen.
- Van Wijk R, Van Wijk EPA (2004) Human photon emission. *Res Dev Photochem Photobiol* 7:139–173.
- Van Wijk EPA, Van Wijk R (2005) Multi-site registration and spectral analysis of spontaneous emission from human body. *Forsch Komplementarmed Klass Naturheilkd* 12:96–106.
- Van Wijk R, Kobayashi M, Van Wijk EPA (2006a) Spatial characterization of human ultraweak photon emission. *J Photochem Photobiol B* 83: 69–76.
- Van Wijk EPA, Koch H, Bosman S, Van Wijk R (2006b). Anatomic characterization of ultraweak photon emission in practitioners of Transcendental Meditation and control subjects. *JACM* 12:31–38.
- Van Wijk R, Kobayashi M, Van Wijk EPA (2007) Spatial characterization of human ultraweak photon emission. In: Belousov LV, Voeikov VL, Martynyuk VS (eds) *Biophotonics and Coherent Systems in Biology*. Springer, New York. Pp. 177–190.
- Van Wijk R, Van Wijk EPA, Schroen Y, van der Greef J (2013) Imaging human spontaneous photon emission: historic development, recent data and perspectives *Trends Photochem Photobiol* 15:27–40.
- Van Wijk R, Van Wijk EPA, van Wietmarschen HA, van der Greef J (2014) Towards whole-body ultraweak photon counting and imaging with a focus on human beings: a review. *J Photochem Photobiol B* 139:39–46. doi: <https://doi.org/10.1016/j.jphotobiol.2013.11.014>.
- Van Wijk R, Van Wijk EPA, Pang J, Yang M, Yan Y, Han J (2020) Integrating Ultraweak Photon Emission Analysis in Mitochondrial Research. *Front Physiol* <https://doi.org/10.3389/fphys.2020.00717>
- Weber R, Taylor B, Engelman D (2011) Laser induced tissue reactions and dermatology. *Curr Probl Dermatology* 42:24–34.
- Zhao X, Van Wijk EPA, Yan Y, Van Wijk R, Yang H, Zhang Y, Wang J (2016) Ultraweak photon emission of hands in aging prediction. *J Photochem Photobiol B* 162:529–534.



Chronobiological Aspects of Spontaneous Ultra-Weak Photon Emission in Humans: Ultradian, Circadian and Infradian Rhythms

17

Felix Scholkmann

17.1 Introduction

Living organisms, from cells to humans, exhibit autoluminescence, i.e. spontaneous ultra-weak photon emission (UPE) in the ultraviolet to visible/near-infrared spectral range (approx. 200–1300 nm) without photoexcitation and with intensity in the order of 10^1 – 10^4 photons/s cm^2 (Mei 2011; Cadenas 1988; Cifra and Pospíšil 2014; Havaux et al. 2006).

The UPE signal can be regarded as a non-stationary multicomponent signal with (i) a non-linear trend (in the medium- and long-term time scale, i.e. longer than minutes) in the form of fluctuations and oscillations, (ii) Poisson distributed intensity fluctuations (in the short-term time scale, i.e. seconds/minutes), (iii) non-Poisson and non-Gaussian distributed intensity fluctuations (also in the short-term time scale, i.e. seconds/minutes) and (iv) an added non-Poisson distributed detector noise component (affecting all time scales) (Cifra and Pospíšil 2014; Dlask et al. 2019). As discussed by Cifra and Pospíšil (2014), disentangling these components is important for a proper analysis and interpretation of biological UPE signals.

In this chapter, I will give a review about the findings with regard to the first component, i.e. the *non-linear trend of spontaneous* (i.e. not induced) UPE obtained from measurement on humans.

17.2 Rhythms in Ultra-Weak Photon Emission in Humans: A Review of the Published Work

When measuring spontaneous UPE from human tissue, e.g. the hands, at several time points over the day or successively on several days, one can notice that the intensity values vary. This variability of UPE can be regarded as a sum of a nonlinear trend due to changes in biochemical and biophysical processes involved in the generation of UPE as well as signal changes caused by the detector equipment affected by environmental factors. The first component, i.e. the biological relevant trend in UPE, can be obtained by normalizing the data with dark count measurement performed in parallel or intermittently, and by shielding the detector equipment properly. The obtained signal represents then mainly the UPE long-term fluctuation with biological meaning.

According to literature research performed, *seven* studies have been published so far reporting long-term (> several hours) measurement of spontaneous UPE in humans (Cifra et al. 2007; Cohen and Popp 1997; Jung et al. 2005; Kobayashi et al. 2009; Van Wijk et al. 2006; Scholkmann et al. 2018; Zheng 1986). Non-random long-term fluctuations, i.e. oscillations, were detected in UPE data from several body locations and performed over different time frames (for an overview of the studies see Fig. 17.1).

The non-linear trend and oscillations of UPE reported by these studies are of interest since they seem to demonstrate that they reflect primarily chronobiological processes happening in humans.

Chronobiological rhythms span from *ultradian* (with a period shorter than 1 day) over *circadian* (with a period of about a day) to *infradian* (with a period longer than 1 day) (Koukkari and Sothorn 2006). The available studies published about fluctuations in UPE signals measured from humans cover all of these three categories of chronobiological rhythms (Fig. 17.1).

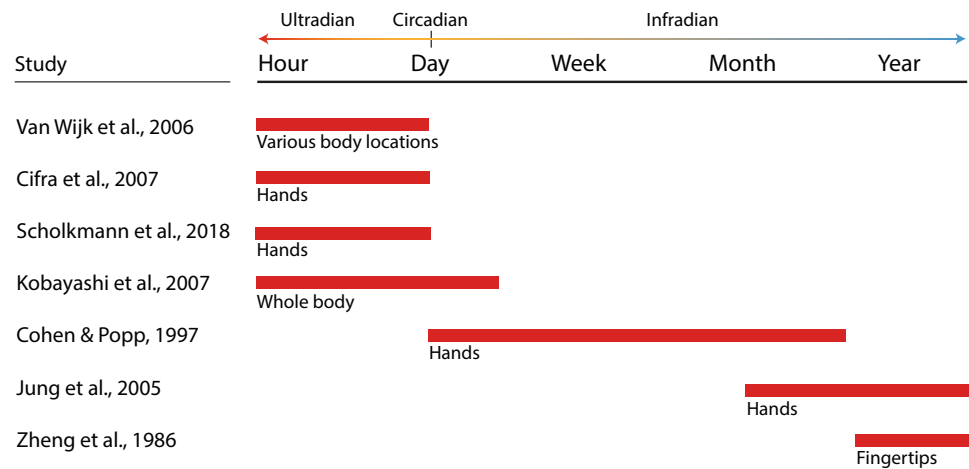
F. Scholkmann (✉)

Biomedical Optics Research Laboratory, Department of Neonatology, University Hospital Zurich, University of Zurich, Zurich, Switzerland

Institute of Complementary and Integrative Medicine, University of Bern, Bern, Switzerland

e-mail: Felix.Scholkmann@usz.ch

Fig. 17.1 Visualization of the UPE rhythms reported in the seven studies discussed in this chapter. The references refer to the studies of Van Wijk et al. (2006), Cifra et al. (2007), Scholkmann et al. (2018), Kobayashi et al. (2009), Cohen and Popp (1997), Jung et al. (2005) and Zheng (1986)



For the present review, data from the seven published studies were extracted and re-analysed by fitting oscillatory modes to the data. To this end, Fourier series with a varying number of harmonics as well as polynomials and power functions were used, depending on the particular data set. This approach enabled to detect multicomponent oscillations, i.e. oscillations as a sum of several single oscillatory modes, that would be not optimally captured by the classical cosinor analysis (Cornelissen 2014).

17.2.1 Circadian and Ultradian Rhythms

The circadian and ultradian rhythms of UPE measured at different parts of the human body were reported in *four* studies (Cifra et al. 2007; Kobayashi et al. 2009; Van Wijk et al. 2006; Scholkmann et al. 2018).

Van Wijk et al. measured three times per day (morning [9:00–10:30], early afternoon [13:00–14:30], evening [18:00–19:30]) spontaneous UPE from 30 different positions on the human body of one subject. Each recording was 2 min long with a window of 1 s for photon emission count registration. As Fig. 17.2 shows, there was a general pattern obvious in the UPE changes from all body locations: the UPE intensity in the morning was lower compared to the early afternoon and evening – with one exception, the measurement at the left upper back showed a global minimum in early afternoon. With regard to the differences of UPE between early afternoon and evening the pattern was dependent on the body position with the largest increase in the evening at several sites (forehead, cheek, abdomen, knee, foot, lower back and thigh) and similar intensities in the early afternoon and evening (elbow, hand (palm), upper leg, hand (dorsum) and popliteal). At some position, a right-left asymmetry in the pattern was detected (thorax, upper back and lower back). The findings of Van Wijk et al. show clearly that the UPE intensity at different body parts varies in a circadian way with

generally a minimum in the morning and a maximum in the evening.

A detailed study of circadian changes of UPE from the hand was conducted by Cifra et al. (2007). In this study, UPE was measured at the right and left dorsal and palm position of the hand of subjects (the exact number of subject is not given in the publication) during 24 h (every 2 h one measurement). Five 24 h measurements were performed (resulting in 60 single measurements for each measurement location). Figure 17.3 shows the normalized (i.e. the deviations from the mean) and averaged data for the 24 h period. The UPE from the palm and dorsum of the hand shows a clear circadian variation with a global minimum in the evening and a global maximum at night (Fig. 17.3a and b). The circadian fluctuations at the palm and dorsum are in phase. The right and left hand, however, show a different pattern with an ultradian rhythm present at the right hand (with a period of about half a day) (Fig. 17.3c) and a circadian rhythm similar to the pattern at the palm and dorsum at the left hand (Fig. 17.3d). The difference in UPE intensities between the palm and dorsum exhibits also an ultradian rhythm with a period of a bit less than one half a day (Fig. 17.3e), while the difference in UPE intensities between the right and the left hand shows a clear circadian rhythm which a right hand dominance in the time between around noon and midnight and a left dominance between around midnight to noon (Fig. 17.3f).

When comparing now the results from the study of Cifra et al. (2007) with those of Van Wijk et al. (2006), one can note that the UPE pattern detected differ. While the data of Van Wijk et al. (2006) show a circadian variation of UPE at the hand (palm and dorsum), with a minimum in the morning and a maximum in the evening, the data of Cifra et al. (2007) show a circadian variation at the palm and dorsum, with a minimum in the evening and a maximum in the night.

Another study that investigated circadian changes of UPE from the hand was conducted by myself with data from the

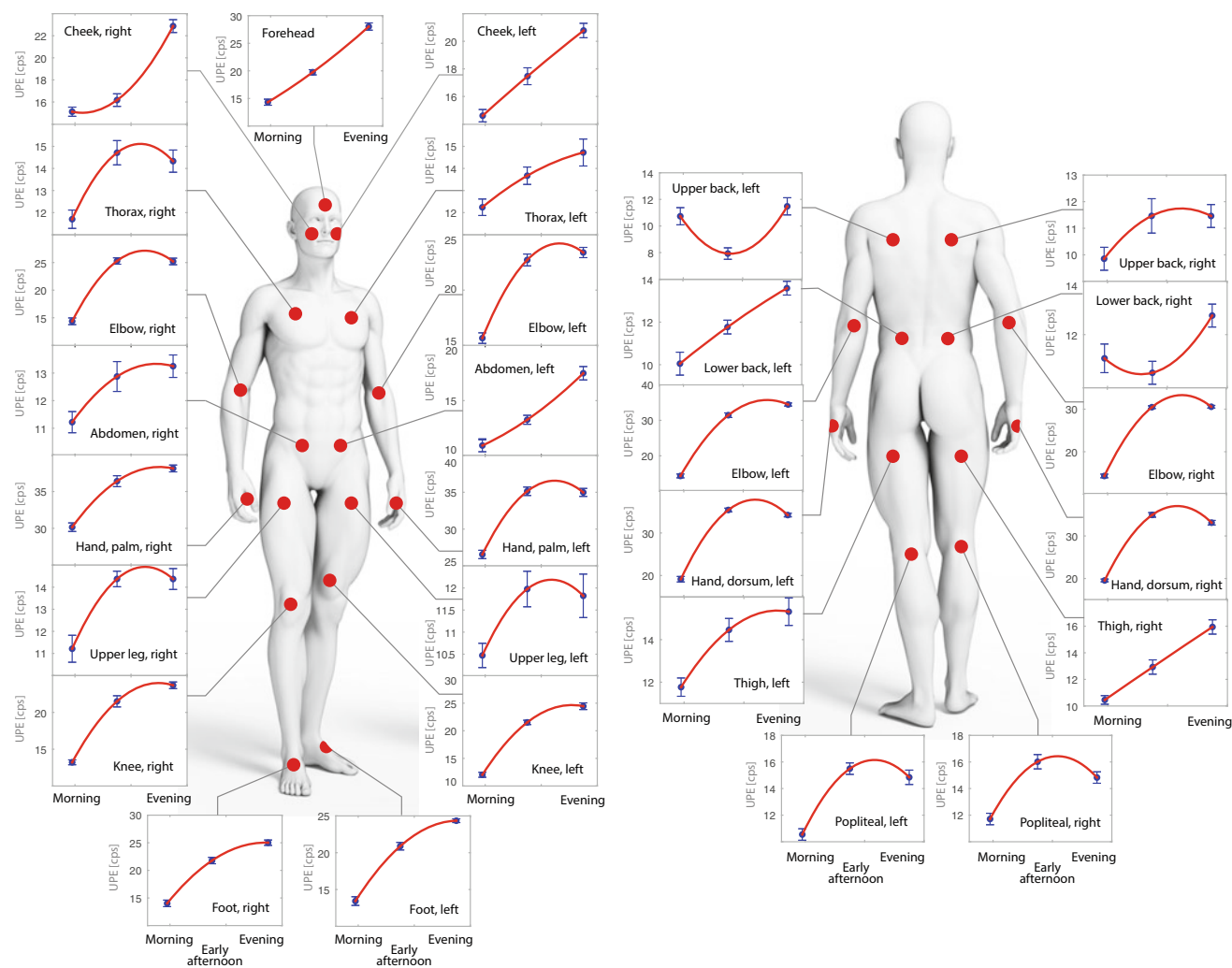


Fig. 17.2 Circadian changes in spontaneous UPE of the human body measured at 30 different body positions in one human according to the study results of Van Wijk et al. (2006). (Data extracted from Fig. 2 of (Van Wijk et al. 2006) and fitted with a second-order polynomial)

research group of Roeland and Eduard Van Wijk (Scholkmann et al. 2018). By analysing UPE images from 10 UPE measurements performed at different days and different times of day (two subjects) (Fig. 17.4a), an ultradian fluctuation was detected based on averaged data with a global minimum around noon (Fig. 17.4b). With this study, three *different* UPE patterns at the hands (dorsum) have been published so far. In each study (Cifra et al. 2007; Van Wijk et al. 2006; Scholkmann et al. 2018), a different pattern has been obtained (see Fig. 17.4b-d). An indication for a possible reason for this might be seen in the UPE images shown in Fig. 17.4a: Subject 1 showed a higher UPE intensity in the *afternoon* at the dorsum at day 2 and 3 but a slightly higher UPE intensity in the morning at day 1. Furthermore, at day 3, the UPE intensity of the whole hand was much higher compared to the other days. This indicates that the circadian UPE variation from the hand is modulated also by larger rhythms causing a day-to-day (infradian) variation of the

circadian amplitude (and possible also a change in sign). That the mean UPE intensity at the hands indeed shows ultradian rhythms that will be discussed in Sect. 17.2.2.

Another study investigating circadian changes of UPE measured at humans was conducted by Kobayashi et al. (2009) (Fig. 17.5). In this study, the team measured spontaneous UPE from the human body (upper frontal side of the body) with a CCD camera (exposure time for each measurement: 20 min) at five different times per day in five healthy males. In addition, a three-day-long measurement with five measurements per day was conducted in one subject, in parallel with measurements of oral temperature and cortisol concentration in saliva. An ultradian UPE rhythm with a period of about 6 h from the whole upper part of the body was found in the group data (Fig. 17.5k) as well as by averaging the three-day long data from the single subject (Fig. 17.5g). By comparing Fig. 17.5k with Fig. 17.5g, one can note clearly that the ultradian change in UPE is much

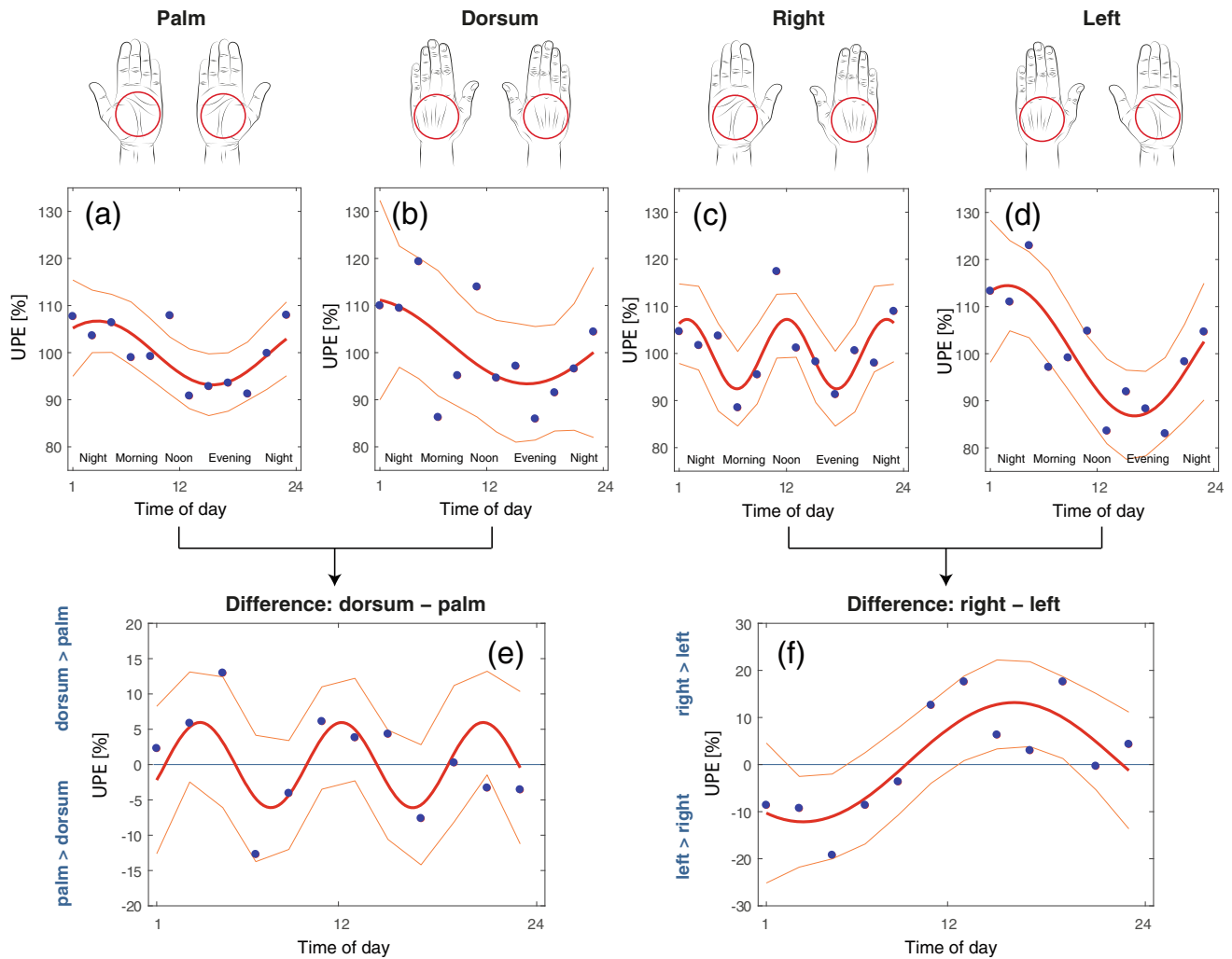


Fig. 17.3 Circadian and ultradian changes of UPE of the hands of one human according to the study of Cifra et al. (2007). (Data extracted from Figs. 2 and 3 of (Cifra et al. 2007) and fitted with a Fourier series with

one harmonic). The 95% confidence bounds for the fitted coefficients are shown as thin red lines

clearer in visibility in the single-subject average (Fig. 17.5g) compared to the average from five subjects (Fig. 17.5k). This indicates that the inter-subject variability of the ultradian UPE dynamics is larger than the inter-trial variability in one single subject (especially when the linear trend of UPE during the 3 days of measurement was removed before calculating the average, as performed in this analysis). In both ultradian profiles, the maximum UPE intensity is found to be in the afternoon with minima during the night and in the morning. Since no measurements were performed in the night, an ultradian profile was more evident instead of a circadian one. However, the 3-day long UPE measurement provided enough data to show a circadian pattern (Fig. 17.5g). In addition, a linear trend was evident in the data set as well (Fig. 17.5f), proving also an infradian change in UPE. Therefore, it seems to be the case that the dynamics of spontaneous UPE from the upper human body exhibits

three rhythms: ultradian, circadian and infradian. The results of Kobayashi et al. provide evidence for this.

Interestingly, Kobayashi et al. found also that the change in UPE was anticorrelated with the change in concentration of cortisol in saliva (Fig. 17.5f-i). The anticorrelation is evident in both oscillatory modes: (i) UPE intensity increased over 3 days (Fig. 17.5f) while cortisol decreased (Fig. 17.5h), and (ii) the circadian changes in UPE and cortisol were in antiphase (Fig. 17.5g, i). A correlation with oral temperature was not evident (Fig. 17.5j).

17.2.2 Infradian Rhythms

Through the literature research conducted, four studies were found that reported UPE changes in humans on a time scale

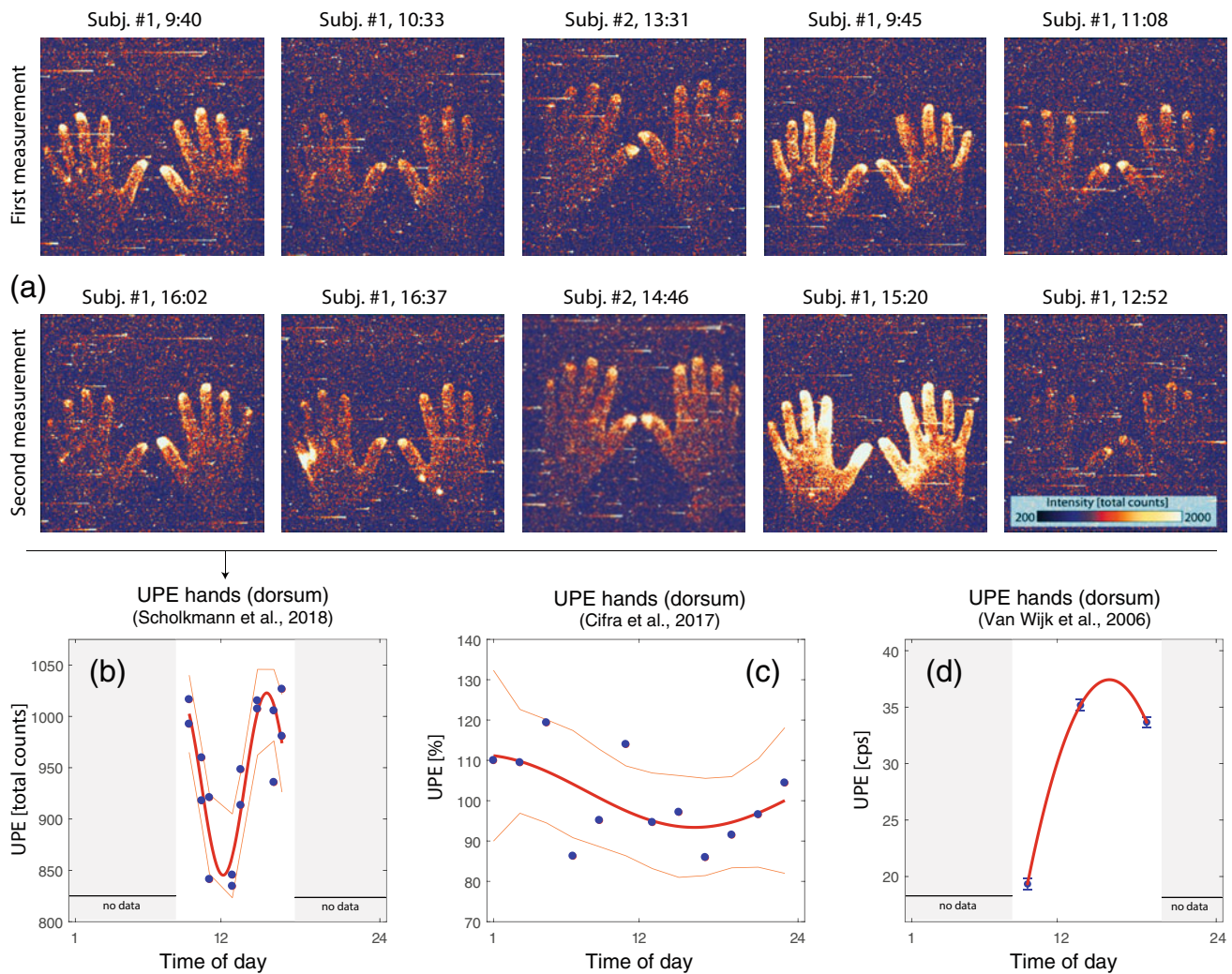


Fig. 17.4 (a, b) Circadian changes of UPE of the hands of five humans according to the study of Scholkmann et al. (2018). The subfigures show UPE images of the hand of two subjects measured twice a day as well as on different days. (c, d) Comparison with the findings of Cifra et al. (2007) and Van Wijk et al. (2006). (Data of (a, b) extracted from Fig. 1

of (Scholkmann et al. 2018). Data of (c) extracted of (Cifra et al. 2007) and (d) of (Van Wijk et al. 2006). Data shown in (b) and (c) fitted with a Fourier series with one harmonic and in (d) with a second-degree polynomial function). The thin red lines in (b) and (c) mark 95% confidence bounds for the fitted coefficients

larger than 1 day (Cohen and Popp 1997; Jung et al. 2005; Kobayashi et al. 2009; Zheng 1986) (see Fig. 17.1).

As already mentioned in the previous section, in the study of Kobayashi et al. (2009), an infradian rhythm of UPE from the upper part of the body was noted in the form of an increasing trend over the 3 day measurement period (see Fig. 17.5f). This infradian change can be described as an amplitude modulation of the circadian UPE changes with an increase in magnitude of the circadian UPE changes as well as a constant increase in the overall intensity over the 3 days. As shown in Fig. 17.5h, a slight constant decrease in cortisol concentration during the 3 days has been observed, being anticorrelated with the infradian UPE change.

In another study, Cohen and Popp (1997) reported measurements of spontaneous UPE from the hands (which

side of the hands, palm or dorsum, is not mentioned in the publication) and forehead of a women (27 years of age) performed once a day over 9 months (starting in August 1995 and ending in March 1996). Over this time period, an infradian UPE rhythm at the hand could be detected in the form of an increase in late summer, early autumn and a decrease in the winter (Fig. 17.6a, b). Surprisingly, the measurements at the forehead showed a different pattern: a global minimum at the end of the year and a sharp increase in the first quarter of the successive year (Fig. 17.6c). The sharp increase at the end of the UPE measurements from the forehead is curious and unexpected, possibly reflecting not an endogenous chronobiological process but more a transitional change of physiology, maybe triggered by an external influence. A discussion of this aspect is unfortunately lacking in

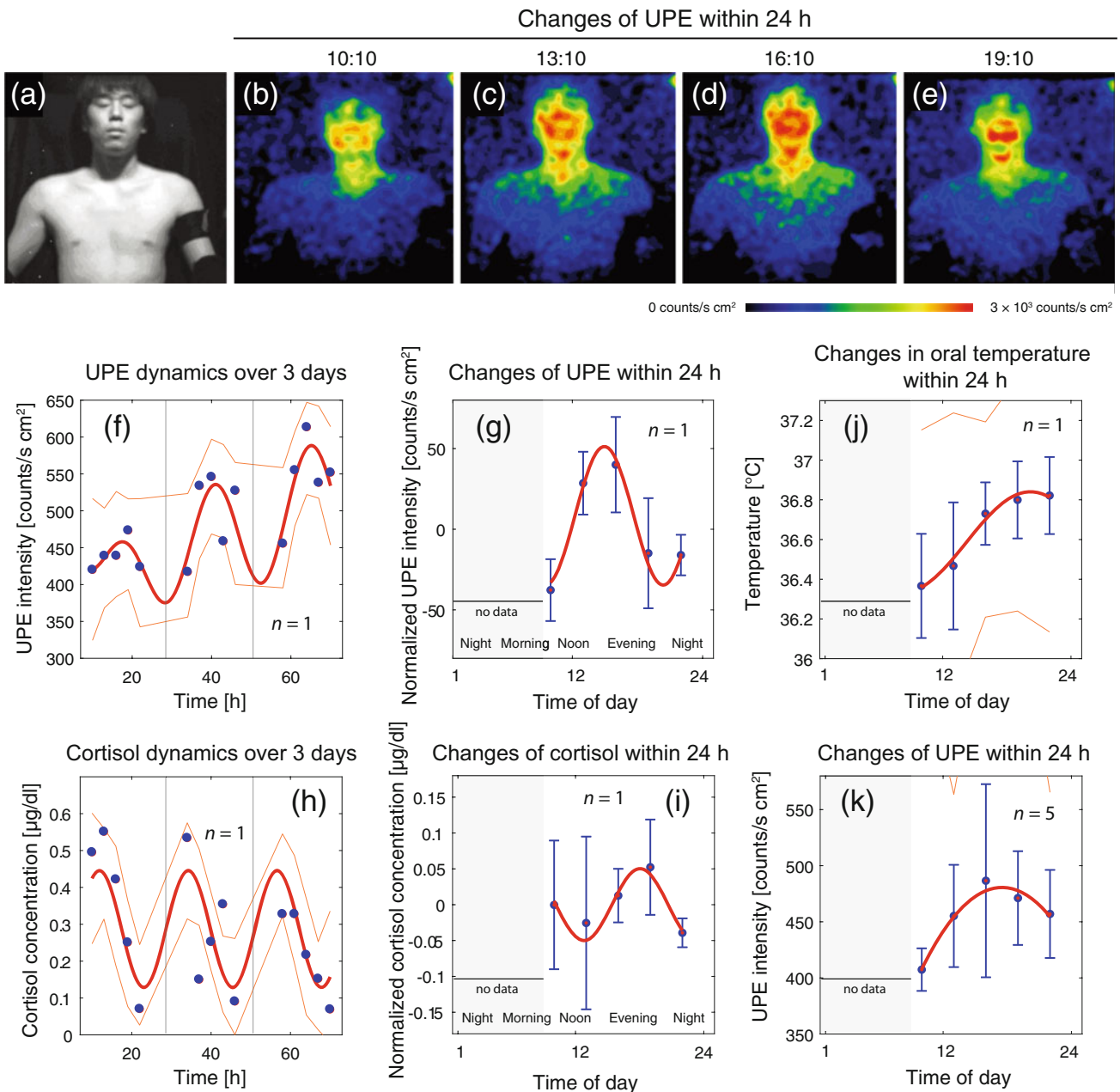


Fig. 17.5 Circadian and ultradian changes of UPE measured from the upper part of the frontal side of the human body in one human according to the study of Kobayashi et al. (2009). (a) Black and white images of the person measured. (b-e) UPE images taken at different times of day. (Image source: Fig. 1 of Kobayashi et al., with permission from the author). (f) UPE changes over 3 days. (g) Average of values shown in (f) on a 24 h scale. The normalized UPE intensity is shown, i.e. the UPE intensity where the mean UPE value for each day was subtracted to remove the trend. (h) Saliva cortisol concentration change over 3 days.

(i) Average of values shown in (h) on a 24 h scale. Also here, the intensity values shown were normalized with respect to each day. (k) Group average (five subjects) of UPE intensity values throughout the day. (Data shown in (f-k) extracted from Fig. 1 of Kobayashi and redrawn. Data shown in (f) fitted with a Fourier series with three harmonics, (g-k) fitted with a Fourier series with one harmonic). The thin red lines in (f), (j), (h) and (k) mark 95% confidence bounds for the fitted coefficients

the original paper of Cohen and Popp. The authors reported finding different infradian rhythms in the UPE data from the hands as well as the forehead; periodicities with periods of 7, 14, 21, 27, 80 and 270 days were detected by performing a spectral analysis (however, the spectral analysis was

performed only with a low resolution and the statistical significance of the detected oscillations was not evaluated by the study, limiting the significance of this finding). Interestingly, the infradian UPE rhythm from the hands was different from that at the forehead with a more pronounced

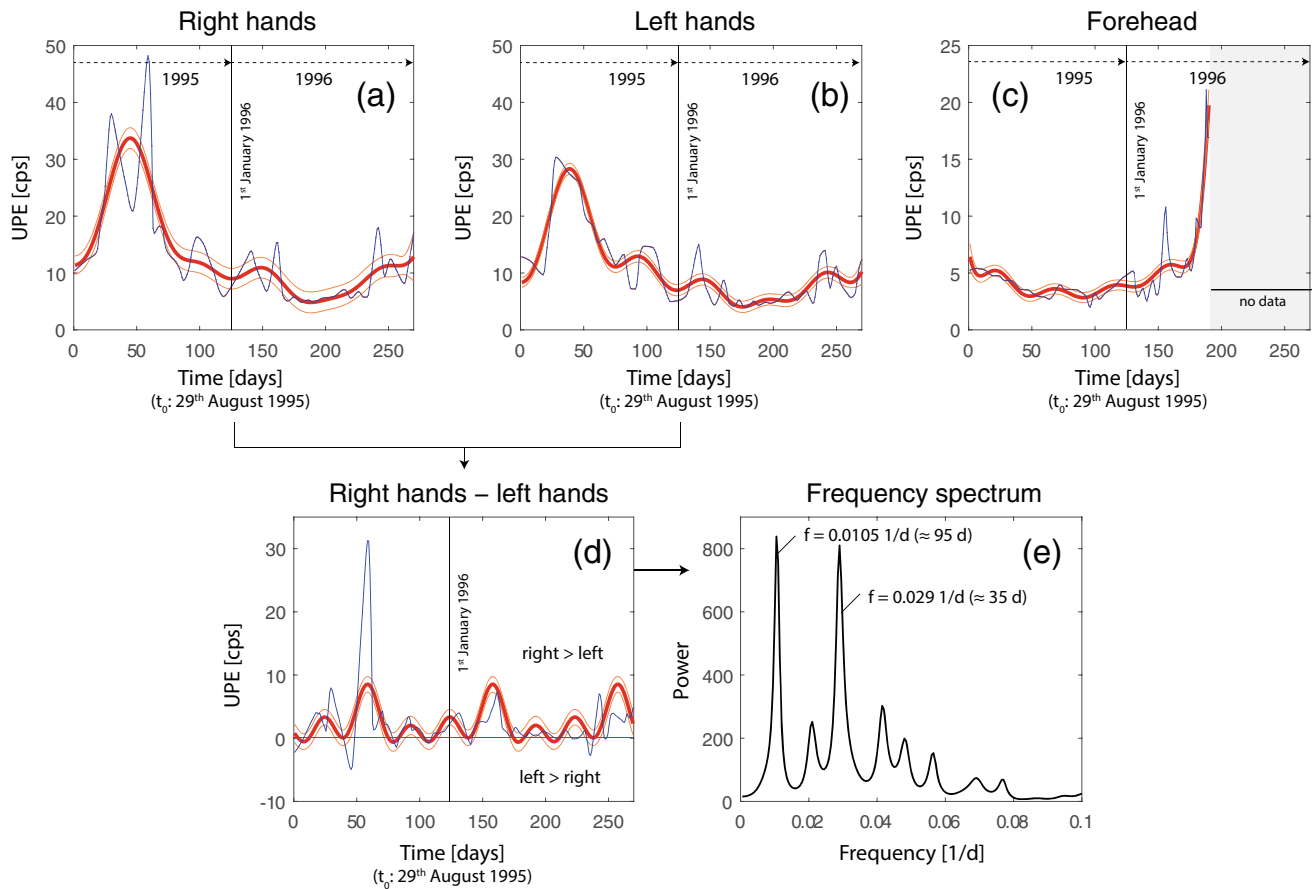


Fig. 17.6 Infradian changes of UPE measured at the hands (a, b) and forehead (c) of a woman according to the study of Cohen and Popp (1997). (d) Changes in the difference of UPE between the right and left hand. (e) Frequency spectrum of the data shown in (d). (Data extracted

from Fig. 1 of (Cohen and Popp 1997). The data shown in (a–c) were fitted with a Fourier series with five harmonics, the data in (d) – with a Fourier series with three harmonics). The thin red lines mark 95% confidence bounds for the fitted coefficient

multi-oscillatory dynamics at the hands compared to the forehead.

Our own analysis of the data of Cohen and Popp revealed that the difference of UPE intensity between the right and left hand shows also an infradian rhythm: the time series can be modelled by a Fourier series with three harmonics (Fig. 17.6d). Analysing the data with a modern high-resolution spectral analysis approach (maximum entropy spectral analysis (Ulrych and Bishop 1975; Fong Chao 1990; Dowse 2013), MESA) clearly shows two peaks: one with a period of about 95 days (a rhythm with four peaks per year) and one with about 35 days (a circa monthly rhythm) (Fig. 17.6e).

Another study investigating the long-term changes of spontaneous UPE from human hands has been conducted by Jung et al. (2005). In this study, measurements from the dorsal and palmar side of both hands were made each week for 1 year (from September 2002 to September 2003) in three subjects. As shown in Fig. 17.7, a clear circannual rhythm could be detected with emission maxima from the palm sides in summer (subject 1) or spring (subjects 2 and 3) and

emission maxima from the dorsal side at spring in all three subjects. A phase shift of about 2–3 months between the maxima of the circannual rhythms from the palm sides with respect to the dorsum is noticeable. Our own analysis of the differences between the left and right hands (dorsum and palm) revealed additional information not reported in the original publication: (i) while subject 1 showed no visible rhythm in the right-left UPE difference, subjects 2 and 3 did (Fig. 17.8a–f); both subjects showed also circannual rhythms in the right-left UPE difference, both for the palm and the dorsum. While in subject 2 the circannual rhythm of right-left UPE difference had different maxima when comparing the two parts of the hand (dorsum vs. palm) (Fig. 17.8c, d), in subject 3 the circannual oscillation is in phase (Fig. 17.8e, f). Also the position of the maxima is different: the largest difference of the emission from the right compared to the left hand is visible in the early summer (palm) and late summer (dorsum) for subject 2 and in late winter in subject 3 (palm and dorsum). This study shows nicely that (i) there is an ultradian, i.e. circannual, rhythm in the spontaneous UPE from human hands (dorsum and palm sides), (ii) the phase of

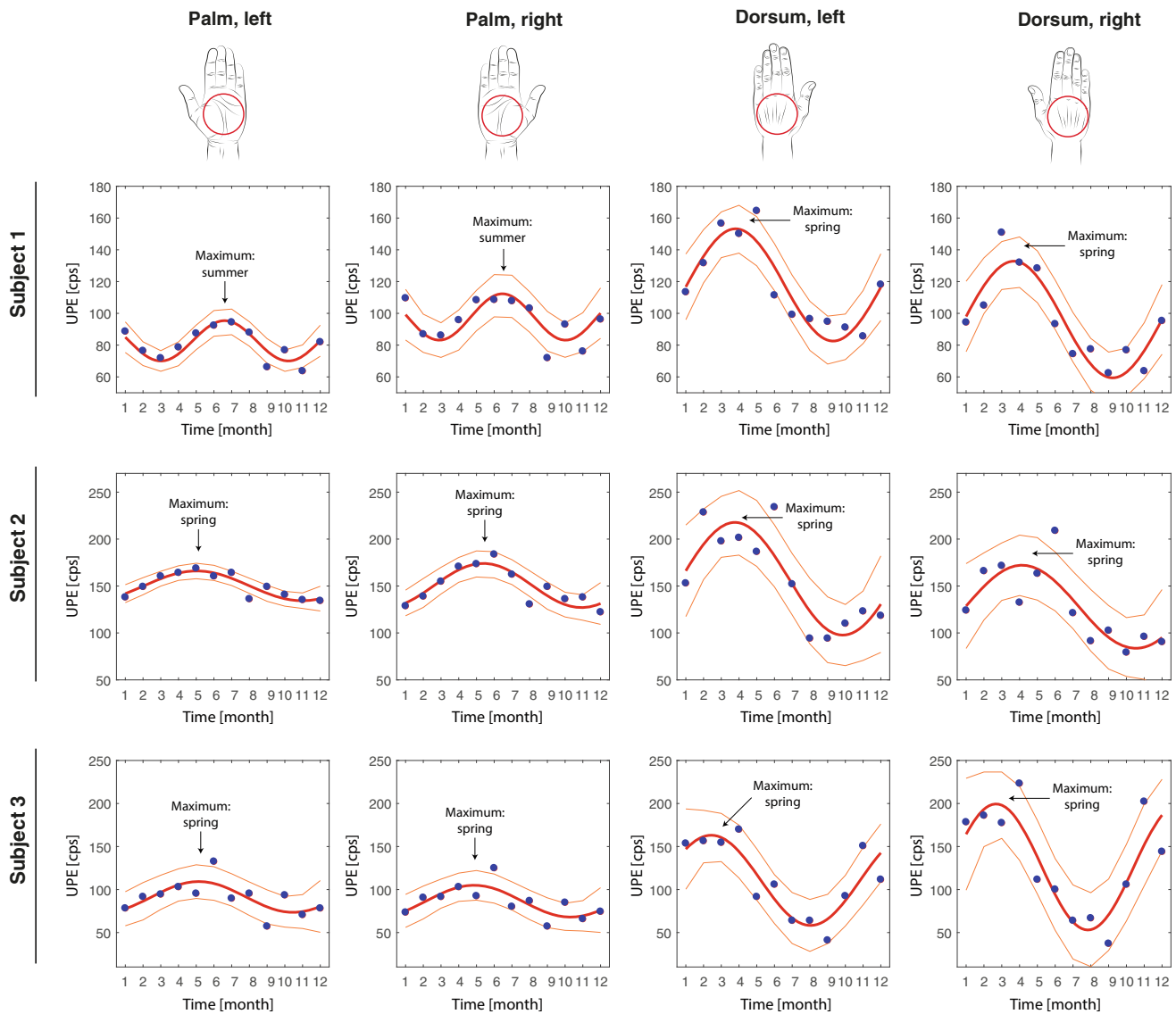


Fig. 17.7 Infradian (circannual) changes of UPE measured at the hands (right, left, palm and dorsum) on three subject according to the study of Jung et al. (2005). (Data extracted from Fig. 2 of (Jung et al. 2005)). The

data shown were fitted with a Fourier series with one harmonic). The thin red lines mark 95% confidence bounds for the fitted coefficients

the circannual rhythm is different at the palm with respect to the dorsum, (iii) the phases of the circannual rhythms depends slightly on the individual subject and (iv) the right-left UPE difference at the palm and dorsum is either absent (subject 1) or also shows a circannual rhythm (subjects 2 and 3) with different phase shifts for each subject.

The study of Jung et al. seems to be the only study that measured UPE from the human body continuously for 1 year.

Unfortunately, infradian rhythms in UPE from the human body with a period longer than 1 year have not been investigated (or at least not published) with longitudinal studies yet. However, studies have been published describing age-related changes of UPE from human hands (Zheng 1986; Zhao et al. 2016; Sauermann et al. 1999). Since the

development and aging of an organism is also governed by infradian rhythm (Diambra and Menna-Barreto 2009; Clayton et al. 2014; Scholkmann and Wolf 2019; Mahoney et al. 2018; Pitfield et al. 2019; Bott 1985; Rohen 1984a, b, c), age-related changes in UPE can in principle be also regarded from the chronobiological viewpoint.

In the study of Zheng (1986) (published in Chinese), reviewed by He et al. (2016), the authors measured spontaneous UPE from the fingertips of humans of seven age groups (0–10 years, $n = 20$; 11–14 years, $n = 47$; 20–30 years, $n = 47$; 31–40 years, $n = 12$; 41–50 years, $n = 16$; 51–60 years, $n = 26$; 61–75 years, $n = 24$). A non-linear increase in UPE over the age range was noticed which was different for both sexes (Fig. 17.9a, b). Males showed a

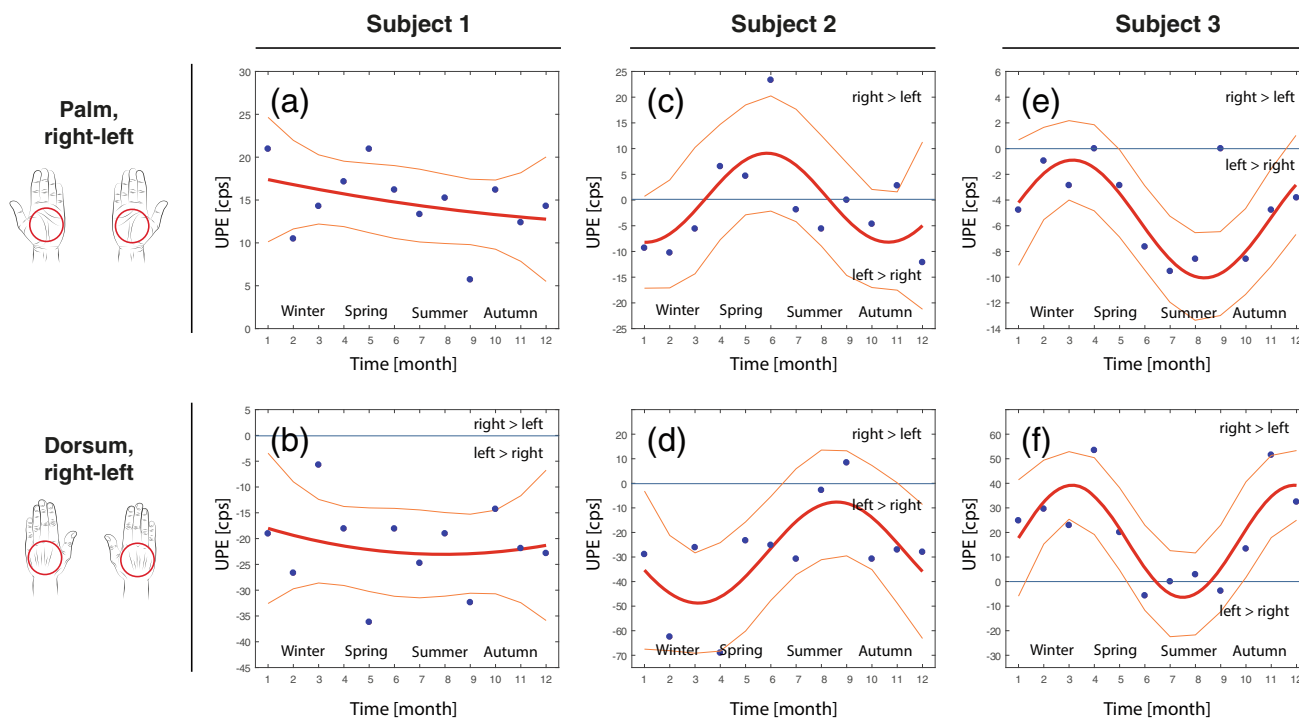


Fig. 17.8 Time-dependent changes in UPE difference values (right-left hand) for the palm and dorsum of three subjects according to the study of Jung et al. (2005). (Data extracted from Fig. 2 of (Jung et al. 2005). The data shown were fitted with a Fourier series with one harmonic)

steeper increase in UPE with age compared to women. Above approximately 40 years of age, a flattening of the UPE age-associated UPE increased can be noticed. That in older subject a higher UPE can be measured compared to younger ones was confirmed by Sauermann et al. (1999), who measured UPE from the arms of two age groups (18–25 years vs. 60–72 years), and by Zhao et al. (2016), who measured UPE from the hands also from two age groups (29.0 ± 1.2 years vs. 56.2 ± 0.7 years).

17.3 On the Possible Origins of Rhythms in Ultra-Weak Photon Emission in Humans

The study results discussed in the previous section clearly show that the intensity of spontaneous UPE from the human body varies with time and is modulated by ultradian, circadian and infradian rhythms. But what is the origin of these rhythms? Which biological, biochemical or environmental processes are linked to or causing this phenomenon? In the following section, possible origins of rhythms in UPE measured from humans will be discussed. To this end, the focus will be on discussing physiological processes with similar frequency and phase characteristics as the rhythms in UPE found by the studies reviewed in the previous section.

17.3.1 Circadian and Ultradian Rhythms

Of the studies reviewed, only Kobayashi et al. (2009) reported concurrent measurements of UPE from the hand and also measurements of oral temperature as well as saliva cortisol concentration. A statistically significant correlation between the *circadian* UPE changes and circadian changes in oral temperature or saliva cortisol concentration changes were not detected; however, the *ultradian* UPE rhythm was statistically significantly anticorrelated (although weakly) with the ultradian change in cortisol concentration ($r = -0.3074$, $p < 0.002$) (Fig. 17.5). These study findings are important since they demonstrate that the circadian UPE fluctuation seems to be not directly related to temperature changes but more to a metabolic process. However, it needs to be pointed out that in this study the temperature was not measured at the hands but orally. As shown in Fig. 17.10a-d, the temperature of different body parts can have different circadian patterns, i.e. different circadian phases and different ultradian modulations of the circadian changes.

The only study documenting parallel changes in hand UPE and hand temperature available, to my knowledge, was conducted as part of a diploma thesis of M. Cifra (2006) and has not been published in a journal. This interesting work shows that UPE measured over 2 days from the right hand (palm) is correlated with the temperature of the

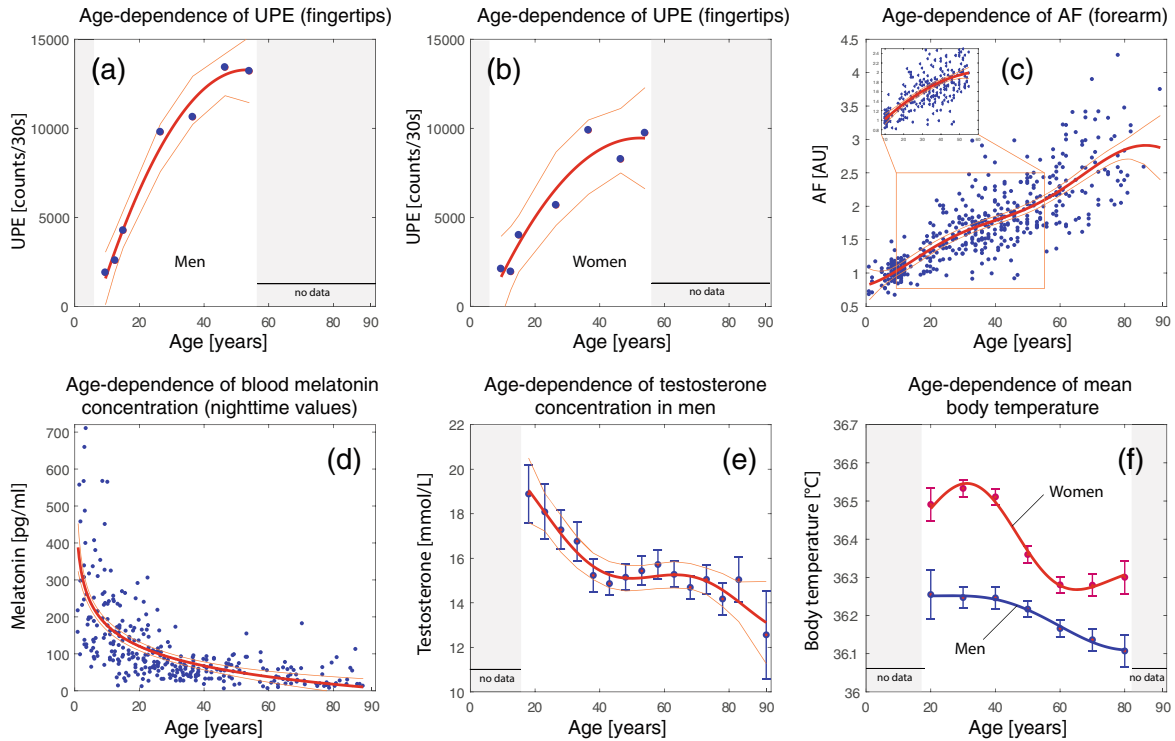


Fig. 17.9 (a, b) Age-related changes of UPE measured at the hands (average UPE from ten fingers; 30 s measurements time, five separate measurements per subject) according to the study of Zheng (1986). (c) Age dependence of skin autofluorescence (AF) from the forearm according to Koetsier et al. (2010). (d) Age dependence of melatonin concentration in the blood during night according to Waldhauser et al. (1998). (e) Age dependence of testosterone concentration in men according to Hughes and Kumari (2019). (f) Age dependence of body temperature in men and women according to Waalen and Buxbaum

(2011). (Data of (a) and (b) extracted from Fig. 1 of (He et al. 2016). Data in (a) and (b) shown were fitted with a polynomial function of second degree. Data of (c) extracted from Fig. 4 of (Koetsier et al. 2010) and fitted with a Fourier series with two harmonics. Data of (d) extracted from Fig. 1 of (Waldhauser et al. 1998) and fitted with a Fourier series with two harmonics. Data of (e) extracted from Fig. 1 of (Hughes and Kumari 2019) and fitted with a Fourier series with two harmonics. Data of (f) extracted from Fig. 4 of (Waalen and Buxbaum 2011) and fitted with a Fourier series with two harmonics)

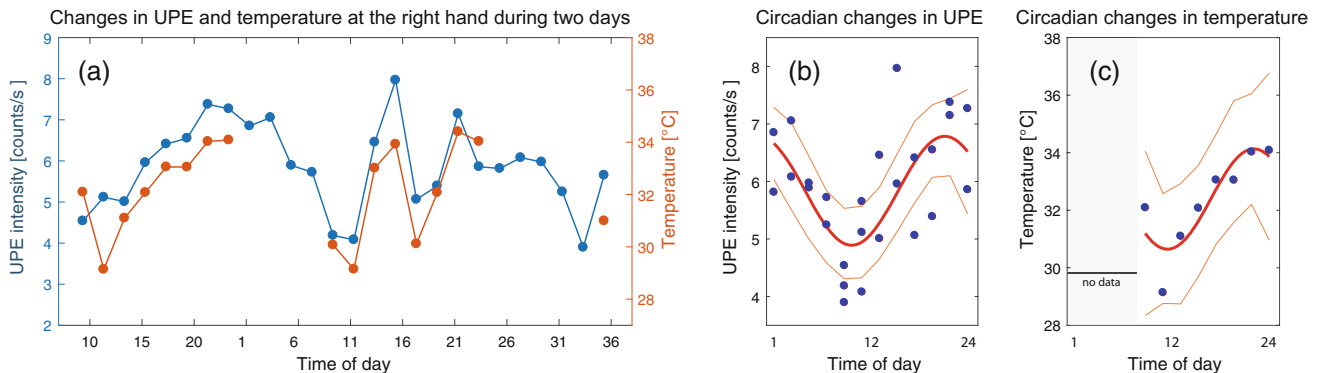


Fig. 17.10 (a) Circadian and infradian changes of UPE from the hand (palm) of one subject. UPE in blue, temperature in orange. (b, c) Circadian changes in UPE and temperature from the first part (first

day) of the data shown in (a). (Data extracted from Fig. 7.11 of Cifra (2006) and fitted with a Fourier series with one harmonic)

hand (Fig. 17.10a). Circadian changes are also clearly visible when analysing the data from the first day (Fig. 17.10b). At the second day, an ultradian fluctuation is present with two minima (around noon and in the evening) (Fig. 17.10c). Based on this study and additional measurements

investigating the effect of induced hand temperature changes on UPE intensity, Cifra concluded that (i) intensity fluctuations of UPE from the hands are correlated with hand temperature changes, whereas the UPE–temperature correlation is not evident for other body parts; (ii) the UPE–

temperature relationship at the hands is non-linear with an additional hysteresis effect (Cifra 2006; Cifra et al. 2008).

The other studies reporting ultradian and circadian changes in UPE in human unfortunately included neither measurement of body or tissue temperature nor metabolic parameters into their experimental protocol. What can be inferred from these studies instead is that there is a large unexplained variability of the phase of the circadian UPE rhythms detected. While in the study of Van Wijk et al. (2006), a general increase in UPE from morning to evening was noticed in almost all body locations measured, the results of Cifra et al. (2007) showed generally a global minimum in the evening and a maximum in the night of the circadian rhythm of UPE measured from the hands, and in the study conducted by Scholkmann et al. (2018) I found a ultradian rhythm from the hand UPE with a minimum at noon and two maxima late in the morning and early in the afternoon. The results about the circadian UPE rhythms therefore seem not to agree with each other.

In order to understand the reason for the discrepancy, a literature research was conducted aiming to collect published circadian rhythms from diverse physiological variables of humans. The aim of this approach was to compare the published circadian physiological rhythm data with the circadian UPE rhythms published by the studies discussed.

Figure 17.11 shows the results of the literature research. Data of circadian rhythm of several physiological parameters were collected including body temperature (core body, proximal temperature and distal temperature), transepidermal water loss and melatonin (Cuesta et al. 2017; Chilcott and Farrar 2000), immune system parameters (concentration of eosinophils, monocytes, platelets, lymphocytes and neutrophils) (Haus and Smolensky 2009) and parameters related to oxidative stress (total antioxidant capacity in saliva, serum uric acid, 8-hydroxy-2'-deoxyguanosine (8-OHdG), malondialdehyde (MDA) and 8-isoprostane) (8-IP) (Borisenkov et al. 2007).

When comparing the circadian UPE rhythm pattern in Figs. 17.2, 17.3, 17.4, and 17.5 with those from the other physiological parameters as shown in Fig. 17.11, several correspondences can be noticed.

The circadian UPE changes from the hand (palm and dorsum) measured by Cifra et al. (2007) are in phase with the circadian rhythm in (i) distal temperature (hands and feet) (Cuesta et al. 2017) (see Figs. 17.3 and 17.11c), (ii) melatonin (Cuesta et al. 2017), (iii) total antioxidant capacity in saliva (Borisenkov et al. 2007) and (iv) some immune parameters (eosinophils and lymphocytes) (Haus and Smolensky 2009). The circadian rhythm of right-left difference of UPE from the hands also discovered in the study of Cifra et al. (Fig. 17.3f) is in phase with the circadian rhythm in (i) core body temperature (Cuesta et al. 2017), (ii) proximal temperature (armpit) (Cuesta et al. 2017),

immune system parameters (monocytes, platelets, neutrophils) (Haus and Smolensky 2009) as well as markers of oxidative stress (8-OHdG, MDA, 8-IP) (Kanabrocki et al. 2009).

The UPE rhythm of an increasing trend from morning to evening observed by Van Wijk et al. (2006) (Fig. 17.2) at several body positions mirrors the pattern in core body temperature (Cuesta et al. 2017) (Fig. 17.11a), two immune system parameters (monocytes and neutrophils) (Haus and Smolensky 2009) (Fig. 17.11i, 1) and two oxidative stress markers (MDA and 8-IP) (Kanabrocki et al. 2009) (Fig. 17.11o, p).

The circadian UPE rhythm detected by the study conducted by myself (Scholkmann et al. 2018) (Fig. 17.4b) is not similar to any circadian pattern shown in Fig. 17.11, except of possibly the change in distal temperature (forearm) (Chilcott and Farrar 2000) (Fig. 17.11d), which shows also a sharp increase from around noon to early afternoon.

In the case of the circadian UPE change of the upper body part as detected by Kobayashi et al. (2009) (Fig. 17.5g), the phase of the rhythm is in phase with the proximal temperature (armpit) (Cuesta et al. 2017) and in antiphase with cortisol concentration (Fig. 17.5i) and two immune system parameters (eosinophils and lymphocytes) (Fig. 17.11h, k) (Haus and Smolensky 2009).

Thus, the comparison between the findings of human studies reporting circadian UPE rhythms and independent studies investigating circadian rhythms of systemic and local physiological parameters shows that some agreements exist, but a general pattern concerning the link between circadian changes in UPE and systemic and local physiological changes is not apparent. What is needed to resolve this issue is a study measuring the UPE intensity at different body parts of a human (or in several human, in the best case) throughout the day (and optimally over several days) with the parallel measurement of local physiological parameters of the body parts investigated (e.g. temperature and oxidative stress) as well as systemic parameters (e.g. core body temperature, hormones, immune system markers and oxidative stress markers).

17.3.2 Infradian Rhythms

From the four studies to be found to report UPE changes in human on a time scale larger than 1 day (Cohen and Popp 1997; Jung et al. 2005; Kobayashi et al. 2009; Zheng 1986) (see Fig. 17.1), the study of Kobayashi et al. (2009) is the only one that provides results of simultaneous measurements of UPE and other physiological variables, saliva cortisol in this case, over 3 days. As already mentioned in Sect. 17.2.1 the cortisol changes was weakly anticorrelated with the infradian UPE change. Unfortunately, oral temperature in

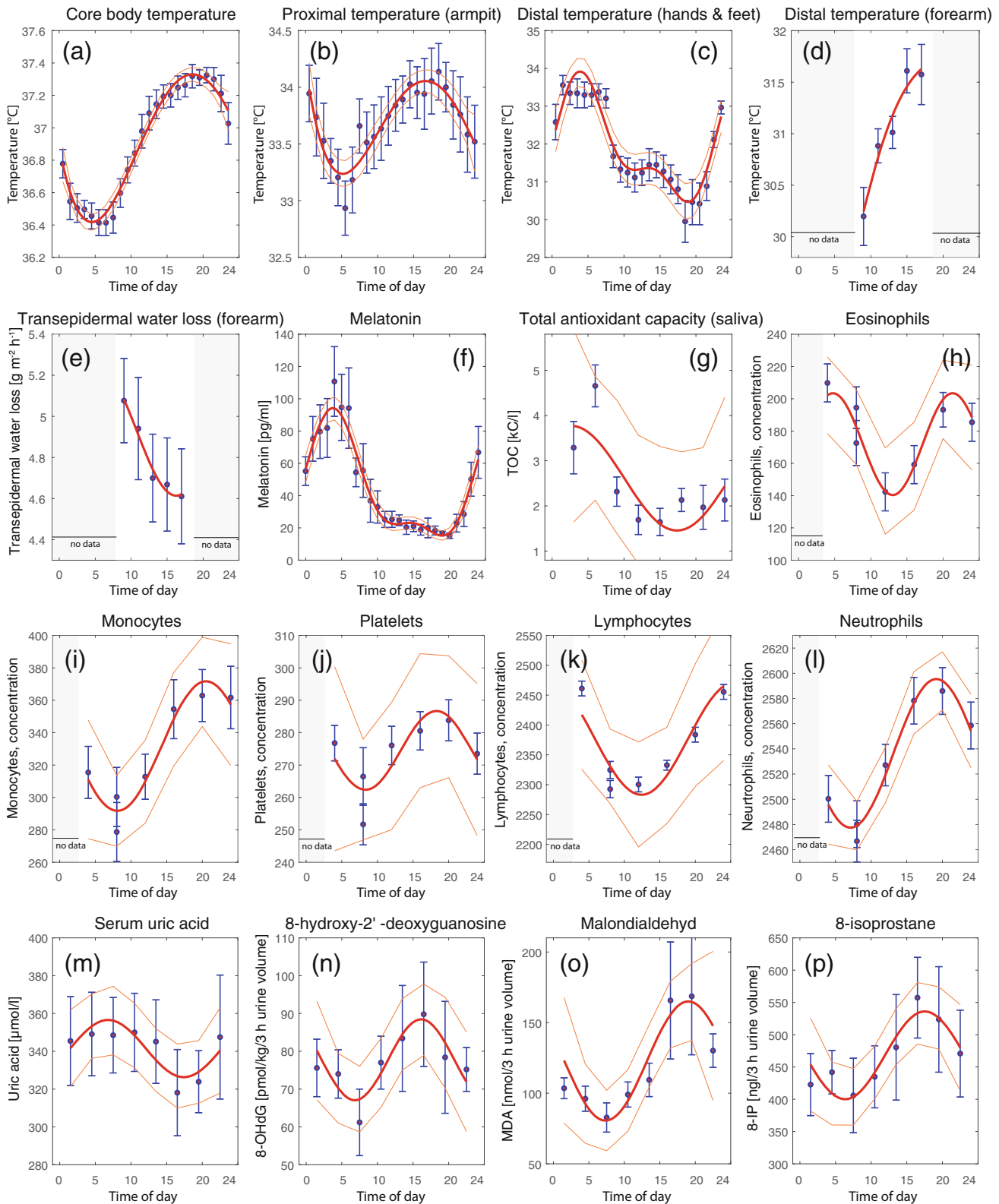


Fig. 17.11 Circadian changes in human temperature, hormone levels, antioxidative capacity, skin water loss, immune system parameters and oxidative stress markers. (Data of (a-c, f) extracted from Fig. 2 of Cuesta et al. (2017), data of (d-e) from Fig. 3 of Chilcott and Farrar (2000), data of (g) from Fig. 1 of Borisenkov et al. (2007), data of (h-l) from Fig. 1 of

Haus and Smolensky (2009), data of (m-p) from Fig. 1-4 of Kanabrocki et al. (2009). Data in (d, e, g-p) shown were fitted with a Fourier series with one harmonic, data in (a-c, f) with a Fourier series with two harmonics)

this study was reported only for the change during 1 day and not for the whole measurement period of 3 days. It is therefore unknown if the oral temperature showed the same ultradian dynamics as UPE did.

Since the other studies presented in Sect. 17.2.1 lack reporting of parallel measurements of additional physiological variables, a comparison with the results of independent studies investigating infradian changes in those variables might be useful. To this end, a literature research was performed aiming to find published results about infradian rhythms of diverse parameters of human physiology. Figure 17.12 provides an overview of study results reporting circannual changes of physiological parameters relevant for our investigation, i.e. total antioxidant activity (in saliva) (Borisovskov 2011), core body temperature (Harding et al. 2019) and markers of oxidative stress (Grešner et al. 2016).

When comparing the infradian changes of UPE measured at the hands and forehead of a women in the study of Cohen and Popp (Fig. 17.6) with the study results visualized in Fig. 17.12, one can notice that the circannual rhythm of UPE from the hands is approximately in phase with the circannual change of core body temperature (Fig. 17.12e, f), with a summer maximum of UPE from the hand corresponding to the summer maximum of core body temperature. Interestingly, such a correspondence is not evident for the infradian fluctuation of UPE from the forehead (Fig. 17.12c). The circannual pattern of the rhythm-adjusted mean (MESOR) of total antioxidant activity in saliva (Fig. 17.12b) is also in phase with the circannual UPE from the hands measured by Cohen and Popp. Circannual variation in the oxidative stress parameters, i.e. the plasma levels of thiobarbituric acid-reactive species (TBARS), ceruloplasmin (Cp), red blood cells' activity of glutathione peroxidase (GPx1) and the ratio of zinc-copper superoxide dismutase (SOD1) to GPx1 ($\ln(\text{SOD1}/\text{GPx1})$) (Fig. 17.12g-l) show also a seasonal dependence, whereas the summer peak of UPE from the hands observed by Cohen and Popp coincides with the circannual minima of TBARS and GPx1 as well as the maxima in Cp and $\ln(\text{SOD}/\text{GPx1})$.

The ultradian variation of the difference of UPE from the right and left hand (Fig. 17.6d) with the detected periods of about 35 d and 95 d may be related to the monthly rhythms of core body temperature in women during the menstrual cycle (Cross and Anderson 2018). The person studied by Cohen and Popp was a woman.

When comparing the results of the infradian UPE changes from hands over 1 year obtained by Jung et al. (2005) with circannual variation of physiological parameters shown in Fig. 17.12g-l the following can be noticed: (i) The circannual change of body temperature (MESOR and amplitude) (Fig. 17.12e,f) is only weekly correlated with the ultradian UPE pattern of the hands (Figs. 17.7 and 17.8). The closest correspondence can be noticed for the UPE changes of

subjects 2 and 3 from the palm that are correlated with the circannual changes of circadian body temperature amplitude (Fig. 17.12f) and anticorrelated with the MESOR and circadian amplitude change of total antioxidant activity in the saliva (Fig. 17.12b, d). The differential changes of UPE (right minus left hand intensities) do not closely resemble the changes in the variables shown in Fig. 17.12 with the exception of the right-left difference of UPE changes from the palm in subject 2 (Fig. 17.8c) that resembling approximately the circannual rhythm in the MESOR of core body temperature (Fig. 17.12e). The oxidative stress markers (Fig. 17.12g-l) show peaks in winter (Cp and $\ln(\text{SOD1}/\text{GPx1})$) or summer (TBARS, GPx1). Assuming that UPE is primarily positively correlated with oxidative stress (the higher UPE, the more oxidative stress) and anticorrelated with the antioxidative defence state (the lower UPE, the lower oxidative stress and/or higher antioxidative protection), the data of Cohen and Popp imply an increase in oxidative stress in spring/summer (UPE maxima). The oxidative stress parameters (Fig. 17.12g-l) reflect this seasonal dependence in general but for a closer analysis the oxidative stress markers would be needed with monthly resolution. Thus, the available data give indications that the circannual UPE changes measured by Jung et al. are correlated with temperature and metabolic markers, while their exact relationship is not directly evident due to the insufficient data available to compare with the UPE changes.

The fact that the *circadian* changes of total antioxidant activity and core body temperature are modulated by an ultradian (i.e. a circannual) rhythm (Fig. 17.12a, d) is also of interest for the interpretation of the circadian UPE changes noticed by the four studies (Cifra et al. 2007; Kobayashi et al. 2009; Van Wijk et al. 2006; Scholkmann et al. 2018) discussed. The seasonal dependence of the circadian changes needs to be also considered for a proper comparison of the study results. However, information on the seasons when the measurements were performed is not reported in the studies.

Concerning the age-related changes of UPE from the hands published by Zheng (1986), a comparison was made with age-related changes of skin autofluorescence (AF; correlated with the concentration of advanced glycation end products in the skin as results of oxidative stress and tissue damage (Mulder et al. 2006; Meerwaldt et al. 2005)), nighttime values of melatonin concentration (indicative of overall health and fitness (Brzezinski and Epstein 1997)), testosterone concentration in men (associated with endocrine health (Booth et al. 1999)) and body temperature (indicative of the general physiological fitness (Kelly 2006, 2007)). The following can be noticed: (i) AF increases linearly whereas UPE quadratically (with a decline in increase above about 40 years of age), (ii) the melatonin concentration decreases according to a power law and is anticorrelated to the UPE change to a specific degree, (iii) the testosterone concentration shows an

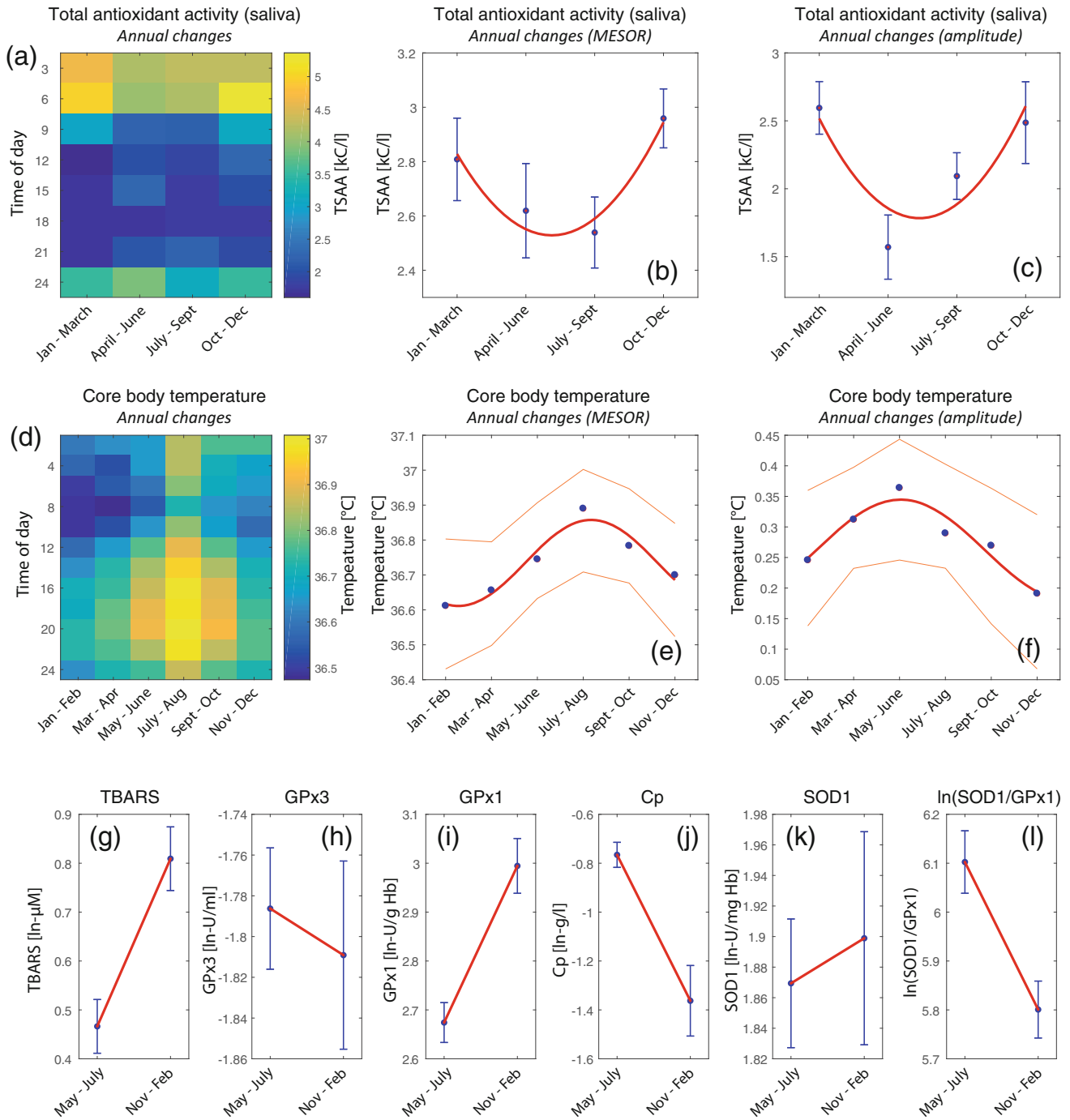


Fig. 17.12 Circannual changes of physiological parameters in humans. (a–c) Changes in total antioxidant activity (saliva) according to Borisenkov (2011). (a) Changes in circadian amplitude with time of year. (b) MESOR (rhythm-adjusted mean). (c) Circadian amplitude. (d–f) Changes in core body temperature according to Hardling et al. (2019). (d) Changes in circadian amplitude with time of year. (e) MESOR. (f)

Circadian amplitude (g–l) Circannual changes in oxidative stress markers in humans according to Grešner et al. (2016). (Data of (a–c) extracted from Fig. 2 of (Borisenkov 2011) and fitted with a polynomial function of fifth degree. Data of (d–f) extracted from Fig. 3 of (Hardling et al. 2019) and fitted with a polynomial function of fifth degree. Data of (g–l) extracted from Fig. 1 of (Grešner et al. 2016))

inflection point around 45 years of age that interestingly coincides with the decrease in UPE with age and (iv) the mean body temperature shows complex trends that do not resemble the trend in UPE. These results indicate the

age-dependent change in UPE partially resembles changes in endocrine function and oxidative stress. Unfortunately, UPE values from subjects in the age range 60–90 years are not available from Zheng (1986) so that a comparison in this

particularly interesting range cannot be made with the other age-dependence changes in physiological parameters.

17.4 Summary, Conclusion and Outlook

The presented analysis of the published data about chronobiological variations of spontaneous UPE from humans revealed several interesting insights that can be summarized as follows:

- (i) According to the literature research performed, *seven* studies have been published so far reporting *chronobiological rhythms* (or age-dependent trend with several age groups) in measurements of spontaneous UPE in humans (Cifra et al. 2007; Cohen and Popp 1997; Jung et al. 2005; Kobayashi et al. 2009; Van Wijk et al. 2006; Scholkmann et al. 2018; Zheng 1986).
- (ii) The UPE rhythms reported span from *ultradian*, *circadian* to *infradian*.
- (iii) There is a *large inter-subject variability* between the UPE rhythms reported both with respect to the period, phase and amplitude.
- (iv) The UPE intensity from the *hands* and *different body parts* follows circadian rhythms (four studies) as well as a circannual one (two studies of UPE emission from hands). The difference of UPE emission from the right and left hand is also modulated with a circadian and circannual rhythm.
- (v) UPE from the hand increases non-linearly with *age*.
- (vi) Key parameters of *human physiology* (i.e. temperature, endocrine function and oxidative stress) show also *circadian and circannual rhythms* and are partially related to the circadian and circannual rhythms in UPE. Most of the studies did not report any physiological parameters in addition to the UPE data so that a general conclusion about the relationship between UPE and other physiological parameters is only partially possible at present, based on the comparison with results from independent studies reporting chronobiological variability of human physiological parameters. However, a correlation of circadian UPE changes of the hands with changes in skin temperature is evident.

Based on these conclusions, the following suggestions for future studies can be formulated:

- (i) It is necessary to perform *multimodal* measurements assessing changes in UPE (from one or several body positions) in a specific time span and other relevant physiological parameters (like tissue and core body temperature, endocrine parameters, immune system parameters, local and systemic oxidative stress markers)

in parallel. Optimally, multimodal measurements (i.e. combination of UPE with other physiological parameters) should be performed to investigate the *complete* chronobiological time frame (ultradian, circadian and infradian), i.e. the *chronome*, and should investigate the inter-subject variability of the chronobiological variability.

- (ii) *Reference ranges* for the chronobiological modulation of UPE changes should be established for all time frames (ultradian, circadian and infradian) from healthy subjects of both sexes and with measurements from several body locations.
- (iii) Studies should be conducted investigating how the chronobiological modulation of UPE from human body parts deviate in subjects with *diseases* and how the modulation changes during a course or treatment of a disease.

In conclusion, in this chapter, I summarized the present knowledge of chronobiological rhythms in spontaneous UPE from humans. The studies available are reviewed and compared to each other.

Acknowledgements I thank my wife, Rachel Scholkmann, for proofreading the manuscript.

References

- Mei, W.P., *About the Nature of Biophotons*. Journal of Biological Systems, 2011. **02**(01): p. 25–42.
- Cadenas, E., *Biological Chemiluminescence*, in *Reactive Oxygen Species in Chemistry, Biology, and Medicine*. 1988. p. 117–141.
- Cifra, M. and P. Pospíšil, *Ultra-weak photon emission from biological samples: Definition, mechanisms, properties, detection and applications*. Journal of Photochemistry and Photobiology B: Biology, 2014. **139**: p. 2–10.
- Havaux, M., C. Triantaphylides, and B. Genty, *Autoluminescence imaging: a non-invasive tool for mapping oxidative stress*. Trends in Plant Science, 2006. **11**(10): p. 480–484.
- Blask, M., et al., *Short-time fractal analysis of biological autoluminescence*. Plos One, 2019. **14**(7).
- Cifra, M., et al., *Spontaneous ultra-weak photon emission from human hands is time dependent*. Radioengineering, 2007. **16**(2): p. 15–19.
- Cohen, S. and F.A. Popp, *Biophoton emission of the human body*. Journal of Photochemistry and Photobiology B: Biology, 1997. **40**(2): p. 187–189.
- Jung, H.-H., et al., *Year-long biophoton measurements: normalized frequency count analysis and seasonal dependency*. Journal of Photochemistry and Photobiology B: Biology, 2005. **78**(2): p. 149–154.
- Kobayashi, M., D. Kikuchi, and H. Okamura, *Imaging of Ultraweak Spontaneous Photon Emission from Human Body Displaying Diurnal Rhythm*. PLoS ONE, 2009. **4**(7).
- Van Wijk, R., E.P.A. Van Wijk, and R.P. Bajpai, *Photocount distribution of photons emitted from three sites of a human body*. Journal of Photochemistry and Photobiology B: Biology, 2006. **84**(1): p. 46–55.
- Scholkmann, F., et al., *Spatio-temporal dynamics of spontaneous ultra-weak photon emission (autoluminescence) from human hands*

- measured with an EMCCD camera: Dependence on time of day, date and individual subject. *Matters*, 2018.
- Zheng, R., *Experimental study related with several physiological and pathological states based on ultraweak luminescence of human body surface (in Chinese)*. Faguang Xuebao, 1986. **7**(1): p. 20-26.
- Koukkari, W.L. and R.B. Sothorn, *Introducing Biological rhythms*. 2006, New York: Springer.
- Cornelissen, G., *Cosinor-based rhythmometry*. *Theoretical Biology and Medical Modelling*, 2014. **11**(1).
- Ulrych, T.J. and T.N. Bishop, *Maximum entropy spectral analysis and autoregressive decomposition*. *Reviews of Geophysics*, 1975. **13**(1).
- Fong Chao, B., *On the use of maximum entropy/autoregressive spectrum in harmonic analysis of time series*. *Pure and Applied Geophysics PAGEOPH*, 1990. **134**(2): p. 303–311.
- Dowse, H.B., *Maximum entropy spectral analysis for circadian rhythms: theory, history and practice*. *Journal of Circadian Rhythms*, 2013. **11**(0).
- Zhao, X., et al., *Ultra-weak photon emission of hands in aging prediction*. *Journal of Photochemistry and Photobiology B: Biology*, 2016. **162**: p. 529–534.
- Sauermann, G., et al., *Ultraweak photon emission of human skin in vivo: Influence on topically applied antioxidants on human skin*. *Methods in Enzymology*, 1999. **300**: p. 419–428.
- Diambra, L. and L. Menna-Barreto, *Infradian Rhythmicity in Sleep/Wake Ratio in Developing Infants*. *Chronobiology International*, 2009. **21**(2): p. 217–227.
- Clayton, P.E., et al., *Translational Neuroendocrinology: Control of Human Growth*. *Journal of Neuroendocrinology*, 2014. **26**(6): p. 349–355.
- Scholkmann, F. and U. Wolf, *The Pulse-Respiration Quotient: A Powerful but Untapped Parameter for Modern Studies About Human Physiology and Pathophysiology*. *Frontiers in Physiology*, 2019. **10**.
- Mahoney, P., et al., *The biorhythm of human skeletal growth*. *Journal of Anatomy*, 2018. **232**(1): p. 26–38.
- Pitfield, R., J.J. Miszkiewicz, and P. Mahoney, *Microscopic markers of an infradian biorhythm in human juvenile ribs*. *Bone*, 2019. **120**: p. 403–410.
- Bott, V., *Der Siebenjahresrhythmus in seiner Bedeutung für bestimmte Kinderkrankheiten*. Beiträge zu einer Erweiterung der Heilkunst nach geisteswissenschaftlichen Erkenntnissen 1985. **38**: p. 24–27.
- Rohen, A., *Rhythmen im Lebenslauf, Teil I*. Beiträge zu einer Erweiterung der Heilkunst nach geisteswissenschaftlichen Erkenntnissen, 1984a. **37**(3): p. 96–102.
- Rohen, A., *Rhythmen im Lebenslauf, Teil II*. Beiträge zu einer Erweiterung der Heilkunst nach geisteswissenschaftlichen Erkenntnissen, 1984b. **37**(4): p. 130–137.
- Rohen, A., *Rhythmen im Lebenslauf, Teil III*. Beiträge zu einer Erweiterung der Heilkunst nach geisteswissenschaftlichen Erkenntnissen, 1984c. **37**(6): p. 240–249.
- He, M., et al., *A Chinese literature overview on ultra-weak photon emission as promising technology for studying system-based diagnostics*. *Complementary Therapies in Medicine*, 2016. **25**: p. 20–26.
- Koetsier, M., et al., *Reference Values of Skin Autofluorescence*. *Diabetes Technology & Therapeutics*, 2010. **12**(5): p. 399–403.
- Waldhauser, F., J. Kovács, and E. Reiter, *Age-related changes in melatonin levels in humans and its potential consequences for sleep disorders*. *Experimental Gerontology*, 1998. **33**(7–8): p. 759–772.
- Hughes, A. and M. Kumari, *Testosterone, risk, and socioeconomic position in British men: Exploring causal directionality*. *Social Science & Medicine*, 2019. **220**: p. 129–140.
- Waelen, J. and J.N. Buxbaum, *Is Older Colder or Colder Older? The Association of Age With Body Temperature in 18,630 Individuals*. *The Journals of Gerontology Series A: Biological Sciences and Medical Sciences*, 2011. **66A**(5): p. 487–492.
- Cifra, M., *Measurement of spontaneous photon emission from the human body: technical aspects, parameters, time and temperature dependent fluctuations of photon emission*. Diploma Thesis. University of Zilina, Faculty of Electrical Engineering, Department of Electromagnetic and Biomedical Engineering, 2006.
- Cifra, M., Van Wijk, E.P.A., Van Wijk, R., *Temperature Induced Changes of Spontaneous Photon Emission from Human Hand*. *Progress in Electromagnetics Research Symposium (PIERS 2008)*, 2008.
- Cuesta, M., et al., *Skin Temperature Rhythms in Humans Respond to Changes in the Timing of Sleep and Light*. *Journal of Biological Rhythms*, 2017. **32**(3): p. 257–273.
- Chilcott, R.P. and R. Farrar, *Biophysical measurements of human forearm skin in vivo: effects of site, gender, chirality and time*. *Skin Research and Technology*, 2000. **6**(2): p. 64–69.
- Haus, E. and M.H. Smolensky, *Biologic Rhythms in the Immune System*. *Chronobiology International*, 2009. **16**(5): p. 581–622.
- Borisenkov, M.F., et al., *Diurnal changes in the total antioxidant activity of human saliva*. *Human Physiology*, 2007. **33**(3): p. 375–376.
- Kanabrocki, E.L., et al., *Circadian variation in oxidative stress markers in healthy and type II diabetic men*. *Chronobiology International*, 2009. **19**(2): p. 423–439.
- Borisenkov, M.F., *Seasonal changes in the circadian rhythm of the total antioxidant activity of human saliva*. *Human Physiology*, 2011. **34**(1): p. 120–122.
- Harding, C., et al., *The daily, weekly, and seasonal cycles of body temperature analyzed at large scale*. *Chronobiology International*, 2019. **36**(12): p. 1646–1657.
- Grešner, P., et al., *Does the Low-level occupational exposure to volatile organic compounds alter the seasonal variation of selected markers of oxidative stress? A case-control study in nail technicians*. *Journal of Occupational Medicine and Toxicology*, 2016. **11**(1).
- Cross, G. and R.J. Anderson, *A 30-year study of body temperature variations correlated with menstrual cycle, seasonality, and aging*. *Biological Rhythm Research*, 2018. **50**(4): p. 505–523.
- Mulder, D.J., et al., *Skin Autofluorescence, a Novel Marker for Glycemic and Oxidative Stress-Derived Advanced Glycation Endproducts: An Overview of Current Clinical Studies, Evidence, and Limitations*. *Diabetes Technology & Therapeutics*, 2006. **8**(5): p. 523–535.
- Meerwaldt, R., et al., *Skin Autofluorescence, a Measure of Cumulative Metabolic Stress and Advanced Glycation End Products, Predicts Mortality in Hemodialysis Patients*. *Journal of the American Society of Nephrology*, 2005. **16**(12): p. 3687–3693.
- Brzezinski, A. and F.H. Epstein, *Melatonin in Humans*. *New England Journal of Medicine*, 1997. **336**(3): p. 186–195.
- Booth, A., D.R. Johnson, and D.A. Granger, *Testosterone and Men's Health*. *Journal of Behavioral Medicine*, 1999. **22**(1): p. 1–19.
- Kelly, G., *Body Temperature Variability (Part 1): A Review of the History of Body Temperature and its Variability Due to Site Selection, Biological Rhythms, Fitness, and Aging*. *Alternative Medicine Reivew*, 2006. **11**(4): p. 278–293.
- Kelly, G., *Body Temperature Variability (Part 2): Masking Influences of Body Temperature Variability and a Review of Body Temperature Variability in Disease*. *Alternative Medicine Reivew*, 2007. **12**(1): p. 49–62.

Cristiano de Mello Gallep

18.1 Introduction

It is now more than 100 years since Alexander G. Gurwitsch discovered that an extremely weak light emission occurs during plant development, by using two onion roots as the ‘source’ and the ‘detector’ (Gurwitsch 1988). But still more decades did pass before the development, in the 1950s, of effective optical detectors able to operate in photon-counting mode with enough efficiency and low noise levels, devices such as the photomultiplier tube (PMT), which came to enable the first quantitative recordings of biological autoluminescence (BAL) in seedlings (Colli and Facchini 1954), where certainly roots do play a dominant role (Devaraj et al. 1997).

So, one may say that such BAL, phenomena also named as ‘biophoton’, or ‘UPE’, for ultraweak photon emission, in seedlings is not a new subject. Some studies have explored applications in agriculture, basic biology and also chronobiology (de Mello Gallep 2014; Cifra and Pospíšil 2014). As a seed prepares to develop into a seedling, taking up water, and as it further grows its leaflets and rootlets, constructing new organic tissues and using its energy reservoirs, it also presents a faint, spontaneous luminescence that can be used to evaluate the seedlings development in real time, in optimal or stressing conditions. This feature can be useful not only for the study of the seedlings growth on its own but also for quantifying the impacts that the environmental conditions can have – chemical or physical. And for chronobiology studies as well, when timing-detailed, long-term data are recorded and available.

The sources of BAL in seedlings can be found, as in other organisms, among the by-products of the metabolic activity where reactive chemical species take part, mainly the ones involving radical-oxygen species (ROS) that are

electronically excited, and that can occur inside living cells and tissues, such as triplet excited carbonyls and singlet oxygen species, most released during enzymatic reactions (Cifra and Pospíšil 2014; Miyamoto et al. 2014) (see more in Chaps. 8, 9, 10, 11, 12, 13, and 14). As discussed in ref. (Cifra and Pospíšil 2014), ROS would react with biomolecules and give unstable intermediates as results – such as dioxetanes and tetroxides – that further would form triplet excited carbonyls and/or singlet oxygen, in forms able to further emit photons in the visible range. In effect, BAL occurs for organisms evolving under normal, optimal conditions as well as in response to chronic or acute stressing conditions, physical or chemical (Ichimura et al. 1989a; Makino et al. 1996a; Rastogi and Pospíšil 2012). For intact seedlings, it was show that the main emitters are the rootlet’s base and tip, regions where the metabolism is more active due to cell division and tissue elongation (Ichimura et al. 1989a).

Before we go to currently developed applications, a little history of achievements in this specific area of BAL from seedlings.

18.2 Historical Developments

The above-mentioned first photon-count recordings of BAL in seedlings were made by Colli and Facchini, using as samples seedlings of wheat, beans, lentils and corn, demonstrating spontaneous photon emission in the range from 400 nm to 700 nm, i.e. the visible light. Their work also pointed out that BAL increases during germination, and it is stronger in roots than in other parts; they realized also that stressing conditions would force seedlings to emit more just after the injury (Colli and Facchini 1954; Colli et al. 1955). They tested large amounts of seeds (up to 60 g) in all the published experiments, probably due to usual constraints in such works: high background noise and low sensitivity setups. These constraints might also have limited the time discretization to the 24-h used, making it hard to compare

C. de Mello Gallep (✉)

Faculdade de Tecnologia, Universidade Estadual de Campinas, Limeira, SP, Brazil

e-mail: gallep@unicamp.br

with actual data, acquired in second-minute windows even for days-long experiments.

In the early 1970s, Inaba and co-workers run the ‘Biophoton Project’ in Tohoku, Japan, working on the development of special setups for BAL experiments (Inaba et al. 1979; Shimizu et al. 1973), further including efficient PMTs and CCD cameras (Inaba et al. 1982; Scott and Inaba 1989). Published works from their group confirmed that physical stress induces BAL increase (Devaraj and Inaba 1997; Suzuki et al. 1991) and that BAL bursts occur together with changes in bioelectric potentials for soybeans tests (Usa et al. 1989). The fact that the spectra of the spontaneous luminescence in mitochondrial respiration is related to the emission spectra of linoleic acid–lipoxygenase reactions did push many to think that lipid peroxidation should be one important source of BAL (Hideg et al. 1991). Although, this same group also showed that imbibed seeds present stronger BAL even for samples without lipoxygenase (Saeki et al. 1989). Later, in the 1990s, this research group was one of the first to present what they named ‘biophoton imaging systems’, enabling now spatiotemporal analysis of BAL, where quick reactions to acute stress can be traced in real time, in living samples (Kobayashi 2005).

In the 1980s, the group of Slawinski confirmed that sprouts and mainly roots are the strongest sources of BAL in seedlings (Slawinski et al. 1981) and that physical and chemical stress do induce BAL bursts, pointing out further toxicological applications to be developed (Slawinski 2005; Slawinski et al. 1992). The group of Boveris made contributions using soybean sprouts, indicating that the radicals related to water uptake and to the lipoxygenase activity might be one of the main sources of BAL (Boveris et al. 1983, 1984). In the following years, the group from Hamamatsu presented their high-sensitive camera system (Ichimura et al. 1989b), used further in plant defense response research (Makino et al. 1996b; Hiramatsu 1998). This research also confirmed that BAL is related to the germination rate (Kai et al. 1994) and to the root growth (Kai et al. 1993), that the suppression/stimulation of seedling’s growth does alter BAL pattern and intensity (Kai et al. 1995) and that BAL can be used to infer, fast and easy, the stress induce over seedlings, both physically (Ohya et al. 2002) and chemically (Ohya et al. 2000).

In the 1990s, works from the group of Musumeci and collaborators indicated that the (induced) luminescence pattern in seeds are related to their further germination vigor (Musumeci et al. 1994). Their work showed that the BAL pattern is related directly to the metabolism (Triglia et al. 1993) and that UV spectral bands can also be detected, mostly at the beginning of the germination process (Grasso et al. 1991). Other contributions in the area were performed in China, already in the 2000s, mostly with soybean sprouts and in response to stress (Chen et al. 2002, 2003; Cheng et al.

2006). Recent data on seedlings have come from the group of Cifra and co-workers, the only one able to do it with arabidopsis so far (Saeidfirozeh et al. 2018). Below we list the works of the Brazilian group at UNICAMP, revisiting already published data.

18.3 Applications at LaFA: UNICAMP

The Applied Photonics Lab – *LaFA (Laboratório de Fotônica Aplicada)* started at the end of 2004, at *Faculdade de Tecnologia / Universidade Estadual de Campinas (UNICAMP)*, with the support of FAPESP (São Paulo State Research Foundation), mostly inspired by the seminar lectures of Prof. Janusz Slawinski, at the former International Institute of Biophysics (IIB, Neuss / Germany), and also by the ones of Yu Yan, who was the first to present long-term, time-detailed measurement of BAL in seedlings (Yan 2005), and with the impulse of a campus where facilities and human resources were more abundant in the area of environmental control and related techniques. As learnt in several visits to the IIB, a set of low-noise PMT and dark chamber are enough to start; and so we did, making two home-made setups, and focused on germination tests, with seedlings being the mediation for applications in toxicology that could be developed with local support.

18.3.1 Toxicology

Our first results were published in 2007, with data of two series of consecutive wheat germination tests, up to 3-days long each, using wastewater sediment solutions as a possible fertilizer; it was shown that the total photon-counting number of each test were directly correlated to their germination rate and vigor (Gallep and dos Santos 2007). In these series of tests, one could note that the BAL (or UPE) time pattern of each germination test is peculiar, differing from day to day even (and mostly) for the control groups. Figure 18.1a presents a typical photon-count time pattern; Fig. 18.1b the BAL (UPE) total count for the last day of germination, on the third day after imbibition, versus the germination rate of each sample with different wastewater solutions, total of 13 germination tests.

Our first results confirmed the data found by Slawinski, Hiramatsu and others: different stress may result in a non-linear BAL response, i.e. small stress could push BAL levels up when the organism can still endure the combat against the hazard; a further intense stress would deprive UPE emission, as the organism gives up in defense response somehow or other.

Next, our group tested toxic solutions of hazards that are abundant in nearby sources: chromium dichromate

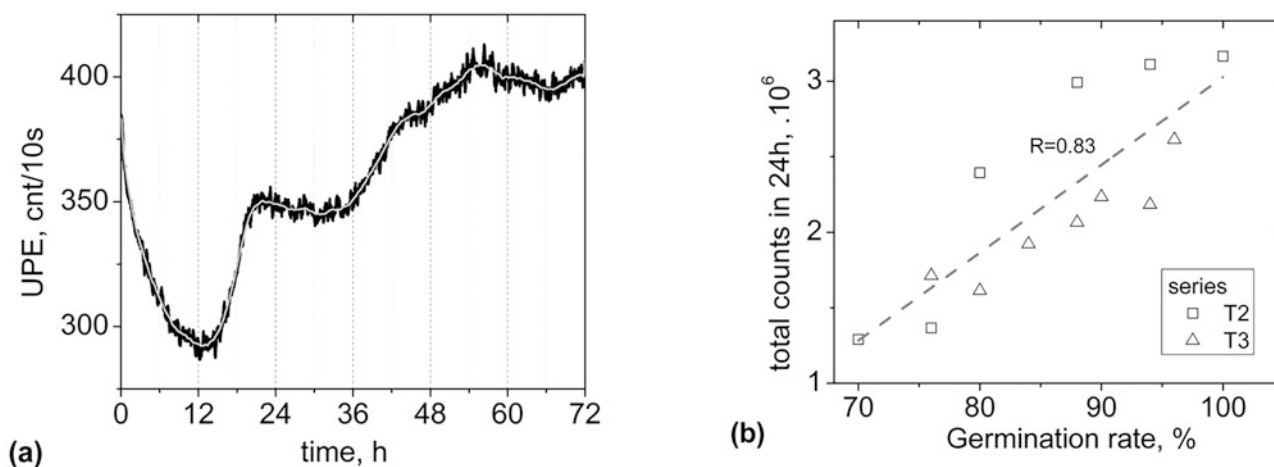


Fig. 18.1 (a) UPE (BAL) photon counts (count /10 s) of 50 wheat seedlings in wastewater sediment (3%), (b) germination rate versus 24-h total count (third day) for two series of tests. (Replicated from (de Mello Gallep 2014))

(K2Cr2O7) and leachate from domestic waste deposit (Moraes et al. 2009, 2010). One more time, the data of these germination series showed that toxic environments do diminish seedlings' growth and total BAL emission, with an almost linear relationship between total photon counts and the germination rates, as shown in Fig. 18.2a and b. Again, a weak stress induced more BAL emissions but did not diminish growth (Fig. 18.2b and 5 ppm and 100 ppm solutions), and stronger solutions depressed both growth and BAL (UPE). However, when just the depressed and control groups were considered, a linear relation could still be traced. Solutions of galvanic ink residues were also tested in 2010 (condensed results at Fig. 18.2c), for two series of tests.

As learnt in those initial series, it is easier to compare the control tests to the strong stressed samples than to the ones embedded in not-so-strong hazards, as when dealing with weak and medium stressing conditions. In order to check this challenge in detail, we endure a long series of germination tests, using small (25 ppm) and medium (150 ppm, EC50) chromium dichromate stressing solutions. As expected, a simple datagram of total count versus germination failed to discriminate between the two different samples, as the daily fluctuations already mentioned might hide tangible differences in those tests that were not performed simultaneously. Trying to answer the question, a multi-fractal analysis of the BAL time patterns was proposed by colleagues, which resulted in a quite successful manner to distinguish the samples by their BAL pattern data (Scholkmann et al. 2011).

We observed that the BAL of consecutive germination tests did vary a lot in pattern/intensity. For that reason, we modified the procedure for a better comparison between stressed and control samples by running simultaneous experiments in similar setups. We also found that an acute instead of a chronic stress could be better analysed and also

save experimental time and material. In chronic tests, the tested solutions are added at the beginning of the germination; in acute tests, it is done after the seedlings have grown for some time (3 days for wheat) in pure water and in a controlled dark chamber. Using this last kind of approach, the BAL from the control and from the stressed samples can be quantified and differentiated more easily using germination rate/size parameters. This procedure was demonstrated for solutions of quicksilver (Hg) and sodium fluoride (NaF), as shown at Fig. 18.3 (Bertogna et al. 2013a, b): Figure 18.3a shows a complete (96 h) double test, showing similar patterns in the first 72 h and the huge difference at the last day, after the second imbibition, when one sample was stressed chemically; Fig. 18.3b shows the germination performance – the average biomass increase and the total sum of the roots lengths – plotted against the angular coefficient of the BAL pattern linear regression, for a series of control and Hg solutions.

The BAL patterns for the NaF series (EC₅₀), after inoculation at 72 h, are presented in Fig. 18.3c – stressed samples present patterns rising in the first 6 h, to decline just after; the respective datagram for this series is shown at Fig. 18.3d.

Figure 18.4 shows the BAL data of single seedlings – mung bean and wheat – in triplicates with diverse growth vigor (see pics) and their correspondent photon-emission, first presented in ref. (Gallep and Robert 2020), confirming the stronger the development, the bigger the BAL detected.

18.3.2 Chronobiology

The daily and monthly oscillations found in BAL patterns, recorded in long series of germination tests, were observed already during the first years of work at the LaFA: two series of consecutive germination tests were presented in 2007,

Fig. 18.2 Total photon counts versus germination rate of wheat seedlings samples, in series of tests for: (a) leachate (solution, %), (b) potassium dichromate (ppm solution, 1.5 and 100 ppm discarded for linear regression) and (c) galvanic ink residues (solution, %). (Replicated from (de Mello Gallep 2014))

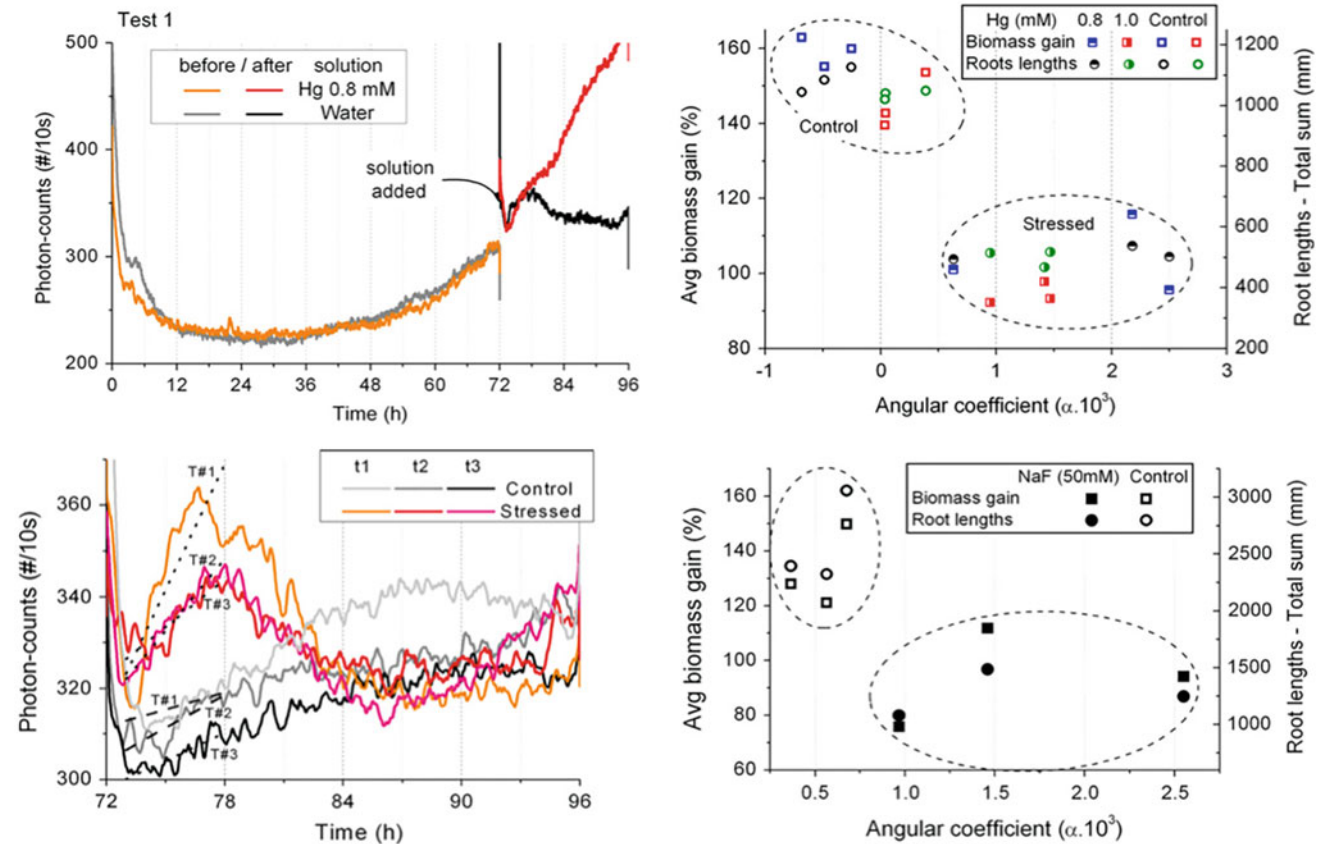
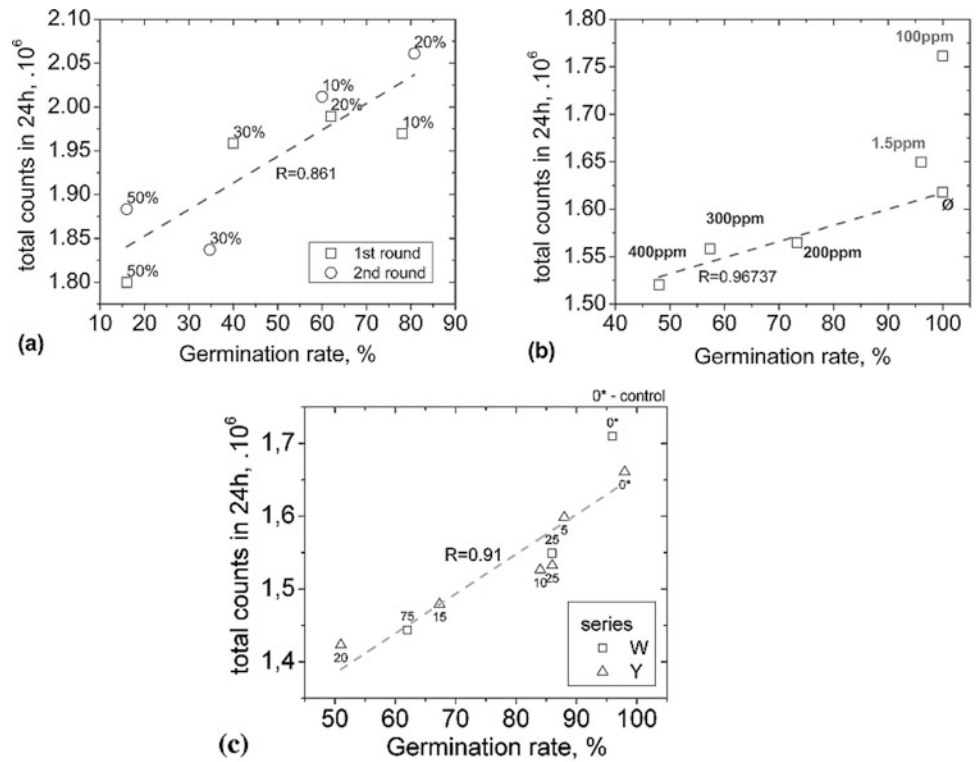


Fig. 18.3 (a) Photon-count data for two simultaneous tests – detail of second imbibition (stress and control) event at 72 h; (b) germination performance (biomass gain and total root length) versus the linear growth (angular) coefficient, for control and stressed series; (c) photon

counts of the last 24 h, data for NaF series (EC_{50}); (d) germination performance (biomass gain and total root length) versus the linear growth (angular) coefficient for 73 h < t < 78 h. (Replicated from (Bertogna et al. 2013a))

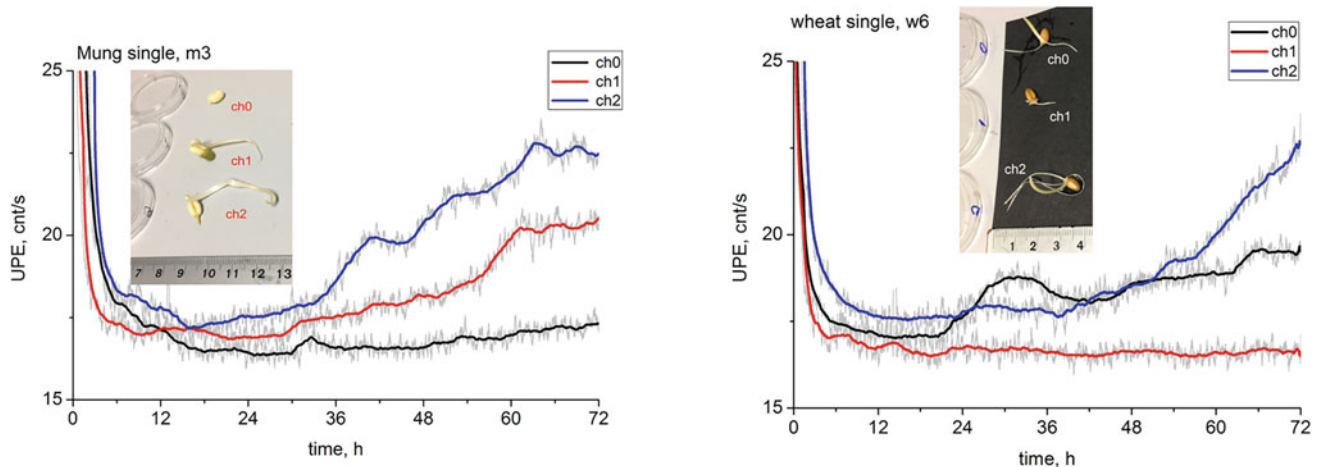


Fig. 18.4 Photon emissions as a function of time, measured in counts/s. (a) mung and (b) wheat. Coloured curves, as roving averages of 100 points, show different seedlings measured simultaneously by three

independent channels, ch0, ch1, ch2. Insert shows pictures of each seedling at time of test termination (72 h). (Replicated from (Galleg and Robert 2020))

showing that the daily and quasi-monthly oscillations of BAL patterns are detected (Galleg et al. 2007). The impact of stress over such periodical cycles were studied later, but results were hard to be reproduced (Bertogna et al. 2010).

So, to better understand these (ultra) circadian rhythms present in the patterns of BAL in germinating samples, we started to use the approach explored by Barlow (Barlow et al. 2010) and previously proposed by Zürcher et al. (1998) to study the daily tree-trunk variations: the relation of plant cycles to the local gravimetric tide, i.e. the daily and monthly oscillations of the total local gravity force due to the relative positioning of Moon and Sun (Longman 1959). Data analysis was used to show that BAL singular points – pattern jumps and plateaus – are synchronous with local peaks/droughts of the local gravimetric (tide) pattern (δg) and that BAL patterns and δg do present equivalent periodical components (Moraes et al. 2012). Further series of germination tests were performed in Brazil and in other countries, working with the contributions of Barlow and colleagues, to compare BAL patterns and local δg cycles (Galleg et al. 2014, 2017). The collected data show that seedlings present variations in BAL intensity directly related to sprout growth and that the BAL patterns are similar to those of the local δg . Further, BAL for a single sunflower seedling, as one example, also appeared to co-vary with the local δg (de Mello Galleg 2014); these single seedling data were revisited recently (Galleg and Robert 2022), as reproduced at Fig. 18.5: the time resolved data displayed in the superposition of consecutive cycles (see ref. (Galleg and Robert 2021) for details), providing evidence of oscillatory periods around but not exactly on a 12-h and 24-h basis, for both the seedlings BAL and the local gravimetric force. Average data in UPE and gravimetric tide profiles highlight the covariance between the gravimetric (tidal) force and the BAL

pattern. The graphs are arranged such that successive gravimetric tides are plotted over each other, keeping the phase of maximal tide coincidental with others. This example does highlight the presence of rhythmicity that looks very much like that of a circadian oscillator, yet in the detail of its time course can be linked to the effect of the gravimetric tide (Galleg and Robert 2022).

Similar approach can be used for the single wheat seedlings BAL data, presented at Fig. 18.4 and ref. (Galleg and Robert 2020): when plotted superposed, cut from the continual time series of germination tests: the BAL appeared to have coincident inflection points to the local gravimetric tide patterns, as presented in Fig. 18.6, where the bell-like gravimetric profiles appear very well correlating with BAL (UPE) profiles, with very coincident inflection points both in individual curves and in the averaged pattern.

So, from the BAL data accumulated along many years, it seems that growing seedlings do follow the local gravimetric tide. We do not have the exact explanations for their behaviour. Although the idea is not new that ions and ion-transport channels are keys in the body time regulation (Njus et al. 1974), it is noteworthy that with the discovery of ‘clock genes’ the research of non-transcriptional oscillators lost evidence in a way that alternative models, such that of redox cycles working autonomously, were recovered just recently (Milev et al. 2018).

Even with ‘clock genes’ being an active cyclic process, the presence of some external cue – a *Zeitgeber* such as light, exercise or food – is needed for the periodic regulation to develop (du Pré et al. 2014). So, the argumentation on internal/mixed/external models are far from being settled, even more that organisms are timing-flexible, able to track the local clues during the year (Hut et al. 2013). Also, the possibility that more than one rhythm could run

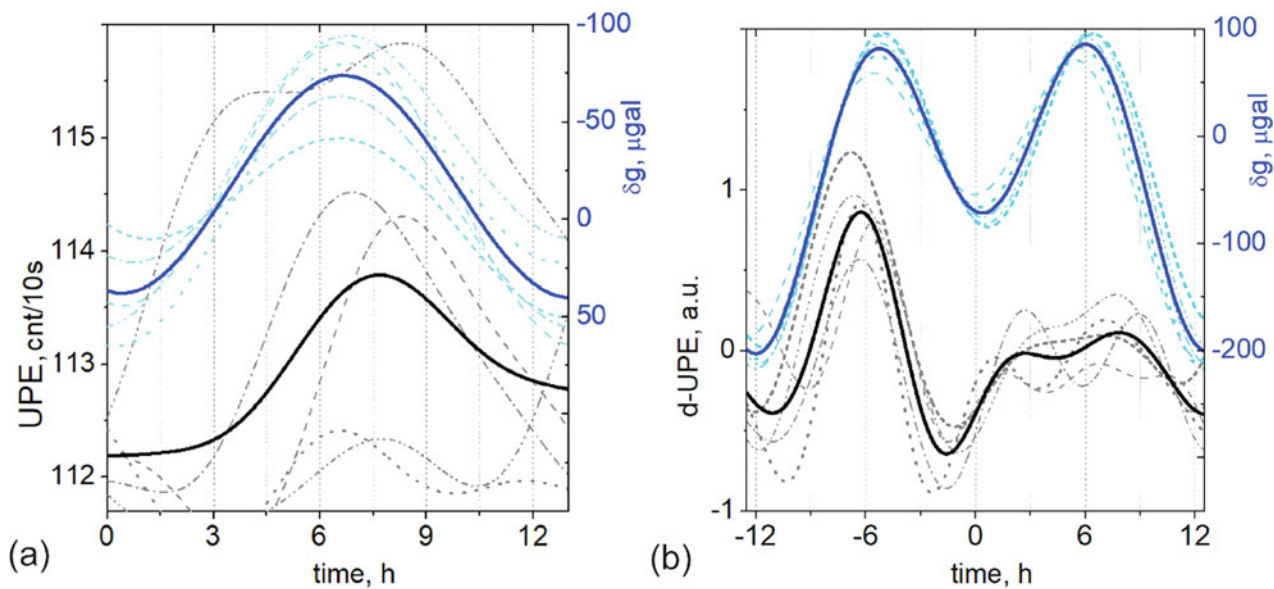


Fig. 18.5 Time patterns of the spontaneous photon emission (UPE, cnt/s) of single sunflower seedlings (grey, stippled lines) and average (solid black line) and of the local gravimetric tide (δg , μGal) at time and location of the experiments (cyan stippled lines: individual tides, blue

solid line: average time course of tide). Measurements for (a) and (b) show two germination tests conducted in controlled conditions, for 13-h and 25-h time scales, respectively, using UPE data (de-trended for (b)). (Replicated from (Gallep and Robert 2022))

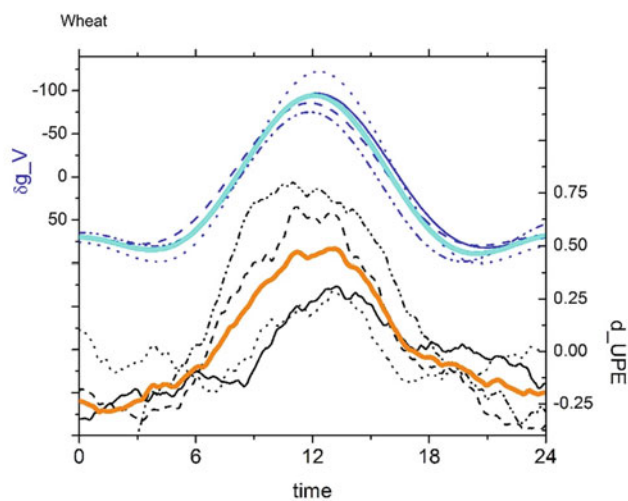


Fig. 18.6 Superposed gravimetric tide profiles (vertical component, μGal) and detrended UPE profiles (d_UPE, a.u.), for single-seedling germination tests of wheat. Respectively, the dark-blue and the black lines comprehend individual data samples for correlated δg and (detrended) UPE (BAL), and the light-blue and the orange lines show the average values in 24-h span

independently in a single cell puts also the idea that there could be a multitude of oscillators, one for each rhythm, and all connect to each other (Roenneberg and Morse 1993; Lillo et al. 2001).

It is easy to conceive the idea that, at cellular level, the interfaces with aqueous domains would have complex properties, where structured water might play a big role

(Hwang et al. 2018; Pagnotta et al. 2005). A better understanding of water clusters and their unusual properties inside the cell would also be necessary to study the possible roles of water properties changes for the interaction with a possible gravimetric tide *Zeitgeber* (Chaplin 2000; Gadre et al. 2014). Even when looking at the basic physical attributes of matter, it is possible to find periodic oscillations related to the Sun–Moon–Earth cycles, such as the conductivity of water (Ageev et al. 2018) and the decay of radioactive isotopes (Fischbach et al. 2009; Sturrock et al. 2014). These physical factors would impact surely over models considering the electrical dimension of life, where ion pumps and electron transport chains play a crucial role (de Toledo et al. 2019), or considering the possible role of quantum coherence in the organism’s interactions with the environment, such as the long-range electron transfer in proteins (Lambert et al. 2013).

If, as said by Szent-Györgyi almost 50 year ago, ‘life is water dancing to the tune of the solids’ (Szent-Györgyi 1971), why wouldn’t the daily/monthly gravimetric tide directly act over organisms, since it acts over the matter all around?

18.4 Conclusions

The use of specific BAL experiments in order to develop practical applications, as briefly presented above for the case of seedlings, is still undergoing and have much to improve, in methods and goals. The possibility to check, in real time and with minimal disturbance, the evolving state of organisms is

a dream, but limited to the constrictions of in-dark sample holding and the sensors sensitivity and noise levels, as well as to the non-specific information that BAL provides (up to now). Studies on the BAL spectral composition, in cooperation with metabolomics tools, might give us more possibilities in the near future. We hope the community keeps pushing the knowledge, with cooperative and supportive scientific exchange.

Acknowledgements The author is very grateful to all students and fellow researchers whom he cooperated with, in exchanging of experiments and ideas, many co-authors of cited papers, from Brazil and abroad. The author thanks the financial support of the National Research Council CNPq, Brazil [grant 301701/2019-9], the São Paulo Research Foundation – FAPESP, Brazil [grants 04/10146-3, 07/00431-0, 14/04232-6, 15/11280-0, 16/50344-6, 18/05300-6], and the Biotechnology and Biological Sciences Research Council (BBSRC), UK (grant number BB/N022556/1).

References

- A.A. Gurwitsch, A historical review of the problem of mitogenetic radiation, *Experientia* 44 (7) (1988) 545–550.
- L. Colli, U. Facchini, Light emission by germinating plants, *Il Nuovo Cimento* 12 (1) (1954) 150–153. <https://doi.org/10.1007/BF02820374>
- B. Devaraj, M. Usa, H. Inaba, Biophotons: ultraweak light emission from living systems, *Current Opinion in Solid State and Materials Science* 2(2) (1997) 188–193. [https://doi.org/10.1016/S1359-0286\(97\)80064-2](https://doi.org/10.1016/S1359-0286(97)80064-2).
- C. de Mello Gallep, Ultraweak, spontaneous photon emission in seedlings: toxicological and chronobiological applications, *Luminescence* 29 (8) (2014) 963–968 <https://doi.org/10.1002/bio.2658>
- M. Cifra, P. Pospíšil, Ultra-weak photon emission from biological samples: definition, mechanisms, properties, detection and applications, *J. of Photochem. and Photobiol. B: Biol.* 139 (2014) 2–10 <https://doi.org/10.1016/j.jphotobiol.2014.02.009>.
- S. Miyamoto, G.R. Martinez, M.H. Medeiros, P. Di Mascio, Singlet molecular oxygen generated by biological hydroperoxides, *J Photochem Photobiol B* 139 (2014) 24–33 <https://doi.org/10.1016/j.jphotobiol.2014.03.028>.
- T. Ichimura, M. Hiramatsu, N. Hirai, T. Hayakawa, Two-dimensional imaging of ultra-weak emission from intact soybean roots, *Photochem. and Photobiol.* 50 (3) (1989a) 283–286 <https://doi.org/10.1111/j.1751-1097.1989.tb04161.x>.
- T. Makino et al. Ultraweak luminescence generated by sweet potato and *Fusarium oxysporum* interactions associated with a defense response, *Photochem. and Photobiol.* 64 (6) (1996a) 953–956 <https://doi.org/10.1111/j.1751-1097.1996.tb01860.x>.
- A. Rastogi, P. Pospíšil, Production of hydrogen peroxide and hydroxyl radical in potato tuber during the necrotrophic phase of hemibiotrophic pathogen *Phytophthora infestans* infection, *J. of Photochem. and Photobiol. B: Biol.* 117 (2012) 202–206 <https://doi.org/10.1016/j.jphotobiol.2012.10.001>.
- Colli L., et al. Further measurements on the bioluminescence of the seedlings. *Experientia* 1955;11(12):479–81.
- Inaba H, Shimizu Y, Tsuji Y, Yamacishi A. Photon counting spectral analyzing system of extra-weak chemi- and bioluminescence for biochemical applications. *Photochem Photobiol* 1979;30:169–75.
- Shimizu Y et al. Measuring methods for ultra-low light intensity and their application to extra-weak spontaneous bioluminescence from living tissues. *IEEE Trans Instrum Meas* 1973;22(2):153–7.
- Inaba H et al. Development of an ultra-high sensitive photon counting system and its application to biomedical measurements. *Opt Lasers Eng* 1982;3(2):125–30.
- Scott RQ, Inaba H. Ultraweak emission imagery of mitosing soybeans. *Appl Physics B* 1989;48(2):183–5.
- Devaraj B, Inaba H. Biophotons: ultraweak light emission from living systems. *Curr Opin Solid State Mater Sci* 1997;2(2):188–93.
- Suzuki S, Nagoshi T, Kobayashi M, Watanabe N, Watanabe H, Inaba H. Two-dimensional imaging and counting of ultraweak emission patterns from injured plant seedlings. *J Photochem Photobiol B Biol* 1991;9(2):211–17.
- Usa M, et al. Simultaneous measurement of biophoton emission and biosurface electric potential from germinating soybean (*Glycine max*). *Protoplasma* 1989;149:64–6.
- Hideg E, Kobayashi M, Inaba H. Spontaneous ultraweak light emission from respiring spinach leaf mitochondria. *Biochim Biophys Acta* 1991;1098:27–31.
- Saeki R, et al. Low-level chemiluminescence of water-imbibed soybean seeds. *Agric Biol Chem* 1989;53:3311–12.
- Kobayashi M. Two-dimensional imaging and spatiotemporal analysis of biophoton. In: Shen X, Wijk R, editors. *Biophotonics: Optical Science and Engineering for the 21st Century*. New York, USA: Springer, 2005:155–71.
- Slawinski J, Grabikowski E, Ciesla L. Spectral distribution of the ultraweak luminescence from germinating plants. *J Lumin* 1981;24:791–4.
- Slawinski J. Photon emission from perturbed and dying organisms: Biomedical perspectives. *Forsch Komplementarmed Klass Naturheilkd* 2005;12:90–95.
- Slawinski J, et al. Stress-induced photon emission from perturbed organisms. *Experientia* 1992;48(11–12):1041–58.
- Boveris A et al. Spontaneous chemiluminescence of soybean embryonic axes during imbibition. *Plant Physiol* 1983;76(2):447–51.
- Boveris A et al. Spontaneous chemiluminescence of soybean embryonic axes during imbibition. *Plant Physiol* 1984;76(2):447–51.
- Ichimura T et al. Two-dimensional imaging of ultra-weak emission from intact soybean roots. *Photochem Photobiol* 1989b;50(3):283–6.
- Makino T, et al. Ultraweak luminescence generated by sweet potato and *Fusarium oxysporum* interactions associated with a defense response. *Photochem Photobiol* 1996b;64(6):953–6.
- Hiramatsu M. Biophotons and defense response in plants. In: Chang J-J, Fisch J, Popp F-A, editors. *Biophotons*. New York, USA: Springer, 1998:45–55.
- Kai S, Mitani T, Fujikawa M. Morphogenesis and bioluminescence in germination of red bean. *Physica A* 1994;210(3):391–402.
- Kai S, Mitani T, Fujikawa M. Anomalous biophoton emission during germination process of red bean. *Jpn J Appl Phys Lett* 1993;32:L-417.
- Kai S, Ohya T, Moriya K, Fujimoto T. Growth control and biophoton radiation by plant hormones in red bean. *Jpn J Appl Phys* 1995;34:6530–8.
- Ohya T et al. Biophoton emission due to drought injury in red beans: possibility of early detection of drought injury. *Jpn J Appl Phys* 2002;41:4766–71.
- Ohya T et al. Early detection of salt stress damage by biophotons in red bean seedling. *Jpn J Appl Phys* 2000;39:3696–700.
- Musumeci F et al. Relation between delayed luminescence and functional state in soya seeds. *Nuovo Cimento D* 1994;16:65–73.
- Triglia A et al. Temperature dependence of the ultraweak spontaneous photon emission from soya seeds. *Nuovo Cimento D* 1993;15(11):1361–70.
- Grasso F, Musumeci F, Triglia A, Pagano M. Spectra of photons emitted from germinating seeds. *Nuovo Cimento* 1991;13(7):891–7.
- Chen WL, Xing D, Tan S, Tang Y, He Y. Imaging of ultraweak biochemiluminescence and singlet oxygen generation in germinating soybean in response to wounding. *Luminescence* 2003;18:37–41.

- Cheng WL, Zhou Q, Li L, Xing D, Van Wijk R, Tang Y. Comparing ultraweak bio-chemiluminescence emission in wounded green and etiolated soybean cotyledons. *SPIE* 2006;6088:60881G–60881G-10.
- Chen WL, Xing D, Wang J. Changes of ultraweak biochemiluminescence from germinating soybean in the wounding defense response. *SPIE* 2002;4920:559–65.
- H. Saeidfirozeh, A. Shafiekhani, M. Cifra, A. Masoudi, Endogenous Chemiluminescence from Germinating Arabidopsis Thaliana Seeds, *Sci. Reports* 8 (1) (2018) 16231 <https://doi.org/10.1038/s41598-018-34485-6>.
- Y. Yan, Biophoton emission and delayed luminescence of plants, in: X. Shen, R. Van Wijk (Eds.), *Biophotonics*, Springer, Boston, 2005, pp. 195–204. https://doi.org/10.1007/0-387-24996-6_15.
- C.M. Gallep, S.R. dos Santos, Photon-counts during germination of wheat (*Triticum aestivum*) in wastewater sediment solutions correlated with seedling growth, *Seed Sci. and Technol.* 35 (3) (2007) 607–614 <https://doi.org/10.15258/sst.2007.35.3.08>.
- Moraes TA, Martins LC, Ramos SR, Garofalo RT, Gallep CM. Spontaneous light emission of wheat seedlings with K2Cr2O7. The Latin America Optics and Photonics Conference, OSA 2010.
- Moraes TA, Garofalo RT, Ramos SR, Martins L, Gallep CM. Spontaneous light emission of wheat seedlings in leachate solutions. In: 2009 SBMO/IEEE MTT-S IMOC-2009; 226–8. <https://doi.org/10.1109/IMOC.2009.5427594>
- Scholkmann F, Cifra M, Moraes TA, Gallep CM. Using multifractal analysis of ultra-weak photon emission from germinating wheat seedlings to differentiate between two grades of intoxication with potassium dichromate. *J Phys Conf Ser* 2011;329:012020.
- Bertogna E, Bezerra J, Conforti E, Gallep CM. Acute stress in seedlings detected by ultra-weak photon emission. *J Photochem Photobiol B* 2013a;118:74–6. <https://doi.org/10.1016/j.jphotobiol.2012.11.005>
- Bertogna E, Conforti E, Gallep CM. Simultaneous Biophoton Measurement of Control and Fluoride Stressed Seedlings Samples. SBMO/IEEE MTT-S International Conference (IMOC) on Microwave and Optoelectronics, Piscataway, USA: IMOC-2013b;1–3.
- Gallep CM, Robert D. Time-resolved ultra-weak photon emission as germination performance indicator in single seedlings. *J Photochem Photobiol*, v. 1, p. 100001, 2020. <https://doi.org/10.1016/j.jpap.2020.100001>
- Gallep CM, Moraes TA, Julião GO, dos Santos SR. Rhythmicities in the spontaneous photon emission of wheat seedlings. SBMO/IEEE MTT-S International Conference on Microwave and Optoelectronics, Piscataway, USA: IMOC-2007;713–15.
- Bertogna E, Moraes TA, Conforti E, Gallep CM. Periodic Time-Components in Spontaneous Ultra-Weak Photon Emission of Wheat Seedlings in Stressing Solutions. The Latin America Optics and Photonics Conference, OSA 2010;MB08.
- Barlow PW, Mikulecký M, Štřeščík J. Tree-stem diameter fluctuates with the lunar tides and perhaps with geomagnetic activity. *Protoplasma* 2010;247:25–43.
- Zürcher E, Cantiani MG, Sorbetti-Guerri F, Michel D. Tree stem diameters fluctuate with tide. *Nature* 1998;392:665–6.
- Longman IM (1959) Formulas for computing the tidal acceleration due to the moon and the sun. *J Geophys Res* 64:2351–2355.
- Moraes TA, Barlow PW, Klingelé E, Gallep CM. Spontaneous ultra-weak light emissions from wheat seedlings are rhythmic and synchronized with the time profile of the local gravimetric tide. *Naturwissenschaften* 2012;99(6):465–72.
- Gallep CM, Moraes TA, Cervinková K, Cifra M, Katsumata M, Barlow PW. 2014. Lunisolar tidal synchronism with biophoton emission during inter- continental wheat-seedling germination tests. *Plant Signaling & Behavior* 9, e28671.
- Gallep CM, Barlow PW, Burgos RC, van Wijk EP. 2017. Simultaneous and intercontinental tests show synchronism between the local gravimetric tide and the ultra-weak photon emission in seedlings of different plant species. *Protoplasma* 254, 315–325.
- Gallep CM; Robert D. Are cyclic plant and animal behaviours driven by gravimetric mechanical forces?, *Journal of Experimental Botany*, Volume 73, Issue 4, 24 February 2022, Pages 1093–1103, <https://doi.org/10.1093/jxb/erab462>
- Gallep, CM; Robert, DI, 2021. Appendix material - are cyclic plant and animal behaviours driven by gravimetric mechanical forces?, <https://doi.org/10.25824/redu/GCPFT7>, REDU, V3
- D. Njus, F. M. Sulzman, and J. W. Hastings, Membrane model for the circadian clock. *Nature*, vol. 248, no. 5444, pp. 116–120, 1974.
- N. B. Milev, S. Rhee, and A. B. Reddy, ‘Cellular Timekeeping: It’s Redox o’Clock’ *Cold Spring Harb. Perspect. Biol.*, vol. 10, no. 5, p. a027698, May 2018.
- du Pré BC, van Veen TA, Young ME, Vos MA, Doevendans PA, van Laake LW. 2014. Circadian rhythms in cell maturation. *Physiology* 29, 72–83.
- R. A. Hut, S. Paolucci, R. Dor, C. P. Kyriacou, and S. Daan, “Latitudinal clines: An evolutionary view on biological rhythms,” *Proc. R. Soc. B Biol. Sci.*, vol. 280, no. 1765, pp. 1–9, 2013.
- T. Roenneberg, D. Morse, “Two circadian oscillators in one cell”, *Nature* 362.6418, pp. 362, 1993.
- C. Lillo, C. Meyer, and P. Ruoff, “The nitrate reductase circadian system. The central clock dogma contra multiple oscillatory feedback loops,” *Plant Physiol.*, vol. 125, no. 4, pp. 1554–1557, 2001.
- S. G. Hwang, J. K. Hong, A. Sharma, G. H. Pollack, and G. W. Bahng, “Exclusion zone and heterogeneous water structure at ambient temperature,” *PLoS One*, vol. 13, no. 4, pp. 1–17, 2018.
- S. E. Pagnotta, R. Gargana, F. Bruni, and A. Bocedi, “Glassy behavior of a percolative water-protein system,” *Phys. Rev. E*, vol. 71, no. 3, p. 031506, Mar. 2005.
- M. F. Chaplin, “A proposal for the structuring of water,” *Biophys. Chem.*, vol. 83, no. 3, pp. 211–221, 2000.
- S. R. Gadre, S. D. Yeole, and N. Sahu, “Quantum chemical investigations on molecular clusters,” *Chem. Rev.*, vol. 114, no. 24, pp. 12132–12173, 2014.
- I. M. Ageev, Y. M. Rybin, and G. G. Shishkin, “Manifestation of Solar–Terrestrial Rhythms in Variations of the Electrical Conductivity of Water,” *Biophys. (Russian Fed.)*, vol. 63, no. 2, pp. 282–288, 2018.
- E. Fischbach et al., “Time-dependent nuclear decay parameters: New evidence for new forces?,” *Space Sci. Rev.*, vol. 145, no. 3–4, pp. 285–335, 2009.
- P. A. Sturrock, E. Fischbach, and J. Jenkins, “Analysis of beta-decay rates for Ag108, Ba133, Eu152, Eu154, Kr85, Ra226, and Sr90, measured at the Physikalisch-Technische Bundesanstalt from 1990 to 1996,” *Astrophys. J.*, vol. 794, no. 1, pp. 9–15, 2014.
- G. R. A. de Toledo et al., “Plant electrome: the electrical dimension of plant life,” *Theor. Exp. Plant Physiol.*, vol. 31, no. 1, pp. 21–46, 2019.
- N. Lambert, Y. N. Chen, Y. C. Cheng, C. M. Li, G. Y. Chen, and F. Nori, “Quantum biology,” *Nat. Phys.*, vol. 9, no. 1, pp. 10–18, 2013.
- A. Szent-Györgyi, “Biology and Pathology of Water,” *Perspect. Biol. Med.*, vol. 14, no. 2, pp. 239–249, 1971.



Application Potentiality of Delayed Luminescence in Medicine, Biology, and Food Quality Researches

19

Rosaria Grasso, Francesco Musumeci, Agata Scordino, and Antonio Triglia

19.1 Introduction

In relatively recent years, the requirements of specific quality requisite arose in many of the fields affecting citizens' everyday life. The presence of products and equipment from countless countries makes this requirement crucial for the development of a society based on respect for the environment and the needs of individuals. In this context, several supranational organizations have developed production chain control protocols and certification criteria, often questionable because based on reductive or obsolete *ex ante* evaluations. There is therefore the necessity of control techniques, if possible, *ex post*, characterized by high reliability, user-friendliness, and reasonably low costs.

A way to try to satisfy this request is suggested by the development of photonics. The use of photons in analysis techniques often allows the realization of nondestructive analyses, capable of giving answers in a short time and which can also be operated by relatively unskilled personnel, thanks to the power of modern user interfaces.

One of the most versatile and powerful analysis techniques is based on the so-called delayed luminescence. Delayed luminescence (DL) consists, like fluorescence and phosphorescence, in the emission of light by a system after illumination. The intensity of the re-emitted light signal, however, is far lower than the other two phenomena and is characterized by a time scale of some orders of magnitude greater than fluorescence (see Chap. 31).¹

¹ According to the generally accepted definition, delayed luminescence is luminescence with characteristic times orders of magnitude longer than standard fluorescence. Thus, phosphorescence belongs to this group of phenomena. However, besides direct $T_1 \rightarrow S_0$ relaxation, DL also includes luminescence generated at $T_1 \rightarrow S_1 \rightarrow S_0$ relaxation, as well as at photochemical reactions. See more in Sects. 3.4, 5.2.5, 12.2 and 12.3 (*editorial note*).

R. Grasso · F. Musumeci (✉) · A. Scordino · A. Triglia
Department of Physics and Astronomy "Ettore Majorana", University of Catania, Catania, Italy
e-mail: fmusumec@dmfci.unict.it

Now we know that it is a ubiquitous phenomenon: practically all condensed matter systems emit delayed luminescence but the first reported data of DL dates to the paper by Strehler and Arnold in 1951 (Strehler and Arnold 1951) and refers to green plants. This delayed light emission (DLE) or delayed fluorescence (DF), as it is named in different papers, was associated with the photosynthetic process just from the beginning (Strehler and Arnold 1951). Schematic representation of the photosynthetic pathway and a possible mechanism for the phenomenon involving the recombination of electrons and holes trapped in a quasicrystalline lattice were proposed (Tollin and Calvin 1957). The interplay between physical and enzymatic processes underlying absorption and emission of light was investigated (Tollin et al. 1958).

The emission spectra of DL and fluorescence in plants are very similar. This suggests that DL can be synthetically described through the general scheme, known as the Jablonski diagram (Jursinic 1986), which explains it through the repopulation of the excited singlet state through a back reaction from an indefinite metastable state, characterized by an energy lower than the excited singlet state one. So, the DL is different from the phosphorescence that originates from the direct decay of the triplet state and is characterized by longer times and longer emission wavelengths.

It has been shown in the literature (Scordino et al. 2000) that the DL is connected to the ordered microscopic structures existing in the illuminated system and that DL enhances when the order parameters increase.

This fact suggested that the DL could be connected to the excitation and subsequent decay of collective states such as excitons, polarons, or solitons present in the system under analysis (Brizhik et al. 2001; Scordino et al. 2010). Its sensitivity to structures and symmetries, often transient, justifies the ability of the DL to provide significant information on the state of many biological systems, despite the irrelevant energies involved in the phenomenon (Niggli 1993; van Wijk et al. 1993; Yamagishi et al. 2018; Mengmeng et al. 2019).

The relationship and the characteristics of prompt (fluorescence) and delayed light emission were further studied in their connection to photosynthesis (Bertsch 1962; Arnold 1965; Clayton 1965; Muller and Lumry 1965; Arnold and Azzi 1968; Clayton 1969), by concluding that the magnitude of delayed light emission reflects the size of the proton motive force across the thylakoid membrane (Neumann et al. 1973). Due to the coupling of DL with the processes and activities of the photosynthetic system, it is able to give information about plant or cyanobacteria physiological states and interactions with their environment. This gives the potentialities for developing biosensors based on DL measurements.

In a short review, Guo and Tan (Guo and Tan 2013a) summarize the main factors that affect DL emission. They report also some application aspects, from the assessment of photosynthesis rate, plant circadian clock and senescence, to detection of stress due to nutrients, salt, chilling or heat, drought, acid rain, herbicide, metal pollution, and in general, to monitoring the condition of aquatic ecosystems.

In this last aspect, DL measurements have been proposed for studying changes in phytoplankton composition in order to monitor and understand phytoplankton population dynamics (Drinovec et al. 2011).

It is worth noting that the research of early indicators of physiological change or damage of plant tissue in response to physiological stress has attracted large interest. The possibility of realizing a rapid and noninvasive technique to evaluate chilling stress (Abbott et al. 1994), water deficiency in plants (Guo and Tan 2013b), or herbicide stress (Guo and Tan 2014a) has been explored. The presence of contaminants as aflatoxins in crops, whose exposure is detrimental to human health, was revealed and the evaluation of their concentration performed (Chen et al. 2005). Delayed fluorescence imaging of potato leaves has been confirmed as a responsive and useful technique for detecting the effects of toxicant as photosynthesis inhibitors (herbicides) and heavy metals (Razinger et al. 2012).

Actually, DL measurements from algae allowed to set tools for evaluating water pollution by herbicides (Scordino et al. 1996; Katsumata et al. 2006) or heavy metals (Scordino et al. 2008), but also to elucidate the action of specific herbicides on the photosystem and on molecular membrane transport in particular (Katsumata and Takeuchi 2017). The possibility of using leaves of garden bean and spinach plants as herbicide sensor was also explored (Guo and Tan 2010; Guo and Tan 2014b).

The relation of DL to physiological status or physiological processes led to the idea that quality aspects of food may be reflected in delayed luminescence. Nowadays an even greater attention is paid to food safety and food quality and their relevant relationship to human health and wellbeing (Hu et al. 2019). In this field, the research ranges from the evaluation of

the effects of growing stage, fertilizing intensity, farming style (biodynamic, organic, and conventional conditions) (Stolz et al. 2019; Wohlers and Stolz 2019) to the assessment of maturity of papaya (Forbus et al. 1987) and tomatoes (Triglia et al. 1998; Forbus et al. 2006), showing the potential use of DL in the automated sorting for fresh produce market. Moreover, it has been successfully used to distinguish medicinal herbs, largely used in the Traditional Chinese Medicine, on the basis of their “cold or heat” properties (Pang et al. 2016) and to evaluate their quality (Sun et al. 2018; Sun et al. 2019).

An actual problem in the use of the DL has been the very low signal intensity, some orders of magnitude lower than the typical values of the fluorescence. To overcome this difficulty, it was necessary to develop and implement dedicated experimental setups, able to reveal this signal. In general, single-photon counting techniques have been used. There was also the need to prevent illumination of both the sample and the detector from spurious sources and to collect as many photons as possible from the re-emitted ones. The developing of instrumentation able to reveal also a very low-level signal, performed several decades after the work of Strehler and Arnold (Strehler and Arnold 1951), allowed to measure DL from mammalian cells, where DL intensities and durations are much lower than in the case of plant or algae. The latter in fact emit more intense signals which decay more slowly over time and which are therefore measurable up to hundreds of seconds after the end of the illumination. They also have an almost constant excitation spectrum from near UV to red wavelength region and an emission spectrum very similar to that of the fluorescence of the same systems. The former, on the other hand, show faster decays and excitation spectra with a maximum in the blue or near ultraviolet region.

The pioneering work of F.A. Popp and coworkers started at the end of the 1980s, showing the possibility of distinguishing between different types of cells (malignant from normal) (Niggli 1993; van Wijk et al. 1993; Scholz et al. 1988). Moreover, the signal was associated to a coherent electromagnetic field inside the cells, according to Frohlich's idea of coherent long-range interactions in biological systems (Zhang et al. 1997; Popp and Yan 2002).

The implementation of the experimental setup ARETUSA (Advanced Research Equipment for fasT Ultraweak luminescence Analysis) (Tudisco et al. 2003) allowed the researchers of Catania University (Catania, Italy) to deeply investigate DL from mammalian cells (Niggli et al. 2005; Musumeci et al. 2005a, b; Lanzaò et al. 2007; Niggli et al. 2008; Baran et al. 2009, 2010, 2012, 2013, 2014a, b; Grasso et al. 2016a, 2019) and confirm the possibility of discriminating between normal and tumor cells (Niggli et al. 2005; Musumeci et al. 2005a, b). Moreover, the possibility to check cell alterations were analyzed in view of developing a technique for optical biopsy (Lanzaò et al. 2007; Niggli

et al. 2008), along with the capacity of evaluating the proapoptotic effects of certain treatments (Baran et al. 2009, 2010, 2012; Scordino et al. 2014a, b). The performed experiments allowed to point out the role of mitochondrion, and in particular the electron transfer steps in the Mitochondrial Respiratory Chain (MRC) Complex I, on DL emission (Baran et al. 2013), which opens the possibility to use DL for monitoring diseases where mitochondrial impairment is involved (Grasso et al. 2016a, 2019).

At present, DL characterization of healthy and pathological tissues continues to be investigated (Chen et al. 2012; Letuta et al. 2016; Kim et al. 2005; Bai et al. 2009), and a new optical noninvasive technique to evaluate in vivo mitochondrial oxygen tension has been settled (Mik et al. 2009; Ubbink et al. 2017; van Dijk et al. 2019).

In the following, some of the most promising results obtained at the laboratories of Catania University are shown and discussed. We will start with applications in the biological and medical fields, including technological solutions and treatment of data adopted, and continue with applications in the quality control for Agriculture. Last but not least, application in water pollution detection will be presented.

19.2 Applications of DL in Biological and Medical Field

19.2.1 The Study of DL from Human Cells and Tissues in View of the Development of a New Technique of Optical Biopsy

There is, by now, a general agreement that the early diagnosis of oncological diseases significantly increases the chances of success of the therapies and therefore the probability of surviving these serious diseases with an acceptable quality of life. Unfortunately, to date, tumors are often identified in an advanced stage, when the functions of one or more vital organs have been altered and the pathology is widespread throughout the body. However, there are general aspects in the onset of this pathology which seems to be generally linked to the body's inability to manage the production and destruction of its various cells. Cancer therefore appears as an alteration of vital processes rather than as the appearance of hostile cells within the body (Bertolaso and Duprè 2018; Bizarri and Cucina 2014). In this context, a technique capable of giving information on the collective states and the processes that take place, at various functional levels within the biological systems, appears to be of considerable importance.

Among the various analysis techniques, optical techniques aroused much interest. In fact, they are generally noninvasive, or slightly invasive, are often able to give information in real time and, from a technological point of view, they rely on a sector of fast development such as photonics. This produces hopes of a fast development of the performances of these techniques and about the possibility of carrying out screening activities on a large part of the population at a reasonable cost, also from the point of view of specialized staff needs. A form of optical biopsy could be able to identify and evaluate the degree of danger of the lesions present in some tissues without requiring their surgical removal, thus quickly and bloodlessly providing information on the progression and invasiveness of tumors. In this frame, some spectroscopic techniques have been proposed in the literature, such as UV-visible fluorescence, Raman spectroscopy, and diffuse reflectance, but their role has been limited to supporting traditional techniques of cytology and immunohistochemistry without being able to replace the traditional surgical biopsy from its role of diagnostic standard. It is therefore of fundamental importance to look for more sophisticated detection procedures. In this context, numerous experimental studies have shown that delayed luminescence (DL) seems to be a promising candidate for the development of a reliable and inexpensive optical biopsy system.

Even if in the specific case of mammalian tissues the signal intensity is lower and the dynamic is faster, introducing more accurate measuring devices and appropriate data analysis techniques have made it possible to obtain reproducible characterizations also for these types of systems. Even in this case, the DL appears to be strictly connected to the functional state of the analyzed systems (van Wijk et al. 1993; Zhang et al. 1997; Niggli et al. 2001). As a matter of fact, specific cultures of human cells (Niggli et al. 2005, 2008) or tissues (Lanzanò et al. 2007) have been examined, showing that it is possible to discriminate between normal and tumor conditions (Musumeci et al. 2005a, b).

In this regard, the growing acknowledgment of the importance of mitochondria, which play a key role in controlling life and death in addition to their established role in generating energy for the cell, is a fact. Indeed, with a few exceptions, mitochondria represent an essential component of many apoptotic pathways (Desagher and Martinou 2000), releasing cytochrome c into the cytosol, thereby activating caspases.²

Summarizing we can say that the research presented here demonstrates the wide potentiality of DL in the early diagnosis of cancer.

²See Chap. 14.

19.2.2 Technological Solutions and Data Treatment

As previously mentioned, the DL extends for relatively long time intervals. Although it is certainly present even during the illumination of the system under analysis, data useful for analysis extends from the end of the illumination to the time when the signal intensity is similar to the background signal of the measure apparatus. The time window for the signal collection therefore depends not only on the system analyzed but also on the equipment performance. A relatively inexpensive solution that guarantees the possibility of making significant measurements is the use of photomultipliers, in single-photon count mode. To reduce the noise, it is necessary to cool down the photomultiplier up to $-30\text{ }^{\circ}\text{C}$ using a cold liquid circulating in direct contact with its surface. In this condition, it is possible to follow the signal dynamics up to a few hundred seconds in the case of vegetal systems. In the case of our interest, regarding tissues and animal cells, the signal decays much more quickly so it is difficult to distinguish it from the background starting from times of the order of the second. It is therefore particularly important to start the measurement as soon as possible after the end of the lighting. The use of mechanical shutters allows starting the measurement a few milliseconds after the end of the lighting, so the analysis of the dynamics is limited to short time intervals (a few magnitude orders in decay time intervals). To overcome this problem, an electronic shutter (Tudisco et al. 2003) has been developed that allows you to start the measurement a few microseconds after the end of the

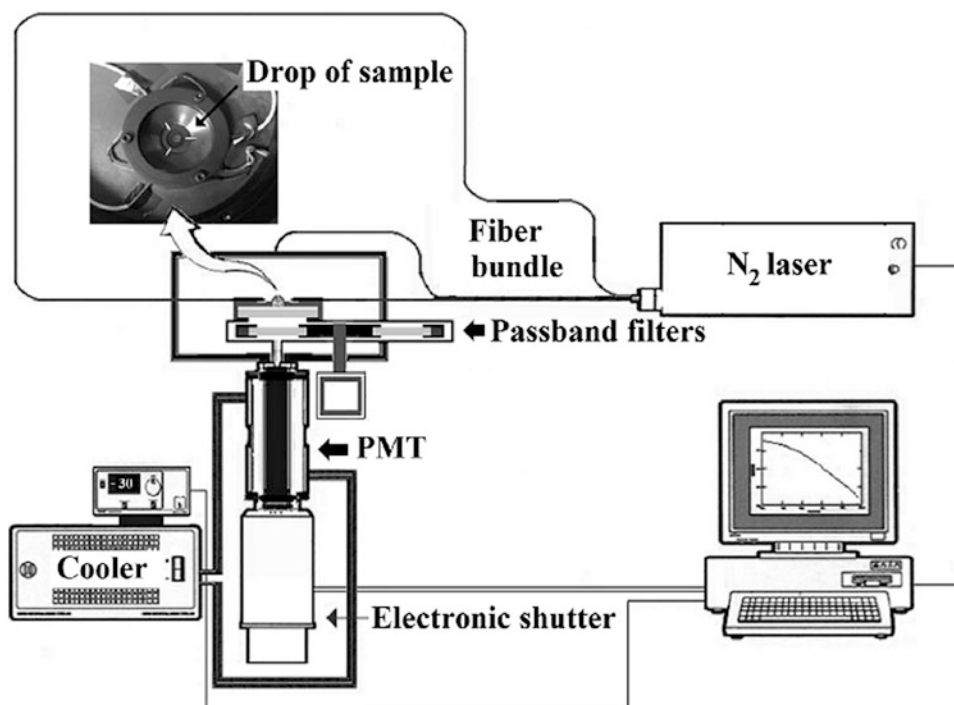
lighting, significantly extending the analyzable dynamics. A further problem that appears in the study of nonplant systems is the presence of an excitation spectrum moved toward the UV region and, therefore, superimposed on the excitation spectrum of the materials commonly used as sample holders, generally plastic or quartz cuvettes, in standard equipment. To overcome this problem, a UV laser can be used. The laser allows to properly manage the photon flows in the input and the output, in order to minimize the influence of the holder. A further requirement is the need to minimize the volume of samples to be analyzed in order to use small quantities of cells. Figure 19.1 shows a system that meets these requirements, described in (Scordino et al. 2014b).

This system uses a multichannel scaler with 65,000 channels and a minimum dwelling time of $2\text{ }\mu\text{s}$. Multichannel operation is managed by a personal computer. In such a way, the dynamics of the DL signal in a time window ranging from $10\text{ }\mu\text{s}$ to about a tenth of a second can be observed. To manage this amount of data it is necessary to apply some statistical reduction treatment. A simple technique consists in averaging groups of experimental points so that $\Delta t_i / t_i$ is constant. This causes the data to be equally spaced on a logarithmic time axis.

In general, the low signal intensity does not allow an accurate spectral analysis. However, the spectrum often provides useful information. A rough spectral analysis can therefore be performed by using a series of broadband interference filters, placed between the sample and the photomultiplier.

Further precautions must be taken to avoid the presence of the DL issued by parts of the setup that are inadvertently lit.

Fig. 19.1 Draft of a setup for DL emitted by cell cultures and animal tissues. PMT is a photomultiplier tube with a wide spectral response (300–850 nm), enhanced for single-photon counting. The excitation source is a high-intensity pulsed nitrogen laser providing pulses at $\lambda = 337\text{ nm}$. During the laser pulse, an electronic shutter turns off the PMT detector minimizing the time delay between the switching off of the laser pulse and the starting of data acquisition



Since the DL is linked to the excitation and subsequent decay of collective states, crystals or quartz, in general, emit much more than biological systems. Attempts have been made to reduce this problem in various ways. Among other improvements, we mention the positioning of tissue samples or drops of cell suspensions directly on the quartz window of a light guide so that only the sample and not the window received the laser light injected onto the sample by means of an optical fiber having the exit end divided into three parts arranged around the drop at constant angles of 120° between them (see Fig. 19.1). Naturally, all the apparatus must be contained in a light tight chamber whose walls are coated on the internal surface with a special low luminescence paint.

The mathematical treatment of data is of fundamental importance.

The most informative characteristics are the time trend of the DL and of its spectral components. It can be obtained by comparing the experimental data to a suitable mathematical function. Generally, as shown in Eq. (19.1), this function is a linear combination of power laws, even if in many cases a simple power law ($k = 1$ in Eq. 19.1) is sufficient.

$$I(t) = \sum_{i=1}^k \frac{I_{0i}}{\left(1 + \frac{t}{t_{0i}}\right)^{m_i}} \quad (19.1)$$

From $I(t)$, one can extract two further parameters:

$$N(t') = \int_{t'}^{\infty} I(t) dt \quad P(t') = \frac{I(t')}{N(t')} \quad (19.2)$$

$N(t')$ represents the number, at time t' , of the excited states that will have a radiative decay, while $P(t')$ represent the probability of radiative decay at time t' . Thanks to the smoothing procedure used in order to reduce random noise, the values P_i of the $P(t')$ function evaluated according to Eq. (19.2) are proportional to the experimental probability that Δn_i levels of the n_i excited ones will decay in a radiative way.

A simpler parameter, able to give information even when the DL signal is very low and the fitting procedures have a poor statistical significance, is the total number of counts collected N_0 . Even the total number of counts collected in presence of the optical filters $N_{0\lambda}$ can be generally used to have a rough evaluation of optical spectrum.

19.2.3 The First Phenomenological Results in Cancer Research

Since the early 2000s, experiments have been carried out to see if it is possible to discriminate, through the DL, between cultures of normal and carcinogenic cells (Niggli et al. 2005).

To ensure the reproducibility of the experiments, well-defined cell lines were used, also relating to different passages. The main purpose of the measurements was to establish the best experimental conditions to highlight, by using the DL, differences between different samples of normal, cancerous, and cancer-prone cells.

Several cell cultures (GM 1717, p 9; CRL 1221 p 16 and p22; 3229, p 13 and p 117; GM05509A p 12; 17; 25% GM05293; p 15; CRL 1223; p 15; CRL 1585; p 5 and CCL 53.1; p 40) have been used and the measurements were performed at room temperature.

Because the normal culture medium emitted some luminescence, all cells were suspended in PBS medium before DL measurements. No significant differences were found in samples of different passages while the difference between different kinds of cells was significant.

The DL dependence from the cell density was tested. In all cases, an increase of the initial DL intensity on increasing cell density was found (Niggli et al. 2005). Interestingly, the differences between normal and cancer cells became more evident on increasing the cell density, suggesting that UVA-induced DL could serve as a marker of carcinogenesis. This is shown in Fig. 19.2 for the total DL counts from normal fibroblast (CRL-1222 p 22) and melanoma (CRL-1585 p 5) human cells.

As said, these measurements were performed at room temperature. However, room temperature is not physiological for human cells. At lower temperatures, the equilibrium between polymerized and nonpolymerized monomers of cytoskeleton is moved favoring free monomers. This must influence DL, which is connected to cytoskeleton structures (Brizhik et al. 2003). So, new measurements have been performed at a temperature of 32°C , close to the physiological one, and at a temperature of 10°C , a storage temperature

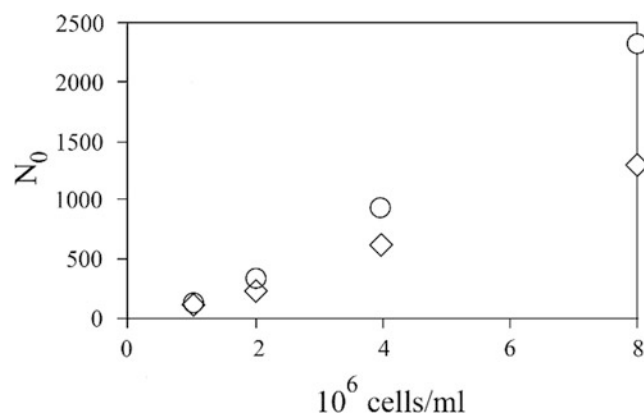


Fig. 19.2 DL total number of counts emitted by two different cell cultures after UVA illumination: (\circ) human white melanoma (CRL-1585, passage 5, cell line), (\diamond) human fibroblasts (CRL-1222, passage 22, cell line). The values reported are the average of three independent experiments. Statistical errors are inside the size of the markers

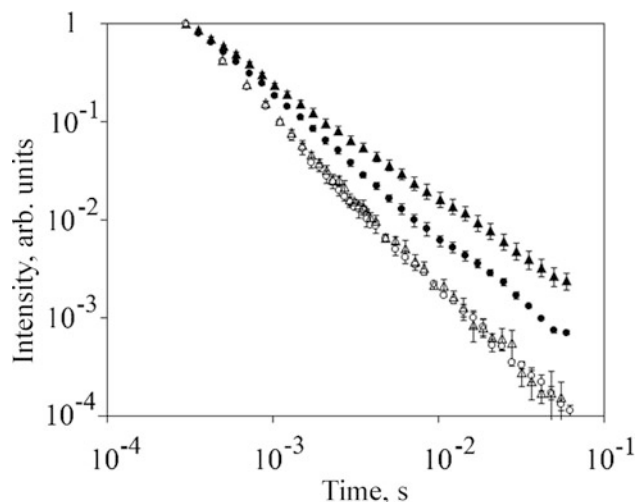


Fig. 19.3 DL dynamics of human cells samples at several temperatures. (●) human fibroblasts at 32 °C, (▲) human melanoma cells at 32 °C, (○) human fibroblasts at 10 °C (△) human melanoma cells at 10 °C. Each set is the average of three independent measurements performed on different samples with the same characteristics (bars denote standard deviations) normalized to 1 at their first point. For each sample, 100 repetitions have been performed

at which cells survive but metabolism is very reduced, comparing the DL time decays of normal and cancer cells (Musumeci et al. 2005a).

Figure 19.3 shows the results of these measurements. The various data has been normalized in order to have the same first point, and outline slope changes. Normal and cancer cells exhibit the same time trend at the lower temperature but are markedly different at the physiological one. So, again, DL could give information on the differences in structure between tumor and normal cells.

Even the spectral analysis of DL allows to outline differences between normal and tumor cell cultures. Due to the low value of the DL intensity, it is possible to perform spectral analysis of the DL only by using broadband filters, and, in general, spectral time trends are not resolved. So, the only spectral information that is possible to achieve is related to the total number of counts collected when using the various filters. Nevertheless, this simple information is able to discriminate very well between normal and cancer cells, as shown in Fig. 19.4.

Figure 19.4 shows the ratio between every spectral component, collected by 80 nm passband filters, and the blue component for human normal fibroblast (CRL-1222 p 22) and melanoma (CRL-1585 p 5) human cells. It is possible to see that the behavior of normal cells is very different from that of tumor. It is worth noting that the evaluation of this parameter does not require the knowledge of time trend of DL and could be performed with a simpler setup.

A further way to discriminate between normal and tumor cells is based on the parameter $P(t')$, which represents the probability of radiative decay at time t' , and has been defined in Eq. (19.2) (Musumeci et al. 2005b).

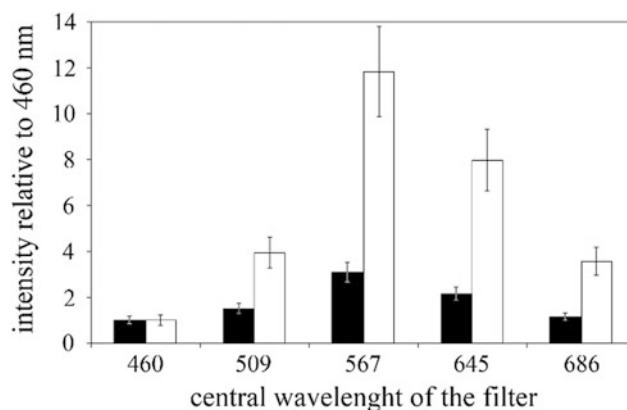


Fig. 19.4 Ratio between every DL spectral component and the component at 460 nm for human cells at 32 °C. (black) normal fibroblasts, (white) human white melanoma cells. Average values and standard deviations of independent measurements performed on four samples with the same characteristics

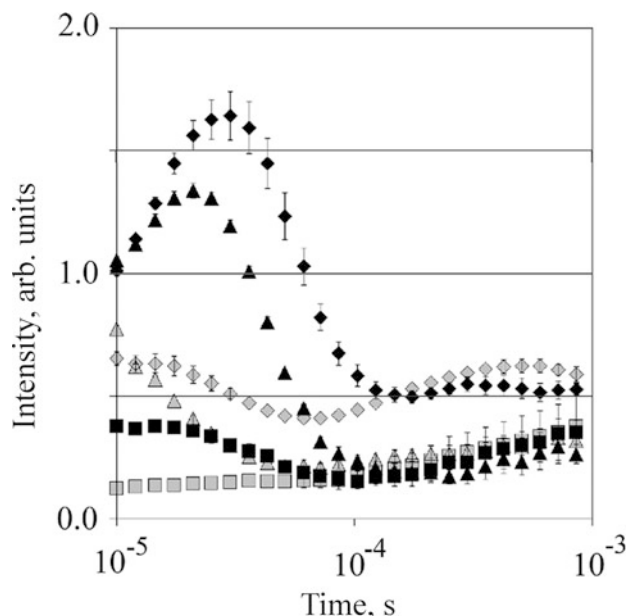


Fig. 19.5 Time trend of the decay probability $P(t)$ (Eq. (19.2)) at different emission wavelengths for foreskin derived human fibroblast cells (gray markers) and human white melanoma cells (black markers). (□) $\lambda_{em} = 460$ nm; (△) $\lambda_{em} = 509$ nm (◇) $\lambda_{em} > 550$ nm. At times > 1 ms, the errors affecting the calculation of $P(t)$ are very big and all the time trends appears similar, so have been not reported

The calculated values of $P(t)$ for various samples appear to be indistinguishable, inside the experimental errors, in the longer time region ($t > 1$ ms), so it has not been reported in Fig. 19.5. On the opposite, in the shorter time region ($t < 1$ ms), the $P(t)$ values relative to fibroblasts and melanoma cells are different and depend on the emission wavelength λ_{em} . As shown in Fig. 19.5, the $P(t)$ values of melanoma cells are greater (about twice) than those of fibroblasts at times of the order of 10 μ s. Moreover, the red component $\lambda_{em} > 550$ nm exhibits a marked maximum at

about 30 μs in melanoma cells, in contrast to fibroblasts. Such a behavior occurs also for the components with $\lambda_{\text{em}} = 509 \text{ nm}$.

19.3 Applications of DL in Quality Control for Agriculture

19.3.1 Tomato Fruits

The consumer selection of fresh fruits, and vegetables in particular, is influenced, without any doubt, by their appearance. External factors, such as the color, often guide the choice, even if it is not always related to the quality. Climacteric fruits as tomatoes are often harvested not yet at the table-ripe stage and left to ripen in controlled conditions. The maturity stage at harvesting influences some important factors, such as sugar or dry matter content, so affecting flavor and nutrient quality of fruits, even if they appear to have similar (final) color. In this respect, it is interesting to study the possibility to assess, in a nondestructive way, fruit quality related to the maturity stage at the harvesting.

A test was performed on Cherry tomato fruits harvest at different ripening stage and kept for 10 days at 20 °C and 80% RH storage in dark conditions (Triglia et al. 1998). Fruits were labeled according to their visual color at harvesting: green-orange (GO), orange-red (OR), light red (LR) and red (R).

The color differences at harvesting disappeared after 10 days: all the samples looked red, and also the measured colorimetric parameters were quite similar. For each fruit, the soluble solid (sugar) content was evaluated as Brix by refractive index. With the exception of the GO samples, for which an increase less than 10% occurred, the sugar content did not change during the 10 days' storage, maintaining the differences that were present at harvesting, as reported in Fig. 19.6. As a matter of fact, sugar content depends on ripening stage at harvesting, so the R samples got the largest value of soluble solid, that did not change during the storage (10 days). Differences were also observed in the DL parameters. In particular, the DL-integral for each DL decay kinetic, DLI, that is the total number of photons emitted, decreased with the fruit maturity at harvesting. The differences in DLI observed immediately after the harvesting, easily connected to different colors, remained after the 10 days' storage period, after that the differences in color were not significant. Data are reported in Fig. 19.6, where an inverse correlation between DLI and solid soluble content with respect the fruit maturity at harvesting is evident.

These results showed the possibility of using, after a standardization procedure, the DL measurements as a tool for both fruits sorting application and food quality evaluation.

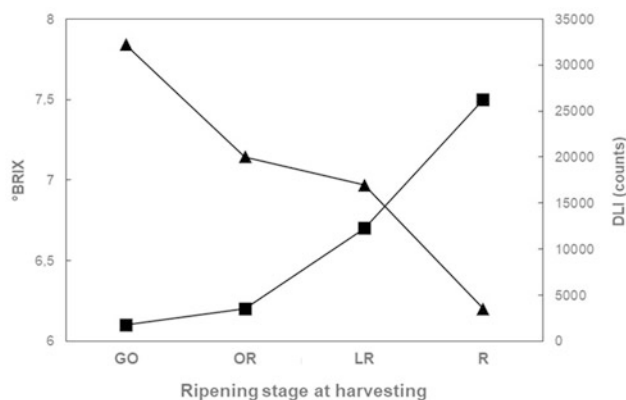


Fig. 19.6 Soluble solids content, Brix, (■) and DL-integral for each DL decay kinetic, DLI, (▲), 10 days after harvesting, as a function of sample ripening stage at harvesting, labeled according to the visual color: green-orange (GO), orange-red (OR), light red (LR) and red (R). Errors are within the marker size

19.3.2 Seeds

In agricultural industry, seed performance, that is the ability of seeds to establish seedlings rapidly, is of great importance. Seed vigor and germination percentage are the principal indexes reflecting seed quality. Stresses due to environmental and biological factors can negatively affect seed viability and vigor and the possibility to assess the germination ability of seeds with simple, not time-consuming and nondestructive methods is of great industrial relevance, being seed the basis for durable and profitable agriculture. In this respect, DL measurements performed on single seeds, which had suffered different type of stress, showed the possibility to selectively discriminate seed viability and/or vigor (Costanzo et al. 2008; Lanzanò et al. 2009; Grasso et al. 2016b, 2018).

19.3.2.1 Effects of Thermal Stress

The effects of a thermal treatment, that simulated artificial aging, were studied in soybean seeds (*Glycine max*). Seeds were set in a stove at the temperature of $75 \pm 2 \text{ }^\circ\text{C}$ and relative humidity less than 10%. Six groups, each of 14 seeds, were treated for 2, 3, 18, 27, 48, and 72 h, respectively. A group of untreated seeds was considered as the native sample. After the treatment, the seeds were sowed by using an experimental apparatus, made by a polycarbonate alveolar plate, that allowed to visually follow the germination and measure the length of every seedling. Growth performance G was evaluated considering the ratio of both the average length L and weight W of each group, 6 days after sowing, to the corresponding average length L_{AV} and weight W_{AV} of the native group:

$$G = \frac{L}{L_{\text{AV}}} + \left(\frac{W}{W_{\text{AV}}} \right)^{\frac{1}{2}} \quad (19.3)$$

The DL decay kinetics from every seed after treatment and before sowing was measured. Changes were studied by evaluating, for each emission spectral component λ , the probability $p_\lambda(t)$ that Δn levels of the n excited (by photo-illumination) ones decay in a radiative way:

$$p_\lambda = \frac{\Delta n_\lambda}{n_\lambda} \quad (19.4)$$

The probability p_λ can be evaluated starting from the experimental point (see Eq. 19.2), after that as overall parameter the R_p parameter was considered, defined as:

$$R_p(\lambda_1/\lambda_2) = \frac{1}{(t_f - t_s)} \int_{t_s}^{t_f} \frac{p_{\lambda_1}(t)}{p_{\lambda_2}(t)} dt \quad (19.5)$$

where t_s and t_f are the first and the last instant of acquisition, respectively, while the spectral components $\lambda_1 = 460$ nm and $\lambda_2 = 650$ nm were considered.

As expected, longer thermal durations induce more severe effects. Studying the correlation between G and R_p , the results showed that three different intervals of the R_p parameter values characterize different germination performance (Costanzo et al. 2008). Moreover, a sigmoidal trend accorded the data (see Fig. 19.7), allowing to identify two different values of the R_p parameter, namely R'_p and R''_p , such that a seed for which it results $R_p > R''_p$ can be rejected with a very high significance level ($p < 0.0001$), while seeds having $R_p < R'_p$ exhibit, with high probability, maximum performances (Lanzanò et al. 2009).

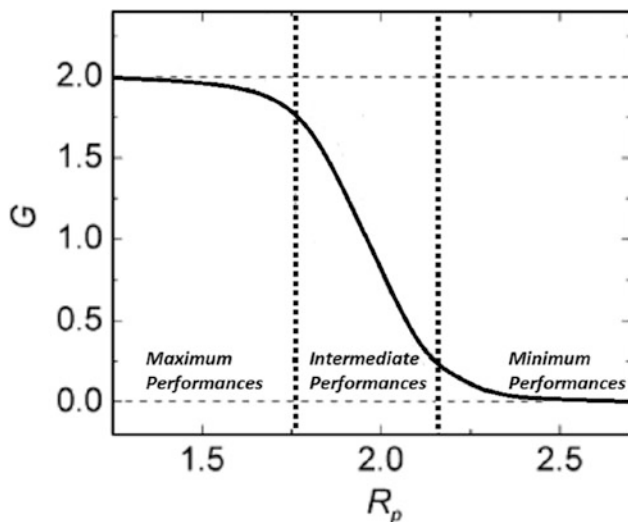


Fig. 19.7 Growth of the performance parameter G as a function of the DL parameter R_p (Eq. 19.5); (solid line) sigmoid-like fit; (dotted lines) vertical lines corresponding to the intersections of line tangent to the inflection point with the lines tangent to the two asymptotes. Intersection points define the R'_p and R''_p values, corresponding to different vegetative performances (see text)

19.3.2.2 Effects of Ion Irradiation

Ion irradiation treatment of biological systems is largely used in different application fields, from therapeutic protocol in cancer research to studies for enhancing the biological diversity. In both cases, the development of noninvasive tools able to rapidly explore the effects of ion beam dose would be welcome. With this aim, the effects of ^{12}C ion beam at the energy of 62 MeV/nucleon on Mung bean (*Vigna radiata*) seeds growth were monitored by delayed luminescence. Dormant seeds were irradiated at different doses: 50, 100, 300, 500, 1000, 5000, and 7000 Gy. After irradiation, DL measurements were performed on each treated seed; simultaneously untreated (nonirradiated) seeds, considered as “control,” were also analyzed. Seedlings growth was carried out under controlled conditions, placing each seed inside a single cell of a polycarbonate alveolar plate, which allowed a visual inspection of the seedling and the measurement of its length.

Six days after the planting of seeds, the average value of the seedlings length for each dose was evaluated and normalized to the average length value of control samples. Such Normalized Growth decreased on increasing the doses, with a dose response curve similar to a typical survival curve (Grasso et al. 2016b).

As it regards the DL measurements, it appeared that DL kinetics did not change with the dose. The effect of different ion beam doses reflected only in the DLI value, that is, the DL-integral for each DL decay kinetic. By normalizing this value to the one obtained for the control sample, it appeared that such Normalized Emission decreased on increasing the doses according to a hyperbolic trend. Figure 19.8 reports the Normalized Growth as a function of the Relative Normalized Emission, that is the relative change of the Normalized Emission of each sample with respect to the control one. Two different spectral components of photon emission, $\lambda_1 = 460$ nm and $\lambda_2 = 650$ nm respectively, were considered.

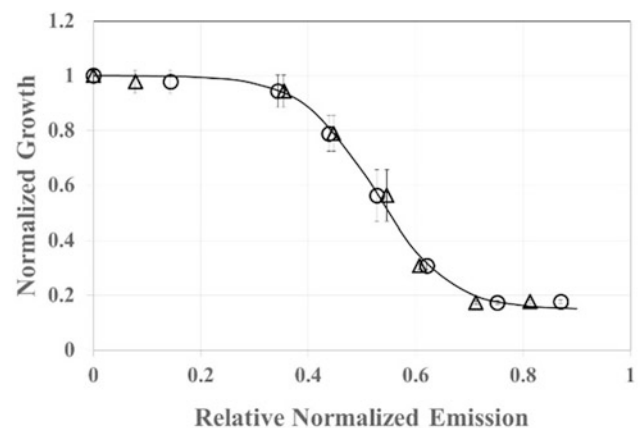


Fig. 19.8 Normalized Growth as a function of the relative normalized emission in DL for two different spectral components: (circle) $\lambda_{\text{emiss}} = 460$ nm, (triangle) $\lambda_{\text{emiss}} = 650$ nm

The trend does not depend on the spectral component and the delayed luminescence intensity and can be correlated with the seedlings elongation by a logistic function that could be able to foresee the behavior of seedling starting from DL measurements on dry seed (Grasso et al. 2016b).

19.3.2.3 Accidental Effects

In the intensive vegetable industry, in order to improve crop production, seeds with rapid and uniform germination and growth are preferred. In particular, when grafting techniques are used to produce hybrid plants, the efficiency of grafting increases by using plants (scions) with high, rapid, and uniform germination. On the other hand, seeds available for sowing come in “lots,” ideally of the same crop, whose characteristics depend on the environment in which the seeds developed and the subsequent harvesting, handling and storage. In this respect, the possibility of testing and quantifying differences between seed lots before sowing them through nondestructive methods are of great industrial relevance.

Two different lots, namely lot A and lot B, of the same cultivar “Mirella” F1 watermelon seeds were chosen (Grasso et al. 2018). The two seed lots, as assessed by the grower, showed different germination performance, the reason for this difference being unknown. Indeed, the germination test performed on 96 seeds randomly selected by each lot, for a duration of 10 days, showed slight differences in the viability of the seed lot, but a relevant difference in the germination uniformity. More precisely, only 7% lot A seeds did not germinate at all, while this percentage became 17% in the case of lot B seeds. More significantly, lot A seeds showed a shorter mean germination time (MGT, considered as the time to reach a 2 mm root length): 76% of Lot A seeds germinated within 2 days, while this percentage dropped to 24% for Lot B seeds.

Before sowing, DL decay kinetics from each seed was measured at three different emission wavelengths $\lambda_{em} = 450$ nm, 550 nm and 650 nm. According to Eq. (19.5), from the experimental data, the three R_p parameters, $R_p(450/550)$, $R_p(450/650)$, and $R_p(550/650)$, sensitive to differences in the decay probabilities between different spectral components, were evaluated. Highly significant differences ($p < 0.001$) between the two seed lots were observed in the $R_p(450/650)$ and $R_p(550/650)$ parameters, as reported in Fig. 19.9. A difference was also observed in the $R_p(450/550)$ parameter, but at a low significant level ($p < 0.05$). The first evidence was that the R_p parameters for seed lot A were always greater than the corresponding values for seed lot B. The idea was to define two limiting values for each R_p parameter, namely a low (R_{pL}) and a high (R_{pH}) value, that were able to discriminate the quality of a new seed lot, in such a way that its goodness is assessed if the average $R_p > R_{pH}$, while the lot might be rejected if the

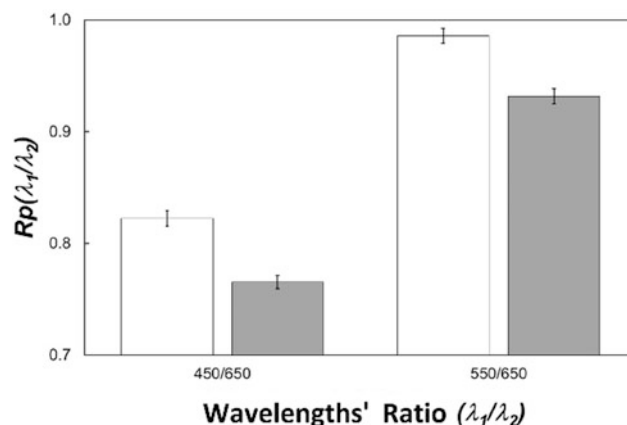


Fig. 19.9 Comparison of the values of the R_p parameter Eq. (19.3) considering the three spectral components at wavelength $\lambda = 450$ nm, 550 nm, and 650 nm, respectively. (white bar) Lot A seeds, (gray bar) Lot B seeds. Data are reported as average of all values within a given lot. Vertical bars denote standard errors. The differences between the two lots are significant at $p < 0.001$

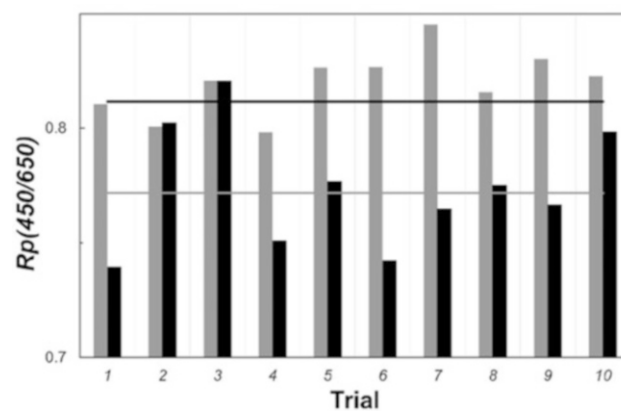


Fig. 19.10 Average values of the R_p parameters for spectral components $\lambda_1 = 450$ nm and $\lambda_2 = 650$ nm as a function of the trial number. (gray bars) trial of ten seeds of Lot A to be compared with the R_{pH} limit (gray solid line) equal to average plus standard error evaluated considering the whole set of Lot B seeds). (black bars) trial of ten seeds of Lot B to be compared with the R_{pL} limit (gray solid line) equal to average-standard error evaluated considering the whole set of Lot A seeds

average $R_p < R_{pL}$. The limiting values R_{pL} and R_{pH} were determined taking into account the whole statistics of the analyzed seeds. More precisely, R_{pH} was considered the average R_p parameter plus its standard error evaluated over the whole statistics of Lot B seeds, and R_{pL} was considered the average R_p parameter minus its standard error evaluated over the whole statistics of Lot A seeds. In order to test this model, for each seed lot ten subsets (trials), each containing 10 seeds, were randomly selected.

Figure 19.10 reports the values of the $R_p(450/650)$ obtained in each trial, along with the limiting values R_{pL} and R_{pH} . It appears that for all the trials of lot A seeds the

R_p value is greater than the R_{p_H} (gray line) value, while for all the trials of lot B seeds (with the exception of trial 3) the R_p value is lower than the R_{p_L} (black line) value. Similar results were obtained by using the $R_p(550/650)$ parameter.

This nondestructive technique could be extended to other seed species, allowing to determine the germination performance of a seed lot by testing a relatively small sample (as small as 10 seeds), so reducing the test time for seed sorting systems.

19.3.3 Water Pollution

Uncontrolled industrial development has carried out increased environmental pollution, and water pollution in particular. The possibility of monitoring pollution in a quick and inexpensive way is of relevant interest.

Among pollutants, metals, and heavy metals in particular, and chemicals, as herbicides, are most frequently identified, especially in aquatic environments. In this respect, metal uptake of heavy metals from polluted water by unicellular algae or other aquatic micro-organisms, has been largely studied. On the other hand, heavy metals exert multiple inhibitory effects on both Photosystem II (PSII) and Photosystem I (PS I). The same occurs in the case of herbicides. The damage to the photosynthetic system could reflect in a change of the DL emitted from aquatic micro-organisms, due to the fact that DL is a sensitive indicator of the many reactions that compose photosynthesis. With the aim to correlate these changes to the pollutant concentration some experimental approaches have been performed.

19.3.3.1 Pollution from Herbicides

In the first experiment, samples of the giant unicellular green alga *Acetabularia acetabulum* were used to test different herbicides (Scordino et al. 1996). Different herbicide concentrations, differing from each other by one order of magnitude, were added to the culture medium (artificial seawater) of the alga. DL measurements were performed, for each alga individual, before adding the herbicide and 30 min after the poison was added. After the poison was added to the culture medium, changes in the initial intensity and in the slope of the DL decay, relatively to the first (control) DL record, were observed. Such changes were more evident on increasing the poison concentration and were correlated to the poison concentration. Figure 19.11 reports the S parameter (defined as the ratio between the slope of DL decay trend after adding the poison to the culture medium and the corresponding value before it (in control)), as a function of the herbicide (Atrazine) concentration. Results reported in Fig. 19.11 are the average of 5 independent experiments performed on different algae, with DL measurement repeated 5 times in each experiment.

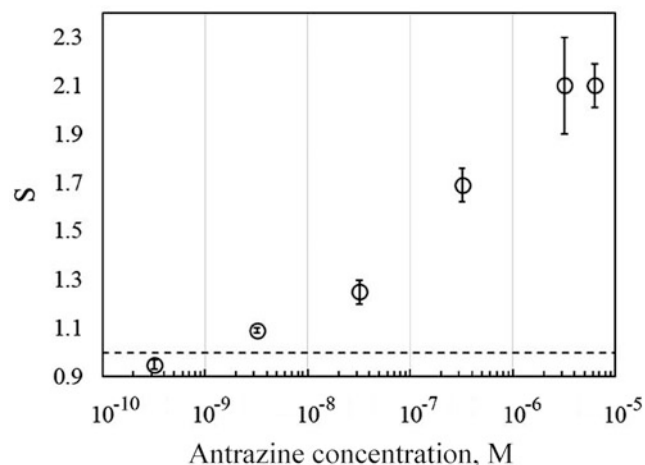


Fig. 19.11 S parameter (relative average slope of DL decay) as a function of herbicides concentration. Results are expressed as mean \pm S.D. of the values of 5 independent experiments; each experiment consisted of 5 runs

Interestingly, it is possible to reveal atrazine concentration as low as 10^{-9} M. It is worth noting that for control purposes it would be sufficient to use standard preconcentration techniques to improve the minimum detectable value.

19.3.3.2 Heavy Metal Pollution

Liquid cultures of the unicellular microscopic fresh water green algae (Chlorophyceae) *Selenastrum capricornutum* were used to test the presence of heavy metals in the medium (Scordino et al. 2008). Cadmium, chromium, copper, and lead solutions were prepared in primary stock solutions 1, 10^{-1} , and 10^{-2} M. The final concentrations of heavy metals were not determined analytically and were nominally based on the initial dosages. For each experiment, a control (native) sample was prepared by adding to the same aliquot of untreated algae a volume of distilled water equal to the one containing the chemicals added to the treated sample. An incubation time as long as 30 min was sufficient to induce changes in DL measurements: longer incubation times were tested, but no significant improvements in pollutant detection were obtained.

Adding metals in the culture medium gave rise to changes in the time trend slopes, depending on the metal concentration. The relative variation in the slope, with respect the native sample, due to the addition of chemical solutions, can be expressed by the overall parameter R_p defined as:

$$R_p = \frac{1}{(t_f - t_s)} \int_{t_s}^{t_f} \frac{p_{\text{treated}}(t) - p_{\text{native}}(t)}{p_{\text{native}}(t)} dt \quad (19.6)$$

where $p(t)$ can be evaluated by the experimental data, according to Eq.(19.4). The above defined R_p parameter

differs from the one defined in Eq.(19.5): it refers to the same spectral component and compares at the same λ_{em} the decay probabilities before (*native*) and after (*treated*) the addition of the toxic agent, by evaluating their relative changes over the decay time interval.

Results for the $\lambda_{em} = 686$ nm spectral component for chromium and cadmium are reported in Fig. 19.12.

Data reported in Fig. 19.12 are the average of 5 independent experiments for each concentration. For cadmium, as well for copper and lead, experimental data can be accorded by a power law trend, while in the case of cadmium, a logarithmic trend better accords the experimental points. The theoretical fit reported as solid line in Fig. 19.12 could allow to make an interpolation and predictions. Taking into account the value R_p^0 that the parameter R_p of Eq. (19.6) assumes in the case of untreated (native) samples, it appears that in the case of chromium the minimum detectable level is very close to the maximum admissible value, especially for sewage (see Fig. 19.12). The same occurs for copper and lead (data not shown). For cadmium, improvement in minimum

detectable level requires the use of preconcentration techniques.

It is worth noting that DL-based technique of water pollutants detection does not require incubation for a long period and is characterized by limited costs and simplicity of operation.

19.4 Conclusion

In this chapter, we reported a short review of the application possibilities offered by DL measurements, and highlighted the connection between changes in DL decay parameters and specific properties of the analyzed biological systems. The reported results obtained at the Catania University laboratories, along with the ones obtained worldwide by others researchers (see references), demonstrate the great potentiality of DL in the analytical field. Considering the fast developments of photonics, these results suggest the possibility of developing experimental tools based on DL measurements as valuable noninvasive tools of investigation and diagnosis in fields ranging from the optical biopsy to the evaluation of food quality with possible application in sorting systems, without disregarding the control of water pollution.

References

- Strehler B L and Arnold W (1951) Light production by green plants, *The Journal of General Physiology* 34(6):809–820
- Tollin G and Calvin M (1957) The luminescence of chlorophyll containing plant material, *PROC. N. A. S.* 43:895–908
- Tollin G, Fujimori E and Calvin M (1958) Delayed light emission in green plants materials: temperature dependence and quantum yield, *PROC. N. A. S.* 44:1035–1047
- Jursinic PA. (1986) Delayed fluorescence: current concepts and status. In Govindjee I, Ames J, Fork DC, editors. *Light Emission by Plants and Bacteria*. Academic Press, New York, p 291–328.
- Scordino A, Triglia A, Musumeci F (2000) Analogous features of delayed luminescence from *Acetabularia acetabulum* and some solid state systems. *J Photochem Photobiol B* 56:181–186. [https://doi.org/10.1016/s1011-1344\(00\)00078-6](https://doi.org/10.1016/s1011-1344(00)00078-6)
- Brizhik L et al (2001) Delayed luminescence of biological systems arising from correlated many-soliton states. *Phys. Rev E* 64: 031902. (<https://doi.org/10.1103/PhysRevE.64.031902>)
- Scordino A et al (2010) Delayed luminescence from collagen as arising from soliton and small polaron states. *Int J Quantum Chem* 110 (1): 221–229. (<https://doi.org/10.1002/qua.22010>)
- Niggli H J (1993) Artificial sunlight irradiation induces ultraweak photon emission in human skin fibroblasts, *J Photochem Photobiol B*. 18 (2–3):281–285 ([https://doi.org/10.1016/1011-1344\(93\)80076-1](https://doi.org/10.1016/1011-1344(93)80076-1))
- van Wijk R et al (1993) Light-induced photon emission by mammalian cells, *Journal of Photochemistry and Photobiology, B: Biology* 18 (1):75–79 ([https://doi.org/10.1016/1011-1344\(93\)80042-8](https://doi.org/10.1016/1011-1344(93)80042-8))
- Yamagishi T et al (2018) Evaluation of the toxicity of leaches from hydrothermal sulfide deposits by means of a delayed fluorescence-based bioassay with the marine cyanobacterium *Cyanobium* sp. NIES-981. *Ecotoxicology*. 27(10):1303–1309. (<https://doi.org/10.1007/s10646-018-1989-2>)

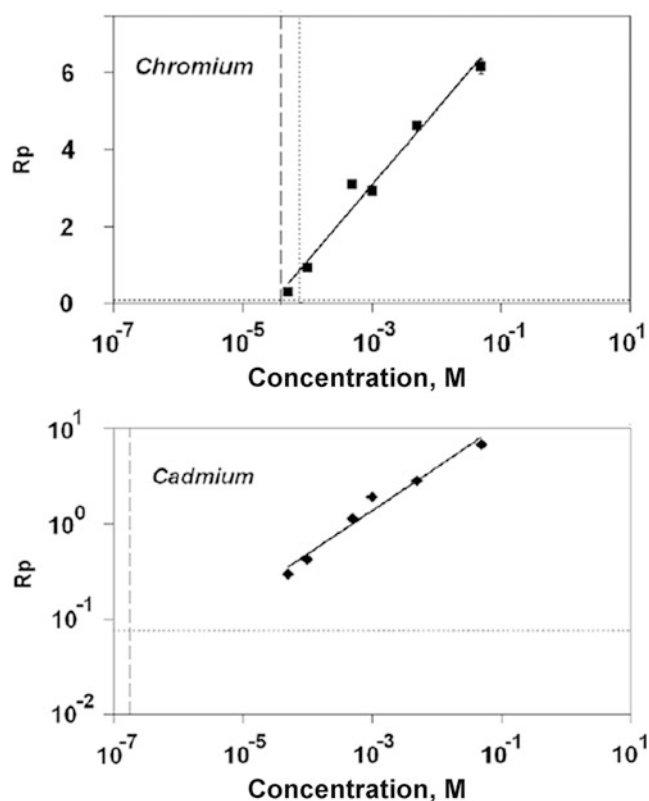


Fig. 19.12 Relative change in decay probability values R_p as a function of the metal concentration in the culture medium, after 30 min incubation. $\lambda_{em} = 686$ nm. (◆) cadmium, (■) chromium. Markers denote the experimental points (errors are within the marker size); solid lines indicate theoretical fits. The horizontal dotted line corresponds to the R_p^0 value obtained without any metal addition. The vertical dashed line and dotted line correspond to the maximum admissible concentrations for surface water and sewage, respectively

- Mengmeng S et al (2019) Characterization of ginsenoside extracts by delayed luminescence, high-performance liquid chromatography, and bioactivity tests. *Photochem. Photobiol. Sci.*, 2019(18): 1138–1146. (<https://doi.org/10.1039/C8PP00533H>)
- Bertsch W F (1962) Two photoreactions in photosynthesis: evidence from the delayed light emission of chlorella, *PROC. N. A. S.* 48: 2000–2004
- Arnold W (1965) An electron-hole picture of photosynthesis. *J. Phys. Chem.* 69 (3):788–791 (<https://doi.org/10.1021/j100887a013>)
- Clayton R K (1965) Characteristics of fluorescence and delayed light emission from green photosynthetic bacteria and algae, *The Journal of General Physiology* 48:633–646
- Muller A and Lumry R (1965) The relation between prompt and delayed emission in photosynthesis, *PROC. N. A. S.* 54:1479–1485
- Arnold W and Azzi J R (1968) Chlorophyll energy levels and electron flow in photosynthesis, *PROC. N. A. S.* 61:29–35
- Clayton R K (1969) Characteristics of prompt and delayed fluorescence from spinach chloroplasts, *Biophysical J.* 9:60–76
- Neumann J, Barber J and Gregory P (1973) The relation between photophosphorylation and delayed light emission in chloroplasts, *Plant Physiol.* 51:1069–1073
- Guo Y and Tan J (2013a) Applications of delayed fluorescence from photosystem II, *Sensors* 13:17332–17345; (<https://doi.org/10.3390/s131217332>)
- Drinovec L et al (2011) Discrimination of marine algal taxonomic groups using delayed fluorescence spectroscopy, *Environmental and Experimental Botany* 73: 42–48 (<https://doi.org/10.1016/j.envexpbot.2010.10.010>)
- Abbott J A, Campbell T A and Massie D R (1994) Delayed light emission and fluorescence responses of plants to chilling, *Remote Sens. Environ.* 47:87–97 (1994)
- Guo Y and Tan J (2013b) A biophotonic sensing method for plant drought stress, *Sensors and Actuators B* 188:519–524 (<https://doi.org/10.1016/j.snb.2013.07.020>)
- Guo Y and Tan J (2014a). On the potential usefulness of Fourier spectra of delayed fluorescence from Plants, *Sensors* 14:23620–23629; (<https://doi.org/10.3390/s141223620>)
- Chen WL, Xing D and Chen WG (2005) Rapid detection of *Aspergillus flavus* contamination in peanut with novel delayed luminescence spectra, *Photochemistry and Photobiology*, 81:1361–1365 (<https://doi.org/10.1562/2005-05-23-RC-538>)
- Razinger J, Drinovec L and Berden-Zrimec M (2012) Delayed fluorescence imaging of photosynthesis inhibitor and heavy metal induced stress in potato, *Cent. Eur. J. Biol.* 7(3):531–541 (<https://doi.org/10.2478/s11535-012-0038-z>)
- Scordino A et al (1996) Influence of the presence of atrazine in water on the in-vivo delayed luminescence of *Acetabularia acetabulum*. *Journal of Photochemistry & Photobiology B* 32 (1–2): 11–17 ([https://doi.org/10.1016/1011-1344\(95\)07213-6](https://doi.org/10.1016/1011-1344(95)07213-6))
- Katsumata M et al (2006) Rapid ecotoxicological bioassay using delayed fluorescence in the green alga *Pseudokirchneriella subcapitata*, *Water Res. Arch* 40: 3393–3400.
- Scordino A et al (2008) Delayed luminescence of microalgae as indicator of metal toxicity, *Journal of Physics D – Applied Physics* 41(15), 155507 (7pp) (<https://doi.org/10.1088/0022-3727/41/15/155507>)
- Katsumata M and Takeuchi I (2017) Delayed fluorescence as an indicator of the influence of the herbicides Irgarol 1051 and Diuron on hard coral *Acropora digitifera*, *Marine Pollution Bulletin* 124:687–693 (<https://doi.org/10.1016/j.marpolbul.2017.08.006>)
- Guo Y and Tan J (2010) A plant-tissue-based biophotonic method for herbicide sensing, *Biosens. Bioelectron.* 25 (8), 1958–1962.
- Guo Y and Tan J (2014b) Fourier transform of delayed fluorescence as an indicator of herbicide concentration, *Journal of Theoretical Biology* 363:271–276 (<https://doi.org/10.1016/j.jtbi.2014.08.023>)
- Hu K et al (2019) Global research trends in food safety in agriculture and industry from 1991 to 2018: A data-driven analysis, *Trends in Food Science & Technology* 85:262–276 (<https://doi.org/10.1016/j.tifs.2019.01.011>)
- Stolz P, Wohlers J and Mende G. Measuring delayed luminescence by FES to evaluate special quality aspects of food samples – an overview. *Open Agriculture*. 2019; 4: 410–417 (<https://doi.org/10.1515/opag-2019-0039>)
- Wohlers J and Stolz P (2019) Differentiation between milk from low-input biodynamic, intermediate-input organic and high-input conventional farming systems using fluorescence excitation spectroscopy (FES) and fatty acids, *Biological Agriculture & Horticulture* 35(3):172–186 (<https://doi.org/10.1080/01448765.2019.1580615>)
- Forbus WR JR, Senter S D and Chan H T Jr (1987) Measurement of papaya maturity by delayed light emission. *Journal of Food Science* 52(2):356–359 (<https://doi.org/10.1111/j.1365-2621.1987.tb06612.x>)
- Triglia A. et al (1998) Delayed luminescence as an indicator of tomato fruit quality, *Journal of Food Science* 63 (3):512–515 (1998) (<https://doi.org/10.1111/j.1365-2621.1998.tb15775.x>)
- Forbus WR JR, Senter S D and Wilson R L (2006). Measurement of tomato maturity by delayed light emission, *Journal of Food Science* 50(3):750–753 (<https://doi.org/10.1111/j.1365-2621.1985.tb13788.x>)
- Pang J et al (2016) Spectral Analysis of Chinese Medicinal Herbs Based on Delayed Luminescence, Evidence-Based Complementary and Alternative Medicine 8469024 (8 pages) (<https://doi.org/10.1155/2016/8469024>)
- Sun M et al (2018) Application of delayed luminescence method on measuring of the processing of Chinese herbal materials, *Chin Med* 13:43 (<https://doi.org/10.1186/s13020-018-0202-0>)
- Sun M et al (2019) Application of delayed luminescence measurements for the identification of herbal materials: a step toward rapid quality control. *Chin Med* 14:47(<https://doi.org/10.1186/s13020-019-0269-2>)
- Scholz W, Staszkievicz U, Popp F A, Nagl W (1988) Light-stimulated ultraweak photon reemission of human amnion cells and wish cells, *Cell Biophysics* 13 (1):55–63 (<https://doi.org/10.1007/BF02797365>)
- Zhang, J et al (1997) Spontaneous and light-induced photon emission from intact brains of chick embryos. *Science in China, Series C: Life Sciences* 40 (1) 43–51 (<https://doi.org/10.1007/BF02879106>)
- Popp F A and Yan Y (2002) Delayed luminescence of biological systems in terms of coherent states. *Physics Letters, Section A: General, Atomic and Solid State Physics* 293 (1–2):93–97 ([https://doi.org/10.1016/S0375-9601\(01\)00831-3](https://doi.org/10.1016/S0375-9601(01)00831-3))
- Tudisco S et al (2003) Advanced research equipment for fast ultraweak luminescence analysis, *Review of Scientific Instruments* 74(10): 4485–4490 (2003) – (<https://doi.org/10.1063/1.1611997>)
- Niggli H J et al (2005) Laser-Ultraviolet-A induced ultraweak photon emission in mammalian cells, *Journal of Biomedical Optics* 10 (2): 024006 (6 pag) (<https://doi.org/10.1117/1.1899185>)
- Musumeci F et al (2005a) Spectral analysis of laser-induced ultraweak delayed luminescence in cultured normal and tumor cells: temperature dependence, *Journal of Photochemistry & Photobiology B* 79(2):93–99 (<https://doi.org/10.1016/j.jphotobiol.2004.12.002>)
- Musumeci F et al (2005b) Discrimination between normal and cancer cells by using spectral analysis of delayed luminescence, *Applied Physics Letters* 86 (15):153902 (3 pag) (<https://doi.org/10.1063/1.1900317>)
- Lanzanò L et al (2007) Spectral analysis of delayed luminescence from human skin as a possible non-invasive diagnostic tool, *European Biophysics Journal with Biophysics Letters* 36 (7):823–829 (<https://doi.org/10.1007/s00249-007-0156-0>)
- Niggli H J et al (2008) Laser-Ultraviolet-A induced ultraweak photon emission in human skin cells: A biophotonic comparison between keratinocytes and fibroblasts. *Indian Journal of Experimental Biology* 46 (5):358–363

- Baran I et al (2009) Effects of nocodazole and ionizing radiation on cell proliferation and delayed luminescence. *Romanian Journal of Physics* 54:557–567
- Baran I et al (2010) Effects of menadione, hydrogen peroxide and quercetin on apoptosis and delayed luminescence of human leukemia Jurkat T-cells - *Cell Biochemistry and Biophysics* 58:169–179 (<https://doi.org/10.1007/s12013-010-9104-1>)
- Baran I et al (2012) Detailed analysis of apoptosis and delayed luminescence of human leukemia Jurkat T cells after proton-irradiation and treatments with oxidant agents and flavonoids. *Oxidative Medicine and Cellular Longevity*, Article ID 498914, 14 pages (<https://doi.org/10.1155/2012/498914>)
- Scordino A et al (2014a) Delayed luminescence to monitor programmed cell death induced by Berberine on thyroid cancer cells, *Journal of Biomedical Optics* 19 (11):117005 (<https://doi.org/10.1117/1.JBO.19.11.117005>)
- Scordino A et al (2014b) Ultra-weak Delayed Luminescence in cancer research: a review of the results by the ARETUSA equipment, *Journal of Photochemistry & Photobiology B- Biology* 139:76–84 (<https://doi.org/10.1016/j.jphotobiol.2014.03.027>)
- Baran I et al (2013) Mitochondrial respiratory Complex I probed by delayed luminescence spectroscopy, *Journal of Biomedical Optics* 18 (12):127006 (<https://doi.org/10.1117/1.JBO.18.12.127006>)
- Grasso R et al (2016a) The delayed luminescence spectroscopy as tool to investigate the cytotoxic effect on human cancer cells of drug-loaded nanostructured lipid carrier, in: *Biophotonics: Photonic Solutions for Better Health* V, Jürgen Popp, Valery V. Tuchin, Dennis L. Matthews, Francesco Saverio Pavone Eds, *Proceedings of SPIE* 9887:988723 (10 pp) (2016) (<https://doi.org/10.1117/12.2227514>)
- Grasso R et al (2019) Delayed Luminescence for in vitro study of mitochondrial dysfunctions in neurodegenerative diseases, in: *Novel Biophotonics Techniques and Applications V*, Arjen Amelink; Seemantini K. Nadkarni. Editor(s), *Proceedings SPIE* 110750K (<https://doi.org/10.1117/12.2526920>)
- Chen P et al (2012) Spectral discrimination between normal and leukemic human sera using delayed luminescence, *Biomed Opt Express*. 3 (8):1787–1792. (<https://doi.org/10.1364/BOE.3.001787>)
- Letuta S N et al (2016) Delayed luminescence of erythrosine in biological tissue and photodynamic therapy dosimetry. *Journal of Photochemistry and Photobiology B: Biology* 163:232–236 (<https://doi.org/10.1016/j.jphotobiol.2016.08.036>)
- Kim H W et al (2005), Spontaneous photon emission and delayed luminescence of two types of human lung cancer tissues: Adenocarcinoma and Squamous cell carcinoma, *Cancer Lett.* 229:283–289.
- Bai H et al (2009) Physical mechanism of delayed luminescence from human serum, in: D.L. Farkas, D.V. Nicolau, R.C. Leif (Eds.), *Imaging, Manipulation, and Analysis of Biomolecules, Cells, and Tissues VII*, Proc. SPIE 7182 71820K
- Mik E G et al (2009). Mitochondrial oxygen tension within the heart, *Journal of Molecular and Cellular Cardiology* 46:943–951. (<https://doi.org/10.1016/j.yjmcc.2009.02.002>)
- Ubbink R et al (2017) A monitor for Cellular Oxygen METabolism (COMET): monitoring tissue oxygenation at the mitochondrial level, *Journal of Clinical Monitoring and Computing* 31 (6):1143–1150 (<https://doi.org/10.1007/s10877-016-9966-x>)
- van Dijk L J D et al (2019) Oxygen-dependent delayed fluorescence of protoporphyrin IX measured in the stomach and duodenum during upper gastrointestinal endoscopy, *Journal of Biophotonics* 12 (10): e2019000251 (<https://doi.org/10.1002/jbio.201900025>)
- Bertolaso M and Duprè J (2018) *A Processual Perspective on Cancer*. In 'Everything Flows' Daniel J. Nicholson and John Duprè' eds. Oxford University Press 321–336
- Bizarri M and Cucina A (2014) Tumor and the Microenvironment: A Chance to Re-frame the Paradigm of Carcinogenesis? *Biomed Res Int* 2014:934038 (<https://doi.org/10.1155/2014/934038>)
- H.J. Niggli, C. Scaletta, F.A. Popp, Y. Yu, L.A. Applegate (2001) Ultraweak photon emission in assessing growth factor efficiency using fibroblastic differentiation, *J. Photochem. Photobiol. B-Biol.* 64:62–68..
- S.Desagher, J.-C. Martinou, Mitochondria as the central control point of apoptosis, *Trends Cell Biol* 10 (2000) 369–377
- Brizhik L et al (2003) Nonlinear dependence of the delayed luminescence yield on the intensity of irradiation in the framework of a correlated soliton model, *Phys Rev E* 67: 021902. (<https://doi.org/10.1103/PhysRevE.67.021902>)
- Costanzo E et al (2008) Single seed viability checked by Delayed Luminescence, *European Biophysics Journal with Biophysics Letters*, 37 (2):235–238 (<https://doi.org/10.1007/s00249-007-0221-8>)
- Lanzanò L et al (2009) Time-resolved spectral measurements of delayed luminescence from a single soybean seed: effects of thermal damage and correlation with germination performance, *Luminescence* 24 (6): 409–415 (<https://doi.org/10.1002/bio.1127>)
- Grasso R et al (2016b) Effects of Ion Irradiation on Seedlings Growth Monitored by Ultraweak Delayed Luminescence, *PLoS ONE* 11 (12):e0167998 (<https://doi.org/10.1371/journal.pone.0167998>)
- Grasso R et al (2018) Non-destructive evaluation of watermelon seeds germination by using Delayed Luminescence - *Journal of Photochemistry & Photobiology, B: Biology* 187, 126–130 (2018) (<https://doi.org/10.1016/j.jphotobiol.2018.08.012>)

Mitogenetic Effect and Related Phenomena: Unresolved Problems of UPE

Preface

The history of mitogenetic research is provided in detail in Chap. 1. Although there is obviously no need to repeat the material from other chapters, we feel that some important information is not only missing but also impossible to add to the historical part. These include the experimental schemes and various methodical approaches used in mitogenetic research. Being obviously of primary importance to any scientific area, such methodical details are crucial for obtaining confident data and their correct interpretation.

As seen in Chap. 1, the mitogenetic literature is full of conflicting issues and misinterpretations, which, taken together, may well create an impression of a false science or pure fallacy (as considered by a number of influential authors – e.g., Langmuir and Hall, 1989). At the same time, as described in Chap. 1, mitogenetic research spanned a huge and saturated period in the history of science, and many serious, respectful workers performed careful, laborious experiments, with an honest mind to find out everything as it is.

Thus, the above discrepancies in mitogenetic data seem impossible to interpret as a result of careless illiterate errors or deliberate falsification by “positive authors.” Moreover, now when many essential conclusions made on the basis of mitogenetic experiments have been proved correct and much ahead of their time (like the discovery of ultraweak photon emission (UPE) itself, the role of free radicals in its generation, peptide tumor markers, etc.), one needs to be extremely careful when analyzing data from early mitogenetic works.

For this reason, we are confident that detailed data on experimental methods used in mitogenetic studies may be of extreme importance for understanding the processes used in them. We do not mean to imply that the results of those works are proven; contrary to that, we are sure that this must be reviewed and verified in detail, with all possible ways to find out what went wrong. However, doing all of this with due attention to the accumulated experience is impossible, and, so, a scrupulous analysis of methods, tips, and tricks should be carried out.

Recently, the characteristics of UV detectors have reached the level needed for an unambiguous final validation or disproof of the key results on ultraviolet UPE. We believe that the next decades will witness a surge of activity in UV-UPE, and the following chapters aim to provide researchers with well-referenced and systematized relevant information on the field, including a large number of studies, which were published in Soviet scientific journals and, as such, are practically inaccessible to an English-speaking reader.

The first chapter (Chap. 20) is devoted to the basic biological effect of mitogenesis, and the second one (Chap. 21) reviews the research of its physical qualities, including instrumental detection. Chapter 22 is dedicated to specific cases of mitogenetic radiation, which seem too

specialized to include in the previous two chapters: mitogenetic radiation (MGR) from mitogenetically INactive cells, stimulated by exposure to external MGR, and MGR from stressed and dying cells. The last chapter (Chap. 23) covers medical aspects of mitogenetic research with a focus on cancer diagnostics.

References

Langmuir I, Hall RN (1989) Pathological science. Phys Today 42. <https://doi.org/10.1063/1.881205>



Ilya Volodyaev, Irina I. Kontsevaya, and Elena V. Naumova

20.1 Definitions and General Scheme of Mitogenetic Experiments

20.1.1 Definitions

The basic *mitogenetic effect (MGE)* is a change in mitotic regime in a cell culture or tissue under external nonchemical influence of another biological object.

MGE recipients (“*biological detectors*”) are cell cultures and tissues, capable of showing MGE under external “mitogenetic” influence.

MGE inductors are those objects that can produce MGE in proper recipients under optimal conditions.

The known recipients are as follows:

- Bacterial and yeast cultures in lag phase (Tuthill and Rahn 1933; Wolff and Ras 1931a; Ferguson and Rahn 1933)
- Bacterial and yeast cultures in growth suppression (prediauxic shift) phase (Baron 1926, 1928)
- Tissue cultures (Guillery 1928)
- Plant meristem (Gurwitsch 1923; Reiter and Gabor 1928a; Siebert and Seffert 1934)
- Eye cornea (Gurwitsch and Anikin 1928; Naville 1929, 1937)
- Eggs (Reiter and Gabor 1928a; Wolff and Ras 1934a) and developing embryos (Magrou and Magrou 1927a, b; Salkind 1929)

The known inductors are as follows:

- Actively growing microbial and tissue cultures (Baron 1930; Magrou and Magrou 1927a, b; Acs 1931; Siebert 1928b)
- Working muscles and heart (Siebert 1928a)
- Excited neurons (Gurwitsch 1934a)
- Blood of healthy people (Pesochensky 1942; Gurwitsch and Salkind 1929; Siebert 1930)
- Malignant tumors (Gurwitsch and Gurwitsch 1934a; Gurwitsch et al. 1947)
- Resorbed and regenerating tissues (Blacher et al. 1932, 1933)
- Certain chemical reactions (Rahn 1934b; Gurwitsch 1968)

Definite noninductors are as follows:

- Not growing or slowly growing cultures (Rahn 1934b)
- Internal parts of the body (collected data in Gurwitsch and Gurwitsch (1934b) and Rahn (1936))
- Blood of cancer patients (Pesochensky 1942, 1947; Gurwitsch et al. 1947; Siebert 1930; Zalkind 1936)
- Blood of people with some other diseases (anemia, sepsis, pneumonia, scarlatina); blood of old and exhausted people (Siebert 1930; Protti 1930)

See more in Rahn (1936) and Gurwitsch and Gurwitsch (1934b), and also in Volodyaev and Belousov (2015), Naumova et al. (2018) and Volodyaev et al. (2021).

20.1.2 General Scheme of MGE Induction

As mentioned in Chap. 2, the mitogenetic effect appeared quite laborious to observe. Besides selecting a suitable inductor and recipient, one needed to prepare both cultures (or organisms), select optimal interaction mode and duration and follow a number of additional experimental conditions. Below, we shortly mention some of them (see more in Rahn (1936) and Gurwitsch and Gurwitsch (1934b)) and also in

I. Volodyaev (✉)
Moscow State University, Moscow, Russia
e-mail: ivolodyaev@gmail.com

I. I. Kontsevaya
Francysk Skaryna Gomel State University, Gomel, Republic of Belarus

E. V. Naumova
Rzhanov Institute of Semiconductor Physics, Siberian Branch of the Russian Academy of Sciences, Novosibirsk, Russia

modern reviews: (Volodyaev and Belousov 2015; Naumova et al. 2018; Volodyaev et al. 2021).

The general experimental scheme was as follows:

1. Preparing the inductor and the recipient (“biological detector”): bringing them to the proper physiological states (e.g., sprouting onion roots, cultivating yeast or bacteria to the appropriate growth phases – usually different for the inductor and the recipient).
2. Exposure (induction) – bringing the recipient into (optical) contact with the MGE inductor (the details of this stage were of primary importance for observing or nonobserving the effect – see next section).
3. The period of MGE manifestation (it takes some time for MGE to manifest itself sufficiently for a quantitative assessment after the end of induction – e.g., for the appearance of detectable yeast buds, or for the recipient yeast or bacterial culture growth detectable by a nephelometer).
4. Quantifying the MGE-characterizing parameter (e.g., calculating the budding index for a yeast culture, or assessing absolute number of cells for yeast or bacterial cultures – microscopically, with a nephelometer or colorimeter, or by mycetocrit¹). Statistical processing of the results. In the 1920s–1940s, the effect was usually quantified as the relative difference between the mean values in the experimental and the control groups.

20.1.3 Induction Conditions

As mentioned above, the MGE was caused by a nonchemical factor: the inductor and the recipient could be totally chemically isolated without losing the effect. However, they had to be rather close (see below), and also there were strict requirements for the material placed between them: a stable MGE was observed only through good-quality quartz, suggesting that the effect was caused by UV radiation of very low intensity.

Concisely, the conditions for observing MGE look like the following:

1. Optical contact

The optical channel between the inductor and the recipient must be transparent to light with $\lambda > 190$ nm. “Even quartz can only be used if it is of very high purity” (Hollaender 1936).

Obviously, reflection, absorption and scattering of radiation in glass, quartz and other materials should be also taken into account, since they can significantly reduce the effect (e.g., if there are several reflecting surfaces between the inductor and the recipient) or give artifactual

stimulation in the control (e.g., if the radiation from the inductor is partially reflected on some surfaces and hits the reference sample).

Importantly, **suspension cultures can only be induced in a very thin layer: <0.5 mm**. This has been emphatically stated in a number of works from Rahn’s and Wolf’s laboratories (e.g., (Rahn 1936; Wolff and Ras 1933a)) and seems the main reason for a number of failures by other authors. As Rahn wrote, “thicker suspension layers absorb the radiation and completely cancel the effect” (Rahn 1936).

2. The inductor–recipient distance

The optimal distance is from 1 to 10 mm; the maximum distance at which MGE is observed depends on the inductor and the recipient, the induction duration and special conditions such as “intermittent induction” (see below). Interestingly, if the distance between them was changed in course of the experiment, the effect changed dramatically. For instance, if the recipient and the inductor were smoothly converged from 10–20 cm to 1–2 mm apart within 3 min, the MGE was stable; if it took 5 to 6 min, the recipient did not react (Gurwitsch and Gurwitsch 1932, 1934b).

3. Aeration and related conditions

Most successful experiments were performed under aerobic conditions, without special saturation of the atmosphere (or medium) with any gas. In many cases, these conditions are not described, but they are highly likely to be generally the same.

Several attempts demonstrated that MGE inductors lost their ability to radiate under anaerobic conditions (for instance, blood (Sorin 1926)).² For a biological object, the ability to induct MGE (i.e., to serve as a primary or secondary MGE inductor³) was found to be an obligatory condition for being MGE recipient as well, thus implying that in anaerobic conditions biological recipients lost their sensitivity to MGR as well. MGE was also not observed when recipient culture was in oxygen-purged atmosphere (Hollaender and Claus 1937), which may have various reasons, including inadequate aeration.

Actually, the above-mentioned requirement to conduct induction only in thin layers (<0.5 mm (Rahn 1936; Wolff and Ras 1933a)) may also be partially due to inadequate aeration in the bulk of the suspension.

¹Mycetocrit is a vessel for accurately measuring the volume of a liquid culture (see, e.g., (Glasser and Barth 1938)).

²Note that it is now generally accepted that spontaneous UPE almost always requires oxygen access, both in model systems (see Chaps. 9, 11, and 12) and in the cell (see Chap. 14). Its two main roles are: (1) initiation of free-radical processes via one-electron reduction, (2) formation of peroxide radicals, which further generate photons at recombination or certain other reactions (see more in Part III).

³See more about secondary radiation in Chap. 22.

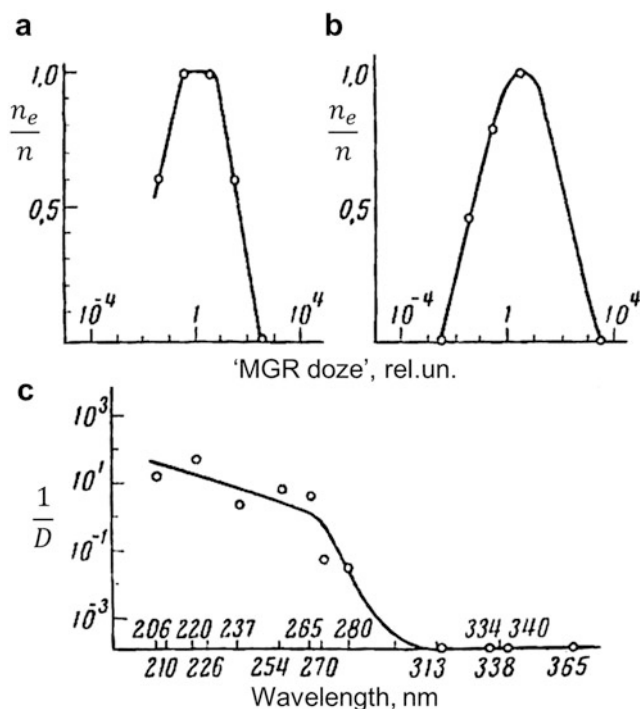


Fig. 20.1 Dose curves and the action spectrum of mitogenetic radiation. (a) Probability of detecting mitogenetic effect (yeast budding) as a function of irradiation dose at 206 nm wavelength; (b) The same, at 220 nm wavelength; (c) Spectrum of action. n_e , number of experiments with a positive mitogenetic effect; n , total number of experiments; $\frac{n_e}{n}$, probability of observing the effect in the current experiment; D , dose corresponding to the maximal mitogenetic effect. (Reprinted from (Vladimirov 1967), with permission from the author; data from (Rodionov and Frank 1934)).

4. Lighting conditions

Induction should be carried out in “diffused daylight” (Potozky 1930).

Besides, MGE is not observed in the presence of external ultraviolet radiation even at relatively low intensities. For example, MGE disappeared in the presence of a gas burner or on a sunny day with open laboratory windows (Ruyssen 1933), but with double shutters closed, and the cultures in the back of the room (i.e., when filtered with two window panes and with significant scattering of ultraviolet), MGE was observed (Gurwitsch and Gurwitsch 1934b).

5. Duration of induction

MGE has a nonlinear dose dependence with a clear suppression effect at high doses (Sussmanowitsch 1928; Gurwitsch and Gurwitsch 1932; Wolff and Ras 1933a) (see Fig. 20.1). The induction duration must be specially selected for each new set of conditions, at least in the range of 1 to 120 min. Sometimes much longer exposures were used, for instance 48 h in (Khruschov 1934).

Examples of the optimal induction duration in the literature:

- from 30 to 40 min and more (Gurwitsch 1929a) up to 2 h (Gurwitsch and Gurwitsch 1934b) – the inductor and the recipient were onion roots;
- 30 min – the inductor and the recipient were yeast cultures (Tuthill and Rahn 1933);
- 6–8 min – the inductor and the recipient were yeast cultures; only very small buds, $<1/10$ of the mother cell, were counted (the approach suggested by M. Baron (1926) and widely used in Gurwitsch’s labs in 1930-s (Gurwitsch and Gurwitsch 1934b; Rahn 1936));
- 15–30 min – the inductor and the recipient were bacterial cultures. An induction of 60 min had no effect; an induction of 120 min resulted in suppression of the culture growth (Wolff and Ras 1933a);
- 5 min – the inductor was a chemical system HCl +NaOH and the recipient was a bacterial culture (Wolff and Ras 1932b).

6. Time mode of induction: “intermittent induction”

A very special condition mentioned in Gurwitsch’s works (Gurwitsch and Gurwitsch 1932, 1934b) and quoted by other researchers (e.g., (Rahn 1936)) was called “intermittent induction.” The authors separated the inductor and the recipient with a rotating nontransparent disc with cut-off slits, so that the recipient was periodically exposed to the inductor and screened from it. The rotation speed, the cuttings number and sizes determined the exposure and screening duration. Surprisingly, certain combinations of these parameters enhanced the observed MGE by several times comparing to the “ordinary” (noninterrupted) induction. This manifested in **decreasing the minimal induction time**, sufficient to get MGE, or in **increasing the maximal inductor–recipient distance**. Thus, while the standard yeast–yeast induction gave consistent MGE only at the minimal time of 6 to 8 min, intermittent induction gave clear effect already after 1 min (with the net induction time being 12–60 s) – see Table 20.1. Moreover, using intermittent induction, the authors managed to obtain MGE at the inductor–recipient distances up to 10 cm (which gave no results otherwise), as well as for certain “very weak inductors,” also incapable of producing MGE with the standard test setup (Gurwitsch and Gurwitsch 1934b).

In the context of these data, Gurwitsch suggested that the greatest MGE efficiency is achieved precisely at the moment of induction “switching on” (Gurwitsch and Gurwitsch 1934b). However, at the same time, he cites data that intermittent induction with a discontinuous rhythm (through a disc with irregularly cut slits of different widths) gave much lower effect, than in steady-rhythm cases, as above (Gurwitsch and Gurwitsch 1934b). Altogether, though these data are quite unclear, greater sensitivity of the recipient to intermittent

Table 20.1 Results of intermittent induction. Inductor, recipient – yeast cultures; standard inductor–recipient distance (not mentioned by the authors, but seemingly 1–2 mm)

| Exposure, msec | Shading, msec | Total cycle, msec | Number of periods | Total induction time, s | Total experiment time, min | Effect | Ref | |
|---------------------------|---------------|-------------------|-------------------|-------------------------|----------------------------|--------|---------------------------------|---------------------------------|
| Constant induction | | | | | <6 | – | Rahn (1936) | |
| | | | | | 6–8 | + | | |
| 50.0 | 50.0 | 100 | 1000 | 50.0 | 1.7 | – | Gurwitsch and Gurwitsch (1934b) | |
| 50.0 | 50.0 | 100 | 1200 | 60.0 | 2.0 | + | | |
| 2.2 | 17.8 | 20 | 5850 | 13.0 | 2.0 | ± | | |
| 2.2 | 17.8 | 20 | 9000 | 20.0 | 3.0 | + | | |
| 1.1 | 2.9 | 4 | 5850 | 6.5 | 0.4 | – | | |
| 1.1 | 3.9 | 5 | 11,250 | 12.5 | 0.9 | + | | |
| 1.1 | 2.9 | 4 | 11,700 | 13.0 | 0.8 | + | | |
| 1.1 | 2.9 | 4 | 14,400 | 16.0 | 1.0 | – | | |
| 1.1 | 2.9 | 4 | 27,000 | 30.0 | 1.8 | + | | |
| 1.1 | 8.9 | 10 | 13,000 | 14.4 | 2.2 | ± | | Rahn (1936) |
| 1.1 | 8.9 | 10 | 20,000 | 22.2 | 3.3 | + | | |
| 0.8 | 3.2 | 4 | 18,000 | 15.0 | 1.2 | – | | Gurwitsch and Gurwitsch (1934b) |
| 0.6 | 1.9 | 3 | 25,000 | 13.9 | 1.0 | + | | Rahn (1936) |
| 0.6 | 19.4 | 20 | 19,000 | 10.6 | 6.3 | + | | |
| 0.4 | 19.6 | 20 | 30,000 | 12.5 | 10.0 | – | | |
| 0.6 | 19.4 | 20 | 23,000 | 12.8 | 7.7 | – | | |
| 0.6 | 19.4 | 20 | 40,000 | 22.2 | 13.3 | + | | |
| 0.3 | 2.2 | 3 | 23,000 | 6.4 | 1.0 | ± | | |
| 0.3 | 3.7 | 4 | 36,000 | 10.0 | 2.4 | – | Gurwitsch and Gurwitsch (1934b) | |
| 0.3 | 2.2 | 3 | 46,000 | 12.8 | 1.9 | + | Rahn (1936) | |
| 0.3 | 3.7 | 4 | 46,800 | 13.0 | 3.1 | + | Gurwitsch and Gurwitsch (1934b) | |
| 0.1 | 1.1 | 1 | 70,000 | 9.7 | 1.5 | – | Rahn (1936) | |
| 0.1 | 1.1 | 1 | 91,000 | 12.6 | 1.9 | + | | |

Recalculated from the data in Gurwitsch and Gurwitsch (1934b) and Rahn (1936)

induction (depending on its parameters), seems to be a fact, that should be taken into account.

7. Dynamics of MGE development after induction

MGE does not manifest immediately. The maximal effect produced by the MGE induction was observed:

- 3–4 h after the end of induction (recipient – corneal epithelium; various inductors; the observed indicator was the number of mitoses) (Gurwitsch and Anikin 1928)
- 1–4 h after the end of induction (recipients – bacterial cultures; culture density observed) (Wolff and Ras 1933a; Ferguson and Rahn 1933)
- 30–120 min after the end of induction (recipients – yeast cultures; budding index observed) (Tuthill and Rahn 1933)
- 5–10 min after the end of induction (recipients – yeast cultures; “Baron’s method”: only buds <1/10 of the mother cell counted) (Gurwitsch and Ereameef 1947; Gurwitsch 1968)

Also, the time of the effect manifestation was shown significantly dependent on the induction duration (Gurwitsch and Ereameef 1947).

20.2 MGE on Plant Meristems

20.2.1 Gurwitsch’s “Onion Experiment”

The very first experiment on MGE was performed on common onion roots (*Allium cepa* L.), which were used as both inductor and recipient (Gurwitsch 1923, 1926). One of the roots (inductor) was located perpendicular to the other one (recipient), the tip of the inductor directed onto the recipient's division zone and separated from it with a quartz plate (see Fig. 20.2). The proportion of cells in mitosis (calculated from the number of mitotic figures) was found significantly higher on the exposed side. Outside the exposure region the distribution of mitotic figures was uniform (Table 20.2).

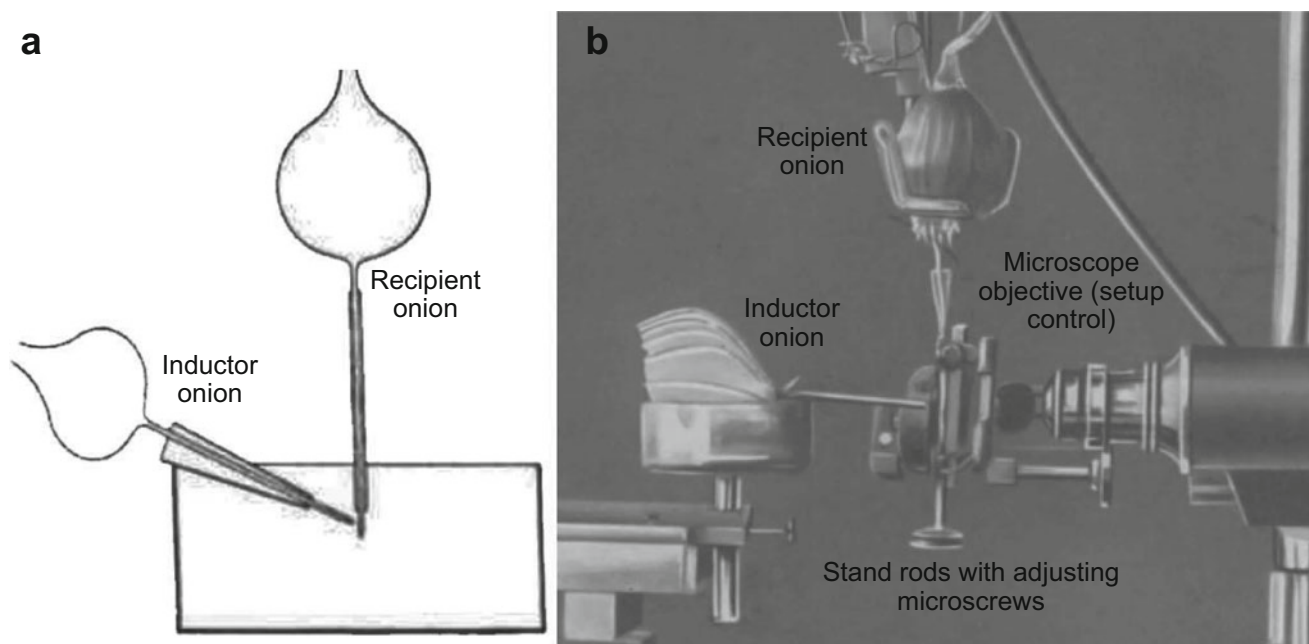


Fig. 20.2 Mitogenetic effect on onion roots. (a) – scheme of experimental setup. (Adapted from (Gurwitsch 1923). Copyright 1923, with permission from SNCSC); (b) – photo of experimental setup. (Adapted from (Gurwitsch 1926). Copyright 1926, with permission from SNCSC)

Table 20.2 Average number of mitoses on cross-sections (10 μm thick) of the exposed and the opposite side of the root

| | % of Cells in mitosis | | |
|----------------------------------|-----------------------|------------------|------------------|
| | Exposed side | Opposite side | Difference |
| Outside of the range of exposure | 54.25 \pm 16.77 | 54 \pm 16.99 | 0.25 \pm 3.97 |
| Exposed part | 65.60 \pm 8.38 | 47.50 \pm 7.45 | 17.83 \pm 6.91 |
| Outside of the range of exposure | 42.86 \pm 8.60 | 43.05 \pm 8.75 | -0.18 \pm 3.16 |

Data from Gurwitsch (1988)

Experiments were carried out in A.G. Gurwitsch's laboratories in Simferopol, Moscow and Leningrad (Gurwitsch 1936) under different temperature, light and seasonal conditions, with different varieties of onion. The total number of such experiments was about 300 (Gurwitsch and Gurwitsch 1948; Zalkind and Frank 1930), with Gurwitsch mentioning only two negative results obtained in his laboratory, which he attributed to extraneous causes (Gurwitsch 1926; Gurwitsch and Gurwitsch 1925). Similar experiments were repeated in other laboratories with positive (Reiter and Gabor 1928a; Siebert 1928b; Loos 1930) or negative results (Moissejewa 1929; Rossmann 1928; Taylor and Harvey 1931). For instance, Reiter and Gabor reported 125 successful experiments (Reiter and Gabor 1928b).

Also, using the onion technique, MGE of various higher plants was demonstrated: pea roots, sunflower, hyacinth, first leaves of sunflower, sunflower cotyledons, potato tubers and leptomes, yellow turnip mush, onion bottom plate, *Sedum* leaves, etc. (Zalkind 1934; Gurwitsch and Gurwitsch 1924, 1934b; Vasilyev 1925; Baron 1926; Borodin 1930; Gurwitsch 1923; Frank and Salkind 1926; Hollaender and

Schoeffel 1931; Loos 1930; Paul 1933; Rawin 1924; Reiter and Gabor 1931; Wagner 1927; Kisliak-Statkewitsch 1927).

Publications (Gurwitsch 1923, 1929a; Gurwitsch and Gurwitsch 1924, 1928; Reiter and Gabor 1928b) outlined the proven experimental methods, described various devices, fixtures and materials, providing photographs and detailed schemes (see Gurwitsch 1926, 1929a; Gurwitsch and Gurwitsch 1927).

Later a methodologically outstanding work on onion roots was published by M. Paul (1933) who analyzed the experiments of other researchers, took all the criticisms into account and suggested new approaches to exclude possible artifacts. In particular, she developed a method for unifying the individual phases of mitosis. Unfortunately, this methodological work has been mostly overlooked by later researchers.

20.2.2 Criticism

Among the studies which have not confirmed Gurwitsch's results, the most significant are the works of B. Rossmann

(1928, 1929), G.W. Taylor and E.N. Harvey (1931), B.P. Tokin (1933) and M.N. Moissejewa (1929, 1931a, b, 1932b), whose opinions were generally that all the positive MGE data were artifacts caused by asymmetric roots, defects in their processing or selecting data consistent with the authors' opinions.

In response to Rossmann's critique, Gurwitsch published more detailed procedures and much statistical material supporting his results (Gurwitsch 1927, 1928a, 1929b, 1968). Gurwitsch also noted that Rossmann did not adhere to his methodology and chose the radiating bioobject (a dicotyledonous plant, the pea) unsuccessfully.

M.N. Moiseeva repeated the basic onion experiment many times, adhering, according to her, to the original methodology in the smallest details (Moissejewa 1929, 1931a, b, 1932b, 1960). Her main conclusions were as follows:

- She was unable to obtain reproducible results.
- Mechanical action on one side of the root stimulated mitoses in its cells.
- Illumination of the roots during the experiment could have caused their phototropic curvature.
- The results of A.G. Gurwitsch et al., T. Reiter and D. Gabor she actually interpreted as deliberate falsification, suggesting that they chose the best roots for the experimental variants and the worst roots for the control, and counted dividing cells only in those microtome sections which corresponded to the expected results.

However, the author included in her critical analysis only those works which confirmed her opinion, neglecting the description of methodological approaches in the main methodical publications (Gurwitsch 1923, 1929a; Gurwitsch and Gurwitsch 1924, 1928; Reiter and Gabor 1928b).

In an influential work (Taylor and Harvey 1931), G.W. Taylor and E.N. Harvey reported surprisingly high heterogeneity and asymmetry of onion roots (up to 50%), which made them conclude that the onion root is unacceptable as an MGR detector, and the results of Gurwitsch's school are incorrect because of the lack of a separate negative control for each new experiment. However, the control root heterogeneity described in (Gurwitsch 1923, 1929a; Gurwitsch and Gurwitsch 1924, 1928, Reiter and Gabor 1928b and Paul 1933) was incomparably less and in most experiments did not exceed 10%, suggesting some gross methodological errors made by Taylor and Harvey (see statistical data in the next section).

Another strong criticism was expressed by B.P. Tokin (1933), who, however, referred in his summary not to the positive results of several hundred experiments of his collaborators mentioned in his own article, but to the above critical works of G.W. Taylor, E.N. Harvey and M.N. Moiseeva.

As these are all matters of the long bygone days, reconstructing all the nuances of experimental work is practically impossible, and one simply cannot get enough evidence to judge pro or contra most of the authors' conclusions. Yet, one can find contemporary data that can be compared to the early publications to make them more understandable and analyzable. For "onion experiments," this is done below.

20.2.3 Analysis of Methodical Details

In order to understand the correctness of the "classic onion test," we compared its technical details with its closest modern counterpart among biological tests – *Allium* test, which has been standardized and is actively used in practice today (Bonciu et al. 2018).

The *Allium* test was developed by A. Levan in 1938 (Levan 1938) and standardized in the 1980s–1990s by G. Fiskesjö (1985, 1993, 1997). Its general approach is quite similar to that proposed by A.G. Gurwitsch, although the methodology is much simpler. However, surprisingly, opinions of researchers (here we've analyzed more than 200 papers) regarding test staging, material incubation conditions, microscopy methodology and analysis of results still vary greatly.

20.2.3.1 Stages of the *Allium* Test and MGE Experiments

Among the stages that have been ignored by the researchers during the experiment setup and/or on which disagreement has been established are the following:

- The choice of onion variety (Loos 1930; Moissejewa 1932a; Borodin 1930)
- Seasonality (Gurwitsch 1923, 1924a, 1929a; Paul 1933; Moissejewa 1932a; Rahn 1936; Siebert 1928b; Puhalsky et al. 2013; Evseeva et al. 2005; Alotaibi and Barnawi 2018; Aslantürk 2019; Ferreira et al. 2020; Ozel et al. 2018; Özkara 2019; Rosculete et al. 2018; Wierzbicka and Antosiewicz 1988)
- Bulb size (Gurwitsch 1929a; Fiskesjö 1985, 1997)
- Onion germination medium (Gurwitsch 1929a; Loos 1930; Lopez-Saez et al. 1969)
- Root germination temperature (Gurwitsch 1929a; Loos 1930; Paul 1933);
- Illumination (Gurwitsch and Gurwitsch 1948; Gurwitsch 1929a; Ghosh et al. 2010; Ferrero and de la Torre 1986; Devnarayan et al. 2016; Özkara 2019; Tedesco and Laughinghouse 2012)
- Root selection for the experiment (Gurwitsch and Gurwitsch 1924, 1999; Loos 1930; Paul 1933; Wagner 1928; Gurwitsch 1929a, 1937; Fiskesjö 1995; Puhalsky et al. 2013);

- Experimental setup (Gurwitsch 1923, 1929a; Wagner 1928; Reiter and Gabor 1928b; Paul 1933)
- Distance from inductor to recipient (Gurwitsch 1923, 1925; Gurwitsch and Gurwitsch 1924)
- Localization of induction effect along the root (Gurwitsch 1922, 1924b; Reiter and Gabor 1928b; Wagner 1927, 1928); length of induction (Gurwitsch 1929a; Gurwitsch and Gurwitsch 1934b; Rusinoff 1925; Wagner 1928; Loos 1930)
- Duration of the effect development (Gurwitsch 1934b; Rahn 1936; Tuthill and Rahn 1933; Reiter and Gabor 1928b; Paul 1933)
- Root fixation time (Gurwitsch and Gurwitsch 1928, 1945, 1948; Gurwitsch 1929a; Rossmann 1929; Paul 1933; Reiter and Gabor 1928b; Evseeva et al. 2005; Pallavi et al. 2008)
- Root fixation and root staining (Gurwitsch 1929a; Gurwitsch and Gurwitsch 1925; Budantsev and Demyanov 2017)

In our opinion, the most important stages are microscopy and statistical analysis.

20.2.3.2 Mitosis Counting

The Gurwitsch-school researchers preferred longitudinal cuts to cross-sections, arguing that they enabled clearer differentiation of mitosis (Gurwitsch 1926, 1929a). The cuts were 10 µm thick, parallel to the direction of induction (Gurwitsch 1926, 1929a; Wassermann 1930).

The cross-sectional method was used by T. Reiter and D. Gabor (1928b). In the experiments of M. Paul (1933), both transverse and longitudinal slices showed the presence of MGE, but the author noted that longitudinal slices were preferable.

In most of the later experiments, Gurwitsch's collaborators limited themselves to counting the number of mitoses in 10 to 15 medial (central) slices (Gurwitsch 1928b). In the negative works, W. Schwarz (1928) and M.N. Moissejewa (1929, 1931b) counted peripheral zones of equal width on either side of the medial plane; N. Wagner (1928) and B. Rossmann (1928) counted all sections of the root.

It should be separately emphasized that mitoses-counting was given special attention in Gurwitsch's school (Gurwitsch 1929a). Each slice was always counted several times, with the average value taken as the result (Gurwitsch 1923, 1928b, 1929b). Moreover, each count was recalculated by another collaborator without knowing the results of the first.

20.2.3.3 Tissues

Concerning the mitosis distribution by the cytohistological zones of the root, information is conflicting. The highest percentage of dividing cells is found in dermatogen and

peripheral layers of periblem (Rostovtseva 1969; Remacle-Dath 1966), other data show the highest mitotic activity of pleroma (Lebedev et al. 1971; Utkina and Sinyagina 1976), or it is stated that there is no essential difference in the mitosis distribution by meristem zones (Savelkoul 1957).

Gurwitsch recommended counting mitotic cells from the root tip to the elongation zone and consider all layers of the growth cone, as there can be a lot of mistakes when visually distinguishing certain tissues (Gurwitsch 1929a). The main effect of induction was found on the dermatogen and subdermatogen and involved 3 to 4 cell layers of the periblem (Gurwitsch 1928b). M. Paul (1933) also performed counts in all tissues of the growth root apex, including calyptrogen and dermatogen, except for the cells of the root cap. In the negative works, the counting methodology differed: N. Wagner (1928) did not count mitoses in the plerome, and B. Rossmann (1928, 1929) ignored dermatogen, calyptrogen and root cap in counts.

20.2.3.4 Cell Cycle Phases

An important point in the methodology is the distinction between the cell cycle phases to be counted (Loos 1930). Here, the researchers' opinions also differed (Paul 1933). According to Gurwitsch's recommendations (Gurwitsch 1928b, 1929a, b), mitoses from the earliest prophase to the late telophase (Gurwitsch and Gurwitsch 1925) should be counted.

Rossmann (1928, 1929) criticized the counting of prophase, which is difficult to distinguish from interphase nuclei; nevertheless, in a number of experiments, he also obtained a dominance of cells with mitoses on the induced root side when counting the prophase as well.

A longer prophase duration in comparison with other phases of mitosis is evidenced in Batikyan and Simonyan (1970) and Stephens (1984). Thus, the effect of MGR on early prophase of mitosis, claimed by Gurwitsch, should really be analyzed first of all when counting nuclei in prophase and can be lost when excluding them from counting.

The methodology of Reiter and Gabor (1928b) differs considerably: they counted "mature nuclei" in addition to mitosis in the usual sense, and their counts cannot be compared with the results of other specialists (Paul 1933).

20.2.3.5 Statistics

The roots heterogeneity in terms of the number of mitoses, even within one bulb, is noted in works of A.G. Gurwitsch (Gurwitsch and Gurwitsch 1924, 1945), O. Rahn (1936) and others. Correspondingly, although statistical methods were poorly used in biology at the time, the authors recognized the need for statistical analysis of the results (see review of this issue in Belousov et al. (1997)).

An independent statistical analysis of all data from Gurwitsch's school by 1929 was performed in Schwemmler

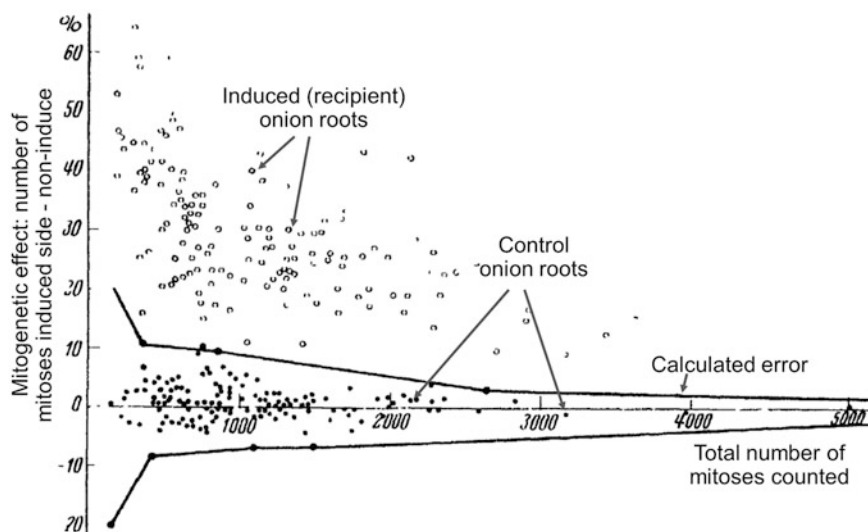


Fig. 20.3 The results of all publications by Gurwitsch's school dealing with MGE on onion roots by 1929. The filled circles are control roots; the hollow circles are recipients in MGE experiments. Each point is the result of one experiment. All control experiments fall within the area of

the calculated error; all induced roots fall outside this area. Thus, in all the experiments analyzed, the result is reliable. (Adapted from (Rahn 1936). Copyright 1936, with permission from SNCSC (data from (Schwemmle 1929)))

(1929) and showed their statistical significance (see Fig. 20.3). The author emphasized that while all control experiments reported by Gurwitsch lied within the calculated error limits (Fig. 20.3, black circles), all the induced roots lied outside these limits (Fig. 20.3, hollow circles) and judged that the results from Gurwitsch's school were reliable (see also tables of raw data in Rahn (1937)).

- Germinate under natural light conditions
- Use only large bulbs
- Select roots that are at least 6 cm long
- Use the described above mitosis counting method by Gurwitsch (i.e., possibly use longitudinal sections, calculate the mitoses numbers blindly and possibly recount them with the help of another worker)

20.2.4 Possibilities of "Upgrading" the Onion Technique to Improve Its Credibility

Based on the heterogeneity of onion roots, O. Rahn (1936) questioned whether it was generally correct to use them as biological detectors and suggested yeast and bacterial cultures as more reliable recipients (the latter had been invented and used by other authors earlier, see below).

However, as was later noted by the Allium test authors (Wierzbicka and Antosiewicz 1988), the described variability in the number of mitotic cells in the onion roots is typical for any biological organism and does not compromise specifically onion roots. Thus, careful analysis of the test material, an appropriate experimental procedure and statistical analysis of the results obtained allow the test to be used with a low risk of error.

We believe that the following recommendations for the "onion method" can be formulated:

- Work with a particular variety of onion by first finding out the maxima and minima of their daily mitotic activity

Of the above, a significant "white spot" is the knowledge of the daily periodicity of mitosis of specific onion varieties. We also assume that it is necessary to work out not only the time of fixation of material for cytological study, but also the time of putting bulbs to germination.

20.3 MGE on Yeast

20.3.1 Baron's and Gurwitsch's Methods

MGE on yeast cultures was first shown by M.A. Baron from Gurwitsch's lab, who used *Saccharomyces ellipsoideus* (Baron 1926) or *Nadsonia julvescence* (Baron 1930). Later they shifted to *Muscat* or *Chablis* wine yeast as more convenient (Gurwitsch and Gurwitsch 1934b, 1945), with no more data on yeast strains.

The inductor cultures were grown on rich media (undefined, mostly "beer wort") and had to be actively growing and budding, to produce reliable MGE in recipients (i.e., were in the exponential or linear growth phases).

20.3.1.1 Recipient Culture

The recipient cultures were grown on lean agar media, to have their budding and growth suppressed in control. In Baron (1926), this medium contained 1% glucose, 1% peptone, 1% Liebig's extract and 0.5% NaCl; in other works, it could be "diluted basic medium" and was often undefined.

The plated recipient culture was grown at mostly undefined temperature: in Baron (1926), it was either room temperature or thermostat, depending on the weather (temperature not mentioned); Gurwitsch used room temperature, casually mentioning 16 °C (Gurwitsch and Gurwitsch 1934b) or 15–20 °C (Gurwitsch and Gurwitsch 1945). He also recommended using suboptimal temperature to get a more confident MGE (Gurwitsch and Gurwitsch 1934b), like the above 15–20 °C for standard yeast strains.

The recipient cultures used for induction experiments were of the following age:

- From 9–12 to 15–20 h (Baron 1926)
- From 6–8 to 10–13 h at optimal temperature (Gurwitsch and Gurwitsch 1934b)
- From 10 to 15 h at summer time, and up to 20 h at 15–18 °C (Gurwitsch and Gurwitsch 1945)

From all these data, the culture real physiological state is quite difficult to assess. The authors usually had 15% to 30% budding in control and specially mentioned that it must be below 40%, in order to "have place" for further mitogenetic stimulation. The upper limit for the culture use as recipient (~15–20 h) was explained by its "aging," associated with losing buds and "vacuolization" (Baron 1926).

From all this, one can conclude that the recipient cultures were in growth suppression phase, after linear-growth, but before diauxic shift (see more on yeast physiology in Herman (2002) and Werner-Washburne et al. (1993)). Besides, the recipient growth was possibly suppressed by lean media and lower temperature.

Later (after O. Rahn's critique – see below) the inoculum culture pretreatment was also standardized (Gurwitsch and Gurwitsch 1945):

- The basic culture was maintained on agar slants with regular passaging every 2 weeks.
- For work, it was inoculated into "standard liquid growth medium," incubated for 1–2 days at 25–28 °C, replated onto "standard agar medium," and incubated for 1–2 days more at 25–28 °C.
- The above agar culture was used for plating the recipient cultures as above.

The standard growth medium used was "unhoped beer wort 15–20 ballings of sugar content."

The authors also tried using hanging drops of freshly-inoculated suspension cultures with the cell density $(8 - 10) \times 10^6$ cells/mL (Baron 1930), but the above yeast-agar method remained the main.

20.3.1.2 Induction

Obviously, the issue of paramount importance is the homogeneity of the recipient cultures – i.e., possibly minimal variation within and between control cultures. The authors paid great attention to it and achieved it as follows:

- A sample from the mother agar culture was thoroughly rubbed in sterile water, and the resulting suspension was poured onto the agar medium
- The excess suspension was carefully drained and aspirated, and the dish was left on a slope for 10–15 h of growth
- Agar blocks ~1 cm² were cut off this dish to be used as recipients or controls cultures, symmetrically about the vertical line, and avoiding the border area, to have them as identical as possible

The recipient blocks were set at the distance of ~10 mm from the inductor and separated with a quartz plate from it. The control blocks were set nearby, screened from the inductor, but with identical lighting conditions.

The lighting conditions are poorly defined, mostly mentioned as "scattered light," with the strictest absence of UV from any sources (no burners, open windows, etc.).

The induction length depended on the inductor and was usually not over 30 min (see Sect. 20.1.3).

After the end of induction, the recipient and control cultures were incubated for 1–2 h to get observable budding, and then spread on glass slides, fixed, stained and analyzed. Importantly, MGE was not observed at too short incubation (because there were no new buds to be counted), or at too long incubation (because by that time the control culture was catching up with the experimental one).

To get reliable results, 1000–2000 cells were counted from different parts of each sample (Baron 1926), with only buds smaller than 50% of the mother cell considered (Baron 1926).

All this gave the authors data with an error of no more than a few percent (Baron 1926).

This method was used in Baron (1926); Salkind and Schabad (1931); Blacher et al. (1932); Blacher and Holzmann (1930); Siebert (1928a, b, 1930); etc. (see also (Gurwitsch and Gurwitsch 1934b, 1945)).

20.3.2 Tuthill–Rahn’s Method

20.3.2.1 General

Obviously, the above method was far from perfect. The authors seemingly didn’t know the basics of yeast physiology and had to investigate it with trials and errors, thus being unable to explain the true necessary conditions for MGE. This made the method hardly standardizable among labs and prone to different mistakes (see also critique in Rahn (1936)).

The yeast method was best optimized by O. Rahn’s group (Tuthill and Rahn 1933, 1934).

The authors used *Burgundy yeast* and began with obtaining the culture control growth and budding curves (see Fig. 20.4), and their temperature dependence. Importantly, increasing the temperature from 20 to 30 °C lengthened the cell generation time from 62 to 156 min, thus prolonging the entire growth and budding kinetics by a factor of 2.5 (Tuthill and Rahn 1933) (this clearly shows how wrong it is to give such vague characteristics as “room temperature”).

20.3.2.2 Recipient Culture

Contrary to the above Baron–Gurwitsch’s method, the authors showed, that the recipient cultures were best to use in their lag-phase, when they had no buds in control, and “had time” to manifest MGE if stimulated by external inductors. For recipient cultures plated from standard inoculum (see below), this was only within the first 30 min after seeding (older cultures, e.g., 60 min after seeding, were no longer

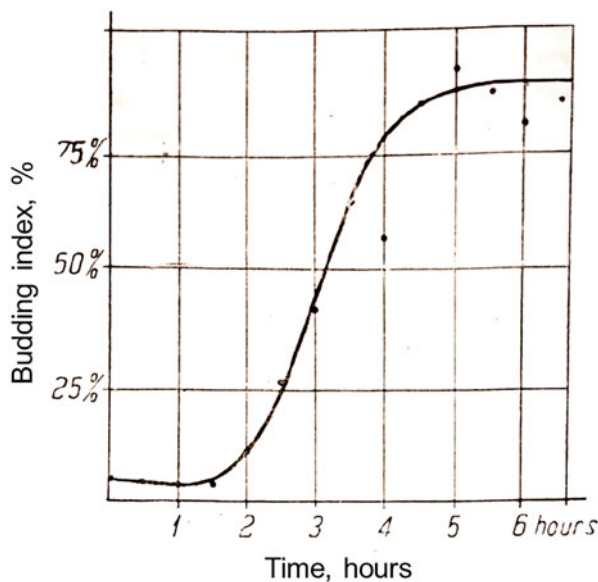


Fig. 20.4 Budding index (% of budding cells; all buds counted) of the *S. ellipsoideus* culture at 30 °C. (Reprinted from (Tuthill and Rahn 1934))

efficient). As the recipient cultures were freshly inoculated, there was no need to lean the medium or lower the temperature for budding suppression. Thus, they were inoculated on the standard “raisin agar” and incubated at 30 °C.

The inoculum culture state was also highly standard. For the best reproducible results, a 24-h suspension culture (grown in the “raisin extract” medium at 30 °C – see (Rahn 1936) for details) was plated onto “raisin agar” and incubated for 24 h at 30 °C. This culture was used for the recipient inoculation as follows: it was washed off the agar with 5 mL sterile water (which gave $\sim 5 \times 10^6$ cells/mL), diluted to 5×10^4 cells/mL, poured onto fresh agar and drained off it (the pretreatment, later copied in Gurwitsch and Gurwitsch (1945) – see above). This approach also made the recipient cultures quite thin and thus diminished possible mutual influence of the cells within the recipient (or control cultures).

The important point here was using the inoculum culture with no budding, but yet not too old (i.e., not too deep in the postdiauxic, or even stationary phase). Liquid cultures of the same age still had a lot of buds and remained them for several days; thus, the recipients plated from them were already budding and had very little opportunity for additional stimulation. Younger agar cultures, or agar cultures grown on less rich media (e.g., Saburo), also had buds and thus showed indistinct MGE at stimulation. On the contrary, if the inoculum culture was physiologically older (e.g., 6-day-old on raisin agar), the lag period after its plating was longer, and the recipient culture was able to start budding only after several hours. Thus, it could either be stimulated 2 h after seeding, or stimulated at once, but left for 2 more hours after induction. Both approaches worked, but were less efficient than the above standard procedure.

20.3.2.3 Induction

For the above standard recipients, it’s optimal to start the induction within 0–30 min after seeding.

The inductors used were 6-h-old agar yeast cultures on raisin agar at 30 °C (exponential growth phase or beginning of linear growth), for which the optimal induction duration was 30 min.

Besides, as there was no budding before induction, all buds were counted, which was easier and less subjective.

After all this optimization, the authors got highly reproducible results, while before that, when strictly following Baron’s recommendations, the results were variable, and the MGE was inconsistent.

In accordance with their experience, the authors specially emphasized the following recommendations:

1. Get the culture growth and budding dynamics before starting the mitogenetic experiments;

2. Start with several independent experiments, inducing the recipient cultures at different ages, to finally select its most sensitive stage. “No reliably positive results can be expected unless the stage of greatest sensitivity has been determined first” (Tuthill and Rahn 1934).

Suspension cultures could also be used as recipients, but only **in very thin layers** (less than 0.6 mm), and plated from the inoculum cultures as above (see more in Rahn (1936)).

20.3.3 Critical and Unsuccessful Works

20.3.3.1 Taylor

A well-known work from Taylor (Richards and Taylor 1932) performed on yeast was done very carefully, but missed a lot of important methodical details, outlined above (see review in Volodyaev and Belousov (2015); our comments are in italics):

1. Suspension cultures were used, with no data on their physiological state (which, according to their experimental tables, was exponential phase).
As said above, MGE is observed only in “aging” (postdiauxic) cultures, or lag-phase cultures inoculated from them. The authors quoted this statement, but preferred to violate it.
2. The medium was optimal for yeast growth, and the temperature was 28 °C.
This is Ok for the lag-phase cultures as in the Tuthill–Rahn method, but totally inapplicable for growing cultures as used by the authors. For such cultures, the only possibility of getting MGE (if any) is to suppress control budding by other means: reduced temperature, poor media, etc.
3. The recipient was put in flasks of 1.5–2 mL, and the flasks were fixed in a big container with the inductor suspension.
MGE on suspension cultures is observed only in very thin recipient layers (Wolff and Ras1933b; Ferguson and Rahn1933).
4. The induction lasted 2–24 h.
Yeast cultures show good MGE only at induction less than 2 h; longer induction gives suppression.
5. The culture density was measured right after the induction.
The induction could affect the culture density no earlier than 1–2 h after its end.
6. Nothing is said about the quartz quality.

Thus, it was impossible to observe MGE in this work for several reasons at once.

Another influential work by this group (Taylor and Harvey 1931) was devoted to physical detection of mitogenetic radiation. The authors used photographic plates and obtained no results. This is also natural, as photographic plates are inappropriate tools to detect UPE (see more in Chap. 21).

20.3.3.2 Quickenden

In the 1970s–1990s, a serious set of works connected to MGE was published by Quickenden et al. The authors detected significant photon emission from growing yeast cultures, in both visible and UV spectral range (see Chap. 21), but couldn’t obtain biological MGE (Quickenden and Tilbury 1985). Here we summarize their technical details (review from (Volodyaev and Belousov 2015); our comments are in italics):

1. They used diploid laboratory strains of *S. cerevisiae*.
2. The inductor culture was in exponential phase.
3. The recipient culture was (1) in stationary (G_0) phase (10 days-old in a rich growth medium at 28 °C and oxygen saturation) or (2) in lag-phase – just after seeding the former (G_0) culture in fresh medium.
As shown above, MGE was not observed in too old cultures. The recipient culture should be plated from a culture close to the diauxic shift, while too old cultures are either insensitive to MGE or have to be carefully investigated for the sensitivity period.
4. The cultures used were (1) suspension, (2) bubbled with oxygen and (3) at 28 °C.
As discussed above (and clearly shown by two independent groups (Wolff and Ras1933b; Ferguson and Rahn1933)), suspension cultures are applicable as recipients only in very thin layers (<0.5–0.6 mm). We do not know the exact reasons for that – MGRabsorption in the suspension, difference in aeration or other physiological conditions, and whether they can be overcome, but anyway the experiment should start from the proven methods, and only optimize later.
5. The induction was performed in “test tubes” of 10 mL volume.
MGE in suspension cultures is observed only in very thin layers.
6. The induction started immediately after inoculating the recipient in a fresh medium. Alternatively, the inoculum culture was induced right before inoculating it into fresh medium.
The receptivity window is one of the principal parameters for MGE and should be specially investigated for the culture used. As shown by Rahn’s group (e.g., Ferguson and Rahn1933), the older the inoculum culture, the later

the induction should start (see above). The true stationary-phase cultures were not used by the authors, and one cannot judge if they are applicable for MGE observation at all. But even if they are, approximation of Rahn's data gives an estimate of the receptivity window >2 h after inoculation.

7. The only time of induction tried here was 30 min.

It should be optimized at least in the diapason 1–120 min for any new conditions.

Thus, the conditions used in these works were not optimized, many of them had not been tried before, and some of them directly contradicted the recommendations in the successful “early works.”

20.3.3.3 Our Mistakes

20.3.3.3.1 The Experimental Setup

Years ago, one of us (IV), who was fortunate enough to be a pupil of the late Lev Belousov, attempted to repeat Gurwitsch's basic MGE experiment on yeast cultures.

We used yeast diploid wine strain, grown in a standard YPD⁴ culture medium on a rotary shaker or on a YPD-agar at 30 °C. The culture reached the growth suppression phase (diauxic shift) in ~15 h (see Fig. 20.5) and was used to inoculate the recipient cultures in the age of 18, 24 and 36 h – in accordance with Tuthill–Rahn's recommendations (see above).

In accordance with observations in Tuthill and Rahn (1934) and Rahn (1936), in the end of active growth (i.e., around diauxic shift), cultures on agar medium were losing buds faster and more synchronously than suspension cultures, and thus allowed to inoculate recipient cultures with practically zero initial budding, obtaining a true lag-phase. This was especially important (and recommended by both Rahn and Wolf) so that the MGE was definite and easily observable.

The recipient cultures were freshly inoculated on different agar media – starting from the standard YPD, and coming down to extremely poor media, like this: CH₃COONa 0.1% + KH₂PO₄ 0.1% + MgSO₄ 0.05% + CaCl₂ 0.01% + NaCl 0.01%, pH 5.5 (the main tested media can be seen in Volodyaev et al. (2013)). To get the recipient culture as homogenous as possible, we washed the inoculum (agar) culture off its dish with still water, thoroughly suspended it (to a specific suspension density), poured onto a Petri dish with the recipient agar media, left for a certain (preselected) time, exactly determining the recipient culture density, carefully withdrew the suspension excess and gently dried the

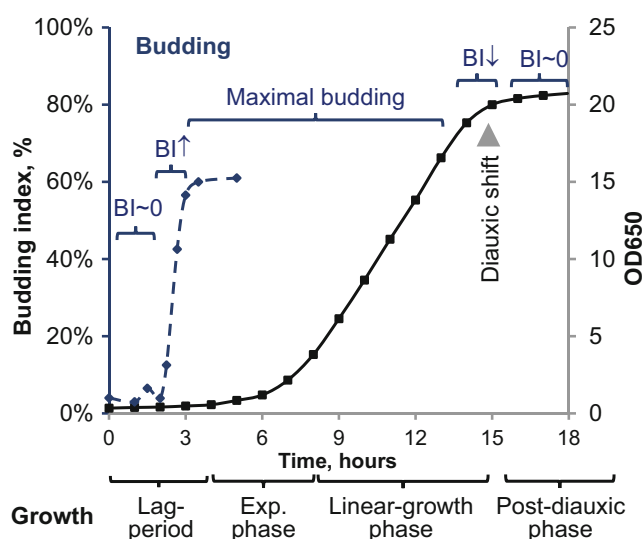


Fig. 20.5 *S. cerevisiae* growth and budding dynamics on YPD-agar medium (glucose 2% + yeast extract 2% + bactopectone 1% + agar 3%). BI – budding index (total number of buds divided by the total number of cells counted, in %). The culture density was assessed by optical density at 650 nm of a thoroughly suspended triple wash from the entire standard dish. (Adapted from (Volodyaev et al. 2013), under Creative Commons license. Copyright 2013, Volodyaev et al.)

dish. We tried various recipient culture densities, as well as various media.

The inductor cultures were in linear growth-phase on YPD-agar (8–10 h old), corresponding to Gurwitsch's recommendations.

The induction was performed at various culture ages, with various duration, the inductor and recipient dishes being (initially) separated with a quartz plate, to exclude chemical interactions (see Fig. 20.6a). The control cultures were identical to recipients in all respects except the (supposed) optical contact with the inductor. After the end of induction, we sampled the recipient and control cultures every 15–30 min, thus obtaining their budding dynamics (see Fig. 20.6b; growth dynamics was also observed, but later, in separate experiments – because it required many identically inoculated and handled dishes with recipient cultures, to assess the total number of cells at each time point by a total flush of one of them).

As is obvious to the reader, we were looking for a set of conditions under which budding and/or growth of the recipient culture would confidently differ from the control. During the first year, we got erratic results: differences between the control and induced cultures were sometimes there and sometimes not, and we kept going through all the possible conditions.

Among our doubts were how good the quartz was and whether its fogging during the induction (which always took place) would interfere with the experiment. We tried several options to combat fogging: slits in the sides of the Petri

⁴YPD medium composition: glucose 2% + yeast extract 2% + bactopectone 1%.

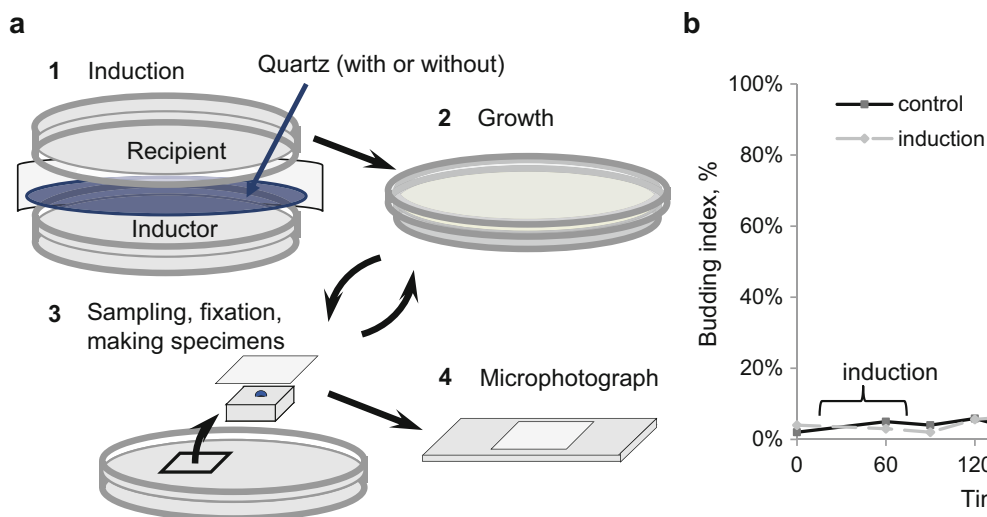


Fig. 20.6 The induction experiment scheme (a) and its results in terms of the culture budding (b). The recipient culture medium in (b) is the above-mentioned CH_3COONa 0.1% + KH_2PO_4 0.1% + MgSO_4 0.05% + CaCl_2 0.01% + NaCl 0.01%, pH 5.5; the induction duration

is 60 min (shown at the plot). The inductor–recipient distance is 10 mm. (Adapted from (Volodyaev et al. 2013), under Creative Commons license. Copyright 2013, Volodyaev et al.)

dishes, side blowing by a fan during induction and predrying the experimental cultures, but none of them led to distinct results. So, we decided to remove the quartz plates for the first time in order to optimize other conditions: medium composition, the cultures growth phase, duration of induction, etc.

Soon after that, a definite MGE was found on 10 times deluded YPD medium (which corresponded to Gurwitsch’s recommendations to work on poor media). Later we lost this effect as well. Finally, a clear reliable difference between the induced and the control cultures, both in terms of budding and growth dynamics, was found on extremely poor media, incompatible with the life of the culture in the long term (see Fig. 20.6b). Though this was quite different from the conditions, ever mentioned before, we continued this line of research and soon got a lot of information on the optimal induction length, start, inoculum cultures, etc. (see (Volodyaev et al. 2013)).

20.3.3.3.2 The Mechanism

Unexpectedly, further research showed that the observed stimulation effect was caused not by radiation, but by carbon dioxide released by the inductor and stimulating the recipient culture, presumably via some signaling paths (Volodyaev et al. 2013).

Why have we not succeeded in getting the real mitogenetic effect? Does this prove that the MGE does not exist?

Although any author of an unsuccessful work is inclined to draw such conclusions, we must give an absolutely different interpretation. Now, after having found and studied much more literature on the topic than at that time, we can draw

several important deviations from the methodology recommended in successful publications:

1. We used extremely poor media, never used before. Though poor media were recommended in several works from the Soviet school as facilitating MGE (see Gurwitsch and Gurwitsch 1934b; Rahn 1934a, b), (1) these media were never as poor as we used, and (2) this approach was tested on cultures of different physiological state (see Sect. 20.3.1 and compare it to Sect. 20.3.2, where lag-phase cultures were used). Thus, the culture state allowed its stimulation by external CO_2 (which we observed), but appeared too weak to react to mitogenetic stimuli (if there were any).
2. Though preliminarily we tested different culture densities and induction duration, our main accent was search for the media that would allow observing MGE. So, in the end neither of these parameters were really optimized.
3. The light conditions were also nonoptimized, though they had been mentioned as important in the early works.
4. The quartz fogging and quartz quality issue was not solved in our experiment. As this is a primarily important step in testing the MGE *per se*, this was a crucial mistake in our work.
5. After obtaining the stimulation effect (which appeared caused by CO_2), we concentrated on investigating it. Thus, if any of the above parameters hindered MGE, we never got the chance to optimize them.

Altogether, we consider our history a good example of diligent research, lacking enough preliminary information on MGE methods, which can and should be studied before any

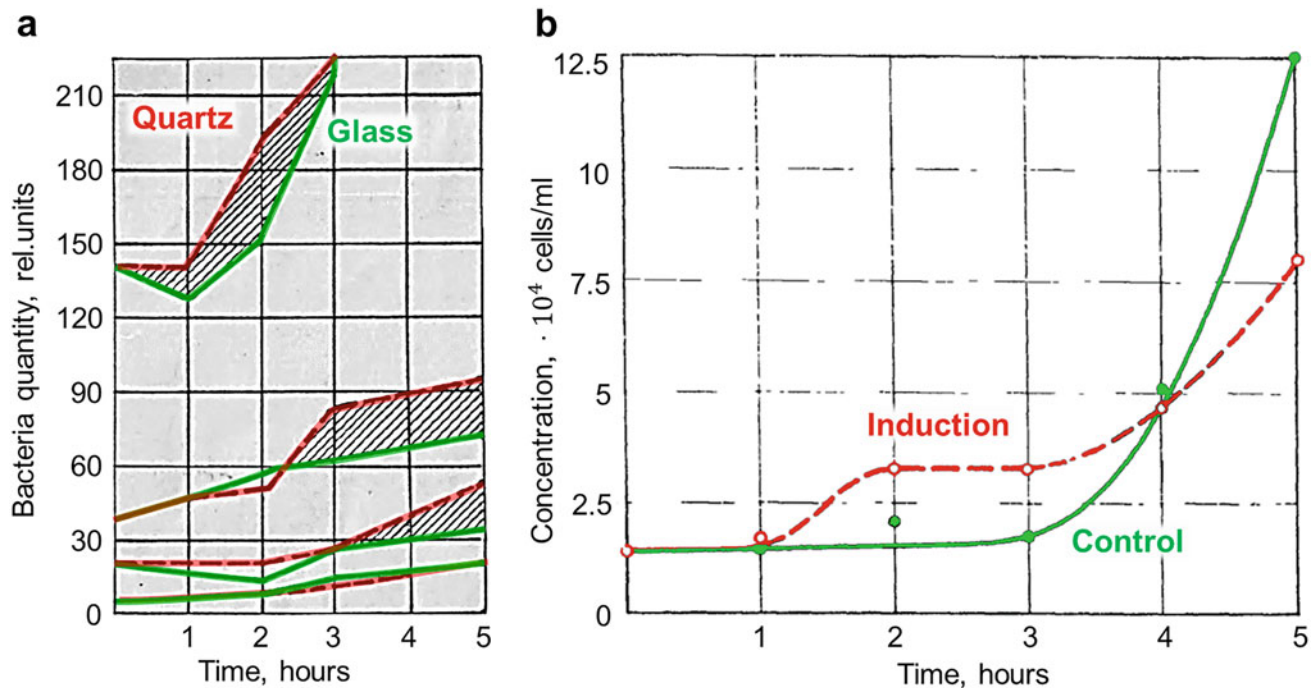


Fig. 20.7 *Staphylococcus* growth curves at mitogenetic induction through quartz or glass (control). (a) – Induction of recipient cultures with different initial density through quartz and glass plates; induction duration is not given directly, but from the authors’ description it looks like constant induction starting from 0 h. (Adapted from Wolff and Ras

1931a); (b) – Constant induction of a recipient culture. Note growth stimulation at 2- and 3-h points and growth suppression at longer times. (Adapted from (Rahn 1936). Copyright 1936, with permission from SNCSC)

experimental work. For the sake of possible attempts of other interested researchers, we have summed up our present knowledge on these issues in this part of the book, as well as in Volodyaev and Belousov (2015); Naumova et al. (2018); Volodyaev et al. (2021) and Naumova et al. (2021).

20.4 MGE on Bacterial Cultures

20.4.1 Wolf’s and Rahn’s Methods

The general logic of getting an observable effect on bacteria repeats that for yeast cultures (see above):

- The recipient culture must be in the lag phase and inoculated from a mother culture in prestationary phase (after the active growth has finished, but before it gets into the quiescent state)
- If the recipient culture is liquid, it should be prepared in very thin layers and in lean media (usually, standard broth diluted 10 times)
- The inductor culture must be in the active growth phase
- The induction duration must be adopted anew for each new set of conditions. Too short induction gives no effect; too long induction leads to suppression

Wolf and Ras used suspension *Staphylococcus* cultures as the recipient (Wolff 1932); Fergusson and Rahn used *E. coli* (Ferguson and Rahn 1933). MGE was detected as a change in the culture growth kinetics (see Fig. 20.7).

To get observable effect, the recipient culture had to be freshly-inoculated (in the **lag-phase**) (Wolff 1932; Wolff and Ras 1932a). Alternatively, the recipient **inoculum culture** can be subjected to induction and further diluted in the fresh medium (usually 1 : 10⁴); the effect is observed as a change in the diluted culture growth (Ferguson and Rahn 1933).

The optimal recipient inoculum culture age depends on the species. For *Staphylococcus*, the optimal age was 12 h; 48-h cultures showed no effect (Wolff 1932). For *E. coli*, the optimal age was 48 h, while 24-h cultures didn’t respond (Rahn 1936).

MGE was observed only on recipient cultures prepared **in lean media** (standard broth diluted 1:10 with water) and **in very thin layers** (<0.6 mm) (Wolff and Ras 1931b; Wolff 1932). Using layers 1 mm and thicker gave no effect; a standard medium for the recipient culture gave no effect even in 0.6 mm layers; a **1:10 diluted medium** in 0.6 mm layers gave reliable MGE (Ferguson and Rahn 1933).

The effect depended on the recipient culture initial density and had to be observed in dynamics not to miss it (see Fig. 20.7a).

The inductor culture gave reliable induction only during active growth (4–18 h for *Staphylococcus* (Wolff and Ras 1932a)), while older cultures gave no effect (Wolff and Ras 1932a).

The optimal induction duration depended on the inductor and its distance to the recipient. Importantly, too long induction led to MGE disappearance and even growth suppression (see Fig. 20.7b).

See a more detailed summary of the methods in Rahn (1936).

20.4.2 Critical Works

One of the most important critical works for the whole topic of MGE is a stunningly thorough research by Hollaender and Claus (1937), published as an almost 100-page manuscript with a lot of tables and scrupulous details. The first impression this work gives to the reader is that the authors have come to the final judgement on the issue, their negative conclusions being the last word on the matter.

However, a detailed review of their work gives quite a different conclusion. Here we summarize their methodical details, with our comments given in italics (see also (Volodyaev and Belousov 2015)):

1. The cultures used were *E. coli* and *Serratia marcescens*, grown on agar media, but the induction and further growth were performed in suspensions.
2. The experiment was set as follows: agar cultures 15–19 h old (they later shifted to cultures 39 h old) were washed off the agar with an inorganic salt solution (NaCl, KCl, CaCl₂ and water), immediately exposed to the inductor, diluted in the culture medium and incubated at 32 °C. Samples were taken from the exposed culture after repeated rapid twirling.
 - *As mentioned above, the inoculum culture age should be optimized anew for any new conditions, starting with its growth curve (which is not given here). Rahn, working with E. coli, found it sensitive to MGE only after 48 h (Rahn 1936).*
 - *The salt solution used as the culture medium during the exposure time had never been tried in mitogenetic research before; thus, no one knew if MGE could be observed in such media at all (here the authors' mistake is exactly the same as the one we later made in our own research – see Sect. 20.3.3.3).*
 - *Recipient cultures have certain periods of sensitivity to the induction. For example, 24-h yeast cultures are sensitive immediately after plating on the new medium, and 6-day cultures – 2 h later (Tuthill and Rahn 1933). No MGE can be seen if the recipient is induced outside this period. Here this was not checked.*

3. Induction was performed in small cups 2 cm in diameter and 1–2 cm high at 37 °C, with constant stirring of the recipient. The induction lasted from 5 s to 12 min.

- *As emphasized by Rahn's and Wolf's groups, the suspension cultures should be induced in very thin layers (<0.6 mm). No effect can be obtained in thicker suspensions.*
- *“Constant stirring” and “rapid twirling” of the recipient culture are very specific conditions. No other worker ever tried MGE under them. The authors argued that this condition mimicked the “interrupted induction” through rotating discs with cut-off slits, that Gurwitsch had proposed as a way to enhance the effect. While the latter assumption is questionable in itself (see more on this issue in Sect. 20.1.3), the authors' suggestion to simulate rotating discs with the culture constant stirring looks like complete nonsense.*
- *Since the conditions were unknown, the induction length should have been tried at least up to 2 h. In successful works, it was always carefully optimized.*

4. The recipient cultures had concentration mostly $1.5\text{--}2 \times 10^5$ cells/mL.

In Wolff and Ras (1933a), it was 2×10^4 cells/mL; in Ferguson and Rahn (1933), the recipient culture was diluted to 50–5000 cells/mL; no effect was obtained on more dense cultures.

5. The work was done under very low light: “in a room without windows . . . [with] a 25-watt globe, contained in a dark green or dark brown bottle” (Hollaender and Claus 1937).

Though this is a good standardization of light conditions (contrary to very vogue description in Gurwitsch's works), it may appear suboptimal, which should be checked at the beginning. In most successful works, it was definitely lighter in the room, with only specific precautions against artificial UV.

Altogether, the authors took a lot of thorough precautions (sometimes doubtful – like, e.g., electrical grounding of the dishes and themselves – see (Hollaender and Claus 1937)), but didn't optimize the conditions of primary importance: the culture age, the induction start and duration, the medium content, the light conditions. Moreover, a number of conditions were definitely against previous recommendations: the recipient layer thickness, the induction duration, the “culture stirring” in course of the induction.

Thus, unfortunately, this laborious meticulous work does not bring any clarity to the question of the existence of the effect.

20.5 MGE on Animal Tissues and Their Cultures

In this subsection, we briefly overview some MGE recipients of animal origin (corneal epithelium, tissue cultures, cancer tissues and embryos). These recipients were much less popular in comparison with yeast, bacteria and onion roots.

20.5.1 Corneal Epithelium

As far as we know, the first report on MGE in animal tissues belongs to L.D. Gurwitsch and A.W. Anikin (1928). They demonstrated MGE in corneal epithelium of mammals (rat) and amphibians (frog and triton) induced by MGR from yeast cultures, and by artificial UV sources (spectral line 203 nm from spark discharge – see more in Sect. 20.6).

For the induction, the authors used either intact eyes of an alive frog, or, alternatively, enucleated eyes ~30 min after the operation; freshly derived eyes were unsuitable for obtaining MGE (Ponomareva 1936; Gurwitsch and Gurwitsch 1999). Interestingly, a similar picture was reported for their induction ability: MGE in yeast cultures could be induced by intact eyes of healthy animals, or by eyes removed from the body, 30 min after the operation (Ponomareva 1936).

A prominent advantage of corneal epithelium as a recipient was a paired well-matched control for each experiment, ensured by little difference in the number of mitoses between the eyes of one animal (Kornfeld 1922). In mitogenetic experiments, such between-eyes variation was first assessed as <12% (Gurwitsch and Anikin 1928) and later refined to 5% to 6%, at decreased temperature (Gurwitsch and Gurwitsch 1945).

This was criticized by A. Hollaender, H. Gay and B. Kauffman, who reported a higher between-eyes difference in control and challenged positive MGE-results (Kaufmann et al. 1944). However, the majority of cases reported by them were still within the 12% deviation stated in Gurwitsch and Anikin (1928), with only rare large outliers that could be explained by some asymmetric abnormalities of particular animals and lack of standardization.

The authors also pointed out that mitoses were distributed highly heterogeneously within an eye: their number was maximal in the corneal center and decreased to periphery by several times (Kaufmann et al. 1944). Thus, an identical position of studied samples from two eyes was crucial to get an honest comparison.

At the same time, several hundred experiments by J.N. Ponomareva (1934, 1936, 1939; Salkind and Ponomareva 1934; Ponomareva 1947) and extensive work of A. Naville (1929, 1937) suggested corneal epithelium as an efficient recipient in mitogenetic experiments. A.G. and L.D. Gurwitsch also mentioned a communication by Dr. Mai

from a Munich clinic, who reported even higher MGE on corneal epithelium than in their own works (Gurwitsch and Gurwitsch 1935).

Corneal epithelium was surely far from the best recipient: first of all, for ethical reasons; second, because it was very labor-intensive and required long working experience. Even a specialist with many years of expertise was treating one pair of eyes for a complete working day (Gurwitsch and Gurwitsch 1945).

One should also point out that even assuming the highest correlation of mitoses between two eyes of one animal (which seems too optimistic), it was impossible to level significant variability of animals to optimize properly the induction parameters (exposure time, development period etc.). For instance, MGE was reported to be more stable in tritons and rats and quite high but too variable in frogs (Gurwitsch and Anikin 1928; Gurwitsch and Gurwitsch 1935). Thus, the induction conditions, which led to stimulation of mitoses (positive MGE) in one frog, could result in depression (i.e., negative MGE) in the others.

20.5.2 Animal Tissue Cultures In Vitro

The first MGE observation on tissue cultures in vitro was reported in 1928 by H. Guillery (1928), without the knowledge of Gurwitsch's works. The author showed a (supposedly) optical interaction between cell cultures from heart of different age chicken embryos. Namely, if there were two or three cell cultures with different growth rate in the same dish, the fastest-growing culture stimulated growth of the others (see Fig. 20.8). The effect disappeared, if they were screened with glass, even without any chemical isolation; moreover, the effect was obviously propagating in a straight line (Guillery 1928) and was "shaded" by glass plates if they were installed. Thus, the author concluded that it was caused by some kind of radiation.

An important series of works was performed by G.K. Khrushov on cell cultures isolated from different animal tissues (Chrustschoff 1930; Khrushov 1934). The author showed their MGE-inducing ability, but appearing many hours after transplantation: 60 h for salamander spleen culture and 12 h for chicken embryo heart fibroblast culture (Chrustschoff 1930).

He also performed an accurate series of works with chicken fibroblast culture used as MGR recipient (Khrushov 1934), which was marked as methodically high-quality even by the most severe critique of MGE, M.N. Moissejewa (1960). The author divided the culture into two or four identical pieces, the induced and control pieces always taken from the same culture; placed them in hanging drops under a single thin quartz plate; and assembled water-tight cameras on top of this quartz plate, with the inductor placed

Fig. 20.8 Daily growth increments of three chicken embryo cultures, grown separately for the first 8 days, and assembled in a single dish with direct optical contact after that (an example of experimental data from Guillery (1928)). (Adapted from (Rahn 1936). Copyright 1936, with permission from SNCSC)

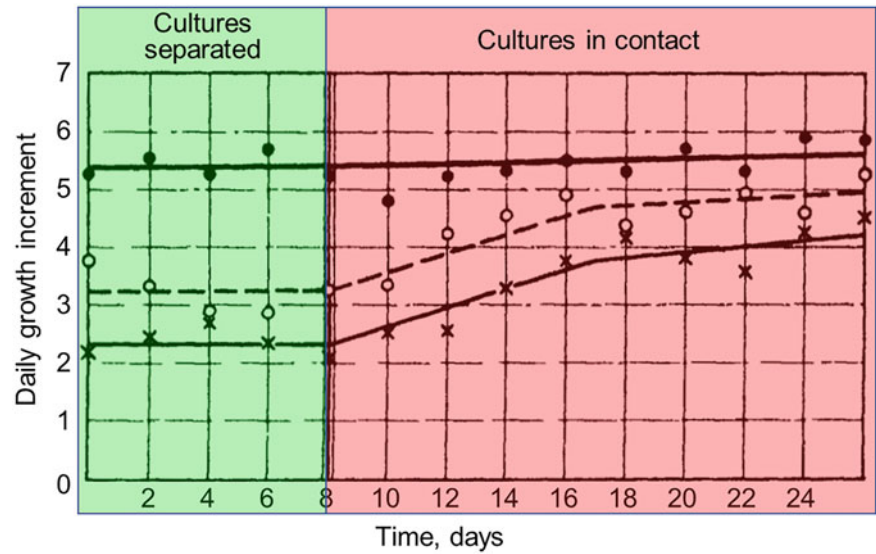
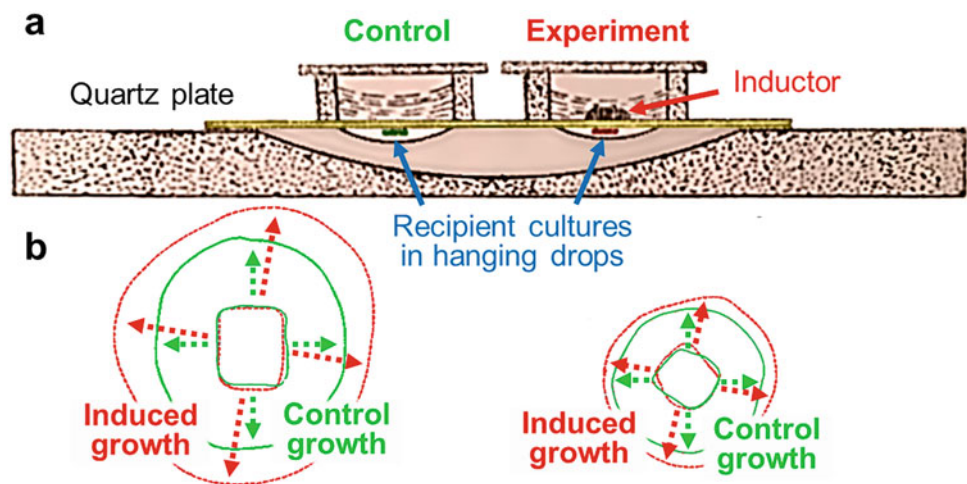


Fig. 20.9 Scheme of the experiment from Khrushchov (1934) (a) and examples of his results: the recipient and control culture growth assessed by planimetric method (b). Inductor – beating chicken hearts (replaced with new ones when stopped beating); recipient – chicken fibroblast culture; induction duration – 48 h, further culture growth – 24 h. (Reprinted from Khrushchov 1934)



above the experimental hanging drop and pure medium placed above the control culture (see Fig. 20.9a).

The inductors were beating chicken hearts, replaced with fresh ones when necessary. The induction lasted 48 h, after which the cultures were incubated for 24 h more to obtain a confident effect. The recipient and control growth were characterized with the so-called planimetric method, well developed by that time for characterization of pure culture growth (see Fig. 20.9b and Table 20.3).

A similar approach was used in Julius (1935). The recipient was chicken fibroblast culture; the inductor was *Staphylococcus* culture; the induction was performed through a quartz plate, with the culture growth assessed by planimetric method as above. The authors also compared induction through quartz with the one through glass, as well as with

the appropriate controls with empty cameras instead of the inductor. No difference was obtained through glass, and a distinct effect similar to the above was shown through quartz, which allowed the authors to suggest that the stimulation effect was caused by ultraweak UV, similarly to Gurwitsch's experiments.

In Zakrzewski (1933), chicken osteoblast cultures (recipient) were exposed to onion sole pulp (inductor), but unlike the above works, the author didn't separate them chemically. However, he tried to level the possible influence of volatile substances from the inductor by placing control and recipient cultures in the same Petri dish. The between-culture deviation in control was 10%, while the induced cultures gave an average excessive growth of 33.4%, supposing a nonchemical influence from the inductor.

Table 20.3 Data from Khrushov (1934)

| Experiment no. | Culture size after 72 h growth, rel.un. | | Effect, % |
|----------------|---|-----------|-----------|
| | Control | Induction | |
| 1 | 35.4 | 53.7 | +51.7 |
| 2 | 31.6 | 52.1 | +64.8 |
| 3 | 28.3 | 41.2 | +45.5 |
| 4 | 36.2 | 49.7 | +37.3 |
| 5 | 27.7 | 42.3 | +52.5 |
| 6 | 28.8 | 43.5 | +51.0 |
| 7 | 38.0 | 37.2 | -2.1 |
| 8 | 30.7 | 50.3 | +63.8 |
| 9 | 38.0 | 54.3 | +43.0 |
| 10 | 27.9 | 38.2 | +37.0 |
| 11 | 26.7 | 39.1 | +46.4 |
| 12 | 24.8 | 32.2 | +29.8 |
| 13 | 22.0 | 34.4 | +56.4 |
| 14 | 22.4 | 20.9 | -6.7 |
| 15 | 32.8 | 49.8 | +51.8 |
| 16 | 20.6 | 30.3 | +47.0 |
| 17 | 37.0 | 40.2 | +8.6 |
| 18 | 36.2 | 50.2 | +38.6 |
| 19 | 34.2 | 39.8 | +16.3 |
| 20 | 32.2 | 41.0 | +27.3 |
| 21 | 34.6 | 36.8 | +6.0 |
| 22 | 32.7 | 51.4 | +57.2 |
| 23 | 27.0 | 39.6 | +46.6 |
| 24 | 32.3 | 39.2 | +21.3 |
| 25 | 32.5 | 38.2 | +17.0 |
| 26 | 34.2 | 40.8 | +19.5 |
| Average | | | +36.5 |

Inductor – beating chicken hearts (replaced with new ones when stopped beating); recipient – chicken fibroblast culture; induction duration – 48 h, further culture growth – 24 h

At the same time, there were a number of unsuccessful attempts to obtain MGE on animal tissue cultures: e.g., (Lasnitzki and Klee-Rawidowicz 1931; Doljanski 1932). Both groups used fibroblast chicken cultures as recipients (plus osteoblast cultures in Doljanski (1932)), and various inductors, repeating the above successful works. Yet, they seemingly violated the recommended recipient media conditions (Khrushov 1934). In Lasnitzki and Klee-Rawidowicz (1931), the medium was too nourishing and provided too favorable conditions for cell division (as mentioned above, suboptimal conditions of recipient were one of crucial requirements to get MGE). In Doljanski (1932), the nutrient medium was too lean for cells to undergo mitosis at all and contained heparin, which may have played an inhibitory role as well (Zakrzewski 1933).

Altogether, one may conclude that MGE could be obtained on animal tissue cultures, but the small number of works on these objects didn't allow to deduce an optimal protocol of the experiment. However, the above-formulated general principles (see Sect. 20.1) are likely to apply here as well.

20.5.3 Tumor Tissues

Tumor tissues were tested as MGE recipients in very few works (e.g., (Ponomareva 1939); see also data reviewed in Gurwitsch (1968)). Overall, they were good inductors, but no recipients (Gurwitsch and Gurwitsch 1934a; Gurwitsch et al. 1947), which is quite understandable for general reasons (see Sect. 20.1).

However, interestingly, metastases in the body of a dead animal became sensitive to external MGR ~1/2 h after the animal death (Ponomareva 1939) (see Table 20.4). Here, the recipient and control objects were two halves of the same metastasis obtained from liver, diaphragm or spleen. At the same time, any two halves of a noninduced metastasis contained very close numbers of mitoses, making the effect quite confident (Ponomareva 1939).

Unfortunately, the author provided no information concerning the inductor and induction details (Ponomareva 1939), but mentioned that the optimal induction duration was 5 min, while 20 min induction gave no effect (similarly to the above data on mitogenetic suppression – see Sects. 20.1.3, 20.3.2, and 20.4.1).

However, in spite of high MGE effects and reliability of controls, tumor tissues also were far from the best recipients: first, for ethical reasons; second, because the animals with experimental cancer were not so easily available as yeast or bacteria.

20.5.4 Embryonal Cells

An important layer of work over the years has been associated with MGE-like effects in embryo development.

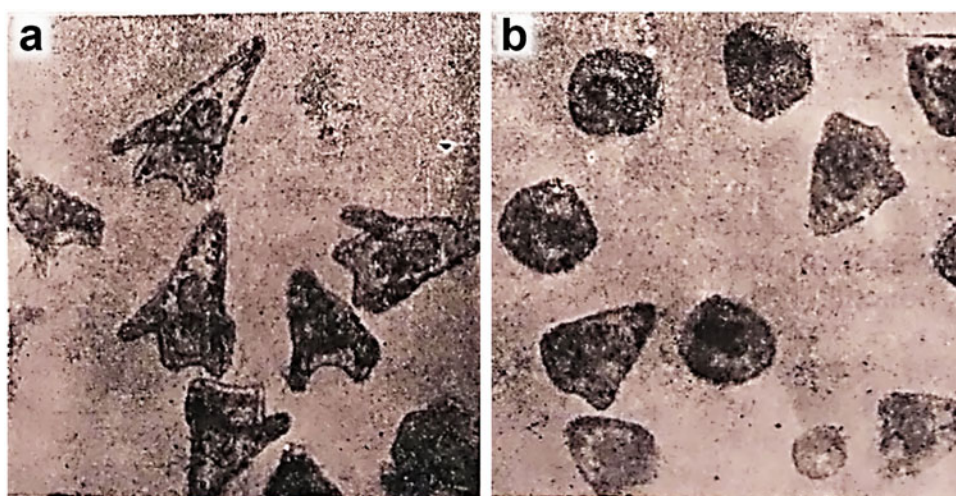
The first observations of this kind were made by J. and M. Magrou (1928), who reported distant nonchemical influence of yeast, bacterial cultures and other previously known MGE inductors on sea urchin embryo development. The role of recipient was played by eggs, semen or zygotes of sea urchin *Paracentrotus lividus*; the inductors were different bacterial (*Bact. tumefaciens*, *Staphylococcus* sp.) and yeast cultures, as well as glucose solutions with different added oxidants and some other chemical systems (Magrou 1930a, b, 1934). The working duration of induction was 2 h for eggs and 30 min for semen (Magrou 1934). The recipient showed severe development abnormalities, which remained if the inductor and the recipient were separated with quartz (see Fig. 20.10), but were not observed when they were separated by glass, or the inductor had been previously killed with heating (Magrou 1930a, b). Importantly, the larvae development was really pathological, and not just stunted or halted, with a pronounced abnormal growth of mesenchyme (Magrou 1934), suggesting specific influence of induction on certain tissues and associated disorders of morphogenesis.

Table 20.4 Number of mitoses in noninduced (control) and induced halves of metastases, in the decapitated mice, with experimentally induced carcinoma, immediately after decapitation and 30 min later (the author provides no data on the inductor and induction details)

| 0 min after death 5 min induction | | | 30 min after death 5 min induction | | | 30 min after death 20 min induction | | |
|--------------------------------------|---------|--------|---------------------------------------|---------|--------|--|---------|--------|
| Control | Induced | MGE, % | Control | Induced | MGE, % | Control | Induced | MGE, % |
| 207 | 203 | 0 | 130 | 218 | 67 | 237 | 236 | 0 |
| 60 | 55 | -4 | 113 | 204 | 80 | 240 | 241 | 0 |
| 322 | 319 | 0 | 196 | 271 | 38 | 242 | 241 | 0 |
| | | | 148 | 236 | 59 | 247 | 246 | 0 |
| | | | 173 | 240 | 38 | 325 | 321 | -1 |
| | | | 170 | 350 | 105 | 324 | 315 | -2 |
| | | | 332 | 399 | 20 | 210 | 209 | 0 |
| | | | 89 | 186 | 100 | | | |
| | | | 123 | 250 | 103 | | | |

Data from Ponomareva (1939)

MGE = (induced - control)/control, %

Fig. 20.10 Sea urchin (*Paracentrotus lividus*) larvae 48-h old: in control (a) and after induction with *Bact. tumefaciens* through a quartz plate (b). (Reprinted from Magrou 1934)**Table 20.5** Hatching of mosquitos *Aedes aegypti* eggs, in control and after mitogenetic induction by bacterial cultures through quartz

| Inductor culture | Control | | Recipient | |
|---------------------------|------------|----------|------------|----------|
| | Total eggs | Hatching | Total eggs | Hatching |
| <i>Bact. Tumefaciens</i> | 203 | 0 | 194 | 31 |
| <i>Staphylococcus sp.</i> | 69 | 0 | 78 | 7 |

Data from Magrou et al. (1931)

However, the authors got contradictory results concerning the physical nature of this influence, supposing either UV or electrostatic interactions (Magrou et al. 1929; Magrou 1934), which nowadays looks quite doubtful. Besides, the effects were strangely temperature-dependent, being quite pronounced at 23 °C, but inconsistent at lower temperatures (e.g., 20 °C) (Magrou et al. 1929). However, with the right set of conditions, the effect was striking and cannot be written off as an accident, which once again shows extreme importance of all experimental details being thoroughly optimized before any interpretation.

The authors also tried similar induction on the resting eggs of mosquitos *Aedes aegypti*. The inductors were cultures of

Bact. tumefaciens (24 h old) and *Staphylococcus sp.* (8 h old), that had been successfully used with sea urchin before. The induction was performed through a quartz layer, with the inductor and the recipient hermetically isolated, at the temperature of 25 °C. The recipient resting eggs were observed for 24–48 h, and the induction was seemingly lasting all this period (it is not clearly outlined) (Magrou et al. 1931). The authors obtained quite certain results, with the control eggs showing 0% hatching, and the recipient eggs hatching in 9% to 16% (see Table 20.5) and also becoming more sensitive to external influences triggering hatching after induction (Magrou et al. 1931).

Altogether, as Hollaender stated, “apparently good effects have been obtained <in these works>, but since sea-urchin eggs are not available the year round and since the laboratories where sea-urchin eggs can be had are few, this method has not been used extensively” (Hollaender 1936). A still more important factor in our opinion was poorly defined experimental conditions, which seem to have been crucial for success.

Another series of works on this topic was performed by Carlo Maxia (1929, 1930, 1932, 1935; Maxia and Vacca 1931; Maxia and Leone 1931), with an honest description of the raw experimental data. However, unfortunately, the reported experiments are variable and unsystematic, which makes it impossible to draw realistic evidence-based conclusions.

The recipient in Maxia’s works was mostly eggs of sea urchin *Paracentrotus lividus*; the inductor – roots of different plants: *Allium sativum*, *Vicia faba*, *Sinapis alba*, *Brassica naous*, *Brassica oleraceae*, as well as mush from these roots. The induction started different time after egg fertilization (from 5 min to several hours) and lasted from 1 to 5 h; the temperature was mostly 10–15 °C; the light conditions were different: from full daylight and light screened with different filters to complete darkness. The recipient eggs were placed in the wells on the slides (200–300 eggs in a set), and the inductor roots were fixed in close proximity; however, the author doesn’t describe this issue, as well as the presence or absence of quartz or glass plates, separating them. He also tried from 1 to several dozen roots used for inducing a single recipient, which makes the results even less interpretable.

The results he observed consisted in accelerated cleavage in the recipients, comparing to control (Maxia 1929), but the degree of acceleration was very different and impossible to formally assess. Thus, although the author has indeed done a great and honest job, it is impossible to draw any real conclusions from his publications.

Actually, attempts of observing nonchemical interaction between embryos or their reaction to external ultraweak nonchemical influences were later undertaken by plenty of researchers in different laboratories. Some of them will be mentioned here in Chaps. 24 and 27; others can be found elsewhere [<https://doi.org/10.1016/j.pbiomolbio.2010.07.003>]. We deliberately avoid describing these works in this chapter because we believe it is necessary to concentrate on the problem of MGE *per se*, as the most elaborated and fundamental phenomenon of this group.

20.6 Stimulation of Mitoses by Artificial UV Sources

20.6.1 Initial Assessments

Since the very first works suggesting UV nature of MGE, there was an obvious task of obtaining a similar effect from artificial UV sources.

Table 20.6 Stimulation of mitoses in an onion root meristem by various spectral lines from aluminum and zinc sparks (the effect is estimated as the difference between the induced half of the root cut and the opposite (control) half, in % of the control half)

| Wavelength, nm | MGE, % |
|----------------|--------|
| 186 | 1 |
| 193 | 28 |
| 199 | 27 |
| 203 | 25 |
| 237 | 20 |
| 267 | –1.2 |

Data from Gurwitsch and Frank (1927)

MGE = (induced – control)/control, %

Such an effect was first successfully demonstrated by G.M. Frank and A.G. Gurwitsch in 1927 (Frank and Gurwitsch 1927; Gurwitsch and Frank 1927). The recipient was onion root (as in Sect. 20.2.1). The role of inductor was played by different spectral lines from aluminum and zinc sparks. The induction intensity was assessed only indirectly: it was 10–200 times lower than the minimal intensity detected by a photographic plate (which in itself is already uncertain) (Frank and Gurwitsch 1927).

For induction, the recipient root was located with the help of a horizontal microscope precisely at the desired spectral band, extracted from the spark emission by a quartz monochromator and previously localized with a photoplate at higher spark intensities. The induction lasted 1 min, after which the root was incubated for 2–2.5 h, with mitoses counted on longitudinal sections (as in Sect. 20.2.1). A reliable mitosis induction was obtained within the spectral range 193–237 nm (see Table 20.6). Notably, later, the 203 nm band appeared to produce an induction effect at even shorter exposure times, from 1 min down to 1 s (Frank 1929) (the intensity was not assessed either, so the radiation dose cannot be compared with the above).

This gave the authors further reasoning that the biological MGR also belonged to the spectral range 190–240 nm and had an intensity not exceeding 1/10–1/200 of the photoplate sensitivity threshold (see Chap. 21 for more data on its physical qualities).

Similar UV-induced MGE was shown for corneal epithelia from frogs, tritons and rats, with one eye used as the recipient, and the other one for control (Gurwitsch and Anikin 1928) (see Sect. 20.5.1). The inductor was 203 nm spectral band from a spark as above; the induction lasted 3–4 min, after which the recipient was incubated for 3–4 h before fixation. In parallel, standard induction by yeast culture was used as a positive control and gave stable results.

Though the authors obtained positive UV-induced MGE (see Table 20.7), it appeared diverse and much less reliable than the standard MGE (especially for frogs – see Table 20.7c). The authors interpreted this as a consequence of too high doses of radiation hitting the threshold of mitogenetic stimulation and depression (see Sect. 20.1.3), at which the natural variability of animals could result in opposite effects under the same conditions (Gurwitsch and Anikin 1928).

Table 20.7 Number of mitoses in corneal epithelium of two eyes and MGE as difference between the induced and noninduced (control) eyes, in % of the control eye

| Number of mitoses | | |
|-------------------|---------|--------|
| Control | Exposed | MGE, % |
| A. Triton | | |
| 27 | 54 | +100 |
| 66 | 134 | +100 |
| 51 | 130 | +150 |
| 30 | 50 | +68 |
| 38 | 53 | +40 |
| 52 | 74 | +38 |
| 23 | 16 | -30 |
| B. Rat | | |
| 1944 | 3086 | +78 |
| 2050 | 3312 | +60 |
| 1187 | 1644 | +40 |
| C. Frog | | |
| 108 | 277 | +158 |
| 2070 | 3200 | +50 |
| 333 | 615 | +85 |
| 221 | 885 | +300 |
| 205 | 695 | +240 |
| 88 | 182 | +106 |
| 169 | 445 | +160 |
| 640 | 552 | -16 |
| 360 | 340 | -6.5 |
| 405 | 354 | -13 |
| 269 | 255 | -6 |
| 60 | 46 | -30 |
| 216 | 156 | -39 |
| 42 | 16 | -108 |

Data from Gurwitsch and Anikin (1928)

Left eye was exposed to spectral line 203 nm from spark for 3–4 min, tissues were fixed 3–4 h after induction. MGE = (induced - control)/control, %

20.6.2 Data from Other Authors

At the same time, Reiter and Gabor gave a different spectral estimate (Reiter and Gabor 1928a, 1931). The recipient used was onion roots, cut from the bulb. The tested inductors were sunshine, carbon arc lamp and mercury arc lamp, all of them producing no effect, unless spectrally decomposed. However, UV, spectrally decomposed with a large quartz spectrograph, produced strong MGE in the range around 340 nm, weak MGE around 280 nm and no MGE in between. Moreover, the 290–320 nm spectral range appeared inhibiting the MGE, simultaneously produced by 340 nm light, thus playing the role of a “mitogenetic suppressor” (see Fig. 20.11).

Notably, the same spectral discrepancy persisted between Reiter and Gabor and Gurwitsch’s school in basic MGE spectral estimates as well (see Chap. 21). Nowadays, it is obviously impossible to find the reasons for this strange contradiction, but we can name several important methodical differences:

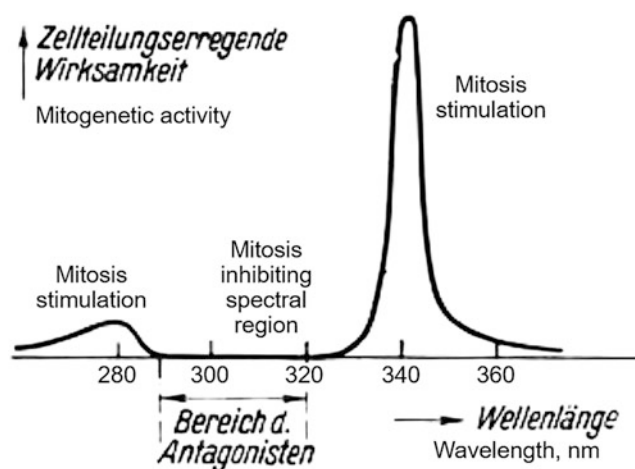


Fig. 20.11 Mitogenetic activity of UV from mercury arc lamp, inducing a cut-off onion root. (Adapted from Reiter and Gabor 1928a)

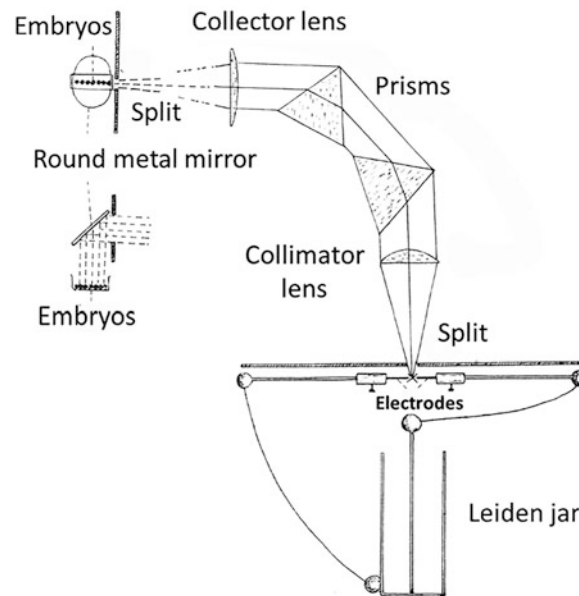


Fig. 20.12 Experimental plant used for exposure of frog and toad embryos to the isolated spectral lines of spark discharge. The upper left part of the figure shows the top view and the side view of embryos and a circle mirror. (Reprinted from Stempell and Romberg 1932)

- The UV intensities, used by Reiter and Gabor, were several orders of magnitude higher, than in the above works by Gurwitsch and Frank.
- The exposure time in Reiter and Gabor (1928a, 1931) was also much longer, up to 1 h.
Thus, the effect observed by the authors could well be a different phenomenon, related to much higher doses of UV (see discussion in Chariton et al. (1930)).
- Reiter and Gabor used cut-off roots, while Gurwitsch used roots, not dissected from the bulb, meaning the whole range of “secondary MGE” phenomena supposedly involved in their results (see more on that in Chap. 22).

Of other workers, R. Ruysen observed mitogenetic effect in bacteria induced by monochromatic UV radiation (250 nm, $50,000 \text{ quanta cm}^{-2} \text{ s}^{-1}$, duration 20 s) (Ruysen 1933). L.K. Wolff and G. Ras from the same laboratory reported that bacteria culture was more sensitive to polarized artificial light than to nonpolarized one (compared for the 253.7 nm spectral line) (Wolff and Ras 1934b).

In Stempell and Romberg (1932), frog (*Rana fusca*) and toad (*Bufo viridis*) embryos freed from tertiary oocyte shells were exposed to the isolated spectral lines from the spark discharge (see Fig. 20.12). For 15-min exposure, a similar stable acceleration of embryo development was obtained for spectral lines 280, 243.8 and 238.3 nm, while 5 min exposure by the same spectral lines had no impact on development, and 30-min exposure produced both acceleration and retardation of embryo development. More intense radiation of the same

UV source without spectral decomposition retarded development and even led to death.

Analogous results were obtained by Reiter and Gabor: irradiation by isolated spectral line accelerated development of eggs of axolotl and toad (*Bufo vulgaris*), while more intense radiation of the same isolated spectral line and nondecomposed radiation retarded their development (Reiter and Gabor 1928b) (as usual these authors reported positive results in the “red-shifted” range, i.e., for wavelengths around 340 nm).

Very clear acceleration of metamorphosis in grown toad larvae (*Bufo vulgaris*) was observed after brief irradiation with a mercury vapor lamp (Barbacci 1929, as cited in Stempell and Romberg 1932). Acceleration of trout eggs development by moderate ultraviolet radiation was reported in Haempel and Lechler 1931 (as cited in Stempell and Romberg 1932).

A number of authors reported negative results in experiments with artificial UV sources at approximately the same ranges of wavelengths and intensities as in positive experiments (Nakaidzumi and Schreiber 1931; Kreuchen and Bateman 1934; Richards and Taylor 1932; Seyfert 1932; Hollaender and Claus 1937, and much later Quickenden et al. 1989). However, all these negative publications violated biological aspects of MGE observation stated in positive works, and none of these authors obtained MGE from biological inductors as well (see Sects. 20.1.3, 20.2.2, 20.3.3, 20.4.2 and (Volodyaev and Belousov 2015)).

20.6.3 Chariton, Frank, Kannegiesser

The most thorough and accurate work on this subject (Chariton et al. 1930) was performed in 1930 by J. Chariton, A.G. Frank and N. Kannegiesser in State Physical-Technical Radiology Institute (now Ioffe Physical-Technical Institute, St. Petersburg) and supervised by A.F. Ioffe.

The recipient was agar yeast cultures (as in Sect. 20.3.1) and onion roots (as in Sect. 20.2.1). The role of inductors was played by aluminum, zinc, cadmium sparks and mercury arc lamp, their intensity measured with sodium photocell and filament electrometer and attenuated by calibrated filters of platinized quartz. Spectral lines within the range of 206–365 nm were isolated by a large dual quartz monochromator, making them nearly monochromatic. The induction lasted 10 min.

The authors obtained stable UV-induced MGE in the spectral range 206–260 nm at intensities $\sim 10^7 - 10^9$ quanta $\text{cm}^{-2} \text{s}^{-1}$ (see Fig. 20.13; 1 arbitrary unit corresponds to 5×10^{-14} A or $\sim 10^8$ quanta $\text{cm}^{-2} \text{s}^{-1}$). Stronger or weaker UV illumination, as well as UV outside this spectral range produced no MGE, including the Reiter-Gabor region around

340 nm (suggesting that the authors observed different phenomena).

Importantly, the minimal MGE-producing intensity ($10^7 - 10^8$ quanta $\text{cm}^{-2} \text{s}^{-1}$) exceeded the estimates for biological inductors ($10 - 10^3$ quanta $\text{cm}^{-2} \text{s}^{-1}$) by many orders of magnitude, suggesting a certain specificity of biological MGR, making biological recipients more sensitive to it than to the used radiation from physical sources. The authors speculated that it could be due to a specific spectral composition, polarization or time dependence of MGR (Chariton et al. 1930) and tested the first hypothesis, repeating the same experiments with less monochromatic radiation. For this, they used an ordinary monochromator with a wider exit slit to get a set of spectral lines within 205–215 nm, which were “mixed” by defocusing. Strikingly, this led to the same mitogenetic response at ~ 15 times lower intensity than in case of the isolated spectral line of 210 nm – see Fig. 20.14 (the received dose here was $10^5 - 10^6$ quanta $\text{cm}^{-2} \text{s}^{-1}$, i.e., a yeast cell received in average about 160 quanta per 10-min exposure) (Chariton et al. 1930; Rodionov and Frank 1934).

However, it was still orders of magnitude greater than the estimated MGR from biological sources, suggesting that simply blurring the irradiation spectrum by 10 nm could not fully simulate biological MGR.

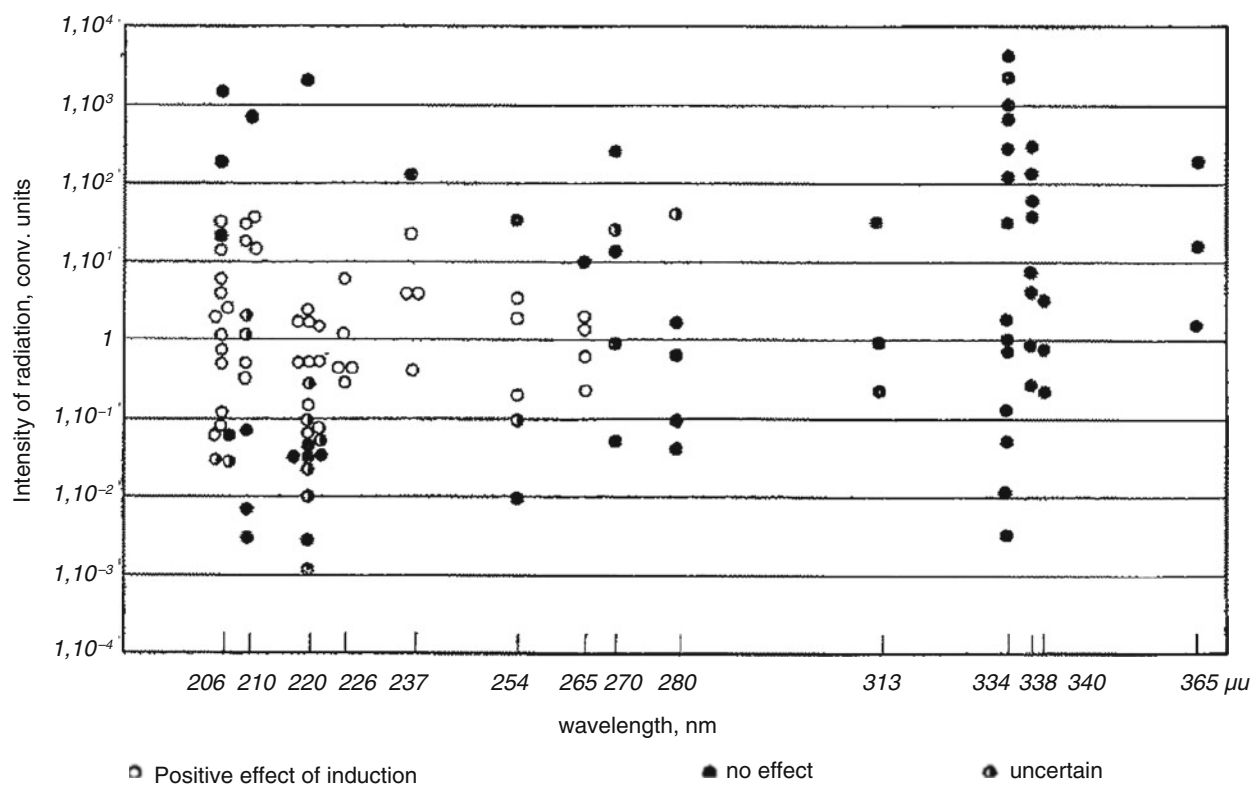


Fig. 20.13 UV-induced MGE on agar yeast cultures depending on the UV wavelength (nm) and intensity (arb.units; 1 arb.unit corresponds to the photoelectric current of 5×10^{-14} A). UV sources – aluminum, zinc,

cadmium sparks and mercury arc lamp. Exposure time: 10 min. ● no MGE; ○ strong MGE; ◐ weak MGE. (Reprinted from (Chariton et al. 1930). Copyright 1930, with permission from SNCSC)

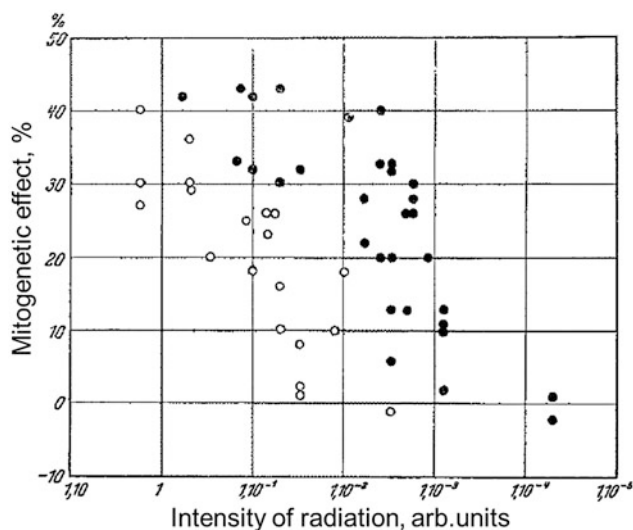


Fig. 20.14 UV-induced MGE on agar yeast cultures by monochromatic 210 nm radiation (●) and 205–215 nm “mixed-wavelength radiation” (○). UV sources – aluminum, zinc, cadmium sparks and mercury arc lamp. Exposure time: 10 min. 1 arb.unit corresponds to the photoelectric current of 5×10^{-14} A. (Reprinted from (Chariton et al. 1930). Copyright 1930, with permission from SNCSC)

20.6.4 The Subtleties of Spectral Composition and the Role of IR

Later, when (1) visible light background was reported very important for MGE (with no MGE observed in complete darkness) (Potozky 1930, 1932), and (2) extensive experiments on MGE spectral analysis showed biological recipients to be better stimulated by certain narrow spectral bands, extracted from the biological MGR (see Chap. 21), the above explanation of “better MGE from a blurred spectrum” appeared unconvincing. This led the authors to a further hypothesis, that the observed greater sensitivity of recipients to mixed-spectrum irradiation was caused not by the spectrum blurring *per se*, but by an increase in the visible light background, a side effect of these additional optical steps (Rodionov and Frank 1934). Indeed, while the above induction with “monochromated UV” (Chariton et al. 1930) was performed in a dark chamber, the “wavelength mixing” procedure was done outside it, and the light background was orders of magnitude higher. This was further tested with other inductors (see below).

The third hypothesis suggested that the threshold MGE-inducing intensity may have been affected by the short-burst character of the light from arc discharges used for induction (Rodionov and Frank 1934). This led the authors to a further modification of the above experiment, with the role of inductor played by a constant UV source, a gas burner. Strikingly, it produced MGE in the recipient at

much lower intensities, thus giving a benefit of several orders of magnitude, but only when the induction was artificially interrupted with a nontransparent disk with cut-off slits, rotating at a certain constant rate (see Sect. 20.1.3). Still, the threshold MGE-producing intensity was still about two orders of magnitude higher than the estimates of biological MGR. For instance, exposing a photographic plate to the 230–235 nm band from a gas burner attenuated to MGE-active intensity, resulted in its darkening after 6–8 h, while biological MGR sources never produced such effect (Rodionov and Frank 1934).

Next, the authors tried eliminating the infrared component of the burner light: with water filter or monochromator, which further halved the exposure threshold time (3 min instead of 6 min) (Rodionov and Frank 1934). Thus, unexpectedly, IR light appeared to have an antagonistic action on MGR recipients, suppressing their sensitivity. This was later reported for MGE from biological inductors as well: both the yeast-recipient sensitivity and the yeast-inductor efficacy decreased in the presence of weak IR light (Rodionov and Frank 1934). Moreover, IR-radiation also reduced biological impact of UV radiation of much higher intensities close to the bactericidal level.

20.6.5 The Role of Visible Light Background

As can be seen in Fig. 20.13, the long-wave threshold of yeast MGE-response to “artificial” UV was found ~265 nm (Chariton et al. 1930). However, as mentioned, the authors were working in total darkness. At the same time, light conditions for MGE induced by biological inductors were usually more favorable (the room usually had diffused light coming in through two window panes or from shielded incandescent bulbs, etc.), and the yeast sensitivity was observed at the longer wavelengths as well. Thus, the maximal wavelength observed in purely biological MGE experiments in Gurwitsch’s school was as high as 291 nm (Eremeev 1947).

To clarify the influence of visible light on the spectral sensitivity of MGE recipients, a series of experiments with yeast recipients and artificial UV sources were performed (Eremeev 1940). The authors used 2 nm wide bands isolated from a hydrogen-tube radiation and attenuated it approximately to the intensity used in Chariton et al. (1930) (as pointed out already in Rodionov and Frank (1934), hydrogen-tube radiation is a more convenient UV source for studying spectral dependence of MGE-response than sparks and mercury lamps, due to its continuous spectrum and higher stability). In the darkness, the long-wave limit of MGE induction was 265 nm (Eremeev 1947), in full

Table 20.8 MGE in yeast induced by isolated UV bands from hydrogen tube radiation with and without visible light background

| Wavelength, nm | Exposure, s | MGE, % | | Current strength, mA |
|----------------|-------------|------------|------------|----------------------|
| | | Light | Darkness | |
| 289–291 | 5 | 42 ± 4.1 | 2 | 8 |
| 349–351 | 15 | 38 ± 7.8 | 7 | 8 |
| 359–361 | 17 | 45 ± 3.8 | 0.55 ± 2.8 | 12 |
| 361–363 | 18 | −1.4 ± 2.2 | 5 ± 2 | 12 |

Data from Eremeev (1940) MGE = (induced – control)/control, %

accordance with (Chariton et al. 1930) (see Fig. 20.13). Strikingly, however, it shifted up to 361 nm, when yeast was additionally illuminated with visible light (see Table 20.8), suggesting a possible explanation of spectral contradictions with (Reiter and Gabor 1928a). Notably, no MGE response was observed for longer wavelengths at similar exposure times either in the dark or in the light (Eremeev 1940).

V.Ph. Eremeev also observed MGE in yeast recipients, induced by UV components of daylight passed through the usual double-pane window, and incandescent lamps, with the exposure times of 10 and 5 min, respectively (Eremeev 1940). UV spectral components down to 360 nm for the daylight after double-pane window and down to 320 nm for the electric light were demonstrated with spectrograph and photo plates. The author pointed out that spectra of these sources surely spread to the shorter wavelengths with intensities nondetectable by photo plate, but probably still detectable by yeast which were known to be more sensitive. However, MGE from biological sources supposedly “overlapped” similar effect from the UV components of the background light, i.e., it had no influence on the usual MGE-response in yeast to the biological inductor (Eremeev 1940).

20.6.6 Konev et al.

Very interesting results on stimulation of cell division by ultraweak UV radiation from artificial sources were obtained much later by S.V. Konev’s group (Konev and Lyskova 1966; Konev 1967a). As far as we know, they were the only group which reported stimulation of mitoses by artificial radiation of the same intensity as they reported for MGR from biological sources. It should be noted that the estimate of the MGR intensity made by Konev’s group was higher ($10^4 - 10^5$ quanta $\text{cm}^{-2} \text{s}^{-1}$) than those by earlier authors ($10 - 10^3$ quanta $\text{cm}^{-2} \text{s}^{-1}$), and this group used longer expositions.

Their method also had some other distinctive features (see Konev and Lyskova 1966; Konev 1967a). Contrary to the early authors, they used synchronized yeast cultures, continuous exposition throughout the experiment instead of short exposures followed by much longer incubation with “MGE development” (see paragraph “Dynamics of MGE

development after induction” in Sect. 20.1.3). Liquid yeast culture was synchronized in the nutrient-deficient media, control and experimental suspensions were poured into usual quartz cuvettes for spectrophotometer $1 \times 1 \times 4$ cm (notably, the condition of induction in thin layers was violated – compare to Sects. 20.3.2 and 20.4.1). The recipient yeast culture was continuously exposed to the 280 nm spectral line of mercury lamp with the intensity of $10^4 - 10^5$ quanta $\text{cm}^{-2} \text{s}^{-1}$, starting with the cell cycle block removal by nutrient addition, and till the end of the experiment (that was about 10 quanta per cell in average). Neither control nor recipient yeast were illuminated by visible light during experiment in spite of the early authors’ recommendations (thus, their conditions are closer to those in Chariton et al. (1930), than to other works). Effect of cell division stimulation by ultraweak UV radiation was characterized by the lag-period shortening (i.e., the time between the cell block removal and the first wave of division): in average it was shortened by 3.1 times comparing to the control culture (see Table 20.9 and Fig. 20.15). With increase of radiation intensity up to 10^8 quanta $\text{cm}^{-2} \text{s}^{-1}$ (Konev and Lyskova 1966)⁵ the effect disappeared (see Table 20.9).

In experiments with exposition of yeast through small diaphragms, the authors obtained the all-or-nothing response typical for MGE. The effect completely disappeared when the exposed area was less than 1 mm^2 (10^5 cells) (Konev 1967a), and the effect for larger exposed areas was the same as for exposure of the whole culture even when only about 1% of yeast was exposed, that agreed well with the conclusions of the early authors about the chain character of mitogenetic response.

20.6.7 Summary

Altogether, mitogenetic stimulation by UV from various physical sources was obtained in a serious number of works from different laboratories. Most of the authors showed UV-induced MGE for wavelengths 200–270 nm (corresponding to spectral estimates of the biological

⁵In Konev (1967a), 10^9 quanta $\text{cm}^{-2} \text{s}^{-1}$ is written in the same context, so there is probably a misprint either in Konev (1967b) or in Konev and Lyskova (1966).

Table 20.9 Change of lag-period (till the first wave of cell division) in synchronized culture *Torula utilis* under the influence of ultraweak UV radiation ($\lambda = 280$ nm)

| | Control culture in darkness. Latent period, min | Induced culture (the same conditions + ultraweak UV). Latent period, min | Shortening of latent period (times) |
|--|---|--|-------------------------------------|
| Radiation intensity: 10^5 quanta $\text{cm}^{-2} \text{s}^{-1}$ | 135 | 25 | 5.4 |
| | 120 | 50 | 2.4 |
| | 120 | 30 | 4.0 |
| | 100 | 60 | 1.7 |
| | 135 | 30 | 4.5 |
| | 135 | 40 | 3.4 |
| | 150 | 35 | 4.3 |
| | 130 | 60 | 2.15 |
| | 180 | 45 | 4.0 |
| | 100 | 30 | 3.3 |
| | 100 | 40 | 2.5 |
| | 120 | 40 | 4.0 |
| | 80 | 20 | 4.0 |
| | 120 | 50 | 2.4 |
| Average for experiments with radiation intensity of 10^5 quanta $\text{cm}^{-2} \text{s}^{-1}$ | 123 | 39.5 | 3.1 |
| Radiation intensity: 10^8 quanta $\text{cm}^{-2} \text{s}^{-1}$ | 135 | 135 | 1.0 |

Data from Konev and Lyskova (1966)

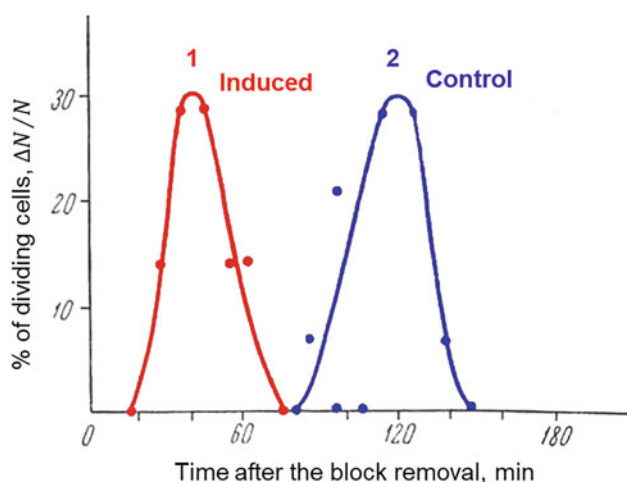


Fig. 20.15 First wave of cell division in synchronized yeast *Torula utilis* after cell block removal: 1 – induced culture (exposed to ultraweak UV radiation: $\lambda = 280$ nm, 10^5 quanta $\text{cm}^{-2} \text{s}^{-1}$); 2 – control culture (in complete darkness). (Reprinted from (Konev 1967b). Copyright 1967, with permission from SNCSC)

MGR – see Chap. 21), while Reiter and Gabor reported MGE stimulation by much longer wavelengths, 330–350 nm. Whether and how this discrepancy can be explained remains unknown: both “parties” were highly competent and have definitely good faith to suspect them of such gross errors in spectrum estimation or data falsification. However, a certain clue to this contradiction can lie in the work by Eremeev, showing huge dependence of recipient sensitivity on background lighting, including both spectral and intensity parameters.

In contrast to the good spectral agreement between biologically- and physically-induced MGE (within the same lab), the MGE-producing intensities of artificial UV appeared orders of magnitude higher than the estimates of biological MGR. The reasons for that could lie in plenty of aspects and were extensively discussed by the authors, but the most convincing ones, to our mind, are the following:

- Biological MGE was usually observed at certain background light, which was highly likely to change the recipient sensitivity both in the sense of spectral range and intensity: the IR component supposedly had MGE-repressing effect, while the visible component was likely MGE-stimulating.
- The UV physical sources had very different characteristics: at least the time structure (meaning continuous radiation or bursts) and spectral composition, which appeared of great importance for biological MGE.

In course of a step-by-step research of these technical issues, different authors managed to decrease the MGE-producing threshold of artificial UV by orders of magnitude, thus giving hope that a full optimization of the UV physical properties could lead to a good simulation of biological inductors.

How can a biological system “sense” so complex emission parameters as time-dependence and spectral composition remain outside our discussion for the reasons of its utter speculation and hollowness.

Acknowledgments We sincerely thank the heirs of Alexander Gurwitsch and his late grandson, Lev Belousov, for unlimited access to their personal library, containing probably the most comprehensive collection of papers on MGE.

References

- Acs L (1931) Über die mitogenetische Strahlung der Bakterien. *Centr Bakt I Abt Orig* 120 (1/2):116-124
- Alotaibi MK, Barnawi IO (2018) Cytogenetic biomonitoring of Almadinah Almunawarah municipal wastewater treatment plant using the *Allium cepa* chromosome aberration assay *Pak J Bot* 50 (6):2245–2249
- Aslantürk ÖS (2019) Cytogenetic effects of Fulvic acid on *Allium cepa* L. root tip meristem cells. *Caryologia* 72 (2):29–35. doi:<https://doi.org/10.13128/cayologia-257>
- Barbacci P (1929). *Atti Accad Fisiocritici Siena* 3:989–993
- Baron MA (1926) Über mitogenetische Strahlung bei Protisten (16. Mitteilung über mitogenetische Strahlung). *Wilhelm Roux' Archiv für Entwicklungsmechanik der Organismen* 108 (4):617–633. doi:<https://doi.org/10.1007/bf02080167>
- Baron MA (1928) Bakterien als Quellen mitogenetischer (ultravioletter) Strahlung. *Zentralbl Bakt Abt 2* 73 (1):373–379
- Baron MA (1930) Analyse der mitogenetischen Induktion und deren Bedeutung in der Biologie der Hefe. *Planta:Archiv für wissenschaftliche Botanik* 10 (1):28-83. doi:<https://doi.org/10.1007/bf01911536>
- Batikyan GG, Simonyan EG (1970) Effect of kinetin on cell division (*Allium cepa*) (In Russian). *Biological Journal of Armenia* 23 (11): 96-103
- Belousov LV, Voeikov VL, Popp FA (1997) Mitogenetic rays of Gurwitsch (In Russian). *Priroda [Nature]* (3):64-80
- Blacher LJ, Holzmann OG (1930) Resorptionsprozesse als Quelle der Formbildung. I. Die Rolle der Mitogenetischen Strahlungen in den Prozessen der Metamorphose der Schwanzlosen Amphibien. *Wilhelm Roux' Archiv für Entwicklungsmechanik der Organismen* 122 (1):48–78. doi:<https://doi.org/10.1007/bf00576965>
- Blacher LJ, Irichimowitsch AI, Liosner LD, Woronzowa MA (1932) Resorptionsprozesse als Quelle der Formbildung. IX Einfluss der mitogenetischen Strahlen auf die Geschwindigkeit der Regeneration. *Roux' Archiv* 127:339-352
- Blacher LJ, Irichimowitsch AI, Liosner LD, Woronzowa MA (1933) Resorptionsprozesse als Quelle der Formbildung. X. Die mitogenetische Strahlung des Regenerats und des Blutes der Kaulquappen während der Regeneration. *Wilhelm Roux' Archiv für Entwicklungsmechanik der Organismen* 127 (1):353–363. doi:<https://doi.org/10.1007/bf01390723>
- Bonciu E, Firbas P, Fontanetti CS, Wusheng J, Karaismailoğlu MC, Liu D, Menicucci F, Pesnya DS, Popescu A, Romanovsky AV, Schiff S, Ślusarczyk J, de Souza CP, Srivastava A, Sutan A, Papini A (2018) An evaluation for the standardization of the *Allium cepa* test as cytotoxicity and genotoxicity assay. *Caryologia* 71 (3): 191-209. doi:<https://doi.org/10.1080/00087114.2018.1503496>
- Borodin DN (1930) Energy emanation during cell division processes (M-rays). *Plant physiology* 5 (1):119-129
- Budantsev AY, Demyanov AY (2017) Deformation of tissues during histological processing I. Methods for morphometric evaluation of deformities (In Russian). *Cytology* 59 (6):447-454
- Chariton J, Frank G, Kannegiesser N (1930) Über die Wellenlänge und Intensität mitogenetischer Strahlung. *Naturwissenschaften* 18 (19): 411-413. doi:<https://doi.org/10.1007/bf01501123>
- Chruschoff GK (1930) Über die Ursachen des Gewebewachstums in vitro. 1. Die Quellen der mitogenetischen Strahlen in Gewebekulturen. *Arch exper Zellforsch* (9):203-213
- Devnarayan G, Marmat S, Rathore H, Qureshi T, Akhand A, Shrivastava S (2016) Influence of Cellular Phone and Tower on Mitosis in *Allium cepa* *Model Int Res J Biological Sci* 5 (8):53-57
- Doljanski L (1932) Das Wachstum der Gewebekulturen in vitro und die Gurwitsch-Strahlung. *Wilhelm Roux' Archiv für Entwicklungsmechanik der Organismen* 126 (1):207-212. doi:<https://doi.org/10.1007/bf00586381>
- Eremeev VF (1940) Determination of the limits of mitogenetic activity of the ultra-violet part of the spectrum. *Comptes Rendus de l'Academie des Sciences de l'URSS* 27 (8):795-796
- Eremeev VF (1947) The mitogenetic regime of streaming protoplasm (In Russian). In: Gurwitsch AG (ed) *Collected volume on mitogenesis and theory of biological field*. Pub.house of the USSR Academy of Medical Sciences, Moscow, pp 65–91
- Evseeva T, Belykh E, Maistrenko T (2005) Toxic and cytogenetic effects induced in *Allium cepa* L. by low concentrations of Cd and ²³²Th. *Bulletin of Institute of Biology* (9):2-7
- Ferguson AJ, Rahn O (1933) Zum Nachweis mitogenetischer Strahlung durch beschleunigtes Wachstum von Bakterien. *Archiv für Mikrobiologie* 4 (1–4):574-582. doi:<https://doi.org/10.1007/bf00407563>
- Ferreira SMCMA, dos Santos HLC, Gomes Jennifer V, Pastura Danilo GN, Pereira Gabriela L, da Rocha EB, de Jesus Costa LM, Alves Raphael S, de Oliveira BL, Borba Helcio R, de Lima VM (2020) *Laurus nobilis* L.: assessment of the cytotoxic and genotoxic potential of aqueous extracts by micronucleus and *Allium cepa* assays *Braz J Pharm Sci* 56:1-9. doi:<https://doi.org/10.1590/s2175-97902019000318302>
- Ferrero ML, de la Torre C (1986) Cell proliferation in *Allium cepa* L. meristems under 8-hydroxyquinoline, a chelating agent that affects DNA and RNA polymerases *J Cell Set* 80:171-180
- Fiskesjö G (1985) The Allium test as a standard in environmental monitoring *Hereditas* 102:99-102
- Fiskesjö G (1993) The allium test in wastewater monitoring *Environmental Toxicology and Water Quality* 8 (3):291-298
- Fiskesjö G (1995) Allium test In: O'Hare S, Atterwill CK (eds) *In vitro toxicity testing protocols, Methods in molecular biology*, vol 43. Humana Press, Totowa, NJ, pp 119-127. doi:<https://doi.org/10.1385/0-89603-282-5:119>
- Fiskesjö G (1997) The Allium test for screening chemicals; evaluation of cytological parameters. In: *Plants for environmental studies*. CRC Press LLC, New York, pp 308-333
- Frank G (1929) Das mitogenetische Reizminimum und -maximum und die Wellenlänge mitogenetischer Strahlen. *Biologisches Zentralblatt* 49:129-141
- Frank G, Salkind S (1926) Die Quellen der mitogenetischen Strahlung im Pflanzenkeimling. *Wilhelm Roux' Archiv für Entwicklungsmechanik der Organismen* 108 (4):596-608. doi:<https://doi.org/10.1007/bf02080165>
- Frank GM, Gurwitsch AG (1927) Zur Frage der Identität mitogenetischer und ultravioletter Strahlen. *Wilhelm Roux' Arch Entwickl Mech Org* 109 (3):451-454. doi:<https://doi.org/10.1007/bf02080806>
- Ghosh M, Bandyopadhyay M, Mukherjee A (2010) Genotoxicity of titanium dioxide (TiO₂) nanoparticles at two trophic levels: Plant and human lymphocytes *Chemosphere* 81:1253–1262
- Glasser O, Barth H (1938) Studies on the problem of mitogenetic radiation. *Radiology* 30 (1):62-67. doi:<https://doi.org/10.1148/30.1.62>
- Guillery H (1928) Über Bedingungen des Wachstums auf Grund von Untersuchungen an Gewebekulturen. *Virchows Archiv für pathologische Anatomie und Physiologie und für klinische Medizin* 270 (2):311-359. doi:<https://doi.org/10.1007/bf01892371>
- Gurwitsch A (1927) Einige Gedanken über die Zellteilung als Wundreaktion. *Deutsch-Russische Medizinische Zeitschrift* 6: 345-348

- Gurwitsch A (1936). *Protoplasma* 26:23
- Gurwitsch A, Gurwitsch L (1925) Weitere Untersuchungen über mitogenetische Strahlungen. *Archiv für mikroskopische Anatomie und Entwicklungsmechanik* 104 (1):109-115. doi:<https://doi.org/10.1007/bf02108493>
- Gurwitsch A, Gurwitsch L (1927) Zur Analyse der Latenzperiode der Zellteilungsreaktion. 19 Mitteilung über mitogenetische Strahlung und Induktion. *Wilhelm Roux' Archiv für Entwicklungsmechanik der Organismen* 109 (3):362-379. doi:<https://doi.org/10.1007/bf02080801>
- Gurwitsch AA (1934a) L'excitation mitogénétique du système nerveux central. *Ann de Physiol et Physicochim Biol* 10 (5):1153-1165
- Gurwitsch AA (1968) [The problem of mitogenetic emission as an aspect of molecular biology] *Problema mitogeneticheskogo izlucheniya kak aspekt molekuliarnoj biologii* (in Russian). Meditsina, Leningrad
- Gurwitsch AA (1988) A Historical Review of the Problem of Mitogenetic Radiation. *Experientia* 44 (7):545-550. doi:<https://doi.org/10.1007/Bf01953301>
- Gurwitsch AG (1923) Die Natur des spezifischen Erregers der Zellteilung. *Archiv für mikroskopische Anatomie und Entwicklungsmechanik* 100 (1-2):11-40. doi:<https://doi.org/10.1007/bf02111053>
- Gurwitsch AG (1924a) Les problèmes de la mitose les rayons mitogéniques. *Bulletin d'histologie appliquée a la physiologie et a la pathologie et de technique microscopique* 1 (11):486-497
- Gurwitsch AG (1924b) Physikalisches über mitogenetische Strahlen. *Archiv für mikroskopische Anatomie und Entwicklungsmechanik* 103 (3-4):490-498. doi:<https://doi.org/10.1007/bf02107498>
- Gurwitsch AG (1925) The Mitogenetic Rays. *Botanical Gazette* 80 (2): 224-226. doi:<https://doi.org/10.1086/333527>
- Gurwitsch AG (1926) Das Problem der Zellteilung physiologisch betrachtet, vol 11. Monographien aus dem Gesamtgebiet der Physiologie der Pflanzen und der Tiere. Julius Springer, Berlin
- Gurwitsch AG (1928a) Einige Bemerkungen zur vorangehenden Arbeit von Herrn B. Rossmann. *Wilhelm Roux' Archiv für Entwicklungsmechanik der Organismen* 113 (2):406-413
- Gurwitsch AG (1928b) Some problems of mitogenetic radiation (In Russian). *Journal of Russian Botanical Society* 13:179-189
- Gurwitsch AG (1929a) Methodik der mitogenetischen Strahlenforschung. In: Abderhalden E (ed) *Handbuch der biologischen Arbeitsmethoden*, vol V, vol 2/2. Urban & Schwarzenberg, Berlin, Wien, pp 1401-1470
- Gurwitsch AG (1929b) Über den derzeitigen Stand des Problems der mitogenetischen Strahlung. *Protoplasma* 6 (3):449-493. doi:<https://doi.org/10.1007/BF01604837>
- Gurwitsch AG (1934b) Der gegenwärtige Stand des mitogenetischen Problems. Paper presented at the Atti del I Congresso Internazionale di electro-radio-biologia 2:689-704
- Gurwitsch AG (1937) Some problems of mitogenesis (in Russian). *Archive of Biological Sciences* 46 (3):3-10
- Gurwitsch AG, Eremeev VF (1947) A contribution to the principles of the mitogenetic method. In: Gurwitsch AG (ed) *Collected volume on mitogenesis and theory of biological field*. Pub.house of the USSR Academy of Medical Sciences, Moscow, pp 5-19
- Gurwitsch AG, Frank GM (1927) Sur les rayons mitogénétiques et leur identité avec les rayons ultraviolets. *Comptes rendus des séances de l' Académie des Sciences* 184:903-904
- Gurwitsch AG, Gurwitsch LD (1928) Zur Energetik der mitogenetischen Induktion und Zellteilungsreaktion. 26 Mitteilung über mitogenetische Strahlung und Induktion. *Wilhelm Roux' Archiv für Entwicklungsmechanik der Organismen* 113 (4): 740-752. doi:<https://doi.org/10.1007/bf02252024>
- Gurwitsch AG, Gurwitsch LD (1932) Die mitogenetische Strahlung, vol 25. Monographien aus dem Gesamtgebiet der Physiologie der Pflanzen und der Tiere. Springer-Verlag Berlin Heidelberg, Berlin. doi:<https://doi.org/10.1007/978-3-662-26146-0>
- Gurwitsch AG, Gurwitsch LD (1934a) Das Mitogenetische Regime der Krebszelle. *Acta Cancrologica* (Budapest) 1 (2):6-18
- Gurwitsch AG, Gurwitsch LD (1934b) Mitogeneticheskoe izlucheniye [Mitogenetic radiation] (in Russian). VIEM publishing house, Leningrad
- Gurwitsch AG, Gurwitsch LD (1935) Mitogenetic method, its theoretical basis and application area (in Russian). *Bulletin of All-Union Institute of Experimental Medicine* (6-7):29-32
- Gurwitsch AG, Gurwitsch LD (1945) [Mitogenetic radiation: physical and chemical bases and applications in biology and medicine] *Mitogeneticheskoe izlucheniye: fizikokhimeskije osnovy i prilozheniya v biologii i meditsine* (in Russian). Medgiz, Moscow
- Gurwitsch AG, Gurwitsch LD (1948) [An introduction to the teaching of 1943 mitogenesis] *Vvedeniye v ucheniye o mitogeneze* (in Russian). USSR Academy of Medical Sciences Publishing House, Moscow
- Gurwitsch AG, Gurwitsch LD (1999) *Twenty Years of Mitogenetic Radiation: Emergence, Development, and Perspectives* (translation from *Uspekhi Sovremennoi Biologii* [Advances in Contemporary Biology], 1943, 16(3):305-334). *21st Century Science and Technology Magazin* 12 (3):41-53
- Gurwitsch AG, Gurwitsch LD, Zalkind SY, Pesochensky BS (1947) [The teaching of the cancer quencher: Theory and clinics] *Ucheniye o rakovom tushitele: Teoriya i klinika* (in Russian). USSR Academy of Medical Sciences Press, Moscow
- Gurwitsch AG, Gurwitsch N (1924) Fortgesetzte Untersuchungen über mitogenetische Strahlung und Induktion. *Archiv für mikroskopische Anatomie und Entwicklungsmechanik* 103 (1):68-79. doi:<https://doi.org/10.1007/bf02107090>
- Gurwitsch L, Anikin A (1928) Das Cornealepithel als Detektor und Sender mitogenetischer Strahlung. 25 Mitteilung über mitogenetische Strahlung und Induktion. *Wilhelm Roux' Arch Entwickl Mech Org* 113 (4):731-739. doi:<https://doi.org/10.1007/bf02252023>
- Gurwitsch LD (1922) Zur Analyse der Arbeit der Nervenzelle. *Pflüger's Archiv für die gesamte Physiologie des Menschen und der Tiere* 197 (1/2):147-158
- Gurwitsch LD, Salkind S (1929) Das mitogenetische Verhalten des Blutes Carcinomatoser. *Biochemische Zeitschrift* 211 (1-3):362-372
- Haempel O, Lechler H (1931) Über die Wirkung von ultravioletter Bestrahlung auf Fischeier und Fischbrut. *Zeitschrift für vergleichende Physiologie* 14 (1):265-272. doi:<https://doi.org/10.1007/BF00348222>
- Herman PK (2002) Stationary phase in yeast. *Current opinion in microbiology* 5 (6):602-607
- Hollaender A (1936) The problem of mitogenetic rays. In: Duggar B (ed) *Biological effects of radiation*, vol 2. 1 edn. McGraw-Hill Book Company, Inc., NY, London, pp 919-958
- Hollaender A, Claus WD (1937) An experimental study of the problem of mitogenetic radiation, vol 100. *Bulletin of the National research council*. National research council of the National academy of sciences, Washington
- Hollaender A, Schoeffel E (1931) Mitogenetic rays. *The Quarterly Review of Biology* 6 (2):215-222
- Julius HW (1935) Do mitogenetic rays have any influence on tissue-cultures? *Acta brevia Neerlandica* 5 (3/4):51-52
- Kaufmann B, Gay H, Hollaender A (1944) Distribution of mitoses in the corneal epithelium of the rabbit and the rat. *The Anatomical record* 90 (2):161-178. doi:<https://doi.org/10.1002/ar.1090900210>
- Khruschov GK (1934) Mitogenetic macroeffect in tissue cultures (In Russian). *Archive of Biological Sciences Ser B* 35 (1):317-324
- Kisliak-Statkewitsch M (1927) Das mitogenetische Strahlungsvermögen des Kartoffelleptoms. *Wilhelm Roux' Archiv für Entwicklungsmechanik der Organismen* 109 (2):283-286. doi:<https://doi.org/10.1007/bf02079703>

- Konev SV (1967a) Electronic Excited States of Biopolymers and Dark Biology (Chapter 7). In: Konev SV (ed) Fluorescence and Phosphorescence of Proteins and Nucleic Acids. Plenum Press, New York, pp 177-191. doi:https://doi.org/10.1007/978-1-4684-0700-6_9
- Konev SV (1967b) Fluorescence and Phosphorescence of Proteins and Nucleic Acids. Plenum Press, New York
- Konev SV, Lyskova TI (1966) On the effect of UV rays of ultra weak intensities on cell division and glycolysis (In Russian). In: Dantsig NM (ed) [Ultraviolet radiation] Ul'trafiol'etovoje izluchenije. Meditsina, Moscow, pp 118-121
- Kornfeld W (1922) Über den Zellteilungsrythmus und seine Regelur Archiv für Entwicklungsmechanik der Organismen 50:526-592
- Kreuchen KH, Bateman JB (1934) Physikalische und biologische Untersuchungen über mitogenetische Strahlung. Protoplasma 22 (1):243-273. doi:<https://doi.org/10.1007/bf01608868>
- Lasnitzki A, Klee-Rawidowicz E (1931) Zur Frage der "mitogenetischen" Induktion von Warmblüterzellen. Zeitschrift für Krebsforschung 34 (1):518-525. doi:<https://doi.org/10.1007/bf01625393>
- Lebedev PV, Melnikova MF, Utkina IA (1971) Diurnal rhythm of mitotic activity in the apical meristem of bromes shoot (In Russian). Cytologia 8 (5):584-592
- Levan A (1938) The effect of colchicine on root mitoses in *Allium Heredias* (24):9-26
- Loos W (1930) Untersuchungen über mitogenetische Strahlen. Jahrb Wiss Bot 72 (4):611-664
- Lopez-Saez JF, Gonzalez-Bernaldez F, Gonzalez-Fernandez A, Garcia Ferro C (1969) Effect of temperature and oxygen tension on root growth, cell cycle and cell elongation. Protoplasma 67:213-221
- Magrou J (1928) Action à distance du Bacterium tumefaciens, sur le développement de l'oeuf d'oursin. Comptes Rendus Acad Sci 186: 802
- Magrou J (1930a) Actions biologiques à distance 1. – Les faits. Bulletin de d'Institut Pasteur 28 (9):393-405
- Magrou J (1930b) Actions biologiques à distance 2. – Les interprétations. Bulletin de d'Institut Pasteur 28 (10):441-448
- Magrou J (1934) Contribution à l'étude des actions à distance en biologie. Archive of Biological Sciences, Ser B 35 (1):297-302
- Magrou J, Magrou M (1927a) Radiations émises par le Bacterium tumefaciens. Rev Path Veg Ent Agr 14:244-244
- Magrou J, Magrou M (1927b) Radiations mitogénétiques et genèse des tumeurs. Comptes Rendus Acad Sci 184:963-965
- Magrou MJ, Magrou MM, Reiss MP (1929) Action à distance de divers facteurs sur le développement de l'oeuf d'Oursin. Comptes Rendus Acad Sci 189:779
- Magrou MJ, Magrou MM, Roubaud ME (1931) Action stimulante à distance, exercée par certaines suspensions bactériennes, à travers le quartz, sur l'éclosion du moustique de la fièvre jaune. Comptes Rendus Acad Sci 192:1134
- Maxia C (1929) Intensificazione della segmentazione di uova di *Paracentrotus lividus* sotto l'influenza di radiazioni mitogenetiche. R Comitato talassografico italiano 155:3-23
- Maxia C (1930) Gli anelli di Liesegang adoprati come detectori negli studi sulle radiazioni mitogenetiche. Atti della Società fra i Cultori delle Scienze Mediche e Naturali in Cagliari, 32 (5):194-198
- Maxia C (1932) Effetti diversi di radiazioni e di gas sugli anelli di Liesegang. Radiobiologia 1 (1):39-48
- Maxia C (1935) Die Wahl der Teste für den Gurwitsch-Effekt. Protoplasma 23 (1):77-80. doi:<https://doi.org/10.1007/bf01603332>
- Maxia C, Leone P (1931) Reazioni di glicolisi e proteolisi e radiazioni mitogenetiche: esperimenti sul latte. Atti della Società fra i Cultori delle Scienze Mediche e Naturali in Cagliari 33:293-294
- Maxia C, Vacca A (1931) Ulteriori studi sulla segmentazione di uova di *Paracentrotus lividus* sotto l'influenza di radiazioni mitogenetiche e di olii eteri. R. Comitato Talassografico Italiano 187
- Moissejewa M (1929) Gurwitsch's mitogenetic rays (In Ukrainian). Ukrainian Botanical Review [Ukrainskyi botanichnyi zhurnal] (5): 41-55
- Moissejewa M (1931a) Zur Theorie der Mitogenetischen Strahlung I. Biochemische Zeitschrift 241:1-13
- Moissejewa M (1931b) Zur Theorie der Mitogenetischen Strahlung II. Biochemische Zeitschrift 243 (1-3):67-87
- Moissejewa M (1932a) More about mitogenetic radiation (in Ukrainian). Visnyk Kyi'vs'kogo botanichnogo sadu [Bulletin of Kiev Botanical Garden] (14):1-15
- Moissejewa M (1932b) Zur Theorie der mitogenetischen Strahlung III. Biochemische Zeitschrift 251:133-140
- Moissejewa MN (1960) [Mitogenetic rays and mitogenetic methods] Mitogeneticheskije luchi i mitogeneticheskij metod (in Russian). Abstract of dissertation (Doctor of Biological Sciences). Kiev
- Nakaidzumi M, Schreiber H (1931) Untersuchungen über das mitogenetische Strahlungsproblem II. Biochemische Zeitschrift (237):358-379
- Naumova EV, Belousov LV, Vladimirov YA, Tuchin VV, Volodyaev IV (2021) Methods of studying ultraweak photon emission from biological objects: I. History, types and properties, fundamental and application significance. Biophysics 66 (5):764-778. doi:<https://doi.org/10.1134/S0006350921050158>
- Naumova EV, Naumova AE, Isaev DA, Volodyaev IV (2018) Historical review of early researches on mitogenetic radiation: from discovery to cancer diagnostics. Journal of Biomedical Photonics & Engineering 4 (4):040201. doi:<https://doi.org/10.18287/JBPE18.04.040201>
- Naville A (1929) Les rayons mitogénétiques. Exposé de quelques résultats. Revue Suisse de Zoologie 36:213-215
- Naville A (1937) Recherches statistiques sur le caryoquinèse sous l'influence de divers facteurs. Arch biol 48:1-28
- Ozel CA, Ozkul M, Unal F, Yuzbasioglu D (2018) Evaluation of genotoxicity of picloram by Allium test in plant tissue culture. Fresenius environmental bulletin 27 (12):8133-8138
- Özkara A (2019) Assessment of cytotoxicity and mutagenicity of insecticide Demond EC25 in *Allium cepa* and Ames Test. Caryologia International Journal of Cytology, Cytosystematics and Cytogenetics 72 (2):21-27. doi:<https://doi.org/10.13128/caryologia-698>
- Pallavi S, Singh M, Rathore HS, Sharma A, Makwana M, Shrivastava S (2008) An Evaluation of the Genotoxic Effects of the Seed Decoction of Cassia tora Linn. (Leguminosae) in an *Allium cepa* Model. Ethnobotanical Leaflets 12:927-933
- Paul M (1933) Zwiebelwurzeln als Detektoren bei Untersuchungen über die Mitogenetische Strahlung. Wilhelm Roux' Archiv für Entwicklungsmechanik der Organismen 128 (1):108-165. doi:<https://doi.org/10.1007/bf00578946>
- Pesochensky BS (1942) The phenomenon of the mitogenetic radiation quenching in blood in cancer and "precancer": Dr. Med. Sci. Dissertation (in Russian). Leningrad Oncological Institute, Leningrad
- Pesochensky BS (1947) Quenching of mitogenetic radiation of blood in cancer and precancerous diseases (In Russian). In: Gurwitsch AG (ed) [Collected volume on mitogenesis and theory of biological field] Sbornik rabot po mitogenezu i teorii biologicheskogo polya. Pub.house of the USSR Academy of Medical Sciences, Moscow, pp 102-114
- Ponomareva JN (1939) Stimulation of mitoses in surviving tissues by physical methods (In Russian). Archive of Biological Sciences 55 (2):108-118
- Ponomareva YN (1934) Direct impact of mitogenetic radiation on the course of the mitosis (reaction of corneal epithelium) (In Russian). Archive of Biological Sciences, Ser B 35 (1):239-248
- Ponomareva YN (1936) Mitogenetic and thermal effect on the mitotic rate of survival cells (In Russian). Bulletin of experimental biology and medicine 2 (1):16-18
- Ponomareva JN (1947) Inhibition of mitoses by treating the cells with quenchers and extinguishers (In Russian). In: Gurwitsch AG

- (ed) [Collected volume on mitogenesis and theory of biological field] Sbornik rabot po mitogenezu i teorii biologicheskogo polya. Pub. house of the USSR Academy of Medical Sciences, Moscow, pp 131-136
- Potozky A (1930) Über Beeinflussung des mitogenetischen Effekts durch sichtbares Licht. *Biologisches Zentralblatt* 50:712-723
- Potozky A (1932) Die Beeinflussung des mitogenetischen Effektes durch sichtbares Licht. Zweiter Teil: Analyse des Effektes. *Biologisches Zentralblatt* 52 (3):129-138
- Protti G (1930) Involuzione senile, oncogenesi e radiazioni ematiche – Esperienze col sarcoma Galliera (Comunicazione alla XIX riunione della Società Italiana per il progresso delle Scienze Venezia Tridentina – Settembre 1930 – VIII).
- Puhalsky VA, Solovyov AA, Badaeva ED, Yurtsev VN (2013) [Practical course on plant cytology and cytogenetics] Praktikum po tsitologii i tsitogenetike rastenij (In Russian). Coloss, Moscow
- Quickenden TI, Matich AJ, Pung SH, Tilbury RN (1989) An attempt to stimulate cell division in *Saccharomyces cerevisiae* with weak ultraviolet light. *Radiat Res* 117 (1):145-157. doi:<https://doi.org/10.2307/3577283>
- Quickenden TI, Tilbury RN (1985) An attempt to stimulate mitosis in *Saccharomyces cerevisiae* with the ultraviolet luminescence from exponential phase cultures of this yeast. *Radiation Research* 102: 254-263
- Rahn O (1934a) The disagreement in mitogenetic experiments, a problem in bacterial physiology. *Journal of bacteriology* 28 (2):153-158
- Rahn O (1934b) The physico-chemical basis of biological radiations. In: Cold Spring Harbor Symposia on Quantitative Biology, vol. 2 Berlin, pp 226-240. doi:<https://doi.org/10.1101/SQB.1934.002.01.029>
- Rahn O (1936) Invisible radiations of organisms, vol 9. Protoplasma-Monographien. Gebrüder Bornträger, Berlin
- Rahn O (1937) Mitogenetic radiation. *Tabulae biologicae* 14 (1):1-35
- Rawin W (1924) Weitere Beiträge zur Kenntnis der mitotischen Ausstrahlung und Induktion. *Archiv für Mikroskopische Anatomie und Entwicklungsmechanik* 101 (1/3):53-61
- Reiter T, Gabor D (1928a) Ultraviolette Strahlen und Zellteilung. *Strahlentherapie* (28):125-131
- Reiter T, Gabor D (1928b) Zellteilung und Strahlung. Sonderheft der Wissenschaftlichen Veröffentlichungen aus dem Siemens-Konzern. Springer-Verlag, Berlin. doi:<https://doi.org/10.1007/978-3-642-50832-5>
- Reiter T, Gabor D (1931) Der heutige Stand des Problems der Gurwitsch-Strahlen. *Arch Exp Zellforsch* 11:21-32
- Remacle-Dath MT (1966) Mise en évidence des variations journalières de l'activité mitotique au niveau du méristème caulinaire de *Sinapis alba* L. . *Bull Soc Royale Sci Liege* 35 (3-4):315-321
- Richards OW, Taylor GW (1932) "Mitogenetic rays" – a critique of the yeast-detector method. *The Biological Bulletin* 63 (1):113-128
- Rodionov SF, Frank GM (1934) Voprosy svetobiologii i izmereniya sveta. [Problems of Light Biology and Light Measurement] (In Russian). Gostekhizdat, Moscow-Leningrad
- Rosculete CA, Bonciu E, Rosculete E, Olaru LA (2018) Determination of the Environmental Pollution Potential of Some Herbicides by the Assessment of Cytotoxic and Genotoxic Effects on *Allium cepa*. *Int J Environ Res Public Health* 16 (1):75. doi:<https://doi.org/10.3390/ijerph16010075>
- Rossmann B (1928) Untersuchungen über die Theorie der mitogenetischen Strahlen. *Wilhelm Roux' Archiv für Entwicklungsmechanik der Organismen* 113 (2):346-405. doi:<https://doi.org/10.1007/bf02081074>
- Rossmann B (1929) Mitogenetische Induktionsversuche mit Hefe als Indikator. *Wilhelm Roux' Archiv für Entwicklungsmechanik der Organismen* 114 (4):583-586. doi:<https://doi.org/10.1007/bf02078920>
- Rostovtseva ZP (1969) Apical meristem. Moscow State University Press, Moscow
- Rusinoff PG (1925) Weitere Untersuchungen über mitogenetische Strahlen und Induktion. *Archiv für mikroskopische Anatomie und Entwicklungsmechanik* 104 (1):121-124. doi:<https://doi.org/10.1007/bf02108495>
- Ruyssen R (1933) Sur l'énergie et les limites de longueur d'onde des rayons mitogénétiques. *Acta Brev Neerl* (3):141-142
- Salkind S (1929) Über den Rhythmus der mitogenetischen Strahlung bei der Entwicklung des Seeigelees. *Wilhelm Roux' Archiv für Entwicklungsmechanik der Organismen* 115 (1):360-362. doi:<https://doi.org/10.1007/bf02080426>
- Salkind S, Ponomarewa J (1934) Der unmittelbare Einfluss der mitogenetischen Strahlen auf den Verlauf der Zellteilung. *Radiobiologia* 1 (4):11-27
- Salkind SJ, Schabad LM (1931) Über die mitogenetische Strahlung des experimentellen Teerkrebses. *Zeitschrift für Krebsforschung* 34 (1): 216-227. doi:<https://doi.org/10.1007/bf01625365>
- Savelkoul RMM (1957) Distribution of mitotic activity within the shoot apex of *Elodea densa*. *Amer J Bot* 44 (4):311-317
- Schwarz W (1928) Zur Theorie der mitogenetischen Strahlung. *Biol Zentralbl* 48:302-308
- Schwemmler J (1929) Mitogenetische Strahlen. *Biologisches Zentralblatt* (49):421-437
- Seyfert F (1932) Über den physikalischen Nachweis von mitogenetischen Strahlen. *Jahrb Wiss Bot* (76):747-764
- Siebert WW (1928a) Über die mitogenetische Strahlung des Arbeitsmuskels und einiger anderer Gewebe. *Biochemische Zeitschrift* 202:115-122
- Siebert WW (1928b) Über die Ursachen der mitogenetischen Strahlung. *Biochemische Zeitschrift* 202:123-132
- Siebert WW (1930) Die mitogenetische Strahlung des Blutes und des Harns gesunder und kranker Menschen. *Biochemische Zeitschrift* 226 (4-6):253-256
- Siebert WW, Seffert H (1934) Zur Frage des Physikalischen Nachweis der Gurwitsch-Strahlung. *Archive of Biological Sciences Ser B* 35 (1):177-181
- Sorin AN (1926) Zur Analyse der mitogenetischen Induktion des Blutes. *Wilhelm Roux' Archiv für Entwicklungsmechanik der Organismen* 108 (4):634-645. doi:<https://doi.org/10.1007/bf02080168>
- Stempell W, Romberg G (1932) Anurenkeime als Detektoren für Organismenstrahlen und die Wirkung ultravioletter Strahlen auf die Anurenentwicklung. *Jenaische Zeitschrift für Naturwissenschaft* Herausgegeben von der medizinisch-naturwissenschaftlichen Gesellschaft zu Jena 67:19-36
- Stephens CE (1984) Daily Mitotic Cycle in the Common Onion, *Allium cepa* *Cytologia* 49:679-684
- Sussmanowitsch H (1928) Erschöpfung durch mitogenetische Induktion. 27 Mitteilung über mitogenetische Strahlung und Induktion. *Wilhelm Roux' Archiv für Entwicklungsmechanik der Organismen* 113 (4):753-758. doi:<https://doi.org/10.1007/bf02252025>
- Taylor GW, Harvey EN (1931) The theory of mitogenetic radiation. *Biolog Bull* 61 (3):280-293
- Tedesco SB, Laughinghouse HD (2012) Bioindicator of genotoxicity: the *Allium cepa* test In: Srivastava J (ed) Environmental contamination. InTech, Croatia, pp 137-156
- Tokin BP (1933) [Mitogenetic rays] Mitogeneticheskije luchi (In Russian). State Medical Publishing House,
- Tuthill JB, Rahn O (1933) Zum Nachweis mitogenetischer Strahlung durch Hefesprossung. *Archiv für Mikrobiologie* 4 (1-4): 565-573. doi:<https://doi.org/10.1007/bf00407562>
- Tuthill JB, Rahn O (1934) Analysis of the bud formation of the Baron Method. *Archive of Biological Sciences Ser B* 35 (1):289-296
- Utkina IA, Sinyagina IM (1976) Daily dynamics of mitosis in barley root meristem. In: [Materials on ecology and physiology of plants of Ural flora] Materialy po ekologii i fiziologii rastenij ural'skoj flory Ural State University, Sverdlovsk, pp 42-50

- Vasilyev LL (1925) Biological rays (In Russian). Vestnik znaniya [Herald of knowledge] (19–20):1185-1194
- Vladimirov YA (1967) Ultraweak luminescence accompanying biochemical reactions (English translation of Sverkhslabye svecheniya pri biokhimicheskikh reaktsiyah (In Russian) USSR Academy of Sciences, Institute of Biological Physics. Izdatel'stvo "Nauka" Moscow, 1966). NASA, C.F.S.T.I., Springfield, Vermont
- Volodyaev IV, Belousov LV (2015) Revisiting the mitogenetic effect of ultra-weak photon emission. *Frontiers in physiology* 6 (00241): 1-20. doi:<https://doi.org/10.3389/fphys.2015.00241>
- Volodyaev IV, Belousov LV, Kontsevaya II, Naumova AE, Naumova EV (2021) Methods of studying ultraweak photon emissions from biological objects. II. Methods based on biological detection. *Bio-physics* 66 (6):920–949
- Volodyaev IV, Krasilnikova EN, Ivanovsky RN (2013) CO2 mediated interaction in yeast stimulates budding and growth on minimal media. *PLoS ONE* 8 (4):e62808. doi:<https://doi.org/10.1371/journal.pone.0062808>
- Wagner N (1927) Über den von A. Gurwitsch entdeckten spezifischen Erreger der Zellteilung (mitogenetische Strahlen). *Biol Zentralbl* 47: 670-678
- Wagner N (1928) Die Induktion von Mitosen auf Entfernung. Über die von A. Gurwitsch entdeckten "mitogenetischen Strahlen". *Planta* 5 (1):70–88. doi:<https://doi.org/10.1007/bf01993735>
- Wassermann F (1930) Die Sogenannten Mitogenetischen Strahlen (Gurwitsch-Strahlung). *Klinische Wochenschrift* 9 (10): 433-435. doi:<https://doi.org/10.1007/bf01748371>
- Werner-Washburne M, Braun E, Johnston GC, Singer RA (1993) Stationary phase in the yeast *Saccharomyces cerevisiae*. *Microbiological reviews* 57 (2):383-401
- Wierzbička M, Antosiewicz D (1988) Allium test – some questions *Acta Soc Bot Pol* 57 (2):201-215. doi:<https://doi.org/10.5586/asbp.1988.020>
- Wolff LK (1932) Mitogenetische stralen. *Nederl Tijdschrift voor Geneeskunde* 76 (27):3278-3287
- Wolff LK, Ras G (1931a) Einige Untersuchungen über die mitogenetischen Strahlen von Gurwitsch. *Ztrbl f Bakt I* 123:257-270
- Wolff LK, Ras G (1931b) Über Gurwitsch-Strahlen bei Bakterien. *Acta Brevia Neerlandica de physiologia, pharmacologia, microbiologia* 1 (7):136-137
- Wolff LK, Ras G (1932a) Eenige onderzoekingen over demitogenetische stralen van Gurwitsch. *Ned Tijdschr Hyg* 6: 265-280
- Wolff LK, Ras G (1932b) Über Gurwitschstrahlen bei einfachen chemischen Reaktionen. *Biochemische Zeitschrift* 250:305-307
- Wolff LK, Ras G (1933a) Über mitogenetische Strahlen. V. Über die Methodik zum Nachweis von Gurwitschstrahlen. *Zentralblatt für Bakteriologie, Parasitenkunde und Infektionskrankheiten* 128: 314-319
- Wolff LK, Ras G (1934a) Effect of Mitogenetic Rays on Eggs of *Drosophila melanogaster*. *Nature* 133 (3361):499-499. doi:<https://doi.org/10.1038/133499a0>
- Wolff LK, Ras G (1934b) Études sur le rayonnement suivant Gurwitsch. VI. Le rayonnement secondaire. *K Akad Wetensch* 37 (1):430–445
- Wolff LK, Ras MG (1933b) De Methodiek voor het aantoonen van Gurwitsch-stralen. *Nederl Tijdschrift voor Geneeskunde* 77 (8): 875–881
- Zakrzewski Z (1933) Über die Wirkung der Gurwitsch-Strahlung auf Gewebekulturen in vitro. *Archive für experimentelle Zellforschung besondes Gewebezüchtung* 14:471-478
- Zalkind SY (1934) The problem of mitogenetic radiation II. Sources of radiation. Manifestation of rays in the body (In Russian). *Priroda [Nature]* (3):11-27
- Zalkind SY (1936) Mitogenetic radiation of blood and diagnosis of malignant neoplasms (in Russian). *Soviet Medical Journal* (17): 15-28
- Zalkind SY, Frank GM (1930) [Mitogenetic rays and cell division] Mitogeneticheskije luchi i delenije kletok (In Russian). «Gosizdat», Moscow – Leningrad



Elena V. Naumova and Ilya Volodyaev

21.1 Introduction

As soon as the mitogenetic effect (MGE) was suggested to be mediated by ultraviolet radiation (mitogenetic radiation, MGR), the challenges of its testing by physical methods and studying the MGR physical properties were set. As the history of this research (and the main difficulties along the way) appeared an important separate area, we decided to arrange it here as a special chapter, continuing the logic of Chap. 20, but standing alone and focusing specifically on the MGR physical properties. The current chapter deals with two main research aspects: (1) MGR detection and intensity estimates with photosensitive modifications of Geiger–Müller counters, and (2) MGR spectral analysis.

Importantly, the first years of MGR studies went in parallel with technical development of the Geiger–Müller counters and methods of handling them. The estimated intensity of MGR ($10\text{--}1000\text{ quanta cm}^{-2}\text{ s}^{-1}$) was close to the sensitivity limits of the best devices of that time, and many of the technical nuances and approaches were discovered right along the way. This led to a significant evolution in the results credibility, and has forced us to separate these data by time periods.

Next, as one can easily estimate from the above intensity data, physical detection of MGR spectra was technically impossible, and the authors of spectral works used biological recipients as detectors, pulling the full range of issues and features of biological detection (see Chap. 20). This let the authors observe MGR spectra in the range of 190–280 nm (usually restricted to 190–250 nm).

Other physical qualities of MGR (temporal characteristics, directivity, polarization) have not been seriously studied, and therefore, for lack of data, we only briefly mention them here and not in the main text.

Temporal characteristics. MGR was often described as temporally organized, consisting of short flashes; however, the only basis underlying this reasoning was the “intermittent induction” data, namely, that periodical shielding of the recipient from the inductor enhanced the observed MGE (see Sect. 20.1.3). While this may hint at an irregular temporal structure of MGR (its periodicity or even aperiodicity), it can in no way be regarded as proof. Thus, as we found no physical data on this topic, this aspect is not discussed in this chapter.

Directivity of MGR was studied only in a few early works with onion roots (for instance, Gurwitsch (1928)). A precise mutual positioning of the inductor and the recipient (with the inductor root tip pointing to the recipient root meristem) was found necessary for observing MGR, which led the authors to a conclusion that MGR is narrow-beamed. However, the requirement of precise mutual positioning of roots itself hardly proves MGR directivity, at least in this form. Both roots have surfaces of high curvatures and when the tip of the inductor is directed precisely to the axis of the root recipient, the energy transfer is more effective even if the cells emit omnidirectional radiation

Of course, in case of isotropic systems (pulp of onion or carcinoma, liquid chemical systems, or liquid microbial cultures), there were no needs to study directionality of MGR, and these issues were never mentioned.

Polarization of MGR was not studied as far as we know. First, there were no reasons to expect any preferential orientation of elementary emitters in most of the inductors studied (like liquid microbial cultures, pulps, or liquid chemical systems), and, thus, linear polarization was out of question. Second, circular polarization (which had already been related to chaotically oriented chiral sources (Pasteur 1850; Lindman 1920)) could not be technically distinguished from nonpolarized emission, at least in the UV range. Finally, the very intensity of MGR was estimated as so low that most of these kinds of questions did not even arise.

For a specific type of MGR called secondary radiation (see Chap. 22), the *propagation velocity* was also studied.

E. V. Naumova (✉)

Rzhanov Institute of Semiconductor Physics, Siberian Branch of the Russian Academy of Sciences, Novosibirsk, Russia

I. Volodyaev

Moscow State University, Moscow, Russia

However, we do not consider it in this chapter as it is not a physical parameter of radiation in the strict sense, but an averaged characteristic of the complex process based on elementary acts of photon absorption, radiation, and chemical reactions in between.

21.2 Physical Detection of Mitogenetic Radiation and Intensity Estimates

21.2.1 The First Attempts of MGR Objective Detection

21.2.1.1 Biological MGR Detection: Merits and Demerits

As discussed in Chaps. 2 and 20, the very notion of mitogenetic radiation (MGR) originated from the effect it produced on biological systems, i.e., specific stimulation of mitoses. Yet, this was not the only biological effect reported from MGR. Other MGR-stimulated effects included: increase of membrane permeability (Potozky 1936), appearance of deformities at embryo development (Magrou et al. 1929), etc. (see Chap. 20), but they have not found wide application for MGR detection.

Biological detectors were useless to estimate the MGR absolute intensity, as the effect could only be evaluated in the yes–no regime. Thus, one could compare MGR intensity from different sources only relatively, by testing MGE from them with the same type of detector (usually, identical yeast cultures) (Blacher and Holzman 1930; Gurwitsch and Gurwitsch 1934b, 1945, 1959) and all conditions as identical as possible, except for a variation of the exposure time. Each inductor was characterized by the minimal exposure time required to produce MGE, and shorter threshold exposure times were supposed to indicate greater MGR intensities.

The main and the only advantage of biological detectors was that they had superior sensitivity, comparing to any other ultraweak photon emission (UPE) detectors of that time. In fact, it was this extremely high sensitivity of biological detectors that made possible the very discovery of MGR.

Yet, biological detectors had innate variability and demonstrated high vulnerability to the influence of external environmental conditions and preceding cultivation. Biological detection of MGR was time-consuming, exacting, and laborious and required experience.

21.2.1.2 Detection by Means of Specific Physicochemical Effects: Unsuccessful Attempts

Skepticism about biological detectors and increasing interest to MGR pushed the search of novel physical and chemical effects for its detection. The MGR was claimed to damp formation of Liesegang rings (concentric circles of

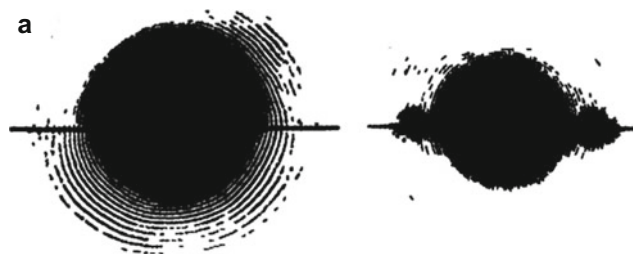


Fig. 21.1 Influence of mitogenetic radiation on Liesegang rings (Stempell 1932). Onion pulp in metal tube with a slit (marked with a line) was used as a source of radiation. Liesegang rings were formed at precipitation of silver chromate in gelatine. (a) exposure through cellophane, which is nontransparent for UV radiation, (b) exposure through a UV-transparent quartz plate. (Reprinted from Rahn (1936). Copyright 1936, with permission from Springer Nature)

precipitate formed at certain reactions, under specific conditions, including the absence of convection) as seen in Fig. 21.1 ((Stempell 1929; Stempell and Romberg 1931), (Stempell 1932) as cited in Rahn (1936)), enhance hydrogen peroxide decomposition ((Stempell 1931), (Stempell 1932) as cited in Hollaender and Claus (1935)), and to accelerate flocculation of unstable colloidal solutions (charged sols of inorganic substances flocculating after the addition of neutral salts) (Heinemann 1934, 1935). The methods of MGR detection based on these effects demonstrated no less drawbacks than biological detectors including the extreme susceptibility to multiple external factors difficult to avoid, that made results doubtful. The Liesegang rings method stirred more active discussion and several series of experiments, both positive (Stempell 1929, 1932; Stempell and Romberg 1931; Zirpolo 1932) and negative (Gigon and Noverraz 1930; Iterson and Heide 1930; Siebert 1930, 1931b; Tokin 1930, 1931a, b, 1933).¹ Other claimed effects were tested in very few works (see more details on these unsuccessful attempts in Rahn (1936) and Hollaender and Claus (1935)).

21.2.1.3 Photographic and Standard Photoelectric Methods: Insufficient Sensitivity

Technically, in the 1920s–1930s, there were two possible approaches to detect weak UV radiation: photographic plates and photoelectric cells. Almost all the leading researchers in this field made attempts to detect MGR by photographic method and failed (see Rahn 1936). Reiter and Gabor (Reiter and Gabor 1928b) were the first who reported positive results with photographic plates, but they pointed out that their data

¹See also some more critique of the method and discussion of factors influencing formation of the Liesegang rings in Maxia (1930, 1932), Schreiber (1933) and Tokin (1933). The extreme susceptibility to multiple external factors making results doubtful was admitted even in some positive works, for instance, Zirpolo (1932).

were only preliminary, these experiments were very few and could not be taken as solid evidence. A number of other researchers claimed successful detection of MGR from biological sources and biochemical models by photographic method as well ((Protti 1932; Copisarow 1932, 1934), (Brunetti and Maxia 1930; Protti 1930; Čech 1932a, b) as cited in Hollaender (1936), Vaccari (1932a, b) as cited in Bateman (1935)).

However, they were offset by a number of negative experiments with photoplates which were mostly more convincing ((Rossmann 1928; Loos 1930; Taylor and Harvey 1931), (Petri 1928; Magrou 1930; Elger 1932; Hauer 1932) as cited in Bateman (1935)). Most probably, the spurious results with photographic plates related to the influence of chemical factors not taken into account, as it was suggested in Taylor and Harvey (1931), or were due to the insufficient darkening. Some positive results were undoubtedly rejected later (Protti 1930b; Brunetti and Maxia 1930).

In some cases, the used MGE inductors were proved not radiating under reported conditions. For instance, growing yeast was found to radiate only in the presence of visible light, and not in the complete darkness (Potozky 1930), which had to be strictly observed when using photoplates.

Among the attempts to detect UV-UPE with photographic method, Lepeschkin's experiments on the so-called necrobiotic radiation are considered in more detail to show significant problems with unambiguous interpretation of results (see Sect. 22.3).

Actually, the negative experiments with photoplates gave a very rough upper estimate for MGR intensity. Indeed, linear summation of radiation dose is not valid for very low intensities and long exposures, and the threshold sensitivity estimate for photographic plates was too coarse.

Sensitivity of photocells was not sufficient for the MGR detection either, as it was shown by several researchers ((Vaccari 1932a, b) as cited in Bateman (1935) and Chariton et al. (1930)). The upper limit of MGR intensity was estimated from the negative experiments with photocells as $<10^5$ quanta $\text{cm}^{-2} \text{s}^{-1}$ (Chariton et al. 1930).

Also, L. Petri made attempts to detect MGR by using a very sensitive microelectroscope connected to a cadmium photocell (Petri 1932, 1933). He reported its discharge rate accelerated up to 30–35% under exposure to germinating wheat (Petri 1933) (it should be noted that L. Petri used photocell in the usual low-voltage mode not producing electron avalanche, contrary to the photocells used as modified Geiger–Müller counters described below). These results were doubted because of the absence of proper statistics and protocols (Bateman 1935).

21.2.2 MGR Detection with Photosensitive Gas-Discharge Counters: The Development Stage (1930–1934)

21.2.2.1 The Geiger–Müller Counters and Their UV-Sensitive Modifications

The first detectors that confidently showed ultraweak UV radiation from biological objects and chemical systems were modified gas-discharge (Geiger–Müller) counters.

The operation principle of gas-discharge counters was suggested and proved by detecting individual α -particles by H. Geiger and E. Rutherford in 1908 (Rutherford and Geiger 1908; Geiger 1913a, b). Practical devices that found wide application as detectors of different ionizing particles were developed two decades later by W. Müller under supervision of H. Geiger (Geiger and Müller 1928a, b).

Possibility to detect UV radiation with gas-discharge counters was shown by P. Pringsheim (Pringsheim 1913) and independently by W. Gerlach and E. Meyer (Gerlach and Meyer 1913). They irradiated the point cathode (Pt) of Geiger sensors with UV light, photoelectrons accelerated and caused ionization, electric discharges were counted. Yet, such devices were unable to detect ultraweak photon emission, because the photocathode had a very small area.

The first attempt to detect ultraweak radiation (from artificial sources) was undertaken by J. Elster and H. Geitel who used standard photocells with potassium cathode as Geiger counters and demonstrated possibility to detect blue light corresponding to the maximal spectral sensitivity of potassium cathodes, with intensity as low as 650 quanta $\text{cm}^{-2} \text{s}^{-1}$ (Elster and Geitel 1916). Their device had high instability and dark currents and, therefore, did not find practical application.

B. Rajewsky was the first who made a working version of the detector for ultraweak UV radiation and detected MGR from biological objects by adequate physical method (Rajewsky 1930a, 1931b, c) (see also his further works (Rajewsky 1931a, 1932)).² His device was based on the Geiger–Müller counter. The main differences of Rajewsky's design from a usual Geiger–Müller sensor were the cathode material showing photoeffect in the UV range, and a quartz window that allowed radiation to hit the cathode. The internal side of the cathode tube was plated with cadmium, the anode wire was strained along the tube axis on the insulators (Fig. 21.2).

²It is worth noting that B. Rajewsky started this work with prejudice against the very existence of MGR: "At that time (about 2 years ago) my attitude to the question about the radiation nature of the phenomena discovered by Gurwitsch was frankly a negative one. It was based partly on contradicting results of the studies published by different authors, partly on concerns about the methodological side and the evaluation of the test results in some studies." (Rajewsky 1932)

Fig. 21.2 Photosensitive modification of the Geiger–Müller counter proposed by B. Rajewsky (Rajewsky 1931c). (Adapted from Rahn (1936). Copyright 1936, with permission from Springer Nature)

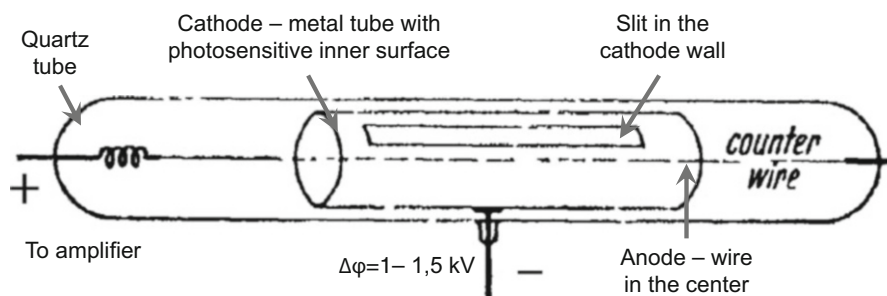


Table 21.1 Detection of ultraweak radiation from murine Ehrlich carcinoma pulp with a modified Geiger–Müller counter. Automatic reading of counts is taken over 2 min periods

| Total time of count | Total number of counts | Number of counts per minute | | Difference | Effect in % of control intensity | Limit of random errors (estimated as 3 standard deviations) |
|---------------------|------------------------|-----------------------------|----------------|------------|----------------------------------|---|
| | | without carcinoma | with carcinoma | | | |
| 104 min | 3058 | 25.4 | 31.7 | 6.3 | 25.2 | 12.5 |

Adapted from Rajewsky (1932). Copyright 1932, with permission from Springer Nature

Using this device, B. Rajewsky detected radiation from a number of known inductors of MGE: onion roots and pulp, carcinomas, etc. Besides that, while searching for the MGR biochemical background, he demonstrated ultraweak UV radiation from aqueous solutions of albumen under various impacts (thermal coagulation, decomposition by acid or by bombardment with alpha-particles), etc. (see an example of Rajewsky's results in Table 21.1).

Notably, B. Rajewsky reported that his design allowed sensing radiation as weak as $12 \text{ quanta cm}^{-2} \text{ s}^{-1}$ (Rajewsky 1932), which is the lowest threshold reported for MGR detection.

All the further modifications of gas-discharge counters used to detect MGR also represented some combinations of a Geiger–Müller counter and a photocell. Some devices were more like Geiger–Müller tubes provided with a sensitive photocathode and a quartz window, like B. Rajewsky's device (see Fig. 21.3), others were designed like a photocell operated in the gas-discharge regime (see the design by S. Rodionov and G. Frank in Fig. 21.4).

However, the operation principle of photon detection was generally the same as in the first device by B. Rajewsky. The potential difference between the cathode and the anode of the counter in operation mode is slightly less than the discharge voltage. The detected UV radiation falls onto the photosensitive cathode (A in Figs. 21.3 and 21.4) through the quartz window (Q in Figs. 21.3 and 21.4) and knocks out an electron. The ejected photoelectron is accelerated by high electric field in the gas media between the cathode and the anode (A and B in Figs. 21.3 and 21.4) and ionizes molecules at collisions. Being accelerated, the secondary electrons also ionize gas and thus give rise to an electron avalanche (Townsend avalanche). Discharge is registered as

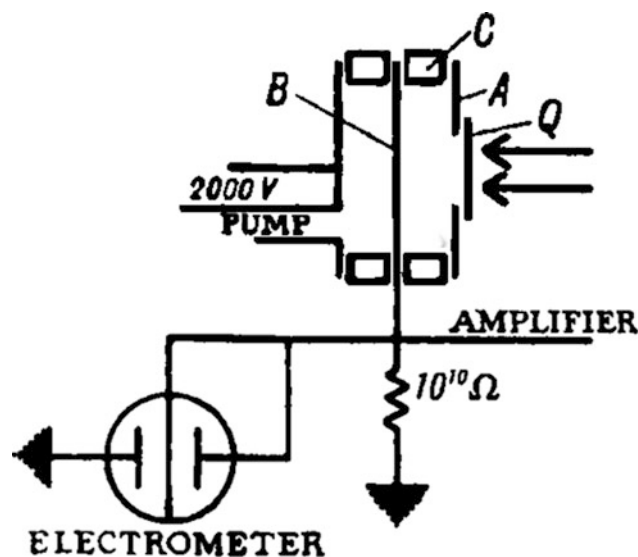


Fig. 21.3 Simplified circuit of Geiger–Müller counter. A – metal tube cathode, B – axial wire anode, C – insulating stoppers, Q – quartz window. (Reprinted from Bateman (1935). Copyright 1935, with permission from John Wiley and Sons)

electrometer filament deflection or crack in a loudspeaker, or counted with special registration schemes. Accumulation of slow positive ions screens the anode from electrons and interrupts discharge. Resistance of about 10^{10} Ohms connecting the anode to the ground, permits the charge to leak off, and in about 10^{-4} s the device is ready for the next count.

21.2.2.2 Basic Characteristics of the Counters

It should be noted, that most of the gas-discharge devices for MGR detection were developed by physicists, well-

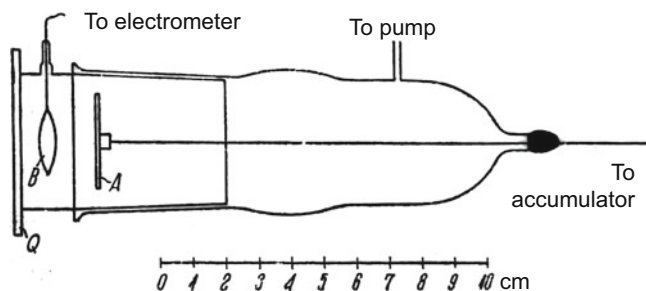


Fig. 21.4 Scheme of modified Geiger–Müller counter by G. Frank and S. Rodionov. A – plate cathode, B – wire loop anode, Q – quartz window. (Reprinted from Rodionov and Frank (1934a))

Table 21.2 Sensitivity of several Al cathodes manufactured in one series (total of 78 cathodes in the series)

| No. of cells | 2 | 6 | 20 | 50 |
|---|---------------------|---------------------|--------------------|--------------------|
| Approx. sensitivity $\text{erg cm}^{-2} \text{s}^{-1}$ | 5×10^{-11} | 5×10^{-10} | 5×10^{-8} | 5×10^{-6} |
| Quanta $\text{cm}^{-2} \text{s}^{-1}$ to give 1 count | 6 | 60 | 6000 | 600,000 |

Adapted from Audubert (1935b). Copyright 1935, with permission from EDPSciences

experienced in the relevant areas (e.g., Fr. Dessauer (Dessauer 1931), W. Gerlach (Gerlach 1933), H. Barth (Barth 1934) – see Table 21.3). However, the devices they built were rather objects of research than reliable measuring tools. Thus, in this period, not only the results obtained with the counters were under discussion, but even more the estimates of their technical parameters (and consequently the measurement validity and MGR intensity estimations).

Here, we summarize some technical parameters and details on the counters that appeared crucial for obtaining valid results: sensitivity spectra, background noise, operation life, and method of calibration.

21.2.2.2.1 Sensitivity

First of all, the counters were characterized by sensitivity (average excess of the counting rate over dark counts divided by intensity of radiation), or counting yield/counting efficiency (average number of counted photons per number of incident photons) at certain calibration wavelengths. Sensitivity depended greatly on the cathode material, its manufacturing method, and further treatment (Barth 1937). Most attention was paid to the material purity, roughness, and surface oxidation.

The technology of photosensitive surface manufacturing was so underdeveloped, that sensitivity of photocathodes from the same series could differ by 5 orders of magnitude (!) (see data from Audubert (1935b) in Table 21.2). H. Barth, who worked both in Germany and in the USSR, mentioned that photosensitive surfaces made of the same material

(copper oxide) in different competent laboratories differed in sensitivity by several orders of magnitude, and thus were either able or completely unable to detect mitogenetic radiation; they even had significantly different colors (Barth 1937). Authors of “positive” works reported that selection of the best cathodes and their regular testing during operation life was a necessary requirement for successful experiments.

The realization that the technology level could not guarantee against a wide deviation in sensitivity and dark counts came only after years of intense debates and extensive study.

21.2.2.2.2 Dark Current

The dark counts are the counter discharges caused by cosmic radiation, radioactivity of used materials, stray emission, thermal electrons, and other factors leading to ionization of gas media in the absence of any source of radiation. When the detected radiation is of extremely low intensity, it can appear comparable or even lower than the dark counts. The proportion between the measured signal and the dark counts corresponds to what is called the signal/noise ratio, largely determining the data validity. For this reason, the dark current also belongs to the parameters of primary importance.

B. Rajewsky reported that his counter had about 100 dark counts per minute in average and that value decreased down to 30 counts per minute with thick-walled tubular lead shield.

Another advancement was introduction of a differential registration scheme based on the correlation of dark counts between the counters (Siebert and Seffert 1933, 1934). In this differential scheme, one counter was exposed to the source of radiation under study and the other was operating in the dark mode. Subtraction of dark counts significantly increased signal/noise ratio (Siebert and Seffert 1933, 1934). The authors studied blood of healthy people and animals, blood of patients with tumors, urine of healthy men, and some oxidation model systems as sources of radiation, and performed about 2000 experiments (Siebert and Seffert 1934) (see examples in Fig. 21.5).

21.2.2.2.3 Calibration

Estimating the device sensitivity was so problematic, because the flux intensity detected by the counters ($\sim 10^2\text{--}10^4$ photons $\text{cm}^{-2} \text{s}^{-1}$) was about $10^7\text{--}10^8$ times less than sensitivity of all standard detectors used for calibration. To calibrate a counter the radiation of certain wavelength (usually, spectral line of 253.7 nm of mercury lamp) was separated by monochromator; its absolute intensity was measured with a thermopile or a graduated photocell, and the same spectral line was attenuated and measured with the counter under calibration.

Inaccuracy of the attenuation was the weakest point of the counter calibration, and various attenuation methods were tried by different authors (see Table 21.3). In the later works, attenuation was made with filters that appeared more accurate, but still far from the desirable precision. As

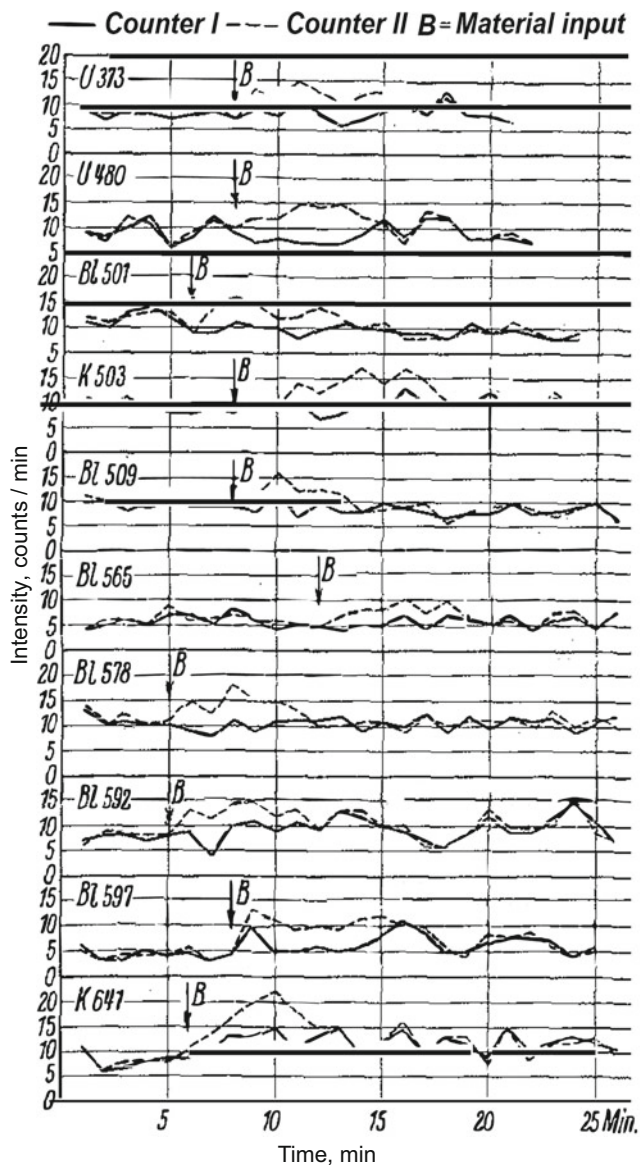


Fig. 21.5 UPE from various biological fluids, detected with two Geiger–Müller counters (differential scheme): U 373, U 480 – urine of a healthy person; BL 501, K 503, BL 509, BL 565, BL 578, BL 592, BL 597 – blood of a healthy person; K 641 – blood of a healthy dog (data of Siebert and Seffert). (Reprinted from Salkind (1937). Copyright 1932, with permission from Springer Nature)

A. Hollaender wrote, “The great difficulty is that both detector and filter are spectrally selective, so that the effect of an extremely minute amount of impurity in the original beam may be tremendously magnified in the filtered beam. The result is an observed counter sensitivity which bears no resemblance to its actual sensitivity” (Hollaender and Claus 1937).

One more problem of comparing the detected signal to the real MGR sensitivity was discrepancy between the calibration wavelength and MGR spectra. In the first years, counters

were typically calibrated at wavelengths of 250 nm or more (see Table 21.3), while the reported MGR spectra of biological objects mainly belonged to the range of 190–230 nm. Such a mismatch was significant because of an abrupt sensitivity decrease at longer wavelengths and different slopes of sensitivity curves (see Fig. 21.6). For instance, the counters with aluminum and iodized silver photocathodes showed similar sensitivities at the wavelength of 210 nm, while at the wavelength of 250 nm, the aluminum cathode counter was 1000 times more sensitive (Barth 1937).

21.2.2.4 Operation Life

The service life was also a very important characteristic, which strongly depended on the material of photocathode, its treatment, gas media, and operation regime. The cathode sensitivity in some cases was reported deteriorating as quickly as in several hours, that allowed only very few experiments to be carried out (Rodionov and Frank 1934a; Audubert 1938a). In many works, this parameter was not estimated clearly enough.

A significant progress was achieved by the group of G. Frank and S. Rodionov, who managed to prolong the service life of cathodes from a few hours to several weeks (Rodionov and Frank 1934a).

21.2.2.5 Common Notes on the Technical Parameters of Counters

Altogether, it should be noted that comparing sensitivity of the counters used by different research teams is very difficult and sometimes absolutely impossible. The main reasons are the following:

- Sensitivity of the counters was incomparably higher than that of all devices used for their calibration.
- The methods of calibration were different in different labs and still under development.
- The counters operation time was also quite different and not always estimated. In a number of works, it was reported as short as the duration of a single experiment. So, the accuracy of those works in which the counter operation time was not estimated, seem highly questionable.

Details on the development of counters, their calibration and applications for measurement of UPE in this period are presented in the monographs (Rodionov and Frank 1934a; Barth 1936, 1937). See also discussion on calibration problems in Hollaender and Claus (1935) and Hollaender and Claus (1937) and some more technical parameters of particular devices in Haussert and Kreuchen (1934), Karev and Rodionov (1934), Reiss (1935) and Lorenz (1933).

Table 21.3 Summary of published reports (1930–1934) on MGR detection with modified gas-discharge counters

| Reference | Sensitive surface | Inverse counting efficiency (average number of quanta per one count) | Calibration wavelength (nm) | Method of calibration | Materials tested | Result | Estimated intensity, quanta $\text{cm}^{-2} \text{s}^{-1}$ |
|--|--|--|-----------------------------|--|---|-----------------------|--|
| Rajewsky (1930a, b, c, 1932) | Cd | 10^2 – 10^3 | 265 | Cellophane filters | Onion roots Onion pulp Carcinomas Carcinoma pulp Albumen (thermal coagulation, decomposition by acid, etc.) | + + + + + | 10 – 10^2 |
| Schreiber and Friedrich (1930) | K | $>10^4$ | 366 266 254 | Photographic emulsions Crossed Nicol prisms | Yeast | – | <2000 |
| Frank and Rodionow (1931, 1932), Rodionov and Frank (1934a, b) | Al Cd | 6×10^3 | 253.7 | Solution filter of variable thickness | Frog muscle Frog muscle pulp Frog hearts Chemical and biochemical reactions | + + + + | 100 – 2000 |
| Locher (1932) | | | | | Onion roots Bacteria | - - | |
| Seyfert (1932) | Zn-amalgam | 5×10^2 10^5 | 230 340 | Calculated from standard lamp at 260 meters | Onion pulp Onion roots Yeast | - - - | <5 |
| | Al | 3×10^3 | 230 | | Chick embryos | – | <30 |
| | Mg | 5×10^3 | 230 | | Mouse tumors | – | <50 |
| Audubert and Doormaal (1933) | CuI, CuO, Cu ₂ O, cu, Al | Not constant | | | Chemical oxidations in vitro | + | |
| Siebert and Seffert (1933) | Cd | | | | Blood Carcinomas Urine Oxidation models | + + + + | |
| Gerlach (1933) | | | | | $\text{K}_2\text{Cr}_2\text{O}_7 + \text{FeSO}_4$ | + | |
| Gray and Ouellet (1933) | Pt | 6×10^3 | 250 | Calibrated slits | Sea urchin eggs spermatozoa Yeast Oxidation reactions (onion mash + H_2O_2 , alcohol + H_2O_2 , benzaldehyde + H_2O_2 , ether + H_2O_2 , ether + Br_2 + air) | - - - - | <50 |
| Lorenz (1934) | Cd | 1400 2400 | 230 253.7 | Filter of $\text{K}_2\text{Cr}_2\text{O}_7$ solution | Onion pulp and roots Mouse sarcoma Mouse embryo Frog muscle | - - - - | <10 – 15 |
| Barth (1934) | Al Cu CuI | | | | $\text{K}_2\text{Cr}_2\text{O}_7 + \text{FeSO}_4$ Digestive reactions | + + | |
| Kreuchen and Bateman (1934) | Cd, Al Zn | 2×10^4 – 5×10^4 | 253.7 | Filters of ground quartz; multiple reflections from polished quartz surfaces | Yeast Frog muscles | - - | <300 |

Adapted from Hollaender and Claus (1935). Copyright 1935, with permission from Optica Publishing Group

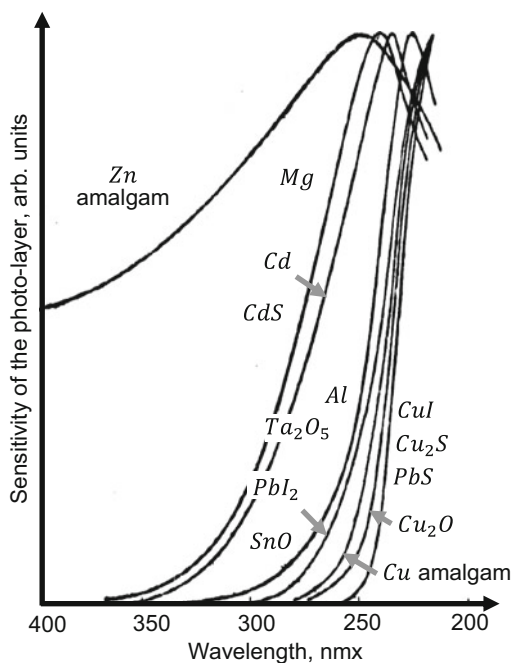


Fig. 21.6 Normalized sensitivity spectra of modified Geiger–Müller counters with various photo-sensitive layers. (Reprinted from Audubert (1938a). Copyright 2006, with permission from John Wiley and Sons)

21.2.2.3 Conflicting Data Obtained during the Development Stage

As mentioned above, by the time of the MGR research, there were no standard devices applicable for its detection, and all research teams were constructing their own counters (with a few exceptions like (Gray and Ouellet 1933), where the authors used Rajewsky’s design). These counters differed in the cathode material and methods of its treatment, gas medium, pressure, electrode geometry, voltage, leakage resistance (determining the lag between the counts), and other features. No wonder that their spectral sensitivity, dark currents, vulnerability to irrelevant influences, operation life, and other parameters varied greatly. Table 21.3 presents the main characteristics of the devices used in these works, as well as their basic results. In the period of the counters’ invention and development, approximately equal amount of negative and positive data on MGR detection were presented by several competent research teams from different countries (see Table 21.3). Yet, data obtained with so different devices are too hard to compare to call them conflicting.

Some authors detected no radiation with the counters, whose sensitivity they estimated to be as good as of those in positive works. However, different methods of calibration, roughness of sensitivity estimations and absence of data on sensitivity in the main MGR spectral range, both in the “negative” and in the “positive” publications (see above), made such comparison unconvincing. Both “negative” and “positive” publications drew lots of criticism.

The weakest point of most “negative” works was inadequate handling of biological inductors. For instance, soon after publication of negative results with yeast cultures (Schreiber and Friedrich 1930), they were shown to lose their ability to radiate in darkness (Potozky 1930), which was an obvious condition in Schreiber and Friedrich (1930). Some unsuccessful attempts to detect MGR with gas-discharge counters were hopeless because of their low sensitivity, relatively high dark counts or vulnerability to irrelevant influences. See also a thorough analysis of negative publications in Barth (1937) and a summary of their mistakes in Volodyaev and Belousov (2015).

Yet, the credibility of some positive works was also questioned. In Kreuchen and Bateman (1934), Gray and Ouellet (1933) and Lorenz (1934), some factors were shown to produce false-positive results, for instance, higher humidity near biological objects or electrostatic disturbances. Later, these effects were thoroughly studied by H. Barth (Barth 1937), who showed that some effects were specific for the modifications used by the authors. For example, the counter used in Kreuchen and Bateman (1934) had too high leakage resistance (10^{16} Ohm instead of the usual 10^9 – 10^{10} Ohm), and conductivity of glass due to the air moisture became a significant factor. E. Lorenz’s design (Lorenz 1934) was more than others vulnerable to electrostatic influences due to poor electrode geometry.

The development stage brought not only technical improvement of the detectors, but also a number of scientific results valuable for the whole MGR studies. G. Frank and S. Rodionov (Frank and Rodionow 1932), W. Gerlach (Gerlach 1933), R. Audubert (Audubert and Doormaal 1933) demonstrated UV chemiluminescence from inorganic and organic oxidative reactions. A major study was performed by Frank and Rodionov’s team in Physical-Technical Institute (Leningrad) (Frank and Rodionow 1931, 1932; Rodionov and Frank 1934a), initiated and supervised by the famous academician A.F. Ioffe. The authors demonstrated UV-component of UPE from a number of biological MGE inductors and chemical systems, estimated and compared their radiation intensities, showed dependence of radiation intensity on the physiological state of the biological objects, and found that chemiluminescence efficiency of some inorganic reactions ($\text{SnCl}_2 + \text{HgCl}_2$, $\text{K}_2\text{Cr}_2\text{O}_7 + \text{FeSO}_4$) increased by 5–6 times in the presence of visible light. A famous physicist W. Gerlach observed radiation of blood samples and confirmed the results obtained by G. Frank and S. Rodionov on inorganic reactions (Gerlach 1933).

Methodical aspects were also developed. To recognize the useful signal in spite of significant natural time variations both of ionizing radiation background and radiation under study, periods of the counter exposure to the object were alternated with “dark counts” (see Fig. 21.7), which was later used in all successful works (see Fig. 21.8).

Fig. 21.7 UPE from MGE inductors, detected with modified Geiger–Müller counters: (a) $K_2Cr_2O_7 + FeSO_4$; (b) sartorius muscle of the frog. The ordinates are the number of counts per 5-min interval, when the counter was alternately exposed to/shielded from the source of radiation: Solid lines – MGR from the sample; Dashed lines – dark counts. (Reprinted from Frank and Rodionow (1932))

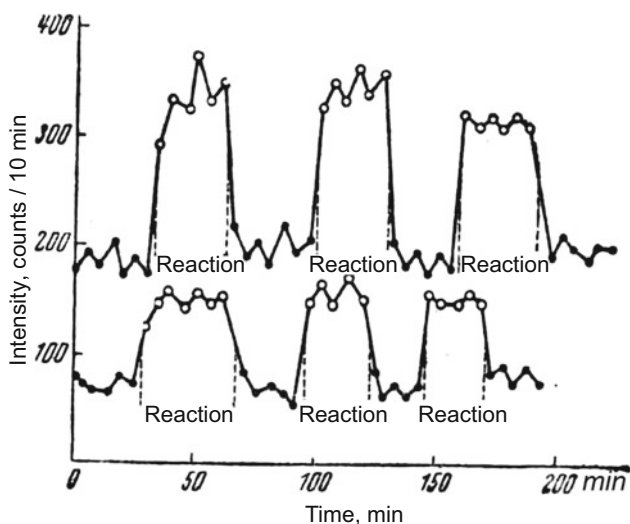
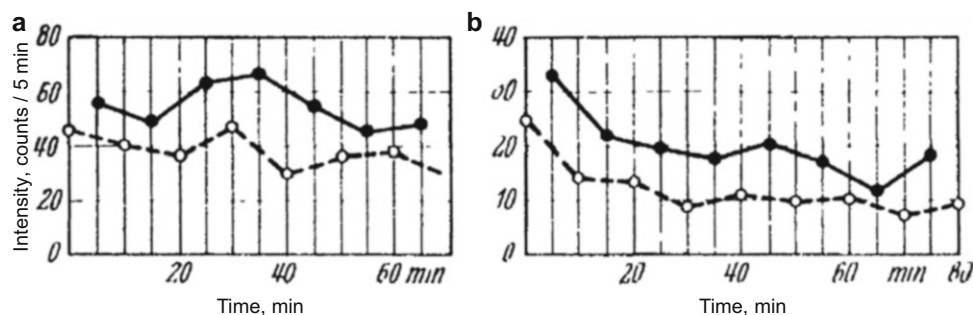


Fig. 21.8 UV-UPE from Na pyrogallate oxidized with oxygen (measurements with the modified gas-discharge counter in alternating periods of exposure to chemical system and dark counts). (Reprinted from Audubert (1938a). Copyright 2006, with permission from John Wiley and Sons)

21.2.2.4 A. Hollaender and W. Claus: “Antimitogenetic Monography”

The publication of A. Hollaender and W. Claus (Hollaender and Claus 1937) is probably the most important of all “negative works” devoted to MGR. It contains the most detailed description of MGE and MGR methods in English and became the most cited work on the topic. As the authors wrote, they aimed “to prove or to disprove the existence of $\langle MGR \rangle$ with the greatest of care and attention to detail” (Hollaender and Claus 1937) and gather sufficient statistics both for biological and physical detection of the phenomenon. The design of experiments, the used materials and methods were presented in exhaustive details in almost a hundred pages, and the reported failures to detect radiation were extensive and seemed impressive. Thus, it made grounds for further prejudice to the whole field of research in the Western countries (e.g., (Metcalf and Quickenden 1967)) in spite of the fact that the authors clearly stated that their work cannot be taken as the final disproof of MGR.

As can be seen from the scrupulous description given by the authors, the work contained a number of critical deviations from the methods of the “positive works.” These were stated in Zalkind (1940) and Gurwitsch and Gurwitsch (1948) and some other publications and nowadays systematized in Volodyaev and Belousov (2015). Here, the biological part of (Hollaender and Claus 1937) is analyzed in Chap. 20, while this section is devoted to the physical part of the work, related to MGR detection with modified Geiger–Müller counters.

The authors studied a number of photocathode surfaces and selected zinc sensitized by glow discharge in hydrogen. Using such photocathodes, they constructed three modifications of gas-discharge counters and clearly stated significant drawbacks of each of them. The first modification was too difficult to calibrate (it was used to detect UPE from water electrolysis, reaction $HCl + NaOH$, action of rennet on milk). The second one showed high and unstable dark counts, supposedly due to metal defects which “permitted spurious electrical discharges to leak from one electrode to the other” (no data obtained with this counter were considered satisfactory by the authors). The third modification had too high leakage resistance that made it too vulnerable to humidity changes and electrically ungrounded bodies near the photon counter (it was used in experiments with *Escherichia coli*, reaction of $HCl + NaOH$, and electrolysis of water containing a small amount of $NaCl$).

Trying to be as precise as possible, the authors grounded their experiments on the wrong assumptions about the reproducibility of experiments with Geiger–Müller counters: “In our investigations on mitogenetic rays, we thought it advisable to use methods and procedures which, from the experience of others and of ourselves, would. . . (1) be so arranged that duplicates or triplicates might be maintained,. . . (2) be so well controlled that repetition would permit an interchange of controls,. . . (3) yield all the data that might be required by anyone wishing to check on this problem, using similar materials” (Hollaender and Claus 1937).

As it was clearly shown by Barth and Audubert (see below), slow natural changes of the dark count could be as high as orders of magnitude, which made it a priory

impossible to make all controls interchangeable. For this reason, the successful works either presented an alternation of UPE measurements with dark counts, estimating the difference between their nearest pairs (see Figs. 21.7 and 21.8), or used an additional counter for simultaneous detecting of dark counts to be subtracted (see Fig. 21.5), which made the useful signal distinctive. Hollaender and Claus also alternated 2-min periods of signal registration (“exposed”) with 2-min periods of shaded cathode (“dark”), but treated them separately as follows: “The standard deviation of the difference between two means is:

$$SD = \sqrt{\left(\frac{\sum n'x^2}{n^2}\right)_{\text{dark}} + \left(\frac{\sum n'x^2}{n^2}\right)_{\text{exposed}}}$$

It is then generally accepted that if $\frac{\bar{N}_{\text{exp}} - \bar{N}_{\text{dark}}}{SD} > 3$, a real difference exists between the two means” (Hollaender and Claus 1937). Here, n is the total number of observations, n' is the frequency of occurrence of any particular observed rate of N , \bar{N} is the average of N , $x = \bar{N} - N$.

As Hollaender and Claus reported for their best counter with zinc hydride cathode surface, “the sensitivity is 1 count for 41,000 quanta at 2300 Å under optimum conditions.” As far as the upper estimate of MGR intensity was 1000 quanta $\text{cm}^{-2} \text{s}^{-1}$, and the working area was about 1 cm^2 , no more than 1 useful count per 41 s could be expected, while the dark counts were 1 per 7.4 s in average. Thus, the signal-to-noise ratio was no more than 0.18. The lower estimate of MGR intensity of 10 quanta $\text{cm}^{-2} \text{s}^{-1}$ would produce 1 count per 740 s and the signal-to-noise ratio of 1.8×10^{-3} .

Using this approach, the authors claimed the ability to clearly detect 1.45 discharges / 2 min (600 quanta $\text{cm}^{-2} \text{s}^{-1}$), if 100 2-min observations were made on both dark and exposed rates. It should be mentioned that the authors omitted counts greater than 30/2 min in the analysis, since “these differ from the average by more than three times the standard deviation.”

Reporting the absence of radiation from chemical reactions, the authors grounded on too high expectations of the chemiluminescence quantum yield: “All results were null, indicating an emission of less than 1 quantum per 10^4 pairs of reacting HCl and NaOH ions, and of less than 1 quantum during the electrolytic production of $3 \cdot 10^{12}$ pairs of ions in salt water.” As it is well known by now (see Chaps. 9 and 10), the chemiluminescence quantum yield in visible and IR ranges is usually about $10^{-8} - 10^{-10}$ (for hydrocarbon oxidation) and up to $10^{-12} - 10^{-15}$ (for aqueous systems), and there is no reason to expect that it would be higher in the ultraviolet range. Moreover, the extensive data by R. Audubert (see below, and also Chap. 9) give an estimated quantum yield of UV chemiluminescence of $10^{-14} - 10^{-15}$.

Hollaender and Claus doubted that authors of positive works managed to make more sensitive counters: “We are tempted to generalize with the statement that it is difficult to see how any of these workers³ could have had counters of sensitivity materially greater than our own since, judging by published reports, they all used photosensitive surfaces of approximately the same type.” As shown above, the used technology of photocathode fabrication could provide extremely poor reproducibility, and comparison of the obtained sensitivities in MGR range was very inaccurate. See also critique of some other mistakes made in experiments (Hollaender and Claus 1937) in Volodyaev and Belousov (2015).

Thus, notwithstanding the impressive volume and scrupulousness of Hollaender and Claus (1937), it turned out to be untenable in criticizing “positive works.” The authors’ negative results were only evidence that MGR was not observed under their conditions, instead of being a refutation of the phenomenon itself.

21.2.3 Advanced Designs and Approved Results

21.2.3.1 H. Barth

By 1935, important methodical aspects became generally recognized (see above, Sect. 21.2.2.2) and a number of extraneous factors leading to false-positive effects were found. Calibration within MGR range was proved obligatory (for instance, in Barth (1935)), advanced schemes of counters and procedures of their calibration were developed (Glasser and Barth 1938). Also, biological methods were improved (see Chap. 20).

The questions about external influences possibly leading to false-positive results were cleared up in a scrupulous experimental work by H. Barth (Barth 1937), who took into account all the criticism and developed advanced novel schemes. First, he showed that a number of factors claimed as possible reasons of spurious positive results were due to specific drawbacks of the counters design used by the critics (Kreuchen and Bateman 1934; Gray and Ouellet 1933; Lorenz 1934). Then, he demonstrated that UPE from the tested mitogenetically active systems is still well-detected after all these factors have been eliminated or made negligible (Barth 1937). This included:

- Biological objects: carcinomas, human blood
- Inorganic chemical reactions: $\text{K}_2\text{Cr}_2\text{O}_7 + (\text{FeSO}_4 + \text{H}_2\text{SO}_4)$,
Al + HCl

³B. Rajewsky (Rajewsky 1934), G. Frank and S. Rodionov (Frank and Rodionow 1932), H. Barth (Barth 1934), and R. Audubert (Audubert 1935b).

- Enzymatic reactions: chicken protein + gastric juice, blood fibrin + pepsin + HCl, blood fibrin + trypsin + HCl, blood fibrin + trypsin and NaHCO_3 , fibrin + trypsin + Na_2CO_3

The scheme by Barth (Barth 1936) was further successfully used by other researchers. For instance, in Rabinerson and Filippov (1938), MGR from several chemical reactions was simultaneously detected by modified gas-discharge counters and biological yeast detectors. Importantly, data from physical and biological detection of UPE demonstrated full coincidence:

- UPE +; MGE +: coagulation of $\text{Fe}(\text{OH})_3$, V_2O_5 sols, sodium oleate
- No UPE; no MGE: coagulation of As_2S_3 sol, dilution of various sols and salts

This work also should be marked for detailed description of methods and results and their clear statistical treatment, that was often omitted in the early works.

Also, among the physical proofs of mitogenetic radiation of the late 1930s, Grebe et al. (1937) should be marked out for well-developed methods and extensive uniform data.

21.2.3.2 R. Audubert

The most extensive and convincing research on detection of ultraweak UV radiation from chemical systems and biological objects with gas-discharge counters was carried out by R. Audubert (mainly famous for his works in physical chemistry and Audubert law) (Audubert and Doormaal 1933; Audubert 1935a, b; Audubert and Lévy 1935a, b; Audubert and Riethmuller 1935; Lévy and Audubert 1936; Audubert 1936a, b, c, d; Audubert and Prost 1936; Audubert and Viktorin 1936; Audubert 1937a, b, c; Audubert and Muraour 1937; Audubert and Viktorin 1937; Audubert 1938a, b; Audubert and Mattler 1938a, b; Audubert 1939; Audubert and Racz 1939; Audubert and Ralea 1939; Audubert and Verdier 1939; Audubert 1943).

Together with C. Riethmuller, he undertook a complex experimental study of many materials, showing photoelectric effect in the UV range (Audubert and Riethmuller 1935), and analyzed sensitivity, stability and other characteristics of counters with cathodes made of these materials (see, e.g., Fig. 21.6).

Audubert developed his own modifications of counters and together with his colleagues demonstrated ultraweak UV emission from a great number of chemical reactions and many biological sources: anodic oxidation of Al, Hg, Ta, Si, etc. (Audubert and Viktorin 1937); quinine sulfate hydrogenation/dehydrogenation processes (Audubert and Prost 1936); oxidation of hydrosulfite, pyrogallol, and

alcohols with chromic acid; water decomposition by amalgams of K, Na, NH_4 , and Hg; aluminum oxidation in atmosphere (Audubert and Doormaal 1933); thermal decomposition of azides (Audubert and Muraour 1937; Audubert 1937c, 1938b), neutralization of strong acids (H_2SO_4 , HNO_3) with strong bases (NaOH, KOH); oxidation of lemon salt with bromine and iodine; oxidation of glucose with permanganate; atmospheric oxidation of sodium pyrogallate (see Fig. 21.8), sodium and potassium sulfites (Audubert 1938a); excited nerves (see Fig. 21.9); and developing frog eggs and some other systems (Audubert and Lévy 1935a, b; Audubert 1938a).

Also Audubert made comparative analysis of UPE intensity from various sources, and determined the *chemiluminescence quantum yield* (named “actinochemical yield” in his works). For instance, oxidation of pyrogallol and hydrosulfite produced 1 photon per $\sim 10^{14} - 10^{15}$ oxygen molecules on average; a similar proportion was obtained for anodic oxidation of aluminum, quinine sulfate dehydrogenation and other chemical reactions (see similar assessments in Chaps. 9, 10, and 11).

MGR detection with the use of counters having different spectral sensitivities allowed Audubert to make rough estimations of the MGR spectral range from different sources that agreed well with the data obtained earlier by MGE spectral analysis. For instance, using counters with Al cathode (sensitive in the range $\sim 210-280$ nm) and with CuI cathode (sensitive in the range $\sim 180-240$ nm), he divided many chemical reactions and some biological processes into

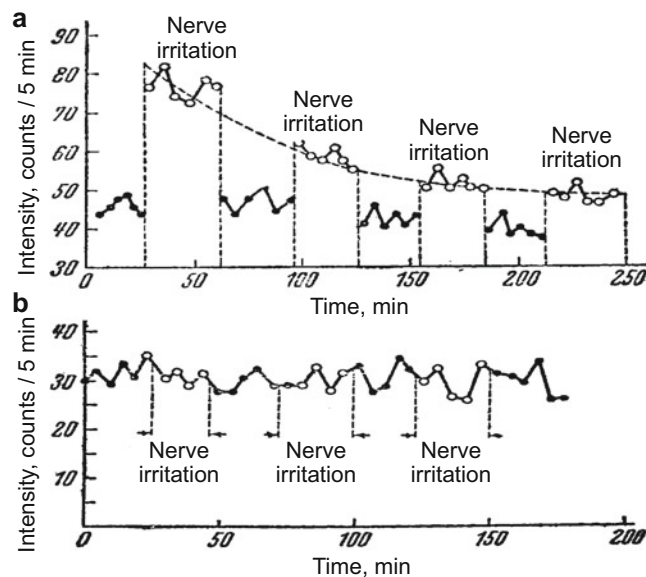


Fig. 21.9 UV-UPE from periodically irritated frog nerves: (a) alive; (b) killed with ethanol. Measurements were made with a modified gas-discharge counter having aluminum photocathode (see sensitivity spectrum in Fig. 21.6). (Reprinted from Audubert (1938a). Copyright 2006, with permission from John Wiley and Sons)

groups with dominating shorter wave radiation (detected only with CuI), longer wave radiation (detected only with Al) and “wide-range radiation” detected with both cathodes. For instance, ultraweak radiation from developing frog eggs was detected both with Al and CuI cathodes, while oxidation of glucose by permanganate – only with CuI cathode (Audubert and Prost 1936).

21.2.3.3 “Final Proofs”: Recognition of R. Audubert’s Work by the Scientific Community

Thus, by the end of the 1930s, the discrepancies in MGR physical detection were mostly overcome, and reliable detection devices and methods were developed and published. Of all the works of this period, those by R. Audubert appeared the most convincing and widely appreciated (though at least the works by H. Barth and L. Grebe et al. are also very well done).

These works were recognized by leading specialists in luminescence of that time on the Conference of the Faraday Society in 1939 (Garner et al. 1939). S.I. Vavilov, codiscoverer of the Vavilov-Cherenkov radiation, Head of the Lebedev Physical Institute, future president of the USSR Academy of Sciences, said: “The results of very interesting investigations of Audubert... enable us to consider the emission of ultra-violet radiation by many chemical reactions as well as by many biological processes as definitely proven by usual physical methods. These investigations constitute a very conclusive confirmation of the important discovery made by Gurwitsch... Since 1931, several scientists (Rajewsky, Frank and Rodionov, Barth, etc.),... have corroborated these discoveries using photo-electric counters instead of the biological detectors of the radiation; however, their work was not as conclusive as desirable. Only the investigation of Audubert and his collaborators has finally proved that the results obtainable with biological detectors are perfectly consistent with the results of refined purely physical measurements.” (Garner et al. 1939).

R.G.W. Norrish, Nobel Prize Winner, Chair of Physical Chemistry at Cambridge University, visited R. Audubert’s laboratory in France and supported validity of his results after observation of experiments: “I was among a few to whom Professor Audubert demonstrated his experiments in some

detail. It did not appear to me that there can be any doubt as to the reality of the phenomena observed” (Garner et al. 1939).

As far as we know, the late Audubert’s works have not drawn any criticism or been discredited in any way. Thus, although the instrumental basis of these works is very different from that currently accepted, they must be considered reliable.

21.2.4 Single Attempts of MGR Physical Detection after the “Golden Age” of Mitogenetic Research

21.2.4.1 S.V. Konev et al.

As discussed in Chap. 2, “The golden age” of mitogenetic research can be described as the period from the late 1920s till the beginning of World War II, after which the mitogenetic works mostly ceased for various historical reasons (see Chap. 2). Later (after the War), there were very few works dealing with physical detection of UPE in middle UV range and a gradually increasing swell of work on ultraweak luminescence in visible light and underlying it free-radical processes. The history of this is described in Chap. 3, and a detailed review of the data is given in Chaps. 9, 10, 11, and 12. Here, we briefly mention the most important groups of works specifically on UV-UPE, which, unfortunately, still haven’t resulted in a universal acceptance of the phenomenon, although we do find some of them very convincing (as well as the above works in Sect. 21.2.3).

Among these works, gas-discharge counters were used by S.V. Konev and his coauthors (Troitskii et al. 1961; Konev et al. 1961, 1963, 1966; Konev 1965). The authors detected UV-UPE from various biological objects (Troitskii et al. 1961) with a self-quenching gas photon counter (similar to the Geiger tube), whose platinum photocathode was sensitive only within the 200–300 nm spectral range (Shelkov et al. 1959). The authors provided a well-described methodical section, with clear and well-defined controls, and good precautions against different artifacts, including electrostatic effects. With this design they managed to detect reliable UV-UPE from a number of biological objects (see some of their data in Table 21.4), including the yeast cultures, frequently used by Gurwitsch et al. It is also interesting to note

Table 21.4 Relative intensity of UV-UPE from some biological objects (data from Troitskii et al. (1961))

| Object | Mean UPE intensity \pm SE, counts/ min | | Excess over background, % |
|--|--|-----------------|---------------------------|
| | Object | Background | |
| Alcohol yeast (suspension culture in wort, 24 h) | 12 \pm 1.7 | 8.3 \pm 0.7 | 47 \pm 22 |
| Alcohol yeast (agar culture on wort-agar, 24 h) | 7.2 \pm 0.1 | 5.2 \pm 0.5 | 42 \pm 10 |
| Dandelion inflorescence in sunny weather | 6.44 \pm 0.11 | 5.25 \pm 0.18 | 20.2 \pm 3.9 |
| Dandelion inflorescence in cloudy weather | 5.4 \pm 0.18 | 5.35 \pm 0.18 | -- |
| Dandelion inflorescence after exposure to UV | 6.3 \pm 0.1 | 5.35 \pm 0.18 | 17.8 \pm 3.6 |

Adapted from Konev (1967). Copyright 1967, with permission from Springer Nature

that they detected UPE from contracting heart of a frog (exceeding the background by 35%), which disappeared with stopping the heart, and UPE from the frog's crushed muscle (20% above the background), while the undamaged muscle at physiological rest showed no UPE (Troitskii et al. 1961) (both of these results are exactly the same as the MGR data reported in many "early works" – see Chap. 20).

21.2.4.2 Anna Gurwitsch et al.

Similar works, but with the use of PMT, were continued in Anna Gurwitsch's lab (Gurwitsch et al. 1965; Gurvich et al. 1968). Contrary to the Konev's group, the authors didn't manage to construct a photodetector sensitive *solely in UV* and had to compare measurements conducted through quartz and glass vessels (with the corresponding controls subtracted) (Gurwitsch et al. 1965). The device was equipped with a liquid nitrogen-cooled PMT with an antimony–caesium cathode (selected among many PMTs of the same type for the best characteristics) and a uviol window, spectral characteristics taking into account the vessel material are given in Fig. 21.10. With this, the authors obtained clear results on both visible and UV-UPE at oxidation of glycine by hydrogen peroxide, $\sim 10^4$ and $\sim (4 - 8) \cdot 10^3$ photons \cdot cm $^{-2}$ \cdot s $^{-1}$, correspondingly (Gurwitsch et al. 1965). Thus, they both confirmed the data on ROS-dependent visible chemiluminescence (see Chaps. 8 and 9) and the UV-UPE component, stated in mitogenetic works (see Chap. 20 and Sect. 21.2.3). In another work, they showed a flash of UPE from a synchronized yeast culture in the lag period, 10–20 min before the first wave of budding; however, the UV vs. visible components here were not discriminated (Gurvich et al. 1968).

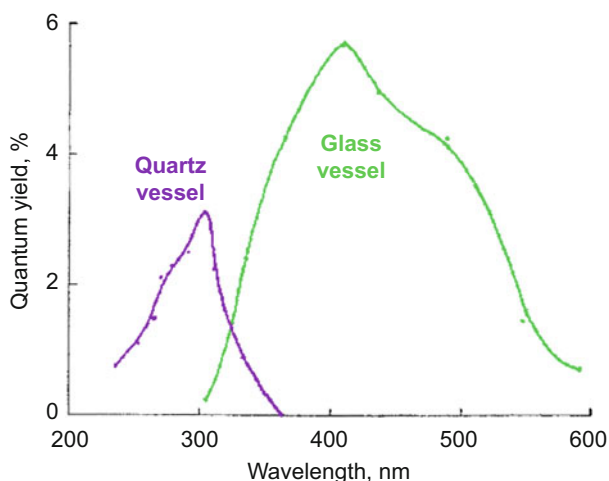


Fig. 21.10 Spectral characteristics of the photosensitive device, used in Anna Gurwitsch's lab, taking into account the material of the vessel with the tested bioobject. (Adapted from Gurwitsch et al. (1965). Copyright 1965, with permission from Springer Nature)

21.2.4.3 T.I. Quickenden et al.

Another attempt to repeat the MGR detection by PMT was performed in 1967 by W.S. Metcalf and T.I. Quickenden, who obtained no results and published an influential negative report (Metcalf and Quickenden 1967). However, in a further work from the same lab (Quickenden and Que Hee 1971), the authors managed to improve the photosensitive device, which resulted in a reliable UPE detected from *S. cerevisiae* at two distinct phases: (1) exponential and linear growth phase, and (2) stationary phase (Quickenden and Que Hee 1974) (see Fig. 21.11a). Later, similar growth-dependent UPE was shown for other microbial species: *S. cerevisiae*, *S. pombe*, *C. utilis* and *E. coli* (Quickenden and Tilbury 1983; Quickenden et al. 1985; Tilbury and Quickenden 1988b, 1992) (see for instance Fig. 21.11b). Moreover, using optical filters and accumulation of experimental replications, the authors managed to obtain rough spectra of UPE from all the tested cultures (Quickenden and Hee 1976; Quickenden et al. 1985; Tilbury and Quickenden 1988a; Quickenden and

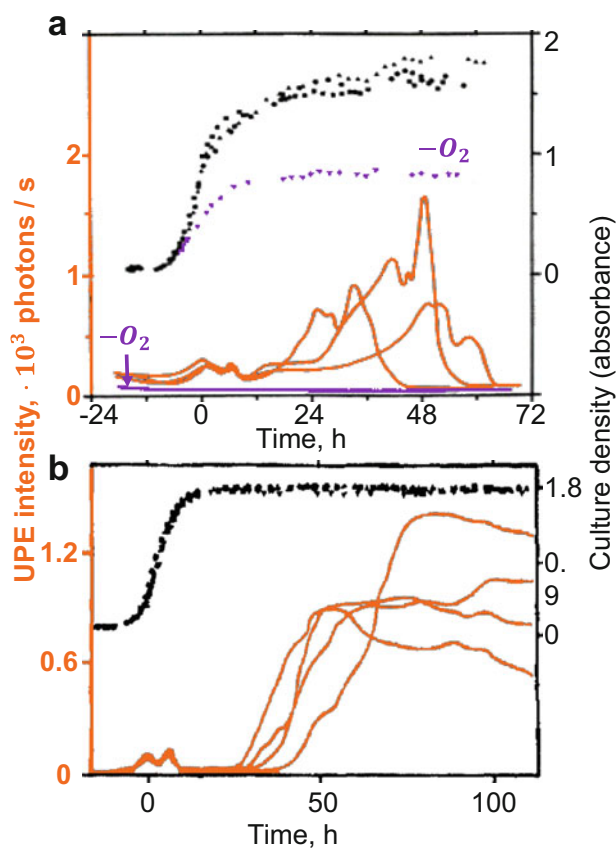


Fig. 21.11 Growth and UPE kinetics of *S. cerevisiae* (a) and *C. utilis* (b) (T 33 °C): black dots – growth (right axis); orange lines – UPE intensity (left axis). Purple dots and line in a – growth and UPE intensity of a nitrogen saturated culture. (a – Adapted from Quickenden and Tilbury (1983). Copyright 1983, with permission from John Wiley and Sons; b – Adapted from Tilbury and Quickenden (1992). Copyright 1992, with permission from John Wiley and Sons)

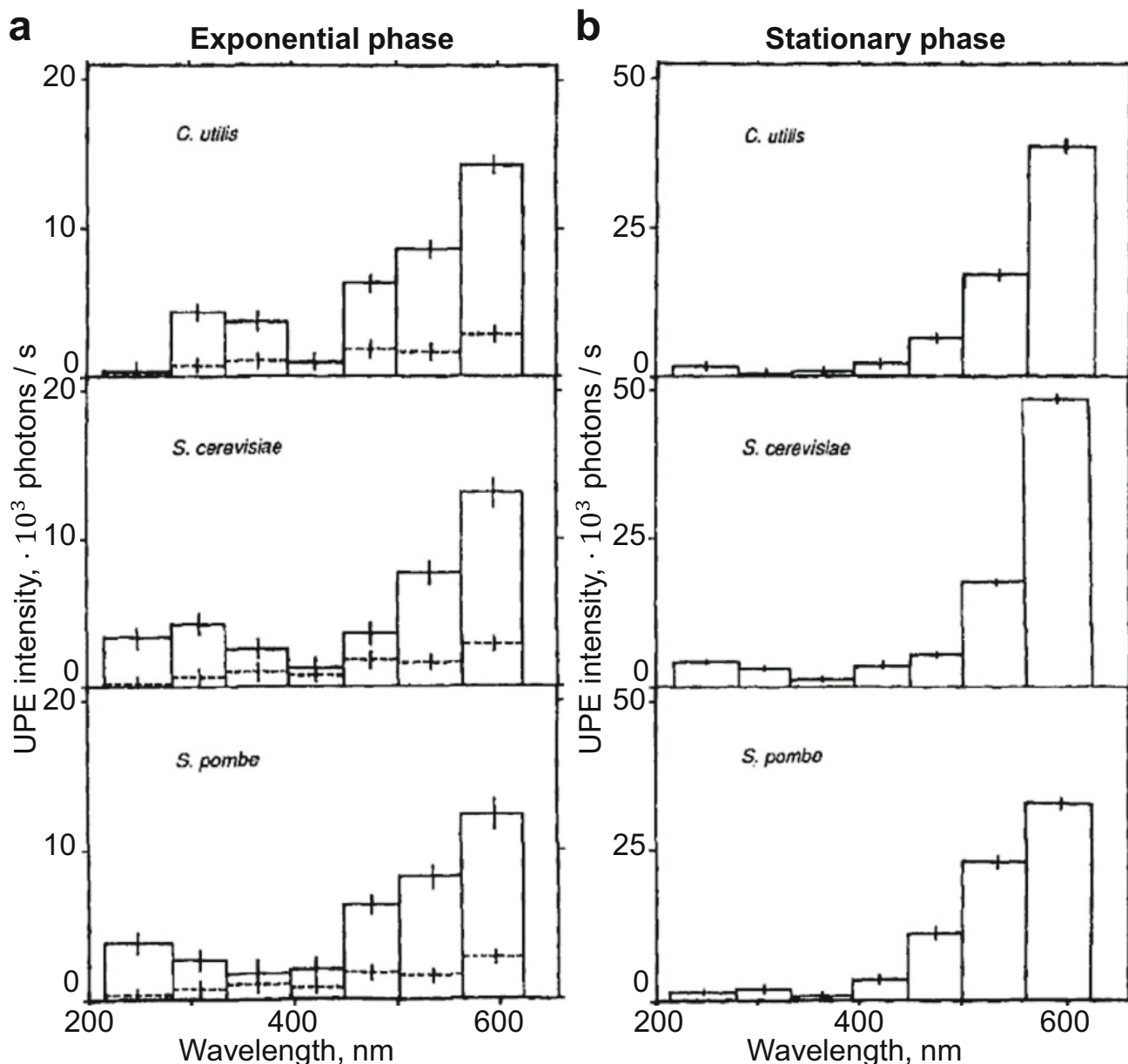


Fig. 21.12 Spectra of UPE from different microbial cultures: *S. utilis*, *S. cerevisiae*, *S. pombe* (T 33 °C): (a) in exponential growth phase; (b) in stationary phase. Error bars – 50% confident intervals; dotted lines –

background (cuvette with medium). (Adapted from Tilbury and Quickenden (1992). Copyright 1992, with permission from John Wiley and Sons)

Tilbury 1991) (see examples in Fig. 21.12). Unfortunately, due to the extremely low UPE intensity, the obtained spectra were not as reliable as desired: the error bars in Fig. 21.12 represent only 50% confident intervals. However, some important features of UPE kinetics and spectra can still be identified:

1. All the tested microbial cultures emit detectable UPE in two distinct growth phases: (1) active growth (exponential–linear growth phases); (2) stationary phase

(several days old cultures, supposedly in quiescent start (G0 cell cycle phase – see, e.g., (Gray et al. 2004)).

2. The active-growth UPE is lasting from several hours to one day and is very well repeated for different cultures of the same species.

It has *one or two distinct* (species-specific) *maxima* (Fig. 21.11) with two major spectral components: $>400\text{ nm}$ (likely generated by peroxidation processes – see Chaps. 11 and 12), and a weaker *UV component* (200–300 nm).

- The growth-phase UPE intensity is $\sim 10\text{--}10^2$ photons $\cdot \text{cm}^{-2} \cdot \text{s}^{-1}$; 20% to 40% of these are in the UV component.
- The stationary-phase UPE starts after the culture density saturation (i.e., after the diauxic shift in yeast), and usually 1–4 days later, i.e., close to the real quiescent state. However, unlike the active-growth UPE, its kinetics is highly variable and shows no species specificity (see Fig. 21.11). The stationary-phase UPE intensity is $\sim 10^2\text{--}10^3$ photons $\cdot \text{cm}^{-2} \cdot \text{s}^{-1}$, i.e., an order of magnitude higher than in the active-growth phase. Practically, all of these are $>400\text{--}450$ nm (corresponding to the mentioned peroxidation processes – see Chaps. 11 and 12).
 - A respiratory-deficient strain of *S. cerevisiae* also shows a generally similar picture of UPE, with some specificity: (1) the active-growth UPE peaks appear ~ 3 h later than in the wild-type strain, and (2) the second active-growth UPE peak in respiratory deficient yeast appears several times higher than in the wild-type cultures (Quickenden and Tilbury 1983, 1991).
Importantly, it is the visible UPE component that appears enhanced in respiratory deficient cultures, but not the UV one.
 - Lack of oxygen (nitrogen purging) of both wild-type and respiratory-deficient strains leads to a complete UPE suppression.

Thus, UPE from microbial cultures is oxygen-dependent, and the visible component is enhanced in the respiratory-deficient cultures. Together with the spectral data, it fits well the lipid (and probably partially peptide) peroxidation mechanisms discussed in Chaps. 8, 9, 10, 11, and 12, and the respiratory chain origin of the primary radicals in them.

However, the UV component in the active-growth phase UPE may well be of a different origin, particularly, the authors pointed out that the spectral range, intensity and observed regularities in behaviour of this component (like emergency at specific stage of growth, absence during stationary phase, etc.) make it similar to the mitogenetic radiation described in the “early works.”

21.3 Spectral Studies of MGR

21.3.1 Rough Estimations of MGR Spectral Range

First of all, rough estimates of the MGR spectral range were obtained by separating the inductor and the recipient with materials transparent in different ranges (quartz, glass, mica, gelatin, wood, 0.5% KNO_3 and 0.02% $\text{Mg}(\text{NO}_3)_2$ aqueous

solutions, etc.). These experiments with filters attributed MGR mostly to $190\text{--}230 \div 250$ nm (Gurwitsch 1923, 1924, 1925; Rawin 1924; Gurwitsch and Gurwitsch 1925; Wolff and Ras 1931a, b, 1932; Siebert 1931a) (weaker components with longer wavelengths were also assumed possible). D. Gabor and T. Reiter were the only research group that attributed MGR to longer wavelengths (mainly >300 nm) in such experiments, and all their later experiments also corroborated their first estimate (Reiter and Gabor 1928a, b). This discrepancy of spectral estimations seems one of the most significant disagreements in the early MGE observations and may relate to the difference in biological aspects of used methods discussed in Chap. 20. Modifications of Geiger–Müller counters (Rajewsky 1930a, 1931c; Dessauer 1931) with photocathodes sensitive to radiation below 300 nm (see spectral sensitivities of the most popular photocathodes in Fig. 21.6) supported the spectral estimation obtained with filters by the majority of authors.

UV range of MGR was indirectly confirmed by demonstration of the same effect of mitotic rate stimulation by ultra-weak middle UV radiation from artificial sources (Frank and Gurwitsch 1927; Chariton et al. 1930; Ruysen 1933; Frank and Rodionov 1932) (see Sect. 20.6).

21.3.2 Mitogenetic Spectral Analysis: Method Development

21.3.2.1 The First Data

The first attempt of MGR spectral analysis was made by D. Gabor and T. Reiter (Reiter and Gabor 1928b). An onion pulp was taken as an inductor, its MGR was spectrally decomposed by means of a quartz spectrograph and detected with a row of MGE recipients (onion roots) placed instead of the usual photographic plate detector. Thus, each recipient was exposed to a narrow spectral band. The maximal MGE was observed near 340 nm (see Fig. 2.15 in Chap. 2), and a weaker spectral band was supposed to be near 280 nm. This result was not repeated by other authors, and was criticized by A.G. Gurwitsch (Gurwitsch and Gurwitsch 1934b) for the biological part of method. However, the basic experimental scheme with spectrograph suggested in Reiter and Gabor (1928b) was used later with just minor modifications in all further works (see Fig. 21.13).

It is the series of experiments by G.M. Frank (Frank 1929) that is considered the first successful spectral analysis of MGR; the obtained results agree well with all the further works by other authors. G.M. Frank used a set of agar blocks of yeast recipient as detectors and an electrically stimulated frog muscle as the MGR source (Frank 1929) (Fig. 21.13). In his scheme, separate agar blocks were cut in such a way that they were exposed to the spectral bands of different widths (from 5 nm to 25 nm). In later works, the width of recipients

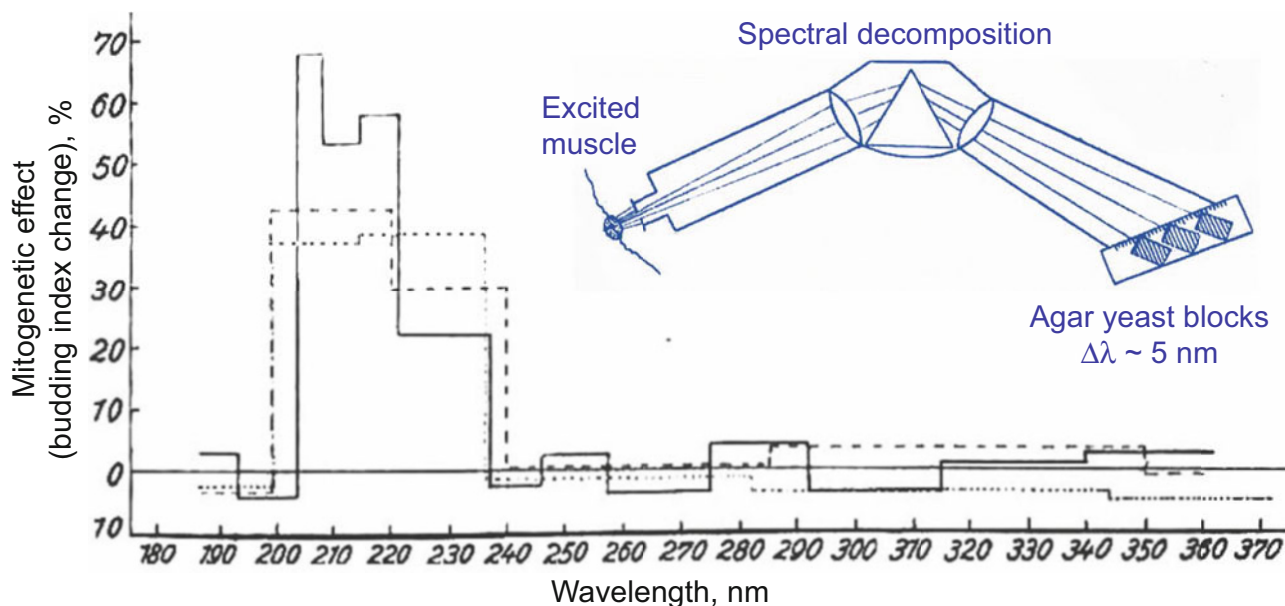


Fig. 21.13 Mitogenetic spectral analysis. Scheme of experimental setup includes an electrically excited frog sartorius muscle as the MGR source, spectrograph, and a series of agar blocks with yeast culture as recipients (“biological detectors”). Here, mitogenetic effect

means a change of budding index relative to the control yeast culture. Three MGR spectra from the frog’s sartorius have different step widths because of nonprecise cutting of yeast blocks. (Adapted from Frank (1929))

was usually controlled precisely so that any MGE recipients in the row of detectors were exposed to the spectral bands of the same width, that was convenient for comparison of spectra.

21.3.2.2 Increasing Spectral Resolution

Significant miniaturization of yeast blocks was impossible, because it would make the amount of yeast culture too small for definite results. To improve spectral resolution, it was suggested to expose yeast recipients one by one to 1 nm wide spectral bands, sequentially isolated with a monochromator (Ponomarewa 1931). This approach obviously required much more time. Moreover, to gather valid statistics, usually no less than 10 recipients were used to study each band of 1 nm width, which made this method even slower and more labour intensive (when recipients were exposed one after another, the studied inductor usually had to be replaced with a similar one for every experiment that increased dispersion of results due to the variability of inductors, while in case of simultaneous induction of a row of recipients, less number of experimental replicates were required).

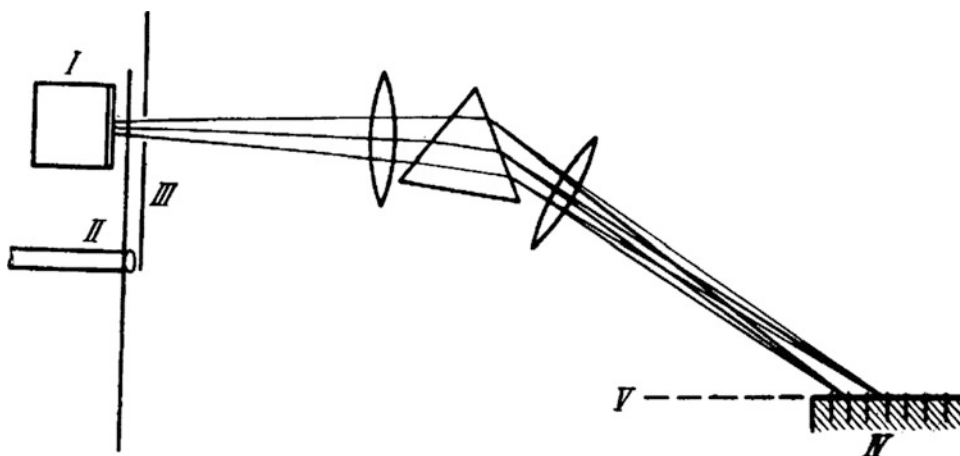
Still, some authors supposed that the resolved 1 nm bands had further unresolved fine structure. An attempt of further spectral resolution increase was made in Decker (1936) (with yeast cultures used both as inductors and as recipients). The authors managed to get some spectral bands as narrow as

2–3 Å. Yet, as such work was too laborious and slow, spectra with so high resolution were later taken very rarely, and only for the short-wave bands of MGR spectra (Gurwitsch and Gurwitsch 1948). Researchers mostly preferred spectra with the resolution of 1 nm (see examples in Fig. 21.16, 21.17, 21.18, 21.19, 21.20, 21.21 and 21.22).

Though a possibility of further unresolved fine structure in MGR spectra within bands of 1 nm and even 3 Å could not be excluded, resolution of such spectra was limited by the ultraweak MGR intensity, that made further spectral decomposition meaningless because of intensity decrease. It should be noted that even spectral measurements with low resolution seem some sort of paradox, because MGE was observed at inductor-recipient distance limited by a few cm (see Chap. 20), while spectral measurements required some tens of cm, and decomposition decreased its intensity even more. The early researchers stated that this problem was resolved by the so-called MGR fractioning (“intermittent induction,” see Fig. 21.14), introduced into the spectral analysis scheme in Kannegiesser (1931) and used mainly with biological MGR sources⁴ (see more in Sect. 20.1.3).

⁴“MGR fractioning” was reported to increase sensitivity of MGR recipients and thus allow its observation at longer distances. This effect was reported in many works of Gurwitsch’s school (Gurwitsch and Gurwitsch 1934b); however, it seems one of the most mysterious and unexplainable effects claimed in MGE studies.

Fig. 21.14 Scheme of MGR spectral analysis. I. Source of MGR in a chamber with quartz window; II. Rotating disk with cut-off windows; III. Entrance slit of the spectrograph; IV. Agar blocks with the surface layer of yeast-blocks separated from each other by celluloid strips; V. Plate holder. (Reprinted from Gurwitsch and Gurwitsch (1932). Copyright 1932, with permission from Springer Nature)



To make the high-resolution spectral measurements less time-consuming and laborious, spectral analysis was usually performed in two steps:

1. The whole spectrum was obtained at low resolution (with a row of recipients simultaneously exposed to MGR).
2. The mitogenetically active bands were further analyzed at high resolution with the monochromator scheme and sequential exposure of recipients.

21.3.2.3 Special Adaptations

To increase resolution and avoid time-consuming sequential exposure of recipients one by one to the narrow bands, the following scheme was developed. Special plates with narrow slits (see Fig. 21.15), narrower than the recipient blocks, were placed in front of the yeast recipients. The mitogenetic effect was observed in yeast beyond the slits, over the whole recipient, due to the so-called secondary radiation effect (see Chap. 22). Thus, every yeast recipient had enough volume, and the mitogenetic response could be detected from rather narrow bands (5–10 nm). Several (usually 3–5) such plates were used to cover the whole investigated spectral range: the lower spectral boundary was 190–200 nm (that was limited by the quartz transparency); the upper spectral boundary was initially 260 nm, yet by 1948, it was shifted to 330 nm.

At the same time, as some authors preferred liquid yeast or bacterial recipients, they also invented special devices for liquid culture-based spectral MGE analysis. For instance, in Potozky (1932), a long multiple-section capillary cell was designed (see Fig. 21.16), with sections corresponding to different spectral bands, filled independently with liquid yeast cultures. It was used only for low-resolution spectra (5 nm), while higher resolution spectra were obtained with the use of agar yeast recipients as above.

See more details on methodical aspects of MGE spectral analysis in Kannegiesser (1931), Gurwitsch and Gurwitsch (1934a), Gurwitsch and Gurwitsch (1945, 1948).

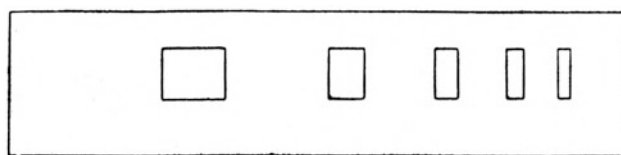


Fig. 21.15 An example of the plate with slits for 10 nm bands that was used as a mask for the accelerated spectral analysis. A set of three masks covered the whole mitogenetic range continuously (190–330 nm). (Reprinted from Gurwitsch and Gurwitsch (1959). Copyright 1959, with permission from Springer Nature)

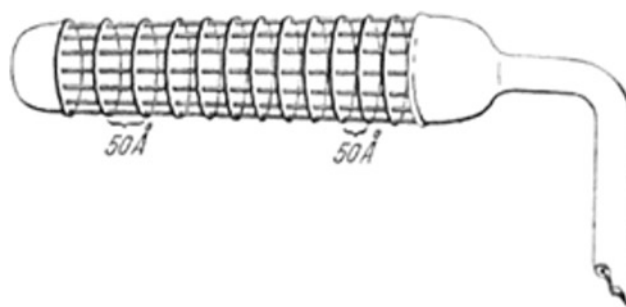


Fig. 21.16 Multiple-section capillary cell for liquid yeast recipient (from Potozky (1932)). (Reprinted from Potozky (1932). Copyright 1932, with permission from Springer Nature)

21.3.3 Mitogenetic Spectra: Their Identification and Interpretation

21.3.3.1 Inorganic Processes

Besides biological inductors, spectral analysis was applied to study MGR from a number of inorganic chemical systems (Figs. 21.17, 21.18, and 21.19).

Analysis of reactions showing similar spectra allowed drawing some generalizations. For instance, hydrogen reduction in reactions of any metal with any acid and its electrochemical reduction on cathode (electrolysis of water) produced the same spectra (see Figs. 21.18 and 21.19)

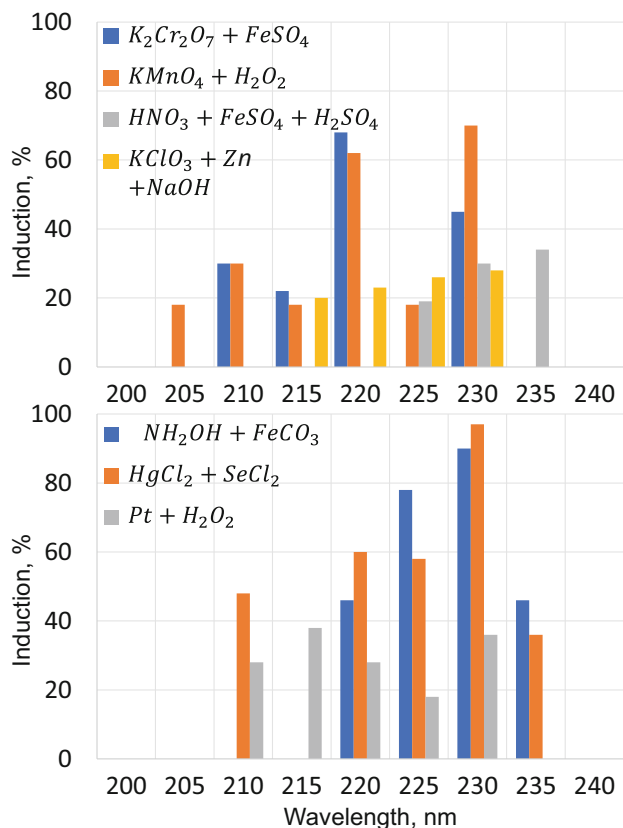


Fig. 21.17 MGR spectra of inorganic redox reactions, obtained with liquid yeast recipients. (Adapted from Potozky (1932). Copyright 1932, with permission from Springer Nature)

(Braunstein and Potozky 1934). In various electrochemical redox reactions, MGR was observed only at the cathode and not at the anode (Braunstein and Potozky 1934). MGR spectra of reduction in inorganic chemical and electrochemical models showed specificity of spectra to the electron acceptor and identity of spectra for its electrochemical and chemical reduction (Braunstein and Potozky 1934).

21.3.3.2 Biological and Biochemical Processes

The MGR-spectra of biological objects and biochemical model systems were also divided into groups with the same spectral features. For instance, the same spectrum was observed for lactic-acid fermentation, alcoholic fermentation, rabbit laky blood, and rabbit eye (Ponomarewa 1931) (Fig. 21.20), which was called “glycolytic spectrum.” See also spectra of lipolysis (Fig. 21.21), urea-urease reaction (Fig. 21.22), and some other basic spectra (Fig. 21.23).

Biological sources of MGR often had more complex spectra. These spectra were identified by the authors as a superposition of the simple basic spectra (see a typical example of analysis of a complex spectrum in Fig. 21.24).

For rough estimations related to the most commonly encountered spectra (the so-called glycolytic, proteolytic, oxidative and phosphatase ones), the analysis procedure was significantly simplified with the use of masks (as in Sect. 21.3.2.3) having slits corresponding to the specific spectral lines of these spectra, with each line absent in

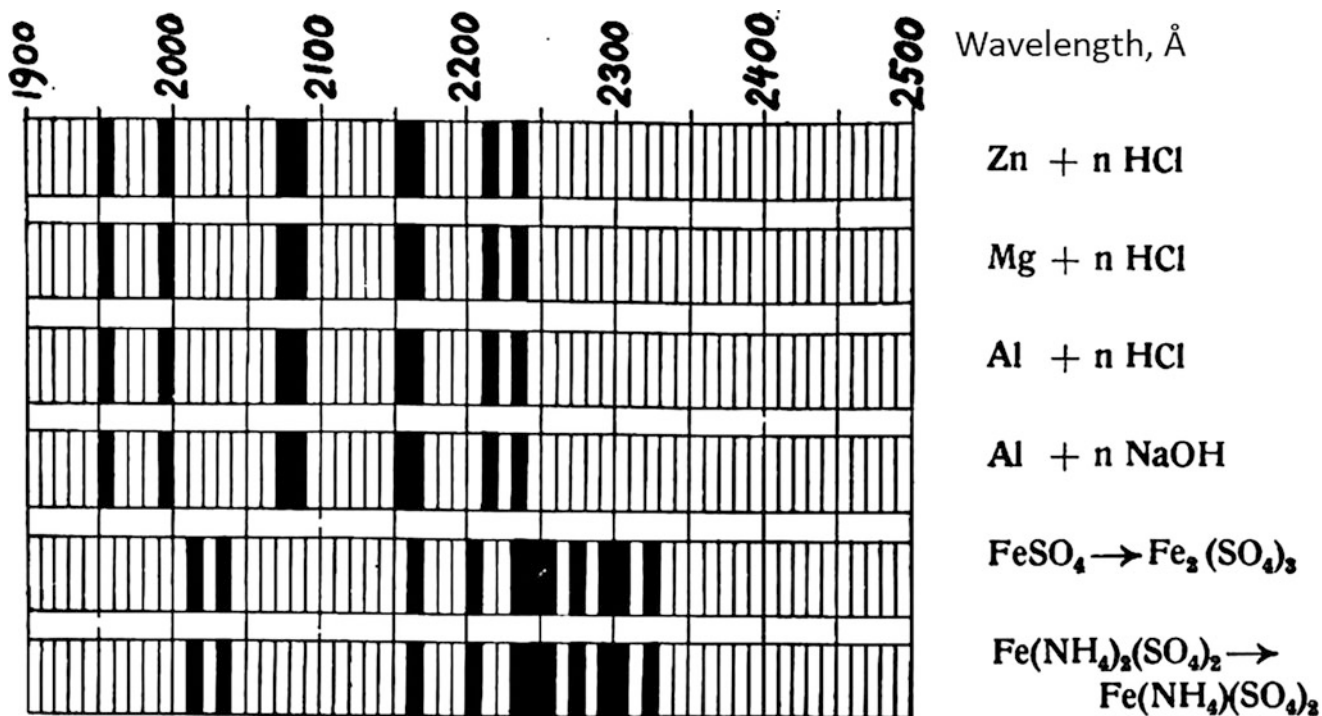


Fig.21.18 MGR spectra of H^+ reduction and Fe^{2+} oxidation in different chemical reactions. Black painted rectangles – positive effect, unpainted rectangles – no effect (data from Braunstein and Potozky (1934)). (Reprinted from Rahn (1937))

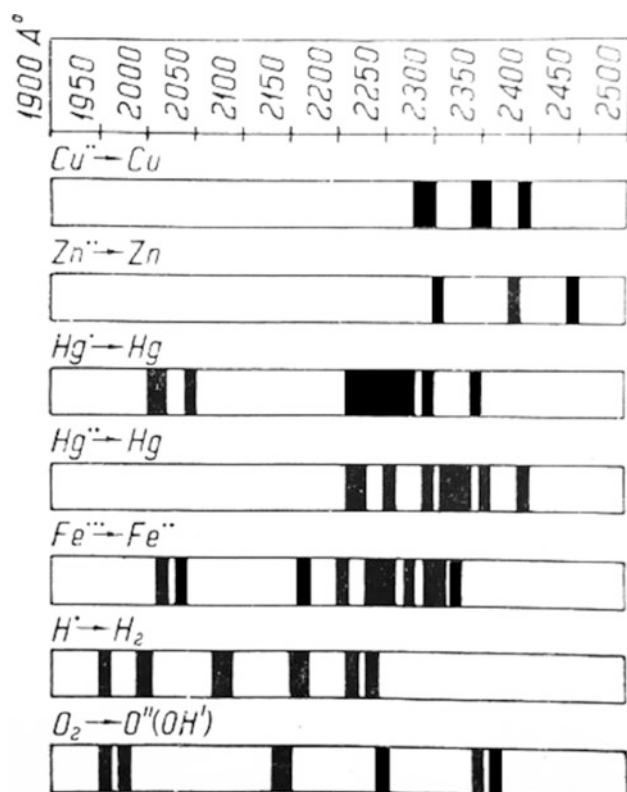


Fig. 21.19 MGR spectra of reduction in inorganic chemical and electrochemical processes. Black painted rectangles – positive effect. (Reprinted from Braunstein and Potozky (1934))

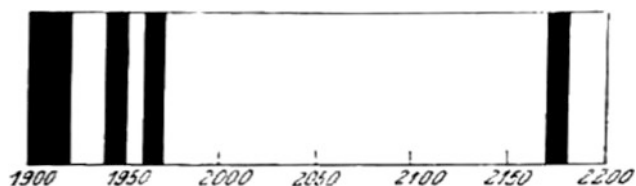


Fig. 21.20 MGR spectrum of glycolysis (lactic-acid fermentation, alcoholic fermentation, rabbit laky blood, rabbit eye). (Reprinted from Ponomarewa (1931))

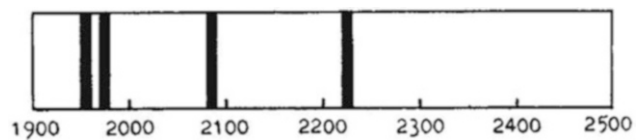


Fig. 21.21 MGR spectrum of lipolysis (splitting of monobutyryn by pancreatic lipase). The spectrum is based on more than 200 experiments. (Reprinted from Braun (1934). Copyright 1932, with permission from Springer Nature)

the spectra of the other three. These lines were detected simultaneously with yeast recipients behind the plate with four spectral slits (see a similar plate in Fig. 21.15) (Gurwitsch 1934), which reduced the number of experiments per one spectral measurement by several times.

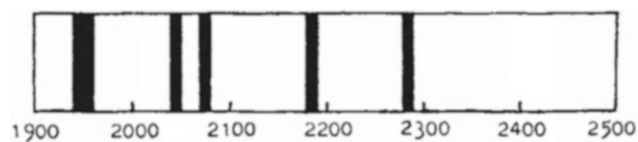


Fig. 21.22 MGR spectrum of urea-urease system (based on 300 experiments). (Reprinted from Prokofiewa (1934). Copyright 1932, with permission from Springer Nature)

21.3.3.3 Spectra Interpretation

Initially, the spectra specificity related to rather simple model systems allowed A.G. Gurwitsch hypothesize that mitogenetic spectra can be used for identification of chemical/biochemical processes taking place in the studied system: e.g., “phosphatase spectrum” was explained as a result of breaking ether bonds by phosphatase (Gurwitsch and Gurwitsch 1932) (see also Gurwitsch and Gurwitsch (1999) for the history of this issue). However, this didn’t explain the mechanisms of its formation and anyway looked more like a temporary hypothesis, needing further clarification.

In 1933 J. Frankenburger formulated the chemiluminescence energy paradox: high-energy MGR quanta (>100 kcal/mol) are generated in course of low-enthalpy reactions (mostly ~ 0 – 30 kcal/mol) occurring within the system (Frankenburger 1933). This led him suggest the free-radical mechanism of photon generation, supported and further developed by R. Audubert (Audubert 1939). According to this concept, photons (of MGR, and later – of UPE/chemiluminescence in general) are generated in course of rare highly energetic side reactions, which involve free radicals appearing within the system. Appearance of photons is likely associated with recombination of such free radicals (see energy considerations in Sect. 9.1). Moreover, the energy liberated at free-radical recombination could be either emitted at once or transferred to some fluorescent substances (taking part in the reaction or not) and then emitted by them with their own specific spectrum: “...ultra-violet luminescence could here either be caused directly by recombination of atoms with radicals, or indirectly by transferring the energy balance to “molecules capable of radiating” (citation from Frankenburger (1933) as translated in Gurwitsch and Gurwitsch (1939)). Obviously, this kind of energy transfer meant that the actual MGR spectrum could be determined not by the reacting radicals, but by the fluorescent substances (participating in the reaction or not), that finally emitted the quanta. Strikingly, this completely anticipated what is known about the mechanisms of UPE/chemiluminescence today (see Parts II–III, particularly Chaps. 5, 9 and 10).

Further mitogenetic data were consistent with this suggestion. MGR spectra were found to change greatly when certain substances were added (even those, not involved in the

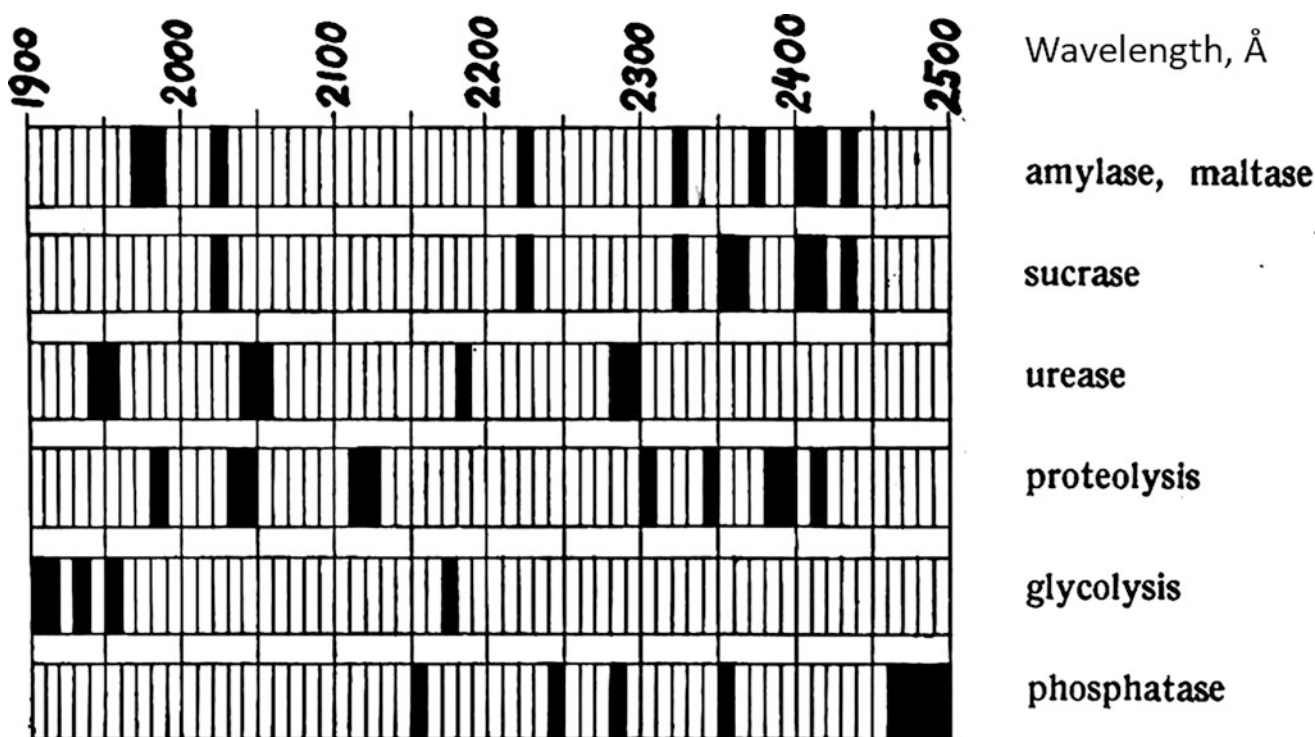


Fig. 21.23 MGR spectra of some enzymatic reactions. (Data from Gurwitsch and Gurwitsch (1934a). Reprinted from Rahn (1937))

reaction) in quite small amounts. For instance, addition of glucose to the urea-urease system led to certain features of the “glycolytic spectrum” in the system’s MGR, though glucose was not participating in the main reaction (Gurwitsch and Gurwitsch 1959). The same bands appeared when glucose was added to the aqueous solution of irradiated glycine⁵ (Gurwitsch et al. 1939; Gurwitsch and Gurwitsch 1939) (see Fig. 21.25). Thus, the “glycolytic spectrum” was concluded to evidence some excited state of glucose molecules (Gurwitsch et al. 1939; Gurwitsch and Gurwitsch 1939, 1945, 1948). Contrary to that, the spectrum of nucleic acid splitting was associated not with the whole molecule

excitation, but with the excitation of one of the split products. Addition of nucleic acid to irradiated glycine solution did not produce “phosphatase” bands, while the splitting of nucleic acid and lecithin by phosphatase resulted in identical spectra, which the authors attributed to the phosphate ion. Addition of sodium phosphate to irradiated glycine solution produced the whole phosphatase spectrum and the specific spectrum of sodium ion⁶ (Fig. 21.25).

Experiments with various substances and mitogenetic sources (Gurwitsch and Gurwitsch 1939, 1934a, 1948; Gurwitsch 1968) allowed to divide the studied substances into “fluorescent” and “nonfluorescent.” The “fluorescent” substances were small molecules and their residues such as monosaccharides (glucose, fructose, mannose), sucrose, tryptophan, phosphate radical, sodium and chlorine ions, while all “nonfluorescent” substances were high-molecular compounds (glycogen, pure albumin, nucleic acids). Emission of substances excited due to the transfer of energy released in chemical reactions was called sensitized fluorescence (the term suggested by the physicist A.N. Filippov (Gurwitsch 1968)).

⁵Irradiated glycine solution was widely used in experiments as a source of mitogenetic radiation with the simplest emission spectrum: it contained only one band of 229–230 nm (Gurwitsch and Gurwitsch 1934a), which Gurwitsch related to its desamination (Gurwitsch and Gurwitsch 1938). Though it is too early to speculate on the real origin of such spectral bands, we have to admit that they cannot be explained by the process per se. Contrary to that, a distinct band in the luminescence spectrum can only mark a certain electron-excited state, appearing in the system and undergoing radiational relaxation. Obviously, such states can well be standard and characteristic for a certain process, like Russel’s tetroxide at recombination of hydrocarbon peroxy radicals (see Sect. 10.5.1, 10.5.2), or (supposedly) some specific state at glycine desamination in the above example. However, all this reasoning is currently based on unverified primary data on MGR, so is somehow ahead of time.

⁶Both “excited glucose molecule” and “excited phosphate/sodium ions” may seem naïve, but the mode of reasoning is remarkably close to the modern one.

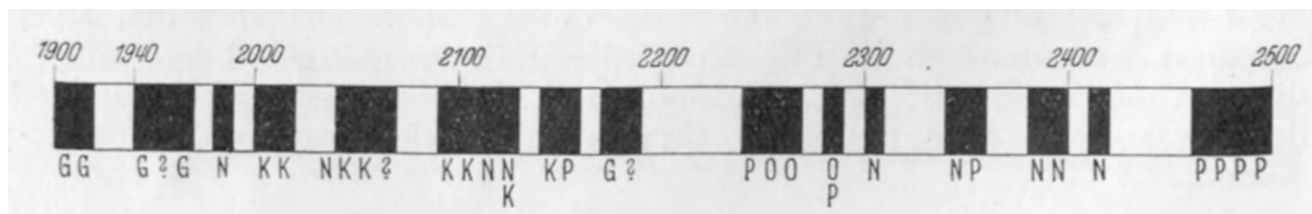


Fig. 21.24 Mitogenetic spectral analysis of MGR from rabbit blood. The spectral features were identified as follows: G – glycolytic spectrum; N – spectrum of peptide cleavage (referred to as NH_3 spectrum), K – spectrum of creatine-phosphate cleavage; P – phosphatase

spectrum; O – oxidation spectrum; ? – lines of unknown origin. (Reprinted from Golischewa (1933). Copyright 1933, with permission from Springer Nature)

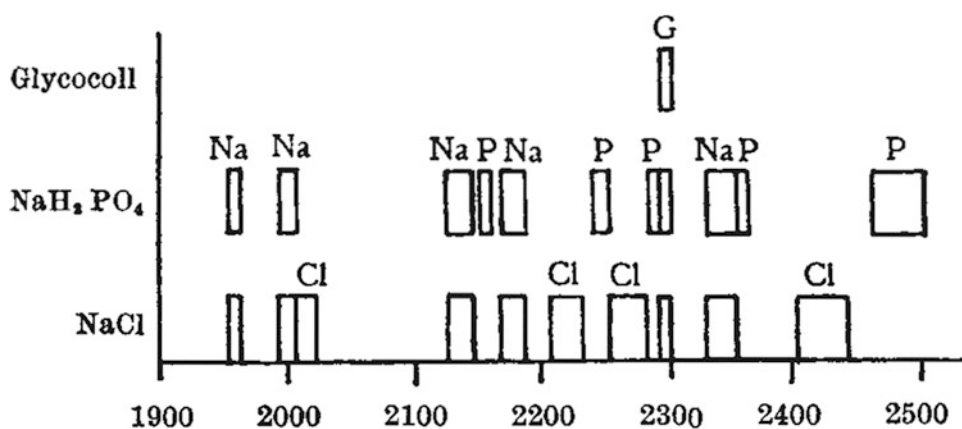


Fig. 21.25 MGR spectra of irradiated glycine (first row), and irradiated glycine with addition of NaH_2PO_4 (second row) and NaCl (third row). The PO_4 spectrum (denoted by “P”) as found here is identical with that of nucleic acid fermentation. (Reprinted from Gurwitsch and Gurwitsch

(1934a). Copyright 1933, with permission from Springer Nature, see also details of experiment in Gurwitsch et al. (1939); Gurwitsch and Gurwitsch (1939) and the method description in Gurwitsch and Gurwitsch (1934a))

21.4 Conclusions

Thus, notwithstanding great technical difficulties, the factor producing the mitogenetic effect in biological recipients was physically characterized. It was shown to be ultraweak UV photon emission and designated as mitogenetic radiation (MGR). Here is the summary of its main physical properties:

- Intensity: $\sim 10\text{--}1000 \text{ photons} \cdot \text{cm}^{-2} \cdot \text{s}^{-1}$.
- Spectrum: $\sim 190\text{--}250 \text{ nm}$ (rarely up to 340 nm)
- Polarization not investigated
- Temporal structure: Supposed to consist of short bursts, but based only on the data on “intermittent induction” (see Chap. 20), without direct proofs

The attempts of physical MGR detection gave rise to development of photosensitive modifications of Geiger–Muller counters and advanced techniques.

This type of devices and later photo multiplying tubes (PMT) were successfully used to detect MGR from different

objects, producing biological MGE, which appeared a good confirmation of the biological data (see Chap. 20).

However, the MGR spectral estimates using such physical detectors as gas-discharge counters were very rough and could be based only on the sensitivity spectra of different photodetectors used. The spectrally decomposed MGR could not be measured with these devices for its extremely low intensity. Much later, this issue was partially solved by using PMTs with photo filters and signal accumulation in experimental replicates (see Sect. 21.2.4.3).

Yet, the real MGR spectral decomposition appeared possible if replacing physical detectors with biological MGR recipients (see Sect. 21.3.2). How the detection of spectrally decomposed ultraweak photon emission, even by biological recipients, can be physically possible at such low intensities remains an open question. The authors used “intermittent induction,” but the mechanism of the increasing effect of this is also unclear to us. Chapters 24, 25, 26, and 27 provide a discussion of various possibilities (or impossibilities) of ultra-weak light detection, and maybe some of this does take part in the biological detection of MGR. Anyway, the biological recipients of MGE appeared to have unexpectedly

high sensitivity to ultraweak UV, supposedly, with certain specific features. Schemes with biological MGE recipients as detectors inherited all the drawbacks of biological principle of detection like laboriousness, sensitivity of biological recipients to numerous extraneous factors and necessity of multiple repeats; however, the obtained spectral features impress with their high reproducibility in an extensive series of experiments.

Acknowledgments We sincerely thank the heirs of Alexander Gurwitsch and his late grandson, Lev Belousov, for unlimited access to their personal library, containing probably the most comprehensive collection of papers on MGE.

References

- Audubert R (1935a) Sur la sensibilité des compte-photons. *Comptes Rendus Acad Sci* 200:918–920
- Audubert R (1935b) Sur quelques propriétés des compteurs photoélectriques. *J. Phys. Radium* 6:451–456. doi:<https://doi.org/10.1051/jphysrad:01935006011045100>
- Audubert R (1936a) Sur le domaine spectral d'émission des réactions chimiques. *Comptes Rendus Acad Sci* 202:131–133
- Audubert R (1936b) Die Strahlung bei chemischen Reaktionen. *Document Sci* 5:267–274
- Audubert R (1936c) Émission de rayonnement par les réactions chimiques. *J Chim Physique* 33:507–525
- Audubert R (1936d) Sur le mécanisme d'émission de la lumière par les réactions chimiques. *Comptes Rendus Acad Sci* 202:406–407
- Audubert R (1937a) Étude de l'émission du rayonnement ultraviolet au cours de la décomposition lente des azotures. *J Chim Phys* 34:405–416 (erratum 615)
- Audubert R (1937b) Sur l'énergie d'activation des réactions photogéniques accompagnant la thermolyse des azotures. *Comptes Rendus Acad Sci* 204:1192–1194
- Audubert R (1937c) Sur les spectres d'émission ultraviolet de la dissociation thermique lente de l'azoture d'argent. *Comptes Rendus Acad Sci* 205:133–135
- Audubert R (1938a) Die Emission von Strahlung bei chemischen Reaktionen. *Angewandte Chemie* 51 (11):153–163. doi:<https://doi.org/10.1002/ange.19380511102>
- Audubert R (1938b) Sur le spectre d'émission ultraviolet de la dissociation thermique lente de l'azoture de sodium. *Comptes Rendus Acad Sci* 206:748–750
- Audubert R (1939) Emission of ultraviolet rays by chemical reactions. *Transactions of the Faraday Society* 35 (213):197–206
- Audubert R (1943) Sur le mécanisme de l'émission de rayonnement ultraviolet par polarisation anodique. *Comptes Rendus Acad Sci* 216:880–882
- Audubert R, Doormaal V (1933) Sur l'émission de rayonnement par les réactions chimiques. *Comptes Rendus Acad Sci* 196:1883–1885
- Audubert R, Lévy R (1935a) Émission de rayonnement par l'excitation nerveuse. *Comptes Rendus Acad Sci* 200:1634–1636
- Audubert R, Lévy R (1935b) Émission de rayonnement par les œufs de *Discoglossa* en cours de développement. *Comptes Rendus Acad Sci* 201 (3):236–239
- Audubert R, Mattler J (1938a) Influence des vapeurs sur la courbe de sensibilité spectrale des compteurs photoélectriques. *Comptes Rendus Acad Sci* 206:1005–1007
- Audubert R, Mattler J (1938b) Action des gaz sur les réactions photogéniques accompagnant la thermolyse de l'azoture de sodium. *Comptes Rendus Acad Sci* 206:1639–1641
- Audubert R, Muraour H (1937) Étude de l'émission du rayonnement ultraviolet au cours de la décomposition lente des azotures. *Comptes Rendus Acad Sci* 204:431 — 432
- Audubert R, Prost M (1936) Sur le rayonnement émis dans la déshydratation et l'hydratation et du sulfate de quinine. *Comptes Rendus Acad Sci* 202:1047 — 1049
- Audubert R, Racz C (1939) Emission de rayonnement ultraviolet et thermolyse de l'azoture de thallium. *Comptes Rendus Acad Sci* 208 (23):1810–1811
- Audubert R, Ralea R (1939) Effet photogénique et activation électronique du radical $N\equiv N$. *Comptes Rendus Acad Sci* 208 (23): 983–985
- Audubert R, Riethmuller C (1935) Sur la sensibilité spectrale des compteurs photoélectriques. *Comptes Rendus Acad Sci* 200:389–391 (erratum 596)
- Audubert R, Verdier ET (1939) Sur l'émission du rayonnement ultraviolet par l'électrolyse de solutions d'acide azotrique et d'azoture de sodium. *Comptes Rendus Acad Sci* 208 (25):1984–1986
- Audubert R, Viktorin O (1936) Émission de lumière ultraviolette pendant l'oxydation anodique de l'aluminium. *C R hebdomadaire Séances Acad Sci* 200:1504–1507
- Audubert R, Viktorin O (1937) Sur l'émission de lumière ultra-violette par l'oxydation anodique de l'aluminium. *J Chim physique* 34:18–27
- Barth H (1934) Versuche zum physikalischen Nachweis von mitogenetischer Strahlung. *Archive of Biological Sciences Ser B* 35 (1):29–36
- Barth H (1935) Novel method of studying mitogenetic problem by means of photoelectron counter (in Russian). *Bulletin of All-Union Institute of Experimental Medicine* (8):12–15
- Barth H (1936) Physikalische Versuche zum Problem der mitogenetischen Strahlung. *Biochemische Zeitschrift* 285:311–339
- Barth H (1937) Physical studies on the question of mitogenetic radiation problem (in Russian). *Archive of Biological Sciences* 46 (1): 153–177
- Bateman JB (1935) Mitogenetic radiation. *Biological Reviews* 10 (1): 42–71. doi:<https://doi.org/10.1111/j.1469-185X.1935.tb00476.x>
- Blacher LA, Holzman OG (1930) Resorption processes as a source of morphogenesis. 1. Role of mitogenetic radiation in processes of metamorphosis of batrachians (In Russian). *Medico-biological Journal* (3):150–170
- Braun AD (1934) Lipolysis as a source of mitogenetic radiation. *Nature* 134 (3388):536. doi:<https://doi.org/10.1038/134536d0>
- Braunstein AE, Potozky AP (1934) About specificity of mitogenetic radiation spectra in oxidation-reduction reactions (In Russian). *Archive of Biological Sciences, Ser B* 35 (1):73–86
- Brunetti R, Maxia C (1930) Sulla fotografia e la eccitazione delle radiazioni del Gurwitsch. *Atti della Società fra i Cultori delle Scienze Mediche e Naturali in Cagliari* 32 (2):50–57
- Čech A (1932a) Gurwitsch's rays and their connection with lytic ferments and rickets (In Czech). *Čas. Lék. česk.* 71:70–74
- Čech A (1932b) Gurvitch rays (In Czech). *Čas. Lék. česk.* 71:585–587
- Chariton J, Frank G, Kannegiesser N (1930) Über die Wellenlänge und Intensität mitogenetischer Strahlung. *Naturwissenschaften* 18 (19): 411–413. doi:<https://doi.org/10.1007/bf01501123>
- Copisarow M (1932) Radiation and enzyme activity. *Nature* 130:1001–1002. doi:<https://doi.org/10.1038/1301001b0>
- Copisarow M (1934) Metabolic oxidation and radiation. *Protoplasma* 21 (1):73–80. doi:<https://doi.org/10.1007/bf01984466>
- Decker G (1936) Über die Schärfe mitogenetischer Spektren. *Protoplasma* 25 (1):515–527. doi:<https://doi.org/10.1007/bf01839124>
- Dessauer F (1931) Bemerkung über den physikalischen Nachweis der mitogenetischen Strahlung von Gurwitsch. *Archiv für exper Zellforschung, besonders Gewebzüchtung* 11:33–37
- Elger L (1932) Conditions of photographic registration of Gurwitsch radiation (In Czech). *Čas lék česk* 71:418–421

- Elster J, Geitel H (1916) Über Stromschwankungen in Vakuumröhren bei Gegenwart von Alkalimetallen, ihre Bedeutung für den Entladungsvorgang und für die Messung äusserst kleiner Lichtintensitäten. *Phys Z* 17:268–276
- Frank G (1929) Das mitogenetische Reizminimum und -maximum und die Wellenlänge mitogenetischer Strahlen. *Biologisches Zentralblatt* 49:129–141
- Frank G, Rodionow S (1931) Über den physikalischen Nachweis mitogenetischer Strahlung und die Intensität der Muskelstrahlung. *Die Naturwissenschaften* 19 (30):659–659. doi:<https://doi.org/10.1007/BF01516035>
- Frank G, Rodionow S (1932) Physikalische Untersuchung mitogenetischer Strahlung der Muskeln und einiger Oxydationsmodelle. *Biochemische Zeitschrift* 249 (4/6):323–343
- Frank GM, Gurwitsch AG (1927) Zur Frage der Identität mitogenetischer und ultravioletter Strahlen. *Wilhelm Roux' Arch Entwickl Mech Org* 109 (3):451–454. doi:<https://doi.org/10.1007/bf02080806>
- Frankenburger W (1933) Neuere Ansichten über das Wesen photochemischer Prozesse und ihre Beziehungen zu biologischen Vorgängen. *Strahlenther Onkol* 47 (2):233–262
- Garner WE, Polanyi M, Emelús H, Norrish RGW, Vavilov S (1939) General discussion. *Transactions of the Faraday Society* 35:204–206. doi:<https://doi.org/10.1039/TF9393500204>
- Geiger H (1913a) Demonstration einer einfachen Methode zur Zählung von α - und β -Strahlen. *Physikalische Zeitschrift* 14:1129
- Geiger H (1913b) A method of counting alpha and beta rays. *Deutsch Phys Ges* 15:534–539
- Geiger H, Müller W (1928a) Das Elektronenzählrohr. *Physikalische Zeitschrift* 29:839–841
- Geiger H, Müller W (1928b) Elektronenzählrohr zur Messung schwächster Aktivitäten. *Die Naturwissenschaften* 16 (31):617–618
- Gerlach W (1933) Physikalisches zum Problem der mitogenetischen Strahlung. *Sitzungsber Ges Morphol und Physiol [München]* 42:1–10
- Gerlach W, Meyer E (1913) Über die Auslösung von Spitzenentladungen durch ultraviolettes Licht. *Verhandlungen der Deutschen Physikalischen Gesellschaft* 15:1037
- Gigon A, Noverraz M (1930) Organe als Strahlensender. *Schweiz Med Wochensh* 60:584–590
- Glasser O, Barth H (1938) Studies on the problem of mitogenetic radiation. *Radiology* 30 (1):62–67. doi:<https://doi.org/10.1148/30.1.62>
- Golischewa KP (1933) Die mitogenetische Spektralanalyse der Blutstrahlung am lebenden Tier. *Biochemische Zeitschrift* 260:52
- Gray J, Ouellet C (1933) Apparent mitogenetic inactivity of active cells. *Proceedings of the Royal Society of London Series B, Containing Papers of a Biological Character* 114 (786):1–9. doi:<https://doi.org/10.1098/rspb.1933.0067>
- Gray JV, Petsko GA, Johnston GC, Ringe D, Singer RA, Werner-Washburne M (2004) “Sleeping beauty”: quiescence in *Saccharomyces cerevisiae*. *Microbiology and molecular biology reviews* 68 (2):187–206. doi:<https://doi.org/10.1128/MMBR.68.2.187-206.2004>
- Grebe L, Krost A, Peukert L (1937) Versuche zum physikalischen Nachweis der mitogenetischen Strahlung. *Strahlenther Onkol*, 60: 575–581
- Gurvich AA, Eremeev V, Karabchievskii Iu A (1968) Measurement of mitogenetic radiation of yeast culture by photoelectric multipliers. The relation between radiation and cell division and the suppression of radiation by cancer quencher (In Russian). *Doklady Akademii nauk SSSR* 178 (6):1432–1435
- Gurwitsch A, Gurwitsch L (1934a) L'analyse mitogénétique spectrale. *Actualités scientifiques et industrielles, vol. 150 - Exposés de physiologie, vol 4*. Hermann & Cie, Paris
- Gurwitsch A, Gurwitsch L (1938) Über Anreicherung (Neubildung) von Fermenten auf Kosten von Aminosäuren. *Enzymologia* 5:17–25
- Gurwitsch AG, Gurwitsch LD, Sliusarev AA (1939) Mitogenetic radiation regarded as “sensitized fluorescence”. Experimental confirmation of Frankenburger's hypothesis on the origin of mitogenetic radiation (In Russian). *Archive of Biological Sciences* 55(2): 104–107
- Gurwitsch AA (1968) Problema mitogeneticheskogo izluchenija kak aspekt molekuliarnoj biologii (The problem of mitogenetic emission as an aspect of molecular biology). *Meditsina, Leningrad*
- Gurwitsch AA, Eremeev VF, Karabchievsky YA (1965) Ultra-weak emission in the visible and ultra-violet regions in oxidation of solutions of glycine by hydrogen peroxide. *Nature* 206:20–22
- Gurwitsch AG (1923) Die Natur des spezifischen Erregers der Zellteilung. *Archiv für mikroskopische Anatomie und Entwicklungsmechanik* 100 (1–2):11–40. doi:<https://doi.org/10.1007/bf02111053>
- Gurwitsch AG (1924) Physikalisches über mitogenetische Strahlen. *Archiv für mikroskopische Anatomie und Entwicklungsmechanik* 103 (3–4):490–498. doi:<https://doi.org/10.1007/bf02107498>
- Gurwitsch AG (1925) The Mitogenetic Rays. *Botanical Gazette* 80 (2): 224–226. doi:<https://doi.org/10.1086/333527>
- Gurwitsch AG (1928) Some problems of mitogenetic radiation (In Russian). *Journal of Russian Botanical Society* 13:179–189
- Gurwitsch AG, Gurwitsch LD (1925) Über die präsumierte Wellenlänge mitogenetischer Strahlen. *Wilhelm Roux' Archiv für Entwicklungsmechanik der Organismen* 105 (2):473–474. doi:<https://doi.org/10.1007/bf02080850>
- Gurwitsch AG, Gurwitsch LD (1932) Die mitogenetische Strahlung, vol 25. *Monographien aus dem Gesamtgebiet der Physiologie der Pflanzen und der Tiere*. Springer-Verlag Berlin Heidelberg, Berlin. doi:<https://doi.org/10.1007/978-3-662-26146-0>
- Gurwitsch AG, Gurwitsch LD (1934b) Mitogeneticheskije izluchenije [Mitogenetic radiation] (in Russian). VIEM publishing house, Leningrad
- Gurwitsch AG, Gurwitsch LD (1939) Ultra-Violet Chemi-Luminescence. *Nature* 143 (3633):1022–1023. doi:<https://doi.org/10.1038/1431022b0>
- Gurwitsch AG, Gurwitsch LD (1945) Mitogeneticheskije izluchenije: fizikokhimeskije osnovy i prilozhenija v biologii i meditsine (Mitogenetic radiation: physical and chemical bases and applications in biology and medicine). *Medgiz, Moscow*
- Gurwitsch AG, Gurwitsch LD (1948) Vvedenije v uchenije o mitogeneze (in Russian) [An introduction to the teaching of mitogenesis]. *USSR Academy of Medical Sciences Publishing House, Moscow*
- Gurwitsch AG, Gurwitsch LD (1959) Die mitogenetische Strahlung (Mitogenetic radiation). *VEB Gustav Fischer Verlag, Jena*
- Gurwitsch AG, Gurwitsch LD (1999) Twenty Years of Mitogenetic Radiation: Emergence, Development, and Perspectives (translation from *Uspekhi Sovremennoi Biologii /Advances in Contemporary Biology*, 1943, Vol.16, No. 3, pages 305–334). *21st Century Science and Technology Magazin* 12 (3):41–53
- Gurwitsch LD (1934) Mitogenetic spectrum at excitation of proprioceptive nerve filaments (In Russian). *Archive of Biological Sciences Ser B* 35 (1):141–144
- Hauer F (1932) Über mitogenetische Strahlung. *Verh Deut Physikal Ges* 13:11
- Hausser KW, Kreuchen KH (1934) Quantenausbeuten bei Lichtzählern *Zeits f tech Physik* 15:20–23
- Heinemann M (1934) Physico-chemical test for mitogenetic (Gurwitsch) rays. *Nature* 134:701. doi:<https://doi.org/10.1038/134701b0>
- Heinemann M (1935) Physico-chemical test for mitogenetic (Gurwitsch) rays. *Acta Brevia Neerland* 5:15

- Hollaender A (1936) The problem of mitogenetic rays. In: Duggar B (ed) *Biological effects of radiation*, vol 2. 1 edn. McGraw-Hill Book Company, Inc., NY, London, pp 919–958
- Hollaender A, Claus WD (1935) Some Phases of the Mitogenetic Ray Phenomenon. *Journal of Optical Society of America* 25:270–286
- Hollaender A, Claus WD (1937) An experimental study of the problem of mitogenetic radiation, vol 100. *Bulletin of the National research council. National research council of the National academy of sciences*, Washington
- Iterson Gv, Heide Hvd (1930) Stempell's Versuche zum Nachweis der mitogenetischen Strahlung mit Hilfe der Liesegang'schen Ringe. *Proceedings Koninklijke Akademie van Wetenschappen te Amsterdam* 33 (7):702–706
- Kannegiesser N (1931) Die mitogenetische Spektralanalyse. I. *Biochemische Zeitschrift* 236:415–424
- Karev MW, Rodionov SF (1934) Die Empfindlichkeit von Lichtzählern. *Zeits f Physik* 92:615–621
- Konev SV (1965) The nature and biological importance of ultraweak luminescence of a cell (In Russian). In: *Bioluminescences. Trudy MOIP (Bioluminescence. MOIP Reports)*, vol 21. "Nauka", Moscow, pp 181–185
- Konev SV (1967) *Fluorescence and Phosphorescence of Proteins and Nucleic Acids*. Plenum Press, New York
- Konev SV, Lyskova IT, Nisenbaum GD (1966) Very weak bioluminescence of cells in the ultraviolet region of the spectrum and its biological role. *Biophysics* 11 (2):410–413
- Konev SV, Lyskova TI, Bobrovich VP (1963) On the nature of the ultraviolet luminescence of cells (in Russian). *Biofizika* 8: 433–440
- Konev SV, Troitskii NA, Katibnikov MA (1961) Chemiluminescence of proteins and biological objects in the visible and ultraviolet region of the spectrum: Report presented at the V International biochemical congress (Moscow, 1961). Central Statistical Office of the B.S.S.R., Minsk (see also Report abstract 14.56 In: *Proceedings of the 5 International Congress of Biochemistry, Moscow, 1961*) (1963) *Academic Press*, pp 343
- Kreuchen KH, Bateman JB (1934) Physikalische und biologische Untersuchungen über mitogenetische Strahlung. *Protoplasma* 22 (1):243–273. doi:<https://doi.org/10.1007/bf01608868>
- Lévy R, Audubert R (1936) Émission de rayonnement par les œufs de Discoglossa en cours de développement. *Protoplasma* 25 (1): 25–31. doi:<https://doi.org/10.1007/BF01839027>
- Lindman KF (1920) Über eine durch ein isotropes System von spiralförmigen Resonatoren erzeugte Rotationspolarisation der elektromagnetischen Wellen. *Annalen der Physik* 63:621–644
- Locher G (1932) Photoelectric quantum counters for visible and ultraviolet light. *Phys Rev.* 42:525–546
- Loos W (1930) Untersuchungen über mitogenetische Strahlen. *Jahrb Wiss Bot* 72 (4):611–664
- Lorenz E (1934) Search for mitogenetic radiation by means of the photoelectric method. *The Journal of general physiology* 17 (6): 843–862. doi:<https://doi.org/10.1085/jgp.17.6.843>
- Lorenz E (1933) Investigation of mitogenetic radiation by means of a photoelectric counter tube. *Pub Hlth Rep* 48:1311–1318
- Magrou J (1930) Sur l'interprétation des actions biologiques à distance. *Compt Rend Acad Sci (Paris)* 190:84–87
- Magrou MJ, Magrou MM, Reiss MP (1929) Action à distance de divers facteurs sur le développement de l'œuf d'Oursin. *Compt Rend Acad Sci* 189:779
- Maxia C (1930) Gli anelli di Liesegang adoprati come detectori negli studi sulle radiazioni mitogenetiche. *Atti della Società fra i Cultori delle Scienze Mediche e Naturali in Cagliari* 32 (5):194–198
- Maxia C (1932) Effetti diversi di radiazioni e di gas sugli anelli di Liesegang. *Radiobiologia* 1 (1):39–48.
- Metcalf WS, Quickenden TI (1967) Mitogenetic Radiation. *Nature* 216 (5111):169–170. doi:<https://doi.org/10.1038/216169a0>
- Pasteur L (1850) Recherches sur les propriétés spécifiques des deux acides qui composent l'acide racémique. *Annales de chimie et de physique* 28(3):56–99
- Petri L (1928) Sopra le radiazioni mitogenetiche del Gurwitsch. *R C Accad Lincei, Ser VI* 7:891–896
- Petri L (1932) Di un metodo fotoelettrico per mettere in evidenza le radiazioni mitogenetiche del Gurwitsch. *R C Accad Lincei, Ser VI* 15:919–925
- Petri L (1933) Nachweis der Mitogenetischen Strahlung durch Eine Physikalische Methode. *Protoplasma* 19 (1):365–369. doi:<https://doi.org/10.1007/bf01606234>
- Ponomarewa J (1931) Die mitogenetische Spektralanalyse. III. Mitteilung: Das detaillierte glykolytische Spektrum. *Biochemische Zeitschrift* 239:424
- Potozky A (1930) Über Beeinflussung des mitogenetischen Effekts durch sichtbares Licht. *Biologisches Zentralblatt* 50:712–723
- Potozky A (1932) Untersuchungen über den Chemismus der mitogenetischen Strahlung. II. Mitteilung: Die mitogenetischen Spektren der Oxydationsreaktionen. *Biochemische Zeitschrift* 249: 282–287
- Potozky A (1936) Über Beeinflussung der Zellpermeabilität durch mitogenetische Bestrahlung. *Protoplasma* 25 (1):49–55. doi:<https://doi.org/10.1007/bf01839030>
- Pringsheim P (1913) Über die Beobachtung lichtelektrischer Schwankungen mit Hilfe empfindlicher Spitzen. *Verhandlungen der deutschen physikalischen Gesellschaft* 15:705
- Prokofiewa EG (1934) Mitogenetic Radiation of the Urea-Urease System. *Nature* 134 (3389):574–574. doi:<https://doi.org/10.1038/134574a0>
- Protti GI (1930) I raggi mitogenetici nell' emoinnesto e prime loro fotografie. In: *Comunicazione alla Seduta scientifica dell'Ospedale Civile di Venezia, XVIII*. Stamperia Carlo Rertotti, Venezia
- Protti G (1930b) Il fenomeno della emoradiazione applicato alla clinica. *Radiobiologia* 1 (4):49–49
- Protti G (1932) Effetti fotografici intraorganici I (2):61–65
- Quickenden TI, Comarmond MJ, Tilbury RN (1985) Ultraweak bioluminescence spectra of stationary phase *Saccharomyces cerevisiae* and *Schizosaccharomyces pombe*. *Photochem Photobiol* 41 (5):611–615. doi:<https://doi.org/10.1111/j.1751-1097.1985.tb03534.x>
- Quickenden TI, Hee SSQ (1976) The spectral distribution of the luminescence emitted during growth of the yeast *Saccharomyces cerevisiae* and its relationship to mitogenetic radiation. *Photochem Photobiol* 23 (3):201–204. doi:<https://doi.org/10.1111/j.1751-1097.1976.tb07242.x>
- Quickenden TI, Que Hee SS (1971) The luminescence of water excited by ambient ionizing radiation. *Radiat Res* 46 (1):28–35
- Quickenden TI, Que Hee SS (1974) Weak luminescence from the yeast *Saccharomyces cerevisiae* and the existence of mitogenetic radiation. *Biochem Biophys Res Commun* 60 (2):764–770
- Quickenden TI, Tilbury RN (1983) Growth dependent luminescence from cultures of normal and respiratory deficient *Saccharomyces cerevisiae*. *Photochem Photobiol* 37 (3):337–344
- Quickenden TI, Tilbury RN (1991) Luminescence spectra of exponential and stationary phase cultures of respiratory deficient *Saccharomyces cerevisiae*. *Journal of photochemistry and photobiology B, Biology* 8 (2):169–174. doi:[https://doi.org/10.1016/1011-1344\(91\)80055-M](https://doi.org/10.1016/1011-1344(91)80055-M)
- Rabinerson AJ, Filippov MV (1938) Short-wavelength ultraviolet emission in structurization processes (In Russian). *Zhurnal Fizicheskoi Khimii* 11(5):688–701
- Rahn O (1936) Invisible radiations of organisms, vol 9. *Protoplasma-Monographien*. Gebrüder Bornträger, Berlin
- Rahn O (1937) Mitogenetic radiation. *Tabulae biologicae* 14 (1):1–35
- Rajewsky B (1930a) Anordnung zur Messung kleinster Lichtintensitäten. *Zeits f Physik* 63:576

- Rajewsky B (1930b) Eine neue Messanordnung für kleinste Lichtintensitäten. *Strahlenther Onkol* 39:194–200
- Rajewsky B (1931a) Über einen empfindlichen Lichtzähler. *Physikalische Zeitschrift* 32:121–124
- Rajewsky B (1931b) Ultraviolett-Strahlung des Eiweiss. *Klinische Wochenschrift* 10 (36):1672–1673. doi:<https://doi.org/10.1007/bf01755391>
- Rajewsky B (1931c) Zur Frage des physikalischen Nachweises der Gurwitsch-Strahlung. In: Dessauer F (ed) *Zehn Jahre Forschung auf dem physikalisch-medizinischen Grenzgebiet*. Georg Thieme Verlag, Leipzig, pp. 244–257
- Rajewsky B (1932) Zum Problem der mitogenetischen Strahlung. *Zeitschrift für Krebsforschung* 35 (1):387–394. doi:<https://doi.org/10.1007/bf01792230>
- Rajewsky B (1934) Weitere Erfahrungen mit dem Lichtzähler. I. Teil: Beschreibung verschiedener Lichtzählertypen. *Ann d Physik* 412: 13–32
- Rawin W (1924) Weitere Beiträge zur Kenntnis der mitotischen Ausstrahlung und Induktion. *Archiv für Mikroskopische Anatomie und Entwicklungsmechanik* 101 (1/3):53–61
- Reiss KH (1935) Über eine neuartige lichtelektrische Apparatur speziell zur Untersuchung von Lichtzählern. *Zeitschrift für Physik* 93 (5-6): 411–415
- Reiter T, Gabor D (1928a) Ultraviolette Strahlen und Zellteilung. *Strahlenther Onkol* (28):125–131
- Reiter T, Gabor D (1928b) Zellteilung und Strahlung. Sonderheft der Wissenschaftlichen Veröffentlichungen aus dem Siemens-Konzern. Springer-Verlag, Berlin. doi:<https://doi.org/10.1007/978-3-642-50832-5>
- Rodionov SF, Frank GM (1934a) *Voprosy svetobiologii i izmereniya sveta* (Problems of Light Biology and Light Measurement). Gostekhizdat, Moscow-Leningrad
- Rodionov SF, Frank GM (1934b) On the measurements of mitogenetic radiation by means of a photoelectron register (In Russian). *Archive of Biological Sciences Ser B* 35 (1):277–288
- Rossmann B (1928) Untersuchungen über die Theorie der mitogenetischen Strahlen. *Wilhelm Roux' Archiv für Entwicklungsmechanik der Organismen* 113 (2):346–405. doi:<https://doi.org/10.1007/bf02081074>
- Rutherford E, Geiger H (1908) An electrical method of counting the number of α particles from radioactive substances. *Proceedings of the Royal Society Series A* 81 (546):141–161
- Ruyssen R (1933) Sur l'énergie et les limites de longueur d'onde des rayons mitogenetiques. *Acta Brev Neerl* (3):141–142
- Salkind S (1937) Der gegenwärtige Stand des mitogenetischen Problems. *Protoplasma* 28 (1):435–468. doi:<https://doi.org/10.1007/bf01625014>
- Schreiber H (1933) Zur Theorie der "mitogenetischen Strahlung". *Protoplasma* 19 (1):1–25. doi:<https://doi.org/10.1007/bf01606160>
- Schreiber H, Friedrich W (1930) Über Nachweis und Intensität der mitogenetischen Strahlung. *Biochem Zeitsch* (227):386–400
- Seyfert F (1932) Über den physikalischen Nachweis von mitogenetischen Strahlen. *Jahrb Wiss Bot* (76):747–764
- Shelkov LS, Prager IA, Kostin AG (1959) Photon counters for precise measurements of ultraviolet radiation (In Russian). *Pribory i tehnika eksperimenta* (Devices and techniques for experiments) (3):50–56
- Siebert WW (1930) Das Stempell-Phänomen an den Liesegang'schen Ringen. *Biochemische Zeitschrift* 220 (4.-6.):487–492
- Siebert WW (1931a) Bericht über eigene Untersuchungen zum Problem der mitogenetischen Strahlung (2. Internat. Zellforscher-Kongress 1930, Amsterdam). *Arch f experim Zellforschung* 11:52–55
- Siebert WW (1931b) Untersuchungen über mitogenetische Strahlen. *Strahlenther Onkol* 40:780–783
- Siebert WW, Seffert H (1933) Physikalischer Nachweis der Gurwitsch-Strahlung mit Hilfe eines Differenzverfahrens. *Naturwissenschaften* 21 (9):193–194. doi:<https://doi.org/10.1007/bf01504200>
- Siebert WW, Seffert H (1934) Zur Frage des physikalischen Nachweises der Gurwitsch-Strahlung. *Archive of Biological Sciences Ser B* 35 (1):177–181
- Stempell W (1929) Nachweis der von frischem Zwiebelsohlenbrei ausgesandten Strahlen durch Störung der Liesegang'schen Ringbildung. *Biologisches Zentralblatt* 49:607
- Stempell W (1931) Das Wasserstoffsperoxyd als Detektor für Organismenstrahlung und Organismengasung. *Protoplasma* 12: 538–548. doi:<https://doi.org/10.1007/BF01618778>
- Stempell W (1932) Die unsichtbare Strahlung der Lebewesen (Mitogenetische oder Organismenstrahlung). Verlag von Gustav Fischer, Jena
- Stempell W, Romberg GV (1931) Über Organismenstrahlung und Organismengasung. *Protoplasma* 13 (1):28–235. doi:<https://doi.org/10.1007/bf01599624>
- Taylor GW, Harvey EN (1931) The theory of mitogenetic radiation. *Biolog Bull* 61 (3):280–293
- Tilbury RN, Quickenden TI (1988a) Spectral and Time-Dependence Studies of the Ultraweak Bioluminescence Emitted by the Bacterium *Escherichia-Coli*. *Photochem Photobiol* 47 (1):145–150. doi:<https://doi.org/10.1111/j.1751-1097.1988.tb02704.x>
- Tilbury RN, Quickenden TI (1988b) Spectral and time dependence studies of the ultraweak bioluminescence emitted by the bacterium *Escherichia coli*. *Photochem Photobiol* 47 (1):145–150. doi:<https://doi.org/10.1111/j.1751-1097.1988.tb02704.x>
- Tilbury RN, Quickenden TI (1992) Luminescence from the yeast *Candida utilis* and comparisons across 3 genera. *Journal of bioluminescence and chemiluminescence* 7 (4):245–253. doi:<https://doi.org/10.1002/bio.1170070404>
- Tokin BP (1930) Über die mitogenetischen Strahlen und die Liesegang'schen Ringe. *Biol Zentralbl* 50:641–671
- Tokin BP (1931a) Mitogenetic rays and Liesegang Rings (In Russian). In: *Trudy po dinamike razvitiya* (Proceedings on Development Dynamics) vol 6. Medgiz, Moscow, pp 117–143
- Tokin BP (1931b) Über die mitogenetischen Strahlen und die Liesegang'schen Ringe (Vortrag auf dem 2. Internat. Zellforscherkongress 1930, Amsterdam). *Arch f experim Zellforschung* 11:65–66
- Tokin BP (1933) Mitogeneticheskiye luchi (In Russian) (Mitogenetic rays). Medgiz, Moscow
- Troitskii NA, Konev SV, Katibnikov MA (1961) Investigation of the ultraviolet chemiluminescence of biological systems. *Biophysics* 6 (2):80–81
- Vaccari A (1932a). *Zbl ges Radiol* 13
- Vaccari A (1932b) Ricerche sulle radiazioni mitogenetiche. *Arch Fisiol* 30:350–365
- Volodyaev IV, Belousov LV (2015) Revisiting the mitogenetic effect of ultra-weak photon emission. *Frontiers in physiology* 6(00241): 1–20. doi:<https://doi.org/10.3389/fphys.2015.00241>
- Wolff LK, Ras G (1931a) Einige Untersuchungen über die mitogenetischen Strahlen von Gurwitsch. *Ztrbl f Bakt I* 123:257–270
- Wolff LK, Ras G (1931b) Über Gurwitsch-Strahlen bei Bakterien. *Acta Brevia Neerlandica de physiologia, pharmacologia, microbiologia* 1 (7):136–137
- Wolff LK, Ras G (1932) Eenige onderzoekingen over demitogenetische stralen van Gurwitsch. *Ned Tijdschr Hyg* 6:265–280
- Zalkind SY (1940) Antimitogenetic monography (in Russian). *Archive of Biological Sciences* 57 (2–3):124–127
- Zirpolo G (1932) Studi sulla bioluminescenza batterica. XI. - Batteri luminosi ed Anelli di Liesegang. *Bollettino della Società dei Naturalisti in Napoli* 44:221–228

Elena V. Naumova and Ilya Volodyaev

22.1 Secondary Radiation

22.1.1 The Phenomenon of Secondary Radiation

The first attempts to classify biological objects by their ability to emit mitogenetic radiation into inductors and noninductors (see Chap. 20) appeared incomplete. Some objects, not inducing MGE by themselves, became stable inductors when ‘stimulated’ by other MGE inductors. This phenomenon was called ‘secondary mitogenetic radiation’ (see Gurwitsch and Gurwitsch 1932b, 1948).

The ‘secondary radiation’ was discovered (Gurwitsch and Gurwitsch 1927) and further studied in more detail (Potozky and Zoglina 1928) in experiments with onion roots. Being cut from the bulb, a root stopped emitting immediately. Yet, irradiation of its meristem or elongation zone with usual MGE inductors (e.g., root-inductors (Gurwitsch and Gurwitsch 1927) (see Fig. 22.1), blood or yeast (Gurwitsch 1931d) or UV radiation from artificial sources (separate spectral line of 202 nm in Potozky and Zoglina (1928)) restored MGR from the tip of the cut root (Table 22.1).¹

Technically, the above scheme with four roots required their strict positioning without microscope (Gurwitsch 1929), which was obviously a challenge limiting this kind of works. Similar experiments with artificial radiation instead of the primary inductors was also difficult to perform, with the

¹It should be noted that the ‘artificial radiation’ used in experiments was quite intensive, and thus, a stray lighting of the recipient from the artificial source could not be completely excluded *a priori* (Potozky and Zoglina 1928). However, the authors report no MGR from roots 45 minutes after the cutting, suggesting that the source of stimulation in the above experiments was not stray light.

E. V. Naumova (✉)
Rzhanov Institute of Semiconductor Physics, Siberian Branch of the Russian Academy of Sciences, Novosibirsk, Russia
e-mail: naumova@yandex.ru

I. Volodyaev
Moscow State University, Moscow, Russia

main problems being dose selection and proper attenuation of radiation. Thus, in Potozky and Zoglina (1928) the authors reported 18 of 53 negative experiments (with an artificial primary radiation source), which is obviously unsatisfactory. The authors explained such cases by improper or diseased roots and technical mistakes mainly during irradiation and further recipient root treatment (like wrong slicing, etc.) This explanation seems valid taking into account multistage and laborious recipient treatment, natural root variability and no data on the primary radiation intensity and stability of its source (that may well have been uncontrolled, and whose instability could result in negative results as well). However, none of these negative experiments resulted in significant prevalence of mitoses on the back side of the recipient root, and none of the recipient roots in control series showed such a high asymmetry, so it is unlikely that the obtained positive results are outliers.

The same phenomenon was manifested when onion roots, bacteria or yeast cultures were irradiated through a narrow slit or hole and showed mitogenetic response far outside the exposed area (see Fig. 22.2) (Gurwitsch and Gurwitsch 1934b).

22.1.2 Prevalence of the Secondary MGR

In further work, a large number of different biological and biochemical systems were tested for secondary radiation (see the setup for such experiments in Fig. 22.3).

All competent recipients of mitogenetic radiation as well as many known inductors demonstrated ability to serve as secondary emitters, for instance:

- Bacteria (Wolff and Ras 1932, 1933, 1934a, b)
- Yeast cultures (Gurwitsch 1931a; Gurwitsch and Gurwitsch 1932b)
- Blood (Gurwitsch and Gurwitsch 1934b; Ryazanskaya 1936) and blood serum (Wolff and Ras 1933)
- Nerves (Latmanisowa 1933; Gurwitsch 1934b)

Generally speaking, ability to emit secondary radiation appeared more common for biological objects than ability to emit spontaneous MGR and imposed less conditions on the inductor's biological state and ambient conditions. For instance, nutrient deficient and old yeast lost their ability to radiate spontaneously, while were still able to emit secondary radiation (data by E. Kannegisser, taken from (Gurwitsch and Gurwitsch 1934b)). Obvious secondary radiation, and at the same time the absence of primary radiation, was observed from onion meristem (Gurwitsch and Gurwitsch 1927; Potozky and Zoglina 1928), cornea of frog (Gurwitsch and Anikin 1928), and Lieberkühn's glands (Gurwitsch 1932).

The only exception to this rule were malignant tumours, which emitted the most intense spontaneous MGR, and no secondary radiation (Gurwitsch 1932).

In addition to biological objects, the secondary inductors could be solutions of bioorganic substances, e.g. nucleic

acids (Gurwitsch and Gurwitsch 1932a). The experiment scheme on the secondary radiation of nucleic acid solutions, excited by spontaneous MGR of carcinoma (with yeast cultures used as recipients) is presented in Fig. 22.4.

Secondary radiation was also shown for other substrates:

- Aqueous solutions/emulsions of glucose (Gurwitsch and Gurwitsch 1934a)
- Some fats (tributyryn, triolein and castor oil) (Braun 1934), cholesterol (Braun 1936)
- Albumen (Gurwitsch and Gurwitsch 1934b, 1936)
- Urea (Prokofiewa 1934)
- Lecithin (Gurwitsch and Gurwitsch 1934b)
- Filtrate of nutrient broth after bacteria cultivation (sterile nutrient broth before bacteria inoculation produced no secondary radiation) (Wolff and Ras 1933)
- All the tested organic substrates subjected to enzymatic cleavage (Gurwitsch 1934a; Gurwitsch and Gurwitsch 1936)

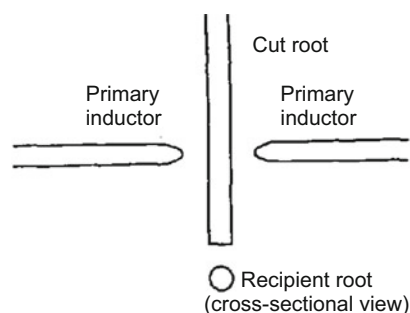


Fig. 22.1 Scheme of secondary radiation observation with onion root. Two primary inductors (connected to bulbs not drawn here) directed to the axis of the vertical root (cut from the bulb) induce secondary radiation, detected with a root-recipient. Here the tip of the vertical root is cut; however, an intact tip induced MGE in the recipient root as well. (Reprinted from Gurwitsch and Gurwitsch (1927). Copyright 1969, with permission from Springer Nature)

22.1.3 Secondary Radiation Properties

22.1.3.1 Intensity

Surprisingly, intensity of the secondary inductors did not depend on the intensity of the primary radiation that initiated it, in a wide range of intensities – i.e. it was fully determined by the secondary inductor itself. However, if the exciting MGR intensity was slowly and smoothly increased, starting from subthreshold values (e.g. MGR of the root elongation zone carried out through an elliptical slowly rotating disk (Gurwitsch 1931b)), then the secondary radiation was not observed (analogous to the lack of basic MGE under the same conditions – see Sect. 20.1.3).

Table 22.1 MGR from an onion root used as a 'secondary inductor'. Irradiation: separated spectral line 202 nm

| | Numbers of mitoses on the two sides of a normal onion root exposed to the supposed MGR from: | | | | | | | | |
|------------|--|------------------|------------|--|------------------|------------|---|------------------|------------|
| | A cut onion root | | | A cut onion root whose elongation zone is irradiated | | | A cut onion root whose meristem is irradiated | | |
| | Exposed side | Non-exposed side | % increase | Exposed side | Non-exposed side | % increase | Exposed side | Non-exposed side | % increase |
| | 286 | 283 | 1.1% | 328 | 258 | 27.1% | 623 | 499 | 24.8% |
| | 836 | 840 | -0.5% | 195 | 142 | 37.3% | 812 | 698 | 16.3% |
| | 833 | 827 | 0.7% | 784 | 687 | 14.1% | 517 | 415 | 24.6% |
| | 650 | 654 | -0.6% | 468 | 342 | 36.8% | 701 | 583 | 20.2% |
| | 475 | 474 | 0.2% | 527 | 398 | 32.4% | | | |
| | 474 | 472 | 0.4% | 589 | 489 | 20.4% | | | |
| | 603 | 605 | -0.3% | 362 | 276 | 31.2% | | | |
| | 258 | 251 | 2.8% | 534 | 393 | 35.9% | | | |
| Altogether | 4415 | 4406 | 0.2% | 3787 | 2985 | 26.9% | 2653 | 2195 | 20.9% |

Data from Potozky and Zoglina (1928). Copyright 1969, with permission from Springer Nature

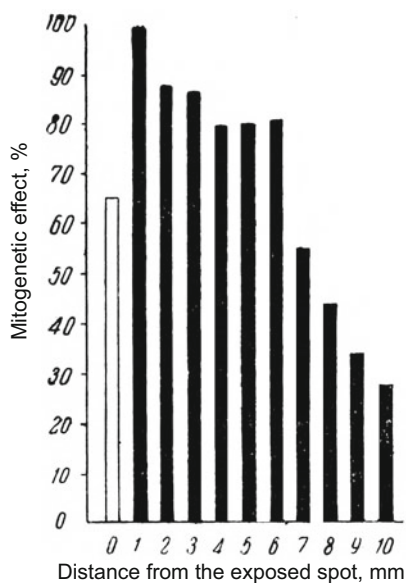


Fig. 22.2 Mitogenic effect on agar yeast cultures, induced at a narrow area, and its 'spreading'. A large yeast block was irradiated through a 1 mm wide slit, with a usual mitogenetic inductor. Effect was studied by taking samples in strips distanced by 1 mm with a micromanipulator. The maximal mitogenetic effect is observed 1–6 mm away from the exposed spot (note that the MGE value cannot be used as a direct measure of the MGR intensity, since the doze-effect curves could be very far from linear (see Chap. 20, Fig. 20.1)). (Reprinted from Gurwitsch and Gurwitsch (1948), with the permission of the heirs of the authors)

At the same time, intensity² of the secondary MGR strongly depended on the system used as the secondary inductor. Thus, in Wolff and Ras (1932, 1933) secondary MGR induced in bacterial cultures and nucleic acid solutions of various concentrations (0.001%, 0.004%, 0.02%, 0.1%, 0.25%, 0.5%, 0.75%, 1% for NA) was investigated. First of all, for any secondary inductor, there was a threshold concentration, below which the secondary MGR could not be observed (for NA it was 0.02%). Second, its intensity appeared the highest at the minimal concentration when it was observed and became weaker at higher concentrations (Wolff and Ras 1933).

Interestingly, the secondary radiation intensity was approximately the same as that of primary MGR, produced at enzymatic cleavage of the same substrate (Gurwitsch and Gurwitsch 1935). Some researchers reported secondary radiation of higher intensity than the primary radiation from the same object (both for biological and chemical systems) (Wolff and Ras 1933; Gurwitsch and Gurwitsch 1934b, 1935, 1945) (see discussion below).

²Because of the obvious impossibility to assess MGR intensity using biological effect alone, MGR intensities were compared indirectly, by the minimal exposure time producing MGE in identical (as possible) recipients and conditions: the shorter the time, the higher the intensity was assumed.

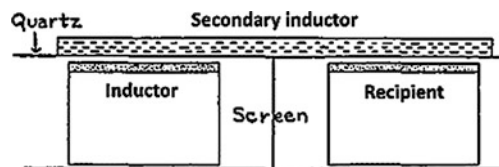
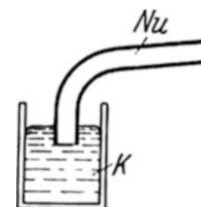


Fig. 22.3 Diagram illustrating mitogenetic effect induced with a secondary inductor. (Reprinted from Hollaender and Claus (1935). Copyright 1935, with permission from Optica Publishing Group)

Fig. 22.4 Scheme of secondary radiation experiment in a nucleic acid solution irradiated by a carcinoma pulp. Nu – nucleic acid solution; K – carcinoma pulp. Bent glass tube 2.5 mm in diameter and 3 cm long was filled with 1% nucleic acid solution and submerged into carcinoma pulp by 2–3 mm. Secondary radiation from the horizontal end of the tube was detected with an agar yeast culture, which is not shown in the scheme. (Reprinted from Gurwitsch (1932). Copyright 1969, with permission from Springer Nature)



22.1.3.2 Spectra

Spectra of the secondary MGR were assessed in a standard way (see Chap. 21, Sect. 21.3.2). They were found specific for each of the secondary inductors and largely independent of the exciting MGR (Gurwitsch and Gurwitsch 1947). Importantly, secondary MGR could be excited only by external radiation containing at least one spectral band coinciding with its spectrum (Braun 1936; Gurwitsch and Gurwitsch 1948) (in case of intense exciting light this was no longer a prerequisite (Gurwitsch and Gurwitsch 1948)).

Very strange, but some workers reported secondary MGR with shorter wavelengths than the exciting light (Gurwitsch and Gurwitsch 1932a). For instance, gelatinized 3% nucleic acid solutions, induced by the 322–324 nm spectral band of the copper arc, emitted secondary MGR with a clear spectral band of 245–250 nm (Gurwitsch and Gurwitsch 1932a). This obvious violation of the Stokes' law led to sharp criticism (Bateman 1935) and much discussion (Gurwitsch and Gurwitsch 1948) (see below, Sect. 22.1.4.1).

Importantly, characteristic spectral bands of the secondary MGR were preserved during its propagation in the secondary inductor over long distances and at different intensities of the exciting (primary) light. They were called spectra of selective secondary conduction (or selective scattering) of the secondary inductor. Using this quality, the authors reduced intensity of background and stray lighting, by using long, specifically shaped tubes with the secondary inductor (Fig. 22.5) and very

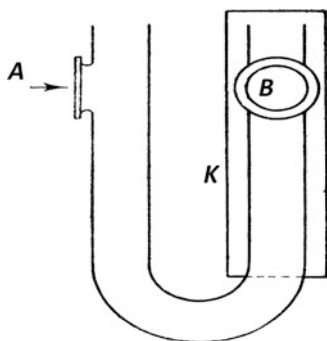


Fig. 22.5 A device for studying selective secondary conduction. The test liquid was poured into a glass U-shaped tube and locally irradiated with weak broadband UV radiation through a quartz window (A) as indicated by the arrow. A hydrogen lamp or a carbon arc was used as the source of the exciting light. Quartz window B was facing the collimator slit of the spectrograph with a set of biological recipients, used for detection of the secondary MGR spectrum (see more details on MGE spectral analysis in Chap. 21). The U-shaped tube and the cylindrical shield K are designed to eliminate the scattered primary radiation. (Reprinted from Gurwitsch and Gurwitsch (1948), with the permission of the heirs of the authors)

low intensity of the incident primary light (Gurwitsch and Gurwitsch 1948).

Analogous to the usual MGR, the secondary MGR spectra could be decomposed into elementary spectra, each of which corresponded to a specific molecule or functional group: hydroxyl, carbonyl, amino groups, etc. (Gurwitsch and Gurwitsch 1948; Gurwitsch 1968). Such superposition of spectra was claimed characteristic of open chains – alcohols, fatty acids, amino acids, peptides, proteins (Gurwitsch 1968), while cyclic and heterocyclic compounds, as well as some molecules of simple structure (hydroxylamine, hydrazine, formaldehyde, and formic acid) gave integral spectra characterizing them as a whole and not reflecting individual groups (Gurwitsch 1968; Gurwitsch and Gurwitsch 1948, 1959).

The basic spectra of functional groups were obtained by comparison of different spectra. For instance, comparing selective secondary conduction spectra of urea and guanidine solutions (Fig. 22.6), the authors suggested spectral lines, characteristic of C = O, C = N, and NH₂ groups (Gurwitsch and Gurwitsch 1947, 1948). This assumption was confirmed by studies of other compounds: fatty acids, amino acids, acetone, and peptone for the C = O group, amino acids for the NH₂ group, creatine, arginine for the C = N group (opposite to creatinine and other amino acids and amines not containing C = N) (Gurwitsch and Gurwitsch 1947, 1948). Basic spectra of hydroxyl, phenyl, and some other groups were assumed in a similar way.

These spectra were further used to determine the presence of various substances in biochemical and biological systems

and changes in their composition (Gurwitsch and Gurwitsch 1948).

The advantage of selective secondary conduction spectra over conventional MGR spectra was the ability to characterize the biochemistry of a number of objects that did not have their own MGR.

22.1.3.3 Propagation

The secondary radiation propagated over considerable distances. For example, Yu.A. Zysin demonstrated propagation of secondary radiation along a 6 m long pipe with 5% glucose solution (glucose solution was the most studied secondary inductor) (Gurwitsch and Gurwitsch 1948). Moreover, during the first dozen centimeters, the radiation propagated with an increase in intensity (Gurwitsch and Gurwitsch 1945, 1948). Contrary to that, secondary radiation in the gelatinous jelly was attenuated as it spread out (Gurwitsch and Gurwitsch 1945).

It was also shown that, depending on the medium structure, secondary radiation can propagate both isotropically and anisotropically. For example, it effectively propagated along the root of an onion and practically did not spread in the transverse direction (Gurwitsch 1931c). However, in solutions, the radiation naturally propagated isotropically (Gurwitsch and Gurwitsch 1936).

22.1.3.4 Temporal Characteristics

To study temporal parameters of the secondary radiation propagation, a scheme with rotating discs with slits (Gurwitsch 1931c, d) was proposed (Fig. 22.7).

The first slit periodically exposed one locus of the secondary inductor to the exciting primary MGR, and the second slit exposed another locus of the secondary inductor to the detector after a short delay. By varying the angular dimensions and the relative position of the slits, as well as the disk rotation speed, it was possible to set the exposure time and the delay between them, and thus to analyze the propagation speed of the secondary emission. Thus, if the primary radiation was delivered in the form of a short pulse, the secondary radiation also had the character of a short pulse, observed after a certain time (Gurwitsch 1931c). Dividing the distance travelled by the secondary MGR in the sample, by this delay time, the authors calculated the speed of its propagation, which was always found tens of meters per second (Gurwitsch 1968; Gurwitsch and Gurwitsch 1934b, 1935, 1936, 1948) (for instance, approximately 30 m/s for nerves (Latmanisowa 1933) and onion roots (Gurwitsch 1931d)).

22.1.3.5 Exhaustion of Secondary Inductors

All secondary emitters were functioning only during a certain period (usually around 5–10 – up to dozens of minutes), after which they lost their ability for secondary emission and stopped conducting MGR. Such exhaustion happened faster

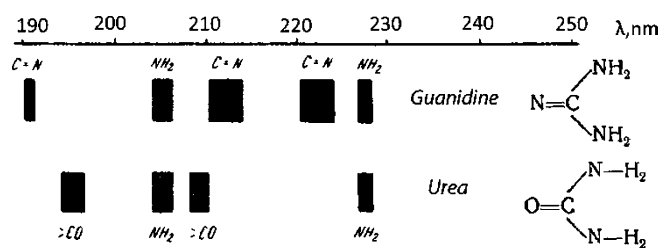


Fig. 22.6 Spectra of secondary MGR from urea and guanidine solutions. (Adapted from Gurwitsch and Gurwitsch (1948), with the permission of the heirs of the authors)

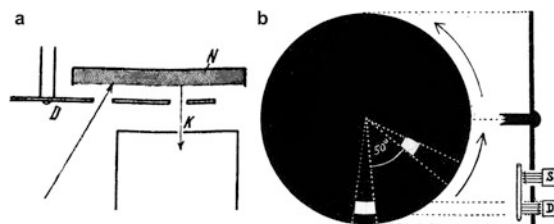


Fig. 22.7 Experimental schemes for the study of secondary radiation using rotating disks with slits. (a) Scheme for studying the secondary radiation of a nucleic acid solution with MGE spectral analysis, under monochromatic primary irradiation. Reprinted from Gurwitsch (1932). Incident radiation indicated by the arrow – copper arc radiation, inducing MGR in the secondary inductor (322–324 nm and 242–244 nm spectral bands, isolated with a monochromator, the radiation source is not shown in the diagram). The width of the irradiated zone of the liquid column is ~1 mm. D is a rotating disk with sectorial slots (see panel b, left). K is the collimator slit of the spectrograph with yeast detectors (not

shown in the scheme), N-nucleic acid solution (1% and 3%), distance along the liquid column from the irradiated strip to the collimator slit is ~15–18 mm. (b) Left: rotating disk with sectorial slits; right: side view of setup for secondary radiation study in onion roots: S – primary inductor (yeast; mouse, horse, rabbit, and human blood; onion root), D – recipient (yeast). (Illustration for experiment Gurwitsch AA (1931d), also used in Gurwitsch AG (1931c). Adapted from Rahn (1937) and Gurwitsch and Gurwitsch (1959). Copyright 1959, with permission from Springer Nature)

when the primary radiation was more intense (Sussmanowitsch 1928; Wolff and Ras 1933). Possibility of recovering after some ‘rest’ also was shown (Gurwitsch 1940; Gurwitsch and Gurwitsch 1959; Gurwitsch et al. 1974). For instance, after 30–45 min of exposure to mitogenetic radiation *staphylococcus* suspensions ceased to produce secondary radiation and on the next day restored this ability (Wolff and Ras 1933), nucleic acid solutions restored the ability to generate secondary radiation in a few hours after exhaustion (Gurwitsch 1940).

Moreover, as Gurwitsch wrote, “the ability to generate secondary radiation was observed only in relatively fresh solutions. So, for example, solutions of glucose, urea, nucleic acids, protein, when stored in the light and in the presence of atmospheric oxygen, retain their ability to generate secondary radiation only for several hours, and in complete darkness they were suitable for more than a day” (Gurwitsch and Gurwitsch 1945).

22.1.3.6 Physical Detection of Secondary Radiation

Secondary radiation was also detected with modified Geiger–Müller counters (Fig. 22.8) (Barth 1937).

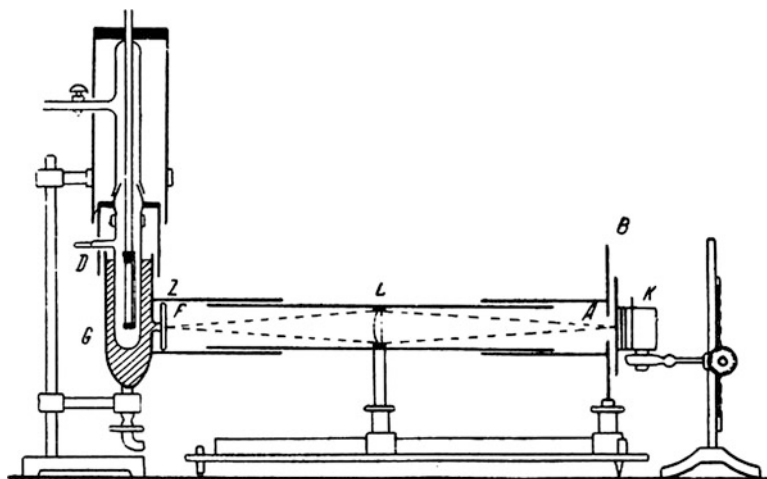
The author used glucose solution as the secondary inductor, and the Al + HCl chemical system (proposed as an MGE inductor in Braunstein and Potozky (1934)) and mouse carcinoma in Ringer’s solution with glucose, as the primary MGR sources. AgI was used as the photocathode material (see more details on physical detection of MGR in Chap. 21). The counter detected photon emission from the glucose solution only when it was exposed to the primary inductor, i.e. when it was functioning as the secondary inductor. When the glucose solution was not exposed to the primary sources of MGR, it gave no photon emission, in full accordance with biological data.

22.1.4 Criticism and Explanation: Hypothetical Mechanisms of the Secondary Radiation

22.1.4.1 Anti-Stokes Processes

The concept of the secondary radiation caused no less and even more criticism than the MGE itself. As mentioned above, some authors argued that irradiation of secondary inductors with primary MGR could not excite secondary processes leading to emission of light with shorter wavelengths, i.e. higher energy of quanta, thus violating the

Fig. 22.8 Detection of secondary radiation with a photon counter. D – photon counter submerged into the vessel G with 5% glucose solution, F – quartz window for the radiation beam from the source of mitogenetic radiation (Al+HCl) in the shielded chamber K, L – quartz lens. Photocathode is AgI. (Adapted from Barth (1937) and Gurwitsch and Gurwitsch (1959). Copyright 1959, with permission from Springer Nature)



Stokes' law. At that time such statements seemed physically so absurd, that, for instance, J.B. Bateman (Cambridge), a well-known critic of MGR, called a chapter of his review 'The Gurwitsch demon: secondary radiation and the propagation of the mitogenetic impulse' (Bateman 1935).

Anti-Stokes processes were theoretically justified by L. Landau more than a decade later (Landau 1946) and experimentally shown by N. Bloembergen when MGR research had already been ceased (Bloembergen 1959). A well-known example is anti-Stokes luminescence of pre-UV-irradiated frozen aromatic amino acids, induced by red light (Vladimirov 1965; Vladimirov et al. 1970a, b) (see Chap. 12). Nowadays specially prepared systems, capable of anti-Stokes luminescence, are used in a number of applications (Moffatt et al. 2019) (see Chap. 30). Though none of that is directly related to the works on secondary MGR, this definitely refutes criticism related to an impossibility of Stokes's law violation.

22.1.4.2 Chain Reactions

Analogous to the chain-reaction hypothesis of the primary MGR (see Gurwitsch and Gurwitsch 1934b, 1959), A.G. Gurwitsch suggested that the secondary emission was generated by branched-chain reactions, induced by the incident light: "Each secondary emitted photon is the final link in a long chain of 'dark' processes affecting a huge number of molecules in the system" (Gurwitsch 1940). This concept resolved contradictions both in terms of the spectrum and the intensity of the secondary radiation (sometimes reported stronger than the incident light, causing it (Gurwitsch and Gurwitsch 1932a)). It was indirectly confirmed by the coincidence of the secondary MGR spectrum from nucleic acid solutions with the MGR spectrum of their hydrolysis (Ponomarewa 1931) (see more in Gurwitsch and Gurwitsch (1948) and Gurwitsch (1968)).

22.1.4.3 Structural Ordering in the Medium

Another, more complicated suggestion was some structural ordering of molecules, supposedly necessary for nonradiative transfer of energy between them. As Gurwitsch wrote, "The secondary radiation (which is a result of chain reactions) is carried over more or less significant distances only in a 'molecularly ordered medium'" (Gurwitsch 1940). He also hypothesized that in biological systems, MGR propagates due to certain molecular structures arranged as chains or films.

In this regard, a number of studies have been devoted to the specificity of secondary radiation inside thin capillaries and in very thin films, where the breaks of the chain process are favored by a large specific surface area. Indeed, homogeneous solutions of biochemical secondary emitters lost the ability to emit in capillaries with submillimeter diameter (Gurwitsch and Gurwitsch 1945, 1948). However, in capillaries with solutions of 'thread-like molecules' (slightly denatured proteins), aligning of molecules under the action of electric field (about 100 V/cm at the capillary wall) or due to the flow, restored their ability to secondary radiation. In a glucose solution, in which there is no such ordering of molecules, secondary radiation did not appear. Secondary radiation also disappeared in very thin films of cedar oil (Braun 1936), stearic acid and anilide (Chetverikov 1939) but could be well observed from films of lecithin and cholesterol (Braun 1936).

Long mitogenetic irradiation of monofilm secondary inductors (for instance, lecithin (Engel and Gurwitsch 1936)) led to increase of their transparency to mitogenetic radiation that the authors explained by their degradation.

22.1.5 Fundamental and Applied Role of Secondary Radiation in Mitogenetic Research

The greatest problem in interpretation of the first experiments on MGE was to explain how a UV UPE, generated in highly absorbing and scattering biological media, could propagate through them. The concept of secondary radiation resolved this contradiction, suggesting that MGR propagates through biological media not directly, but through chain photochemiluminescent processes (see more about photochemiluminescence in Chaps. 5 and 12). The secondary MGR became one of the key concepts in the entire area of mitogenetic effect.

In fact, the phenomenon of secondary MGR was involved even in the very first onion experiments (Gurwitsch 1923). According to the Gurwitsch, the primary MGR was produced not by the tip or meristem, but by the onion sole (Gurwitsch and Gurwitsch 1924), and its UV radiation could not pass several centimeters along the highly absorbing root without secondary radiation. For agar yeast recipients, the role of secondary radiation was also considered extremely important: ‘The effect itself, that is, the preponderance in the number of yeast buds, is localized in the middle layers of the culture (consisting of several dozens of cell layers); several upper layers consist of senescent cells that are unable to divide – these are the “secondary emitters” that determine the conditions for the mitogenetic effect upon irradiation.’ (Gurwitsch and Gurwitsch 1948).

Interestingly, A.G. Gurwitsch supposed secondary radiation to be an obligatory first stage in the mechanism of biological reception of MGR (Gurwitsch and Gurwitsch 1928, 1936; Gurwitsch 1940).

It should be noted that some other observations on secondary radiation have found analogies later. For instance, exhaustion after long irradiation with the following recovery of luminescence, demonstrated by mitogenetic secondary inductors, seems rather ordinary among anti-Stokes luminescent materials.

The effect of secondary radiation was used for spatial mapping of MGR of nerves and cerebral cortex (Gurwitsch and Gurwitsch 1948). A scheme of the device used for it is shown in Fig. 22.9.

A bundle of capillaries with funnel-shaped openings were filled with solutions of secondary inductors (usually, glucose, proteins or nucleic acids) and placed over the surface of the studied object. The MGR of the investigated object excited secondary radiation in the capillaries, which was recorded by biological detectors placed on the other side of the capillaries, at the capillary sockets (Gurwitsch and Gurwitsch 1948). The

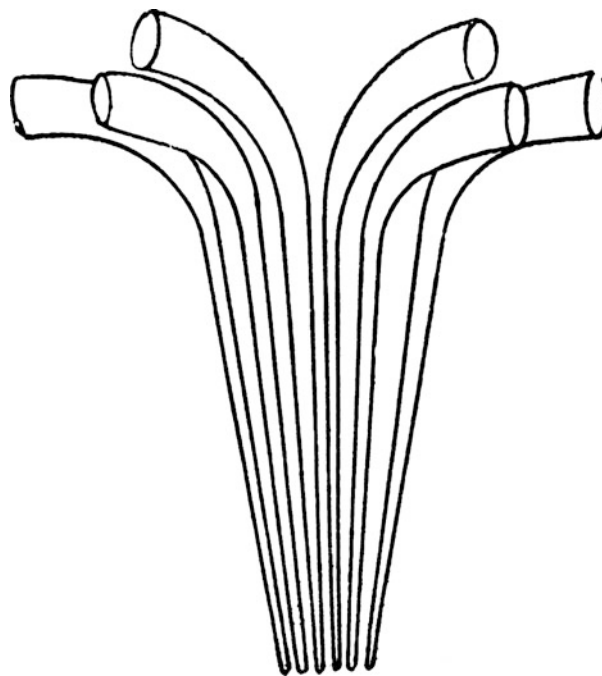


Fig. 22.9 Diagram of a device for spatial mapping of MGR. Glass capillaries were filled with a glucose solution or other secondary inductor, the lower thin ends were placed at the surface under study, and the upper sockets were directed to biological detectors. (Reprinted from Gurwitsch and Gurwitsch (1948), with the permission of the heirs of the authors. Identical figures are present in Gurwitsch and Gurwitsch (1936) and some other works)

resolution of such devices was limited by the minimal diameter of capillaries in which secondary radiation could propagate, approx. 1 mm.

This approach was used in a number of investigations, primarily, of the brain and neural activity (Gurwitsch and Gurwitsch 1936) (Fig. 22.10).

This was obviously the first attempt of noncontact mapping of neural activity.

Significance of secondary radiation for applied research also related to the selective scattering analysis (see above). The authors placed tubes with different secondary inductors in close proximity to the source of the primary MGR, and by analyzing the presence or absence of secondary radiation from each of them, made conclusions about chemical sources of radiation in the primary inductor (Gurwitsch and Gurwitsch 1936). As Gurwitsch wrote, “the study of chain processes (*associated with MGE – authors note*) became possible only due to the secondary radiation” (Gurwitsch and Gurwitsch 1999).

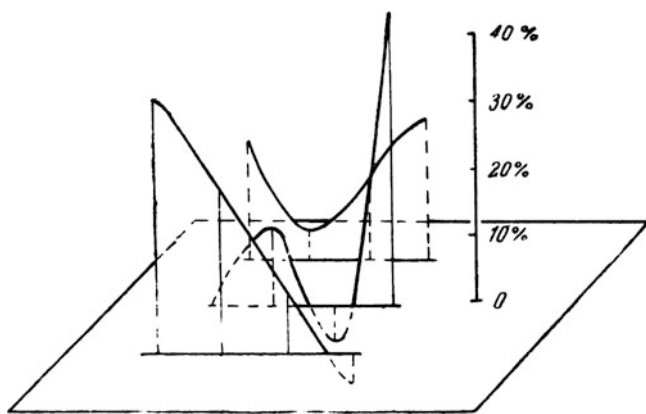


Fig. 22.10 The visual area of the rabbit's cerebral cortex when illuminating the eyes (MGR measured in 12 points). (Reprinted from Gurwitsch and Gurwitsch (1948), with the permission of the heirs of the authors)

22.2 Degradation Radiation and the Concept of Non-equilibrium Molecular Constellations

22.2.1 Definition and Prevalence of Degradation Radiation

Another very important concept was 'degradation radiation' (dMGR), that is MGR from stressed or dying cells.

It was first observed by J. Ponomareva on corneal epithelium of frog as a 5-min burst of MGR immediately after its fast cooling to 2–5 °C (Ponomareva 1936). Later, dMGR was detected from different living objects as a response to a sudden cooling, physiologically active substances (mainly anesthetics, like ether), mechanical stresses (for instance, centrifugation at 2500–3000 rpm), application of weak direct or alternating current (0.02–0.05 mA) (Gurwitsch and Gurwitsch 1937a, b, 1999, 1945, 1959; Gurwitsch 1937b, c).

dMGR was found much more universal than spontaneous MGR. It was observed from all tested plant and animal tissues (including known non-inductors): chicken embryos, corneal epithelium, liver (mice, frogs and rabbits), kidney (mice), spleen and brain (mice, frogs and rabbits), mucous coat of stomach and skeletal muscles, yeast, roots of onion, sunflower and bean, onion skin and others (Gurwitsch 1937a; Frenkel and Gurwitsch 1943; Gurwitsch and Shalagin 1947; Gurwitsch and Gurwitsch 1945, 1959, 1999).

22.2.2 Properties of Degradation Radiation

Degradation radiation significantly differed from spontaneous MGR in several respects. First, it had different spectra: highly variable and irreducible to the basic spectra of

enzymatic reactions (see Chap. 21) (Gurwitsch and Gurwitsch 1937b, 1948). This difference was especially clear for plant sprouts, whose physiological spectra were referred to fluorescence of glucose, peptides and phosphatides, and degradation spectra obtained by cooling had none of the lines from their physiological spectra (Gurwitsch and Gurwitsch 1945, 1959, 1999). Another example was dMGR of frog brain that had no common lines with its spontaneous MGR (Gurwitsch 1937c). Second, dMGR appeared immune to the quenchers of spontaneous MGR (see cancer quencher in Chap. 23). This quality was used for testing if any given MGR had some 'inner degradation nature' (see below).

22.2.2.1 Duration

When a biological object was exposed to some stressing stimuli, the degradation radiation appeared in the form of a burst, lasting from dozens of seconds (Gurwitsch and Gurwitsch 1959) to dozens of minutes (Gurwitsch and Gurwitsch 1937b, 1945), or even up to an hour (Gurwitsch 1937c) – depending on the biological object and the stressor (Gurwitsch and Gurwitsch 1959). Stronger stresses (for instance, deeper cooling) caused shorter and supposedly more intense response (evaluated by the minimal exposure time required to get MGE in biological detectors – see Chaps. 20 and 21). For instance, the following data were reported in different sources (see Gurwitsch and Gurwitsch 1945, 1959) (Table 22.2)

Importantly, if stressors were applied one immediately after another, the second and further stresses produced no effect. For instance, weak electric current did not lead to radiation after fast cooling (Gurwitsch and Gurwitsch 1945, 1959). However, alive biological objects and freshly extirpated internals or tissues, subjected to 'weak stress', restored their ability for degradation radiation after some refractory period (Gurwitsch and Gurwitsch 1945, 1948, 1959).

22.2.2.2 Spectra

Generally speaking, spectra of dMGR appeared much more variable than those of the primary (or secondary) MGR. Thus, degradation spectra of various internals or tissues of the same biological organism were different, as well as spectra of degradation MGR from the same object, stimulated by different stressors (e.g. liver of the same animal – rabbit or mouse, subjected to cooling and weak alternate current (Gurwitsch and Gurwitsch 1959)). Analogous tissues/internals of different animals or plants (for instance, liver of mice and rabbit, roots of bean and onion) had different spectra of degradation radiation, contrary to the similarity of their physiological mitogenetic spectra (Gurwitsch and Gurwitsch 1945, 1948, 1959). Yeast races also showed

Table 22.2 Degradation MGR at different influences

| Object | Stimulation of dMGR | Duration of the dMGR burst |
|--------------------------|-------------------------|----------------------------|
| Plant tissues | Cooling to 5 °C | 10–15 min |
| Plant tissues | Cooling to 0 °C | 1–2 min |
| Mouse liver | Cooling to 5–7 °C | ≤30 min |
| Frog brain | Cooling to 5–7 °C | ≤30 min |
| Beans roots | Centrifugation 3000 rpm | Several min |
| Liver and kidney of mice | Centrifugation 3000 rpm | Several min |

Adapted from Gurwitsch and Gurwitsch (1959). Copyright 1959, with permission from Springer Nature

Fig. 22.11 Spectra of dMGR from various yeast races, subjected to sudden cooling (After Billig; reprinted from Gurwitsch and Gurwitsch (1959). Copyright 1959, with permission from Springer Nature)



variety of degradation spectra (Fig. 22.11) (Gurwitsch and Gurwitsch 1948, 1959).

Spectra of dMGR from mucous coat of murine stomach showed dependence on dietary patterns (Gurwitsch and Gurwitsch 1959) (Fig. 22.12).

Thus, despite all attempts to strictly maintain experimental conditions and avoid additional external stresses (Gurwitsch and Gurwitsch 1945, 1948, 1959), in general, dMGR spectra were much less reproducible than the usual MGR spectra.

Evolution of degradation spectra under the action of physiologically active substances was studied on animal internals (see Gurwitsch and Gurwitsch 1948). The most detailed of these studies was undertaken by J.N. Ponomareva on livers of rabbits and mice *in vivo* (described in Gurwitsch and Gurwitsch (1945, 1948, 1959)). The stress factor was weak alternate current ~0.05 mA, applied directly to the liver. The degradation spectra were detected in 'normal' physiological state, and after subcutaneous injection of small doses of cocaine or glucose. The degradation spectra showed significant change just 5 min after the injections in spite of the fact that the concentration of injected substance in liver could not increase much for that time. Difference between degradation radiation spectra after glucose and cocaine injections was also reported.

In general, the authors claimed, that abrupt changes in metabolism had impact on degradation spectra, while larger but slower changes produced no effect. Injection of glucose even in small doses resulted in distinct evolution of degradation spectra, while slow changes of glucose concentration to even much higher level exerted no influence. Repeated study of degradation spectra evolution with glycogen accumulation in liver also proved no relation between its absolute concentration

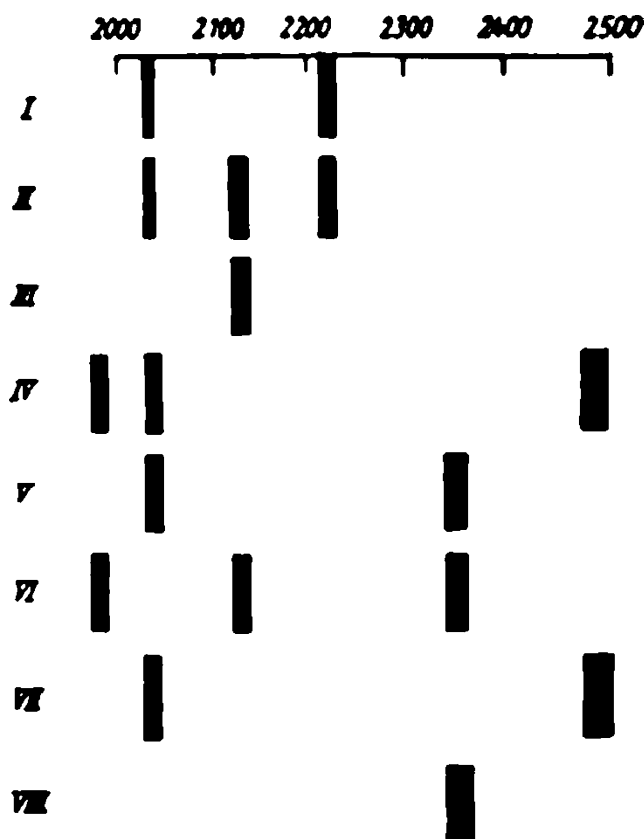


Fig. 22.12 Spectra of dMGR from mucous coat of murine stomach after different types of diet. The authors complained about the impossibility of strict adherence to the diet and compensated for this uncertainty by assessing the contents of the mice stomach (see Table 22.3). (Reprinted from Gurwitsch and Gurwitsch (1959). Copyright 1959, with permission from Springer Nature)

and spectra of degradation radiation (Yu.G. Sherezhevskaya, data reported in Gurwitsch and Gurwitsch (1959)).

22.2.3 Hypothetical Mechanism of Degradation MGR: Non-equilibrium Molecular Constellations

Data on degradation radiation led Gurwitsch to formulate the hypothesis of non-equilibrium structures in biological objects ('non-equilibrium molecular constellations', as he called them) (Gurwitsch 1937b). Here we briefly represent it according to his monographies (Gurwitsch and Gurwitsch 1945, 1948, 1959).

The term 'non-equilibrium molecular constellation' (Gurwitsch 1937b) meant an ordered association of molecules:

- Not bonded chemically
- Having common energy levels as a whole
- Maintained in the non-equilibrium state (implying higher energy than disordered molecules) due to continuous energy inflow (that could be gained from normal metabolic processes, visible light etc.)
- Having rather labile composition and geometry

Later, formation of analogous non-equilibrium states was suggested for large individual biomolecules, such as proteins (Gurwitsch and Gurwitsch 1959).

Along with E. Bauer's theory of stable nonequilibrium (deformed states of protein molecules, that store energy during life and release them at death) (Bauer 1935), this was among the earliest formulations of the concept of dissipative structures, as it was described in the self-organization theory decades later (Nicolis and Prigogine 1977). Yet, A.G. Gurwitsch himself stated that both his and E. Bauer's concepts were preceded by the ideas of O. Warburg on nonequilibrium structures (Warburg 1910).

Mechanisms of normal physiological and degradation MGR were generally hypothesized in Gurwitsch's school as follows (Gurwitsch and Gurwitsch 1945, 1948, 1959). Exothermic enzymatic processes were considered the main original source of energy for both normal physiological and degradation radiation. In case of normal physiological metabolism, the energy liberated in exothermal processes is finally transferred to some fluorescent molecule, group or ion, and soon after that emitted with its own specific spectrum. Cooling or anesthesia dramatically retards enzyme and other reactions, and normal physiological MGR ceases. In case of degradation radiation, statistically continuous inflow of energy from exothermal processes supports the non-equilibrium molecular states of higher energy, and when this inflow is interrupted, 'molecular constellations'

relax to a less ordered state of lower energy, with the energy excess emitted as dMGR. At the same time, some parts of 'constellations' may still remain in excited states, with their energy levels different from those in equilibrium.

The observed diversity of degradation spectra was explained by the great variety of possible spatial arrangements ('deformations') of molecular non-equilibrium constellations, that were specific for species and tissues. Moreover, their states could change specifically in response to various abrupt changes in metabolism and be a link in the chain of processes underlying complex macro-reaction of alive system to different events. Recovery of normal metabolism restored non-equilibrium 'constellations' and possibility to degradation radiation.

The molecules of the 'constellations' were hypothesized to acquire both small portions of energy released in exothermal metabolic processes (with energy yield $\lesssim 20$ kcal), and those from higher energy processes like recombination of free radicals or absorption of light. The energy absorbed by the constellation belongs to the whole of it, and thus sequentially absorbed quanta can sum up, and migrate along the 'constellation'.

Interestingly, physiological mitogenetic radiation of muscles, elements of nervous system (Gurwitsch and Gurwitsch 1959, 1999), and streaming protoplasm (Eremeev, 1947 #4160; Eremeev, 1958 #11627) were also interpreted to be of degradation character, as it was not suppressed with the quenchers, opposite to standard MGR and analogous to degradation radiation (Gurwitsch and Gurwitsch 1959).

Of course, all this was speculation, but much of this found one or another parallel in the subsequent development of science – both molecular biology and synergetics:

- The non-equilibrium state of living systems
- 'Deformed' states of proteins during their functioning
- 'Elements of degradation processes' during muscle functioning, and in conducting a nerve impulse

22.3 Necrobiotic Radiation

22.3.1 Definition

Perhaps, a special (extreme) case of degradation radiation is 'necrobiotic radiation', proposed in 1932 by a prominent plant physiologist and biochemist W.W. Lepeshkin (Lepeschkin 1932a, b). 'Necrobiotic radiation', according to his definition, is ultraweak UV emission from cells dying from toxins or heating (see details in Lepeschkin (1933, 1934, 1935)).

The author detected radiation with photosensitive silver compounds. In most of his experiments, these substances (or even reagents for their formation) were added to the

studied biological suspensions³ before their killing (in experiments) or after that (in controls), and difference in photosensitive substance response was taken as evidence of radiation from dying cells. In our opinion, this is the main methodical inconsistency of Lepeschkin's works that makes his results too doubtful to analyze them except for a few publications (see below). At the same time, these works are sometimes cited alongside MGE research, inaccurately and without understanding the subject, which indirectly discredits the latter. Moreover, references to W.W. Lepeschkin's papers on necrobiotic radiation in the top-rated journals including 'Science' (Lepeschkin 1932a) add persuasiveness to completely fallacious papers on the subject, which often misinterpret mitogenetic research as well. Therefore, here we provide a review of these works, with an accent on the best-quality series, probably related to degradation radiation.

22.3.2 Setup and Critique of Experiments

22.3.2.1 Doubtful Experiments with Mixtures of the Studied Biological Suspensions and Photosensitive Materials

As mentioned above, in most of the works, photosensitive compounds were added directly to the investigated suspension (Lepeschkin 1933, 1934, 1935), which completely entangled chemical and physical effects. Photosensitivity is well known to be determined by the so-called sensitivity centres (sensitivity specks) – defects of crystal structure, highly dependent on the chemical contaminants. The obvious difference in the chemical environments of photosensitive microcrystals before and after killing the cells makes it fundamentally impossible to understand whether the darkening

³In the first experiments, suspensions of unicellular organisms or pieces of multicellular organisms which have a large surface (yeast cells, *Elodea* leaves, flower petals, etc.) in water were mixed with potassium bromide and silver nitrate in an absolutely dark room, killed by ether (before or after addition of reagents for silver bromide formation – authors' note), and exposed to diffuse sunlight. The suspensions in which the cells were killed after formation of silver bromide showed a quicker darkening than the suspensions in which the cells had been killed before formation of silver bromide' (Lepeschkin 1932a). Multiple variation of this method (addition of AgBr/KBr + AgNO₃/KBr (before killing) + AgNO₃ (before and after killing); various concentrations of these substances, cell killing by ether/heating/alcohol) were described in details with example of yeast in Lepeschkin (1933), and the author applied this method for detection of necrobiotic radiation in thick bacterial suspensions of *Bacillus subtilis*, *Elodea* leaves, *Papaver* petals, etc. Lepeschkin also suggested a more sophisticated method, where silver nitrate served both as a toxin for cell killing and as a reagent for formation of organic and inorganic photosensitive silver compounds with cell substances (Lepeschkin 1933), that further complicated the matter. The last method was used in Lepeschkin (1934) for studying relative intensities of necrobiotic radiation of different yeast strains, dependency of radiation intensity on the number of alive cells and influence of external UV-radiation.

of the photosensitive substance was caused by radiation or it was a purely chemical effect.

The author admitted these problems and was constantly trying to improve the setup. For instance, in Lepeschkin (1934) he showed direct influence of toxins used in previous works, on photosensitivity, and found that even cork stoppers used in Lepeschkin (1933) emanated volatile substance facilitating silver reduction during development process.

He made some efforts to distinguish chemical and radiation impacts on silver reduction, referring to the time dependencies of the response to these impacts (Lepeschkin 1933). Nevertheless, the controls in these experiments without chemical isolation of photosensitive substance from cells cannot be taken as valid, which makes the whole setup totally unconvincing (see more in Lepeschkin (1932a, b, 1933, 1934, 1935)).

22.3.2.2 Experiments with Chemical Isolation of Photosensitive Materials from the Studied Objects (Biological Suspensions)

A more convincing method used in some of W.W. Lepeschkin's works included chemical isolation of photosensitive substance (silver bromide suspensions) (Lepeschkin 1932a, b). It was described in details on yeast cultures (Lepeschkin 1933), and also used on horse erythrocytes and flower petals (Lepeschkin 1935). Here we present its description according to Lepeschkin (1933).

Dilute suspension of silver bromide⁴ was put into two quartz tubes⁵ and sealed with glass stoppers in an absolutely dark room. Yeast suspension⁶ was put into two glass flasks. In one flask (control), yeast were killed by heating or toxin.⁷ Sealed quartz tubes with silver bromide were introduced into the flasks with dead and alive yeast suspensions.⁸ Then alive yeast was killed. In some experiments, control yeast was killed by heating and cooled before the quartz tube introduction, then toxin was added both to the dead and alive yeast. In other experiments, the control yeast was killed by toxin, and after introduction of the quartz tubes, the toxin was added only to alive yeast.

⁴Silver bromide was prepared by mixing aqueous solutions of silver nitrate (10 drops of 0.1 standard solution of silver nitrate per 45 drops of water) and potassium bromide (10 drops of 0.1 standard solution of potassium bromide per 45 drops of water).

⁵Quartz tubes: 48 mm length; 4 mm internal diameter, 5.8 mm external diameter. Tubes had identical volume (22 drops of distilled water) and slightly different shapes so as to identify them in the darkness.

⁶Yeast suspension: 72 g compressed yeast + 110 ml water.

⁷Toxin: 20 cm³ of saturated solution of mercuric chloride or 25 cm³ of ether per flask.

⁸Identical positioning of quartz tubes was secured by their fastening to the resin plugs of flasks with an aluminium wire.

Table 22.3 Contents of the mice stomach, used in dMGR experiments

| Mouse No | Pyloric part of the stomach | Lower part of the stomach |
|----------|-----------------------------|---------------------------|
| I | Bread in large quantities | Bread in large quantities |
| II | Milk in large quantities | Milk in large quantities |
| III | Empty | Empty |
| IV | Empty | Hay |
| V | Bread in small quantities | Bread in large quantities |
| VI | | |
| VII | Bread in small quantities | Milk in small quantities |
| VIII | empty | Milk in small quantities |

Adapted from Gurwitsch and Gurwitsch (1959). Copyright 1959, with permission from Springer Nature

After addition of toxin, both quartz tubes were shaken⁹ (there was no visual difference with control if the tube exposed to dying cells was still). Then quartz tubes were taken from flasks, washed, dried, opened, put into the cylinders with developer and shaken.¹⁰ After that, the fixing agent¹¹ was added, and reduction of silver bromide suspension was evaluated qualitatively by several visual parameters (see results presented by the author as typical in Table 22.4). All the stages were performed in the darkness besides the final evaluation made in the daylight.

If the quartz tube with silver bromide was exposed to renewed suspensions of dying yeast for 3–4 times one after another, the silver reduction was greater (Lepeschkin 1933).

Besides the obvious fact that color, turbidity and thicknesses are no quantitative parameters and were evaluated subjectively, detection method cannot be reproached on condition that both experimental and control tubes were treated identically (precise dosing and timing, temperature maintenance, etc.).

However, this was not always so. When working with horse erythrocytes and *Dahlia* petals, killed with ether, the author used a similar method, but control quartz tubes with silver bromide suspension were left in the black box instead of shaking (Lepeschkin 1935). This strange detail was not explained by the author and could obviously introduce additional errors.

22.3.2.3 Estimation of Spectral Range and Intensity of Necrobiotic Radiation

In the above experiments, the difference between experimental and control tubes with photosensitive suspension was observed only when the tubes were made of quartz; glass

⁹After addition of toxin the quartz tubes were shaken with frequency about 5–6 Hz for 15–30 min.

¹⁰Cylinders (length 8 cm, volume 12 ml, sealing stoppers) contained 3 ml of developer and were shaken with frequency of 2 Hz for 5–10 min. Developer composition: 200 ml water; 0.01 g metol (4-(methylamino)phenol sulfate); 0.75 g sodium sulphite; 0.09 g hydroquinone; 0.25 g sodium carbonate and 0.05 g potassium bromide.

¹¹Fixing agent: 1 ml 10% acetic acid.

tubes gave no effect (Lepeschkin 1933). From this, the author estimated the radiation spectrum mainly belonging to 180–230 nm. This also explained failures to detect necrobiotic radiation with ordinary photographic plates, covered with gelatin, which is strongly absorbing light with wavelengths below 230 nm.

Silver reduction in suspension exposed to dying horse erythrocytes was approximately the same as for exposure to 75 W electric lamp at the distance of 7 cm for 1.5 s (no other data for estimation of the lamp radiation spectrum or intensity were presented) (Lepeschkin 1935). Thus, the author concluded the luminous flux from 25 ml of suspension of dying horse erythrocytes to be approximately equal to that of the lamp. Nowadays, this estimate obviously seems questionable, to say the least, taking into account all results on intensity of UPE of biological objects and data of early authors on mitogenetic radiation (Lepeschkin's estimate exceeds all of them by too many orders of magnitude).

22.3.3 Relation Between Mitogenetic and Necrobiotic Radiation

In all his publications, Lepeschkin supposed that the discovered phenomenon related to mitogenetic radiation. He suggested that necrobiotic radiation “was produced in the decomposition of the principal compounds of protoplasm in the process of death” (Lepeschkin 1932a) and assumed that mitogenetic radiation was generated in similar processes, i.e. partial decomposition having place in any structural reconstruction in the cell (Lepeschkin 1932a, b).

The author reported detection of mitogenetic radiation from growing yeast (beer yeast mixed with sugar solution) by his method with silver bromide suspension in sealed quartz tubes and stated that difference of silver reduction with control was still visible, but less than in case of dying yeast (Lepeschkin 1933). He explained it by higher intensity of necrobiotic radiation due to more complete and intensive decomposition of biological structures at death than during mitosis (Lepeschkin 1932a). Lepeschkin also stated that contrary to growing yeast, compressed yeast had no effect on photosensitive emulsion, which agreed with Gurwitsch's results (Gurwitsch and Gurwitsch 1932b).

In the leading scientific teams on MGR, experimental works inspired by Lepeschkin's experiments were very few, in spite of the reported greater intensity allowing simpler detection (photosensitive silver salts) and the supposed close relation of these phenomena (Rahn 1936). Researchers from Gurwitsch's laboratory used the earliest Lepeschkin's method without chemical isolation of silver salt (Lepeschkin 1932b), repeated his experiments with dying yeast and got similar results for protein coagulation (Sukhov and Sukhova

Table 22.4 Detection of necrobiotic radiation of yeast with silver bromide suspension in quartz tubes

| Exp. No | Toxin | Time of shaking yeast with quartz tubes (min) | Development time (min) | Yeast | Colour of suspension after development | Turbidity | Colour of sediment | Thickness of silver layer on the tube wall |
|---------|-------------------|---|------------------------|-------|--|-----------------|--------------------|--|
| 10 | Ether | 30 | 8 | Alive | White | Clear | Black | Thick |
| | | | | Dead | Violet | Turbid | Grey | Thin |
| 11 | Ether | 30 | 8 | Alive | White | Clear | Black | Thick |
| | | | | Dead | White | Turbid | Grey | Thin |
| 12 | HgCl ₂ | 15 | 6 | Alive | White | Slightly turbid | Dark grey | Thick |
| | | | | Dead | White | Very turbid | Grey | Medium |
| 13 | HgCl ₂ | 15 | 6 | Alive | White | Slightly turbid | Dark grey | Thick |
| | | | | Dead | White | Very turbid | Grey | Medium |

Reprinted from Lepeschkin (1933). Copyright 1969, with permission from Springer Nature

1934; Sukhov and Lanshina 1933). They suggested this process to be a possible source of necrobiotic radiation.¹²

Besides these works, directly inspired by Lepeshkin's experiments, a number of quite independent works conducted by researchers of Gurwitsch's school seems relevant to the necrobiotic radiation, that is all the studies on mitogenetic radiation explained by proteolysis: autolysis of batrachians (Blacher and Holzman 1930), digestion of proteins, radiation from necrotic lesions of tumours (Kisliak-Statkewitsch 1929) and different mashed tissues (onion sole, etc.) (Gurwitsch 1925; Gurwitsch and Gurwitsch 1925). A special study of autolysis of normal tissues in vitro conducted by A. and L. Gurwitsch demonstrated that fragments of corneal epithelium, liver and kidney as well as their pulp became sources of MGR 8 h after the beginning of autolysis, and radiation of kidney was reported to be more intensive, that agreed well with more intensive autolysis in them (Blacher and Holzman 1930).

Generally, necrobiotic radiation was considered in Gurwitsch's school as an ultimate case of degradation radiation. Yet, as mentioned above, only a few works on necrobiotic radiation can be considered convincing enough to analyze their results.

Acknowledgements We sincerely thank the heirs of Alexander Gurwitsch and his late grandson, Lev Belousov, for unlimited access to their personal library, containing probably the most comprehensive collection of papers on MGE.

¹²It should be noted that several years later protein coagulation was shown to produce MGR, and its spectrum was studied with yeast detectors (flocculation of aqueous solution of dried horse serum with alcohol was used as a coagulation model, MGR was detected by the usual method of yeast on agar with bud counting) (Billig 1938).

References

- Barth H (1937) Physical studies on the question of mitogenetic radiation problem (in Russian). *Archive of Biological Sciences* 46 (1): 153–177
- Bateman JB (1935) Mitogenetic radiation. *Biological Reviews* 10 (1): 42–71. <https://doi.org/10.1111/j.1469-185X.1935.tb00476.x>
- Bauer E (1935) *Teoreticheskaja biologija (Theoretical Biology)*. VIEM Publishing House, Moscow-Leningrad
- Billig ES (1938) Mitogenetic spectral analysis of radiation from protein coagulation with alcohol. *Bulletin of experimental biology and medicine* 5 (4):314–315
- Blacher LA, Holzman OG (1930) Resorption processes as a source of morphogenesis. 1. Role of mitogenetic radiation in processes of metamorphosis of batrachians (In Russian). *Medico-biological Journal* (3):150–170
- Bloembergen N (1959) Solid state infrared quantum counters. *Physical review letters* 2 (3):84–85
- Braun AD (1934) Lipolysis as a source of mitogenetic radiation. *Nature* 134 (3388):536. <https://doi.org/10.1038/134536d0>
- Braun AD (1936) Die mitogenetische Sekundärstrahlung an monomolekularen Filmen. *Protoplasma* 26 (1):338–343. <https://doi.org/10.1007/bf01628662>
- Braunstein AE, Potozky AP (1934) About specificity of mitogenetic radiation spectra in oxidation-reduction reactions (In Russian). *Archive of Biological Sciences, Ser B* 35 (1):73–86
- Chetverikov DA (1939) Mitogenetic regime of monomolecular films of stearic acid anilide (In Russian). *Physiological Journal of USSR* 27 (5):618–622
- Engel FL, Gurwitsch A (1936) Über die mitogenetischen Erscheinungen an monomolekularen Filmen. *Protoplasma* 26 (1):331–337. <https://doi.org/10.1007/bf01628661>
- Frenkel YI, Gurwitsch AG (1943) The physico-chemical basis of mitogenetic radiation. *Transactions of the Faraday Society* 39:201–204
- Gurwitsch A, Gurwitsch L (1925) Weitere Untersuchungen über mitogenetische Strahlungen. *Archiv für mikroskopische Anatomie und Entwicklungsmechanik* 104 (1):109–115. <https://doi.org/10.1007/bf02108493>
- Gurwitsch A, Gurwitsch L (1927) Zur Analyse der Latenzperiode der Zellteilungsreaktion. 19 Mitteilung über mitogenetische Strahlung und Induktion. *Wilhelm Roux' Archiv für Entwicklungsmechanik der Organismen* 109 (3):362–379. <https://doi.org/10.1007/bf02080801>

- Gurwitsch A, Gurwitsch L (1932a) Die Fortleitung des mitogenetischen Effektes in Lösungen und die Beziehungen zwischen Fermenttätigkeit und Strahlung. *Biochemische Zeitschrift* 246 (1–3):127–133
- Gurwitsch A, Gurwitsch L (1934a) L'analyse mitogénétique spectrale. *Actualités scientifiques et industrielles*, vol. 150 - Exposés de physiologie, vol 4. Hermann & Cie, Paris
- Gurwitsch A, Gurwitsch L (1936) Die mitogenetische Sekundärstrahlung. *Protoplasma* 25 (1):1–15. <https://doi.org/10.1007/bf01839025>
- Gurwitsch AA (1968) Problema mitogeneticheskogo izluchenija kak aspekt molekuliarnoj biologii (The problem of mitogenetic emission as an aspect of molecular biology) (in Russian). *Meditsina*, Leningrad
- Gurwitsch AA, Eremeev VF, Karabchievsky YA (1974) Energeticheskije osnovy mitogeneticheskogo izluchenija i ego registratsija na fotoelektronnikh umnozhiteliakh (Energy bases of mitogenetic radiation and its registration on photomultipliers) (In Russian). *Meditsina*, Moscow
- Gurwitsch AG (1923) Die Natur des spezifischen Erregers der Zellteilung. *Archiv für mikroskopische Anatomie und Entwicklungsmechanik* 100 (1–2):11–40. <https://doi.org/10.1007/bf02111053>
- Gurwitsch AG (1929) Methodik der mitogenetischen Strahlenforschung. In: Abderhalden E (ed) *Handbuch der biologischen Arbeitsmethoden*, vol V. vol 2/2. Urban & Schwarzenberg, Berlin, Wien, pp 1401–1470
- Gurwitsch A (1931a) Die Intensität mitogenetischer Strahlung und das Zustandekommen des mitogenetischen Effektes. *Naturwissenschaften* 19 (20):423–424. <https://doi.org/10.1007/bf01516396>
- Gurwitsch AG (1931b) Basic laws of mitogenetic excitation (In Russian). *Archive of Biological Sciences* 31 (1):149–159
- Gurwitsch AG (1931c) To analysis of secondary mitogenetic radiation (In Russian). *Archive of Biological Sciences* 31 (1):85–87
- Gurwitsch AG (1932) Die mitogenetische Strahlung der pflanzlichen und tierischen Meristeme. *Radiobiologia* 1 (1):15–19
- Gurwitsch AG (1934a) Der gegenwärtige Stand des mitogenetischen Problems. In: Capelli L (ed), *Atti del I Congresso Internazionale di electro-radio-biologia*, vol. 2, Venezia pp 689–704
- Gurwitsch AG (1937a) Mitogenetic Analysis of the Excitation of the Nervous System. N. V. Noord-Hollandsche Uitgeversmaatschappij, Amsterdam
- Gurwitsch AG (1937b) On degradation radiation of the central nervous system (In Russian). *Archive of Biological Sciences* 45 (2):53–57
- Gurwitsch AG (1937c) Some problems of mitogenesis (in Russian). *Archive of Biological Sciences* 46 (3):3–10
- Gurwitsch AG (1940) About macro-and microphotobiology (In Russian). *Physiological Journal* 29 (4):243–248
- Gurwitsch AG, Gurwitsch LD (1924) Mitogenetic rays and induction of mitoses (In Russian). *Meditsynskij arkhiv (Medical archive)* 1 (2): 173–178
- Gurwitsch AG, Gurwitsch LD (1928) Zur Energetik der mitogenetischen Induktion und Zellteilungsreaktion. 26 Mitteilung über mitogenetische Strahlung und Induktion. *Wilhelm Roux' Archiv für Entwicklungsmechanik der Organismen* 113 (4): 740–752. <https://doi.org/10.1007/bf02252024>
- Gurwitsch AG, Gurwitsch LD (1932b) Die mitogenetische Strahlung, vol 25. *Monographien aus dem Gesamtgebiet der Physiologie der Pflanzen und der Tiere*. Springer-Verlag Berlin Heidelberg, Berlin. <https://doi.org/10.1007/978-3-662-26146-0>
- Gurwitsch AG, Gurwitsch LD (1934b) Mitogeneticheskije izluchenije [Mitogenetic radiation] (in Russian). VIEM publishing house, Leningrad
- Gurwitsch AG, Gurwitsch LD (1935) Mitogenetic method, its theoretical basis and application area (in Russian). *Bulletin of All-Union Institute of Experimental Medicine* (6–7):29–32
- Gurwitsch AG, Gurwitsch LD (1937a) Degradation mitogenetic radiation (In Russian). *Bulletin of experimental biology and medicine* 4 (6):471–473
- Gurwitsch AG, Gurwitsch LD (1937b) Rayonnement mitogénétique de dégradation. *Bulletin de Biologie et de Médecine expérimentale de l'U.R.S.S.* 4 (6):459–460
- Gurwitsch AG, Gurwitsch LD (1945) Mitogeneticheskije izluchenije: fizikokhimicheskije osnovy i prilozhenija v biologii i meditsine (Mitogenetic radiation: physical and chemical bases and applications in biology and medicine). *Medgiz*, Moscow
- Gurwitsch AG, Gurwitsch LD (1947) Selective dispersion of ultraviolet as a method of analysis chemical structures (In Russian). In: Gurwitsch AG (ed) *Collected volume on mitogenesis and theory of biological field*. Pub.house of the USSR Academy of Medical Sciences, Moscow, pp 20–26
- Gurwitsch AG, Gurwitsch LD (1948) Vvedenije v uchenije o mitogeneze (An introduction to the teaching of mitogenesis). USSR Academy of Medical Sciences Publishing House, Moscow
- Gurwitsch AG, Gurwitsch LD (1959) Die mitogenetische Strahlung (Mitogenetic radiation). *VEB Gustav Fischer Verlag*, Jena
- Gurwitsch AG, Gurwitsch LD (1999) Twenty Years of Mitogenetic Radiation: Emergence, Development, and Perspectives. *21st Century Science and Technology Magazin* 12 (3):41–53 (translation from *Uspekhi Sovremennoi Biologii (Advances in Contemporary Biology)*, 1943, 16(3):305–334)
- Gurwitsch AG, Lydia (1925) Über den Ursprung der mitogenetischen Strahlen. *Wilhelm Roux' Archiv für Entwicklungsmechanik der Organismen* 105 (2):470–472. <https://doi.org/10.1007/bf02080849>
- Gurwitsch AG, Shalagin MM (1947) Mitogenetic method of diagnosis and evaluation of septic infections (In Russian). In: *Ognestrel'nyje rany grudnoj kletki (Gunshot wounds of thorax)*. Tatgosizdat, Kazan, pp 73–85
- Gurwitsch AA (1931d) Die Fortpflanzung des mitogenetischen Erregungszustandes in den Zwiebelwurzeln. *Wilhelm Roux' Archiv für Entwicklungsmechanik der Organismen* 124 (2):357–368. <https://doi.org/10.1007/bf00652480>
- Gurwitsch L, Anikin A (1928) Das Cornealepithel als Detektor und Sender mitogenetischer Strahlung. 25 Mitteilung über mitogenetische Strahlung und Induktion. *Wilhelm Roux' Arch Entwickl Mech Org* 113 (4):731–739. <https://doi.org/10.1007/bf02252023>
- Gurwitsch LD (1934b) Mitogenetic spectrum at excitation of proprioceptive nerve filaments (In Russian). *Archive of Biological Sciences Ser B* 35 (1):141–144
- Hollaender A, Claus WD (1935) Some Phases of the Mitogenetic Ray Phenomenon. *Journal of Optical Society of America* 25:270–286
- Kisliak-Statkewitsch M (1929) Die mitogenetische Strahlung des Carcinoms – I. Mitteilung. *Zeitschrift für Krebsforschung* 29 (3): 214–219. <https://doi.org/10.1007/bf01634487>
- Landau L (1946) On the thermodynamica of photoluminescence. *J Phys USSR* 10:503–506
- Latmanisowa LW (1933) Die mitogenetische Sekundärstrahlung des Nerven. *Pflüger's Archiv für die gesamte Physiologie des Menschen und der Tiere* 231 (1):265–279. <https://doi.org/10.1007/bf01754550>
- Lepeschkin WW (1932a) Necrobiotic Rays. *Science* 76 (1964):168. <https://doi.org/10.1126/science.76.1964.168>
- Lepeschkin WW (1932b) Nekrobiotische Strahlen. *Berichte der Deutschen Botanischen Gesellschaft* 50 (7):367–370. <https://doi.org/10.1111/j.1438-8677.1932.tb00072.x>
- Lepeschkin WW (1933) Nekrobiotische Strahlen. *Protoplasma* 20 (1): 232–250. <https://doi.org/10.1007/bf02674831>
- Lepeschkin WW (1934) Nekrobiotische Strahlen. *Protoplasma* 21 (1): 594–614. <https://doi.org/10.1007/BF01984547>

- Lepeschkin WW (1935) Nekrobiotische Strahlen. *Protoplasma* 22 (1): 561–580. <https://doi.org/10.1007/BF01608923>
- Moffatt JE, Tsiminis G, Klantsataya E, de Prinse TJ, Ottaway D, Spooner NA (2019) A practical review of shorter than excitation wavelength light emission processes. *Applied Spectroscopy Reviews*:1–23. <https://doi.org/10.1080/05704928.2019.1672712>
- Nicolis G, Prigogine I (1977) *Self-Organization in Nonequilibrium Systems*. Wiley, New York-London
- Ponomareva YN (1936) Mitogenetic and thermal effect on the mitotic rate of survival cells (In Russian). *Bulletin of experimental biology and medicine* 2 (1):16–18
- Ponomarewa J (1931) Die mitogenetische Spektralanalyse. III. Mitteilung: Das detaillierte glykolytische Spektrum. *Biochemische Zeitschrift* 239:424
- Potozky A, Zoglina I (1928) Über mitogenetische Sekundärstrahlung aus abgeschnittenen Zwiebelwurzeln. 28. Mitteilung über mitogenetische Strahlung und Induktion. *Wilhelm Roux' Archiv für Entwicklungsmechanik der Organismen* 114 (1):1–8. <https://doi.org/10.1007/bf02080336>
- Prokofiewa EG (1934) Mitogenetic Radiation of the Urea-Urease System. *Nature* 134 (3389):574–574. <https://doi.org/10.1038/134574a0>
- Rahn O (1936) Invisible radiations of organisms, vol 9. *Protoplasma-Monographien*. Gebrüder Bornträger, Berlin
- Rahn O (1937) Mitogenetic radiation. *Tabulae biologicae* 14 (1):1–35
- Ryazanskaya BS (1936) Secondary mitogenetic radiation of healthy and cancer patients (In Russian). *Vestnik rentgmologii i radiologii (Bulletin of Roentgenology and Radiology)* 17:536–542
- Sukhov K, Sukhova M (1934) Coagulation rays (In Russian). *Archive of Biological Sciences, Ser B* 35 (1):303–308
- Sukhov KS, Lanshina MN (1933) Ultraviolet radiation from protein coagulation (In Russian). *Biological journal* 2 (2–3):528
- Sussmanowitsch H (1928) Erschöpfung durch mitogenetische Induktion. 27 Mitteilung über mitogenetische Strahlung und Induktion. *Wilhelm Roux' Archiv für Entwicklungsmechanik der Organismen* 113 (4):753–758. <https://doi.org/10.1007/bf02252025>
- Vladimirov YA (1965) Fotokhimiya i lyuminescenciya belkov (Photochemistry and luminescence of proteins) (In Russian). Nauka, Moscow
- Vladimirov YA, Roshchupkin DI, Fesenko EE (1970a) Mechanism of ultraviolet radiation effects on proteins (In Russian). *Biofizika* 15 (2):254–264
- Vladimirov YA, Roshchupkin DI, Fesenko EE (1970b) Photochemical reactions in amino acid residues and inactivation of enzymes during UV-irradiation. A review. *Photochem Photobiol* 11 (4):227–246
- Warburg O (1910) Über Beeinflussung der Sauerstoffatmung. *Zeitschrift für Physikalische Chemie* 70 (6):413–432. <https://doi.org/10.1515/bchm2.1910.70.6.413>
- Wolff LK, Ras G (1932) Sekundäre Gurwitschstrahlung *Acta Brevia Neerlandica* 2:127–129
- Wolff LK, Ras G (1933) Über mitogenetische Strahlen. IV. Über Sekundärstrahlung. *Zentralblatt für Bakteriologie, Parasitenkunde und Infektionskrankheiten* 128:305–313
- Wolff LK, Ras G (1934a) Etudes sur le Rayonnement suivant Gurwitsch. VI. Le rayonnement secondaire. *Koninklijke Nederlandse Akademie van Wetenschappen* 37 (1):430–445
- Wolff LK, Ras G (1934b) Le rayonnement secondaire suivant Gurwitsch. II Communication. *Archive of Biological Sciences, Ser B* 35 (1):51–64



Mitogenetic Research in Medicine: Radiation of Blood and Cancer Diagnostics

23

Elena V. Naumova, Maira S. Aristanbekova, and Ilya Volodyaev

23.1 Introduction. Medical Aspects of Mitogenetic Radiation Research

As detailed in the previous chapters, mitogenetic effect (MGE) and mitogenetic radiation (MGR)¹ are two concepts that appeared in the scientific space in the 1920s. Despite over 1000 works in a dozen countries during the following 25 years, both of them remained in the strange position of “either/or” till now (see historical lines, review and critical analysis of results on MGE and MGR in Chaps. 2, 20, and 21, reviews (Gurwitsch 1988; Voeikov and Belousov 2007; Volodyaev and Belousov 2015; Naumova et al. 2018, 2021, 2022; Volodyaev et al. 2021; Gurwitsch and Gurwitsch 1999; Hollaender and Claus 1935; Hollaender 1936) and old monographs (Reiter and Gabor 1928; Gurwitsch and Gurwitsch 1932, 1945, 1948, 1959; Rahn 1936)). At least one-fourth to one-third of all MGR-related works were dealing with medicine. Here, after a brief introduction to the whole field, we will concentrate on the two main (largely overlapping) areas of this research – blood MGR and cancer diagnostics. They were extensively studied for many years and, in our opinion, require much attention because of their potential diagnostic possibilities.

¹MGR is a (claimed) endogenous ultraweak photon emission of biological systems in the middle UV range, stimulating division of certain cells (the phenomenon called MGE). The MGR-emitting objects are called “MGE-inductors,” the objects able to exhibit MGE under their action are “MGE-recipients” (see more in Chap. 20).

E. V. Naumova (✉)
Rzhanov Institute of Semiconductor Physics, Siberian Branch of the Russian Academy of Sciences, Novosibirsk, Russia
e-mail: naumova@yandex.ru

M. S. Aristanbekova
Saratov Regional Center for the Prevention and Control of AIDS, Saratov, Russia

I. Volodyaev
Moscow State University, Moscow, Russia

23.1.1 Research Objects

23.1.1.1 Organs, Tissues and Tumours

Of biological systems, various actively dividing cells (tissues or cell cultures) were the first reported MGE inductors (see Chap. 20), which naturally gave rise to research on MGR from malignant neoplasms. The latter was almost simultaneously reported by W. Siebert (1928a, b), T. Reiter and D. Gabor (1928), A.G. and L.D. Gurwitsch (1928) on freshly prepared pulps of sarcoma and carcinoma. Moreover, malignant tumours appeared the strongest² MGE inductors (Kisliak-Statkewitsch 1929; Gurwitsch and Gurwitsch 1929; Ypsilanti and Paltauf 1930; Klenitzky 1933a; Klenitzky 1933; Protti 1934), while healthy adult internals were no MGE inductors and no sources of MGR (see reviews in (Gurwitsch and Gurwitsch 1934, 1948, 1959)).

Good inductors were eye cornea (Gurwitsch and Anikin 1928; Gurwitsch 1931; Ponomareva 1934, 1936, 1939; Salkind and Ponomarewa 1934; Ponomarewa 1947; Naville 1929, 1937) (which was mostly used as recipient – see Sect. 20.5), nerves (Wassiliew et al. 1931; Gurwitsch 1933a, b, c, 1934a, b, 1938; Braines and Galperin 1934; Braines 1934, 1936) and muscles (Frank and Rodionow 1932, 1931; Siebert 1928a, b, 1929, 1931; Frank and Popoff 1929b), with both nerves and muscles reported as reliable sources of MGR when working and no MGR sources at rest. The latter made them very convenient objects for physical detection of MGR, as the intensity of MGR in them was relatively high, and repeated stimulation and rest allowed “switching it on” and “switching it off,” i.e., modulating the signal and separating it from noise (see Chap. 21, Fig. 21.9). Besides, they were

²Since, until the mid-1930s, MGR intensities were orders of magnitude below the sensitivity threshold of any photodetector, the inductor “strength” was estimated indirectly by the minimum induction time required to produce reliable MGE in a standard MGE-recipient (see more in Chaps. 20 and 21). While for the majority of “standard” inductors, the optimal induction time was 10 to 30 min, for malignant tumours, it was only seconds (e.g., 5 s for adenocarcinoma of alive mice (Gurwitsch and Gurwitsch 1948)).

popular subjects for MGR research due to considerable progress in studies of neural and muscle physiology at that time.

Nerves were also found reliable sources of the secondary radiation³ (Latmanisowa 1933), which was found to propagate along the nerve at about the speed of the nerve impulse.

Importantly, all internals (liver, kidney, stomach, spleen) were found capable of degradation radiation (dMGR)⁴ both in vivo and in vitro (Gurwitsch and Gurwitsch 1945, 1948, 1959), as well as all other tissues except tumours (see Chap. 22). Some of the authors also speculated that MGR from working nerves and muscles had mechanism similar to dMGR (Gurwitsch and Gurwitsch 1945, 1959).

A good source of MGR were also different regenerating tissues, studied in a long-lasting series of works, mostly from the group of L.J. Blyakher (Blacher and Bromley 1930; Samarajew 1932a; Blacher et al. 1932, 1933).

23.1.1.2 Blood

As mentioned in Chap. 20, blood of healthy animals and humans appeared a stable source of MGR (Gurwitsch and Gurwitsch 1926). Soon after it was demonstrated, blood and its various components became the most popular objects of MGE-based medical research, as a widely used and easily accessible fluid for medical diagnostics. Moreover, at first it attracted additional attention due to the erroneous assumption that blood is the universal source of MGR in adult organisms (Gurwitsch and Anikin 1928).⁵

Altogether, by the mid-1930s, MGE experiments with blood had numbered several thousand (Golshmid 1934) and had been performed in many top-rated medical institutions, like Charité clinics (Berlin, Germany) and All-Union Institute of Experimental Medicine (which later became the basis of the USSR Academy of Medical Sciences), and presented in textbooks/handbooks on general biology and haematology (e.g., Siebert 1934).

- No MGR detected from adult internals (Gurwitsch and Gurwitsch 1934)
- MGR from chicken embryos, appearing only with emergence of hematopoiesis (Sorin 1928)

let him speculate that blood is a universal source of MGR in adult organisms (Gurwitsch and Anikin 1928). However, some of these data appeared to be artifacts, caused by UV from the burners used, and this idea was abandoned.

³Secondary MGR is MGR whose generation is stimulated by irradiating the object with external MGR (see Chap. 22). That is, secondary inductors are no inductors by themselves and become MGE inductors only under external irradiation.

⁴Degradation MGR is MGR arising after stimulation by various factors (see Chap. 22).

⁵As mentioned in Chap. 2, Gurwitsch considered MGR to be a prerequisite for mitoses. This, plus the following experimental results:

Blood of young, healthy people and mammals was considered one of the most reliable MGE inductors (Gourvitch 1935). As H. Gesenius wrote, “Healthy blood never fails. If a failure occurs, it is time to test either the yeast or the apparatus” (Gesenius 1932).

However, it stopped emitting MGR if the animals or people were hungry, exhausted or suffering from different diseases, including cancer, diabetes, sepsis, etc. (see Table 23.1 in Sect. 23.2.5). Unlike other conditions, in case of cancer the authors attributed this lack of MGR to a certain highly-specific substance named “cancer quencher,” which appeared the first mentioned blood tumour marker⁶ (see below). This has spawned a huge field of cancer diagnostics, which stands alone among other medical applications of MGE as the most widely studied, supported by the most extensive clinical data, and showing unexpectedly high specificity and sensitivity, $\geq 95\%$ (Pesochensky 1942; Nagorianskaia 1945; Orlova 1949; Avchina 1950; Nudolskaja 1945; Gurwitsch and Gurwitsch 1945; Gurwitsch et al. 1947). This diagnostic tool was tested in practically all the main oncological institutions and clinics of the USSR⁷ and got positive reports from the leading oncologists (see below).

23.1.1.3 Other Body Fluids

In addition to blood, various other body fluids have been tested for ability to induce MGE in normal and pathological conditions:

- Urine (Zarkh 1934; Siebert 1930; Siebert and Seffert 1934; Orlova 1949)
- Saliva ((Ferguson 1932) as cited in (Rahn 1936))
- Cerebrospinal fluid (Lotsman 1940, 1941)
- Human and animal semen (experiments of Dorphman et al. as cited in (Zalkind 1934))

The authors mainly reported similar results for different fluids in respect to physiological conditions (see Table 23.4 for blood).

23.1.2 Methods and Applications

In the vast majority of all MGR studies, it was detected by the mitogenic effect obtained on standard recipients: yeast and,

⁶Cancer quencher was claimed in 1937, 26 years before alpha-fetoprotein, which is commonly regarded as the first tumour marker discovered in blood.

⁷Oncological Institute of Academy of Medical Sciences, the Second Moscow Medical Institute, Scientific Research Institute of Obstetrics and Gynecology, Army Medical Academy, Middle-Asia Oncological institute, X-raying and Radiology Hospital, Clinics at the Kiev Medical Institute and some others.

Table 23.1 MGE induction by blood in some diseases and physiological states

| Blood induces MGE | | Blood does not induce MGE | |
|--|--|---|--|
| Condition | References | Condition | References |
| Tuberculosis | Gurwitsch and Salkind (1929), Gesenius (1929, 1930), Markovsky (1931), Biddau (1932), Heinemann (1932), Verdina (1933), Yudeles (1944), and Pesochensky (1939) | Cancer diseases | Gurwitsch and Salkind (1929), Siebert (1930), Salkind and Schabad (1931), Gesenius (1930, 1932), Klenitzky (1933b), Heinemann and Seyderhelm (1933, 1934), Siebert and Seffert (1934, 1937), Blyakher et al. (1935), Golysheva (1934), Shlyapnikov and Komissar (1934), Pavlova (1935), Goldberg (1936), Nudolskaja (1936, 1937b), Pesochensky (1942), and Gurwitsch et al. (1947) |
| Lues | Gurwitsch and Salkind (1929) and Siebert (1930) | Pernicious anemia | Gesenius (1932) and Chmutova (1938, 1940) |
| Typhus | Gurwitsch and Gurwitsch (1932) | Leukemia | Gesenius (1932) and Storti and de Filippi (1936) (the latter as cited in (Maxia 1940)) |
| Gastritis | Voikhansky (1933) and Gesenius (1934) | Lymphogranuloma | Gesenius (1932) |
| Colitis, duodenal ulcer, stomach ulcer | Voikhansky (1933) | Sepsis | Gurwitsch and Salkind (1929) and Gesenius (1929, 1932) |
| Pneumonia | Zolotova-Kostomarova and Lyass (1936) and Gesenius (1934) | Pellagra | Golshmid (1934) |
| Hyperthyroidism (Basedow's disease) | Samarajew (1932b) | Chronic tonsillitis (MGR restores after tonsillectomia) | Heinemann (1932) |
| Mania | Brainess (1934) | Diabetes | Gurwitsch and Salkind (1929) and Chmutova (1946) |
| Mental fatigue | Vasil'ev (1934) | Liver cirrhosis | Gesenius (1934) |
| | | Rickets | Biddau (1932) and Mai (1934) |
| | | Menstruation period | Siebert (1934) and Heinemann and Seyderhelm (1933) |
| | | Starvation | Gurwitsch and Gurwitsch (1934) |
| | | Depression | Brainess (1934) |
| | | Senility | Heinemann (1932) and Brainess (1934) |
| | | Data on blood MGR ceasing in mental fatigue (Yefimov and Letunov 1934) were later explained by nonexcluded easy physical labor in experiments (Vasil'ev 1934) (thus, see mental fatigue in the left column) | |

Based on Gurwitsch et al. (1947) and Maxia (1940)

less frequently, bacteria or eye cornea (see Chap. 20 for more on methods). Several investigators have used modified gas-discharge counters: to study MGR from carcinoma (Rajewsky 1931; Siebert and Seffert 1933), blood and urine (Siebert and Seffert 1933), frog muscle and heart, frog muscle pulp (Frank and Rodionow 1931), nerves (Audubert 1938) (see Chap. 21 for more on methods). Some authors have tried to detect MGR photographically (Protti 1930, 1932; Acqua 1935; Brunetti and Maxia 1930), but we do not address these works here, as we consider them false positives (see Chap. 21 for details).

As discussed below, the strong dependence of MGR on various physiological conditions, its potential noninvasiveness (apart from the issue of access to a specific MGR source in the body) and the potential ability to observe it “here and now” made it an attractive tool for medical diagnostics. Besides that, there have also been attempts at

its therapeutic applications, such as (Brainess 1934, 1936), but the lack of double-blind trials (not accepted at the time) and insufficient statistical sample size cast doubt on the claimed positive results.

23.1.3 The Research Prevalence and Fate

The absolute majority of medicine-related research of MGR were performed in three countries: the USSR (A.G. and L.D. Gurwitsch, S.J. Salkind, A. Potozky, Yu.N. Ponomareva, V.P. Nagorianskaia, B.S. Pesochensky, S.N. Brainess, Ya.S. Klenitsky, M.B. Novikov, G.M. Frank), Germany (M. Heineman, T. Reiter, D. Gabor, W.W. Siebert, H. Seffert, R. Seyderhelm) and Italy (G. Protti, L. Castaldi, R. Brunetti, G. Zirpolo, C. Maxia).

In Germany, medical MGR research almost ceased after Hitler came to power⁸ and completely stopped (as well as in Italy) by the beginning of World War II. In the USSR, it was almost terminated after the famous “VASKHNIL session” in August 1948 (see Chap. 2, Section “After 1948”), where mitogenetic research was persecuted together with genetics. It should be noted that despite practically blocking biological MGE research, papers on cancer diagnostics were still published for several more years (Zalkind 1950; Pesochensky 1950; Nechaeva 1952, 1953; Maleeva and Nechaeva 1951) and even a few dissertations were defended (Avchina 1950; Orlova 1949; Sneshko 1955). Later, medicine-related MGE researches were performed only in Anna Gurwitsch’s group, mainly focusing on nerves and muscles (Lazurkina 1982, 1987; Gurvich 1966, 1976; Gurvich et al. 1966; Gurvich and Ereemeev 1966; Gurwitsch 1962) and to a less extent on cancer (Ereemeev 1961) and other subjects (Gurwitsch 1968; Gurwitsch et al. 1974).

Here, we review two main areas of medicine-related MGE/MGR research: blood MGR and cancer diagnostics. These works are hardly remembered by now, and the whole area appears frozen in a strange state of “non-proven but with great promise,” the latter mainly related to cancer diagnostics. It was this, as well as fortunate access to the original publications and clinical protocols, that has prompted us to collect and review these data now.

23.2 Mitogenetic Radiation from Blood

23.2.1 Blood as a Source of MGR and Some Methodical Specifics of Its Study

Stable MGR was detected from:

- Whole blood of amphibia (frogs (Gurwitsch and Gurwitsch 1926), tadpoles (Blyakher et al. 1934a), axolotls at metamorphosis (Blyakher et al. 1934b)), mammals (rats, dogs) (Potozky and Zoglina 1929), chicken (Potozky and Zoglina 1929), hemolymph of invertebrates: crabs and mollusks (Salkind et al. 1930; Potozky et al. 1930).
- Hemolyzed blood and blood with added heparin or $MgSO_4$ (Potozky and Zoglina 1929).
- Blood cell suspension in a suitable buffer solution (Klenitzky 1932; Rylova 1935) (however, the work by Rylova (1935) looks quite doubtful in itself).
- Blood serum with added H_2O_2 (Potozky and Zoglina 1929).

MGR from blood was first reported in (Gurwitsch and Gurwitsch 1926; Sorin 1926) on frogs *Rana temporaria* and *esculenta*: both whole blood and deluded with saline. Interestingly, MGR could be also detected from live open frog vessels (both veins (Gurwitsch and Gurwitsch 1926) and arteries (Sorin 1926)) containing blood (ligated blood-free vessels showed no MGR). A.N. Sorin (1926) reported some (undetermined) oxidising substances in lymph and serum and referred MGR from frog blood to oxidation.

Hemolymph of invertebrates (arthropoda and molluscs) also emitted MGR, which was supposedly caused by oxidation processes in blood cells (Potozky et al. 1930).

Blood of rats, chickens and pigeons was investigated in (Potozky and Zoglina 1929). The authors detected MGR from the whole blood, hemolyzed blood, serum, serum ultrafiltrate, when adding heparin, KCN, $MgSO_4$ or H_2O_2 , and obtained its spectra (see more on methods in Chap. 21). From these, the authors concluded that sources of mammalian blood MGR are (unlike frog blood) glycolysis and oxidation of polypeptides and (possibly) amino acids. They also suggested that cessation of blood MGR under starvation is caused by slowing down of these enzymatic processes.

More than two thousand successful experiments with human and animal blood (both in vitro and in vivo) and urine have been performed in the famous Charité Clinic in Berlin (Siebert and Seffert 1934) (see, e.g., Fig. 23.1). The authors used a differential measurement scheme with two counters, which greatly improves the signal/noise ratio.

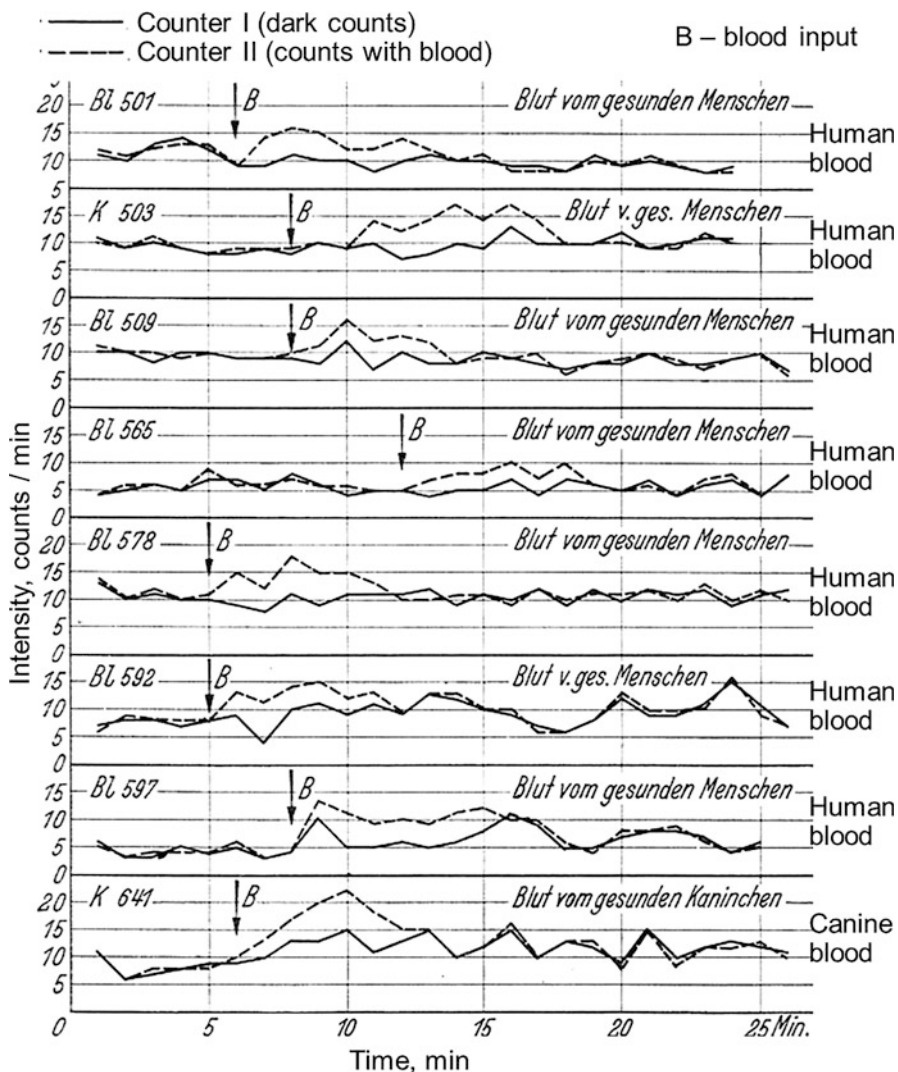
In most works, MGR from fresh blood was observed within 10 to 15 min after collection (Potozky et al. 1930; Rahn 1936); however, some authors reported shorter times, down to 2 to 3 min (Golshmid 1934). Yet, there is no significant contradiction between these data, because methods, animals, and their states were different.

For MGR studies, blood was usually mixed with an equal amount of a 4% $MgSO_4$ solution to prevent clotting, or hemolyzed with distilled water (Potozky and Zoglina 1929; Gurwitsch and Gurwitsch 1934). Because of the short storage time of fresh blood, many studies used blood dried on blotting paper and mixed with water before experiments (Karpas and Lanschina 1932). The storage period of dried blood was 2 to 3 days; the redeluded blood after addition of water retained its induction ability for about 15 min (Karpas and Lanschina 1932) (see method details in (Gurwitsch and Gurwitsch 1932) and its brief description in (Rahn 1936)).

Even trace amounts of disinfectants were reported to stop radiation, so usually the blood was drawn with a Francke needle without disinfection or after complete evaporation of disinfectant (10–15 min after disinfection with 96% alcohol), both of which look strange now.

⁸M. Heinemann and D. Gabor emigrated in 1934, later followed by T. Reiter and some other leading researchers of medical aspects of MGR.

Fig. 23.1 Detection of blood MGR with a differential scheme: simultaneous use of two Geiger-Müller counters, one of which measures radiation background. (Data of Siebert and Seffert (1934) arranged in (Salkind 1937). Reprinted from (Salkind 1937). Copyright 1932, with permission from Springer Nature)



23.2.2 MGE Spectral Analysis of Blood

To study MGR spectra the usual spectrographs of those times were used, but with rows of yeast recipients as detectors instead of photographic plates (see Chap. 21, (Volodyaev et al. 2021; Gurwitsch and Gurwitsch 1945)). MGR spectra of bioobjects usually represented superposition of a few basic spectra, which were interpreted as fingerprints of excited states of specific molecules or functional groups. These elementary spectra were named by processes taking place in some simple biochemical systems, like glycolytic spectrum or the spectrum of creatine-phosphate cleavage.

Blood radiation itself and its spectra depended on the physiological state of the organism. The blood spectra most often coincided with the so-called glycolytic spectrum (see Fig. 23.2), and these spectral features were later interpreted as fingerprints of the glucose excited state (Gurwitsch et al. 1939; Gurwitsch and Gurwitsch 1939b, 1945, 1948).

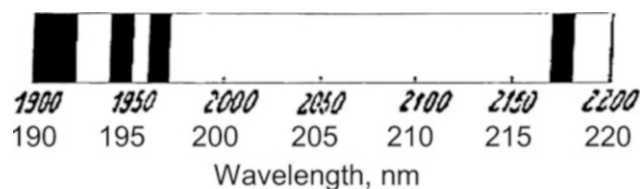


Fig. 23.2 MGE-spectrum of rabbit's laky blood. (Reprinted from Ponomarewa 1931)

Importance of glucose for blood MGR was shown in (Potozky and Zoglina 1929). The animal starvation led to the fading of glycolytic spectral lines, while injection of glucose restored glycolytic spectra almost immediately (Gurwitsch and Gurwitsch 1945). In case of long starvation after complete ceasing of glycolytic component and a week's absence of MGR, "proteolytic" components aroused (Gurwitsch and Gurwitsch 1932).

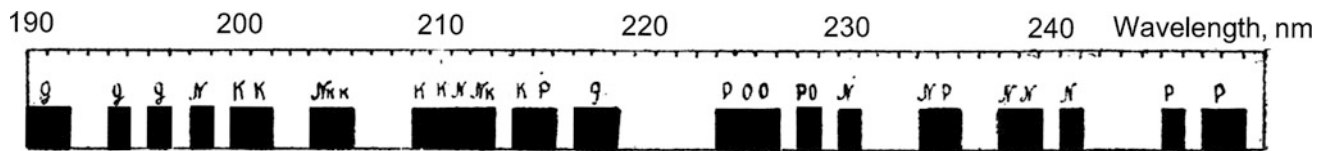
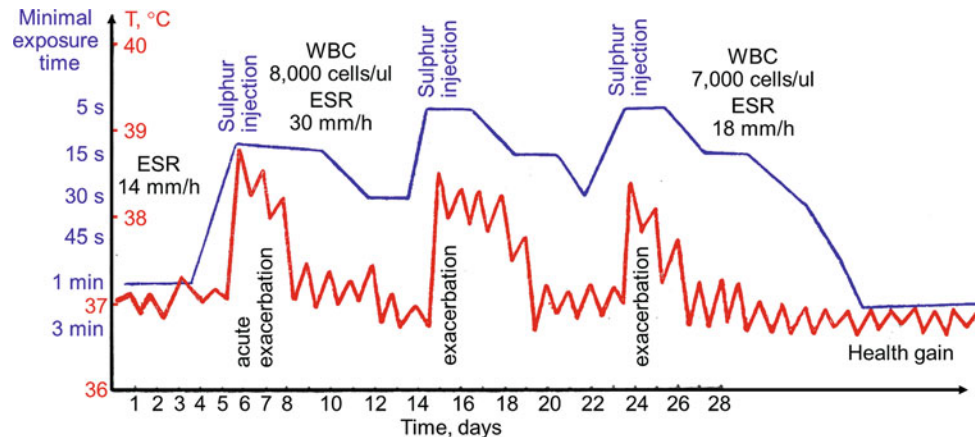


Fig. 23.3 Mitogenetic spectral analysis of MGR from the streaming blood in the rabbit vein. The spectral features were identified as follows: g, glycolytic; N, proteolytic, also referred to as NH_3 spectrum; K,

creatine-phosphate cleavage; P, phosphatase; O oxidation. We should note that spectral features caused by secondary MGR of the vein cannot be excluded here. (Reprinted from Golysheva 1933)

Fig. 23.4 Dynamics of blood MGR intensity (evaluated by the minimal exposure time of a standard yeast recipient to the blood sample, inducing a reliable MGE in it) and temperature of rheumatic patient as a reaction to provocation with sulphur injections. ESR, erythrocyte sedimentation rate (mm/h); WBC, white blood cells. (Adapted from Zolotova-Kostomarova and Lyass 1936)



Sometimes, blood MGR demonstrated spectral lines of the so-called oxidative, phospholytic spectra and some others (see an example of such multicomponent spectrum in Fig. 23.3).

The MGR of white blood elements (polynuclears as well as lymphocytes) manifested spectral features of glycolytic, oxidation and phosphatase spectra (Klenitzky 1932).

23.2.3 Blood MGR under the Influence of Chemical Agents

A number of works have focused on the effects of chemical agents on blood MGR. First, they aimed at studying the chemical bases of MGR generation. For instance blood MGR stopped in oxygen-free media, suggesting that the source of chemical energy released as MGR may be oxidative processes (Sorin 1926). Second, the prospects of diagnostic based on the changes in blood MGR prompted to search for other factors that can influence it.

Some substances were supposed to have a direct impact on MGR generation or absorbance. For instance, quinine was shown to stop MGR when added to blood in vitro, after oral intake and injections (playing the role of a UV absorber) (Billig 1931; Gurwitsch and Gurwitsch 1945). A similar effect was produced by the other mid-UV absorbing substances: iodine, arsenic, KCN, lactic acid, etc. (Siebert and Seffert 1934; Salkind 1937; Gurwitsch and Gurwitsch 1945; Pesochensky 1942; Nagorianskaia 1945).

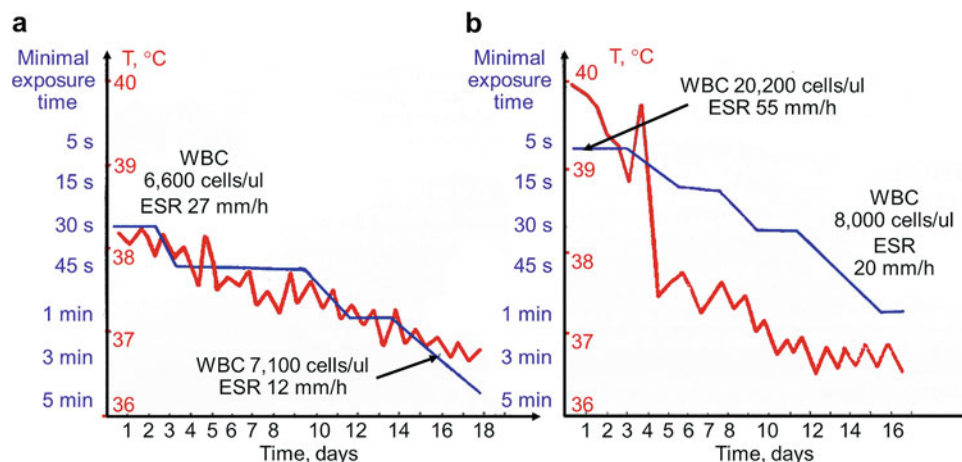
Glucose served as an MGR enhancer (Gurwitsch and Gurwitsch 1945). MGR of blood was shown to cease at starvation due to the lack of glucose and to restore immediately after glucose injections (Gurwitsch and Gurwitsch 1945). Addition of glucose to the blood of cancer patients also restored MGR (Gurwitsch and Salkind 1929; Potozky and Zoglina 1929), while addition of glucose to blood with quinine did not (Billig 1931).

Addition of citagenin (Heinemann 1932), hemoglobin, polypeptides with H_2O_2 (Potozky and Zoglina 1929) restored MGR of blood in case of its absence caused by various reasons, or even gave rise to MGR from blood serum (Potozky and Zoglina 1929), which usually was no MGE inductor (Sorin 1926).

Oral intake or injections of some other substances were expected to influence MGR through some complex physiological response of the body. For instance, sulphur injections to rheumatic patients were shown to cause exacerbation, increase of temperature and erythrocyte sedimentation rate (ESR) that correlated with the blood MGR increase (see Fig. 23.4) (Zolotova-Kostomarova and Lyass 1936). Effect of injections of twelve different hormones on blood MGR was studied in (Engel and Morelli 1936).⁹

⁹The authors used a specific modification of the MGE observation methods, suggested by J. Morelli and significantly differed from Gurwitsch's method. It was used only by Morelli and his coauthors, making their results difficult to compare with the others (see more about Morelli's method in Sect. 23.3.4).

Fig. 23.5 Dynamics of blood MGR intensity (characterized by the minimal exposure time producing MGE in a standard recipient) in rheumatism (left) and pneumonia (right). (Adapted from Zolotova-Kostomarova and Lyass 1936)



23.2.4 Blood MGR in Various Physiological States

Blood of healthy people of various ages and physiological states was studied widely. MGR was observed from blood of all groups and from any mixtures thereof except for the mixture of A and B groups (Siebert and Seffert 1936, 1937). Blood MGR was not observed at starvation (Gurwitsch and Gurwitsch 1934), senility (Heinemann 1932; Brainess 1934), physical (Brainess 1931, 1932a, 1934; Heinemann and Seyderhelm 1933) and mental (Yefimov and Letunov 1934) fatigue. Especially extensive data were obtained on the dynamic of blood MGR ceasing and further restoration in physical and mental fatigue (Brainess 1931, 1932a, b, 1934; Yefimov and Letunov 1934; Vasil'ev 1934; Heinemann and Seyderhelm 1933). In case of physical fatigue, it was explained by the influence of milk acid, whose injections also suppressed blood MGR (Brainess 1932a). Blood MGR ceasing in case of hard mental work accompanied by easy physical labor (Yefimov and Letunov 1934) was later referred to the physical, but not to the mental part of the job (Vasil'ev 1934).

Absence of blood MGR during menstruation was reported in (Siebert 1934; Heinemann and Seyderhelm 1933). Blood of pregnant women was shown to emit more intensive MGR (MGE was observed already after 10 to 15 s exposure) and kept ability to induce MGE for much longer time after hemolysis (up to 2 h) (Lintvareva 1940a, b). The author even suggested to use this method for determination of gestational dynamics.

Blood MGR dynamics was also studied during childbirth (Klenitsky 1934a). In the dilating stage of labour, MGR remained normal, while the author expected its ceasing in response to the obvious muscle work. The contradiction was explained by the very specific rhythm of work: in dilating stage, the short strong muscle contraction alternated with significant rest periods that differed from monotonous work usually studied in previous research on blood MGR in

physical fatigue (Brainess 1932a, 1934). Ceasing of blood radiation during the expulsion period in labor was explained by lactic acid accumulation. The mother's peripheral blood appeared to emit more intensive MGR than that of the new-born child (Marconi 1931).

23.2.5 Blood MGR in Various Pathologies

Besides the above physiological conditions, blood MGR was found to cease in certain pathologies: cancer, sepsis, diabetes, starvation, and depression, as well as for elderly people (see Table 23.1). At the same time, blood MGR remained well-detectable in tuberculosis, lues, typhus and some other diseases (see Table 23.1), and even increased¹⁰ in cases of induced and spontaneous hyperthyroidism (Basedow's disease) (Samarajew 1932b), mania and some forms of schizophrenia (Brainess 1934), pneumonia and rheumatism¹¹ (Zolotova-Kostomarova and Lyass 1936) (see Fig. 23.5).

Interestingly, while at that time complains of neurotics on physical fatigue after the full-night sleeping were considered illusory, the MGR experiments demonstrated that they had quite a real biochemical ground manifesting in a decrease or termination of blood MGR (Brainess 1934). Another interesting observation by S.N. Brainess related to the disappearance of blood MGR after it has been drawn from a vein. While in healthy individuals it occurred within half an hour, for manic patients, it remained for 3 to 4 h more (as described in (Gurwitsch 1937; Gurwitsch and Gurwitsch 1999)).

¹⁰While in most works, the blood MGR was assessed simply in "yes or no" terms, some authors took into account the changes in its relative intensity as well. As stated above (see Chaps. 20 and 21) in case of biological detection, it was characterised by the minimal exposure time needed to obtain MGE in the recipient.

¹¹The authors claimed that intensification of MGR was even more reliable evidence of acute process than increase of such blood values as erythrocyte sedimentation rate (ESR) and white blood cell count (WBC) (Zolotova-Kostomarova and Lyass 1936).

23.2.6 Blood MGR in Cancer

Naturally, of all the above, it was the disappearance of MGR in cancer that attracted the most attention. This phenomenon was observed in all types of cancer, both for humans and animals (Gurwitsch and Salkind 1929; Siebert 1930), and by means of both biological and physical detection with gas-discharge counters (see, for instance data from (Siebert and Seffert 1933) in Table 23.2, compare to Table 23.3 as an MGR-positive control).

Importantly, though (as mentioned above) lack of blood MGR was not a specific indication of cancer, in cancer patients and animals it happened very early and correlated with the course of the disease. Thus, in works with experimentally induced cancer in mice (Klenitzky 1933b) and rats (Goldberg 1936), blood MGR stopped in a few days after tumour inoculation and disappeared several days after its radical extirpation. In most clinical works, blood MGR was reported to stop at very early stages of carcinogenesis and restore in a few months after successful surgery or radiotherapy (assessed clinically). Importantly, in cases of persistent absence of MGR even with a favourable clinical picture, recurrence of the primary tumour or metastases was diagnosed later (Chochia and Zhirmunskaya 1938). The only exception that we've found was a paper on experimental

tar cancer in which the authors observed blood radiation till metastases occurred (Zalkind and Shabad 1931).

Cancer blood temporarily restored its mitogenetic activity in 2 to 3 h after injection of citagenin (Heinemann 1932) and

Table 23.2 MGR from blood of cancer patients on blotting paper (a differential scheme with two gas-discharge counters registering counts with and without sample was used)

| Exp. no | $\frac{\text{Counts with sample} - \text{Dark counts}}{\text{Dark counts}}, \%$ |
|---------|---|
| 93 | -0.6 |
| 95 | -1.4 |
| 111 | -3.5 |
| 113 | -1.4 |
| 118 | -0.9 |
| 125 | +0.7 |
| 136 | -2.3 |
| 137 | +3.7 |
| 176 | +2 |
| 177 | 0 |
| 250 | -1.5 |
| 253 | -3.1 |
| 392 | -0.7 |
| 400 | -1.9 |
| 485 | +2.5 |

Data from Siebert and Seffert (1934)

Table 23.3 MGR from blood of healthy humans on blotting paper (a differential scheme with two gas-discharge counters registering counts with and without sample was used)

| Exp. no | Counting period, min | Number of counts | | Difference, % | Exp. no | Counting period, min | Number of counts | | Difference, % |
|---------|----------------------|-----------------------|-------------|---------------|---------|----------------------|-----------------------|-------------|---------------|
| | | Without sample (dark) | With sample | | | | Without sample (dark) | With sample | |
| 77 | 7 | 70 | 91 | +30 | 214 | 6 | 38 | 56 | +47.4 |
| 79 | 5 | 50 | 72 | +43.9 | 226 | 6 | 42 | 58 | +38 |
| 92 | 6 | 60 | 79 | +31.6 | 233 | 5 | 35 | 49 | +40 |
| 94 | 7 | 64 | 98 | +53.1 | 241 | 4 | 26 | 40 | +53.8 |
| 101 | 6 | 80 | 112 | +40 | 244 | 4 | 31 | 51 | +64.5 |
| 114 | 6 | 46 | 64 | +39 | 246 | 5 | 30 | 41 | +31.6 |
| 121 | 5 | 43 | 58 | +35.1 | 252 | 6 | 30 | 48 | +60 |
| 124 | 6 | 78 | 105 | +34.6 | 254 | 5 | 40 | 60 | +50 |
| 131 | 6 | 62 | 88 | +42 | 261 | 5 | 26 | 41 | +47.6 |
| 157 | 7 | 122 | 165 | +34.7 | 262 | 5 | 37 | 55 | +48.7 |
| 167 | 5 | 37 | 55 | +48.6 | 268 | 5 | 36 | 53 | +47.2 |
| 172 | 6 | 53 | 78 | +47 | 272 | 6 | 46 | 72 | +56.7 |
| 183 | 5 | 30 | 42 | +40 | 273 | 5 | 43 | 63 | +46.4 |
| 186 | 5 | 44 | 64 | +45.5 | 279 | 5 | 33 | 48 | +45.4 |
| 190 | 6 | 30 | 47 | +56.5 | 280 | 6 | 42 | 62 | +47.6 |
| 192 | 5 | 23 | 38 | +65 | 281 | 5 | 35 | 59 | +68.4 |
| 195 | 5 | 31 | 46 | +49 | 282 | 6 | 47 | 73 | +55 |
| 196 | 5 | 30 | 42 | +40.2 | 357 | 6 | 72 | 108 | +50 |
| 200 | 5 | 35 | 49 | +40 | 358 | 5 | 44 | 66 | +50 |
| 209 | 6 | 43 | 60 | +41.6 | | | | | |
| 213 | 5 | 34 | 48 | +41.2 | • | | | | |

Data from Siebert and Seffert (1934)

Table 23.4 Excerpt from the summary table on cessation of MGR from human and animal blood in cancer (22 authors, about 1200 cases)

| Authors | References (if available) | Institute or clinic | Material | Number of cases | % of concordance with clinical diagnosis |
|--------------------------|---|---|--------------------------|------------------------|--|
| Gurwitsch and Zalkind | Gurwitsch and Salkind (1929) | Histological Institute | Mice with adenocarcinoma | 28 | 100 |
| | | First Moscow Medical Institute | Clinical | 17 | 100 |
| Gesenius | Gesenius (1930) | Clinic Charité in Berlin | Clinical | 47 | 98 |
| Gesenius | Gesenius (1934) | Clinic Charité in Berlin | Clinical | 74 people 124 cases | 87 |
| Siebert | Siebert (1930) | Clinic Charité in Berlin | Clinical | 30 | 100 |
| Siebert | Siebert and Seffert (1934) | Clinic Charité in Berlin | Clinical | 15 | 100 |
| Seiderhelm and Heinemann | Heinemann and Seyderhelm (1933, 1934) | Clinical hospital in Frankfurt am Main | Clinical | 60 | 100 |
| Pavlova | Pavlova (1935) | Cancer Institute in Tashkent | Clinical | 116 | 93.5 |
| Nudolskaya | J. Obs. Gyn. (USSR), 1935 (ref. not found) | Obstetrics and Gynecology Clinic of the Second Moscow Medical Institute | Gynecological cancer | 47 | 86 |
| | Nudolskaja (1936) | | | 105 | 96 |
| Klenitsky | Klenitzky (1933a) | All-USSR Institute of Experimental Medicine | Gynecological cancer | 14 | 100 |
| Klenitsky | Klenitzky (1933b) and Klenitsky (1934b) | All-USSR Institute of Experimental Medicine | Mice with adenocarcinoma | 48 | 100 |
| Golysheva | Golysheva (1934) | All-USSR Institute of Experimental Medicine | Clinical | 35 | 90 |
| | | | Mice | 8 | 100 |
| Shlyapnikov | Shlyapnikov and Komissar (1934) | Saratov Medical Institute | Clinical | 42 | 95 |
| Voykhansky | Voikhansky (1933) | Institute for the Improvement of Doctors in Leningrad | Clinical | 36 | 95 |
| Blyakher | Blyakher et al. (1935) | Institute of Experimental Morphology | Clinical | 14 | 100 |
| | | | Mice | 19 | 100 |
| Lazaris | Bogdanovich and Lazaris (1935) | Dnepropetrovsk Medical Institute | Mice | 20 | 95 |
| Chochia | Chochia and Zhirmunskaya (1938) | Radiological Institute in Leningrad (clinic of Prof. Schaak) | Clinical | 50 | 91.3 |
| Nagorianskaia | Nagorianskaia (1938) | Cancer Institute (Moscow?) | Clinical | 172 | 98.2 |
| Goldberg | Supposedly, Goldberg (1936) | Tomsk Medical Institute | Transplanted rat cancer | 94 | 100 |
| Levina | In manuscript; supposedly, later published as Levina (1938) | Institute of Endocrinology in Kharkov | Grafted mouse cancer | 30 | 100 |
| Ryazanskaya | Ryazanskaya (1936) | Radiological Institute in Leningrad | Clinical | 12 | 100 |
| Zalkind | In manuscript | Radiological Institute in Leningrad | Clinical | 19 | 100 |
| Chernevskaya | Supposedly, Chernevskaya (1940a, b) | Cancer Institute in Voronezh | Clinical | 64 | 70 |
| Kuraev | In manuscript; supposedly, unpublished | Cancer Institute in Dnepropetrovsk | Clinical | 49 | 94 |
| Krasovskaya | Supposedly, Weller and Krasovskaya (1936) and Krasovskaya and Weller (1936) | Institute of Endocrinology in Kharkov | Rat sarcoma | 30 | 100 |

Based on (Zalkind 1936), data from (Gurwitsch and Zalkind 1936), with appropriate references added (including later published ones, and available only as manuscripts at the time the table was published)

immediately after adding glucose into it (Gurwitsch and Salkind 1929; Potozky and Zoglina 1929).

Interestingly, MGR of corneal epithelium (Gurwitsch and Gurwitsch 1934) and urine (Siebert 1930; Orlova 1949) also stopped with cancer.

In 1936, the above conclusions were supported by a generalized report of approx. 1200 experiments with blood

of cancer patients and animals, obtained by 22 authors from different countries, presented by L.D. Gurwitsch and S.Ya. Salkind at the Second international congress on cancer research (Gurwitsch and Zalkind 1936; Pesochensky 1942) (see an extract from their report in Table 23.4).

Table 23.5 Difference between cancer quencher and absorbers of blood MGR found in other conditions

| Name | Absorbers | Quencher |
|--------------------------|---|---|
| Conditions when detected | Noncancerous diseases; physiological conditions accompanied by the absence of MGR | Cancer only |
| Specificity | No | High |
| UV absorbance | Yes | Comparatively negligible |
| Thermostability | Heat-resistant (100 °C) | Destroyed by heating |
| Molecular properties | Low-molecular substances | High-molecular substance, supposedly peptide or a group of peptides with a certain quenching group in their structure |

23.3 Cancer Quencher and Cancer Diagnostics

23.3.1 Discovery of MGR Quenching. Differences between Absorbers and Quenchers, Their Physical and Chemical Properties

Needless to say, the disappearance of MGR in the above physiological and pathological conditions has led researchers to question the mechanisms of this phenomenon. In all cases except cancer, absence of blood MGR was referred to the substances actively absorbing UV (similarly to the presently known reabsorption – see Sect. 5.3.3). Usually these products of pathological or physiological metabolism had low molecular weight: e.g., ketone bodies in diabetes (Chmutova 1946), bile pigments in jaundice (Gurwitsch et al. 1947), etc.

Contrary to that, in cancer, the substance responsible for MGR suppression had quite different physical and chemical properties (Gurwitsch and Gurwitsch 1937, 1945; Zalkind 1937; Gurwitsch et al. 1947; Siebert and Seffert 1937).

First of all, it practically did not absorb UV (although it efficiently suppressed the blood MGR), so it had a different mechanism than simple reabsorption.

Second, it was concentrated in the anodic (but not cathodic) fraction during electrophoresis, indicating its negative charge.

Third, it could not spontaneously diffuse through a collodion film with pores of ~2 to 3 nm, but did diffuse through it during electrophoresis. This suggested that it is a high-molecular-weight filamentous molecule at least 3 nm long.

Interestingly, it could be subjected to hydrolysis, but retained its quenching ability. However, after hydrolysis, the substance with quenching properties diffused well through the same collodion film without voltage application, indicating that the quenching effect was caused by a relatively small group in the molecule.

The quenching substance was found in albumen-free blood fraction and retained its quenching properties after careful drying at 37 °C. However, a short boiling or longer heating to 80 °C completely removed its quenching ability.

Also, it could be adsorbed by kaolin and washed out from it with an alkaline solution.

All this led the authors to assume that it was a peptide or a group of peptides (its chemical structure surely could not be sequenced in the time).

Importantly, this substance was specifically detected only in cases of cancer, allowing the authors suggest it as a highly specific cancer marker and call it “cancer quencher” (Gurwitsch and Gurwitsch 1937; Zalkind 1937; Gurwitsch et al. 1947) (see Table 23.5 for the summary of the above properties and their comparison with those of MGR absorbers, and (Novikov 1938; Gurwitsch and Gurwitsch 1945; Gurwitsch et al. 1947; Pesochensky 1942; Nudolskaja 1945; Maleeva and Nechaeva 1951) for more methods of cancer quencher detection).¹²

Importantly, isolated from blood (see methods below) and added to any MGE inductor, cancer quencher stopped its MGR. Injected into healthy animals (mice), it also stopped MGR from their blood for ~4 days, after which its MGR was spontaneously restored (Boukatina 1939).

Cancer quencher was also detected in healthy organs (Salkind and Novikov 1938) and urine (Orlova 1949) of cancer patients and animals.

Usually, the priority in cancer quencher discovery is given to Gurwitsch (Gurwitsch and Gurwitsch 1937) and Siebert (Siebert and Seffert 1937) who reported it almost simultaneously. However, an observation that MGR from a “normal blood” disappears when mixed with a “cancer blood” had been made ~5 years earlier by Lapchinsky and Martynov (Gurwitsch and Gurwitsch 1932) (see Table 23.6) and Voikhansky (1933) (without any conclusions on the quenching substance).

Cancer quencher was used in experiments proving the necessity of MGR for mitosis. Addition of quencher to an MGE inductor damped not only its MGR, but mitoses as well (Ponomarewa 1947; Zalkind 1937; Gurwitsch et al. 1947), and exposure of this system to external MGR restored mitoses (Zalkind 1937; Gurwitsch et al. 1947).

¹²It should be noted that the existence of a tumour marker in blood was a revolutionary statement for the 1930s. It was claimed about 25 years before the discovery of alpha-fetoprotein as a tumour marker (Tatarinov 1963), which is now generally accepted as the first tumour marker in blood (Nikulina et al. 2015).

Table 23.6 Suppression of normal blood MGR with cancer blood (assessed via biological MGE, %)

| MGE, % Normal blood | MGE, % Cancer blood | MGE, % Mixture of normal and cancer blood |
|------------------------|------------------------|--|
| 30 | -1.2 | 0.7 |
| 60 | -1 | 5 |
| 28 | -3 | -10 |
| 40 | -9 | -1 |
| 38 | -3 | 2 |
| 38 | -3 | 10 |
| 48 | 5 | 6 |

Data by Lapchinsky and Martynov

Adapted from (Gurwitsch and Gurwitsch 1932). Copyright 1932, with permission from Springer Nature

23.3.2 Experimental Cancer and Clinical Data on Cancer Diagnostics

23.3.2.1 Animal Models

An even more important feature of the cancer quencher (referred to herein as CQ, for brevity) was that it appeared long before clinically diagnosable diseases, i.e., could be used for very early diagnostics. These conclusions were made from a series of experimental works with cancer inoculation or application of carcinogens to different animals (see below).

In experiments with mice (inoculated Ehrlich adenocarcinoma), cancer quencher was detected in a few days after carcinoma implantation, long before any histological sign of malignization or possibility of tumour palpation (Novikov 1938; Gurwitsch et al. 1947). Then, if radical surgery was applied, CQ also disappeared a few days after surgery. However, if CQ persisted in the blood after surgery or reappeared after some time, a recurrence of the primary tumour or metastases was subsequently diagnosed.

Cancer induced by injections of carcinogens in mice was developing slower; however, CQ was also detected much earlier than the first clinical signs of the tumour (Pesochensky 1947):

- CQ by week 6 of the experiment
- Clinically detectable tumour after 6 months or later

Regular skin application of carcinogens in mice showed that CQ appeared in blood not only long before any histological sign of malignization, but at the still reversible stages of carcinogenesis (Pesochensky 1942):

- CQ at approx. week 6 of the experiment.
- Clinically detectable tumour after 5 to 6 months.

If the carcinogen applications were stopped just after CQ appeared (when papillomas already grew on the bald patches,

but the tumour was not palpated), some mice recovered. Their papillomas disappeared, bald patches were covered with fur and CQ disappeared again. Tumours developed further only in mice with persistent blood CQ. Moreover, tumours were not formed in the mice, in whose blood CQ did not appear (Pesochensky 1942).

CQ was also detected in healthy internals of animals with experimental cancer: liver and kidney (Salkind and Novikov 1938; Novikov 1938), brain (Salkind and Novikov 1938), spleen (Novikov 1938). Very special role of the spleen in CQ formation was shown in Sneshko (1955). The author showed that in case of the spleen extirpation CQ did not emerge in blood of cancer animals. Unpublished paper of Z.V. Maleeva (from A.G. Gurwitsch's archive) showed that CQ appeared also in the liver, and even earlier than in blood (in the first days after carcinogen injections).

Thus, in the above experimental animal models, CQ has proved not only a means of early cancer diagnostics, but also a marker of cancer progression or remission. Moreover, its presence in different healthy organs suggests its important role in the general metabolism in cancer.

23.3.2.2 Clinical Models

Compliant results were obtained in clinics. CQ was found only in blood of patients with malignant tumours and in those precancerous states that further led to malignization. For instance, CQ was observed in blood of women with myoma only in those cases that later developed into cancer. Importantly, CQ was detected in their blood before malignization could be diagnosed by any other method (Pesochensky 1942).

If the therapy was successful, CQ disappeared and blood MGR was completely restored in a few months, which reliably indicated the patients' recovery (Pesochensky 1942; Avchina 1950).

In case of persistent absence of blood MGR for longer periods, a recurrence of the primary tumour or metastases were usually stated later (though some patients relocated in course of the trial and their further history is unknown) (Gurwitsch et al. 1947; Pesochensky 1942; Avchina 1950). If the quencher was still found in blood 3 months after the radiotherapy/chemotherapy course, the tumour recurrence or metastases were diagnosed later (Gurwitsch et al. 1947); thus, it could be used as a predictor.

Also, consistent results on blood MGR disappearance and recovery (without CQ detection) had been obtained in animals (Klenitzky 1933b; Goldberg 1936) and in humans in cancer (Golysheva 1934; Chochia and Zhirmunskaya 1938; Pavlova 1935) earlier.

Publications on CQ presented a huge amount of clinical and experiment cancer data: for instance, (Pesochensky 1947) alone presented data on CQ detection in 527 patients and 220 mice (a follow-up control).

23.3.3 Antiquencher

In a number of works (Gurwitsch and Gurwitsch 1938, 1939a; Boukatina 1939; Zalkind and Lomovskaya 1941; Zalkind 1950; Sneshko 1955), the authors reported another specific substance appearing in the blood of a healthy animal injected with CQ, and compensating its effect (i.e., restoring blood MGR). Moreover, addition of this substance (which they called “antiquencher”) to any inductor previously quenched with CQ, also restored its MGR, both in vitro and in vivo. In vitro (as discussed above) adding CQ to any MGE inductor stopped its MGR, but further addition of the antiquencher restored MGR (see Table 23.7). In vivo administration of antiquencher to animals with cancer restored MGR from their blood in 20 to 30 min and sustained it for 6 to 7 days.

Antiquencher was found in the fresh serum and albumen-free fraction of blood, but its physicochemical properties were poorly investigated and contained contradictory results. For instance, Gurwitsch and Gurwitsch (1938) reported it to have no charge, while Sneshko (1955) stated that its charge is positive. However, the authors agreed that boiling deactivated it (see Table 23.7).

Altogether, the data available on this issue are not enough to draw any conclusions, and anyway its testing can only be performed after having definitely repeated the CQ data. However, in the event that this proves to be the case, the antiquencher may turn out to be a CQ-specific antibody fraction.

23.3.4 Alternative MGE-Related Cancer Diagnostics: Heinemann and Morelli

It should be noted that there were two other MGE-related methods of cancer diagnostics. The first one was proposed by M. Heinemann and R. Seyderhelm (Heinemann and Seyderhelm 1933, 1934), who observed the following effects:

Table 23.7 MGE from the rabbit blood, assessed by a standard yeast recipient. The rabbit blood: fresh, with added CQ, and with further added antiquencher

| MGE from fresh rabbit blood | Adding CQ | Adding antiquencher |
|-----------------------------|-----------|--|
| 60% | 9% | 52% |
| 53% | −5% | −5% (adding boiled antiquencher) 62% (adding native antiquencher) |

Reprinted from Gurwitsch and Gurwitsch (1938)

- Blood of healthy people induced MGE in yeast both in chemically isolated (quartz) and open cuvettes (corresponding to the standard MGE/MGR).
- Blood of people with noncancer diseases accompanied by appearance of UV-absorbers in blood never induced MGE: neither in open nor in isolated cuvettes (corresponding to the blood MGR being absorbed within it).
- Blood of cancer patients produced no effect in isolated cuvettes (corresponding to blood MGR being quenched), and when placed in open cuvettes, first damped mitoses in yeast, and then stimulated them (obviously by some volatile compounds).

The Heinemann-Seyderhelm effect was reproduced in other laboratories (Novikov 1937) and successfully used in practice in Clinics of Heiligen Geist Hospital in Frankfurt am Main. There Heinemann studied 1200 cases, including patients with cancer and noncancer diseases and healthy people, and demonstrated high efficiency of this method, but unfortunately, after migration to London in 1934, had to stop practicing it.

The other cancer diagnostics suggested by J. Morelli (1936) was much less convincing. The author used a strangely modified MGE-observation method with extremely long exposure (1 h!) of recipient (*Nadsonia fulvescens*) to blood which was highly diluted (1 drop of blood per 1 ml of distilled water). The author claimed that in such conditions no effect was induced by normal blood, while cancer blood stimulated its growth. Statistics was too small (66 people and 85 animals with and without cancer) and as far as we know there were no further attempts to reproduce this effect.

23.3.5 Cancer Quencher and Cancer Diagnostics: Resume

23.3.5.1 Scope of Work and Data

In the 1940s, the cancer diagnostics based on the cancer quencher detection was successfully tested in all leading cancer institutions and clinics of the USSR: Oncological Institute of Academy of Medical Sciences, X-raying and Radiology Hospital, the Second Moscow Medical Institute, Scientific Research Institute of Obstetrics and Gynecology, Army Medical Academy, Clinics of Kiev Medical Institute, Middle-Asia Oncological Institute and others. In most cases, CQ was tested when the new patients were admitted, long before the final diagnoses. Altogether, the authors describe thousands of cases, with a remarkably high concordance between the CQ data and clinical diagnoses: e.g., >95% in (Pesochensky 1942; Gurwitsch et al. 1947), and > 98% in (Nudolskaja 1945).

While preparing this chapter, we have come across an impressive 80-page document from the unpublished part of A.G. Gurwitsch's archive, entitled "Memorandum report." It is a summary of clinical data, including approx. 1200 clinical cases and CQ data, supposedly a copy of an application to the governmental authorities to reinstate R&D on cancer diagnostics, which we can date not earlier than 1951. Separate tables within the report are devoted to diagnosis of cancer patients (see fragment in Fig. 23.6), patients with innocent tumours and non-tumour diseases (see fragment in Fig. 23.7), healthy people, cases reporting discrepancies between primary clinical and CQ diagnoses resolved in favour of CQ data (Fig. 23.8), as well as false CQ diagnostics.

The obvious main drawback of the method was the use of biological detectors. First, it required strict observation of laborious procedures. Second, biological detectors had an obvious natural variability, and detection had to be repeated

several times. That's why this method was time-consuming, with a single specialist being able to treat only 4 to 6 cases in a day. Finally, and most importantly, the biological detectors were evaluated by humans, which is fundamentally subjective and can only be objectified by a double-blind method, analogous to medical research. However, the authors seem to have made every effort to overcome this problem and obtain objective data (see discussion on MGE in general in (Gurwitsch and Gurwitsch 1934, 1959; Gurwitsch 1945), and cancer quencher in (Gurwitsch et al. 1947)).

Systematic experimental studies of cancer quencher and its application to cancer diagnostics were presented in more than 15 dissertations (e.g., (Gamer 1938; Pesochensky 1939, 1942; Nagorianskaia 1945; Orlova 1949; Avchina 1950; Klenitsky 1940; Pavlova 1943; Yudeles 1944; Nudolskaja 1937a, 1945; Kushnirov 1947; Nechaeva 1948; Snesenko 1955)), several books and book chapters (Gurwitsch and

| Case No | Hospital | Patient | Age | Primary diagnosis | CQ +/- | Final diagnosis | Verification method | |
|---------|---------------------------------|---------|-------|---|-------------------------------|---|---|--------|
| 113 | Leningrad Institute of Oncology | ЕВМ | 48 | Рак желудка II Stomach c-r | + | Аденокарцинома Аденокарцинома | δ | |
| 114 | | ЕГВ | 56 | Рак мочевого пузыря в 1938 г. C-r (resected in 1938) | + | Солитарный медуллярный Solid medullary c-r | Biopsy | |
| 115 | | ЕВВ | 48 | Рак желудка II Stomach c-r | + | Рак мочевого пузыря то солитарный Glandular + diffuse c-r | | |
| 116 | | ЕФФ | 60 | Рак пищевода II Esophageal c-r | + | Рак желудка Stomach c-r | 4 | |
| 117 | | ЕЕЕ | 54 | Рак желудка " | + | Аденокарцинома Adenocarcinoma | 4 | |
| 118 | | ЕОК | 50 | " Stomach c-r | + | Аденокарцинома Adenocarcinoma | 4 | |
| 119 | | ЕНН | 51 | Рак желудка мочевого пузыря в 1938 г. Stomach c-r (resected in 1938) | + | Аденокарцинома Adenocarcinoma | 4 | |
| 120 | | ИИ.ЕВ | 54 | Рак желудка Stomach c-r | + | Аденокарцинома Adenocarcinoma | 4 | |
| 121 | | ИИ.ВУ | 41 | Рак желудка III Stomach c-r | + | Рак мочевого пузыря то солитарный Glandular + diffuse c-r | 4 | |
| 122 | | " | ИИ.ЕМ | 48 | Рак желудка IV Stomach c-r | + | Рак мочевого пузыря завис C-r + mts. | " |
| 123 | | " | УФН | 45 | " Stomach c-r | + | Рак мочевого пузыря то солитарный Glandular + diffuse c-r | " |
| 124 | | " | УТФ | 54 | " Stomach c-r | + | Аденокарцинома Adenocarcinoma | " |
| 125 | | " | ОМФ | 36 | Рак желудка Stomach c-r | + | Или не Adenocarcinoma | Clin. |
| 126 | | " | АЕУ | 64 | Stomach c-r | + | Идиопатический рак Colloidal c-r | Biopsy |
| 127 | | " | ИИ.ВЗ | 63 | Stomach c-r | + | Идиопатический Colloidal c-r | Clin. |
| 128 | " | ИИ.НН | 64 | Рак желудка с метастазами в сальник Stomach c-r + omental mts. | + | Идиопатический Colloidal c-r | Clin. | |
| 129 | " | ЕЕА | 48 | Рак желудка Stomach c-r | + | Рак мочевого пузыря завис то идиопатический Solid + colloidal c-r | Biopsy | |

Fig. 23.6 Excerpt from the "Memorandum report" comparing clinical data and blood test results for the presence of CQ: Cancer cases. (From the personal archive of A.G. Gurwitsch, with the permission of the heirs)

| Case No | Hospital | Patient | Sex | Age | Primary diagnosis | CQ +/- | Final diagnosis | Verification method |
|---------|--------------|---------|-----|-----|--|--------|-----------------|---------------------|
| 26 | ВМА 1 | ГВД | Ж | 33 | Гипоплазия матки, послеоперационная кастрация. | - | TOT Same | /КЛ/ Clin |
| 22 | " 1 | ИРП | " | 35 | Симп. преждев. климакса | - | TOT Same | /КЛ/ Clin |
| 28 | " 1 | МСП | " | 31 | тоже | - | TOT Same | /КЛ/ Clin |
| 29 | " 1 | СИГ | " | 26 | тоже | - | TOT Same | " |
| 30 | " 1 | ЮМА | " | 61 | Недостаток аорт. клапанов. | - | TOT Same | " |
| 31 | " 1 | СЛЕ | " | 18 | Недост.: и стеноз двухств. кл. Декомпенсация. | - | TOT Same | " |
| 32 | " 1 | ЦСВ | " | 43 | Язва желудка | - | TOT Same | /б/ Biopsy |
| 33 | ВИЭМ 2 | ЕАА | " | 42 | Сахарн. диабет | - | TOT Same | /КЛ/ Clin |
| 34 | ВМА 1 | РММ | " | 35 | тоже | - | TOT Same | " |
| 35 | " 1 | СИД | " | 39 | " " | - | " " | " |
| 36 | " 1 | ЕНС | " | 41 | " " | - | " " | " |
| 37 | ВИЭМ 2 | ЯЕА | " | 54 | Атр. цирроз печени | - | " " | " |
| 38 | " 2 | МСИ | " | 52 | " " | - | " " | " |
| 39 | 3 Онкр. ин-т | ИММК | Ж | 36 | Эндометрит | - | " " | " |
| 40 | 3 " " | СЕИ | " | 40 | Метроэндометрит | - | " " | /б/ Biopsy |
| 41 | 3 " " | МАР | " | 28 | " " | - | " " | " |

1 – Army Medical Academy
2 – All-Union Institute of Experimental Medicine
3 – Oncological institute

Fig. 23.7 Excerpt from the “Memorandum report” comparing clinical data and blood test results for the presence of CQ: Noncancerous diseases. (From the personal archive of A.G. Gurwitsch, with the permission of the heirs)

Gurwitsch 1937, 1945, 1959; Gurwitsch et al. 1947) and more than 100 articles.

Prominent Soviet oncologists like N.N. Petrov (1948), A.I. Serebrov (1948) and many other clinicians approved the method as valuable and made conclusions that the developed diagnostics was promising for early cancer screening and evaluation of the therapy effectiveness.

Active development of this cancer diagnostics was interrupted in the late 1940s mainly due to several historical reasons (see Chap. 2 and recent reviews (Volodyaev and Belousov 2015; Naumova et al. 2018, 2021)) in spite of highly positive conclusions from oncologists, and thousands of studied medical cases proving its high reliability, high prognostic value for early cancer screening and assessing the effectiveness of the medical care provided. In 1948,

the MGE research was pursued simultaneously with genetics and was interrupted, while in some cancer institutes and clinics, a few medicians kept working on the developed cancer diagnostics for about 5 years more.

23.3.5.2 Timetable and Conclusion

Here is a brief timetable of the reviewed works.

- End of 1922 – Discovery of mitogenetic radiation (MGR) from biological objects.
- 1926 – MGR from blood of healthy people and animals
- 1929 – Ceasing of blood MGR in cancer (biological detection)
- 1934 – Ceasing of blood MGR in cancer is confirmed with modified Geiger-Müller counters

| Case No | Hospital | Patient | Sex | Age | Primary diagnosis | CQ +/- | Final diagnosis | Verification method |
|---------|------------------------------|---------|--------|--|--|---|---|---------------------|
| 66. | " | В.М.И.ж | | | Гипертония и холецистит Hypertension, cholecystitis | + | Рак желчн.пузыря Gallbladder c-r | /с/ Wash |
| 67 | X-ray and Radiology Hospital | Б.Ф.Г. | | | Лимфогрануломатоз Hodgkin's disease | + | Миклобластич.лейкоз Mycloblastic leukemia | /б/ Biopsy |
| 68 | | К.Н.Н. | | | тбц легкого? Pulmonary tuberculosis | + | Рак легкого Lung c-r | /кл/ Clin |
| 69 | | Л.Е.И. | | | Рак печени Liver c-r | - | Кистозное перерожд Cystic degeneration | /с/ Wash |
| 70 | | Ш.Н.Е. | | | Опухоль верхн.чел. Upper jaw tumour | - | Киста верхн.челюс. Maxillary cyst | /б/ Biopsy |
| 71 | | К.И.И. | | | Бластома желудка? Stomach blastoma | - | Гипертроф.гастрит Hypertrophic gastritis | " / Biopsy |
| 72 | | Т.А.А. | | | Бластома легкого? Lung blastoma | - | ТБЦ легкого Pulmonary tuberculosis | |
| 73 | | " | К.В.Л. | | Рак желудка/скир/ Stomach c-r | - | Анацидный гастрит Anacid gastritis | |
| 74 | | " | К.А.И. | | Опухоль средостения? Mediastinal tumour | - | Лимфаденит тбц Tbc lymphadenitis | |
| 75 | | " | Ю.К.В. | | Бластома пищевода Esophageal blastoma | - | пищевода Tbc lymphadenitis (esophagus) | |
| 76 | | " | В.А.М. | | "- желудка Stomach blastoma | - | Анацидн.гастрит Anacid gastritis | |
| 77 | - | И.Г.И. | | Опух.толстой кишки Colon tumour | - | Холецистогепатит Cholecystohepatitis | | |
| 78 | " | М.И.Ф. | | Бластома пр.легкого Lung blastoma (right) | - | Бронхоэтазия Bronchoethasia | | |
| 79 | " | В.Л.З. | | Бластома легкого Lung blastoma | - | тбц легкого Pulmonary tuberculosis | | |

Fig. 23.8 Excerpt from the "Memorandum report" comparing clinical data and blood test results for the presence of CQ: Discrepancies in the primary diagnoses resolved in favour of CQ diagnoses. (From the personal archive of A.G. Gurwitsch, with the permission of the heirs)

- 1930s – Active studies of blood MGR in various pathological and physiological states, including MGR spectral analysis
- 1937 – Discovery of "cancer quencher," the first blood tumour marker
- 1938–1948 – Extraction of cancer quencher and study of its physical and chemical properties, development of cancer diagnostics and its application in clinics
- 1948 – Persecution of biological research in the USSR (the famous August session of VASKhNIL)
- 1948–1954 – very few publications on cancer diagnostics.

Further research on ultraweak chemiluminescence of blood in visible, near-ultraviolet and near-infrared ranges have shown its practical value for medical diagnostics and

basic science (see (Serkiz et al. 1984; Sidorik et al. 1989; Izmailov and Vladimirov 2017; Vladimirov and Proskurnina 2009; Vladimirov and Archakov 1972)). Academician Yu.A. Vladimirov, internationally famous for his fundamental works on ultraweak biological chemiluminescence (see Chaps. 3, 8, 9, 10, 11, 12 and 14 of this book), drew an analogy between the data on cancer quencher and the increase in plasma antioxidant activity in cancer shown by A.E. Zakaryan and B.N. Tarusov (Zakarian et al. 1970; Zakarian and Tarusov 1965; Zakarian and Tarusov 1967) in his book (Vladimirov and Archakov 1972). He also noted that the properties of the cancer quencher resemble a lipoprotein with antioxidant properties studied by the authors.

The early cancer diagnostics was the most developed practical application of mitogenetic research. Unfortunately,

almost all results based on the detection of cancer quencher were published only in Russian and remained unknown abroad. In the USSR, the access to them was forbidden in libraries for decades. We believe it important to draw attention to these works, which have been almost completely forgotten and unknown to the scientific readership of our times. They have not been digitized, and practically not available in the Internet. Analogous to MGE in general, these large-scale experimental and clinical data have been neither proved nor disproved on a modern level. The claimed methodology “worked” effectively, and if the scientific explanation for this turns out to be quite different from that of the earlier authors, this does not detract from the practical value and relevance of diagnostics with such high parameters. Verification of the claimed cancer diagnostics is promising for the early cancer screening, estimation of efficacy of medical treatment and prognosis of metastases and tumour recurrence.

Acknowledgements We sincerely thank the heirs of Alexander Gurwitsch and his late grandson, Lev Belousov, for unlimited access to their personal library, containing probably the most comprehensive collection of papers on MGE.

References

- Acqua C (1935) Sulla eventuale emissione di raggi mitogenetici, capaci d'impressionare la lastra fotografica durante lo sviluppo delle uova di *Bombyx mori*. *Boll R staz sper Gels. e Bachicolt* 14:159–164
- Audubert R (1938) Die Emission von Strahlung bei chemischen Reaktionen. *Angewandte Chemie* 51 (11):153–163. doi:<https://doi.org/10.1002/ange.19380511102>
- Avchina EE (1950) On the prognostic value of the reaction of quenching of the mitogenetic radiation of blood in the treatment of uterine cancer: Cand. Med. Sci. dissertation (in Russian). Leningrad
- Biddau I (1932) Studio sulle radiazioni mitogenetiche del sangue del bambino. Nota 1: Ricerche sul neonato e lattante con speciale riguardo al potere radiante del sangue materno. *Radiobiologia* 1 (2):3–18
- Billig ES (1931) Effect of quinine on mitogenetic radiation of blood (In Russian). *Archive of Biological Sciences* 31 (6):540–543
- Blacher LJ, Bromley NW (1930) Resorptionsprozesse als Quelle der Formbildung. II. Mitogenetische Ausstrahlungen bei der Regeneration des Kaulquappenschwanzes. *Wilhelm Roux' Archiv für Entwicklungsmechanik der Organismen* 122 (1):79–87. doi:<https://doi.org/10.1007/bf00576966>
- Blacher LJ, Irichimowitsch AI, Liosner LD, Woronzowa MA (1932) Resorptionsprozesse als Quelle der Formbildung. IX Einfluss der mitogenetischen Strahlen auf die Geschwindigkeit der Regeneration. *Roux' Archiv* 127:339–352
- Blacher LJ, Irichimowitsch AI, Liosner LD, Woronzowa MA (1933) Resorptionsprozesse als Quelle der Formbildung. X. Die mitogenetische Strahlung des Regenerats und des Blutes der Kaulquappen während der Regeneration. *Wilhelm Roux' Archiv für Entwicklungsmechanik der Organismen* 127 (1):353–363. doi:<https://doi.org/10.1007/bf01390723>
- Blyakher LY, Liozner LD, Chmutova AP (1935) Studies on mitogenetic radiation of blood.V. Mitogenetic radiation of blood in cancer (In Russian). In: *Proceedings of the State Research Institute of Morphogenesis*, vol 3. Moscow, pp 125–137
- Blyakher LY, Vorontsova MA, Irikhimovich AI, Liozner LD (1934a) Resorption processes as a source of morphogenesis. X. Mitogenetic radiation of regenerate and blood tadpoles of *Pelobates fuscus* during regeneration (In Russian). In: *Proceedings of the State Research Institute of Experimental Morphogenesis*, vol 1. Moscow-Leningrad, pp 85–95
- Blyakher LY, Vorontsova MA, Liozner LD (1934b) Spectral analysis of the mitogenetic radiation of axolotl blood during metamorphosis (In Russian). In: *Proceedings of the State Research Institute of Experimental Morphogenesis* vol 1. Moscow-Leningrad, pp 127–132
- Bogdanovich V, Lazaris Y (1935) On analysis of disappearance of mitogenetic radiation in the blood of animals in cancer (In Ukrainian). *Experimental medicine* 10:32–44
- Boukatina AA (1939) Effets d'injection de «l'extincteur» du sang cancéreux dans l'organisme normal. *Bulletin of experimental biology and medicine* 7 (5):402–403
- Brains SN (1934) Analysis of mitogenetic excitation of the nerve (In Russian). *Archive of Biological Sciences, Ser B* 35 (1):65–72
- Brains SN (1936) Mitogenetic radiation of the rabbit central nervous system (In Russian). *Byull Eksp Biol Med* 2 (1):12–13
- Brains SN, Galperin SI (1934) Mitogenetic radiation of the cat's sympathetic nerve (In Russian). *Physiological Journal of USSR* 17 (1):81–83
- Brainess S (1932a) Die mitogenetische Strahlung als Methode zum Nachweis und Analyse der Ermüdungserscheinungen. *Arbeitsphysiologie* 6 (1):90–104. doi:<https://doi.org/10.1007/bf02009856>
- Brainess SN (1931) Problem of variability of mitogenetic radiation of blood depending on physiological state of organism (In Russian). *Archive of Biological Sciences* 31 (5):432–437
- Brainess SN (1932b) On application of mitogenetic method for study of fatigue phenomena (In Russian). *Archive of Biological Sciences* 32 (5–6):513–516
- Brainess SN (1934) Problems of fatigue and activity, and mitogenetic radiation (In Russian). *Archive of Biological Sciences Ser B* 35 (1):325–340
- Brainess SN (1936) Analysis of mitogenetic radiation of blood in psychotic diseases as basis for therapy (In Russian). *Archive of Biological Sciences* 40 (2):11–31
- Brunetti R, Maxia C (1930) Sulla fotografia e la eccitazione delle radiazioni del Gurwitsch. *Atti della Società fra i Cultori delle Scienze Mediche e Naturali in Cagliari* 2:21–28
- Chernevskaya NA (1940a) Mitogenetic radiation as method of early diagnostic of cancer (In Russian). In: *Roentgenology and oncology*, vol 1. Voronezh, pp 51–66
- Chernevskaya NA (1940b) Study of mitogenetic radiation as method of early diagnostic of cancer (In Russian). *Khirurgia [Surgery]* 1:89–91
- Chmutova AP (1938) Mitogenetic radiation of blood in Addison-Biermer anemia (In Russian). *Clinical Medicine* 16 (8):1010–1014
- Chmutova AP (1940) Mitogenetic radiation of blood in Addison-Biermer anemia (In Russian). In: *Modern problems of hematology and blood transfusion [Sovremennyye problemy gematologii i perelivaniya krovi]*, vol 17–18. Moscow-Leningrad, pp 116–122
- Chmutova AP (1946) Mitogenetic radiation of blood in diabetes (In Russian). *Arch Path* 8 (1–2):34–39
- Chochia KN, Zhirmunskaya KM (1938) Mitogenetic radiation of blood in radical therapy of malignant tumours (in Russian). *Bulletin of Roentgenology and Radiology [Vestnik rentgenologii i radiologii]* 19:138–145
- Engel P, Morelli JE (1936) Einfluss von Hormonen auf die mitogenetische Strahlung. *Klinische Wochenschrift* 15 (20):716–716. doi:<https://doi.org/10.1007/bf01779454>

- Eremeev VF (1961) Analysis of the mechanism governing mitogenetic radiation of the liver in mice with implanted cancers. *Bull Exp Biol Med* 51(4):486–489. doi:<https://doi.org/10.1007/BF00779540>
- Ferguson AJ (1932) Morphological changes in yeasts induced by biological radiation, Thesis, Cornell University.
- Frank G, Popoff M (1929a) Die mitogenetische Strahlung des Muskels und ihre Verwertung zur Analyse der Muskelkontraktion. *Pflüger's Archiv für die gesamte Physiologie des Menschen und der Tiere* 223 (3):301–328. doi:<https://doi.org/10.1007/bf01794089>
- Frank G, Popoff M (1929b) Le rayonnement mitogénétique du muscle en contraction. *Compte Rendu de l'Academie des Sciences* 188: 1010
- Frank G, Rodionow S (1931) Über den physikalischen Nachweis mitogenetischer Strahlung und die Intensität der Muskelstrahlung. *Die Naturwissenschaften* 19 (30):659–659. doi:<https://doi.org/10.1007/BF01516035>
- Frank G, Rodionow S (1932) Physikalische Untersuchung mitogenetischer Strahlung der Muskeln und einiger Oxydationsmodelle. *Biochemische Zeitschrift* 249 (4/6):323–343
- Gamer MM (1938) Diagnostic value of the mitogenetic quenching reaction in malignant neoplasms of the female genital area: Dissertation (in Russian). Leningrad
- Gesenius H (1929) Über Stoffwechselwirkungen mitogenetischer Strahlen. *Biochemische Zeitschrift* 212 (1–3):240
- Gesenius H (1930) Über die Gurwitsch-Strahlung menschlichen Blutes und ihre Bedeutung für die Carcinom-Diagnostik. *Biochemische Zeitschrift* 226 (4–6):257–272
- Gesenius H (1932) Blutstrahlung und Carcinomdiagnostik. *Radiobiologia* 1 (2):33–36
- Gesenius H (1934) Klinische Erfahrungen mit der Blutfemwirkung. *Archiv für Gynäkologie* 155 (2):500–516. doi:<https://doi.org/10.1007/bf01765589>
- Goldberg GI (1936) Mitogenetic radiation of blood after transplantation and surgical extirpation of malignant tumours in mice (In Russian). *Archive of pathological anatomy and pathological physiology [Arkhiv patologicheskoi anatomii i patologicheskoi fiziologii]* 2 (3):13–27
- Golshmid KL (1934) Mitogenetic radiation of blood in pellagra (In Russian). In: *Collected works of Perm Medical Institute "Pellagra"*. Perm Medical Institute, Perm, pp. 105–137
- Golysheva KP (1933) Mitogenetic spectrum of streaming blood (In Russian). *Archive of Biological Sciences* 33 (1–2):107–115
- Golysheva KP (1934) Analysis of the inhibition of blood radiation in carcinomatous patients (In Russian). *Archive of Biological Sciences, Ser B* 35 (1):113–125
- Gourvitch AG (1935) Le rayonnement mitogénétique. *Annales de l'Institute Pasteur* 54:259–267
- Gurvich AA (1966) Mitogenetic radiation spectra of muscles as an indicator of the dynamic molecular organization of the sarcoplasm. *Bulletin of experimental biology and medicine* 62 (2):894–896. doi:<https://doi.org/10.1007/bf00810720>
- Gurvich AA (1976) "Molecular organization" of the vagus nerves and cardiac muscle in different functional states (In Russian). *Biulleten' eksperimental'noi biologii i meditsiny* 81 (6):689–691
- Gurvich AA, Eremeev VF (1966) Mitogenetic irradiation of animal cardiac muscle (In Russian). *Biulleten' eksperimental'noi biologii i meditsiny* 61 (6):56–58
- Gurvich AA, Eremeev VF, Sobieva ZI (1966) Mitogenetic irradiation of partially de-afferented cardiac muscle (In Russian). *Biulleten' eksperimental'noi biologii i meditsiny* 62 (7):55–59
- Gurwitsch A (1933a) Die mitogenetische Strahlung der optischen Bahn bei adäquater Erregung. *Pflüger's Archiv für die gesamte Physiologie des Menschen und der Tiere* 231 (1):255–264. doi:<https://doi.org/10.1007/bf01754549>
- Gurwitsch A (1933b) Die mitogenetische Strahlung des markhaltigen Nerven. *Pflüger's Archiv für die gesamte Physiologie des Menschen und der Tiere* 231 (1):234–237. doi:<https://doi.org/10.1007/bf01754546>
- Gurwitsch A (1933c) Mitogenetic radiation of nerve. *Nature* 131 (3321): 912–913. doi:<https://doi.org/10.1038/131912a0>
- Gurwitsch A, Gurwitsch LD (1939a) Further study of quencher in cancer blood and anti-quencher (In Russian). *Archive of Biological Sciences* 56 (3):93–100
- Gurwitsch A, Gurwitsch LD, Sliussarew AA (1939) Deutung der mitogenetischen Strahlung als „sensibilisierte Fluoreszenz“ (Eine experimentelle Bestätigung der Theorie der mitogenetischen Strahlung von Frankenburger). *Acta physicochimica URSS* 10: 719–724
- Gurwitsch AA (1934a) L'excitation mitogénétique du système nerveux central. *Ann de Physiol et Physicochem Biol* 10 (5):1153–1165
- Gurwitsch AA (1934b) L'excitation mitogénétique du système nerveux pendant l'éclairage monochromatique de l'œil. *Annales de Physiologie et de Physicochimie biologique* 10 (5):1166–1169
- Gurwitsch AA (1938) Les phénomènes mitogénétiques de l'écorce cérébrale. *Annales de Physiologie et de Physicochimie biologique* 14 (2):182–199
- Gurwitsch AA (1962) Unbalanced molecular orderliness of the substrate of living systems and its significance for the regulation of certain metabolic processes. (A.G. Gurwitsch's "physiological" theory of protoplasm and its reference to the analysis of some processes in muscle). *Enzymologia* 24:237–251
- Gurwitsch AA (1968) Problema mitogeneticheskogo izlucheniya kak aspekt molekuliarnoj biologii (The problem of mitogenetic emission as an aspect of molecular biology). *Meditzina, Leningrad*
- Gurwitsch AA (1988) A Historical Review of the Problem of Mitogenetic Radiation. *Experientia* 44 (7):545–550. doi:<https://doi.org/10.1007/Bf01953301>
- Gurwitsch AA, Eremeev VF, Karabchievsky YA (1974) Energeticheskije osnovy mitogeneticheskogo izlucheniya i ego registratsiya na fotoelektronnikh umozhiteliakh (Energy bases of mitogenetic radiation and its registration on photomultipliers). *Meditzina, Moscow*
- Gurwitsch AG (1937) Some problems of mitogenesis (in Russian). *Archive of Biological Sciences* 46 (3):3–10
- Gurwitsch AG (1945) Physical and chemical bases of mitogenetic radiation (in Russian). *Bulletin of the USSR Academy of Sciences: Physics* 9 (4–5):335–340
- Gurwitsch AG, Gurwitsch LD (1926) Die Produktion mitogener Stoffe im erwachsenen tierischen Organismus 13 Mitteilung über mitogenetische Strahlung und Induktion. *Wilhelm Roux' Archiv für Entwicklungsmechanik der Organismen* 107 (4):829–832. doi:<https://doi.org/10.1007/BF02079917>
- Gurwitsch AG, Gurwitsch LD (1928) Über ultraviolette Chemolumineszenz der Zellen im Zusammenhang mit dem Problem des Carcinoms. *Biochemische Zeitschrift* 196 (4.–6.):257–275
- Gurwitsch AG, Gurwitsch LD (1932) Die mitogenetische Strahlung, vol 25. Monographien aus dem Gesamtgebiet der Physiologie der Pflanzen und der Tiere. Springer-Verlag Berlin Heidelberg, Berlin. doi:<https://doi.org/10.1007/978-3-662-26146-0>
- Gurwitsch AG, Gurwitsch LD (1934) Mitogeneticheskije izlucheniya [Mitogenetic radiation] (in Russian). VIEM publishing house, Leningrad
- Gurwitsch AG, Gurwitsch LD (1937) Mitogeneticheskij analiz biologii rakovoj kletki (Mitogenetic analysis of cancer cell biology). VIEM publishing house, Moscow
- Gurwitsch AG, Gurwitsch LD (1938) Quencher in cancer patients' blood, its value for diagnostic value and anti-quencher (in Russian). *Archive of Biological Sciences* 51 (3):40–44
- Gurwitsch AG, Gurwitsch LD (1939b) Ultra-Violet Chemi-Luminescence. *Nature* 143 (3633):1022–1023. doi:<https://doi.org/10.1038/1431022b0>

- Gurwitsch AG, Gurwitsch LD (1945) Mitogeneticheskoje izluchenije: fizikokhimicheskiye osnovy i prilozheniya v biologii i meditsine (Mitogenetic radiation: physical and chemical bases and applications in biology and medicine). Medgiz, Moscow
- Gurwitsch AG, Gurwitsch LD (1948) Vvedeniye v ucheniye o mitogeneze (An introduction to the teaching of mitogenesis). USSR Academy of Medical Sciences Publishing House, Moscow
- Gurwitsch AG, Gurwitsch LD (1959) Die mitogenetische Strahlung (Mitogenetic radiation). VEB Gustav Fischer Verlag, Jena
- Gurwitsch AG, Gurwitsch LD (1999) Twenty Years of Mitogenetic Radiation: Emergence, Development, and Perspectives. 21st Century Science and Technology Magazin 12 (3):41–53 (translation from Uspekhi Sovremennoi Biologii (Advances in Contemporary Biology), 1943, Vol. 16, No. 3, pages 305–334)
- Gurwitsch AG, Gurwitsch LD, Zalkind SY, Pesochensky BS (1947) Ucheniye o rakovom tushitele: Teorija i klinika (The teaching of the cancer quencher: Theory and clinics). USSR Academy of Medical Sciences Press, Moscow
- Gurwitsch L, Anikin A (1928) Das Cornealepithel als Detektor und Sender mitogenetischer Strahlung. 25 Mitteilung über mitogenetische Strahlung und Induktion. Wilhelm Roux' Arch Entwickl Mech Org 113 (4):731–739. doi:<https://doi.org/10.1007/bf02252023>
- Gurwitsch L, Gurwitsch A (1929) Die mitogenetische Strahlung des Carcinoms – II. Mitteilung. Zeitschrift für Krebsforschung 29 (1–2): 220–233. doi:<https://doi.org/10.1007/bf01634488>
- Gurwitsch LD (1931) Die mitogenetische Spektralanalyse. II. Mitteilung: Die mitogenetischen Spektren des Carcinoms und des Cornealepithels. Biochemische Zeitschrift 236 (4–6):425–431
- Gurwitsch LD, Salkind S (1929) Das mitogenetische Verhalten des Blutes Carcinomatoser. Biochemische Zeitschrift 211 (1–3): 362–372
- Gurwitsch LD, Zalkind SY Report at the 2nd International Anti-Cancer Congress. In: 2nd International Cancer Congress, Brussels, 1936.
- Heinemann M (1932) Cytagenin und „mitogenetische Strahlung“ des Blutes. Klinische Wochenschrift 11 (33):1375–1378. doi:<https://doi.org/10.1007/bf01815913>
- Heinemann M, Seyderhelm R (1933) Weitere Untersuchungen Über die Mitogenetische Strahlung des Blutes Unter Besonderer Berücksichtigung der „Strahlungen“ des Blutes von Carcinomkranken. Klinische Wochenschrift 12 (25):990–990. doi:<https://doi.org/10.1007/bf01876282>
- Heinemann M, Seyderhelm R (1934) Mitogenetische Strahlung des Blutes und „Strahlungen“ des Blutes Carzinomkranker. Archive of Biological Sciences Ser B 35 (1):106–112
- Hollaender A (1936) The problem of mitogenetic rays. In: Duggar B (ed) Biological effects of radiation, vol 2. 1 edn. McGraw-Hill Book Company, Inc., NY, London, pp 919–958
- Hollaender A, Claus WD (1935) Some Phases of the Mitogenetic Ray Phenomenon. Journal of Optical Society of America 25:270–286
- Izmailov DY, Vladimirov YA (2017) Chemiluminescence as a method of study of free radicals (Chapter 2). In: Sources and targets of free radicals in human blood. MAX Press, Moscow,
- Karpas AM, Lanschina MN (1932) Über den Verlust des mitogenetischen Strahlungsvermögens des Blutes: a) bei längerem Stehen in vitro, b) nach der Bestrahlung mit ultraviolettem Licht. Biochem Zeitsch 253:313–317
- Kisliak-Statkewitsch M (1929) Die mitogenetische Strahlung des Carcinoms – I. Mitteilung. Zeitschrift für Krebsforschung 29 (3): 214–219. doi:<https://doi.org/10.1007/bf01634487>
- Klenitsky JS (1934a) Effect of childbirth on mitogenetic radiation of blood. Journal of obstetrics and gynecopathies 45 (5):322–325
- Klenitsky YS (1933) Mitogenetic radiation of cervical cancer (In Russian). Archive of Biological Sciences 33 (1–2):115–120
- Klenitsky YS (1934b) Effect of the surgical tumour removal on the mitogenetic radiation of blood (In Russian). Archive of Biological Sciences Ser B 35 (1):213–218
- Klenitsky YS (1940) Experimental cancer of uterus: Dissertation (in Russian). All-Union Institute of Experimental Medicine
- Klenitzky J (1932) Die mitogenetische Strahlung der weißen Blutelemente. Biochemische Zeitschrift 252 (1–3):126–131
- Klenitzky J (1933a) Die mitogenetische Strahlung des Collumcarcinoms. Zeitschrift für Krebsforschung 39 (1): 60–65. doi:<https://doi.org/10.1007/bf01674140>
- Klenitzky JS (1933b) Einfluss der Karzinomextirpation auf das mitogenetische Austrahlungsvermögen des Blutes. Radiobiologia 1 (4)
- Krasovskaya EN, Weller NS (1936) On the inconstancy of mitogenetic radiation of blood (In Russian). Archive of Biological Sciences 41 (2):143–151
- Kushnirov PV (1947) On the value of the mitogenetic radiation quenching reaction for the early diagnosis of cancer: Cand. Med. Sci. Dissertation (in Russian). Odessa
- Latmanisowa LW (1933) Die mitogenetische Sekundärstrahlung des Nerven. Pflüger's Archiv für die gesamte Physiologie des Menschen und der Tiere 231 (1):265–279. doi:<https://doi.org/10.1007/bf01754550>
- Lazurkina NN (1982) Molecular organization of the sarcoplasm of skeletal muscles in different functional states (In Russian). Biulleten' eksperimental'noi biologii i meditsiny 94 (11):43–45
- Lazurkina NN (1987) Sympathetic influences on skeletal muscle studied by recording mitogenetic radiation. Bulletin of experimental biology and medicine 103 (2):196–197. doi:<https://doi.org/10.1007/bf00840330>
- Levina RI (1938) Observation of restoration of disappeared mitogenetic radiation of blood of cancerous mice (In Russian). Medical practice [Vrachebnoye delo] 7:507–510
- Lintvareva NI (1940a) Detection of pregnancy dynamics by mitogenetic method (In Russian). Akusherstvo i ginekologija [Obstetrics and Gynecology] (3–4):10–12
- Lintvareva NI (1940b) Duration of mitogenetic activity of blood of pregnant women (In Russian). Akusherstvo i ginekologija [Obstetrics and Gynecology] 3–4:12–15
- Lotsman LA (1940) Mitogenetic radiation of blood and cerebrospinal fluid of patients with chronic epidemic encephalitis (In Russian). Archive of Biological Sciences 59 (3):41–44
- Lotsman LA (1941) Mitogenetic radiation of cerebrospinal fluid in diseases of the nervous system (In Russian). Zhurnal nevropatologii i psikiatrii [Journal of neuropathology and psychiatry] 10 (2): 81–84
- Mai H (1934) Die Bedeutung der mitogenetischen Strahlung für die Kinderheilkunde. Archive of biological sciences, 35 (1):237–238
- Maleeva ZV, Nechaeva ID (1951) Cancer quencher as diagnostic method (In Russian). In: Rann'aya diagnostika raka [Early cancer diagnostics]. Moscow, pp 11–16
- Marconi E (1931) Ricerche sulle radiazioni mitogenetiche del sangue umano col *Micrococcus prodigiosus* come detectore. Pathologica 23 (481)
- Markovsky Y (1931) On mitogenetic radiation of blood of tuberculous patients (in Russian). Clinical Medicine 9 (11–12):444–449
- Maxia C (1940) Quadro sinottico delle ricerche sull "effetto Gurwitsch". Scritti biologici 15:186–220
- Morelli JE (1936) Mitogenetische Strahlung und Krebsproblem. Acta Cancrol (2):93–106
- Nagorianskaia VP (1938) Mitogenetic radiation of blood of patients with malignant neoplasms (In Russian). In: Voprosy klinicheskoy i eksperimental'noy onkologii [Problems of clinical and experimental oncology], vol 1. Medgiz, pp 38–63

- Nagorianskaia VP (1945) Mitogenetic radiation of blood of patients with malignant neoplasms: Diss. Cand.Med.Sc. (In Russian). Moscow
- Naumova EV, Belousov LV, Vladimirov YA, Tuchin VV, Volodyaev IV (2021) Methods of studying ultraweak photon emission from biological objects: I. History, types and properties, fundamental and application significance. *Biophysics* 66 (5):764–778. doi:<https://doi.org/10.1134/S0006350921050158>
- Naumova EV, Naumova AE, Isaev DA, Volodyaev IV (2018) Historical review of early researches on mitogenetic radiation: from discovery to cancer diagnostics. *Journal of Biomedical Photonics & Engineering* 4 (4):040201. doi:<https://doi.org/10.18287/JBPE18.04.040201>
- Naumova EV, Vladimirov YA, Tuchin VV, Namiot VA, Volodyaev IV (2022) Methods of studying ultraweak photon emission from biological objects: III. Physical methods. *Biophysics* 67 (1):27–58
- Naville A (1929) Les rayons mitogénétiques. Exposé de quelques résultats. *Revue Suisse de Zoologie* 36:213–215
- Naville A (1937) Recherches statistiques sur le caryoquémèse sous l'influence de divers facteurs. *Arch biol* 48:1–78
- Nechaeva ID (1948) The quenching reaction in the blood of patients with precancerous diseases of the mammary gland: Dissertation (in Russian). Leningrad
- Nechaeva ID (1952) Quencher in blood of patients with precancerous diseases of mammary gland (In Russian). In: *Voprosy onkologii [Questions of oncology]*, vol 5. AMN SSSR [Publishing House of Academy of Medical Sciences of the USSR], Moscow, pp 31–40
- Nechaeva ID (1953) Quencher in blood in stomach diseases (In Russian). In: *Voprosy onkologii [Questions of oncology]*, vol 6. AMN SSSR [Publishing House of Academy of Medical Sciences of the USSR], Moscow, pp 124–132
- Nikulina D, Terentyev A, Galimzyanov K, Jurišić V (2015) Fifty years of discovery of alpha-fetoprotein as the first tumor marker. *Srpski arhiv za celokupno lekarstvo* 143 (1–2):100–104. doi:<https://doi.org/10.2298/sarh1502100n>
- Novikov MB (1937) On depressing action of cancer blood on the yeast budding (Heinemann-Seyderhelm effect). *Bulletin of experimental biology and medicine* 4 (3):281–283
- Novikov MB (1938) The effect of extirpation of a cancer tumour on the presence of mitogenetic radiation quencher in blood and organs of white mice (In Russian). *Archive of Biological Sciences* 51 (3): 56–63
- Nudolskaja OE (1936) Mitogenetic radiation of blood and its significance in the early diagnosis of uterine cancer (In Russian). *Zhurnal akusherstva i ginekologii [Journal of Obstetrics and Gynecology]* 5: 551–568
- Nudolskaja OE (1937a) Diagnostic significance of mitogenetic radiation for cancer and pre-cancerous states of the female genitalia: Cand. Med. Sci. Dissertation (in Russian). 2nd Obstetrics and Gynecology Clinics of 2nd Moscow State Medical Institute, Moscow
- Nudolskaja OE (1937b) Die mitogenetische Ausstrahlung des Blutes und ihre Bedeutung in der frühen Diagnostik des Gebärmutterkrebses. *Archiv für Gynäkologie* 163 (1):30–49. doi:<https://doi.org/10.1007/bf01714831>
- Nudolskaja OE (1945) Precancer state of neck and body of uterus: Dr. Med. Sci. Dissertation (in Russian). 2nd Obstetrics and Gynecology Clinics of 2nd Moscow State Medical Institute, Moscow
- Orlova AI (1949) Reaction of quenching mitogenetic radiation in cancer and precancerous states: Diss. Cand. Med. Sc. (in Russian). Moscow
- Pavlova EV (1935) Early diagnosis of malignant tumours by mitogenetic radiation of blood (In Russian). *Za sotsialisticheskoye zdravookhraneniye Uzbekistana [To socialist health care of Uzbekistan]* 1:53–56
- Pavlova EV (1943) Early diagnosis of malignant tumours with use of mitogenetic radiation: Cand. Med. Sci. dissertation (in Russian).
- Pesochensky BS (1939) Experimental and clinical data for the evaluation of blood mitogenetic quenching reactions in malignant neoplasms of the female genitalia: Cand. Med. Sci. Dissertation (in Russian). Leningrad
- Pesochensky BS (1942) The phenomenon of the mitogenetic radiation quenching in blood in cancer and “precancer”: Dr.Med. Sci. Dissertation (in Russian). Leningrad Oncological Institute, Leningrad
- Pesochensky BS (1947) Quenching of mitogenetic radiation of blood in cancer and precancerous diseases. In: Gurvitsch AG (ed) *Collected volume on mitogenesis and theory of biological field*. Pub.house of the USSR Academy of Medical Sciences, Moscow, pp 102–114
- Pesochensky BS (1950) The role of quencher of mitogenetic radiation in malignization process (In Russian). In: *Voprosy onkologii [Questions of oncology]*, vol 2. Publishing House of Academy of Medical Sciences of the USSR, Moscow, pp 501–506
- Petrov NN (1948) Mitogenetic radiation and quencher (In Russian). In: *Malignant tumours [Zlokachestvenniye opukholi]*, vol 1, part 2 (practical). Medgiz, Leningrad, pp 17–18
- Ponomareva YN (1939) Stimulation of mitoses in surviving tissues by physical methods (In Russian). *Archive of Biological Sciences* 55 (2):108–118
- Ponomareva YN (1934) Direct impact of mitogenetic radiation on the course of the mitosis (reaction of corneal epithelium) (In Russian). *Archive of Biological Sciences, Ser B* 35 (1):239–248
- Ponomareva YN (1936) Mitogenetic and thermal influence on the mitotic rate of survival cells (In Russian). *Bulletin of experimental biology and medicine* 2 (1):16–18
- Ponomareva YN (1931) Die mitogenetische Spektralanalyse. III. Mitteilung: Das detaillierte glykolytische Spektrum. *Biochemische Zeitschrift* 239:424
- Ponomareva YN (1947) Inhibition of mitoses by treating the cells with quenchers and extinguishers (in Russian). In: Gurvitsch AG (ed) *Collected volume on mitogenesis and theory of biological field*. Pub.house of the USSR Academy of Medical Sciences, Moscow, pp 131–136
- Potozky A, Salkind S, Zoglina I (1930) Die mitogenetische Strahlung des Blutes und der Gewebe von Wirbellosen. *Biochemische Zeitschrift* 217 (1–3):176–185
- Potozky A, Zoglina I (1929) Untersuchungen über die mitogenetische Strahlung des Blutes. *Bioch Ztschr* 211 (4–6):352–361
- Protti G (1930) I Raggi mitogenetici nell' emoinnesto e prime loro fotografie. In: *Comunicazione alla Seduta scientifica dell' Ospedale Civile di Venezia, XVIII, Stamperia Carlo Rertotti, Venezia*
- Protti G (1932) Effetti fotografici intraorganici. *Radiobiologia* 1 (2): 61–65
- Protti C (1934) Das Verhalten einiger Tumoren gegenüber dem Saccharomyces cerevisiae. *Archive of Biological Sciences, Ser. B* 35 (1): 255–268
- Rahn O (1936) Invisible radiations of organisms, vol 9. *Protoplasma-Monographien*. Gebrüder Bornträger, Berlin
- Rajewsky B (1931) Zur Frage des physikalischen Nachweises der Gurvitsch-Strahlung. In: Dessauer F (ed) *Zehn Jahre Forschung auf dem physikalisch-medizinischen Grenzgebiet*. Georg Thieme Verlag, Leipzig, pp 244–257
- Reiter T, Gabor D (1928) Zellteilung und Strahlung. Sonderheft der *Wissenschaftlichen Veröffentlichungen aus dem Siemens-Konzern*. Springer-Verlag, Berlin. doi:<https://doi.org/10.1007/978-3-642-50832-5>
- Ryazanskaya BS (1936) Secondary mitogenetic radiation of healthy and cancer patients (In Russian). *Bulletin of Roentgenology and Radiology [Vestnik rentgmologii i radiologii]* 17:536–542
- Rylova M (1935) Mitogenetic radiation of blood components (In Russian). *Archive of Biological Sciences* 37 (1):311–321
- Salkind S (1937) Der gegenwärtige Stand des mitogenetischen Problems. *Protoplasma* 28 (1):435–468. doi:<https://doi.org/10.1007/bf01625014>

- Salkind S, Ponomarewa J (1934) Der unmittelbare Einfluß der mitogenetischen Strahlen auf den Verlauf der Zellteilung. *Radiobiologia I* (4):11–27
- Salkind S, Potozky A, Zoglina I (1930) Die mitogenetische Beeinflussung der Eier von *Protodrilus* und *Saccocirrus*. *Wilhelm Roux' Archiv für Entwicklungsmechanik der Organismen* 121 (4): 630–633. doi:<https://doi.org/10.1007/bf00583343>
- Salkind SJ, Schabad LM (1931) Über die mitogenetische Strahlung des experimentellen Teerkrebses. *Zeitschrift für Krebsforschung* 34 (1): 216–227. doi:<https://doi.org/10.1007/bf01625365>
- Salkind SY, Novikov MB (1938) Quencher of mitogenetic radiation in healthy organs of cancer animal (In Russian). *Archive of Biological Sciences* 51 (3):45–55
- Samarajew WN (1932a) Die mitogenetische Ausstrahlung bei der Regeneration des Regenwurms. *Wilhelm Roux' Archiv für Entwicklungsmechanik der Organismen* 126 (4):633–635. doi:<https://doi.org/10.1007/bf00573792>
- Samarajew WN (1932b) Die mitogenetische Strahlung des Blutes bei künstlicher Hyperthyreose und bei Basedowscher Krankheit. *Endokrinol* 2:335–343
- Serebrov AI (1948) Cervical cancer [Rak scheijki matki] (in Russian). Academy of Medical Sciences of the USSR, Moscow
- Serkiz YI, Chebotarev EE, Baraboy VA, Orel VE, Chebotarev GE (1984) Blood chemiluminescence in experimental and clinical oncology (in Russian). “Naukova dumka”, Kiev
- Shlyapnikov NF, Komissar IG (1934) Mitogenetic radiation of blood of cancer patients and healthy people (In Russian). *Kazan Medical Journal* (2):180–183
- Sidorik EP, Bagley EA, Danko MI (1989) Cell biochemiluminescence during tumour process (in Russian). *Naukova dumka*, Kiev
- Siebert W (1934) Die “mitogenetische” Strahlung des Blutes. In: Hirschfeld H, Hittmair A (eds) *Handbuch der allgemeinen Hämatologie*, vol 2. Urban & Schwarzenberg, Berlin, Wien, p 1339
- Siebert W, Seffert H (1937) Zur Frage der Blutstrahlung bei Krankheiten, insbesondere bei Geschwülsten. *Biochemische Zeitschrift* 289 (6/2):292–293
- Siebert WW (1928a) Über die mitogenetische Strahlung des Arbeitsmuskels und einiger anderer Gewebe. *Biochemische Zeitschrift* 202:115–122
- Siebert WW (1928b) Über eine neue Beziehung von Muskeltätigkeit und Wachstumsvorgängen. *Zeitsch Klin Med* (109):360–370
- Siebert WW (1929) Aktionsstrahlung des Muskels und Wachstumswirkung des elektrodynamischen Feldes. *Biochem Zeitsch* 215 (1–3):152–161
- Siebert WW (1930) Die mitogenetische Strahlung des Blutes und des Harns gesunder und kranker Menschen. *Biochemische Zeitschrift* 226 (4–6):253–256
- Siebert WW (1931) Zur Wachstumswirkung des Arbeitsmuskels. *Biol Gen* 7:69–70
- Siebert WW, Seffert H (1933) Physikalischer Nachweis der Gurwitsch-Strahlung mit Hilfe eines Differenzverfahrens. *Naturwissenschaften* 21 (9):193–194. doi:<https://doi.org/10.1007/bf01504200>
- Siebert WW, Seffert H (1934) Zur Frage des Physikalischen Nachweis der Gurwitsch-Strahlung. *Archive of Biological Sciences Ser B* 35 (1):177–181
- Siebert WW, Seffert H (1936) Blutgruppen und Blutstrahlung. *Biochemische Zeitschrift* 287:109–112
- Sneshko LI (1955) The role of the spleen in the dynamics of cancer quencher (experimental study): *Cand. Med. Sci. dissertation* (in Russian) Dnepropetrovsk State Medical Institute, Dnepropetrovsk
- Sorin AN (1926) Zur Analyse der mitogenetischen Induktion des Blutes. *Wilhelm Roux' Archiv für Entwicklungsmechanik der Organismen* 108 (4):634–645. doi:<https://doi.org/10.1007/bf02080168>
- Sorin AN (1928) Über mitogenetische Induktion in den frühen Entwicklungsstadien des Hühnerembryo. *Wilhelm Roux' Archiv für Entwicklungsmechanik der Organismen* 113 (4):724–730. doi:<https://doi.org/10.1007/bf02252022>
- Storti E, de Filippi P (1936) Das Verhalten des Strahlungsvermögens des Blutes und der blutbildenden Gewebe bei einigen Blutkrankheiten. *Wiener klinische Wochenschrift* 49 (2):1494–1496
- Tatarinov YS (1963) Detection of embryospecific alpha-globulin in serum of patients with primary liver cancer. In: 1st All-Union Biochem Congress Abstract Book. Moscow – Leningrad, p 274
- Vasil'ev LL (1934) On the question of the effect of mental activity on the mitogenetic effect of blood (In Russian). *Archive of Biological Sciences, Ser B* 35 (1):95–105
- Verdina C (1933) Recherches sur les radiations mitogénétiques du sang des tuberculeux. *Boll Soc Int di Microbiologia Sez It* 5:211–218
- Vladimirov YA, Archakov AI (1972) Perekisnoe okislenie lipidov v biologicheskikh membranakh (Lipid peroxidation in biological membranes). *Nauka*, Moscow
- Vladimirov YA, Proskurnina EV (2009) Free radicals and cell chemiluminescence. *Biochemistry (Moscow)* 74 (13):1545–1566. doi:<https://doi.org/10.1134/s0006297909130082>
- Voekov VL, Belousov LV (2007) From Mitogenetic Rays to Biophotons. In: *Biophotonics and Coherent Systems in Biology*. Springer US, Boston, MA, pp 1–16. doi:https://doi.org/10.1007/978-0-387-28417-0_1
- Voikhansky PY (1933) Gurwitsch's rays in internal medicine (In Russian). *Soviet Clinic* 19 (105):3–15
- Volodyaev IV, Belousov LV (2015) Revisiting the mitogenetic effect of ultra-weak photon emission. *Frontiers in physiology* 6 (00241): 1–20. doi:<https://doi.org/10.3389/fphys.2015.00241>
- Volodyaev IV, Belousov LV, Kontsevaya II, Naumova AE, Naumova EV (2021) Methods of studying ultraweak photon emissions from biological objects. II. Methods based on biological detection. *Biophysics* 66 (6):920–949
- Wassiliew LL, Frank GM, Goldenberg EE (1931) Versuche über die mitogenetische Strahlung des Nerven. *Biologisches Zentralblatt* 51 (5):225–231
- Weller NS, Krasovskaya EN (1936) On the inconstancy of mitogenetic radiation of blood (In Ukrainian). In: *Eksp. endokrin [Experimental Endocrinology]*, vol 10. Kharkiv, pp 203–210
- Yefimov VV, Letunov SP (1934) Effects of work, fatigue, and rest on the blood emission of Gurwitsch's rays (In Russian). *Archive of Biological Sciences Ser B* 35 (1):157–168
- Ypsilanti HP, Paltauf R (1930) Zur Frage des Nachweises von Wachstumstrahlen in malignen tierischen Tumoren. *Zeitschrift für Krebsforschung* 32 (1–2):372–376. doi:<https://doi.org/10.1007/bf01636847>
- Yudeles AL (1944) Clinico-physiological and toxicological significance of studies on haemoglycolysis and mitogenetic radiation of blood: *Dr. Med. Sci. Dissertation* (in Russian). Sverdlovsk Institute of Occupational Health and Occupational Diseases, Sverdlovsk
- Zakarian AE, Tarusov BN (1967) Study of antioxidant activity of serum fractions by chemiluminescence inhibition during malignization (In Russian). *Biofizika* 12 (4):739–741
- Zakarian AY, Kochur NA, Tarusov BN (1970) Ultraweak chemiluminescence of blood serum of cancer patients. In: *Fiziko-khimicheskije mekhanizmy zlokachestvennogo rosta. Trudy MOIP [Physico-chemical mechanisms of malignant growth. MOIP Reports]*, vol 32. MOIP Press, p 99
- Zakarian AY, Tarusov BN (1965) Inhibition of chemiluminescence by blood plasma in malignant growth (In Russian). *Biofizika* 10 (5): 919–921
- Zalkind SY (1934) The problem of mitogenetic radiation II. Sources of radiation. Manifestation of rays in the body (In Russian). *Priroda [Nature]* (3):11–27
- Zalkind SY (1936) Mitogenetic radiation of blood and diagnosis of malignant neoplasms (in Russian). *Soviet Medical Journal* (17): 15–28

- Zalkind SY (1937) Mitogenetic radiation is indispensable for cell division (In Russian). *Archive of Biological Sciences* 47 (2):153–160
- Zalkind SY (1950) Experimental study of anti-quencher (In Russian). *Biulleten' eksperimental'noi biologii i meditsiny* [Bulletin of experimental medicine and biology] 2:153–156
- Zalkind SY, Lomovskaya EG (1941) Long-term action of quencher of mitogenetic radiation on biological objects. *Collected works of Military Veterinary Academy of the Red Army* 3:165–180
- Zalkind SY, Shabad LM (1931) On mitogenetic radiation of tar cancer (In Russian). *Bulletin of Roentgenology and Radiology* [Vestnik rentgenologii i radiologii] 9 (5–6):359–369
- Zarkh MN (1934) Mitogenetic radiation of urine and influence of physical work on it (In Russian). *Physiological Journal of the USSR* 17 (5):1035–1038
- Zolotova-Kostomarov MI, Lyass M (1936) Mitogenetic radiation of blood in rheumatism and pneumonia. *Clinical Medicine* 14 (11): 1629–1633

Nonchemical Distant Interaction Hypothesis: Pro et Contra

Preface

This part (as well as the previous one) significantly differs from the others in this book. Here, in contrast to the proven and well-established data summarized in the major part of the monography, we provide material that requires full-scale experimental verification and revision, namely, different viewpoints and theoretical analysis of the possibility or impossibility of nonchemical interactions in biological systems.

As all human beings, each of the authors has his or her own inner beliefs that determine the intonation with which they speak about such complex and ambiguous matters. At the same time, we all share the belief that scientific truth is one, which means that the arguments of each of the authors will sooner or later find their place in the general picture of the world. We consider the pluralism of (reasoned) opinions a necessary condition for the preparation of future scientific discoveries – or a reasoned closure of untenable areas.



Daniel Fels

24.1 Introduction

More and more scientists develop a basic interest in a comprehensive understanding of life that includes electromagnetic (EM) fields. Technology and therewith methods exist as well as a theory about life that includes EM fields.

The Theory A cell with its billions of atoms and molecules cannot avoid being electric as (i) atoms appear mainly in an ionised state, (ii) most molecules are electrically charged, (iii) chemical reactions can cause the release of EM fields (i.e. exothermic reactions) and (iv) mechanical vibrations of subcellular structures can act as dipole sources producing EM fields (Fels et al. 2015). In parallel, atoms and molecules, owing to the electric charge they contain, are affected by EM fields, whether these being electrostatic or electrodynamic. Hence, cells generate EM fields and these fields feedback to the cells or the community of cells they are located with. With thousands of catalysed cell reactions and corresponding transcriptions, we can assume a multitude of EM signals being released and perceived by cells, and therefore, probably a multitude of EM-based processes as part of a cybernetic organisation of cellular functions (Fels et al. 2015).

Indirect Evidence for the Function of Endogenous EM Signals To this day, several research works reported the detection of EM fields of different frequencies emitted from different types of cells, tissues or organisms (Colli et al. 1955; Galle et al. 1991; Belousov 2007; Van Wijk et al. 2007; Cifra et al. 2011; Sun et al. 2010; Tzambazakis 2015, Tab1) and, in parallel, we find more and more photoreceptors, too (Briggs and Spudich 2005; Van der Horst et al. 2007; Idnurm and Crosson 2009; read also Laager 2015). Note that the visible range together with weak UV-A is assumed as ... *a very efficient frequency window for electromagnetic cell*

communication ... because ... the thermal noise ... has a low intensity in the visible and UV range, and so the signal-to-noise ratio can be very high in that range (Fels 2015) with the energy content of photons in that range being high enough to trigger chemical reactions. There is, furthermore, a growing understanding about the origin of cell endogenous EM waves (sometimes referred to as biophotons) (Mei 1994; Bokkon et al. 2010; Rastogi and Pospisil 2010; Prasad and Pospisil 2011, 2015). As cells use their metabolites also as signals, we assume that emitted EM fields can serve as signals as well. Yet, testing for function(s) of these signals contains an obstacle opposite to testing functions of chemical signals. In the later nineteenth century, it was easy to test, e.g. the function of hormones, first by isolating them and, second, testing them, e.g. by applying isolated thyroxin from tadpoles on early tadpoles thereby inducing (to early) metamorphosis in the latter. With EM fields, there is the obstacle that we cannot (yet) catch, store and deliver these potential signals (Fels 2015). An elegant way to gain combined certainty about the nature and the function of the signal was shown by Reiter and Gabor (1928): They deduced emitted frequencies from a natural source (onions) applied these but from technical sources and found effects like those coming from the natural source, delivering thereby *quasi-direct evidence*. However, the impossibility of measuring those emitted photons that will be signals demands that we generally speak of *indirect evidence for a most probably electromagnetic signal*. This state of the art should by far not be discouraging as selected studies will demonstrate.

Every experiment with pairs of cells or tissues, chemically but not physically separated from each other that shows effects from one onto the other delivers *indirect evidence* for cellular self-organization based on (most probably) endogenous EM fields. In other words, we can find cell systems under the influence of physical signals emitted by the cell system itself. Into this we go, starting with history.

D. Fels (✉)

Independent Researcher, Binningen, Basel, Switzerland
e-mail: daniel.fels@breitband.ch

24.2 Disentangling an Early Definition of the Function

Gurwitsch, as a morphologist, was driven by the question of what is giving form (*morpha*). He deduced (Gurwitsch and Gurwitsch 1926; Gurwitsch 1988) that hormones alone – or we may say metabolites in general – cannot be fully responsible for the whole process of form-giving, hence referred to and began – inspired by Einstein’s field theory – to look for fields as an additional factor playing a major role in development. In 1912, he suggested a *field of force* effectively guiding development in multicellular organisms (Belousov 1997, 2015; Volodyaev and Belousov 2015; read also in this book Chap. 2). In addition to this force, Gurwitsch postulated (1923) – based on strong evidence – a cell-emitted radiation that induces cell divisions and named it, therefore *mitogenetic radiation*; the radiation and its effect (the function) was a simultaneous discovery.

Today, his suggested *field of force* is referred as to EM fields of both cells and whole organisms and instead of cellular *radiation* we speak of EM waves (or biophotons; Voikov and Belousov 2007). What is giving form to multicellular life throughout its development points today clearly at the electrostatic fields and regards cell migration and orientation (Funk 2015; Levin et al. 2017). Note that cell differentiation, a crucial aspect of development in multicellular organisms, too, is observed as changes in membrane voltage(s) (Levin 2014; Duran et al. 2017). So, Gurwitsch was basically right with his idea about the effect of a *field of force*. However, what are the functions of the EM waves that are emitted by cells? If Gurwitsch’s definition that the *radiation* generates *mitosis* is correct, then EM fields would also play a major role in development as a form-giving factor for cell division is a *conditio sine qua non* in developmental processes of multicellular organisms. However, development is not only resulting from cell division.

Albrecht-Bühler (1992) worked with baby hamster kidney (BHK) cells and observed traversing cells, a phenomenon well known in tissues of bone, intestine or cornea as well as in confluent cultures of BHK cells. The phenomenon regards differences in cell orientation between consecutive layers of cells, while they are parallel within one layer, the cells of the next layer will be transversally to the former with the potential function of *force distribution*. What is interesting is that Albrecht-Bühler observed this transversal positioning of two layers of BHK cells that were separated from each other by two glass slides that were lying on top of each other with one cell layer on one side and the other layer on the other side of the *double slide*. When he placed a metallic foliage in between the *double slide*, the effect was annihilated and he so concluded an electromagnetic signalling between the cells. Note that the study of Albrecht-Bühler shows not only

another function of cell-emitted EM waves than altered cell division rates, it also shows that referring orientation, migration and stem cell differentiation singly to electrostatic fields might be a too narrow view.

Yet, coming back to the early days of the discovery of cell *radiation*, Gurwitsch might have erred what regard the *single function* of the radiation. Soon after his first publications Reiter and Gabor (1928) confirmed (by repeating his major experiment) the emission of cellular EM fields and concluded frequencies responsible for the alterations in cell division rates in exposed tissue regions. Yet, the emitted frequencies would not induce cell divisions but rather regulate them. To fully see the difference with respect to Gurwitsch’s work, it is worth to describe – in a nutshell – his major experiment that led to the term of *mitogenetic radiation*: The famous onion-root experiment.

24.2.1 The Onion-Root Experiment

Gurwitsch exposed in a rectangular way two onion roots to each other, one vertically and the inducer root horizontally with its tip pointing at the middle section of the vertically positioned tester root (see also Chaps. 2 and 20). Both roots were ‘engaged’ in cuvettes of quartz (to avoid chemical signalling). After exposure, he made slides of the middle section of induced roots and counted how many cells were either starting or being already in *mitosis*. He observed that the one half-section of the slides looking towards the inducer root showed many more mitotic cells than the opposed half-section. Hence, he concluded – and at first sight correctly – a mitosis-inducing effect coming from the tip of the inducer root. As chemical signals could not be the cause – recall, the roots were in quartz cuvettes – and as no effects were found when the roots were ‘engaged’ in cuvettes consisting of normal glass (i.e. in quartz with amorphous structure), he concluded (i) a radiation as effector and – as UV is absorbed by ‘normal glass’ but not by quartz with a crystalline structure – (ii) a radiation in the UV-range (Gurwitsch 1923).

Reiter and Gabor (1928) repeated his design and found the same effects but also realized that the opposed half section not only showed less cells in *mitosis* but observed also a reduction in the rate of mitotic cells compared to ‘backside-regions’ of the root that were further away from the effected region. Reiter and Gabor have not directly tested for this reduced mitotic rate in the opposed backside region (as they declare) but concluded that the total rate of cell divisions in the growing root was not altered; it was augmented in the exposed half section and reduced in the opposed half. So, rather than talking of a *mitogenetic radiation*, we can – based on Reiter and Gabor – speak of a *mitosis regulating radiation*. Later in this chapter, the reader will find additional

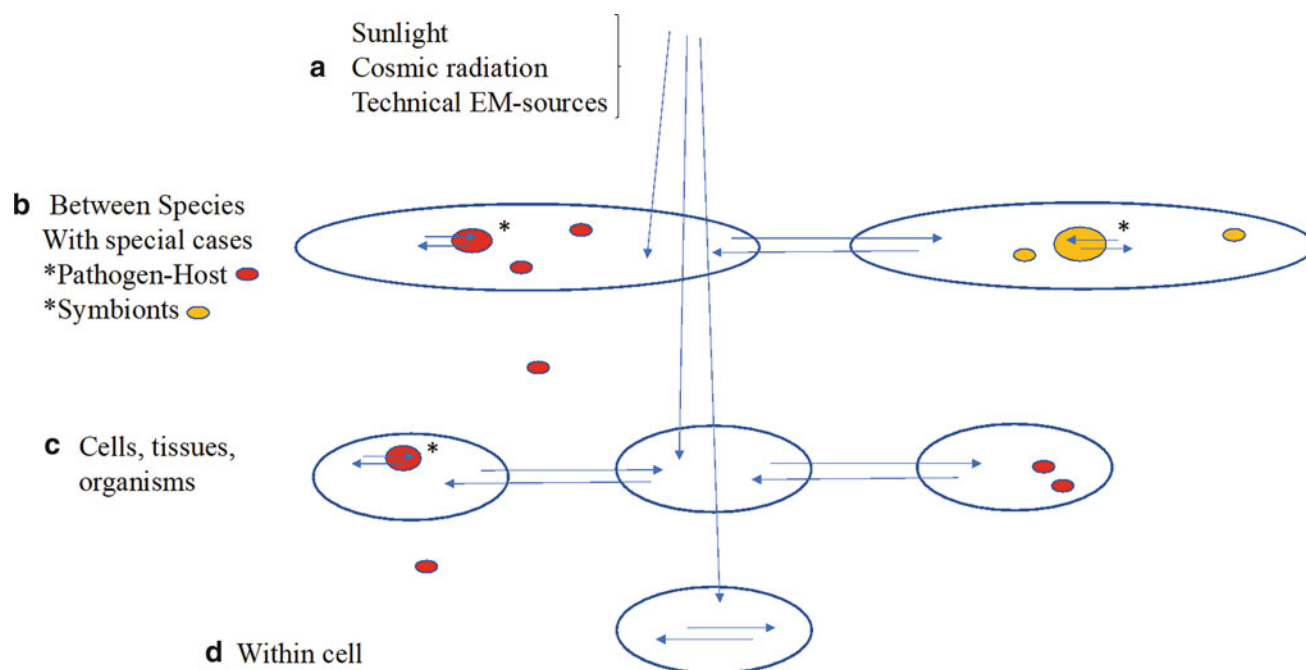


Fig. 24.1 The figure represents the different levels where EM interactions or -effects (arrows) are either observed or still demand our shared interest. Panel (a) refers to solar EM waves but intends to look at cosmic radiation in general as well as at technical sources. Panel (b) refers to those studies that revealed EM-based effects across the species

border and hints on species relations (*) where functions can be expected. Panel (c) represents the level on which most studies worked on, it, however, offers to look there as well at e.g. host–pathogen interactions or symbiotic relationships. Panel (d) is the living cell itself, the smallest unit of living EM–field–matter interaction

evidence for this *new* definition, more precisely for its regulatory function, yet in a surprising multitude!

Accepting for a moment this *new* definition we may still ask: Is regulation the full answer? If we would let the tester root grow, it would – due to its asymmetric growth – curve away from the inducer root as if *avoiding competition*. So, apart from growth regulation as immediate response, we find a simultaneous ecological interpretation. Throughout the following two sections, I will continue to disentangle the early definition of cell radiation away from *mitosis only*, thereby guiding the reader’s attention towards a higher and a lower level of the cell, i.e. towards ecology and cell dynamics (Fig. 24.1).

24.3 The Ecological Dimension of Electromagnetic Cell Signals

24.3.1 Between Species

To move away cell radiation from being directly relevant to development, we see a rather ecological function in the above interpretation of *avoiding competition*, which, nonetheless, can also be interpreted as a regulation. Yet, even though this early experiment gave literally insight into the potential of cell- or tissue-intrinsic regulation based on EM fields, it

describes at the same time also an effect between two organisms when looking at both *sender* and *receiver*.

Somewhat surprising is the fact that effects on cell division rates were also observed across the species border! And with that we move even further away from development. Soon after Gurwitsch’s pioneering works one could read about bacteria influencing – via an assumed radiation – sea urchin eggs (Choucrun 1930) or tadpoles influencing onion roots in a similar way as the inducer root did on the tester root (Reiter and Gabor 1928). More recent and most striking is the work of Jaffe (2005). Under the title *Marine Plants May Polarize Remote Fucus Eggs via Luminescence*, he reports to finally have found the signal that directs proliferation of *Fucus* eggs towards the substrate they need for settlement. Note that Jaffe reports of a many years lasting search for chemical signals but then found (responsible for the known directional growth of *Fucus* eggs towards marine plants) a non-chemical signal that did not work when marine plants and *Fucus* eggs were shielded against presumed endogenous electromagnetic signals (Jaffe 2005) emitted by the marine plants. Even though the eggs of *Fucus* begin cell division when they grow towards the required substrate, the substrate did not induce cell division as in the absence of a shield the eggs grow as well, but in all directions. Jaffe’s study about a presumed endogenous electromagnetic signal is better understood in an ecological than development-regarding context:

Fucus eggs sense an EM field that guides them to a substrate onto which they will attach (before developing into a fully grown brown algae).

Note The term luminescence, as Jaffe uses it, refers to a phenomenon we know, e.g. from fire flies. It is a visible cold monochromatic light and used to a much greater extent in the aphotic zones of the Deep Sea than on land and this by a multitude of species from different phyla either for attraction, deception or swarm coherence. Yet, all studies described here (including Jaffe's) refer to ultra-weak photon emission (UPE), hence, a light not visible for the naked eye and emitted in many frequencies. Imagining host–pathogen interactions, where interspecific contact is extremely close, the unavoidably appearing electromagnetic communication would be based on UPE.

Jaffe's work is wonderful because it regards two species where one depends on the other, allowing to think about a function. Yet, we are faced by the fact that most *between species experiments* did not test for functions but for effects as the following studies will show.

The group of Rossi et al. (2011) worked with isolated mammalian cells, namely immortalized mouse fibroblasts (NIH3T3) and adult human microvascular endothelial cells (HMVECad) and found effects between the two cell types when chemically but not physically separated from each other by Petri dishes. The effects regarded cell number and morphology and were absent when a black filter was placed between the dishes.

In a recent work on effects across the species border I suggested (Fels 2016) to develop . . . *theories on electromagnetic (despite chemical) organization of whole ecosystems* In my work, I exposed the unicellular algae *Euglena viridis* and the unicellular heterotrophic ciliate *Paramecium caudatum* to each other and observed that *Euglena* would have a reducing effect on cell division rates in *Paramecia*. I also exposed the multicellular Rotifer *Rotatoria* sp. (a little aquatic worm) to *Paramecium caudatum* and found that they could influence each other in proliferation in either way, accelerating or decelerating and this also in dependence of normal glass or quartz separation. It is not immediately clear what was the function of affecting proliferation across the species border. We may (i) speculate that it regards species density regulation and (ii) carefully conclude here that the phenomenon of a physical, most probably electromagnetic effect across the species border hints on a *universal character* of nonchemical cell signalling.

The between species experiments of the future should be biased towards two-species systems such as host and pathogen, or plant root and mycorrhiza or unicellular prey and predator systems.

24.3.2 Within Species

In 2009, I published my first work – motivated by the studies of Gurwitsch – on communication between *Paramecium caudatum* populations across normal and quartz glass. Expecting increase in growth, i.e. cell division rates, and only across quartz barriers still following the assumption that derived from the term *mitogenetic radiation*, the results were surprising. First, there was increase in growth but also decrease in growth observed. Second, the effects were found across both normal and quartz glass, hence indicating that EM waves ranging below UV would also induce effects from one population onto another one across a chemical barrier; surprisingly, the effects across normal glass were different from those across quartz glass (see in Fels 2009). And third, depending on the number of neighbours and the separating material, *Paramecia* would produce via phagocytosis different numbers of vacuoles containing their food: bacteria. With this latter and double-blind performed experiment and together with the above-mentioned results, it then became clear that the 'old' definition (*mitogenetic radiation*) is too narrow.

Based on these 2009 results, I (i) developed a test for direct assessment of a regulative function (2017) and (ii) in an a posteriori analysis (2012) focused on an unknown environmental factor that remains active when the separated populations do not affect each other (across chemical barriers) but becomes inactive when inducer populations do affect tester populations. The following two paragraphs elaborate this a bit further.

Regulation The 2009 results had a pattern when just looking at quartz-separated pairs of populations: The population that consisted in more cells had a decreasing effect on cell division rates or energy consumption in the smaller populations. Beginning to look for a meaning, i.e. a function, this was interesting for two reasons. First, as quartz absorbs effectively deeper in UV (Fels 2009) than glass this was closer to natural conditions than separation with glass as a frequency filter. Second, *Paramecia* regulate their density when kept in microcosms (50 mL Falconer-tubes), thereby reaching a maximum of about 300 cells per mL. How do they organize this maximum density? The reader may refer to the original work but find here in short that tester populations (5 cells at the beginning) grew more, the less neighbours (300, 200, 100 or 50 cells at the beginning) they had. This reads the other way around, the closer the inducer populations were to their *carrying capacity* the less would also tester cells grow (Fels 2017). This indicated the function of a density regulation (most probably) based on EM signals and with this supports the assumption of Reiter and Gabor, namely that the cell radiation does not induce but regulate *mitosis*. Yet, as we look here at a unicellular organism,

regulation refers in the case of *Paramecia* to ecology rather than to the organization of cells within a multicellular organism. Are we, nonetheless, looking at a phenomenon that may explain, how cell densities are stabilised in multicellular organisms?

Unknown Environmental Factor The reader may note that ecological experiments, when repeated over time (no matter how standardized they are) always show a tremendous variation across repetitions. This variation is bigger than the one between replicates in an experimental block and is often bigger than the effects coming from the treatment itself (Fels 2005). To reduce this unknown cause of (tremendous) variation, one either cares for a statistically satisfying great number of replications within one single experiment or one repeats the same experiment accepting that an unknown environmental factor will induce variation; I did the latter for reasons of data-handling (Fels 2009). Across three different experiments with several replications in each, I found that inducer populations when affecting a tester population (in cell division rates) would be freed from the effect of the unknown environmental factor while the tester population would still show great variation across the repetitions of the experiment. For cases of no effect from inducer on tester populations both would display tremendous variation across the repeats of experimental blocks. Hence, as soon as a cell population affects another one, it becomes, on the one hand, part of the other's population environment but, on the other hand, decouples itself from the effect of that unknown environmental factor. The meaning of this *decoupling* is unclear. However, the above-described pattern resembles patterns of typical two-photon entanglement experiments (described in detail in Fels 2012) and hence we might speculate to look here at a law working on a quantum level as well as on a *microscopic* (if not *macroscopic*) level (Fels 2015). Note that we are not only looking at a function between sender and receiver but also at a function within the sender: the *decoupling* from an unknown environmental factor. What that factor is, remains still unclear. Suggested candidates are altering intensities of cosmic rays (read also Kozlov 2000) or – due to changes in global flashing rates – altered intensity of Schumann waves.

24.4 The Cellular Dimension of Electromagnetic Signals

So far, we disentangled the narrow definition of cellular EM signals from *inducers* to *regulators* of mitosis and described evidence-based effects between species that look like regulation in an ecological context hinting thereby at a *universality* of cellular electromagnetic signals. We continue with three

studies revealing functions in cell dynamics. These studies all start with the induction of chemicals but then look for electromagnetically induced responses.

The group of Galantsev (1993) applied neurotransmitters (acetylcholine and noradrenaline) to isolated mouse mammary cells that were maintained in one cuvette and reported of *induced protein synthesis* also in the neighbouring cuvette that contained the same cells. Note, that the latter was shielded chemically but not optically from the former. When the two cuvettes were shielded optically from each other, no induction of protein synthesis in the tester population was observed. Protein synthesis allows to deduce that the – most probably – electromagnetic signal had a regulatory effect on the gene level.

The group of Shen et al. (1994) added PMA (*phorbol myristate acetate*) to cells of the immune systems (neutrophils) and reported two effects in a neighbouring cuvette containing neutrophils as well (but with no PMA application). First, the cells produced *superoxide radicals*, which is of significant meaning as these substances play a major role in the cellular metabolism leading to em-wave emission (in the visible range; Prasad and Pospíšil 2015, see also Chaps. 8 and 14). And in fact, second, the tester cells emitted *photons* (measured with photomultipliers). Shen argues... *that a long-range optical coupling of biological significance between living cells exists*. Most interesting would have been a third cuvette with neutrophils for testing whether the photons emitted by the tester neutrophils would have induced the production of superoxide radicals and the emission of photons as well. Such a chain-of-reaction-like process could demonstrate the potential of photon-based signal transduction across tissues; a type of experiment awaiting future scientists. We note here that a chemical signal (PMA) led (i) to a metabolic reaction (production of superoxide radicals) and (ii) the release of light (photons in the visible range). So, one function can be that EM fields induce the release of further EM fields, maybe to produce synchronicity in the response of a whole tissue.

The group of Farhadi et al. (2007), working with malign gut epithelial Caco-2-cells, used a standard method that provokes the release of photons from a tissue or isolated cells: the application of H₂O₂. They report of similar effects in the inducer cells (with H₂O₂ application) and the detector cells (without H₂O₂ application). Most striking about this study are significant effects on the nuclear transcription factor NFκB, generally known for gene regulation regarding chemical signaling in immunity, inflammation, cancer and nervous system function (Karin and Ben-Neriah 2000) and with evidence for NFκB-activity contributing to overall function inside and outside of mitochondria as well (Albensi 2019). These are the results of the Farhadi-group: *Exposing inducer cells to H₂O₂ resulted in a significant reduction in total protein content (–50%), an increase in nuclear NFκB*

activation (+38%) and structural damage (56%) compared to controls. There was a similar reduction in total protein content (−48%), increase in the nuclear fraction of NFκB (+35%) and structural damage (25%) in detector cells. Farhadi explains further that this . . . signaling system possibly plays a role in synchronous, stimulus-appropriate cell responses to noxious stimuli and may explain a number of cellular behaviors that are hard to explain based only on conventional cell signaling systems. In this study, we can interpret the function of EM signals as organizing synchronicity between cells.

24.5 Conclusion

Combining both subchapters, the ecological and the cellular dimension of electromagnetic signals, we can conclude that the studies point towards regulation; from gene regulation to cell density and synchronicity regulation and probably also (at least partly) to species density regulation. Regulation might thus be the major, the above-all function of endogenous electromagnetic signals emitted by cells. However, when we delve into different studies, we immediately see that a multitude of different regulatory processes occur on different levels of life, each one differently organized.

We still know very little about the electromagnetic field parameters these processes depend on (or are accompanied by), whether these parameters are modulated or combinations of different parameters are needed. What we know is that cells do emit electromagnetic fields at various spectral ranges and that cells have photoreceptors sensitive to a certain range of the electromagnetic spectrum. Even though, cells regulate incredible numbers of processes, it is pretentious to claim that all of them are regulated by electromagnetic field parameters as we know as well of molecular regulators such as, e.g. hormones or transcription factors.

Under the assumption of the general hypothesis regarding the *fields of the cell*, it is understood that cell processes lead to (electrostatic and) electrodynamic fields and that these fields feedback on cell processes. Consequently, a chicken egg question, namely who regulates, chemicals or em-waves, is not of help: Both do. Yet, it is suggested to look at the processes of life as an ongoing sequence of action and reaction, as a reciprocal causality between the electric and the molecular aspects of life. The understanding of reciprocal causality follows directly from an understanding about the physics of field forces and resonance. For the latter, there are theoretical thoughts regarding morphogenesis (Pietak 2015) as well as there is . . . *the first evidence in support of sequence-specific resonance signaling in the genome* (Savelev and Myakishev-Rempel 2020).

Once we delve into single processes, it might be that we sometimes find a molecule as the key signal and probably

more often than previously thought of, a *field-component* involved in it. Taking the latter, we can conclude that there is a multiple functionality of the endogenous electromagnetic waves of cells, all of which having to do with regulation, either within or between cells (or even species). However, this regulation splits into a multitude of individual processes depending on the organisation level and the system under study. So, it is one function and at the same time many.

To be clear, under the hypothesis presented here, I do not consider a hierarchy between chemical and EM signals. Both are in use. Which one may depend on the receiver and the distance between the receiver and the sender. A level description may illustrate this. Flowers reflect sunlight, i.e. electromagnetic waves in the visible and UV range. These are perceived by photoreceptors of pollinators. As they approach the flower, the pollinators get further attracted by chemicals, the odour of the flower and for which they have receptors, too. In some cases, and when getting still closer, electrostatic pollination occurs, which means that pollen flies along *field-lines* towards the oppositely charged surface of the pollinator (Vaknin et al. 2000). The pollen then releases its tube that is guided chemically towards the female gamete. It might be electromagnetically embedded on this way; once its nucleus has entered the egg cell and conjugation occurred, the male DNA enters the reciprocal causality system between the material and electrodynamic world of the fertilised egg.

24.6 Outlook

To study life without including EM fields is as if looking at galaxies without including the gravitational field they generate. Both systems' dynamics are assumed to be based on reciprocal causality. I believe it is only a question of time until we generally include EM fields in our theory of life and teach future generations of students about how to do it, in theory and in practice.

What we learn and already learned enlarges our basic understanding of life and the government of its processes touching in today's times at least two major issues: The effects of technically generated electromagnetic waves on organisms (e.g. Cammaerts et al. 2011; Fels 2018) and hand in hand with it, non-invasive therapies (Saliev et al. 2014; Markov 2015; Funk 2017) or diagnostics (Esmaeilpour et al. 2020; Murugan et al. 2020).

An open question and a provocative answer: I am often puzzled by viruses about how they manage (i) without kinetic abilities by their own to be transported from the place of infestation to their host cells (as, e.g. in the case of rabies or polio), then (ii) to be incorporated by the host cell and eventually and (iii) be moved therein to the nucleus region (as, e.g. in HIV infection), all of which being actions the cells themselves can do but – again – not the viruses. Certainly,

knowledge exists, e.g. about the *mechanistic* contact of the virus with the host cell membrane (in the case of the bacteriophage Lambda followed by DNA-injection) or of capsid proteins clinging onto motor proteins that transport the capsid along microtubules (Cunningham et al. 2006; Patarroyo et al. 2013). Yet, could it be, if all the cell dynamics occur in company of and with EM fields that viruses interfere with these fields in such (evolved) ways that cell kinetic processes are guided towards the virus's goal? If so, do viruses have senders or receivers to interfere in such proposed ways? Very interesting in this context is the research of virus transportation to (nonbiological) surfaces of physiological ionic strength (Docoslis et al. 2007). While this regard electrostatic adherence, theoretical work exists on frequency-based resonant recognition of pathogen proteins (Cosic et al. 2015) as well as on considering antibodies also as antennas (Madl and Egot-Lemaire 2015). One may suggest that the interaction between cellular EM fields of both host cells and pathogens in general will give us a closer insight into host–pathogen interactions. It is worth, in this context, to recall that the *coats of molecules*, hence including proteins, consist of electric charges: the electrons. In general, electric charges are capable to generate as well as to respond to electromagnetic fields.

References

- Albensi BC (2019) What is nuclear factor Kappa B (NF- κ B) doing in and to the mitochondrion? *Front Cell Dev Biol*. <https://doi.org/10.3389/fcell.2019.00154>
- Albrecht-Buehler G (1992) Rudimentary form of cellular ‘vision’. *Proc Natl Acad Sci USA* 89: 8288–8292
- Belousov LV (2007) Ultraweak photon emission as a tool for analysing collective processes in cells and developing embryos. In: Belousov LV, Voeikov VL, Martynyuk VS (eds) *Biophotonics and Coherent Systems in Biology*. New York Springer, p 139–157
- Belousov LV (1997) Life of Alexander G. Gurwitsch and his relevant contribution to the theory of morphogenetic fields. *Int J Dev Biol* 41: 771–779
- Belousov LV (2015) Morphogenetic fields: History and relations to other concepts. In: Fels D, Cifra M, Scholkmann F (eds) *Fields of the Cell*, Research Signpost, Trivandrum, p 267–278
- Bokkon I, Salari V, Tuszynski JA, Antal I (2010) Estimation of the number of biophotons involved in the visual perception of a single-object image: Biophoton intensity can be considerably higher inside cells than outside. *J Photochem Photobiol (B, Biology)* 100(3): 160–166
- Briggs WR, Spudich JL (eds) (2005) *Handbook of Photosensory Receptors*. Wiley, Weinheim
- Cammaerts M-C, Debeir O, Cammaerts R (2011) Changes in *Paramecium caudatum* (Protozoa) near a switched-on GSM telephone. *Electromagnetic Biol Med* 30: 57–66
- Choucrun N (1930) On the hypothesis of mitogenetic radiation. *J Marine Biol Ass UK* 17(1):65–74
- Cifra M, Fields Z, Farhadi A (2011) Electromagnetic cellular interactions. *Prog Biophys Mol Biol* 105: 223–246
- Colli L, Facchini U, Guidotti G, Dugnani-Lonati R, Orsenigo M, Sommariva O (1955) Further Measurements on the Bioluminescence of the Seedlings. *Experientia* 11:479–481
- Cosic I, Caceres JLH, Cosic D (2015) Possibility to interfere with malaria parasite activity using specific electromagnetic frequencies. *EPJ Nonlin Biomed Physics* 2015. <https://doi.org/10.1140/epjnbp/s40366-015-0025-1>
- Cunningham AL, Diefenbach RJ, Miranda-Saksena M, Bosnjak L, Kim M, Jones C, Douglu MW (2006) The cycle of human herpes simplex virus infection: Virus transport and immune control. *J Infect Diseases* 194:s11–18
- Docoslis A, Espinoza LAT, Zhang B, Chen LL, Israel BA, Alexandridis P, Abbott NL (2007) Using nonuniform electric fields to accelerate the transport of viruses to surfaces from media of physiological ionic strength. *Langmuir* 23:3840–3848
- Duran F, Morokuma J, Fields C, Williams K, Adams DS, Levin M (2017) Long-term, stochastic editing of regenerative anatomy via targeting endogenous bioelectric gradients. *Biophys J* 112:2231–2243
- Esmailpour T, Fereydouni E, Dehghani F, Bókkon I, Panjehshahin M-R, Császár-nagy N, Ranjbar M, Salari V (2020) An experimental investigation of ultraweak photon emission from adult murine neural stem cells. *Sci Rep* 10:463. <https://doi.org/10.1038/s41598-019-57352-4>
- Farhadi A, Forsyth C, Banan A, Shaikh M, Engen P, Fields JZ, Keshavarzian A (2007) Evidence for non-chemical, non-electrical intercellular signaling in intestinal epithelial cells. *Bioelectrochemistry* 71:142–148
- Fels D (2005) The effect of food on microparasite transmission in the waterflea *Daphnia magna*. *Oikos* 109:360–366
- Fels D (2009) Cellular communication through light. *PLoS ONE* 4: e5086
- Fels D (2016) Physical non-contact communication between microscopic aquatic species: Novel experimental evidences for an interspecies information exchange. *J Biophys*, article ID 7406356. <https://doi.org/10.1155/2016/7406356>
- Fels D (2012) Analogy between quantum and cell relations. *Axiomathes* 22:509–520. <https://doi.org/10.1007/s10515-011-9156-x>
- Fels D (2017) Endogenous physical regulation of population density in the freshwater protozoan *Paramecium caudatum*. *Sci Rep* 7:13800
- Fels D (2015) Electromagnetic cell communication and the barrier method. In: Fels D, Cifra M, Scholkmann F (eds) *Fields of the Cell*, Research Signpost, Trivandrum, p 149–162
- Fels D (2018) The double-aspect of life. *Biol* 7(2):28. <https://doi.org/10.3390/biology7020028>
- Fels D, Cifra M, Scholkmann F (eds) (2015) *Fields of the Cell*. Research Signpost Trivandrum
- Funk RHW (2015) Endogenous electric fields as guiding cue for cell migration. *Front Physiol* 6:143. <https://doi.org/10.3389/fphys.2015.00143>
- Funk RHW (2017) Does electromagnetic therapy meet an equivalent counterpart within the organism? *J Transl Sci* 3:1–6
- Galantsev VP, Kovalenko SG, Moltchanov AA, Prutskov VI (1993) Lipid peroxidation, low-level chemiluminescence and regulation of secretion in the mammary gland. *Experientia* 49:870–875
- Galle M, Neurohr R, Altmann G, Popp F-A, Nagl W (1991) Biophoton emission from *Daphnia magna*: A possible factor in the self-regulation of swarming. *Experientia* 47:457–460
- Gurwitsch A (1923) Die Natur des spezifischen Erregers der Zellteilung. *Arch Mikrosk Anat Entwicklungsmechanik* 100:11–40
- Gurwitsch A, Gurwitsch L (1926) Das Problem der Zellteilung physiologisch betrachtet. In: *Gildmeister M, Goldschmid R, Neuberg C, Parnas J, Ruhland W (eds) Monographien aus dem Gesamtgebiet der Physiologie der Pflanzen und der Tiere*. Springer, Berlin, p 1–221
- Gurwitsch AA (1988) A historical review of the problem of mitogenetic radiation. *Experientia* 44:545–550
- Idnurm A, Crosson S (2009) The photobiology of microbial pathogenesis. *PLoS Pathog* 5:e1000470

- Jaffe LF (2005) Marine plants may polarize remote *Fucus* eggs via luminescence. *Luminescence* 20:414–418
- Karin M, Ben-Neriah Y (2000) Phosphorylation meets Ubiquitination: The Control of NF- κ B Activity. *Ann Rev Immunol* 18:621–663
- Kozlov AA (2000) The role of natural radiation background in triggering cell division. In: Belousov L, Popp F-A, Voeikov V, van Wijk R (eds) *Biophotonics and Coherent Systems*. Moscow University Press, p 241–248
- Laager F (2015) Light based cellular interactions: Hypotheses and perspectives. *Front Phys* 3:55
- Levin M, Pezzulo G, Finkelstein JM (2017) Endogenous bioelectric signaling networks: Exploiting voltage gradients for control of growth and form. *Annu Rev Biomed Eng* 19:353–387
- Levin M (2014) Endogenous bioelectrical networks store non-genetic patterning information during development and regeneration. *J Physiol* 592:2295–2305
- Madl P, Egot-Lemaire S (2015) The Field and the Photon from a physical point of view. In: Fels D, Cifra M, Scholkmann F (eds) *Fields of the Cell*. Research Signpost Trivandrum, p 29–54
- Markov MS (ed) (2015) *Electromagnetic Fields in Biology and Medicine*. Taylor & Francis, Boca Raton
- Mei W-P (1994) On the Biological Nature of Biophotons. In: Ho M-W, Popp F-A, Warnke U (eds) *Bioelectrodynamics and biocommunication*. Singapore World Scientific, p 269–291
- Murugan N J, Persinger M A, Karbowski L M, Blake T, Dotta BT (2020) Ultraweak Photon Emissions as a Non-Invasive, Early-Malignancy Detection Tool: An In Vitro and In Vivo Study. *Cancers* 12:1001. <https://doi.org/10.3390/cancers12041001>
- Patarroyo C, Laliberté J-F, Zheng H (2013) Hijack it, change it: how do plant viruses utilize the host secretory pathway for efficient viral replication and spread? *Front Plant Sci* 3:308, p 1–8. <https://doi.org/10.3389/fpls.2012.00308>
- Pietak A (2015) Electromagnetic resonance and morphogenesis. In: Fels D, Cifra M, Scholkmann F (eds) *Fields of the Cell*. Research Signpost Trivandrum, p 303–320
- Prasad A, Pospisil P (2011) Linoleic acid-induced ultra-weak photon emission from *Chlamydomonas reinhardtii* as a toll for monitoring of lipid peroxidation in the cell membranes. *PLoS ONE* 6:e22345
- Prasad A, Pospisil P (2015) The photon source within the cell. In *Fields of the Cell*. In: Fels D, Cifra M, Scholkmann F (eds) *Fields of the Cell*. Research Signpost Trivandrum, p 113–129
- Rastogi A, Pospisil P (2010) Effect of exogenous hydrogen peroxide on biophoton emission from radish root cells. *Plant Physiol Biochem* 48:117–123
- Reiter T, Gabor D (1928) *Zellteilung und Strahlung*. Springer, Berlin
- Rossi C, Foletti A, Magnani A, Lamponi S (2011) New perspectives in cell communication: Bioelectromagnetic interactions. *Semin Cancer Biol* 21:207–214
- Vaknin Y, Gan-Mor S, Bechar A, Ronen B, Eis D (2000) The role of electrostatic forces in pollination. *Plant Syst Evol* 222:133–142
- Van der Horst MA, Key J, Hellingwerf KJ (2007) Photosensing in chemotrophic, non-phototropic bacteria: Let there be light sensing too. *Trends Microbiol* 15:554–562
- Van Wijk R, Kobayashi M, Van Wijk EPA (2007) Spatial characterization of human ultra-weak photon emission. In: Belousov LV, Voeikov VL, Martynyuk VS (eds) *Biophotonics and Coherent Systems in Biology*. Springer, New York, p 177–189
- Voeikov V V, Belousov LV (2007) From mitogenetic rays to biophotons. In: Belousov LV, Voeikov VL, Martynyuk VS (eds) *Biophotonics and Coherent Systems in Biology*. Springer, New York, p 1–16
- Volodyaev I, Belousov LV (2015) Revisiting the mitogenetic effect of ultra-weak photon emission. *Front Physiol*. <https://doi.org/10.3389/fphys.2015.00241>
- Saliev T, Mustapova Z, Kulsharova G, Bulanin D, Mikhlovsky S (2014) Therapeutic potential of electromagnetic fields for tissue engineering and wound healing. *Cell Prolif* 47:485–493
- Savelev I, Myakishev-Rempel M (2020) Possible traces of resonance signaling in the genome. *Prog Biophys Mol Biol* 151:23–31. <https://doi.org/10.1016/j.pbiomolbio.2019.11.010>
- Shen X, Mei W, Xu X (1994) Activation of neutrophils by a chemically separated but optically coupled neutrophil population undergoing respiratory burst. *Experientia* 50:963–968
- Sun Y, Wang C, Dai J (2010) Biophotons as neural communication signals demonstrated by *in situ* biophoton autography. *Photochem Photobiol Sci* 9(3):315–22
- Tzambazakis A (2015) The evolution of the biological field concept. In: Fels D, Cifra M, Scholkmann F (eds) *Fields of the Cell*. Research Signpost Trivandrum, p 1–28



Understanding Fritz-Albert Popp's Biophoton Theory from the Viewpoint of a Biologist

25

Yu Yan

25.1 Introduction

I met Fritz for the first time in 1993 in my hometown Hangzhou, a city around a beautiful lake. It was my final year of undergraduate study in Hangzhou. Even after so many years, I still remember the many scenes of our meeting. He presented me with a gift, a book with the title *Recent Advances in Biophoton Research and Its Applications*, which led me into a totally new world of scientific research and changed my career fundamentally. Since then, I have been studying and working in the field of biophoton research. Fritz and many other authors of that book became my teachers and colleagues in those exciting years of research. The researchers were from different nations and from different disciplines. They all contributed to the understanding of biophotons. With the experimental findings and the mathematical formulas, Fritz and colleagues introduced the quantum physical principles in biology. They paved a new way of thinking about “what is life?”

25.2 Biophotons

A biophoton is a photon. A photon is itself an interesting phenomenon. In his lectures, Fritz often described a photon in the following way: “If a photon propagates in a light beam, you can't see it at all; only if a photon hits your retina and its energy is absorbed, and the multiplication product of the absorbed energy and the absorption time is equal to or larger than the Planck's constant, you may see it, but at that time, it is not a photon anymore.” Two important aspects of a photon are described here: (1) a photon can transit from one form (wavelike) to another (particle-like) and (2) a photon can only be detected by chance when its energy is absorbed within a

Y. Yan (✉)
Meluna Research B.V. Business & Science Park Wageningen,
Wageningen, The Netherlands
e-mail: yan@melunaresearch.nl

certain time, which is dependent on its frequency and phase. Both aspects are important for understanding the interaction between photons and biomolecules. Their importance will be discussed later in the text.

Fritz-Albert Popp's concept of biophotons was inspired by Alexander Gurwitsch's finding of mitogenetic radiation (see Chap. 2) (Gurwitsch and Gurwitsch 1959). Mitogenetic radiation was not directly measured but detected via a bioindicator (onion roots). It was related to cell division and hypothesized as an emission in the ultraviolet (UV) range. Based on the direct measurements of ultraweak photon emission from biological samples, Fritz and colleagues extended the term “biophoton” to a general phenomenon of almost all living organisms (Rattemeyer et al. 1981; Li and Popp 1983; Popp et al. 1988, 1992; Chang et al. 1998), in all cell cycles, and in a broad band 200–800 nm (whole visible range + partially UV and infrared (IR)). Furthermore, they developed a set of theories to explain the origin and meaning of the biophotons.

25.3 The Spectrum of Biophotons

In the literature, biophotons are observed in the 200–800-nm range, which includes the full visible light range with narrow extensions into the ultraviolet and infrared range. Is it just a coincidence for the overlapping of biophoton spectral range to the visible range? Or is the biophoton spectral range just specified by the photon detector's spectral sensitivity range? After a careful study of Fritz's biophoton theory, the answer is “no.” This spectral range is only a tiny fraction of the electromagnetic wave spectra but has a special meaning to living organisms on Earth.

In Fritz's publications and lectures, he postulated that one of the most important functions of biophotons is triggering (Popp et al. 1992; Chang et al. 1998; Belousov et al. 2007). Biophotons that are emitted from a part can trigger further activities of another part within a biological system or within

a population of living organisms. In fact, Gurwitsch's mitogenetic radiation pointed to the same postulation: cells in division can trigger cell division in another root via photons. If a biophoton functions as a kind of trigger signal, then it should fulfill three conditions: (1) it can propagate through the media without or with a low loss of its signal strength, (2) it can be generated by the sender and absorbed by the receiver, and (3) the generation and absorption of the signal will not destroy the sender and the receiver.

In a living organism, the most important medium is water. On an average, water makes up 70% of the total cell mass. It is a strong absorber for a wide range of electromagnetic waves (<200 nm or >800 nm). However, it has low absorption exactly in the range of 200–800 nm. This is the reason why water appears transparent to the human eye because visible light can transmit through it with almost no loss. The photons in the 200–800-nm range fulfill the first condition.

Activities in a cell are based on chemical reactions. A chemical reaction is a procedure of rebuilding the bonds of a molecule. A bond (for example, a C–C bond) is a sharing electron pair of the outer electron shell of two atoms. In a reaction, an electron first needs to be activated to a higher energy level so that the old bond can be broken; then, this electron can build a new bond with another electron and turn to a lower energy level. The energy level changes are fueled by quantum energy, which is equivalent to a photon's wave. However, not all photons have the same energy and not all photons can interact with the outer electrons. The wavelength of a photon corresponds to its energy and determines the size of its absorber (Fig. 25.1). Long-wave photons (from mid-infrared to microwave) have such long wavelengths that they can only interact with a molecule and trigger its motion and vibration. On the other side, short-wave photons (from extreme ultraviolet to gamma rays) represent ionizing radiation. Each of these photons can simply deliver enough energy for an electron to escape from an atom and cause damage of biological molecules. Therefore, neither of the above photon types can fulfill the second and third conditions at the same time.

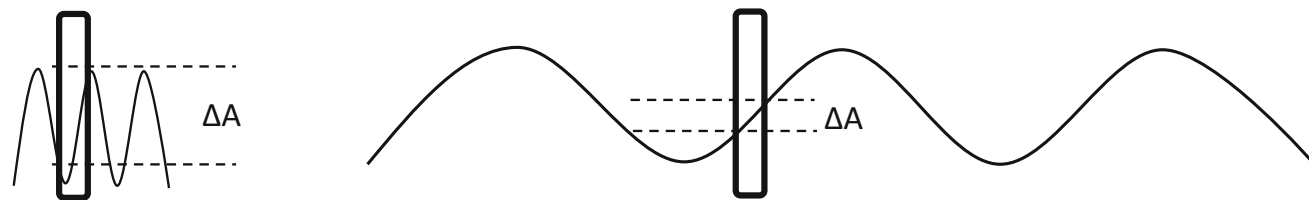


Fig. 25.1 When a wave travels through an absorber, the amplitude change ΔA within the space of the absorber is dependent on the ratio between its wavelength and the size of the absorber. A photon is a quantum wave, which means that its amplitude cannot be partially

Visible light and near-UV and near-IR range photons can interact with the outer electrons of an atom. Each of these photons can deliver energy for an electron to change its energy level but will not hit it away from its atom. The photons in this range fulfill the abovementioned second and third conditions. The most prominent examples for the interaction between photons and biological chemical reactions are photosynthesis and visual perception. In both cases, photons in the visible range interact with the electrons of biomolecules and trigger a sequence of chemical reactions. Fritz and colleagues presented experimental results showing that this kind of triggering effect also exists in other biological processes (Popp et al. 1992; Chang et al. 1998; Shen and van Wijk 2005; Belousov et al. 2007).

25.4 Photons and the Negentropy of Life

Erwin Schrödinger was Fritz's most favorite physicist. In his book *What is Life*, Schrödinger emphasized the relationship between the second law of thermodynamics and life (Schrödinger 1944). What does this physical law say? The simplest explanation is that nature is undergoing an irreversible process. This means, in nature, many processes have only one direction, i.e., $A \rightarrow B$. For example, when we open a gas bottle, the gas will spread to the environment. However, the gas will not return back to the bottle spontaneously. The direction of a process is determined by entropy. If the entropy of B is larger than that of A , then the process can happen in nature. Otherwise, it cannot happen without external influences. Higher entropy means more homogeneity and more randomness, whereas lower entropy means less homogeneity and less randomness (more structure and order). In this sense, we can call high entropy "chaos" and low entropy as "order."

It is possible to make an irreversible process reversible only with external forces and energy input. For example, we can use a compressor to force the gas back into a bottle. Besides these man-made machines, there is a single type of

absorbed like a classical wave. A photon can be either absorbed or not absorbed as a portion (quantum) by chance. The chance is only high if the wavelength matches the size of the absorber

system in nature that can make irreversible processes reversible: life. A plant can use sunlight, CO₂ and water to produce sugar (wood) and O₂ through photosynthesis. In fact, wood can be burned with O₂ easily to produce CO₂ and water in nature, but this process is irreversible according to the second law of thermodynamics. In this sense, a plant can reduce entropy. Schrödinger introduced the term “negentropy” in his book to describe the most fundamental process of life.

Fritz extended the concept of “negentropy” in his book *Die Botschaft der Nahrung* from a more biological view (Popp 2005). The food uptake of heterotrophic organisms (e.g., animals) is not only a simple energy input but also a process of negentropy feeding. Foods are composed of biomolecules with high order (carbohydrates, proteins, fats, etc.), whereas defecated wastes are composed majorly of small molecules with low order. Heterotrophic organisms keep their own entropy low through the entropy difference between foods and wastes. Interestingly, if we analyze both foods and wastes, we will find that their compositions of atoms are almost the same. The input and output of elements (N, O, C, H atoms, etc.) are kept roughly in balance. What is left in the organism's body are the connection forces between these atoms – bonds – which connect those atoms to biomolecules. If we trace along the food chain on Earth back to the origin of these bonds, we will end up with phototrophs (e.g., plants). Unlike animals, plants use sunlight (photons) as the driving force to create negentropy. In photosynthesis, photons are absorbed, which drive the formation of new bonds between the elements (H, C, and O) of CO₂ and water to build carbohydrates, a process from low to high order. Where are the absorbed photons after the photosynthesis? To answer this question, we need to remember one of the two aspects about photons, which are mentioned in the previous text. A photon is a wave but, at the same time, is also a particle (wave-particle duality). When a photon propagates, it behaves like a wave. When it is absorbed by the photosynthetic system, it behaves more like a particle and is bound to an electron, in the form of the so-called “energy level” or “excited state.” Through a complex electron transport chain, the excited electron is built into an electron pair (bond) of adenosine triphosphate (ATP) or nicotinamide adenine dinucleotide phosphate (NADPH), which, in turn, transfers the “energy level” to build a bond of sugar in the Calvin cycle. In this sense, the absorbed photons become a part of the bonds that connect the elements in a sugar molecule, which are further transferred to animals along the food chain.

Why can photons create order (negentropy) in life?

25.5 Coherence

Fritz and some physicists independently but also inevitably started to search the answers for the above questions in one property of photons – coherence. Photons are a kind of

waves – electromagnetic waves. Waves can interfere with each other when they have close frequencies, directions, and polarities. When a bundle of waves have the capability to interfere with each other, they are coherent. By incoherent photons, the intensity is homogeneously distributed in space because it is the result of accumulation of independent photon waves. On the contrary, by coherent photons, the intensity can be locally high (constructive interference) or locally low (destructive interference) in space. If the total intensity in this space is the same, then the coherent photons show lower entropy than do the incoherent ones because they have less homogeneity and randomness.

This means that coherent photons can bring about negentropy (order). One important aspect for biology is the spatially local synergetic effect of coherent photons. The intensity can be diminished through destructive interference at a location when the photons are not needed and can be amplified through constructive interference at another location when the photons are needed. This kind of local synergetic effect can bring about precision and efficiency.

A living cell carries out thousands of reactions simultaneously. These reactions happen in certain compartments in a cell, in certain directions, and in certain times with high precision and high efficiency. The cell compartments are mainly built from the membrane system and cytoskeleton. Both reaction directions and time are mainly controlled by the active sites of enzymes. The structures of these compartments and active sites are well-studied at the molecular level. However, to explain why these structures can facilitate high precision and efficiency, we have to go beyond the molecular level. For Schrödinger, this precision in life is related to quantum coherent systems (Schrödinger 1944). He suggested that life processes make use of coherent mechanisms because such mechanisms are much more precise and able to operate below the statistical (chance) phenomenon of thermal noise. In recent years, the quantum coherence phenomenon and its role in the high efficiency of biological systems have been discovered and intensely studied. One of the most popular topics in this field is the highly efficient light-harvesting ability of photosynthetic systems of plants (Engel et al. 2007; Lee et al. 2007; Tzu-Chi Yen and Cheng 2011; Nelson et al. 2018). The quantum efficiency of these systems can reach an unbelievably high rate of >95%. Based on experimental evidence, e.g., two-dimensional (2D) electronic spectroscopy, researchers have revealed that the energy transfer in photosynthetic complexes is a wavelike coherent motion between the excitons (one excited state). Based on the experimental findings on delayed luminescence (DL) and ultraweak photon emission (UPE), Fritz and colleagues (Belousov, van Wijk, Li, Gu, Musumeci et al.), in their numerous publications, postulated that such quantum coherence generally exists in biological systems, not only in light-harvesting systems (Li and Popp 1983; Popp et al. 1988, 1992; Chang et al. 1998; Scordino et al. 2000; Popp and Yan

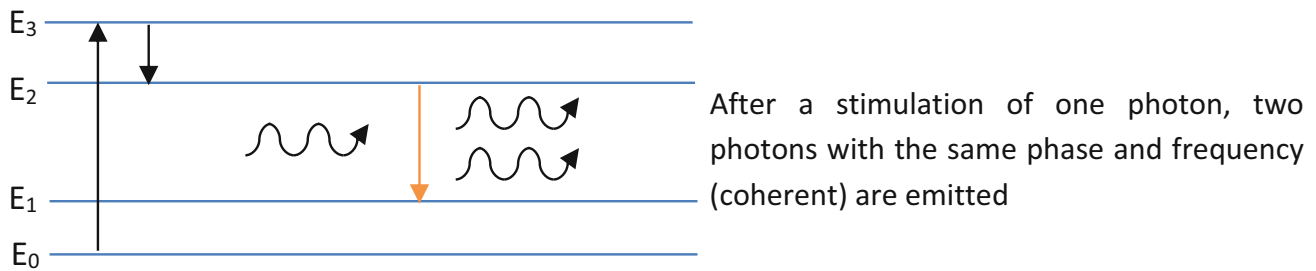


Fig. 25.2 The principle of stimulated photon emission (laser). E_0 is the ground state and E_1 , E_2 , and E_3 are the excited states. E_3 is an unstable state and will drop to the more stable state E_2

2002; Popp and Belousov 2003; Brizhik et al. 2003; Shen and van Wijk 2005; Belousov et al. 2007; van Wijk 2014).

How can the classical and mechanical motions of chemicals in a cell produce quantum coherence? To answer this question, we first look at the principle of laser – a quantum coherent light. Laser is a stimulated photon emission, which has two special aspects: (1) it needs a stimulation (photon) and (2) the emitter (an electron or a molecule) is in an excited state (Fig. 25.2).

By laser, coherent light emission is produced when a photon stimulates a metastable excited electron or a molecule (in the excited state E_2). Then, two coherent photons are emitted when the electron or molecule jumps to a lower excited state, i.e., E_1 . To understand this process, we can look at an analogue in our classic world. Some of us play the guitar, and most of us have seen others playing a guitar. Before playing, one important task is to tighten the strings. When a string is tightened, no matter how strongly a player plucks the string, it will always produce a sound with the same tone (a specific package of frequencies). However, when a string is loose, depending on how strong a player plucks the string, it will produce different tones or even no tone. Compared to laser, the loose string is the ground state E_0 , the tightened string is the metastable excited state E_2 , whereas the player's plucking finger is the stimulating photon. The tightened string or the excited electron (or molecule) functions as a resonator, which produces coherent waves. They are in the so-called metastable state because they need certain force or energy to keep the state. In case of the guitar string, as soon as the tightening force disappears, it will become loose (back to its ground state).

If we understand the above principle, we can imagine how a biological system could generate quantum coherence. Fritz and colleagues suggested a four-state model of biomolecules, which is analogous to the principle of laser (Fig. 25.2) (Popp et al. 1992). A biomolecule is pumped to the excited state E_3 and then stays in the stable excited state E_2 . Such biomolecules in excited states give rise to the coherent features in DL and UPE. To understand the coherent features in a biological system, three major questions need still to be clarified:

1. What kinds of physical structures facilitate the quantum coherent phenomenon?
2. How are these physical structures formed?
3. What is the pumping energy to keep the coherent metastable excited states?

If we take the analogue of the guitar again, the first question is about what the guitar string is made of, the second question is about what construction keeps the string tight, and the third question is about who tightens the string.

25.5.1 The Coherence Facilities

In his theory on coherence in biology, Fröhlich suggested that the metastable highly polar states of proteins are the excited states responsible for the coherence in a biological system (Fröhlich and Kremer 1983; Fröhlich 1988).

Fritz and colleagues postulated that the exciplexes (a well-known excited metastable state) in biomolecules, for example, DNA, are the basic structures for the quantum coherence in a cell. An exciplex exists when two atoms or molecules build a dimer, whereby one atom or molecule is in the excited state and the other one is in the ground state. If both are strongly polarized, then they will build a metastable complex (an exciplex) (Popp et al. 1992).

In the study of photosynthetic systems, the researchers suggested that the excitons among the chlorophyll complexes are the structures for the coherent energy transfer (Lee et al. 2007; Nelson et al. 2018). An exciton is a bound state of an electron/electron hole, as we may have heard from semiconductor theory.

In general, these metastable excited states suggested by the physicists have some common features: (a) electric force (Coulomb force) is involved and (b) they are polarized. In case of a guitar, mechanic force creates certain tension on the string and allows it to produce resonant tones. In the microscopic structures in a cell, the electric force also creates a kind of “tension,” which may give rise to coherent electromagnetic waves.

25.5.2 The Formation of the Metastable Excited States

All of the above researchers mentioned the roles of conformation of biomolecules in the formation of metastable excited states. Fröhlich suggested that the conformation of proteins gives rise to metastable highly polar states. The researchers of photosynthetic systems also postulated the role of proteins in the protection of excitonic states. Fritz and colleagues described the theory and experimental evidence of the relationship between DNA conformation and the exciplex state (Rattemeyer et al. 1981; Li 1992).

25.5.3 Pumping Energy to Keep the Coherent Metastable Excited States

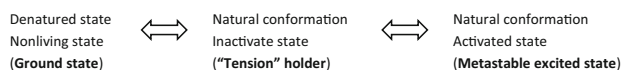
Fröhlich et al. suggested that there exists a loss-free energy transport between proteins, which excites the metastable state. Fritz and colleagues postulated that either incident photons or energy metabolism (ATP, glycolysis, etc.) delivers the pumping energy required for keeping the metastable excited states (Gu 1992).

25.5.4 A Summary of the Coherence Model in Biology

After the above reviews, we may have a rough picture of how a biological system develops coherence, from the viewpoint of Popp and colleagues.

First, a kind of electric force needs to be established in order to create "tension." The electric force that creates tension is not a novel occurrence for a biologist. In a cell, there are several pumping systems that create proton or ion membrane gradients. The most prominent ones are the proton pumps of the mitochondria. In a macromolecule, electric polarizations and charges play an important role for its function. One example is chlorophyll that has a core of a magnesium ion, which is fixed in the center of four chlorins through electric force.

Second, the macromolecules in a cell should be capable of forming metastable excited states, which is crucial for a possible coherent energy transfer. The formation of a metastable excited state requires two more conditions: (1) a mechanism to keep the state and (2) pumping energy for excitation. Analogous to the guitar, to tighten a string, you need: (1) a holder to keep the tightness of the string and (2) force to tighten the string. Interestingly, we can find an analogue in molecular biology. A macromolecule (protein, DNA, etc.) has three different states:



Proteins and DNA will lose their conformation at high temperatures and become long strings without biological functions. In this form, their atoms and functional groups are mostly in their ground state because of the loss of hydrophilic force. We can consider this state as the ground state of a macromolecule. As soon as the temperature drops below a critical point, the macromolecules will form their natural conformation in an aqueous environment. The hydrophilic force plays a crucial role in building the natural conformation. It is in fact a kind of electric force caused by polarized molecules (e.g., water) and polarized chemical groups on the macromolecules. The stability of the hydrophilic force is dependent on the motions of molecules. At high temperatures, the random motions of the molecules are so fast that the hydrophilic forces between them cannot be maintained. Only when the temperature drops below a critical point can the random motions become slow and the hydrophilic forces be maintained again so that the macromolecules form their natural conformations. This kind of behavior of macromolecules resembles well a guitar string made of nylon (polyamide). At room temperature, it is tough and elastic so that it can be tightened and hold tension, which is crucial for generating a tone. However, when a nylon guitar string is heated above its glass-transition temperature (>50 °C), it becomes soft and cannot hold tension anymore. Without tension, it cannot generate a specific tone either.

The natural conformation of a macromolecule builds the "tension" holder to maintain the excited state. When it receives energy from ATP or through other ways, it will enter the activated state: the metastable excited state. In this state, the macromolecule will have its full function with a high precision and efficiency.

25.6 Perspectives

In 2018, Fritz left us. During the funeral held at his hometown Coburg, I recalled our first meeting in my hometown. At one point, it seemed that our meeting was a coincidence. However, after so many years of research work together with Fritz, I have a feeling that our meeting was somehow inevitable.

The biophoton research of Fritz and colleagues opened my mind and answered a lot of my questions about life from the viewpoint of a biologist. Furthermore, it has also brought about the emergence of far more questions about life. To address these questions, a close collaboration between physicists and biologists is crucial. For me, one major

question is essential for our further journey in the study of this mind-opening field: How can we improve the communication between biologists and physicists? In the research on biophotons, physicists think in the way of quantum mechanics, whereas biologists do so in the way of classical physics. On the other side, biologists are familiar dealing with complex systems, whereas physicists tend to deal with simplified systems. We need to find a way to understand the language used by the each side and develop a kind of coherence between the two different disciplines.

References

- Belousov L. V., Voeikov V. L., Martynyuk V. S. (2007): *Biophotonics and Coherent Systems in Biology*, Springer
- Brizhik L., Musumeci F., Scordino A., Tedesco M., Triglia A. (2003): Nonlinear dependence of the delayed luminescence yield on the intensity of irradiation in the framework of a correlated soliton model, *Phys. Rev. E* 67, 021902
- Chang J. J., Fisch J., Popp F. A. (1998): *Biophotons*, Springer Netherlands
- Engel G. S., Calhoun T. R., Read E. L., Ahn T. K., Mancal T., Cheng Y. C., Blankenship R. E., Fleming G. R. (2007): Evidence for wavelike energy transfer through quantum coherence in photosynthetic systems, *Nature*, volume 446, pages 782–786
- Fröhlich, H. (1988): *Biological Coherence and Response to External Stimuli*, Springer
- Fröhlich, H., Kremer, F. (1983): *Coherent Excitations in Biological Systems*, Springer
- Gu Q. (1992): Quantum theory of biophoton emission, in *Recent Advances in Biophoton Research and its Application*, eds. Popp F. A., Li K. H. and Gu Q. (World Scientific Publishing Co.), 59–112
- Gurwitsch, A. G., and Gurwitsch, L. D. (1959): *Die Mitogenetische Strahlung, ihre physikalisch-chemischen Grundlagen und ihre Anwendung auf die Biologie und Medizin*. G. Fischer, Jena.
- Lee H., Cheng Y. C., Fleming G. R. (2007): Coherence Dynamics in Photosynthesis: Protein Protection of Excitonic Coherence, *Science*, Vol. 316, Issue 5830, pp. 1462–1465
- Li K. H. (1992): Coherent radiation from DNA molecules, in *Recent Advances in Biophoton Research and its Application*, eds. Popp F. A., Li K. H. and Gu Q. (World Scientific Publishing Co.), 157–195
- Li K. H. and Popp F. A. (1983): Non-exponential decay law of radiation systems with coherent rescattering, *Phys. Lett. A* 93, 262–266
- Nelson T. R., Ondarse-Alvarez D., Oldani N., Rodriguez-Hernandez B., Alfonso-Hernandez L., Galindo J. F., Kleiman V. D., Fernandez-Alberti S., Roitberg A. E., Tretiak S. (2018): Coherent exciton-vibrational dynamics and energy transfer in conjugated organics, *Nature Communications*, volume 9, Article number: 2316
- Popp F. A. (2005): Die Botschaft der Nahrung, *Zweitausendeins*
- Popp F. A., Yan Y. (2002): Delayed luminescence of biological systems in terms of coherent states, *Physics Letters A* 293, 93–97
- Popp F. A., Belousov L. V. (2003): *Integrative Biophysics Biophotonics*, Springer Netherlands
- Popp F. A., Gurwitsch A. A., Inaba H., Slawinski J., Cilento G., van Wijk R., Chwirot W. B., and Nagl W. (1988): Multi-author Review on biophoton emission, *Experientia* 44, 543–600
- Popp F. A., Li K. H. and Gu Q. (1992): *Recent Advances in Biophoton Research and its Application*, World Scientific Publishing Co.
- Rattemeyer M., Popp F.A., Nagl, W. (1981): Evidence of photon emission from DNA in living systems. *Naturwissenschaften* 68 (11), 572–573
- Schrödinger E. (1944): *What Is Life?*, Cambridge University Press
- Scordino A., Triglia A., Musumeci F. (2000): Analogous features of delayed luminescence from *Acetabularia acetabulum* and some solid state systems, *Journal of Photochemistry and Photobiology B: Biology*, Volume 56, Issues 2–3, Pages 181–186,
- Shen X., van Wijk R. (2005): *Biophotonics Optical Science and Engineering for the 21st Century*, Springer US
- Tzu-Chi Yen T. C., Cheng Y. C. (2011): Electronic coherence effects in photosynthetic light harvesting, *Procedia Chemistry* 3, 211–221
- van Wijk R. (2014): *Light in shaping life: Biophotons in biology and medicine*, Meluna



Limits to Information Transfer Through Biological Autoluminescence

26

Ondřej Kučera

26.1 Introduction

“...and now I watch for the light, the signal-fire breaking out of Troy, shouting Troy is taken,” says a poor watchman in “Agamemnon,” an old Greek play by Aeschylus (1984). The watchman waits for a signal of the relay of beacon fires, which were arranged by Queen Clytemnestra, informing the town of Mycenae about the Greek victory in Troy and warning the faithless queen herself about the return of her cheated husband. While the message about the fate of Troy is rather complex, it is transmitted by a binary signal, darkness or fire, because the sender in Troy and the receiver in Mycenae had a priori knowledge about the meaning of the signal. No further complexity was needed provided that there were no other fires in that particular part of the horizon, which could be mistakenly read as an anticipated signal, and that the signal was sent at night under favorable atmospheric conditions in order to be visible from a long distance. Although doubtlessly fabulated by Aeschylus, this story charmingly exemplifies the problems of the hypothesis on biocommunication through ultraweak photon emission (UPE).

UPE, which is likely a side product of oxidative metabolism (Cifra and Pospíšil 2014), is a “cold light” of biological origin that has an extremely low intensity. Unlike bioluminescence, which is visible to the naked eye and has been known since ancient times, as reported by Aristotle (Wilson and Hastings 1998), UPE is not perceivable by the human eye and is not generated by a dedicated enzymatic system. It was suggested as a mechanism to explain the correlative effects between chemically separated cell cultures (Laager 2015;

Scholkmann et al. 2013) because these effects were present only under the condition of optical connection between the cultures and, strikingly, they disappeared after blocking of the optical path. Although this hypothesis is logically plausible, in the following, we show that it challenges our understanding of the physical theory of communication. We argue that alternative ways of signaling shall be sought to explain these effects and that UPE is unlikely to be a general mechanism of biocommunication in typical biological contexts.

26.2 Biocommunication Through Light

Communication through light is a common feature in nature. Mostly, however, such communication uses reflected sunlight as a means of signaling and the signals are interpreted by visual perception. Seeing a wolf that bares its teeth to signal its intentions is a trivial, yet vitally important, example of signaling using reflected sunlight. More sophisticated examples include aposematism, i.e., signaling of toxicity or harmfulness by intense coloration, mimicry of this coloration by other species, or dynamic change of the skin coloration of chameleons that serves not only as camouflage but also as a behavioral signal to other chameleons (Ligon and McGraw 2013). Less commonly, some organisms produce signaling light themselves. Bioluminescent signaling has been observed in various forms of aquatic life and some terrestrial organisms. Fireflies, a well-known terrestrial example, employ bioluminescence to attract mates. In summary, as many species use natural or endogenous light as a means of communication, the hypothesis that UPE might be used for communication too is biologically uncontroversial. Since UPE is readily available in many organisms as discussed elsewhere, it could serve as a more general mechanism than bioluminescence.

The UPE biocommunication hypothesis suggests that some cells employ UPE for signaling purposes. This hypothesis, in other words, assumes that (i) cells, cell cultures, or

O. Kučera (✉)

Institut de recherche interdisciplinaire de Grenoble, Commissariat à l'énergie atomique et aux énergies alternatives (CEA), Grenoble, France

Department of Engineering Technology, South East Technological University, Waterford, Ireland
e-mail: ondrej.kucera@setu.ie

tissues (referred to as the sender in the following for the sake of simplicity) can modulate the UPE-generating mechanism in order to encode information in UPE and efficiently emit UPE and (ii) other cells (the receiver) can receive UPE, and decode the information it bears. It also assumes that the physical conditions of an environment allow for the transmission of UPE. Unlike radio-frequency electromagnetic fields, light is indeed a more plausible mechanism of signaling at a distance (Kučera and Cifra 2016). In the following, we will dissect the hypothesis along these lines and discuss its feasibility. We deliberately use general language to describe the mathematical and physical concepts behind this reasoning in order to make the text accessible to a broader readership, particularly life scientists. We kindly ask readers interested in a more rigorous description of the concept of communication in noisy environments to refer to the literature on information and communication theory (Shannon 1949; Chaaban and Hranilovic 2020).

26.3 Information Contents of UPE

The central part of any communication or signaling is the message that is to be transmitted. This message carries information, which is unknown to the receiver. The information contents of the message and its meaning, however, can be two different things. Using the example of Agamemnon, the light of the fire from Troy carried binary information contents of 1 bit (“yes” or “no” to whether Troy was conquered), but its extensive meaning could not be interpreted from the message itself. Similarly, the biological information contents of a UPE signal may not be lengthy if the receiver already has instructions on how to interpret it (that is to say, the signal would elicit a unique message-specific response of the molecular machinery of the cell). It comes as no surprise then that the detailed response of the receiver to the UPE signal cannot be deduced from the pure information contents of the UPE itself. What nevertheless could be ascertained from UPE is how many different messages it can carry.

In many natural systems, the observed UPE is a quasi-stationary signal, stable over a range of minutes. This would suggest that the number of messages carried by UPE is somewhat limited. In an extreme case, UPE might serve as an always-on sign that would signal the presence of the sender cell. The absence of this signal would be a sign that the sender is either not around anymore or is no more. The optical separation and the death of one of the populations would be indistinguishable and shall produce similar correlative effects. Although this could be a realistic scenario, it has not been tested to our knowledge.

The nonstationary development of UPE has a timescale of changes in the order of tens of seconds (Rossetto Burgos et al.

2018) or more (Gallep et al. 2013). Rapid variations of UPE on the scale of seconds usually follow drastic external chemical stimuli, such as treatment with hydrogen peroxide (Rác et al. 2015) or triggered respiratory burst (Rossetto Burgos et al. 2017, 2018). These changes of the waveform of UPE resemble and follow the kinetics of the underlying chemistry (Rossetto Burgos et al. 2016). In light of the observations as mentioned earlier, UPE intensity is proportional to the rate of the underlying chemical reactions, and this is the information it carries.

The spectral content of UPE was only sparsely analyzed in the works on UPE. Theoretical analysis of the molecular pathways, which are likely involved in the generation of UPE, specifies several principal wavelengths of the emission (Pospíšil et al. 2014). It would be unrealistic, however, to expect the UPE following these pathways to have extremely sharp line spectra. The inherent uncertainty of the radiative decay leads to line broadening, and, we may, therefore, expect these principal wavelengths to create effectively overlapping bands. Indeed, a rare experimental example indicates that the emissions from both yeasts and neutrophil-like cells are broader than 100 nm within the visible spectrum (Nerudová et al. 2015). A study of UPE from the skin of mice reported similar results (Zhao et al. 2017). In other published works, also, we may deduce from the sensitivity of the used detection techniques that UPE covers broad parts of the visible spectrum. Although there have also been claims about the emission in near-ultraviolet and infrared regions, no spectrometric data have been provided. On the one hand, no molecular mechanism that could generate ultraviolet photons is known in a biological context nor does it seem feasible due to the lethal effects of ultraviolet radiation. On the other hand, the infrared region is dominated by thermal emission. Although the measured spectra of UPE are mostly missing, we may conclude that the emission is likely bounded within the near-infrared and visible part of the spectrum. Although a broad spectrum of the emission could indicate significant information contents, and it is indeed a good strategy for communication over the noisy environment (Shannon 1949), the underlying line-broadening phenomena disprove such a hypothesis.

The information contents of UPE were also studied by fractal analysis with limited success (Dlask et al. 2019). As the claims about the coherence of UPE are not substantiated (Cifra et al. 2015), the photo-count statistics of UPE seems to follow the classical Poisson distribution (Rafieiolhosseini et al. 2016). UPE is also likely transmitted uniformly in all directions. All these observations support the view that UPE is a fingerprint of chemical reactions that have limited capacity to encode a large amount of information. As the variance of UPE is rather low at biologically relevant timescales, we conclude that should UPE play a role in signaling, its

alphabet of keys, or, in other words, the number of different messages it might carry, is likely to be highly limited.

26.4 UPE Modulation

Above, in the discussion of the information contents of UPE, we focused on the signal properties of the emission. Now, we will direct our attention to the same property from a different point of view. With the exception of the always-on scenario described above, the ability of the sender to modulate the emission of UPE is a crucial prerequisite for signaling. What is modulation in this context, and why is it so important? By modulation, we mean the ability to regulate the intensity and the wavelength of an emission. In a minimal case, this would mean the ability to initiate and inhibit the emission. In a maximum scenario, we could envision some version of amplitude and frequency modulation that would enable virtually unlimited variability of messages to be sent. However, could some form of more complex modulation have a benefit even for the sender, which has, as we argued above, highly limited alphabet?

As we discuss in more detail later, the main problems with signaling via UPE are the lack of specificity and transmission in a noisy environment. A strategy to overcome these limitations is to transmit a signal of higher complexity than that of the message to be transmitted. This can be achieved by encoding the message in a redundant way. To improve the reliability of the relay from Troy, two beacon fires simultaneously or a blinking fire (by blocking the view) could be used, for instance, to minimize the risk of the signal to be mistakenly interpreted as noise (for instance, a bonfire made by shepherds). Similar strategies are used in information technology, and redundancy is also widespread in living systems and molecular signaling.

The requirement of redundancy for reliable information transfer brings us to an important conclusion about the hypothesized UPE signaling: the information contents of UPE are an upper estimate of the real information contents of the signals. As UPE itself has not been proven to be rich in information contents, this conclusion further limits the possibility of the hypothesized signaling based on UPE.

26.5 Transmission

Once emitted, the transmission of light is something that the sender can hardly control. In theory, of course, the sender can actively influence the environment in which the signal is propagating, but it seems far-fetched to expect a sender to use UPE for signaling if it was already able to control the whole path to the receiver physically. In the reported observations, moreover, the sender could not govern the

separating medium, typically glass or quartz. We are therefore left with the assumption that the UPE signal propagates freely from the sender to the receiver with no interference from the sender or the receiver, just like in the case of the relay from Troy.

Along its path, the signal can be attenuated, scattered, or diverted by the environment, thus distorting the fidelity of the transmission and limiting the possibility of detection by the receiving cells. Moreover, the presence of other transmitters would lead to interference or cross talk. Any advanced free-space communication strategy has to compensate for these adverse effects. Such a strategy requires some degree of synchronization between the transmitters and some knowledge about the properties of the optical path. As this is unlikely to happen, UPE signaling would have to be free of any communication complexity. This fact adds to our previous conclusion about the extremely limited alphabet of UPE.

Importantly, the path, over which the signal propagates, is subject to background light, the noise. This natural light masks the UPE light from the sender. A level of background light is context-dependent, naturally varying by many orders of magnitude depending on the environment and day time. The level of this noise is not uniform along the spectrum; however, it is never too low so that some wavelengths could be considered silent (absent from noise). In all relevant settings, therefore, the background light is always much stronger than UPE (Kučera and Cifra 2013). Therefore, as there are no indications that the energy (wavelength) or the angular momentum (polarization, spatial distribution) of the UPE photons and their statistical properties would differ from those of the natural background, the latter simply adds to the former. This is an important feature that undermines the feasibility of signaling via UPE as we will now show.

26.6 Reception

Cells possess photosensitive complexes such as rhodopsin that can play a role in the reception of light and make the reception of UPE theoretically possible (Laager 2015). There are, however, fundamental physical constraints that limit the amount of information per unit of time that can be transmitted over a noisy environment and detected by the receiver (Shannon 1949). As UPE photons (the signal) are indistinguishable from other photons (the noise) by principle, this limit applies to the possibility of UPE signaling too. Intuitively, it is easier to see the light of fire at night than in the daylight, so the limit clearly depends on the ratio of the intensities of the signal to the background noise. As the noise becomes stronger than the signal, the amount of transferable information decreases. Observations that are long enough, however, enable us to assess the statistical difference between the signal and the noise. Put in another way, using a

broader band of wavelengths increases the amount of information that can be sent and correctly received (Shannon 1949; Chaaban and Hranilovic 2020; Kučera and Cifra 2013). However, here, we hit another physical limitation.

All molecular processes, as we showed earlier, have line emission spectra that are not continuous. Moreover, these lines are spread by the uncertainty principle and limited efficacy. The available bandwidth is, therefore, rather limited because the spectrum cannot be efficiently covered. The same is true for the excitation spectra, meaning that the distinguishability of near wavelengths is drastically limited and so is the bandwidth that can be used for the reception of the signal. Finally, there is no up-to-date knowledge of a biological mechanism that could detect the multi-wavelength optical signal, process the input on each wavelength to extract the useful signal from noise, and translate it into a biochemical signal at a single-cell level. One may argue that multiple cells can cooperatively overcome these limitations. However, as the cells would have to share the same communication channel, the signal would be subject to interference and cross talk, adding another complexity to the already difficult task to receive the message.

Under the unfavorable conditions, we have just described, the receiver would have to put in all the efforts to compensate for the low probability of detection of a UPE photon. It would have to maximize the detection sensitivity on the one hand and minimize the number of false detections, on the other hand. However, do the cells actually do it? An experiment may provide the answer rather easily. On the hypothesized detection side, the UPE signal should be prone to masking by external light, as we have discussed above. The reported correlative effects in experiments could, therefore, possibly be disturbed by an external illumination of suitable properties. This experimental direction, which could bring about invaluable resolution to the controversy, nevertheless, was not followed.

The watchman in Mycenae had an easy task because he knew where on the horizon the fire was to be lighted. He could, therefore, apply what engineers call spatial filtering and focus only on that particular spot on the horizon, ignoring other fires that might interfere from other directions. In the reported experiments, however, it is unrealistic to expect that cells, the sender, and the receiver had knowledge about their respective positions. Therefore, they could not have used the same trick. It is also doubtful whether the benefits of UPE communication would counterweigh the costs for the machinery required for establishing this narrow line of sight. Although we may not rule out the possibility that cells in highly organized tissues could establish some form of spatial filtering, it is quite an unrealistic scenario, for example, in paramecia (Fels 2009). Moreover, spatial filtering would likely require some alignment and beamforming of the emission. Finally, the optical properties of biological

systems seem to imply a rather diffuse mode of light propagation. A wide field-of-view signaling is, therefore, a more realistic option.

26.7 Conclusions

We have discussed the hypothesis that biological systems could utilize UPE for biocommunication. Although this communication can be in the form of simple signaling, and, as such, there might be no need to send lengthy messages, the hypothesis fails to explain how could biosystems distinguish UPE signals from ambient noise. Photons simply do not have the specificity of biomolecules. The theoretical possibility of information transfer by UPE is further undermined by the fact that UPE signals themselves do not exhibit any nontrivial properties, which could improve the unfavorable situation.

The biocommunication hypothesis was motivated by observation. Here, we argued that UPE, due to its extremely low intensity, does not seem to be the signaling mechanism that could explain such observations and thus be, at the same time, a general phenomenon with occurrence in various biological contexts. We may only speculate about the influence of volatiles (Pichersky and Gershenzon 2002; Schmidt et al. 2015) or vibrations (Mathijssen et al. 2019) in the experiments. Nevertheless, we assume that alternative mechanisms can provide a more suitable explanation of the observations.

If the watchman in Mycenae were a cell, he would not see just one beacon fire on the horizon. He would see millions of lights, having almost no chance to say which of them are lighthouses marking safe harbors and which single one is the signaling fire he ought to patrol.

References

- Aeschylus, *Agamemnon* (Penguin Books, New York, 1984).
- M. Cifra, P. Pospíšil, Ultra-weak photon emission from biological samples: Definition, mechanisms, properties, detection and applications. *J. Photochem. Photobiol. B Biol.* **139**, 2–10 (2014).
- T. Wilson, J. W. Hastings, Bioluminescence. *Annu. Rev. Cell Dev. Biol.* 197–230 (1998).
- F. Laager, Light based cellular interactions: hypotheses and perspectives. *Front. Phys.* **3**, 1–9 (2015).
- F. Scholkmann, D. Fels, M. Cifra, Non-chemical and non-contact cell-to-cell communication : a short review. *Am. J. Transl. Res. Res.* **5**, 586–593 (2013).
- R. A. Ligon, K. J. McGraw, Chameleons communicate with complex colour changes during contests: Different body regions convey different information. *Biol. Lett.* **9** (2013), <https://doi.org/10.1098/rsbl.2013.0892>.
- O. Kučera, M. Cifra, Radiofrequency and microwave interactions between biomolecular systems. *J. Biol. Phys.* **42**, 1–8 (2016).
- C. E. Shannon, Communication in the Presence of Noise. *Proc. IRE.* **37**, 10–21 (1949).

- A. Chaaban, S. Hranilovic, Capacity of Optical Wireless Communication Channels. *Philos. Trans. R. Soc. A* (2020).
- R. C. Rossetto Burgos, R. Ramautar, E. P. A. Van Wijk, T. Hankemeier, J. Van Der Greef, A. Mashaghi, Pharmacological targeting of ROS reaction network in myeloid leukemia cells monitored by ultra-weak photon emission. *Oncotarget*. **9**, 2028–2034 (2018).
- C. M. Gallego, T. A. Moraes, S. R. dos Santos, P. W. Barlow, Coincidence of biophoton emission by wheat seedlings during simultaneous, transcontinental germination tests. *Protoplasma*. **250**, 793–796 (2013).
- M. Rác, M. Sedlářová, P. Pospíšil, The formation of electronically excited species in the human multiple myeloma cell suspension. *Sci. Rep.* **5**, 1–8 (2015).
- R. C. Rossetto Burgos, W. Zhang, E. P. A. van Wijk, T. Hankemeier, R. Ramautar, J. van der Greef, Cellular glutathione levels in HL-60 cells during respiratory burst are not correlated with ultra-weak photon emission. *J. Photochem. Photobiol. B Biol.* **175**, 291–296 (2017).
- R. C. Rossetto Burgos, E. P. A. van Wijk, R. van Wijk, M. He, J. van der Greef, Crossing the boundaries of our current healthcare system by integrating ultra-weak photon emissions with metabolomics. *Front. Physiol.* **7**, 1–7 (2016).
- P. Pospíšil, A. Prasad, M. Rác, Role of reactive oxygen species in ultra-weak photon emission in biological systems. *J. Photochem. Photobiol. B Biol.* **139**, 11–23 (2014).
- M. Nerudová, K. Červinková, J. Hašek, M. Cifra, Optical spectral analysis of ultra-weak photon emission from tissue culture and yeast cells. *Proc. SPIE*. **9450**, 94500O (2015).
- X. Zhao, M. Yang, Y. Wang, J. Pang, E. Van Wijk, Y. Liu, H. Fan, L. Zhang, J. Han, Spectrum of spontaneous photon emission as a promising biophysical indicator for breast cancer research. *Sci. Rep.* **7**, 1–12 (2017).
- M. Dlask, J. Kukul, M. Poplová, P. Sovka, M. Cifra, Short-time fractal analysis of biological autoluminescence. *PLoS One*. **14**, 1–17 (2019).
- M. Cifra, C. Brouder, M. Nerudová, O. Kučera, Biophotons, coherence and photocount statistics: A critical review. *J. Lumin.* **164**, 38–51 (2015).
- N. Rafeiolhosseini, M. Poplová, P. Sasanpour, H. Rafii-Tabar, M. R. Alhossaini, M. Cifra, Photocount statistics of ultra-weak photon emission from germinating mung bean. *J. Photochem. Photobiol. B Biol.* **162**, 50–55 (2016).
- O. Kučera, M. Cifra, Cell-to-cell signaling through light: just a ghost of chance? *Cell Commun. Signal.* **11**, 87 (2013).
- D. Fels, Cellular communication through light. *PLoS One*. **4** (2009), <https://doi.org/10.1371/journal.pone.0005086>.
- E. Pichersky, J. Gershenzon, The formation and function of plant volatiles: Perfumes for pollinator attraction and defense. *Curr. Opin. Plant Biol.* **5**, 237–243 (2002).
- R. Schmidt, V. Cordovez, W. De Boer, J. Raaijmakers, P. Garbeva, Volatile affairs in microbial interactions. *ISME J.* **9**, 2329–2335 (2015).
- A. Mathijssen, J. Culver, M. S. Bhamla, M. Prakash, Collective intercellular communication through ultra-fast hydrodynamic trigger waves. *Nature*, 428573 (2019).



Sergey Mayburov

27.1 Introduction

It is well known that the development and functioning of large biological systems is performed quite consistently even at large distances between their parts. For example, in the kidney and liver cells, blood erythrocytes identify and attract the proper partner cells and reject the wrong ones at a distance of several microns, which is much larger than the range of chemical forces (Vitiello 2001). Another notorious example is the morphogenesis problem, i.e. proportional and optimal growth of plants and animal organisms. Up to now the mechanism which regulates spontaneous cell division in a necessary and optimal way at significant distances between them is poorly understood. It's difficult to admit that such long-distance coherence can be achieved via chemical messengers only, so it was argued long ago that some other physical mechanism can be responsible for that. In particular, it was proposed that a coherent electromagnetic field, similar to a laser field, can exist inside the biosystem and perform such communications (Frohlich 1968; Popp 1998). However, it seems doubtful that such electromagnetic field coherence can be conserved in a wide frequency range during long time periods of the order of minutes and hours. To support the biological coherence paradigm, Frohlich and others applied the methods of solid-state physics and quantum optics to biological systems, but their arguments do not seem watertight (Frohlich 1968; Vitiello 2001). In principle, such functions can be performed also by intricate noncoherent electromagnetic signaling mechanisms between organism constituents, but no conclusive theory for that was proposed (Kucera and Cifra 2013).

Meanwhile, an alternative idea explaining biological coherence origin was proposed earlier, namely, that it is induced by the fundamental nonlocality of quantum mechanics (QM) (Primas 1982; Josephson and Pallikari-Viras 1991;

Bischof 2003). This phenomenon was first formulated as the famous EPR-Bohm paradox and later developed as Bell's theorem (Jauch 1968; Peres 2002). By now, such effects have been confirmed experimentally and applied in quantum communications and computing (Sudbery 1986; Peres 2002). In fact, this mechanism permits to realize some form of nonlocal correlations (NC) or "action at a distance" between distant subsystems of quantum system S . NC realization in EPR-Bohm variant demands that initially S subsystems S_1, \dots, S_n should interact with each other, while after such interaction has seized, such NC conserves the correlations between S_i uncertain parameters even at a large distance between these S subsystems. Obviously, such conditions are quite difficult to fulfill for communications in dense and warm biological systems. Therefore, the particular EPR-Bohm nonlocality mechanism doesn't look like a suitable candidate for biological coherence explanation. However, it was supposed for long that quantum NC can be a more general concept than the standard QM formalism admits and, in principle, some other NC effects, besides EPR-Bohm one, can exist (Stapp 1997; Cramer 1986; Bell 2004; Norsen 2009; Korotaev 2011). Below we'll discuss experimental results which presumably support this hypothesis, basing on them, novel NC mechanism was proposed (Mayburov, 2021b; Mayburov 2022). Note that this approach is principally different from hidden parameter theories (Sudbery 1986).

Let's consider first the conditions that such a nonstandard NC mechanism should generally obey. Plainly, besides causality demands, such NC should agree with all standard invariance principles i.e. time, space shift, and rotation symmetries. For simplicity, we'll suppose that NC by itself can't transfer energy, momentum, or orbital momentum between distant objects. Hence the system's average energy, momentum, and orbital momentum should not change during such communications. It will be shown below that application of nonlinear NC Hamiltonians permits us to obey such constraints (Doebner and Goldin 1992; Mayburov 2021a, b).

S. Mayburov (✉)

Lebedev Institute of Physics, Moscow, Russia
e-mail: mayburov@sci.lebedev.ru

More complicated NC model variants for which these constraints are absent will be considered elsewhere. Let's analyze which quantum systems can be most vulnerable to such NC influence. Suppose that states of two distant objects S_1 and S_2 begin to differ from standard QM predictions due to their conjugate NC influence during arbitrary time intervals $\{t_0, t_f\}$. As follows from the described assumptions, according to QM rules the initial S_1 and S_2 states can't be stationary, because such states are ground ones and possess minimal energy, so only some energy transfer can make them evolve to another state which will be an excited one. Hence, the reasonable option is that S_1 and S_2 are degenerate systems, i.e. they have several states with the same energy and during interval $\{t_0, t_f\}$ can evolve from the initial state to another one with the same energy. In this case, due to NC influence some S_1 and S_2 parameter values, in principle, can deviate from the standard QM predictions. A simple example of such a system is a particle with energy level E confined in symmetric double well potential divided by potential wall U_0 with $E \leq U_0$. Suppose that such S_1 has two degenerate states g_1 and g_2 in these two wells with the same energy E , and at t_0 it is in state g_1 confined in one well. Thereon, due to under-barrier tunneling it would spread gradually into the other well, so that it will evolve with the time to some g_1, g_2 superposition (Peres 2002). In this case, the hypothetical S_2 NC influence on S_1 can change its tunneling rate in comparison with QM predictions, so that it would influence S_1 state parameters, in particular, resulting in g_1, g_2 probabilities at t_f . Analogous variations would occur with S_2 if it possesses a similar degenerate structure. In this chapter, a phenomenological model of such NC processes involving quantum tunneling will be considered in its framework, with NC effects described by QM evolution equations with specific nonlinear Hamiltonians.

27.2 Experimental Motivations

Experiments considered here concerned situations when a quantum system undergoes abrupt transformations, in particular, this occurs in chemical and nuclear reactions, for example, decays of unstable nuclei. It was acknowledged previously that due to strong nuclear forces no environmental influence can change the isotope decay parameters significantly (Martin 2011). However, recent results indicate that some cosmophysical factors related to Earth's motion along its orbit can influence them, in particular, their lifetime and decay rate at 10^{-3} to 10^{-4} scale (Alekseev et al. 2016; Fischbach et al. 2009). The first results, indicating deviations from exponential β -decay rate dependence, were obtained during the precise measurement of ^{32}Si isotope lifetime. In addition to the standard decay exponent, sinusoidal annual oscillations with an amplitude of about 6×10^{-4} relative to

the total decay rate and maxima at the end of February were found during 5 years of measurements. Since then, annual oscillations of β -decay rate for different heavy nuclei from Ba to Ra were reported, for most of them the oscillation amplitudes are of the order of 5×10^{-4} with their maximum on the average in the middle of February (Fischbach et al. 2009). Lifetime of α -decay isotopes ^{212}Po , ^{213}Po , and ^{214}Po was measured directly, the annual and daily oscillations with amplitude of the order of 7×10^{-4} and annual minima at February–March for different isotopes and daily maxima around 6 a.m. were found during 6 years of measurements (Alekseev et al. 2016). It was shown also that decay rates of ^{53}Mn , ^{55}Fe e -capture, and ^{60}Co β -decay correlate with solar activity, in particular, with intense solar flare moments, preceding them for several days; in this case, observed decay rate variations are of the order of 10^{-3} (Fischbach et al. 2009; Bogachev et al. 2020).

Parameters of some chemical reactions also demonstrate a similar dependence on solar activity and periodic cosmophysical effects. The first results were obtained for bismuth chloride hydrolysis, its reaction rate was shown to correlate with the solar Wolf number and intense solar flare moments (Piccardi 1962). It was demonstrated that for biochemical unithiol oxidation reaction, its rate correlates with solar activity, in particular, with intense solar flares and it grows proportionally to the Wolf number. It was found also that its rate correlates with periodic Moon motion and Earth axis nutation (Troshichev et al. 2004). Takata biochemical blood tests also indicate a strong influence of solar activity and Sun position in the sky (Takata 1951). It is performed via human blood reaction with sodium carbonate Na_2CO_3 resulting in blood flocculation. Its reaction rate parameter demonstrates fast gain for blood samples taken from organisms starting from 6 to 8 min before astronomic sunrise moment, such gain continues during the following 30 min. Such reaction parameter behavior is independent of a mountain or cloud presence at the eastern horizon sector, which can screen the Sun. This parameter demonstrates approximate invariance for blood taken during the solar day and slow decline after sunset, such daily dependence is conserved even in complete isolation from electromagnetic fields and solar radiation. This parameter also demonstrates the gain for larger solar Wolfe numbers and for the test location shift in the direction of Earth's equator. Significant parameter correlation with Sun eclipse moments also was observed; some of these results were confirmed by other groups (Gierhake 1938; Jezler and Bots 1938; Koller and Muller 1938; Kaulbersz et al. 1958; Sarre 1951). Similar daily variations were reported for deuterium diffusion into palladium crystal (Scholkman et al. 2012). The possible connection of these effects with the NC mechanism for chemical reactions will be discussed in the final section.

Experiments of other kinds also exploit some biochemical and organic-chemical reactions. An example is the reaction of ascorbic acid with dichlorophenolindophenol. First, the authors noticed that the dispersion of their reaction rates can change dramatically from day to day, sometimes by one order of value, whereas the average reaction rate practically does not change (Shnoll 1973, 2009; Shnoll and Kolombet 1980). Further studies have shown the connection of this effect with some cosmophysical factors, first of all with solar activity, solar wind, and orbital magnetic field. In particular, average rate dispersion becomes maximal during solar activity minima of the 11-year solar cycle (Shnoll and Chetverikova 1975; Shnoll 2009). It supposes that high solar activity makes such chemical reaction processes more ordered and regular in time. Shielding chemical reactors from the external electromagnetic field in iron and permalloy boxes practically does not change the reaction dispersions, hence such cosmophysical influence can't be transferred by electromagnetic fields. Individual nuclear decay or chemical reaction acts are supposedly normally independent of each other; such stochastic processes are called Poissonian and described by Poisson probability distribution (Korn and Korn 1968). For this distribution, at any time interval dT the dispersion of decay count number $\sigma_p = N^{\frac{1}{2}}$, where N is the average count number per dT . If the resulting dispersion $\sigma < \sigma_p$, which means that this process becomes more regular and self-ordered and is described by the sub-Poisson statistics with the corresponding distribution (Mandel and Wolf 1995). For $\sigma \rightarrow 0$ the time intervals between events become fixed, i.e. the process tends to become maximally ordered. If on the opposite $\sigma_p < \sigma$, such process corresponds to the super-Poisson statistics, which is typical for collective chaotic processes. In both cases, it can be supposed that solar activity acts on reaction volume as a whole, similarly to crystal lattice excitations. For quantum systems such dispersion variations are typical for squeezed states (Paul 1982; Mandel and Wolf 1995); this approach will be applied in our model below. This analysis evidences that high solar activity makes molecular systems perform chemical reactions in a more self-ordered and regular way. In general, these considerations are applicable to arbitrary probability distributions of the studied systems, and not only Poisson-like ones. Some results evidence that squeezed photon states are produced also in biophoton emission (Popp 1998; Popp et al. 2002). Summing up, the cited results permit us to suppose the existence of unknown distant interactions of non-electromagnetic origin, which can be attributed to hypothetical NC effects.

27.3 Theoretical NC Premises

Here we will consider possible NC properties for large systems like a set of noninteracting molecules or metastable nuclei. In standard QM formalism, the system evolution operator is defined mainly by quantum-to-classical correspondence (Jauch 1968), for NC effects such guidelines are absent and we'll construct it based only on general QM principles and the cited experimental results. We will construct here a phenomenological model of NC effects, it can't directly describe the discussed experimental results, but it can simulate analogous effects for simple quantum systems. Below we'll consider an NC model for the system $\{A_i\}$ of N unstable α -decay nuclei, its initial state is $\{A_i\}$ product state. In fact, similar considerations are applicable to the evolution of arbitrary metastable systems, like atoms, molecules, or biological systems, yet for a nucleus α -decay its description is the simplest example. In QM formalism the system in a pure state is described by the Dirac complex vector ψ in Hilbert space denoted also as ket-vector $|\psi\rangle$. For any system in a pure state ψ its evolution is described by the Schroedinger equation

$$i\hbar \frac{\partial \psi}{\partial t} = H\psi \quad (27.1)$$

where \hbar is the Plank constant and H is the Hamiltonian operator (Peres 2002). Gamow's theory of nucleus α -decay admits that before the decay act occurs, the α -particle with average kinetic energy E already exists as an independent entity inside the nucleus (Gamow 1928; Newton 1961). It supposes that Coulomb and nuclear forces constitute a potential barrier with the maximal height U_m on the nucleus periphery, so that $E \leq U_m$. Hence, an α -particle can leave the nucleus volume only by means of underbarrier tunneling, which explains large lifetimes of such isotopes. Therefore, like in the double well example, the state energy is the same inside and outside the nucleus, and the corresponding inside-outside states $\psi_{0,1}$ are degenerate and orthogonal to each other. Such energy degeneration permits, in principle, some hypothetic NC mechanism to change nucleus decay parameters without any energy transfer to the α -particle, but just changing the barrier transmission rate. Such a mechanism is considered below. In the Gamow theory, an α -particle Hamiltonian is

$$H = \frac{\vec{P}^2}{2m} + U(r) \quad (27.2)$$

where $\vec{P} = -i\hbar \vec{\nabla}$ is its momentum operator, m is the α -particle mass, U is the nucleus barrier potential, and r is the

distance from the nucleus center (Gamow 1928; Newton 1961). If at t_0 α -particle was in an initial state $\psi_0^i = \psi_0$, inside A_i nucleus, then the solution of Eq. (27.1) for A_i state $\psi^i(t)$ gives decay probability rate at a given decay moment t for nucleus A_i ; $i = 1, \dots, N$

$$p_i(t) = \lambda \exp[-\lambda(t - t_0)] \quad (27.3)$$

which is the time derivative of the total A_i decay probability from t_0 to t . Here λ depends on m , U , and on the Gamow kinematic factor n_d related to the α -particle motion inside the nucleus (Gamow 1928; Newton 1961). Thus, at $t \rightarrow \infty$ the nucleus state evolves to the final state $\psi_1^i = \psi_1$, so that $\langle \psi_0^i | \psi_1^i \rangle = 0$ and $p_i(t)$ is the transition rate for such nucleus transformation. Note that in chemical reaction models, their reagents pass over potential barriers mainly due to thermal fluctuations, which transfer to them kinetic energy exceeding the barrier height, while the role of tunneling is supposed to be negligible. However, they also would suffer barrier scattering, hence it's possible that a similar model can be applied to them as well.

The described experimental results indicate that the hypothetic NC influence perturbs the system transitions; the examples are chemical reactions and nucleus decay. It's reasonable to suppose that NC influence should be reciprocal and symmetric so that NC influence of inductor system S_1 on detector system S_2 is supposedly induced by similar transitions in S_1 . An example of such reciprocal NC influence on tunneling rate in quantum systems was discussed in Sect. 27.1. It's reasonable to suppose that such S_1 influence on an arbitrary S_2 system would change S_2 transition rate, and vice versa for S_2 NC influence on S_1 , because in that case, division into inductor/detector systems is conditional. We will consider here only the simplest system transitions, i.e. from the initial to the final state directly without passing through intermediate stages. For the beginning, our heuristic assumption is that in that case, the NC effect intensity induced by the inductor system S_1 will be proportional to the S_1 transition rate from its initial internal state ψ_{in} to the final one ψ_f , such that $|\langle \psi_{in} | \psi_f \rangle| < 1$. In particular, according to that assumption, NC influence intensity induced by A_i nucleus decay is proportional to $p_i(t)$ of Eq. (27.3). This assumption will be reconsidered below in the QM formalism framework, it will be shown that it is applicable only as an approximation and in general, with the NC influence described by the corresponding QM operator. It is notable that some standard QM interactions are also induced by analogous transition processes. An example is the charged transition current in weak interactions, it stipulates, in particular, neutron β -decay (Martin 2011).

The experimental results discussed in the previous section indicate that NC influence can make their evolution less chaotic and more regular, in particular, it can result in

squeezed states with sub-Poisson statistics. It's notable that self-ordering is quite a general feature of quantum dynamics, examples are crystal lattice formation or atomic spin order in ferromagnets. Another example is elastic particle scattering, in that case, the final state possesses higher angular symmetry than the incoming plane wave state. These analogies together with the cited experimental data permit us to suppose that for an arbitrary system evolution such NC influence tends to make its evolution most symmetric and self-ordered, our choice of NC Hamiltonians will be prompted by these assumptions. Then, one can suppose that any large system would gain its own self-ordering via the NC mechanism, in particular, making its own evolution more regular and ordered. Besides the self-ordering, corresponding to more regular time intervals between events, other forms of the system evolution symmetrization, can in principle be induced by NC effects. In particular, the enlargement of average time intervals between events can be also treated as the growth of temporary symmetry since event distribution becomes more homogeneous in time, its asymptotic limit is $p(t) \rightarrow const$ for $t > t_0$. It is notable that the above experimental results demonstrate enlargement of nucleus lifetime induced by solar activity (Fischbach et al. 2009; Bogachev et al. 2020); the same is true for its influence on some chemical reactions (Piccardi 1962; Troshichev et al. 2004). It's natural to suppose that the NC effect for any system of restricted or fixed size grows with the number of system constituents N involved in reactions. For the case of two nearby systems $S_{1,2}$ it's reasonable to expect that S_1 evolution due to NC effects would result in its own self-ordering and influences S_2 in a similar way and vice versa. For the case of two nearby systems one of which – S_1 is large and the other one – S_2 is small, NC effects are supposedly realized in the master regime, i.e. S_1 can significantly influence the S_2 state and make its evolution more ordered, whereas S_2 practically doesn't influence S_1 state evolution. Then, the resulting NC effect in S_2 should depend on the S_1 evolution properties and S_1, S_2 distance R_{12} .

Typical experimental accuracy of nucleus decay time measurement Δt is several nanoseconds (Martin 2011). Formally, such measurement is described as a sequence of two consequent A_i state measurements divided at least by Δt interval. If the first one shows that A_i is in the ψ_0 state, and the next one shows that it is in the ψ_1 state, it means that A_i decay has occurred during this time interval (Sudbery 1986). In QM formalism, a general state of quantum system S is described by the density matrix ρ , for pure states $\rho = |\psi\rangle\langle\psi|$. If A_1 and A_2 nuclei are its components, the partial $A_{1,2}$ density matrixes $\rho_{1,2}$ can be defined. For each A_i , it follows that if other S components were measured previously, then its decay probability rate would differ from p_i of Eq. (27.3) and becomes

$$\gamma_i(t) = \frac{\partial}{\partial t} \text{Tr} \rho_i(t) P_1^i \quad (27.4)$$

where P_1^i is projector on A_i final state (Sudbery 1986).

27.4 Nonlinear QM Formalism

It was supposed that NC effects should not change the system average energy, however, if the corresponding NC Hamiltonian is a linear operator, then for α -decay this condition will be violated (Mayburov 2021a, b). It will be shown here that nonlinear Hamiltonians can satisfy this condition much better and so it's sensible to apply them to the NC effect description. Nonlinear QM Hamiltonians were introduced initially as effective theories describing collective quantum effects, but now it's acknowledged that such hypothetical nonlinear corrections to standard QM formalism can exist also at the fundamental level (Weinberg 1989). In nonlinear QM formalism, a particle evolution is described by a nonlinear Schroedinger equation of the form

$$\begin{aligned} i\hbar \frac{\partial \psi}{\partial t} &= -\frac{\hbar^2}{2m} \nabla^2 \psi + V(\vec{r}) \psi + F(\psi, \bar{\psi}) \psi \\ &= H^L \psi + F(\psi, \bar{\psi}) \psi \end{aligned} \quad (27.5)$$

where m is the particle mass, V is the system potential, and F is an arbitrary function of the system state. In our case, H^L is the Gamow Hamiltonian with $V = U$. Currently, the most popular and elaborated nonlinear QM model is the one by Doebner and Goldin (DG) (Doebner and Goldin 1992, 1996). In its formalism, a simple variant of nonlinear term is $F = \frac{\hbar^2 \Gamma}{m} \Phi$, where

$$\Phi = \nabla^2 + \frac{|\nabla \psi|^2}{|\psi|^2} \quad (27.6)$$

is a nonlinear operator, Γ is a real or imaginary parameter which, in principle, can depend on time or other external factors, here only real Γ will be exploited. The main properties of Eq. (27.5) were studied by (Doebner and Goldin 1992; Mayburov 2021a, b), and they can be summarized as follows:

- The probability is conserved.
- The equation is homogeneous.
- The equation is Euclidian – and time-translation invariant for $V = 0$.
- A noninteracting particle subsystem remains uncorrelated (separation property).

- For $V = 0$, the particle plane waves are solutions both for real and imaginary Γ .

Since $\int \bar{\psi} F \psi d^3x = 0$ for an arbitrary ψ , the energy functional for the solution of Eq. (27.5) is $\langle i\hbar \partial_t \rangle = \langle H^L \rangle$. Hence, the average system energy would change insignificantly if at all, if F is added to the initial Hamiltonian H^L , so it advocates DG ansatz application to NC models. In particular, it will be shown that in WKB approximation, which is the main formalism for decay calculus, the energy expectation value doesn't change in the presence of such a nonlinear term F .

It is notable that the nonlinear term F in the particle Hamiltonian can modify the particle tunneling rate through the potential barrier. In particular, an analytic solution to this problem was obtained for a rectangular potential barrier, in that case, the barrier transmission rate depends exponentially on Γ (Mayburov 2021a, b). To calculate corrections to the Gamow model for arbitrary potential U , WKB approximation for nonlinear Hamiltonian of Eq. (27.5) can be used. In this ansatz for rotation invariant U , the α -particle wave function was reduced to

$$\psi = \frac{1}{r} \exp\left(\frac{i\sigma}{\hbar}\right)$$

Function $\sigma(r)$ can be decomposed in \hbar order as $\sigma = \sigma_0 + \sigma_1 + \dots$, where r is the distance from the nucleus center (Peres 2002; Sakurai 1994). Given an α -particle with the average energy E , one can calculate the distances $R_{0,1}$ from the nucleus center at which $U(R_{0,1}) = E$. Then, for our nonlinear Hamiltonian of Eq. (27.5) the resulting equation for σ_0 is:

$$\left(\frac{1}{2m} - \Lambda\right) \left(\frac{\partial \sigma_0}{\partial r}\right)^2 = E - U(r)$$

where $\Lambda = 2m\Gamma$ for $R_0 \leq r \leq R_1$; $\Lambda = 0$ for r outside this interval. Its solution for $R_0 \leq r \leq R_1$ results in

$$\psi(r) = \frac{1}{r} \exp\left(\frac{i\sigma_0}{\hbar}\right) = \frac{C_r}{r} \exp\left[-\frac{1}{\hbar} \int_{R_0}^r q(u) du\right] \quad (27.7)$$

where C_r is the normalization constant,

$$q(u) = \left\{ \frac{2m[U(u) - E]}{1 - 4\Gamma} \right\}^{\frac{1}{2}}$$

Account of higher order σ terms practically doesn't change transmission coefficient D

$$D = \exp \left[-\frac{2}{\hbar} \int_{R_0}^{R_1} q(u) du \right] = \exp \left[-\frac{\phi}{(1-4\Gamma)^{\frac{1}{2}}} \right]$$

$$\cong \exp[-\phi(1+2\Gamma)]$$

Here ϕ is a constant for a given nucleus, whereas Γ can depend on time and other parameters. Note that Λ term induced by H nonlinearity doesn't change the particle energy in comparison with corresponding linear H^L . To calculate the nucleus decay parameter, D multiplied by the number of α -particle kicks n_d into the nucleus potential wall per second, it gives $\lambda = n_d D$ (Gamow 1928), for DG model n_d doesn't depend on the F term (Mayburov 2021a, b).

27.5 Quantum-Mechanical NC Model

As was noticed above, besides more regular time intervals between events, described by sub-Poisson statistics, NC effects can in principle induce other forms of symmetrization of the system evolution. In particular, the growth of average time intervals between events can be also considered as the enlargement of the system evolution symmetry. Really, the event distribution of Eq. (27.3) on time half-axis $\{t_0, \infty\}$ becomes maximally homogeneous for $\lambda \rightarrow 0$, hence the evolution temporary symmetry grows in this limit. Let's study first how such an NC influence is described in the master regime approximation. Consider two nuclei systems S_1 and S_2 with the average distance between S_1 and S_2 elements R_{12} , which is supposedly much larger than the S_1 and S_2 size. For simplicity, we will consider here only static situations when all the object positions are fixed. S_1 is a set of N_1 unstable nuclei $\{A_i\}$ prepared at t_0 with decay probability described by Eq. (27.3). However, S_1 internal NC self-influence can change it to some $p_i^m(t)$. S_2 includes just one unstable nuclide B prepared also at t_0 , with its evolution described by the Gamow Hamiltonian H_b , analogous to H of Eq. (27.2), but its decay constant λ_b and decay probability rate $p_b(t)$ can differ from λ and $p_i(t)$ of Eq. (27.3). In such a set-up, corresponding to the master regime, NC induced by the system S_1 supposedly influences B evolution, in particular, it can change its average lifetime. Suppose that all geometric factors of such an NC influence for the given S_1 are described by phenomenological real propagation function $\chi(R_{12})$ in B Hamiltonian; its absolute value is supposedly reduced with R_{12} and grows with N_1 . The resulting corrections to H_b presumably are small and so can be accounted for only up to the first order of χ . Based on assumptions discussed above, in particular, that the resulting NC effect is proportional to the S_1 transition rate and described by a nonlinear Hamiltonian term B, it follows that the parameter Γ in the F term becomes a function

$\Gamma(R_{12}, t) = \chi(R_{12})p_i^m(t)$, so that the phenomenological B Hamiltonian looks like:

$$H_b^d(t) = H^L + \frac{\hbar^2}{m} \chi(R_{12})p_i^m(t)\Phi \quad (27.8)$$

where Φ is the operator of Eq. (27.6) for B. For simplicity, we admit that $p_i^m(t) \approx p_i(t)$ of Eq. (27.3) because in our model S_1 NC self-influence effects aren't expected to be large. Hence, for such an ansatz, B Hamiltonian and consequently B lifetime depend on the S_1 nuclei decay probability rate. Solving the Schrodinger equation with such a Hamiltonian in WKB approximation for B state $\psi^b(t)$, we get B decay probability rate:

$$p_b^f(t) = C_b \exp[-(t-t_0)\epsilon(t)] \quad (27.9)$$

where C_b is a normalization constant

$$\epsilon(t) = \lambda_b \left(\frac{\lambda_b}{n_d} \right)^{2\Gamma(R_{12}, t)}$$

Then, under S_1 NC influence, the resulting B nucleus lifetime for $\chi > 0$ becomes larger than the initial one. Such an S_2 evolution modification can be interpreted as an enlargement of S_2 evolution symmetry so that the resulting decay probability $p_b^f(t)$ would become more homogeneous in time.

Now, such an NC effect can be considered on a more fundamental level, beyond the master regime. Let's suppose now that $N_1 = 1$ and the nucleus A_1 , B states are described by the wave functions ψ^1 , ψ^b , correspondently. Then for the same initial conditions as above, the system initial wave function $\psi_s = \psi^1_0 \psi^b_0$ at the moment of preparation t_0 . In accordance with our previous analysis, it is reasonable to assume that in general A_1 NC influence on B state evolution is proportional to the A_1 transition rate from its initial state to the final one. In the QM framework, such a rate is described by the operator $\frac{dP_1^1}{dt}$ for projector P_1^1 exploited in Eq. (27.4); it can be calculated from the Ehrenfest theorem (Peres 2002). Conjugal B NC influence on the A_1 evolution has analogous dependence which is defined by the corresponding projector P_1^b for the B state. As a result, A_1 , B Hamiltonian in the first χ order

$$H_S(t) = H^L + \frac{\hbar^2}{m} \chi(R_{12}) \frac{dP_1^1}{dt} \Phi + H_1 + \frac{\hbar^2}{m} \chi(R_{12}) \times \frac{dP_1^b}{dt} \Phi_1 \quad (27.10)$$

where Φ_1 is the operator of Eq. (27.6) for A_1 , R_{12} is A_1 , B distance; parameter Γ is substituted by A_1 , B operators. It follows that for our system

$$\left\langle \frac{dP_1^{1,b}}{dt} \right\rangle = p_{1,b}(t)$$

Since A_1 and B operators commute, transition rate operators can be replaced by their expectation values

$$H_S(t) = H^L + \frac{\hbar^2}{m} \chi(R_{12}) p_1(t) \Phi + H_1 + \frac{\hbar^2}{m} \chi(R_{12}) p_b(t) \Phi_1 \quad (27.11)$$

The solution of the evolution equation for such a Hamiltonian would give the probability rate for B decay described by Eq. (27.9) with $p_i^m(t) = p_i(t)$ of Eq. (27.3); A_1 decay probability rate can be calculated analogously. Note that the Gamow kinematic factor n_d doesn't change in this case. Thus, the obtained ansatz supports the applicability of Eq. (27.5) for NC influence description for S_1 nuclei ensemble in the master regime. It also demonstrates that our initial hypothesis that the NC effect intensity is related to the system transition rate, is reasonable because any other option would demand much more complicated Hamiltonians. The obtained A_1 and B states are correlated but aren't entangled, so that the system state $\psi_s(t) = \psi_1(t) \psi_b(t)$ at an arbitrary time, however, in the next χ order A_1 , B state entanglement can appear. Under NC influence for $\chi > 0$, the resulting A_1 , B nucleus life-times become larger than the initial one. Such an A_1 , B evolution modification can be interpreted as the growth of their evolution symmetries, such that the resulting decay probabilities become more homogeneous in time in comparison with the initial A_1 , B decay probabilities. It can be supposed also that the inverse process, i.e. A_1 nucleus synthesis via reaction of α -particle with the remnant nucleus would induce the opposite NC effect on B, reducing the B nucleus lifetime and so reducing its evolution symmetry. Hence, the proposed NC mechanism can change, in principle, the evolution symmetry in both directions enlarging or reducing it. The proposed model exploits the NC dynamics based on nonlinear α -decay Hamiltonian, which, in fact, is used as an effective Hamiltonian demonstrating how the decay rates can change under NC influence. It was assumed above that NC doesn't change any system average energy, in our model this condition is fulfilled for WKB approximation. The system momentum and orbital momentum are also conserved due to the rotational symmetry of the studied systems.

27.6 Squeezed State Production

The formal solution of QM evolution Eq. (27.1) is:

$$\psi(T) = W(T) \psi(t_0)$$

where the integral operator of evolution is:

$$W(T) = \exp \left[-\frac{i}{\hbar} \int_{t_0}^T H(t') dt' \right] \quad (27.12)$$

If one considers a set of N -independent nuclei, their joint decay probability is described by Poisson distribution (Martin 2011). Consider now the case $N = 2$, for the system of two independent nuclei A_1, A_2 , with its initial state $\psi_A = \psi_0^1 \psi_0^2$, where $\psi_0^{1,2} = \psi_0$. If their evolution is independent, then the evolution operator is the product of two right-side terms of Eq. (27.9), but it can be also formally written as

$$W(T) = C_t \exp \left\{ -\frac{i}{\hbar(T-t_0)} \iint_{t_0}^T [H_1(t_1) + H_2(t_2)] dt_1 dt_2 \right\} \quad (27.13)$$

In our case, $H_{1,2}$ are A_1, A_2 Gamow Hamiltonians with the corresponding $r_{1,2}, U_{1,2}$, etc. Both integrals here are from t_0 to T , the same double integral limits are used below, and C_t is the time-ordering (chronological) operator (Feynman 1961). In a sense, here the second integration for each term is a dummy, giving just multiplier $T - t_0$, yet such an ansatz is used here because NC effects will be treated via time-dependent Hamiltonians below, for which using multiple time parameters is a standard approach (Sakurai 1994).

Let us consider just one system S of N nuclei. As supposed, due to conjugal NC influence between its elements, its evolution can become more regular and self-ordered practically without nucleus lifetime change. Because of it, S evolution can differ from the case of independent nuclei and would result in the temporary correlation between decays of S nuclei. Let's start from the simplest case $N = 2$ with A_1, A_2 nuclei prepared at t_0 at the distance of R_{12} . The modified S evolution operator can be chosen from the analogy with squeezed photon state production in atomic resonance fluorescence (Mandel and Wolf 1995). In that case, the photon production rate is suppressed if the time interval between two consequently produced photons is less than some fixed Δt . Due to it, the resulting photon detection becomes more regular, and their distribution would become sub-Poissonian. Suppose that the A_1 NC influence rate on A_2 is characterized by a real scalar function $k(R_{12})$, its absolute value diminishes as R_{12} grows, the same function describes A_2 NC influence on A_1 , $k(R_{12})$ can be regarded as the coordinate NC Green function. For simplicity, we choose the NC correlation of

A_1, A_2 decay moments such that its evolution ansatz can be factorized into A_1, A_2 terms. For example, if no measurement of the A_1 state is done, then the resulting phenomenological A_2 Hamiltonian supposedly becomes

$$H_2^c(T) = H_2 + \int_{t_0}^T k(R_{12}) \varphi(T-t') \frac{dP_1^1}{dt} \Phi_2 dt' \quad (27.14)$$

Here $\Phi_{1,2}$ is the nonlinear term of Eq. (27.6) for $A_{1,2}$, φ is the causal Green function chosen as

$$\varphi(\tau) = \eta(\tau - \nu) - \eta(\tau) \quad (27.15)$$

its possible dependence on A_1, A_2 distance neglected, assuming that it is accounted by $k(R_{12})$ function. Thus, the

$$W(T) = C_i \exp \left\{ - \frac{i}{\hbar(T-t_0)} \iint_{t_0}^T [H_1(t_1) + H_2(t_2) + (T-t_0)G(t_1, t_2)] dt_1 dt_2 \right\} \quad (27.16)$$

The third term in this equality is the NC term, its simple ansatz suppresses nucleus decays at small time intervals between them. Due to A_1, A_2 operator commutativity, $\frac{dP_1^{1,2}}{dt}$ operators in it can be replaced by their expectation values $\gamma_{1,2}(t)$

$$G(t_1, t_2) = \frac{\hbar^2}{m} k(R_{12}) \times [\varphi(t_1 - t_2) \gamma_2(t_2) \Phi_1 + \varphi(t_2 - t_1) \gamma_1(t_1) \Phi_2]$$

Note that the second right-side term corresponds to H_2^c Hamiltonian of Eq. (27.14), $\gamma_i(t_i)$ is of Eq. (27.4). If no measurement of A_i state was performed for $t_f < T$, then $\gamma_i(t_i) = p_i(t_i)$ of Eq. (27.3), i.e. the NC influence rate is proportional to the A_i decay rate. Otherwise, if such a measurement were performed at some t_f , and A_i was found to be in the final state, then for $t_i > t_f$ it follows that $\gamma_i(t_i) = 0$. For $t_i \leq t_f$ resulting $\gamma_i(t_i)$ follows from the decay moment measurement ansatz of Eq. (27.4) described above (Sudbery 1986). Thus, for $i = 1, 2$ the nucleus A_i NC term in the first k order is proportional to the decay rate of the neighbor nucleus A_{2-i} of Eq. (27.3). As a result, for $k > 0$, the solution for the joint $A_{1,2}$ decay probability rate p_s will differ from the independent case when $p_s(t_1, t_2) = p_1(t_1) p_2(t_2)$ and becomes

$$p_s(t_1, t_2) = C \lambda^{2+2\theta} \exp[-g(t_1, t_2)(t_1 + t_2 - 2t_0)] \quad (27.17)$$

where C is the normalization constant. Under these conditions, the Gamow kinematic factor n_d for α -particle

corresponding NC time dependence is described as the difference of two-step functions $\eta(\tau) = \{0, \tau < 0; 1, \tau \geq 0\}$ which is a simple variant of such ansatz (Korn and Korn 1968). $\nu > 0$ is an NC phenomenological parameter, it corresponds to the time range in which A_1 and A_2 decays are correlated; ν supposed to be much larger than the effective nucleus transition time (Newton 1961). As a result, the current A_2 Hamiltonian is a time-dependent operator, so that at a given time it depends on the A_1 decay probability rate at earlier time moments. An analogous modification occurs for the A_1 Hamiltonian with the corresponding index change. Hence, the NC influence on A_1 and A_2 Hamiltonians results in $W(T)$ modification in comparison with Eq. (27.13)

motion inside the nucleus changes insignificantly (Gamow 1928). Then, both for WKB approximation (Peres 2002) and analytic solution of the Gamow problem (Lubenets 1977)

$$g(t_1, t_2) = \exp[(1 + \vartheta) \ln \lambda]$$

where λ is from Eq. (27.3) and

$$\vartheta = \frac{k(R_{12})}{2} \times [\eta(t_1 - t_2) \varphi(t_1 - t_2) \gamma_2(t_2) + \eta(t_2 - t_1) \varphi(t_2 - t_1) \gamma_1(t_1)] \quad (27.18)$$

Due to it, if the time interval between two decay events is less than ν , the nucleus decay rate for $k > 0$ will be suppressed and the resulting decay event distribution will become more ordered. Here the second-order correction of the kind $\gamma_1 \rightarrow \gamma_2 \rightarrow \gamma_1 + d\gamma_1$ is neglected. For independent nucleus decays with $N = 2$ described by Eq. (27.13) their joint decay probability corresponds to a Poisson process, whereas the NC dynamics term in Eq. (27.16) would transform it into a sub-Poisson one, resulting in less stochastic and more ordered event distribution. Note that the resulting $A_{1,2}$ states are correlated but not entangled. For $N > 2$ the considered NC dynamics term in $W(t)$ would change to

$$G(t_1, \dots, t_N) dt_1 \dots dt_N$$

with the corresponding integration over N independent time parameters. As a result, for an analogous G ansatz, the joint

decay probability of arbitrary consequent decays will be suppressed for small time intervals between them, and the decay time distribution of the whole event set will be sub-Poissonian. In a general case, such a correlation can involve all N decays resulting in more self-ordered decay moment distribution.

Two considered symmetrization mechanisms – lifetime enlargement and event sub-Poisson symmetrization, in principle, can coexist and act simultaneously in some systems. Here the system self-ordering NC effect was considered, however, some distant system S_m also can induce, in principle, analogous NC evolution symmetrization in system S , as evidenced by experimental results (Shnoll 1973, 2009; Shnoll and Kolombet 1980). It can be supposed that the analogous NC effect description is applicable also to chemical reactions and other atomic and molecular systems. Non-linear Hamiltonians were used here for NC effect description, however, it's possible also that in collective systems NC effects can be described by linear Hamiltonians, so that nonlinearity appears as the corresponding effective theory (Doebner and Goldin 1996).

27.7 Discussion

The considered experimental results and theoretical analysis evidence that a novel communication mechanism between distant quantum systems can exist. It is based on a new form of QM nonlocality, principally different from the well-known EPR-Bohm nonlocality mechanism. In this paper, NC effects were studied for the system of metastable states, in particular, unstable nuclei ensemble. It was assumed that such a mechanism can be applicable also to chemical reactions. Additional arguments in favor of this hypothesis supposedly demonstrate Takata blood test studies. Taking blood samples at different altitudes up to several km and analyzing them together with results cited in Sect. 27.2, the authors concluded that the influence source is not the Sun itself, but the Earth atmosphere at an altitude above 6–7 km (Kiepenheuer 1950; Takata 1951). It is well established that from sunrise to sunset at such altitude intense photochemical reactions occur, in particular, SO_2 and NO_2 molecule destruction by UV solar radiation, which results in ozone and other compound synthesis (McEven and Phylips 1975). Hence it can be supposed that those chemical reactions induce NC influence which changes blood activity in distant human organisms promptly, in its turn such changes result in variations of blood reaction with sodium carbonate. In particular, it supposedly explains the start of reaction rate gain 6–8 min before astronomic sunrise, because at that time solar radiation already reaches the Earth's atmosphere at such altitudes.

An important feature of such an NC mechanism is that such communications, in principle, can function effectively even in dense and warm media which is characteristic of biological systems. There are many confirmed effects of distant correlations in biological systems which still have no satisfactory explanation, some of them reviewed in the first section. Besides, multiple publications indicate that cosmophysical effects influence also biological system development and functioning (Galleg 2014; Hayes 1990). Of them, it is worth noticing especially the significant influence of moon tide gravity variations δg on seedling photon emission rate and tree stem diameter variations (Barlow et al. 2010; Galleg 2014; Galleg et al. 2018). There is no consistent explanation now of how such small gravitational force variations $\frac{\delta g}{g} \approx 10^{-7}$ can seriously affect these subtle biological processes. It is worth noticing especially that photon emission data show an essential intensity dependence on δg time derivative (Galleg et al. 2018). Meanwhile, the model of nonlinear gravitational field interaction with quantum systems predicts similar gravity influence on arbitrary quantum systems, in particular, it describes in this framework the observed lifetime and decay rate variations of unstable nuclear isotopes (Mayburov 2021a, b). It is established now that such ultraweak photon emission is stipulated mainly by biochemical reactions of lipid and protein oxidation (Popp 1998; Galleg 2014). Hence, it can be assumed that δg time derivative performs an analogous influence on molecular states involved in these reactions.

Another example of unsolved biophysics problems is Gurwitsch's mitogenetic effect which demonstrates that cell division in one organism or plant can stimulate cell division in another (distant) one, separated from the first by a quartz wall (Bischof 2003). Such wall is transparent for ultraviolet (UV) photons, and their emission by living species and plants, called also ultraweak biochemiluminescence, was reported by many groups (Quickenden and Que Hee 1976; Popp et al. 2002) and reviewed in (Popp 1998). However, the detected UV photon intensity is quite low, the irradiation of an animal organism or plant by a UV lamp with similar light intensity doesn't result in any sizable effect. However, the existence of NC influence between such biosystems supposedly can constitute, in fact, the additional communication channel between them. First of all, it follows from the considered NC properties that they can stimulate similar self-organization-processes in the neighboring detector biosystem if such self-organization in the form of cell division occurs in the inductor biosystem. Suppose that cell division occurs in the inductor biosystem so that the cell number grows. We can assume that an NC self-ordering mechanism regulates it inside the inductor. It is possible also that an exchange of excitons with UV energy is also necessary for cell proliferation in it. Plainly, such excitons on

the inductor border can convert into UV or optical photons, and some part of them can be absorbed by the detector system. In addition, the NC effect produced by inductor cells can also influence detector cells at some distance. Hence the simultaneous presence of these two effects can become the reason for the cell proliferation gain inside the detector system stipulated by these two different external effects. In summary, the NC influence and the UV radiation constitute, in fact, two independent communication channels between the inductor and the detector.

Such quantum NC influence supposedly has a universal character, in particular, such nonlocal effects can appear for systems of scattering particles. However, for metastable systems, its effects are expected to be more easily accessible for practical detection due to their relatively long duration. EPR-Bohm paradox and Bell inequalities demonstrate that quantum measurement dynamics is essentially nonlocal (Bell 2004; Norsen 2009; Gillis 2011). It seems doubtful yet that dynamics of quantum measurements differ principally from the rest of QM dynamics. It is more reasonable to expect that both of them can be described by some universal QM formalism, therefore, the presence of nonlocal terms in it would be plausible. Concerning causality for NC communications, at the moment it is still possible to assume that such NC can spread between systems at the speed of light. But even if this spread is instant, it's notable that usually superluminal signaling in QM is discussed for one bit of yes/no communications (Norsen 2009). In our case, to define the resulting change of some continuous parameter expectation value or dispersion, one should collect significant event statistics which can demand significant time for its storing, so it makes causality violation quite a doubtful possibility. In addition, NC dependence on the distance between two systems expressed by k , χ functions can be so steep that it also would suppress effective superluminal signaling. The situation can be similar to QFT formalism where some particle propagators spread beyond the light cone, but due to analogous factors, it doesn't lead to superluminal signaling (Blokhintsev 1973).

References

- Alekseev E et al. (2016) Results of search for daily and annual variations of ^{214}Po half-life at the two year observation period. *Phys. Part. Nucl.* 47, 1803–1815
- Barlow P W et al (2010) Tree stem diameter fluctuates with lunar tide. *Protoplasma* 247, 25–43
- Bell J S (2004) *Speakable and Unspeakable in Quantum Mechanics*. Cambridge University Press, Cambridge
- Bischof M (2003) in *Integrative Biophysics*, Popp F-A, Belousov, L V (eds.) Kluwer Academic Publishers, Dordrecht
- Blokhintsev D I (1973) *Space and Time in the Microworld*. Springer, Berlin
- Bogachev S A et al. (2020) Search for of x-ray solar activity correlations with ^{55}Fe , ^{60}Co nucleus decay rates. *J. Phys.: Conf. Series* 1690, 012028–012035
- Cramer J (1986) Transactional interpretation of quantum mechanics. *Rev. Mod. Phys.* 58, 647–66
- Doebner H and Goldin G (1992) On general nonlinear Shrodinger equation admitting diffusion currents. *Phys. Lett. A* 162, 397–402
- Doebner H and Goldin G (1996) Nonlinear gauge transformations in a family of nonlinear Schroedinger equations. *Phys. Rev. A* 54, 3764–3772
- Feynman P R (1961) *Quantum Electrodynamics*. Benjamin, Inc., N-Y
- Fischbach E et al (2009) Time dependent nuclear decay parameters. *Space Sci. Rev.* 145, 285–335
- Frohlich H. (1968) Long-range coherence and energy storage in biological systems. *Int. J. Quant. Chem.* 2, 641–649
- Gallep C (2014) Ultraweak, spontaneous photon emission from seedlings. *Luminiscence* 29, 963–974
- Gallep C et al (2018) P.Barlow insights and contributions to study of tidal gravity variations. *Ann. Botany* 122, 757–766
- Gamow G (1928) Theory of radioactive nucleus α -decay. *Zc. Phys.* 51, 204–218
- Gierhake E (1938) Diskussionsbemerung. *Arch. fur Gynak.* 166, 249–255
- Gillis E J (2011) Causality, measuremnts and elementary interactions. *Found. Phys.* 41, 1757–1785
- Hayes D K (1990) *Chronobiology: its Role in Clinical Medicine, General Biology and Agriculture*. John Wiley & Sons, N-Y
- Jauch J M (1968) *Foundations of quantum mechanics*. Addison-Wesley, Reading
- Jezler A and Bots P (1938) Uber die Fockungszahl in serum. *Klin. Wschr.* 17, 1140–1148
- Josephson B.D., Pallikari-Viras F. (1991) Biological utilization of quantum nonlocality. *Found. Phys.* 21 197–208
- Kaulbersz J et al (1958) Alterations of some blood reactions during total Sun eclipse. *Proc. VIII Int. Austronaut. Cong.* ed F Hecht Springer-Verlag, Berlin
- Kiepenheuer K O (1950) Zur beeinflussung der menschlichen blutserums durch die sonne. *Naturwiss.* 37 234–245
- Koller T and Muller H (1938) Serologische Untersuchungen. *Zbl. Gynak* 62, 2642–2649
- Korotaev S M (2011) *Causality and reversibility in irreversible time*. Scientific Results Publishing, Irvine, Ca
- Korn G A, Korn T M (1968) *Mathematical Handbook*. McGraw Hill, N-Y
- Kucera O, Cifra M (2013) Cell-to-cell signaling through light. *Cell Comm. Sign.* 11, 87–98
- Lubenets E R (1977) On unstable state decay problem in quantum mechanics. *Theor. Math. Phys.* 32 279–288
- Mandel L, Wolf E (1995) *Optical coherence and quantum optics*. Cambridge University Press
- Martin B R (2011) *Nuclear and particle physics: An introduction*. John Wiley & Sons, N-Y
- Mayburov S N (2021a) Nuclear decay oscillations and nonlinear quantum dynamics. *Int. J. Theor. Phys.* 60 630–639
- Mayburov S N (2021b) Quantum nonlocality – possible cosmophysical effects. *J.Phys.: Conf. Series* 2081 012025–012034
- Mayburov S N (2022) Nonlinear quantum nonlocality and its cosmophysical tests. Submitted to *Int. J. Mod. Phys. A*; ArXiv:2211.03520
- McEven M J, Phylips L F (1975) *Chemistry of the Atmosphere*. Edward Arnold, N-Y
- Newton R R (1961) Dynamics of unstable systems and resonances. *Ann. of Phys.* 14 333–358

- Norsen T (2009) Local causality and completeness. *Found. Phys.* 39 273–294
- Paul H (1982) Nonclassical optical photon production. *Rev. Mod. Phys.* 54 1061–1083
- Peres A (2002) *Quantum Theory: Concepts and Methods*. Kluwer, N-Y
- Piccardi G (1962) *The chemical basis of medical climatology*. Charles Thomas, Springer
- Popp F-A (1998) in *Biophotons*, Chang J J, Fisch J, Popp F A (eds.) Kluwer, Netherlands
- Popp F-A et al (2002) Evidence of nonclassical (squeezed) light in biological systems. *Physics Letters A* 293 98–102
- Primas H (1982) Chemistry and complementarity, *Chimia* 36 293–300
- Quickenden T I, Que Hee S S (1976) The spectral distribution of the luminescence emitted during growth of the yeast *Saccharomyces cerevisiae* and its relationship to mitogenetic radiation. *Photochem. Photobiol.* 23. V. 3. 201–204
- Sakurai J J (1994) *Modern quantum mechanics*. Addison-Wesley, Reading, MA
- Sarre H (1951) Solare einflüsse auf die Takata-reaction. (1951) *Medizin-Meteorol. Hefte* 5, 25–31
- Scholkman F et al (2012) Analysis of daily variations in electrochemical reactions. *J. Cond. Mat. Nucl. Sci* 8, 37–49
- Shnoll S E (2009) *Cosmophysical factors in stochastic processes*, Svenska fysikarkivet, Stockholm (in Russian)
- Shnoll S E (1973) Conformational oscillations in protein macromolecules. In: *Biol. and Biochemical Oscillators*, Ed. by B. Chance, Acad. Press, N.Y., p. 667–669.
- Shnoll S E and Kolombet V A (1980) Macroscopic fluctuations and statistical spectral analysis and the states of aqueous protein solutions. In: *Sov. Sci. Rev.*, Ed. by V. P. Sculachev, OPA, N.Y.
- Shnoll S E and Chetverikova E P (1975) Synchronous reversible alterations in enzymatic activity (conformational fluctuations) in actomyosin and creatine kinase preparations. *Biochem. Biophys. Acta*, 403, 8997–9006
- Stapp H P (1997) Nonlocal nature of quantum mechanics, *Am. J. Phys.* 65 300–311
- Sudbery A (1986) *Quantum mechanics and particles of nature*. Cambridge university press, Cambridge
- Takata M (1951) *Über eine neue biologisch wirksame*. *Archiv für Meteor., Geophys. Bioklimatologie B2*, 486–508
- Troshichev O A et al. (2004) Variation of gravitation field and rhythms of biochemical processes *Adv. Space Res.* 34 1619–1624
- Vitiello G (2001) *My Double Unveiled*. John Benjamins, Amsterdam
- Weinberg S (1989) Testing quantum mechanics nonlinearity. *Ann. Phys. (N.Y.)* 194, 336–352

Part VII

Perspectives



Integrating Ultraweak Photon Emission in Mitochondrial Research

28

Roeland Van Wijk and Eduard Van Wijk

28.1 Introduction

The mitochondrion is a multifunctional life sustaining organelle. Each cell of the body, except for red blood cells that transport oxygen, contains hundreds to thousands of mitochondria. They are most widely known as the powerhouses of the cell (Alberts 2015). In recent years, the interest in mitochondria is rising (Picard et al. 2016). The rising interest for mitochondria stems from the recognition that they are the only organelles to house their own genome and from a growing number of medical conditions recognized to be caused or promoted by mitochondrial DNA (mtDNA) defects. Beside energy production, mitochondria produce signals that convey information between mitochondria and the nucleus including reactive oxygen species (ROS) and reactive metabolites derived from mitochondrial metabolism. Likewise, tools to grasp mitochondrial morphology transitions have suggested rapid information exchange across mitochondria. An often-forgotten aspect of mitochondria is that they produce the majority of cellular ultraweak photon emission (UPE), which has long been considered an important marker for quality of mitochondrial respiratory activity (Van Wijk 2014). In this article, we focus on the classical aspects – UPE in relation to respiration and ROS – but also on emerging aspects of mitochondrial biology and their relevance to the specific area of noncommunicable diseases. The overview begins with the situation around 1960 (Sect. 28.2), when three areas of mitochondria-related research began to develop, largely independent from each other: (a) respiration and energy production, (b) production of free radicals and other, nonradical reactive oxygen species (ROS), and (c) ultraweak photon emission (UPE). Later, these areas became interrelated, but not immediately integrated. The integration has been a stepwise development in two distinct

time periods: (a) 1980–2000 (Sect. 28.3), and (b) 2000–2020 (Sect. 28.4). In Fig. 28.1, we conceptualize the development and integration process of knowledge utilizing the 1960s–1980s building blocks of knowledge as piles to erect a stable (evidence based) structure of a “light house,” as a metaphor. In the second building layer (1980–2000), we extend and interconnect these piles. The booming of mitochondrial research focused on the critical role of mitochondrial DNA (mtDNA) for mitochondrial functioning and the specific sensitivity of mtDNA for ROS resulting in the vicious cycle theory of mitochondrial ROS production and increasing probability for damage and disease as demonstrated in the identification of stress-related and age-related metabolic and degenerative diseases. On the other hand, the interconnectedness of ROS and UPE in stress and aging strongly progressed. In the third building layer (2000–2020), integration progresses as presented by the dome of the mitochondrial lighthouse with its light signaling. In Sect. 28.5 on “Future Perspectives,” the authors include data on noninvasive UPE recording in vivo to illustrate the analysis of recent research on single-photon counting time profiles suggesting that ROS-directed photon emission may play a valuable role in health and disease.

28.2 Historical Aspects: The Three Piles (1960–1980)

28.2.1 Mitochondria Are Powerhouses

In 1949, mitochondrial oxidation was demonstrated. Mitochondria contain the enzymes of the citric acid cycle as well as the respiratory assembly (Kennedy and Lehninger 1949). The first high-resolution (electron microscopic) images of mitochondria were published in the early 1950s (Palade 1952; Sjöstrand 1953). A typical mitochondrion is about the size of a bacterial cell with a diameter of 0.2 to 0.8 micrometer and a length of 0.5 to 2 micrometer.

R. Van Wijk · E. Van Wijk (✉)
Meluna Research, Wageningen, The Netherlands
e-mail: evanwijk@melunaresearch.nl; <https://www.melunaresearch.nl/>

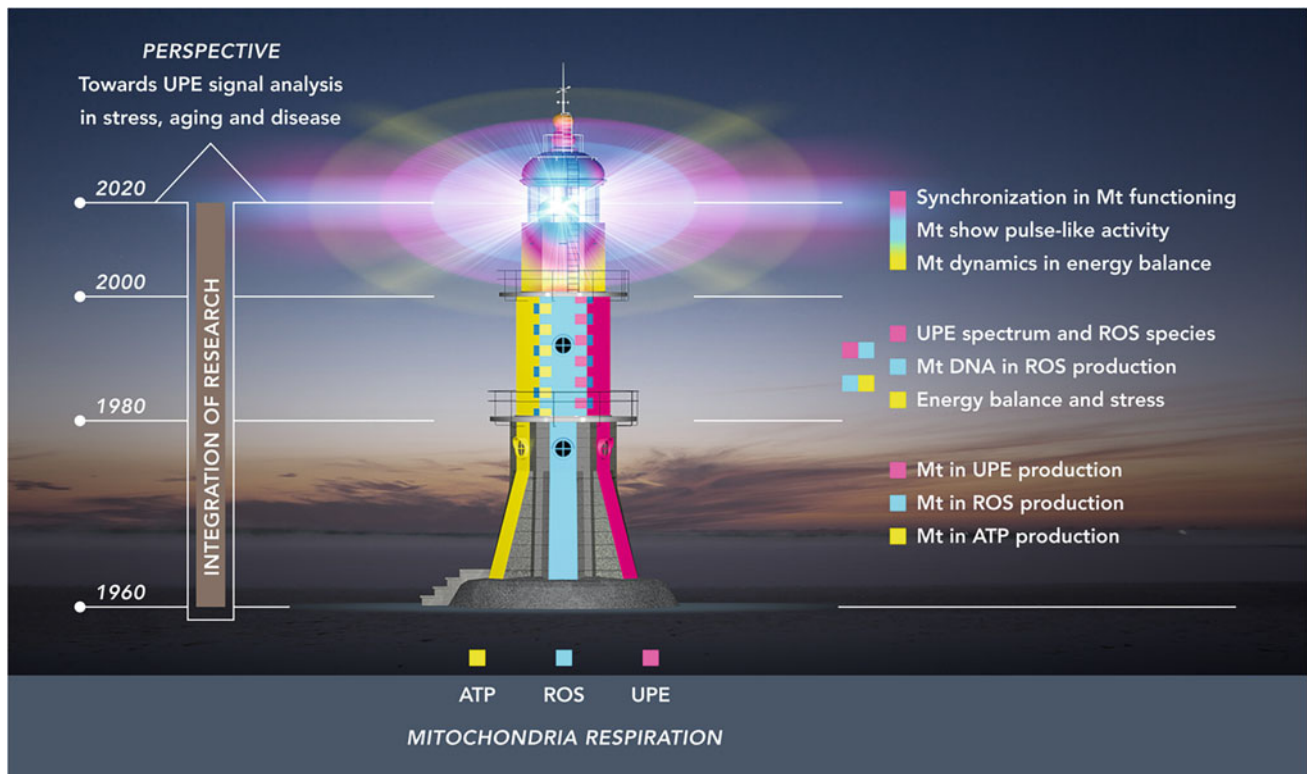


Fig. 28.1 The light house from base till top represents three periods of 20 years: 1960–1980 (the lowest floor); 1980–2000 (mid-floor); 2000–2020 (top floor). The colors illustrate three developing fields of research related to mitochondria: energy (ATP) production (yellow); ROS production (cyan blue); UPE production (magenta red). These research fields originally developed independently in the first period.

Mitochondria have two membrane systems with markedly different biochemical properties. The outer mitochondrial membrane has few proteins, the major proteins form channels through this membrane allowing free diffusion of ions and small water-soluble metabolites. The inner mitochondrial membrane is rich in protein. It is a barrier to protons and larger polar and ionic substances which cross this membrane only via specific transporters. This inner membrane is folded into a series of internal ridges called cristae. Hence, there are two compartments in mitochondria: (1) the space between the outer and the inner membrane, and (2) the matrix which is bounded by the inner membrane. The reactions of the citric acid cycle take place in the matrix, which also contains a pool of NAD^+ and NADP^+ that remains separate from pyridine nucleotide enzymes of the cytosol. Oxidative phosphorylation takes place in the inner mitochondrial membrane. This cellular respiration starts with the formed strong reducing agents NADH and FADH_2 and is the culmination of a series of oxidation–reduction transformations utilizing the four enzyme complexes (I to IV) of the mitochondrial respiration chain (Fig. 28.2).

The flow of electrons from NADH or FADH_2 to O_2 through these protein complexes leads to the pumping of

protons out of the mitochondrial matrix. The resulting uneven distribution of protons generates a pH gradient and a trans-membrane electrical potential that creates a proton motive force. Finally, these protons flow through ATP synthase to generate ATP from ADP and inorganic phosphate (Mitchell 1961).

28.2.2 Respiration as Major Producer of Reactive Oxygen Species (ROS)

In 1954, Gerschman and Gilbert proposed that most of the damaging effects of elevated oxygen concentrations in living systems is attributed to the formation of free oxygen radicals (Gerschman et al. 1954; Gerschman 1981). In 1956, Harman published the “free radical theory of aging” that proposed that oxygen radicals, by damaging cellular macromolecules, are responsible for the aging process (Harman 1956). This idea did not capture the interest of many biologists until 1969 when the enzyme superoxide dismutase (SOD), was discovered which catalytically removes specific free radicals (McCord and Fridovitch 1969). In living systems, superoxide anion ($\text{O}_2^{\cdot -}$) is the primary ROS which can generate

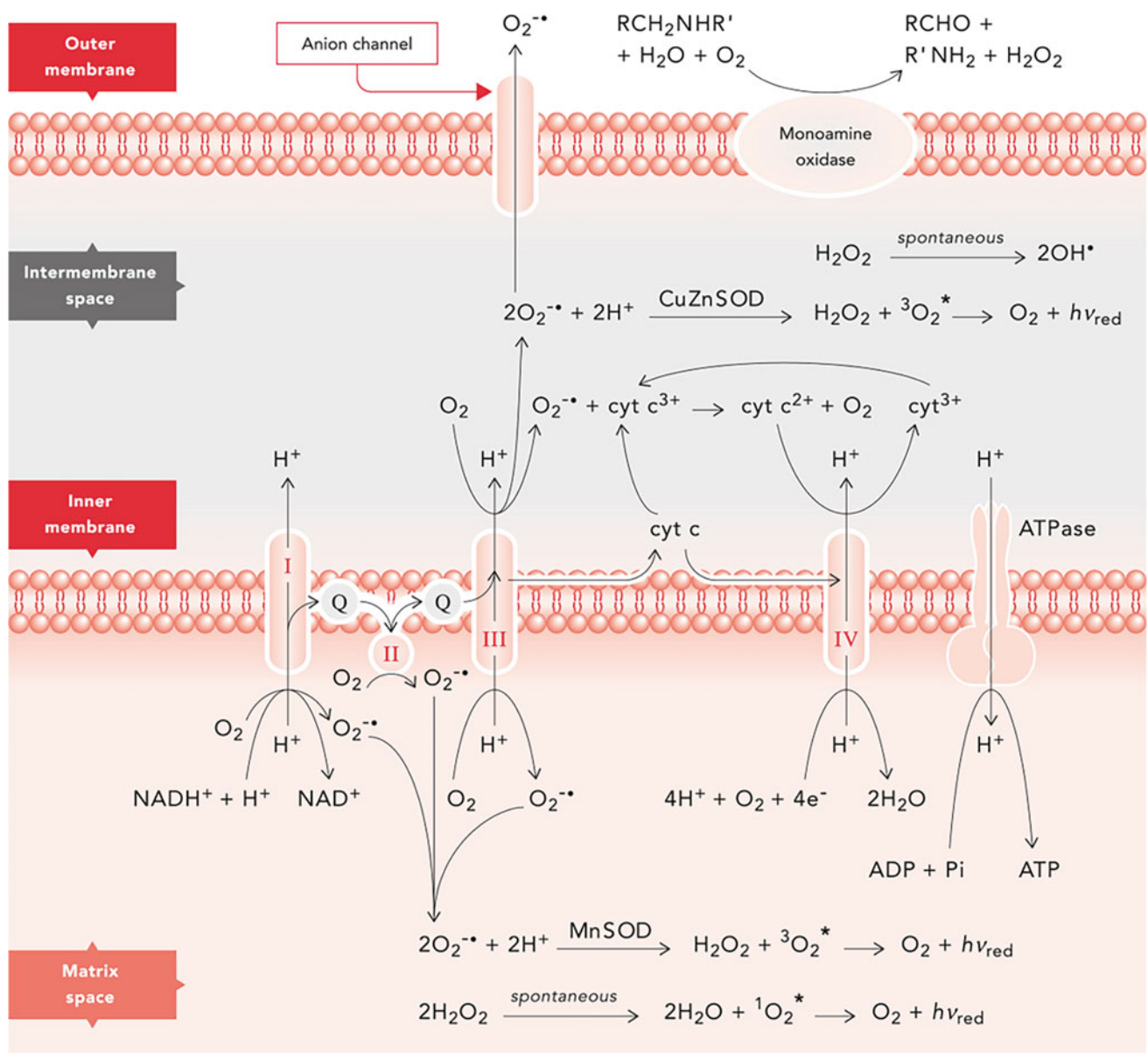


Fig. 28.2 Transport of electrons and protons by the four enzyme complexes (I to IV) of the mitochondrial respiration chain. ATP is synthesized from ADP and Pi by ATP-synthase, taking advantage of the proton gradient (proton motive force) established between the intermembrane space and the matrix by the four protein complexes of the respiration chain. Complete reduction of oxygen is accomplished at complex IV, leading to $O_2^{\bullet -}$ which reacts with protons to generate water at the matrix-oriented site of the inner membrane. But at Complex I, II and III electrons can leak to oxygen at the matrix side generating superoxide anions ($O_2^{\bullet -}$). Dismutation of $O_2^{\bullet -}$ is catalyzed by a manganese containing superoxide dismutase (*MnSOD*) enzyme at the matrix side, leading to hydrogen peroxide (H_2O_2) and excited oxygen in the triplet state (${}^3O_2^*$) which upon decay to the ground state

(O_2) emits photons ($h\nu_{red}$). At the intermembranous space, electrons can leak from cytochrome c to oxygen forming $O_2^{\bullet -}$. At the intermembranous space, $O_2^{\bullet -}$ is dismutated by a *CuZnSOD* to H_2O_2 and ${}^3O_2^*$. Oxygen in the triplet state can contribute to the emission of photons when decaying to the ground state. Hydrogen peroxide is also a reaction product of monoamine oxidase situated at the outer mitochondrial membrane. Hydrogen peroxide may be spontaneously reduced to water and singlet oxygen (${}^1O_2^*$) and when singlet oxygen decays to the ground state it emits photons ($h\nu_{red}$). Hydrogen peroxide may also be reduced to the hydroxyl radical OH^\bullet by reduced transition metals, which in turn may be re-reduced by $O_2^{\bullet -}$, propagating this process

secondary highly reactive substances (Chance et al. 1975; Kellogg and Fridovitch 1975).¹ Notwithstanding their efforts, many scientists in the 1970s, unfamiliar with free radicals, regarded the field as irrelevant to mainstream biology, till experimental data in the 1980s emphasized that the reactive species actually do produce alterations in DNA, proteins, and lipids (Halliwell 2007).

The central role of molecular oxygen in the production of ROS can be easily understood because a single oxygen atom is unstable, which is why each one tends to bind a twin atom, forming molecular oxygen, in which one pair of electrons is shared and two unpaired electrons remain; oxygen therefore is actually a free biradical (Jamieson 1989). If the oxygen atom does not find a twin atom, it can accept hydrogen to form water (H₂O). The reduction of O₂ requires the transfer of four electrons providing two molecules of H₂O.² Such a complete strategy for the full reduction of O₂ is accomplished vis-à-vis the cytochrome c oxidase complex which does not release partly reduced intermediates by holding O₂ tightly between *Fe* and *Cu* ions. If this protection is not present, an only partial reduction of O₂ would be generated. In living systems, superoxide anion (O₂⁻) is created from oxygen by an electron addition within the mitochondrial respiratory chain (Taylor et al. 1986; Halliwell 1991). Superoxide anion can generate secondary highly reactive substances, interacting with other molecules and giving rise to chain reactions. The chain reactions following superoxide anion production include both oxygen radicals and certain nonradicals that are easily converted into radicals [singlet oxygen (¹O₂) and hydrogen peroxide (H₂O₂)]. The collective term for this group of oxidizing agents is ROS, what means that all oxygen radical species are ROS, but not all ROS are oxygen radicals (Halliwell 2007). Nowadays, different free-radical species are distinguished – the oxygen-centered, nitrogen-centered, carbon-centered and sulfur-centered radicals; however, in living systems, oxygen radicals represent the most important class of radical species generated (Buonocore et al. 2010)³.

28.2.3 Respiration as Major Producer of Ultraweak Photon Emission (UPE)

The first documentations without doubt of radiation emanating from living organisms began in 1955 in Italy, and in the early 1960s in Russia, when sensitive photomultiplier tubes were utilized to study the photon emission from biological organisms and tissues (Colli and Facchini 1954; Veselowskii et al. 1963; Popov and Tarusov

1963; Tarusov and Zhuravlev 1965). The advances in photodetection with extremely sensitive photomultiplier tube technology have confirmed that many, if not all, living systems emit very low levels of ultraviolet [UV], visible (VIS) and near infrared [NIR] photons (Van Wijk 2014). The biological emission was originally described as spontaneous ultraweak chemiluminescence and later as spontaneous ultraweak photon emission (UPE). It was demonstrated that the intensity of photon emission is dependent on the concentration of oxygen in the atmosphere. In searching for biological compounds that could produce chemiluminescence, carefully controlled tissue homogenization procedures were carried out that break up tissues facilitating cell organelles to remain intact (depending on the procedure) and hence, facilitated the study of which cellular parts were responsible for the photon emission (Tarusov and Zhuravlev 1965). Mitochondria seemed to be the main source of photon emission. It was demonstrated that the luminescence of mitochondria is associated with oxidative phosphorylation (Vladimirov and L'vova 1964). These classic data were reviewed in 1969 (Barenboim et al. 1969). It took until the early 1970s for photomultiplier equipment to be in demand by research laboratories outside Russia eager to study ultraweak photon emission from biological organisms. The research first began to provide experimental data from three other groups, in Japan, Australia, and Poland. They were shortly followed by teams in Germany, United States, and China. A recent overview demonstrates that, in 1980, this resulted in a worldwide research addressing ultraweak photon emission (Van Wijk 2014). In the next section, we will learn how mitochondrial research started to boom, and ultraweak photon emission research was integrated with: (a) production of ROS, and (b) energy production in stress (and adaptation).

28.3 Extending Piles and Beginning of Integration (Period 1980–2000)

28.3.1 ROS in Mitochondrial Functioning and Aging

The complexity of the “mitochondrial task” became more clear when mitochondrial DNA research boomed in the 1980s. Since the early 1960s, it was known that mitochondria house their own DNA (mtDNA); in human cells one or more small 16.6 kb circles of double stranded mtDNA are present in each mitochondrion. The mtDNA is considered a vestige of bacterial heritage. In 1981, the entire human mtDNA sequence was determined (Anderson et al. 1981). It appeared to contain genes that are critical for mitochondrial functioning, coding for 13 respiratory chain polypeptides and 24 nucleic acids (two ribosomal RNAs and 22 transfer

¹ See Chap. 8.

² See Sect. 8.3.

³ See Sect. 8.4.

RNAs) that are needed for intramitochondrial protein synthesis. All mtDNA-encoded proteins are subunits of the respiratory chain complexes I, III, IV and V. It then also appeared that both mitochondrial DNA (mtDNA) and nuclear DNA (nDNA) encode mitochondrial proteins. Nuclear genes code for the majority of mitochondrial respiratory chain polypeptides and complex II (succinate dehydrogenase) is fully encoded by the nuclear genome.

The mtDNA is more simple and is much less protected than the coiled and chromatin packaged nuclear DNA. In comparison to the nuclear genome, it is more susceptible to damage. Mutagens bind to mitochondrial DNA up to 1000 times more strongly than to nuclear DNA whereas the mutation rate in mitochondria is 10–20 times that of the nuclear DNA. Also, DNA repair mechanisms are much less efficient in mitochondria. These observations mean that mtDNA damage and mutation could relatively easily happen and then impair respiration and hence could have a considerable impact on mitochondrial functioning in cell's energy demands. If we combine this with data on the relatively high production of ROS in mitochondria, it suggests a high chance for mtDNA damage (Fleming et al. 1982, 1985; Marcus et al. 1982; Miquel and Fleming 1986). Accumulating levels of ROS in mitochondria may be produced by the reactions of ROS species with mitochondrial membranes, as a result of the chain reactions of lipid peroxidation in which the lipid radicals formed at a previous stage can react with oxygen and hence produce another lipid peroxyl radical and so on (Halliwell and Gutteridge 1985; Halliwell 1991)⁴.

ROS not only can disturb the mitochondrial membrane structure, it is also a continuous source of danger for proteins causing proteotoxicity and for mtDNA. What such mtDNA damage means for cell functioning is only understood if one takes into account that a cell contains many copies of mtDNA, from 1000 to 100,000, depending on the cell type. These mtDNA copies are to a great deal identical in a healthy individual at birth. It means that a single mtDNA mutation or deletion does not lead to a diseased cell state. Patients harboring pathogenic mtDNA defects often have a mixture of mutated and nonmutated (wild-type) mtDNA. The percentage of mutated mtDNA can vary widely from organ to organ, and even between cells within the same individual. To understand mtDNA damage in cell function, we must therefore not only focus on the “vicious cycle theory of mitochondrial ROS production,” but also on time. Mitochondria generate large amounts of ROS directly exposing mtDNA to damage; if ROS causes mtDNA damage, then such damage may result in mitochondrial dysfunction leading to an increase in ROS production, which subsequently elevates the accumulation rate of mtDNA mutations, which will further impair

respiratory chain function. This had led to the above conclusion that within a mitochondrion the oxidative mitochondrial DNA damage accumulates in time. This “normal” aging process may be then the risk factor for the development of age-associated disorders, such as cancer and neurodegenerative diseases.

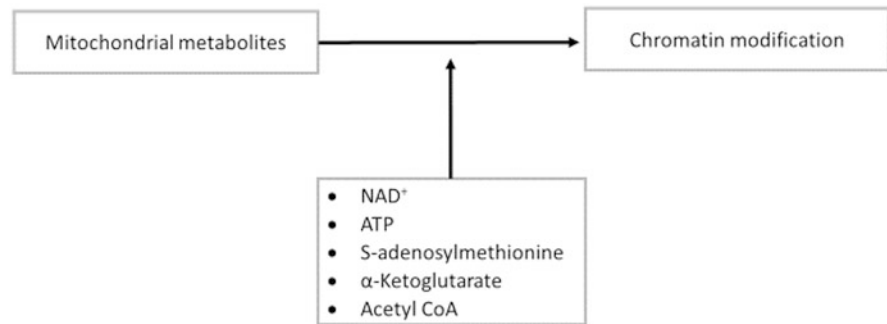
In the long term, an increasing source of dangerous products develop: the major secondary products of lipid peroxidation are dangerous mutagenic aldehydes, malondialdehyde (MDA) and 4-hydroxynonenal/4-hydroxy-2-nonenal (HNE). These products which are sometimes considered markers of the oxidative stress, have unique properties compared with ROS because the noncharged structure of aldehydes allows them to easily migrate through membrane and cytosol and, consequently, to cause far-reaching damaging effects inside or outside the cells. HNE and MDA do not only modify the amino acid residues leading to protein damage, they can also form covalent adducts with nuclei acids leading to various types of DNA damage: double and single-strand breaks, intra- and inter-strand DNA crosslinks, DNA adduct formation and DNA modifications.

A further understanding of the long-term effects of mitochondrial malfunctioning on nuclear gene expression and possible health outcomes, is another type of pathway in the functional interaction between mitochondria and nucleus. In the functional interaction, we must distinguish the anterograde and the retrograde signals. The anterograde signals are defined, as mentioned before, as the signals from nucleus to mitochondria. They control the import of proteins in mitochondria, availability of substrates, the maintenance of the mtDNA and the expression of its genes in accordance with the energy and growth requirements of the cell. The retrograde feedback is defined as the signals from mitochondria to nucleus. In a healthy cell, under physiological conditions, this retrograde feedback is likely to be the normal mitochondrial output of ATP, metabolic intermediates and basal reactive oxygen radicals. On the other hand, mitochondrial retrograde signaling, which is activated under stress, may have the ability to bring about global changes in the nuclear gene expression and phenotype changes in cells.

One such pathway refers to “metabolic epigenetics”: the nuclear alterations of chromatin and other factors that regulate nuclear gene expression resulting from changes in mitochondrial energetics and metabolism. Thus, mitochondria provide key metabolites, for example beta-nicotinamide adenine dinucleotide (NAD⁺), ATP, alpha-ketoglutarate and acetyl coenzyme A that are cosubstrates required for numerous transcriptional and epigenetic processes. These metabolites mediate gene expression changes that control cellular processes via chromatin structure changes and dynamics, DNA methylation, histone modification and

⁴See Chaps. 10 and 11.

Fig. 28.3 Mitochondrial metabolites involved in chromatin modification and epigenetic regulation



noncoding RNA expression. Epigenetic modifiers include DNA methyltransferases, histone acetyltransferases, histone deacetylases, sirtuins (SIRTs), histone demethylases, poly (ADP-ribose) polymerase and other enzymes that work coordinately in regulating gene expression (Fig. 28.3).

The last type of pathway resulting in retrograde signaling is the one which is initiated by unfolded proteins, the unfolded protein response initiated signaling. Mitochondrial stress affects protein homeostasis, in which oxidatively damaged proteins and unfolded proteins are degraded by mitochondrial proteases for quality control. The latter requires that the matrix unfolded protein response is communicated to the nucleus in order to induce the appropriate stress response which involves the gene expression and synthesis of a special group of proteins: the stress or heat shock proteins (HSP). These proteins function as chaperones to recover the cell against the ravages of abuse by preventing incorrect interactions with other proteins, and assist in their correct refolding (Ellis et al. 1989; Pardue et al. 1989).

That in responses to mitochondrial dysfunction the cell may not only age but also may change its nuclear gene expression was actually demonstrated since the second breakthrough in mitochondrial DNA research in 1988 when the first pathogenic mtDNA mutations and deletions were identified which cause human disease (Wallace et al. 1988; Holt et al. 1988). Since the mtDNA codes for the central genes of the mitochondrial energy-generating process of oxidative phosphorylation (OXPHOS) the diseases are commonly metabolic and degenerative diseases. The milder mtDNA variants can affect caloric metabolism and result in metabolic abnormalities such as diabetes and obesity and/or affect the most energy-demanding organs such as the brain and lead to late-onset degenerative diseases, such as psychiatric disorders, Parkinson disease and Alzheimer disease. The more severe mtDNA mutations, like MERRF (myoclonic epilepsy with ragged fibers syndrome) and MELAS (mitochondrial encephalopathy, lactic acidosis, and stroke-like episodes syndrome), cause progressive multisystem diseases, frequently resulting in premature death. The most severe mtDNA mutations can lead to lethal childhood diseases, such as Leigh syndrome (also called subacute necrotizing

encephalomyelopathy). The growing list of defects has pushed mitochondriopathies into the realm of many medical specialties including endocrinology, gastroenterology, immunology, neurology, oncology and others (Chinnery 1993; Schon et al. 1997; Wallace 1999).

28.3.2 Connecting Ultraweak Photon Emission with Metabolic Adaptation and Stress

Extra-ordinary ROS production and the associated ROS-induced molecular damage are the basis of cellular stress and possible shift in health. The term “stress” is broadly used and applied to several types of conditions, which need some clarification within the context of this overview. We use the term stress to focus on a state of the cell in which it meets a (life-threatening) disbalance in the functional interaction between mitochondria and nucleus; in other words, in the balance between the anterograde signals (from nucleus to mitochondria) and the retrograde signals (from mitochondria to nucleus). For a cell in a complex, multicellular organism – plant, animal, or human – such demand may reach the cell via a hormone (or other signaling substance) demanding for a production of energy (ATP) which is extraordinarily high or lasting longer than “normal.” Another stress condition is stress from “within.” Functional macromolecular structures and complexes may be damaged and either be repaired or handled by organized decay systems since, as nonfunctional structures, they may obstruct normal functioning of the cell. Finally, the term stress is also utilized when cells are exposed to “toxic” compounds (for example heavy metals) which may react with enzymes (or macromolecules) and disturb normal working capacities and threaten cell’s life unless adaptation results in protection by inducing stress tolerance (Schamhart et al. 1984; Wiegant et al. 1993, 1995; Ovelgönne et al. 1995a, b). Anyway, in stress, the cell meets a disbalance between energy demand and production which, if not solved, becomes life-threatening. In the early 1980s, the typical molecular stress response has moved to center stage in cell and molecular biology (Schlesinger et al. 1982). Heat shock proteins (hsps)

in tolerance development (Schamhart et al. 1984; Van Dongen et al. 1986) with their role as chaperones (and chaperonins) in protein folding and trafficking, and hence in mitochondria and other organelle functioning (Welch et al. 1989) as well as the mechanism of ROS-induced expression of genes coding for stress proteins (Burdon et al. 1990; Ovelgönne et al. 1995a, b), became the focus of investigations in many areas of cell biology.

Automatically, this has raised questions about ultraweak photon emission in biological stress conditions. The answer was presented in a multiauthor review on “Photon emission, stress and diseases” (Van Wijk et al. 1992). This series of reviews covered three decades of research on ultraweak photon emission of perturbed organisms, including bacteria (Tilbury 1992), yeast (Tilbury 1992; Slawinski et al. 1992), amoeba (Tilbury 1992; Fisher et al. 1991; Fisher and Rosenberg 1988), and perturbed plants (Slawinski et al. 1992; Gu and Popp 1992) and animals (Slawinski et al. 1992; Inaba 1988; Van Wijk and Schamhart 1988). Organisms were exposed to mechanical, electrical, temperature, oxidative and metabolic/nutritional, chemical and photochemical (UV)-induced perturbations. In most instances, the perturbation resulted in an increase in photon emission. A few classic examples in the plant, animal, and microorganism arena will be presented to illustrate the phenomenon of increased UPE in stress.

In case of plants, the classic studies of photon emission in temperature stress of grain seedling illustrate that if temperature conditions become life-threatening, it is associated with increased emissions. The UPE intensity of seedlings increased dramatically both at an “upper temperature growth limit” and at a “lower temperature growth limit.” At both temperature limits, associated with a UPE glow, the life of the seedlings was threatened. The upper and lower glow limits of different grain species were associated with their heat resistance and frost resistance, respectively (Tarusov and Veselovski 1978).

In case of animal tissues and organs, the earliest studies focused on UPE of nerve and muscle during activation by electrical or mechanical stimulation. The activation requires a certain threshold. In the case of subthreshold stimulation, no increase in the light emission could be detected. UPE was associated only in case of real stimulation. This was demonstrated in sciatic nerve of a frog emitting light when it was excited by electric pulses (Artemy et al. 1967). An increase in photon emission was also observed upon activation of the contraction of a frog heart, both when isolated and when still in the thorax (Perlygin and Tarusov 1966). A similar effect was reported for UPE intensity from isolated rectus abdominal muscles (Shtrankfel'd et al. 1968) and the gastrocnemius and sartorius muscles after stimulation (Blokha et al. 1968).

Yeast cultures as simple model systems have also been explored for the connection between stress and UPE in metabolic adaptation. In yeast, UPE was studied during growth of oxygenated cultures on glucose-rich media from their exponential state into the stationary state. This requires a metabolic shift when glucose becomes limiting, the phenomenon is termed “glucose effect” or “catabolite repression” (Polakis and Bartley 1965; Polakis et al. 1964; Van Wijk et al. 1969). Yeast cells start to grow preferentially with glucose if that substrate is available; strongly repressing the formation of mitochondrial structures and the synthesis of respiratory and disaccharide (maltose) splitting enzymes. When glucose has been consumed, the yeast cells adapt to the alcohol excreted in the medium developing mitochondria and using alcohol for their final growth in the stationary phase. Such a model system has demonstrated increased UPE during the adaptation vis-à-vis mitochondrial development (Quickenden and Tilbury 1983).

The toxin-induced stress studies not only have suggested that the photon emission response may serve as a rapid indicator of perturbation of homeostasis, but has also demonstrated that the kinetic pattern of UPE is dose-dependent and contains information on the severity of stress. At lower doses, when the homeostasis is weakly and reversibly perturbed, this is manifested as a gradual increase of UPE reaching a new quasi-stationary level several times higher than that of the original (nontreated) culture. At high doses, the inhibitor results in a single peak of UPE reflecting an irreversible perturbation of homeostasis. This phenomenon has been confirmed regardless of the type of life-threatening stress (Slawinski et al. 1992; Ruth and Popp 1976).

28.3.3 Differentiating UPE: Connecting ROS Species with Spectral Bands

In 1980, several important papers demonstrated that UPE from mammalian tissues could serve as a noninvasive assay for oxidative radical reaction (Boveris et al. 1980, 1981; Cadenas et al. 1980a, b). This stimulated the studies on identification of the chemical reactions which are responsible for increased photon emission after perturbation to the extent that spectral analyses were included. This state of the art was the central topic of a number of reviews plus a multiauthor review (Slawinska and Slawinski 1983, 1985; Cadenas 1984; Popp et al. 1988).

In some reviews, the identification of the chemical reactions which are responsible for increased photon emission after perturbation has been discussed to the extent that experimental data about endogenous ROS and spectral analyses were included. The combination of superhigh sensitivity photon-counting systems and spectral analysis

techniques in the mid-1980s made it possible to identify various ultraweak photon emission bands in the range of 400–800 nm (Slawinska and Slawinski 1983, 1985; Cadenas et al. 1984; Cadenas 1984; Inaba 1988).

To summarize the connection between the production of superoxide anions and the spectrum of photon emission, we begin with superoxide anions. This may appear on both sides of the inner mitochondrial membrane and hence also in the matrix space. Within both compartments, enzymes are present that may specifically react with superoxide anion ($O_2^{\cdot -}$). These are two different superoxide dismutase (SOD) enzymes, a manganese containing one (located at the matrix side), and a copper zinc-containing enzyme (located at the intermembrane space). Both SOD's transform superoxide anions (vis-à-vis protons) to hydrogen peroxide and excited oxygen in the triplet state ($^3O_2^*$). This excited, high-energy state of O_2 is able to emit a red photon in the transition to O_2 .

Another radiation comes from hydrogen peroxide when it spontaneously dismutates to water and excited singlet oxygen ($^1O_2^*$) which (upon decay to the ground state) may also emit a red photon. Excited singlet oxygen molecules can emit in the 780 nm or in bands that lie even further into the infrared. Other emission bands, centered on 634 and 703 nm, arise after dimerization of excited singlet oxygen. Such emission is most compatible with red emissions observed from the different organisms (Fig. 28.1).

The excited singlet oxygen molecules may excite a secondary emission by reacting with lipids (especially unsaturated fatty acids) wherein the methylene groups in double bonds possess reactive hydrogen atoms. By the dismutation reactions of peroxy radicals and the cleavage of peroxides, the most common emitters of UPE are produced: carbonyl compounds ($>C=O$) in the excited singlet and triplet states as well as excited dimers (dimols) of the singlet molecular oxygen $^1O_2^*$. Excited carbonyl groups may be responsible for the emissions at wavelengths within the 350–500 nm range. Upon incomplete reduction of H_2O_2 , the hydroxyl radical (OH^*) is generated (one of the strongest oxidants in nature). The hydroxyl radical (OH^*) may also lead to the emission of photons when it reacts with lipids, resulting in the formation of excited carbonyl species (ROO^*) wherein oxygen is in the excited singlet or triplet states. Upon decay to the ground state, carbonyl species emit photons. It is also emphasized that recombination reactions of certain radicals may release up to 480 kJ/mol energy, which is sufficient to generate UV-photons in the 230–300 nm range (Slawinski 1988; Slawinski et al. 1992).

The application of this knowledge in experimental stress research was dependent on the accuracy of the experimental technology for spectral analysis. In the studies on UPE during the metabolic transition (Tilbury 1990, 1992), UPE is not only more bright, but the analysis of the spectrum reveals that

the brighter emission mainly occurs in a spectral band from 450 to 600 nm. A similar spectral increase was detected when yeast cells were grown in the presence of appropriate dyes resulting in respiratory deficiency. In such conditions, the UPE transition peak was about ten times as intense. Spectral distributions studies indicated that the brightness is dominated by a band around 600 nm (Quickenden and Tilbury 1983, 1991) indicating that lipid peroxidation reactions are involved in UPE. However, more details were not presented because the spectral area of interest, ranging from 210 nm to 630 nm, was only resolved in 7 spectral areas with a broadness of roughly 70 nm. Other researchers have estimated the spectral analysis of UPE of yeast with more resolving power utilizing 11 spectral areas with a broadness of roughly 20 nm within the 470 nm to 700 nm range (Ezzahir et al. 1992; Slawinski et al. 1992). They exposed yeast to formaldehyde stress which leads to intra- and intermolecular crosslinking and subsequent denaturation of proteins (Slawinsky 1990, 1991). The intensity of UPE increases with the increase of the concentration of formaldehyde in the range 0.06–7% by a factor up to 70, while oxygen consumption by yeast cells decreases. The observed photonic response from stressed yeast cells was assigned to both excited carbonyl groups and excited singlet oxygen formed during the decomposition of hydroperoxides.

28.4 Enhanced Integration Vis-à-Vis Research of Mitochondrial Dynamics (Period 2000–2020)

28.4.1 Mitochondrial Structural Dynamics

Novel (confocal scanning and deconvolution) microscopic techniques allowing three-dimensional visualization of live cells, revealed that mitochondria do not sit idle within the cell as static bean-like organelles according to traditional textbooks. The mitochondria change their form as the result of fusion and fission. A mitochondrion could be separated in parts by fission; but a mitochondrion could also increase in size by fusion. The picture of a mitochondrial network which undergoes extensive remodeling in a constant dynamic process has appeared (reviewed in Liesa et al. 2009).

The molecular biology of the movement, tethering, fusion and fission events have been extensively studied. Proteins mediating mitochondrial fission are: Dynamin-related protein 1 (Drp 1, is mostly cytosolic and translocates to the outer mitochondrial membrane during fission), Fission 1 protein (Fis 1, located in the outer mitochondrial membrane) and Mitochondrial fission factor (Mff, also located in the outer mitochondrial membrane) (Frank et al. 2001; Lee et al. 2004). In fact, Mff and Fis 1 mediate fission by recruiting

Drp 1 to the mitochondria which requires GTP hydrolysis. Mitochondrial fusion is mediated by the Optic Atrophy gene 1 (Opa 1, located in the inner membrane) and Mitofusins (Mfn1 and Mfn2, located in the outer mitochondrial membrane) (Lee et al. 2004; Ishihara et al. 2006). These three proteins require GTPase activity to mediate fusion and remodel the internal cristae structure.

The fusion and fission machinery is a vital part of the continuing Mitochondrial Life Cycle which occurs under steady state nutrient conditions. The continuous changes to mitochondrial architecture enable the reorganization of mitochondrial components. Hence, maintaining both fusion and fission sequentially in a repeating cycle is the key to optimal bioenergetic functioning of the mitochondrial population within the cell (Twig et al. 2008a; Molina et al. 2009; Mouli et al. 2009). Studies of mitochondrial dynamics have identified an intriguing link between the mitochondrial architecture and the energy supply (Benard et al. 2007). Cells exposed to rich nutrient environments tend to keep their mitochondria in a fragmented state and mitochondria in cells under starvation tend to remain for a longer duration in the connected state. It has suggested that the functionality of the shift in the fusion–fission balance is related to damage and repair. In metabolic rich environments that may result in excessive ROS generation and molecular damage, the formation of inefficient ATP-producing parts of mitochondria may be avoided through the process of fission. Thus, fission allows dilution by exchanging such materials between separate regions of the network and hence allows optimal repair of defective mitochondria. Moreover, fission may also isolate dysfunctional mitochondrial parts to avoid the accumulation of damaged mitochondria by directing these parts along the autophagy route (Parone et al. 2008). Evidently, upon nutrient depletion, fusion is believed to dilute damaged molecules and may protect mitochondria from engulfment with autophagosomes (Twig et al. 2008b).

A relevant observation to this discussion came from the confocal microscopic visualization of single mitochondria units and tracking them over time utilizing specific fluorescent substances to probe specific mitochondrial activities (see also Sect. 28.4.2). Wikstrom et al. (2007, 2009) observed that a fission event may generate two bioenergetically different mitochondria, one with a higher membrane potential and one with lower membrane potential. Having such a single daughter mitochondrion with lower membrane potential illustrates two future options: (1) recover its membrane potential and regain the capacity to reconnect with the network or (2) remain in the solitary period, depolarized. If membrane potential is not restored, the solitary mitochondria will not be able to re-engage with the network and will be degraded. These solitary and dysfunctional mitochondria, with no fusion capabilities, comprise the preautophagic pool of mitochondria. The effect of nutrient supply on fusion and

fission may be considered an important effect in the formation of a mitochondrial preautophagic pool and on the process of autophagy (Twig et al. 2010). In this context, one can appreciate that the cycle of mitochondrial fusion and fission would be compromised if mitochondria were disabled to allow for bioenergetic adaptation following changes in nutrient availability, i.e., feeding and fasting states. Any prolongation in the fasting state requires a bioenergetic adaptation that will shift the mitochondrial dynamics balance to homogenize the mitochondrial population, preventing segregation, formation of the preautophagic pool and removal of damaged components by mitophagy. In the fed and nutrient excessive state, high respiratory rates can lead to increased ROS generation and accumulation of dysfunctional units and, in addition, to mechanisms affecting the autophagic machinery downstream of the preautophagic pool of mitochondria.

28.4.2 Mitochondrial “Flashing” of Superoxide Formation

The second recent breakthrough in mitochondrial research is the development and application of novel fluorescent tools that probe different mitochondrial activities in individual mitochondria in living cells in real time using confocal scanning or deconvolution microscopy. These tools could be specifically introduced in mitochondria and probe different mitochondrial activities or substances by showing fluorescence in the presence of these specific compounds. The tools make it possible to study different processes in a single mitochondrion over time: formation of superoxide, mitochondrial Ca^{2+} uptake, mitochondrial membrane potential and pH, they all may contain information about the mitochondrial functioning.

The formation of superoxide which is considered the primary ROS, has been probed in a mitochondrion with a mitochondrial-targeted biosensor cpYFP protein (Wang et al. 2008). When tested in living cells and animals, it showed the remarkable phenomenon of acute increases in fluorescence within the mitochondrial matrix. This was a breakthrough because it demonstrated that the probed process, i.e., superoxide formation, is not characterized by a steady-state level, as supposed in the past, but instead, by a “flash,” a transient and stochastic event confined within an individual mitochondrion. The pulsed mitochondrial superoxide formation was observed in a range of mammalian tissues and cells (Wang et al. 2012, 2013). Although the frequency of flash events differed dramatically across different cell types, the kinetic properties of individual flash events were essentially invariant. Because mt-cpYFP detects superoxide but not hydrogen peroxide (Wang et al. 2008), and superoxide in mitochondria is rapidly dismutated to hydrogen peroxide, then the fact that mitochondrial superoxide flashes activity persists over

10–15 seconds is consistent with a robust burst of superoxide production within the mitochondrial matrix during the time frame of the flash.

The development of fluorescent substances for recording other mitochondrial respiration-related processes, such as Ca^{2+} uptake, pH or membrane potential, led to a second discovery. Using specific probes for these other mitochondrial processes, similar pulsatile or flash events were detected with the same kinetic features as were detected with cpYFP (Wei and Dirkson 2012; Wang et al. 2016). This culminated in studies monitoring simultaneously two or more probes and showing synchronized flashing. The synchronized flashing has been confirmed of different mitochondrial targeted fluorescent indicators within a mitochondrion, illustrating that a single flash event involves multiple transient concurrent changes within the mitochondrion, including changes in ROS generation, Ca^{2+} homeostasis, membrane potential and pH. It resulted in the picture that not only all respiration-related processes but also the associated ROS signaling (and, presumably, also UPE) in a mitochondrion is an on-off phenomenon. They all share the common feature of a strong dependence on electron flow of the mitochondrial electron transport chain (Azarias and Chatton 2011; Breckwoldt et al. 2014; Gong et al. 2015; Santo-Domingo et al. 2013; Schwarzlander et al. 2012; Wang et al. 2008; Wei-LaPierre et al. 2013). The finding is also in agreement with the notion that the electron flow of the mitochondrial electron transport chain underlies ROS production⁵.

It has been argued that mitochondrial flash activity can be used as a biomarker for mitochondrial respiration. Several studies have reported that mitochondrial flashes in living cells, tissues and animals are stimulated by physiological respiration substrates, including oxygen, glucose, fatty acids, and specific substrates for the electron transport chain complexes (Fang et al. 2011; Gong et al. 2015; Pouvreau 2010; Santo-Domingo et al. 2013; Shen et al. 2014; Wang et al. 2008; Wei et al. 2011a, b). Moreover, recent reports using genetic animal models have provided evidence that mitochondrial flash activity is dependent on electron transport chain components. In these studies, knock out (KO) of electron transport chain components or related mitochondrial proteins resulted in decreased or abolished mitochondrial flash activity in live cells and animals (Gong et al. 2015; Karamanlidis et al. 2013).

28.4.3 Toward Coherence in Mitochondrial Flash Activity

Mitochondrial flashes reflect a fundamental physiological phenomenon that has a significant functional impact on the

type of regulation in bioenergetic adaptation at mitochondrial level. This type of regulation offers the possibility to adjust an increased or decreased energy demand of a cell by changing the frequency and number of its pulsing ATP producing mitochondria. Several studies have clearly shown that mitochondrial flash activity contributes to both local physiological signaling and pathological conditions in skeletal muscle and heart. The characterization of mitochondrial superoxide flash properties in skeletal muscle cells regarding the spatial dynamics was performed by Pouvreau (2010) and Wei et al. (2011a, b) utilizing automated detection and analysis program for characterization of flash events during time lapse. This program identifies and quantifies flash frequency, amplitude, full duration at half maximum, time constant of decay and spatial area during the time series. These recordings of flash activity in skeletal muscle fibers demonstrated that individual events exhibit a variety of spatial morphological appearances. Some seemed to involve a single mitochondrion, point shaped or column-shaped, longitudinal or transversal, arranged adjacent mitochondria. A third type of appearances of flash events encompassed large clusters of mitochondria and involved thick longitudinal columns. Hence, thick longitudinal columns were often involved in large clusters. On the other hand, point shaped and column shaped events were found in longitudinal thin columns or transversal paired slender mitochondria. Even the larger cluster-sized flashes presented a striking homogeneity in terms of increase of fluorescence intensity. Furthermore, the same cluster could flash several times during a 3 min record, the shape of the successive flashes being identical. These units have well-defined boundaries and are stable in time. Active units are surrounded by quiescent ones; this shows that superoxide does not diffuse randomly to adjacent mitochondria. Overall, results show the existence of intermyofibrillar mitochondrial units of variable size, characterized by their superoxide production.

Another important finding was that repetitive tetanic stimulation exerts an increase in frequency. However, the effect on superoxide flash production is biphasic when comparing moderate stimulation with an intense activity, the latter resulting in a reduction in frequency, amplitude (Imamura et al. 2009). The marked reduction in flash frequency and amplitude was unlikely due to irreversible damage of the mt-cpYFP probe, since flash activity recovered to control levels 5–8 min after the termination of stimulation. Even more surprising was the observation that total cellular ROS levels increase substantially during repetitive high-frequency stimulation and thus contribute to a decrease in force production associated with fatigue (Allen et al. 2008; Powers and Jackson 2008; Jackson et al. 2002). In any event, the decrease in superoxide flash activity that occurs after stress by severe (prolonged) tetanic stimulation suggests that increased cellular levels of ROS that occur during muscle fatigue is not

⁵See also Chap. 14.

related to superoxide flash activity but is beyond the coherent portion and is representing an increase in the tonic level.

This has also been illustrated for heart (Wang et al. 2012). A continuous pumping function of the heart demands for high levels of cytosolic energy and hence mitochondrial respiration. Under these conditions, the required increase in mitochondrial respiration is associated with increased generation of mitochondrial flashes. Several studies have explored the role of mitochondrial flash activity under pathological conditions. During heart failure, mitochondrial flash activity is decreased, which likely reflects compromised mitochondrial metabolism (Gong et al. 2014). During reperfusion following cardiac ischemia, mitochondrial flash activity mirrors the burst in mitochondrial ROS production and mPTP openings (Murphy and Steenbergen 2018; Wang et al. 2008).

To conclude this section, it can be stated that mitochondrial flash activity may reflect a “switch” between a quiescent state and an excited state within each mitochondrion. An increase in energy demand is sensed and translated into a transient burst or acceleration in aerobic respiration (Aon et al. 2003; Azarias and Chatton 2011; Kembro et al. 2013; Li et al. 2012; Wang et al. 2008; Wei et al. 2011a, b). In this regard, individual (or interconnected) mitochondria are regulated and work autonomously. At the whole cell level, controlling the autonomy of individual mitochondria could enable precise and prompt manipulation of energy production to match fluctuations in energy demand. Under certain conditions, such as during whole cell ROS oscillations, individual mitochondrion could function in synchrony or form functional networks (Aon et al. 2003, 2008; Glancy et al. 2015; Kembro et al. 2013; Kurz et al. 2010, 2015; Wei et al. 2011a, b). In that regard, the current paradigm that views mitochondria as passive energy producers may shift to a more active participant and regulator of whole cell energy metabolism.

28.5 Perspective on Integration: Noninvasive UPE Recording In Vivo

A further integration is most likely expected to be based on the characterization of dynamic ROS regulation utilizing the ROS produced emission of photons. This should broaden and deepen our understanding of the complex role of mitochondria in health and disease. In most studies, the mean intensity or strength of the photon signal was utilized to quantify the signal. This is only one of many variables of the signal. Its value is limited. Therefore, another strategy is under development that has focused on the distribution of counts in a photon signal and the discovery of novel photon count distribution parameters to describe combination of amplitude and frequency modes of ROS, and hence, number

of photons emitted in subsequent short periods of time. The “digitized” photon production allows the distinction of “frequency-modulatory (FM) modes” of photons (from FM modes of ROS) and sustained or steady-state photon emission (from ROS production in amplitude-modulatory (AM) mode). As mentioned earlier, accumulating evidence is suggesting that the FM mode of ROS regulation is uniquely suitable to regulate local signals such as EC coupling under physiological conditions (Gong et al. 2015; Ying et al. 2016). Under extreme conditions or strong stresses, such as ischemia-reperfusion or cell damage, the FM mode activity becomes uncontrolled and significantly augments global or whole cell ROS signaling (Aon et al. 2003; Wang et al. 2008; Ying et al. 2016; Zorov et al. 2000).

A few of the possible novel variables have been studied for human photon signals. In one study, the photon count distribution was described as “Best fitting” according to the squeezed state model with its specific variables (Orszag 2000; Bajpai 2005). A first calculation of these squeezed state model parameters was based on photon count distribution of three human body sites (Van Wijk et al. 2006). The squeezed state parameters of different body locations were not different for a single subject. This line of research has been continued using large groups of subjects (Van Wijk et al. 2008, 2013; Zhao et al. 2016; Sun et al. 2017; He et al. 2019). Recent studies have extensively described the attributes (parameters) of the photon count distribution of time series of counts according to the squeezed state model: the squeezed state parameters $[\alpha]$, r , θ and ϕ , the squeezed state index, and sum of the squares of residue (Bajpai et al. 2013; Sun et al. 2017; He et al. 2019).

Fano factor (the ratio of variance to the mean of a time series (Fano 1947)) is another property of the photon count distribution in time series. Fano factor of a UPE signal changes with the bin size of the time series. The fluctuations were around a line specified by its slope and intercept. Fano factor properties have been estimated in a few human studies (Bajpai et al. 2013; Van Wijk et al. 2005, 2010; Zhao et al. 2016; Sun et al. 2017; He et al. 2019).

Future studies designed to advance our understanding of the composite nature of the two proposed modes of mitochondrial flash activity in health and disease are crucial for moving this field forward.

References

- Alberts B (2015) *Molecular Biology of the Cell* (6th edition). Garland Science, New York
- Allen DG, Lamb GD, Westerblad H (2008) Skeletal muscle fatigue: cellular mechanisms. *Physiol Rev* 88:287–332
- Anderson S, Bankier AT, Barrell BG et al (1981) Sequence and organization of the human mitochondrial genome. *Nature* 290:457–465

- Aon MA, Cortassa S, Marban E (2003) Synchronized whole cell oscillations in mitochondrial metabolism triggered by a local release of reactive oxygen species in cardiac myocytes. *J Biol Chem* 278: 44735–44744
- Aon MA, Cortassa S, O'Rourke B (2008) Mitochondrial oscillations in physiology and pathophysiology. *Adv Exp Med Biol* 641:98–117
- Artemý VV, Goldobin AS, Gus'kov LN (1967) Recording the optical emission of a nerve. *Biophysics* 12:1278–1280
- Azarias G, Chatton JY (2011) Selective ion changes during spontaneous mitochondrial transients in intact astrocytes. *PLoS One* 6:e28505
- Bajpai RP (2005) Squeezed state description of the spectral decompositions of a biophoton signal. *Physics Letters A* 337:265–273
- Bajpai RP, Van Wijk EPA, Van Wijk R et al (2013) Attributes characterizing spontaneous ultraweak photon signals of human subjects. *J Photochem Photobiol B* 129:6–16
- Barenboim GM, Domanskii AN, Turoverov KK (1969) Luminescence of biopolymers and cells. Plenum Press, New York-London
- Benard G, Bellance N, James D et al (2007) Mitochondrial bioenergetics and structural network organization. *J Cell Sci* 120:838–848
- Blokha VV, Kossova GV, Sizov AD et al (1968) Detection of ultraweak glow of muscles on stimulation. *Biophysics* 13:1084–1085
- Boveris A, Cadenas E, Reiter R et al (1980) Organ chemiluminescence: Noninvasive assay for oxidative radical reactions. *Proc Natl Acad Sci USA* 77:347–351
- Boveris A, Cadenas E, Chance B (1981) Ultraweak chemiluminescence: a sensitive assay for oxidative radical reactions. *Fed Proc* 40:195–198
- Breckwoldt MO, Pflster FM, Bradley PM et al (2014) Multiparametric optical analysis of mitochondrial redox signals during neuronal physiology and pathology in vivo. *Nat Med* 20:555–560
- Buonocore G, Perrone S, Tataranno ML (2010) Oxygen toxicity: chemistry and biology of reactive oxygen species. *Seminars in Fetal & Neonatal Medicine* 15:186–190
- Burdon RH, Gill V, Evans CR (1990) Active oxygen species and heat shock protein induction. In: Schlesinger MJ, Santoro MG, Garaci E (eds), *Stress Proteins*, Springer Verlag, Berlin/Heidelberg, p 19–25
- Cadenas E, Boveris A, Chance B (1980a). Low-level chemiluminescence of bovine heart submitochondrial particles. *Biochem J* 186: 659–667
- Cadenas E (1984) Biological chemiluminescence. *Photochem Photobiol* 40:823–830
- Cadenas, E, Boveris A, Chance, B (1980b) Hydroperoxide-dependent chemiluminescence of submitochondrial particles and its relationship to superoxide anion and other oxygen radicals. In: Bannister JV, Hill HAO (eds) *Developments in Biochemistry*. Elsevier, North Holland, New York, p 92–10
- Cadenas E, Boveris A, Chance B (1984) Low level chemiluminescence of biological systems. In: Pryor WA (ed) *Free Radicals in in Biology*, Academic Press, Orlando, p 211–242
- Chance B, Sies H, Boveris A (1975) Hydroperoxide metabolism in mammalian organs. *Physiol Rev* 59:527–605
- Chinnery PF (1993) Mitochondrial disorders overview. In: Adam MP, Ardinger HH, Pagan RA et al (eds) *Gene Reviews*. University of Washington, Seattle
- Colli L, Facchini U (1954) Light emission by germinating plants. *Nuovo Cimento* 12:150–155
- Ellis RJ, van der Vies JM, Hemmingsen SM (1989) The molecular chaperone concept. *Biochem Soc Symp* 55:145–153
- Ezzahir A, Godlewski M, Krol M et al (1992) The influence of environmental factors on the ultraweak luminescence from yeast *Saccharomyces cerevisiae*. *Bioelectrochem Bioenerg* 27:57–61
- Fang H, Chen M, Ding Y (2011) Imaging superoxide flash and metabolism-coupled mitochondrial permeability transition in living animals. *Cell Res* 21:1295–1304
- Fano U (1947) Ionization yield of radiations. II The fluctuations of the number of ions. *Phys Rev* 72:26–29
- Fisher PR, Rosenberg LT (1988) Chemiluminescence in *Dictyostelium discoideum*. *FEMS Microbiol Lett* 50:157–161
- Fisher PR, Karampetsos P, Wilczynska Z et al (1991) Oxidative metabolism and heat shock enhanced chemiluminescence in *Dictyostelium discoideum*. *J Cell Sci* 99:741–750
- Fleming JE, Miquel J, Cottrell SF, Yengoyan JS et al (1982) Is cell aging caused by respiration dependent injury to the mitochondrial genome? *Gerontology* 28:44–53
- Fleming JE, Miquel J, Bensch KG (1985) Age dependent changes in mitochondria. *Basic Life Sci* 35:143–156
- Frank S, Gaume B, Bergmann-Leitner ES et al (2001) The role of dynamin-related protein 1, a mediator of mitochondrial fission, in apoptosis. *Dev Cell* 1:515–525
- Gerschman R (1981) Historical introduction to the 'free radical theory' of oxygen toxicity. In: Gilbert DL (ed) *Oxygen and living processes, an interdisciplinary approach*. Springer, New York, p44–46
- Gerschman R, Gilbert DL, Nye SW et al (1954) Oxygen poisoning and x-irradiation: a mechanism in common. *Science* 119:623–626
- Glancy B, Hartnell LM, Malide D et al (2015) Mitochondrial reticulum for cellular energy distribution in muscle. *Nature* 523:617–620
- Gong G, Liu X, Wang W (2014) Regulation of metabolism in individual mitochondria during excitation-contraction coupling. *J Mol Cell Cardiol* 76:235–246
- Gong G, Liu X, Zhang H et al (2015) Mitochondrial flash as a novel biomarker of mitochondrial respiration in the heart. *Am J Physiol Heart Circ Physiol* 309:H1166–H 1177
- Gu Q, Popp FA (1992) Nonlinear response of biophoton emission to external perturbation. *Experientia* 48:1069–1081
- Halliwell B (1991) Reactive oxygen species in living systems: Source, biochemistry and role in human disease. *Am J Med* 91:S14–S22
- Halliwell B (2007) Biochemistry of oxidative stress. *Biochem Soc Trans* 35:1147–1150
- Halliwell B, Gutteridge JM (1985) The importance of free radicals and catalytic metal ions in human diseases. *Mol Aspects Med* 8:89–108.
- Harman D (1956) Aging, a theory based on free radical and radiation chemistry. *J Gerontology* 11:298–300
- He M, Sun M, Koval S et al (2019) Traditional Chinese medicine-based subtyping of early-stage type 2 diabetes using plasma metabolomics combined with ultra-weak photon emission. *Engineering* 5:916–923
- Holt I, Harding AE, Morgan-Hughes JA (1988) Deletion of muscle mitochondrial DNA in patients with mitochondrial myopathies. *Nature* 331:717–719
- Inamura H, Nhai KP, Togawa H et al (2009) Visualization of ATP levels inside single living cells with fluorescence resonance energy transfer-based genetically encoded indicators. *Proc Natl Acad Sci USA* 106:15651–15656
- Inaba H (1988) Super-high sensitivity systems for detection and spectral analysis of ultraweak photon emission in biological cells and tissues. *Experientia* 44:550–559
- Ishihara N, Fujita Y, Oka T (2006) Regulation of mitochondrial morphology through proteolytic cleavage of OPA 1. *EMBO J* 25:2966–2977
- Jackson MJ, Papa S, Bolanos J (2002) Antioxidants, reactive oxygen and nitrogen species, gene induction and mitochondrial function. *Mol Aspects Med* 23:209–285
- Jamieson B (1989) Oxygen toxicity and reactive oxygen metabolites in mammals. *Free Radical Biol Med* 7:87–108
- Karamanlidis G, Lee CF, Garcia-Menendez L et al (2013) Mitochondrial complex I deficiency increases protein acetylation and accelerates heart failure. *Cell Metab* 18:239–250
- Kellogg EW, Fridovich I (1975) Superoxide, hydrogen peroxide, and singlet oxygen in lipid peroxidation by xanthine oxidase system. *J Biol Chem* 250:8812–8817

- Kembro JM, Aon MA, Winslow RL et al (2013) Integrating mitochondrial energetics redox and ROS metabolic networks: a two-compartment model. *Biophys J* 104:332–343
- Kennedy EP, Lehninger AL (1949) Oxidation of fatty acids and tricarboxylic acid intermediates by isolated rat liver mitochondria. *Journal of Biological Chemistry* 179:957–972
- Kurz FT, Aon MA, O'Rourke B et al (2010) Spatio-temporal oscillations of individual mitochondria in cardiac myocytes reveal modulation of synchronized mitochondrial clusters. *Proc Natl Acad Sci USA* 107:14315–14320
- Kurz FT, Dernings T, Aon MA et al (2015) Mitochondrial networks in cardiac myocytes reveal dynamic coupling behavior. *Biophys J* 108:1922–1933
- Lee YL, Jeong SY, Karbowski M et al (2004) Role of the mammalian mitochondrial fission and fusion mediators Fis1, Drp1, and OPA1 in apoptosis. *Mol Biol Cell* 15:5001–5011
- Li K, Zhang W, Fang H (2012) Superoxide flashing reveal novel properties of mitochondrial reactive oxygen species excitability in cardiomyocytes. *Biophys J* 102:1011–1021
- Liesa M, Palacin M, Zorzano A (2009) Mitochondrial dynamics in mammalian health and disease. *Physiol Rev* 89:799–845
- Marcus DL, Ibrahim NG, Freedman L (1982) Age-related decline in the biosynthesis of mitochondrial inner membrane proteins. *Exp Gerontol* 17:333–341
- McCord JM, Fridovich I (1969) Superoxide dismutase. An enzymic function for erythrocyte hemocuprein. *J Biol Chem* 244:6049–6055
- Mitchell P (1961) Coupling of phosphorylation to electron and hydrogen transfer by a chemical-osmotic type of mechanism. *Nature* 191:144–148
- Miquel J, Fleming J (1986) Theoretical and experimental support for an 'oxygen radical-mitochondrial injury' hypothesis of cell aging. In: Johnson JE, Walford R, Harman D et al (eds), *Free radical, ageing, and degenerative diseases*, Alan R. Liss, New York, p 51–74
- Molina AJ, Wikstrom JD, Stiles L et al (2009) Mitochondrial networking protects beta-cells from nutrient-induced apoptosis. *Diabetes* 58:2303–2315
- Mouli PK, Twig G, Shirihai OS (2009) Frequency and selectivity of mitochondrial fusion are key to its quality maintenance function. *Biophys J* 96:3509–3518
- Murphy E, Steenbergen C (2018) Mechanisms underlying acute protection from cardiac ischemia-reperfusion injury. *Physiol Rev* 88:581–609
- Orszag M (2000) *Quantum Optics*, Springer, Berlin, Heidelberg, p 29–45
- Ovelgonne H, Bitorina M, Van Wijk R (1995a) Stressor-specific activation of heat shock genes in rat hepatoma cells. *Toxicology and Applied Pharmacology* 135:100–109
- Ovelgonne JH, Souren JEM, Wiegant FAC et al (1995b) Relationship between cadmium induced expression of heat shock genes, inhibition of protein synthesis and cell death. *Toxicology* 99:19–30
- Palade GE (1952) An electron microscope study of the mitochondrial structure. *Journal of Histochemistry and Cytochemistry* 1:188–211
- Pardue ML, Feramisco JR, Lindquist S (eds) (1989) *Stress-Induced Proteins*. Alan R. Liss, New York
- Parone PA, Da CS, Tondera D et al (2008) Preventing mitochondrial fission impairs mitochondrial function and leads to loss of mitochondrial DNA. *PLoS One* 3:e3257
- Perelygin VV, Tarusov BN (1966) Flash of very weak radiation on damage to living tissues. *Biofizika* 11:539–541
- Picard M, Wallace DC, Burelle Y (2016) The rise of mitochondria in medicine. *Mitochondrion* 30:105–116
- Polakis ES, Bartley W (1965) Changes in enzyme activities of *Saccharomyces cerevisiae* during aerobic growth on different carbon sources. *Biochem J* 97:284–297
- Polakis ES, Bartley W, Meek GA (1964) Changes in the structure and enzyme activity of *Saccharomyces cerevisiae* in response to changes in the environment. *Biochem J* 90:369–374
- Popp FA, Cilento G, Chwirot WB et al (1988) Biophoton emission – multi-author review. *Experientia* 44:543–601
- Popov GA, Tarusov BN (1963) Nature of spontaneous luminescence of animal tissues. *Biophysics (USSR)* 8:372
- Pouvreau S (2010) Superoxide flashes in mouse skeletal muscle are produced by discrete arrays of active mitochondria operating coherently. *PLoS One* 5:e13035
- Powers SK, Jackson MJ (2008) Exercise-induced oxidative stress: cellular mechanisms and impact on muscle force production. *Physiol Rev* 88:1243–1276
- Quickenden TI, Tilbury RN (1983) Growth dependent luminescence from cultures of normal and respiratory deficient *Saccharomyces cerevisiae*. *Photochem Photobiol* 37:337–344
- Quickenden TI, Tilbury RN (1991) Luminescence spectra of exponential and stationary phase cultures of respiratory deficient *Saccharomyces cerevisiae*. *J Photochem Photobiol B* 8: 69–174
- Ruth B, Popp FA (1976) Experimentelle Untersuchungen zur ultraschwachen Photonemission biologischer Systeme. *Z. Naturforsch* 31:741–745
- Santo-Domingo J, Giacomello M, Poburko D et al (2013) OPA1 promotes ph. flashes that spread between contiguous mitochondria without matrix protein exchange. *EMBO J* 32:1927–1940
- Schamhart DHJ, Van Walraven HS, Wiegant FAC et al (1984) Thermotolerance in cultured hepatoma cells: cell viability, cell morphology, protein synthesis and heat shock proteins. *Radiation Research* 98:82–95
- Schlesinger MJ, Ashburner M, Tissières A (eds) (1982) *Heat Shock From Bacteria to Man*. Cold Spring Harbor Laboratory, New York
- Schon EA, Bonilla E, DiMauro S (1997) Mitochondrial DNA mutations and pathogenesis. *J Bioenerget Biomemb* 29:131–149
- Schwarzlander M, Logan DC, Johnston IG et al (2012) Pulsing of membrane potential in individual mitochondria; a stress-induced mechanism to regulate respiratory bioenergetics in *Arabidopsis*. *Plant Cell* 24:1188–1201
- Shen EZ, Song CQ, Lin Y et al (2014) Mitoflash frequency in early adulthood predicts lifespan in *Caenorhabditis elegans*. *Nature* 508:128–132
- Shtrankfel'd IG, Klimensko LL, Komarow NN (1968) Very weak luminescence of muscles. *Biophysics* 13:1082–1084
- Sjöstrand FS (1953) Electron microscopy of mitochondria and cytoplasmic double membranes. *Nature* 171:30–32
- Slawinski J (1988) Luminescence research and its relation to ultraweak cell radiation. *Experientia* 44:559–571.
- Slawinski J (1990) Ultraweak luminescence and perturbations of bio-homeostasis. In: Jezowska-Trzebiatowska B, Kochel B, Slawinski J et al (eds), *Biological Luminescence*, World Scientific, Singapore, p 197–212
- Slawinski J (1991) Stress-induced biological luminescence. *Trends Photochem Photobiol* 2:289–308
- Slawinska D, Slawinski J (1983) Biological chemiluminescence. *Photochem Photobiol* 37:709–715
- Slawinska D, Slawinski J (1985) Low-level luminescence from biological objects. In: Burr JG (ed) *Chemiluminescence and Bioluminescence*, M. Dekker, New York, p 495–531
- Slawinski J, Ezzahir A, Godlewski M et al (1992) Biophoton emission, stress and disease - multi-author review. *Experientia* 48:1041–1058
- Sun M, Van Wijk E, Koval S et al (2017) Measuring ultra-weak photon emission as a non-invasive diagnostic tool for detecting early-stage type 2 diabetes: a step toward personalized medicine. *J Photochem Photobiol B* 166:86–93
- Tarusov BN, Zhuravlev AI (1965). *Bioluminescence of Lipids*. In: Zhuravlev AI (ed) *Bioluminescenciya*, Nauka, Moscow, p 125–133

- Tarussov BN, Veselovski WA (1978) *Ultraweak Luminescence from Plants and its Application*. Moscow State Publ House, Moscow
- Taylor AE, Matalon S, Ward PA (eds) (1986) *Physiology of Oxygen Radicals*. Williams and Wilkins, Baltimore
- Tilbury RN (1990) Ultraweak luminescence of yeast and bacteria. In: Jezowska-Trzebiatowska B, Kochel B, Slawinski J et al (eds), *Biological Luminescence*, World Scientific, Singapore, p 49–77
- Tilbury RN (1992) The effect of stress factors on the spontaneous photon emission from microorganisms. *Experientia* 48:1030–1041
- Twig G, Hyde B, Shirihai OS (2008b) Mitochondrial fusion, fission and autophagy as a quality control axis: the bioenergetic view. *Biochim Biophys Acta* 1777:1092–1097
- Twig G, Elorza A, Molina AJ et al (2008a) Fission and selective fusion govern mitochondrial segregation and elimination by autophagy. *EMBO* 27:433–446
- Twig G, Liu X, Liesa M et al (2010) Biophysical properties of mitochondrial fusion events in pancreatic beta-cells and cardiac cells unravel potential control mechanisms of its selectivity. *Am J Physiol Cell Physiol* 299:C477–C487
- Veselowskii VA, Sekamova YN, Tarusov BN (1963) Mechanism of ultraweak spontaneous luminescence of organisms. *Biophysics (USSR)* 8:147
- Van Dongen G, Geilenkirchen WLM, Van Rijn J et al (1986) Increase of thermoresistance after growth stimulation of resting Reuber H35 hepatoma cells. Alteration of nuclear characteristics, non-histone chromosomal protein phosphorylation and basal heat shock protein synthesis. *Experimental Cell Research* 166:427–435
- Van Wijk R (2014) *Light in Shaping Life – Biophotons in biology and Medicine*. Meluna Research, Geldermalsen. https://scholar.google.com/scholar_lookup?title=Light+in+shaping+life%E2%80%9494Biophotons+in+biology+and+medicine&author=R.+Van+Wijk&publication_year=2014&
- Van Wijk R, Schamhart DHJ (1988) Regulatory aspects of low intensity photon emission. *Experientia* 44:586–593
- Van Wijk R, Ouwehand J, Van de Bos T et al (1969) Induction and catabolite repression of α -glucosidase synthesis in protoplasts of *Saccharomyces carlbergensis*. *Biochimica Biophysica Acta* 186:178–191
- Van Wijk R, Tilbury RN, Slawinski J et al (1992) Biophoton emission, stress and disease - multi-author review. *Experientia* 48:1029–1102
- Van Wijk R, Van Wijk EPA, Bajpai RP (2006) Photon count distribution of photons emitted from three sites of a human body. *J Photochem Photobiol B* 84:46–55
- Van Wijk EPA, Ackerman JM, Van Wijk R (2005) Effect of meditation on ultra-weak photon emission from hands and forehead. *Forsch Komplementarmed Klassik Naturheilkd* 12:96–106
- Van Wijk EPA, Van Wijk R, Bajpai RP (2008) Quantum squeezed state analysis of spontaneous ultra-weak photon emission of practitioners of meditation and control subjects. *Ind J Exp Biol* 46:345–352
- Van Wijk EPA, Van Wijk R, Bajpai RP et al (2010) Statistical analysis of the spontaneous emitted signals from palm and dorsal sides of both hands in human subjects. *J Photochem Photobiol B* 99:133–143
- Van Wijk EPA, van der Greef J, Van Wijk R (2013) Human photon dynamics determined by using photon count statistics In: Jung H (ed), *New Developments in Photon and Material Research*, Nova Publishers, New York, p 61–82
- Vladimirov YA, L'vova OF (1964) Superweak luminescence and oxidative phosphorylation in mitochondria. *Biophysics (USSR)* 9:548
- Wallace DC (1999) Mitochondrial diseases in mouse and man. *Science* 283:1482–1488
- Wallace DC, Singh G, Lott MT et al (1988) Mitochondrial DNA mutation associated with Leber's hereditary optic neuropathy. *Science* 242:1427–1430
- Wang W, Fang H, Groom L et al (2008) Superoxide flashes in single mitochondria *Cell* 134:279–290
- Wang X, Jian C, Zhang X et al (2012) Superoxide flashes elemental events of mitochondrial ROS signaling in the heart. *J Mol Cell Cardiol* 52:940–948
- Wang X, Fang H, Huang Z et al (2013) Imaging ROS signaling in cells and animals. *J Mol Med (Berl)* 91:917–927
- Wang W, Gong G, Wang X et al (2016) Mitochondrial flash: integrative reactive oxygen species and pH signals in cell and organelle biology. *Antioxidants Redox Signaling* 25:534–549
- Wei AC, Aon MA, O'Rourke B (2011a) Mitochondrial energetics pH regulation, and ion dynamics; a computational approach. *Biophys J* 100:2894–2903
- Wei L, Salahura G, Boncompagni S et al (2011b) Mitochondrial superoxide flashes metabolic biomarkers of skeletal muscle activity and disease. *FASEB J* 25:3068–3078
- Wei L, Dirkson RT (2012) Perspectives on SGP symposium on mitochondrial physiology and medicine; mitochondrial superoxide flashes from discovery to new controversies. *J Gen Physiol* 139:425–434
- Wei-LaPierre L, Gong G, Gerstner BJ (2013) Respective contribution of mitochondrial superoxide and pH to mitochondria-targeted circularly permuted yellow fluorescent protein (mt-cpYFP) flash activity. *J Biol Chem* 288:10567–10577
- Welch WJ, Mizzen LA, Arrigo AP (1989) Structure and function of mammalian stress proteins. In: Pardee ML, Feramisco JR, Lindquist S (eds) *Stress-Induced Proteins*, Alan R Liss Inc, New York
- Wiegant FAC, Souren JEM, Van Rijn H et al (1993) Arsenite-induced sensitization and self-tolerance of Reuber H35 hepatoma cells. *Cell Biology and Toxicology* 9:49–59
- Wiegant FAC, Souren JEM, Van Rijn J et al (1995) Stressor-specific induction of heat shock proteins in rat hepatoma cells. *Toxicology* 94:143–159
- Wikstrom JD, Twig G, Shirihai OS (2009) What can mitochondrial heterogeneity tell us about mitochondrial dynamics and autophagy? *Int J Biochem Cell Biol* 41:1914–1927
- Wikstrom JD, Katzman SM, Mohamed H et al (2007) Beta-cell mitochondria exhibit membrane potential heterogeneity that can be altered by stimulatory or toxic fuel levels. *Diabetes* 56:2569–2578
- Ying Z, Chen K, Zheng L et al (2016) Transient activation of mitoflashes modulates nanog at the early phase of somatic cell reprogramming. *Cell Metab* 23:220–226
- Zhao X, Van Wijk E, Yan Y et al (2016) Ultra-weak photon emission of hands in aging prediction. *J Photochem Photobiol B* 162:529–534
- Zorov DB, Filburn CR, Klotz LO et al (2000) Reactive oxygen species (ROS)-induced ROS release: a new phenomenon accompanying induction of the mitochondrial permeability transition in cardiac myocytes. *J Exp Med* 192:1001–1014



Selected Biophysical Methods for Enhancing Biological Autoluminescence

29

Hadi Sardarabadi, Fatemeh Zohrab, Petra Vahalova, and Michal Cifra

Abbreviations

| | |
|-----|-----------------------------|
| BAL | Biological autoluminescence |
| ECL | Electrochemiluminescence |
| LFE | Low field effect |
| NP | Nanoparticle |
| ROS | Reactive oxygen species |

29.1 Introduction

Biological autoluminescence (BAL) is known to be generated by electronically excited states of molecules in biosystems (Burgos et al. 2017; Wang et al. 2015; Gabe et al. 2014; Cilento and Adam 1995; Van Wijk 1992; Nakamura and Hiramatsu 2005; Okano et al. 2001; Rastogi and Pospíšil 2011; Cifra and Pospíšil 2014; Cadenas and Sies 1984; Boveris et al. 1980; Nakano 1989). The typical intensity is $<1000 \text{ photons} \cdot \text{s}^{-1} \cdot \text{cm}^{-2}$. These rays cover a range of the electromagnetic wave spectrum 350–1270 nm (depending on the type of emitter molecule), which includes a significant portion of the visible range, and hence is also called ultraweak photon emission, biophotons, endogenous bioluminescence, autoluminescence, weak luminescence, low-level chemiluminescence, spontaneous chemiluminescence, spontaneous ultraweak light emission, or ultraweak bioluminescence (Cifra and Pospíšil 2014). BAL is

endogenously generated and, unlike other luminescence phenomena, does not depend on exogenous chemical, physical, or electrical excitations. In fact, BAL is emitted from endogenously excited biomolecules. Extensive indirect investigation of BAL as light dates back to the 1920s (Belousov et al. 2004; Gurwitsch 1988) when it was referred to as mitogenetic rays (Volodyaev and Belousov 2015). The existence of this phenomenon was controversial until the 1950s, when the first photomultiplier tubes were used to reliably confirm this phenomenon in a number of species (Coil 1995; Colli and Facchini 1954) and further supported using charge-coupled device camera systems in the 1990s (Scholkmann et al. 2018). To date, a widely accepted view regarding the origin of BAL is that the oxidative reactions of biomolecules initiate the generation of electron-excited molecular species. There are also other hypotheses: one of them, which is not accepted by the wider scientific community because of the lack of experimental evidence, claims that endogenous biological light emanates from a coherent electromagnetic field and the main source of these emissions could be inside the DNA molecule and other intracellular cavity resonators (Popp 2005). Although profiling the genes (genomics), proteins (proteomics), and other cellular biomarkers (metabolomics) provides promising methods to detect different physiological states, these methods depend on applying invasive sampling methods. Therefore, the monitoring of intracellular and intercellular events at the appropriate time and location without the use of invasive methods is a major goal of future research in various disciplines. As all metabolically active cells (both eukaryotic and prokaryotic) generate electronically excited biomolecules during their metabolism as the main source of BAL, it can be considered as a new noninvasive diagnosis approach (Bókkon et al. 2016a). A significant increase in the BAL signal intensity of in vivo implanted tumors has been observed (Takeda et al. 2004). Researchers have shown that there is a strong relationship between the enhancement of the BAL signals intensity and an increase in tumor size (Takeda et al. 1998). In normal tissue,

H. Sardarabadi
Faculty of Medicine, Qom University of Medical Sciences, Qom, Iran
Cellular and Molecular Research Center, Qom University of Medical Sciences, Qom, Iran

F. Zohrab
Department of Medical Science, Qom Branch, Islamic Azad University, Qom, Iran

P. Vahalova · M. Cifra (✉)
The Czech Academy of Sciences, Institute of Photonics and Electronics, Prague, Czech Republic
e-mail: cifra@ufe.cz

generated ROS are quickly eliminated by the enzymatic (as self-defense antioxidant mechanisms of living cells) or nonenzymatic pathways (Agarwal et al. 2012). Compared with normal tissue, cancer tissue has a lower concentration of ROS eliminators, such as superoxide dismutase and catalase (Oberley and Spitz 1984). Such evidence shows the potential application of BAL as a noninvasive monitoring method for the early detection of cancer. Recently, cancer biomarkers have also been successfully detected by the analysis of BAL intensity. Among all human tissues, the skin is the most prone to oxidative damage. Considering the powerful relationship between the BAL intensity and oxidative processes, skin-related diseases could also be studied using BAL (Khabiri et al. 2008; Ou-Yang et al. 2004; Prasad and Pospíšil 2012; Rastogi and Pospíšil 2010; Sauermann et al. 1999). Several studies have shown that neuronal tissue activity can be studied by BAL (Salari et al. 2015; Bókkon et al. 2016b; Esmailpour et al. 2020). In agriculture, the intensity and the spectrum of biologically generated photons can be used to evaluate plant responses to pathogens (Iyozumi et al. 2002), drought stress (Ohya et al. 2002), salinity stress (Ohya et al. 2000) and herbicides (Inagaki et al. 2008). The researchers also indicate it is possible to study physiological changes during metamorphosis noninvasively by imaging of BAL (Usui et al. 2019). Despite widespread efforts to optimally exploit the valuable properties of BAL, the weak intensity of these signals is considered as a major constraint both in *in vivo* and *in vitro* applications (Cifra and Pospíšil 2014; Pospíšil et al. 2014; Non-equilibrium and coherent systems in biology, biophysics and biotechnology 2000; Popp et al. 1992; Belousov et al. 2007). Hence, BAL signal enhancement studies are strongly required.

In this chapter, selected biophysical approaches for modulating the BAL signal intensity are introduced. First, the related mechanisms that are involved in the generation of electronically excited species are described. Then, we reviewed selected experimental studies that are related to the field of BAL signal enhancement.

29.2 Mechanisms of the BAL Generation as a Starting Point for Signal Enhancement

Radiative relaxation of chemically generated electronically excited states of molecules (generated during the oxidative cell metabolism or stress) are recognized as the main sources of endogenous radiative processes we term here as BAL (Pospíšil et al. 2019). The general working hypothesis is displayed in Fig. 29.1 and is described in the following text.

There are several pathways that lead to the formation of various ROS, reactive molecules standing at the beginning of the BAL generation. The one-electron reduction of molecular

oxygen leads to the formation of a superoxide anion radical ($O_2^{\cdot-}$) and occurs in the mitochondria during cellular respiration, in the chloroplast during light exposure, and in the membrane-bound enzyme complex NADPH oxidase during the oxidative burst (Auchère and Rusnak 2002).¹ Although $O_2^{\cdot-}$ is preferentially formed at a neutral pH, it is converted into HO_2^{\cdot} in an acidic microenvironment because $pK_a(HO_2^{\cdot}) = 4.8$ (Bielski et al. 1985). One-electron reduction of $O_2^{\cdot-}$ (occurring spontaneously or catalyzed by various types of superoxide dismutases in mitochondria, peroxisomes, and cytoplasm) (Auchère and Rusnak 2002) or two-electron oxidation of H_2O (in water splitting manganese complex in photosystem II in chloroplasts) (Kale et al. 2017) lead to the creation of hydrogen peroxide (H_2O_2). A hydroxyl radical (HO^{\cdot}) is formed through the one-electron reduction of H_2O_2 mediated by free metal ions such as Fe^{2+} (Prousek 2007).² Triplet-singlet energy transfer from excited triplet chromophores ($^3C^*$) to molecular oxygen leads to the formation of singlet oxygen (1O_2). Radical ROS with unpaired electrons have high positive redox potential so they are highly reactive. An appropriate amount of ROS in the right place plays an important role in cellular signaling pathways, immune defense systems, apoptosis, or aging.³ On the other hand, undesirable reactions with biomolecules lead to the damage of cells.

ROS, especially HO^{\cdot} and HO_2^{\cdot} , can react with organic matter RH and form organic radicals R^{\cdot} . In the presence of molecular oxygen, peroxy radicals ROO^{\cdot} can be created. The hydrogen abstraction from another RH by ROO^{\cdot} leads to $ROOH$, and R^{\cdot} formation. $ROOH$ can be also created “directly” from RH during reaction with 1O_2 via an “ene” reaction. If transition metals, such as Fe^{2+} , Mn^{2+} , Cu^+ , or Zn^+ , and reducing agents are in proximity to $ROOH$, reduction of $ROOH$ leads to the creation of alkoxy radicals RO^{\cdot} (Pospíšil et al. 2019).

The recombination of peroxy radicals ROO^{\cdot} results in the formation of unstable high-energetic tetroxide $ROOOOR$, which is decomposed either to ground-state carbonyl, 1O_2 , and organic hydroxide ROH, or to triplet excited carbonyl $^3R=O^*$, molecular oxygen, and ROH.⁴ Cyclization of ROO^{\cdot} or cycloaddition of 1O_2 to polyunsaturated fatty acids or amino acids lead to the creation of another high-energetic intermediate, 1,2-dioxetane ROOR, which decomposes to $^3R=O^*$ and $R=O$ (Pospíšil et al. 2014).

Excited triplet carbonyls $^3R=O^*$ can relax to the ground state and emit light in the spectrum region 350–550 nm. In the presence of natural chromophores, such as tetrapyrroles (porphyrin, bilirubin), flavins (FMN, RAD), pyridine nucleotides (NADH, NADPH), melanin, urocanic acid, or

¹See more in Chap. 14.

²See also Chap. 8.

³See Chap. 14.

⁴See Sect. 10.5.

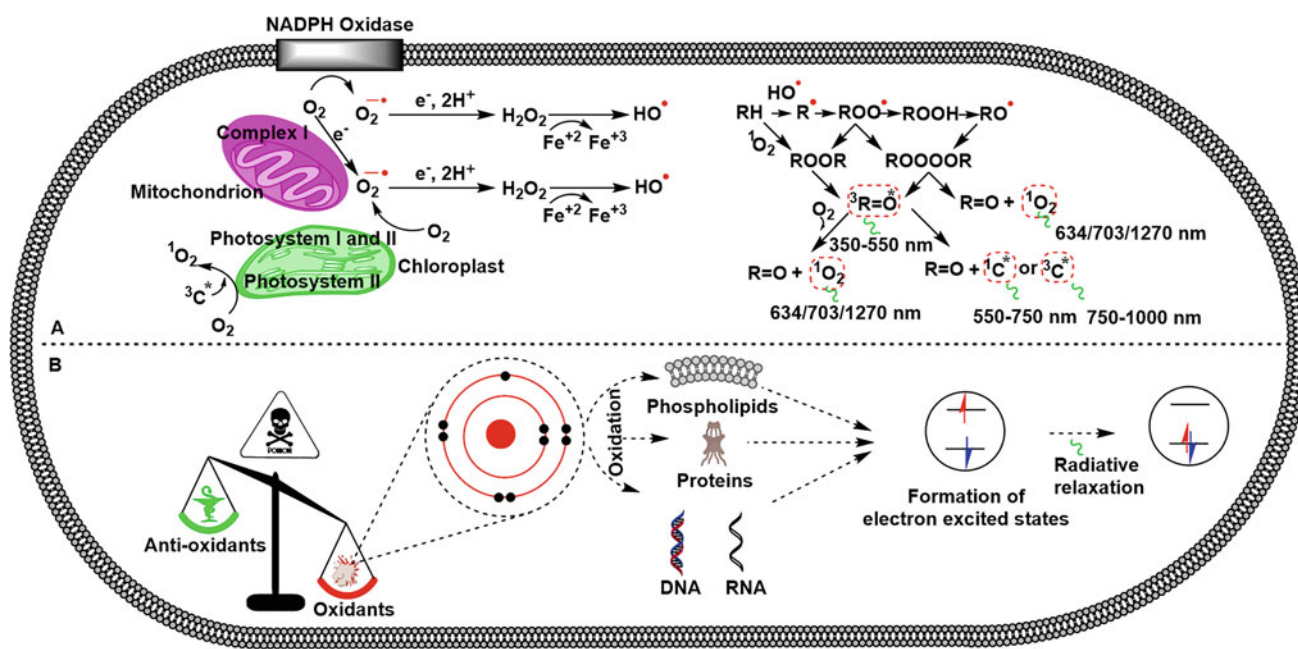


Fig. 29.1 Biological autoluminescence during dynamic metabolic processes. (a) Formation of ROS and electronically excited states of molecules in metabolically active cells. (b) The BAL emission from

electron-excited states of molecules caused by an imbalance between oxidants and antioxidants

pterins, excitation energy can be transferred from $^3R=O^*$ to the chromophore. As a consequence of the triplet–singlet or triplet–triplet energy transfer, singlet ($^1C^*$) or triplet excited ($^3C^*$) chromophores are formed. During their radiative transition to the ground state, they emit photons in the range 550–750 nm ($^1C^*$) or 750–1000 nm ($^3C^*$). For example, excited chlorophylls emit in the red part of the spectrum (670–740 nm) (Hideg and Inaba 1991). In aerobic conditions, the triplet–singlet energy transfer from $^3R=O^*$ and $^3C^*$ to molecular oxygen causes the formation of 1O_2 . Its transition to the ground triplet state is accompanied by monomol photon emission at 1270 nm. A collision of two 1O_2 results in dimol photon emission at 634 and 703 nm. However, not all emitters are created with the same probability. For example, the formation of $^3R=O^*$ is lower by 3–4 orders of magnitude than the generation of 1O_2 (3–14%) during recombination of two ROO^{\cdot} (Pospíšil et al. 2019). However, measurement of BAL is focused on the near UV and visible part of the spectrum because BAL intensity in the near infrared region is comparable with photon emission caused by thermal excitation (Fig. 29.1a). In general, BAL generation stems from oxidation reactions of the ROS with practically all types of biomolecules, such as lipids, proteins, or DNA (Fig. 29.1b).

29.3 The BAL Signal Enhancement Strategies

Here we review several biophysical approaches that could lead to an increase of the intensity of BAL by modulating the rate of processes across the whole chain of reactions leading to BAL: from the production of free radicals to radiative transitions of the electronically excited species.

29.3.1 Application of the Magnetic Fields

The most important possible biophysical mechanism involved in magnetic field modifying effects on biological responses to UV radiation and other oxidizing agents is the “radical-pair mechanism” (Barnes and Greenebaum 2015). Based on this mechanism, the low (below approximately 1 mT) and high field magnetic field can affect specific types of chemical reactions, which involve pair of radical molecules, by generally increasing or decreasing the concentration of free radicals in low and high fields, respectively. The low field effect (LFE) could explain the effects reported at 100 μ T. Experimental studies have shown that the radical-pair mechanism is involved not only in cell-free biochemical

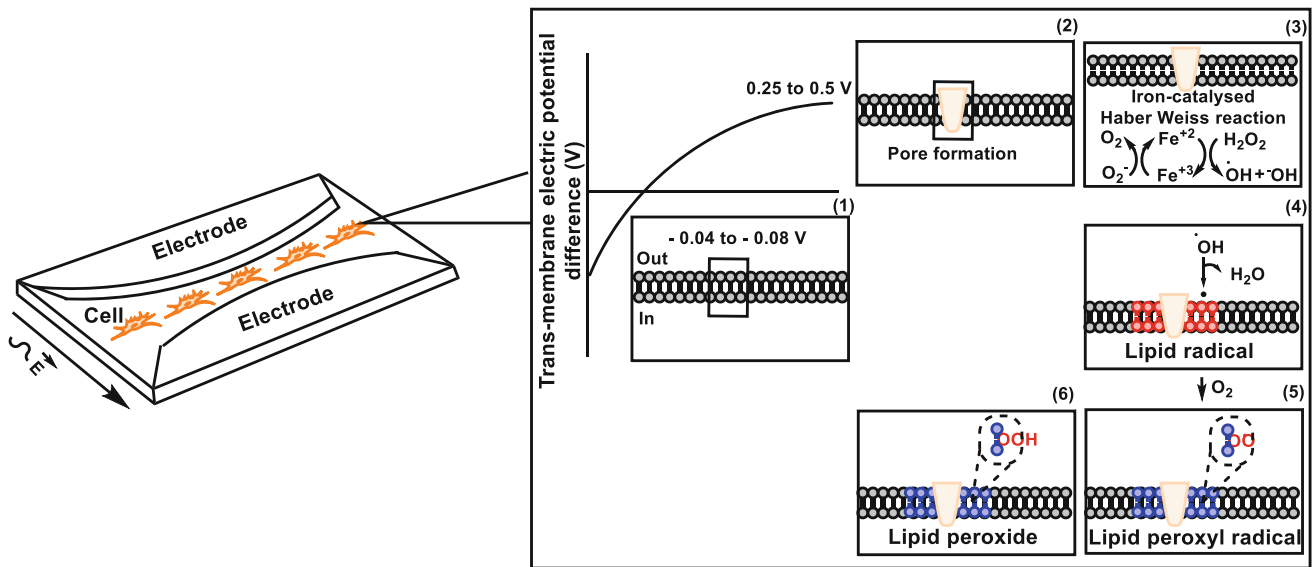


Fig. 29.2 Molecular mechanism of lipid peroxidation and ROS generation in the presence of a pulsed electric field. Increasing the transmembrane potential (1) caused the temporary formation of the pore (2). Generated hydroxyl radical near the pore (3) can produce lipid radical

(4), and such a radical eventually can generate the lipid peroxyl radical (5) and lipid peroxide (6) in the presence of molecular oxygen as BAL-generating source

systems but also has bioeffects in cells. For example, some studies have shown that the 50-Hz magnetic fields of approximately 100 μT have been able to alter the biological responses to ultraviolet (UV) radiation in yeast cells (Markkanen et al. 2001) and in mouse skin (Kumlin et al. 1998, 2002). Also, several other studies of biological samples treated with physical or chemical agents and exposed to a magnetic field indicate a similar radical-pair mechanism. Therefore, considering the ability of a small-magnitude LFE to generate a high radical level, LFE potentially has multiple effects on biological functions. In a normal cell, a crucial balance exists between the generation and elimination of radicals. If any external or internal agent disturbs this balance, the oxidative stress phenomenon will occur. Because the initial outcome of LFE exposure is generation of high radical levels, the oxidative stress is not unexpected and has meaningful effects on biological functions (Pizzino et al. 2017) and can also affect BAL intensity (Bereta et al. 2021; Cheun et al. 2007).

29.3.2 Application of Electric Fields

29.3.2.1 Pulsed Electric Field

Pulsed electric field has been used for a long time to generate electroporation or electroporabilization, with potential biomedical applications leveraging the delivery of various molecules such as exogenous genetic material and proteins into cells (Rols 2006). The permeability of the eukaryotic (human, animal, plant) cell membrane could be transiently

increased by applying monopolar electric pulses or polarity alternating (bipolar) pulses (Fig. 29.2) (Sweeney et al. 2018). It has also been shown that by reducing the duration of the applied electric pulses, some vital organelles such as mitochondria can be temporarily more permeable.

In theory, electric field can directly or indirectly generate ROS. Direct generation is owing to reduction-oxidation (redox) reactions of the molecules at the electrode-electrolyte interface, when voltage is applied and exceeds a certain electrochemical threshold, which is almost always the case for intense electric pulses (Pataro et al. 2016). Indirect ROS generation by an electric field could also occur from electric field-induced cellular stress (permeabilization of membranes, leakage of ions) (Pakhomova et al. 2012). There are experimental works that support both the direct and indirect regime of ROS generation (Teissie 2017; Gabriel and Teissie 1994). Several works employing direct physical contact of electrodes with a biological sample have shown that pulsed electric fields cause oxidation in bio(molecular) systems. Interestingly, increased oxidation of biomolecules has also been found after delivery of intense electric pulses without contact through the antenna (Breton Marie et al. 2016). Furthermore, electric pulses have been demonstrated to induce cellular stress and biological production of ROS (Gabriel and Teissie 1994).

The generated ROS are able to oxidize cellular biomolecules (lipids, proteins, or DNA) and very likely initiate reactions leading to the formation of electron-excited states and eventually to BAL (Ou-Yang et al. 2004, 2009; Barnard et al. 1993; Sander et al. 2002). The factors

Table 29.1 The oxidation effect of short intense electric pulses

| Cell type | Pulsing buffer | Cell/ml concentration | Signal time interval (ns) | Electric field strength (kV·cm ⁻¹) | Voltage (V) | Distance between electrodes or gap size (cm) | Signal enhancement mechanism | Ref. |
|-----------|---|------------------------|---------------------------|--|---------------|--|---|----------------------------|
| WTT CHO | (A): sucrose, potassium phosphate MgCl ₂ ; (B): buffer A treated with Chelex-100 resin; (C): sucrose, potassium phosphate; (D): buffer C treated with Chelex-100 resin; (E): sucrose, potassium phosphate, MgCl ₂ , 69 mM KCl | 4 · 10 ⁸ | 10 ⁵ | 1.4 | Not-specified | Not-specified | Chemiluminescence: Metal-ion-catalyzed Haber–Weiss reaction | Gabriel and Teissie (1994) |
| K562 | RPMI 1640 with 10% fetal bovine serum | 1.25 · 10 ⁶ | Not specified | 1.1 | 300 | 0.4 | Chemiluminescence: Lipid peroxidation and generation of singlet oxygen and excited triplet carbonyl | Maccarrone et al. (1995) |
| PIEC | RPMI 1640 with 10% fetal bovine serum | 1.1 · 10 ⁶ | 100 | 5, 10 and 20 | 60,000 | 0.2 | Chemiluminescence: ROS generation | Zhang et al. (2018) |

influencing the effects of pulsed electric field on cells and on BAL include the cell type and cell concentration, time duration, pulsing buffer conductivity and osmolarity, temperature, signal time interval, electric field strength, distance between electrodes or gap size and electrode material. The oxidation effects of short intense electric pulses on BAL signal enhancement are summarized in Table 29.1.

Although it has not yet been possible to visualize all the mechanisms involved in the electroporation process in detail, evidence from various studies has shown that the localized generated ROS in the permeabilized part of the plasma membrane causes the direct or indirect production of further ROS.

29.3.2.2 Electrochemiluminescence

The direct generation of ROS and consequent BAL might be conceptually very similar to the phenomenon of electrochemiluminescence (synonymous with electrogenerated chemiluminescence) (ECL) (Bard et al. 1980; Bard 2004), which is a widely explored research topic (Fig. 29.3).

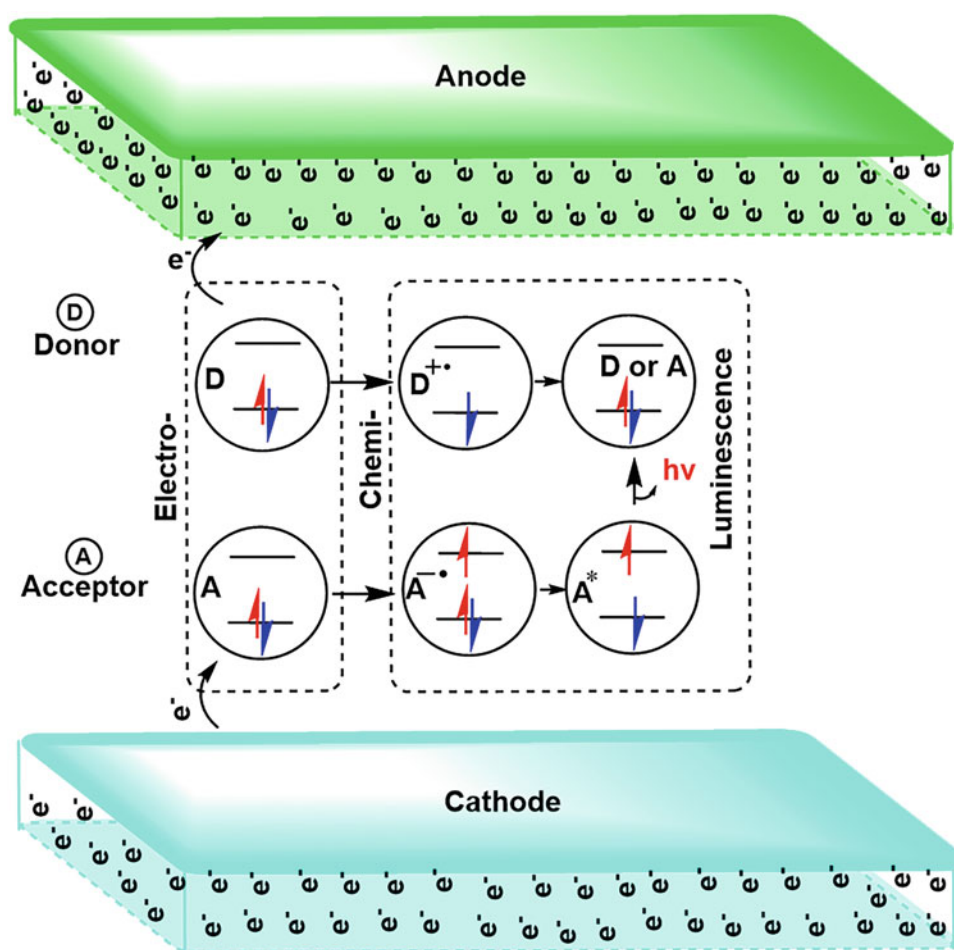
29.3.2.2.1 Definition Box

In electrochemiluminescence (ECL), electrogenerated species undergo electron-transfer reactions (in the vicinity of a working electrode) to form excited species, and these species relax to the ground state with the release of energy in the form of light. Fundamental research on ECL since the mid-1960s with smart compounding of electrochemistry with chemiluminescence has revealed that ECL is a powerful potential diagnosis tool over optical methods (Bouffier and Sojic 2019). First, because ECL does not require any external

light as a triggering source, this not only simplifies ECL devices but also eliminates the background noise that originates from internal luminous impurities and scattered light. Second, ECL responses aren't affected by luminous position changes because the ECL emission occurs close to the surface of the electrode; hence, ECL shows preferable control toward the position. Third, due to the relationship between the ECL luminophore and coreactants, ECL has an excellent specificity. Because the luminophore-excited states can be operated by using an alternative applied potential, ECL has satisfactory selectivity. Finally, ECL reproducibility is related to its controllability over time. Considering the high sensitivity, low background, and excellent controllability of ECL signals, ECL has attracted much attention in various fields of analysis including bioassay (DNA sensing, enzymatic detection), clinical diagnostics, drug screening, biodefense (Bruno and Cornette 1997), environmental monitoring (such as food and water safety), and other application such as solid-state electrochemiluminescence sensor (Kong et al. 2017; Spehar-Délèze et al. 2015). Furthermore, the combination of ECL with other analytical techniques such as capillary electrophoresis, flow injection analysis, high-performance liquid chromatography, and micrototal analysis has brought good results (Rizwan et al. 2017; Inoue et al. 2017; Roy et al. 2016; Yao et al. 2017; Cui et al. 2016; Bist et al. 2017).

However, in contrast to typical electrochemiluminescent systems, in which donor and acceptor molecules are selected by design, endogenous ECL might involve a plethora of endogenously present donor and acceptor molecules and complex reaction dynamics taking place.

Fig. 29.3 Schematic diagrams showing the general principles of electrochemiluminescence. Electron is transferred from the cathode to electron acceptor to form a radical. Electron donor transfers an electron to the anode and becomes a radical. The acceptor-based radical transfers a ground state electron to the donor radical and electron-excited state of an acceptor is generated. The excited state can decay radiatively to generate luminescence



29.3.3 Application of Nanoparticles into the Cell

The size similarity between nanoparticles and various intracellular components not only facilitates the delivery of particles into the cell (Blanco et al. 2015), but can also cause subtle interactions with various intracellular molecules and organelles (Cai et al. 2017; Nel et al. 2009). Therefore, we consider nanoscale particles as a promising tool for manipulating processes leading to BAL, potentially leading to BAL signal enhancement.

Here, we review two main classes of mechanisms for the prospective BAL signal enhancement by nanoscale particles, then a combination of electric field and nanoparticles and finally the current evidence of BAL enhancement using nanoparticles in cells.⁵

29.3.3.1 Nanoparticle-Mediated Increase of ROS Production

Nanoscale particles contribute to the increase of BAL intensity via ROS production. Increased formation of reactive groups on the nanoparticle (NP) surface with decreasing

particle size (Fu et al. 2014; Xia et al. 2008; Nel et al. 2006), active redox cycling on the surface of the NPs (Li et al. 2008; Huang et al. 2010) and the interaction of NPs with different intracellular components (Risom et al. 2005; Knaapen et al. 2004) are probably three main possibilities of how metal NPs could affect the BAL through ROS production. Some studies have shown that gold nanoparticles (AuNPs) are able to promote oxidation of biomolecules within the cell (Wang et al. 2015; Khan et al. 2012). How AuNPs can enhance the BAL signal through the production of electron-excited species is summarized in Fig. 29.4. Interaction of the free radicals ($CO_3^{\cdot-}$ and $O_2^{\cdot-}$) and AuNP results in the formation of emissive intermediate complex (Gold (I)), carbon dioxide dimers and singlet oxygen molecular pairs (Fig. 29.4a) (Cui et al. 2005). These intermediate species relax to their ground state via radiative relaxation.

Also, during the mitochondrial metabolism, this organelle produces various free radicals (mainly superoxide anion radical) (Razzaq et al. 2016). In the presence of AuNPs, it is possible to form a complex between AuNPs and superoxide radicals. After formation of this complex, the superoxide radical acts as an electron donor and transfers its $2\pi^*$ electron

⁵See also next chapter (Chap. 30).

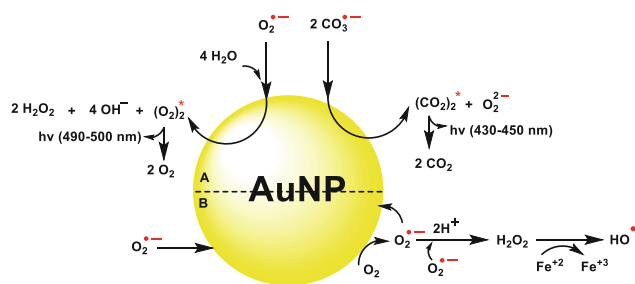


Fig. 29.4 Formation of emissive intermediate gold(I) complex. AuNP interaction with CO_3^- and O_2^- causes formation of excited molecules on AuNP surface (Cui et al. 2005)

to the gold conducting bond (Fig. 29.4b). Mitochondria are the main molecular oxygen consumption organelle within the cell. By the arrival of the molecular triplet oxygen to the AuNP surface, this molecule is able to receive one electron from the conducting electron band and finally convert to another superoxide radical. This superoxide radical can go to two distinct routes: combine with another superoxide radical and form hydrogen peroxide (by action of mitochondrial superoxide dismutase (SOD) enzyme) or return to the surface of the AuNP. Because the absorption spectra of the Au surface plasmon band remain unchanged upon adsorption of the radicals, the electron density at the surface remains essentially unchanged. The mechanism is likely based on the exchange interactions between the unpaired electrons of radicals and conduction-band electrons of the metal. The superoxide radical can convert to singlet oxygen in two processes. First, it can act as a donor and transfer one of its $2\pi^*$ electron to the conducting band. Second, this molecule can be converted to the singlet oxygen via spin conversion relaxation. (Note: singlet oxygen has the same electron spin on its $2\pi^*$) (Razzaq et al. 2016).

29.3.3.2 Nanoparticle-Mediated Manipulation of the Radiative Yield of Electron-Excited Species

From a chemical point of view, owing to the low efficiency of reactions that generate BAL, several strategies have been developed to enhance the BAL intensity. In this chapter, we do not consider fluorescent molecules (such as fluorescein (White et al. 1964) or DBAS (9,10-dibromoanthracene-2-sulfonic acid) (Velosa et al. 2007)), which can accept electron excitation energy from otherwise weakly emitting endogenously generated electron-excited states and emit the energy in the form of a photon with high efficiency.⁶ Rather, we focus on more “physical,” material science-based and nano-scale approaches for BAL enhancement.

One such physical approach is metal-enhanced chemiluminescence, which is another novel strategy in which

plasmonic nanoparticles such as gold, silver and platinum are used for the enhancement of chemiluminescence (Aslan and Geddes 2009; Chowdhury et al. 2006a, b). In metal-enhanced chemiluminescence, excitation of the metal surface plasmons by electronically excited molecules of chemiluminescent species can enhance the chemiluminescence intensity. Two mechanisms have been proposed for the enhancement effect of plasmonic nanoparticles: (1) increasing the local electromagnetic field (Abel et al. 2015) and (2) interaction of the plasmons with chemiluminescence species (Chowdhury et al. 2006a, b).

This mechanism for the BAL signal enhancement in the presence of AuNPs is based on the plasmonic antenna effects of the AuNPs. The metal nanoparticles have been shown to modulate and to potentially enhance the radiative yield of electron-excited molecules (Park et al. 2017). Triplet excited carbonyls, one of the primary excited states produced chemically in the process preceding BAL emission, have very low radiative yield because of quenching by molecular oxygen (Cilento and Adam 1995). Hence, enhancing radiative yield of triplet excited state due to AuNPs antenna effects (Herrmann et al. 2016) could be another potential mechanism for the BAL signal enhancement in the presence of AuNPs.

Quantum dots (QDs) are zero-dimensional nanoparticles that have been used as potential alternatives to chemiluminescence emitters owing to their excellent electronic and optical properties (Chen et al. 2014). There are three possible mechanisms for QDs as chemiluminescence enhancers: (1) modulators of the radiative relaxation rate of chemically generated excitons after direct electron- and hole-injection, (2) acting as the catalysts or energy acceptor, and (3) acting as emitter species after chemiluminescence resonance energy transfer (CRET).

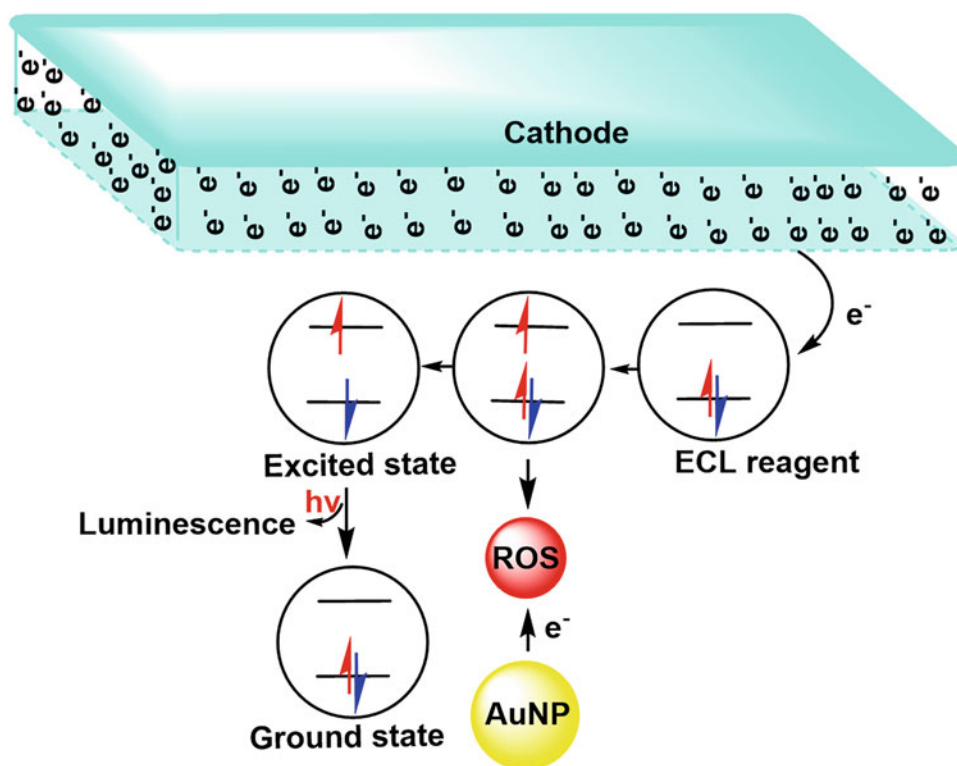
29.3.3.3 Combination of Electric Field and Nanoparticles

Since the first report of ECL on silicon QDs, ECL enhancement using other alloyed or core–shell structure QDs including CdSe, CdS, CdTe, ZnS, and Ag₂Se has also been reported (Huan et al. 2015; Zhang et al. 2004, 2016; Jie and Jie 2016; Lv et al. 2014; Stewart et al. 2015; Jie et al. 2015). Furthermore, polymer dots, carbon nanodots, graphite like carbon nitride, upconversion nanoparticles, and noble metal nanoclusters such as Au (Zhang et al. 2004; Richter and Bard 1996), Ag (Lei et al. 2018; Chowdhury et al. 2007; Bruno et al. 1998; Jingru and Jinming 1991), Cu (Bolleta et al. 1982; Vogler and Kunkely 1987; McCall et al. 2001), Pd (Tokel-Takvoryan and Bard 1974), and Pt (Vogler and Kunkely 1984, 1987; Gross et al. 2002; Kim et al. 1985; Bonafede et al. 1986) are other ECL emitters. In this section, we discuss metal nanoparticles as a new ECL component.

Because of the unique properties of metal nanoclusters, including high electrical conductivity, good water solubility,

⁶See more on that in Chap. 6.

Fig. 29.5 AuNP surface can generate ROS and these species are ultimately able to produce ECL by combination with ECL reagent. ECL reagent accepts an electron from cathode. Subsequently, ROS gains the low-energy electron from the intermediate ECL reagent and convert it to the excited state. The final excited species radiatively relax and emit a photon



and stability, they are ECL luminophores, quenchers, and catalysts (Wang et al. 2006, 2008; Sun et al. 2005). For example, the discrete electronic energy level (due to the comparable size to the Fermi wavelength of electrons) and direct electron transition of gold nanoclusters (GNCs) caused their use as new ECL nanomaterial. However, because of the low ECL efficiency of GNCs, increasing the ECL efficiency of GNCs by decreasing the nonradiative transition and complications from mass transport between the reactants has been investigated (Wang et al. 2016; Han et al. 2016). Functionalization of gold nanocluster with luminol resulted in up to 100-fold enhancement in ECL intensity for alkaline phosphatase detection (Nie et al. 2015). Hybrid gold nanocluster (AuNCs/graphene) showed a low detection limit (0.1 fM to 0.1 nM) of pentachlorophenol (Luo et al. 2014). AuNPs-modified ECL electrode showed high sensitivity and good stability in immunoassays and DNA assays (Zhang et al. 2007; Yin et al. 2005; Li et al. 2009). Although enhancement of the ECL signals of cell with a AuNPs-modified electrode is mainly attributed to its high surface area, the powerful electrons transfer properties of AuNPs caused sensitivity enhancements of 10- and 6-fold for detection of some biological material such as bovine serum albumin (BSA) and immunoglobulin G (IgG) (Zhao et al. 2018). Also, the catalytic effect of AuNPs on the redox of ECL-emitting species is considered as another reason for the enhancement of the ECL intensity in the presence of AuNPs. By using the gold nanorods, the intensities of ECL

peaks were enhanced approximately 2- to 10-fold on a gold-nanorod-modified gold electrode (Dong et al. 2006). AuNP also shows catalytic activity for the generation of ROS. Actually, AuNP surface can generate the ROS and these species are ultimately able to produce ECL by combination with ECL reagent (Fig. 29.5) (Higashi et al. 2017).

29.3.3.4 Nanoparticle-Mediated BAL Enhancement: Evidence from Cells

In this section, we briefly outline recent reports in which nanoparticle-mediated BAL enhancement has been demonstrated.

BAL signal enhancement by metal nanoparticles under in vitro conditions has revealed a few valuable endpoints related to the importance of manipulating the ROS as the main source of BAL. An exponential increase in the BAL signal was observed when prostate cancer cells (10^5 cell·ml⁻¹) were treated with a 10 nM silver nanoparticle (AgNPs) solution (6–20 nm in diameter). The main reason for such an enhancement is related to the increase in the number of ROS, especially singlet oxygen in the presence of AgNPs (Hossu et al. 2013). Similarly, the treatment of 5 mm thick disks of sweet potato roots with 1 nM AgNPs (8–15 nm in diameter) resulted in BAL signal enhancement through two proposed mechanisms: ROS generation and energy resonance transfer (Hossu et al. 2010).

Given that mitochondria are the most important source of BAL (approximately 90% of ROS are produced by

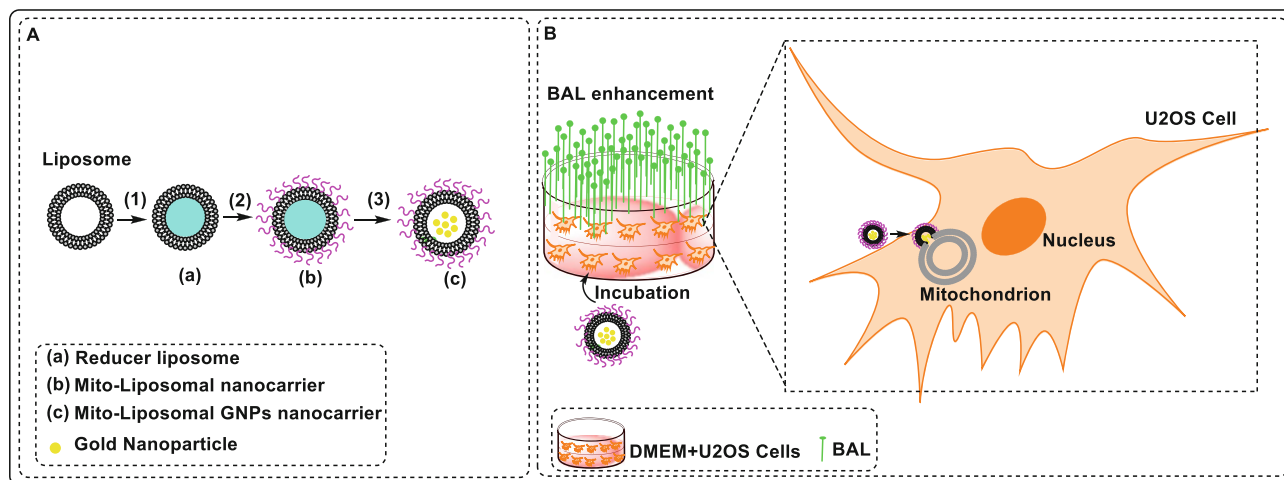


Fig. 29.6 Mitoliposomal gold nanoparticles nanocarriers for the enhancement of the BAL signal. (a) Functionalization of reducer liposome (1) with mitochondrial penetrating peptides (2) produced the mito-

mitochondria (Zhang et al. 2019)), it is expected that the amount of generated BAL can be increased by affecting this vital organelle. For example, in a recent study, we showed that mitochondrial-targeted delivery by liposomal gold nanoparticles nanocarriers could significantly increase the intensity of BAL in a completely safe manner (Fig. 29.6) (Sardarabadi et al. 2020).

29.4 Conclusion

Biological autoluminescence detection is a potentially important noninvasive diagnostic method. However, owing to the ultraweak intensity of BAL signals, it is necessary to enhance it to be able to detect an unknown biological condition. Here, we reviewed novel approaches for the enhancement of the BAL signal by selected biophysical means by focusing on the application of electric and magnetic fields and metal nanoscale particles.

Acknowledgments MC and PV thank the Czech Science Foundation project no. 20-06873X for the support, and they are also participating in the bilateral exchange project between the Czech and Slovak Academy of Sciences, no. SAV-18-11. The Science Editorium is acknowledged for the language check.

References

Burgos, R.C.R., et al., *Ultra-weak photon emission as a dynamic tool for monitoring oxidative stress metabolism*. Scientific reports, 2017. 7(1): p. 1229.

liposomal GNPs nanocarrier (3). (b) Incubated mitoliposomal GNP nanocarriers can enhance the UPE of U2OS cells by affecting the mitochondria

Wang, P., et al., *Interaction of gold nanoparticles with proteins and cells*. Science and technology of advanced materials, 2015. 16(3): p. 034610.

Gabe, Y., O. Osanai, and Y. Takema, *The relationship between skin aging and steady state ultraweak photon emission as an indicator of skin oxidative stress in vivo*. Skin Research and Technology, 2014. 20(3): p. 315–321.

Cilento, G. and W. Adam, *From free radicals to electronically excited species*. Free Radical Biology and Medicine, 1995. 19(1): p. 103–114.

Van Wijk, R., *Introduction: biophoton emission, stress and disease*. Cellular and Molecular Life Sciences, 1992. 48(11): p. 1029–1030.

Nakamura, K. and M. Hiramatsu, *Ultra-weak photon emission from human hand: influence of temperature and oxygen concentration on emission*. Journal of Photochemistry and photobiology B: Biology, 2005. 80(2): p. 156–160.

Okano, Y., H. Masaki, and H. Sakurai, *Pentosidine in advanced glycation end-products (AGEs) during UVA irradiation generates active oxygen species and impairs human dermal fibroblasts*. Journal of dermatological science, 2001. 27: p. 11–18.

Rastogi, A. and P. Pospíšil, *Spontaneous ultraweak photon emission imaging of oxidative metabolic processes in human skin: effect of molecular oxygen and antioxidant defense system*. Journal of Biomedical Optics, 2011. 16(9): p. 096005.

Cifra, M. and P. Pospíšil, *Ultra-weak photon emission from biological samples: definition, mechanisms, properties, detection and applications*. Journal of Photochemistry and Photobiology B: Biology, 2014. 139: p. 2–10.

Cadenas, E. and H. Sies, *[26] Low-level chemiluminescence as an indicator of singlet molecular oxygen in biological systems*, in *Methods in enzymology*. 1984, Elsevier. p. 221–231.

Boveris, A., et al., *Organ chemiluminescence: noninvasive assay for oxidative radical reactions*. Proceedings of the National Academy of Sciences, 1980. 77(1): p. 347–351.

Nakano, M., *Low-level chemiluminescence during lipid peroxidations and enzymatic reactions*. Journal of bioluminescence and chemiluminescence, 1989. 4(1): p. 231–240.

- Belousov, L.V., J.M. Opitz, and S.F. Gilbert, *Life of Alexander G. Gurwitsch and his relevant contribution to the theory of morphogenetic fields*. International Journal of Developmental Biology, 2004. **41**(6): p. 771–777.
- Gurwitsch, A., *A historical review of the problem of mitogenetic radiation*. Experientia, 1988. **44**(7): p. 545–550.
- Volodyaev, I. and L.V. Belousov, *Revisiting the mitogenetic effect of ultra-weak photon emission*. Frontiers in physiology, 2015. **6**: p. 241.
- Coil, L., *Further measurement of the bioluminescence of the seedlings*. Experientia, 1995. **11**: p. 479–481.
- Colli, L. and U. Facchini, *Light emission by germinating plants*. II Nuovo Cimento (1943-1954), 1954. **12**(1): p. 150–153.
- Scholkmann, F., et al., *Spatio-temporal dynamics of spontaneous ultra-weak photon emission (autoluminescence) from human hands measured with an EMCCD camera: Dependence on time of day, date and individual subject*. Matters, 2018. **4**(3): p. e201803000001.
- Popp, F.-A., *Quantum phenomena of biological systems as documented by biophotonics*, in *Quo Vadis Quantum Mechanics?* 2005, Springer. p. 371–396.
- Bókkon, I., et al., *Endogenous spontaneous ultraweak photon emission in the formation of eye-specific retinogeniculate projections before birth*. Reviews in the Neurosciences, 2016a. **27**(4): p. 411–419.
- Takeda, M., et al., *Biophoton detection as a novel technique for cancer imaging*. Cancer Sci, 2004. **95**(8): p. 656–61.
- Takeda, M., et al., *A novel method of assessing carcinoma cell proliferation by biophoton emission*. Cancer Lett, 1998. **127**(1–2): p. 155–60.
- Agarwal, A., A. Hamada, and S.C. Esteves, *Insight into oxidative stress in varicocele-associated male infertility: part I*. Nature Reviews Urology, 2012. **9**(12): p. 678–690.
- Oberley, L.W. and D.R. Spitz, *[61] Assay of superoxide dismutase activity in tumor tissue*. Methods in enzymology, 1984. **105**: p. 457–464.
- Khabiri, F., et al., *Non-invasive monitoring of oxidative skin stress by ultraweak photon emission (UPE)-measurement. I: mechanisms of UPE of biological materials*. Skin Research and Technology, 2008. **14**(1): p. 103–111.
- Ou-Yang, H., et al., *A chemiluminescence study of UVA-induced oxidative stress in human skin in vivo*. Journal of investigative dermatology, 2004. **122**(4): p. 1020–1029.
- Prasad, A. and P. Pospíšil, *Ultraweak photon emission induced by visible light and ultraviolet A radiation via photoactivated skin chromophores: in vivo charge coupled device imaging*. Journal of biomedical optics, 2012. **17**(8): p. 085004.
- Rastogi, A. and P. Pospíšil, *Ultra-weak photon emission as a non-invasive tool for monitoring of oxidative processes in the epidermal cells of human skin: comparative study on the dorsal and the palm side of the hand*. Skin research and technology, 2010. **16**(3): p. 365–370.
- Sauermann, G., et al., *Ultraweak photon emission of human skin in vivo: influence of topically applied antioxidants on human skin*, in *Methods in enzymology*. 1999, Elsevier. p. 419–428.
- Salari V, Valian H, Bassereh H, Bókkon I, Barkhordari A. *Ultraweak photon emission in the brain*. Journal of integrative neuroscience. 2015;14(03):419–29.
- Bókkon I, Scholkmann F, Salari V, Császár N, Kapócs G. *Endogenous spontaneous ultraweak photon emission in the formation of eye-specific retinogeniculate projections before birth*. Reviews in the Neurosciences. 2016b;27(4):411–9.
- Esmailpour T, Fereydouni E, Dehghani F, Bókkon I, Panjehshahin M-R, Császár-Nagy N, et al. *An experimental investigation of ultraweak photon emission from adult murine neural stem cells*. Scientific reports. 2020;10(1):1–13.
- Iyozumi, H., K. Kato, and T. Makino, *Spectral Shift of Ultraweak Photon Emission from Sweet Potato During a Defense Response*. Photochemistry and photobiology, 2002. **75**(3): p. 322–325.
- Ohya, T., et al., *Biophoton emission due to drought injury in red beans: possibility of early detection of drought injury*. Japanese journal of applied physics, 2002. **41**(7R): p. 4766.
- Ohya, T., et al., *Early detection of salt stress damage by biophotons in red bean seedling*. Japanese Journal of Applied Physics, 2000. **39**(6R): p. 3696.
- Inagaki, H., et al., *Difference in ultraweak photon emissions between sulfonylurea-resistant and sulfonylurea-susceptible biotypes of Scirpus juncoides following the application of a sulfonylurea herbicide*. Weed biology and management, 2008. **8**(2): p. 78–84.
- Usui, S., M. Tada, and M. Kobayashi, *Non-invasive visualization of physiological changes of insects during metamorphosis based on biophoton emission imaging*. Scientific reports, 2019. **9**(1): p. 1–7.
- Cifra, M. and P. Pospíšil, *Ultra-weak photon emission from biological samples: definition, mechanisms, properties, detection and applications*. J Photochem Photobiol B, 2014. **139**: p. 2–10.
- Pospíšil, P., A. Prasad, and M. Rác, *Role of reactive oxygen species in ultra-weak photon emission in biological systems*. J Photochem Photobiol B, 2014. **139**: p. 11–23.
- Non-equilibrium and coherent systems in biology, biophysics and biotechnology. *2nd International Alexander Gurwitsch Conference. Moscow, Russia, September 6-10, 1999. Abstracts*. Riv Biol, 2000. **93**(1): p. 103–61.
- Popp, F.A., K. Li, and Q. Gu, *Recent advances in biophoton research and its applications*. 1992: World Scientific.
- Belousov, L.V., V.L. Voeikov, and V.S. Martynyuk, *Biophotonics and coherent systems in biology*. 2007: Springer Science & Business Media.
- Pospíšil, P., A. Prasad, and M. Rác, *Mechanism of the formation of electronically excited species by oxidative metabolic processes: role of reactive oxygen species*. Biomolecules, 2019. **9**(7): p. 258.
- Auchère, F. and F. Rusnak, *What is the ultimate fate of superoxide anion in vivo?* JBIC Journal of Biological Inorganic Chemistry, 2002. **7**(6): p. 664–667.
- Bielski, B.H., et al., *Reactivity of HO₂O– 2 radicals in aqueous solution*. Journal of physical and chemical reference data, 1985. **14**(4): p. 1041–1100.
- Kale, R., et al., *Amino acid oxidation of the D1 and D2 proteins by oxygen radicals during photoinhibition of Photosystem II*. Proceedings of the National Academy of Sciences, 2017. **114**(11): p. 2988–2993.
- Prousek, J., *Fenton chemistry in biology and medicine*. Pure and applied chemistry, 2007. **79**(12): p. 2325–2338.
- Pospíšil, P., A. Prasad, and M. Rác, *Role of reactive oxygen species in ultra-weak photon emission in biological systems*. Journal of Photochemistry and Photobiology B: Biology, 2014. **139**: p. 11–23.
- Hideg, E. and H. Inaba, *Biophoton emission (ultraweak photoemission) from dark adapted spinach chloroplasts*. Photochemistry and photobiology, 1991. **53**(1): p. 137–142.
- Barnes, F.S. and B. Greenebaum, *The effects of weak magnetic fields on radical pairs*. Bioelectromagnetics, 2015. **36**(1): p. 45–54.
- Markkanen, A., et al., *Effects of 50 Hz magnetic field on cell cycle kinetics and the colony forming ability of budding yeast exposed to ultraviolet radiation*. Bioelectromagnetics: Journal of the Bioelectromagnetics Society, The Society for Physical Regulation in Biology and Medicine, The European Bioelectromagnetics Association, 2001. **22**(5): p. 345–350.
- Kumlin, T., et al., *p53-independent apoptosis in UV-irradiated mouse skin: possible inhibition by 50 Hz magnetic fields*. Radiation and environmental biophysics, 2002. **41**(2): p. 155–158.
- Kumlin, T., et al., *Effects of 50 Hz magnetic fields on UV-induced skin tumorigenesis in ODC-transgenic and non-transgenic mice*. International journal of radiation biology, 1998. **73**(1): p. 113–121.
- Pizzino, G., et al., *Oxidative stress: harms and benefits for human health*. Oxidative medicine and cellular longevity, 2017. **2017**.

- Bereta, M., et al., *Biological autoluminescence as a noninvasive monitoring tool for chemical and physical modulation of oxidation in yeast cell culture*. Scientific reports, 2021. **11**(1): p. 1–11.
- Cheun, B., et al., *Biophoton emission of MDCK cell with hydrogen peroxide and 60 Hz AC magnetic field*. Journal of environmental biology, 2007. **28**(4): p. 735–740.
- Rols, M.-P., *Electroporation, a physical method for the delivery of therapeutic molecules into cells*. Biochimica et Biophysica Acta (BBA)-Biomembranes, 2006. **1758**(3): p. 423–428.
- Sweeney, D.C., T.A. Douglas, and R.V. Davalos, *Characterization of cell membrane permeability in vitro part II: computational model of electroporation-mediated membrane transport*. Technology in cancer research & treatment, 2018. **17**: p. 1533033818792490.
- Pataro, G., G. Donsi, and G. Ferrari, *Modeling of Electrochemical Reactions During Pulsed Electric Field Treatment*, in *Handbook of Electroporation*, D. Miklavcic, Editor. 2016, Springer International Publishing: Cham. p. 1–30.
- Pakhomova, O.N., et al., *Oxidative effects of nanosecond pulsed electric field exposure in cells and cell-free media*. Archives of biochemistry and biophysics, 2012. **527**(1): p. 55–64.
- Teissie, J., *Involvement of reactive oxygen species in membrane electroporation*. Handbook of Electroporation, 2017: p. 1–15.
- Gabriel, B. and J. Teissie, *Generation of reactive-oxygen species induced by electroporation of Chinese hamster ovary cells and their consequence on cell viability*. European Journal of Biochemistry, 1994. **223**(1): p. 25–33.
- Breton Marie, A.C., René Vezinet L, Luis M. Mir, *Chemical Study of the Effects of UltraWide Band and Narrow Band Signals on Membranes*, in *Proceedings of BIOEM2016*. 2016. p. 17–19.
- Barnard, M.L., et al., *Protein and amino acid oxidation is associated with increased chemiluminescence*. Archives of biochemistry and biophysics, 1993. **300**(2): p. 651–656.
- Ou-Yang, H., G. Stamatias, and N. Kollias, *Dermal contributions to UVA-induced oxidative stress in skin*. Photodermatology, photoimmunology & photomedicine, 2009. **25**(2): p. 65–70.
- Sander, C.S., et al., *Photoaging is associated with protein oxidation in human skin in vivo*. Journal of Investigative Dermatology, 2002. **118**(4): p. 618–625.
- Maccarrone, M., N. Rosato, and A.F. Agrò, *Electroporation enhances cell membrane peroxidation and luminescence*. Biochemical and biophysical research communications, 1995. **206**(1): p. 238–245.
- Zhang, Y., et al., *Nanosecond pulsed electric fields promoting the proliferation of porcine iliac endothelial cells: An in vitro study*. PloS one, 2018. **13**(5): p. e0196688.
- Bard, A.J., et al., *Electrochemical methods: fundamentals and applications*. Vol. 2. 1980: Wiley New York.
- Bard, A.J., *Electrogenerated chemiluminescence*. 2004: CRC Press.
- Bouffier, L. and N. Sojic, *Introduction and Overview of Electrogenerated Chemiluminescence*. 2019.
- Bruno, J.G. and J.C. Cornette, *An Electrochemiluminescence Assay Based on the Interaction of Diaminotoluene Isomers with Gold (I) and Copper (II) Ions*. Microchemical journal, 1997. **56**(3): p. 305–314.
- Kong, S.H., et al., *Light-Emitting Devices Based on Electrochemiluminescence: Comparison to Traditional Light-Emitting Electrochemical Cells*. ACS Photonics, 2017. **5**(2): p. 267–277.
- Spehar-Délèze, A.-M., S. Almadaghi, and C.K. O'Sullivan, *Development of solid-state electrochemiluminescence (ECL) sensor based on Ru (bpy) 3²⁺-encapsulated silica nanoparticles for the detection of biogenic polyamines*. Chemosensors, 2015. **3**(2): p. 178–189.
- Rizwan, M., et al., *A highly sensitive and label-free electrochemiluminescence immunosensor for beta 2-microglobulin*. Analytical Methods, 2017. **9**(17): p. 2570–2577.
- Inoue, Y., et al., *Sensitive detection of glycated albumin in human serum albumin using electrochemiluminescence*. Analytical chemistry, 2017. **89**(11): p. 5909–5915.
- Roy, S., et al., *A novel, sensitive and label-free loop-mediated isothermal amplification detection method for nucleic acids using luminophore dyes*. Biosensors and Bioelectronics, 2016. **86**: p. 346–352.
- Yao, J., et al., *Quantum dots: from fluorescence to chemiluminescence, bioluminescence, electrochemiluminescence, and electrochemistry*. Nanoscale, 2017. **9**(36): p. 13364–13383.
- Cui, H., et al., *Analytical electrochemiluminescence*. 2016, Springer.
- Bist, I., K. Bano, and J.F. Rusling, *Screening Genotoxicity Chemistry with Microfluidic Electrochemiluminescent Arrays*. Sensors, 2017. **17**(5): p. 1008.
- Blanco, E., H. Shen, and M. Ferrari, *Principles of nanoparticle design for overcoming biological barriers to drug delivery*. Nat Biotech, 2015. **33**(9): p. 941–951.
- Cai, K., et al., *Bio-nano interface: The impact of biological environment on nanomaterials and their delivery properties*. Journal of Controlled Release, 2017.
- Nel, A.E., et al., *Understanding biophysicochemical interactions at the nano-bio interface*. Nat Mater, 2009. **8**(7): p. 543–557.
- Fu, P.P., et al., *Mechanisms of nanotoxicity: generation of reactive oxygen species*. Journal of food and drug analysis, 2014. **22**(1): p. 64–75.
- Xia, T., et al., *Comparison of the mechanism of toxicity of zinc oxide and cerium oxide nanoparticles based on dissolution and oxidative stress properties*. ACS nano, 2008. **2**(10): p. 2121–2134.
- Nel, A., et al., *Toxic potential of materials at the nanolevel*. science, 2006. **311**(5761): p. 622–627.
- Li, N., T. Xia, and A.E. Nel, *The role of oxidative stress in ambient particulate matter-induced lung diseases and its implications in the toxicity of engineered nanoparticles*. Free Radical Biology and Medicine, 2008. **44**(9): p. 1689–1699.
- Huang, Y.-W., C.-H. Wu, and R.S. Aronstam, *Toxicity of transition metal oxide nanoparticles: recent insights from in vitro studies*. Materials, 2010. **3**(10): p. 4842–4859.
- Risom, L., P. Møller, and S. Loft, *Oxidative stress-induced DNA damage by particulate air pollution*. Mutation Research/Fundamental and Molecular Mechanisms of Mutagenesis, 2005. **592**(1): p. 119–137.
- Knaapen, A.M., et al., *Inhaled particles and lung cancer. Part A: Mechanisms*. International Journal of Cancer, 2004. **109**(6): p. 799–809.
- Khan, H.A., et al., *Effect of gold nanoparticles on glutathione and malondialdehyde levels in liver, lung and heart of rats*. Saudi journal of biological sciences, 2012. **19**(4): p. 461–464.
- Cui, H., Z.-F. Zhang, and M.-J. Shi, *Chemiluminescent reactions induced by gold nanoparticles*. The Journal of Physical Chemistry B, 2005. **109**(8): p. 3099–3103.
- Razaq, H., et al., *Interaction of gold nanoparticles with free radicals and their role in enhancing the scavenging activity of ascorbic acid*. Journal of Photochemistry and Photobiology B: Biology, 2016. **161**: p. 266–272.
- White, E.H., et al., *Chemiluminescence of luminol: The chemical reaction*. Journal of the American Chemical Society, 1964. **86**(8): p. 940–941.
- Velosa, A.C., et al., *1, 3-diene probes for detection of triplet carbonyls in biological systems*. Chemical research in toxicology, 2007. **20**(8): p. 1162–1169.
- Aslan, K. and C.D. Geddes, *Metal-enhanced chemiluminescence: advanced chemiluminescence concepts for the 21st century*. Chemical Society Reviews, 2009. **38**(9): p. 2556–2564.
- Chowdhury, M.H., et al., *Metal-enhanced chemiluminescence*. Journal of fluorescence, 2006a. **16**(3): p. 295–299.

- Chowdhury, M.H., et al., *Metal-enhanced chemiluminescence: Radiating plasmons generated from chemically induced electronic excited states*. Applied physics letters, 2006b. **88**(17): p. 173104.
- Abel, B., et al., *Enhancement of the chemiluminescence response of enzymatic reactions by plasmonic surfaces for biosensing applications*. Nano biomedicine and engineering, 2015. **7**(3): p. 92.
- Park, J.-E., J. Kim, and J.-M. Nam, *Emerging plasmonic nanostructures for controlling and enhancing photoluminescence*. Chemical science, 2017. **8**(7): p. 4696–4704.
- Herrmann, J.F., et al., *Antenna-Enhanced Triplet-State Emission of Individual Mononuclear Ruthenium (II)-Bis-terpyridine Complexes Reveals Their Heterogeneous Photophysical Properties in the Solid State*. ACS Photonics, 2016. **3**(10): p. 1897–1906.
- Chen, H., et al., *Quantum dots-enhanced chemiluminescence: mechanism and application*. Coordination Chemistry Reviews, 2014. **263**: p. 86–100.
- Wang, T., et al., *Near-infrared electrogenerated chemiluminescence from aqueous soluble lipoic acid Au nanoclusters*. Journal of the American Chemical Society, 2016. **138**(20): p. 6380–6383.
- Huan, J., et al., *Amplified solid-state electrochemiluminescence detection of cholesterol in near-infrared range based on CdTe quantum dots decorated multiwalled carbon nanotubes@ reduced graphene oxide nanoribbons*. Biosensors and Bioelectronics, 2015. **73**: p. 221–227.
- Zhang, X., et al., *Molecular-counting-free and electrochemiluminescent single-molecule immunoassay with dual-stabilizers-capped CdSe nanocrystals as labels*. Analytical chemistry, 2016. **88**(10): p. 5482–5488.
- Jie, G. and G. Jie, *Sensitive electrochemiluminescence detection of cancer cells based on a CdSe/ZnS quantum dot nanocluster by multibranch hybridization chain reaction on gold nanoparticles*. RSC Advances, 2016. **6**(29): p. 24780–24785.
- Lv, X., et al., *Electrochemiluminescent immune-modified electrodes based on Ag₂Se@ CdSe nanoneedles loaded with polypyrrole intercalated graphene for detection of CA72-4*. ACS applied materials & interfaces, 2014. **7**(1): p. 867–872.
- Stewart, A.J., et al., *A cholesterol biosensor based on the NIR electrogenerated-chemiluminescence (ECL) of water-soluble CdSeTe/ZnS quantum dots*. Electrochimica Acta, 2015. **157**: p. 8–14.
- Jie, G., et al., *Autocatalytic amplified detection of DNA based on a CdSe quantum dot/folic acid electrochemiluminescence energy transfer system*. Analyst, 2015. **140**(1): p. 79–82.
- Zhang, J., Z. Gryczynski, and J.R. Lakowicz, *First observation of surface plasmon-coupled electrochemiluminescence*. Chemical physics letters, 2004. **393**(4–6): p. 483–487.
- Richter, M.M. and A.J. Bard, *Electrogenerated chemiluminescence*. 58. *Ligand-sensitized electrogenerated chemiluminescence in europium labels*. Analytical chemistry, 1996. **68**(15): p. 2641–2650.
- Lei, Y.-M., et al., *Silver Ions as Novel Coreaction Accelerator for Remarkably Enhanced Electrochemiluminescence in a PTCA-S₂O₈²⁻-System and Its Application in an Ultrasensitive Assay for Mercury Ions*. Analytical chemistry, 2018. **90**(11): p. 6851–6858.
- Chowdhury, M.H., et al., *First observation of surface plasmon-coupled chemiluminescence (SPCC)*. Chemical physics letters, 2007. **435**(1–3): p. 114–118.
- Bruno, J.G., et al., *Preliminary electrochemiluminescence studies of metal ion–bacterial diazolumelanin (DALM) interactions*. Journal of bioluminescence and chemiluminescence, 1998. **13**(3): p. 117–123.
- Jingru, A. and L. Jinming, *Determination of Trace Silver (I) in Basic Aqueous Solution by Electrochemiluminescence of a New Reagent 6-(2-Hydroxy-4-Diethylaminophenylazo)-2, 3-Dihydro-1, 4-Phthalazine-1, 4-Dione*. CHEMICAL RESEARCH IN CHINESE UNIVERSITIES, 1991. **7**(1): p. 32–36.
- Bolleta, F., et al., *Polypyridine transition metal complexes as light emission sensitizers in the electrochemical reduction of the persulfate ion*. Inorganica Chimica Acta, 1982. **62**: p. 207–213.
- Vogler, A. and H. Kunkely, *Electrochemiluminescence of organometallics and other transition metal complexes*. 1987.
- McCall, J., et al., *Electrochemiluminescence of Copper (I) Bis (2, 9-dimethyl-1, 10-phenanthroline)*. Analytical chemistry, 2001. **73**(19): p. 4617–4620.
- Tokel-Takvoryan, N.E. and A.J. Bard, *Electrogenerated chemiluminescence. XVI. ECL of palladium and platinum α , β , γ , δ -tetraphenylporphyrin complexes*. Chemical Physics Letters, 1974. **25**(2): p. 235–238.
- Vogler, A. and H. Kunkely, *Electrochemiluminescence of tetrakis (diphosphonato) diplatinate (II)*. Angewandte Chemie International Edition in English, 1984. **23**(4): p. 316–317.
- Gross, E.M., N.R. Armstrong, and R.M. Wightman, *Electrogenerated chemiluminescence from phosphorescent molecules used in organic light-emitting diodes*. Journal of the Electrochemical Society, 2002. **149**(5): p. E137–E142.
- Kim, J., et al., *Electrogenerated chemiluminescence on the electrogenerated chemiluminescence (ECL) of tetrakis (pyrophosphito) diplatinate (II), Pt₂ (P₂O₅H₂)₄–*. Chemical physics letters, 1985. **121**(6): p. 543–546.
- Bonafede, S., et al., *Electrogenerated chemiluminescence of an orthometalated platinum (II) complex*. The Journal of Physical Chemistry, 1986. **90**(16): p. 3836–3841.
- Wang, H., et al., *Electrogenerated chemiluminescence detection for deoxyribonucleic acid hybridization based on gold nanoparticles carrying multiple probes*. Analytica chimica acta, 2006. **575**(2): p. 205–211.
- Sun, X., et al., *Method for effective immobilization of Ru (bpy)₃²⁺ on an electrode surface for solid-state electrochemiluminescence detection*. Analytical chemistry, 2005. **77**(24): p. 8166–8169.
- Wang, X., et al., *A controllable solid-state Ru (bpy)₃²⁺ electrochemiluminescence film based on conformation change of ferrocene-labeled DNA molecular beacon*. Langmuir, 2008. **24**(5): p. 2200–2205.
- Han, S., et al., *Chemiluminescence and electrochemiluminescence applications of metal nanoclusters*. Science China Chemistry, 2016. **59**(7): p. 794–801.
- Nie, F., et al., *Novel preparation and electrochemiluminescence application of luminol functional-Au nanoclusters for ALP determination*. Sensors and Actuators B: Chemical, 2015. **218**: p. 152–159.
- Luo, S., et al., *Ultrasensitive detection of pentachlorophenol based on enhanced electrochemiluminescence of Au nanoclusters/graphene hybrids*. Sensors and Actuators B: Chemical, 2014. **194**: p. 325–331.
- Zhang, L., et al., *A novel alcohol dehydrogenase biosensor based on solid-state electrogenerated chemiluminescence by assembling dehydrogenase to Ru (bpy)₃²⁺-Au nanoparticles aggregates*. Biosensors and Bioelectronics, 2007. **22**(6): p. 1097–1100.
- Yin, X.-B., et al., *4-(Dimethylamino) butyric acid labeling for electrochemiluminescence detection of biological substances by increasing sensitivity with gold nanoparticle amplification*. Analytical chemistry, 2005. **77**(11): p. 3525–3530.
- Li, Y., et al., *Detection of DNA immobilized on bare gold electrodes and gold nanoparticle-modified electrodes via electrogenerated chemiluminescence using a ruthenium complex as a tag*. Microchimica Acta, 2009. **164**(1–2): p. 69.
- Zhao, C., et al., *Electrochemiluminescence of gold nanoparticles and gold nanoparticle-labelled antibodies as co-reactants*. RSC advances, 2018. **8**(63): p. 36219–36222.
- Dong, Y.-P., H. Cui, and C.-M. Wang, *Electrogenerated chemiluminescence of luminol on a gold-nanorod-modified gold electrode*. The Journal of Physical Chemistry B, 2006. **110**(37): p. 18408–18414.

- Higashi, Y., et al. *Electrochemiluminescence Based Biosensors with AuNP Showing Catalytic ROS Generation*. in *Multidisciplinary Digital Publishing Institute Proceedings*. 2017.
- Hossu, M., et al., *Enhancement of biophoton emission of prostate cancer cells by Ag nanoparticles*. *Cancer nanotechnology*, 2013. **4**(1): p. 21–26.
- Hossu, M., L. Ma, and W. Chen, *Nonlinear enhancement of spontaneous biophoton emission of sweet potato by silver nanoparticles*. *Journal of Photochemistry and Photobiology B: Biology*, 2010. **99**(1): p. 44–48.
- Zhang W, Hu X, Shen Q, Xing D. *Mitochondria-specific drug release and reactive oxygen species burst induced by polyprodrug nanoreactors can enhance chemotherapy*. *Nature communications*. 2019;10(1):1–14.
- Sardarabadi, H., et al., *Enhancement of the biological autoluminescence by mito-liposomal gold nanoparticle nanocarriers*. *Journal of Photochemistry and Photobiology B: Biology*, 2020. **204**: p. 111812.



Upconverting Nanoparticles as Sources of Singlet Oxygen

30

Cássio Cardoso Santos Pedroso, Sayuri Miyamoto, Amanda da Annuniação Farhat, Eduardo Alves de Almeida, Hermi Felinto Brito, and Paolo Di Mascio

30.1 Introduction

Singlet oxygen ($^1\text{O}_2$) is one of many photoactive molecules present in biological systems. The importance of $^1\text{O}_2$ molecule is related to its active role in physiologic and pathophysiologic processes within living organisms, e.g., in photosynthetic metabolism or inflammatory response of arthritis, cataracts, and skin cancer (Nonell and Flors 2016; Nathan and Ding 2010; Liou and Storz 2010; Halliwell 2006; Winterbourn 2008). Unsaturated fatty acids, proteins, and nucleic acids are singlet oxygen targets and susceptible to oxidation due to the high $^1\text{O}_2$ reactivity with organic molecules rich in electrons (Nonell and Flors 2016; Di Mascio et al. 2019). For example, in photodynamic therapy (PDT), many strategies use singlet oxygen generation to trigger off apoptosis of cancer cells and keep the healthy cells in the organism intact. Selective cancer cell apoptosis is not an easy task, so many scientific fields investigate strategies to solve this problem (Nonell and Flors 2016; Castano et al. 2006).

Fluorescent dyes, proteins, or quantum dots demonstrate many useful features, but the luminescence of these molecules and materials is based on high energy excitation, in general, by UV radiation, which is potentially harmful and carcinogenic, or high scattering light as blue/green able to excite biomolecules too (Gnach and Bednarkiewicz 2012). These radiations can cause multiple effects on living

organisms interfering with the results of laboratory analysis to technological applications. Considerable effort has been made to develop and implement photoactive materials within the “biological transparency windows” (NIR-I: 750–950 nm; NIR-II: 1000–1300 nm; NIR-III: 1550–1870 nm) (Hemmer et al. 2016). Upconverting nanomaterials are an elegant strategy to overcome this problem due to their characteristic of converting low-energy light to high-energy light in a phenomenon called upconversion (Wang et al. 2010; Liu et al. 2013).

The field of trivalent lanthanides (Ln^{3+} : La^{3+} – Lu^{3+}) based UCNPs focused on just synthesis and spectroscopic characterization of these nanomaterials in the past. Nowadays, the ability of UCNPs to convert low-energy photons to high-energy photons increases the attention of other areas, transitioning the UCNPs from simple optical probes to more complex multifunctional systems. This transition is enabling the application of Ln^{3+} -based UCNPs as a source of singlet oxygen and using these complex systems in photodynamic therapies. Therefore, this chapter will point out the characteristics and properties of upconversion, UCNPs for singlet oxygen sources, and recent applications in this field (Wang et al. 2010; Idris et al. 2012; Hemmer et al. 2017; Zhou et al. 2012; Tessitore et al. 2019).

30.2 Photon Upconversion Phenomenon and Mechanisms

Photon upconversion (UC) is a nonlinear optical phenomenon known as anti-Stokes emission that converts two or more low-energy pump photons to a higher-energy output photon (Auzel 2004). This concept was theoretically described by the physicist Nicolaas Bloembergen in 1959 who was laureated with the 1981’s Nobel Prize in Physics (Bloembergen 1959). Although Bloembergen’s idea was promising, he was not the first scientist to observe the UC phenomenon experimentally. Notably, François Auzel

C. C. S. Pedroso (✉)

The Molecular Foundry, Lawrence Berkeley National Laboratory, Berkeley, CA, USA

Departamento de Bioquímica, Instituto de Química, Universidade de São Paulo, São Paulo, SP, Brazil
e-mail: ccsp@iq.usp.br

S. Miyamoto · A. d. A. Farhat · E. A. de Almeida · P. Di Mascio
Departamento de Bioquímica, Instituto de Química, Universidade de São Paulo, São Paulo, SP, Brazil

H. F. Brito

Departamento de Química Fundamental, Instituto de Química, Universidade de São Paulo, São Paulo, SP, Brazil

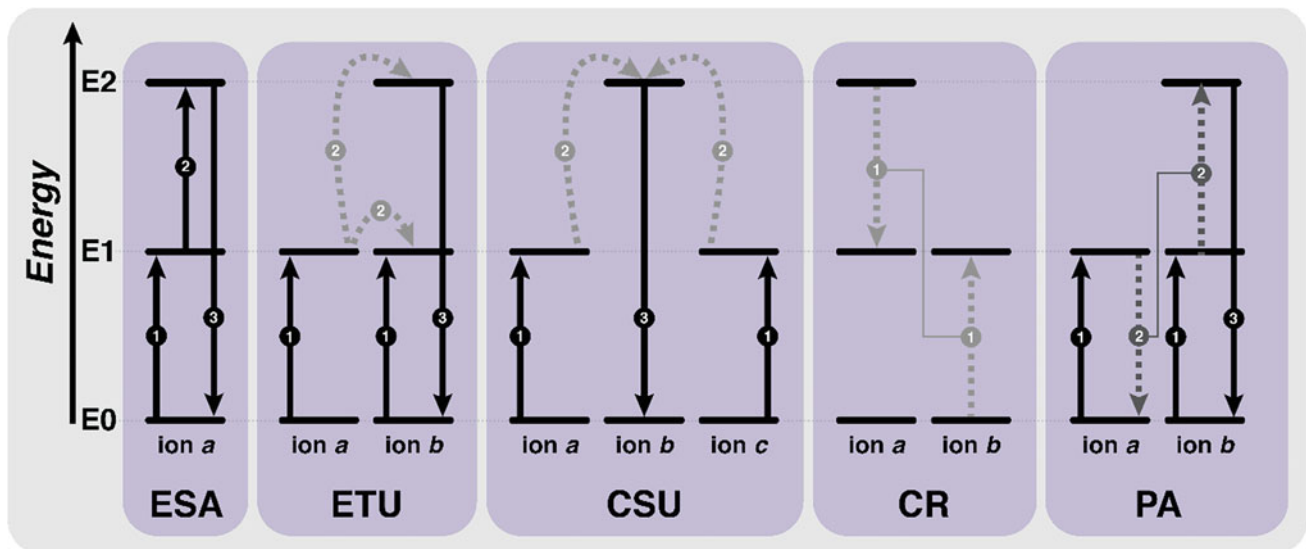


Fig. 30.1 Energy-level diagram containing the main upconversion mechanisms: excited-state absorption (ESA), energy transfer upconversion (ETU), cooperative sensitization upconversion (CSU),

cross-relaxation (CR), and photon avalanche (PA). The numbered arrows are related to the steps of the upconversion mechanisms

reported the experiments proving the upconverted visible emission in 1966 by trivalent ytterbium (Yb^{3+}) energy transfer to trivalent erbium (Er^{3+}) and thulium (Tm^{3+}) ions (Auzel 2004). The photon upconversion process has since inspired the near-infrared (NIR) upconverters design to generate UV-visible-NIR light suitable for many areas of application, e.g., bioimaging probes, photocatalysts, anticounterfeiting devices, and photodynamic therapies (Zhou et al. 2015).

Several different mechanisms have been recognized to be involved in the UC process either alone or in combination, such as excited-state absorption (ESA), energy transfer upconversion (ETU), cooperative sensitization upconversion (CSU), cross relaxation (CR), and photon avalanche (PA) (Auzel 2004; Zhou et al. 2015), as illustrated in Fig. 30.1. In the ESA mechanism, successive photons are absorbed by a ground-state ion. When an ion is excited from the ground state to an excited state called E_1 level, a second photon promotes the ion from E_1 level to a higher lying E_2 level resulting in an upconverted emission. ETU process involves two ions close spatially where ion a is excited to E_1 level and transfers energy to E_1 level of an ion b . The ion b with electrons in the E_1 excited state absorbs the radiation promoting the electrons to E_2 level and emitting upconverted light. The dopant concentration determines the average distance between the neighboring dopant ions and strongly influences the efficiency of ETU upconversion process. In contrast, in an ESA process, the upconversion efficiency is independent of the dopant concentration since that the mechanism affects a single ion (Auzel 2004; Zhou et al. 2015).

Cooperative sensitization upconversion (CSU) involves the interaction among three ion centers where ions a and

c are sensitizers and ion b is the activator ion. After irradiation with excitation photons, both ions a and c are in the excited state E_1 and both will interact with the activator ion b simultaneously and excite ion b to higher energy (state E_2). The excited ion b decays radiatively to its ground state, emitting an upconverted photon. The CSU efficiency is generally orders of magnitude lower than ESA or ETU efficiency because it involves quasi-virtual pair levels during the process (Auzel 2004).

A typical cross-relaxation (CR) is considered a detrimental process in upconversion materials. The mechanism can occur by ion-ion interaction in which ion a transfers part of its energy to ion b . Ions a and b can be either the same or different. Ion b can also be in its excited state in some cases. If ion a and b are the same, CR process will arouse concentration quenching, which significantly decreases emission intensity (Auzel 2004). On the other hand, this physical mechanism can be intentionally used in upconversion color-tuning materials or constructing an efficient photon avalanche (PA) mechanism. PA-induced upconversion features an unusual pump mechanism that requires a power density above a specific threshold value. When the power density is below the threshold, a very low upconverted emission intensity is detected. Photoluminescence intensity increases by orders of magnitude when it is above the pump threshold, however. The PA is a mechanism that involves ETU or ESA process (Fig. 30.1) for excitation light and an efficient CR that produces a feedback emission (Zhou et al. 2015; Lahoz et al. 2005). In addition to high pump intensity, PA-induced upconversion also requires a prolonged irradiation source (da Silva et al. 2020; Lee et al. 2021).

30.3 Lanthanide-Based Upconverting Nanoparticles

Highly efficient bulk upconverting materials can be excited by LED irradiation, but lasers are the most common photon source, especially when it comes to nanomaterials (Zhang 2015). A high photon density is required for upconverter excitation due to its relatively low quantum efficiency. With the advent of inexpensive high-power infrared diode lasers (e.g., 980-nm NIR laser), the UC emission from trivalent lanthanide ions (Ln^{3+}) has been extensively studied (Auzel 2004; Zhang 2015). Besides, the lanthanide spectroscopy properties are suitable for upconverter nanoparticles (UCNP) (Auzel 2004; Zhou et al. 2015; Zhang 2015). These tiny particles have been receiving increase attention as optical imaging probes and theranostic agents from the materials science, chemistry, physics, and biomedical community (Hemmer et al. 2017; Zhou et al. 2015; Zhang 2015; Chen et al. 2018).

Lanthanides are fifteen elements from lanthanum (La) to lutetium (Lu) with empty to completely filled 4f subshells, respectively. Trivalent lanthanide ions (Ln^{3+}) possess a rich energy level structure with transitions in the UV, visible, and NIR spectral regions. Ln^{3+} electronic transitions are responsible for the versatile use and the complexity of lanthanides as spectral converters. The filled and external $5s^2$ and $5p^6$ subshells shield the 4f electrons of Ln^{3+} , resulting in weak electron–phonon coupling responsible for its optical phenomena such as narrow absorption and emission bands from 4f–4f transitions. Also, the optical transitions of the 4f electrons (Stark energy levels) are only marginally affected by the surroundings and appear at nearly the same energies for different host crystalline matrices (materials). Dieke and Crosswhite determined Ln^{3+} energy level structures in the lanthanum chloride matrix (LaCl_3), which can be extended to other host materials due to the small Ln^{3+} energy-level shifts. The 4f–4f transitions are Laporte forbidden,¹ resulting in low transition probabilities and substantially long-lived (up to 0.1 s) excited states. The crystal field acting on an Ln^{3+} ion splits the energy levels into crystal field components called Stark sublevels. Consequently, the sharp Ln^{3+} transitions become slightly broader (Cotton 2006; Chen et al. 2014). Slightly broader bands can help in the overlap of activator and sensitizer transitions for energy transfer in the ETU or PA mechanisms.

Since 4f–4f transitions are Laporte forbidden, the low molar absorption coefficients limit the upconversion luminescence efficiency (Cotton 2006). The light absorption can be

improved by increasing the lanthanide doping concentration in the material. Nonradiative multiphonon relaxation combined with the cross-relaxation process severely limits the range of useful dopant concentrations, however (Chen et al. 2014; Wen et al. 2018; Chen and Wang 2020). It is worth mentioning that in the matrices where lanthanides are heterovalently doping, for example, CaF_2 , ion clusters form, and CR between lanthanides occurs more easily. Thus, the optimized dopant concentration in this kind of UCNPs is usually lower than that in, e.g., NaYF_4 (Zhang 2015).

The nonradiative multiphonon relaxation rate is an essential factor that dictates the population of intermediate and emitting levels and subsequently determines the efficiency of the upconversion process. The multiphonon relaxation rate constant k_{nr} for 4f levels in lanthanide ions is described in Eq. (30.1):

$$k_{nr} \propto \exp\left(-\beta \frac{\Delta E}{\hbar\omega_{\max}}\right) \quad (30.1)$$

where β is an empirical constant of the host lattice, ΔE is the energy gap between the populated level and the next lower-lying energy level in the lanthanide ion, and $\hbar\omega_{\max}$ is the highest energy vibrational mode of the host lattice. The energy gap law implies that the multiphonon relaxation rate constant decreases exponentially with increasing energy gap. The Er^{3+} and Tm^{3+} ions have relatively large energy gaps and low probabilities of nonradiative transitions among various excited levels. In agreement with the energy gap law, the most efficient UCNPs known to date are obtained with Er^{3+} and Tm^{3+} as the activators (Auzel 2004; Zhou et al. 2015; Zhang 2015). The upconversion efficiency of Er^{3+} is exceptionally high due to the similar energy gap in different energy levels. For example, the energy difference in Er^{3+} ($10,350 \text{ cm}^{-1}$) between the $^4\text{I}_{11/2}$ and $^4\text{I}_{15/2}$ levels is similar to that ($10,370 \text{ cm}^{-1}$) between the $^4\text{F}_{7/2}$ and $^4\text{I}_{11/2}$ levels. Thus, the $^4\text{I}_{15/2}$, $^4\text{I}_{11/2}$, and $^4\text{F}_{7/2}$ energy levels can be used to generate upconversion emissions under 980-nm excitation. In addition, the energy difference between $^4\text{F}_{9/2}$ and $^4\text{I}_{13/2}$ states is close to $10,000 \text{ cm}^{-1}$. Therefore, at least three different transitions in Er^{3+} ions are induced by 980 nm excitation, which leads to the green and red emission colors after the sequential absorption of two 980-nm photons (Fig. 30.2) (Auzel 2004).

30.3.1 Sensitizers and Activators in UCNPs

The upconversion luminescence efficiency can be significantly enhanced using a sensitizer with high absorption cross section. A sensitizer is usually used along with an

¹Laporte rule: spectroscopic selection rule applied to electronic transitions of atoms or centrosymmetric molecules that considers allowed transitions of a change in parity, either $g \rightarrow u$ or $u \rightarrow g$ ($\Delta l: +1$ or -1).

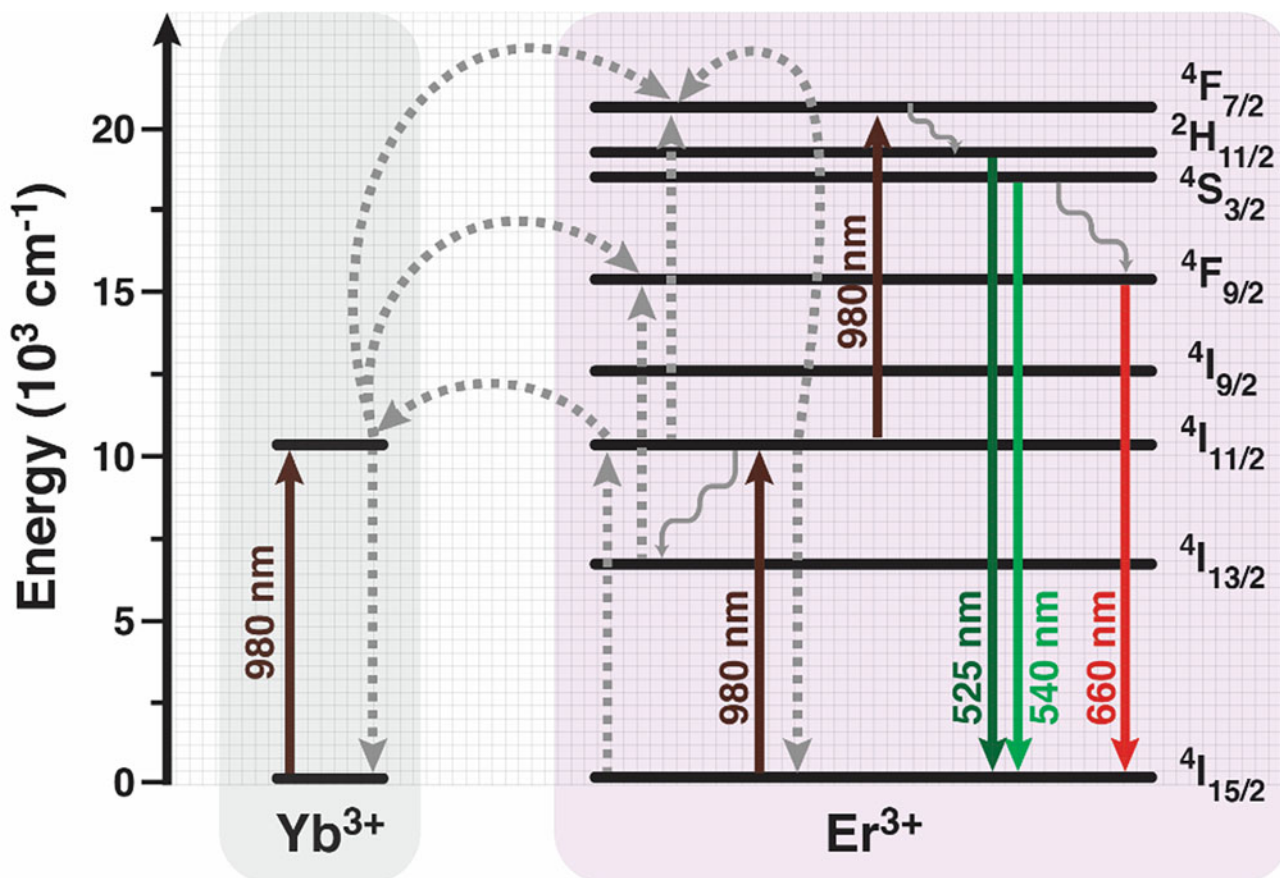


Fig. 30.2 Schematic energy-level diagrams showing typical upconversion processes for the pair Yb^{3+} - Er^{3+} . (Reference Auzel 2004)

activator to take advantage of the efficient ETU process. The most widely used sensitizer for Er^{3+} , Tm^{3+} , and trivalent holmium (Ho^{3+}) activators is the Yb^{3+} ion. Yb^{3+} possesses an extremely simple energy-level scheme with only one excited 4f level attributed as $^2\text{F}_{5/2}$ (Fig. 30.2). The energy gap between the $^2\text{F}_{7/2}$ ground state and $^2\text{F}_{5/2}$ excited state of the Yb^{3+} ion matches the energy gap between the $^4\text{I}_{11/2}$ - $^4\text{I}_{15/2}$ and the $^4\text{F}_{7/2}$ - $^4\text{I}_{11/2}$ states of Er^{3+} ion. Thus, these similar energy gaps allow an efficient energy transfer between these two lanthanide ions and electron excitation for higher energy levels (Auzel 2004; Zhou et al. 2015; Zhang 2015). A similar principle can be used in Tm^{3+} and Ho^{3+} . The small energy gap mismatches of Tm^{3+} and Ho^{3+} concerning Yb^{3+} can decrease the energy transfer exponentially from the Yb^{3+} sensitizers. However, it can be partially compensated by a process termed phonon-assisted energy transfer. When the energy gap is not too large, the matrix phonons participate in the process and balance the energy mismatches (Auzel 2004; Zhou et al. 2015, 2018; Zhang 2015).

The incorporated impurities in crystalline matrices may generally serve as sensitizers such as Yb^{3+} , modify the local crystal field around activators, or dissociate ion clusters in nanoparticles. This last one occurs typically in host matrices

heterovalently doped, leading to the upconversion enhancement (Zhang 2015). Another approach to enhance the Ln^{3+} emission is distorting the crystal field in the host lattice by co-substitution of inert Ln^{3+} with slightly smaller and larger ionic radii to disturb the crystal field without the generation of crystal defects. The large size mismatch between the dopant and the host is likely to cause local distortion in the crystal lattice and reduce activator ions' site symmetry. Consequently, this may lead to an increase in the probability of 4f-4f optical transitions (Wisser et al. 2016). Other impurities like Gd^{3+} ions may also participate in energy transfer within the matrix. For example, gadolinium sublattice-mediated energy migration can facilitate efficient upconverter emissions from a series of Ln^{3+} ions (terbium, Tb^{3+} ; europium, Eu^{3+} ; dysprosium, Dy^{3+} ; and samarium, Sm^{3+}) without intermediary energy levels by a mechanism called energy migration upconversion (EMU; Fig. 30.3) (Wang et al. 2011a).

30.3.2 Host Matrix in UCNPs

Host materials with low phonon energies are appropriate for lanthanide doping to achieve efficient upconverter emission,

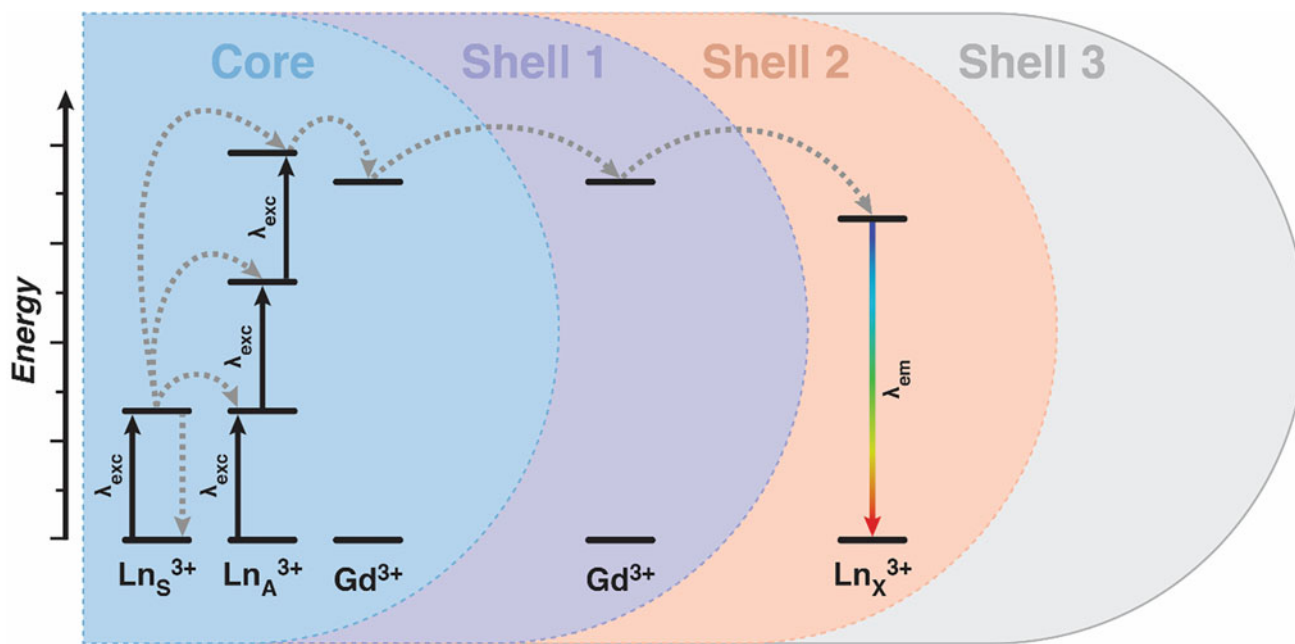


Fig. 30.3 Energy migration upconversion (EMU) mechanism showing the upconversion between a sensitizer lanthanide (Ln_S^{3+}) and activator lanthanide (Ln_A^{3+}), the energy transfer from Gd^{3+} in the core to Gd^{3+} in

Shell 1, and, the energy transfer to a lanthanide emitter (Ln_X^{3+} : Tb^{3+} , Eu^{3+} , Dy^{3+} , and Sm^{3+}) in the shell 2. Shell 3 is an inert shell to avoid energy losses. (Wang et al. 2011a)

as the low-energy phonons assure low multiphonon relaxation rates and low nonradiative losses. Chlorides, bromides, and iodides, with phonon energies of 144, 172, and 260 cm^{-1} , respectively, are theoretically ideal host matrices for upconverter emission. However, these materials often suffer from poor chemical stability and are liable for the deliquescence process under ambient conditions, which exclude them as bioapplicable UCNPs. Oxides, despite their excellent chemical stability, possess high phonon energies over 600 cm^{-1} . It makes the activator's multiphonon relaxation rates comparable to the radiative emission rates and thus are not ideal host matrices for this phenomenon either. Nevertheless, the upconversion process may sometimes require phonon assistance, so there is a balance between phonon properties and upconversion efficiency. Fluorides are considered the most efficient host matrices for lanthanide doping to achieve desirable upconverter emission for versatile applications due to their high chemical stability and suitably low phonon energies ($<350\text{ cm}^{-1}$). So far, NaYF_4 has been well established as the most efficient host material for this purpose (Auzel 2004; Zhang 2015).

In addition to phonon energy, the host matrix's crystalline structure also plays a critical role in the upconverter efficiency enhancement. For example, hexagonal-phase NaYF_4 (beta) bulk materials exhibit around an order of magnitude enhancement of upconverter efficiency relative to their cubic phase (alpha). The phase-dependent optical property can be ascribed directly to the different crystal fields around Ln^{3+} ions in the host material. Low-symmetry sites typically exert

a crystal field containing odd components around the dopant ions as compared to high-symmetry sites containing the center of inversion. The odd components enhance the electronic coupling between 4f and 5d opposite parity states, increasing 4f–4f transition probabilities of the Ln^{3+} dopant ions. Besides, the decrease in Ln^{3+} site size causes an increase in the crystal field strength around the dopant ions and can lead to enhanced upconversion efficiency (Zhang 2015).

30.3.3 Core–Shell Structures of UCNPs

Ln^{3+} -based UCNPs usually have a high proportion of superficial dopant ions in incomplete coordination environments. Luminescence of the dopant ions in the particle surface is readily quenched by high-energy oscillators arising from weakly bound surface impurities, ligands, or solvents due to a lack of effective protection by the host lattice. The excitation energy of interior ions can also be transferred to the surface through energy migration and eventually dissipate nonradiative energy. In addition, incomplete coordination environments result in a decrease of the crystal field strength around the superficial dopant ions and consequently lead to low upconverter efficiency. Therefore, it is generally believed that upconverter emission of nanoparticles is less efficient than the respective in bulk materials. The introduction of an inert crystalline shell based on an undoped material around each doped UCNPs provides an effective way to improve the upconverter efficiency. The shell usually has the same

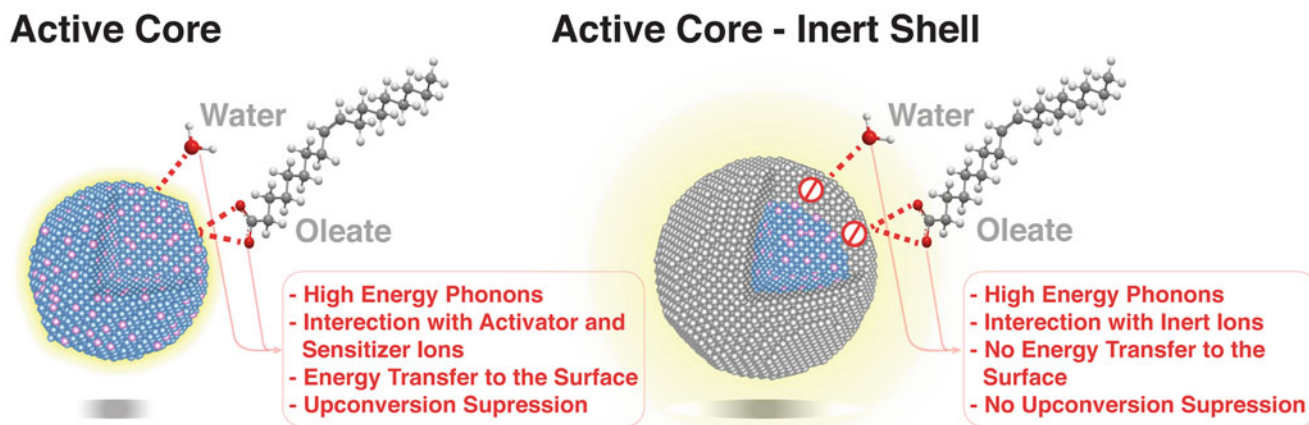


Fig. 30.4 Illustration of active core and active core-inert shell UCNPs interacting with water and oleate molecules on the surface

composition as the host matrix. In such structures, all dopant ions are confined in the interior core of the UCNPs, effectively suppressing energy transfer to the crystal surface (Fig. 30.4) (Heer et al. 2004).

30.3.4 Preparation Methods of UCNPs

Usually, the synthesis process of UCNPs requires the participation of organic ligand molecules. The ligand molecules bound in the nanoparticle surface control the particles' growth during synthesis and prevent the aggregation of the UCNPs. The repulsive force stabilizing the particles can, in principle, be due to electrostatic repulsion, steric exclusion, or a hydration layer on the surface. The choice of surface ligands is essential to keep the particles stable and dispersed in the solvent. Like most of the synthesis methods for high-quality nanoparticles, synthetic approaches for UCNPs with uniform size distributions usually involve organic ligands, resulting in hydrophobic UCNPs (Johnson et al. 2012; Suter II et al. 2014). Therefore, their hydrophobic ligands compromise their water solubility and their compatibility with the biological medium. The UCNPs surface engineering is essential to obtain hydrophilic and biocompatible nanoparticles for various biomedical applications. In turn, this goal is almost entirely dependent on the surface modification's properties approach designed to provide aqueous stability to the UCNPs and facilitate their integration within the biological environment. To this end, a variety of surface modification strategies such as ligand exchange, ligand oxidation, ligand-free synthesis, ligand attraction, electrostatic layer-by-layer assembly, and surface silanization have been designed to prepare high stable UCNPs in aqueous solutions over the past decade (Fig. 30.5). For biological applications, UCNP should exhibit high upconversion efficiency and have hydrophilic surface

characteristics that are compatible with biomolecules or biomolecular assemblies such as live cells and organisms (Sedlmeier and Gorris 2015).

30.4 Advantages of UCNPs for Biological Applications

The field of Ln^{3+} -based UCNPs focused on the synthesis and spectroscopic characterization of these nanomaterials in the past. Now, the area experiences a transition from simple optical probes to more complex multifunctional systems. Consequently, current research efforts focus on nanoplatforms not only suitable for optical imaging but also providing additional functional features. These include the application of Ln^{3+} -based UCNPs as (i) temperature sensors and heaters for potential applications in photothermal therapy (PTT) and as (ii) photochemical agents targeting photodynamic therapies (PDTs) (Wang et al. 2010; Idris et al. 2012; Hemmer et al. 2017; Zhou et al. 2012; Tessitore et al. 2019; Tajon et al. 2018).

When biological tissue is irradiated with light, photon absorption and scattering attenuate the signal proportionally with the tissue depth. Biomolecules and water induce these attenuation effects. This kind of attenuation is especially severe in the visible region (400–750 nm). As a result, the visible imaging region's penetration depth is limited to 1–3 mm. To overcome this deficiency, considerable effort has been made to develop and implement imaging agents within the "biological transparency window" or the NIR window (NIR-I; 750–950 nm). The tissue optical penetration depth is determined by the absorption and scattering of the excitation and emission light. Bashkatov et al. proposed an equation (Eq. 30.2) to calculate this value (Zhang 2015; Bashkatov et al. 2005).

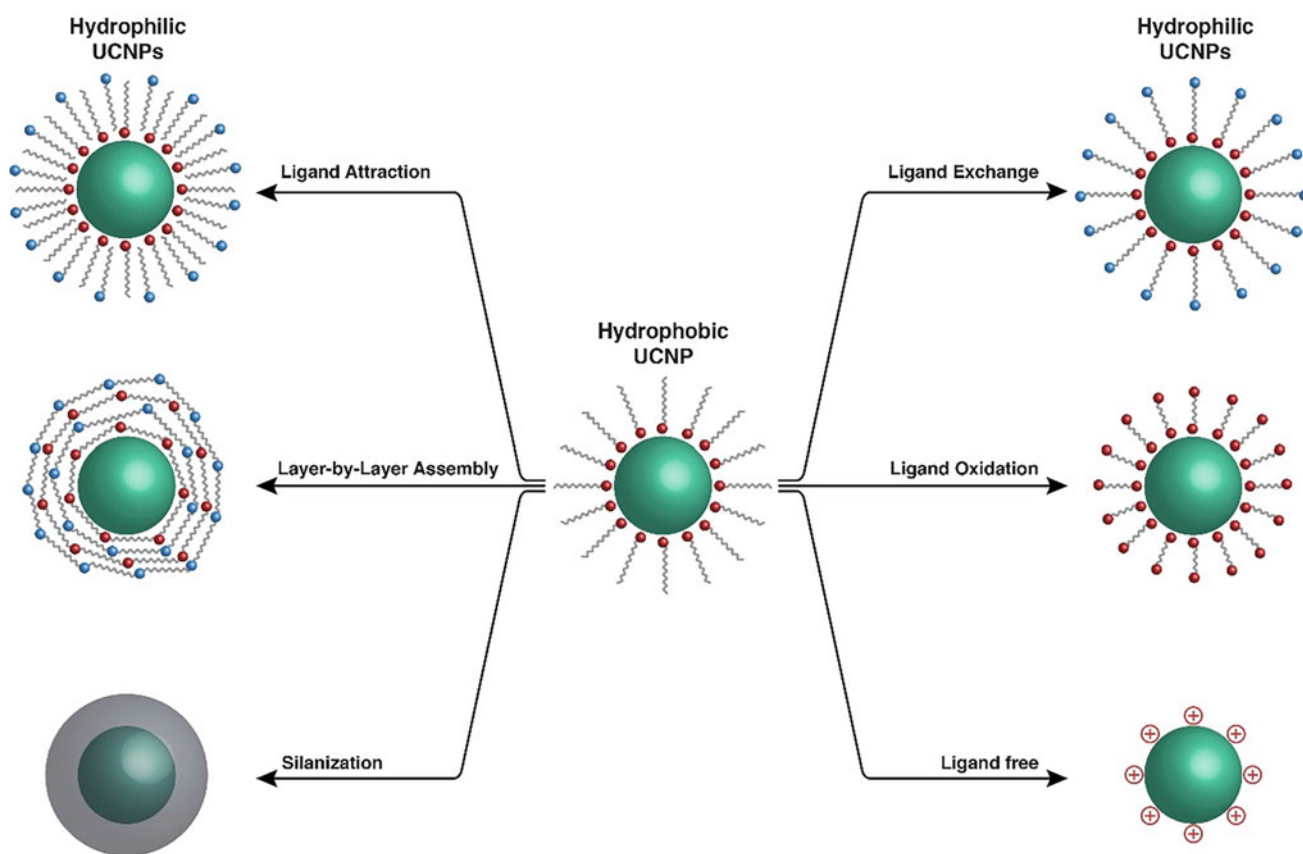


Fig. 30.5 Surface modification of hydrophobic UCNPs to hydrophilic UCNPs by ligand exchange, ligand oxidation, ligand removal (ligand-free), silanization, layer-by-layer assembly, and ligand attraction. (Sedlmeier and Gorris 2015)

$$\delta = (3\mu_a(\mu_a + \mu'_s))^{-1/2} \quad (30.2)$$

The optical absorption extinction coefficient is μ_a , which depends on the wavelength, μ'_s ($\sim \lambda^{-w}$) is the reduced scattering coefficient, and δ is the resulting penetration depth. The exponent (w) is intrinsic to tissue scatterers' size and concentration (from 0.22 to 1.68). We know that in most cases, water absorption and tissue scattering are higher in the visible range than in the NIR range, demonstrating the superiority of NIR light in this case. Since the 1990s, NIR biomedical imaging has obtained extensive attention because of its deeper penetration into biological tissue than visible light (Zhang 2015; Bashkatov et al. 2005).

Ln^{3+} -based UCNPs can efficiently absorb and convert NIR light to visible/UV/NIR light through an upconversion process, leading to many unique advantages for optical imaging and bioassay, such as low background auto-fluorescence, deep light penetration depth, and minimal photodamage in living organisms. Thus, UCNPs are interesting for bioapplications since they provide high sensitivity and spatial

resolution. Second, the above-mentioned optical properties of biological tissue demonstrate that the most critical obstacle to optical imaging is the limited penetration depth, which is not a problem in this case. UCNPs have moved into the spotlight as efficient materials for constructing multifunctional nanoprobe (Wang et al. 2010; Idris et al. 2012; Hemmer et al. 2017; Zhou et al. 2012; Tessitore et al. 2019; Zhang 2015; Tajon et al. 2018).

Traditional organic dyes, such as fluorescent dyes or proteins, and quantum dots, demonstrate many useful features. On the other hand, the luminescence mechanisms of these molecules and materials are based on energy downshifting that has to be excited in general by UV radiation, which is potentially harmful and carcinogenic, or blue/green visible radiation (Fig. 30.6) (Gnach and Bednarkiewicz 2012). As is widely known, the strong tissue scattering and biomolecule absorption of these short-wavelength excitation light limit the light penetration depth. Possible photodamage of biomolecules or cell death may also be induced by long-term exposure to relatively high-energy photons. Under UV-Vis photoexcitation, most endogenous biocomponents, such as flavins, porphyrins, NADH, and FAD^+ , exhibit auto-fluorescence, which decrease the signal-to-noise detection

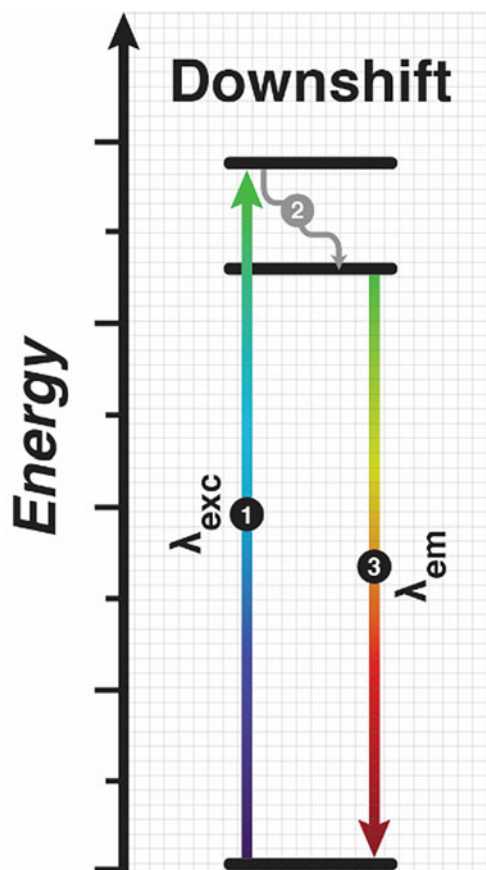


Fig. 30.6 Mechanism of downshift photon luminescence conversion process

ratio. Due to their nature, different fluorescent organic molecules show broad absorption and emission bands with low Stokes shifts, which overlap between each other and with biomolecules. This feature makes them not very suitable for multiplexed bio-labeling. Therefore, complicated spectral deconvolution methods need to be applied. Moreover, organic dyes exhibit short detection times and high photobleaching rates. Their quantum yield and spectral properties may also be affected by local chemical environments, making them difficult to analyze (Wang et al. 2010; Liu et al. 2013).

Quantum dots possess relatively narrow size-tunable emission, bright photoluminescence, good photostability, broad UV excitation, and relatively narrow emission bands. However, quantum dots are restrained because of their toxicity and chemical instability (Hardman 2006; Auffan et al. 2009). Therefore, UCNPs are a promising alternative to traditional fluorophores and quantum dots. The advantageous properties of UCNPs, such as nontoxicity, photostability, and chemical stability, complement the ability of lanthanide ions to efficiently upconvert NIR radiation into shorter wavelengths. It must also be pointed out that, compared

with dyes and quantum dots, UCNPs demonstrate sufficiently large Stokes shift in order to photoexcite and detect its luminescence selectively. Also, they are resistant to photobleaching or biochemical degradation, allowing prolonged luminescence detection *in vivo*. The different doping compositions in UCNPs enable the generation of various spectral profiles that can distinguish between them in a single sample for multiplexing detection. Lastly, the availability of bio-functionalization and bio-conjugation on the UCNP surface also adds to the superiority of UCNPs being used in biosensing (Fig. 30.7) (Wang et al. 2010; Zhou et al. 2012, 2015; Zhang 2015; Heer et al. 2004).

30.5 Singlet Oxygen Generation by Energy Transfer from UCNPs to Photosensitizers

By the basic concepts and principles of energy transfer mentioned below (Sects. 30.5.1 and 30.5.2), it is possible to engineer UCNPs as a source of singlet oxygen. Usually, the energy transfer from an excited energy donor to the acceptor may occur by radiative or nonradiative processes. The radiative energy transfer involves emission of photons from the donor and the subsequent absorption of photons by the acceptor. On the other hand, the nonradiative energy transfer occurs by the energy transfers through coulombic interactions with simultaneous donor's deactivation and the acceptor's excitation without the emission and re-absorption of photons. This mechanism is described by relative long distance (ca. 10 to 100 Å) between the donor and acceptor, such as the case of core-shell UCNPs and molecules around their surface, compared to the mechanisms to generate the upconversion where the lanthanide ions are close to each other (< 10 Å). As a result, nonradiative energy transfer is also termed resonance energy transfer. This mechanism indicates that the energy is transferred due to the resonance between the donor and the acceptor (Chen et al. 2018; Blasse and Grabmaier 1994).

30.5.1 Förster Resonance Energy Transfer and UCNPs

Since Theodor Förster formulated the theoretical description of nonradiative energy transfer between organic fluorophores in 1948, Förster resonance energy transfer (FRET) has become an essential method for biological studies (Förster 1948). FRET can be used to study a variety of biomolecular interactions by labeling biological species with optical probes. FRET-based assays are able to transduce a near-field interaction into a far-field signal by emitting light, which can be captured by a sensor to assess biological phenomena far below the resolution limit of standard optical

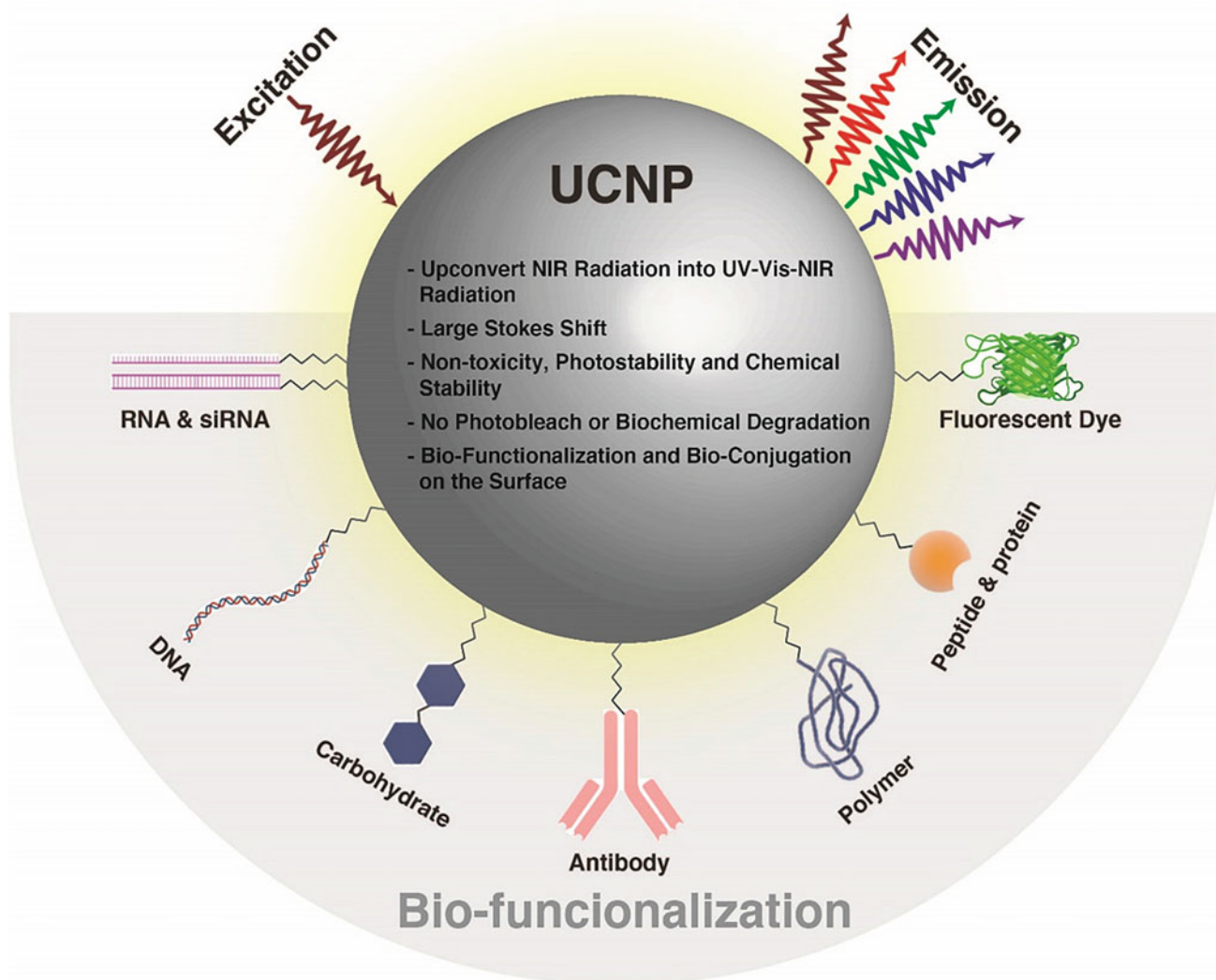


Fig. 30.7 Advantages of UCNPs as luminescent probes and illustration of bio-functionalization or bio-conjugation with RNA, siRNA, DNA, carbohydrate, antibody, polymer, peptide, protein, and fluorescent dye

microscopy. So, FRET is a spectroscopic phenomenon able to detect ionic/molecular interactions to structural changes of proteins or nucleic acids (Fig. 30.8). For example, FRET-based biosensors have been used in monitoring cellular physiology and detecting molecular dynamics. When combined with other techniques (e.g., electrochemistry), these sensors can achieve more variety of applications (Chen et al. 2018).

In a typical FRET process of two fluorophore pairs, not only the fluorophore donor's emission directly excited by an external source can be detected. The emission light from the fluorophore acceptor will also be observed. The occurrence of FRET is not simple, and it needs to satisfy two criteria between the pair of optical materials: (1) there is appreciable spectral overlap between the emission spectrum of the donor

and the absorption spectrum of the acceptor and (2) the materials are close of each other, less than a critical distance (Förster distance, R_0) that is determined by the optical characteristics of the donor-acceptor pair. The FRET efficiency (E_{FRET}) is strongly dependent on these two criteria. The spectral overlap is measured by the overlap integral $J(\lambda)$ in Eq. (30.3):

$$J(\lambda) = \frac{\int F(\lambda) \varepsilon(\lambda) \lambda^4 d\lambda}{\int F(\lambda) d\lambda} \quad (30.3)$$

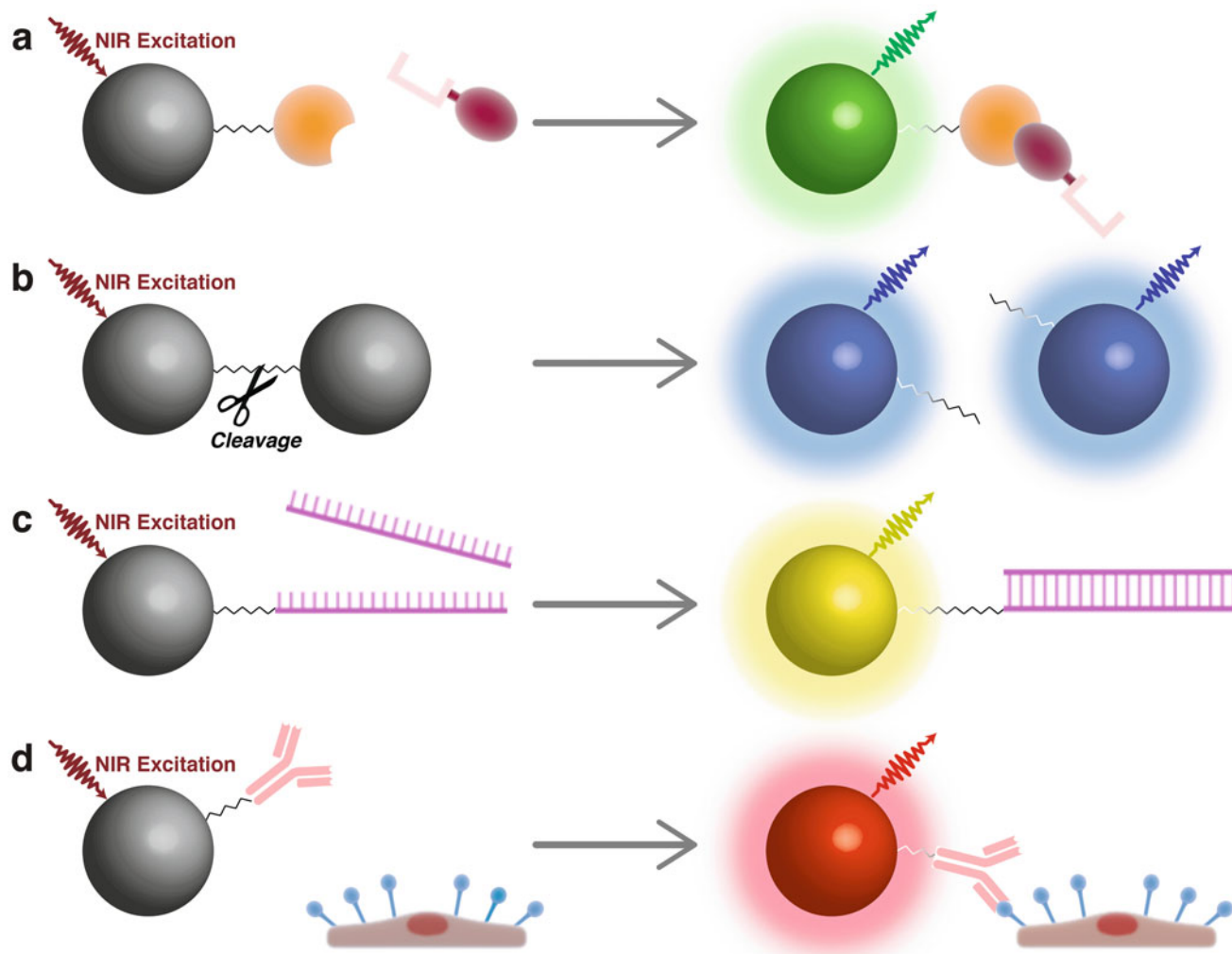


Fig. 30.8 FRET-based biosensors integrated with UCNP for (a) protein conjugation, (b) bond cleavage, (c) DNA double strain formation, and (d) antibody interaction

where $F(\lambda)$ is the emission intensity of the donor at wavelength λ , and $\varepsilon(\lambda)$ is the absorption coefficient of the acceptor. For an efficient FRET, the donor fluorophore emission and the acceptor fluorophore excitation have to overlap by at least 30%. E_{FRET} varies as the sixth power of the distance between the donor–acceptor pair (R), and Eq. 30.4 elucidates the relationship between E_{FRET} and the distance R :

$$E_{\text{FRET}} = \frac{1}{1 + \left(\frac{R}{R_0}\right)^6} \quad (30.4)$$

where R_0 is the Förster radius or the distance between the donor and acceptor at which $E = 50\%$. R_0 is a constant for a given combination of the donor–acceptor pair and is

calculated by Eq. 30.5 (Chen et al. 2018; Förster 1948; Patterson et al. 2000):

$$R_0^6 = \frac{9}{4(2\pi)^5} \frac{2303}{N_A} k^2 \varphi_D n^{-4} J(\lambda) \quad (30.5)$$

where N_A is Avogadro's constant, n is the average refractive index of the medium, φ_D is the quantum yield of the donor material without the acceptor material, and k^2 is the orientation factor of the transition dipoles. Thus, for an efficient FRET to proceed, the donor–acceptor distance should meet $R \leq R_0$. FRET-based sensors monitor FRET efficiencies by detecting the emission characteristics (e.g., intensity and lifetime) of energy donors and acceptors that serve as optical probes (Chen et al. 2018; Förster 1948).

The development of UCNPs as optical probes in recent years has greatly enhanced the capability of FRET techniques. Compared with conventional organic luminescent probes, UCNPs have better photostability, larger Stokes shift, and narrow and tunable emission bands controlled by the dopant composition. These nanomaterials combined with organic dyes can form efficient FRET pairs with modulated excitation and emission spectra as well as energy transfer characteristics (Wang et al. 2010; Liu et al. 2013; Idris et al. 2012; Zhou et al. 2012; Zhang 2015; Chen et al. 2018; Sedlmeier and Gorris 2015; Neto et al. 2019).

30.5.2 UCNPs Photosensitizers

One of the most common acceptors in FRET from UCNPs is photosensitizers (PSs). After the energy transfer, the light absorbed by the PSs generates a short-lived excited singlet state (S_1) from the ground state (S_0) and subsequently to a relatively long-lived excited triplet state (T_1) by intersystem crossing (Fig. 30.9). Alternatively, the excited PS molecule can return to the S_0 state by a radiative process emitting the absorbed energy as fluorescence or by a nonradiative pathway (internal conversion). From T_1 excited state, the PS can also present the energy decay to S_0 ground state, leading to the phosphorescence phenomenon or by a non-radiative process (intersystem crossing). The resulting fluorescence and phosphorescence phenomena may be used to track PS localization in the biological system. In the second step, the sufficiently long-lived T_1 state can react in two ways to generate reactive oxygen species (ROS), defined as type I and type II mechanisms. The PS can undergo electron (or hydrogen) transfer reactions with a biological substrate, such as the cell membrane, molecule oxygen, or another sensitizer, to form radicals and radical ions. These reactive radical species can further interact with oxygen to produce ROS such as superoxide anion radical ($O_2^{\cdot -}$), hydrogen peroxide (H_2O_2), and hydroxyl radical ($OH \cdot$) by type I mechanism (Nonell and Flors 2016; Di Mascio et al. 2019; Zhang 2015; Wang et al. 2011b; Liu et al. 2012; Thanasekaran et al. 2019).

Type II mechanism involves the energy transfer from the excited state of the sensitizer to the ground-state oxygen $O_2(\sum_g^-)$, generating the first excited state of the molecular oxygen, singlet oxygen $O_2(\Delta_g)$. Meanwhile, the second excited singlet state of molecular oxygen, $O_2(\sum_g^+)$, can also be formed in competition with $O_2(\Delta_g)$ and rapidly deactivated to the relatively long-lived $O_2(\Delta_g)$ species in solution (Nonell and Flors 2016; Di Mascio et al. 2019). The first excited state $O_2(\Delta_g)$ has an energy of 94 kJ mol⁻¹ above the ground state $O_2(\sum_g^-)$, thus requiring that PSs have excited state energy higher than 94 kJ mol⁻¹. The singlet oxygen has a lifetime of ~3 μs in the biological environment, corresponding to a short diffusion distance of ~100 nm (Hatz

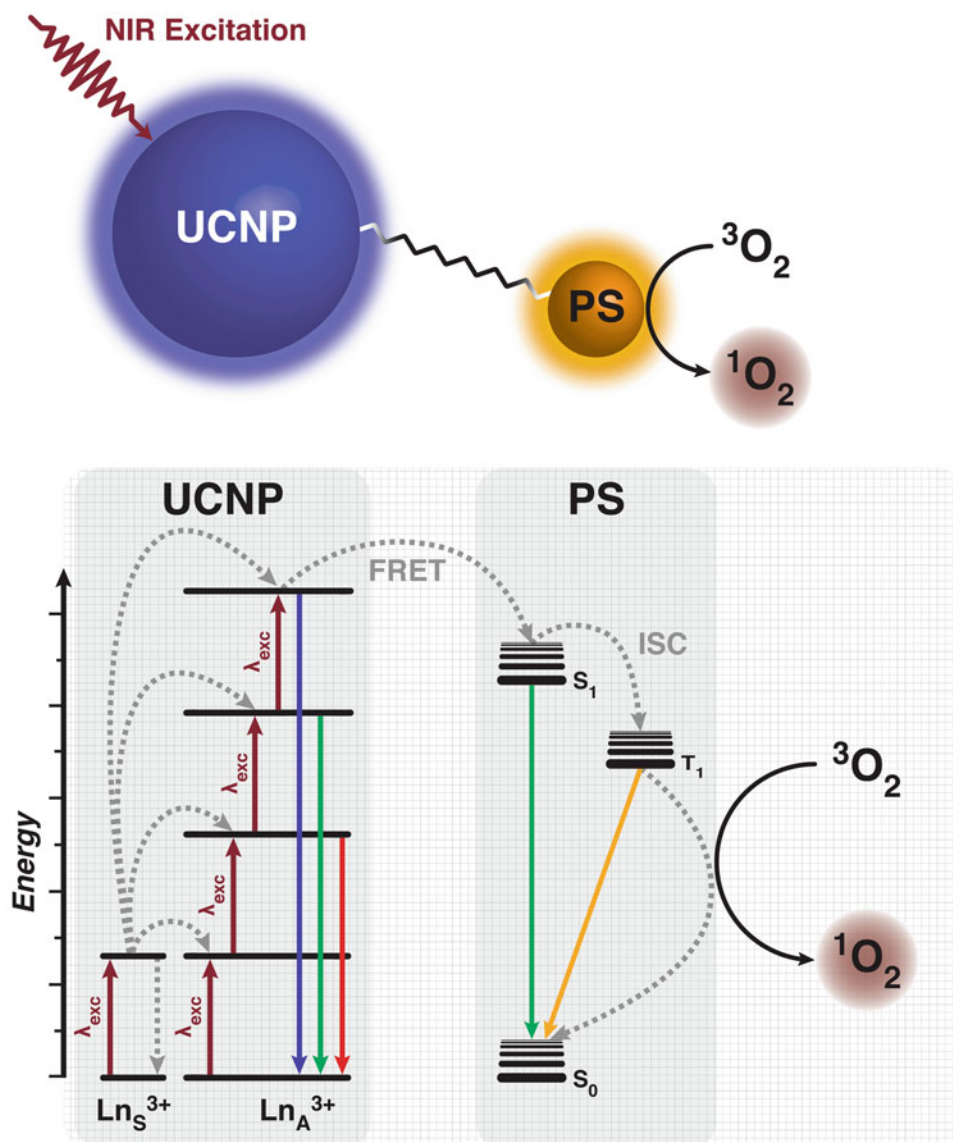
et al. 2008). Therefore, the oxidative damage resulting from 1O_2 is limited to sites of PS localization. Notably, PSs should act catalytically as they can return to the ground state ($^1PS \rightarrow ^1PS^* \rightarrow ^3PS^* + ^3O_2 \rightarrow ^1PS + ^1O_2$). Both type I and type II mechanisms occur simultaneously, and the type II mechanism is generally considered dominant in most cases. Type I mechanism becomes more critical at low oxygen and high substrate concentrations (Nonell and Flors 2016; Di Mascio et al. 2019).

An ideal PS should be a single substance with known and constant composition and a high degree of chemical purity and stability as well as nontoxic without light irradiation and relatively rapid clearance from healthy tissues, thereby minimizing side effects. A high photochemical reactivity, with a high triplet-state yield and long triplet-state lifetime, is also needed to generate in this case singlet oxygen efficiently. The pair UCNP-PS is ideal in this case due to the low UCNP toxicity, low phototoxicity of the NIR excitation, a high lifetime of Ln^{3+} , tunable UCNP emission in UV-Visible-NIR changing the Ln^{3+} composition, UCNP surface capable to link PSs, and FRET efficiency capable to indicate the PS bleaching during the application (Fig. 30.9). The structural optimization of an UCNP sensitizer for singlet oxygen generation is a challenging task; however, researchers have been making efforts to synthesize an ideal structure in this sense.

In order to realize their full potential in NIR-induced singlet oxygen source, high-quality UCNPs should be fabricated with high phase purity, uniform morphology, and good dispersibility. It is noteworthy that hexagonal-phase $NaYF_4$ is the most popular host matrix in UCNP-based singlet oxygen source. $NaYF_4$ has been reported as the most efficient NIR-to-UV-visible-NIR upconversion host so far. Also, the upconversion efficiency of hexagonal-phase nanocrystals is much higher than that of cubic-phase nanocrystals. Optimal amounts of photosensitizers and/or targeting moieties should be attached to hydrophilic UCNPs by either noncovalent interactions or covalent conjugation (Zhang 2015; Heer et al. 2004; Tajon et al. 2018; Tian et al. 2018).

In general, current UCNP-based singlet oxygen source designs can be divided into five types by PS-loading approaches: (i) photosensitizers are encapsulated into silica shell coated onto the surface of UCNPs; (ii) photosensitizers are deposited in pores of mesoporous silica shell via physical adsorption or covalent conjugation; (iii) photosensitizers are loaded into “hydrophobic pocket” on the UCNP surface, which is formed by noncovalent interactions between the hydrophobic segments of polymers and UCNP surface ligands, e.g., oleic acid; (iv) photosensitizers are covalently bonded to UCNPs capped with amino-/carboxyl-functionalized capping agents; and (v) photosensitizers are directly attached to the positively charged surface of UCNPs or loaded onto porous UCNPs via noncovalent interactions

Fig. 30.9 Illustration and schematic energy-level diagram showing singlet oxygen ($^1\text{O}_2$) formation by upconversion luminescence in a UCNP and FRET energy transfer to a photosensitizer (PS). *ISC* intersystem crossing, Ln_S^{3+} sensitizer lanthanide, Ln_A^{3+} activator lanthanide



without an interlayer between UCNPs and the loaded photosensitizers. Up to now, the most efficient PS loading is the molecules covalently bonded to capping agents or coordinated to UCNP surface. The covalent bond is important to avoid the leaching of the photosensitizers. The UCNP most commonly used in the literature are the Yb^{3+} , Er^{3+} -doped nanoparticles due to the high intensity of the upconversion process. On the other hand, it is possible to find a range of photosensitizers used to generate singlet oxygen molecules, such as rose bengal (RB), methylene blue (MB), phthalocyanine (ZnPc), Chlorin e6 (Ce6), cyanine (Cy5), and doxorubicin (DOX) (Zhang 2015; Wang et al. 2011b, 2016; Liu et al. 2012; Gnanasammandhan et al. 2016; Li et al. 2016; Ai et al. 2016).

30.6 New Approaches Based on UCNP Photosensitizers for Singlet Oxygen Generation

The design of UCNP core–shell structure is essential for an efficient singlet oxygen source. The design of layers containing the sensitizer and activator ions plays an important role where they needed to be optimized to generate an efficient upconversion as well as FRET to the photosensitizers. Wang et al. (2015) prepared $\text{NaYF}_4:\text{Yb}^{3+}$, $\text{Ho}^{3+}@\text{NaYF}_4:\text{Nd}^{3+}@\text{NaYF}_4$ capping with polymer covalently bonded with rose bengal. The authors observed that 1.5 nm was the optimal layer thickness of $\text{NaYF}_4:\text{Nd}^{3+}$ containing 20% of

dopant. In addition, the passive layer presents an important role in the FRET process. This layer can be modulated to create an optimum distance between the activator-sensitizer in FRET as well as decrease nonradiative processes by vibrational modules in NP surface (Tajon et al. 2018).

The structure UCNP-PS can generate a variety of ROS molecules, such as $^1\text{O}_2$, H_2O_2 , superoxide anion radical ($\text{O}_2^- \cdot$), and hydroxyl radical ($\text{OH} \cdot$). The selective detection of singlet oxygen can be performed by molecular capture. This methodology is based on the oxidation of a molecule by the singlet oxygen. The molecular probe used in this reaction needs to attend to some specifications such as water solubility and $^1\text{O}_2$ specificity. The oxidizing process cannot compete with other reactions, and the reaction products need to be stable, unique, and easily detectable in small quantities. Currently, researchers have used, e.g., 9,10-dimethylanthracene, 1,3-diphenylisobenzofuran, p-nitroso-dimethylaniline, and 9,10-anthracenediyl-bis(methylene)dimalonic acid for singlet oxygen detection (Wang et al. 2011b, 2015, 2016; Liu et al. 2012, 2019; Thanasekaran et al. 2019; Gnanasammandhan et al. 2016; Li et al. 2016).

It is difficult to obtain a singlet oxygen probe applicable in vivo covering all the required characteristics. This fact discourages the use of the molecular capture method. Browne and Ogryzlo discovered a $^1\text{O}_2$ emission at approximately 1270 nm generated by the singlet oxygen decay to the triplet state. The $^1\text{O}_2$ monomolecular emission can be detected by a spectrofluorometer with a germanium photodetector and the concentration is determined by luminescence intensity. The $^1\text{O}_2$ spectroscopic methodology became a simple and direct way to detect and quantify this molecule (Browne and Ogryzlo 1964).

The scientific community has developed theranostic devices that can be the future of nanomedicine based on singlet oxygen generation by UCNP-PS (Tajon et al. 2018; Li et al. 2016; Wang et al. 2015, 2016; Ai et al. 2016; Liu et al. 2019; Browne and Ogryzlo 1964; Mi et al. 2019). These complex systems can be applied in photodynamic therapies (PDT), for example. Wang et al. (2016) prepared a UCNP-PS with the β -cyclodextrin linked in mesoporous silica surface. The NIR radiation is able to produce singlet oxygen by photoexcitation of rose bengal and release β -cyclodextrin at the same time. The β -cyclodextrin acts as a drug delivery molecule able to release biologically active compounds under specific conditions. Most of UCNP-PS devices are designed to generate singlet oxygen and emit light at the same time. However, Mi et al. (2019) developed a UCNP-PS system based on the diarylethene conversion emitting upconversion by 980-nm excitation and upconversion with singlet oxygen release by dual excitation in 980 and 808 nm. This device allows to track the nanostructure and produce singlet oxygen controllably. Ai et al. (2016) synthesized a UCNP-PS

material generating $^1\text{O}_2$ in tumor-specific cathepsin protease. The cleavage of peptides induces covalent cross-linking between the exposed cysteine and 2-cyanobenzothiazole on neighboring particles. Enzyme-triggered cross-linking of UCNP-PS leads to enhanced upconversion emission under 808 nm amplifying the singlet oxygen generation from the photosensitizers attached on UCNPs.

30.7 Conclusion

Lanthanide-based nanoparticles showing the upconversion phenomenon (UCNPs) have the ability to convert low-energy photons to high-energy photons efficiently. This unusual property is providing a new approach for $^1\text{O}_2$ generation. UCNPs combined with photosensitizers (PS) are able to produce singlet oxygen molecules without competing with other harmful processes in living organisms. These features have indicated that $^1\text{O}_2$ is generated and can be triggered in tumor cells using specially designed UCNP-PS. The design optimization of these complex nanodevices, localized generation, and direct quantification of $^1\text{O}_2$ as well as nanomaterials delivery in subcellular compartments are topics to be assessed in the future to establish these nanosystems as a wide applicable technology. However, the current approaches presented by the scientific community are demonstrating the potential of UCNP-PS nanodevices, such as in photodynamic therapies.

Acknowledgments We thank FAPESP (Fundação de Amparo à Pesquisa do Estado de São Paulo) – C.C.S.P. No. 2017/09774-0 and No. 2018/15011-1, P.D.M. No. 2012/12663-1, S.M. No. 2013/07937-8, A.A.F. No. 2019/17363-5, H.F.B.; CEPID Redoxoma – C.C.S.P., P.D.M., S.M., A.A.F.; CNPq (Conselho Nacional de Desenvolvimento Científico e Tecnológico) – P.D.M. No. 2021/08111-2 Temático FAPESP, H.F.B., P.D.M.; No. 302120/2018-1, H.F.B.; PRPUSP (Pro-Reitoria de Pesquisa da Universidade de São Paulo) – NAP Redoxoma – P.D.M. No. 2011.1.9352.1.8; and John Simon Guggenheim Memorial Foundation (P.D.M. Fellowship) for financial support.

References

- Ai, X.; Ho, C.J.; Aw, J.; Attia, A.B.; Mu, J.; Wang, Y.; Wang, X.; Wang, Y.; Liu, X.; Chen, H.; Gao, M.; Chen, X.; Yeow, E.K.; Liu, G.; Olivo, M.; Xing, B. (2016) In vivo covalent cross-linking of photon-converted rare-earth nanostructures for tumour localization and theranostics. *Nat. Commun.* 7:10432.
- Auffan, M.; Rose, J.; Bottero, J.Y.; Lowry, G.V.; Jolivet, J.P.; Wiesner, M.R. (2009) Towards a definition of inorganic nanoparticles from an environmental, health and safety perspective. *Nat. Nanotechnol.* 4(10):634–641.
- Auzel, F. (2004) Upconversion and anti-Stokes processes with f and d ions in solids. *Chem. Rev.* 104(1):139–73.
- Bashkatov, A.N.; Genina, E.A.; Kochubey, V.I.; Tuchin, V.V. (2005) Optical properties of human skin, subcutaneous and mucous tissues

- in the wavelength range from 400 to 2000 nm. *J. Phys. D: Appl. Phys.* 38(15):2543–2555.
- Blasse, G.; Grabmaier, B.C. (1994) *Luminescent Materials*. Springer-Verlag, Berlin.
- Bloembergen, N. (1959) Solid state infrared quantum counters. *Phys. Rev. Lett.* 2:84–85.
- Browne, R.J.; Ogryzlo, E.A. (1964) Chemiluminescence from the Reaction of Chlorine with Aqueous Hydrogen Peroxide. *Proc. Chem. Soc.* 4:117.
- Castano, A.P.; Mroz, P.; Hamblin, M.R. (2006) Photodynamic therapy and anti-tumour immunity. *Nat. Rev. Cancer* 6(7):535–545.
- Chen, B.; Wang, F. (2020) Combating Concentration Quenching in Upconversion Nanoparticles. *Acc. Chem. Res.* 53(2):358–367.
- Chen, X.; Liu, Y.; Tu, D. (2014) *Lanthanide-doped luminescent nanomaterials: from fundamentals to bioapplications*. Springer-Verlag, Berlin.
- Chen, B.; Su, Q.; Kong, W.; Wang, Y.; Shi, P.; Wang, F. (2018) Energy transfer-based biodetection using optical nanomaterials. *J. Mater. Chem. B* 6(19):2924–2944.
- Cotton, S. (2006) *Lanthanide and actinide chemistry*. John Wiley & Sons, West Sussex.
- da Silva, J.F.; da Silva, R.F.; Santos, E.P.; Maia, L.J.Q.; Moura, A.L. (2020) Photon-avalanche-like upconversion in NdAl₃(BO₃)₄ nanoparticles excited at 1064 nm. *Appl. Phys. Lett.* 117(15):151102 (1–6).
- Di Mascio, P.; Martinez, G.R.; Miyamoto, S.; Rosein, G.E.; Medeiros, M.H.G.; Cadet, J. (2019) Singlet Molecular Oxygen Reactions with Nucleic Acids, Lipids, and Proteins. *Chem. Rev.* 119(3):2043–2086.
- Förster, T. (1948) Zwischenmolekulare Energiewanderung und Fluoreszenz. *Ann. Phys.* 2:55–75.
- Gnach, A.; Bednarkiewicz, A. (2012) Lanthanide-doped up-converting nanoparticles: Merits and challenges. *Nanotoday* 7(6):532–563.
- Gnanasamandhan, M.K.; Idris, N.M.; Bansal, A.; Huang, K.; Zhang, Y. (2016) Near-IR photoactivation using mesoporous silica-coated NaYF₄:Yb, Er/Tm upconversion nanoparticles. *Nat. Protoc.* 11(4): 688–713.
- Halliwell, B. (2006) Oxidative stress and neurodegeneration: where are we now? *J. Neurochem.* 97(6):1634–1658.
- Hardman, R. (2006) A toxicologic review of quantum dots: toxicity depends on physicochemical and environmental factors. *Environ. Health Perspect.* 114(2):165–172.
- S. Hatz; L. Poulsen; P.R. Ogilby (2008) Time-resolved Singlet Oxygen Phosphorescence Measurements from Photosensitized Experiments in Single Cells: Effects of Oxygen Diffusion and Oxygen Concentration. *Photochem. Photobiol.* 84(5):1284–1290.
- Heer, S.; Kömpe, K.; Güdel, H.-U.; Haase, M. (2004) Highly efficient multicolour upconversion emission in transparent colloids of lanthanide-doped NaYF₄ nanocrystals. *Adv. Mater.* 16(23–24): 2102–2105.
- Hemmer, E.; Benayas, A.; Légaré, F.; Vetrone, F. (2016) Exploiting the biological windows: current perspectives on fluorescent bioprobes emitting above 1000 nm. *Nanoscale Horiz.* 1(3): 168–184.
- Hemmer, E.; Acosta-Mora, P.; Méndez-Ramos, J.; Fisher, S. (2017) Optical nanoprobe for biomedical applications: shining a light on upconverting and near-infrared emitting nanoparticles for imaging, thermal sensing, and photodynamic therapy. *J. Mater. Chem. B* 5(23):4365–4392.
- Idris, N.M.; Gnanasamandhan, M.K.; Zhang, J.; Ho, P.C.; Mahendran, R.; Zhang, Y. (2012) In vivo photodynamic therapy using upconversion nanoparticles as remote-controlled nanotransducers. *Nat. Med.* 18(10):1580–1585.
- Johnson, N.J.; Korinek, A.; Dong, C.; Van Veggel, F.C. (2012) Self-focusing by Ostwald ripening: a strategy for layer-by-layer epitaxial growth on upconverting nanocrystals. *J. Am. Chem. Soc.* 134(27): 11068–11071.
- Lahoz, F.; Martín, I.R.; Alonso, D. (2005) Theoretical analysis of the photon avalanche dynamics in Ho³⁺-Yb³⁺ codoped systems under near-infrared excitation. *Phys. Rev. B* 71:045115.
- Lee, C.; Xu, E.Z.; Liu, Y.; Teitelboim, A.; Yao, K.; Fernandez-Bravo, A.; Kotulska, A.M.; Nam, S.H.; Suh, Y.D.; Bednarkiewicz, A.; Cohen, B.E.; Chan, E.M.; Schuck, P.J. (2021) Giant nonlinear optical responses from photon-avalanching nanoparticles. *Nature* 589: 230–235.
- Li, Y.; Tang, J.; Pan, D.X.; Sun, L.D.; Chen, C.; Liu, Y.; Wang, Y.F.; Shi, S.; Yan, C.H. (2016) A Versatile Imaging and Therapeutic Platform Based on Dual-Band Luminescent Lanthanide Nanoparticles toward Tumor Metastasis Inhibition. *ACS Nano* 10(2):2766–2773.
- Liou, G.-Y.; Storz, P. (2010) Reactive oxygen species in cancer. *Free Radic. Res.* 44(5):479–496.
- Liu, K.; Liu, X.; Zeng, Q.; Zhang, Y.; Tu, L.; Liu, T.; Kong, X.; Wang, Y.; Cao, F.; Lambrechts, S.A.; Aalders, M.C.G.; Zhang, H. (2012) Covalently Assembled NIR Nanoplatform for Simultaneous Fluorescence Imaging and Photodynamic Therapy of Cancer Cells. *ACS Nano* 6(5):4054–4062.
- Liu, Y.; Tu, D.; Zhu, H.; Ma, E.; Chen, X. (2013) Lanthanide-doped luminescent nano-bioprobes: from fundamentals to biodetection. *Nanoscale* 5(4):1369–1384.
- Liu, S.; Li, W.; Dong, S.; Gai, S.; Dong, Y.; Yang, D.; Dai, Y.; He, F.; Yang, P. (2019) Degradable Calcium Phosphate-Coated Upconversion Nanoparticles for Highly Efficient Chemo-Photodynamic Therapy. *ACS Appl. Mater. Interfaces* 11(51): 47659–47670.
- Mi, Y.; Cheng, H.-B.; Chu, H.; Zhao, J.; Yu, M.; Gu, Z.; Zhao, Y.; Li, L. (2019) A photochromic upconversion nanoarchitecture: towards activatable bioimaging and dual NIR light-programmed singlet oxygen generation. *Chem. Sci.* 10(44):10231–10239.
- Nathan, C.; Ding, A. (2010) SnapShot: Reactive Oxygen Intermediates (ROI). *Cell* 140(6):951–951.e2.
- Neto, A.N.C.; Teotonio, E.E.S.; de Sá, G.F.; Brito, H.F.; Legendziewicz, J.; Carlos, L.D.; Felinto, M.C.F.C.; Gawryszewska, P.; Moura Jr., R.T.; Longo, R.L.; Faustino, W.M.; Malta, O.L. (2019) Modeling intramolecular energy transfer in lanthanide chelates: A critical review and recent advances (Chapter 310). In Bünzli, J.-C.G.; Pecharsky, V.K. (ed) *Handbook on the Physics and Chemistry of Rare Earths, Volume 56* Elsevier, Amsterdam, p 55–162.
- Nonell, S.; Flors, C. (2016) *Singlet Oxygen: Applications in Biosciences and Nanosciences Volume 1*. The Royal Society of Chemistry, Cambridge.
- Patterson, G.H.; Piston, D.W.; Barisas, B.G. (2000) Förster Distances between Green Fluorescent Protein Pairs. *Anal. Biochem.* 284(2): 438–440.
- Sedlmeier, A.; Gorris, H.H. (2015) Surface modification and characterization of photon-upconverting nanoparticles for bioanalytical applications. *Chem. Soc. Rev.* 44(6):1526–1560.
- Suter II, J.D.; Pekas, N.J.; Berry, M.T.; Stanley May, P. (2014) Real-Time-Monitoring of the Synthesis of β-NaYF₄:17% Yb,3% Er Nanocrystals Using NIR-to-Visible Upconversion Luminescence. *J. Phys. Chem. C* 118(24):13238–13247.
- Tajon, C.A.; Yang, H.; Tian, B.; Tian, Y.; Ercius, P.; Schuck, P.J.; Chan, E.M.; Cohen, B.E. (2018) Photostable and efficient upconverting nanocrystal-based chemical sensors. *Opt. Mater.* 84:345–353.
- Tessitore, G.; Mandl, G.A.; Brik, M.G.; Park, W.; Capobianco, J.A. (2019) Recent insights into upconverting nanoparticles: spectroscopy, modeling, and routes to improved luminescence. *Nanoscale* 11(25):12015–12029.
- Thanasekaran, P.; Chu, C.H.; Wang, S.B.; Chen, K.Y.; Gao, H.D.; Lee, M.M.; Sun, S.S.; Li, J.P.; Chen, J.Y.; Chen, J.K.; Chang, Y.H.; Lee, H.M. (2019) Lipid-Wrapped Upconversion Nanoconstruct/

- Photosensitizer Complex for Near-Infrared Light-Mediated Photodynamic Therapy. *ACS Appl. Mater. Interfaces* 11(1):84–95.
- Tian, B.; Fernandez-Bravo, A.; Najafiaghdam, H.; Torquato, N.A.; Altoe, M.V.P.; Teitelboim, A.; Tajon, C.A.; Tian, Y.; Borys, N.J.; Barnard, E.S.; Anwar, M.; Chan, E.M.; Schuck, P.J.; Cohen, B.E. (2018) Low irradiance multiphoton imaging with alloyed lanthanide nanocrystals. *Nat. Commun.* 9(1):3082.
- Wang, F.; Banerjee, D.; Liu, Y.; Chen, X.; Liu, X. (2010) Upconversion nanoparticles in biological labeling, imaging, and therapy. *Analyst* 135(8):1839–1854.
- Wang, F.; Deng, R.; Wang, J.; Wang, Q.; Han, Y.; Zhu, H.; Chen, X.; Liu, X. (2011a) Tuning upconversion through energy migration in core-shell nanoparticles. *Nat. Mater.* 10(12):968–973.
- Wang, Y.; Liu, K.; Liu, X.; Dohnalová, K.; Gregorkiewicz, T.; Kong, X.; Aalders, M.C.G.; Buma, W.J.; Zhang, H. (2011b) Critical Shell Thickness of Core/Shell Upconversion Luminescence Nanoplatform for FRET Application. *J. Phys. Chem. Lett.* 2(17):2083–2088.
- Wang, D.; Xue, B.; Kong, X.; Tu, L.; Liu, X.; Zhang, Y.; Chang, Y.; Luo, Y.; Zhao, H.; Zhang, H. (2015) 808 nm driven Nd³⁺-sensitized upconversion nanostructures for photodynamic therapy and simultaneous fluorescence imaging. *Nanoscale* 7(1):190–197.
- Wang, H.; Han, R.L.; Yang, L.M.; Shi, J.H.; Liu, Z.J.; Hu, Y.; Wang, Y.; Liu, S.J.; Gan, Y. (2016) Design and Synthesis of Core–Shell–Shell Upconversion Nanoparticles for NIR-Induced Drug Release, Photodynamic Therapy, and Cell Imaging. *ACS Appl. Mater. Interfaces* 8(7):4416–4423.
- Wen, S.; Zhou, J.; Zheng, K.; Bednarkiewicz, A.; Liu, X.; Jin, D. (2018) Advances in highly doped upconversion nanoparticles. *Nat. Commun.* 9(1):2415.
- Winterbourn, C.C. (2008) Reconciling the chemistry and biology of reactive oxygen species. *Nat. Chem. Biol.* 4(5):278–286.
- Wisser, M.D.; Fischer, S.; Maurer, P.C.; Bronstein, N.D.; Chu, S.; Alivisatos, A.P.; Salteo, A.; Dionne, J.A. (2016) Enhancing Quantum Yield via Local Symmetry Distortion in Lanthanide-Based Upconverting Nanoparticles. *ACS Photonics* 3(8):1523–1530.
- Zhang, F. (2015) *Photon Upconversion Nanomaterials*. Springer-Verlag, Berlin.
- Zhou, J.; Liu, Z.; Li, F. (2012) Upconversion nanophosphors for small-animal imaging. *Chem. Soc. Rev.* 41(3):1323–1349.
- Zhou, B.; Shi, B.; Jin, D.; Liu, X. (2015) Controlling upconversion nanocrystals for emerging applications. *Nat. Nanotechnol.* 10(11):924–36.
- Zhou, J.; Wen, S.; Liao, J.; Clarke, C.; Tawfik, S.A.; Ren, W.; Mi, C.; Wang, F.; Jin, D. (2018) Activation of the surface dark-layer to enhance upconversion in a thermal field. *Nat. Photonics* 12:154–158.



Delayed Luminescence as a Tool to Study the Structures of Systems of Biological Interest and Their Collective Long-Living Excited States

31

Rosaria Grasso, Francesco Musumeci, Agata Scordino, and Antonio Triglia

31.1 Introduction

31.1.1 The Mechanistic Approach to the Study of Biological Systems

Modern science has represented the redemption of atomistic models in the description of reality. According to the mechanistic models, explicitly introduced and formalized from a mathematical point of view by Descartes, it is possible to study any system only through the analysis of its parts and the interactions between these parts. A repeated application of this method of analysis will lead to the study of interactions between indivisible parts. The knowledge of these interactions would allow, according to Laplace, to foresee the time trend of any system if one knows the positions and the impulses of its components at a given instant. As a matter of principle, a superior intelligence, able to collect and process an extremely large number of data, would be able to know the temporal evolution of the entire universe, starting from the knowledge of the positions and impulses of its parts at a given moment. This point of view, known as a mechanism, has been successful for centuries, favoring the development of classical physics and related sciences, including life sciences. Descartes, for example, considered animals as real machines, unable to feel sensations and pain. However, the mechanistic approach has received a serious blow precisely from researches and evidences developed in the physical field. Think of the partial solution of the three-bodies problem, at the basis of the theory of deterministic chaos and of the consequent theory of complex systems or to the development of quantum mechanics with its uncertainty principle. So, since the beginning of the twentieth century, Physics has emancipated itself from the mechanistic vision. Yet, mechanism continues to constitute the backbone of modern

biology, especially after the development, crowned by undoubted successes, of molecular biology. Moreover, the current mechanistic description of the functioning of living systems is heavily influenced by the organization of today's human society. Indeed, the single cell is often depicted as a modern factory in which proteins are described as complex molecular machines connected among themselves by intricate metastable circuits and coordinated through the execution of a genetically fixed deterministic program whose only degree of freedom is due to the presence of mutations induced by fortuitous interactions with the environment.¹ However, this kind of view of biological systems appears to be useful to develop a conventional description of some of the possible phenomena, but up to date, has not been able to describe most of the complex phenomenology that concerns even the simplest of living systems, despite the use of exceptionally powerful computing means. Here are some particularly significant examples.

31.1.2 Problems Unresolved by the Mechanistic Descriptions of Biological Systems

The first significant problem concerns the transmission of information and coordination of chemical species. Within a single cell, there is a continuous flow of chemical species and dynamically unstable structures that guarantee the survival of the cell itself within a generally hostile environment. The organization of these flows and structures depends on the knowledge of the state of the cell and of its environment and provides that different chemical species move within the cell in a way coordinated in time and space. To date how this process occurs is unclear, even in the case of elementary organisms. Another problem concerns

R. Grasso · F. Musumeci · A. Scordino (✉) · A. Triglia
Department of Physics and Astronomy "Ettore Majorana", University of Catania, Catania, Italy
e-mail: ascordin@dmfci.unict.it

¹This is a highly personalized view of the authors. Applying the notion of 'degrees of freedom' to self-organizing systems like genome, is quite contradictive in general, and in any case such a system can have several dynamic solutions (editor's note).

morphogenesis: it is not yet clear how the complicated topologies of biological systems develop and maintain.² In the early twentieth century, it was suggested that these processes were organized by a special kind of field called the morphogenetic field. This field would occupy both space and time in a dynamic way, influencing the cells included in it. The concept of morphogenetic field has been more recently abandoned, due to the identification of biochemical agents near the growth zones.³ However, up to now, even if, thanks to great strides made by molecular cell biology and genetics, a lot has been discovered concerning signaling cascades and mechanical guidance of these processes, a generalized rational control of shape is beyond actual capabilities, and a full understanding of what guarantees the logistic and morphological coordination in this phenomenon is missing.⁴ A further unclear question concerns the control of energy flows. It is now well established that biological organisms are dissipative systems crossed by the flow of metabolic energy. However, the problem of how energy is accumulated and transferred within living systems constitutes up to now one of the main problems of biophysics. The process from which most of the biological energy comes is the hydrolysis of adenosine triphosphate (ATP) in adenosine diphosphate (ADP). The quantum of energy released under normal conditions, as is well known, is equal to about 12 times the thermal energy and, if the process should occur freely in the intracellular environment, as described by molecular biochemistry, the energy obtained would be rapidly thermalized. This is expected in most cases, due to the relatively large distance between the place of production and that of use of energy. However, this does not happen at all and the mechanistic model is not able to explain how it is possible.⁵ The last fundamental problem concerns the genesis

of living systems. Since ancient times the problem of how living systems may develop from non-living matter has been examined. In the most remote age, this problem seemed of no particular importance: people believed that the mud in the canals could generate worms or that the dirt could generate flies. The discovery of microorganisms by Antonie van Leeuwenhoek, around 1670, questioned this type of belief, and about 200 years later Pasteur showed experimentally that microorganisms do not form spontaneously and that only living systems can generate other living systems. Nevertheless, today many researchers believe that for a very long time, thanks to very unusual environmental conditions, microorganisms could form spontaneously. Stanley Miller experimentally tested this hypothesis, by using a special set-up simulating the conditions of the primitive terrestrial atmosphere. Even if he obtained racemic mixtures of numerous amino acids, many of which are non-proteogenic, many proteogenic amino acids were missing and no peptide was detected. So, nowadays nobody has an idea of how a living system, even an extremely elementary one, could develop from a suitable set of chemicals. This series of unsolved questions shows that there is no global model able to describe various aspects of biological systems accurately, therefore a satisfactory description of their behavior still appears far away. From the point of view of their material constitution, biological systems differ from other systems in the condensed state due to the significant presence of ephemeral and complicated structures, defined by Schrödinger in his essay “What Is Life?” as aperiodic structures, to underline the presence of symmetries different from those, relatively simpler, normally used in Physics. A fundamental aspect of these structures, from the functional point of view, is their continuous variability over time, which is at the basis of the vital processes of living organisms. Freezing of these dynamics causes generally the system death. So, the existing analysis techniques, generally based on a mechanistic approach, exhibit huge difficulties to achieve valuable information on the system behavior from an experimental point of view. Indeed, even if these techniques are able to describe the ‘frozen’ system from a microscopic point of view, they are nevertheless unable to detect further qualities emerging in the living system thanks to its dynamic complexity (Turner et al. 2018).

²Though there are definitely a lot of unresolved problems in all areas of biology, this is too defeatist a statement. A lot of morphogenetic processes have been explained and modelled sufficiently well by now (see e.g. <https://www.sciencedirect.com/journal/biosystems/vol/173/suppl/C> and <https://link.springer.com/book/10.1007/978-3-319-13990-6>) – editor’s note.

³This is a personal term of the authors. Though e.g. plant roots really have specific zones of cell division and growth, this term is not used in general (editor’s note).

⁴This is not exactly so. Morphogenetic processes are largely understood in terms of mechanical guidance and morphomechanical feedbacks (see also <https://www.sciencedirect.com/journal/biosystems/vol/173/suppl/C> and <https://link.springer.com/book/10.1007/978-3-319-13990-6>), though there are definitely a lot of issues still under question (editor’s note).

⁵The energy ‘stored’ in the ADP-P bond of ATP is typically estimated as 7.3 kcal/mol, which is approx. 12 times the thermal oscillations energy at room temperature ($RT = N_A kT = 0.593$ kcal/mol). However, the ATP molecule is quite stable at neutral pH, which allows its relatively long lifetime in the cell, and performing both energy and signaling functions (see e.g. <https://www.ncbi.nlm.nih.gov/books/NBK553175/>).

There are many ATP-producing processes in the cell, including the famous F_0F_1 ATP synthase (see e.g. <https://academic.oup.com/jb/>

[article/149/6/655/2182760](https://academic.oup.com/jb/article/149/6/655/2182760)). The general principle, allowing the $ADP + P_i \rightarrow ATP$ reaction, notwithstanding the thermal and chaotic environment is its direct mechanistic association with the ‘fuel process’ (here – the proton gradient relaxation). A similar principle can be traced in all ATP-using reactions (see more in <https://www.norton.com/books/9780393884821>) – editor’s note.

31.1.3 What We Know About the Behavior of Living Systems

Living systems possess many specific properties distinguishing them from usual inanimate matter. They are able to adapt to the environment thanks to fine control and coordination of all the chemical and physical processes occurring inside them. The number of complex structures working inside even simple biological systems is astonishing but they are based on quite a limited set of structures: hundred thousand proteins are built up by about 20 amino acids while genetic code is based on four types of molecules. Even if in principle practically no one denies that the global behavior of these complicated structures obeys the laws of Physics and Chemistry, it is not possible to apply the mechanistic principle to describe their behavior at all. As a matter of fact, analysis of complex systems' behavior has demonstrated that on increasing the system's complexity new properties emerge (Thurner et al. 2018). A simple example of a complex system is a cloud: a formation that cannot be described through analyzing microscopic interactions between individual molecules but which arises from the cooperation of various fields, functions of time and space, such as the gravitational field, the fields of pressure and velocity present in the atmosphere and humidity. This system is activated by the flows of thermal energy coming from the sun or radiated from the earth.

Therefore, in the case of complex systems, it is not possible to study the system as constituted of parts interacting only between close neighbor atoms, but it is necessary to take into account a great number of weaker and often long-range interactions. Some of these interactions are due to the ubiquitous presence of water inside living systems.

A fundamental property of all known living systems is the ability to manage changes both inside and outside the organism. As soon as this capacity is lost, the biological system slips toward its final state of equilibrium: death. During the lifetime of the organism, every cell of it maintains homeostasis by managing space and time inside a, to some extent, undetermined environment. It is, therefore, necessary to adequately understand the foundations of homeostasis and of its evolution during the life of a system, which, through development, reaches aging. The multiplicity of possible scenarios clearly tells us that these processes are managed by information that cannot be traced back to the genetic information of individual cells. Clearly, there is more than one way to integrate the same combination of signals into a phenotype, making the result of the overall process very robust (Bissell et al. 2003). The understanding of this kind of phenomenology probably cannot be achieved through a mechanistic investigation taking into account the interactions between single molecules. An in-depth analysis of the temporal

evolution of the spatial structures of tissues and biological systems will be necessary (Nelson and Bissell 2006).

Nevertheless, even if it should seem that also the simplest of biological systems never should be described *ab initio* using the quantum mechanics formalism, even employing very powerful modern computers,⁶ a possible way is individuated starting from the very characteristics of living systems.

As Linus Pauling said: "Life is a relationship among molecules and not a property of any one molecule."

Many life processes are associated with variations in degrees of freedom related to collective properties. These processes are often characterized by relatively long relaxation times because their degrees of freedom are relatively isolated from the other degrees of freedom of the system.

As an example, the memory process is associated with the collective interaction of a large number of neurons. In a similar way, the muscle contraction process is the result of the action of many structural elements whose action is coordinated in space and time and likely allows the transmission of non-linear excitations propagating along the proteins structure.

The study of the behavior of these degrees of freedom, which can often be described as quasi-particles, could allow the explanation of a vast number of experimental facts related to biological systems, favoring a dynamic non-mechanistic view of their functioning. The migration of these collective states, such as solitons, excitons, and polarons along low-dimensional structures, which abound in biological systems, can be revealed and described by studying the photons that are emitted when these excited states decay. These signals, due to their nature and function, are of extremely low intensity, at the level of single photons, so it is necessary to increase their intensity. The solution to this problem does not appear to be simple. We need to identify analytical techniques able to explore not the behavior of individual molecules but the global response of the systems in terms of collective states, that allow to follow the time evolution of the examined systems. An analysis technique that has shown in many cases to be able to give functional information on the state of biological organisms is delayed luminescence (DL) (Jursinic 1986; Niggli 1993; Van Wijk et al. 1993; Chirvony et al. 2017; Yamagishi et al. 2018; Mengmeng et al. 2019; Yagura et al. 2019; Stolz et al. 2019).

⁶We cannot agree with this too strict a statement. Although the authors' reflections on self-organizing systems generally coincide with our understanding, they do not exclude the application of classical and quantum physics approaches. Moreover, self-organization in quantum systems is a vast and developing part of science (see e.g. <https://iopscience.iop.org/article/10.1088/1742-6596/966/1/012027>) – editor's note.

31.1.4 DL and Its Potentiality

DL is the emission of photons, by condensed systems, following the illumination of the systems through a source that emits in the UV-VIS range. This emission, detectable after turning off the excitation source, is generally very weak, some orders of magnitude lower than the fluorescence. On the other hand, the time window in which the phenomenon can be analyzed ranges from microseconds to seconds or, in some cases, to hundreds of seconds. To take into account so long-lasting times the DL has been described through the Jablonski diagram (Jursinic 1986), which connects DL to the repopulation of an excited singlet state via a back reaction from an undefined metastable state, where the energy is stabilized.⁷ This description does not explain why DL from biological systems is strongly connected with the system state but a correlation between the DL signals and the ordered dynamic structures of the samples has been assessed (Scordino et al. 2000, 2010; Brizhik et al. 2000, 2001, 2003). Thanks to this connection, application tools in plant breeding (Costanzo et al. 2008; Lanzanò et al. 2009; Grasso et al. 2016), environment control (Yamagishi et al. 2018; Yagura et al. 2019; Scordino et al. 2008) and cancer research (Baran et al. 2010, 2012, 2013, Scordino et al. 2014a, b) have been proposed. To explain the characteristics of the DL signals, a theoretical model has been developed. It explains the DL from biological samples as due to the excitation and decay of non-linear coherent localized electron states (excitons or solitons) in low dimensional biological macromolecules (Brizhik et al. 2000, 2001, 2003; Scordino et al. 2010). These results suggest the possibility to use DL to investigate the processes that underlie the behavior of living systems and the dynamics of their ordered structures. In this paper indeed we analyze this possibility.

31.2 Relation Between Delayed Luminescence and Structures of Simple Biological Systems

31.2.1 General Description of the DL

As already mentioned, the DL phenomenon consists of illuminating a system and measuring the re-emitted light after the end of the lighting period. Various DL parameters can provide useful information on the analyzed system. One of the most used of them is the time trend of the re-emitted light intensity $I(t)$, measured in counts per second. In the general case this trend is described by a linear combination of power laws (see Eq. 31.1), in the simplest case, for

⁷See also Sects. 3.4, 5.2.5, 12.2 and 12.3.

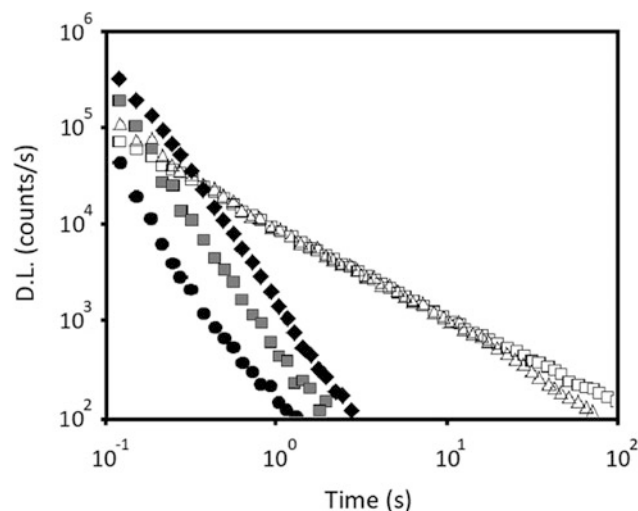


Fig. 31.1 Typical time trend of DL from some biological systems (●) yeast, (□) *A.a.* alga, (Δ) tomato fruit, (◆) soya seeds, (■) pepper seeds. (Reprinted from Musumeci et al. 2000)

instance in the case of *Acetabularia acetabulum* (*A.a.*) alga, a simple power law ($k = 1$ in Eq. 31.1) is sufficient.⁸

$$I(t) = \sum_{i=1}^k \frac{I_{0i}}{\left(1 + \frac{t}{t_{0i}}\right)^{m_i}} \quad (31.1)$$

The time trend and its parameters are usually able to give significant information on the biological system under analysis. Figure 31.1, for example, shows the DL time trend of some biological systems with or without a photosystem. It is possible to see that in the case of organisms having photosystems, the re-emission is shifted to longer times, revealing that the probability of decay of the excited states is lower than that of the systems without photosystems.

Experiments have shown that I_0 , t_0 , and m are useful for studying the connections between DL and some physiological parameters. For example, the damage induced in the unicellular alga *Acetabularia acetabulum* (*A.a.*) by atrazine is detectable by the parameter m variations (Scordino et al. 1996), while the vitality of some seeds can be controlled through the parameter I_0 (Costanzo et al. 2008) and t_0 is connected to the gender and the age in the case of DL from human skin in vivo (Lanzano et al. 2007).

Other parameters that can be used, even if with a quite larger instrumental error, are the excitation and emission spectra of the DL. Figure 31.2 shows that in photosynthetic systems the emission spectrum is similar to the one of chlorophyll while that of excitation differs notably being, within

⁸Although a function can be decomposed into different series, the natural way of analyzing DL trends should include exponential functions, reflecting monomolecular processes of relaxation – compare to Sects. 12.2 and 12.3 (editor's note)

Fig. 31.2 Excitation (continuous line) and emission (dotted line) spectra for fluorescence. Delayed luminescence spectra are respectively reported as dark grey and light grey boxes. (Reprinted from Musumeci et al. 1996)

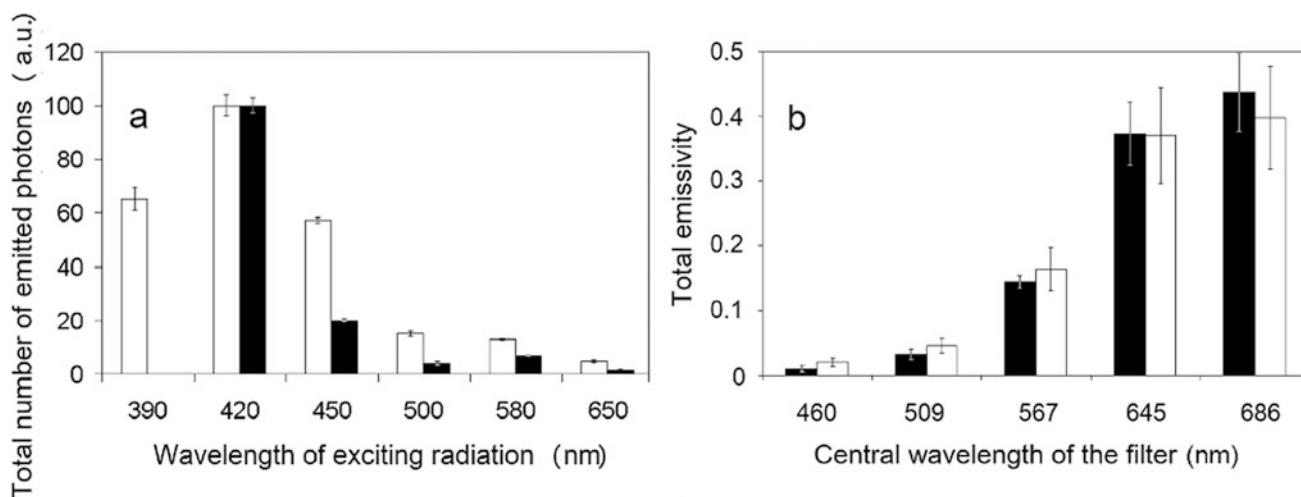
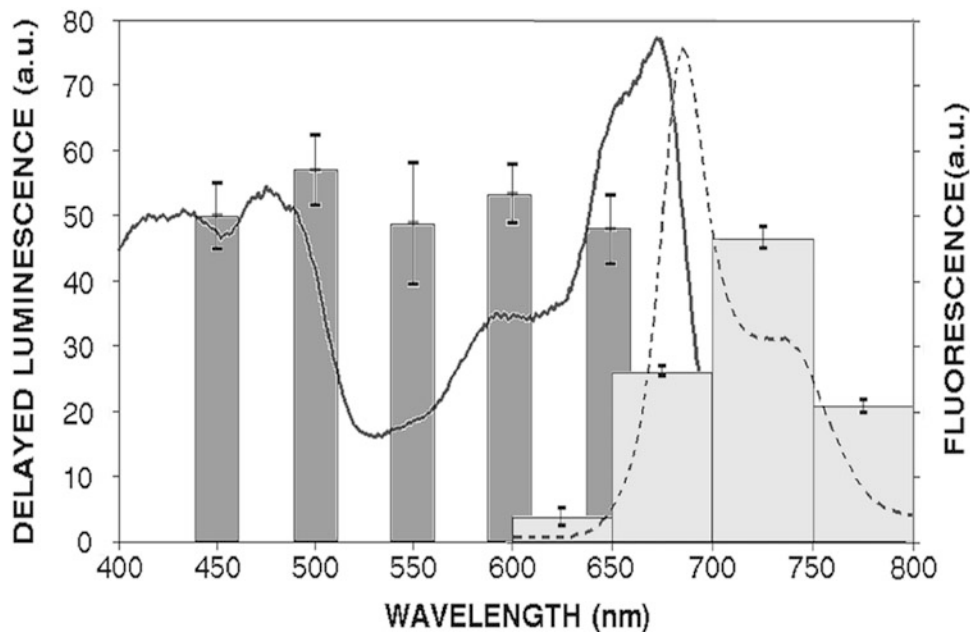


Fig. 31.3 Excitation (a) and emission (b) spectra of Delayed Luminescence of yeast cells (black) and human fibroblasts (white) cultures

experimental errors, almost constant in the range of 400–700 nm. In systems in which photosynthesis is not present the emission and absorption spectra are quite different, but similar to each other for various systems, as shown in Fig. 31.3 for yeast and human fibroblast cells.

Figure 31.4 shows that in some unicellular algae, two of the decay parameters (t_0 and m) are independent of the emission wavelength, so different spectral components decay with the same dynamics (Scordino et al. 2000). This result is in accordance with a model that connects DL to the excitation and decay of collective states within the biological structure (Brizhik et al. 2000).

31.2.2 The DL and the State of Some Living Structures

In order to support the idea that DL could be useful to investigate the processes that underlie the behavior of living systems and the dynamics of their ordered structures, we present a series of results that demonstrate how the DL is closely related to many aspects of the biological systems' functional state. These evidences could be the basis for developing a new vision of their functioning, an alternative to the mechanistic one.

As the first evidence, Fig. 31.5 demonstrates the connexion between the DL and very fundamental processes in the

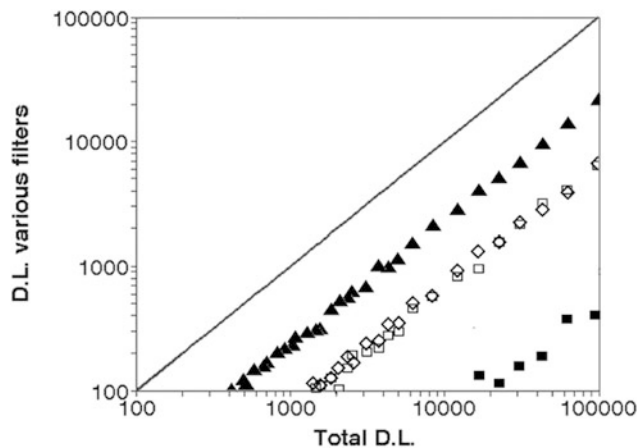


Fig. 31.4 Time trends of spectral components of the emission spectrum of *Acetabularia acetabulum* alga. (■) 600–650 nm, (□) 650–700 nm, (▲) 700–750 nm, (◇) 750–800 nm. (Reprinted from Scordino et al. (2000). Copyright 2000, with permission from Elsevier)

life world, the complex fluxes of energy, matter, and information present in the cell cycle. Figure 31.5 shows precisely how different is the DL from synchronized yeast cells in various cellular phases (Tudisco et al. 2004). The G1 phase in which the cells grow up, by synthesizing polypeptides and nucleic acids and increasing also the number of organelles, exhibits a DL trend very similar to that of the S phase, in which the synthesis and the duplication of genetic material happens. A similar trend is present in the G2 phase, characterized by the full production of genetic material and the appearance of the centrioles and chromosomes. Only the total intensity of DL increases, perhaps due to the growth of the number of excitable states connected with the emission of more and more structures. Very different is the behavior of DL in the M phase: the separation of a big part of the cell produces a decrease in the DL intensity and a faster time trend decay. This first example gives an idea of how sensible DL is to the biological processes inside the living systems, even if it is difficult to understand the genesis of this phenomenon.

31.2.3 DL and Cytoskeleton Dynamics

Within the *A.a.* alga, as within many other plant cells, cytoplasmic streaming is observed, a continuous movement of organelles such as chloroplasts and mitochondria, associated in clusters, connected to their dynamic organization. This movement arises from the flow of metabolic energy connected to the hydrolysis of nucleoside triphosphates. In the *A.a.* alga, it is possible to observe two currents of clusters that move in the opposite direction with velocities that change continuously and whose average value is around $0.25 \pm 0.15 \mu\text{m/s}$ (Van Wijk et al. 1999). Cytoplasmic

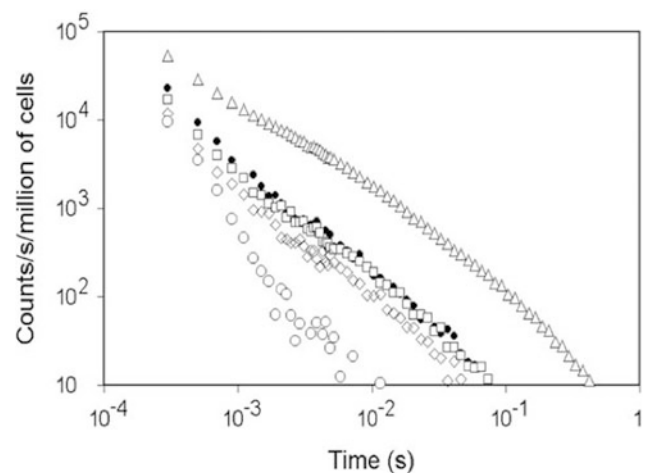


Fig. 31.5 DL from yeast cells in different stages of the cellular cycle: (●) unsynchronized, (□) G1, (◇) S, (Δ) G2 and (○) M. (Reprinted from Tudisco et al. (2004). Copyright 2004, with permission from Elsevier)

streaming is likely connected to the action of the motor proteins, which act on the dynamically unstable polymers that constitute the cytoplasm. The energy flux is ensured by hydrolysis of ATP, able to activate motor proteins and to favor the building of actin filaments, and of Guanosine Triphosphate (GTP) able to favor the formation of microtubules. Organelles and other molecules can move through the cytoplasm thanks to motor proteins. It remains unclear up till now which process constructs the well-ordered actin configurations required for a coherent flow.⁹ DL is able to follow the time evolution of this phenomenon because, during every measurement, the spatial distribution of clusters appears to be ‘frozen’, due to the slow speed which characterizes their movement.

Experiments show that DL is connected to this phenomenon: if one dips an *A.a.* alga in liquid air and then brings it back to the standard culture medium, it is possible to observe with a microscope that the spatial distribution of organelles at a given instant is very similar to the one before the dive. However, the cytoplasm streaming has disappeared. Correspondingly, the effect on the DL is dramatic, as shown in Fig. 31.6a: only about 3% of the original signal survives and then disappears in about a day (Van Wijk et al. 1999).

This kind of procedure is used to isolate chloroplasts and study their fluorescence. In this case, the fluorescence remains almost unchanged (about 80% of the undamaged cytoplasm fluorescence) so it is evident that the collapse of DL is strictly connected to the disappearance of the streaming or, better, to the alteration of the dynamic organization of the cell. This evidence has been further investigated by choosing

⁹Though there are definitely a lot of unresolved questions in this issue, molecular mechanisms of cytoplasmic streaming are generally understood and well demonstrated (see e.g. <https://doi.org/10.1016/j.pbi.2015.06.017>) – editor’s note.

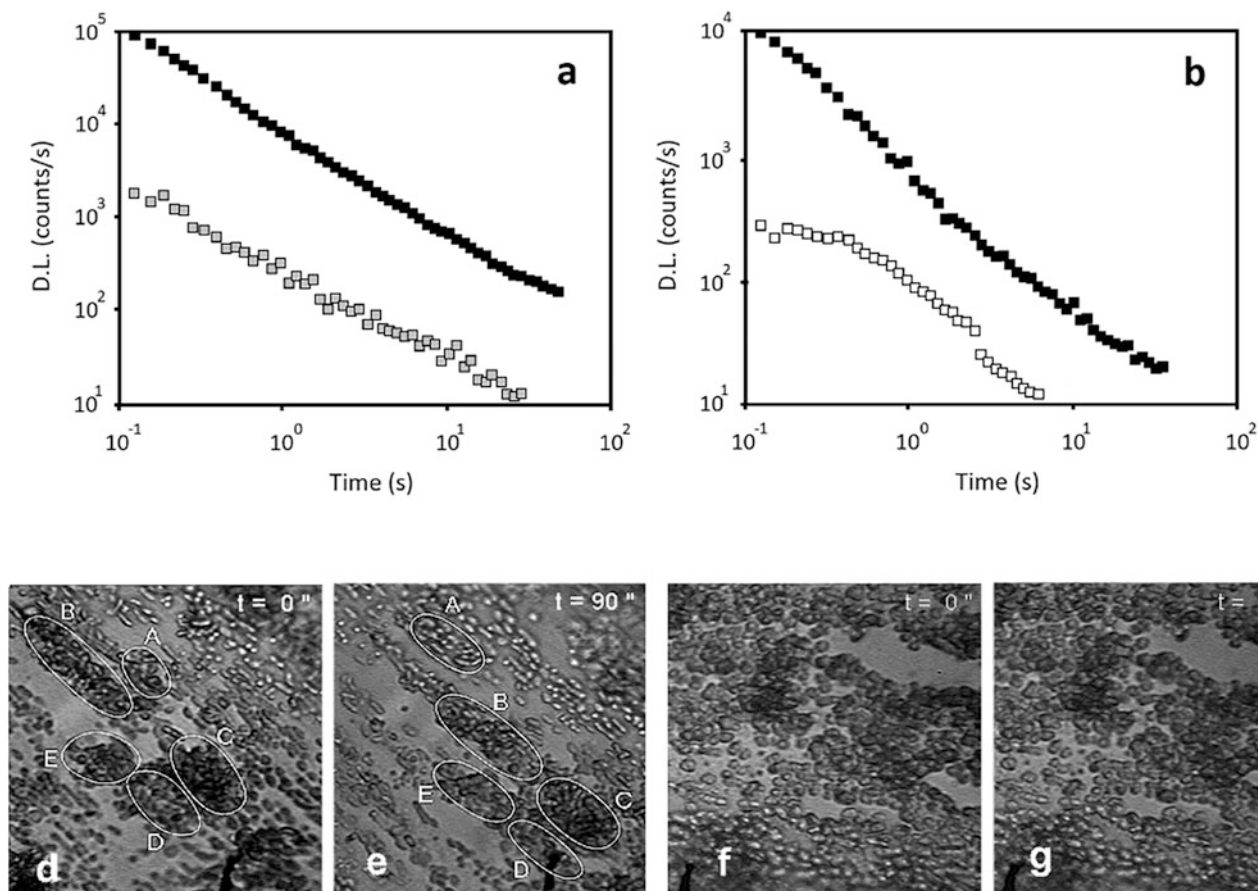


Fig. 31.6 (a) DL of *A.a.* alga. (black square) native, (grey square) after immersion in liquid air. (b) DL of *A.a.* alga (black square) native, (white square) after cooling and immersion in chloroform solution. (d) and (e) photomicrographs of organelles movement, due to cytoplasmic streaming, inside intact *A.a.* Time interval between (d) and (e) is 90 s, square

side dimension is 74 μm . (f) and (g) photomicrographs of organelles inside *A.a.* after freezing and thawing procedure: no cytoplasmic streaming is present. (Reprinted from Van Wijk et al. (1999). Copyright 1999, with permission from Elsevier)

a different method to influence the dynamic organization of the cytoplasm, a reversible one that would allow the possibility of recovering the alga. In this second case, two different types of general anesthetics have been used: chloroform and thiopental sodium. The mechanism of action of general anesthetics is still not fully understood since they do not seem to have alike chemical structures and actions. They were chosen following Penrose and Hameroff (Penrose 1995; Hameroff et al. 1987), who suggested that they could act through van der Waals interactions by altering the normal dynamics of microtubules and therefore the entire phenomenon of the cytoplasmic streaming. Since chloroform is highly volatile, the medium containing the algae was cooled to 4 $^{\circ}\text{C}$, and chloroform was then added until it reached the concentration of 1 mM. In seaweed at low temperatures, cytoplasmic streaming is present. The DL is reduced to about 50% of its value at 20 $^{\circ}\text{C}$. The introduction of chloroform radically changes the situation: the streaming disappears and the DL decreases over time, reaching 10% of the initial value in 5 min (Fig. 31.6b). After that, if the alga is washed and placed

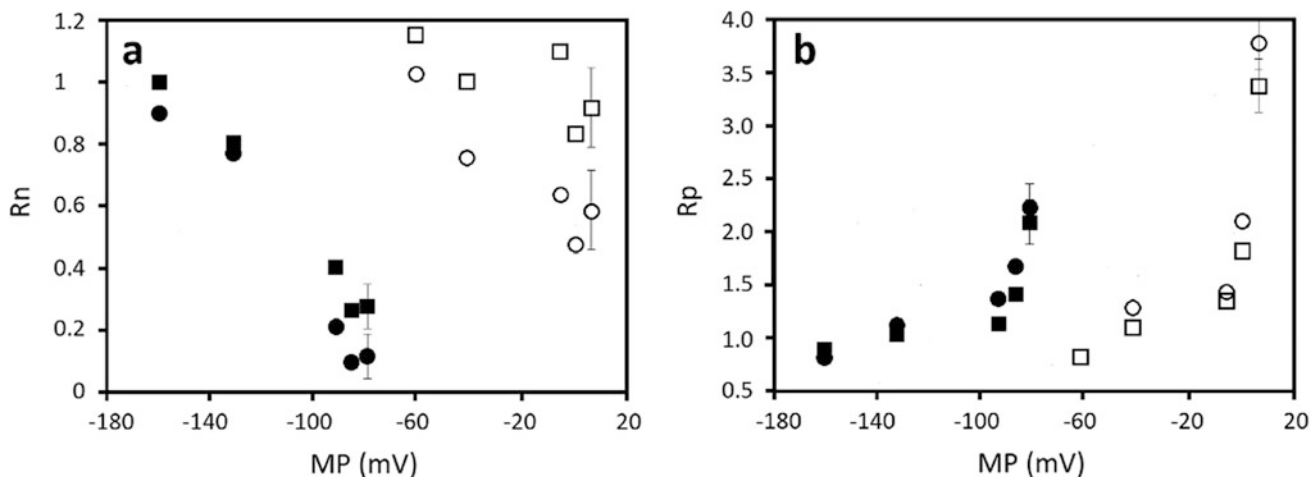
again in its normal culture medium, the protoplasm streaming restarts and DL, both in the total number of counts and time trend, increases returning back to the initial values, that can be hardly distinguished from the initial one (Van Wijk et al. 1999). A longer exposure instead causes an irreversible block of the streaming and death of the alga. A similar result was obtained (Tudisco et al. 2003) when 10 g/l of Thiopental sodium was dissolved in the culture medium of the alga *Scenedesmus subspicatus*. In this case, the presence of the anesthetic also reduces the total number of photons emitted to 2% of those emitted when the alga is in the standard culture medium and the phenomenon is also reversible for short exposure times (data not shown).

31.2.4 Delayed Luminescence and Membrane Potential

Some studies have shown that specific ions dissolved in the culture medium (Ho et al. 1998) affect the structure of the

Table 31.1 Salt contents of test solutions (mM) and membrane potentials (mV)

| Solution | NaCl | KCl | MP (at 25 °C) |
|----------|------|-----|---------------|
| A | 479 | 10 | -160 |
| B | 438 | 50 | -132 |
| C | 238 | 250 | -93 |
| D | 168 | 320 | -87 |
| E | 88 | 400 | -81 |

**Fig. 31.7** (a) Relative number of excited states R_n (a) and Relative probability of decay R_p (b) as a function of the membrane potential (MP). At 0.5 h after immersion and 25 °C (■) or 5 °C (□) and at 2 h after

immersion and 25 °C (●) or 5 °C (○). To avoid confusion in the drawing, the error bars are drawn on only one point. (Reprinted from Ho et al. (2000). Copyright 2000, with permission from Elsevier)

cytoskeleton and the characteristics of the cytoplasmic streaming in the *A.a.* alga. In particular, if the medium contains some basic salts such as NaCl (480 mM), KCl (10 mM), MgCl₂ (20 mM), and CaCl₂ (10 mM), the alga perfectly survives for a few weeks and, at a microscopic analysis, exhibits a normal cytoskeletal structure and cytoplasm streaming. Varying the ratio between the amounts of NaCl and KCl, with MgCl₂ and CaCl₂ concentrations and total osmolarity maintained, one gets the following solutions (see Table 31.1) which allow survival of the alga and apparent conservation of both the structure and the cytoplasm dynamics from the microscopic point of view.

In these conditions, the membrane potential (MP) varies in a considerable way and this affects the biological system evolution over time. These variations influence, among other things, the processes of energy accumulation and exchange within the alga and are dramatically linked to the temperature value (Ho et al. 2000). It has been experimentally seen that the DL is able to provide information on these processes. In principle, we could use the parameters present in Eq. 31.1 but it is simpler to use some parameters which present a more immediate physical meaning. So, two parameters derived from the time trend of the DL were used. The first one $N(t')$ is connected to the total number of excited levels which decay in a radiative way after the time t' after the end of illumination while $P(t')$ represents the probability of decay per excited level at time t'

$$N(t') = \int_{t'}^{\infty} I(t) dt \quad P(t') = \frac{I(t')}{N(t')} \quad (31.2)$$

$N(t')$ and $P(t')$, normalized with respect to the corresponding values for the alga kept in darkness for 12 h in solution A, become respectively the parameters R_n (Relative number of excited states) and R_p (Relative probability of decay).

R_n is connected to the energy stored within the system available for radiative decay, and R_p is inversely related to the capacity of the system to prevent both radiative and non-radiative decay. The results presented in Fig. 31.7 are the average of the values obtained measuring four samples each consisting of three individuals (Ho et al. 2000). The samples were placed in different solutions at 25 °C when the plant is actively metabolizing, and at 5 °C when both the electrogenic pump, which overcomes passive diffusion, and the metabolic pump,¹⁰ which maintains the ATP pool, are inactive. Measurements were performed at 0.5, 1, 2, and 4 h after the sample's immersion in their specific solution. Figure 31.7 reports only data related to 0.5 h and 2 h after the algae immersion in the solutions.

¹⁰These are the authors' personal terms for a set of ion pumps and molecular processes generating ATP (editor's note).

In solution A, which gives the maximum membrane potential of -160 mV at 25 °C, the two parameters deviated only slightly from the value at the starting point (equal to 1) and tend to return to it. This means that homeostasis is maintained in both Rn and Rp . The homeostasis is particularly good at 25 °C, nevertheless, even when the temperature is 5 °C and the intensity of DL is reduced to about 40% of the value at 25 °C, the values of Rn and Rp remain close to 1.

DL parameters change in solutions B, C, D, and E at both 25 °C and 5 °C. Figure 31.7 shows that a progressive increase of Rp (especially at 25 °C) and a decrease of Rn occur, on changing the membrane potentials. This behavior is also influenced by temperature. As a matter of fact, the electrogenic pump, which opposes passive diffusion, and the metabolic pump, which maintains the ATP pool, are both active at 25 °C and inactive at 5 °C. The quasi-linear decrease of Rn vs membrane potential at higher temperatures suggests that energy stored in excited levels is strongly connected to the membrane potential and is weakly influenced by the time spent in the test solution. Regarding lower temperatures, the influence of the immersion time becomes significant. Regarding the relation between Rp and membrane potential, at both temperatures, Rp is constant inside experimental errors up to a certain value of MP and then becomes nearly independent of MP itself.

31.2.5 Delayed Luminescence and Temperature

The connection between the DL and the dynamic nature of cell structures is illustrated also by the behavior of DL at changing the system temperature. Inside the temperature interval that characterizes cell survival, an increase in temperature favors the hydrophobic condensation reaction at the basis of the formation of the cytoplasmic polymers, such as actin filaments and microtubules.

So, on increasing the temperature, a kind of ‘phase transition’¹¹ happens because more and more cytoskeleton proteins are involved in the formation of cytoplasmic structures (Scordino et al. 2000). DL reveals this process by an increase of the yield, as shown in Fig. 31.8 in the case of the *A.a.* alga. It is interesting to compare this behavior with that of DL from the alga after immersion in liquid air and subsequent thawing in the standard culture medium. In the latter case, even if the basic monomers of cytoskeleton structure are present and some organelles, as chloroplasts, appear undamaged, the DL yield is strongly reduced and is about insensitive to the temperature change. So, DL response results are correlated to the flux of energy and material present in normal living cells.

¹¹This is also the authors’ personal interpretation: there are no generally accepted data on phase transitions under these conditions (editor’s note).

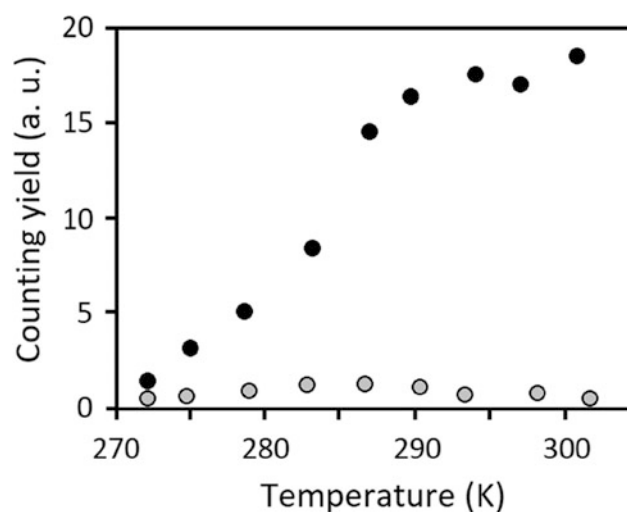


Fig. 31.8 Behavior of DL yield of *A.a.* alga on changing temperature: (black dots) native, (grey dots) after immersion in liquid air and thawing in standard culture medium. (Reprinted from Scordino et al. (2000). Copyright 2000, with permission from Elsevier)

One can calculate the energy associated with this monomers-polymers transition with the Arrhenius plot. It is difficult to perform a complete quantitative evaluation of the microscopic parameters. Nevertheless, it is interesting to observe that, in the case of *A.a.* alga, this energy is of the order of 1 eV, so similar to the value of the free energy of polymerization of the 13 tubulin couples necessary to build up a microtubule layer (Desai and Mitchison 1997). Analogous results have been obtained (data not shown) comparing the DL of human cells at 32 °C, close to the normal working temperature of the cells, which are characterized by a polymer-rich cytoplasm, and 10 °C when metabolic reactions are drastically reduced and the cytoskeleton proteins appears prevalently as monomers. At the higher temperature, the DL emission of normal fibroblast and melanoma cells cultures are different both in the yield and in the time trend while at the lower temperature, the DL of these cultures becomes the same, further confirming the DL potentiality in the analysis of living processes (Musumeci et al. 2005).

31.2.6 The DL and the Structure of Biological Polymers

A crucial problem in the study of biological systems is how water affects the structure of polymers immersed in it. If a material is insoluble in water, the influence of water is often taken into account by considering water as a continuum, characterized by a high dielectric constant. To check the validity of this approach the DL of dry cellulose, a well-known glucose polymer, has been compared with the DL of the same cellulose sample after imbibition (Grasso et al.

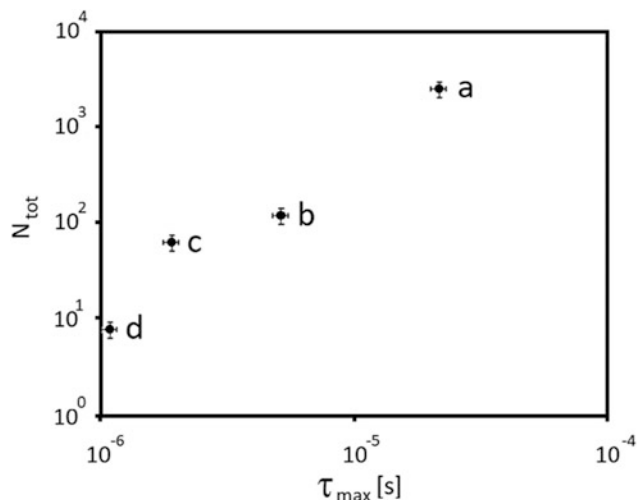


Fig. 31.9 DL Yield as a function of τ_{\max} . (a) Cellulose type 50, (b) Wet Cellulose type 50, (c) α -D-glucose power, (d) D-Glucose water solution. (Reprinted from Grasso et al. (2019). Copyright 2019, with permission from Elsevier)

2019). Due to its hydrophilicity, imbibed cellulose is able to contain about 30 water molecules per every glucose of the chain without any loss. Moreover, the DL of a glucose solution in water characterized by the same number of water molecules per glucose molecule has been measured. These measurements show that water indeed affects both the total number of photons measured N_{tot} as well as the time trend of DL. The DL time trend $I(t)$ can also be described as a convolution of a suitable distribution of exponential decays (Berberan-Santos et al. 2005):

$$I(t) = I_0 \int_0^{\infty} h(\tau) e^{-t/\tau} d\tau \quad (31.3)$$

where $h(\tau)$ represents the lifetime probability density function. Starting from the DL time trend the lifetimes probability density function $h(\tau)$ was evaluated. It resulted that the presence of water changes the lifetime's distribution, which moves to shorter lifetimes going from dry to wet conditions. Figure 31.9 shows the dependence of the total number of counts N_{tot} and of the time τ_{\max} corresponding to the maximal value of the lifetime's probability density. N_{tot} is connected to the number of states excited during the initial illumination that decay in a radiative way, while τ_{\max} is connected to the capacity of the excited states to survive within the system structure.

It is interesting to note that DL parameters appear to be able to discriminate between different polymeric structures: in Fig. 31.9 the parameters related to different structures are allocated in very distinct positions within the N_{tot} vs τ_{\max} plan even if, as in the case of (b) and (d) they present the same

chemical composition. This fact could favor the development of an analysis technique able to follow the formation or demolition of certain structures inside non-equilibrium systems. Moreover, this result underlines the importance of water's role inside biological systems: one must expect that the structure of biological polymer is always strongly influenced by the presence of water and this should be taken into account when the connection between structure and function is studied.

31.3 A Possible Origin of DL

To better understand the characteristics of the DL emission from living organisms and its connection to the dynamical structures and the energy fluxes inside the systems, a full set of measurements on a relatively simple organism has been performed. For this purpose, the *A.a.* alga has been chosen, because it is simple to manage and characterized by a noticeable DL emission. The DL from the alga was measured by changing the exciting light intensity, duration, and wavelength. Every sample consisted of a single individual of *A.a.* alga cell and each measurement required a rather long time: it takes 400 s to collect about 95% of the total DL yield and a further 1800 s to reach the unperturbed (before illumination) value.

As expected from the excitation spectrum of Fig. 31.2, the sample response was independent of the incident radiation wavelength (Scordino et al. 1993). This result suggests that the DL is not related to absorption by *A.a.* alga pigments which, in the *A.a.* alga extracts, exhibit two peaks in the fluorescence excitation spectrum at around 433 and 663 nm. Moreover, the DL trends of different *A.a.* alga individuals were very similar to each other, differing only for the total number of counts, so they have been normalized according to a factor that took into account the biological differences between different samples such as size and age. This factor was ranging between 0.6 and 1.7. Figure 31.10 shows the total counting yield values for an *A.a.* alga individual as a function of the incident photon dose (the light intensity times the illumination time). The plot covers an incident photon flux range of five orders of magnitude and a time-interval range of three orders (Scordino et al. 1993).

The four different groups are related to different illumination times. In order to improve the visualization, markers related to the same illumination time have been connected by lines. It appears that the measured trends are different from what one could expect. As a matter of fact, one could foresee a well-determined number of excitable levels and, consequently, a linear increase of the signal as a function of the incident dose, followed by saturation when the incident light dose is enough to saturate all the possible levels.

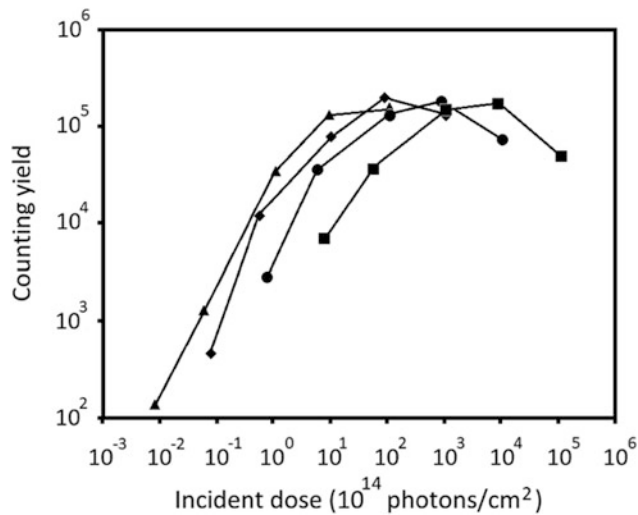


Fig. 31.10 Counting yield of an *A.a* algae vs the incident photon dose achieved at various illumination times: (▲) 1 s, (◆) 10 s, (●) 100 s, (■) 1000 s. (Reprinted from Scordino et al. (1993). Copyright 1993, with permission from Springer Nature)

Most of the above-reported characteristics of DL, including the non-linear response with impinging dose, can be explained within a soliton model. More precisely, the dependence of DL on the system-organized structure suggested the idea that this phenomenon in biological systems could be connected with collective electron states. Indeed, in a biological cell, there is a large variety of low-dimensional macromolecules (as, for instance, alpha-helical polypeptide proteins, actin filaments, etc.) whose structure is represented by the arrays of parallel quasi-one-dimensional (quasi-1D) polypeptide chains formed by periodically placed peptide groups along the chain of hydrogen bonds. From the point of view of electronic structure, these macromolecules are semiconductor-like quasi-1D systems with a filled valence band and empty conduction band, separated by the gap of finite width.

These characteristic properties favor the existence of coherent collective electron and exciton states, in general, and solitons in particular.

In view of the long DL duration, the model assumes that the DL is connected with the formation and dissociation of non-linear coherent self-trapped (localized) electron states (solitons and electro-solitons). These states are much more stable than the corresponding delocalized ones and can be created, in low-dimensional macromolecular structures during the charge and energy transfer processes, by the pre-illumination of the sample.

The simplest energy scheme of the process in the presence of solitons is given in Fig. 31.11 (Brizhik et al. 2001), along with the following group of rate equations:

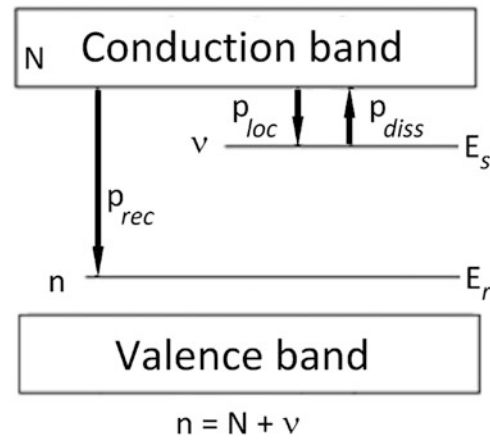


Fig. 31.11 Jablonski diagram that illustrates the electronic states and the transitions originating the DL. (Reprinted from Brizhik et al. (2001). Copyright 2001 by the American Physical Society)

$$\frac{dn}{dt} = -p_{rec}Nn$$

$$\frac{dN}{dt} = p_{diss}\nu - p_{rec}Nn - p_{loc}N(\nu_0 - \nu) \quad (31.4)$$

$$\frac{d\nu}{dt} = -p_{diss}\nu + p_{loc}N(\nu_0 - \nu)$$

where N is the number of free electrons in the conduction band, n is the number of the ionized reaction centers, ν is the number of solitons (occupied soliton levels), ν_0 is the number of available soliton levels, p_{diss} is the rate of soliton photodissociation, p_{rec} is the rate of electron-hole recombination at the reaction center, p_{loc} is the rate of a single soliton formation.

In such a model the intensity of the DL from *A.a.* algae is determined by the electron-hole recombination processes at the reaction center of Photosystem II, according to the equation $I(t) = -dn/dt$. The rate of electron localization p_{loc} depends on the energy of localization E_{loc} , which in turn cannot be considered constant in the case of strongly correlated coherent electrons as it occurs at a relatively high level of excitation (Brizhik et al. 2001).

In these conditions, by introducing dimensionless variables $\tau = p_{diss}t$, $z = n/\nu_0$ and $\gamma = p_{loc}/p_{rec}$, in the steady state regime (p_{diss} much smaller than the decay rate of band electron), we can take into account the effect of pumping on the DL yield, that is the value of $z_{tot} = z(\tau_{ill})$, by integrating $dz/d\tau$ from $\tau = 0$ to $\tau = \tau_{ill}$ (Brizhik et al. 2003). It appeared that:

- (i) in the case of linear pumping (not very high illumination intensity or photon flux, such that the total number of ionized reaction centers is expected to be less than the maximum value n_{max} and constant level of pumping P_0

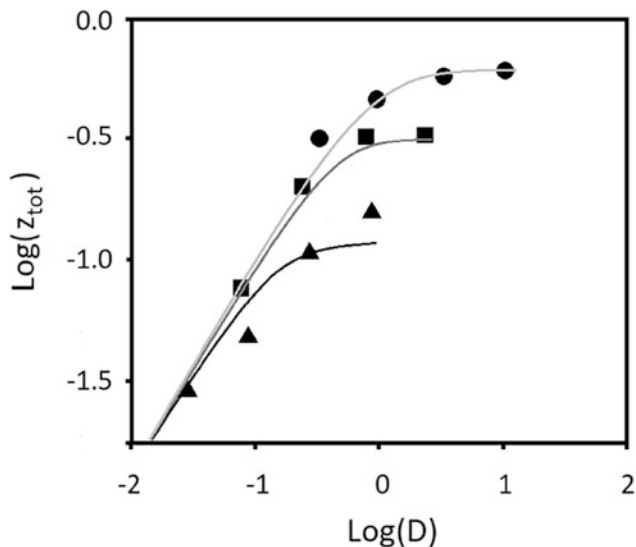


Fig. 31.12 Quantum yield of the DL $z_{\text{tot}} = z(\tau_{\text{III}})$ as function of dose $D = P_0 \cdot \tau_{\text{III}}$ in a Log-Log scale. Markers correspond to the experimental data (in arbitrary units) at different illumination intensities I_{III} : 0.08 (▲), 0.58 (■), 10.87 (●) $\times 10^{13}$ photons/($\text{cm}^2 \text{ s}$). Lines correspond to the theoretical prediction for the corresponding values of pumping level P_0 : 0.05 (black line); 0.36 (gray line); 6.75 (light gray line) at $\gamma = 10$. (Reprinted from Brizhik et al. (2003). Copyright 2001 by the American Physical Society)

can be considered) z_{tot} increases linearly with the dose D till the saturation value depending on the γ value;

- (ii) in the opposite case of non-linear pumping (high intensity of illumination) the numerical analysis shows that a change occurs, due to photoinhibition, in the dependence of z_{tot} on the dose: after an increase up to a maximum value, there is a decrease till the saturation level.

Figure 31.12 shows the accord between experimental data and theoretical predictions.

As can be seen from the figure, the agreement between the experimental data and the theoretical predictions is very good. This reinforces the hypothesis that the DL originated from the excitation and subsequent decay of collective states present within the dynamic structures characterizing the biological systems. Considering the existing relationship, from an experimental point of view, between the DL and various basilar physiological parameters characterizing the vital processes, it can be understood that the DL is potentially able to illuminate these processes by capturing them in their dynamic specificity that, probably, represents one of the discriminatory traits between living and non-living systems.

31.4 Conclusion

The recent successes of biochemistry and molecular biology have not been able to explain a whole series of empirical observations of the phenomena underlying the behavior of

the living system. The fundamental reason for this current inability lies in the fact that the experimental observations and the consequent theoretical elaborations start from an old idea, the mechanism, which has proved extremely useful both in the description of a large part of the physical and chemical world and in the microscopic analysis of basic biological structures. However, this type of approach and the related experimental techniques are hardly capable of analyzing many aspects of living systems because of their dynamic nature. Biological systems can be better represented as systems far from equilibrium, crossed by flows of energy and matter, rather than as particularly refined thermal machines.

This chapter highlights the possibilities offered by delayed luminescence in the experimental study of living systems. It appeared that there is a close connection between DL and dynamical structural organization of the emitting sample. This opens the possibility of monitoring, by DL, the living systems during their biological activity and exploring collective properties of the whole biological multicomponent system.

Finally, many cases have been shown in which drastic changes in some of the parameters that describe DL can be connected to fundamental aspects of biological systems, which allows us to propose DL as a valuable aid in developing a better understanding of the phenomenon we call life.

References

- Baran I et al (2010) Effects of menadione, hydrogen peroxide and quercetin on apoptosis and delayed luminescence of human leukemia Jurkat T-cells. *Cell Biochem Biophys* 58:169–179. <https://doi.org/10.1007/s12013-010-9104-1>
- Baran I et al (2012) Detailed analysis of apoptosis and delayed luminescence of human leukemia Jurkat Tcells after proton-irradiation and treatments with oxidant agents and flavonoids. *Oxidative Medicine and Cellular Longevity* 2012:498914. <https://doi.org/10.1155/2012/498914>
- Baran I et al (2013) Mitochondrial respiratory complex I probed by delayed luminescence spectroscopy. *J Biomed Opt* 18(12):127006. <https://doi.org/10.1117/1.JBO.18.12.127006>
- Berberan-Santos MN, Bodunov EN, Valeur B (2005) Mathematical functions for the analysis of luminescence decays with underlying distributions: 2. Becquerel (compressed hyperbola) and related decay functions. *Chem Phys* 317, 57–62. <https://doi.org/10.1016/j.chemphys.2005.05.026>
- Bissell, MJ et al. (2003) Tissue-specificity: Structural cues allow diverse phenotypes from a constant genotype. In: Müller, GB.; Newman, SA., editors. *Origination of Organismal Form: Beyond the Gene in Developmental and Evolutionary Biology*. Vol. 7. MIT Press, Cambridge, MA, p 103–117.
- Brizhik L et al., (2000) The soliton mechanism of the delayed luminescence of biological systems. *Europhysics Letters* 52 (2), 238–244. <https://doi.org/10.1209/epl/i2000-00429-5>
- Brizhik L, Scordino A, Triglia A, Musumeci F (2001) Delayed luminescence of biological systems arising from correlated many-soliton states. *Phys Rev E* 64 (3): 031902. <https://doi.org/10.1103/PhysRevE.64.031902>

- Brizhik L et al (2003) Nonlinear dependence of the delayed luminescence yield on the intensity of irradiation in the framework of a correlated soliton model. *Phys Rev E* 67: 021902. <https://doi.org/10.1103/PhysRevE.67.021902>
- Chirvony VS et al (2017) Delayed Luminescence in Lead Halide Perovskite Nanocrystals. *J. Phys. Chem. C*, 121(24): 13381–13390. <https://doi.org/10.1021/acs.jpcc.7b03771>
- Costanzo E et al (2008) Single seed viability checked by delayed luminescence. *Eur Biophys J* 37:235–238. <https://doi.org/10.1007/s00249-007-0221-8>
- Desai A and Mitchison TJ (1997) Microtubule polymerization dynamics. *Annu Rev Cell Dev Biol* 13:83–117. <https://doi.org/10.1146/annurev.cellbio.13.1.83>
- Grasso R et al (2016) Effects of Ion Irradiation on Seedlings Growth Monitored by Ultraweak Delayed Luminescence. *PLoS ONE* 11 (12): e0167998. <https://doi.org/10.1371/journal.pone.0167998>
- Rosaria Grasso et al (2019) Impact of structure on the delayed luminescence of D-Glucose based polymer chains. *J Photochem Photobiol B: Biol* 198: 111589. <https://doi.org/10.1016/j.jphotobiol.2019.111589>
- Hameroff SR, Watt RC, Schneiker CW (1987) Models of information processing in microtubules. *Biophysical J* 51(2A): 524.
- Ho MW et al (1998) Influence of cations in extracellular liquid on delayed luminescence of *Acetabularia acetabulum*. *J Photochem Photobiol B: Biol* 45:60–66. [https://doi.org/10.1016/S1011-1344\(98\)00161-4](https://doi.org/10.1016/S1011-1344(98)00161-4)
- Ho MW et al (2000) Change in membrane potential and delayed luminescence in *Acetabularia acetabulum*. *J Photochem Photobiol B: Biol* 55:70–73. [https://doi.org/10.1016/S1011-1344\(00\)00033-6](https://doi.org/10.1016/S1011-1344(00)00033-6)
- Jursinic PA. (1986) Delayed fluorescence: current concepts and status. In Govindjee I, Ames J, Fork DC, editors. *Light Emission by Plants and Bacteria*. Academic Press, New York, p 291–328.
- Lanzano L et al (2007) Spectral analysis of Delayed Luminescence from human skin as a possible non-invasive diagnostic tool. *Eur Biophys J* 36:823–829. <https://doi.org/10.1007/s00249-007-0156-0>.
- Lanzano L et al (2009) Time-resolved spectral measurements of delayed luminescence from a single soybean seed: effects of thermal damage and correlation with germination performance. *Luminescence*. 2009; 24: 409–15. <https://doi.org/10.1002/bio.1127>
- Mengmeng S et al (2019) Characterization of ginsenoside extracts by delayed luminescence, high-performance liquid chromatography, and bioactivity tests. *Photochem. Photobiol. Sci.*, 2019(18): 1138–1146. <https://doi.org/10.1039/C8PP00533H>
- Musumeci F, Scordino A Triglia A (1996) Interaction between the visible electromagnetic field and the living matter: experimental basis for a biophysical approach in “ Current development of Biophysics” Zang C, Popp F A, Bischof M eds Capter 9 Hangzhou University press ISBN 7-81035-903-7
- Musumeci F, Scordino A Triglia A (2000) Delayed luminescence and structure of simple biological systems in “ Biophotonics and coherent systems” Belousov L, Popp F A, Voeikov V, van Wijk R eds Capter 11 Moscow University press ISBN 5-211-04313-8
- Musumeci F et al (2005) Spectral analysis of laser-induced ultraweak delayed luminescence in cultured normal and tumor human cells: temperature dependence. *J Photochem Photobiol B: Biol* 79: 93–99.
- Nelson, C.M. and Bissell, MJ (2006) Of Extracellular Matrix, Scaffolds, and Signaling: Tissue Architecture Regulates Development, Homeostasis, and Cancer. *Annu Rev Cell Dev Biol*. 22:287–309. <https://doi.org/10.1146/annurev.cellbio.22.010305.104315>.
- Niggli H.J. (1993) Artificial sunlight irradiation induces ultraweak photon emission in human skin fibroblasts. *J. Photochem. Photobiol. B* 18:281–285. [https://doi.org/10.1016/1011-1344\(93\)80076-1](https://doi.org/10.1016/1011-1344(93)80076-1)
- Penrose R. (1995) *Shadows of the mind*. Vintage science pp 367–371. ISBN-10: 9780099582113; ISBN-13: 978-0099582113
- Scordino A et al (1993) Physical aspects of delayed luminescence in *Acetabularia acetabulum*. *Experientia* 49:702–705. <https://doi.org/10.1007/BF01923955>
- Scordino A et al (1996) Influence of the presence of atrazine in water on in vivo delayed luminescence of *Acetabularia acetabulum*. *J Photochem Photobiol B* 32:11–17. [https://doi.org/10.1016/1011-1344\(95\)07213-6](https://doi.org/10.1016/1011-1344(95)07213-6)
- Scordino A, Triglia A, Musumeci F (2000) Analogous features of delayed luminescence from *Acetabularia acetabulum* and some solid state systems. *J Photochem Photobiol B* 56:181–186. [https://doi.org/10.1016/S1011-1344\(00\)00078-6](https://doi.org/10.1016/S1011-1344(00)00078-6)
- Scordino A et al (2008) Delayed luminescence of micro-algae as indicator of metal toxicity. *J Phys D: Appl Phys* 41 (15): 155507. <https://doi.org/10.1088/0022-3727/41/15/155507>
- Scordino A et al (2010) Delayed luminescence from collagen as arising from soliton and small polaron states. *Int J Quantum Chem* 110 (1): 221–229. <https://doi.org/10.1002/qua.22010>
- Scordino A et al (2014a) Ultra-weak delayed luminescence in cancer research: A review of the results by the ARETUSA equipment. *J Photochem Photobiol B* 139:76–84. <https://doi.org/10.1016/j.jphotobiol.2014.03.027>
- Scordino A et al (2014b) Delayed luminescence to monitor programmed cell death induced by berberine on thyroid cancer cells. *J Biomed Opt* 19 (11):117005. <https://doi.org/10.1117/1.JBO.19.11.117005>
- Stolz P, Wohlers J, Mende G (2019) Measuring delayed luminescence by FES to evaluate special quality aspects of food samples – an overview. *Open Agriculture*. 4:410–417. <https://doi.org/10.1515/opag-2019-0039>
- Thurner S, Klimek P and Hanel R (2018) *Introduction to the theory of complex systems*, Oxford University Press ISBN 9780198821939
- Tudisco S et al (2003) Advanced research equipment for fast ultraweak luminescence analysis. *Rew Sci Instrum* 74(10):4485. <https://doi.org/10.1063/1.1611997>
- Tudisco S et al (2004) ARETUSA – advanced research equipment for fast ultraweak luminescence analysis: new developments. *NIM A*: 518 (1–2): 463–464. <https://doi.org/10.1016/j.nima.2003.11.056>
- Van Wijk R, Van Aken H, Mei WP, Popp FA (1993) Light-induced photon emission by mammalian cells. *J. Photochem. Photobiol. B* 18: 75–79. [https://doi.org/10.1016/1011-1344\(93\)80042-8](https://doi.org/10.1016/1011-1344(93)80042-8)
- Van Wijk R et al. (1999) Simultaneous measurements of Delayed luminescence and chloroplast organization in *Acetabularia acetabulum*. *J Photochem. Photobiol B Biol* 49:142–149. [https://doi.org/10.1016/S1011-1344\(99\)00048-2](https://doi.org/10.1016/S1011-1344(99)00048-2)
- Yagura R, Imanishi J, Ikushima Y, Katsumata M (2019) Delayed fluorescence as a new screening method of plant species for urban greening: an experimental study using four bryophytes. *Landscape and Ecological Engineering*. 15:437–445. <https://doi.org/10.1007/s11355-019-00393-8>
- Yamagishi T et al (2018) Evaluation of the toxicity of leaches from hydrothermal sulfide deposits by means of a delayed fluorescence-based bioassay with the marine cyanobacterium *Cyanobium* sp. NIES-981. *Ecotoxicology*. 27(10):1303–1309. <https://doi.org/10.1007/s10646-018-1989-2>.

Index

- A**
Activated chemiluminescence, 114, 253
Aging, 3, 30, 120, 221, 277, 296, 319, 337, 461, 462, 465, 476
Animal, 12, 20, 27, 33, 34, 40–42, 50, 101, 123, 127, 160, 167, 236, 265–275, 316, 344, 348, 365, 394, 395, 404, 406, 407, 410–414, 416, 437, 447, 455, 466, 467, 469, 470, 478, 505
- B**
Biochemiluminescence (BCL), 1–3, 50–52, 189, 267, 455
Bio-functionalization, 496
Biological action of ultraweak UV, 345, 353, 363
Biological autoluminescence (BAL), 1–3, 63, 64, 107, 113, 125, 135, 198, 265–268, 275, 305–307, 309–311, 475–483
Biological coherence, 447
Biological detection of radiation, 15–17, 381, 416
Biological oxidation, 27, 87, 144
Biological window, 489, 494
Biophotonics, 55, 61
Biophotons, 1, 49, 51, 52, 54, 55, 95, 284, 305, 306, 427, 428, 435–440, 449, 475
- C**
Cancer diagnostics, 21, 22, 328, 403, 404, 406, 413–418
Cancer research, 320, 411, 508
Carbonyls, 116, 126–127, 140, 141, 144, 145, 147, 149, 150, 152, 153, 173, 195, 201, 213–216, 305, 390, 468, 476, 479, 481
Cells, 1, 27, 49, 87, 102, 109, 125, 131, 157, 189, 219, 266, 277, 289, 305, 328, 329, 361, 393, 403, 427, 435, 441, 447, 461, 475, 489, 505
Chemiluminescence, 30, 32, 33, 39, 40, 42, 222, 251, 252, 417
Chemiluminescence of animal tissues, 265–275
Chemiluminescence of plant oils, 265–275
Chemiluminescent techniques, 91
Chronobiology, 305, 307–310
Circadian, 289–303, 309, 314
Classification of free radical, 110, 111
Coherence, 50, 430, 438, 440, 442, 447–456, 470–471
Coherent states, 508
Collective excited states, 505–516
Communication, 1, 50, 51, 344, 427, 430, 440–444, 447, 455, 456
Connective tissue, 277, 278, 281–284, 286, 287
- D**
Degradation radiation, 394–397, 399, 404
Delayed luminescence (DL), 53, 63, 69–70, 102, 190, 195, 313–323, 437, 438, 507–516
Diagnosis, 17, 86, 90, 95, 315, 323, 411, 414, 415, 417, 475, 479
- Dioxetane, 147, 151–153, 170, 213, 215, 267, 305
DL applications, 34–38, 53, 63, 69, 102, 190, 195, 313–323, 437, 505–516
- E**
Electromagnetic fields, 49–51, 54, 61, 314, 432, 433, 442, 447–449, 475, 481
Electron excitation, 107, 213, 250, 267, 481, 492
Energy transfer, 2, 3, 62–64, 73, 77–81, 103, 137, 148–150, 202, 206, 213, 361, 379, 437–439, 448, 449, 476, 477, 481, 490–494, 496–500, 515
Environment, 30, 62, 68, 76, 85, 116, 214, 216, 217, 229, 236, 251, 253, 268, 279, 307, 310, 313, 314, 321, 322, 397, 431, 436, 439, 442, 443, 469, 493, 494, 496, 499, 505–508
Enzymatic sources of free radicals, 219–253
Enzymatic sources of ROS, 235–253
Exciplex, 438, 439
- F**
Fascia, 281–286
Food quality, 314, 319, 320, 323
Förster resonance energy transfer (FRET), 103, 496–501
Free-radical processes, 1, 3, 4, 8, 23, 34, 43, 79, 86, 87, 89, 127, 128, 134, 148, 150, 164, 169, 170, 176, 180, 195, 198, 221, 243, 245, 253, 274, 372
Free radicals in the cell, 120, 157
- G**
Gaussian, 214
Germination tests, 306, 307, 309, 310, 321
Gurwitsch radiation, 23
- H**
History of science, 327
Holistic approach, 50
Human, 4, 50, 53, 95, 98, 99, 102, 103, 110, 115, 197, 234, 236, 240, 275, 277–280, 282–284, 286, 287, 289–292, 294–297, 299–301, 303, 306, 314, 315, 317, 318, 370, 406, 411, 425, 430, 436, 441, 448, 455, 464, 466, 471, 476, 478, 505, 508, 509, 513
- I**
Imaging, 95–99, 101–104, 277, 280, 284, 286, 287, 306, 314, 476, 491, 494, 495
Information contents, 442–443
Information transfer, 55, 441–444

- Infradian, 289, 291–303
 International Institute of Biophysics (IIB), 49–55, 306
- K**
 Kinetic chemiluminescence, 84
- L**
 Lanthanides, 269, 489, 491–494, 496, 500
 Laws of luminescence, 64–65
 Lipid peroxidation, 31, 34, 40, 41, 86, 89, 91–93, 103, 110, 112, 113, 115, 116, 157, 158, 165–168, 170, 174, 175, 179, 181, 183, 189, 203, 252, 268, 277, 306, 465, 468, 478, 479
 Luminescence, 20, 31, 51, 83, 107, 123, 134, 167, 189, 219, 265, 305, 372, 392, 429, 464, 475, 489
 Luminescence of amino acids, 30, 42, 190, 195
 Luminescence of proteins, 193
 Luminescence quenching, 3, 71–77, 137
- M**
 Mechanisms of hydrocarbon oxy-chemiluminescence, 131–153
 Metastable states, 36, 37, 63, 313, 438, 439, 455, 508
 Methods of free-radical research, 116
 MGR applied research, 20, 393
 MGR physical properties, 20, 361, 381
 Mitochondria, 30, 40, 41, 220, 231, 234–236, 238, 240, 246–248, 252, 253
 Mitogenetic effect (MGE), 4, 7, 8, 10–15, 17–23, 329, 361–364, 368, 369, 371, 375–377, 381, 382, 387–391, 393, 394, 397, 399, 403–409, 412–418, 455
 Mitogenetic radiation (MGR), 1, 4, 7, 8, 10–23, 49, 123, 327, 328, 330, 334, 335, 339, 344, 346, 348, 351–354, 361–381, 387–396, 398, 399, 403–414, 416, 417, 428, 430, 435, 436
 Modulation, 61, 68, 293, 297, 303, 443
 Molecular mechanisms, 4, 71, 77, 107, 442, 478, 510
- N**
 Nanoparticles (NPs), 480–483, 489–501
 Near-infrared (NIR), 99, 108, 140, 289, 417, 442, 464, 490, 491, 494–496, 499, 501
 Necrobiotic radiation, 363, 396–399
 Negentropy, 436–437
 Non-chemical distant interaction, 1, 50, 51, 344, 348, 427–433, 440–446, 449
- O**
 One-electron oxygen reduction, 41, 107–108, 170, 183, 245, 275
 Oxychemiluminescence (OCL), 135–136, 138–153, 189, 190, 195, 198–209, 219
 Oxychemiluminescence of amino acids, 198–209
 Oxychemiluminescence of fatty acids, 172
 Oxy-chemiluminescence of hydrocarbons, 135, 136, 140, 142, 148, 172
 Oxychemiluminescence of lipids, 172, 219
 Oxychemiluminescence of proteins, 190, 198–209
- P**
 Phosphorescence, 2, 3, 17, 33–38, 42, 62–65, 69, 70, 78, 79, 137, 140, 144, 147–150, 152, 190–193, 195, 196, 200, 213, 217, 313, 499
 Photodynamic therapy (PDT), 489, 501
 Photon detection, 364, 453
 Photon emission, 1–3, 7, 32, 35–38, 40, 49–53, 55, 131, 135–153, 189, 190, 199, 215, 271, 310, 320, 461–471, 477
 Photonics, 52, 267, 306, 313, 315, 323, 468
 Photon sucking, 53, 54
 Photosensitizers (PSs), 322, 496–501
 Physical theory of communication, 441
 Physics of light, 61
 Plant, 4, 7, 101–102, 123, 127, 235, 271, 273, 305, 306, 309, 313, 314, 321, 329, 333, 348, 350, 394–396, 429, 430, 437, 447, 455, 466, 467, 476, 478, 508, 510, 512
 Popp, F.A., 1, 50–53, 55, 279, 284, 290, 293–295, 301, 314, 435, 436, 439
- Q**
 Quantum nonlocality, 447–456
- R**
 Radiative and non-radiative relaxation, 2, 3, 36, 37, 62, 63, 65, 66, 71–81, 137, 153, 199, 476, 480, 481
 Reactive oxygen species (ROS), 3, 43, 49, 86, 90, 95, 102, 108–110, 125, 127, 128, 131, 132, 153, 219, 269, 270, 277, 305, 461–471, 476–482, 499, 501
 Regulation, 49–52, 111, 120, 223, 225, 226, 235, 238, 241, 247, 309, 429–432, 466, 470, 471
 ROS in the cell, 43, 131, 223, 226, 235, 236
- S**
 Secondary mitogenetic radiation, 350, 387
 Self-organization, 396, 427, 455
 Short intense electric pulses, 479
 Signal enhancement, 476–483
 Signal properties, 443
 Singlet oxygen, 79, 108–109, 140–146, 150, 153, 173, 174, 184, 196–197, 200, 202, 204, 213, 221, 268, 275, 305, 463, 464, 468, 476, 479–482, 489, 496–501
 Skin, 102, 103, 277, 278, 280–284, 286, 287, 298, 300, 301, 303, 394, 413, 441, 442, 476, 478, 489, 508
 Spectral analysis, 12, 14, 15, 21, 99–103, 195, 294, 295, 316, 318, 352, 361, 371, 375–377, 381, 390, 391, 407–408, 417, 467, 468
 Squeezed states, 449, 450, 453–455, 471
 Steps in chemiluminescence analysis, 87–89
 Stress, 3, 4, 15, 52, 86, 95, 102, 120, 223, 226, 236, 238, 239, 247, 273–274, 284, 299–303, 306–309, 314, 319, 394, 395, 461, 464–468, 470, 471, 476, 478
- T**
 Transmission of light, 443
 Triplet-emission spectra, 213, 216
- U**
 Ultradian, 289–292, 294, 295, 297–299, 301, 303
 Ultraviolet (UV) chemiluminescence, 368, 370
 Ultraweak photon emission (UPE), 1, 2, 4, 7, 8, 11–12, 17–19, 22, 23, 50, 51, 54, 63, 64, 66, 69, 95–104, 123–128, 131, 135, 137, 139, 141–143, 189, 191, 198–199, 204, 265, 267–275, 277–287, 289–299, 301–303, 305–307, 309, 310, 327, 339, 362, 363, 366, 368–375, 379, 381, 393, 398, 430, 437, 438, 441–444, 455, 461, 462, 464, 467–468, 470, 471, 475, 483

Ultra-weak photon emission and detection, 32
Ultra-weak radiation detection, 363, 364, 371
Upconversion, 481, 489–495, 499–501
Upconverting nanoparticles (UCNPs), 489, 491–501
UPE anatomical pattern, 277–287
UPE generation, 42, 125, 139, 141
UPE physical properties, 11
UV UPE, 327, 363, 369, 371–373, 393

W

Water pollution, 314, 315, 322, 323
Whole-body UPE, 277–287